World Geomorphological Landscapes

Olav Slaymaker *Editor*

Landscapes and Landforms of Western Canada

Springer

World Geomorphological Landscapes

Series editor

Piotr Migoń, Wroclaw, Poland

More information about this series at http://www.springer.com/series/10852

Olav Slaymaker
Editor

Landscapes and Landforms of Western Canada

Springer

Editor
Olav Slaymaker
Department of Geography
The University of British Columbia
Vancouver, BC
Canada

ISSN 2213-2090 ISSN 2213-2104 (electronic)
World Geomorphological Landscapes
ISBN 978-3-319-44593-9 ISBN 978-3-319-44595-3 (eBook)
DOI 10.1007/978-3-319-44595-3

Library of Congress Control Number: 2016948113

© Springer International Publishing Switzerland 2017
This work is subject to copyright. All rights are reserved by the Publisher, whether the whole or part of the material is concerned, specifically the rights of translation, reprinting, reuse of illustrations, recitation, broadcasting, reproduction on microfilms or in any other physical way, and transmission or information storage and retrieval, electronic adaptation, computer software, or by similar or dissimilar methodology now known or hereafter developed.
The use of general descriptive names, registered names, trademarks, service marks, etc. in this publication does not imply, even in the absence of a specific statement, that such names are exempt from the relevant protective laws and regulations and therefore free for general use.
The publisher, the authors and the editors are safe to assume that the advice and information in this book are believed to be true and accurate at the date of publication. Neither the publisher nor the authors or the editors give a warranty, express or implied, with respect to the material contained herein or for any errors or omissions that may have been made.

Printed on acid-free paper

This Springer imprint is published by Springer Nature
The registered company is Springer International Publishing AG
The registered company address is: Gewerbestrasse 11, 6330 Cham, Switzerland

This book is dedicated to the memory of Robert Gilbert (1945–2015), Professor Emeritus, Geography, Queen's University.
Bob was engaged in co-authoring Chap. 22 of this volume when he was stricken with cancer. He died on 27 April 2015 and we have all lost an extraordinary scientist and friend. He was one of my most outstanding Ph.D. students who taught me more than I was able to teach him. During his time at UBC, Alberta and Queen's he led his colleagues and students by example through his passion for research and a deep commitment to teaching at all levels. The sediment cascade and the physical mechanisms by which sediments are delivered to, distributed through, and deposited in water bodies in the Great Lakes region, western Canada, the Canadian Arctic, Greenland, Antarctica, Nepal and the southern USA were the foci of his research. Bob was a highly respected physical limnologist of arctic and periglacial environments whose work will stand the test of time.

Olav Slaymaker

Preface

The inspiration for this volume is a "love of landscape" (Goudie and Viles 2010), specifically the geomorphological landscapes of western Canada. Although the word landscape has many rich and varied meanings, I am here referring to "the total character of a region of the Earth's surface which includes landforms, vegetation (ecosystems), and fields and buildings (anthropogenically modified land)" (von Humboldt 1845). Landscape is the dynamic backdrop to people's lives. Landscapes inspire awe, aesthetic pleasure and scientific curiosity. In my experience, coastal landscapes have been most influential: the island archipelago (skerry guard) and fjords of Norway; the raised beaches, limestone headlands and ria coastline of Wales; and the dramatic fjords and paraglacial coastline of British Columbia have all excited my imagination. These coastal landscapes compel the observer to look beyond immediate surroundings and towards the neighbouring landscapes of Denmark, England, Ireland, Vancouver Island and Asia. All the landscapes in which I have lived have been significantly influenced by glaciation in the geologically recent past, and contemporary processes of coastal and anthropogenic change are self-evident. Geomorphological landscapes are a natural heritage of great aesthetic appeal and are intrinsically valuable (Gray 2003). The threat of degradation from unwise economic development is everywhere real.

The terrestrial surface of Canada is the subject of this two volume series on western and eastern Canada. This first volume deals exclusively with western Canada, an area of approximately 4.65 million km^2. Western Canada is herein defined as British Columbia, Alberta, Saskatchewan, almost all of Manitoba, Northwest Territories, Yukon and a few enclaves of Nunavut. This vast area contains a splendid variety of landscapes and landforms almost all of which have been profoundly influenced by one or more of three continental ice sheets during the Quaternary Period: the Laurentide, the Cordilleran and the Innuitian ice sheets.

The Northwest Territories contain some of the oldest rocks at the Earth's surface. Some 300 km north of Yellowknife and to the east of Great Bear Lake is found the Acasta gneiss with an estimated age of 4 billion years, which is close to the absolute age of the Earth. However, only a tiny fraction of the landscape that is visible today provides clues to the interpretation of palaeolandscapes older than a few hundred million years. Rocks which underlie the Northwest Territories have undergone numerous mountain building episodes, have been sutured along former plate collision zones and have experienced a series of erosion cycles. Today, these landscapes are topographically subdued and some have suggested that they are the most genuine peneplains, or end points of erosion cycles, that exist on the planet (Ambrose 1964).

This book is about landscapes that are larger than individual landforms and smaller than continental scale (Slaymaker et al. 2009). Landform assemblages of western Canada that form uniquely distinctive landscapes are the essence of the volume. These distinctive landscapes include the presence of ice caps and glaciers (almost 30,000 km^2); permafrost underlying 50 % of the region; glacivolcanism and volcanic landscapes; spectacular karst landscapes; structurally controlled landscapes in sedimentary rock sequences; unparalleled variety of mass movement phenomena in paraglacial and periglacial landscapes; fossil sand dune fields and some of the world's finest pingos and patterned ground landscapes; arctic and temperate coastal landscapes adjoining the Arctic and Pacific oceans and magnificent fluvial landscapes,

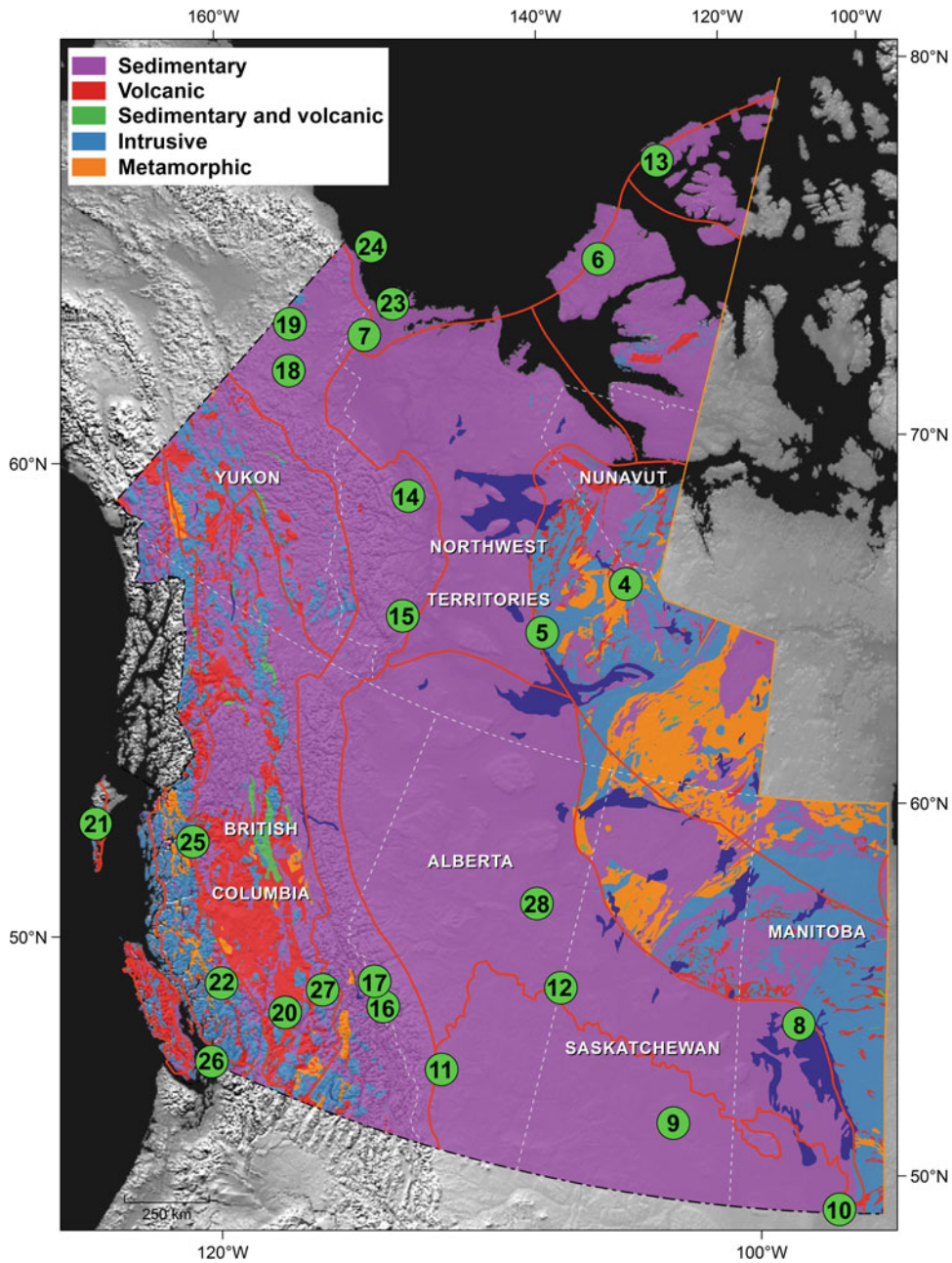

Fig. 1 Distribution of major rock types in western Canada (after Wheeler et al. 1997) and approximate locations of case studies in Chaps. 4–28. Numbers at the sites correspond to the chapter number in this book. Chapter numbers: *4* Slave Geological Province; *5* Great Slave Lowland; *6* Banks Island; *7* Peel Plateau; *8* Little Limestone Lake; *9* Assiniboine River watershed; *10* Red River valley; *11* Foothills Erratics Train; *12* Prairie Dune archipelago; *13* Prince Patrick Island; *14* Canol Road corridor, Mackenzie Mountains; *15* South Nahanni National Park; *16* Castleguard Cave, Banff National Park; *17* Glaciers in Canadian Rockies; *18* Northern Interior, Yukon, *19* Old Crow Flats; *20* Southern Fraser Plateau; *21* Haida Gwaii; *22* Lillooet–Harrison river basin; *23* Mackenzie Delta; *24* Herschel Island; *25* Terrace-Kitimat area; *26* Fraser Lowland; *27* Fraser River; *28* Alberta Oil Sands. Not shown are Chaps. 1–3 and 29. Chapters 1 through 3 are introductory and Chap. 29 deals with the intrinsic value of geomorphological landscapes and the evolution of western Canada's parks and natural heritage sites. The *red lines* represent geomorphological landscape regions and the *orange line* is the boundary between western and eastern Canada (see Chap. 1)

highlighted by the Mackenzie River basin, the fourth largest polar river basin in the world. Anthropogenic change in a thinly populated region such as western Canada (fewer than 2 people per km^2) is nevertheless significant and rapidly intensifying (Slaymaker et al. 2009).

The complexity of geology at the scale of western Canada precludes a discussion of detailed lithological variations. We map the broadest categories of rock types (sedimentary, volcanics, metamorphic and intrusives), thereby giving the reader only a first-order statement about western Canada's geological complexity that must be complemented with details of historical and structural geology at individual sites (Wheeler et al. 1997) (Fig. 1).

Part I (Chaps. 1–3) provides a general overview of the range of outstanding western Canadian landscapes arranged by scale, by tectonic structure and by dominant processes of change. Part II (Chaps. 4–28) consists of case studies of outstanding representative landscapes from which original, field-based research is reported. The locations of these case studies are shown in Fig. 1. Part III (Chap. 29) addresses the question "Wherein lies the intrinsic value of landscape?"

This book could not have been completed without the assistance and technical skills of Dori Kovanen, Research Associate in the Department of Geography at the University of British Columbia. She spent countless hours processing data and designing effective ways of illustrating the landscapes and landforms of western Canada. The Book Series editor, Piotr Migoń, provided valuable advice at all times during the process of book preparation, and Robert Doe and Marielle Klijn of Springer Verlag were consistently supportive. The following expert reviewers gave freely of their time to ensure the scientific quality of the text: Chris Burn (Ottawa), Norm Catto (St. John's), Mike Church (Vancouver), John Clague (Burnaby), Bob Gilbert (Kingston), Vic Levson (Victoria), Piotr Migoń (Wroclaw), Pascale Roy-Léveillée (Sudbury), Jim Teller (Winnipeg), Harvey Thorleifson (St. Paul), Paul Williams (Auckland), Mike Wilson (Vancouver), and Ming-ko (Hok) Woo (Hamilton). To all I express my personal thanks. Whatever errors of interpretation and fact remain are solely the responsibility of the author.

Vancouver, Canada Olav Slaymaker
2016

References

Ambrose JW (1964) Exhumed paleoplains of the Precambrian shield of North America. Am J Sci 262:817–857

Goudie A, Viles H (2010) Landscapes and geomorphology: a very short introduction. Oxford University Press Inc., New York

Gray M (2003) Geodiversity: valuing and conserving abiotic nature. Wiley, Chichester

Slaymaker O, Spencer T, Embleton-Hamann C (eds) (2009) Geomorphology and global environmental change. Cambridge University Press, Cambridge

von Humboldt A (1845) Kosmos: a sketch of a physical description of the universe (vol.1) (trans: from the German by Otté EC). Harper and Brothers, New York

Wheeler JO, Hoffman PF, Card KD, Davidson A, Sanford BV, Okulitch AV, Roest WR (compilers) (1997) Geological map of Canada. Geol Surv Can, Map D1860A, Ottawa

Series Editor Preface

Landforms and landscapes vary enormously across the Earth, from high mountains to endless plains. At a smaller scale, Nature often surprises us creating shapes which look improbable. Many physical landscapes are so immensely beautiful that they received the highest possible recognition—they hold the status of World Heritage properties. Apart from often being immensely scenic, landscapes tell stories which not uncommonly can be traced back in time for tens of million years and include unique events. In addition, many landscapes owe their appearance and harmony not solely to the natural forces. Since centuries, or even millennia, they have been shaped by humans who modified hillslopes, river courses, and coastlines, and erected structures which often blend with the natural landforms to form inseparable entities.

These landscapes are studied by Geomorphology—"the Science of Scenery"—a part of Earth Sciences that focuses on landforms, their assemblages, surface and subsurface processes that moulded them in the past and that change them today. Shapes of landforms and regularities of their spatial distribution, their origin, evolution and ages are the subject of research. Geomorphology is also a science of considerable practical importance since many geomorphic processes occur so suddenly and unexpectedly, and with such a force, that they pose significant hazards to human populations and not uncommonly result in considerable damage or even casualties.

To show the importance of geomorphology in understanding the landscape, and to present the beauty and diversity of the geomorphological sceneries across the world, we have launched a new book series *World Geomorphological Landscapes*. It aims to be a scientific library of monographs that present and explain physical landscapes, focusing on both representative and uniquely spectacular examples. Each book will contain details on geomorphology of a particular country or a geographically coherent region. This volume is the first among two planned to show the geomorphology of the second largest country in the world—Canada. It focuses on the western part of this enormous territory, presenting highly diverse geomorphology, with the legacy of tectonics, volcanism, glaciation, periglaciation, karst and river action. Western Canadian landscapes range from extremely rugged mountain terrains in the west through permafrost-dominated lowlands in the north to nearly featureless plains in the east. But even the latter record a fascinating story of geomorphic change which this book will undoubtedly help to understand.

The World Geomorphological Landscapes series is produced under the scientific patronage of the International Association of Geomorphologists—a society that brings together geomorphologists from all around the world. The IAG was established in 1989 and is an independent scientific association affiliated with the International Geographical Union and the International Union of Geological Sciences. Among its main aims are to promote geomorphology and to foster dissemination of geomorphological knowledge. I believe that this lavishly illustrated series, which sticks to the scientific rigour, is the most appropriate means to fulfil these aims and to serve the geoscientific community. To this end, my great thanks go to

the Editor, Prof. Olav Slaymaker, past President of the IAG, who enthusiastically responded to the invitation to coordinate the volume (and eastern Canada at a later date) and produced it remarkably quickly. I am also grateful to all individual contributors who agreed to add the task of writing chapters to their busy agendas and delivered high-quality final products.

Piotr Migoń

Contents

Part I Introduction to the Geomorphological Landscapes of Western Canada

1 Long-Term Geomorphic History of Western Canada 3
Olav Slaymaker and Dori J. Kovanen

2 Pleistocene Landscapes of Western Canada 27
Olav Slaymaker and Dori J. Kovanen

3 Holocene and Anthropocene Landscapes of Western Canada 49
Olav Slaymaker and Dori J. Kovanen

Part II Case Studies of Periglacial, Aeolian, Fluvial, Glacial, Karst, Coastal and Anthropogenic Landscapes and Landforms Under the Influence of Geological Structure, Climate, and Land Use/Land Cover

4 Slave Geological Province: An Archetype of Glaciated Shield Terrain 77
Stephen A. Wolfe, Daniel E. Kerr, and Peter D. Morse

5 Great Slave Lowland: The Legacy of Glacial Lake McConnell 87
Stephen A. Wolfe, Peter D. Morse, Steve V. Kokelj, and Adrian J. Gaanderse

6 The Banks Island Tundra 97
Hugh M. French

7 The Peel Plateau of Northwestern Canada: An Ice-Rich Hummocky Moraine Landscape in Transition 109
Steven V. Kokelj, Jon F. Tunnicliffe, and Denis Lacelle

8 Little Limestone Lake: A Beautiful Marl Lake in the Interlake Region, Manitoba 123
Derek Ford

9 Landscapes of the Assiniboine River Watershed 131
W.F. Rannie

10 Red River Valley, Manitoba: The Geomorphology of a Low-Relief, Flood-Prone Prairie Landscape 143
Gregory R. Brooks

11 The Foothills Erratics Train Region 157
Lionel E. Jackson Jr.

12 The Prairie Dune Archipelago 167
Stephen A. Wolfe

13 The Polar Desert Landscape of Prince Patrick Island 177
Hugh M. French

14 Cold Climate, Canyons and Karst Along the Canol Road Corridor, Mackenzie Mountains, NWT 187
D.C. Ford and J.P. Hamilton

15 The Many Landscapes of South Nahanni National Park 205
D.C. Ford

16 Castleguard Cave and Karst, Columbia Icefield, Alberta and British Columbia 227
D.C. Ford and C.C. Smart

17 Glacier Landscapes in the Canadian Rockies 241
Brian Henry Luckman

18 The Northern Interior Yukon: An Example of Periglaciation 257
Hugh M. French

19 Old Crow Flats: Thermokarst Lakes in the Forest–Tundra Transition 267
Pascale Roy-Léveillée and Christopher R. Burn

20 The Deglacial Landscape of the Southern Fraser Plateau, British Columbia 277
Tracy A. Brennand and Andrew J. Perkins

21 The Diverse Landscapes of Haida Gwaii 291
Alexandre Bevington, John J. Clague, Thomas Millard, Ian J. Walker, and Marten Geertsema

22 Lillooet-Harrison Drainage Basin: Variable Landscapes Within the Coast Mountains 303
Olav Slaymaker, John J. Clague, Robert Gilbert, Pierre A. Friele, Peter Jordan, Brian Menounos, and Erik Schiefer

23 Mackenzie Delta: Canada's Principal Arctic Delta 321
C.R. Burn

24 Herschel Island (Qikiqtaryuk), Yukon's Arctic Island 335
C.R. Burn

25 The Landslide-Modified Glacimarine Landscape of the Terrace–Kitimat Area, BC 349
Marten Geertsema, David M. Cruden, and John J. Clague

26 The Fraser Lowland: A Polygenetic Paraglacial Landsystem 363
Dori J. Kovanen and Olav Slaymaker

27 Fraser River: History in a Changing Landscape 381
Michael Church

28 Landscapes of the Alberta Oil Sands 395
Nigel Atkinson

Part III The Intrinsic Value of Our Geomorphological Heritage

29 Geomorphological Landscapes and Geoconservation 413
Olav Slaymaker, Norm Catto, and Dori J. Kovanen

Editor and Contributors

About the Editor

Olav Slaymaker Member of the Order of Canada, is a professor emeritus of geography in the Department of Geography at the University of British Columbia, Vancouver, BC. His 20+ co-authored and edited monographs and 160+ refereed papers reflect three distinct styles of work. First, he has pursued original field research for 40 years on sediment systems in the Canadian Cordillera and the European Alps, strongly supported and enhanced by his stellar doctoral and postdoctoral students and international colleagues. Second, he has produced papers and books summarising trends in land use and environmental change in mountain regions. Third, he has edited monographs with invited international contributions on major environmental and geomorphological themes. He is a former President of the Canadian Association of Geographers and a former President of the International Association of Geomorphologists.

Contributors

Nigel Atkinson is a Quaternary scientist and section leader of the Quaternary geology section of the Alberta Geological Survey, Alberta Energy Regulator, in Edmonton, Alberta.

Alexandre Bevington is a research earth scientist with the BC Ministry of Forests, Lands and Natural Resource Operations Prince George, British Columbia, Canada. He is a guest lecturer at the University of Northern British Columbia. His main research interest is the application of thermal models and satellite remote sensing to better understand natural hazards in mountain environments.

Tracy A. Brennand is a professor and chair of geography at Simon Fraser University, Burnaby BC, and a former President of the Canadian Geomorphological Research Group. A geomorphologist and sedimentologist by training, her field-intensive research programme probes the palaeoenvironmental record contained within glacigenic sediments and landforms. Her main interest is in understanding how ice sheets operated in the past, with a view to better understanding how present-day ice sheets may behave in the future. Her research programme integrates geomorphology, digital terrain modelling, topographic surveying, remote sensing, sedimentology, shallow geophysical techniques and geochronology.

Greg Brooks is a research scientist with the Geological Survey of Canada, Earth Sciences Sector, Natural Resources Canada, Ottawa, ON. A geomorphologist by training, his research interests have focused on natural hazard topics, including the effects of high-magnitude flooding, the chronology of prehistoric sensitive clay landslides and palaeoseismicity. He has conducted research in many regions of Canada.

Chris Burn is a professor of geography at Carleton University in Ottawa, Canada. His research concerns relations between climate and permafrost in northwestern Canada, where he is committed to long-term investigations on frozen ground, especially in central Yukon and the Mackenzie Delta area.

Norm Catto is a professor of geography at Memorial University of Newfoundland, St. John's, Newfoundland and Labrador. His research and teaching interests include natural hazards and risk assessment; coastal landforms, erosion, and sea level change; and the impacts of climate and weather events on marine communities, transportation, infrastructure, fisheries, agriculture, and tourism. He has written two textbooks, one on natural hazards in Canada, and another focused on Canadian landforms and associated hazards.

Michael Church Fellow of the Royal Society of Canada, is a professor emeritus in the Department of Geography at the University of British Columbia in Vancouver, BC. His research interests focus on the morphodynamics of rivers at all scales from steepland streams to large rivers. He is engaged in long-term studies of sediment transport and stability in Fraser and Peace rivers. Sediment transport is also studied in an experimental programme conducted in UBC's environmental hydraulics laboratory. In addition, he is interested in fluvial landscape evolution over intermediate timescales (order 10,000 years) and in the history and methodology of geomorphology.

John J. Clague Fellow of the Royal Society of Canada, is a professor of earth science and holds the Shrum Chair in Science at Simon Fraser University, Burnaby, BC; he is also an emeritus scientist, Geological Survey of Canada, and has 40 years experience in surficial/terrain mapping, Quaternary stratigraphic investigations, engineering and environmental interpretations of surficial geological information and natural hazard studies. Clague has published more than 300 papers, reports and monographs on a wide range of earth science topics of regional and national importance. He has had numerous television and radio interviews and has been featured in newspaper and magazine articles. He is a past President of the Association of Professional Engineers and Geoscientists of British Columbia (APEGBA) and a former President of Geological Association of Canada (GAC) and the International Association for Quaternary Research (INQUA).

David M. Cruden Fellow of the Engineering Institute of Canada, is a professor emeritus of the Department of Civil and Environmental Engineering and the School of Mining and Petroleum Engineering at the University of Alberta in Edmonton, AB. His research interests include landslides, slope stability, engineering geology, rock mechanics, geological hazards, geomorphological mapping and geotechnical materials. He has won numerous awards, including the Stermac Award, Canadian Geotechnical Society, and was Legget Medallist of Canadian Geotechnical Society and Varnes Medalist of the International Consortium on landslides.

Derek Ford Fellow of the Royal Society of Canada, is a professor emeritus of geography and earth sciences at McMaster University in Hamilton, ON. His chief interests are in karst processes and landforms, cave genesis and karst aquifers, and palaeoclimate studies of speleothems. These days he is most interested in applied consulting, advising on conservation and UNESCO World Heritage applications. He is author/co-author of $\sim$200 journal papers, many reports to Canadian and foreign government agencies, co-author or co-editor of twelve scientific books, one coffee table book, and producer of a movie for the National Film Board of Canada. He is a former President of the Canadian Association of Geographers and of the International Union of Speleology, and Gold Medallist of the Royal Canadian Geographical Society.

Hugh M. French is a professor emeritus, University of Ottawa, and currently an adjunct professor, Department of Geography, University of Victoria. He is an earth scientist with a special interest in the terrain conditions and landscapes of the cold non-glacial regions of the world. Between 1968 and 1998, he undertook geomorphic research in the western Canadian

Arctic. He has received the Roger Brown Award of the Canadian Geotechnical Society for outstanding contributions to permafrost science and engineering (1989), the Canadian Association of Geographers award for scholarly distinction (1995) and the Lifetime Achievement Award of the International Permafrost Association (2016). He was the founding editor-in-chief of the Wiley journal, *Permafrost and Periglacial Processes,* 1990–2005, and President of the International Permafrost Association, 1998–2003. He is the author of *The Periglacial Environment*, first published in 1976 and now in its 3rd edition (2007), and is co-author with Olav Slaymaker of *Canada's Cold Environments*, published in 1993, and *Changing Cold Environments*, published in 2012.

Pierre A. Friele is a self-employed professional geoscientist in Squamish, BC, and specialises in engineering geology. Pierre's work assignments typically include terrain and slope stability mapping, hazard and risk assessment, flood and erosion protection, and palaeoenvironmental reconstruction. His research has focused on the Quaternary geology and volcanic hazards of the Sea-to-Sky Corridor.

Adrian J. Gaanderse is an agricultural soil science researcher at Cainthus Corporation in Ottawa, with a background in permafrost science. His research focused on lithalsa morphology in the Great Slave Lowland, Northwest Territories, and he currently investigates crop analytics based on aerial imagery.

Marten Geertsema is a research geomorphologist with the BC Ministry of Forests, Lands and Natural Resource Operations in Prince George, BC, and is an adjunct professor at the University of Northern BC in Prince George, BC. His primary focus is on natural hazards and terrain analysis. He is interested in the influence of landslides on biophysical diversity. He is also interested in the effects of climate change on natural hazards, and studies past and present hazard regimes.

Robert Gilbert (deceased) was a professor emeritus of geography at Queen's University in Kingston, ON. He was a highly productive, dedicated and creative scientist. His research focused on sedimentology, limnology and marine systems in the Great Lakes region, western Canada, the Canadian Arctic, Greenland and Antarctica. This book is dedicated to his memory with profound respect.

James P. Hamilton is an associate professor in the Department of Geography at Wilfrid Laurier University, Waterloo, ON. His research interests include climate change and palaeoclimatology; hydrology and geomorphology of karst terrains in cold regions.

Lionel E. Jackson, Jr., is an emeritus scientist, Geological Survey of Canada (GSC) in Vancouver, BC, and is an adjunct professor at Simon Fraser University in Burnaby, BC. He is an authority on the surficial geology of the Rocky Mountain Foothills and southern Yukon. He is a continuing authority in the recognition and evaluation of debris flow hazards in the Canadian Cordillera and he has investigated debris flow and rock avalanche hazards in California, Venezuela, Ecuador, Peru, Bolivia and Argentina. He led an expedition on behalf of the United Nations and GSC to the Republic of Seychelles in 2005 to investigate the effects of the 2004 Indian Ocean tsunami on that island nation. He is currently investigating the glacial and postglacial geology of the Greater Vancouver area of British Columbia.

Peter Jordan is an emeritus scientist with the British Columbia Ministry of Forests, Lands and Natural Resource Operations, based in Nelson, BC. His primary research interests are slope stability, erosion and sedimentation, and watershed sediment budgets. Recent research has focused on large landslides in south-eastern BC, and post-wildfire erosion and mass movement processes.

Daniel E. Kerr is a research scientist with the Geological Survey of Canada in Ottawa, ON. His research focuses on surficial geology mapping and drift exploration techniques for gold, diamonds and other commodities, within the Northwest Territories and Nunavut.

Steven V. Kokelj is a permafrost scientist with the Northwest Territories Geological Survey in Yellowknife, Northwest Territories. He has conducted numerous studies on the physical and thermal conditions of permafrost, thermokarst processes, and the influence of anthropogenic disturbance on permafrost. His research interests include understanding the patterns and processes of permafrost landscape change and improving the compilation, management and synthesis of permafrost information to support northern decision-making.

Dori J. Kovanen is a professional engineering geologist and research associate in the Department of Geography at the University of British Columbia, Vancouver, BC. She is a specialist in Quaternary geomorphology and has written extensively on Late Glacial and Holocene history of the Pacific Northwest as well as contemporary environmental changes in the region.

Denis Lacelle is an associate professor of geography at the University of Ottawa, Ottawa, ON. His research interests include investigation on near-surface permafrost disturbances on water quality under changing climate; origin, stability and habitability of ancient ground ice and permafrost; ice dynamics; and polar environments as planetary analogues.

Brian Henry Luckman is a professor emeritus of geography at the University of Western Ontario in London, ON. He was one of Canada's pioneers in the field of dendro-palaeoclimatology and was seconded as Global Change Coordinator, Terrain Sciences Division, Geological Survey of Canada. He established some of the longest, and regionally extensive, proxy dendroclimatic records in the world. He was the President of the Canadian Geomorphological Research Group and was awarded the CAG Award for Scholarly Distinction in Geography.

Brian Menounos is a professor of geography and holds the Canada Research Chair on Glacier Change at the University of Northern British Columbia in Prince George, BC. His research interests include glaciers and glacier change, process geomorphology, palaeoenvironmental reconstruction, Quaternary and surficial geology and surface hydrology. His research programme focuses on Holocene glacier fluctuations; environmental controls of proglacial lake sedimentation; and recent and future changes to the cryosphere.

Thomas H. Millard is a research scientist with the BC Ministry of Forests, Lands and Natural Resource Operations in Nanaimo, BC.

Peter D. Morse is a research scientist with the Geological Survey of Canada, Ottawa, ON. His interests include biophysical controls on variation of permafrost thermal and physical conditions, the influences of climate change and anthropogenic disturbance on permafrost, and remote sensing of the cryosphere.

Andrew J. Perkins is a lecturer in the Department of Geography at Simon Fraser University in Burnaby, BC. A field-based geomorphologist by training, his research in palaeoenvironmental reconstruction integrates traditional fieldwork with the combined application of remote sensing, geophysical and geochronological tools in understanding landform genesis.

Bill Rannie is a retired professor of geography and senior scholar at the University of Winnipeg in Winnipeg, MB. His research has focused on the historical hydrometeorology of the Red and Assiniboine Rivers, the nineteenth-century environment of the Red River Settlement and the evolution of the lower Assiniboine River.

Pascale Roy-Léveillée is an assistant professor of geography at the Laurentian University School of Northern and Community Studies in Sudbury, ON. Her research focuses on permafrost conditions and thermokarst processes in central and northern Yukon.

Erik Schiefer is an associate professor in the Department of Geography, Planning and Recreation, at Northern Arizona University in Flagstaff, AZ. His research focuses on watershed geomorphology, lacustrine sedimentology, glaciology, remote sensing and GIS applications in the environmental sciences. He has worked in the American Southwest, Alaska,

British Columbia and Alberta. He also teaches graduate courses on advanced geographical methods and professional development.

Chris Smart is a professor of geography at the University of Western Ontario, London, ON. Following a doctorate under Derek Ford's supervision on Castleguard, he has continued work in alpine regions including the Rockies, the Swiss Alps and Southern Alps of New Zealand. His academic focus is on environmental monitoring and instrumentation, coupled with work on glacier hydrology and hydraulics, karst groundwater contamination and landscape evolution.

Jon F. Tunnicliffe is a lecturer in the School of Environment at University of Auckland in Auckland, New Zealand. His research focuses on fluvial and glacial processes and the roles they have played in shaping the Canadian and New Zealand landscapes over timescales of decades to millennia. Jon is presently working on questions relating to climate change impacts in the western Canadian Arctic, including hillslope stability, river sedimentation and permafrost hydrology.

Ian J. Walker is a professor of geography in the Department of Geography at the University of Victoria, Victoria, BC. He is a geomorphologist with expertise in beach and dune systems, sedimentary processes, environmental fluid dynamics, wind (aeolian) processes, coastal erosion, climate change impacts and Holocene landscape interpretation. His research focuses on the British Columbia coast from Haida Gwaii to Pacific Rim National Park and the southern Gulf Islands.

Stephen A. Wolfe is a research scientist with the Geological Survey of Canada, Ottawa, ON, and is an adjunct professor at Carleton University in Ottawa, ON. His research focuses on cold climate processes in Canada, including permafrost and aeolian geomorphology.

Part I

Introduction to the Geomorphological Landscapes of Western Canada

Long-Term Geomorphic History of Western Canada

1

Olav Slaymaker and Dori J. Kovanen

Abstract

Geological timescales and large spatial landscape units of Canada are introduced. The tectonic framework of western Canada is sketched with specific attention to the north–northwest to south–southeast orientation of western Canadian mountain landscapes and the east–west grain of much of the western arctic islands. Structural, physiographic, and geomorphological landscape units of western Canada are defined, and the distinctive landscape impact of volcanic and carbonate lithologies is discussed. A descriptive account of each of the geomorphological landscape units of western Canada provides a general background for the individual case studies reported in Chaps. 4–28.

Keywords

Western Canada • Structural units • Physiographic regions • Geomorphological landscapes • Landforms

1.1 Scale Typology

The terrestrial surface can be considered within four time and space scales as follows. Plate tectonics has been the dominant driver of change over geological time and at the largest and oldest landscape scales (up to 10^8 year and 10^5 km^2); glaciation has superimposed its effects on tectonics at intermediate landscape scales (up to 10^6 year and 10^3 km^2); paraglaciation, defined as non-glacial processes conditioned by glaciation, has modified glaciated land systems at scales of up to 10^4 year and 10^1 km^2; and finally, at up to 10^2 year and 10^{-1} km^2 scales, the effects of local relief, hydroclimate, and human activity are superimposed on older morphologies. The timescales involved correspond closely to the Late Cretaceous–Quaternary periods (this chapter), the Pleistocene Epoch (Chap. 2), and the Holocene and Anthropocene epochs (Chap. 3).

O. Slaymaker (✉) · D.J. Kovanen
Department of Geography, University of British Columbia, 1984 West Mall, Vancouver, BC V6T 1Z2, Canada
e-mail: olav.slaymaker@ubc.ca

D.J. Kovanen
e-mail: djkovanen@comcast.net

The cumulative effect of all drivers (tectonics, climate, lithology, glaciation, paraglaciation, local relief, hydroclimate, and human activity) has produced the polygenetic landscape we see today. This chapter emphasizes the effects of tectonics, climate, and lithology over millions of years and over thousands of square kilometers.

1.2 Terrestrial Structural Units, Physiographic Regions, and Geomorphological Landscapes of Canada

1.2.1 Terrestrial Structural Units

The largest elements of the surface morphology of Canada are determined by long-term tectonic history. These elements are here referenced as the main terrestrial structural units of Canada (Stearn 1975). They have evolved around the core area known as the Canadian Shield and form a concentric pattern of highly folded and faulted mountain systems as well as relatively flat-lying sedimentary platforms. The eight terrestrial

© Springer International Publishing Switzerland 2017

O. Slaymaker (ed.), *Landscapes and Landforms of Western Canada*,
World Geomorphological Landscapes, DOI: 10.1007/978-3-319-44595-3_1

structural units are as follows: Canadian Shield, surrounded by the Arctic, Interior, Hudson, and St. Lawrence platforms; and these platforms are in turn surrounded by the Innuitian, Cordilleran, and Appalachian mountain systems (Fig. 1.1).

1.2.2 Physiographic Regions

Physiography is the land surface morphology, in so far as it summarizes the effects of lithology and available relief superimposed on the tectonic history. The eleven physiographic regions of Canada are the Canadian Shield, the lowlands identified as Arctic Lowlands, Interior Plains, Hudson Bay Lowlands, and St. Lawrence Lowlands, the mountains of Innuitian, Cordillera, and Appalachia, and the coastal areas of the Arctic Coastal Plain, the Pacific Coastal Lowlands, and the Maritime Plain. These regions, with the exception of the last three, are recognizably associated with the eight largest structural units of Canada (Bostock 2014; Fig. 1.2).

1.2.3 Geomorphological Landscapes

Geomorphological landscapes are built on the physiographic foundation of tectonic history and surface morphology but also incorporate the role of permafrost, vegetation cover, and human activity in so far as they affect geomorphological processes of erosion and sedimentation (Smith et al. 2001; Environment Canada 1995; Meidinger and Pojar 1991). The Canadian Shield structural and physiographic region is divided into four geomorphological landscapes on the basis of relief, permafrost, and forest cover; the Interior Plains' structural and physiographic region is divided into three geomorphological landscapes on the basis of permafrost, forest cover, and grasslands; the Hudson Bay Lowlands' structural and physiographic region comprises two geomorphological landscapes on the basis of permafrost and forest cover; Innuitia is divided into two geomorphological landscapes on the basis of relief; and the Cordillera is divided into five geomorophological landscapes based on relief,

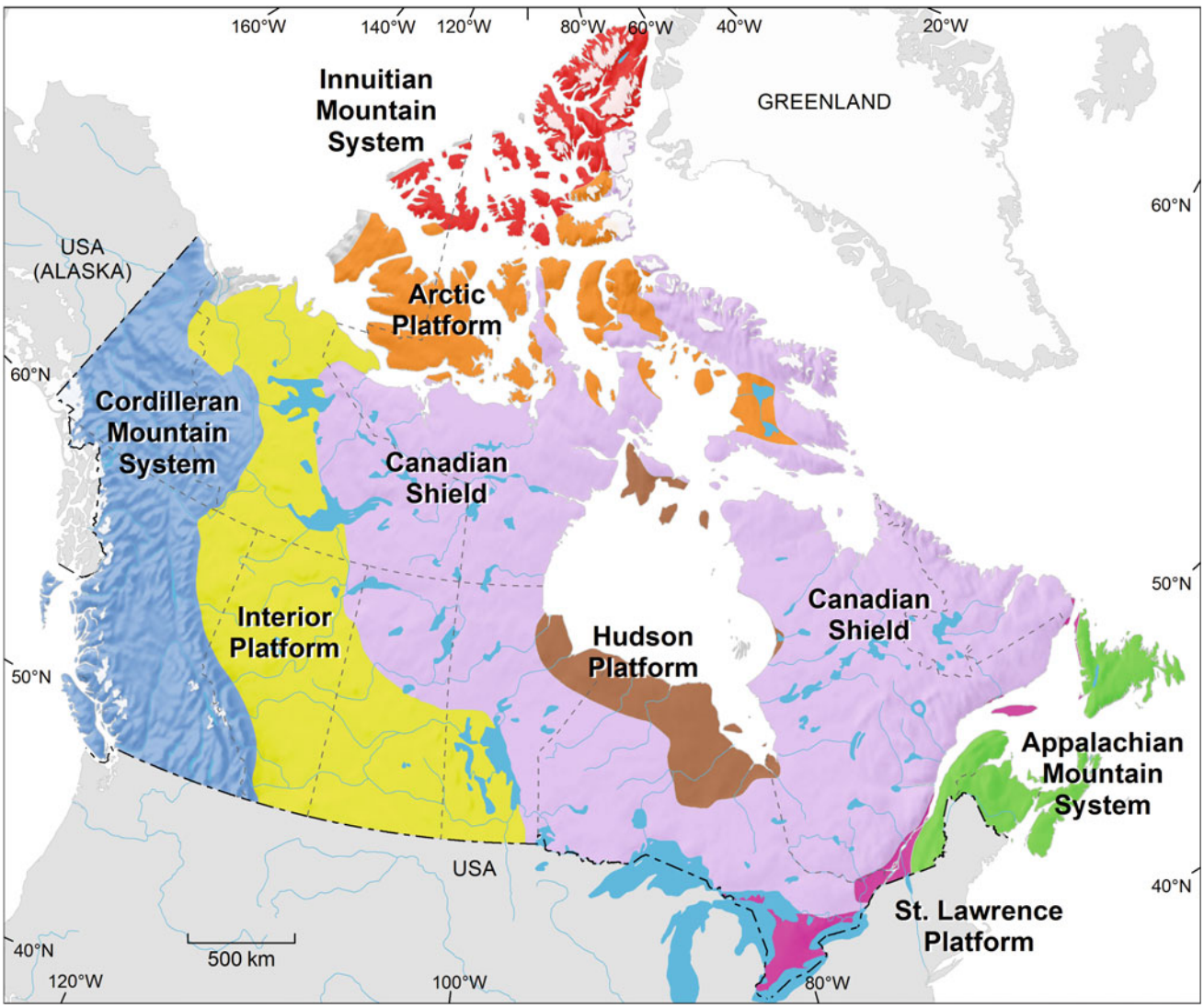

Fig. 1.1 Main structural units of Canada (adapted from Bostock 2014)

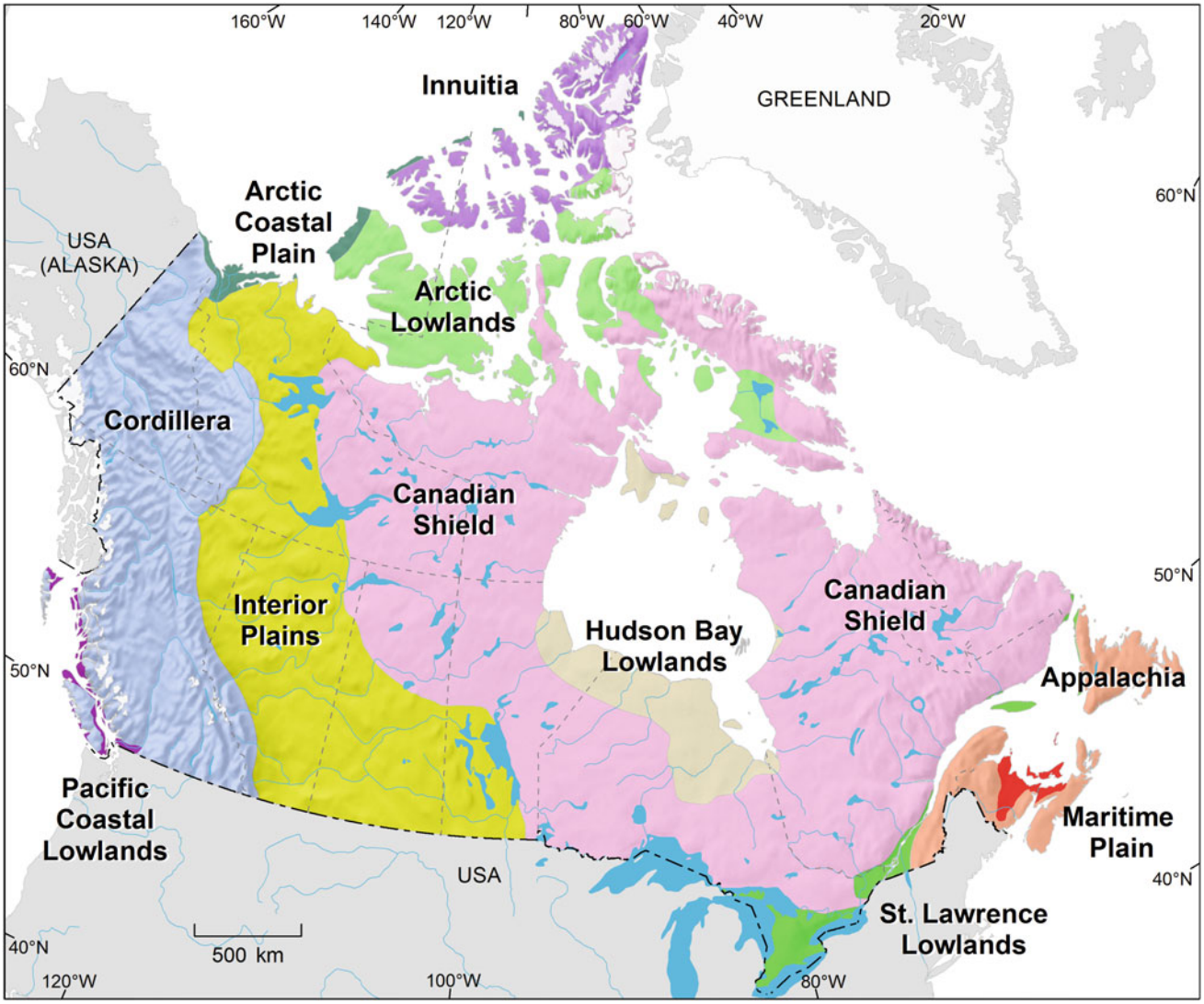

Fig. 1.2 Physiographic regions of Canada (derived from Bostock 2014)

permafrost, forest cover, and grasslands. This brings the total number of geomorphological landscape regions of Canada to twenty-two (Fig. 1.3).

1.3 Plate Tectonics of Western Canada

1.3.1 Pre-100 Ma

The Alberta Plateau, the Rocky Mountains, and the Cassiar–Columbia Mountains began to develop on a zone of continental shelf-slope sedimentation on the west side of the North American craton in Precambrian time [1.6–0.5 Ga (billion years ago)] with a period of mountain building (East Kootenay orogeny) about 0.9 Ga ago. Between 500 Ma (million years) and 200 Ma ago, a complex sequence of island arc activity developed to the west as crustal subduction became more active. Successive, westerly stepping subduction zones defined the Interior Cordillera, the Coast Mountains, and the Insular Ranges. Mathews (1992) considered that the middle or late Jurassic was the starting point of the geomorphic development of the Canadian Cordillera (175–150 Ma ago). The ancestral North America collided with a previously existing intermontane superterrane along its western margin so as to form the Omineca morphogeological belt. Later in the Mesozoic Era (c. 100 Ma ago), a similar collision gave rise to the Coast morphogeological belt.

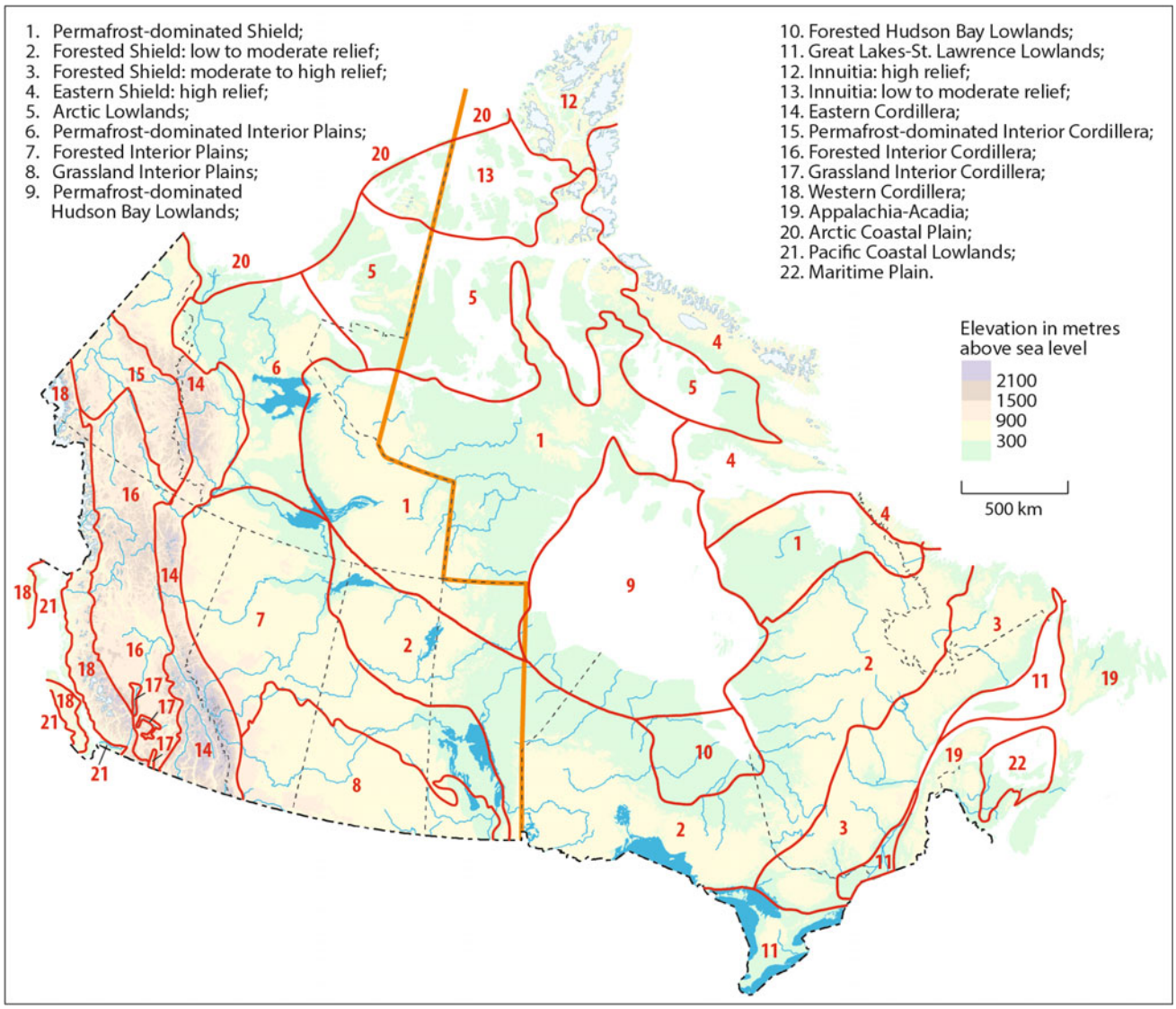

Fig. 1.3 Geomorphological landscapes of Canada. Data sources include physiographic regions of Canada (Bostock 2014), permafrost limits in Canada (Smith et al. 2001), and ecozones of Canada (Environment Canada 1995). Cartography by E. Leinberger

1.3.2 The Emergence of the Contemporary Cordilleran Landscape

Extensive mountain building in late Mesozoic and earliest Cenozoic eras (c. 75–35 Ma ago) was followed by erosion of the mountain landscapes during the bulk of the Cenozoic Era. Topography west of the Rocky Mountains was reduced to gentle slopes and broad valleys with up to 500 m of local relief. Remnants of this eroded landscape are found widely distributed as high surfaces in the Cordillera. The contemporary landscape of the Cordillera began to develop during the most recent phase of uplift and river incision commencing in the Miocene Epoch about 10 Ma ago (Parrish 1981; Mathews 1992).

Summit surfaces in the Juan de Fuca–Georgia Strait area and in the Interior Cordillera represent relict fragments of mid-Cenozoic erosion surfaces (Ryder 1981). Gravel-capped pediment fragments east of the Eastern Cordillera represent Pliocene and early Quaternary fluvial surfaces that have escaped glacial obliteration. The surface of the Beaufort Formation (Miocene) of the Queen Elizabeth Islands presents a similar denudation history.

The present-day plate tectonic regime at the tectonically active western boundary of the North American Plate consists of three contrasting segments:

(1) The southern segment is a subduction zone, along which slabs of oceanic lithosphere of the Juan de Fuca Plate and the Explorer Plate are slipping northeastward under southern British Columbia at 20–46 km Ma^{-1}.
(2) The central segment, which extends northward into the Gulf of Alaska from just south of the Queen Charlotte Islands, consists of the Queen Charlotte and Fairweather transform faults, along which the Pacific Plate and the Yakutat "block" are slipping northwestward or northward relative to the North American Plate at about 55 km Ma^{-1} (Riddihough and Hyndman 1992).
(3) The northern segment of the Cordillera consists of a tectonic "collage" of allochthonous terranes. The larger terranes (Quesnellia, Stikinia, Wrangellia, and Alexander) are laterally persistent tectonostratigraphic assemblages.

1.3.3 The Innuitian–Greenland Plate Connection

The Queen Elizabeth Islands archipelago is a subplate, bounded by major shear zones, that was broken by rifting in the late Cretaceous and Paleogene periods (75–50 Ma; Hodgson 1989). The islands are largely underlain by the deformed sediments of the Innuitian Province lying between the Arctic Ocean basin to the northwest, the stable Arctic Platform in the southeast, and Greenland in the northeast. Initial fragmentation started possibly by the late Paleozoic (c. 300 Ma), and deformation parallel to the present northeast–southwest topographic grain continued late into the Cenozoic (c. 25 Ma). Prince Patrick Island, the southwesternmost member of the Queen Elizabeth Islands, has an east–west topographic orientation.

1.4 Major Lineaments of Western Canada

The net effect of western Canada's tectonic history is that much of the landscape, with the exception of the Innuitian region, is aligned in a general north–northwest to south–southeast direction. The main orientations of the major valleys in the Coast Mountains, including the fjords, define the principal conjugate failure planes for the stresses established by onshore movement of the Juan de Fuca and Explorer plates, demonstrating their specific influence over the topography of coastal British Columbia (Church and Ryder 2010) and also, in a more general sense, their extensive influence over most western Canadian landscapes (Brew and Ford 1978).

1.4.1 Thrust Faults

One of the most dramatic expressions of western Canada's tectonic history is the surface trace of the thrust faults that separate the Rocky Mountain Foothills to the east and the Rocky Mountains proper to the west. The morphological expression of this surface trace is illustrated in Sect. 1.7.3. Older rocks have traveled more than 100 km over the top of younger rocks. For example, the McConnell Thrust, at Mount Yamnuska (65 km west of Calgary, Alberta), is a nearly horizontal thrust fault. There is a remarkably thin deformation zone of only about 1 m in thickness that separates overlying Cambrian carbonates from underlying Cretaceous sandstones and shales. It forms the easternmost surface thrust fault in a sequence that first started forming with the docking of the first superterrane (the Intermontane Belt) onto the western margin of the North American craton.

1.4.2 Trenches

A second even more dramatic landscape expression of western Canada's tectonic history is the presence of three semi-continuous linear valleys, each at least 500 km long, and oriented in a north–northwestern to south–southeastern direction. These trenches are known as the Rocky Mountain, Tintina, and Shakwak trenches. Running parallel between the peaks of the Columbia and Rocky mountains and ranging 3–16 km wide and about 1400 km long, the Rocky Mountain Trench (Fig. 1.4) extends past Mount Robson, the highest peak in the Canadian Rockies at 3954 masl. The trench likely formed due to underlying normal faults that emerged as a result of tectonic collisions that pushed up the mountains.

Characteristically, these trenches are straight, flat-bottomed, and several kilometers wide and have steep, nearly vertical sides that are often 700–1000 m high. They contain Cretaceous and Cenozoic non-marine sediments and glacifluvial and glacilacustrine deposits. (Leech 1966; Clague 1975).Within these large trenches, the upper reaches of many of western Canada's largest rivers flow as misfit streams, such as the Columbia (Fig. 1.5a), Fraser, Finlay, Kechika, and Pelly rivers. The Rocky Mountain Trench is drained by six major rivers, including the Kootenay, Columbia, Upper Fraser (Fig. 1.5b), and Finlay–Parsnip (Peace).

Three hundred and fifty km northwest of the Liard River, the Tintina Trench extends for 700 km past Dawson City into Alaska. The Shakwak Trench, the shortest of the three

Fig. 1.4 **a** The Rocky Mountain Trench, a tectonic graben in western Canada. Running parallel between the peaks of the Columbia and Rocky mountains and ranging 3–16 km wide and about 1400 km long, the trench extends past Mount Robson, the highest peak in the Canadian Rockies at 3954 masl. The trench likely formed due to underlying normal faults that emerged as a result of tectonic collisions that pushed up the mountains. In this image, snow and ice appear *turquoise*; vegetation is *green,* exposed rock in *grays*, *browns,* and *tans*; and liquid water is *dark blue*. The area has been shaped by a combination of rivers and glaciers. *Source* MDA Federal (2004). **b** Aerial oblique view of the southern Rocky Mountain Trench. *Source* © Province of British Columbia. All rights reserved. BC767:18. The inset image here and elsewhere in this chapter is extracted from NASA, Visible Earth (Stöckli et al. 2005)

trenches, parallels the Tintina Trench in the southwestern Yukon and contains Kluane Lake.

1.4.3 Major Mountain Divides

Another striking expression of the landscape impact of western Canada's tectonic history is the approximate parallelism of the major mountain divides. The Coast Mountains parallel the Rocky Mountains as do, for example, the Cassiar, Skeena, Omineca, and Mackenzie mountains. Individual mountain ranges, such as the St. Elias Mountains and the Alsek and Boundary ranges of the Coast Mountains, have the same orientation and form the international boundary between British Columbia and Alaska (Fig. 1.6).

1.4.4 Significant Tertiary Drainage Reversals

In spite of the clear control exerted by the geological structure on major lineaments of the landscape, there were numerous drainage reversals before those associated with glacial effects during the Pleistocene. Eisbacher et al. (1974) described the early Cretaceous rivers forming an alluvial

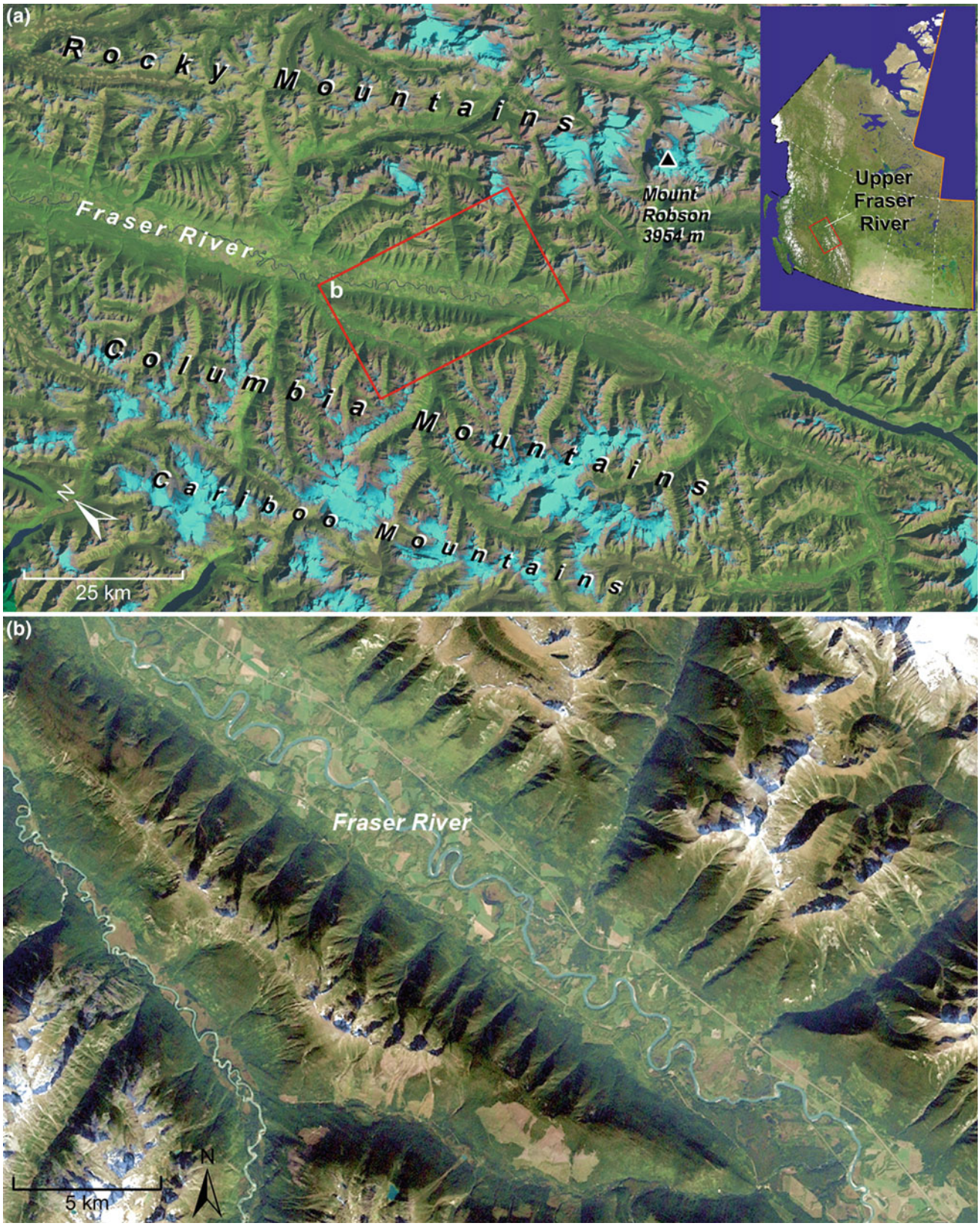

Fig. 1.5 **a** Upper Fraser River. *Source* NASA Landsat Program (2003). **b** The misfit Fraser River in the southern Rocky Mountain Trench. *Source* © Department of Natural Resources Canada. All rights reserved. Government of Canada, Centre for Topographic Information, CanImage—Landsat 7 Orthoimage, 083e04

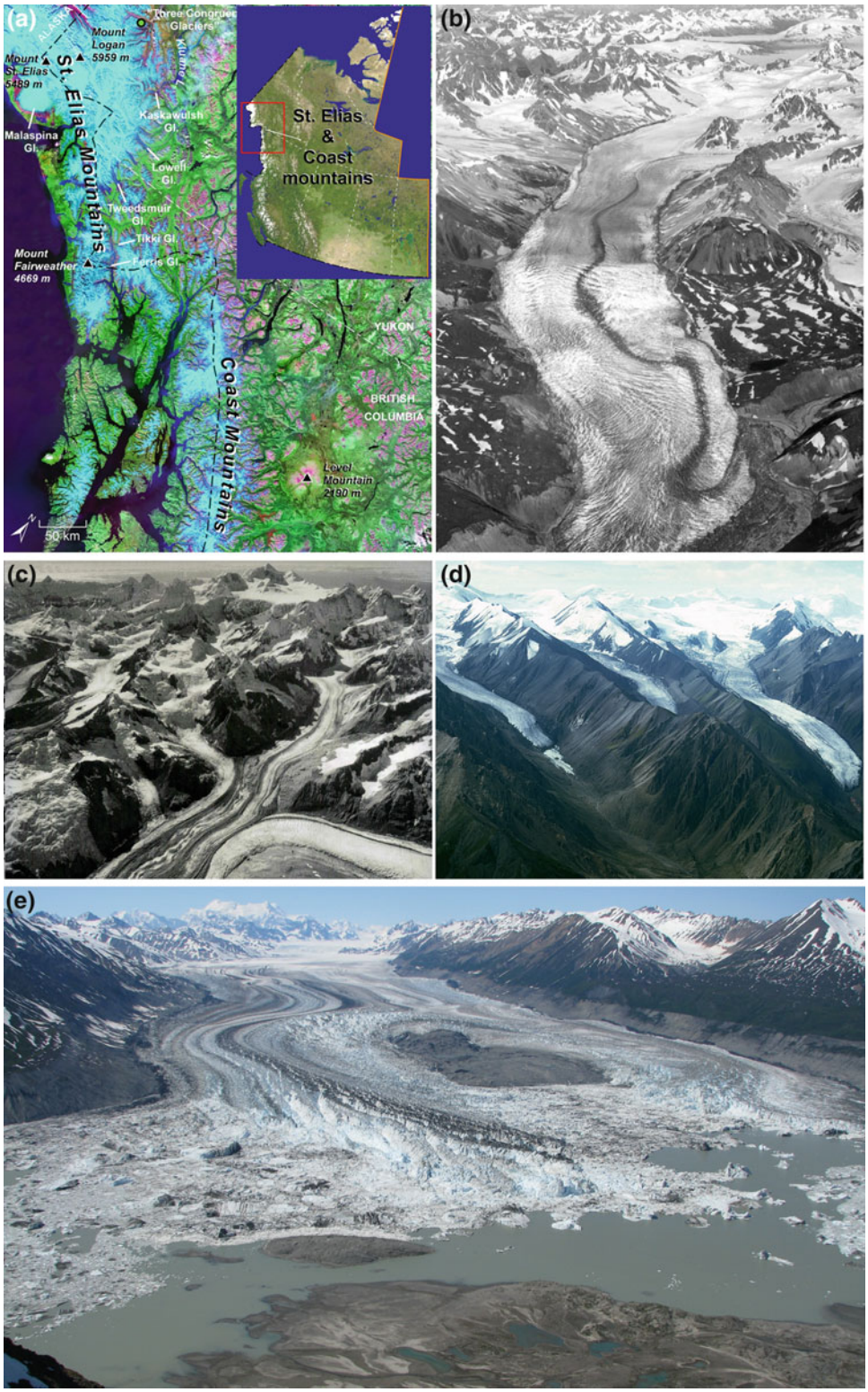

Fig. 1.6 **a** Saint Elias Mountains hold the world's most extensive ice fields outside the polar ice caps. Many peaks exceed 5200 masl, including Mount Logan (5959 masl, the highest in Canada) and Mount St Elias. *Source* MDA Federal (2004). **b** Aerial oblique view of the Tikki Glacier in the Boundary Ranges of the Coast Mountains in British Columbia. Tikki Glacier is one of many glaciers in Canada which can be expected to form hazardous lakes periodically (*Source* US Geological Survey, Department of the Interior; photograph by Austin Post 1966). **c** Aerial oblique view of the Ferris Glacier. Medial moraines are clearly formed at the juncture of the glacier's adjacent tributaries. In the background is Mount Fairweather (4669 masl). *Source* © Province of British Columbia. All rights reserved. BC 688:16. **d** "Three Congruent Glaciers" in the St. Elias Mountains in Yukon. These glaciers originate from similar firn basins and flow along nearly identical parallel valleys. Their history has shown that their lengths have markedly different responses to changes in mass balance. Reproduced with the permission of Natural Resources Canada, 2015 (photograph: NRCan 2002-678 by Robert Bélanger). **e** Panoramic view of the terminus of Lowell Glacier from Goatherd Mountain in Kluane National Park and UNESCO World Heritage Site (June 14, 2010; © Government of Yukon, Panya Lipovsky. Image reproduced with permission). Mount Kennedy (4238 masl) is part of the white massif in the background

apron on the western and westward flowing side of the Omineca Belt, whereas Yorath and Cook (1981) focused on the tributaries of the Mackenzie in the northern Interior Plains and Duk-Rodkin and Hughes (1994) discussed the evolution of the gravel-capped pediplains of the late Tertiary landscape of the eastern Rocky, Mackenzie, and Richardson mountains. During the uplift of the mountains during the Laramide Orogeny, two major drainage systems developed:

one to the Atlantic Ocean and another to the Arctic Ocean. The Atlantic drainage is composed of the northwestern tributaries of an integrated drainage system that flowed toward Hudson Bay. Traces of this drainage are found in the Canyon Ranges of the Mackenzie Mountains, Iroquois upland, and in the Norman Range of the Franklin Mountains (see Chap. 14). The arctic drainage included two main basins —the Porcupine basin that drained from west to east across the Richardson Mountains (see Chap. 19) and the Anderson basin that included the Peel (see Chap. 7) and Snake rivers as its tributaries (Duk-Rodkin and Hughes 1994). Tempelman-Kluit (1980) and Jackson et al. (2012) have differing views on the evolution of the Miocene drainage pattern of the Yukon. Mathews (1992) showed the effects of volcanic diversion of the upper Stikine. Lay (1940/41) made an early study of the reversal of the Fraser River flow based on placer gold evidence (see Chap. 27), and Tribe (2005) has made an exhaustive analysis of drainage evolution on the central Interior Plateau.

1.5 Volcanic Landscapes of Western Canada

Within the Cordilleran structural and physiographic region, there has been and continues to be much volcanism. Active volcanism extends across BC and Yukon from the Cascade Mountains (Hickson 2000) to Wells Gray Provincial Park (Neuffer et al. 2006), the Anahim Plateau (Cassidy et al. 2011), northern BC (Edwards and Russell 2000), and north to Fort Selkirk in central Yukon (Jackson et al. 2012). More than 200 potentially active volcanoes exist in western Canada, and 49 have erupted in the last 10,000 years (Stasiuk et al. 2003). Not only all standard volcanic landforms are represented, but also, more unusually, volcanic landforms created beneath the Cordilleran Ice Sheet are present (Fig. 1.7).

1.5.1 The Northern Cordilleran Volcanic Province

Possibly the oldest volcanic events in the Northern Cordilleran Volcanic Province (NCVP) are represented by Miocene age volcanics of 27–16 Ma around Atlin Lake. More than 100 eruptions have occurred in the past 20 Ma with a broad range of eruptive styles. These volcanic processes have created a range of different volcanic landforms, including stratovolcanoes, shield volcanoes, lava domes, and cinder cones along with a few isolated examples of rarer volcanic forms such as tuyas. Tuyas are flat-topped subglacially formed volcanoes (Mathews 1947). Four large volcanoes have formed: Hoodoo Mountain (Fig. 1.8), the Mt. Edziza volcanic complex, the Level Mountain Range, and Heart Peaks.

At least three types of volcanic zones are present in the NCVP, including large persistent lava plateaus like those found at the Mount Edziza volcanic complex, polygenetic volcanoes such as Hoodoo Mountain, and monogenetic volcanoes such as the basaltic cinder cones found throughout the volcanic province.

Basaltic shield volcanoes throughout the central NCVP form lava plateaus and are the largest volcanoes of the volcanic zone. The massive Level Mountain Range shield volcano, occupying an area of 1800 km^2, forms a broad cliff-bounded lava plateau. The Mount Edziza volcanic complex covers an area of 1000 km^2. Just west of the Level Mountain Range lies Heart Peaks, the third largest volcano of the NCVP with an area of 275 km^2. Glacial ice and streams have since dissected the >2000 masl volcanoes into a series of valleys with intervening ridges that constitute the Level Mountain Range proper.

In northern British Columbia, remnants of a shield volcano are found throughout the western Cassiar Mountains. This prehistoric shield volcano, known as Maitland Volcano, erupted from 5–4 Ma ago on a mature eroded surface. Remnants of this prehistoric shield volcano include a cluster of 14 volcanic plugs and scattered cliff-bounded basaltic lava flows. A series of lava domes was constructed in the Level Mountain Range alpine valley system 4.5–2.5 Ma ago. Headward erosion has modified the Level Mountain Range shield by incising youthful V-shaped stream canyons into the lava plateau margin.

1.5.2 The Garibaldi Volcanic Belt

To the northwest of Mt. Garibaldi, the Mount Cayley massif constitutes the largest and most persistent volcano in the central Garibaldi Volcanic Belt. It is a highly eroded stratovolcano composed of lava that was deposited during three phases of volcanic activity. The first eruptive phase started about 4 Ma ago with the eruption of lava flows and pyroclastic rock. This resulted in the creation of Mount Cayley proper. Subsequent volcanism during this volcanic phase constructed a significant lava dome.

To the northwest, the Franklin Glacier complex is volcanic bedrock that encompasses an area 20 km long and 6 km wide. Volcanics include breccia and lava flows associated with tuffs that reach 450 m thick. Potassium–argon dates obtained from some of the subvolcanic intrusions

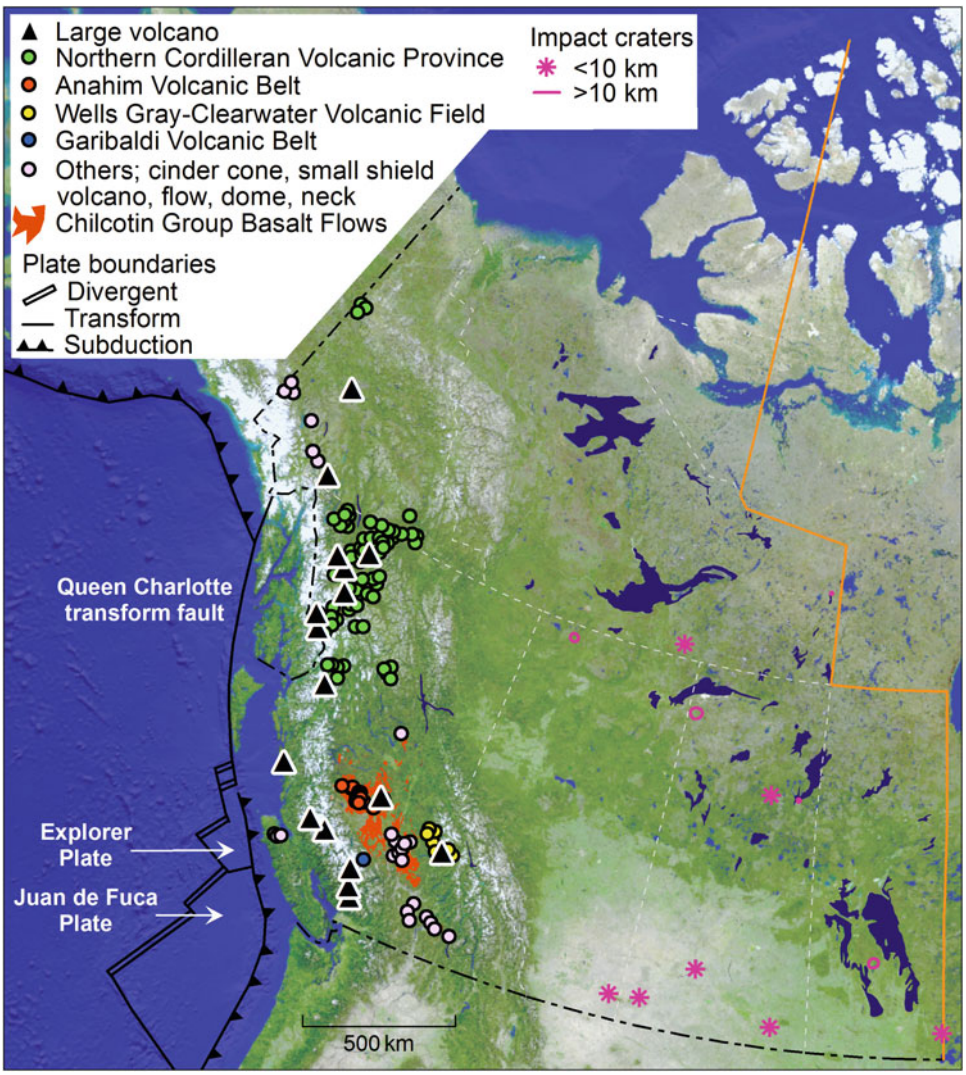

Fig. 1.7 Distribution of selected volcanic landforms and impact structures in western Canada. Data sources include Volcanoes of the World dataset (Siebert and Simkin 2002), regional volcanic centers (modified from Edwards and Russell 2000), Chilcotin Group basalts (Massey et al. 2005), and Earth Impact Database (2015). *Background image*: NASA, Visible Earth

indicate that Franklin formed during two volcanic events, each separated by about 5 Ma of dormancy. The first event occurred between 6 and 8 Ma ago. When the Garibaldi Volcanic Belt moved to its current location 5 Ma ago, another volcanic event occurred at the Franklin complex. This final and most recent volcanic event occurred between 2 and 3 Ma ago, about a million years after Mount Cayley to the south began its formation.

Silverthrone Caldera is the larger and better preserved of the two caldera complexes in the northern Garibaldi chain, the other being the Franklin Glacier complex 55 km to the east–southeast. The caldera has a diameter of 20 km and contains breccia, lava flows, and lava domes. Near-vertical flanks extend from near sea level to more than 3000 m in elevation.

1.5.3 Anahim Volcanic Belt

The Anahim Volcanic Belt is a 600-km-long volcanic belt, stretching from Vancouver Island to near Quesnel. It has had three main magmatic episodes, dated at around: 15–13, 9–6, and 3–1 Ma. The volcanoes generally become younger eastward at a rate of 2–3.3 cm a year. The Nazko Cone, which last erupted only 7200 years ago, is the youngest Anahim volcano. These volcanoes are thought to have formed as a result of the North American Plate sliding westward over a long-lived center of upwelling magma called the Anahim Hotspot.

The volcanic belt is defined by 37 Quaternary basalt centers and three large shield volcanoes called the Rainbow,

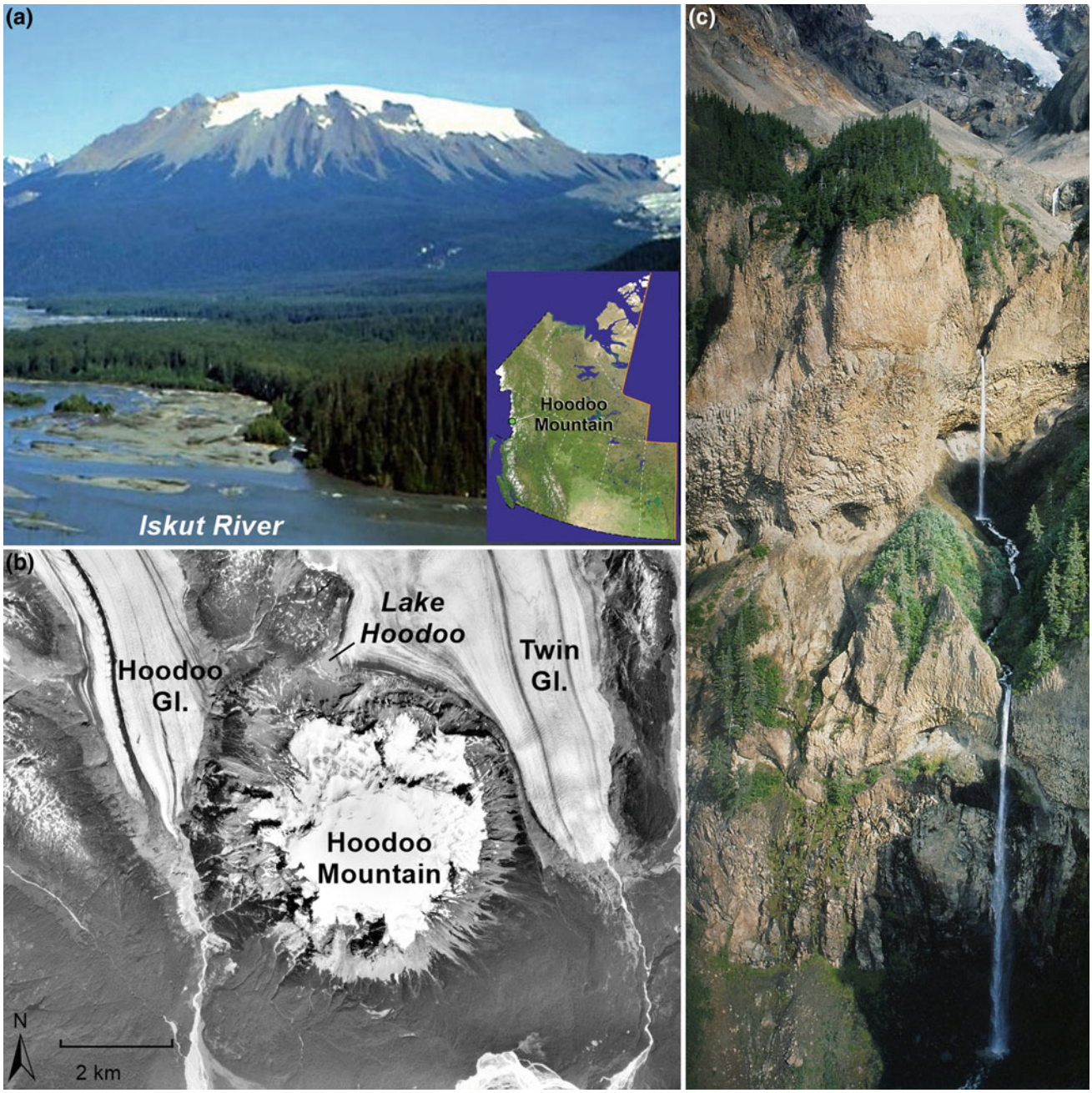

Fig. 1.8 **a** Hoodoo Mountain is a classic flat-topped glacivolcanic edifice (tuya) that rises to 1850 masl on the north side of the Iskut River, in the Coast Mountains of northwestern British Columbia. The volcano formed under glacial ice within the Cordilleran Ice Sheet during the Quaternary. *Photograph* by Ben Edwards, 1994. **b** Aerial photograph of Hoodoo Mountain volcano, the Hoodoo and Twin valley glaciers, and Lake Hoodoo. At present, the summit region is covered by a 3–4 km diameter ice cap above 1700 masl. *Source* © Province of British Columbia. All rights reserved. BC82022:206. **c** On Hoodoo's south face, meltwater cascades from the ice-filled crater and drops over vertical volcanic cliffs. The stratigraphy of the volcano is dominated by thick lava flows. *Photograph* by Gary Fiegehen

Ilgachuz, and Itcha ranges (Fig. 1.9). These three large volcanoes have built up dome-like piles of lava and fragmental rocks to a height of 2478 masl at Tsitsutl Peak in the Rainbow Range, 2400 masl at Far Mountain in the Ilgachuz Range, and 2365 masl at Mt. Downton in the Itcha Range. The Rainbow Range is a low dome-like cone about 36 km diameter, with Anahim Peak an obsidian plug on its northeast flank. The Ilgachuz Range is 24 km or more in diameter, and the Itcha Range is 16 km wide and about 64 km long.

Fig. 1.9 **a** Three large shield volcanoes called the Rainbow Range, Ilgachuz Range, and the Itcha Range in the central part of the east-trending Anahim Volcanic Belt located on the Interior Plateau in central British Columbia. Also shown (*orange dots*) are locations of younger cinder cones. *Source* MDA Federal (2004). **b** A highly dissected shield volcano within the Rainbow Range. *Source* © Department of Natural Resources Canada. All rights reserved. Government of Canada, Centre for Topographic Information, CanImage—Landsat 7 Orthoimage, 09c12. **c** View looking north from north side of the Itcha Range. *Source* © Province of British Columbia. All rights reserved. Reproduced with permission of the Province of British Columbia (*photo*: 9456-00CBD0001)

1.6 Karst Landscapes of Western Canada

Karst landscapes are present in each of the eight terrestrial structural units of Canada. Karst topography develops where the chemical dissolution of carbonate limestone or dolostone of chemically precipitated evaporite rocks is a significant process (Ford and Williams 2007). There are widespread outcrops of carbonate and sulfate rocks in temperate, arctic, and alpine environments of western Canada although they are often buried under glacial deposits. In this region, there

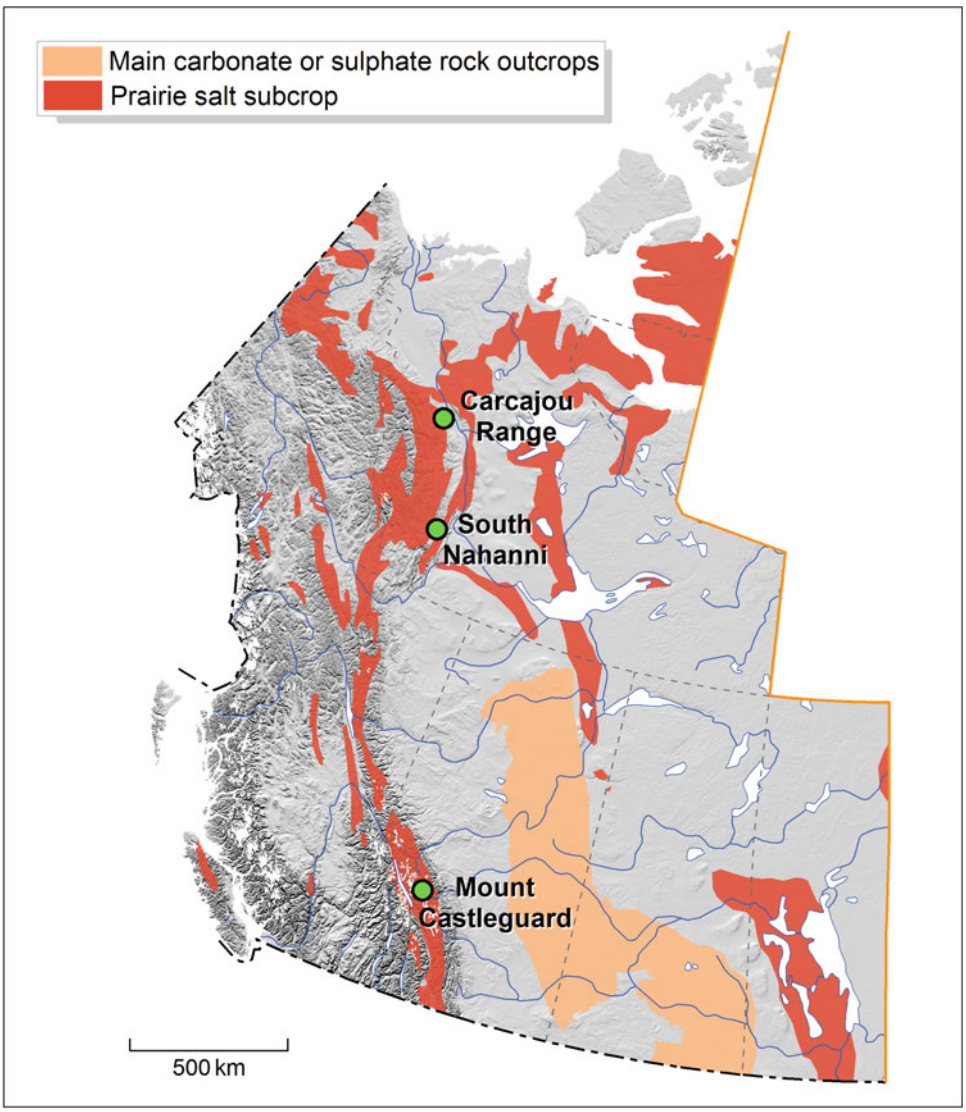

Fig. 1.10 Distribution of karst rocks in western Canada (Williams and Fong 2015; also see Ford and Williams 2007). Extensive karstified carbonate rock also exists in subcrop (Prairie Evaporite; after Meijer Drees 2008)

are at least 8×10^5 km^2 of limestone and marble outcrops or 18 % of the area (Ford 1987; Fig. 1.10).

Karst landscapes are dominated by subterranean drainage, facilitated by the solution of highly soluble rocks, producing caves and underground diversion of river systems across topographic boundaries. The most widespread surface karst landforms are small solution pits, grooves, and runnels, collectively called karren. In metropolitan Winnipeg, approximately 3500 km^2 of limestone pavement is preserved beneath glacial lake clays and serves as an important industrial water store. There are spectacular subarctic pavements in the Carcajou Range west of Norman Wells, Northwest Territories (see Chap. 14). Further north, ice penetration into cracks in the bedrock is common; the bedrock becomes shattered into rubble fields that are widespread on the extensive carbonate rock terrains of arctic Canada.

The most recognizable karst landform is the sinkhole or doline. The length or diameter of sinkholes ranges from 10 to 2000 m. Most are formed by chemical solution in the funnel or by collapse of the roof of an underlying cave. In southern Saskatchewan, collapse-solution cavities in salt have extended through as much as 1000 m of overlying insoluble rocks to produce shallow sinkholes at the surface. Sinkholes often occur in lines or clusters. In some karsts their frequency exceeds 500 per km^2, giving the terrain a shell-pitted appearance. Thousands of sinkholes exist in limestone on Vancouver Island. There are many large, spectacular examples in Wood Buffalo National Park, in the Franklin Mountains, and west of Great Bear Lake where limestones and dolomites have collapsed into cavities in gypsum.

Larger karst landforms include dry valleys and gorges, carved by past rivers that now flow underground, and poljes,

which are major sinkholes with flat floors and steep walls. Maligne Lake in Jasper National Park is a polje measuring 6 km by 1–2 km. The Maligne River drains into it and floods it to a depth of 25 m during the summer melt season. In winter, the lake reduces to small pond sinkholes in the polje floor. The sinking water is discharged 16 km northwest at some 60 springs in the floor of Maligne Canyon. With an aggregate discharge that may exceed 65 m^3 of water each second, these are the largest karst springs known in Canada.

Karst landform development is rather limited in Canada when compared to countries that have not undergone repeated glaciation (Ford 1987). Glacier action has eroded or infilled much karst. Canada's finest karstland, Nahanni Karst, is found in a region of the Mackenzie Mountains, Northwest Territories (see Chap. 15), which has escaped glaciation for the past several hundred thousand years. Major karst forms have developed and include hundreds of sinkholes up to 150 m deep, giant solution grooves intersecting to form a natural labyrinth, several poljes, and dry canyons. Parts of the karst have reached a very advanced stage, displaying residual rock towers and natural bridges, features rarely seen in northern latitudes. A dense karstland of karren, small sinkholes, and innumerable caves has developed on steep limestone tracts clad in Douglas fir in northern Vancouver Island. The landforms pose some hazard to forestry practices, while clear-cutting may severely damage both surface and underground karst.

Alpine karst, comprising fields of karren and shaft sinkholes above the tree line that drain into deep caves, is well developed in parts of the Rocky Mountains and Vancouver Island. Crowsnest Pass offers very good examples of classical alpine karst forms: Major springs issue from active water caves in the floor of the pass, while fragments of drained, relict caves are scattered at higher elevations up to the mountain summits (Ford et al. 1981). The largest ice field in the Rockies, Columbia Icefield, is mostly drained by sinkholes surviving in the limestone and dolostone beneath it. The waters flow in great caves through Mount Castleguard to emerge as spectacular springs in the valley of Castleguard River (a headwater of the North Saskatchewan River; see Chap. 16). It is the world's preeminent example of modern subglacial karst.

1.7 Geomorphological Landscapes of Western Canada

As indicated in Sect. 1.2.3, geomorphological landscapes are built on the physiographic foundation of tectonic history and surface morphology and incorporate the role of permafrost, vegetation cover, and human activity in so far as they affect geomorphological processes of erosion and sedimentation. Of the 22 geomorphological landscapes found in Canada, fourteen are found in western Canada (Table 1.1).

Table 1.1 Geomorphological landscape regions of western Canada

Region	Geomorphological landscapes	Area (thousands of km^2)
Canadian Shield		
	1. Permafrost-dominated Shield	380
	2. Forested (Taiga) Shield: low-moderate relief	550
Lowlands, Plateaus and Interior Plains		
	5. Arctic Lowlands	220
	6. Permafrost-dominated Interior Plains	320
	7. Forested (Taiga) Interior Plains	950
	8. Grassland (Prairie) Interior Plains	550
	13. Innuitia: low-moderate relief	100
Mountains		
	14. Eastern Cordillera	580
	15 Permafrost-dominated Interior Cordillera	200
	16. Forested Interior Cordillera	450
	17. Grassland Interior Cordillera	20
	18. Western Cordillera	260
Coastal Plains		
	20. Arctic Coastal Plain	40
	21. Pacific Coastal Lowlands	30

Numbers 1–21 refer to geomorphological landscapes in Fig. 1.3

1.7.1 Shield Landscapes

These geomorphological landscapes present an "even, monotonous skyline interrupted by rounded or flat-topped monadnocks and ranges of hills" (Bostock 1970). Much of the Canadian Shield in western Canada is an erosion surface with local relief of no more than 100 m. Some parts of the erosion surface are considered an exhumed surface, exposed after the pre-Paleozoic (or younger) cover deposits were stripped. Even though parts of the Canadian Shield are geologically distinct, a regional surface truncating these different geological units emerged (Ambrose 1964; Fig. 1.11).

Permafrost-dominated Shield (geomorphological landscape region 1; see Fig. 1.3) includes plains, such as Athabasca Plain formed on areas of unmetamorphosed rocks more or less flat-lying sandstones and conglomerates; hills, such as the East Arm Hills, composed of low grade metamorphic rocks, generally tilted or gently folded sediments or sills; and uplands, such as Bear-Slave Upland, treeless and underlain by massive rocks, with numerous lakes and monadnocks.

In the following text, "permafrost-dominated" is taken to mean the presence of extensive discontinuous permafrost underlying 50–80 % of the landscape (Smith et al. 2001; Fig. 1.12).

Forested Shield (2) has low-moderate relief. The Kazan and Severn Uplands are underlain by Archean crystalline rocks and form rolling, lake-studded landscape. Toward the southwest, they are mantled with glacial lake deposits. The forested shield becomes progressively less permafrost rich from northwest to southeast (see Chaps. 4 and 5). Sporadic permafrost (10–50 % according to Smith et al. 2001) is succeeded by isolated patches of permafrost in northern Saskatchewan and Manitoba. In southern Manitoba, the landscape is permafrost-free.

1.7.2 Lowlands, Plateaus, and Interior Plains Landscapes

Arctic Lowlands (5), Permafrost-dominated Interior Plains (6), Forested Interior Plains (7), Grassland Interior Plains (8), and Low-moderate relief Innuitia (13) are shown in Fig. 1.3. They are almost entirely low-moderate relief landscapes and are differentiated into four categories The Arctic Lowlands are treeless and dominated by permafrost (see Chap. 6). Victoria Lowland and the Shaler Mountains are included. The Shaler Mountains reach an elevation of 800 masl, are composed of Proterozoic stratified rocks intruded by gabbro sills, which form cuestas, and are capped by flat-lying volcanics. Victoria Lowland is a smooth undulating erosion surface covered by a variety of glacial deposits with drumlinoid ridges and moraines forming irregular hills.

The Permafrost-dominated Interior Plains are present in Northwest Territories and include the Horton, Anderson, Peel, Great Bear, and Great Slave plains. Anderson Plain is covered by glacial drift and outwash, and the Peel Plateau rises in three steps. Thin drift deposits, small, scattered lakes, and several large entrenched meltwater channels are evident. The Forested Interior Plains in northern Alberta and northeastern BC (Fig. 1.13) are eventually replaced by the Grassland Interior Plains (Prairies) of southern Alberta and Saskatchewan (Fig. 1.14; see Chaps. 9, 10, and 11). The Cypress Hills are the remnants of the Tertiary erosion surface formed during the initial uplift of the Rocky Mountains.

The lowlands and plateaus of low-moderate relief Innuitia enjoy a polar desert climate with thick permafrost (see Chap. 13). The terrain of Parry Plateau is strongly ridged on Bathurst Island. The wide, flat-floored longitudinal valleys are transected by ravine-like cross valleys. The Sverdrup Lowland contains dissected domes and ring structures that have developed on gypsum anhydrite diapirs and igneous intrusions.

1.7.3 Mountain Landscapes

The Eastern Cordillera (14), Permafrost-dominated Interior Cordillera (15), Forested Interior Cordillera (16), Grassland Interior Cordillera (17), and the Western Cordillera (18) are dominantly mountain landscapes. The Canadian Cordillera is divided into three great belts: Eastern System, Interior System, and Western System. Each has its characteristic geology and physiography and hence its own geomorphological landscapes. The Eastern System (Rocky Mountains) consists almost entirely of folded sedimentary strata and is a classic example of a foreland fold-and-thrust belt (Fig. 1.15).

The Interior System (which includes geomorphological landscape regions 15, 16, and 17; see Fig. 1.3) has folded sedimentary and volcanic strata, igneous rocks intruded into extensive metamorphics with local areas of flat-lying

Fig. 1.11 Canadian Shield erosion surface with till veneer. Both of the images are from the transition zone between Permafrost-dominated and Forested Shield. **a** The Selwyn Upland forest cover is patchy on boulder till veneers and polygonal peat plateaus on poorly drained flats. **b** The Dubawnt Plain is characterized by a gently undulating boulder till plain with open black spruce woodlands. *Source* © Government of the Northwest Territories /D. Downing

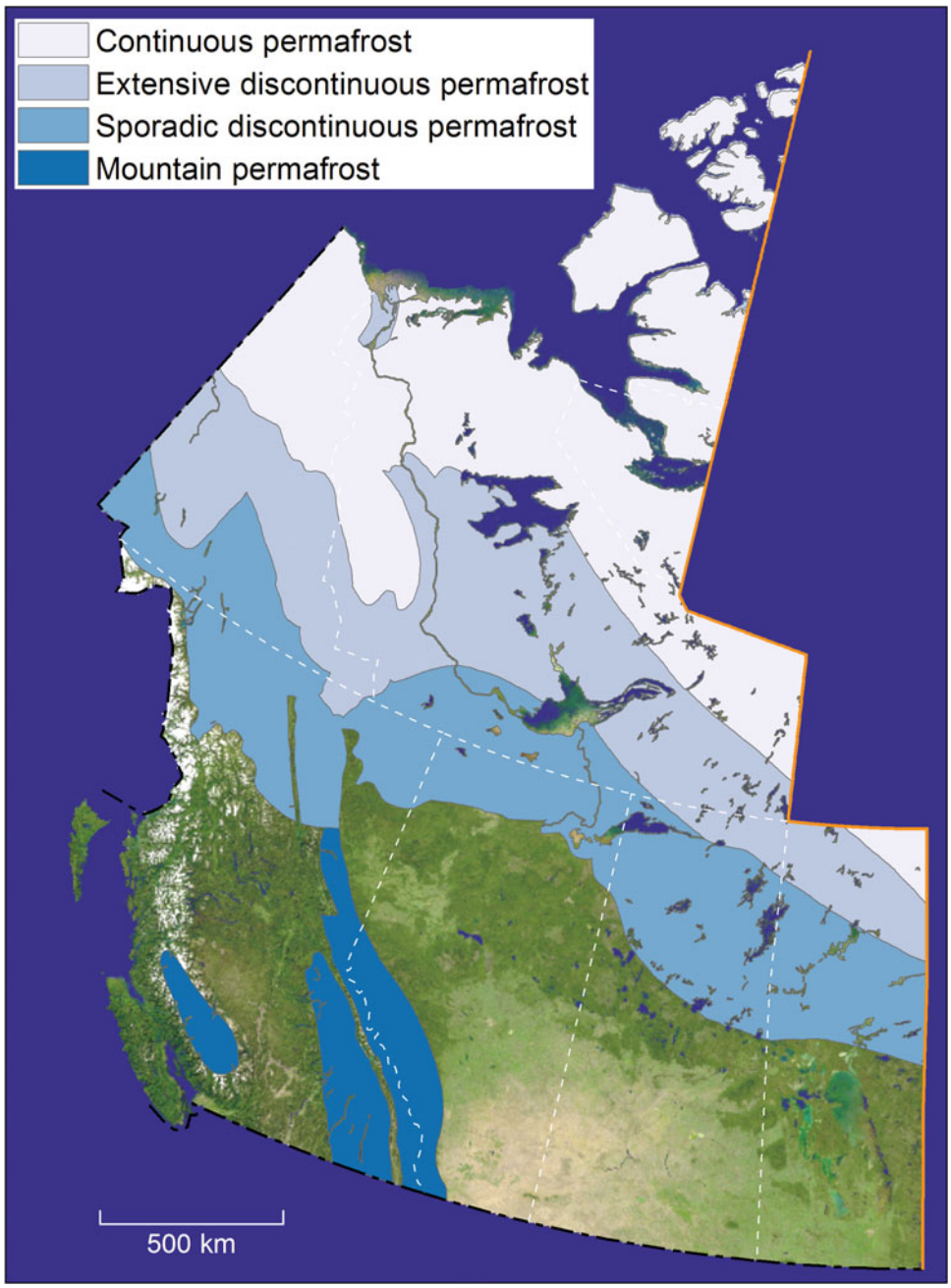

Fig. 1.12 Distribution of permafrost in western Canada (adapted from Smith et al. 2001; Government of Canada 2008). *Background image*: NASA, Visible Earth

volcanics. In the Western System, the Coast Mountains are composed mainly of plutonic rocks whereas other parts are a mixture of volcanic and sedimentary strata intruded by igneous rocks (Fig. 1.16).

The Cordilleran region contains the most varied landscapes—ranging from the high relief Western and Eastern Cordillera to moderate-high relief Interior Cordillera. Added to this variety of physiography is the gradation from north to south of the tundra, forested and grassland landscapes. The Eastern Cordillera, including the Columbia, Rocky, Mackenzie, Franklin, and Richardson mountains, is best known for the castellated carbonate peaks of the central

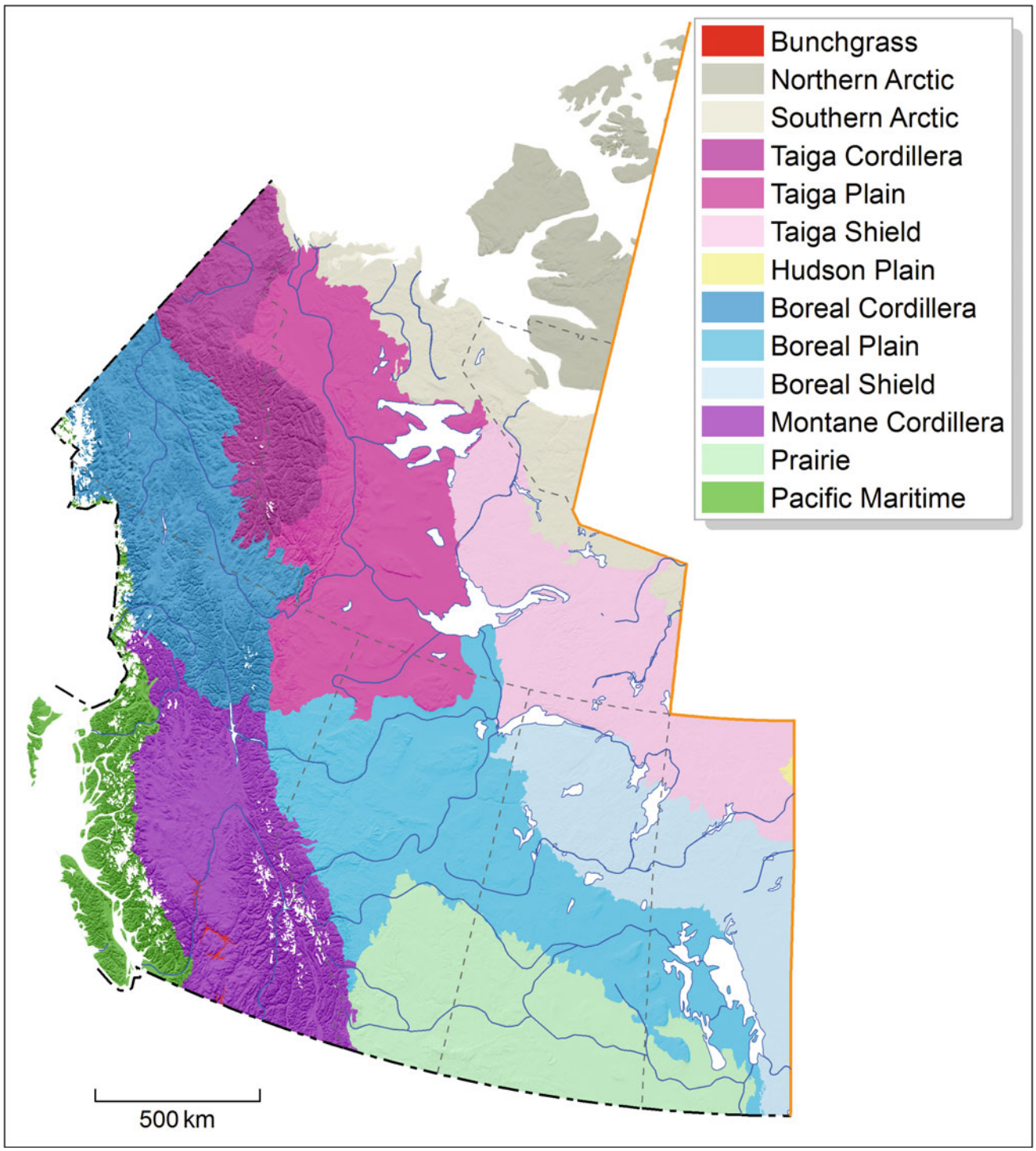

Fig. 1.13 Terrestrial Ecozones of western Canada (derived from Environment Canada 1995; Government of British Columbia 2014)

Rockies (see Chap. 17), but there is great variety of lithology and relief within this region. The Interior Cordillera contains mountain ranges as dramatic as the Eastern Cordillera alongside extensive plateaus and lowlands. But the unique feature of the Interior Cordillera is the occurrence of widespread volcanism and, specifically, volcanic landscapes that were created while the Cordilleran Ice Sheet was present. The Northern Cordilleran Volcanic Province (Edwards and

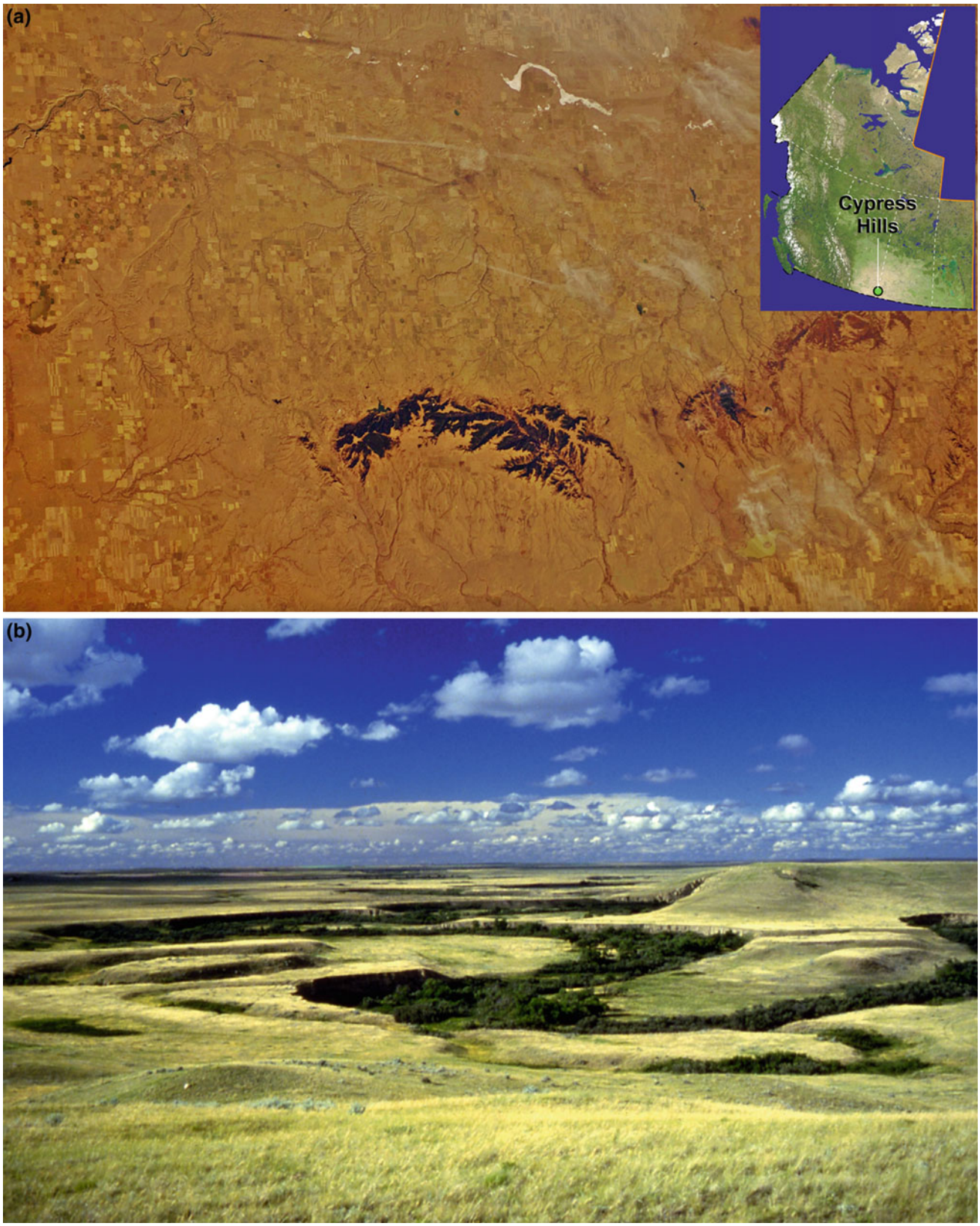

Fig. 1.14 Grassland Interior Plains (Prairies) in southern Alberta and Saskatchewan. **a** View from space of the landscape in southeastern Alberta and southwestern Saskatchewan. Cypress Hills (1466 masl) in the lower part of the image rise 600 m above the surrounding prairies. *Source* NASA Earth's Observatory, ISS017-E-19645. **b** Along Lower Gap Creek, Alberta, the landscape has been modified to form glacilacustrine, glacifluvial, and postglacial alluvial surfaces. Reproduced with the permission of Natural Resources Canada, 2015 (*photograph*: NRCan 1999-043C by W.J. Vreeken)

Fig. 1.15 **a** View from space of the Eastern Cordillera. *Source* NASA Earth's Observatory, ISS040-E-129996, September 6, 2014. **b** Fault-related folds in Mount Kidd (2972 masl). Reproduced with the permission of Natural Resources Canada, 2015 (*photograph*: NRCan 2012-066 by M.E. McMechan)

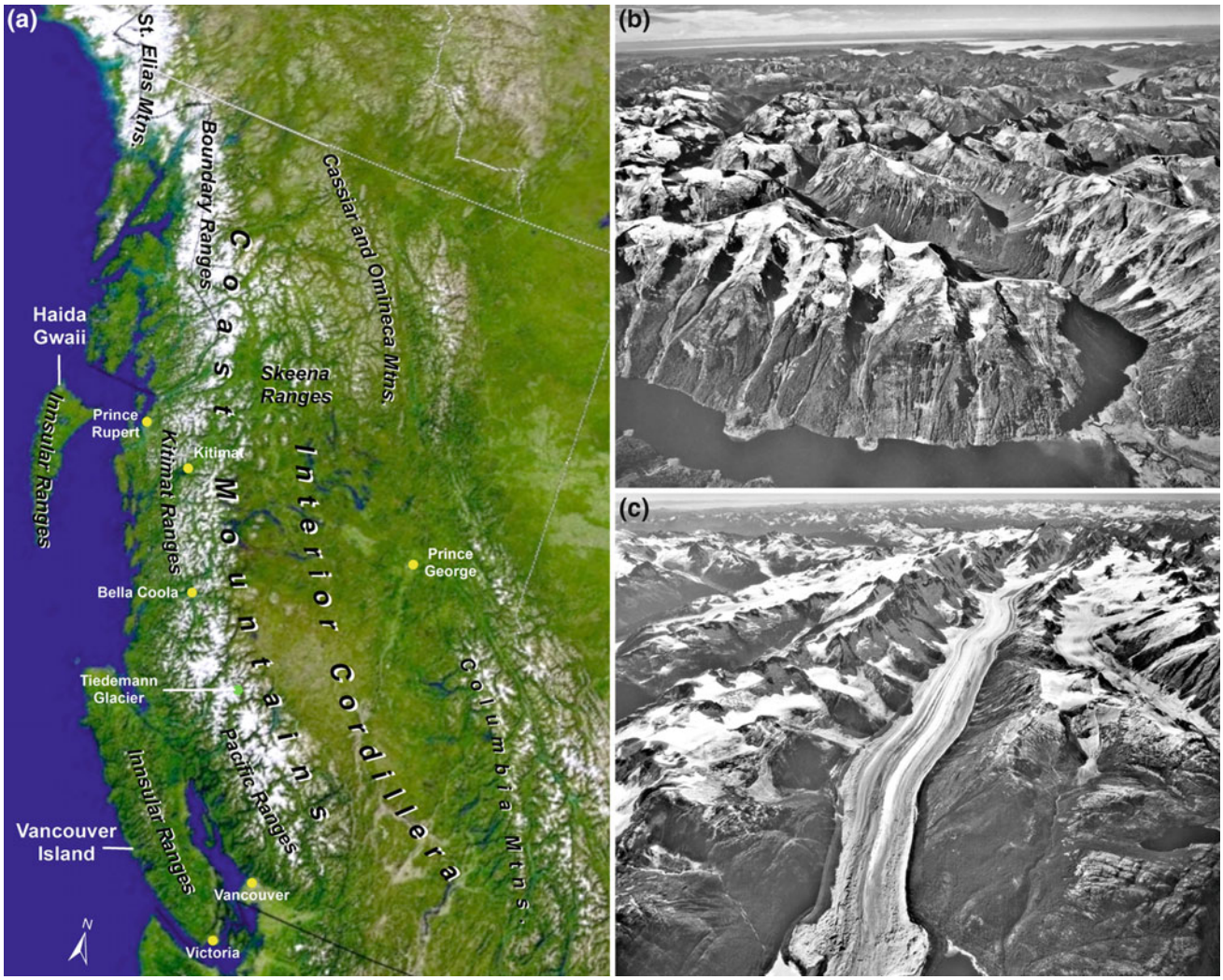

Fig. 1.16 **a** Image of the Interior and Western Cordillera. *Source* NASA, Visible Earth. **b** Oblique view of the Kitimat Ranges of the Coast Mountains west of Kitimat. **c** Looking westward up the Tiedemann Glacier toward Mount Waddington (4030 masl), Pacific Ranges of the Coast Mountains. *Source* © Province of British Columbia. All rights reserved. BC 688:16 and BC528:21

Russell 2000) has a rich assemblage of volcanic landscapes, culminating in the Mt. Edziza complex and the Spectrum Range (Fig. 1.17). The Western Cordillera, which includes the Coast and St. Elias mountains as well as the Insular Ranges, has the highest available relief in Canada (>5000 m) and contains the most glacier ice outside the Canadian Arctic (30,000 km^2) and steep-sided fjords, reminiscent of the Norwegian fjords (Peacock 1935; see Chaps. 21, 22, and 25).

1.7.4 Coastal Plains

Regions 20 and 21 are the Arctic Coastal Plain and Pacific Coastal Lowlands. The Arctic Coastal Plain is dominated by the delta of Mackenzie River, comparable with the delta landscapes of Lena and Yukon rivers in Siberia and Alaska, respectively (see Chaps. 23 and 24). The Pacific Coastal Lowlands include the fascinating strandflat landscape of

Fig. 1.17 **a** Looking north toward the snow-covered Mount Edziza volcanic complex from the Spectrum Range (*foreground*) in northwestern British Columbia. Mount Edziza is one of four large composite volcanoes making up the Mount Edziza-Spectrum Range volcanic complex, a large volcanic plateau or shield (65 km long and 20 km wide). The volcano contains both subglacial and subaerial lava domes, lava flows, and pyroclastic cones such as the one seen below. *Source* © Province of British Columbia. All rights reserved. Reproduced with permission of the Province of British Columbia (*photograph*: 0238-00HQLD0017). **b** Eve Cone on the northern flank of Edziza, north of Telegraph Creek. Reproduced with the permission of Natural Resources Canada, 2015 (photo: KGS-1511 by J. M. Harrison)

Milbanke Flats, south of Prince Rupert, and the 10,000 year old delta of Fraser River (see Chaps. 25 and 26). The most distinctive feature of this landscape is that it sits below the so-called Marine Limit, which means that it has been raised and inundated by the sea multiple times during the Pleistocene Epoch (see Chaps. 2 and 3).

Acknowledgment Cartography (with the exception of Fig. 1.3) by D. Kovanen.

References

Ambrose JW (1964) Exhumed paleoplains of the Precambrian Shield of North America. Am J Sci 262:817–857

Bostock HS (1970) Physiographic regions of Canada. Geol Surv Can Map 1254A (1st and 2nd edn), scale 1:5,000,000. doi:10.4095/293408

Bostock HS (2014) Physiographic regions of Canada. Geol Surv Can Map 1254A (1st and 2nd edn), scale 1:5,000,000. doi:10.4095/293408

Brew DA, Ford AB (1978) Megalineaments in southwest Alaska marks southwest edge of Coast Range batholithic complex. Can J Earth Sci 15:1763–1772

Cassidy JF, Balfour N, Hickson C, Kao H, White R, Caplan-Auerbach J, Mazzotti S, Rogers GC, Al-Khoubbi I, Bird AL, Esteban L, Kelman M, Hutchinson J, McCormack D (2011) The 2007 Nazko BC earthquake sequence: injection of magma deep in the crust beneath the Anahim volcanic belt. B Seismol Soc Am 101:1732–1741

Church M, Ryder JM (2010) Physiography of British Columbia. In: Pike RG, Redding TE, Moore RD, Winkler RD, Bladon KD (eds) Compendium of forest hydrology and geomorphology in British Columbia, vol 1. Land Management Handbook 66, BC Min Forest Range Res Branch, pp 17–45

Clague JJ (1975) Late Quaternary sediments and geomorphic history of the southern Rocky Mountain Trench. Can J Earth Sci 12:595–605

Duk-Rodkin A, Hughes OL (1994) Tertiary-Quaternary drainage of the pre-glacial Mackenzie Basin. Quatern Int 22(23):221–241

Earth Impact Database (2015) University of New Brunswick, Planetary and Space Science Centre. http://www.unb.ca/passc/ImpactDatabase/faq.html. Accessed 15 Feb 2015

Edwards BR, Russell JK (2000) Distribution, nature, and origin of Neogene—Quaternary magmatism in the northern Cordilleran volcanic province, Canada. Geol Soc Am Bull 112:1280–1295

Eisbacher GH, Carrigy MA, Campbell RB (1974) Paleodrainage pattern and late-orogenic basins in the Canadian Cordillera. In: Dickinson WR (ed) Tectonics and sedimentation. SEPM Special Paper 22, pp 143–166

Environment Canada (1995) Ecozones of Canada (version 1). http://sis.agr.gc.ca/cansis/nsdb/ecostrat/gis_data.html. Accessed 21 Jan 2015

Ford DC (1987) Effects of glaciations and permafrost upon the development of karst in Canada. Earth Sur Processes 12:507–521

Ford DC, Williams PW (2007) Karst hydrogeology and geomorphology. Wiley, Chichester

Ford DC, Schwarcz HP, Drake JJ, Gascoyne M, Harmon RS, Latham AG (1981) Estimates of the age of the existing relief of the Rocky Mountains of Canada. Arctic Alpine Res 13:1–10

Government of British Columbia (2014) Biogeoclimatic ecosystem classification (BEC) zone/subzone/variant/phase map (version 9). Published by the Ministry of Forests, Lands and Natural Resource Operations, Victoria, British Columbia. http://www.for.gov.bc.ca/hre/becweb/resources/maps. Accessed 21 Jan 2015

Government of Canada (2008) Canadian permafrost thickness, Geological Survey of Canada. Natural Resources Canada; Earth Sciences Sector; Canada Centre for Mapping and Earth Observation. http://geogratis.gc.ca/api/en/nrcan-rncan/ess-sst/092b663d-198b-5c8d-9665-fa3f5970a14f.html. Accessed 30 Jan 2015

Hickson CJ (2000) Physical controls and resulting morphological forms of Quaternary ice-contact volcanoes in western Canada. Geomorphology 32:239–261

Hodgson DA (1989) Quaternary Geology of the Queen Elizabeth Islands. In: Fulton RJ (ed) Quaternary Geology of Canada and Greenland. Geol Surv Can. Geology of Canada Series, no 1, pp 441–478

Jackson LE, Nelson FE, Huscroft CA, Villeneuve M, Barendregt RW, Storer JE, Ward BC (2012) Pliocene and Pleistocene volcanic interaction with Cordilleran icesheets, damming of the Yukon River and vertebrate paleontology, Fort Selkirk volcanic group, west-central Yukon. Quatern Int 260:3–30

Lay D (1940/41) Fraser River Tertiary drainage history in relation to placer gold deposits. BC Department of Mines, Bulletins 3 and 11

Leech GB (1966) The Rocky Mountain Trench. Geol Surv Can Paper 66–14:307–329

Massey NWD, MacIntyre DG, Desjardins PJ, Cooney RT (2005) Digital Map of British Columbia: Whole Province, B.C., British Columbia Ministry of Energy, Mines and Petroleum Resources, Geofile 2005-1. http://www.mapplace.ca/. Accessed 6 Jan 2015

Mathews WH (1947) Tuyas, flat-topped volcanoes in northern BC. Am J Sci 245:560–570

Mathews WH (1992) Physiographic evolution of the Canadian Cordillera. In: Gabrielse H, Yorath CJ (eds) Geology of the Cordilleran orogen in Canada. Geol Surv Can, Geology of Canada 4:403–418

MDA Federal (2004) Landsat GeoCover ETM + 2000 Edition Mosaics Tiles N-06-60, N-7-55, N-08-55, N-08-60, N-11-50. ETM-EarthSat-MrSID, 1.0, USGS, Sioux Falls, South Dakota, 2000. Data available at the Global Land Cover Facility, www.landcover.org

Meidinger DV, Pojar J (eds) (1991) Ecosystems of British Columbia. BC Ministry of Forests and Lands

Meijer Drees NC (2008) Distribution of Lower Givetian Strata (GIS data, polygon features, version 2). Geological Survey of Canada, FIG 2008-0088. http://www.ags.gov.ab.ca/publications/DIG/ZIP/DIG_2008_0088.zip. Accessed 21 Feb 2015

Neuffer DP, Schultz RA, Walters RJ (2006) Mechanisms of slope failure on Pyramid Mountain, a subglacial volcano in Wells Gray Provincial Park BC. Can J Earth Sci 43:147–155

NASA Landsat Program (2003) Landsat ETM+ scene LE70460232000269EDC00, USGS, Sioux Falls, 10/26/2003. Data available from the Global Land Cover Facility, www.landcover.org

Parrish RR (1981) Uplift rates of Mount Logan, Yukon Territory and BC's central Coast Mountains using fission track dating methods. EOS 62:59–60

Peacock MA (1935) Fjordlands of British Columbia. Geol Soc Am Bull 46:633–696

Riddihough RP, Hyndman RD (1992) Modern plate tectonic regime of the continental margin of western Canada. In: Gabrielse H, Yorath CJ (eds) Geology of the Cordilleran orogen in Canada. Geol Surv Can, Geology of Canada, vol 4, pp 437–455

Ryder JM (1981) Geomorphology of the Coast Mountains of BC. In: Slaymaker O (ed) High mountains. Z Geomorphol Supp 37:120–147

Siebert L, Simkin T (2002) Volcanoes of the World—Data from Global Volcanism Program Digital Information Series, GVP 4.3.3, Smithsonian Institution, Washington, D.C. http://www.volcano.si.edu/. Accessed 21 Feb 2015

Smith SL, Burgess MM, Heginbottom JA (2001) Permafrost in Canada: a challenge to northern development. In: Brooks GR (ed) A synthesis of geological hazards in Canada. Geol Surv Can Bulletin, vol 548, pp 241–264

Stasiuk MV, Hickson CJ, Mulder T (2003) The vulnerability of Canada to volcanic hazards. Nat Hazards 28:563–589

Stearn CW (1975) Canada. In: Fairbridge RW (ed) Encyclopedia of World Regional Geology. Dowden, Hutchinson and Ross, Stroudsburg, Pa, pp 139–144

Stöckli R, Vermote E, Saleous N, Simmon R, Herring D (2005) The Blue Marble Next Generation—A true color earth dataset including seasonal dynamics from MODIS. NASA, Earth Observatory

Tempelman-Kluit D (1980) Evolution of physiography and drainage in southern Yukon. Can J Earth Sci 17:1189–1203

Tribe S (2005) Eocene paleophysiography and drainage directions, southern Interior Plateau, BC. Can J Earth Sci 42:215–230

Williams PW, Fong YT (2015) World map of carbonate rock outcrops (version 3.0). http://web.env.auckland.ac.nz/research/karst.shtml. Accessed 23 Feb 2015

Yorath CJ, Cook DG (1981) Cretaceous and Tertiary stratigraphy and paleogeography, northern Interior Plains, District of Mackenzie. Geological Survey of Canada, Memoir 398

Pleistocene Landscapes of Western Canada

2

Olav Slaymaker and Dori J. Kovanen

Abstract

A brief summary of western Canada's late Quaternary history emphasizes the period from the Last Glacial Maximum to the start of the Holocene Epoch. Almost all of Canada was covered by ice at the Last Glacial Maximum. Canada's contemporary landscapes are deeply imprinted with the Quaternary legacy. The general concept of a glacial landsystem is the prism through which western Canadian landscapes are seen. The concept recognizes three glacial landsystems: the Shield terrain, the sedimentary lowlands and the glacial valley terrain. Within the glacial landsystems, individual landscapes and landform assemblages subject to supraglacial, englacial and subglacial processes are described. Glacivolcanic landscapes are exceptionally important in western Canada and are discussed separately. The 5 % of western Canada that was not glaciated in the Quaternary has distinctive landscapes. The increasing importance of fluvial and proglacial lake processes towards the end of the Pleistocene requires separate treatment.

Keywords

Western Canada • Quaternary • Landscape • Landform assemblages • Glacial landsystem • Glacivolcanism

2.1 Pleistocene History

In late Tertiary and Quaternary time, uplift of order 1 km has emphasized the high relief of the Canadian Cordillera, and during the Quaternary the region was repeatedly glaciated. The presently glacierized regions of the Western Cordillera and, to a lesser extent, the Eastern Cordillera indicate the core accumulation zones of the Cordilleran Ice Sheet. Major valleys and individual mountain masses have been extensively modified by glacial erosion and deposition. The coastal fjords and the interior lakes are the most obvious glacial erosional legacy. The fact remains, however, that most of Quaternary time has been much like today so that the main dissection of the landscape has been achieved by rivers. Clague (1986) directed attention to the episodic nature of fluvial activity during the Pleistocene. Mathews (1989) has summarized the geomorphic processes that were effective during the Quaternary in bringing about physiographic change in the Cordillera under the headings of (1) glaciation; (2) subaerial erosion and deposition; (3) diastrophism; and (4) volcanism. Ford (1987) reminded us of the specific effects of glaciation and permafrost on karst landform evolution.

2.1.1 The Distribution of Ice Sheets and Stages of Deglaciation

Glaciers formed first in the northern part of the Western Cordillera about 9 Ma ago (Denton and Armstrong 1969) and since then have profoundly altered the landscape. Classic alpine landforms were created, including cirques and over-deepened valley heads, horns and comb ridges. The

O. Slaymaker (✉) · D.J. Kovanen
Department of Geography, University of British Columbia, 1984 West Mall, Vancouver, BC V6T 1Z2, Canada
e-mail: olav.slaymaker@ubc.ca

D.J. Kovanen
e-mail: djkovanen@comcast.net

© Springer International Publishing Switzerland 2017

O. Slaymaker (ed.), *Landscapes and Landforms of Western Canada*,
World Geomorphological Landscapes, DOI: 10.1007/978-3-319-44595-3_2

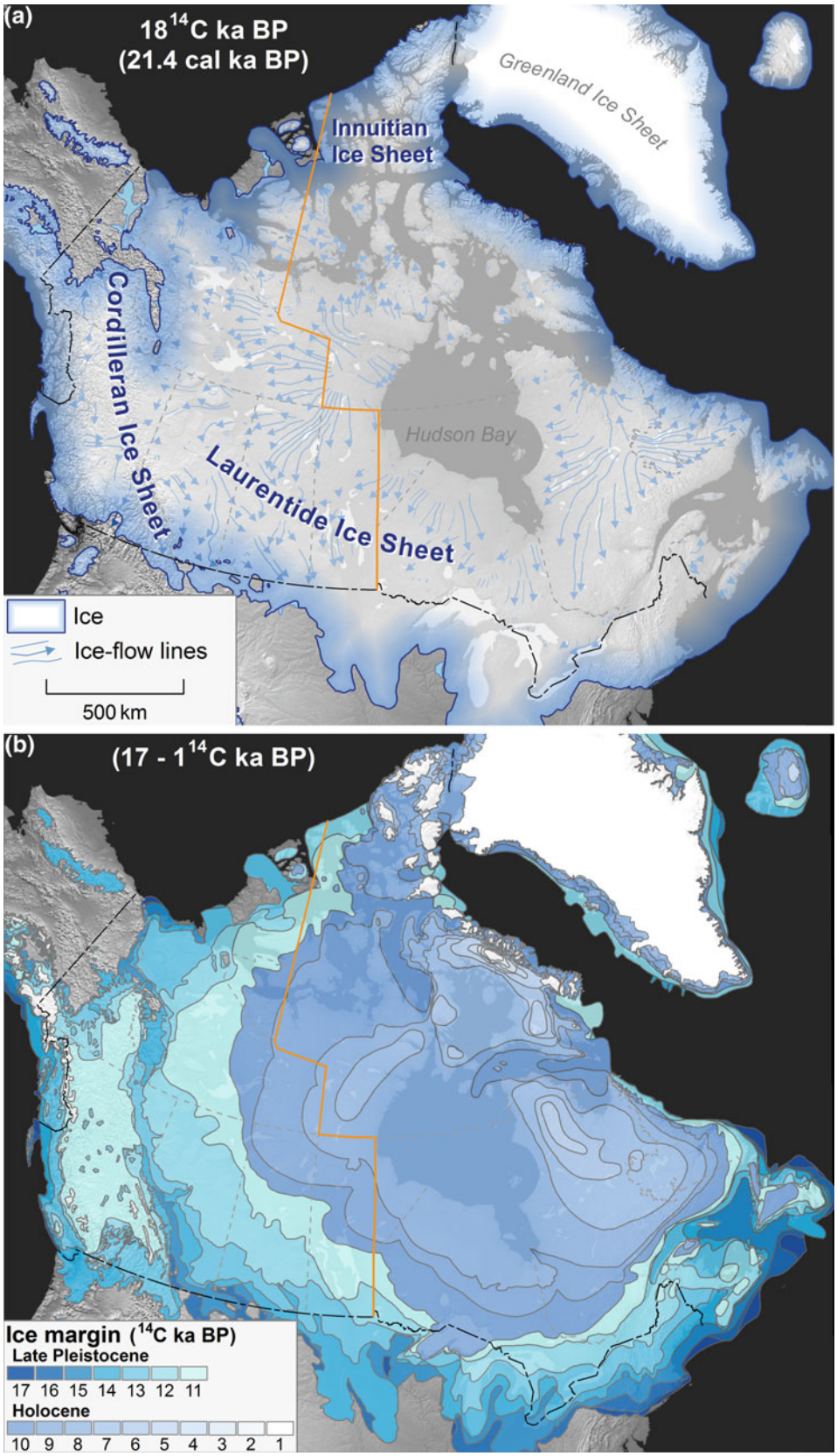

Fig. 2.1 Ice masses in Canada. **a** Distribution of Cordilleran, montane, plateau and continental ice coverage and generalized ice flow direction (modified from Shaw et al. 2000) of glaciers covering the last ice age, called the "Late Wisconsinan Glaciation." The only ice-free areas were in Yukon, and on Banks, Prince Patrick and Melville islands in the western Arctic. **b** Extent of ice coverage at various stages of deglaciation. Ice margins from Dyke et al. (2003)

coastline is highly indented by fjords extending as much as 150 km inland and as much as 755 m deep (Peacock 1935). The continental shelf between Vancouver Island and Haida Gwaii is crossed by three major U-shaped troughs. On the eastern side of the Coast Mountains, there are fjord lakes up to 125 km long and over 400 m deep. Three ice sheets (Laurentide, Cordilleran and Innuitian) influenced western Canada (Fig. 2.1).

At the Last Glacial Maximum (LGM), the Laurentide Ice Sheet was the second largest (to Antarctica) in the world. It therefore contributed most to global sea-level fall during the last ice age. In its coalescence with the Cordilleran and Innuitian ice sheets, one-third of the world's glacial cover was based in North America. The only ice-free areas were in Yukon, and on Banks, Prince Patrick and Melville islands in the western Arctic. There continues to be debate about the precise sequence of events as the ice sheets retreated. The various stages of deglaciation and the extent of ice coverage have been estimated from ice margins by Dyke et al. (2003) (Fig. 2.1b). For discussion of the Innuitian Ice Sheet, see England et al. (2006). The complexity of landform and landscape evidence in those areas where ice sheets interacted is illustrated in Fig. 2.2 (Gordey and Makepeace 1999; Duk-Rodkin and Froese 1999; Dyke and Evans 2003).

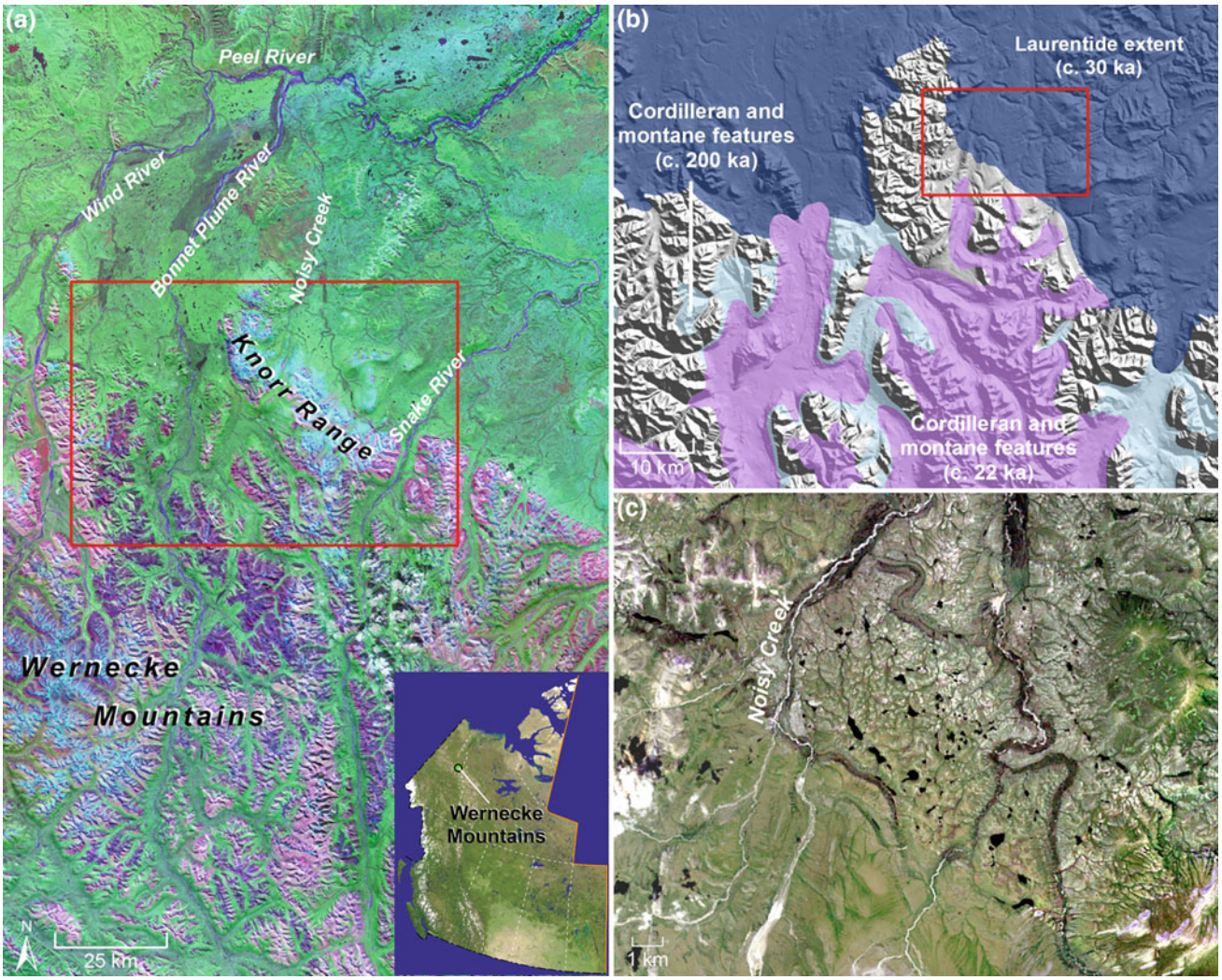

Fig. 2.2 Laurentide and Cordilleran Ice Sheet interactions, **a** and **b** against the north flank of Knorr Range, Wernecke Mountains, in Yukon, the area contains the limits of several glaciations (Gordey and Makepeace 1999). *Source* MDA Federal (2004). **c** At this site, hummocky moraine deposited at the southern margin of a small lobe of Laurentide ice is separated from colluvial slopes to the south by ice marginal channels and glacifluvial deposits. *Source*: © Department of Natural Resources Canada. All rights reserved. Government of Canada, Centre for Topographic Information, CanImage—Landsat 7 Orthoimage, extracted from 106e08, 09 and 106f05. The inset image here and elsewhere in this chapter is extracted from NASA, Visible Earth (Stöckli et al. 2005)

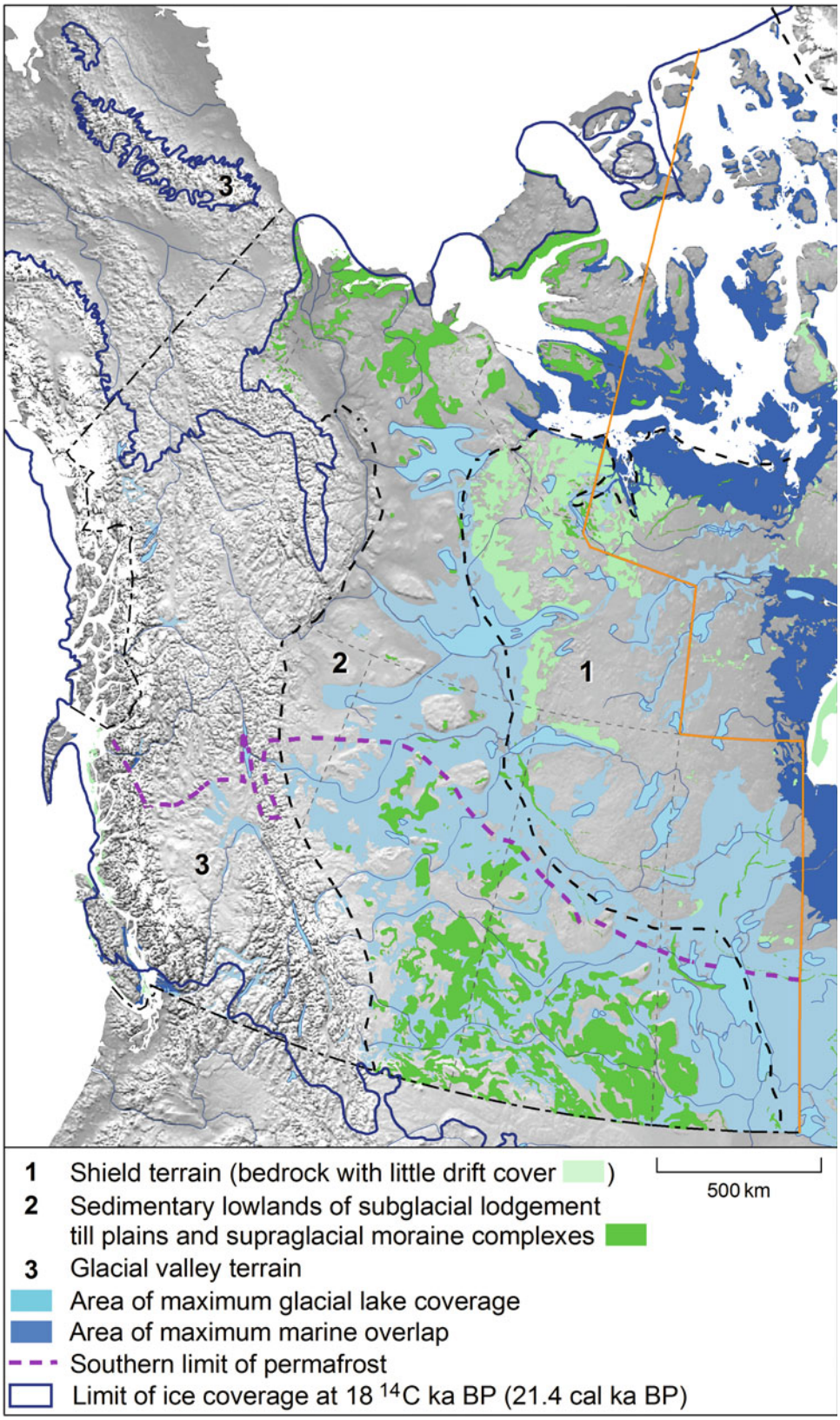

Fig. 2.3 Glacial landsystems in western Canada. The maximum outermost limit of glaciation is after Dyke et al. (2003) at 18 ^{14}C ka BP. This is not the maximum extent for the Cordilleran Ice Sheet (see Puget Lobe), which is at 14 ^{14}C ka BP, but we used 18 ka for consistency. Also see Eyles et al. (1983)

2.1.2 Subaerial Erosion and Deposition

Most Cordilleran valleys were probably initially cut by streams prior to glaciation. In unglaciated northern Yukon, streams alone controlled erosion. Stream diversions and reversals took place frequently during the Quaternary. Many diversions resulted from the blockage of stream courses by glaciers, but also by glacial and fluvial deposits, lava flows and landslides (Mathews 1989). Periglacial processes, such as solifluction, cryoplanation and thermokarst development, were more widespread during cooler non-glacial stages of the Pleistocene and during early parts of glacial cycles. A low, coastal rock platform abutting against a sharply rising slope (known as a strandflat) is found along the Pacific coast from Vancouver Island northwards. It averages 10 km wide and reaches a maximum elevation of 150 masl (Mathews 1989). Accelerated Pleistocene frost weathering is the favoured explanation (Holtedahl 1960) but debate continues because of the astonishing width of the rock platform cut, in many cases, across rocks of greatly differing strength.

2.1.3 Diastrophism and Volcanism

Miocene lavas in the northeastern St. Elias Mountains and southern Coast Mountains have been tilted, faulted and uplifted. On the basis of apatite fission track dates, uplift of 0.2–0.3 m ka^{-1} has continued for 10–15 Ma (Parrish 1981, 1983). Dissected gravel-capped pediplains overly folded and faulted rocks of the eastern foothills of the Rocky Mountains from Montana to the Richardson Mountains. They were uplifted and incised from Late Tertiary through Quaternary times as the mountains to the west rose (Rampton 1982). Volcanism generated widespread basaltic lava flows in the BC Interior during Late Tertiary. Most Quaternary volcanoes in the Cordillera are localized in four relatively narrow belts (Souther 1977 and see Sect. 2.6 below).

2.2 Glacial Landsystems in Western Canada

As mentioned in Chap. 1, the emphasis in Chap. 2 would be on shorter timescales of order 10^4–10^6 years and smaller areas of 10^3–10^5 km^2. But before focusing on these different scales, a brief reference to the larger glacial landsystems provides context. The idea of a glacial landsystem was developed by Eyles et al. (1983) and elaborated by Evans (2003) (Fig. 2.3). Landsystems are strictly defined as areas of common terrain attributes, different from those of adjacent areas, in which recurring patterns of topography, soils and vegetation reflect the underlying geology, past erosional and depositional processes and climate. The landsystem is the upper level in a hierarchy of terrain classification. At the lowest level are land elements or individual landforms; at the intermediate level are land facets or groups of land elements; and landsystems are composites of linked land facets (Eyles 1983; Kovanen and Slaymaker 2015).

Three glacial landsystems were defined by Eyles (1983): (a) Shield terrain, dominated by subglacial processes; (b) sedimentary lowlands, dominated by supraglacial processes and landforms which were draped over the former glacier bed during ice retreat; and (c) glacial valley terrain, which is characteristic of mountain areas (Benn and Evans 2010).

2.3 The Shield Terrain

Quaternary glaciations, especially the last, have created a concentric landscape zonation on the Canadian Shield. The entire shield has been extensively scoured by ice sheets, and this process has created countless lake basins. Overprinted on this is a zonation of landform–sediment associations centred on the final area of ice retreat from western Canada in the District of Keewatin. This retreat centre is characterized by large fields of ribbed moraine formed in association with flutings and drumlins. Beyond these are broad zones of thick and nearly continuous drift composed mostly of streamlined till and large eskers. The outer shield is largely bare bedrock (Fulton 1989).

2.3.1 Landscapes of Little or no Glacial Erosion

Some preglacial landforms, sediments and weathering horizons have survived intact in spite of repeated occupation by ice (Sugden 1974). Cold-based ice caps and ice sheets are generally assumed to be the reason. But much remains to be explained with respect to the survival of tors, saprolites and block fields as discussed by Dyke (1993) for the Canadian Arctic. His argument was that uplands in the Canadian Arctic islands supported Late Wisconsinan ice caps that developed two landscape zones reflecting basal thermal conditions regulated by long-sustained ice flow patterns. Central cold-based zones protected older glacial and preglacial landscapes while peripheral warm-based zones scoured and otherwise altered their beds.

2.3.2 Subglacial Chemical Weathering

The effectiveness of subglacial chemical weathering has been underestimated in the literature because of the logistical difficulties in securing field data, the intrinsic complexity of the environment and the fact that most geomorphologists are better trained in physics than in chemistry. Glacier beds are

complex, dynamic mosaics whose rate of chemical weathering is controlled by bedrock and till lithology and the availability of reactants such as free oxygen and carbon dioxide. Much research needs to be done on solute budgets of glacierized basins.

2.3.3 Areal Scouring

Landscapes of areal scouring consist of subglacially eroded bedrock, such as rock knobs, roches moutonnées and over-deepened rock basins. Extensive tracts of subglacially eroded bedrock occur on the Canadian Shield (Fig. 2.4). The distribution of hard and soft subglacial beds, ice sheet dynamics and sediment dispersal patterns are the major causative factors. Hollows and rock basins occur where joint density of the underlying bedrock is high or where less resistant rocks outcrop. They develop under wet-based ice where glacial meltwater run-off is laterally extensive.

2.3.4 Subglacial Bedforms

Subglacial bedforms are longitudinal or transverse accumulations of sediment formed below active ice. Longitudinal forms are streamlined features aligned parallel to ice flow and can be divided into drumlins, flutings and megaflutings. Transverse bedforms are classified as Rogen or ribbed moraines.

(a) **Flutings, Drumlins and Megascale Glacial Lineations (MSGL)** Flutings are elongated, streamlined ridges of sediment aligned parallel to former glacier flow. They tend to consist of subglacial till. Drumlins, megaflutings and MSGLs are among the most enigmatic of glacial landforms. The former bed of the Dubawnt Lake palaeo-ice stream in Keewatin is a classic site to illustrate MSGLs (Stokes and Clark 2003). The drumlins and megalineations have a pattern of convergence towards a narrow corridor of highly elongate, closely packed and parallel lineations followed by a pattern of divergence (Fig. 2.5). A similar pattern was observed by Kovanen and Slaymaker (2004) in the Okanagan Lobe. Boulton (1987) proposed a qualitative model of drumlin formation based on the principles of sediment erosion and redistribution within subglacial deforming layers. He used the drumlins of northern Saskatchewan to illustrate his theory. Megaflood explanation of subglacial bedforms (Shaw et al. 1989, 2000) cited this same drumlin field as evidence for a completely different theory of drumlin formation, Shaw's megaflood explanation.

(b) **Transverse Bedforms such as Ribbed or Rogen Terrain** Rogen moraines are fields of coalescent crescentic ridges up to 30 m high and up to 100 m wide lying transverse to former ice flow (Fig. 2.6a). In North America, these features are usually referred to as ribbed terrain. Keewatin provides many classic examples of ribbed terrain (Aylsworth and Shilts 1989). Dunlop and Clark (2006) recognized 16 different types of ribbed terrain. The close association of ribbed terrain with drumlins and flutings suggests that they can predate, postdate and be contemporaneous with each other. Gravenor and Kupsch (1959) described linear disintegration ridges which are intersecting ridges oriented parallel, transverse and oblique to former ice flow from western Canada.

(c) **Eskers** Eskers are elongated, sinuous ridges of glaciofluvial sand and gravel (Fig. 2.7). Some of the longest esker ridges in Canada are several hundred kilometres long, stand more than 50 m above the surrounding terrain and are up to several kilometres wide (Shilts et al. 1987). Brennand (2000) recognized four basic esker types: (1) tunnel fills, formed in englacial and subglacial conduits; (2) ice-channel fills, formed in supraglacial ice-walled channels; (3) segmented tunnel fills, formed during pulsed glacier retreat; and (4) beaded eskers, formed during pulsed retreat of a water terminating glacier.

2.4 The Sedimentary Lowlands

The Interior Plains are a low relief area lying between the Canadian Shield and the Cordillera. Bedrock relief plays a role in large scale physiographic features, but small scale elements, which are largely depositional, are primarily related to Quaternary glaciation. Deposition of drift was more important, in general, than glacial erosion and has resulted in thick Quaternary successions (Vincent and Klassen 1989). The Interior Plains region occupies the western margin of the Keewatin sector of the Laurentide Ice Sheet. In fact it contains the limits of advance of many of the Quaternary glaciers, both Laurentide and Cordilleran. Because the lithology of the underlying beds was deformable and the glaciers were highly mobile, hummocky moraine and ice-thrusted sheets of bedrock and Quaternary materials are better developed here than in any other region of Canada (Vincent and Klassen 1989).

Fig. 2.4 Shield bedrock landscape with till or lacustrine veneers. **a** Dubawnt Plain with open white spruce—dwarf birch woodlands and wetlands (*lighter green tones*). **b** Great Slave Upland with bedrock-dominated landscape. The forest grows in rock fractures and on discontinuous till and lacustrine deposits between bedrock exposures. *Source* © Government of the Northwest Territories/D. Downing

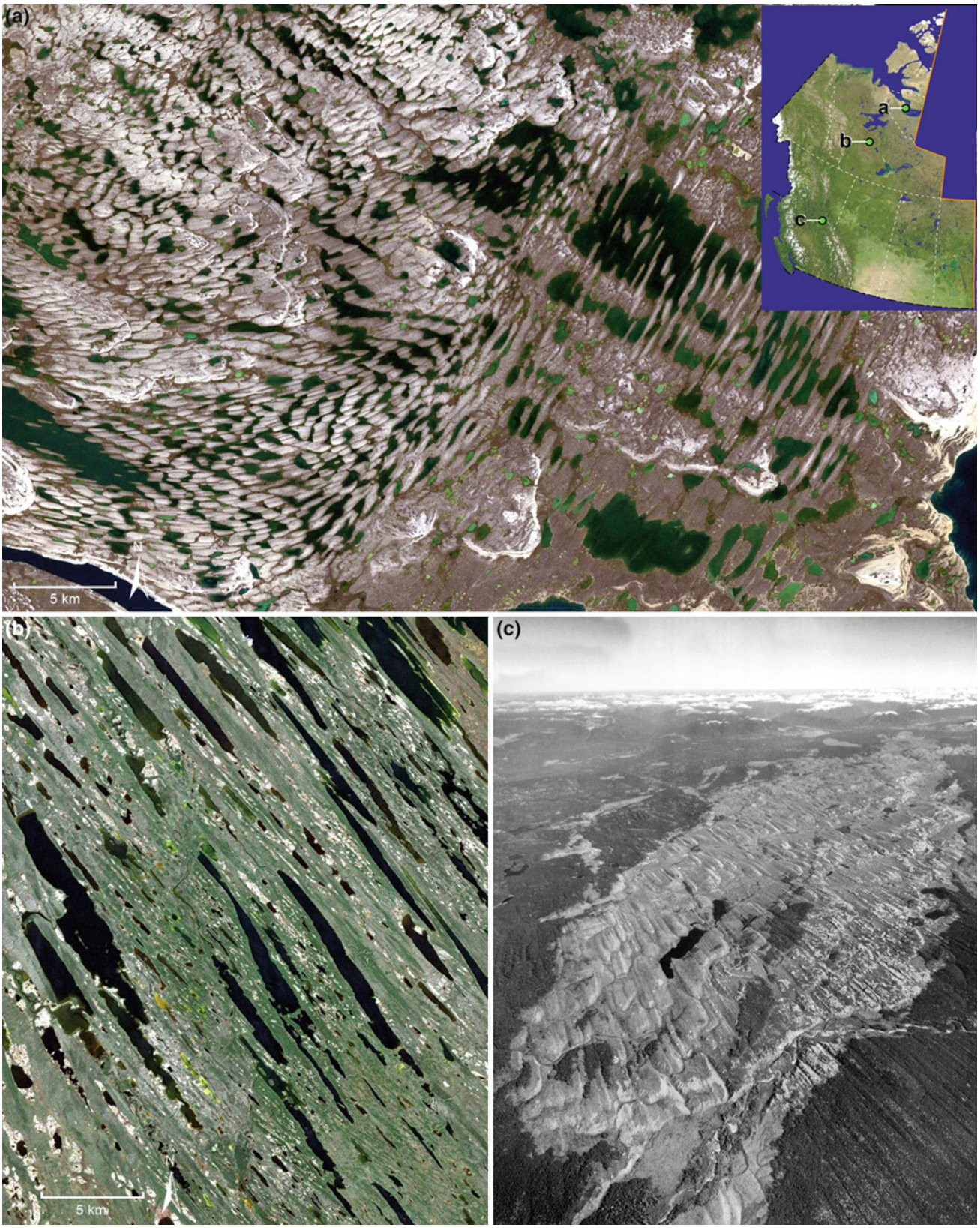
(a)
a
b
c
5 km
(b)
5 km
(c)

◀ **Fig. 2.5** Megascale lineations. **a** Cross-cutting drumlins along the Amundsen Gulf in northwest Nunavut. These elongated hills or streamlined landforms were formed below the Laurentide and Cordilleran Ice Sheets during the last ice age. They are aligned parallel to the flow of ice and often dictate the locations of lakes and the path of rivers. *Source* © Department of Natural Resources Canada. All rights reserved. Government of Canada, Centre for Topographic Information, CanImage—Landsat 7 Orthoimage, 087a06. **b** Elongate drumlinized landforms south of Great Bear Lake, Northwest Territories. *Source* © Department of Natural Resources Canada. All rights reserved. Government of Canada, Centre for Topographic Information, CanImage—Landsat 7 Orthoimage, 095b16. **c** Interior Plateau, McGregor Plateau. Looking eastward across Angusmac Creek and over the drumlinized surface of the McGregor Plateau northeast of Prince George, British Columbia. The fluting and drumlins in the unconsolidated material and the drumlin-like rock ridges trend north 40 degrees east. *Source* © Province of British Columbia. All rights reserved. BC761:70

2.4.1 The Supraglacial Landsystem

(a) **Supraglacial Hummocky Moraine** The term hummocky moraine is restricted to moraines deposited during the melt-out of debris-mantled glaciers (Sharp 1985; Fig. 2.6b). Some hummocky moraines, such as controlled moraines, have pronounced transverse linear elements because their morphology was controlled by the former pattern of debris concentration in the parent ice (Gravenor and Kupsch 1959). The ice-cored (controlled) morainic topography in the continuous permafrost zone of northern Canada is a modern analogue for the development of ancient hummocky moraines in lowland terrain (Dyke and Savelle 2000). The circular rimmed mound (known as rim ridges, doughnuts or ring forms) may be either supraglacial or subglacial moraine forms (Johnson and Clayton 2003).

(b) **Kame Terraces** Kame terraces are gently sloping depositional terraces, located on valley sides, and deposited by meltwater streams flowing between glacier margins and the adjacent valley wall. (Levson and Rutter 1989).

(c) **Kame and Kettle Topography** Kame and kettle topography comprises variously shaped mounds and ridges (kames) and intervening hollows (kettles; Fig. 2.8). It is formed by supraglacial or ice-contact glacifluvial deposition. Classic examples of these mounds and ridges and intervening hollows are found in the lower Fraser Valley.

(d) **Pitted Outwash or Sandar** Pitted sandar, kettled sandar or kettled outwash plains are sandar that are cratered by hollows left by the melt out of isolated blocks of glacier ice. The difference between kame and kettle topography and pitted outwash reflects the relative importance of glacifluvial deposition and the melt-out of buried ice in the form of the final landform assemblage.

2.4.2 Ice Sheet Margins

Landform zonation in western Canada has been explained by Evans (2009) as a product of changing thermal regimes in the receding south-western margin of the Laurentide Ice Sheet. Three partially overprinted suites of moraines and landforms occur in the McGregor Lake moraine belt in southwestern Alberta indicating that readvances took place during overall ice sheet recession. The outermost suite is interpreted as controlled moraine produced when the ice sheet base was cold. The innermost suite consists of recessional push moraine at a warm-based ice margin. Possibly the intermediate suite relates to a period when ice marginal conditions were changing from polythermal to temperate (Fig. 12.88 in Benn and Evans 2010).

2.4.3 Glacitectonic Forms

Erosional basins also occur in areas underlain by soft sediments. If sediments form a rigid bed, erosion by plucking may occur. Glacitectonic thrusting near glacier margins can excavate large basins, and erosion may occur on deformable beds. The following four glacitectonic sediment landform associations have been recognized by Aber et al. (1989): hill-hole pairs; thrust block moraines; cupola hills; and megablocks. One of the largest hill-hole pairs so far recognized at the Earth's surface, with an area >100 km^2, is found at Herschel Island (Rampton 1982; see Chap. 24); Evans and England (1991) have noted the common occurrence of thrust block moraines in permafrost in the Canadian Arctic; cupola hills that are aligned in arcuate or transverse belts are widespread in Alberta where the advancing Laurentide Ice Sheet dislocated soft sedimentary bedrock, and megablocks are widespread in southern Alberta (e.g. the Cooking Lake megablock near Edmonton) and have been described classically by Stalker and Mac (1976) (see Chap. 11).

2.5 Glacial Valley Terrain

2.5.1 Glaciated Mountain Landscapes

Alpine landscapes have formed in areas of repeated valley glaciation and are essentially networks of troughs and cirques deeply incised into mountain massifs. During glacial occupancy, the interfluves were commonly ice-free and were typically reduced to narrow aretes and sharp horns. As pointed out by Porter (1989) and Benn and Evans (2010), it

Fig. 2.6 Ribbed moraine and hummocky moraine landscapes. **a** Ribbed moraines near Kasmere Lake, northwestern Manitoba, evidence of retreating ice margin. **b** Hummocky moraines south of the Cypress Hills, southwestern Saskatchewan. Reproduced with the permission of Natural Resources Canada, 2015 (*photographs*: NRCan 2001-358 by Denis St-Onge and NRCan 2001-068 by Lynda Dredge)

Fig. 2.7 Sandy-textured till, outwash deposits and eskers in northwestern Manitoba (**a**) and the Northwest Territories (**b**), related to the Laurentide Ice Sheet flow. Reproduced with the permission of Natural Resources Canada, 2015 (*photograph*: NRCan 2001-6106 by Lynda Dredge) and © Government of the Northwest Territories/D. Downing

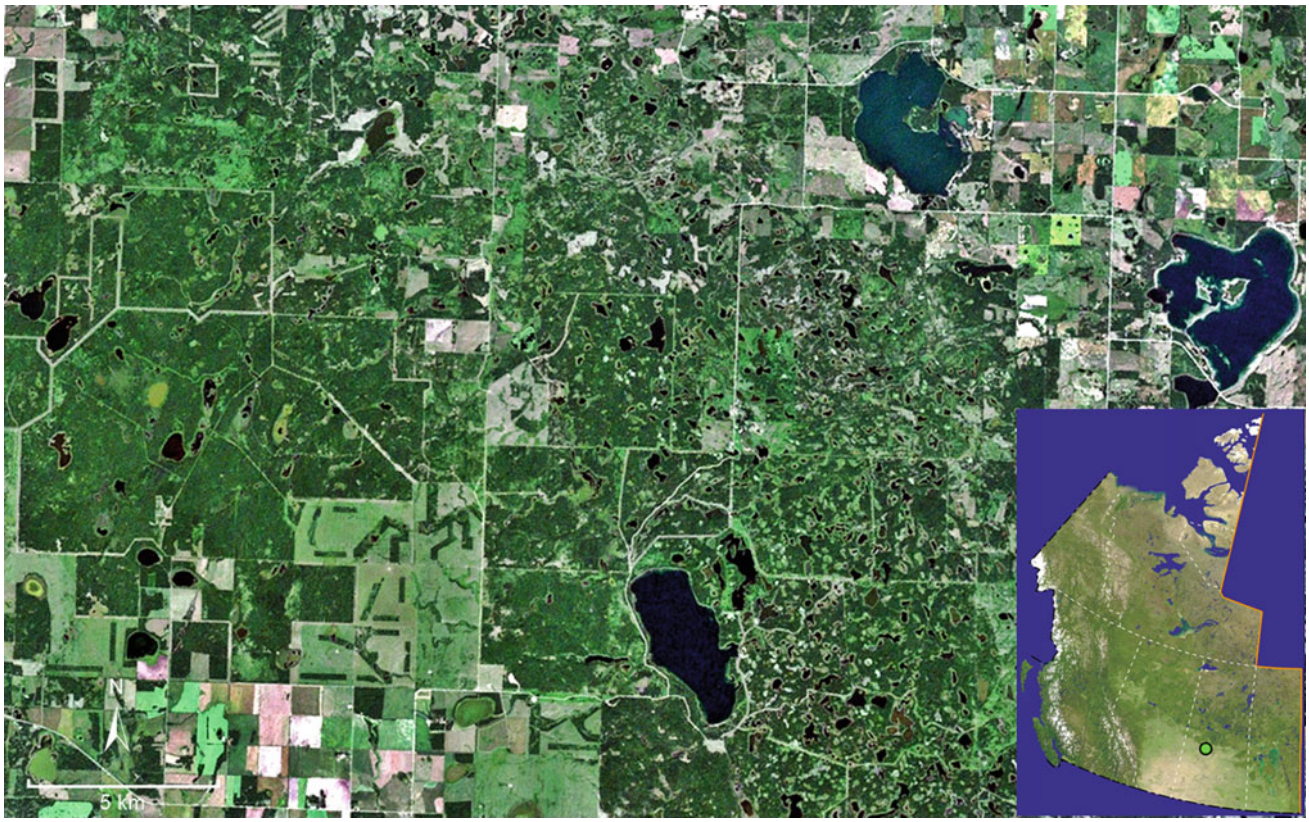

Fig. 2.8 Kame and kettle topography, Witchekan Lake, Saskatchewan. *Source* © Department of Natural Resources Canada. All rights reserved. Government of Canada, Centre for Topographic Information, CanImage—Landsat 7 Orthoimage, 073g06

is not the duration of ice sheet cover but the period of occupancy of alpine styles of glacier cover that develops alpine landscapes.

In the Canadian Cordillera, available relief is commonly between 2000 and 2500 m, with maximum relief of nearly 5000 m in the Western Cordillera where Alaska, Yukon and British Columbia converge near the Pacific coast. High throughput of water and ice leads to high erosion rates (Hallet et al. 1996). The glacial "buzz saw" effect has been endorsed by Mitchell and Montgomery (2006) and Tomkin (2007) using numerical modelling that couples rock uplift and erosion rates in the Washington Cascades. It remains to be seen how general a phenomenon this is (French and Slaymaker 2012).

(a) **Rock Basins and Overdeepenings** Basins can be eroded into bedrock by glaciers at a wide variety of scales from small hollows between roches moutonnées to large overdeepenings, occupying the full width of cirques and troughs. Large overdeepenings are common in deglaciated valleys, where they are generally occupied by lakes (e.g. Lillooet and Harrison Lakes in the Coast Mountains, Chap. 22) and have been identified under many existing glaciers. The formation, size and shape of rock basins are controlled by glaciological variables, such as the thermal regime and stress conditions at the glacier bed, and substrate conditions such as bedrock structure and lithology. Lithological controls on rock basin development have been emphasized by Evans (1994) in the Cayoosh Range, Pacific Ranges of the Coast Mountains.

(b) **Troughs and Fjords** The most spectacular glacial erosion is illustrated by troughs and fjords (Fig. 2.9). Troughs and fjords are carved by ice flow through major rock channels which have in most cases been initiated by fluvial erosion. The location and nature of trough heads is influenced by (1) a pre-existing valley step (2) increase in ice discharge due to convergence of glacier tributaries or (3) lithological or structural variation in the bedrock leading to down-glacier increase in erodibility. Troughs and fjords commonly have overdeepenings on their floors. Over-deepened sections terminate at a sill or threshold. Roberts and Rood (1984) have characterized British Columbia fjords. The pattern of erosion intensity is often inherited from preglacial fluvial networks.

(c) **Cirque Landscapes** Cirques are the most characteristic forms of glacial erosion in mountainous terrain. The

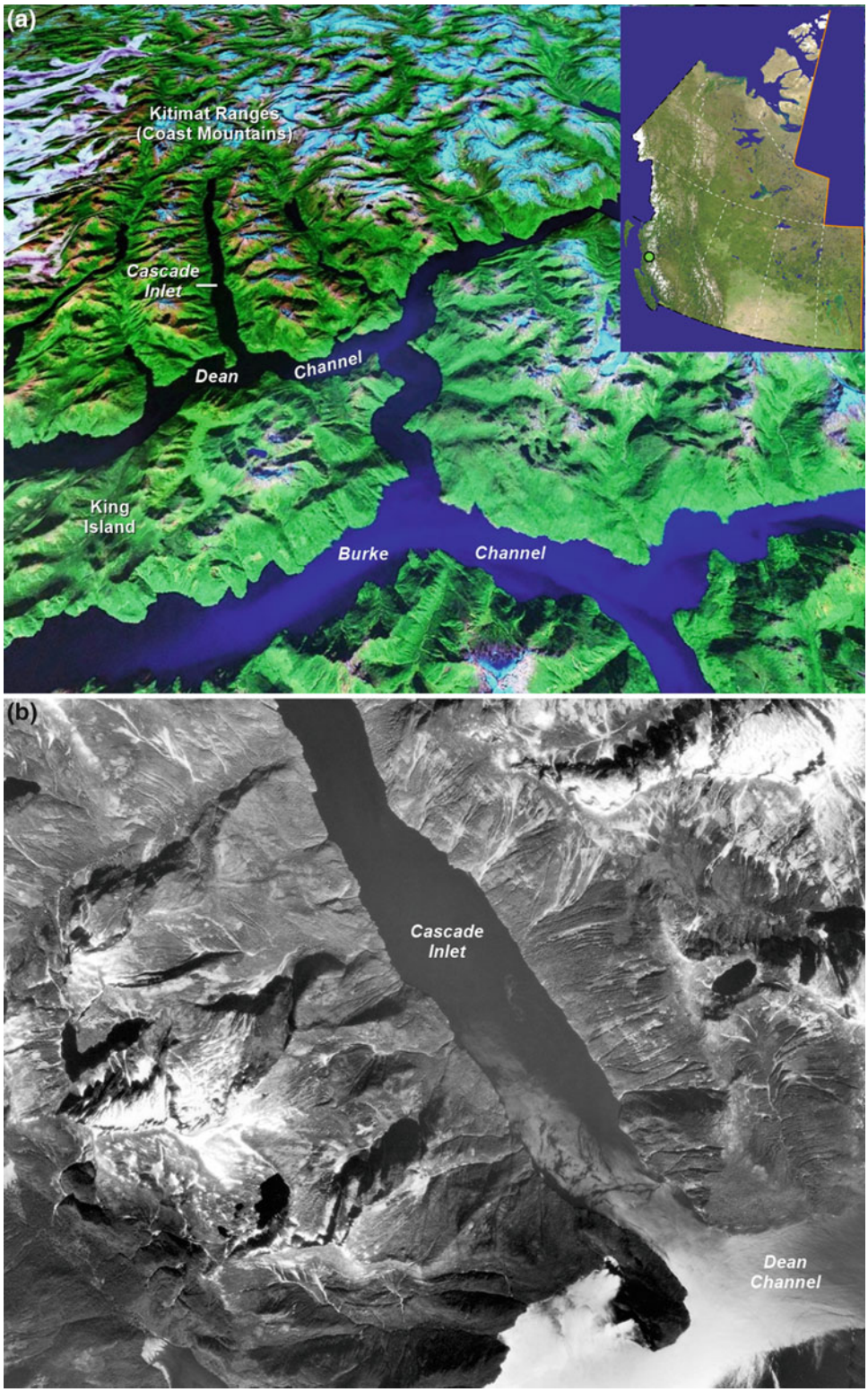

Fig. 2.9 Fjords in BC. **a** Burke and Dean channels and Cascade Inlet. *Source* MDA Federal (2004). **b** Looking north-west into the Kitimat Ranges up the Cascade Inlet, a fjord tributary of Dean Channel. Note the straightness of the channel, the steep slopes extending to the water's edge and the absence of beaches. *Source* © Province of British Columbia. All rights reserved. BC86098:235

typical cirque profile (flat floor, over-deepened basin connected to a steep backwall by a concave slope) is a product of subglacial erosion on the cirque floor and lower backwall and subaerial frost action on the upper backwall. Increasing evidence shows that large rock wall failures also play an important role. The connection between snow patches in a nivation hollow through a larger snow patch in a nivation cirque to a

glacier in a true cirque is a controversial model. Cirques in British Columbia have been characterized by Evans (1990) (Pacific Ranges of the Coast Mountains) and by Brardinoni and Hassan (2006) for the North Shore mountains, West Vancouver. Cirque landscapes are characterized by independent cirques incised into upland terrain (Fig. 2.10). Because of their assumed association with small glaciers, cirques have been used as indicators of long-term average palaeoclimate conditions (e.g. Evans 1999).

Fig. 2.10 Cirque landscapes in the Canadian Rocky Mountains. **a** Muskwa Ranges, Northern Rocky Mountains and Protected Area (cf. Figs. 3.8 and 29.10). **b** Front Ranges, Canadian Rocky Mountains. *Sources* © Department of Natural Resources Canada. All rights reserved. Government of Canada, Centre for Topographic Information, CanImage—Landsat 7 Orthoimage, 094k07 and 082g01

2.5.2 Valley Bottom Glaciated Landscapes

(a) **Moraine Landscapes** There is a range of moraine building processes in marginal positions at glacier snouts leading to the recognition of three main types of moraines. Ice pushing is simply the bull dozing of ice marginal sediment by an advancing glacier snout. Squeezing results from the pressure gradient between sediment that is overlain by glacier ice and unconfined sediment, producing push and squeeze moraines. Material accumulating at the surface of a glacier gets remobilized by mass movement and fluvial transport and is then dumped. Dump moraine size is related to supraglacial moraine volume and the length of the glacier still-stand period. Dumping of large quantities of debris around glacier margins builds up lateral frontal dump moraines. The accumulation of dump moraine at the margin of a thickening glacier results in a wedge-shaped moraine. Lateral dump moraines on steep valley sides have poor preservation potential due to rapid paraglacial reworking. Lateral moraines tend to be asymmetrically developed. Four reasons for within-valley asymmetry are (Evans 1999) as follows: (1) differential mass movement on opposite valley sides; (2) differences in thickness and type of sediment; (3) cross valley differences in lithology and structure; and (4) glacier dynamics influenced by insolation. Medial moraines do not have good preservation potential because they contain relatively little debris and are subject to intensive reworking processes.

(b) **Strandflats** Perhaps the least understood of all glacial landforms is the strandflat. Strandflats are extensive undulating rock platforms cut across variably resistant lithologies located close to sea level. Strandflats in western Canada are up to 10 km wide and usually end abruptly at an inland cliff line or break of slope. When viewed parallel to the coast, strandflats are remarkably horizontal, but usually have a small seaward slope due to postglacial glaci-isostatic displacement (Holtedahl 1960). A combination of frost action, sea ice rafting, marine erosion, subaerial erosion and subglacial erosion processes are commonly invoked, but the great width of the strandflat and its modest relief presents problems of explanation (Fig. 2.11).

2.6 Glacivolcanic Landscapes

2.6.1 Tuyas: Volcano–Ice Interaction

One of the most distinctive landscapes in western Canada is that associated with volcano–ice interaction. Throughout the Pleistocene Epoch 2.6 Ma to 10,000 ka ago, there was volcanism in the Northern Cordilleran Volcanic Province (NCVP). The first volcano–ice interaction resulted in tuyas, including Tuya Butte, on the Tanzilla Plateau and in the Cassiar Mountains in the northern interior of British Columbia. These tuyas commonly reach more than 100 m in elevation. Flat-topped tuya volcanoes developed under glacial ice between 1 Ma and 730 ka ago (Hickson 2000). The Mathews Tuya, in northern BC, pays tribute to the *locus classicus* that was described by Mathews (1947).

2.6.2 Complex Volcano–Ice Interactions

A second more complicated type of volcano–ice interaction is geographically restricted to the Level Mountain Range, the Mount Edziza volcanic complex and Hoodoo Mountain (in the Boundary Ranges of the Coast Mountains; Figs. 1.8 and 1.17). All three volcanoes are broad enough to hold ice caps that likely altered regional ice flow while still being altered by the Cordilleran Ice Sheet at individual periods. At the Edziza and Level Mountain Range complexes, glacier hydrology of the Cordilleran Ice Sheet was influenced by a complicated interaction between drainage on the flat plateaus under relatively thinner ice and drainage within nearby steep valleys filled with much thicker ice. Within the Mt. Edziza volcanic complex, Ice Peak began to form when the Cordilleran Ice Sheet began retreating around 1.6 Ma ago. It is a stratovolcano that was constructed when large areas of the Edziza lava plateau were free from glacial ice. As Ice Peak began to form, lava spread to the flanks of Ice Peak where it formed meltwater lakes. Mount Edziza, a steep-sided stratovolcano overlapping the northern flank of Ice Peak, began to form 1 Ma ago. Its smooth northern and western flanks are only slightly channelled by erosion and they curve up to a circular 2700 masl summit ridge which surrounds a central ice-filled caldera 2 km in diameter. Active cirques on Edziza's eastern flank have breached the caldera rim, exposing the remnants of several lava lakes that ponded in the caldera 900 ka ago.

Near the border between British Columbia and the Alaska Panhandle, lava flows and eight small volcanoes form a volcanic field known as the Iskut–Unuk River Cones. Lava flows date back 70 ka ago during the Pleistocene Epoch, but the eight volcanoes were likely formed between 9 ka and a few hundred years ago. At least five volcanoes sent lava 20 km down the Iskut and Unuk River valleys and their tributaries. Volcanism in the Iskut River area has created at least ten lava flows.

2.6.3 The Garibaldi Chain

Dominating the Garibaldi chain are volcanoes and other volcanic formations that formed during periods of intense

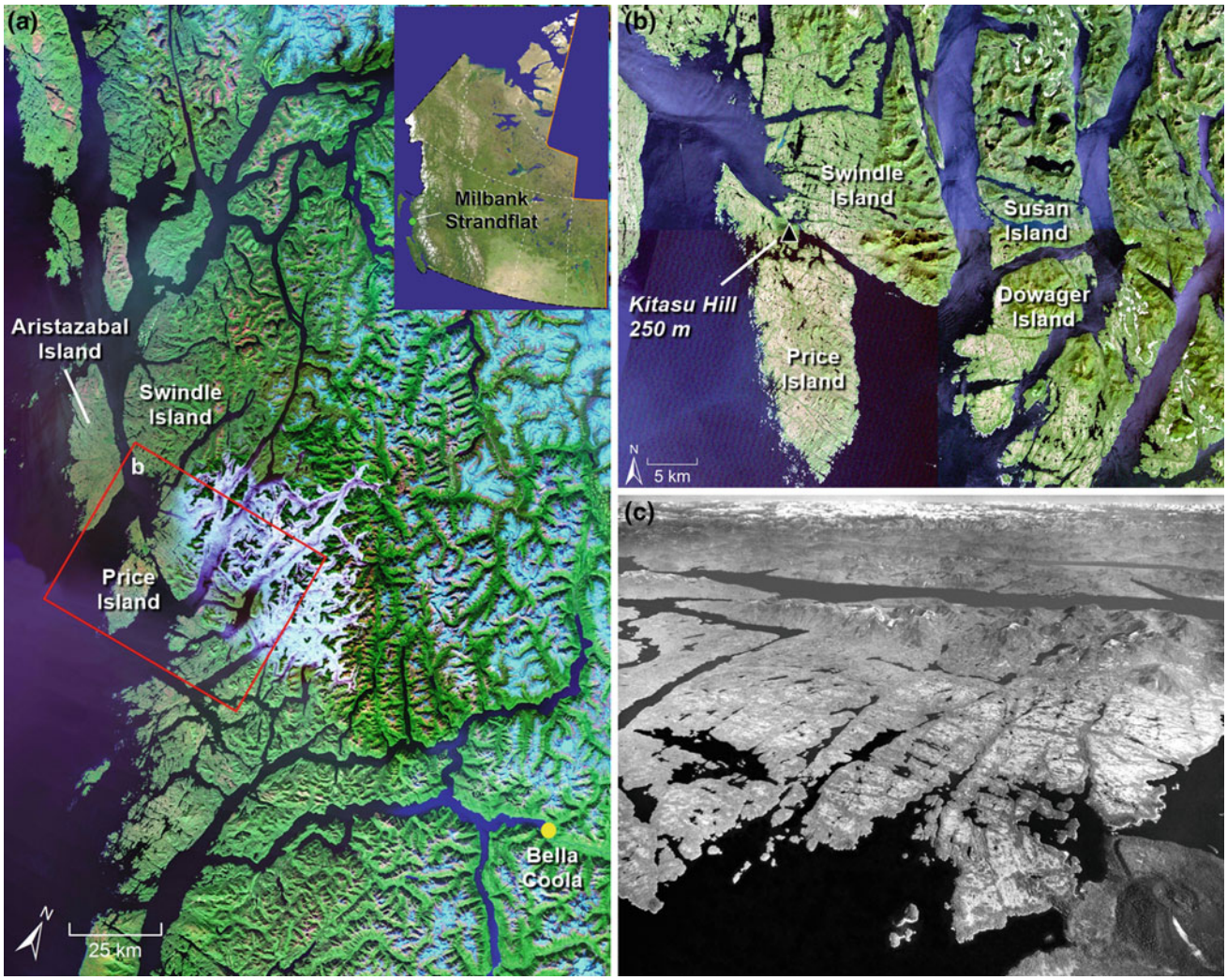

Fig. 2.11 Swindle and Price islands strandflat, components of the Milbanke Flats strandflat. **a** Regional overview. *Source* MDA Federal (2004). **b** Swindle and Price islands in relation to fjorded Coast Mountains. *Source*: © Department of Natural Resources Canada. All rights reserved. Government of Canada, Centre for Topographic Information, CanImage—Landsat 7 Orthoimage, 103a07, 103a08, 103a09, 103a10. **c** Oblique view of scoured bedrock looking northeast across Milbanke Strandflat on Swindle Island toward Finlayson Channel. Kitasu Hill in the right foreground is a post-Pleistocene volcanic cone. *Source* © Province of British Columbia. All rights reserved. BC 501.47

glaciation. This includes flow-dominated tuyas, subglacial lava domes and ice-marginal lava flows. Lava domes that were formed mainly during subglacial activity have steep flanks. Ice-marginal lava flows form when lava erupts from a subaerial vent and ponds against glacial ice. The Barrier, a lava dam impounding Garibaldi Lake in the southern segment, is the best represented ice-marginal lava flow in the Garibaldi Belt. Mount Garibaldi has a volume of 6.5 km^3 and erupted within the last 300 ka. It was constructed when volcanic material erupted onto a portion of the Cordilleran Ice Sheet (Fig. 2.12).

On the western shore of Garibaldi Lake, Mt. Price is a stratovolcano which was constructed during three periods of activity. The first phase 1.2 Ma ago formed the stratovolcano. Volcanism then moved towards the west where a series of lava flows was extruded during a period of Peléan activity 300 ka ago. Lava flows that extend 6 km to the northwest and southwest occurred 9 ka ago. These flows were dammed against glacial ice to form an ice-marginal lava flow more than 250 m thick known as The Barrier. Black Tusk (2136 masl) is the glacially eroded remnant of a much larger volcano that formed during two periods of volcanic activity (Fig. 2.12c). The first occurred between 1.1 and 1.3 Ma ago and the second between 170 and 210 ka ago. The ice-marginal lava flows form 100-m cliffs. Subsequently, the regional Late Pleistocene Ice Sheet carved a deep north-trending U-shaped valley into the eastern flank of the second-stage cone.

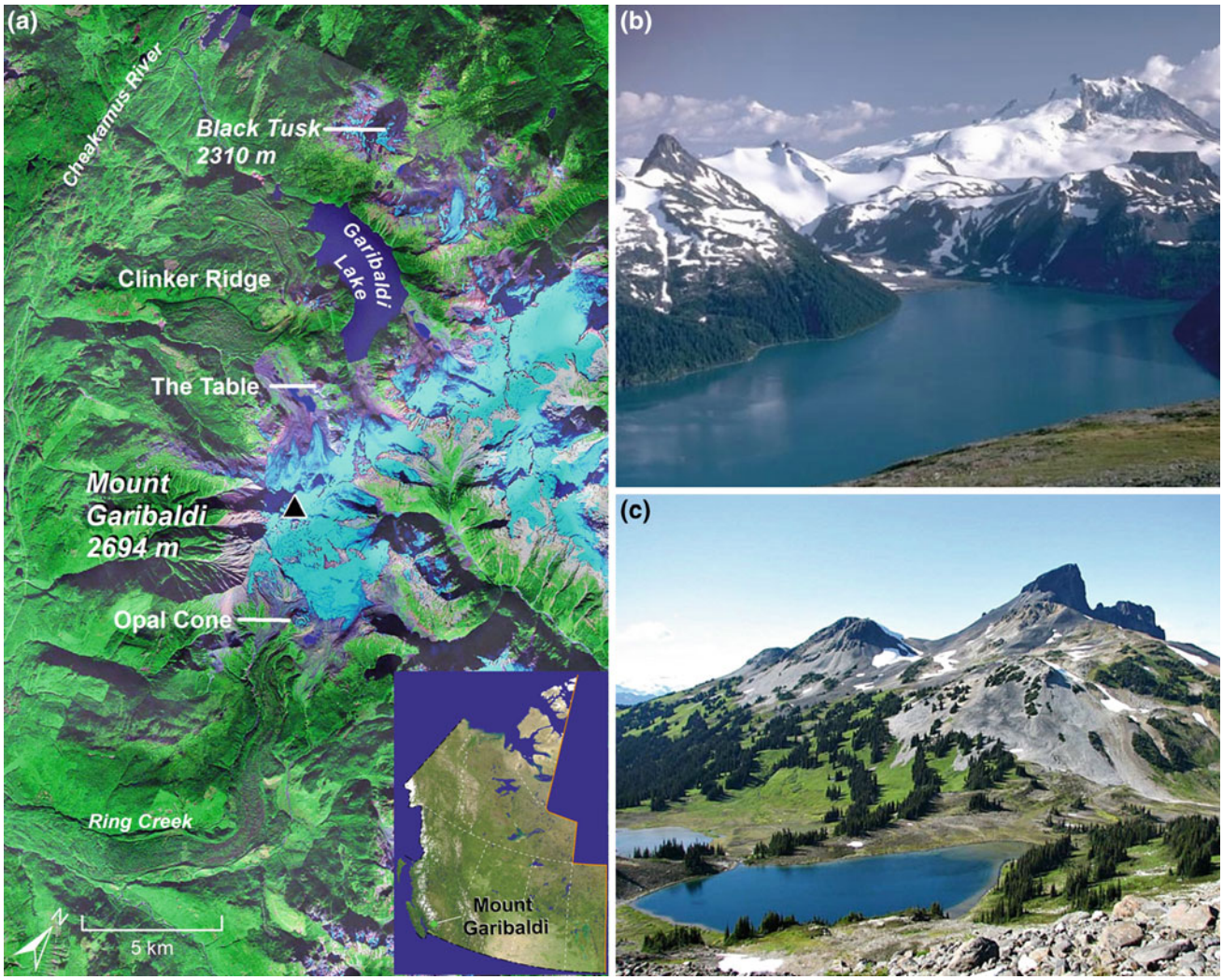

Fig. 2.12 The Garibaldi Lake volcanic field **a** consists of nine small stratovolcanoes and volcanic vents of Pleistocene to Holocene age around Garibaldi Lake. Mount Garibaldi, a Pleistocene stratovolcano, was partially constructed over the Cordilleran Ice Sheet and displays many ice-contact features. Eruptions during the early Holocene included the emission of lava flows, on both sides of Clinker Ridge and from Opal Cone. *Source* MDA Federal (2004). **b** Mount Garibaldi rising above Garibaldi Lake (1433 masl). The Table, the dark, flat-topped ridge in the foreground is the southernmost vent of the Garibaldi Lake volcanic field and is a "tuya." Photograph by Lee Siebert, 1983, Smithsonian Institution, Global Volcanism Program, http://www.volcano.si.edu. **c** Black Tusk (2319 masl) towering above a mountain meadow is a stratovolcano formed more than a million years ago and has since been glacially eroded. *Source*: © Province of British Columbia. All rights reserved. Reproduced with permission of the province of British Columbia

The Mount Meager massif is the most voluminous composite volcano in the Garibaldi chain as well as the most recent to erupt. It has a volume of 20 km^3 and consists of an eroded stratovolcano. Several dissected lava domes and volcanic plugs are present on its glaciated summit, as well as a volcanic crater with a lava dome placed within it. At least eight volcanic vents compose the complex and have been the sources for volcanic activity throughout Meager's 2.2 Ma history. A well-documented history of volcanism is present at Meager, with its most recent eruption about 2350 years ago. This is the largest recorded Holocene explosive eruption in Canada. Subsequent pyroclastic flows travelled 7 km down Mount Meager's slopes. This created thick agglutinated rubble that successfully blocked the adjacent Lillooet River to form a lake. Subsequently, the breccia dam collapsed to produce a catastrophic flood that deposited house-sized boulders more than 1 km downstream. After the flood took place, a small lava flow was erupted that later solidified to form a series of well-preserved columnar joints. This is the last phase of the 2350-year BP eruption, and subsequent stream erosion has cut through this lava flow to form a waterfall (see chap. 22).

2.7 Unglaciated Landscapes

A few areas of western Canada remained unglaciated during the Pleistocene Epoch, notably the Beaufort Plain, Banks Island and interior Yukon. Although Yukon has been glaciated at least six times, approximately one-third of its area (primarily in central and northern Yukon) escaped the effects of the Cordilleran and Laurentide ice sheets. Northwest Banks Island has experienced uninterrupted cold climate conditions throughout at least the last one million years (French 2007; see Chap. 6); it was an ice-marginal location in the Late Pleistocene and evolved as a fluvial plain underlain by thick gravels and sands. River valleys are cut as much as 160 m below the plain surface, and the valleys are separated by broad areas of flat plain which are completely free of lakes. Large polygons bounded by shallow troughs

Fig. 2.13 Cathedral Provincial Park. **a** Overview. *Source* © Department of Natural Resources Canada. All rights reserved. Government of Canada, Centre for Topographic Information, CanImage—Landsat 7 Orthoimage, 092h01. **b** Nunatak on Cathedral Ridge. **c** Deeply weathered granodiorite on Cathedral Ridge. **d** Patterned ground in the form of stone stripes also on Cathedral Ridge. Photographs by O. Slaymaker

are common. The Barn Mountains of northern interior Yukon also lie beyond the limit of Pleistocene glaciation (see Chap. 18). The mountains are structurally controlled upland massifs surrounded by extensive pediments. These pediments are dissected by streams draining towards the arctic coast (Hughes 1972); they truncate the dip of the underlying rock and occasionally cross fault lines. The Barn Mountains' landscape is old, probably Middle–Late Tertiary, and is characterized by "glacis" slopes, pediments cut in bedrock with a protective veneer of detritus.

The majority of the placer gold deposits of Yukon are located in never or rarely glaciated fluvial systems of central Yukon. The only other areas of western Canada that remained beyond ice cover were the highest peaks of the Cordillera which remained as nunataks at the LGM. An interesting example is Cathedral Provincial Park (Fig. 2.13) which contains distinctive erratics below the highest peaks, indicating the maximum height of the Cordilleran Ice Sheet during LGM.

2.8 Disturbed Fluvial Landscapes

In preglacial time, drainage extended from the mountains eastward across the entire northern Interior Plains. The modern Mackenzie River formed much later primarily as a result of glacial erosion and drainage diversion. The region presently drained by Mackenzie River formerly contributed to two major drainage systems, one entering the North Atlantic as the Bell system, the other entering the Arctic Ocean via the Porcupine and Anderson rivers (Fig. 2.14). The Porcupine River drained across the Richardson Mountains to the Mackenzie Delta, starting in the early Eocene. The Peel and Snake rivers were tributaries to the Anderson

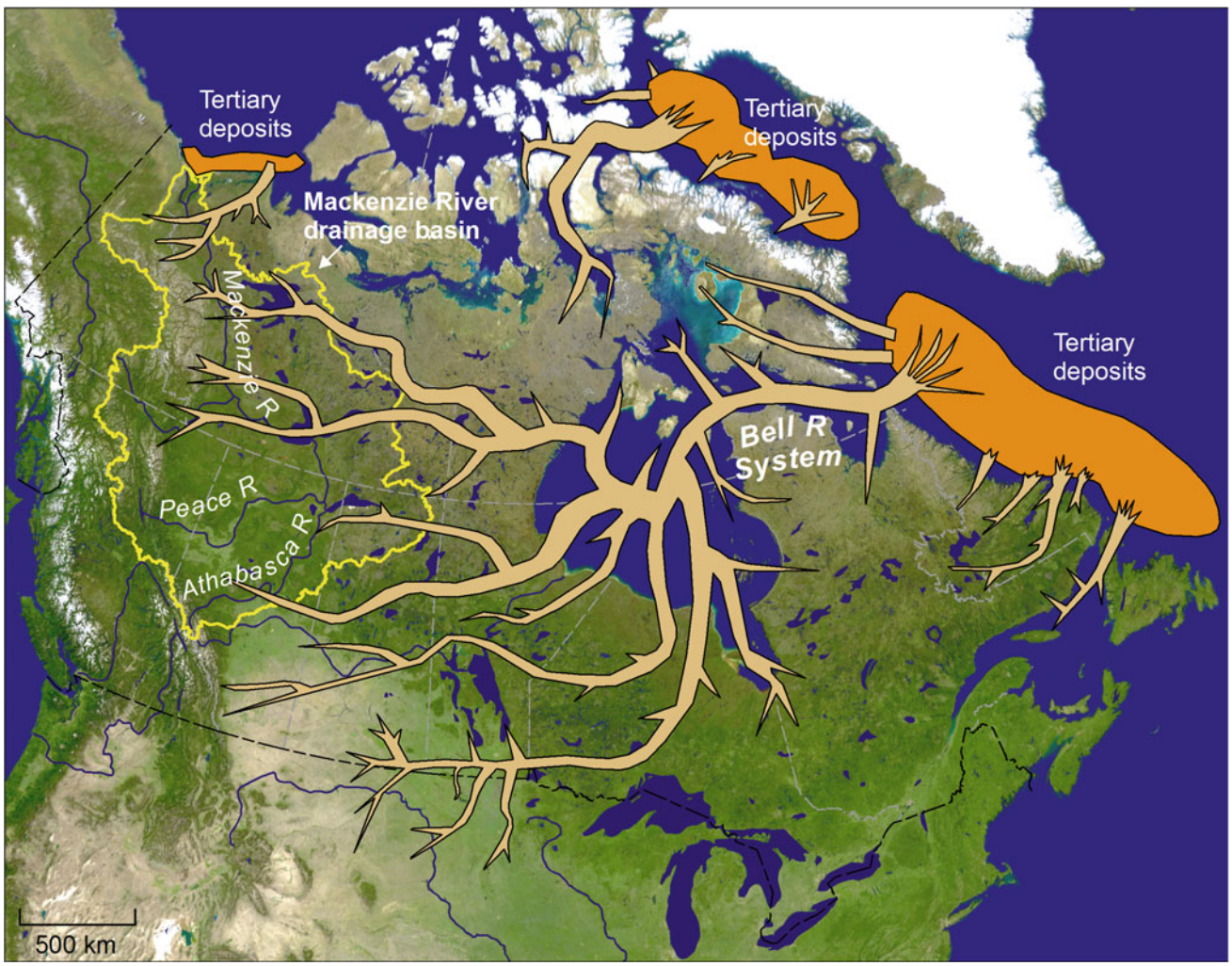

Fig. 2.14 Reconstruction of the preglacial Bell River system, Canada, and the glacial diversion of the headwaters to form the modern Mackenzie River drainage basin (after Duk-Rodkin and Hughes 1994). *Background image*: NASA, Visible Earth

River. Advance of the late Wisconsinan Laurentide Ice Sheet diverted these preglacial drainage systems. The Porcupine River was diverted to the Arctic Ocean via Yukon River; drainage from as far south as Athabasca and Peace rivers was diverted into the Arctic Ocean. A series of ice marginal and proglacial channels associated with retreat of the late Wisconsinan Laurentide Ice Sheet integrated drainage to form Mackenzie River. Most of the rivers occupying the foothills and plains of the Mackenzie region follow former ice-marginal channels for at least part of their modern course.

2.9 Proglacial Lakes in Western Canada

Retreat of ice sheets was accompanied by the development of large glacial lakes and deposition of glacilacustrine silts and clays across large areas. The changing geometry of the

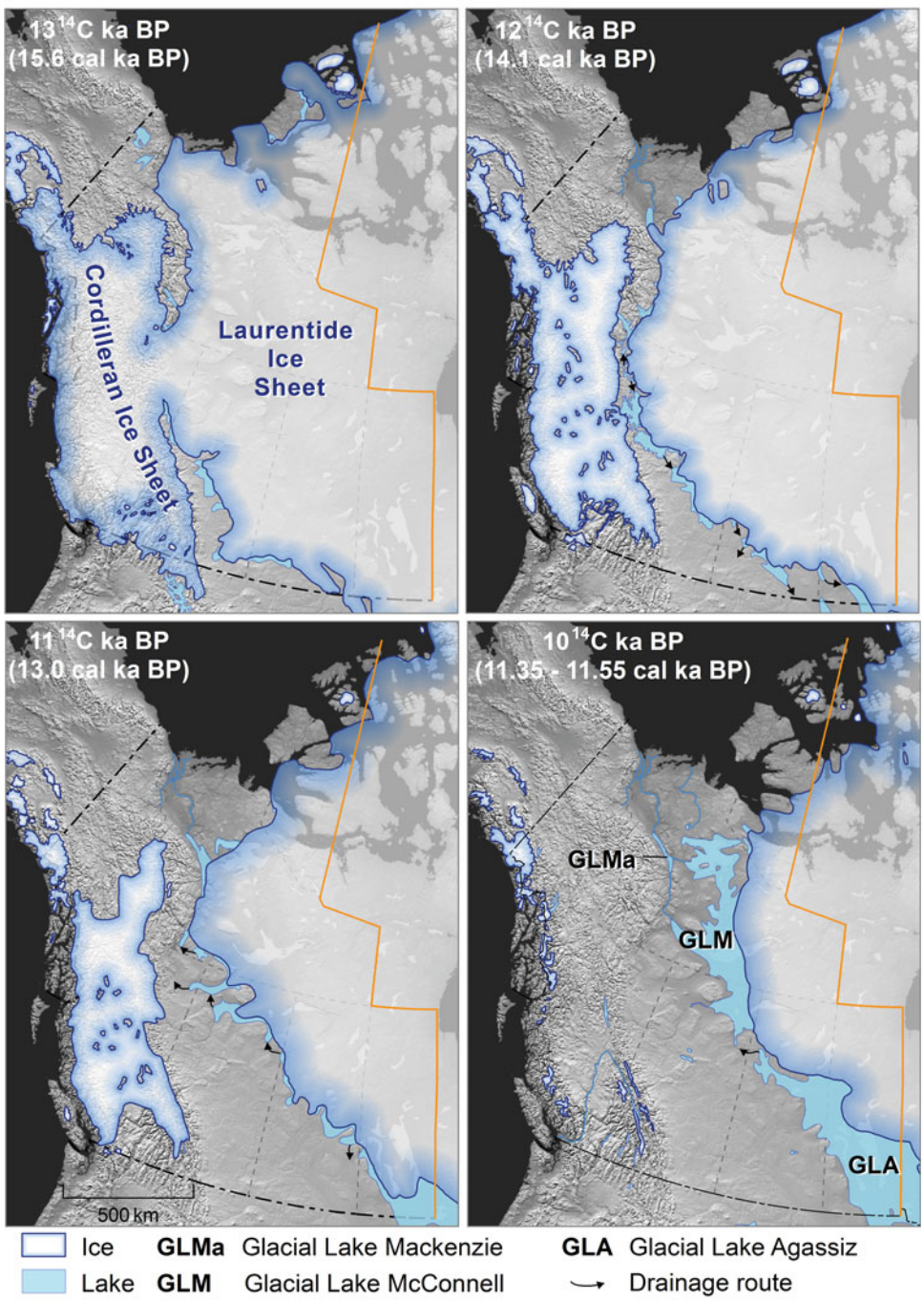

Fig. 2.15 Proglacial lakes in western Canada. Ice margins from Dyke et al. (2003). The Pleistocene Epoch formally ended around 11,350–11,550 calendar years before present (as in the lower right panel) but locally, as in areas still covered by ice, the Holocene Epoch has yet to commence

Laurentide Ice Sheet during deglaciation along with the associated differential isostatic rebound caused the configuration of proglacial lakes and their drainage routeways to evolve. Figure 2.15 shows the locations and maximum extent of glacial lakes Agassiz, McConnell and Mackenzie at various stages of deglaciation (from Dyke et al. 2003). The largest of the glacial lakes was Glacial Lake Agassiz, which covered an area of >260,000 km^2, and the level of the lake was about 215 m above the present level of Lake Winnipeg (22,000 km^3 of water). Between 10.1 and 9.4 ^{14}C ka BP, Glacial Lake Agassiz discharged through a north-western outlet into Glacial Lake McConnell, then Glacial Lake Mackenzie before reaching the Arctic Ocean via Mackenzie River (see Chap. 9).

Deglaciation of the Cordilleran Ice Sheet was mainly by downwasting, with the uplands emerging through the ice while tongues remained in the valleys (see Chap. 20 for a contrary view). This completely disrupted the drainage pattern, causing large glacial lakes, ponded by stagnant ice tongues and active ice lobes to develop in major valleys and small glacial lakes to form in many upland valleys and marginal to the ice. Many of the Cordilleran Ice Sheet-associated proglacial lakes are mapped by Prest et al. (1968).

Acknowledgments Cartography by D. Kovanen.

References

Aber JS, Croot DG, Fenton MM (1989) Glaciotectonic landforms and structures. Glaciology and Quaternary Geology Series, Kluwer Academic Publishers, Dordrecht

Aylsworth JM, Shilts WW (1989) Bedforms of the Keewatin ice sheet. Sediment Geol 62:407–428

Benn DI, Evans DJA (2010) Glaciers and glaciation. Arnold, London

Boulton GS (1987) A theory of drumlin formation by subglacial sediment deformation. In: Menzies J, Rose J (eds) Drumlin symposium. Balkema, Rotterdam, pp 25–80

Brardinoni F, Hassan M (2006) Glacial erosion, evolution of river long profiles and the organization of process domains in mountain drainage basins of coastal British Columbia. J Geophys Res 111: F01013. doi:10.1029/2005JF000358

Brennand TA (2000) Deglacial meltwater drainage and glacio-dynamics: inferences from Laurentide eskers, Canada. Geomorphology 32:263–293

Clague JJ (1986) The Quaternary stratigraphic record of BC: evidence for episodic sedimentation and erosion controlled by glaciation. Can J Earth Sci 23:885–894

Denton and Armstrong (1969) Miocene-Pliocene glaciations in southern Alaska. Am J Sci 267:1121–1141

Duk-Rodkin A, Hughes OL (1994) Tertiary-Quaternary drainage of the preglacial Mackenzie Basin. Quater'n' Int 22(23):221–241

Duk-Rodkin A, Froese DG (1999) Yukon glacial history. In: Froese DG, Duk-Rodkin A, Bond JD (eds) Field guide to Quaternary research in central and western Yukon Territory, pp 14–16

Dunlop P, Clark CD (2006) The morphological characteristics of ribbed moraine. Quat Sci Rev 25:1668–1691

Dyke AS (1993) Landscapes of cold-centred Late Wisconsinan ice caps, Arctic Canada. Prog Phys Geog 17:223–247

Dyke AS, Evans DJA (2003) Ice-marginal terrestrial landsystems: northern Laurentide and Innuitian ice sheet margins. In: Evans DJA (ed) Glacial landsystems. Arnold, London, pp 143–165

Dyke AS, Savelle JM (2000) Major end moraines of Younger Dryas age on Wollaston Peninsula, Victoria Island, Canadian Arctic: implications for paleoclimate and for formation of hummocky moraine. Can J Earth Sci 37:601–619

Dyke AS, Moore A, Robertson L (2003) Deglaciation of Canada. Geol Surv Can Open File 1574. Thirty-two digital maps at 1:7,000,000 scale with accompanying digital chronological database and one poster (two sheets) with full map series; 1 CD-ROM. doi:10.4095/214399

England J, Atkinson N, Bednarski J, Dyke AS, Hodgson DA, O Cofaigh C (2006) The Innuitian ice sheet: configuration, dynamics and chronology. Quat Sci Rev 25:689–703

Evans DJA (1999) Glacial debris transport and moraine deposition: a case study of the Jardalen cirque complex, Sogn og Fjordane, Norway. Z Geomorphol 43:203–234

Evans DJA (ed) (2003) Glacial landsystems. Arnold, London

Evans DJA (2009) Controlled moraines: origins, characteristics and paleoglaciological implications. QuatSci Rev 28: 183–208

Evans DJA, England J (1991) Canadian landform examples 19: high Arctic thrust block moraines. Can Geogr 35:93–97

Evans IS (1990) Climatic effects on glacier distribution across the southern Cast Mountains. Ann Glaciol 14:58–64

Evans IS (1994) Lithological and structural effects on forms of glacial erosion: cirques and lake basins. In: Robinson DA, Williams RBG (eds) Rock weathering and landform evolution. Wiley, Chichester, pp 455–472

Eyles N (1983) Glacial geology: a landsystems approach. In: Eyles N (ed) Glacial geology. Pergamon, Oxford, pp 1–18

Eyles N, Dearman WR, Douglas TD (1983) The distribution of glacial landsystems in Britain and North America. In: Eyles N (ed) Glacial Geology. Pergamon, Oxford, pp 213–228

Ford DC (1987) Effects of glaciation and permafrost upon the development of karst in Canada. Earth Surf Proc Land 12:507–521

French HM (2007) The periglacial environment, 3rd edn. Wiley, Chichester

French HM, Slaymaker O (2012) Changing cold environments: a Canadian perspective. Wiley, Chichester

Fulton RJ (1989) Summary (Chapter 3: Quaternary geology of the Canadian Shield). In: Fulton RJ (ed) Quaternary geology of Canada and Greenland. Geological Survey of Canada. Geology of Canada Series no. 1, pp 177–178

Gordey SP, Makepeace AJ (comp) (1999) Yukon bedrock geology in Yukon digital geology, S. P. Gordey and A. J. Makepeace (comp.). Geological Survey of Canada Open File D3826 and Exploration and Geological Services Division, Yukon, Indian and Northern Affairs Canada, Open File 1999-1(D)

Gravenor CP, Kupsch WO (1959) Ice disintegration features in western Canada. J Geol 67:48–64

Hallet B, Hunter L, Bogen J (1996) Rates of erosion and sediment evacuation by glaciers: a review of field data and their implications. Global Planet Change 12:213–235

Hickson CJ (2000) Physical controls and resulting morphological forms of Quaternary ice-contact volcanoes in western Canada. Geomorphology 32:239–261

Holtedahl H (1960) Mountain, fjord, strandflat: geomorphology and general geology of parts of western Norway 21st. International Geological Congress (Norden) Guide to Excursions A6 and C3, 29 pp

Hughes OL (1972) Surficial geology of northern Yukon Territory and northwestern District of Mackenzie, NWT. Geological Survey of Canada Paper 69-36
Johnson MD, Clayton L (2003) Supraglacial landsystems in lowland terrain. In: Evans DJA (ed) glacial landsystems. Arnold, London, pp 228–258
Kovanen DJ, Slaymaker O (2004) Glacial imprints of the Okanagan Lobe, southern margin of the Cordilleran Ice Sheet. J Quat Sci 19:547–565
Kovanen DJ, Slaymaker O (2015) The Fraser lowland as a complex paraglacial landsystem. Geomorphology 232:78–93
Levson VM, Rutter MW (1989) Late Quaternary stratigraphy, sedimentology and history of the Jasper town site. Can J Earth Sci 26:1325–1342
Mathews WH (1947) "Tuyas": flat-topped volcanoes in northern BC. Am J Sci 245:560–570
Mathews WH (1989) Development of Cordilleran landscapes during the Quaternary (Chapter 1: Quaternary Geology of the Canadian Cordillera). In: Clague JJ (compiler) Quaternary geology of the Canadian Cordillera; Fulton RJ (ed) Quaternary geology of Canada and Greenland. Geol Surv Can, Geology of Canada Series no. 1, pp 32–34
MDA Federal (2004) Landsat GeoCover ETM + 2000 Edition Mosaics Tiles N-06-60, N-7-55, N-08-55, N-08-60, N-08-65, N-08-70, N-09-50, N-10-45, N-10-50, N-10-65, N-10-70, N-12-55. ETM-EarthSat-MrSID, 1.0, USGS, Sioux Falls, South Dakota, 2000. Data available at the Global Land Cover Facility, www.landcover.org
Mitchell SG, Montgomery DR (2006) Influence of a glacial buzzsaw on the height and morphology of the Cascade Range in central Washington State. Quat Res 65:96–107
Parrish RR (1981) Uplift rates of Mt. Logan, Y.T. and BC's Coast Mountains using fission track dating methods. EOS 62:59–60
Parrish RR (1983) Cenozoic thermal evolution and tectonics of the Coast Mountains of BC. I. Fission track dating, apparent uplift rates and patterns of uplift. Tectonics 2:601–631
Peacock MA (1935) Fordland of British Columbia. Geol Soc Am Bull 46:633–696
Porter SC (1989) Some geological implications of average Quaternary glacial conditions. Quat Res 32:245–261
Prest VK, Grant DR, Rampton VN (1968) Glacial map of Canada. Geological Survey of Canada Map 1253
Rampton VN (1982) Quaternary geology of the Yukon Coastal Plain. Geol Surv Can Bull 317
Roberts MC, Rood RM (1984) The role of ice contributing area in the morphology of transverse fjords, BC. Geogr Ann A 66:381–393
Sharp MJ (1985) "Crevasse-fill" ridges: a landform type characteristic of surging glaciers? Geogr Ann A 67:213–220
Shaw J, Kvill D, Rains RB (1989) Drumlins and catastrophic subglacial floods. Sediment Geol 62:177–202
Shaw J, Faragini DM, Kvill DR, Rains RB (2000) The Athabasca fluting field, Alberta, Canada: implications for the formation of large scale fluting (erosional lineations). Quat Sci Rev 19:959–980
Shilts WW, Aylsworth JM, Kaszycki CA, Klassen RA (1987) Canadian Shield. In: Graf WL (ed) Geomorphic systems of North America. Geol Soc Am, Centennial Spec 2, pp 119–161
Souther JG (1977) Volcanism and tectonic environments in the Canadian Cordillera: a second look. In: Baragar WRA, Coleman LC, Hall JM (eds) Volcanic Regimes in Canada Geological Association of Canada Special Paper 16, p 3–24
Stalker A, Mac S (1976) Mega blocks, or the enormous erratics of the Albertan Prairies. Report of Activities, Part C, Geological Survey of Canada, Paper 76-1C, pp 185–188
Stöckli R, Vermote E, Saleous N, Simmon R, Herring D (2005) The blue marble next generation—a true color earth dataset including seasonal dynamics from MODIS. NASA, Earth Observatory
Stokes CR, Clark CD (2003) The Dubawnt lake paleo ice stream: evidence for dynamic ice sheet behavior on the Canadian Shield and insights regarding the controls on ice stream location and vigour. Boreas 32:263–279
Sugden DE (1974) Landscapes of glacial erosion in greenland and their relationship to ice, topographic and bedrock conditions. Inst Br Geogr Spe 7:177–195
Tomkin JH (2007) Coupling glacial erosion and tectonics at active orogens: a numerical modelling study. J Geophys Res. doi:10.1029/2005JF000332
Vincent JS, Klassen RW (1989) Introduction (Chapter 2: Quaternary Geology of the Canadian Interior Plains). In: Fulton RJ (ed) Quaternary geology of Canada and Greenland. Geological Survey of Canada, Geology of Canada Series no. 1, pp 99–100

Holocene and Anthropocene Landscapes of Western Canada

3

Olav Slaymaker and Dori J. Kovanen

Abstract

A brief review of Holocene history of western Canada is followed by a description of the deglaciation of the western Canadian landscape within the framework of the paraglacial model. The landforms and landform assemblages of the Holocene are more localized than those of the previous chapters and include landscapes impacted by volcanism, periglaciation, aeolian, mass movement, fluvial and coastal processes. The proposed Anthropocene epoch is discussed under landscapes modified by human activity, climate change and associated hazards and risks.

Keywords

Holocene • Paraglacial • Landforms and landscapes • Anthropocene • Hazards • Risks

3.1 Holocene History

Periodic sedimentation and erosion was a feature of the Canadian Cordillera throughout the Quaternary Period (Clague 1986). The formal starting point for the Holocene Epoch is 10,000 radiocarbon years BP or approximately 11,450 calibrated calendar years BP, but it is well understood that the actual transition date varies from place to place depending on the presence or absence of ice. The Holocene climate has been by no means constant. Warm, dry conditions characterized the earlier half of the period but a continuing modulation of climate with cooler, wetter conditions recurred approximately every 2500 years. Landscape effects are preserved in records of renewed alpine glaciation (Ryder 1998). Cold phases are approximately centred on 8000, 5500 and 3000 years BP and within the last millennium (Church 1998). Each of these cold phases has been more severe than the last so that the "Little Ice Age" of the last millennium, culminating in the eighteenth century, represents the most severe "Neoglacial" advance of the Holocene Epoch. Within the last three centuries, alpine glaciers attained their greatest Holocene extent but since the early nineteenth century increasingly rapid retreat has been the norm. The last three centuries have also seen the greatest acceleration in anthropogenic processes, leading many to propose a new epoch called the Anthropocene (Crutzen and Stoermer 2000; Lewis and Maslin 2015; Ruddiman et al. 2015).

Proglacial and paraglacial processes have influenced the landscape for as much as 10,000 years and at spatial scales of order 1000 km^2, anthropogenic processes have become globally noticeable over the past few hundreds of years, especially at local scales up to 10 km^2. These temporal and spatial scales are, respectively, shorter and larger (sic) than those in Chaps. 1 and 2. Data relevant to these temporal and spatial scales can be accessed in, for example, Fisheries and Environment Canada (1978), Meidinger and Pojar (1991), Environment Canada (1995), and Smith et al. (2001).

3.2 Proglacial and Paraglacial Landscapes

Church and Ryder (1972) defined paraglaciation as "non-glacial processes of sediment redistribution conditioned by glaciation" and identified the earliest stages of

O. Slaymaker (✉) · D.J. Kovanen
Department of Geography, University of British Columbia, 1984 West Mall, Vancouver, BC V6T 1Z2, Canada
e-mail: olav.slaymaker@ubc.ca

D.J. Kovanen
e-mail: djkovanen@comcast.net

© Springer International Publishing Switzerland 2017
O. Slaymaker (ed.), *Landscapes and Landforms of Western Canada*, World Geomorphological Landscapes, DOI: 10.1007/978-3-319-44595-3_3

paraglaciation as a proglacial phase marking the earliest transition from the Pleistocene to the Holocene Epoch (Fig. 3.1a). Ballantyne (2002) extended the paraglacial concept to include lacustrine, mass movement, aeolian and coastal environments. Kovanen and Slaymaker (2015) have proposed a category of complex paraglacial land system which also incorporates the effects of glaci-isostatic rebound, a non-glacial process conditioned by glaciation. Glaci-isostatic rebound sets in motion a sequence of inter-related non-glacial processes, all of which are directly or indirectly conditioned by glaciation.

The period following deglaciation of the western Canadian landscape was characterized by the presence of extensive and unstable glacial deposits on hillslopes and

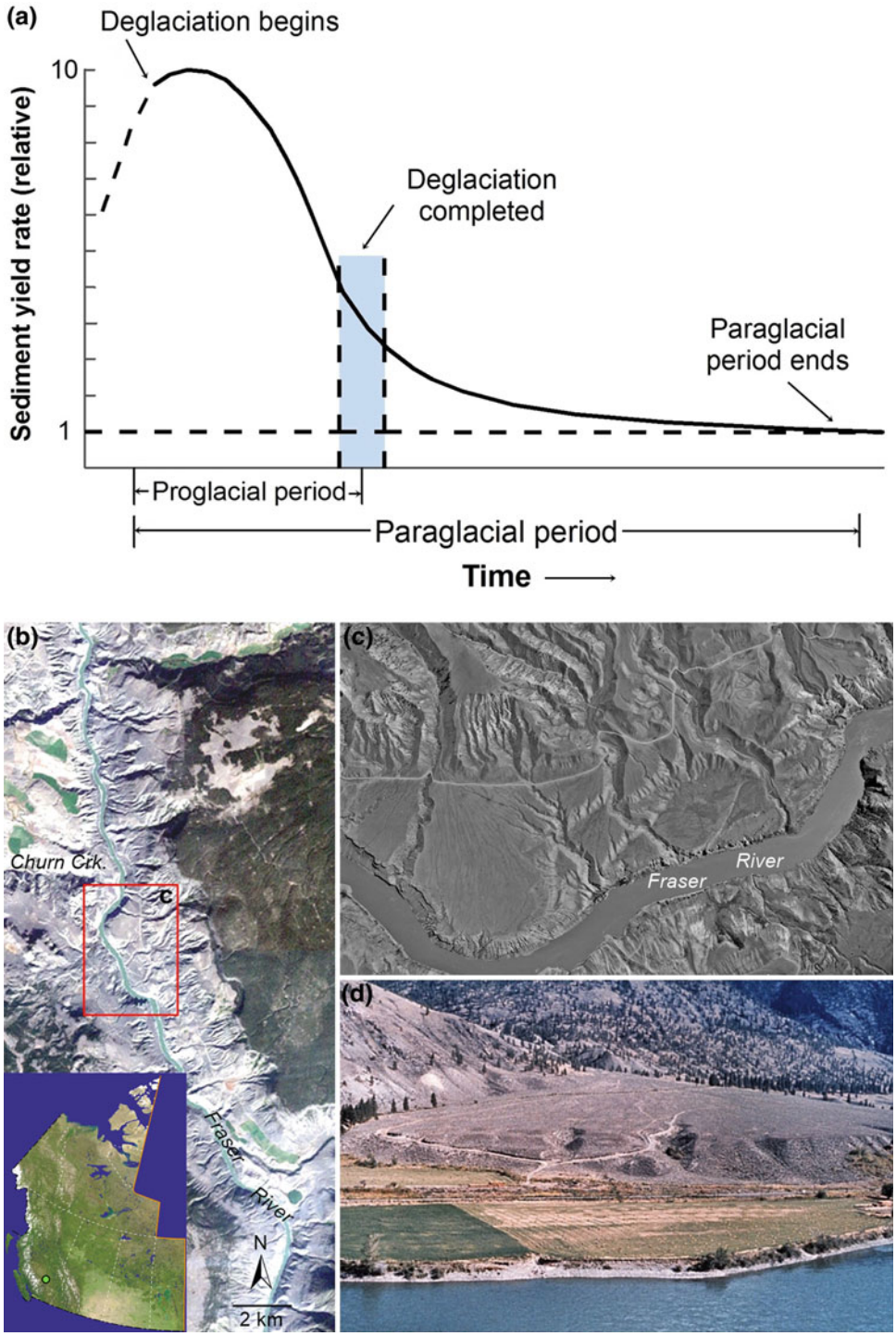

Fig. 3.1 Middle Fraser Valley, British Columbia: **a** original paraglacial model according to Church and Ryder (1972), showing the overlapping proglacial and paraglacial periods. **b** Overview of middle Fraser Valley between Dog Creek and Big Bar Creek, Fraser Plateau, Interior Cordillera. *Source* © Department of Natural Resources Canada. All rights reserved. Government of Canada, Centre for Topographic Information, CanImage—Landsat 7 Orthoimage, extracted from 092o08 and 092o09. **c** Dissected paraglacial debris fan, Fraser Valley, near Churn Creek. Formerly more extensive fan has been dissected and segmented by falling base level in the Early Holocene. *Source* © Province of British Columbia. All rights reserved. BC7713:219. **d** Undissected paraglacial alluvial fan in Thompson River Valley near Spences Bridge. Photograph by O. Slaymaker. The inset image here and elsewhere in this chapter is extracted from NASA, Visible Earth (Stöckli et al. 2005)

along valleys (e.g. Fig. 3.1b; Tunnicliffe et al. 2012). Substantial mass movement and fluvial, lacustrine and aeolian reworking of these deposits created a major "pulse" of sediment movement in the early post-glacial landscape (Fig. 3.1c, d). This pulse of sediment redistribution had major impact on the morphology of western Canada's landscapes both in the Interior Plains (e.g. Jackson et al. 1982) and in the Cordillera. During the retreat of the Cordilleran and Laurentide ice sheets, huge proglacial lakes lasting in some cases for several thousand years were formed by glacial meltwaters dammed around the edges of the ice sheets (see Chaps. 9 and 19). Evidence of the extent and timing of those lakes that were associated with the retreat of the Laurentide Ice Sheet is shown in Fig. 3.2a, b.

The transition from glacial through marine/lacustrine/aeolian to fluvial process dominance was driven by ice sheet recession and relative sea level change. The flights of multiple raised beaches, especially evident in Northwest Territoies (Fig. 3.3) and Nunavut, provide spectacular evidence of relative sea level change in northwestern Canada in the early Holocene. The transition, which continues more slowly today (Church and Slaymaker 1989; Kovanen and Slaymaker 2015), is essentially a transformation in mode of landscape evolution from dominantly glacial to dominantly fluvial and mass movement.

3.2.1 Glacimarine Landscapes

There was widespread sea level recession from the maximum post-glacial marine limit at about 200 masl. Glacimarine landscapes were created as sediments were delivered from four main sources: (1) supraglacial, englacial and subglacial debris; (2) unfrozen subglacial sediment; (3) glacial meltwater runoff; and (4) fluvial and slope sediments, which can be considered to be paraglacially reworked glacigenic sediments. Glacimarine sediments are commonly laminated as a result of alternating overflow and interflow plumes of sediment due to the buoyancy of fresh meltwater in dense saline seawater. Perhaps the most distinctive feature of glacimarine sediments is the presence of ice-rafted debris, ranging in size from clay to boulders (Gilbert 1990) (see Chaps. 25 and 26 for regional landscape examples). Deglaciated fjords, such as Howe Sound and the Fraser Valley embayment, contain thick deposits of glacimarine sediments that extend along the eastern and western shores of the Pacific Coastal Lowlands (see Chaps. 25 and 26).

3.2.2 Glacilacustrine Landscapes

Glacilacustrine landscapes reached a maximum extent around 8200 calibrated calendar years BP, when Lake

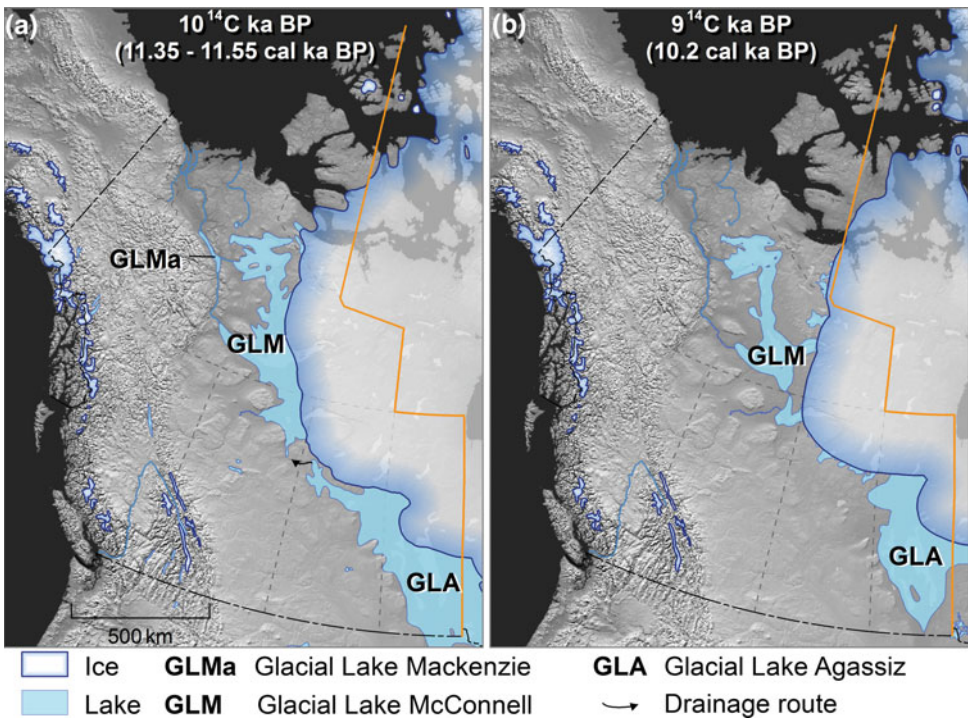

Fig. 3.2 Distribution of large proglacial lakes associated with the retreat of the Laurentide Ice Sheet in western Canada. **a** 11,350–11,550 calendar years before present, and **b** 10,200 calendar years before present. Ice margins from Dyke et al. (2003)

Agassiz drained into the North Atlantic Ocean. In proglacial and glacier contact lakes, the same varied sources of sediments produced well-laminated glacilacustrine deposits which typically show proximal-to-distal fining and thinning. The laminae reflect fluctuations in the grain size and quantity of the incoming sediments due to daily or annual water and sediment discharge cycles (Church and Gilbert 1975). Glacilacustrine landscapes are most extensively developed in the Interior Plains of Saskatchewan and Manitoba (see Chaps. 9 and 10 for regional landscape examples). The Peace River Valley and the Interior Cordillera also boast extensive glacilacustrine landscapes.

3.2.3 Glacifluvial Landscapes

In making the analogy between early Holocene Interior Cordillera of British Columbia and contemporary sandur development on Baffin Island in Nunavut, Church and Ryder (1972) made explicit the importance of the transition between glacier-dominated Pleistocene landscapes and the emerging river-dominated Holocene landscapes which they recognized as glacifluvial landscapes. Their definition of paraglacial expresses this transition perfectly as glacially conditioned non-glacial sedimentation. Most proglacial rivers carry large amounts of sediment, have a braided habit and deposit these sediments in gently sloping outwash plains known as sandar. The Alexandra River, tributary of the North Saskatchewan River in Banff National Park, illustrates this feature well (Fig. 3.4). Narrow tracts of outwash hemmed in by valley sides in mountainous terrain are called valley trains. Some sandar are periodically inundated by Glacial Lake and Outflow Floods (GLOFs), a phenomenon which occurs most commonly within Canada in northwestern British Columbia (Boundary Ranges of the Coast Mountains and the St. Elias Mountains; Clague and Evans 2000).

3.3 Holocene Volcanism

Landscape effects of volcanic eruptions since the beginning of the Holocene Epoch are widely distributed through the cordillera. Mount Edziza and Hoodoo Mountain in the Northern Cordilleran Volcanic Province (NCVP) and Mount Meager in the Garibaldi Volcanic Belt have been the three most active volcanoes during the Holocene. Mount Meager produced a large-scale eruption 2350 years ago that sent ash as far as central Alberta (Hickson and Edwards 2001).

At least five volcanoes have experienced seismic activity since 1985, including the Mount Edziza volcanic complex (eight events), Castle Rock (two events), Hoodoo Mountain (eight events), Crow Lagoon (four events) and The Volcano (five events; Hickson and Edwards 2001). The flat summit of Hoodoo Mountain is covered by an ice cap more than 100 m thick. An eruption from Hoodoo's summit would cause considerable melting of the ice cap to create large floods and lahars. This includes the Iskut River just on the southern flank of Hoodoo Mountain, which is the host for a large amount of salmon, logging operations and a large mining and mineral exploration camp. At the southernmost end of the NCVP, Tseax Cone or Aiyansh Volcano lies in a valley above and east of the Tseax River (Fig. 3.5a, b). It is a young Holocene age cinder cone that was the source of a major basalt lava flow eruption in the mid-to-late eighteenth century that travelled into the Tseax River, damming it and forming Lava Lake. The lava flow subsequently travelled 11 km north to the Nass River, where it filled the flat valley floor for an additional 10 km making the entire lava flow 22.5 km long. Native legends from Nisga'a people in the area tell of a prolonged period of disruption by the volcano, including the destruction of two Nisga'a villages. Nisga'a people dug pits for shelter but at least 2000 Nisga'a people were killed due to volcanic gases and poisonous smoke. The Tseax Cone is now part of the Nisga'a Memorial Lava Beds Provincial Park.

3.4 Periglacial Landscapes

Whereas 95 % of western Canada was covered by ice sheets at various times in the Pleistocene Epoch, the 5 % which was not covered experienced extremely dry and cold conditions during that same period. Such conditions are characterized as periglacial and are associated with specific suites of landforms (French 2007; see Chaps. 18 and 19). The presence of permafrost and high freeze-thaw activity are considered essential components, and patterned ground, palsas and pingos are diagnostic landforms in periglacial landscapes (Fig. 3.6a, b). Whereas the transition from glacial through marine/lacustrine/aeolian to fluvial environments is dramatic in formerly ice-covered environments, the transition from LGM periglacial to Holocene periglacial is more subtle. The absence of glacigenic sediments means that there is no recognizable sediment flux pulse associated with unglaciated periglacial landscapes. Thorn and Loewenherz (1987) have described a periglacial paraglacial model (Fig. 3.7a) whose application is best illustrated by the patterned ground created on hillslopes. Plateau Mountain in the Alberta Rocky Mountains (Fig. 3.7b, c) and Cathedral Lakes Provincial Park in British Columbia (Chap. 2) are good examples of periglacial environments that have not been overrun by the Cordilleran Ice Sheet.

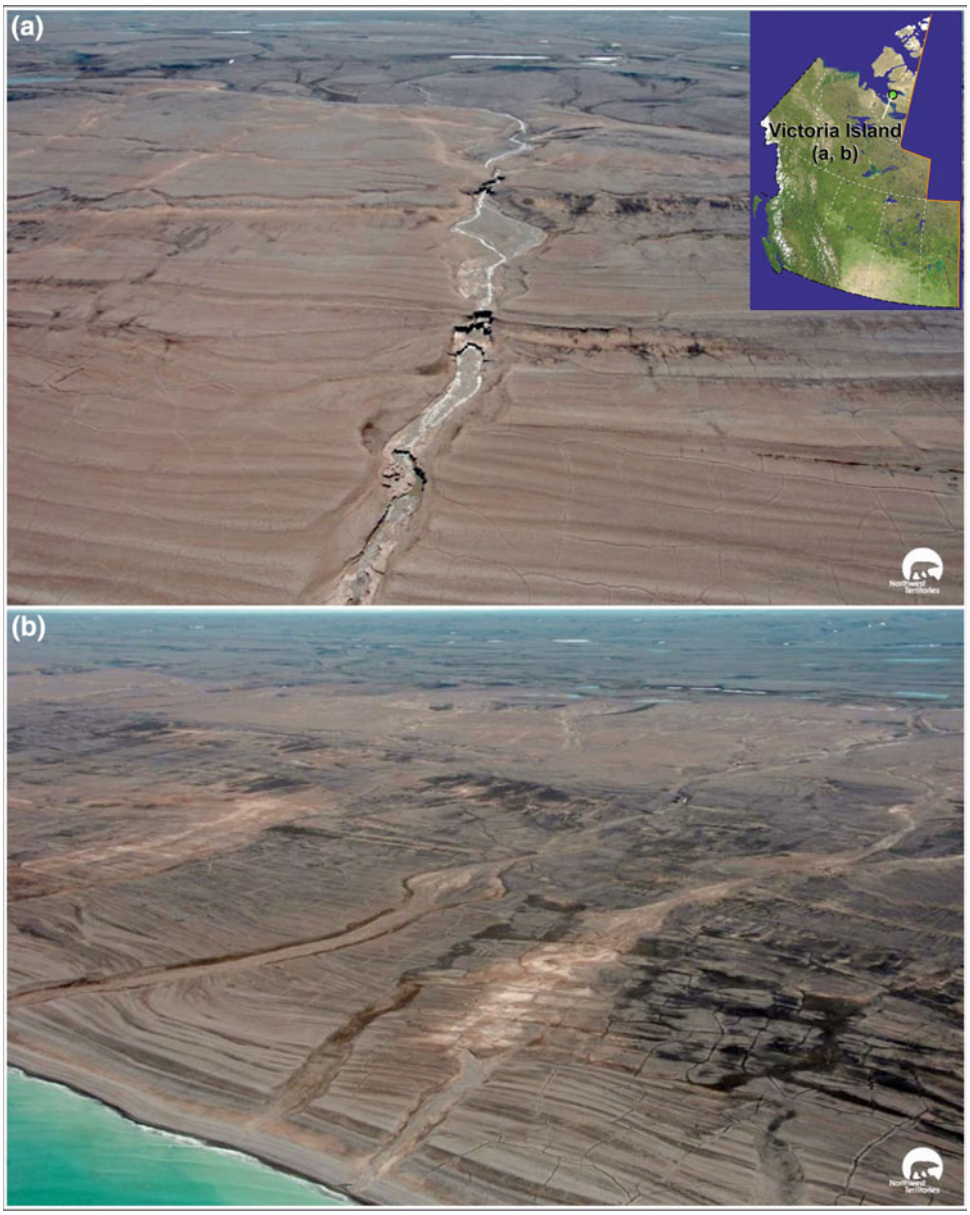

Fig. 3.3 **a**, **b** Paraglacial raised beaches on Victoria Island, arctic Canada demonstrating the glaci-isostatic and glaci-eustatic response to early Holocene sea level changes. *Source* © Government of the Northwest Territories/D. Downing

3.5 Aeolian Landscapes

Another mode of redistribution of glacial and paraglacial sediments is by wind action. Wind erosion and deposition are important processes in cold climates because of sparse vegetation. During the transition from pleni-glacial to post-glacial time, there was widespread loess and finer sediment available for deflation, transportation, and abrasion. In contrast to aeolian processes in subtropical deserts, for example, frost and snow also played important roles in enhancing aeolian processes in western Canada during the Holocene. Large sand dunes and immense loess deposits owe their origins to aeolian processes controlled by snow cover and frost formation (Seppala 2004; see Chap. 12).

3.6 Mass Movement Terrain

The western Canadian landscape is still adjusting after more than 10,000 years since the ice sheets began their last retreat (Figs. 3.8, 3.9; Church and Slaymaker 1989). In the case of steep rock hillslopes, high instability results from glacial

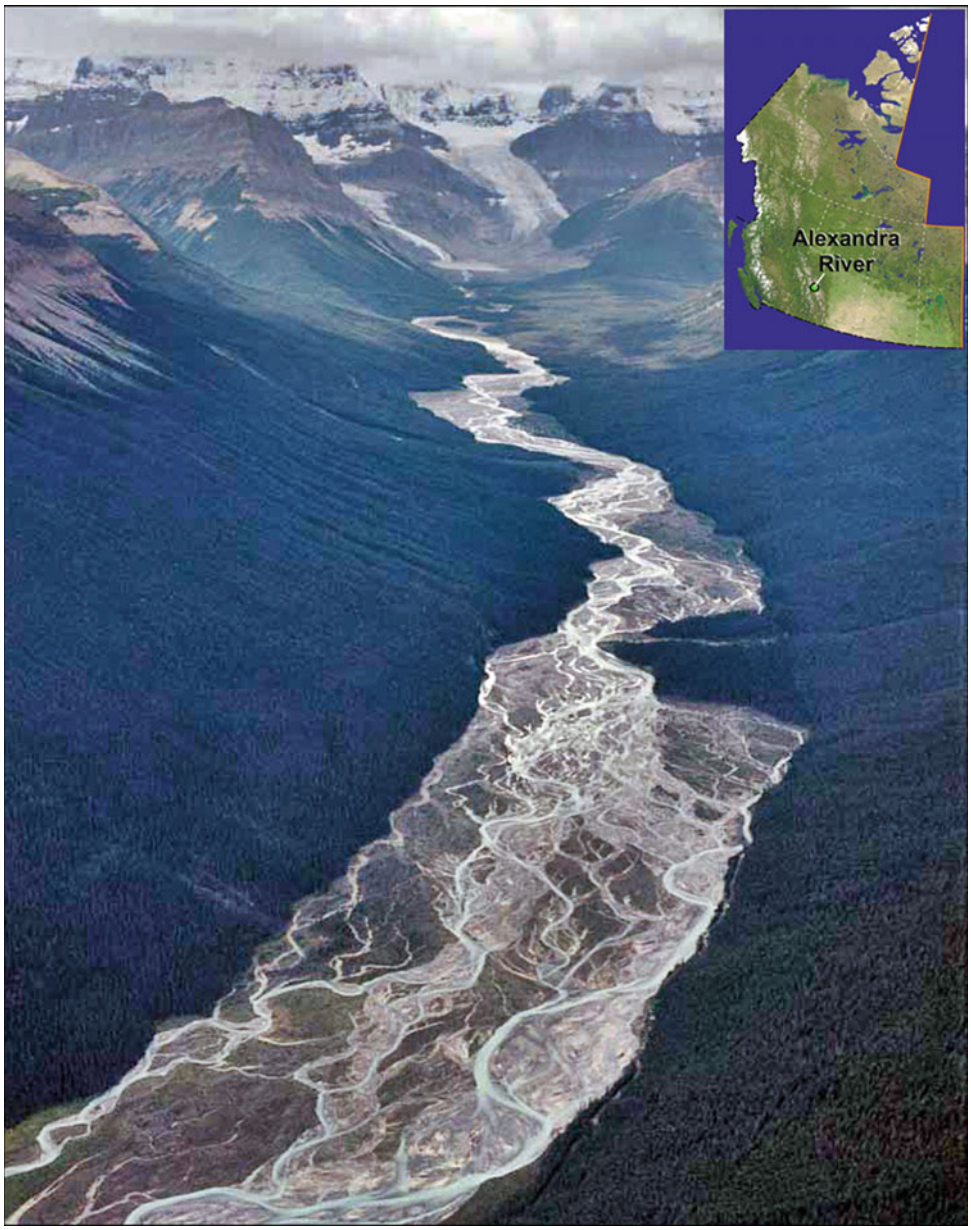

Fig. 3.4 Looking west towards Mount Alexandra (3388 masl) on the continental divide at the head of Alexandra Glacier, Banff National Park. Photograph by R.W. Sandford, United Nations University Institute for Water, Environment and Health

unloading which reactivates pre-existing discontinuities and modifies the stress distribution on glacially oversteepened slopes. This effect is variously termed the debuttressing effect (Evans and Clague 1994) or paraglacial readjustment (Ballantyne 2002). Climate change which sees interaction of deglaciated, debuttressed slopes together with permafrost thawing and/or increased precipitation intensities also decreases slope stability (Fig. 3.8a, b; Harris and Gustafson 1993).

In the case of gentler slopes, underlain by paraglacial and proglacial sediments, mass movements are encouraged by the rapid alternation of sediments with variable mass strength properties, such as till and glacimarine, glacilacustrine and glacifluvial sediments. Overconsolidation of subglacially deposited sediments can be a source of extensive slope failure (Benn and Evans 2010; see Chap. 25).

Mass movements are the most obvious form of landscape instability (Figs. 3.8, 3.9). It is rare to find exclusively "mass movement landscapes" or "landslide terrain" (Gerath and Hungr 1983) because most mass movement phenomena are confined to a small percentage of the overall landscape (Fig. 3.9a, b). Nevertheless, mass movements have a disproportionately high influence on the morphology of

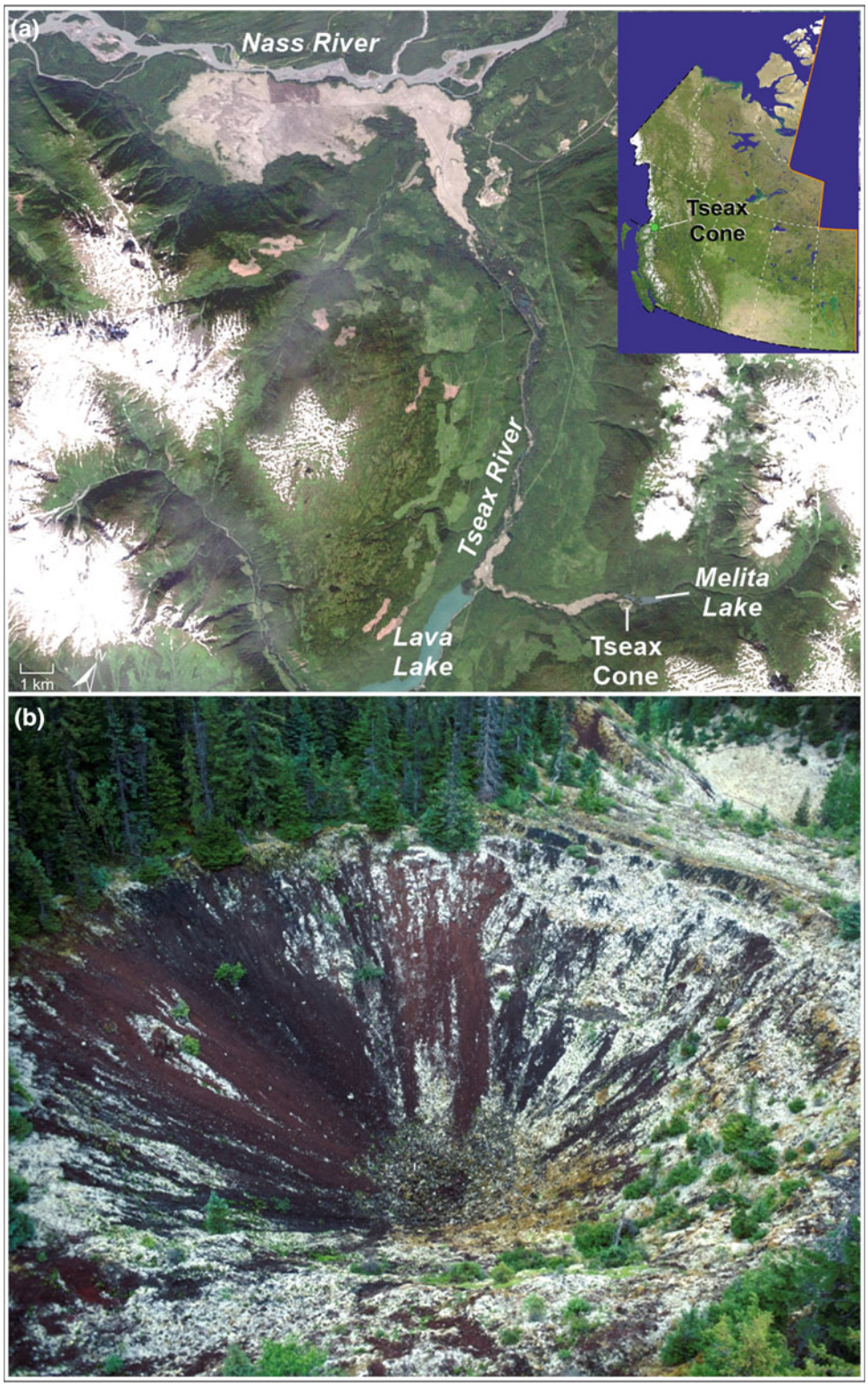

Fig. 3.5 Tseax Cone and Nisga'a Lava Bed Memorial Provincial Park are situated in the Nass River Valley, British Columbia, and are the sites of Canada's most recent volcanic eruption. **a** The Tseax Cone was the source of a lava flow eruption about 300 years ago (mid-to-late eighteenth century). *Source* © Department of Natural Resources Canada. All rights reserved. Government of Canada, Centre for Topographic Information, CanImage—Landsat 7 Orthoimage, extracted from 103i14, 103p02, 03, 06, and 07. **b** Crater on Tseax Cone. *Source* © Province of British Columbia. All rights reserved. Reproduced with permission of the Province of British Columbia

landscape. Mass movements associated with volcanic eruptions (Hickson and Edwards 2001; Friele et al. 2005); GLOFs (Clague and Evans 2000); catastrophic landslides (Geertsema et al. 2006; see Chap. 25); debris flows (Van Dine 1985; Kovanen and Slaymaker 2008); and mass movements strongly affected by Pleistocene history (Bovis 1990; Bovis and Jones 1992) are widespread throughout the Cordillera.

Fig. 3.6 **a** Periglacial environment of the Tuktoyaktuk Peninsula, Northwest Territories, which is part of the Arctic Coastal Plain. Thick Pleistocene marine and fluvial sediments, generally capped by till, which contain ground ice, have been modified by thermokarst. *Source* MDA Federal (2004). **b** Incipient pingo in foreground and small pingo in middle distance. *Source* © Government of the Northwest Territories/D. Downing

3.7 Fluvial Landscapes

3.7.1 Hydroclimate of Western Canada

The term hydroclimate incorporates the prevailing temperature, precipitation, evaporation and soil moisture conditions. Little is known about the precise variations in temperature and precipitation regimes over the Holocene though at least four Neoglacial events have caused glaciers to advance into adjacent currently subalpine areas (e.g. Desloges and Ryder 1990). Only a limited number of monitoring stations provide data on hydroclimate; at those stations only a limited number of aspects of the hydroclimate are measured (Fig. 3.10).

Broad differences in hydroclimate reflect the influence of latitude, distance from the sea, the presence of mountain

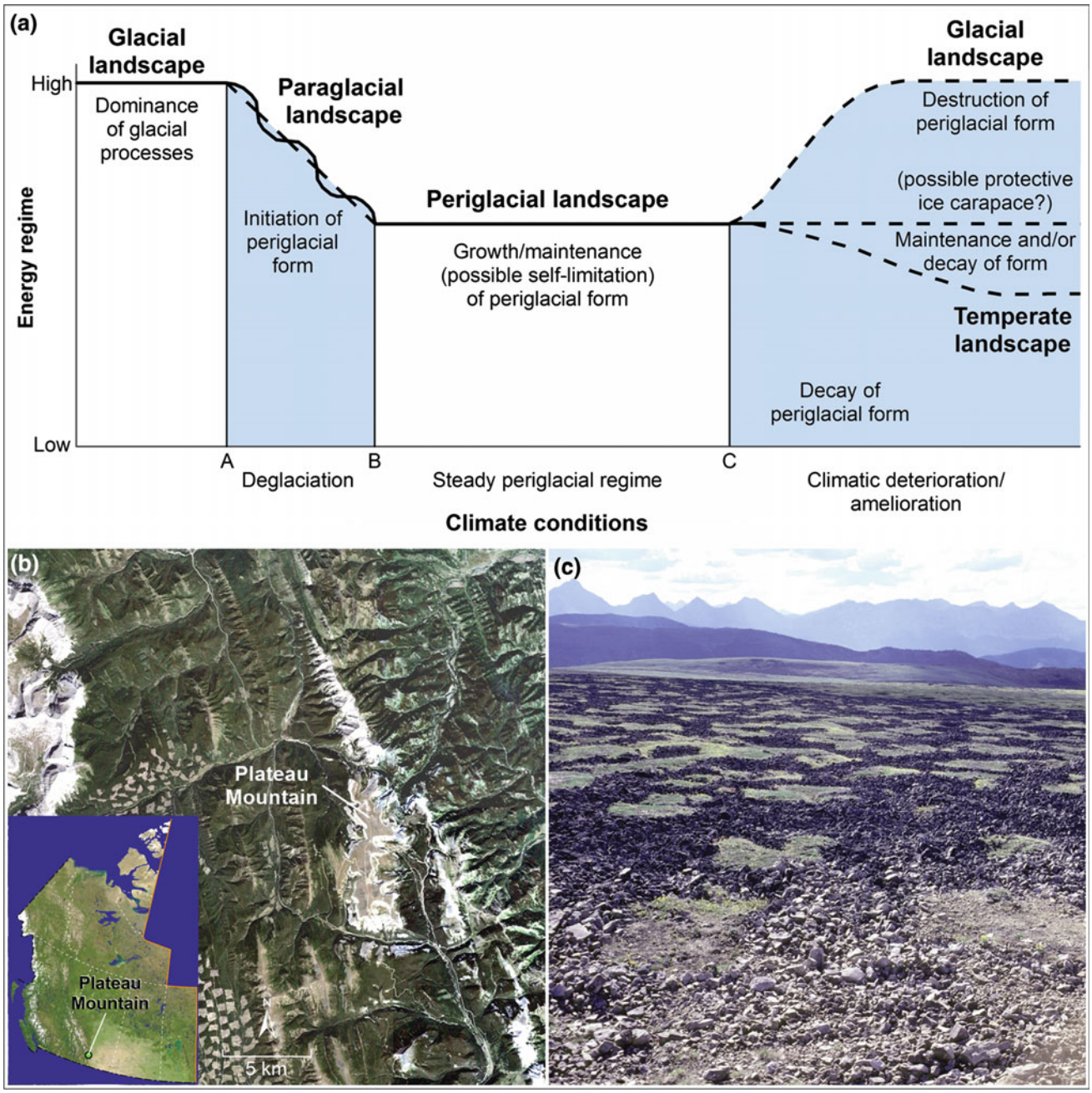

Fig. 3.7 **a** Periglacial paraglacial model according to Thorn and Loewenherz (1987). **b** The alpine area around Plateau Mountain (2519 masl), situated in the Front Ranges of the Rocky Mountains, Alberta. Patch-cut logging is responsible for the patterning visible in the western half of the image. *Source* © Department of Natural Resources Canada. All rights reserved. Government of Canada, Centre for Topographic Information, CanImage—Landsat 7 Orthoimage, extracted from 082j01, 002, 07 and 08. **c** Sorted stone polygons on the surface of Plateau Mountain, Alberta. Image courtesy of the Royal Alberta Museum

barriers and the extent to which areas can be invaded by cold and warm air masses (Fig. 3.10a). Western Canada can be considered to be divided into (a) a wet western Cordillera, including the Insular Ranges, the west facing slopes of the Coast and St. Elias mountains (Fig. 3.10b), (b) a moderately wet and permafrost-rich northern Interior Cordillera, (c) the warmer and drier to semi-arid southern Interior Cordillera, (d) the generally drier Eastern Cordillera, including the Rocky and Mackenzie mountains, (e) the arctic semi-arid climate of the tundra zone, north and east of the widespread permafrost boundary (Smith et al. 2001), including the arctic islands, (f) the continental climate of the boreal (taiga) zone

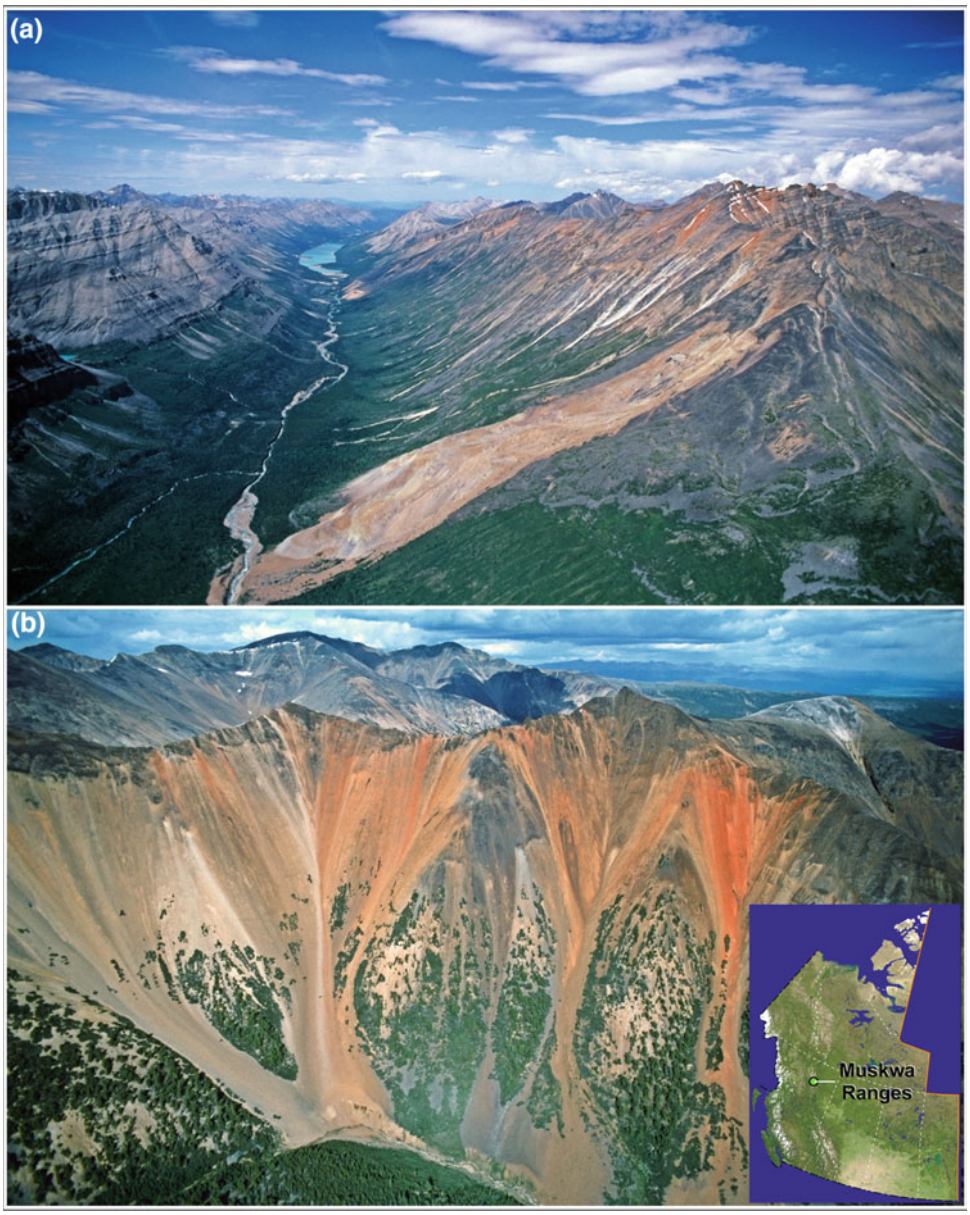

Fig. 3.8 Northern Rocky Mountains Provincial Park and protected area: mass movement in the Muskwa Ranges. Photographs by Gary Feigehen

south of the southern boundary of widespread permafrost and (g) the continental climate of the Prairie grasslands (Environment Canada 1995).

3.7.2 Regional Variations in Geomorphic Process

Because the Canadian Cordillera extends over 20° of latitude and 28° of longitude, there are wide variations in physiography, hydroclimate and lithology which promote highly variable geomorphic processes. The six geomorphological landscapes express something of this variability; Ryder (1998), in a detailed study of potential climate change impacts on Canada's alpine regions, has proposed twelve alpine process regions within the mountain regions of the Cordillera. These process regions are based on total precipitation, snowfall, seasonality of precipitation, January temperature and temperature range and presence or absence of permafrost (Fig. 3.11). Ryder's alpine process regions retain the northwest–southeast pattern of the cordilleran terrain but they are not identical with those geomorphological process regions defined in Chap. 1. Her methodology is semi-quantitative, given the absence of hydroclimate monitoring stations in the mountains. The value of her discussion is that it emphasizes the importance of absolute precipitation amounts in the western Cordillera (regions 1, 2 and 3); of the huge snowpacks in the coastal mountains (2 and 3) and the

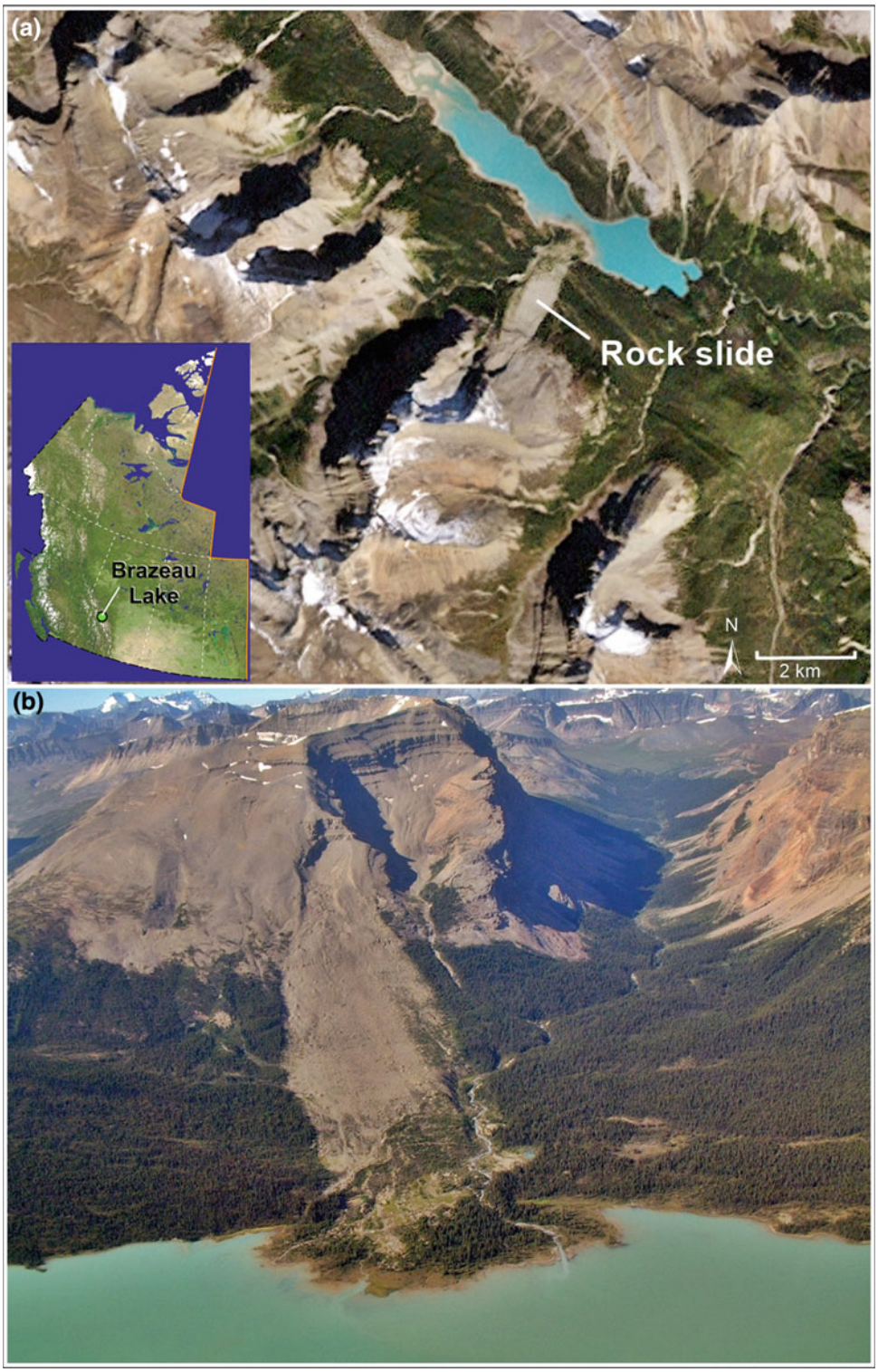

Fig. 3.9 **a** Brazeau Lake, headwaters of North Saskatchewan River, Jasper National Park, Alberta. *Source* © Department of Natural Resources Canada. All rights reserved. Government of Canada, Centre for Topographic Information, CanImage—Landsat 7 Orthoimage, extracted from 083c06. **b** Oblique view of rock slide at Brazeau Lake. Reproduced with the permission of Natural Resources Canada, 2015 (photograph 2002-594 by Réjean Couture)

Columbia Wet Belt (6) and the increasing importance of January cold, large annual temperature range and presence of permafrost in the more continental (7 and 8) and more northern mountains (9, 10, 11 and 12).

3.7.3 Western Canadian Rivers

The western Canadian landscape has evolved from a 95 % glacierized landscape to a dominantly fluvial and mass

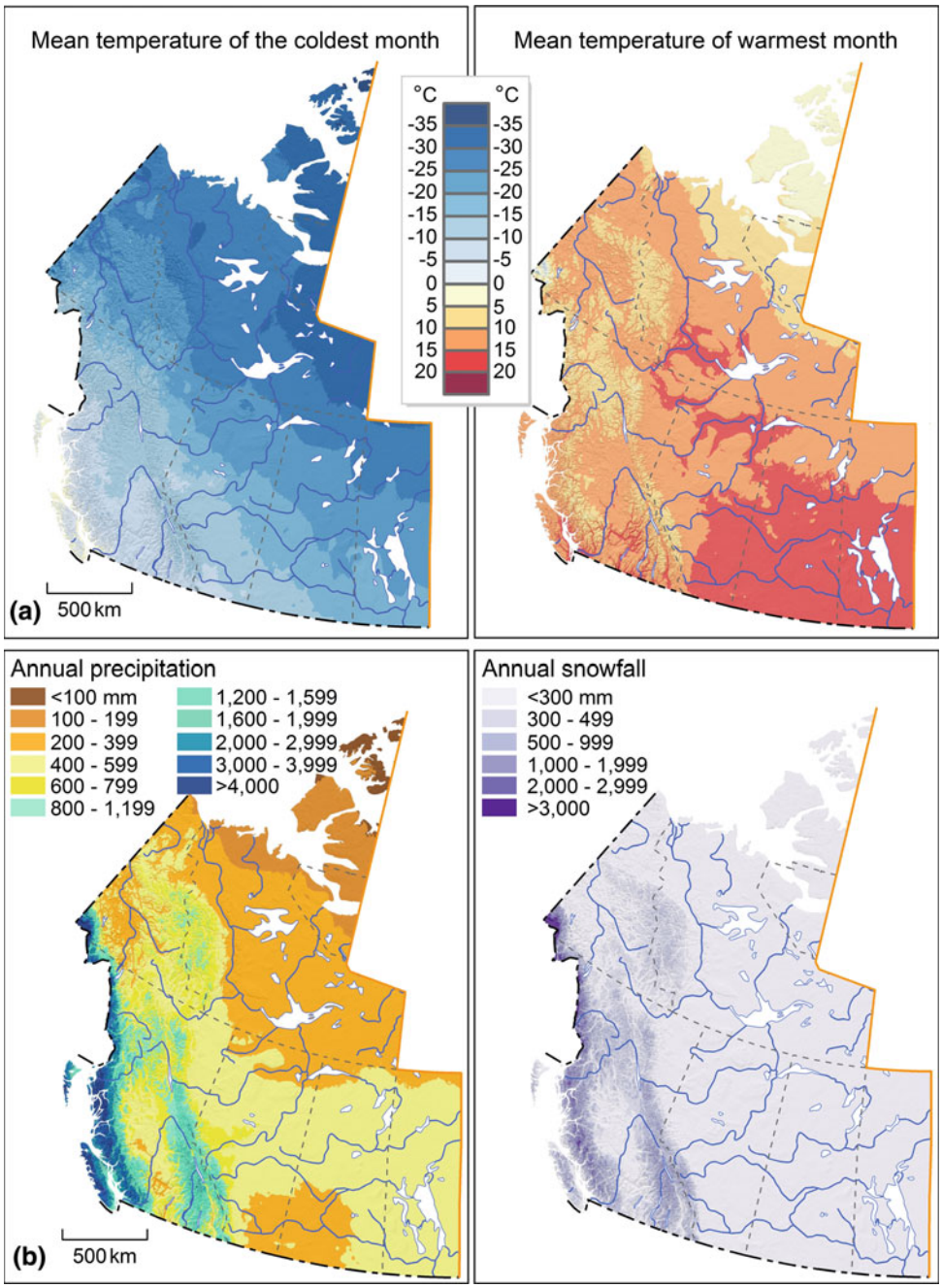

Fig. 3.10 **a** Mean daily temperature of the coldest and warmest months and **b** annual mean total precipitation and average maximum snowfall for western Canada from 1961 to 1990 (climate data have been generated with the ClimateNA v5.10 software package available at http://tinyurl.com/ClimateNA, based on the methodology described by Hamann et al. 2013)

movement landscape during the Holocene. Rivers and river networks have become by far the dominant agents of erosion, sediment transport and sedimentation (Desloges and Church 1989; Slaymaker 1990; Moore et al. 2009). This generalization does not ignore the huge importance of local mass movement processes, especially with respect to influencing the morphology of landscape, but when the total work done by rivers (sediment flux per unit area per unit time) is compared with that done by mass movement, fluvial activity is clearly dominant. The major rivers of western Canada and their mean annual discharges are shown in Fig. 3.12.

Large variations in magnitude and frequency of floods occur within relatively short distances in the mountain regions. For example, the mean annual flood varies by two orders of magnitude within British Columbia and seven distinct flood regions have been identified, ranging from the perhumid exposed coast and fjord region to the semi-arid Okanagan Valley and Princeton Basin (French and Slaymaker 2012). Snowmelt arrives in early May in the south and in late May in the north; as a result, there is a tendency for ice jams to exacerbate the flooding in northward flowing rivers (e.g. Fraser River at Prince George). Ice jam break-up

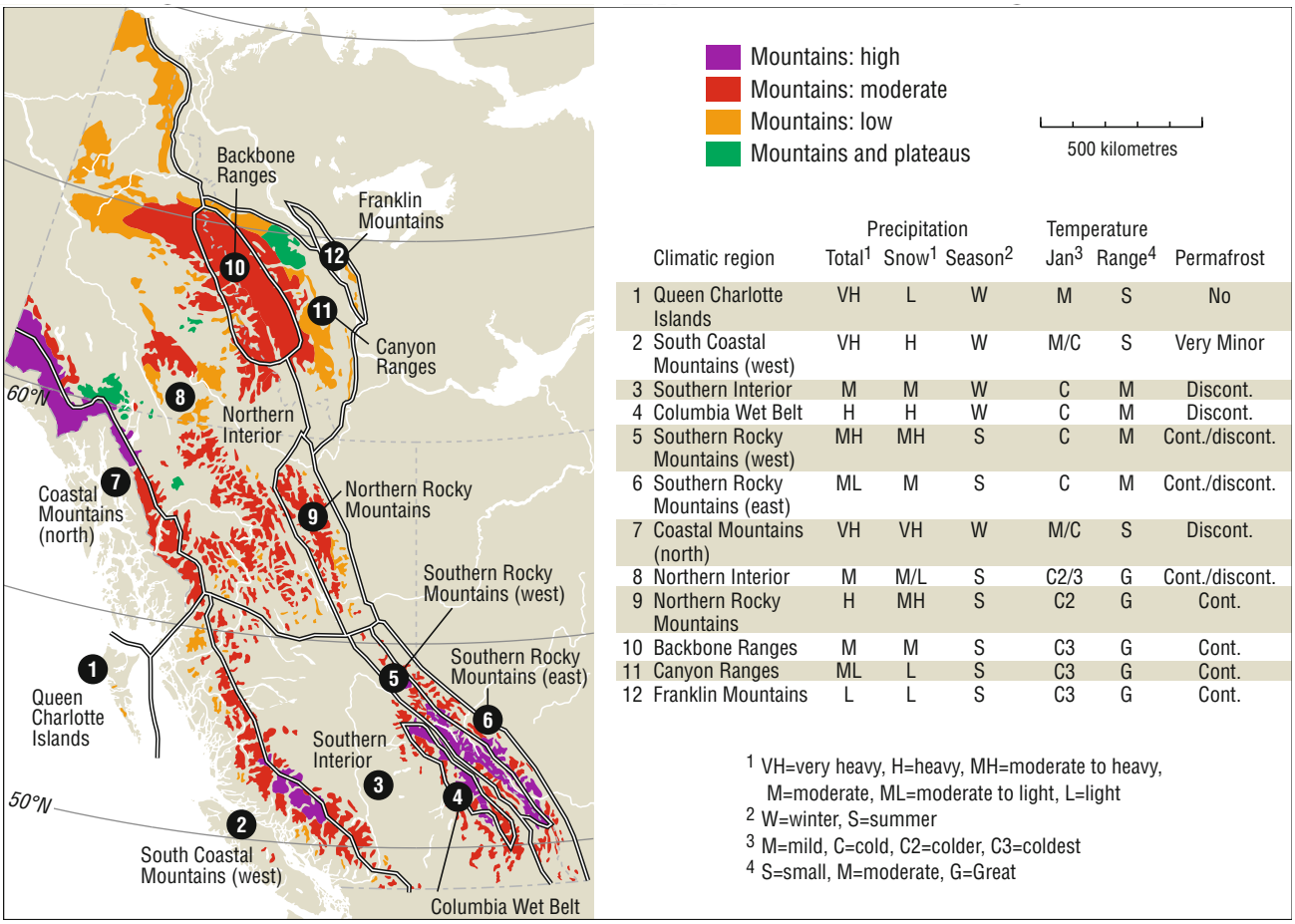

	Climatic region	Precipitation Total[1]	Snow[1]	Season[2]	Temperature Jan[3]	Range[4]	Permafrost
1	Queen Charlotte Islands	VH	L	W	M	S	No
2	South Coastal Mountains (west)	VH	H	W	M/C	S	Very Minor
3	Southern Interior	M	M	W	C	M	Discont.
4	Columbia Wet Belt	H	H	W	C	M	Discont.
5	Southern Rocky Mountains (west)	MH	MH	S	C	M	Cont./discont.
6	Southern Rocky Mountains (east)	ML	M	S	C	M	Cont./discont.
7	Coastal Mountains (north)	VH	VH	W	M/C	S	Discont.
8	Northern Interior	M	M/L	S	C2/3	G	Cont./discont.
9	Northern Rocky Mountains	H	MH	S	C2	G	Cont.
10	Backbone Ranges	M	M	S	C3	G	Cont.
11	Canyon Ranges	ML	L	S	C3	G	Cont.
12	Franklin Mountains	L	L	S	C3	G	Cont.

[1] VH=very heavy, H=heavy, MH=moderate to heavy, M=moderate, ML=moderate to light, L=light
[2] W=winter, S=summer
[3] M=mild, C=cold, C2=colder, C3=coldest
[4] S=small, M=moderate, G=Great

Fig. 3.11 Distribution of Canada's western temperate mountains and their hydroclimatic and geomorphic characteristics (adapted from Ryder 1998). Cartography by E. Leinberger

also has geomorphic consequences with ice floes ripping up riparian vegetation, ice shove armouring the banks with boulder pavements, elevated river level permitting erosion of higher riparian zones and the morphology of the floodplain being frequently altered.

There are also wide variations in the concentrations of suspended sediments and dissolved solids in western Canadian rivers. The average annual concentrations show two orders of magnitude variation in dissolved solids and three orders of magnitude variation in suspended sediments. More importantly, as discussed by Church et al. (1999), these values are scale dependent and, because the data quoted are taken from a wide variety of basin areas, they should be interpreted with caution. In the largest rivers, the ratio of dissolved solids to suspended sediment averages 1:2 with minor bedload in non-carbonate terrain; in the smallest rivers and in the steepest terrain, the bedload becomes substantially greater than 10 % of the total flux. The presence of carbonate terrain generates dissolved solid fluxes that exceed clastic sediment fluxes (Slaymaker 1987).

3.7.4 Process Domains

Montgomery and Foufoula-Georgiou (1993) were successful in defining a technique to describe the quantitative relationship between hillslopes and their tributary sediment-contributing areas and demonstrated that, on a graph of mean slope versus sediment-contributing area, domains subject to certain geomorphic processes are regionally consistent. Application of this technique in the southern Coast Mountains landscape (Fig. 3.13a) has shown that watershed headwater areas (the smallest domains) show maximum variability with high sediment yields driven by mass movements followed by an apparent decline in sediment yield where high-elevation glacial troughs occur (Fig. 3.13b). Sediment-contributing areas around 1 km^2 in the southern Coast Mountains show further increase in sediment yield because of debris flows which dominate basins up to about 10 km^2. Beyond that, fluvial processes become dominant. Uptake of sediments residual from glacial erosion and paraglacial sedimentation ensures that specific

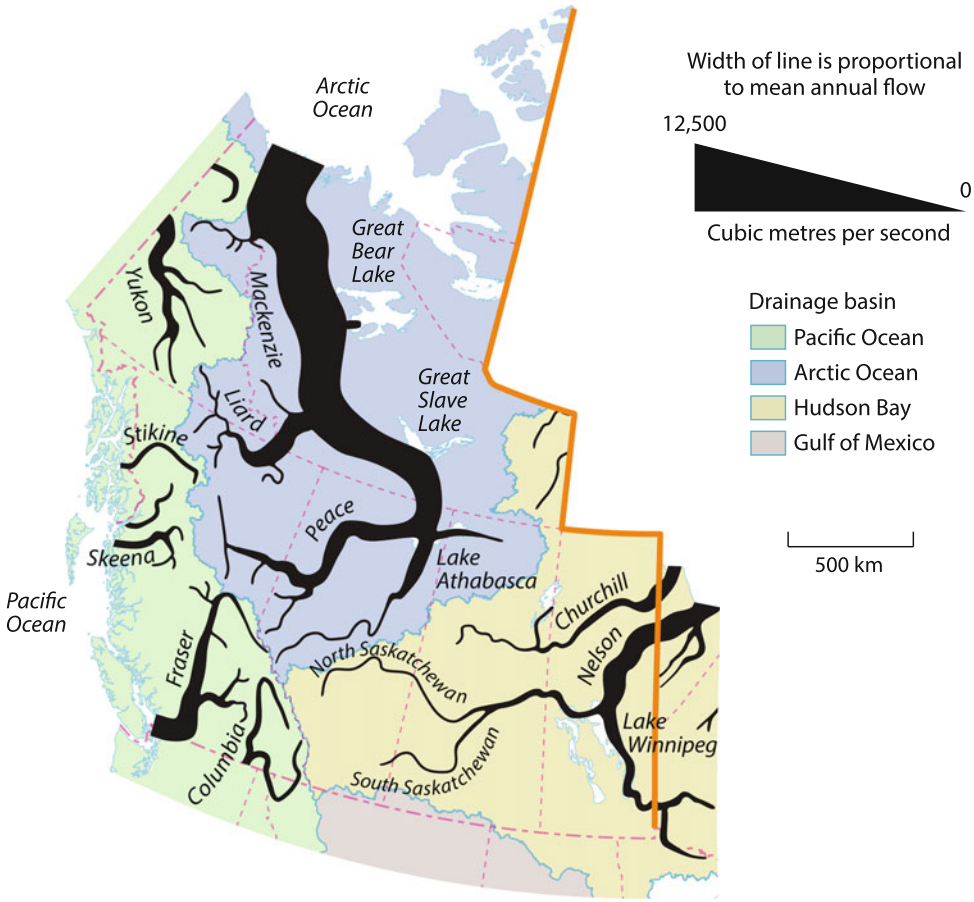

Fig. 3.12 Major rivers of western Canada with river channels depicted proportionate to mean annual discharge (Fisheries and Environment Canada 1978). Cartography by E. Leinberger

sediment yield continues to increase between about 10 and 30,000 km^2. Beyond 30,000 km^2, the conventional pattern of declining specific sediment yield prevails (Church et al. 1999). Church and Ryder (2010) showed that process domains in the Canadian Cordillera are consistent with regional suspended sediment yield patterns (Fig. 3.13c).

3.7.5 Mackenzie Basin Landscapes

The Mackenzie River basin includes five geomorphological landscapes within its 1.8 million km^2: (i) The Shield; (ii) Interior Plains; (ii) Eastern Cordillera; (iv) Interior Cordillera and (v) Arctic Coastal Plain (Fig. 3.14a). These landscapes extend from the Arctic Ocean to temperate southern Alberta.

The Eastern Cordillera (Mackenzie, Richardson and Northern Rocky mountains) and the Interior Cordillera (Liard and Peace river basins) produce the bulk of the runoff (60 from 40 % of the basin area) while the Interior Plains and the Shield contribute only about 40 % of the runoff from 60 % of the basin. Myriad lakes and wetlands in the Interior Plains and the Shield also dampen streamflow response to rainfall. Lake Athabasca is notably effective in modifying the flow of the Mackenzie system. The complex channel network of the Peace–Athabasca delta responds to the rapidly fluctuating discharge of the Peace and Athabasca rivers. Where the Slave River emerges from Athabasca Lake, it has a much dampened streamflow regime (Woo and Thorne 2003).

The Eastern and Interior cordilleras, which produce the highest proportion of Mackenzie basin runoff, produce an even higher proportion of the clastic sediment load of Mackenzie River (Carson et al. 1998; Fig. 3.14b; see Chap. 7). The extensive glacilacustrine sediments of proglacial Lake Peace in the Interior Plains are also important contributors of clastic sediment, as illustrated by the Attachie landslide (Fig. 3.15). Both Lake Athabasca and Great Slave Lake in the Interior Plains trap much of the clastic sediment generated by the Northern Rocky Mountains, the western Interior Plains and southern Interior Cordillera (Fig. 3.14a, b).

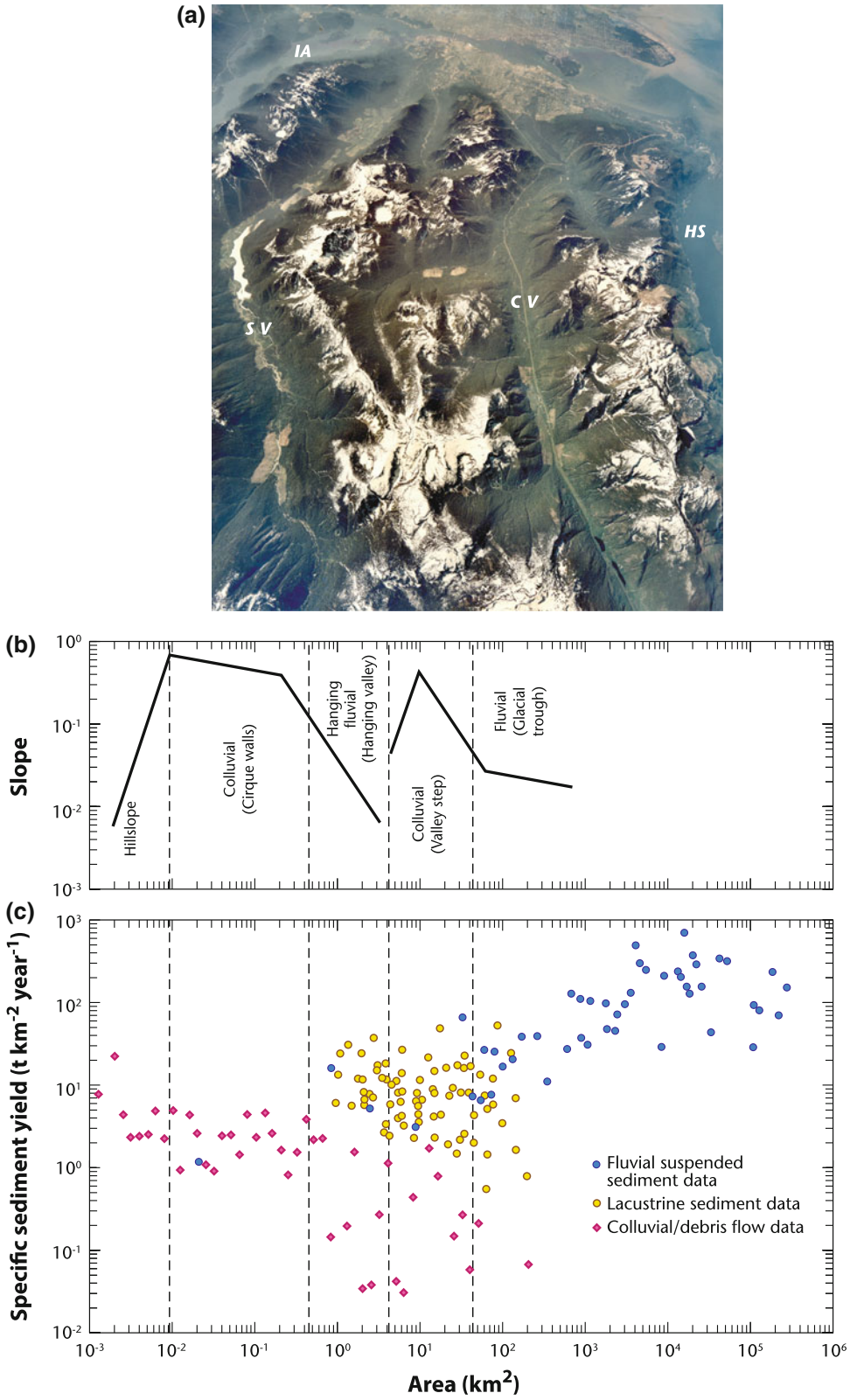

Fig. 3.13 Process domains in the western Cordillera. **a** Oblique photograph of cirque landscape north of Vancouver (*Source* Province of British Columbia). **b** Process domains defined by slope–area relations in British Columbia and Washington State (*Sources* Montgomery and Foufoula-Georgiou 1993; Brardinoni and Hassan, 2006). **c** Regional-specific sediment yield patterns (*Sources* Church et al. 1989; Schiefer et al. 2001; Brardinoni et al. 2009). Cartography by E. Leinberger

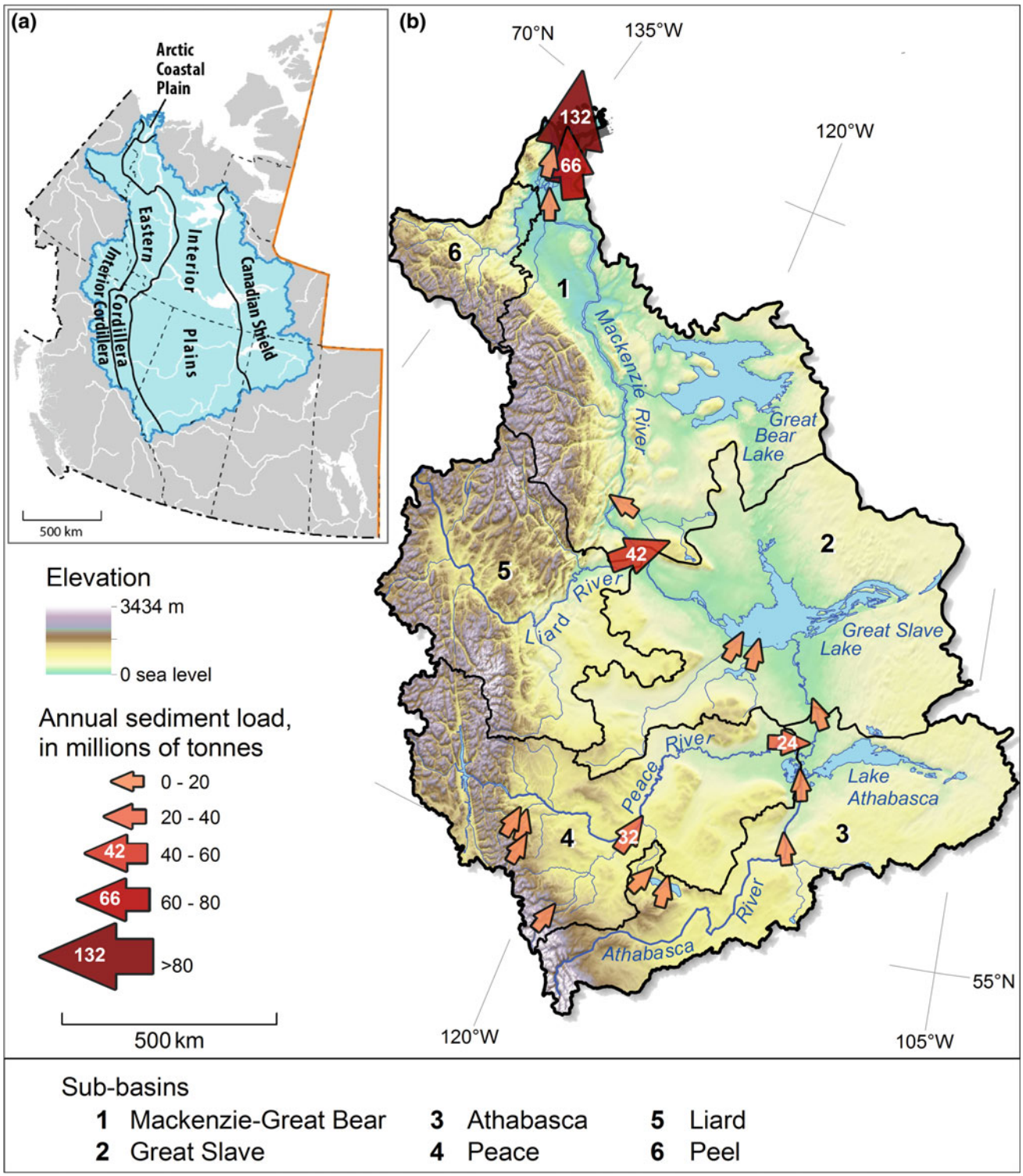

Fig. 3.14 **a** Geomorphological landscapes of the Mackenzie Basin (see Fig. 1.3). **b** Sediment loads of rivers in the Mackenzie Basin (Carson et al. 1998)

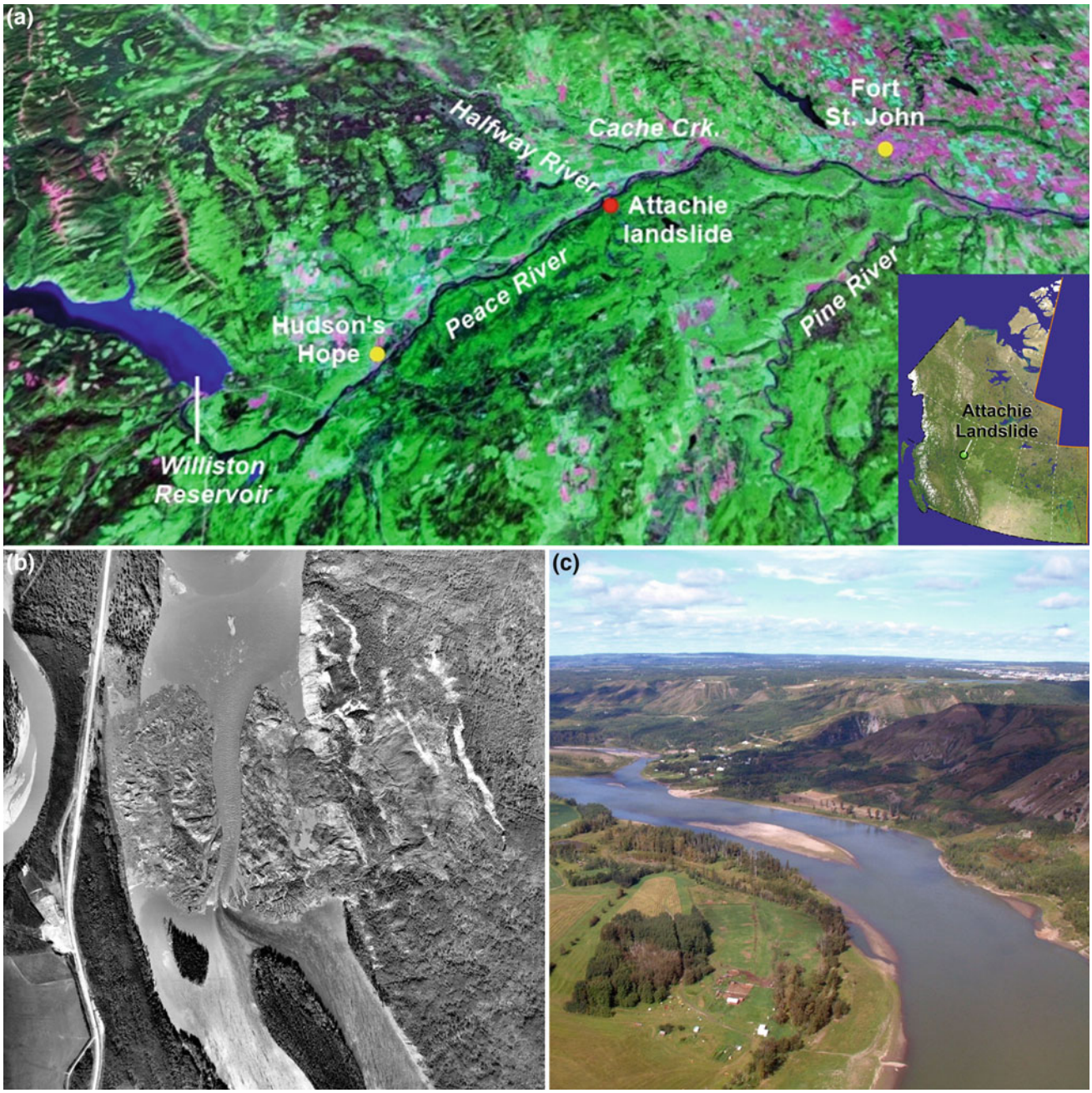

Fig. 3.15 **a** Perspective view of the Peace River area. *Source* MDA Federal (2004). **b** The Attachie landslide that occurred in 1973 on the southeast wall of the Peace River, northeastern British Columbia. © Province of British Columbia. All rights reserved. BC5529:075. **c** Peace River Valley a few kilometres south of Fort St. John. Reproduced with the permission of Natural Resources Canada, 2015 (photographs NRCAN 2000-593 by R. Couture and G. B. Fasani)

3.8 Coastal Landscapes

3.8.1 The Pacific Coast of Canada

A rocky, rugged area of islands, inlets and fjords is flanked by mountain ranges (Fig. 3.16). The morphology of the coast is controlled by the structural trends of the western Canadian Cordillera. Three physiographic regions are commonly recognized: (1) the outer mountain area, including the Insular Ranges of Haida Gwaii and Vancouver Island (see Fig. 1.16); (2) the coastal trough (or Pacific Coastal Lowlands), including parts of Haida Gwaii, Vancouver Island, the northern mainland coast and the Georgia Depression and (3) the Coast Mountains.

Glacial erosion of unconsolidated sediments and bedrock and deposition of till and stratified drift occurred during the

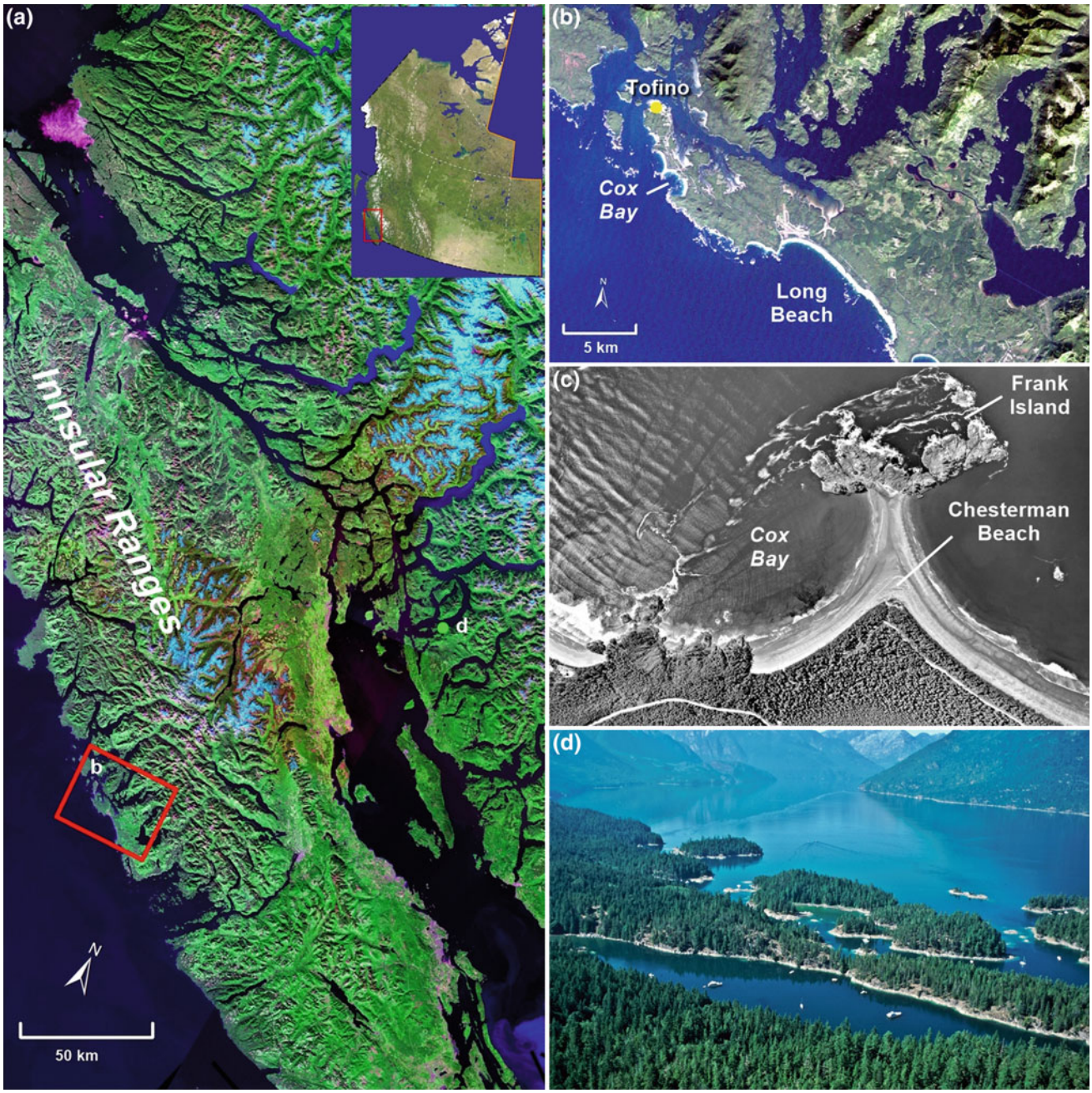

Fig. 3.16 **a** Vancouver Island and adjacent Pacific Ranges, Coast Mountains. *Source* MDA Federal (2004). **b** Long Beach and Tofino. *Source* © Department of Natural Resources Canada. All rights reserved. Government of Canada, Centre for Topographic Information, CanImage—Landsat 7 Orthoimage, 092f04. **c** Tombolo south of Tofino. *Source* © Province of British Columbia. All rights reserved. BC5368-109. **d** Desolation Sound. *Source* © Province of British Columbia. All rights reserved. Reproduced with the permission of the Province of British Columbia

Pleistocene Epoch. During the Holocene Epoch, the redistribution of unconsolidated sediments occurred in many local areas, especially (1) in areas backed by cliffs of unconsolidated Pleistocene sediments; (2) in fjords and protected embayments where deltas have been forming; (3) in exposed coastal areas where deltas are forming such as the Fraser and Skeena River deltas or where littoral currents transport sediment from river mouths; (4) at pocket beaches between resistant headlands and (5) at sheltered, very low energy sites characterized by intertidal flats. This Holocene redistributional activity was encouraged by the marine regression from a maximum relative elevation of about 200 m, achieved largely as a result of glaci-isostatic rebound. Middle and Late Holocene sea levels were

relatively lower than at present on the inner coast but were higher than at present on the outer coast. Recently, rise in sea level on the inner coast has induced erosion (Clague and Bornhold 1980).

3.8.2 The Arctic Coastal Plain

A narrow strip of land stretching from the western boundary of Yukon through Northwest Territories to Nunavut is known as the Arctic Coastal Plain. Relief is generally less than 30 m and much of the western plain is a pediment mantled by glacial drift. Herschel Island and Mackenzie Delta form distinctive landscapes within the Arctic Coastal Plain (see Chaps. 23 and 24). Moving north the Arctic Coastal Plain continues through the Tuktoyaktuk and Bathurst peninsulas to the western third of Banks Island and the northwesternmost fringes of the Queen Elizabeth Islands. Between Tuktoyaktuk and Bathurst peninsulas, the smooth outline of the western Arctic coast is interrupted by a large river delta, the Horton River delta, which has accumulated over the past 300–400 years (Fig. 3.17). The delta was initiated by the avulsion of the Horton River and provides an unusual opportunity to document the nature of geomorphic change in a permafrost environment and the role of river and sea ice in affecting changes. The delta was mapped in 1826, by which date the surface area of the delta was 10–15 km^2; today, the delta surface area is about 40 km^2 (Mackay and Slaymaker 1989).

3.9 The Anthropocene and Modified Landscapes Under the Influence of Climate Change

During the Anthropocene of the past three centuries, interest has shifted towards the direct impact of human activity on the landscape. Western Canadian landscapes are impacted by urban landslides (Evans 1982), agricultural gully erosion (De Boer 1997), mining surface disturbance (Hooke 2000) and forest management practices (Guthrie 2002). Because of global warming induced by human activity (Smith et al. 2001; Slaymaker 2001; Slaymaker and Kelly 2007), coastal landscapes of western Canada are subjected to rising sea level everywhere, except at the outer coast of Vancouver Island, with a maximum rate of rise at Prince Rupert at 3.3 mm a^{-1}. Clague (1989) stated that even a 2 m rise in sea level would have little effect on 85 % of the British Columbia coastline. Only the Fraser delta and east Graham Island, Haida Gwaii are seen to have high sensitivity to anticipated sea level rise. On the Beaufort coast, the two most sensitive areas are Liverpool Bay-Tuktoyaktuk Peninsula and Mackenzie Delta (Shaw et al. 1998).

The potential impact of hydroclimate change on rivers and river processes in Canada has been investigated by Ashmore and Church (2001). They suggested that the greatest threat from natural hydroclimate change was change in the magnitude and frequency of flood flows. The consequences of changes in flow include changes in channel dimensions, gradient, channel pattern, sedimentation, bank erosion rates and channel migration rates. The most sensitive and vulnerable regions are in southern Canada, particularly those regions at risk of substantial increases in rainfall intensity and duration. In northern rivers, thawing of permafrost and changes in river ice conditions are important concerns.

3.9.1 Mountain Landscapes

Mountain landscapes are expected to be subject to more frequent landslides and flooding. (Brooks 2001). The work of Jakob and Jordan (2001) in specifying the need for a geomorphic approach to mountain flood hydrology estimates and that of Ryder (1998) for a comprehensive review of hydroclimatic effects specific to alpine regions recognize the need for new ways of planning and managing mountain landscapes. Sediment budgets and longitudinal studies of debris flow events are also needed (Van Dine 1985; Kovanen and Slaymaker 2008). The work of Evans and Clague (1994) and Clague and Evans (2000) on the incidence and distribution of catastrophic events is especially notable. Shrinking glaciers and glacier dam bursts are the objects of increasing concern (Moore et al. 2009; Clarke et al. 2013, 2015). In response to the mounting evidence of anthropogenically modified landscapes, disturbance regime models have been developed (Hewitt 2006; Nakamura et al. 2000).

3.9.2 Forested Landscapes

Forest hydrology and geomorphology consider the dynamic interactions between hydrologic and geomorphic processes in forested landscapes and the extent to which watersheds, water resources and aquatic habitats can be protected during the harvesting of timber. Although forest cover is renewable after responsible harvesting, Vancouver Island, Haida Gwaii and the southern coast of the British Columbia mainland provide numerous examples of unsustainable forest management practices. Growing concern about forest management has led to intensified research on the relations between forest hydrology and geomorphology (Pike et al. 2010).

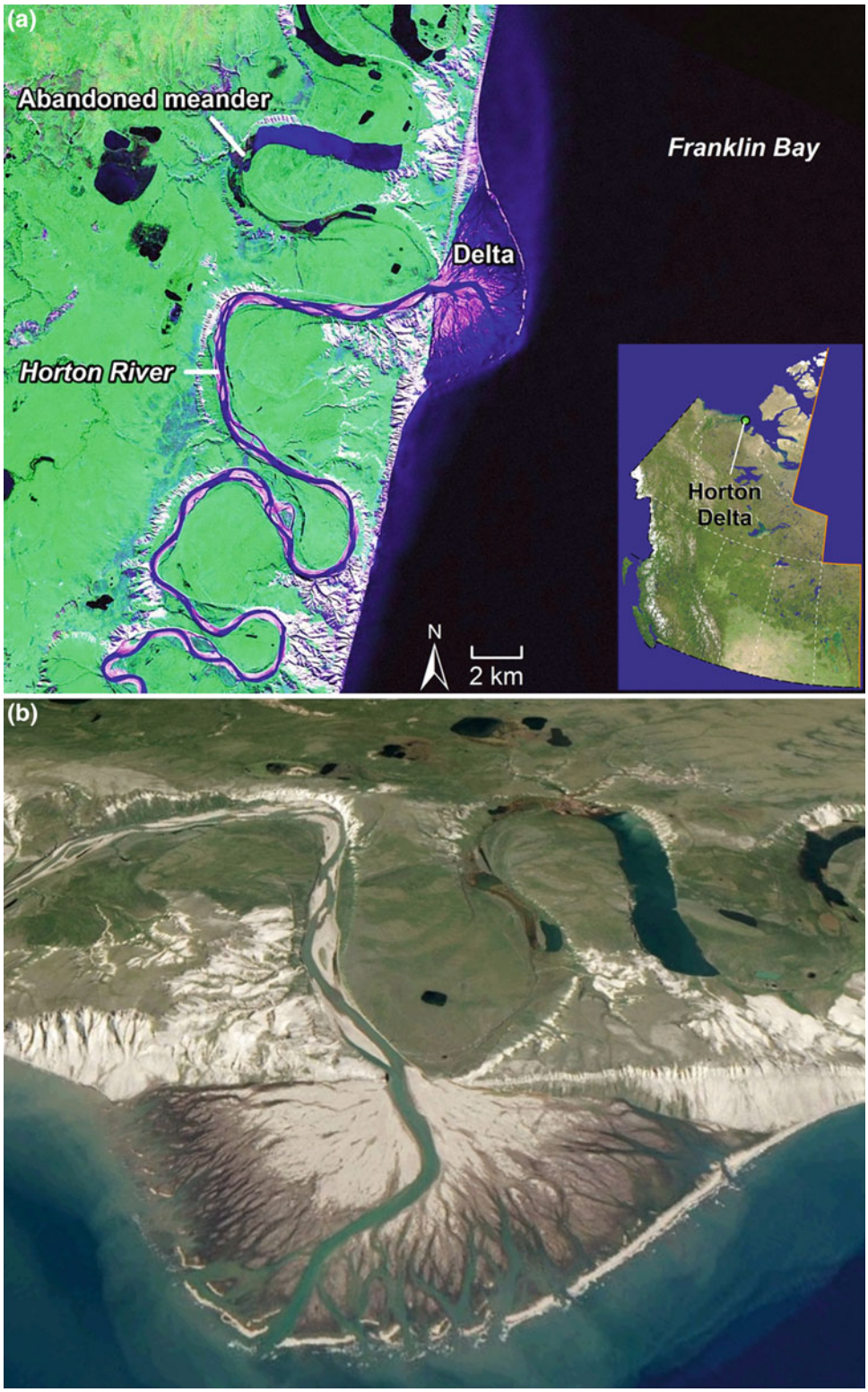

Fig. 3.17 **a** The Horton River, which now flows into Franklin Bay, Northwest Territories, formerly discharged into Harrowby Bay (not shown) about 60 km northwest of the present mouth. The Horton River abandoned its old channel and began to form a delta by about 1750 (Mackay and Slaymaker 1989). *Source* MDA (2004). **b** Horton delta, July 12, 2012. *Source* NASA's Earth Observatory by J. Allen and R. Simmon using EO-1-ALI

3.9.3 Agricultural Landscapes

Settlement of Canada's Prairies during the nineteenth and early twentieth centuries by dominantly Caucasian immigrants and erosional impacts on the landscape has been described by De Boer (1997). Assessment of contemporary rates of degradation in the badlands of Dinosaur Provincial Park (see Chap. 29) has been reported by Campbell (1987).

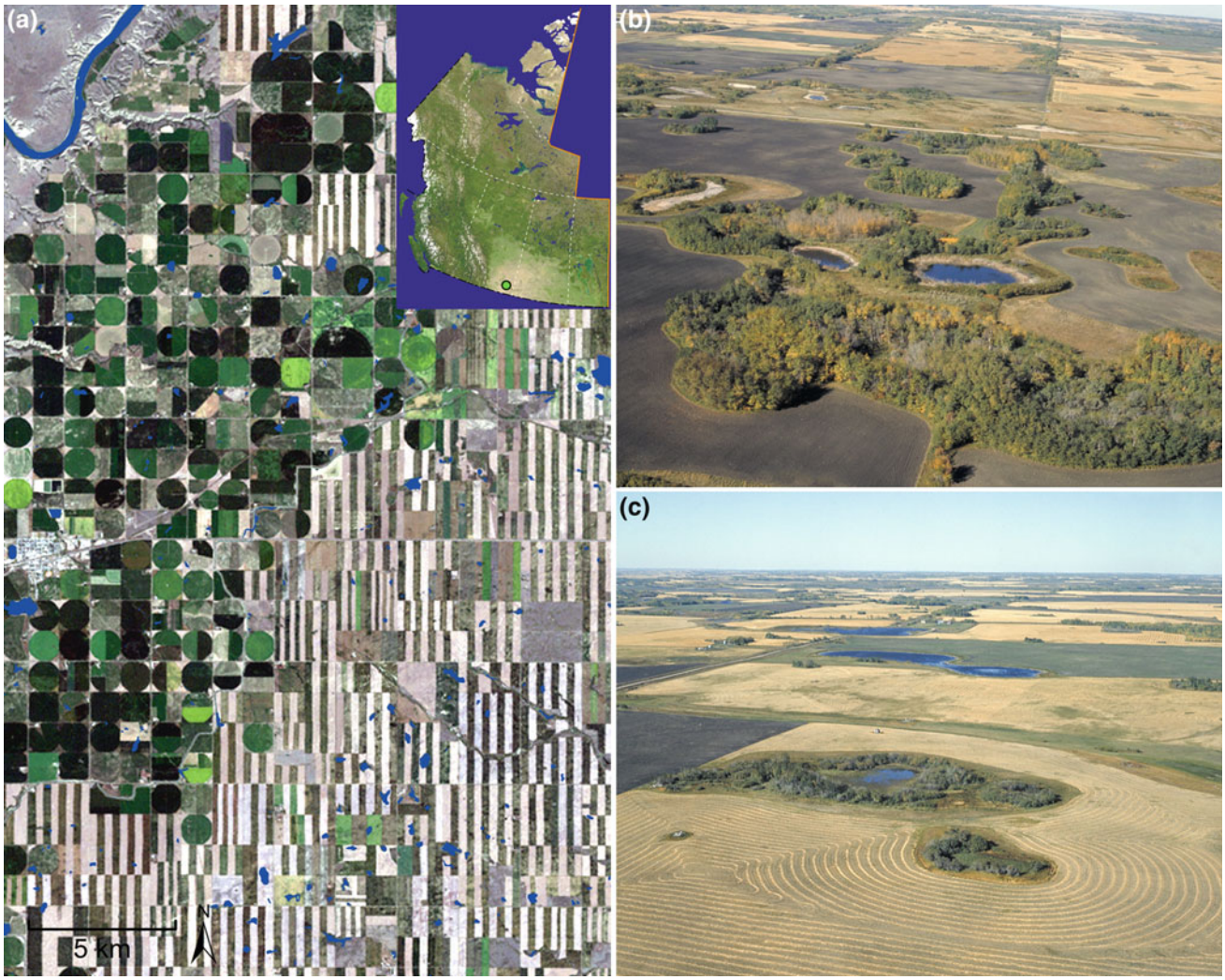

Fig. 3.18 Prairie agriculture patterns showing **a** central pivot irrigation and rectangular agricultural fields. *Source* © Department of Natural Resources Canada. All rights reserved. Government of Canada, Centre for Topographic Information, CanImage—Landsat 7 Orthoimage, 072e14. **b**, **c** Oblique photographs of the prairie pothole area showing geomorphological constraints on agriculture. Reproduced with the permission of Natural Resources Canada, 2015 (photographs NRCAN-2052 and NRCAN-2053)

It is also important to note that landscape elements such as Prairie potholes (Fig. 3.18; see Chaps. 2 and 9) provide physical constraints on agricultural development.

3.9.4 Mining Landscapes

The environmental impact of mining includes erosion and contamination of soil, groundwater and surface water by chemicals from mining processes. In some cases, additional forest logging is done in the vicinity of mines to increase the available room for the storage of the created debris and soil (Fig. 3.19). Erosion of exposed hillsides, mine dumps, tailings dams (see Chap. 28) and resultant siltation of drainages, creeks and rivers can significantly impact the surrounding areas, a prime example being the Mount Polley tailings storage facility breach in the Interior Cordillera of BC that occurred in 2014 (BC Government Ministry of Energy and Mines 2015). Mining may cause destruction and disturbance of ecosystems and habitats, and in areas of farming it may disturb or destroy productive grazing and croplands. In urbanized environments, mining may produce noise pollution, dust pollution and visual pollution.

3.9.5 Urban Landscapes

Because of the increasing population densities in western Canada's major cities natural hazard susceptibility has increased proportionately, whether the hazard be

Fig. 3.19 Mining town of Port Alice, Vancouver Island, British Columbia, showing debris deflection dykes constructed in 1976 to protect town from debris flows. Reproduced with the permission of Natural Resources Canada, 2015 (photographs NRCAN 2000-082 by SG Evans)

liquefaction potential (Fig. 3.20a) and landslides as in Vancouver (Evans 1982; Mustard et al. 1998); river flooding as in Calgary (Fig. 3.20b, c) (Osborn and Rajewicz 1998) or Winnipeg (see Chap. 10); subsidence from collapse as a result of dissolution of Devonian salts as in Saskatoon (Christiansen and Sauer 1998) or natural landslides that occur along river banks as in Edmonton (Rutter et al. 1998).

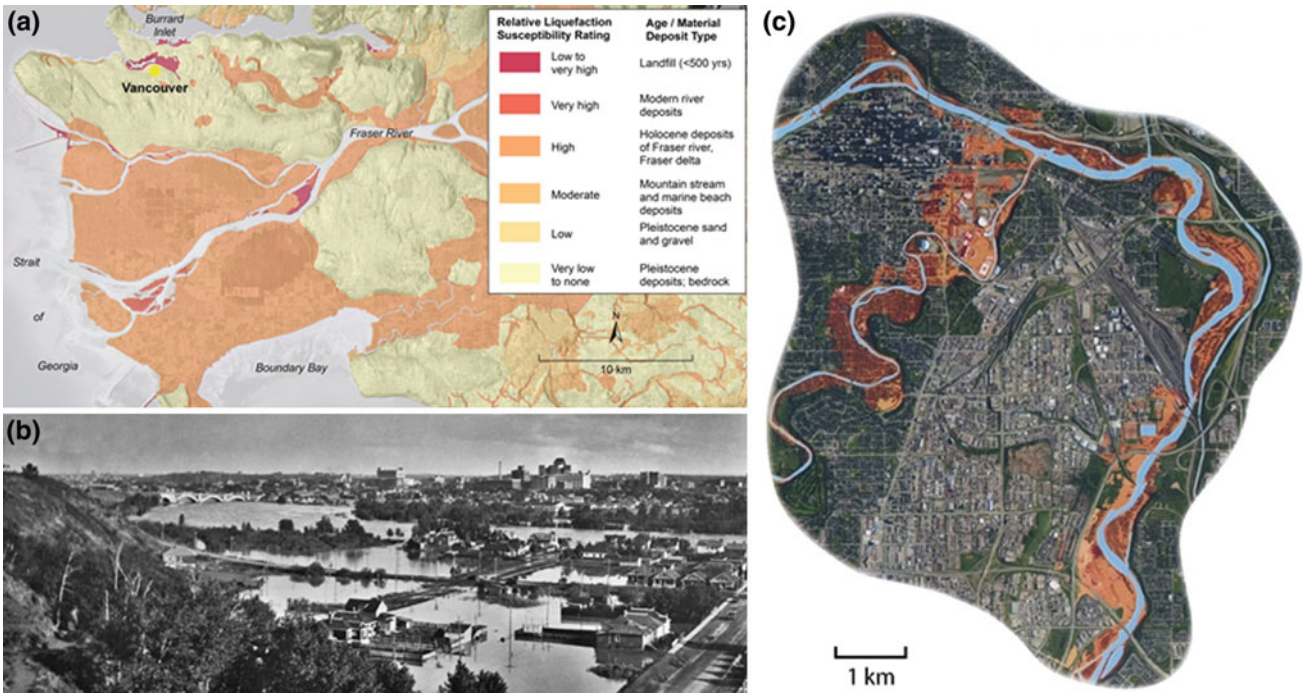

Fig. 3.20 Urban hazards. **a** Generalized liquefaction hazard map of Greater Vancouver area (modified from Mustard et al. 1998). **b** Flooding on the north bank of the Bow River in Calgary, summer flood of 1932: Sunnyside. *Source* Glenbow Archives, NA 1044-3. **c** Highest flood level achieved in the 2013 Calgary flood around the junction of Elbow and Bow rivers. *Source* Chris Brackley, Canadian Geographic

3.10 Conclusion

The Holocene landscapes of western Canada are indelibly marked by proglacial and paraglacial processes. The period following deglaciation of the western Canadian landscape was characterized by rapid relative sea level change, the presence of huge proglacial lakes and extensive and unstable glacial deposits on hillslopes and along valleys (Kovanen and Slaymaker 2015). Substantial mass movement and fluvial, lacustrine and aeolian reworking of these deposits created a major "pulse" of sediment movement in the early post-glacial landscape. This pulse of sediment redistribution had major impact on the morphology of western Canada's landscapes both in the Interior Lowlands and in the Cordillera. Superimposed on these paraglacial processes was repeated volcanism in the Cordillera, most recently exemplified by a major basalt lava flow eruption around the mid-to-late eighteenth century that travelled into a tributary of the Nass River and disrupted the lives of the Nisga'a First Nation. Finally, Anthropocene landscapes as influenced by population growth, mismanagement of the land and climate change are considered but by comparison with much of the developed world, western Canada is lightly populated and, if responsibly managed, can become a model of sustainable development (Slaymaker 2001; Pike et al. 2010).

Acknowledgment Cartography (with the exception of Figs. 3.11, 3.12, 3.13) by D. Kovanen

References

Ashmore PE, Church M (2001) The impact of climate change on rivers and river processes in Canada. Geol Surv Can Bull 555

Ballantyne CK (2002) Paraglacial geomorphology. Quat Sci Rev 21:1935–2017

BC Government Ministry of Energy and Mines (2015) Independent Expert Engineering Investigation and Review Panel, Report on Mount Polley Tailings Storage Facility Breach. Province of British Columbia. Available via https://www.mountpolleyreviewpanel.ca/final-report

Benn DI, Evans DJA (2010) Glaciers and glaciation. Arnold, London

Bovis MJ (1990) Rock slope deformation at Affliction Creek, southern British Columbia. Can J Earth Sci 27:243–254

Bovis MJ, Jones P (1992) Holocene history of earthflow mass movement in southern British Columbia. Can J Earth Sci 29:1746–1755

Brardinoni F, Hassan MA (2006) Glacial erosion, evolution of river long profiles and the organization of process domains on mountain drainage basins of coastal British Columbia. J Geophys Res. doi:10.1029/2005JF000358

Brardinoni F, Hassan MA, Rollerson T, Maynard D (2009) Colluvial sediment dynamics in mountain drainage basins. Earth Planet Sci Lett 284:310–319

Brooks GR (ed) (2001) A synthesis of geological hazards in Canada. Geol Surv Can Bull 548
Campbell I (1987) Canadian Landform examples: 3. Badlands of Dinosaur Provincial Park. Can Geogr 31:82–87
Carson MA, Jasper JN, Conly FM (1998) Magnitude and source of sediment input to the Mackenzie Delta, 1974–1994. Arctic 51:116–124
Christiansen EA, Sauer EK (1998) Geotechnique of Saskatoon and surrounding area, Saskatchewan. In: Karrow PF, White OL (eds) Urban geology of canadian cities. Geol Assoc Can Special Paper 42, pp 117–145
Church M (1998) The landscape of the Pacific Northwest. In: Hogan D, Tschaplinski, PJ, Chatwin S (eds) Carnation creek and queen Charlotte Islands fish/forestry workshop: applying 20 years of coastal research to management solutions. Land Management Handbook 41. BC Ministry of Forests, Research Branch, Victoria, pp 13–22
Church M, Gilbert R (1975) Proglacial fluvial and lacustrine environments. In: Jopling AV, McDonald BC (eds) Glaciofluvial and Glaciolacustrine Sedimentation. Society of Economic Paleontologists and Mineralogists Special Publication No 23. Oklahoma, pp 22–100
Church M, Ryder JM (1972) Paraglacial sedimentation: a consideration of fluvial processes conditioned by glaciation. Geol Soc Am Bull 83:3059–3072
Church M, Ryder JM (2010) Physiography of British Columbia. In: Pike RG, Redding RD, Moore RD, Winkler RD, Bladon KD (eds) Compendium of forest hydrology and geomorphology in British Columbia. Land Management Handbook 66, vol 1. BC Ministry of Forest and Range Research Branch, pp 17–45
Church M, Slaymaker O (1989) Disequilibrium of Holocene sediment yield in glaciated British Columbia. Nature 337:452–454
Church M, Kellerhals R, Day TJ (1989) Regional clastic sediment yield in British Columbia. Can J Earth Sci 26:31–45
Church M, Ham D, Hassan M, Slaymaker O (1999) Fluvial clastic sediment yield in Canada: scaled analysis. Can J Earth Sci 6:1267–1280
Clague JJ (1986) The quaternary stratigraphic record of British Columbia: evidence for periodic sedimentation and erosion controlled by glaciation. Can J Earth Sci 23:885–894
Clague JJ (1989) Sea levels on Canada's Pacific coast. Episodes 12:29–33
Clague JJ, Bornhold BD (1980) Morphology and littoral processes of the Pacific coast of Canada. In: McCann SB (ed) The Coastline of Canada, Littoral Processes and Shore Morphology, Halifax, May 1–3, 1978. Geological Survey of Canada Paper 80-10, pp 339–380
Clague JJ, Evans SG (2000) A review of catastrophic drainage of moraine-dammed lakes in British Columbia. Quat Sci Rev 19:1763–1783
Clarke GKC, Anslow FS, Jarosch AH, Radić V, Menounos B, Bolch T, Berthier E (2013) Ice volume and subglacial topography for western Canadian glaciers from mass balance fields, thinning rates, and a bed stress model. J Clim 26:4282–4303
Clarke GKC, Jarosch AH, Anslow FS, Radic V, Menounos B (2015) Projected deglaciation of western Canada in the twenty-first century. Nat Geosci. doi:10.1038/NGEO2407
Crutzen PJ, Stoermer EF (2000) The "Anthropocene." In: Steffen W (ed) Global change newsletter 41. IGBP, pp 17–18
De Boer DH (1997) Changing contributions of suspended sediment sources in small basins resulting from European settlement in the Canadian prairies. Earth Surf Process 22:623–639
Desloges JR, Church MA (1989) Canadian landform examples: 13 Wandering gravel bed rivers. Can Geogr 33:360–364
Desloges JR, Ryder JM (1990) Neoglacial history of the Coast Mountains near Bella Coola, British Columbia. Can J Earth Sci 27:281–290
Dyke AS, Moore A, Robertson L (2003) Deglaciation of Canada. Geological Survey of Canada, Open File 1574, 2 sheets; 1 CD-ROM. doi:10.4095/214399
Environment Canada (1995) Terrestrial Ecozones and Ecoregions of Canada. NRC of Canada, Ottawa
Evans SG (1982) Landslides and superficial deposits in urban areas of British Columbia. Can Geotech J 19:269–288
Evans SG, Clague JJ (1994) Recent climatic change and catastrophic geomorphic processes in mountain environments. Geomorphology 10:107–128
Eyles N (1983) Glacial geology: a landsystems approach. In: Eyles N (ed) Glacial geology. Pergamon, Oxford, pp 1–18
Fisheries and Environment Canada (1978) Hydrological Atlas of Canada. NRC of Canada, Ottawa
Ford DC, Schwarz HP, Drake JJ, Gascoyne M, Harmon RS, Latham AG (1981) Estimates of the age of the existing relief within the southern Rocky Mountains of Canada. Arct Alp Res 13:1–10
Friele PA, Clague JJ, Simpson K, Stasiuk M (2005) Impact of a Quaternary volcano on sedimentation in Lillooet River valley, British Columbia. Sedim Geol 176:305–322
French HM (2007) The periglacial environment. Wiley, Chichester
French HM, Slaymaker O (2012) Changing cold environments: a Canadian perspective. Wiley, Chichester
Geertsema M, Clague JJ, Schwab JW, Evans SG (2006) An overview of recent large catastrophic landslides in northern British Columbia. Eng Geol 83:120–143
Gerath R, Hungr O (1983) Landslide terrain, Scatter River valley, northeastern British Columbia. Geosci Can 10:30–32
Gilbert R (1990) Rafting in glacimarine environments. In: Dowdeswell JA, Scourse JD (eds) Glacimarine environments, processes and sediments. Geological Society of London Special Paper 53, pp 105–120
Guthrie RH (2002) The effects of logging on frequency and distribution of landslides in three watersheds on Vancouver Island, British Columbia. Geomorphology 43:273–292
Hamann A, Wang T, Spittlehouse DL, Murdock TQ (2013) A comprehensive, high-resolution database of historical and projected climate surfaces for western North America. B Am Meteorol Soc 94:1307–1309
Harris SA, Gustafson CA (1993) Debris flow characteristics in an area of continuous permafrost, St. Elias Range, Yukon. Z Geomorphol 37:41–56
Hewitt K (2006) Disturbance regime landscapes: mountain drainage systems interrupted by large rockslides. Prog Phys Geog 30:365–393
Hickson CJ, Edwards BR (2001) Volcanoes and volcanic hazards. In: Brooks GR (ed) A synthesis of geological hazards in Canada. Geol Surv Can Bull 548, pp 183–206
Hogan DL, Tschaplinski PJ, Chatwin S (eds) (1998) Carnation creek and queen Charlotte Islands fish/forestry workshop: applying 20 years of coastal research to management solutions. Land Management Handbook 41. BC Ministry of Forests, Research Branch, Victoria, pp 41–48
Hooke L (2000) On the history of humans as geomorphic agents. Geology 28:843–846
Jackson LE, MacDonald GM, Wilson MC (1982) Paraglacial origin for terraced river sediments in Bow valley, Alberta. Can J Earth Sci 19:2219–2231
Jakob M, Jordan P (2001) Design flood estimates in mountain streams: the need for a geomorphic approach. Can J Civil Eng 28:425–439

Jordan P, Slaymaker O (1991) Holocene sediment production in Lillooet River basin: a sediment budget approach. Geogr Phys Quat 45:45–57

Kovanen DJ, Slaymaker O (2008) The morphometric and stratigraphic framework for estimates of debris flow incidence in the North Cascades foothills, Washington State. Geomorphology 99:224–245

Kovanen DJ, Slaymaker O (2015) The Fraser Lowland as a complex paraglacial landsystem. Geomorphology 232:78–93

Lewis SL, Maslin MA (2015) Defining the anthropocene. Nature 519:171–180

Mackay JR, Slaymaker O (1989) A Horton River breakthrough and resulting geomorphic changes in a permafrost environment, Western Arctic Coast, Canada. Geogr Ann A 71:171–184

MDA Federal (2004) Landsat GeoCover ETM + 2000 Edition Mosaics Tiles N-08-65, N-08-70, N-10-55, N-10-65, N-10-70, N-12-55. ETM-EarthSat-MrSID, 1.0, USGS, Sioux Falls, South Dakota, 2000. Data available at the Global Land Cover Facility, www.landcover.org

Meidinger DV, Pojar J (eds) (1991) Ecosystems of British Columbia. BC Ministry of Forests, Special Report Series 6. Victoria

Montgomery DR, Foufoula-Georgiou E (1993) Channel network source representation using digital elevation models. Water Resour Res 29:3925–3934

Moore RD, Fleming SW, Menounos B, Wheate R, Foundtain A, Stahl K, Holm K, Jakob M (2009) Glacier change in western North America: influences on hydrology, geomorphic hazards and water quality. Hydrol Process 23:42–61

Mustard PS, Clague JJ, Woodsworth GJ, Hickson CJ, Jackson LE, Lutenauer JL, Monger JWH, Ricketts BD, Turner RJW, Hunter JA, Monahan PA (1998) Geological and geological hazards of the greater vancouver area. In: Karrow PF, White OL (eds) Urban geology of Canadian cities. Geol Assoc Can Special Paper 42, pp 39–70

Nakamura F, Swanson FJ, Wondzell SM (2000) Disturbance regimes of stream and riparian systems: a disturbance cascade perspective. Hydrol Process 14:2849–2860

Osborn G, Rajewicz R (1998) Urban geology of Calgary. In: Karrow PF, White OL (eds) Urban geology of canadian cities. Geol Assoc Can Special Paper 42, pp 93–115

Pike RG, Redding TE, Moore RD, Winkler RD, Bladon KD (eds) (2010) Compendium of forest hydrology and geomorphology in British Columbia. BC land management handbook 66. BC Ministry of Forests and Range, Forest Science Program, Victoria and FORREX Forum for Research and Extension in Natural Resources, Kamloops

Ruddiman WF, Ellis EC, Kaplan JO, Fuller DQ (2015) Defining the epoch we live in. Science 348:38–39

Rutter NW, Andriashek LD, Stein R, Fenton MM (1998) Engineering geology of the Edmonton area. In: Karrow PF, White OL (eds) Urban geology of Canadian cities. Geol Assoc Can, Special Paper 42, pp 71–92

Ryder JM (1998) Geomorphic processes in the alpine areas of Canada: the effects of climate change and their impacts on human activities. Geol Surv Can Bull 524

Seppala M (2004) Wind as a geomorphic agent in cold climates. Cambridge University Press, Cambridge

Schiefer E, Slaymaker O, Klinkenberg B (2001) Physiographically controlled allometry of specific yield in the Canadian Cordillera: a lake sediment-based approach. Geogr Ann A 83:55–65

Shaw J, Taylor RB, Forbes DL, Ruz MH, Solomon S (1998) Sensitivity of the coasts of Canada to sea-level rise. Geol Surv Can Bull 505

Slaymaker O (1987) Sediment and solute yields in British Columbia and Yukon: their geomorphic significance re-examined. In: Gardiner V (ed) Geomorphology '86. Wiley, Chichester, pp 925–945

Slaymaker O (1990) Climate change and erosion processes in mountain regions of western Canada. Mt Res Dev 10:171–182

Slaymaker O (2001) Why so much concern about climate change and so little attention to land use change? Can Geogr 45:71–78

Slaymaker O, Kelly REJ (2007) The cryosphere and global environmental change. Wiley, Chichester

Smith SL, Burgess MM, Heginbottom JA (2001) Permafrost and ground ice conditions in Canada. In: Brooks G (ed) A synthesis of geological hazards in Canada. Geol Surv Can Bull 548, pp 241–264

Stöckli R, Vermote E, Saleous N, Simmon R, Herring D (2005) The blue marble next generation: a true color earth dataset including seasonal dynamics from MODIS. NASA, Earth Observatory

Thorn CE, Loewenherz DS (1987) Spatial and temporal trends in alpine periglacial studies: implications for paleo-reconstruction. In: Boardman J (ed) Periglacial processes and landforms in Britain and Ireland. Cambridge University Press, Cambridge, pp 57–65

Tunnicliffe J, Church M, Enkin RJ (2012) Postglacial sediment yield to Chilliwack Lake, British Columbia. Boreas 41:84–101

Van Dine DF (1985) Debris flow and debris torrents in the southern Canadian Cordillera. Can Geotech J 22:44–68

Woo M-K, Thorne R (2003) Streamflow in the Mackenzie basin, Canada. Arctic 56:326–340

Part II

Case Studies of Periglacial, Aeolian, Fluvial, Glacial, Karst, Coastal and Anthropogenic Landscapes and Landforms Under the Influence of Geological Structure, Climate, and Land Use/Land Cover

Slave Geological Province: An Archetype of Glaciated Shield Terrain

4

Stephen A. Wolfe, Daniel E. Kerr, and Peter D. Morse

Abstract

The Slave Geological Province of the Tundra Shield is a Late Archean craton extending from the north shore of Great Slave Lake in the Northwest Territories to the Coronation Gulf in Nunavut. Underlain by metavolcanic and metasedimentary rocks intruded by granitoid plutons, the region is rich in gold, base metals, and diamonds and hosts numerous historic, active, and prospective mines. Most recently glaciated in the Late Wisconsinan, till and glacifluvial sediments form the most prevalent surficial materials. Glacial landscape features reflect complex ice flow patterns recording several different events. Raised post-glacial marine sediments are significant in the north along the Coronation Gulf at elevations below 200 masl, whereas glacilacustrine sediments related to glacial Lake McConnell are abundant in the south. Ground ice in glacigenic sediments has been preserved since deglaciation as much of the region also lies well within the zone of continuous permafrost. Segregated ice occurs separately within glacimarine and glacilacustrine sediments, and polygonal terrain is abundant on outwash sediments. Glacially derived ground ice includes buried glacial ice within glacifluvial outwash deposits and buried glacial and meltwater ice within eskers. Sediment-rich ice has also been encountered within hummocky till terrain during mine development operations. Surficial features attributed to partial thawing, and creep of massive ground ice, are regionally apparent. Although massive ice has been encountered in only a few locations to date, ground ice may be common within this glaciated region of the Tundra Shield.

Keywords

Slave province • Canadian Shield • Permafrost • Ground ice • Till • Eskers • Outwash

4.1 Introduction

Metamorphic Archean rocks of volcanic and sedimentary origin with granitoid intrusions define the Slave Craton of the northwestern Canadian Shield. Along with the vast majority of the Canadian landscape, the Slave Geological Province (Fig. 4.1) was affected by Late Wisconsinan glaciation. It exemplifies the effects of glacial erosion and deposition, and post-glacial landscape modifications within the northwestern Canadian Shield. Glacial terrain features provide indicators of past ice flow directions and glacial ice conditions, whereas glacifluvial deposits provide insight into late glacial processes. Through cold climate conditions prevailing since deglaciation, permafrost has been preserved in much of this terrain where till and glacifluvial sediments have insulated underlying materials including massive ground ice of glacial and meltwater origin. In particular, hummocky till, ice-contact delta sediments, and esker deposits all have the potential to preserve discrete occurrences of buried ice within the region. Marine inundation in the north and glacilacustrine incursion in the south, combined with subsequent permafrost aggradation, further give

S.A. Wolfe (✉) · D.E. Kerr · P.D. Morse
Geological Survey of Canada, Natural Resources Canada, 601 Booth St., Ottawa, ON K1A OE8, Canada
e-mail: stephen.wolfe@canada.ca

© Springer International Publishing Switzerland 2017

O. Slaymaker (ed.), *Landscapes and Landforms of Western Canada*,
World Geomorphological Landscapes, DOI: 10.1007/978-3-319-44595-3_4

rise to post-glacial landscape modifications. Herein, the glacial and post-glacial landscape of the Slave Geological Province is described with special attention to the uniqueness of buried ground ice within glacifluvial sediments.

4.2 Geographic Setting

4.2.1 Underlying Bedrock

The northwestern Canadian Shield consists predominantly of Archean rocks that form the Slave Province and younger Proterozoic rocks of the Bear Province to the northwest (Fig. 4.1). The Slave Geological Province is predominantly a bedrock defined 210,000 km^2 Late Archean craton, characterized by a depositional and volcanic history that has been overprinted by multiple phases of deformation and intruded by granitoid plutons (Bleeker 2002). Major units include basement gneisses, metavolcanic and metasedimentary rocks, and widespread gneissic–granitoid plutons (Padgham and Fyson 1992; Helmstaedt 2009) including the Acasta Gneiss, which at 4.03 Ga are the world's oldest exposed rocks (Stern and Bleeker 1998).

World-class kimberlite fields in the Lac de Gras area and adjoining kimberlite clusters contain the vast majority of all kimberlites within the Slave Geological Province. Kimberlites are a rare variety of ultra-basic igneous rock, typically occurring in the form of carrot-shaped volcanic pipes and dykes, originating from deep in the Earth's mantle by way of rapidly rising magmas during kimberlite volcanic eruption. A kimberlite pipe is typically expressed on the surface as a small lake-filled depression, which may be more circular and deeper than surrounding lakes. Kimberlite significance is their diamond content, with individual crystals ranging from a fraction of a millimeter to greater than one centimeter. These diamonds are classified into gem, near-gem, and industrial grade. Several hundred kimberlite pipes in the Lac de Gras area range in age from Late Cretaceous to Early

Fig. 4.1 Slave Geological Province of the northwestern Canadian Shield showing chronology of major ice flow directions (*red* = earlier), post-glacial marine limit, limit of glacial Lake McConnell, the southern limit of continuous permafrost, active and abandoned mines, and locations referred to in text. Geology from Wheeler et al. (1996) and ice flow directions from Dredge et al. (1997)

Tertiary (Pell 1994). The Slave Province is host to the majority of Canada's producing diamond mines, including Ekati, Diavik, Gahcho Kue, and Snap Lake, as well as numerous past producing gold mines (Fig. 4.1).

4.2.2 Physiography and Climate

The Slave Geological Province falls within the Bear–Slave Upland physiographic region of the Canadian Shield (Bostock 1970), extending across more than 800 km from the north shore of Great Slave Lake to the coast of the Coronation Gulf (Fig. 4.1). Elevations vary from about 155 m above sea level (masl) at Great Slave Lake, increasing to 250 masl within the southern uplands, then rising to a height of 650 masl in the central interior uplands north of Contwoyto Lake. From there the land declines in elevation northward to sea level along the Arctic Coastal Plain bordering the Coronation Gulf. Relief is variable, commonly between <10 and 30 m in areas of outcrop, although escarpments and cuestas >50 m high are found in the north. Relief on glacial terrain shaped by eskers, streamlined till, and hummocky till is on the order of 10–20 m. The region forms a gently undulating glaciated landscape, with glacial deposits constituting the most prevalent surficial material, although rugged bedrock outcrops dominate in many areas. Raised post-glacial marine sediments are common along the Coronation Gulf, below 200 masl, and glacilacustrine sediments occur in the south below about 350 masl in association with glacial Lake McConnell (Fig. 4.1; Kerr et al. 2014).

The present-day climate ranges from cold continental to maritime arctic. Although climate data are sparse, mean annual air temperatures are warmest in the south near Yellowknife (−4.1 °C), coldest toward the central region at Lupin mine (−12 °C), and slightly warmer to the north at Kugluktuk (−11.6 °C). Precipitation generally declines northward, ranging from about 270 mm at Yellowknife to about 200 mm at Kugluktuk, with about 50 % falling as snow.

The southwestern part of the Slave Province lies within tree line and below the southern limit of continuous permafrost (Fig. 4.1; Heginbottom et al. 1995) and includes stunted spruce and jack pine woodland vegetation with some peatlands. The remainder of the area above tree line supports tundra heath vegetation, with the addition of denser grassy vegetation along the coastal plain underlain by fine-grained marine sediments.

4.3 Glaciation

All glacial features in the Slave Geological Province are related to the Late Wisconsinan glaciation. Ice flow patterns are complex and record several different events (Fig. 4.1; Dredge et al. 1997). The earliest recorded ice flow is present in the central and southern regions, indicating a southwestward movement. This was followed by a dominant regional westward to west–southwestward flow in the same area and northwestward to north–northwestward flow in the Takijuq Lake region. During the last phases of deglaciation, topography and local ice conditions were responsible for minor variations in regional ice flow patterns, such as southwestward ice flow southeast of Lac de Gras, northward ice flow into the Coronation Gulf west of Kugluktuk, and westward ice flow on offshore islands in Coronation Gulf.

Till veneers, undulating till blankets, and streamlined rock and till forms, including crag and tail features (Fig. 4.2) and drumlinoid ridges up to 30 km long (Fig. 4.3), are the principal glacial landforms in the region. These features may be indicative of warm-based ice conditions. Hummocky till, formed to some extent by partial meltout of ice-rich till, marks areas of ice stagnation. Most sand and gravel outwash deposits are in the form of pads flanking or splaying from eskers, or less commonly as proglacial fans and ice-contact deltas. Trunk eskers and tributary eskers mark the location of major and minor meltwater conduits within the late glacial ice sheet and include the Thelon Esker, likely the longest esker in the world, which extends westward for nearly 800 km from Dubawnt Lake, NU, to Great Bear Lake, NT. Eskers with flanking outwash pads developed in relatively thin ice near retreating ice fronts, whereas extensive voluminous eskers lacking these forms probably developed farther within the glacier, where ice was warm-based.

Throughout the Slave Province, the abundance of glacifluvial meltwater corridors testifies to the significant amount of water that resulted from glacial ice melting (St-Onge 1984; Rampton 2000). On the northern coastal plain, a series of ice-contact deltas developed where northward flowing esker conduits deposited glacial sediments into the

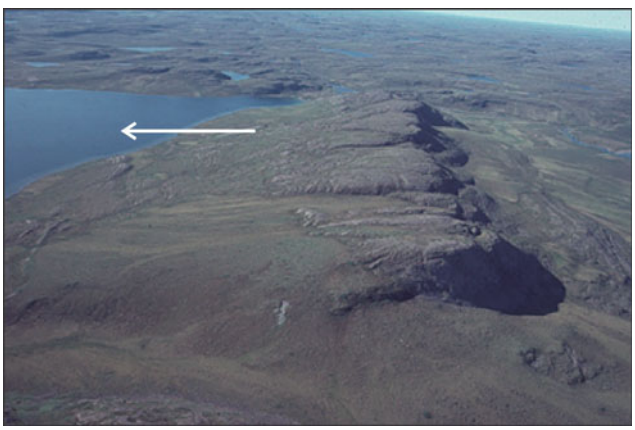

Fig. 4.2 Crag and tail landforms south of Takijuq Lake, north. Ice flow, as indicated by *arrow*, is from right to left. Photograph by Daniel Kerr

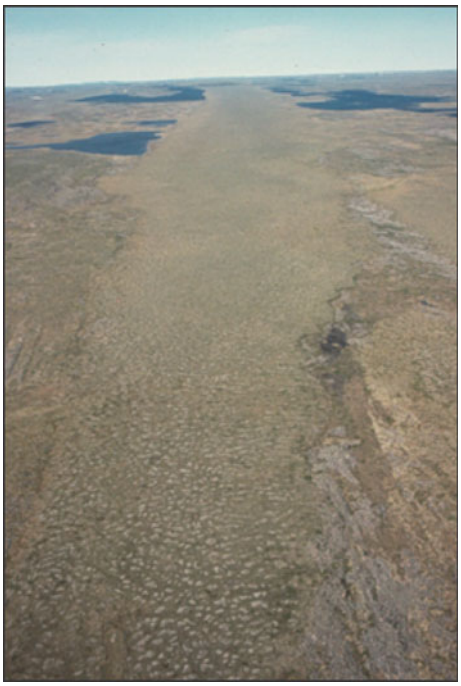

Fig. 4.3 A 22-km-long elongate drumlinoid feature trending north–northwest toward Coronation Gulf, southeast of Kugluktuk. View to the north. Photograph by Stephen Wolfe

high-level sea. Finer glacimarine and subsequent marine sediments were carried into open waters farther from the ice front. As sea level fell to successively lower elevations, numerous beaches formed where suitable sediments for strandlines were available (Fig. 4.4). Raised marine sediments, up to 40 m thick and deposited during post-glacial emergence due to crustal rebound, form coastal lowlands that extend from sea level up to elevations of 170–210 masl and from Coronation Gulf inland to a distance of up to 40 km in the Tree River valley. The region is still experiencing glaci-isostatic uplift (Kerr 1996), accompanied by permafrost aggradation into emerging sediments.

Inundation of coastal glaci-isostatically depressed terrain (Fig. 4.1) progressed across the northern part of the region, following the eastward retreat of the ice lobe occupying the Coronation Gulf. Marine shells west of the Tree River indicate that deglaciation began about 10,500 ^{14}C year BP (Dredge et al. 1999). Marine limit, defined by ice-contact deltas and limits of wave erosion, ranges from about 170 masl west of Kugluktuk to 210 masl near western Bathurst inlet (Fig. 4.1). Northward flowing ice remained near the coast until between 10,100 and 9620 BP, while sea level dropped by 30–50 m. Twigs in ice-contact deposits in hummocky till east of the Lac de Gras area indicate that the southern areas were deglaciated and vegetated by about 8500 BP, although relict glacier ice masses lay southwest of Contwoyto Lake in an area of divergent ice flow (Dredge et al. 1999).

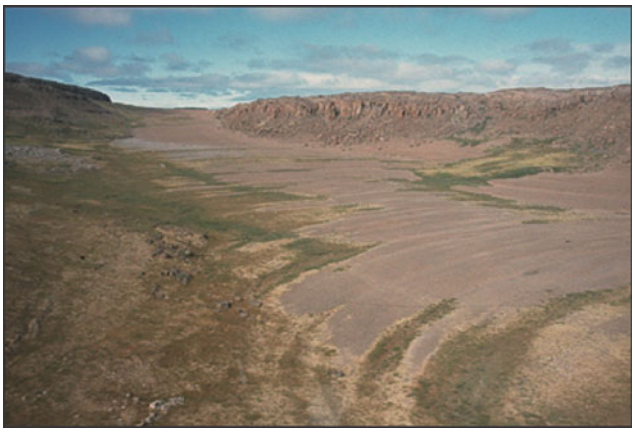

Fig. 4.4 Raised beaches inland of Coronation Gulf coast, 10 km west of the mouth of the Tree River. Photograph by Stephen Wolfe

The southern part of the region was inundated by glacial Lake McConnell (Fig. 4.1), which formed along the retreating glacial margin between about 13,000 and 9500 years ago (Lemmen et al. 1994). Evidence of the glacial lake exists in the form of raised deltas, strandlines, beaches and wave washed eskers and drumlinoid landforms. With lake level recession, the glacial lake separated into distinctive basins, and waves and rivers of ancestral Great Slave Lake reworked and redeposited glacilacustrine sediments in nearshore environments. Consequently, within this area till cover is sparse, whereas glacilacustrine and lacustrine deposits are broadly distributed across the region. Much like the Coronation Gulf coast, the Great Slave Lake region is still experiencing uplift accompanied by permafrost aggradation into emergent terrain (see Chap. 5, this volume).

4.4 Permafrost

Permafrost in the region attains thicknesses of 160 m to more than 400 m (Judge et al. 1981; Lytton Minerals Ltd 1996), but varies considerably depending on local site conditions. Mean annual ground temperatures range from −5 to −7 °C along the coastal plain east of Coronation Gulf and −6 °C at Jericho and Lac de Gras (Wolfe 1997). Summer active layer depths depend on vegetation cover, subsurface material type, and moisture conditions, but typically range from about 15 cm in areas supporting a thick organic mat to more than 120 cm in areas where vegetation cover is thin or lacking.

Evidence exists for at least two warm phases in the region during the Holocene, which may have affected permafrost and surface terrain conditions through an increase in active layer thickness and thawing of excess ice. In the northwestern coastal region, wood from the base of a thermokarst depression on a marine delta 32 km southwest of Kugluktuk

indicates that vegetation development had begun in this area by at least 9150 BP (Geurts 1985). This radiocarbon date is comparable to, but slightly later than, the onset of early Holocene warming which initiated mass wasting in the Mackenzie Delta region to the west, between 10,000 and 9500 BP (Mackay and Dallimore 1992). Toward the south, at the present forest tundra boundary near Lac de Gras, lake cores obtained by Moser and MacDonald (1990) and MacDonald et al. (1993) indicate that tundra predominated from about 7000–5000 BP, with an abrupt transition to forest tundra at approximately 5000 BP. Based on the proportion of organic to inorganic sediment in these lake cores, this warmer forest tundra phase is thought to have lasted until 3500 BP, with tundra subsequently dominating in the region until present (Moser and MacDonald 1990). Peat in kettle holes in an esker north of the Izok mine site indicates that tundra conditions have persisted in this area since 3100 BP (Dredge et al. 1997). The extent to which either the Early or Mid-Holocene warm phases affected the region as a whole is presently unknown. Modern active layer detachment failures and retrogressive thaw slumps are common on fine-grained marine deposits, particularly on slopes in river valleys along the coast (Fig. 4.5).

4.5 Ground Ice

Ground ice in the Slave Geological Province occurs as several primary types within glacigenic sediments. Ground ice is likely present within till terrain in the region and may include wedge ice, aggradational ground ice, and buried glacial ice, especially within hummocky till. Ground ice is generally more evident in the Slave region, however, within other glacigenic materials including glacimarine, glaciolacustrine, and glacifluvial sediments. This includes wedge ice, segregated ice, and buried ground ice. Buried ground ice associated with glacifluvial sediments may be of two main types: buried glacial ice, capped by glacifluvial outwash sediments (Wolfe 1998), or buried ice of glacial meltwater origin deposited contemporaneously within eskers (Wolfe et al. 1997).

4.5.1 Polygonal Ground and Wedge Ice

Polygonal ground is a prominent feature on glacifluvial deposits and within peatlands in the Slave Geological Province. Within the discontinuous permafrost zone below tree line, polygonal terrain on flat-topped glacifluvial sediments is commonly associated with sand wedges, rather than ice (Fig. 4.6). These wedges, which are filled by sand, typically extend to a depth of <1 m below the ground surface, suggesting they are associated with seasonally frozen ground but not permafrost. Within tundra in continuous permafrost, polygonal terrain is also most evident on glacifluvial deposits. The polygonal terrain is characteristically large, with polygons on the order of 10–40 m wide and troughs up to 2 m deep. These polygons are associated with wedge ice, as is evident by thawing and associated subsidence due to disturbance, following the removal of surface granular materials at a number of development sites (Fig. 4.7).

The prominence of polygonal terrain on glacifluvial sediments within both discontinuous and continuous permafrost terrains indicates that these sediments are conducive to thermal contraction cracking, perhaps more so than other

Fig. 4.5 Active layer detachments (indicated by *arrows*) and erosional surfaces in marine sediments along the Tree River. Photograph by Stephen Wolfe

Fig. 4.6 Sand wedge, approximately 70 cm deep, formed within glacifluvial sands. Photograph by Stephen Wolfe

Fig. 4.7 Meltout of an ice-wedge trough, following the removal of the surface granular materials for construction, Jericho mine site. Photograph by Stephen Wolfe

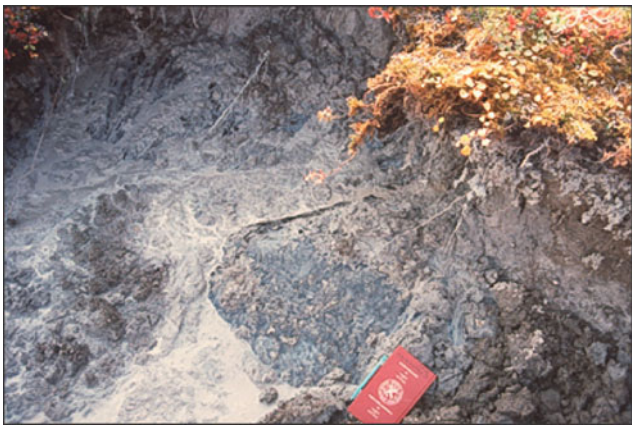

Fig. 4.8 Near-surface ground ice at the top of permafrost within raised marine sediments along the Coronation Gulf Coast. Photograph by Stephen Wolfe

sediment types in the region. Indeed, thermal conductivity of moist sand is high under both unfrozen and frozen conditions in comparison with other common material types such as clay, till, and peat that occurs within the Slave region. They, therefore, likely undergo significant seasonal temperature variations in the near surface. In addition, the sandy and coarse-grained deposits are typically insulated by only thin vegetation cover, if any, and are also commonly swept clear of snow by wind in winter. Consequently, glacifluvial deposits may allow rapid cooling conducive to thermal contraction cracking in winter and thus the development of ice wedges within continuous permafrost and sand wedges within discontinuous permafrost. Although these sites may be cold in winter, they may also be warmer than other terrain types in summer due to the thermal properties and lack of insulating vegetation cover.

4.5.2 Segregated Ice

Segregated ice, formed as permafrost aggrades into saturated fine-grained sediments, is locally prominent in two distinctly separate regions of the Slave Geological Province. In the north, along the Coronation Gulf coast, segregated ice occurs below the marine limit (Fig. 4.1) within raised fine-grained marine sediments. On these tundra surfaces, active layers are about 25 cm thick, and underlying sediments contain in excess of 70 % ice by volume within 1 m of the surface (Fig. 4.8). Thawing of this upper layer of permafrost is responsible for numerous active layer detachments (Fig. 4.5).

In the southern portion of the region, ice-rich terrain occurs in fine-grained lacustrine and glacilacustrine sediments within the glacial Lake McConnell limit of the discontinuous permafrost zone (Fig. 4.1). Lithalsas, which are permafrost mounds up to 8 m high and several hundred meter long, have formed within the area as permafrost aggraded into the fine-grained lacustrine sediments following lake level recession. Lithalsas here are most common within the first few tens of meters above the present level of Great Slave Lake, indicating that many are Late Holocene in age and some <1.000 years (see Chap. 5, this volume).

4.5.3 Buried Glacial Ice

Discrete bodies of massive ice occur beneath glacifluvial outwash delta deposits at the Jericho mine site in the northern Contwoyto Lake area (Fig. 4.1). Locally, an extensive, steep-sided, sandy outwash plain resides immediately north of Carat Lake, rising to a height of about 20 m above the lake (Fig. 4.9a, b). Massive ice, up to 15 m thick, occurs at several locations beneath these sediments (Fig. 4.9b). This ice is overlain by subhorizontally stratified silty sand and coarse-grained bottomset sands, and overlying foreset beds that are attributable to delta progradation (Fig. 4.9c).

The flat-topped surface topography of the fan delta sediments suggests that post-depositional formation of massive ice did not occur. Instead, isolated bodies of ground ice were buried and preserved in situ by prograding outwash sediments. An outflow channel between Contwoyto Lake and an esker complex indicates that a high-energy outflow was discharged from the lake basin. Ice appears to have been buried and thermally preserved by these outwash sediments. As well, kettle lakes, within and around the margins of the glacifluvial deposits (Fig. 4.9a), are further indicative of thawing of massive ice (Benn and Evans 2010).

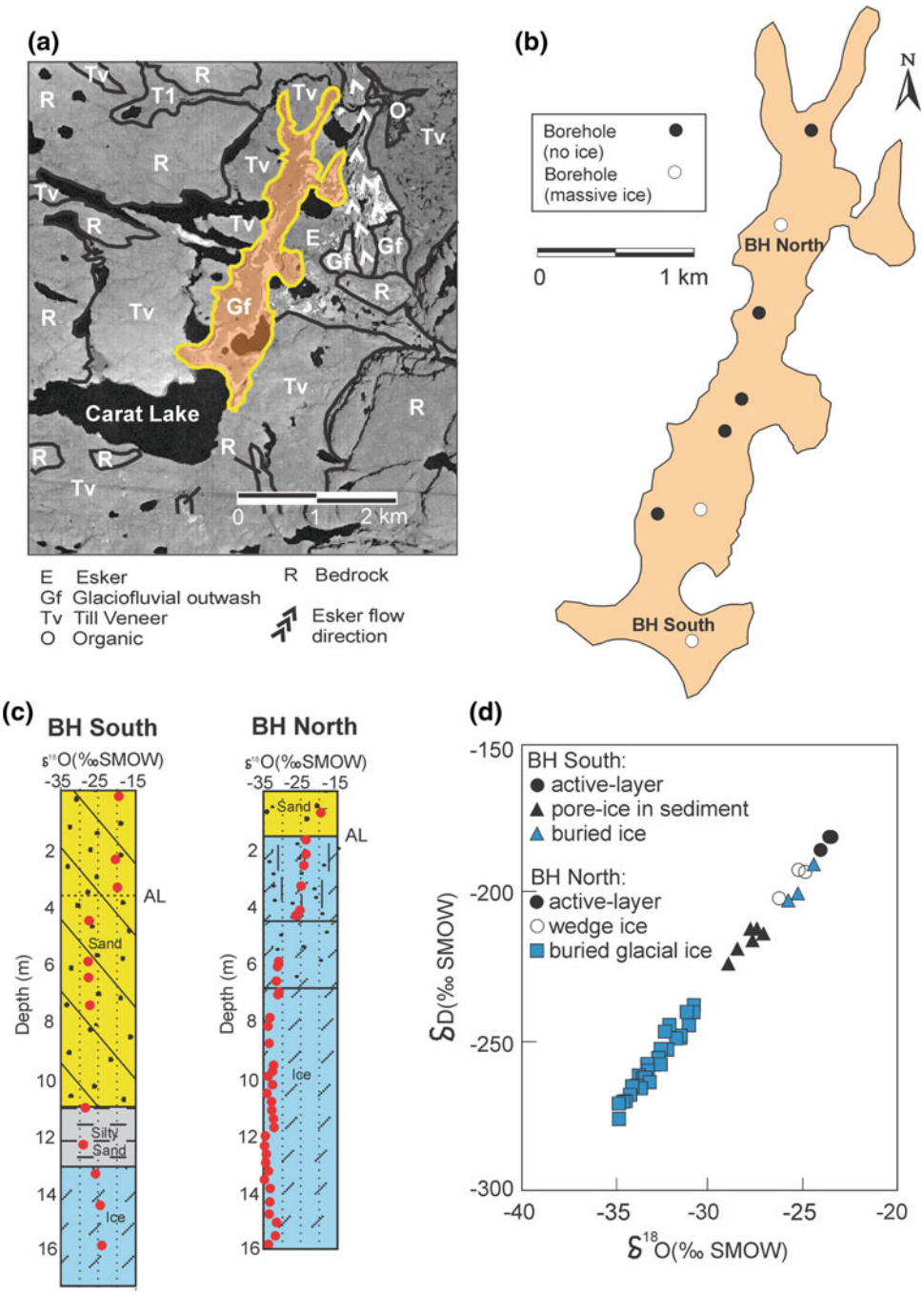

Fig. 4.9 Example of ground ice in glacifluvial fan delta sediments at Jericho mine site on northern Contwoyto Lake. **a** Surficial geology of the local area; **b** outline of glacifluvial fan delta sediments with borehole locations; **c** borehole stratigraphy and oxygen isotope values (*red dots*); **d** co-isotope plot of oxygen and deuterium values of massive ice and pore ice in boreholes. *AL* active layer (Wolfe et al. 1997; Wolfe 1998)

Co-isotopic, oxygen–deuterium relations indicate several ice types associated with this system. These include the following: active layer pore ice and wedge ice near the surface with values consistent with modern precipitation; ice within and beneath outwash sediments, possibly of glacifluvial origin; and lower ice with values consistent with Wisconsinan-aged glacial ice (Fig. 4.8d). Elemental concentrations within this lower ice are further consistent with ice originating as precipitated snow (Langley 1967), with only trace amount of cations such as Al, Si, Na, Ca, and no measurable Fe concentrations, unlike higher cation amounts in overlying ice and sediments (Wolfe 1998).

Thus, rapid deposition of sediments over blocks of glacial ice followed by permafrost aggradation accounts for the preservation of buried ice within these glacifluvial sediments.

4.5.4 Buried Meltwater Ice

Massive ice in glacifluvial sediments has also been noted within an esker residing on till-mantled terrain near Lac de Gras, connecting to a larger east–west-trending esker system. Locally, this esker rises to about 18 m above the surrounding terrain and dams a small lake on its eastern side (Fig. 4.10a). Excavation of granular materials for road and airport construction originally exposed ground ice within the sediments (Fig. 4.10b). Boreholes drilled on the esker encountered stratified sands and gravels, additionally stratified with ice below 9 m depth (Fig. 4.10c). In general, this ice was relatively free of sediment, but contained occasional sand and gravel bands inclined up to 50° to the horizontal.

Whereas isotopic values for ice encountered in the near surface of the esker may be reflective of modern water sources of combined rain and snow, isotopic values for lower pore ice and ground ice in the esker indicate a cold water origin (Fig. 4.10d), similar to the ice contained within outwash sediments in the Contwoyto Lake area (Fig. 4.9d). Oxygen isotopic values in the range of −28 to −30 ‰ suggest that the source for the ground ice is likely glacially derived meltwater. Thus, the lower massive ice identified in the boreholes may represent ice that was buried by esker sediments and preserved by permafrost since deglaciation. Elemental cation concentrations also indicate potentially different water sources for the two ground ice types, with the upper ice having similar concentrations to lake and surface waters in the area and the lower ice showing dissimilarities, indicative of a separate water source for this ice (Wolfe et al. 1997).

Overall, sediments in the esker are well-graded sand and gravels, but with distinctive and frequent changes in stratigraphy. These stratigraphic changes continue at depth, but with interlayering of ice. This cryostratigraphy indicates that the ice was emplaced contemporaneously with

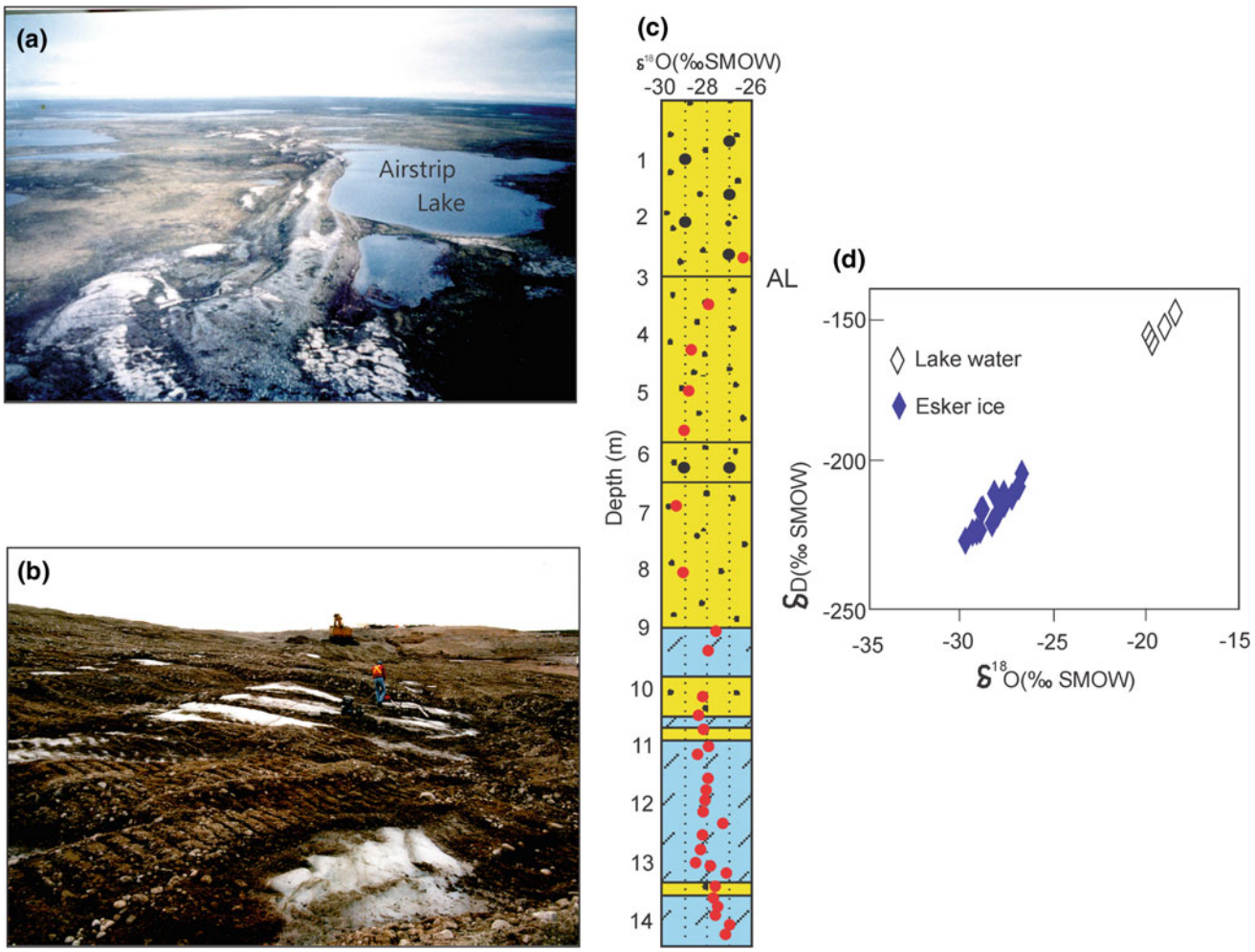

Fig. 4.10 Example of ground ice in esker sediments at the Ekati mine site near Lac de Gras. **a** Esker and lake; **b** ground exposed by aggregate extraction; **c** borehole stratigraphy and oxygen isotope values (*red dots*); **d** co-isotope plot of oxygen and deuterium values in esker ice and nearby lake (Wolfe et al. 1997)

deposition of the esker sediments as water froze within the esker conduit and has since been preserved within permafrost. The isotopic and cation concentrations are indicative of a cold water source in contact with sediments and thus likely of glacial meltwater origin. Comparable esker deposits are geographically widespread but limited in extent and may contain similarly preserved ice.

4.5.5 Ground Ice and Terrain Sensitivity

Ground ice within permafrost is a main factor influencing terrain sensitivity, which is defined as the potential and extent of ground subsidence, slope movement, or thermokarst due to thawing of permafrost. In till veneers and till blankets, ground ice content may be low, as evident by the general absence of thermokarst features. However, distinctive surface relief features in hummocky till including kettle depressions, rim ridges, and thaw slump scars are likely attributed to massive ice, indicative of sensitive till terrain (Fig. 4.11). Similarly, terrain sensitivity is high, and active layer detachment slides are common in the Arctic coastal plain along the Coronation Gulf coast (Fig. 4.5) where frozen silty clay marine sediments may contain high ice contents (Fig. 4.8). Sandy littoral and estuarine deposits, including those a few meters above present sea level, contain ice-wedge polygons. Solifluction lobes developed in surficial materials with a fine-grained matrix have crept downslope for tens of meters, covering raised beaches along certain parts of the coastline in the last 1000–2000 years.

Although many proglacial outwash deposits have low-to-moderate ice contents near the surface associated with pore ice and wedge ice, massive ice ranging from 5 to 15 m thick or more may occur within eskers and related ice-contact sediments. The terrain sensitivity associated with these deposits is typically moderate, due to the coarse-grained nature of the sediments and rather isolated nature of the ground ice. Specific terrain sensitivities associated with ice in these sediments can include thermokarst, slope movement, and collapse features, all indicative of meltout or creep of large bodies of massive ice. In addition, the removal of granular sediments can expose massive ice, resulting in partial-to-complete thaw and significant localized terrain subsidence.

Fig. 4.11 Stabilized thawslide (outline with *dashed line*) on the surface of a till blanket, indicative of partial thaw of icy sediments. Photograph by Stephen Wolfe

4.6 Conclusions

The Slave Geological Province illustrates the evolution of one of the oldest landscapes in the world, from Archean volcanism, sediment deposition, and plutonic intrusions, to Wisconsinan continental glaciation and subsequent post-glacial modifications and establishment of cold climate conditions. The presence of continuous permafrost through much of the region provides the opportunity to examine preserved glacial features characteristic of the northwestern Canadian Shield, including the presence of segregated ice, ice wedges, and buried ice of glacial and meltwater origins. Although massive ice has been uncovered only within discrete locations in the region to date, ground ice may be common as surficial features attributable to partial thawing and creep of massive ice are regionally apparent. Encounters with massive ice will likely increase as development continues in the region. Massive ground ice occurrences in glacifluvial sediments may limit the amount of material available for granular extraction and pose potential hazards to ground stability and water management upon disturbance.

References

Benn DI, Evans DJA (2010) Glaciers and glaciation, 2nd edn. Routledge, New York, p 802

Bleeker W (2002) Archaean tectonics: a review, with illustrations from the Slave craton. Geol Soc Lond Spec Publ 199:151–181

Bostock HS (1970) Physiographic regions of Canada; Geol Surv Can, "A" Series Map 1254A, 1:5000000, 1 sheet

Dredge LA, Kerr DE, Kjarsgaard IM, Knight RD, Ward BC (1997) Kimberlite indicator minerals in till, central Slave Province, Northwest Territories. Geol Surv Can, Open File 3426, 1 sheet

Dredge LA, Kerr DE, Wolfe SA (1999) Surficial materials and related ground ice conditions, Slave Province, N.W.T. Can J Earth Sci 36:1227–1238

Geurts M-A (1985) Le paysage végétal holocène dans la région d'Escape Rapids, Territoires du nord-ouest. Géogr Phys Quat 39:215–220

Helmstaedt HH (2009) Crust-mantle coupling revisited: the Archean Slave craton, NWT, Canada. Lithos 112:1055–1068

Heginbottom JA, Dubreuil MA, Harker PA (1995) Canada-Permafrost. In: National Atlas of Canada, 5th edn. National Atlas information

service: natural resources Canada, Ottawa, Plate 2.1. MCR 4177, scale 1:7500000

Judge AS, Taylor AE, Burgess MM, Allen VS (1981) Canadian geothermal data collection-Northern Wells 1978–1980. Earth Physics Branch, Geothermal Series Number 12, Ottawa

Kerr DE (1996) Late Quaternary sea level history in the Paulatuk to Bathurst Inlet area, Northwest Territories. Can J Earth Sci 33: 389–403

Kerr DE, Knight RD, Sharpe DR, Cummings DI, Kjarsgaard BA (2014) Surficial geology, Snowdrift, NTS 75-L, Northwest Territories. Geol Surv Can, Canadian Geoscience Map-137, (preliminary), scale 1:125000

Lemmen DS, Duk-Rodkin A, Bednarski JM (1994) Late glacial drainage systems along the northwest margin of the Laurentide ice sheet. Quat Sci Rev 13:805–828

Langley Jr CC (1967) Stratigraphic analysis of a deep ice core from Greenland. US Army, Cold Regions Res and Engineering Lab Res, Rept 77, p 133

Lytton Minerals Limited (1996) Jericho diamond project. Unpublished submission in support of class a land use application. Submitted to DIAND, NWT Region, Yellowknife

Mackay JR, Dallimore SR (1992) Massive ice of the Tuktoyaktuk area, western Arctic coast, Canada. Can J Earth Sci 29:1235–1249

MacDonald GM, Edwards TWD, Moser KA, Pienitz R, Smol JP (1993) Rapid response of treeline vegetation and lakes to past climate warming. Nature 361:243–246

Moser KA, MacDonald GM (1990) Holocene vegetation change at treeline north of Yellowknife, Northwest Territories, Canada. Can J Earth Sci 24:227–239

Padgham WA, Fyson WK (1992) The Slave Province: a distinct Archaen craton. Can J Earth Sci 129:2072–2086

Pell J (1994) Kimberlites and diamond exploration in the Central Slave Province, N.W.T. (75 M, N; 76 C, D, E, F; 85 P; 86 A, H). Department of Indian and Northern Affairs. EGS-1995-1, scale 1:500000

Rampton VN (2000) Large-scale effects of subglacial meltwater flow in the southern Slave Province, Northwest Territories. Can J Earth Sci 37:81–93

Stern RA, Bleeker W (1998) Age of the world' oldest rocks refined using Canada's SHRIMP: the Acasta Gneiss Complex, Northwest Territories, Canada. Geosci Can 25:27–31

St-Onge DA (1984) Surficial deposits of the Redrock Lake Area, District of Mackenzie. Geol Surv Can, Curr Res Part A, Paper No. 84-1A, pp 271–278

Wheeler JO, Hoffman PF, Card KD, Davidson A, Sanford BV, Okulitch AV, Roest WR (1996) Geological map of Canada. Geol Surv Can, "A" Series Map 1860A, scale 1:5000000

Wolfe SA (1997) Permafrost research and monitoring stations northern West Kitikmeot: Slave Geological Province. Unpublished Report of Field Activities 96/97. Prepared for DIAND, NWT Region, Yellowknife

Wolfe SA, Burgess MM, Douma M, Hyde C, Robinson S (1997) Geological and geotechnical investigations of ground ice in glaciofluvial deposits, Slave Geological Province, NWT. Geol Surv Can, Curr Res no. 1997-C, pp 39–50

Wolfe SA (1998) Massive ice associated with glaciolacustrine delta sediments, Slave Geological Province, N.W.T., Canada. In: Proceedings, 7th international conference on permafrost, Yellowknife, N.W.T. Nordicana Publication Number 57, pp 1125–1131

Great Slave Lowland: The Legacy of Glacial Lake McConnell

5

Stephen A. Wolfe, Peter D. Morse, Steve V. Kokelj, and Adrian J. Gaanderse

Abstract

The Great Slave Lowland of the Taiga Shield is an 11,000 km^2 low-elevation granitic bedrock plain along the north shore of Great Slave Lake, Northwest Territories. It is characterized by a mosaic of coniferous and deciduous forest cover, wetlands, sparsely vegetated bedrock outcrops, and peatlands. The region was glaciated until about 13,000 years ago and then inundated by Glacial Lake McConnell and by ancestral Great Slave Lake, which gradually declined towards the present lake elevation. Consequently, fine-grained glacilacustrine and nearshore lacustrine sediments are broadly distributed across the region. Permafrost is widespread within forest-covered sediments and peatlands, but is not sustained beneath bedrock outcrops, leading to an extensive, but discontinuous, permafrost distribution. Lithalsas, which are permafrost mounds up to 8 m in height and several hundred metres in length, are also abundant. These form by ice segregation within mineral soil, as permafrost aggrades into the fine-grained sediments following lake level recession. Lithalsas are most common within the first few tens of metres above the present level of Great Slave Lake, indicating that many are late Holocene in age and some <1000 years. These elevated surfaces favour the establishment of deciduous forests with thin organic ground cover and with mean annual ground temperatures typically between −0.5 and −1.5 °C. With annual mean air temperatures consistently warming since the 1940s, this terrain is vulnerable to thawing and subsidence, with impacts on the ecology, hydrology, and population of the region.

Keywords

Great Slave Lake • Glacial Lake McConnell • Discontinuous permafrost • Ground ice • Lithalsas

S.A. Wolfe (✉) · P.D. Morse
Geological Survey of Canada, Natural Resources Canada,
601 Booth St., Ottawa, ON K1A 0E8, Canada
e-mail: Stephen.wolfe@canada.ca

S.V. Kokelj
Northwest Territories Geological Survey, 4601-B 52 Avenue,
Yellowknife, NT X1A 2L9, Canada

A.J. Gaanderse
Cainthus Corporation, 14A Shehyn Lane, Nepean,
ON K2G 4Y3, Canada

© Springer International Publishing Switzerland 2017

O. Slaymaker (ed.), *Landscapes and Landforms of Western Canada*,
World Geomorphological Landscapes, DOI: 10.1007/978-3-319-44595-3_5

5.1 Introduction

Much of the western Canadian landscape is developed from relatively recent post-glacial processes, initiated after the retreat of late Wisconsinan glacial ice. Throughout western Canada, ice proximal lakes of varying spatial and temporal extent followed the retreating ice margins. Whereas the largest of these was Glacial Lake Agassiz (Teller et al. 1983), others including Glacial Lake Old Crow and Glacial Lake McConnell (Craig 1965; Zazula et al. 2004) were significant in defining the present-day character of regional landscapes. Glacial Lake McConnell covered nearly 15 % of present-day Northwest Territories, and associated fine-grained glacilacustrine and lacustrine sediments have had a profound effect on defining the landscape of the Great Slave Lowland along the north shore of Great Slave Lake. In particular, the distribution of lacustrine sediments largely defines the present-day distribution of permafrost in the region. Furthermore, as these fine-grained sediments are frost susceptible, and water was abundant as permafrost aggraded into emergent terrain, ice-rich terrain is common within the lowland. The region contains the highest population and density of infrastructure in the Northwest Territories, so changes to permafrost and the landscape will have significant impacts. Herein, the post-glacial evolution of the Great Slave Lowland is described, providing insight into the patterns and processes of the present-day landscape and its sensitivity to disturbance and climate change.

5.2 Geographical Setting

The Great Slave Lowland of the Taiga Shield is located along the north-western shore of Great Slave Lake, Northwest Territories, at latitudes of between 62°N and 63°N (Fig. 5.1). It is an 11,000 km^2 low-relief Precambrian granitic bedrock surface with silty clay deposits between bedrock outcrops. The lowland is bordered to the southwest by Great Slave Lake and the Taiga Plain and to the north by the Great Slave Upland of higher relief and bedrock occurrence.

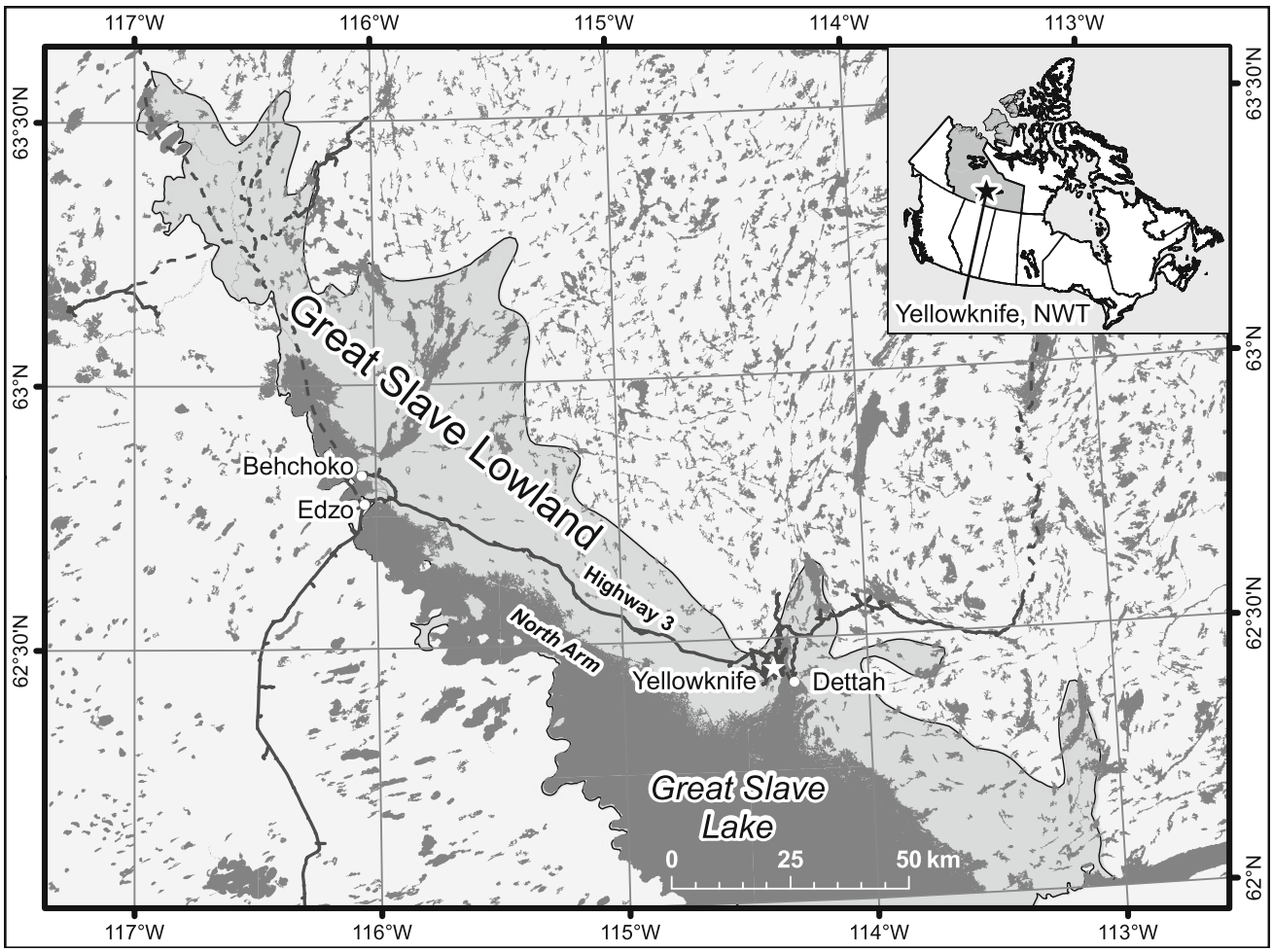

Fig. 5.1 Great Slave Lowland and surrounding area

Fig. 5.2 The Great Slave Lowland along the shoreline of Great Slave Lake. *Note* emergent islands and shorelines in the background, and exposed bedrock, coniferous forest, and deciduous forest cover in foreground

The region has a continental climate, with a mean annual air temperature of −4.1 °C and a mean total precipitation of 291 mm, with 41 % falling as snow. Numerous water bodies within this low-relief, poorly drained terrain separate the mosaic of biophysical environments in lowland (Fig. 5.2), in which forest fires are infrequent. The area is characterized mainly by black spruce (*Picea mariana*) forest with a heath understory on hummocky ground, barren bedrock outcrops with sparse jackpine (*Pinus banksiana*), and mixed black spruce and deciduous forest, which occupy, respectively, about 37, 25, and 25 % of the land. In contrast, white birch (*Betula papyrifera*) forests with herbaceous understory and open peatlands each constitute only about 1 and 2 % of land cover, respectively. The remaining land area consists of fens and bogs. The regional surface hydrology trends from north to south towards Great Slave Lake, but a low topographic gradient, numerous lakes and wetlands, and a rectilinear bedrock fault-controlled drainage pattern contribute to poor hydrological drainage across the area.

5.3 Glacial Lake McConnell

The region was glaciated until about 13,000 years ago and, with the retreat of the Laurentide Ice Sheet, was inundated by Glacial Lake McConnell. This immense lake formed along the retreating glacial margin between about 13,000 and 9500 years ago. Larger than any freshwater lake in existence today, this proglacial lake was named by Craig (1965) after R.G. McConnell, who first recognized the significance of the former high water levels in the Great Slave basin (McConnell 1890). At its maximum extent at about 10.7 ka BP, the lake included the combined basins of Great Bear, Great Slave, and Athabasca lakes (Fig. 5.3; also see Fig. 2.15). Lake McConnell was largely the result of differential glaci-isostatic loading, caused by regional differences in glacial ice thickness. Evidence of the lake exists today in the form of raised deltas, strandlines, beaches, and wave-washed eskers and drumlins. In the Great Slave basin, the maximum lake elevation is about 320 masl along north-eastern Great Slave Lake (Smith 1994), compared to only about 180 masl at Fort Smith (Vanderburgh and Smith 1988). This difference in elevation, due to differential isostatic uplift with greater uplift rates towards the northeast, has caused tilting of the basin towards the Fort Province outlet. The Great Slave Lowland was inundated to an elevation of what is now about 280 masl, a height of more than 100 m above the present-day lake level. During the subsequent recession, the lake first became disconnected from the Great Bear Basin, and then around 9500 years ago, water levels declined sufficiently to separate Great Slave Lake and Lake Athabasca basins (Lemmen et al. 1994). Ancestral

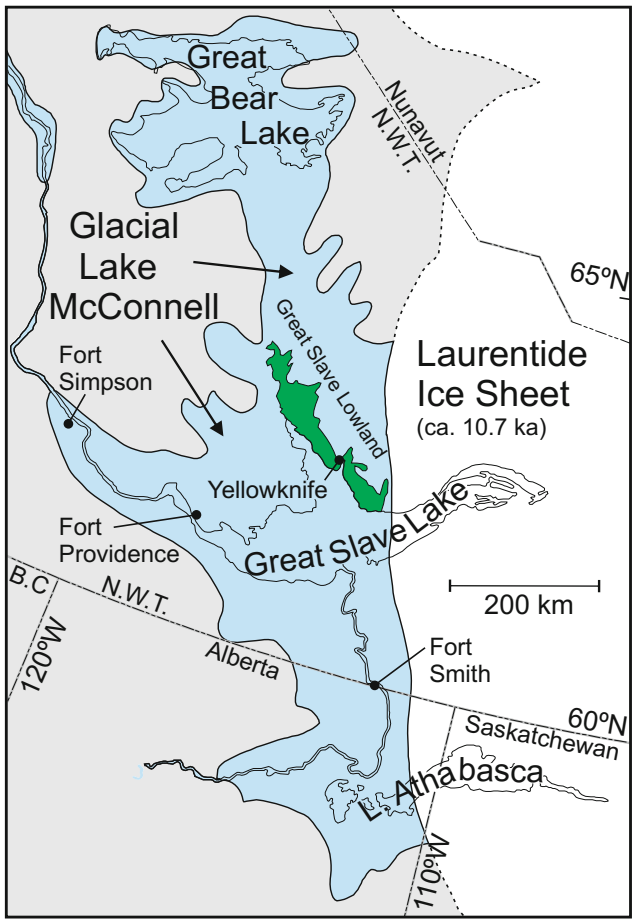

Fig. 5.3 Glacial Lake McConnell at its maximum extent approximately 10.7 ka ago as defined by Smith (1994)

Great Slave Lake continued to decline due to differential uplift, towards its present elevation of 156 masl. The present-day uplift at Yellowknife is reported to be on the order of 6.3 mm/a (Mazzotti et al. 2011). The recession of Great Slave Lake is constrained by Mackenzie River's outlet at Fort Providence, with differential uplift along the southern shore of the lake occurring at a rate of about 2 mm/a (Vanderburgh and Smith 1988).

Glacial Lake McConnell and the subsequent ancestral Great Slave Lake have left prominent signatures on the landscape in the form of extensive silt and clay deposits comprising nearly 70 % of the Great Slave Lowland (Wolfe et al. 2014; Fig. 5.1). Glacilacustrine sediments were deposited within topographic lows in shallow water during submergence and more extensively within deep-water basins. The lowland area, being submerged to depths of about 100 m, represented a depositional basin for the fine-grained sediments. In addition, ancestral Great Slave Lake further reworked and redeposited fine-grained sediments within nearshore environments during recession. Consequently, glacilacustrine and lacustrine deposits are broadly distributed across the region, with a profound influence on the regional distribution of permafrost and sensitivity of the terrain.

5.4 Permafrost Distribution and Thermal Regimes

The present-day permafrost extent within the lowland is considered to be extensively discontinuous, occupying 50–90 % of the land area with permafrost ground temperatures close to 0 °C (Heginbottom et al. 1995). Early studies reported permafrost within peatlands, where the organic layer was at least one metre thick, but not beneath bedrock outcrops or unconsolidated sediments where the organic cover was thin (Brown 1973). Surficial maps show, however, that peatlands occupy <3 % of the lowland area (Wolfe and Kerr 2014; Stevens et al. 2012). The majority of land cover is black spruce forest, or mixed deciduous and coniferous forest with stands of white birch forest (Morse et al. 2016). Geotechnical and geophysical surveys have found that ice-rich sediments are common beneath these forested terrains to depths exceeding 8 m (Wolfe et al. 2011, 2014). Indeed, in order to account for the extensive discontinuous distribution of permafrost in the region, permafrost must occur within most of the unconsolidated fine-grained sediments in the lowland.

Shallow ground thermal regimes under differing vegetation cover types indicate that permafrost exists in all major vegetation cover types underlain by fine-grained sediments in the Great Slave Lowland (Fig. 5.4). Mean annual ground temperatures range from −1.4 °C within black spruce forests to −0.02 °C in a burned peatland. Mean annual ground temperatures at sites with visible signs of permafrost degradation are generally warmer than −0.2 °C.

The depth of zero annual amplitude (DZAA in Fig. 5.4) represents the depth at which seasonal ground temperatures do not vary. Shallow depths (<7 m) indicate considerable damping of the annual surface temperature wave due to low thermal diffusivity of the earth materials. In the study area, this is attributed to the high latent heat content of a saturated active layer and warm, ice-rich permafrost in fine-grained lacustrine sediments. The DZAA is generally deeper at cold sites with thinner active layers and shallower at warmer sites with thick active layers. At the warmest sites, the DZAA is just beneath the permafrost table, and the annual mean ground temperature profile is isothermal near 0 °C. Many sites also demonstrate a temperature inversion in the upper part of the annual mean temperature profile with nearsurface permafrost temperatures being warmer than those at depth (Fig. 5.4). The inverted permafrost temperature profiles suggest non-equilibrium thermal conditions and permafrost warming.

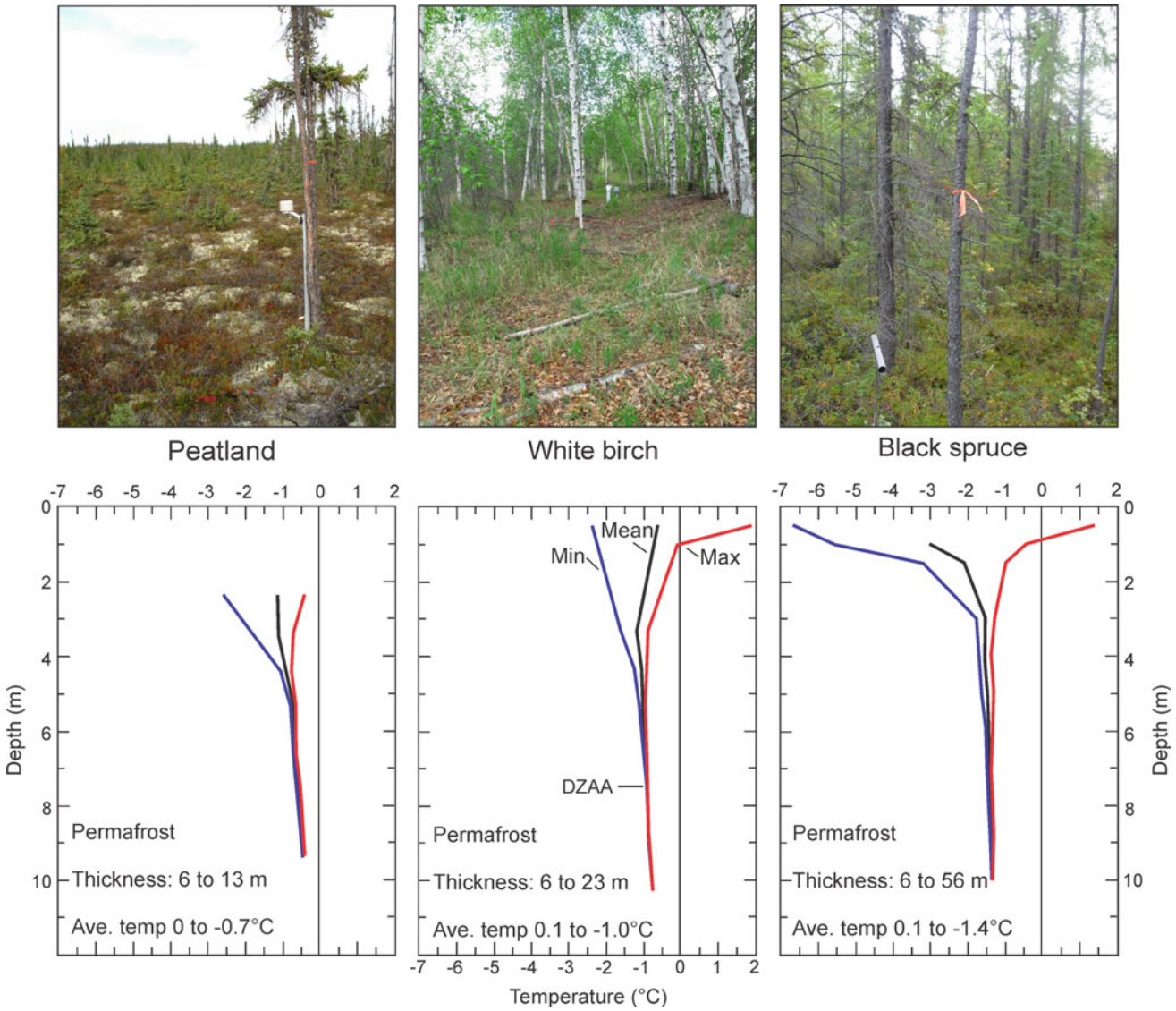

Fig. 5.4 Vegetation cover and thermal regimes within peatlands, black spruce forests, and deciduous birch forests together with associated ground thermal regimes. Temperatures shown are annual mean temperatures at depth, as well as the warmest and coldest annual temperatures that represent the seasonal ground temperature envelop. Also shown is the depth of zero annual amplitude (*DZAA*) for one envelope signifying the depth at which ground temperatures do not vary seasonally. Permafrost thickness and temperatures ranges are from Morse et al. (2016)

5.5 Lithalsas in the Great Slave Lowland

Lithalsas (Fig. 5.5a), first termed as such by Harris (1993), are permafrost mounds formed by ice segregation (i.e. by cryosuction without any hydrostatic pressure) within mineral soil that occur within the zone of discontinuous permafrost (Pissart et al. 1998). Previously referred to as minerogenic palsas (Ahman 1976), cryogenic (mineral) mounds (Payette and Séguin 1979; Lagarec 1982), and mineral palsas (Dionne 1978), lithalsas appear similar to palsas (Seppälä 1986) but lack a surface cover of peat (Pissart 2002). Lithalsas form as permafrost aggrades into saturated fine-grained sediments. Thermally driven moisture migration during soil freezing causes ice segregation, heave of the ground surface, and lithalsa growth (Calmels et al. 2008).

Lithalsas require three conditions to form such as warm but widespread discontinuous permafrost (not limited to organic peatland terrain), a substrate of fine-grained frost susceptible sediment, and available groundwater supplied from nearby taliks (Wolfe et al. 2014). Where these conditions are suitably fulfilled, lithalsas can be widespread and contain significant volumes of ground ice (Fig. 5.5b).

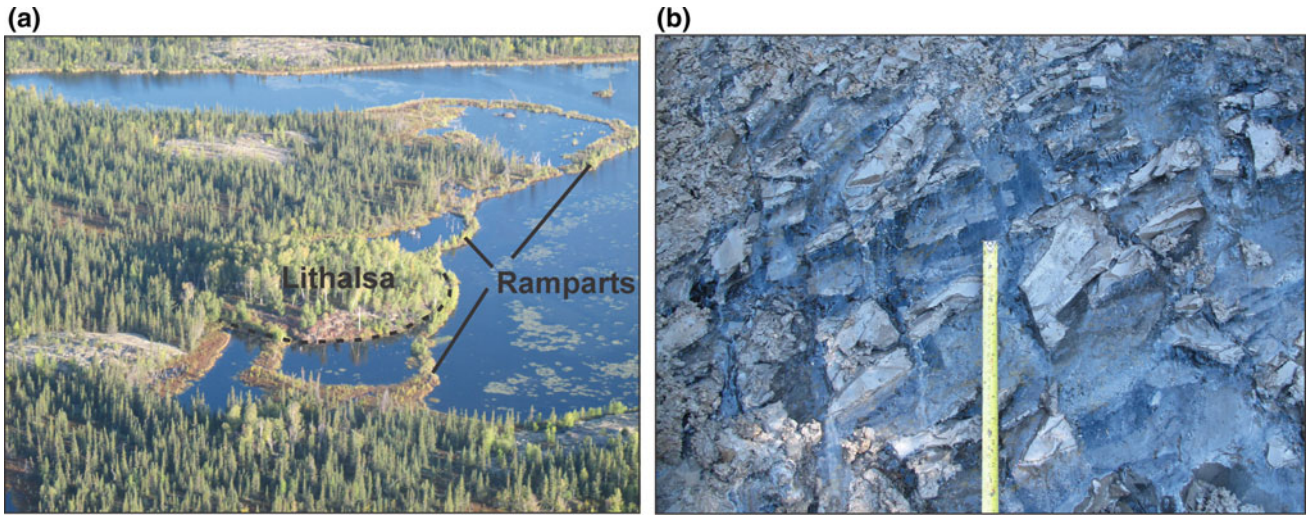

Fig. 5.5 Lithalsas and associated ground ice in the Great Slave Lowland; **a** lithalsa vegetated by white birch forest adjacent to a pond, with bedrock and black spruce forest on surrounding terrain. Ramparts represent shoreline margins of thawed lithalsas; **b** near surface ground ice exposed in the headwall of an active thaw slump in a lithalsa

In the Great Slave Lowland, nearly 1800 potential lithalsas are identified within fine-grained sediments (Wolfe et al. 2014). These lowland lithalsas formed following lake level recession as permafrost aggraded into emerging, saturated, and fine-grained glacilacustrine sediments; a substantial change in conditions that swept over the entire lowland area. They are most common within the first few tens of metres above the present level of Great Slave Lake, indicating that many are late Holocene in age and some <1000 years. They are primarily associated with the deciduous, white birch, forests with a thin organic cover and mean annual ground temperatures of between −0.5 and −1.5 °C. As lithalsas are a product of ice segregation, ground ice is common within a few metres of the ground surface and can exceed 70 % by volume relative to the surrounding mineral soil (Fig. 5.5b). Lowland lithalsas can grow to a height of 8 m and be many hundreds of metres in length.

The legacy of Glacial Lake McConnell and subsequent recession of ancestral Great Slave Lake have thus left clear signatures on the Great Slave Lowland. Permafrost aggradation into fine-grained sediments following lake level recession is related, in a time-transgressive manner, to the elevation above the present level of Great Slave Lake. For example, emergent terrain such as islands and nearshore environments represents conditions for permafrost aggradation (Fig. 5.2), whereas terrain at higher elevations has likely sustained permafrost for centuries to millennia.

Figure 5.6 shows a conceptual history of landscape and permafrost evolution in the Great Slave Lowland. With formation of Glacial Lake McConnell, glacilacustrine clays were deposited into the deep-water basin, until about 10,000 years ago (Fig. 5.6a). With lake level recession, waves and current reworked glacilacustrine clays and underlying sediments on bedrock uplands. These sediments were then redeposited as shallow water clays and nearshore silts within low-lying areas (Fig. 5.6b). With continued recession, topographic highs were terrestrially exposed, but with numerous ponds, shallow wetlands, and streams within the surrounding low-lying areas (Fig. 5.6c). Following emergence, permafrost aggraded into vegetated terrain with underlying fine-grained unconsolidated sediments (Fig. 5.6 d). The combined factors of relatively warm permafrost, gentle thermal gradients at depth, fine-grained sediments, and available groundwater supply were conducive to the development of segregated ice lenses and lithalsa formation (Fig. 5.6d, e). Permafrost degradation, due to fire disturbances, hydrological change, or warmer climate, induces subsidence of ice-rich terrain, leaving remnant ponds and ramparts that represent former margins of lithalsas adjacent to water bodies (Figs. 5.5a, 5.6f).

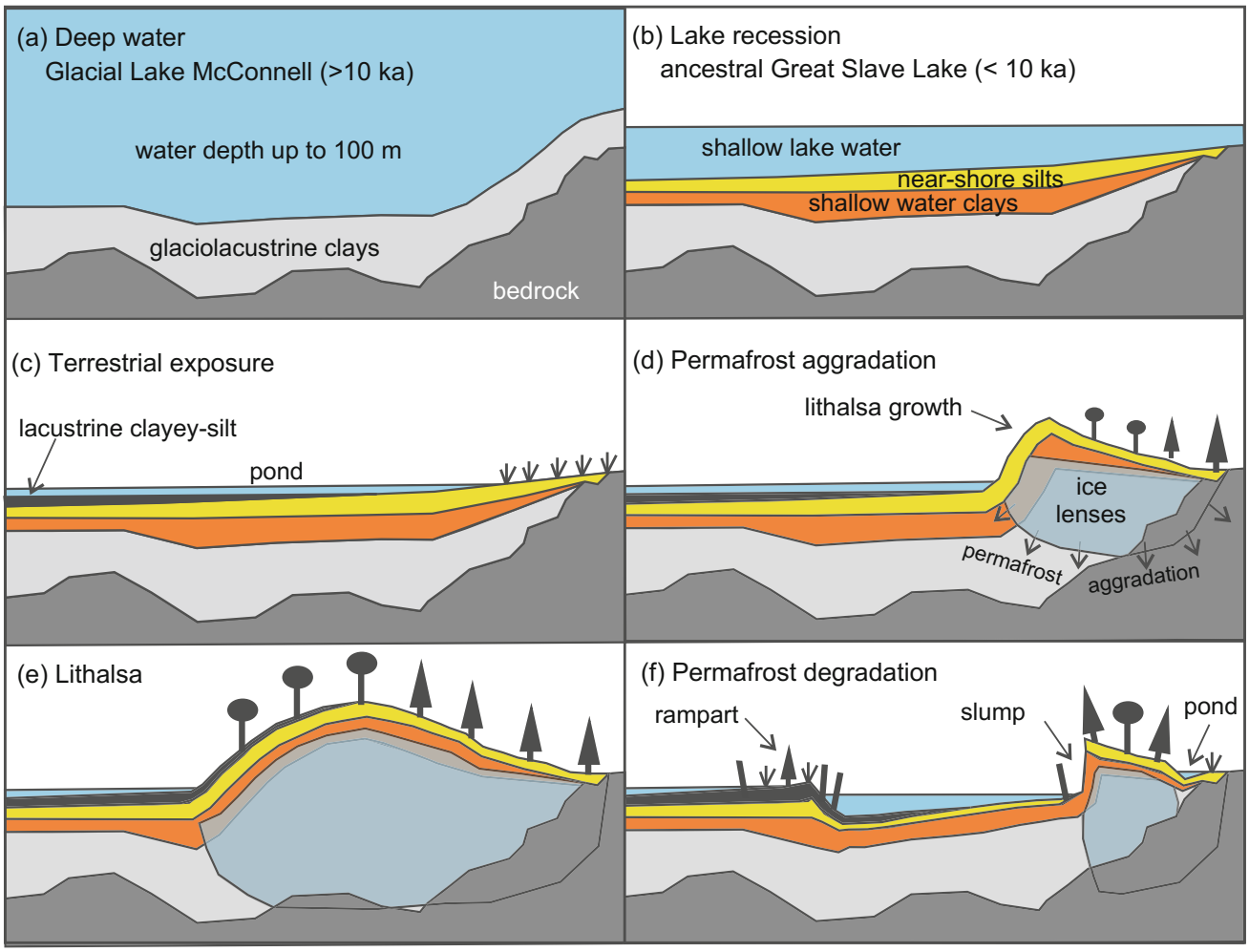

Fig. 5.6 Conceptual diagram of lake level history, terrestrial exposure, permafrost aggradation, lithalsa formation, and decay in the Great Slave Lowland

5.6 Permafrost Disturbance and Change

The Great Slave region is home to over half the population of the Northwest Territories, including the capital city of Yellowknife. In addition, the only overland access to this region is by a highway that traverses the Great Slave Lowland. Changes to permafrost in this region have numerous consequences for the environment and infrastructure. Thawing of permafrost beneath buildings and roadways can lead to ground subsidence and structural damage (Figs. 5.7, 5.8).

Annual mean air temperatures indicate a warming trend of about 0.3 °C per decade since the 1940s and an accelerated trend of about 0.6 °C per decade since 1970. With atmospheric warming, ice-rich terrain is vulnerable to thawing and terrain subsidence, with impacts on the ecology, hydrology, and population of the region. Evidence of permafrost warming and degradation in the lowland is widespread. Warm permafrost temperatures and inversions at the top of the ground temperature profiles are indicative of surface warming (Fig. 5.4) driven by increasing air temperatures and

Fig. 5.7 Thaw of permafrost beneath a heated building leading to loss of soil strength and significant ground subsidence

in some cases surface disturbance. In concert with increases in active layer thickness, this ground warming promotes thaw of nearsurface permafrost. On sloping terrain, thaw of ice-rich sediments can expose ground ice (Fig. 5.5b), leading to shoreline slumping and lithalsa decay together with wetland expansion (Fig. 5.6e, f). The common presence of decayed lithalsa terrain and ramparts within ponds throughout the lowland is indicative of degraded permafrost (Fig. 5.5a). Permafrost thaw in this terrain can significantly alter the structure and function of local ecosystems (Fig. 5.5; Ecosystem Classification Group 2008).

As noted earlier, the occurrence of extensive discontinuous permafrost in the Great Slave Lowland is attributed primarily to the presence of permafrost beneath forested areas underlain by unconsolidated fine-grained sediments and to localized peatlands. Notably, Zhang et al. (2014) have predicted that permafrost extent in this region could be reduced to only about 2.5 % by the end of the century, with permafrost occurring only within peatlands. This projection does not account for the substantive latent heat effect associated with ice-rich permafrost, which may aid to reduce the rate of thaw. Nevertheless, the air temperature-based predictions suggest that a transition to sporadic permafrost, in which frozen ground is restricted solely to peatlands, will have a profound effect on this region. Interestingly, if atmospheric warming also induces hydrological changes that

Fig. 5.8 Example of differential subsidence of highway infrastructure, due to permafrost thaw beneath the highway embankment. Note also significant lateral rotation of the highway embankment as depicted by the curvature of guard rails

saturate peatlands, they could degrade more rapidly than forest sites due to the high latent heat content of the saturated organic matter (Kokelj et al. 2014; Morse et al. 2016).

5.7 Conclusions

The Great Slave Lowlands illustrate the significant influence of a large glacial lake basin on the present-day western Canadian landscape. Conditions of fine-grained glacilacustrine and lacustrine sediments, a poorly drained, gradually emergent landscape, and aggradation of warm but widespread discontinuous permafrost, give rise to notably ice-rich terrain within extensive discontinuous permafrost. Very warm permafrost conditions and evidence of lithalsa decay occurring today suggest that much of this terrain is susceptible to thawing and subsidence under a warming climate. Bearing this in mind, the landscape may undergo profound alteration in the coming century.

References

Ahman R (1976) The structure and morphology of minerogenic palsas in northern Norway. Biul Peryglac 26:25–31

Brown RJE (1973) Influence of climatic and terrain factors on ground temperature at three locations in the permafrost region of Canada. In: Proceedings of the second international conference on permafrost, Yakutsk, USSR, North American Contribution, Washington, DC, National Academy of Science, pp 27–34

Calmels F, Allard M, Delisle G (2008) Development and decay of a lithalsa in Northern Quebec: a geomorphological history. Geomorphology 97:287–299

Craig BG (1965) Glacial Lake McConnell, and the surficial geology of parts of Slave River and Redstone River map-areas, District of MacKenzie. Geol Surv Can Bull 122

Dionne J-C (1978) Formes et phénomènes périglacaires en Jamésie, Québec subarctique. Géogr Phys Quat 32:187–247

Ecosystem Classification Group (2008) Ecological regions of the northwest territories—Taiga Shield. Department of Environment and Natural Resources, Government of the Northwest Territories, Yellowknife, NT, Canada. viii + p 146 + insert map

Harris SA (1993) Palsa-like mounds developed in a mineral substrate. In: Guangzhan W (ed) Sixth international conference on permafrost,

Beijing, China, vol 1. South China University of Technology Press, Guangzhou, pp 238–243
Heginbottom JA, Dubreuil MA, Harker PA (1995) Canada-permafrost. In: National Atlas of Canada, 5th edn. National Atlas Information Service, Nat Resourc Can, Ottawa, MCR 4177
Kokelj SV, Lantz TC, Wolfe SA, Kanigan JC, Morse PD, Coutts R, Molina-Giraldo N, Burn CR (2014) Distribution and activity of ice wedges across the forest-tundra transition, western Arctic Canada. J Geophys Res Earth Surf 119:2032–2047
Lagarec D (1982) Cryogenic mounds as indicators of permafrost conditions, northern Quebec. In: Proceedings of the fourth Canadian permafrost conference. NRC Press, Ottawa, pp 43–48
Lemmen DS, Duk-Rodkin A, Bednarski JM (1994) Late glacial drainage systems along the northwest margin of the Laurentide ice sheet. Quat Sci Rev 13:805–828
Mazzotti S, Lambert A, Henton J, James TS, Courtier N (2011) Absolute gravity calibration of GPS velocities and glacial isostatic adjustment in mid-continent North America. Geophys Res Lett 38: L24311
McConnell RG (1890) Report on an exploration in the Yukon and Mackenzie Basins, N.W.T. Geol Surv Can, Ann Rpt 4, 1888–1889, Part D
Morse PD, Wolfe SA, Kokelj SV, Gaanderse AJR (2016) The occurrence and thermal disequilibrium state of permafrost on forest ecotopes of the Great Slave region, Northwest Territories, Canada. Permafrost Periglacial Process 27:145–162
Payette S, Séguin M-K (1979) Les buttes minérales cryogènes dans les basse terres de la Revière aux Feuilles, Noveau-Québec. Géogr Phys Quatern 33:339–356
Pissart A (2002) Palsas, lithalsas and remnants of these periglacial mounds. A progress report. Prog Phys Geogr 26:605–621
Pissart A, Harris S, Prick A, Vliet-Lanoe V (1998) La signification paleoclimatique des lithalsaes (palses minerals). Biul Peryglac 37:141–152
Seppälä M (1986) The origin of palsas. Geogr Ann A 68:141–147
Smith DG (1994) Glacial Lake McConnell: paleogeography, age, duration and associated river deltas, Mackenzie River Basin, western Canada. Quat Sci Rev 13:829–843
Teller JT, Thorleifson LH, Dredge LA, Hobbs HC, Schreiner BT (1983) Maximum extent and major features of Lake Agassiz. In: Teller JT, Clayton L (eds) Glacial Lake Agassiz. Geol Assoc Can, St. Johns, pp 43–45
Stevens CW, Kerr DE, Wolfe SA, Eagles S (2012) Predictive surficial material and geology derived from LANDSAT 7, Yellowknife, NTS 85J, NWT. Geol Surv Can Open File No. 7106
Vanderburgh S, Smith DG (1988) Slave River delta: geomorphology, sedimentology, and Holocene reconstruction. Can J Earth Sci 25:1990–2004
Wolfe SA, Kerr DE (2014) Surficial geology, Yellowknife area, Northwest Territories, parts of NTS 85-J/7, NTS 85-J/8, NTS 85-J/9 and NTS 85-J/10, Geol Surv Can CGM 183
Wolfe SA, Stevens CW, Gaanderse AJ, Oldenborger GA (2014) Lithalsa distribution, morphology and landscape associations in the Great Slave Lowland, Northwest Territories, Canada. Geomorphology 204:302–313
Wolfe SA, Duchesne C, Gaanderse A, Houben AJ, D'Onofrio RE, Kokelj SV, Stevens CW (2011) Report on 2010–2011 permafrost investigations in the yellowknife area, northwest territories. Geol Surv Can Open File 6983, Northwest Terr Geosci Off NWT Open Report 2011-009, 1 CD-ROM
Zazula GD, Duk-Rodkin A, Schweger CE, Morlan RE (2004) Late Pleistocene chronology of glacial Lake Old Crow and the north-west margin of the Laurentide Ice Sheet. In: Ehlers J, Gibbard PL (eds) Quaternary glaciations: extent and chronology, part II: North America. Elsevier, Amsterdam, pp 347–362
Zhang Y, Olthof I, Fraser R, Wolfe SA (2014) A new approach to mapping permafrost and change incorporating uncertainties in ground conditions and climate projections. Cryosphere 8:2177–2194

The Banks Island Tundra

6

Hugh M. French

Abstract

The Banks Island tundra consists of undulating topography underlain by poorly lithified sand and shale bedrock that is covered by a veneer of Quaternary sediments. This lowland terrain contains a diversity of arctic dwarf shrubs, grasses, sedges and flowering plants that support a productive ecosystem. The landscape consists of broad fluvial surfaces that are currently being modified by weak fluvial incision and mass wasting processes. It is a permafrost landscape that contains ice-wedge polygons, thermokarst lakes and ponds, frost mounds and active-layer phenomena.

Keywords

Tundra • Permafrost • Active layer • Fluvial activity • Ice-wedge polygons • Frost mounds • Thermokarst

6.1 Introduction

Banks Island is located in the western Canadian Arctic between latitudes 72°N and 74°N (Fig. 6.1, inset). It is the fourth largest island in the Canadian Arctic and covers an area of ~70,000 km^2. The southern tip of the island is approximately 500 km north of treeline. The island is separated from the mainland of Canada by Amundsen Gulf, a water body that is ice-covered for more than 8–9 months of the year. The only permanent settlement on Banks Island is the small Inuit community of Sachs Harbour (Ikahuak), located on the southwestern tip of the island. Much of northern Banks Island is within Aulavik National Park, created in 1992 (see Chap. 29).

The tundra lowlands of central and western Banks Island consist of undulating terrain with broad gentle slopes developed upon poorly consolidated Mesozoic age sediments (Thorsteinsson and Tozer 1962; Miall 1979; Fyles et al. 1994). These vary in lithology from shale of the Christopher Formation (Cretaceous age) to sand and gravel of the Eureka Sound (Middle–Tertiary age) and Beaufort (Late Tertiary age) formations. Relative relief varies from less than 50 m to over 250 m. The slopes are covered with an extensive but thin veneer of till and glacifluvial deposits. Much of the landscape consists of broad fluvial surfaces, probably formed by meltwater that flowed westwards away from the decaying Laurentide Ice Sheet to the east.

6.2 Climate

The climate experienced by these tundra lowlands is illustrated by data from Sachs Harbour (72°N), located on the southwest coast. These records (Table 6.1) suggest mean annual air temperature is −14 °C and mean monthly values in the winter fall below −30 °C. During the short 2- to 3-month summer, they range between 1 and 5 °C. Field records from sites in the interior of the island suggest summer air temperatures can exceed 10 °C on occasions.

Total annual precipitation is small, approximately 200 mm per year. In many respects, the tundra environment

H.M. French (✉)
Departments of Geography and Earth Sciences,
University of Ottawa, Ottawa, ON K1N 6N5, Canada
e-mail: hmfrench@shaw.ca

H.M. French
Department of Geography, University of Victoria,
Victoria, BC V8R 3R4, Canada

© Springer International Publishing Switzerland 2017
O. Slaymaker (ed.), *Landscapes and Landforms of Western Canada*,
World Geomorphological Landscapes, DOI: 10.1007/978-3-319-44595-3_6

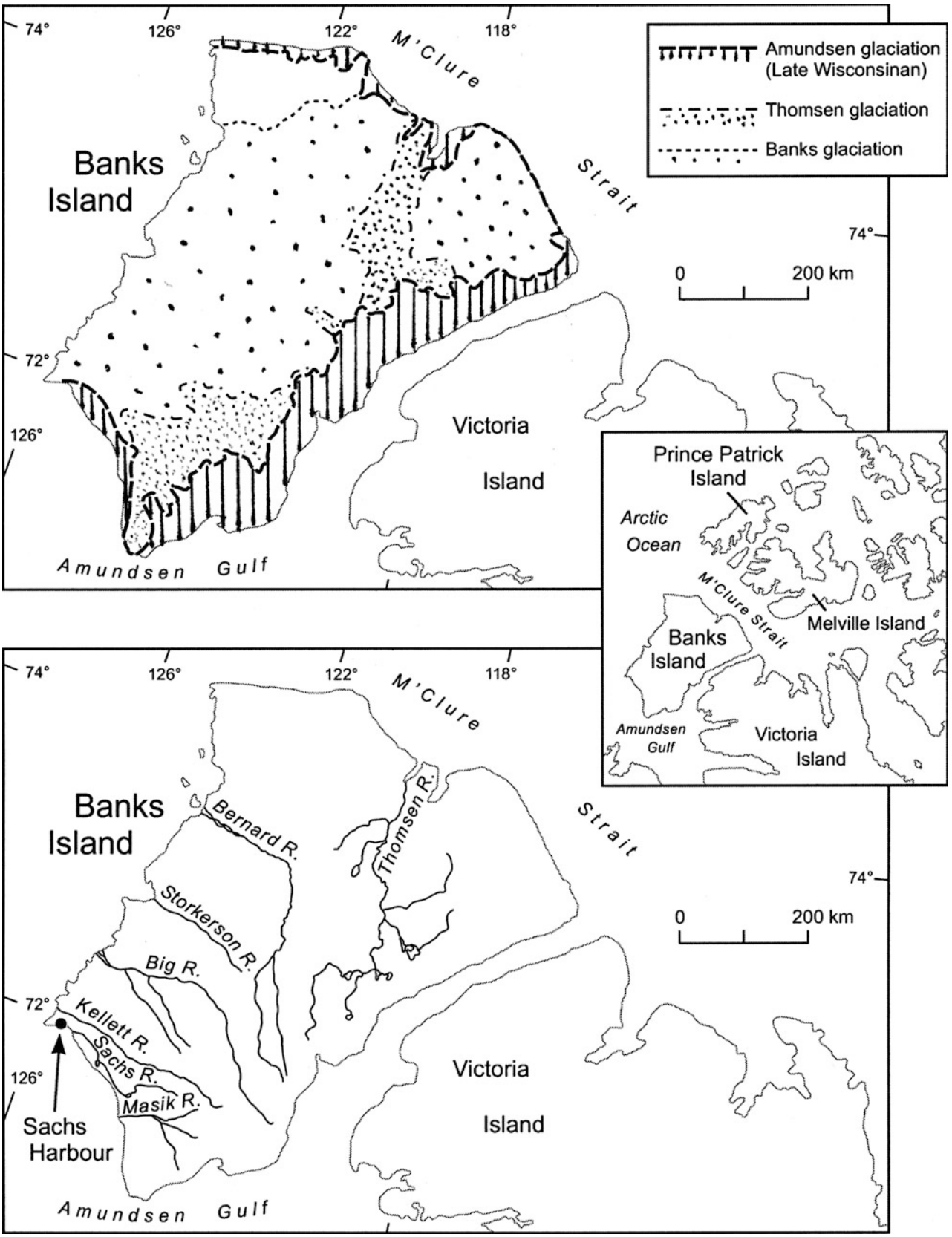

Fig. 6.1 Banks Island, western Canadian Arctic: location (*inset*), limits of Quaternary glaciation (after Vincent 1982, 1983) (*upper*), and major drainage systems (*lower*). Only the northwest corner of the island (the Beaufort Plain) is thought to have been unaffected by glaciation. The location of Sachs Harbour is indicated on the lower map

Table 6.1 Average monthly temperature and precipitation data and frost statistics for Sachs Harbour (lat. 71°57′N; long. 124° 44′W, 92.0 masl) 1955–1970

Month	Temperature (°C)	Precipitation		Frost data	
		Rain (mm)	Snowfall (cm)		
Jan	−29.7	–	41.4	Thawing degree-days (TDD)	~400
Feb	−30.9	–	43.7	Freezing degree-days (FDD)	~5,500
Mar	−27.3	–	46.5	Frost-free period (days)	15
Apr	−19.2	–	49.0	Number of Freeze-thaw cycles, annual average	19.6
May	−7.3	T	55.9		
Jun	+2.2	5.8	57.9		
Jul	+5.6	21.8	2.0		
Aug	+4.3	39.9	6.1		
Sept	−1.8	45.55	14.0		
Oct	−11.6	45.5	27.9		
Nov	−21.7	–	35.1		
Dec	−26.7	–	39.9		
Average	−13.7	–	–		

From Maxwell (1980)

should be regarded as a cold desert (see Chap. 13). Approximately 40 % of the annual precipitation falls as rain during the summer months (see Table 6.1). Because of low temperatures, its effectiveness is high and evaporative losses are relatively small. As a result, summer rain quickly percolates into the seasonally thawed layer (the active layer, see below). The majority of precipitation falls as snow during the rest of the year; much sublimates and wind redistributes the remaining snow into either gullies or lee-slope positions. Thus, during the winter months, many of the interfluves and higher elevations are largely bare of snow. This uneven spatial distribution of snow allows not only frost to quickly penetrate snow-free surfaces in winter but also concentrates snowmelt runoff in a brief 2- to 3-week period during the early summer.

6.3 Late Quaternary History

The Late Quaternary history of the island is still unresolved. Based upon a widespread veneer of glacigenic and surficial materials, a complex sequence of Quaternary glaciations has been proposed (Vincent 1982, 1983). During the latest (Amundsen) advance of the Late-Wisconsinan (Laurentide) Ice Sheet, ice reached the eastern part of the island and ice lobes extended westwards into Amundsen Gulf and McClure Strait. Under this scenario, the central lowlands remained ice-free during the Late Quaternary and only the extreme northwest was unaffected by Quaternary glaciation (see Fig. 6.1, upper).

More recent investigations (England et al. 2009; Lakeman and England 2014) suggest cold-based Laurentide ice extended across the entire island during the Late Quaternary. Such a history might explain anomalous drainage patterns on the island, large palaeo-outwash surfaces and terraces, and the seemingly random occurrence of glacigenic sediments, kame-like features and scattered erratics. A further consideration is the apparent absence of any faunal remains from central Banks Island that can be radiocarbon dated to the last major cold period (~40–20 ka). If this area were ice-free at that time, it would have acted as a refugium for both plants and animals. Yet only a single muskoxen bone, taken from a gravel bar of the Bernard River and dated at >34 ka (Maher 1968), has been found from this time period.

On balance, it seems likely that a thin and stationary (cold-based) ice sheet covered all of central and western Banks Island during the height of the last cold period and that this ice probably disintegrated in situ. What can be assumed with reasonable certainty is that the central and western lowlands have been free of a perennial ice cover for at least 10–15 ka.

6.4 Permafrost and Ground Ice Conditions

Banks Island lies within the zone of continuous permafrost. Deep temperature measurements have been made at only one locality, the Storkerson Bay I-15 exploratory well site located ~110 km north of Sachs Harbour. Here, the mean annual ground temperature at the depth of zero annual amplitude is −13.1 °C (Taylor and Judge 1977). In all probability, permafrost thicknesses exceed 300–500 m on the island. Typically, maximum active-layer thicknesses vary between 50 and 75 cm, depending upon local site conditions.

In areas of continuous and thick permafrost, the presence of water bodies can result in unfrozen zones, or táliks. This is the case on Banks Island where numerous lakes and ponds exist and where large rivers, such as the Thomsen, Bernard and Big, drain the central and western lowlands. In particular, a few of the larger lakes that do not freeze to the bottom in winter are well known to residents of Sachs Harbour because they usually contain arctic char and trout.

In the absence of good exposures and/or detailed borehole sampling, ground ice amounts on the tundra lowlands of central and western Banks Island can only be approximated. Judging by conditions in the Sachs River lowlands (Fig. 6.2), ice may constitute ~50–55 % of the upper 8.0 m of permafrost (French and Harry 1983). This explains the numerous thermokarst lakes and ponds that cover the tundra; most are small, less than 200–300 m in diameter and generally shallow, less than 2.0–3.0 m deep.

6.5 Snow, Soil and Vegetation Interaction

An intimate relationship exists between snow, wind and vegetation in the High Arctic islands. This was first highlighted by the Canadian botanist Porsild (1955, 60–67; 1957, 5–7) and is especially applicable to Banks Island. So-called snowbed habitats are favoured localities for vegetation growth. Other favoured habitats for vegetation growth are gullies, poorly drained valley bottoms and low-level fluvial terraces. All accumulate wind-blown snow in winter. Areas of closed vegetation constitutes anywhere between 60 and 90 % of the island landscape. Woody shrubs occur in a few sheltered localities, but trees are absent.

The lowlands of central and western Banks Island illustrate the climatic and ecological transition between low-arctic tundra, high-arctic tundra and polar semi-desert landscapes (Bliss 1997; Tedrow 1974; Tedrow and Douglas 1964). The vegetation zonations are listed in Table 6.2. The transition is largely controlled by topography, parent material and drainage. For example, Fig. 6.3 illustrates the ecological change along typical mesotopographic profiles across the Banks Island tundra. They portray the progressive transition from bog tundra, sedge-moss tundra and moss-graminoid tundra in the lowlands to cushion plant–lichen communities on the uplands. This transition is accomplished by gentle slopes dominated by mass wasting at snowbank sites while, higher up the slopes, earth hummocks become widespread.

6.6 The Role of Wind

The direct role of wind in fashioning the tundra landscape of Banks Island is relatively small. The main geomorphic effects are to (1) remove fine particles from bare surfaces during winter, (2) encourage the formation of saline and alkaline soil through the rise of capillary moisture and (3) redistribute snow and wind-blown sediment in winter to gullies and valley bottoms where these sediments form localised niveo–aeolian deposits. Additionally, many bare alluvial surfaces within the larger river valleys experience local, thermally induced, winds ('dust devils') that cause deflation and localised cover-sand deposition in summer (Pissart et al. 1977).

The indirect effects of wind are more subtle and most obvious on the northwest and southwest corners of the island that experience consistent south-westerly winds coming from the southern Beaufort Sea. For example, the preferential accumulation of snow on the lee (east facing) slopes results in the asymmetry of stream valleys in the extreme northwest (French 1971a), while the formation of oriented (D-shaped) thaw lakes in southwest Banks Island (see Fig. 6.2) is thought to be related to wind action (Harry and French 1983).

6.7 A Highly Productive Ecosystem

The intense winter cold and the absence of sunlight for 4–5 months each year inhibit plant growth and photosynthesis. Despite this, the Banks Island tundra supports a highly productive ecosystem. This was the major reason why mainland Inuit established a permanent settlement at Sachs Harbour in the late 1940s in order to hunt caribou and trap white fox. While the uplands are dominated by polar desert and semi-desert plant communities, the river valleys and undulating lowlands support arctic dwarf shrubs, grasses, sedges and flowering plants. These tundra meadows attract a diversity of species. For example, more than 15,000 muskoxen live in Aulavik National Park alone and total numbers on the island currently exceed 20–30,000, the highest density for this animal in the entire Arctic. This is all the more remarkable given that the first muskoxen in recent times are thought to have migrated across the ice from Melville Island in the late 1960s. In addition to herds of muskoxen and caribou, arctic fox and wolf range widely, lemmings are

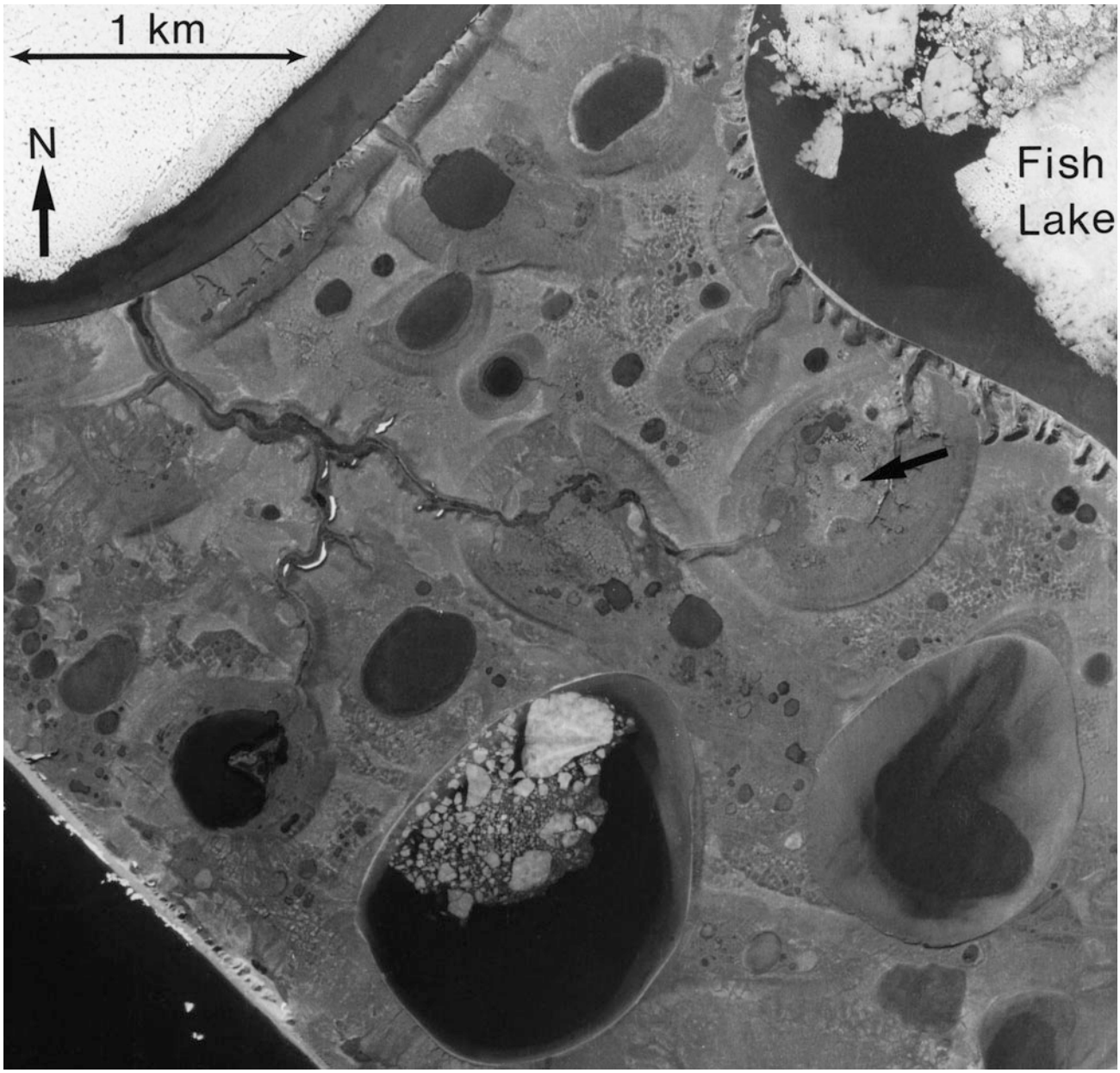

Fig. 6.2 Vertical air photograph of part of the Sachs River lowlands, southern Banks Island (centred on lat. 71°50′N, long 124°35′W) showing elliptical D-shape and preferred orientation of thaw lakes (see Harry and French 1983). There are also numerous drained thaw lake basins, one of which contains a small pingo (*arrow*). National Air Photo Library, Natural Resources Canada, Ottawa, A15980-25

abundant in most years and migratory birds such as snow geese, ducks and snowy owls are numerous in the summer months. Muskoxen meadows, the dens of foxes and the nesting areas of geese, owls and hawks are marked by tundra grasses because of the release of nutrients. Of special geomorphological note are 'owl perches', small mounds of enriched organic matter that may be as much as 0.75 m above the level of the surrounding tundra. In many ways, the tundra landscape of Banks Island is a paradise for northern fauna and flora.

6.8 A Snowmelt-Derived Fluvial Landscape

At first sight, and at the macro-scale, the tundra landscape appears to be snowmelt-derived and fluvially dominated. A number of shallow west- and northwest-aligned valleys dissect the tundra (Fig. 6.1, lower). These valleys contain broad fluvial terraces that reflect previously higher discharges while, in the central part of the island, clearly defined outwash channels and alluvial fans testify to the formerly large meltwater discharges that must have crossed

Table 6.2 Three different vegetation zonations of Banks Island and the main biogeographic zones and major vegetation types within the Russian and North American Arctic

Russian Arctic[a]	Tundra					Polar Desert	
	Subarctic Tundra			*Arctic Tundra*			
	Southern variant	Middle variant	Northern variant	Southern variant	Northern variant	Southern variant	Northern variant
North American Arctic[b]	Low-Arctic Tundra				Mid-Arctic Subpolar Desert	High-Arctic Polar Desert	
North American Arctic[c]	Low Arctic					High Arctic	
			Tundra		*Tundra*	*Polar Semidesert*	*Polar Desert*
	Tall-shrub tundra	Low-shrub tundra	Dwarf-shrub-heath tundra	Dwarf-shrub heath tussock tundra	Graminoid-moss tundra Low-shrub tundra Dwarf-shrub-heath tussock tundra	Cushion-plant cryptogam Cryptogam-herb	Herb-cryptogam
	Graminoid-moss tundra		Cushion-plant cryptogam tundra				
	B a n k s I s l a n d						

Modified from Bliss (1997)

[a]Andreyev and Aleksandrova (1980)
[b]Tedrow (1974)
[c]Bliss (1997)

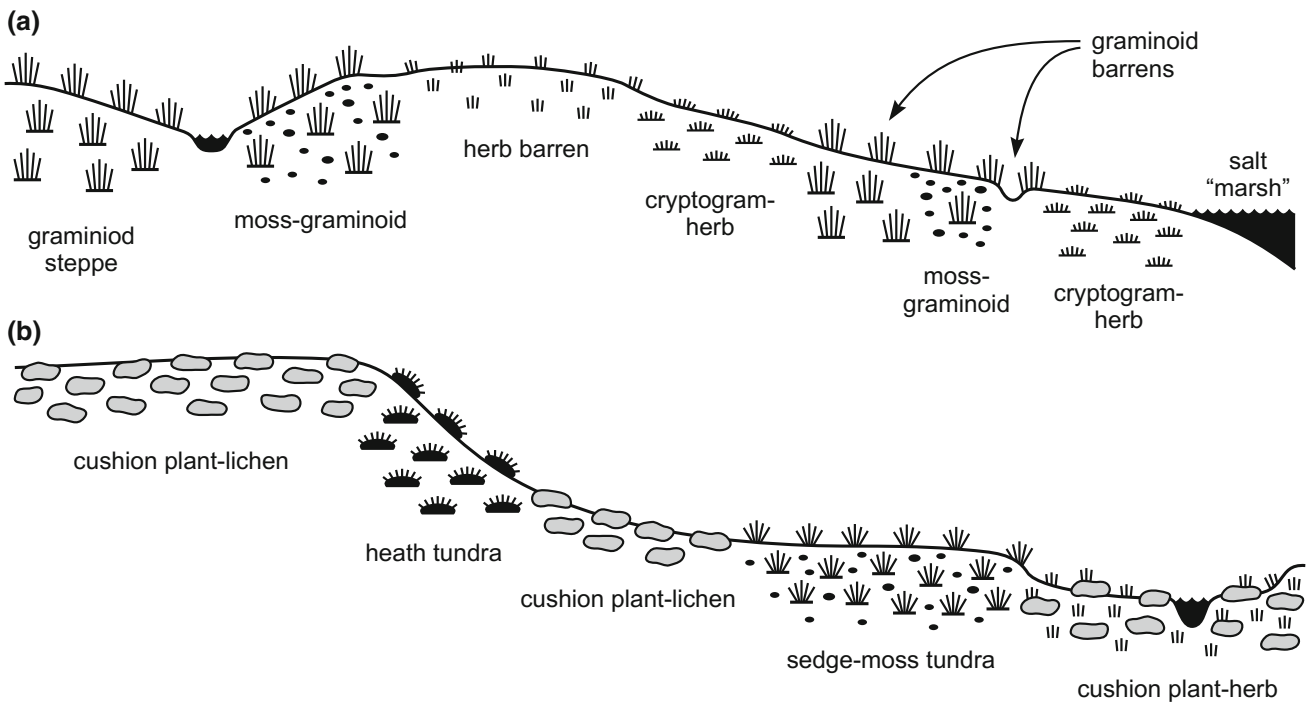

Fig. 6.3 Typical mesotopographic profiles of the vegetation assemblages on **a** the lowland and **b** the upland tundra of Banks Island. Modified after Bliss (1997)

the island as the Laurentide Ice Sheet progressively decayed. Thus, the current drainage system is largely misfit. Only on the Beaufort Plain of northwest Banks Island is there a relatively simple and well-integrated drainage pattern. It is significant that this part of the island is thought to have never been glaciated.

Today, most of the major rivers of the island, such as the Bernard, Storkerson, Kellett and Big, flow in braided channels within broad shallow valleys (Figs. 6.4, 6.5a). The braiding reflects the concentration of runoff in the spring melt combined with the high sediment load derived from the weakly consolidated sands and gravels of the Beaufort and Eureka Sound formations that are exposed in the river banks. Everywhere, the low poorly drained fluvial terraces are characterised by ice-wedge polygons, thaw lakes and ponds (see Fig. 6.2). In places, the formation of seasonal frost mounds and icing blisters can be observed on current floodplains in mid- and late winter (Fig. 6.5b). Elsewhere, the vestiges of palaeo-outwash channels, now abandoned, and the remnants of clusters of seasonal frost mounds can be

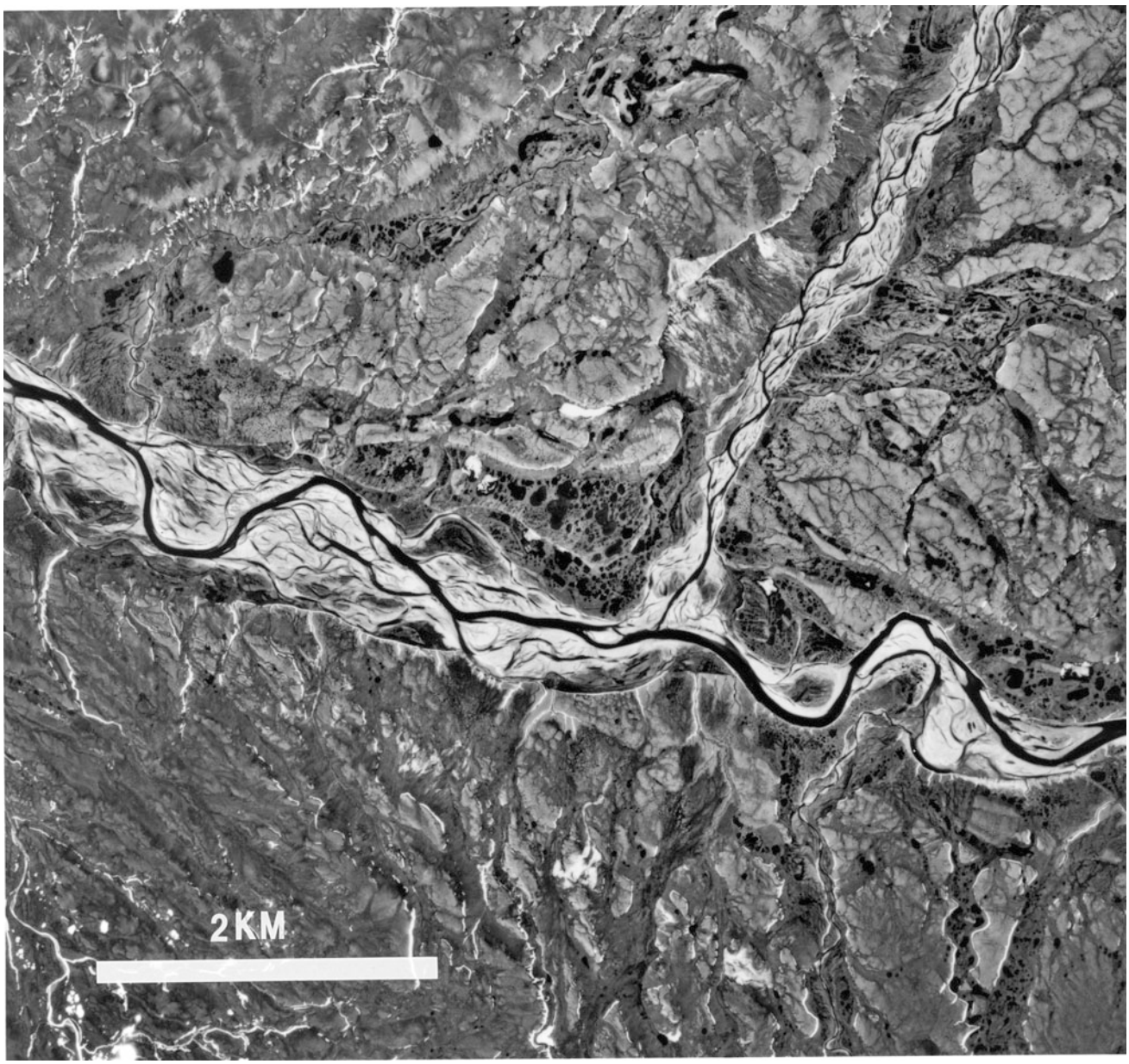

Fig. 6.4 Vertical air photograph of part of the Bernard River, central Banks Island (centred on lat. 73°45′N, long. 122°15′W), showing the braided river channel flanked by an alluvial floodplain and two low-level terraces. The current drainage is misfit. The slopes of former meltwater channels on the surrounding uplands are being modified by mass wasting processes. Thermokarst lakes and ponds occur on the low terraces (see French and Dutkiewicz 1976). National Air Photo Library, Natural Resources Canada, Ottawa, A17564-48

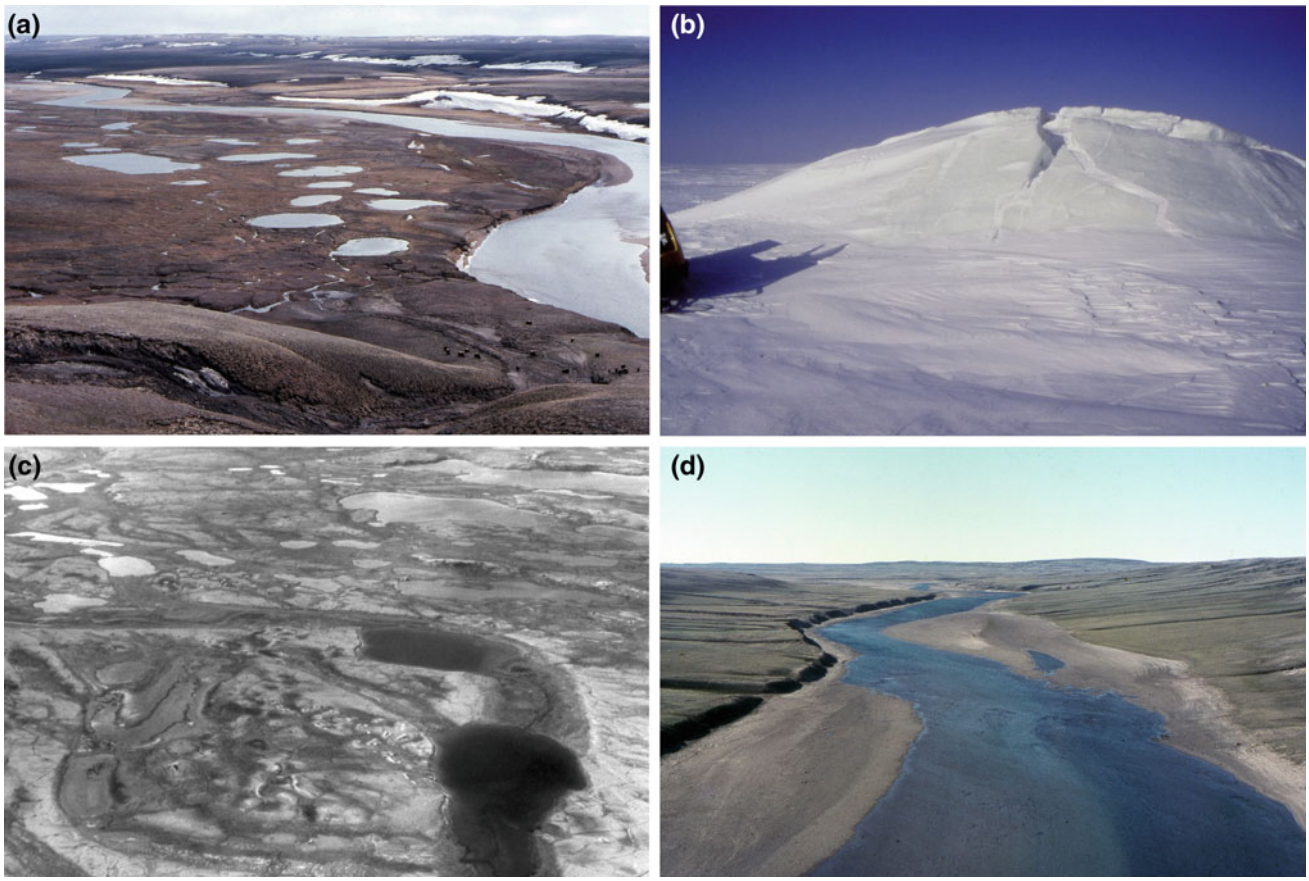

Fig. 6.5 The fluvial landscapes of Banks Island. **a** The Kellett River valley, southern Banks Island, consists of well-vegetated fluvial surfaces that contain thaw lakes, ice-wedge polygons and grazing muskoxen. An active-layer detachment failure can be seen in the immediate foreground. *Photograph*—H.M. French. **b** A seasonal frost mound (icing blister) on the floodplain of the Big River, central Banks Island. The photograph was taken in April 1979 by David Nasagaloak, a member of the Sachs Harbour Hunters and Trappers Association, while inspecting one of his white fox trap lines. Photograph is courtesy of David Nasagaloak. **c** An oblique air view of a palaeo-outwash channel in central Banks Island. A number of small circular and elongate ridges and enclosed depressions on the palaeo-braid-bar surface are thought to be the remnants of seasonal frost mounds and/or icing blisters. *Photograph*—H.M. French. **d** The Thomsen River, the longest on Banks Island, drains the central lowlands. It flows north for much of its length in a single channel. The river is a route for tourists travelling by canoe through Aulavik National Park. The photograph is looking downriver. *Photograph*—H.M. French

identified (Fig. 6.5c). A notable exception to the west-flowing streams is the northward-flowing Thomsen River (Fig. 6.5d). This river has a predominantly single, often straight, channel. The absence of braiding is best explained by the shale bedrock across which it flows for much of its length, the cohesive nature of the river banks and the correspondingly lower sediment load. Where it traverses Aulavik National Park, the Thomsen River is well suited to kayak and canoe adventure camping. Access is via charter plane from either Sachs Harbour or Inuvik.

6.9 A Landscape of Mass Wasting

Closer examination reveals a landscape of gentle slopes upon which slow mass wasting processes dominate (Fig. 6.6a). Today, solifluction sheets and lobes are gradually obliterating the old fluvial channels and terraces. Typical rates of downslope movement range between 0.5 and 2.0 cm/year (French 1974; Egginton and French 1985). Movement is usually greatest below snowbank sites wherever sufficient moisture is available. By moving material from higher to lower elevations, solifluction contributes to a general flattening of the landscape.

Erosion by overland flow is also widespread, especially at, and below, snowbank sites. But there is a complex relationship between the availability of moisture during the melt season and vegetation cover (Lewkowicz 1983; Lewkowicz and Kokelj 2002). Correlation between surface runoff and vegetation cover reaches 100 % at about 300-mm annual runoff but further runoff results in a gradual decrease in vegetation. On Banks Island, quantitative field-derived estimates of erosion via suspended sediment suggest 1–5 mm/1000 years, but this probably increases to between

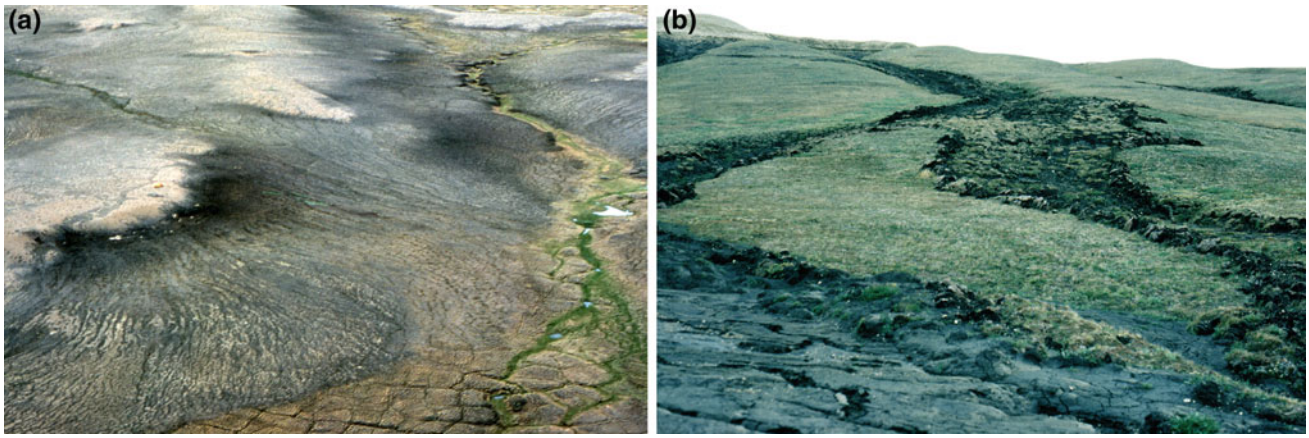

Fig. 6.6 The relationship between lithology and geomorphic processes on the Banks Island tundra. **a** Surfaces underlain by unconsolidated sediments (sand and gravel) favour mass wasting processes and result in gentle slopes characterised by non-sorted stripes and gelifluction sheets. The peaty, ice-wedge polygon terrain in the valley bottom is currently being eroded by a small stream. Location—Thomsen River valley, central Banks Island. *Photograph*—H.M. French. **b** Slopes underlain by shale of the Christopher Formation experience mudflows and active-layer detachment failures in years of exceptional summer thaw and/or after periods of summer rain. Picture was taken in July 1975 following heavy rain, in Masik Valley, southern Banks Island. *Photograph*—H.M. French

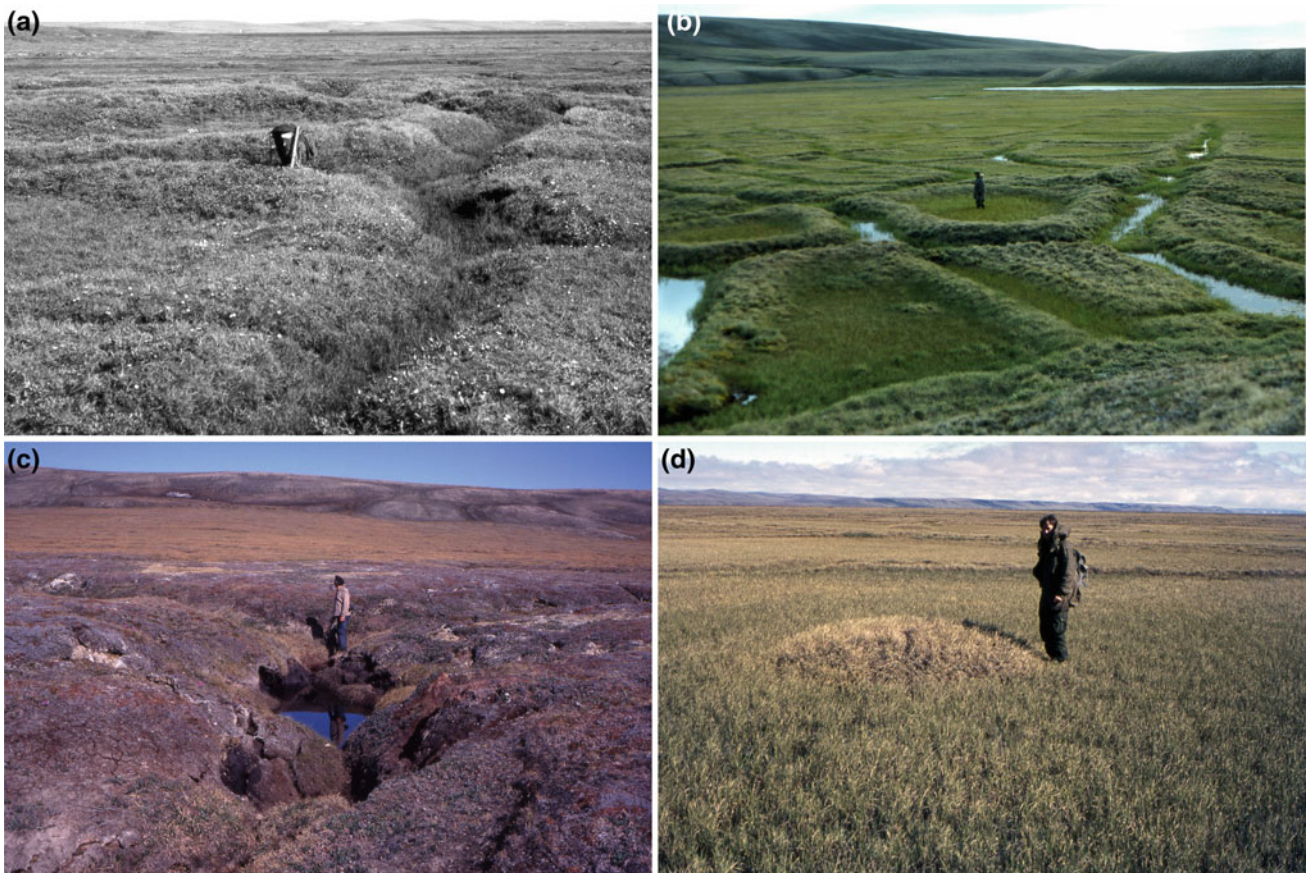

Fig. 6.7 Features of the lowland tundra landscape of Banks Island. **a** Much of the well-vegetated tundra is characterised by low-centred polygons with undulating relief, here covered with grasses, sedges and flowering plants (e.g. *Dryas*, *Papaver, Eriophorum* sp.), central Banks Island. *Photograph*—H.M. French. **b** The growth of ice wedges in very poorly drained tundra results in a distinctive micro-topography (so-called fortress polygons), upper Kellett River catchment, southwest Banks Island. *Photograph*—H.M. French. **c** Rapid snowmelt runoff in spring on the tundra leads to fluvithermal erosion that operates preferentially along ice wedges. This gully developed in early June 1975 near Sachs Harbour. *Photograph*—H.M. French. **d** A small ice-cored mound, or hydrolaccolith, has formed in the wet centre of a low-centred polygon network, Masik Valley, southern Banks Island (see French 1971b). *Photograph*—H.M. French

10–50 mm/1000 years in bare areas more characteristic of the polar desert (Lewkowicz 1983). Where concentrated on low-angled slopes, surface flow erodes shallow linear depressions colonised by vascular plants (*Salix* sp., *Dryas* sp.); this results in the appearance of non-sorted stripes, 0.5–1.0 m in width. More detailed studies are required because measurements from Ellesmere Island on similar fine-grained sediments to those on Banks Island suggest that solute removal can exceed suspended sediment removal on moderately to well-vegetated slopes (Lewkowicz and Kokelj 2002).

Rapid mass movements, such as active-layer detachment failures, occur on slopes where shale of the Christopher Formation outcrops (Fig. 6.6b). These occur during either late spring or after summer rain when the overlying active layer becomes saturated. Evidence of frost heaving and rock shattering is relatively rare due to the lack of coherent bedrock exposed at the surface.

6.10 A Permafrost Landscape

The tundra landscape is also one dominated by permafrost. Many of the old terraces, alluvial surfaces and floodplain surfaces are characterised by large thermal contraction crack polygons, 10–20 m in size (Fig. 6.7a) and numerous shallow tundra lakes and thermokarst ponds. Where these surfaces are poorly drained, a typical micro-relief associated with ice-wedge growth may result (Fig. 6.7b). Although the

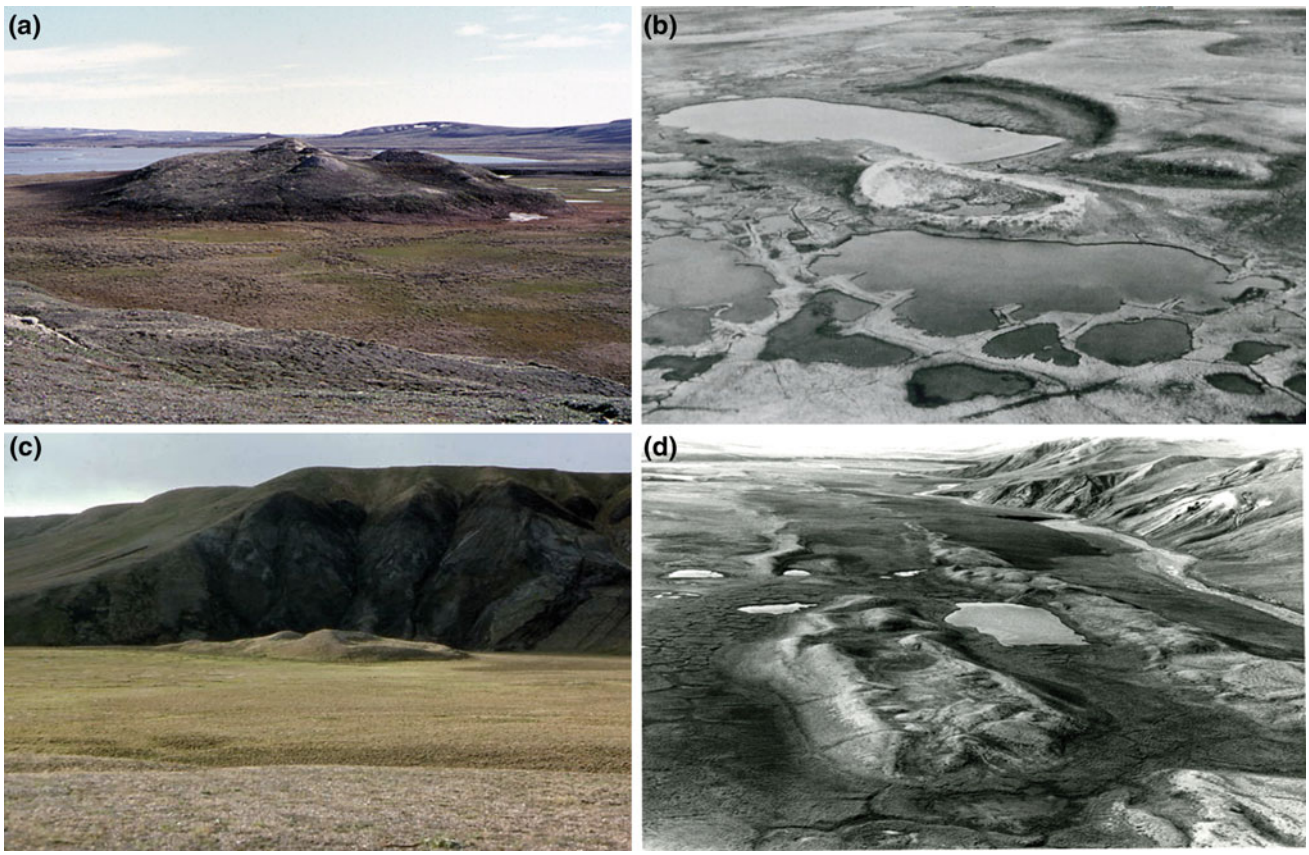

Fig. 6.8 Closed system pingos and pingo-like features on Banks Island occur on low fluvial terraces, in abandoned meltwater channels or in river valleys. **a** Several pingos occur on low terraces within the central part of the Thomsen River valley. The pingo illustrated here (Pingo 15, see Pissart and French 1976) is ~14 m high. The pingos are thought to have formed by the closed system freezing of subchannel taliks following terrace abandonment. Radiocarbon dates suggest pingo growth occurred between ~5.0 and ~2.5 ka. *Photograph*—H.M. French. **b** A collapsed pingo, consisting of a circular ice-cored rampart that surrounds an enclosed depression, is located in an abandoned meltwater channel incised within a low fluvial terrace, Sachs River lowlands, southern Banks Island. The dimensions of the pingo are ~60 m × 100 m and the ramparts rise 7.5 m above the surrounding tundra (see French et al. 1982). The pingo was probably ~20 m in height prior to collapse. It is surrounded by wet tundra with a network of large ice-wedge polygons, ~15–20 m in size. *Photograph*—H.M. French. **c** An oblique air view of a pingo with summit crater and lake in the upper Sachs River valley, southern Banks Island. The feature is ~ 7.5 m high. *Photograph*—H.M. French. **d** An oblique air view of problematic pingo-like ridges in the upper Sachs River catchment, southern Banks Island. The ridges are 1–2 km in length, are aligned parallel to each other, are partially collapsed, contain massive ice with the central depressions and occur on the gentle slope of an asymmetrical valley. They probably reflect the freezing of subchannel taliks following lateral migration of stream channel towards the steeper slope (see French 1976; French and Dutkiewicz 1976). *Photograph*—H.M. French

polygons are known to be underlain by ice wedges, exposures of the ice are rare. But in the spring, melting snow and resulting fluvithermal erosion operates preferentially along the thermal contraction cracks to erode gullies (Fig. 6.7c) where, occasionally, ice wedges can be seen. In especially poorly drained tundra, small ice-cored mounds, or hydrolaccoliths, may be encountered (Fig. 6.7d).

Numerous shallow ponds and lakes characterise the Banks Island tundra (see Fig. 6.2). While the deeper and larger water bodies are usually thermokarstic in nature (French and Harry 1983), many of the smaller and shallower water bodies reflect snowmelt accumulation within low-centred ice-wedge polygons. Sometimes, the ponds result from the amalgamation of adjacent depressions. Some of the deeper lakes do not freeze to their bottom in winter; these may contain char while others attract snow geese, ducks and other migratory birds during the summer months. In the southwest part of Banks Island, many of the lakes have an elliptical D-shape and preferred orientation (see Fig. 6.2). The cause is probably related to dominant winds causing thermokarst erosion of the banks but, in spite of several studies upon other oriented thaw lakes elsewhere in the western Canadian Arctic, the dynamics of this interesting morphology still remains unclear.

A number of pingos and pingo-like forms occur on the Banks Island tundra but, in relation to the size of the island, are not numerous. Nearly all appear related to present or past fluvial activity and most are in varying stages of collapse. Few, if any, appear to be actively growing. Unlike the well-known and conical-shaped pingos of the Mackenzie Delta, those on Banks Island are smaller, more irregular in form and occur in a variety of geomorphic situations (Fig. 6.8a–c). The majority occur on either low fluvial terraces or abandoned channels within the major river valleys. However, some also occur in valley bottom locations or on sloping terrain. Especially problematic are elongated, partially collapsed ice-cored ridges, some several kilometres long (Fig. 6.8d). In all probability, most of these features are of variable ages; they probably formed following the closed system freezing of subriver táliks (unfrozen zones) that must have existed beneath the deeper portions of river channels. This would have occurred during previous times of greater discharge when continued fluvial incision led to terrace abandonment and/or channel migration, or to other landscape modification (Pissart and French 1976; French and Dutkiewicz 1976).

6.11 Conclusions

The lowland tundra of Banks Island illustrates a particularly rich assemblage of cold climate landforms. They reflect the climate and the absence of daylight for several months of the year. Both inhibit photosynthesis and the growth of trees. As a result, the Banks Island tundra supports a surprisingly productive ecosystem even though the tundra is technically a cold desert. The Banks Island tundra is not typical of the majority of tundra landscapes because most lack the diversity of landforms, plants and animals that can be seen in abundance on Banks Island.

Any interpretation of the tundra landscape of Banks Island must consider not only the normal links between rocks, relief and climate but also the complex and subtle relationships that exist between low temperature, aridity, snow, frozen ground, wind and vegetation.

Acknowledgments Field work conducted on Banks Island between 1968 and 1985 was supported by numerous agencies and organisations; these included the Geological Survey of Canada, the Natural Sciences and Engineering Research Council, the Polar Continental Shelf Project (Energy, Mines and Resources Canada), the University of Ottawa, Environment Canada (Indian and Northern Affairs Canada), Elf Aquitaine, Panarctic Oils, and the Arctic Petroleum Operators Association. Figures 6.2, 6.4, 6.6a, 6.7d, and 6.8c are also available in Cuadernos de Investigación Geográfica (No 42(2), 321—340), published by Universidad de La Rioja, Spain(pulicaciones.unirioja.es/revistas/cig).

References

Andreyev VN, Aleksandrova VD (1980) Geobotanical divisions of the Soviet Arctic. In: Bliss DW, Heal, Moore JJ (eds) Tundra ecosystems: a comparative analysis. Cambridge University Press, New York, pp 25–37

Bliss LC (1997) Arctic ecosystems of North America. In: Wielgolaski FE (ed) Ecosystems of the world 3, Polar and Alpine tundra. Elsevier, Amsterdam, pp 551–683

Egginton PA, French HM (1985) Solifluction and related processes, eastern Banks Island, NWT. Can J Earth Sci 22:1671–1678

England JH, Furz MFA, Doupe JP (2009) Revision of the NW Laurentide ice Sheet: implications for paleoclimate, the northeast extremity of Beringia, and Arctic Ocean sedimentation. Quat Sci Rev 28:1573–1596

French HM (1971a) Slope asymmetry of the Beaufort Plain, northwest Banks Island, NWT, Canada. Can J Earth Sci 8:717–731

French HM (1971b) Ice-cored mounds and patterned ground, southern Banks Island. Geogr Ann 53A:32–38

French HM (1974) Mass wasting at Sachs Harbour, Banks Island, N.W. T. Canada. Arct Alpine Res 6:71–78

French HM (1976) Pingo investigations, Banks Island, District of Franklin. Geol Sur Can Paper 76-1A, pp 235–238

French HM, Dutkiewicz L (1976) Pingos and pingo-like forms, Banks Island, Canada. Biuletyn Peryglacjalny 26:211–222

French HM, Harry DG, Clark MJ (1982) Ground ice stratigraphy and late Quaternary events, southwest Banks Island, Western Canadian Arctic. In: French HM (ed) Proceedings Fourth Canadian Permafrost Conference, Calgary, Alberta. National Research Council of Canada, Ottawa, pp 81–90

French HM, Harry DG (1983) Ground-ice conditions and thaw-lake evolution, Sachs River lowlands, Banks Island, Canada. In: Poser H, Chunke E (eds) Mesoformen des reliefs in heutigen Periglazialraumes. Abhandlungen der Akademie der Wissenschaften in Gottingen, vol 35, pp 70–81

Fyles JG, Hills LV, Matthews JV Jr, Barendregt R, Baker J, Irving E, Jette H (1994) Ballast Brook and Beaufort formation (late tertiary) on northern Banks Island, Arctic Canada. Quat Int 22(23):141–171

Harry DG, French HM (1983) The orientation and evolution of thaw lakes, southwest Banks Island, Canadian Arctic. In: Proceedings, Fourth International Conference on Permafrost 17–22 July, Fairbanks, Alaska. National Academy of Science, Washington, DC, pp 456–461

Lakeman TR, England JH (2014) Facies and stratigraphical analyses of glacial and interglacial sediments at Morgan Bluffs, Banks Island, Canadian Arctic Archipelago. Boreas 43:895–913

Lewkowicz AG (1983) Erosion by overland flow. In: Proceedings Fourth International Conference on Permafrost, 17–22 July, Fairbanks, Alaska. National Academy Press, Washington, DC, pp 701–706

Lewkowicz AG, Kokelj SV (2002) Slope sediment yield in arid lowland continuous permafrost environments, Canadian Arctic Archipelago. Catena 46:261–283

Maher WJ (1968) Muskox bone of possible Wisconsin age from Banks Island, Northwest Territories. Arctic 21:260–266

Maxwell JB (1980) The climate of the Canadian Arctic islands and adjacent waters. Climatological Studies, 30, Atmospheric Environment Service, Environment Canada, 531 p

Miall A (1979) Mesozoic and Tertiary geology of Banks Island, Arctic Canada. Geol Surv Can Memoir 387, 234 p

Pissart A, French HM (1976) Pingo investigations, north-central Banks Island, Canadian Arctic. Can J Earth Sci 13:937–946

Pissart A, Vincent JS, Edlund SA (1977) Dépôts et phénomènes éoliens sur l'île de Banks, Territoires du Nord-Ouest, Canada. Can J Earth Sci 14:2452–2480

Porsild AE (1955) The vascular plants of the Western Canadian Arctic Archipelago. Bulletin 135, National Museum of Canada, Ottawa, 226 p

Porsild AE (1957) Illustrated flora of the Canadian Arctic Archipelago. Bulletin 146, National Museum of Canada, Ottawa, 209 p

Taylor AE, Judge AS (1977) Canadian geothermal data collection—northern wells, 1976–1977. Geothermal series no 10, Geothermal Service of Canada, Earth Physics Branch, Department of Energy, Mines and Resources, Ottawa, 194 p

Tedrow JCF (1974) Soils of the high arctic landscape. In: Smiley TL, Zumberge JH (eds) Polar deserts and modern man. University of Arizona Press, Arizona, pp 63–69

Tedrow JCF, Douglas LA (1964) Soil investigations on Banks Island. Soil Sci 98:53–65

Thorsteinsson R, Tozer ET (1962) Banks, Victoria and Stefansson Islands, Arctic Archipelago. Geol Surv Can Memoir 330, 83 p

Vincent J-S (1982) The Quaternary history of Banks Island, NWT, Canada. Géogr physique Quat 36:209–232

Vincent J-S (1983) La géologie du Quaternaire et la géomorphologie de l'ile de Banks, Arctique Canadien. Geol Surv Can, Memoir 405, 118 p

The Peel Plateau of Northwestern Canada: An Ice-Rich Hummocky Moraine Landscape in Transition

7

Steven V. Kokelj, Jon F. Tunnicliffe, and Denis Lacelle

Abstract

The Peel Plateau is a fluvially incised, ice-rich moraine landscape that extends along the eastern margins of the Richardson and Mackenzie Mountains, northwestern Canada. The 24,000 km^2 region demarcates the western boundary of the former Laurentide Ice Sheet (LIS). Landscape form and geomorphic processes are strongly conditioned by terrain assemblages produced during the advance and retreat of the LIS and by the large stores of relict late Pleistocene ground ice preserved in permafrost. Holocene fluvial, slope, and thermokarst activity has reshaped this landscape. Fluvial incision of the plateau and an abundance of ground ice favor the development of retrogressive thaw slumps. Recent warming and increasing rainfall have given rise to large, long-lived instances of these thermokarst features. We discuss the morphology, processes, and climate feedbacks that control their development. Thaw slump activity on the Peel Plateau provides insight on the geomorphic processes that are likely to dominate the evolution of ice-rich glacigenic landscapes under rapidly changing climate conditions.

Keywords

Environmental change • Fluvial valley incision • Glacially conditioned landscape • Hummocky moraine • Ice-rich and ice-cored terrain • Retrogressive thaw slump

7.1 Introduction

Formerly glaciated terrain across northwestern Canada can be organized into large concentric zones of ice-marginal landform assemblages (Dyke and Prest 1987). In Arctic and subarctic regions, the post-glacial climate has maintained continuous permafrost preserving thick layers of relict ground ice in these deposits (Mackay 1971; Rampton 1988; St-Onge and McMartin 1999). This ground ice was emplaced by a suite of processes associated with conditions at the margins of the Laurentide Ice Sheet (LIS) that were conducive to the burial and preservation of glacier ice (Dyke and Evans 2003; Murton et al. 2005) and development of segregated ground ice of glacial meltwater origin (Mackay 1971; Rampton 1988; Lacelle et al. 2004). During the Holocene, fluvial and periglacial processes have modified these landscapes to their present-day form. The preservation of relict ground ice has made these glacigenic environments inherently sensitive to thermokarst and geomorphic change (Lacelle et al. 2010; Lantuit et al. 2012; Kokelj et al. 2015).

In this chapter, we discuss the geomorphology of the Peel Plateau, northwestern Canada (Figs. 7.1, 7.2), where landscape form and processes are strongly influenced by glacial legacy, in particular the large amount of relict late

S.V. Kokelj (✉)
Northwest Territories Geological Survey, 4601-B 52 Avenue, Yellowknife, NT X1A 2L9, Canada
e-mail: Steve_Kokelj@gov.nt.ca

J.F. Tunnicliffe
School of Environment, University of Auckland, Private Bag 92019Auckland, New Zealand

D. Lacelle
Department of Geography, University of Ottawa, 60 University, Ottawa, ON K1N 6N5, Canada

© Springer International Publishing Switzerland 2017
O. Slaymaker (ed.), *Landscapes and Landforms of Western Canada*, World Geomorphological Landscapes, DOI: 10.1007/978-3-319-44595-3_7

Pleistocene ground ice and glacigenic materials sequestered in permafrost (Fig. 7.2d, e). This region extends along the eastern margins of the Richardson Mountains and northeastern Mackenzie Mountains, demarcating the western limit, and recessional positions of the former LIS (Fig. 7.1b) (Duk-Rodkin and Lemmen 2000). Post-glacial incision of the fluvial network provides the relief and erosional environment to make this ice-rich hummocky moraine landscape highly susceptible to thaw slumping and related mass movements (Fig. 7.2) (Lacelle et al. 2010, 2015). Recent warming and increased rainfall have accelerated thaw slump activity leading to the development of very large disturbances (Figs. 7.3, 7.4) (Kokelj et al. 2015; Segal et al. 2016). The stability of the Peel Plateau has far-reaching implications because it constitutes a major sediment source for numerous tributaries of the Peel River and Mackenzie Delta (Kokelj et al. 2013), it is traversed by the Dempster Highway, which links western Arctic Canada with the south (Gill et al. 2014), and it lies at the heart of Gwich'in traditional lands (Slobodin 1981).

7.2 Geologic and Physiographic Setting

The Peel Plateau is situated along the eastern margins of the Richardson and northern Mackenzie Mountains (Fig. 7.1) (Duk-Rodkin and Hughes 1992). The north–south-trending Richardson Mountains rise to a peak of 1575 masl to form the continental divide separating the Northern Interior Platform from the Eagle Fold Belt (Norris 1997). The Peel Plateau slopes gently eastward with elevations ranging from 750 masl in the foothills of the Richardson Mountains to 100 masl west of the Peel River (Catto 1996).

The formerly glaciated foothills of the Richardson Mountains and the Peel Plateau consist mainly of ice-rich tills, and glacifluvial and glacilacustrine deposits emplaced

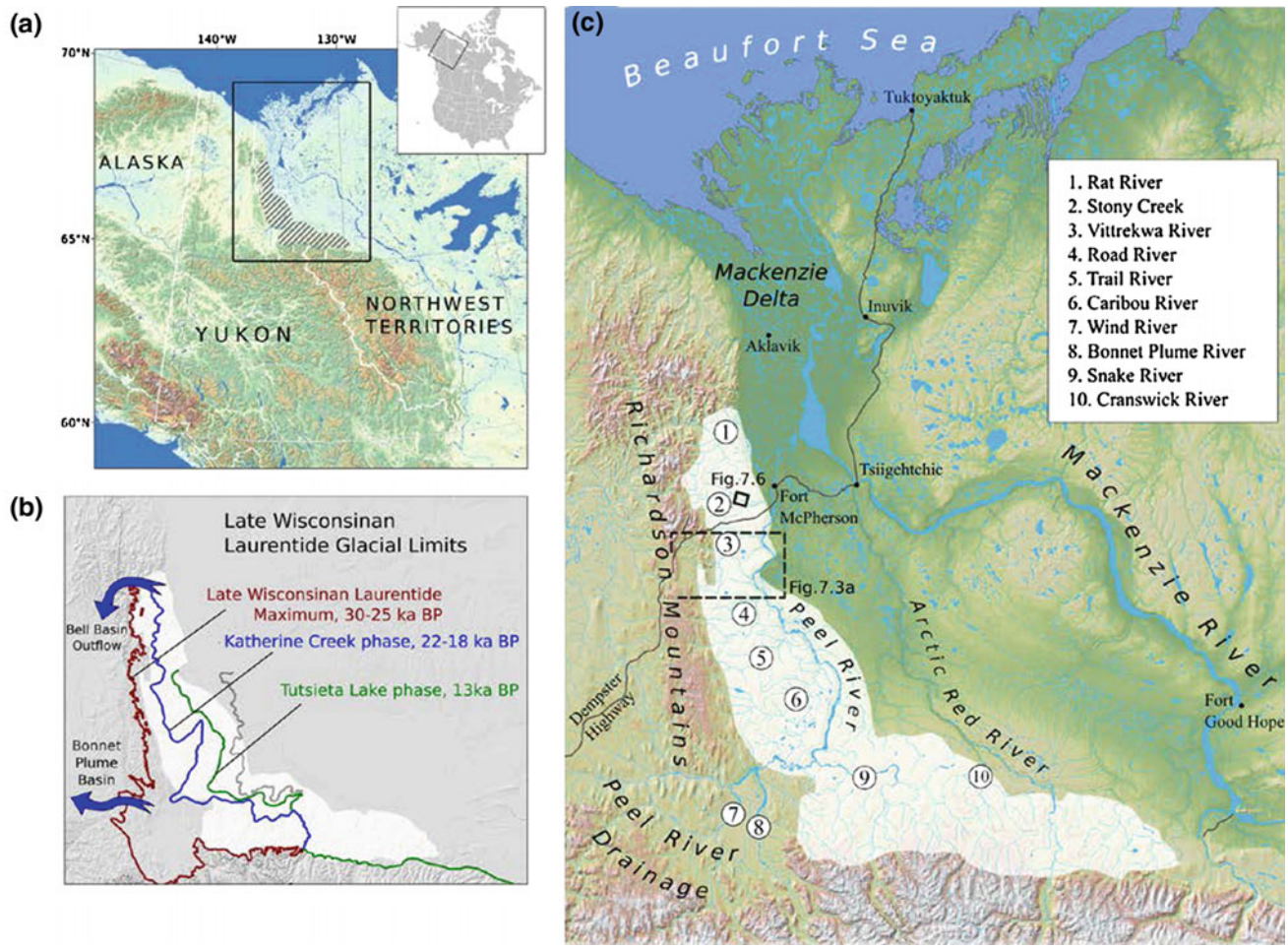

Fig. 7.1 The Peel Plateau region. **a** Map of northwestern North America showing the location of the Peel Plateau. **b** The approximate ice front positions in the Peel Plateau region (Duk-Rodkin and Lemmen 2000). **c** Map of the Peel Plateau (*white*) showing major streams and rivers and the Richardson Mountains

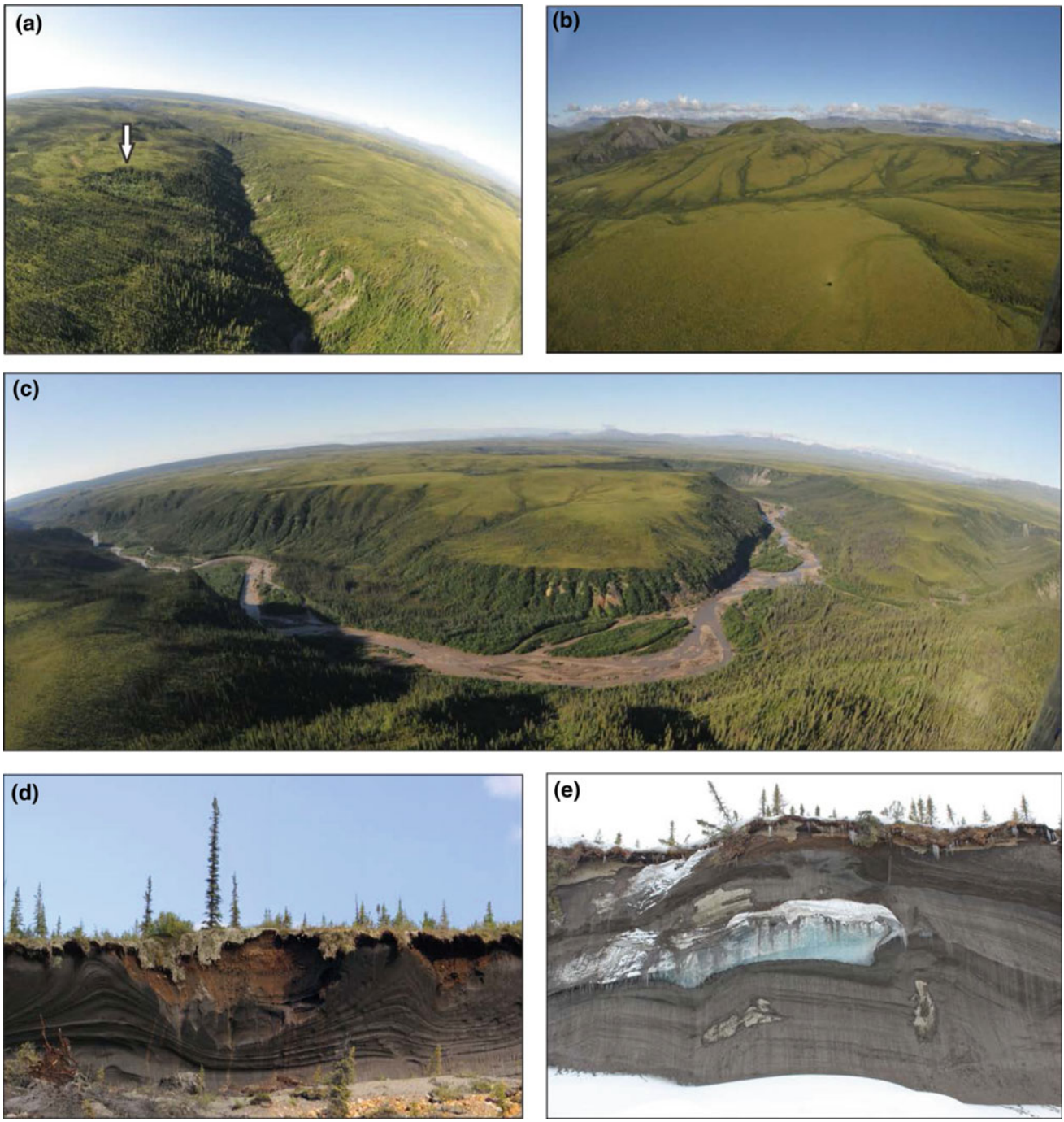

Fig. 7.2 The Peel Plateau. **a** The plateau and an incised valley. Small skin flows are visible on the south-facing slope, and a stable, vegetated thaw slump scar is indicated by the arrow. **b** Rolling moraine upland in the low shrub tundra vegetation zone. Flow tracks and streams are indicated by darker green, tall shrub riparian vegetation. **c** The incised valley and floodplain of a gravel bed stream, Stony Creek. Spruce forest and tall shrub vegetation occur in valleys and on stable slopes. Tundra vegetation occurs on the gently undulating plateau. Some skin flows can be seen on valley sides in background. *Source*: Photographs **a**–**c** NWT Cumulative Impact Monitoring Program, Government of the Northwest Territories. **d** Thaw slump headwalls reveal an ice-rich landscape. Ground ice exposure in fluvial gravel deposit (note the *light colored* boulders in the foreground). **e** Ground ice exposure up to 25 m height showing injection ice (*blue ice*) enclosed in fine-grained, ice-rich sediments overlain by oxidized till

at the western margins of the LIS to form a broad band of ice-rich, hummocky terrain (Figs. 7.2, 7.3). These glacigenic deposits contrast with the alpine slopes, which are veneered by colluvium derived from the weathering of the sandstone, quartzite, and limestone strata that comprise the mountains. The ice-rich tills of the plateau are up to 50 m thick

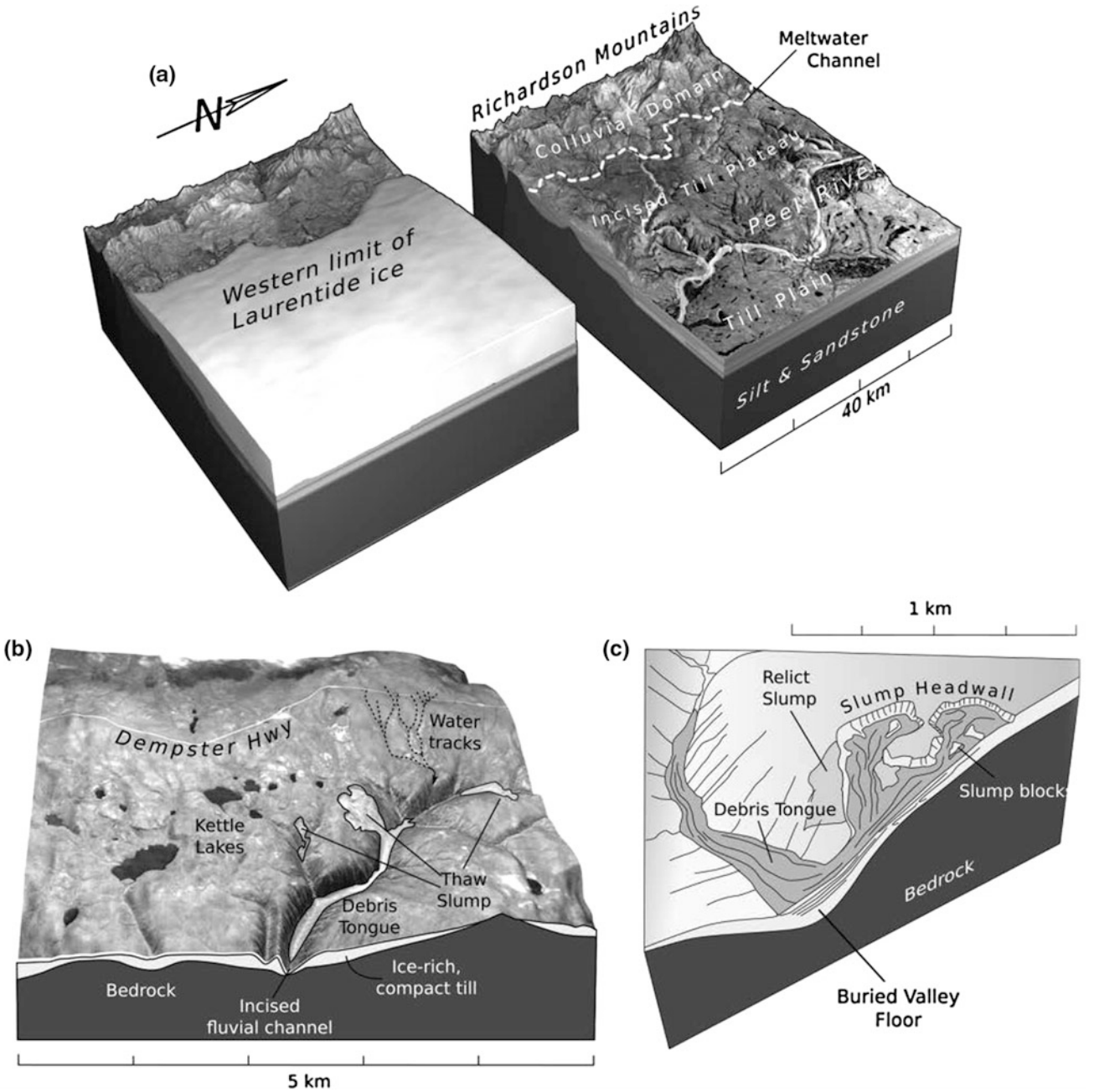

Fig. 7.3 **a** The maximum extent of the Laurentide Ice Sheet (Duk-Rodkin and Lemmen 2000) and the legacy landforms left behind. The block schematic shows the continental divide and colluvial mountain slopes, the incised hummocky till plateau, the Peel River floodplain, and the till plain in the foreground. **b** An active disturbance regime is evident in this glacially conditioned, ice-rich terrain. Fluvial incision and thermal erosion have exposed ice-rich sediments, which has led to the development of large retrogressive thaw slumps and debris tongues within the network of incised valleys in the plateau. Flow tracks convey water downslope from interfluve areas to incised streams. Kettle lakes suggest ice-cored terrain, which is confirmed by the ice-rich permafrost at least 25 m thickness exposed in the nearby slumps. **c** Cross section of a large retrogressive thaw slump and the debris tongue deposit comprised of materials displaced downslope from the valley side and plateau

(Duk-Rodkin and Lemmen 2000) and consist of stony, compact, fine-grained silt or clay material (Bjornson 2003). Distinctive beds of glacifluvial gravel and sand and fine-grained glacilacustrine deposits occur throughout the region (Fig. 7.2) (Smith and Lesk-Winfield 2012). The Mesozoic and Cretaceous silt and sandstone bedrock that underlies the plateau is typically only exposed on the steep slopes or bottoms of incised stream valleys.

Fig. 7.4 Thaw slump photograph montage. a Large thaw slump showing headwall, scar zone, and debris tongue (see Fig. 7.3b, c). The total disturbance area is approximately 39 ha, and the headwall is up to 25 m high. The slump has been on the landscape since the 1950s. Intensified slump activity in the past two decades has resulted in the rapid increase in scar area, an acceleration of scar zone sediment flux, and the development of the large debris tongue deposit. **b** Slump scar zone of the disturbance in previous (**a**). **c** SPOT image of a large thaw slump near the Richardson Mountains. Slump enlargement has captured water tracks, and the runoff has accelerated thermoerosion of headwall. *Source*: NWT Centre for Geomatics (2013). **d** Mega slump, debris tongue, and secondary slumps in foreground. Vegetation patterns on debris tongue show stabilized areas and evidence of sequential flow events. Note the debris-dammed lake and arrows indicating lateral displacement of the trunk stream, which accelerated slope-side erosion and development of secondary slumps visible in the foreground. *Source*: Photographs **a**, **b**, **d** NWT Cumulative Impact Monitoring Program, Government of the Northwest Territories. **e** Enlargement of the slump shown in the previous photograph caused rapid, partial drainage of small lake in summer 2015. The lake is about 170 m wide. Most of the water drained over a 10-m-high waterfall during a period of less than 2 h. Slump development was arrested when the headwall encountered the thawed sediments of the talik which underlies the lake. Photograph by Tom Andrews, Government of the Northwest Territories

7.2.1 Glacial Chronology

During the late Pleistocene, the LIS advanced onto the eastern slopes of the Richardson Mountains depositing tills up to an elevation of about 750 masl (Figs. 7.1, 7.3a) (Duk-Rodkin and Lemmen 2000). It was initially thought that the maximum extent of the LIS in the Peel Plateau region was reached c. 30 ka cal year BP (Duk-Rodkin and Lemmen 2000), but new U/Th ages suggest that this did not occur until c. 18 ka cal year BP (Lacelle et al. 2013). Retreat of the LIS from this region was characterized by at least two standstills or readvances, most notably the ice front positions associated with the Tutsieta Lake Phase and the Katherine Creek Phase situated several kilometers to the west (Duk-Rodkin and Lemmen 2000). The Peel Plateau has been ice-free since about 13 ka cal year BP, as suggested by the dating of *Bison priscus* remains found at Tsiigehtchic (Zazula et al. 2009).

The nature of sediments and morphology of the Peel Plateau reflect a range of conditions at the margins of the former LIS. Advance and retreat of the debris-rich margins of the ice sheet favoured the emplacement of ice-rich hummocky moraine (Dyke and Evans 2003). The occurrence of glacifluvial and lacustrine deposits is a result of the abundant meltwater that was impounded between the mountains and the western margins of the LIS (Duk-Rodkin and Lemmen 2000; Brown 2012). During maximum ice extent, the drainage was diverted westward across the continental divide through McDougall Pass near the headwaters of the Rat River and northwest in the Bonnet Plume basin where glacial Lake Hughes (Fig. 7.1b) spilled into the Bell and Old Crow basins (Catto 1996; Duk-Rodkin and Lemmen 2000). The retreating ice sheet continued to inhibit meltwater drainage, forming small, temporary proglacial lakes and distributing localized lacustrine and glacifluvial deposits across the region (Duk-Rodkin and Lemmen 2000; Brown 2012). Recession of the ice sheet also permitted the northward drainage of glacial meltwater, which cut the prominent S–N-trending meltwater channels that demarcate various positions of the receding ice front (Fig. 7.3a) (Duk-Rodkin and Lemmen 2000). Several major glacifluvial terraces and fans are still in place from this period of major ice retreat. By 12 ka BP, the channel of the Peel River and a topographic base level was established for the development of fluvial networks that incise the plateau (Figs. 7.2, 7.3) (Catto 1996). For example, in the Richardson Mountains, incision of Bonnet Plume Creek started around 9500 cal year BP (Lacelle et al. 2010). The major stream networks are typically diverted northward by the large meltwater valleys where they meander as underfit streams before redirecting eastward to the Peel River or Mackenzie Delta.

7.2.2 Holocene Climate and Vegetation

Holocene climate of the Peel Plateau has been sufficiently cold to maintain large stores of glacigenic sediments in permafrost and preserve thick layers of ground ice (Fig. 7.2d, e), but variation in climate has influenced the intensity of geomorphic activity and landscape evolution. Climate during the early Holocene was warm and dry (Table 7.1) (Lauriol et al. 2002a). The air temperatures were 3–8 °C higher than present (Clark et al. 2004; Kaufman et al. 2004), due to higher solar insolation (Ritchie et al. 1983). At this stage, sea level was lower and the western Arctic coastline was about 150 km north of its present location (Hill et al. 1985). The greater distance from the coast contributed to a warmer, continental climate in the lower Mackenzie Valley (Burn 1997). The higher summer air temperatures increased thaw depths (Burn 1997) and initiated widespread thermokarst and thaw lake development (Rampton 1988; Lacelle et al. 2004). The mid-Holocene climate became cooler and wetter due to a shift in atmospheric circulation, but likely remained warmer than conditions in the 20th Century (Lauriol et al. 2002a, b, 2009). The decrease in solar insolation and over 100 km of coastal retreat have contributed to Holocene cooling in the lower Mackenzie Valley (Burn 1997).

Modern-day climate in the Peel Plateau region is characterized by long cold winters and short cool summers. The mean annual air temperature in Fort McPherson (1986–2010) is −6.8 °C (Environment Canada 2012). Mean July temperature is 15 °C, and the coldest month, January, has a mean temperature of −27 °C. Since the 1970s, mean annual air temperatures have increased at a rate of 0.77 °C per decade in western Arctic Canada (Burn and Kokelj 2009), making this one of the most rapidly warming regions on the planet (Serreze et al. 2000). However, the mean summer air temperatures at Fort McPherson from 1986 to 2012 do not show significant trends. Total annual precipitation in Fort McPherson (1986–2007) averages 295 mm, with rainfall accounting for approximately half (148 mm) (Environment Canada 2012). There has been a significant increase in total June–July rainfall from 1986 to 2012 and a large increase in the frequency and magnitude of extreme rainfall events (Kokelj et al. 2015).

On the Peel Plateau, a cold climate combines with physiography to produce an elevation-driven ecological gradient (Fig. 7.2a–c). These factors result in the transition from open spruce woodlands in valley bottoms and lower elevation south-facing slopes (*Picea* spp., *Populus balsamifera*) to shrub (*Betula* spp., *Alnus* spp., *Salix* spp.) and dwarf shrub tundra (*Cyperaceae* spp., *Eriophorum angustifolium*) on the plateau (Ecosystem Classification Group 2010; Gill et al. 2014).

Table 7.1 Compilation of Holocene climate conditions inferred from various paleoclimate indicators

Age interval	Paleoclimatic evidence		Inferred paleoclimate	
^{14}C yr BP	*Vegetation*	*Lake status*	*Temperature*	*Moisture*
12,000–10,000	Birch zone	Low	Rapid warming	Dry
10,000–8500	Populus and Picea expansion	Intermediate	Warmest (6°C higher than present day)	Gradual increase in moisture
7500–5000	Boreal forest extends further north than present day	Rapid rise in level	Gradual cooling trend	Wetter than during the 20th Century
5000—present	Tree line retreat to present-day position	Intermediate to low	Temperature similar to the 20th Century	Decrease in moisture with increasing dry periods

Studies include data collected from northern Yukon to the west of the study area (Lauriol et al. 2002a, b, 2009)

7.3 Permafrost, Ground Ice, and Patterned Ground

On the Peel Plateau, thick glacigenic deposits have been preserved in permafrost since the retreat of the LIS. The landscape is underlain by continuous permafrost that extends to depths of about 125 m (Mackay 1967; Judge 1973). The annual mean temperature of the permafrost increases with elevation from about −2.5 °C in lowland subarctic forest to about −1.5 °C in upland dwarf shrub tundra due to the prevalence of atmospheric temperature inversions in winter (O'Neill et al. 2015). Tall shrubs that grow on the tundra can trap snow redistributed by winter winds, causing warmer ground temperatures in areas with dense alder and willow along riparian zones, disturbed slopes, or embankments of the Dempster Highway (Gill et al. 2014). The terrain microtopography is hummocky throughout areas with fine-grained, frost susceptible sediments. These soil mounds, 0.70–1.5 m in diameter, are surrounded by organic-rich troughs. The lateral differences in thermal properties of the earth materials in hummocky terrain produce an undulating permafrost table (Mackay 1980). Polygonal terrain and underlying wedge ice are commonly associated with localized organic deposits.

The permafrost underlying the Peel Plateau is ice-rich. A zone of segregated ice enrichment characterizes near-surface permafrost throughout areas with fine-grained frost susceptible sediments (Mackay 1972). At greater depth, the glacigenic deposits host thick layers of relict ground ice (Fig. 7.2d, e), distinguishing this region from the unglaciated terrain to the west, and the Mackenzie Delta and till plains that lie to the east (Fig. 7.1). The relict ground ice is comprised of massive ice and icy sediments (Fig. 7.2d, e) (Lacelle et al. 2004). Investigation of thaw slump headwalls indicates that ice contents in permafrost range from 50 % by volume to massive ground ice up to tens of meters in thickness (Lacelle et al. 2004, 2010; Malone et al. 2013). Some of the ground ice lacks visible stratigraphic structure, while other exposures reveal distinct layering and evidence of deformation. This ground ice typically exhibits an unconformable upper contact with the hosting sediments (Lacelle et al. 2004; Fig. 7.2d, e). The distribution of large thaw slumps across the Peel Plateau (Figs. 7.3b, 7.4) (Lacelle et al. 2015) indicates that ground ice is widespread. A north–south-trending band of kettle lakes immediately to the west of the Tutsieta Phase glacial limit (Figs. 7.1, 7.3) suggests the presence of ice-cored terrain. These inferences are further supported by seismic shothole data, which indicates that ground ice occurs within the uppermost 2 m of permafrost in about 50 % of the 131 shotholes from the study area (Smith and Lesk-Winfield 2012).

The thick zones of ice-rich permafrost that underlie the Peel Plateau reflect the favourable conditions for ground ice development along the western margins of the LIS (Mackay 1971; Dyke and Evans 2003; Murton et al. 2005). Although the origins of ground ice may vary with environmental setting, investigations from across the western Arctic indicate several ground ice forming processes associated with an ice-marginal environment. These include the following: (1) refreezing of meltwater and sediment beneath the ice sheet at the transition from a warm- to cold-based ice sheet (Murton et al. 2005; Evans 2009); (2) permafrost aggradation beneath stagnant basal ice and preservation of glacier ice buried by accumulating sediments (St-Onge and McMartin 1999; Murton et al. 2005); and (3) growth of segregated intrusive ice in aggrading permafrost (Mackay 1971; Rampton 1988; Lacelle et al. 2004). It is probable that a combination of these processes has contributed to ice-rich permafrost on the Peel Plateau (Lacelle et al. 2010).

7.4 Hillslopes and Mass Wasting

The topographic gradient of the Peel Plateau landscape is set by the rocky headwaters in the mountains to the south and west and the base-level influence of the Peel River (Fig. 7.3). The relative relief provided by fluvial incision, an abundance of fine-grained glacigenic sediments, and ice-rich permafrost, combines with a subarctic climate to produce a suite of processes that modify slopes and transfer sediment downslope to the fluvial networks. These freeze–thaw, weathering, slope-wash, and mass wasting processes give rise to colluvium-covered slopes and several characteristic landforms including solifluction lobes, flow tracks, and slope disturbances such as retrogressive thaw slumps (Figs. 7.3b, c, 7.4).

Solifluction lobes are most visible on low shrub tundra highlands; however, this subtle downslope movement of near-surface earth materials is ubiquitous throughout moist sloping terrain. Solifluction is comprised of downslope creep driven by freeze–thaw processes, and gelifluction, which is the plug-like sliding of the thawed active layer over the frost table (Mackay 1981). The relative importance of solifluction as a landscape process is probably greatest in interfluve areas and uplands as suggested by the subdued, rolling terrain morphology (Figs. 7.2b, 7.5a).

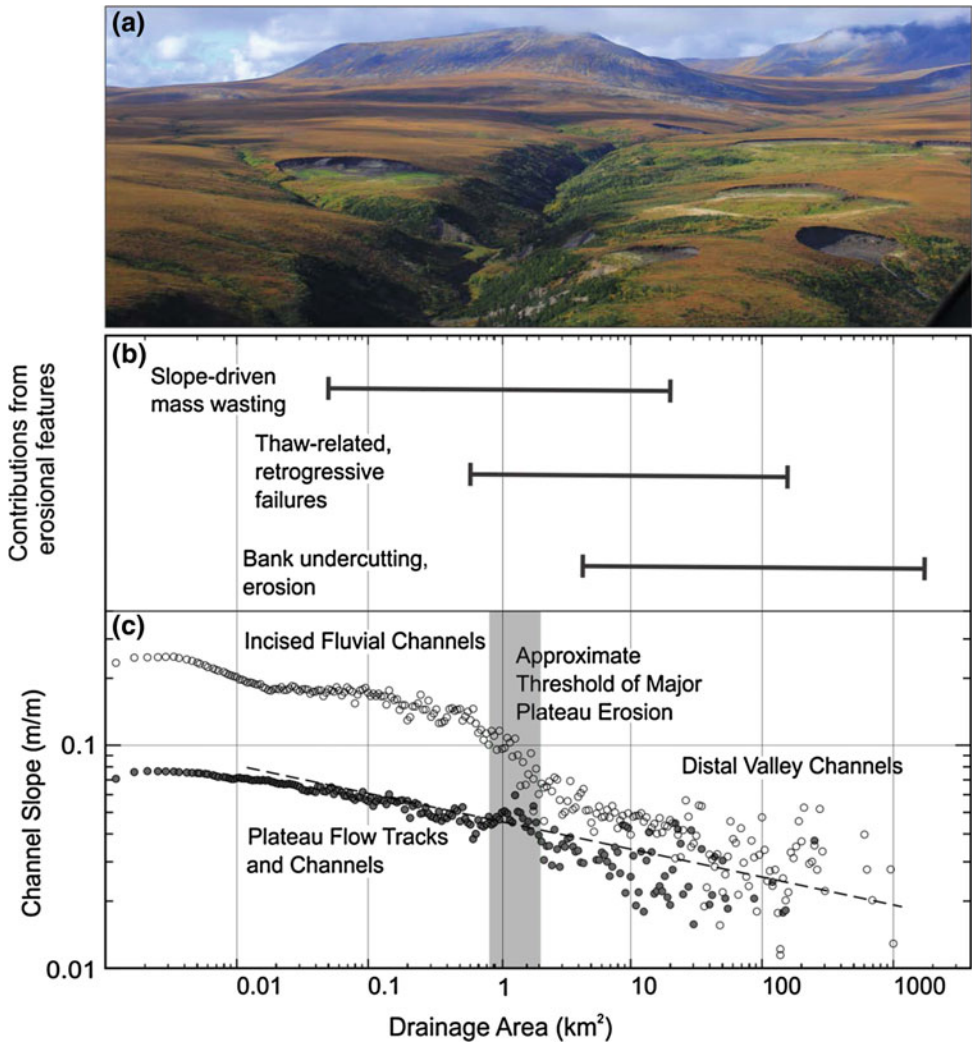

Fig. 7.5 Distribution of sedimentary disturbances within the drainage networks of the Peel Plateau. **a** Oblique photograph showing incised valleys, flow tracks, and abundant thaw slump disturbances on the Peel Plateau. Photograph by Scott Zolkos, University of Alberta. **b** Disturbance inventories throughout the northern Peel Plateau (by Duk-Rodkin and Robertson 2001), and our own work indicates that slides occur mainly within the upper drainages and bedrock-controlled steeplands ($A < 1$ km^2), while retrogressive thaw slumps may occur at relatively larger drainage areas. Bank undercutting and valley wall failures most commonly occur within the distal reaches of the valleys. **c** Tracing the accumulated upstream area and slope along the Stony Creek drainage network on a 30-m DEM reveals the contrasting transport gradients within the upper plateau (mainly flow tracks) and within incised channel settings. The considerable transport potential with the incised plateau gives rise to thermal erosion, slump initiation, and downstream increases in specific sediment yield

Active layer detachment slides are rapid mass movements that involve the downslope translation of thawed materials over frozen ground. On the Peel Plateau, small active layer detachment slides and skin flows occur on steeply sloping, fluvially incised valley sides (Fig. 7.2a, c). Sliding events typically occur due to intense or prolonged periods of rainfall. When the base of the active layer becomes saturated and water cannot drain away, porewater pressures increase to reduce effective stress at the thaw front (Lewkowicz 2007). These disturbances may expose underlying ground ice and initiate thaw slump development (Lacelle et al. 2010).

Retrogressive thaw slumping is a dominant agent of geomorphic change in landscapes underlain by ice-rich permafrost, and it is the most common form of mass wasting on the Peel Plateau (Figs. 7.4, 7.5) (Lacelle et al. 2015). Thaw slumps initiate by a variety of mechanisms that expose ground ice including mechanical and thermoerosion by fluvial processes, thermally driven subsidence along lakeshores, or mass wasting triggered by extreme thaw or precipitation (Kokelj and Jorgenson 2013). Active thaw slumps are comprised of an ice-rich headwall, a low angled scar zone consisting of thawed slurry and in some cases a periodically mobile tongue of debris that develops as the saturated materials flow downslope (Fig. 7.4). Surface energy fluxes, ground ice, and headwall characteristics (size and orientation) control the headwall ablation rate (Lewkowicz 1987; Grom and Pollard 2008; Lacelle et al. 2015), and gravity-driven flows move debris and meltwater to the base of the headwall. The thawed materials are transported from the slump headwall by rill erosion, fluvial transport, and shallow and deep seated mass flows (Figs. 7.3c, 7.4a) (Kokelj et al. 2013, 2015). A thaw slump can enlarge for decades until the exposed ground ice is covered by the accumulation of thawed materials (Kokelj and Jorgenson 2013). Vegetation colonization on the nutrient-rich scar zone soils contributes to stabilizing the slump scar zone (Fig. 7.5a) (Lantz et al. 2009).

The steeply incised valleys and ice-rich permafrost on the Peel Plateau provide favorable conditions for the development of extremely large "mega slumps" (Fig. 7.4). As thaw slumps enlarge, they tend to exhibit greater geomorphic complexity, including different modes of downslope sediment displacement, which operate across a range of temporal and spatial scales. The processes and characteristics associated with these disturbances described in Kokelj et al. (2015) include the following: (1) ablation of large massive ice bodies, backwasting of the headwall by retrogressive failure and supply of sediments and meltwater to a low angled scar zone; (2) evacuation of debris from the scar zone proceeding as a combination of diurnal, meltwater-driven fluvial transport, intermittent rainfall-induced mass wasting, and quasi-continuous fluidized mass flow; (3) base-level erosion, or evacuation of outlet detritus; (4) prolonged slump activity over decades producing disturbances exceeding 15 ha in area; and (5) valley-confined downstream aggradation of debris derived from the scar zone, leading to cascading effects including the development of debris-dammed lakes and enhanced valley side erosion and development of secondary slumps (Fig. 7.4).

Thaw slumps are common throughout the Peel Plateau (Brooker et al. 2014), but several topographic factors appear to control their distribution. Lacelle et al. (2015) report a bimodal distribution of slumps along an elevation gradient with greater landscape normalized frequency of slump occurrence between 300–350 and 450–500 masl. This study also showed that most disturbances develop on slopes of 8–12°, and the population has a preferred eastward orientation, likely related to the regional slope gradient. Figure 7.5 suggests that slumps tend to initiate along small streams, likely coinciding with the threshold for fluvial incision.

7.5 Hydrology and Fluvial Processes

Drainage network form is governed by the capacity of overland flow to incise a channel on the permafrost-affected landscape. Surface runoff is the dominant hydrological flowpath for snowmelt due to the rapid melt and the presence of frozen ground (Woo 2012). However, the high tortuosity of flowpaths through vegetated, hummocky terrain (Quinton and Marsh 1999) diffuses surface flow and, in conjunction with the presence of frozen ground, limits the efficacy of surface wash erosion (Lewkowicz and Kokelj 2002). Solute concentrations in runoff from undisturbed tundra are also typically very low because water rapidly transits over or through a shallow, organic-rich and nutrient poor active layer (Lewkowicz and Kokelj 2002; Malone et al. 2013). Vegetation cover, organic soils, and local topographic gradients lead to a higher threshold for channel incision and different scaling relationships for the initiation of channelization in these drainage networks (Fig. 7.5).

On hillslopes of the Peel Plateau, we find widely spaced linear drainage features known as water tracks or runnels. Water tracks may be distinguished by slightly darker tones on the landscape (Fig. 7.2b, c), owing to the distinctive tall shrub vegetation that develops in these zones of enhanced soil moisture (Hastings et al. 1989; Walker et al. 1989). They develop at flow accumulation areas of between 0.1 and 1 km^2 (Fig. 7.5c) and are recognized as important pathways of water delivery and nutrient transfer within the drainage network. In Fig. 7.5c, the slope of these undissected plateau channels is quite shallow, relative to the steep, incised portions of the river network. There is relatively little fluvial sediment transport activity on the flatter interfluves and first-order catchments where solifluction processes dominate

to produce the subdued topography characteristic of the upper parts of the plateau.

Surface runoff becomes negligible in winter as the active layer freezes. However, aufeis (a.k.a. icing, naled) forms in winter on some rivers of the Richardson Mountains and Peel Plateau caused by an upwelling of water from springs in a river or creek (e.g., Lauriol and Clark 1991; Hu and Pollard 1997). This groundwater floods the frozen river and adjacent valley forming a large, layered ice sheet that can grow to several meters thickness and cover areas of several square kilometers. Thick aufeis deposits may persist for most of the summer.

Increases in the Peel River discharge begin in mid-April with the onset of snowmelt, followed by breakup and flooding in May (Environment Canada; http://wateroffice.ec.gc.ca). During the nival flood, the lower Peel River can experience a backwater effect from ice-jam flooding in the Mackenzie Delta; tributary streams may also experience ice-jam-related backwater effects near their confluence with the Peel River, enhancing sediment deposition in lower reaches. Convective storms can generate rapid runoff from sloping terrain underlain by permafrost. Summer rainfall events can be very important as surface, and bank sediments are thawed and more readily eroded by surface runoff and streams.

Sediment yields in the study region are relatively high for an arctic/subarctic landscape; Mackenzie River carries one of the highest sediment loads among circumpolar rivers (see chapter 3, this volume). The Peel River at Fort McPherson delivers more than 21 Mt a^{-1}, and Mackenzie River at Tsiigehtchic delivers more than 96 Mt a^{-1} (Carson et al. 1998; Holmes et al. 2002). Much of the Peel River sediment load is derived from the mid-reach to lower reach and from rivers that drain the plateau.

Figure 7.5a, b shows the sediment sources for catchments within the northern Peel Plateau and the characteristic scales at which they intersect the fluvial network. Debris flows, rotational slides, small active layer detachment slides, and other slope-driven mass wasting processes generally occur within steeper terrain and are generally coupled with the mountain streams in the upper portions of the catchment. The threshold catchment area for major thaw slump-driven erosion of the plateau is roughly 1 km^2 (Fig. 7.5).

Beyond this drainage basin scale, the dominant sediment sources tend to be related to thermokarst and thermoerosion, namely retrogressive thaw slumps, and areas of bank erosion by the river (Figs. 7.5, 7.6). Thaw slumps are a dominant solute and sediment source for streams and rivers in the Peel Plateau (Kokelj et al. 2013); thus, the highest specific sediment yields likely occur at catchment scales of 5–10 km^2 (Fig. 7.5b). Slump-impacted streams exhibit solute and sediment concentrations up to two orders of magnitude greater than in undisturbed streams. Meltwater pulses and lower frequency high-magnitude mass flows deliver solutes and sediments from thaw slumps to the streams, producing distinct diurnal and seasonal patterns in sediment and solute fluxes (Kokelj et al. 2013; Malone et al. 2013). Large debris tongue deposits, which have infilled stream valleys with deposits several meters in thickness, show evidence of stream diversion and multiple episodes of buildup and down cutting, transferring considerable sediment load downstream (Fig. 7.4).

At catchment scales greater than about 10 km^2, there is sufficient flow in the channel that stream sediment loads remain high. Lateral undercutting of the high valley walls contributes additional sediments to the larger streams which show evidence of considerable bank and valley wall erosion (Figs. 7.5b, 7.6). Thus, the specific sediment yield for streams and rivers that drain the Peel Plateau likely remains high with increasing catchment size.

7.6 Climate-Driven Intensification of Slumping, Feedbacks, and Cascading Effects

The large stores of late Pleistocene ground ice and frozen glacigenic sediments comprise the Peel Plateau. Thaw slumping, a dominant driver of geomorphic change in this ice-rich permafrost landscape, can rapidly degrade thick layers of ice-rich ground and release significant quantities of glacigenic materials downslope to fluvial systems. Since thaw slumping involves the coupling of geomorphic and thermal processes, this disturbance regime is particularly sensitive to climatic variation.

Warmer air temperatures and increasing rainfall can influence thaw slump initiation. Around lakes, rising permafrost and water temperatures can alter talik configuration and thaw ice-rich sediments adjacent to lakeshores causing lake-bottom subsidence, shoreline collapse, and thaw slump initiation (Kokelj et al. 2009). An increase in magnitude and intensity of rainfall can cause active layer detachment slides and accelerate thermoerosion along flow tracks and streams leading to the exposure of ground ice and slump initiation (Figs. 7.4, 7.5).

Several climate factors intensify the processes of thaw slump development. On the Peel Plateau, a recent increase in number and size of active slump surfaces and debris tongue deposits since the mid-1980s has occurred in concert with an increase in the magnitude and intensity of rainfall (Kokelj et al. 2015; Segal et al. 2016). Air temperature and precipitation interact to influence the moisture regime of slump soils and downslope sediment transport from the slump scar zone. Diurnal pulses in meltwater drive high-frequency, low-magnitude surficial sediment movement, and intense rainfall events stimulate major mass flows and downslope

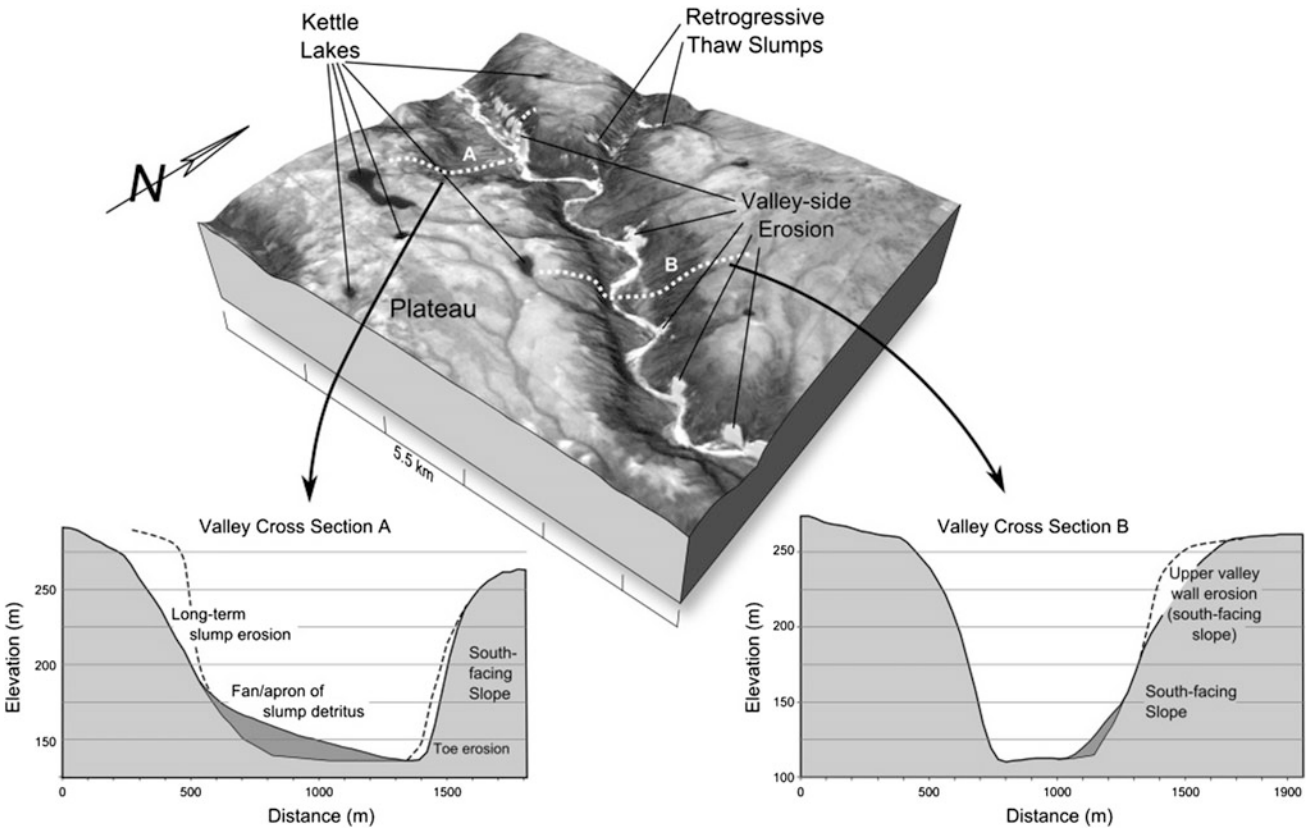

Fig. 7.6 Morphology of the lower incised valleys. The lower reaches of Stony Creek exhibit some notable relief (150 m) and steep valley (>40°) walls. Plateau stratigraphy is exposed where persistent erosion at the outer bends of river meanders erodes the slope base. Sediment eroded from the high valley walls is sufficient to satisfy transport capacity. Some of the larger E–W-oriented valleys exhibit some asymmetry in their cross section, likely due to enhanced thermoerosion of the plateau by thaw slumping. Flow tracks are evident from kettle lakes to the incised channel. See Fig. 7.1c for location

debris tongue enlargement to evacuate sediments from the scar zone, maintain a headwall of exposed ground ice, and inhibit slump stabilization (Kokelj et al. 2015).

The enlargement of thaw slumps initiates feedbacks that amplify this disturbance regime. At decadal timescales, large slumps retreat more rapidly than small ones because they are less likely to accumulate sufficient debris to arrest headwall retreat (Lacelle et al. 2015). The exposure to incoming solar radiation and rate of ground ice ablation also increase with headwall size so that mega slumps are likely to grow more rapidly than smaller disturbances. Large, rapidly thawing headwalls produce saturated scar zone soils that are preconditioned for the occurrence of major rainfall-induced flow events (Kokelj et al. 2015). As thaw slumps enlarge so does their upslope contributing catchment area. Slump growth can capture upslope drainage networks, which contribute additional moisture to the scar zone and further accelerate thermoerosion of the slump headwall and scar surface (Fig. 7.4c).

These feedbacks accelerate scar zone sediment flux to promote the formation of debris tongue deposits, which can intensify fluvial impacts and disturbance of adjacent slopes (Figs. 7.3c, 7.4) (Kokelj et al. 2015). Debris tongue deposits can lead to the development of debris-dammed lakes and channel diversions. Lateral stream displacement commonly initiates valley side thermoerosion and slumping of adjacent slopes to produce areas of high disturbance intensity. Some of the most vigorous erosion of the plateau by mega slumps occurs at watershed scales of roughly 1–10 km^2 (Fig. 7.5).

Intensification of the slump disturbance regime has significant downstream impacts. Regional disturbance inventories indicate that slumping in the Peel and lower Mackenzie River basins impacts hundreds of small- to medium-sized watersheds (Brooker et al. 2014). An increase in the frequency and magnitude of thaw slumps on the Peel Plateau has enhanced the supply of sediments and solutes to fluvial environments (Kokelj et al. 2013; Malone et al. 2013). A significant increase in SO_4 concentrations and the SO_4/Cl ratio in the Peel River between 1960 and 2012 indicate an increase in the availability of weatherable tills, suggesting that the recent acceleration in thaw slump activity is detectable in the geochemical flux of this 70,000 km^2

watershed (Kokelj et al. 2013). The rapid fluvial responses to the slump disturbance regime highlight the efficacy of this process in mobilizing glacigenic materials from slopes to the fluvial system.

7.7 Conclusions: An Ice-Rich Landscape in Transition

The Peel Plateau is strongly conditioned by its glacial legacy. Given the large amounts of glacigenic materials and ground ice and the relatively high topographic gradients on this landscape, there remains considerable potential for climate-driven geomorphic change. In this environment, thaw slumping is an important driver of landscape evolution. The process is sensitive to climate variation and highly effective at reconfiguring slopes and transporting large volumes of sediments to valleys and fluvial systems.

The Peel Plateau is an example of a "glacially conditioned" landscape; however, permafrost has limited sediment availability, dampening the rates and magnitude of post-glacial geomorphic change that is typically associated with paraglacial conditions (Church and Ryder 1972; Ballantyne 2002). Thermokarst processes such as thaw slumping, which mobilize stores of glacigenic materials, are incrementally active, or reactivated over time, and their intensity varies in relation to climatic drivers. Contemporary warming and increased precipitation is proving to be a particularly strong driver of accelerated thaw slumping and geomorphic change in the Peel Plateau. The recent intensification of thaw slump activity and the impacts on slopes and stream sedimentary regimes indicate that this ice-rich permafrost environment may be regarded as a hot spot of landscape change in a warmer and wetter climate.

References

Ballantyne CK (2002) Paraglacial geomorphology. Quat Sci Rev 21:1935–2017

Bjornson J (2003) Les glissements rétrogressifs de fonte de la rivière Willow, Territoires du Nord-Ouest, Canada: Caractéristiques sédimentologiques, distribution spatiale et temporelle (Unpublished MSc Thesis). University of Ottawa

Brooker A, Fraser RH, Olthof I, Kokelj SV, Lacelle D (2014) Mapping the activity and evolution of retrogressive thaw slumps by tasselled cap trend analysis of a Landsat satellite image stack. Permafrost Periglac 25:243–256

Brown V (2012) Ice stream dynamics and pro-glacial lake evolution along the north-western margin of the Laurentide Ice Sheet. (Doctoral Thesis). Durham University

Burn CR (1997) Cryostratigraphy, paleogeography, and climate change during the early Holocene warm interval, western Arctic coast, Canada. Can J Earth Sci 34:912–925

Burn CR, Kokelj SV (2009) The environment and permafrost of the Mackenzie Delta area. Permafrost Periglac 20:83–105

Carson MA, Jasper JN, Conly FM (1998) Magnitude and sources of sediment input to the Mackenzie Delta, Northwest Territories, 1974–94. Arctic 51:116–124

Catto NR (1996) Richardson Mountains, Yukon-Northwest Territories: the northern portal of the postulated "ice-free corridor". Quat Int 32:3–19

Church MA, Ryder JM (1972) Paraglacial sedimentation: a consideration of fluvial processes conditioned by glaciation. Geol Soc Am Bull 83:3059–3072

Clark I, Lauriol B, Marschner M, Sabourin N, Chauret Y, Desrochers A (2004) Endostromatolites from permafrost karst, Yukon, Canada: paleoclimatic proxies for the Holocene hypsithermal. Can J Earth Sci 41:387–399

Duk-Rodkin A, Hughes OL (1992) Pleistocene montane glaciations in the Mackenzie Mountains, Northwest Territories. Géog Phys Quatern 46:69–83

Duk-Rodkin A, Lemmen S (2000) Glacial history of the Mackenzie region. In: Dyke LD, Brooks GR (eds) The physical environment of the Mackenzie Valley, Northwest Territories: a base line for the assessment of environmental change. Geol Surv Can Bull, pp 11–20

Duk-Rodkin A, Robertson T (2001) Landslide inventory, Mackenzie corridor (central part), Northwest Territories. Geol Surv Can, Open File No. 3916

Dyke A, Evans D (2003) Ice-marginal terrestrial landsystems: northern Laurentide and Innuitian ice sheet margins. In: Evans DJA (ed) Glacial landsystems. Arnold, London, pp 143–165

Dyke AS, Prest VK (1987) Late Wisconsinan and Holocene history of the Laurentide ice sheet. Géog Phys Quat 41:237–263

Ecosystem Classification Group (2010) Ecological regions of the Northwest Territories—Cordillera, Department of Environment and Natural Resources, Government of the Northwest Territories, Yellowknife, NT, Canada

Environment Canada (2012) National climate data and information archive, fort McPherson, NWT. http://climate.weatheroffice.gc.ca

Evans D (2009) Controlled moraines: origins, characteristics and palaeoglaciological implications. Quat Sci Rev 28:183–208

Gill HK, Lantz TC, O'Neill B, Kokelj SV (2014) Cumulative impacts and feedbacks of a gravel road on shrub tundra ecosystems in the Peel Plateau, Northwest Territories, Canada. Arctic Antarct Alp Res 46:947–961

Grom J, Pollard W (2008) A study of high Arctic retrogressive thaw slump dynamics, Eureka Sound Lowlands, Ellesmere Island. In: Proceedings of the ninth international conference on permafrost, pp 545–550

Hastings SJ, Luchessa SA, Oechel WC, Tenhunen JD (1989) Standing biomass and production in water drainages of the foothills of the Philip Smith Mountains, Alaska. Ecography 12:304–311

Hill PR, Mudie PJ, Moran K, Blasco SM (1985) A sea-level curve for the Canadian Beaufort Shelf. Can J Earth Sci 22:1383–1393

Holmes RM, McClelland JW, Peterson BJ, Shiklomanov IA, Shiklomanov AI, Zhulidov AV, Gordeev VV, Bobrovitskaya NN (2002) A circumpolar perspective on fluvial sediment flux to the Arctic ocean. Glob Biogeochem Cycles 16:45-1–45-14

Hu X, Pollard WH (1997) The hydrologic analysis and modelling of river icing growth, North Fork Pass, Yukon Territory, Canada. Permafrost Periglac 8:279–294

Judge AS (1973) The thermal regime of the Mackenzie valley: observations of the natural state (No. 73–38), Environmental Social Committee Northern Pipeline (Canada), Task Force on Northern Oil Development, Ottawa

Kaufman DS, Ager TA, Anderson N, Anderson PM, Andrews JT, Bartlein PJ, Brubaker LB, Coats LL, Cwynar LC, Duvall ML, Dyke AS, Edwards ME, Eisner WR, Gajewski K, Geirsdóttir A, Hu FS, Jennings AE, Kaplan MR, Kerwin MW, Lozhkin AV, MacDonald GM, Miller GH, Mock CJ, Oswald WW, Otto-Bliesner BL, Porinchu DF, Rühland K, Smol JP, Steig EJ, Wolfe BB (2004) Holocene thermal maximum in the western Arctic (0–180°W). Quat Sci Rev 23:529–560

Kokelj SV, Jorgenson MT (2013) Advances in thermokarst research. Permafrost Periglac 24:108–119

Kokelj SV, Lantz TC, Kanigan J, Smith SL, Coutts R (2009) Origin and polycyclic behaviour of tundra thaw slumps, Mackenzie Delta region, Northwest Territories, Canada. Permafrost Periglac 20:173–184

Kokelj SV, Lacelle D, Lantz TC, Tunnicliffe J, Malone L, Clark ID, Chin KS (2013) Thawing of massive ground ice in mega slumps drives increases in stream sediment and solute flux across a range of watershed scales. J Geophys Res Earth Surf 118:681–692

Kokelj SV, Tunnicliffe JF, Lacelle D, Lantz TC, Chin KS, Fraser R (2015) Increased precipitation drives mega slump development and destabilization of ice-rich permafrost terrain, northwestern Canada. Glob Planet Change 129:56–68

Lacelle D, Bjornson J, Lauriol B, Clark ID, Troutet Y (2004) Segregated-intrusive ice of subglacial meltwater origin in retrogressive thaw flow headwalls, Richardson Mountains, NWT, Canada. Quat Sci Rev 23:681–696

Lacelle D, Bjornson J, Lauriol B (2010) Climatic and geomorphic factors affecting contemporary (1950–2004) activity of retrogressive thaw slumps on the Aklavik Plateau, Richardson Mountains, NWT, Canada. Permafrost Periglac 21:1–15

Lacelle D, Lauriol B, Zazula G, Ghaleb B, Utting N, Clark ID (2013) Timing of advance and basal condition of the Laurentide Ice Sheet during the last glacial maximum in the Richardson Mountains, NWT. Quat Res 80:274–283

Lacelle D, Brooker A, Fraser RH, Kokelj SV (2015) Distribution and growth of thaw slumps in the Richardson Mountains-Peel Plateau region, northwestern Canada. Geomorphology 235:40–51

Lantuit H, Pollard WH, Couture N, Fritz M, Schirrmeister L, Meyer H, Hubberten H-W (2012) Modern and late Holocene retrogressive thaw slump activity on the Yukon Coastal Plain and Herschel Island, Yukon Territory, Canada. Permafrost Periglac 23:39–51

Lantz TC, Kokelj SV, Gergel SE, Henry GHR (2009) Relative impacts of disturbance and temperature: persistent changes in microenvironment and vegetation in retrogressive thaw slumps. Glob Change Biol 15:1664–1675

Lauriol B, Clark JCMEID (1991) Localisation, Genèse et Fonte de Quelques Naleds du Nord du Yukon (Canada). Permafrost Periglac 2225–2236

Lauriol B, Cabana Y, Cinq-Mars J, Geurts M-A, Grimm FW (2002a) Cliff-top eolian deposits and associated molluscan assemblages as indicators of Late Pleistocene and Holocene environments in Beringia. Quat Int. Holocene Studies, INQUA Commission Meeting, Sevilla 2000 87, pp 59–79

Lauriol B, Duguay CR, Riel A (2002b) Response of the Porcupine and Old Crow rivers in northern Yukon, Canada, to Holocene climatic change. Holocene 12:27–34

Lauriol B, Lacelle D, Labrecque S, Duguay CR, Telka A (2009) Holocene evolution of lakes in the Bluefish Basin, Northern Yukon, Canada. Arctic 62:212–224

Lewkowicz AG (1987) Headwall retreat of ground-ice slumps, Banks Island, Northwest Territories. Can J Earth Sci 24:1077–1085

Lewkowicz AG (2007) Dynamics of active-layer detachment failures, Fosheim Peninsula, Ellesmere Island, Nunavut, Canada. Permafrost Periglac 18:89–103

Lewkowicz AG, Kokelj SV (2002) Slope sediment yield in arid lowland continuous permafrost environments, Canadian Arctic Archipelago. Catena 46:261–283

Mackay JR (1967) Permafrost depths, lower Mackenzie Valley, Northwest Territories. Arctic 20:21–26

Mackay JR (1971) The origin of massive icy beds in permafrost, western Arctic Coast, Canada. Can J Earth Sci 8:397–422

Mackay JR (1972) The world of underground ice. Ann Assoc Am Geogr 62:1–22

Mackay JR (1980) The origin of hummocks, western Arctic coast, Canada. Can J Earth Sci 17:996–1006

Mackay JR (1981) Active layer slope movement in a continuous permafrost environment, Garry Island, Northwest Territories, Canada. Can J Earth Sci 18:1666–1680

Malone L, Lacelle D, Kokelj S, Clark ID (2013) Impacts of hillslope thaw slumps on the geochemistry of permafrost catchments (Stony Creek watershed, NWT, Canada). Chem Geol 356:38–49

Murton J, Whiteman C, Waller R, Pollard W, Clark I, Dallimore S (2005) Basal ice facies and supraglacial melt-out till of the Laurentide Ice Sheet, Tuktoyaktuk Coastlands, western Arctic Canada. Quat Sci Rev 24:681–708

Norris DK (ed) (1997) Geology and mineral and hydrocarbon potential of northern Yukon Territory and northwestern District of Mackenzie. Geol Surv Can Bull 422

NWT Centre for Geomatics (2013) GNW spot mosaic. Data available at http://apps.geomatics.gov.nt.ca//arcgis/rest/services/Mosaics/GNWT_SPOT_Mosaic/MapServer. Accessed January 2015

O'Neill HB, Burn CR, Kokelj SV, Lantz TC (2015) "Warm" tundra: Atmospheric and near-surface ground temperature inversions across an alpine treeline in continuous permafrost, western Arctic, Canada. Permafrost Periglac 26:103–118

Quinton W, Marsh P (1999) A conceptual framework for runoff generation in a permafrost environment. Hydrol Process 13:2563–2581

Rampton VN (1988) Quaternary geology of the Tuktoyaktuk Coastlands, Northwest Territories. Geol Surv Can Mem, No. 423

Ritchie JC, Cwynar LC, Spear RW (1983) Evidence from north-west Canada for an early Holocene Milankovitch thermal maximum. Nature 305:126–128

Segal RA, Lantz TC, Kokelj SV (2016) Acceleration of thaw slump activity in glaciated landscapes of the western Canadian Arctic. Environ Res Lett 11:34025–34036

Serreze MC, Walsh JE, Iii FSC, Osterkamp T, Dyurgerov M, Romanovsky V, Oechel WC, Morison J, Zhang T, Barry RG (2000) Observational evidence of recent change in the northern high-latitude environment. Clim Change 46:159–207

Slobodin R (1981) Kutchin [Gwich'in]. In: Helm J (ed) Handbook of North American Indians: vol. 6 Subarctic. Smithsonian, Washington, pp 514–532

Smith IR, Lesk-Winfield K (2012) An updated assessment of ground ice and permafrost geology-related observations based on seismic shothole drillers' log records, Northwest Territories and northern Yukon (Open File No. 7061). Geol Surv Can Open File, No. 7061

St-Onge DA, McMartin I (1999) The Bluenose Lake Moraine, a moraine with a glacier core. Géog Phys Quat 53:287–296

Walker DA, Binnian E, Evans BM, Lederer ND, Nordstrand E, Webber PJ (1989) Terrain, vegetation and landscape evolution of the R4D research site, Brooks Range Foothills, Alaska. Ecography 12:238–261

Woo M (2012) Permafrost hydrology. Springer, New York

Zazula GD, MacKay G, Andrews TD, Shapiro B, Letts B, Brock F (2009) A late Pleistocene steppe bison (Bison priscus) partial carcass from Tsiigehtchic, Northwest Territories, Canada. Quat Sci Rev 28:2734–2742

Little Limestone Lake: A Beautiful Marl Lake in the Interlake Region, Manitoba

8

Derek Ford

Abstract

Marl lakes are those accumulating fine-grained bottom sediments including at least 25 % $CaCO_3$. Visually attractive examples have higher proportions of $CaCO_3$, with crystallites precipitating in the water to give it a rich and opaque duck-egg blue colouration. Such lakes are largely limited to recently glaciated carbonate rock terrains. Most are also shallow, with much or all of the water column being in the photic zone. Little Limestone Lake (lat. 53°47′ N, long. 99°19′W) is the finest example that the author has seen. It occupies a shallow glacial trough scoured in a plain of flat-lying cyclothem dolomites. It is ~12 km long, 1–5 km wide, and rarely >7 m deep. Including bordering wetlands, it occupies ~45 % of the area of an elongated, narrow topographic basin. Recharge is through impoverished boreal forest with little soil cover; it discharges chiefly as springs and seeps along and below the shore. Mean annual temperature is ~1 °C, and precipitation is ~475 mm/year. Springs in the surrounding region show groundwaters to be simple bicarbonate composition, with TDS = 230–300 mg/L. Grab sampling throughout the lake found its waters degassed to 125–135 mg/L. Little Limestone Lake is visually spectacular because it is almost entirely groundwater fed, with a ratio of recharge area to lake area that is low. In contrast, nearby lakes are regularly flushed by channelled surface storm water and thus cannot maintain high densities of crystallites in suspension. The lake became protected as a provincial park in June 2011.

Keywords

Marl lake • Glaciated karst • Superlative colour • Park protection

8.1 Introduction

The *raison d'être* for this contribution can be seen clearly in Fig. 8.1a, a MODIS image taken on 6 October 2004. Amongst the many lakes of central Manitoba, Little Limestone Lake stands out very sharply even from space due to its intense duck-egg blue colour. It is a 'marl' lake, defined sensu stricto as one in which the sediment accumulating on the bottom is a mixture of 25–75 % calcium carbonate with clay or silt or non-carbonate organic debris (Schurrenberger et al. 2003). Marl has the feel and appearance of soft mud or ooze. Some authorities would extend the term to include sediments with up to 95 % calcium carbonate provided that they remain soft, i.e. unconsolidated. An essential feature of the most attractive marl lakes everywhere is that there are also calcium carbonate micro-crystals ('crystallites') in suspension in sufficient concentration in the water column to scatter sunlight and so create strong and opaque blue colouration.

Lakes where marl contributes between 5 and 95 % of the bottom sediments (marl lakes sensu lato) are found in every region of the world where there are large quantities of limestone and/or dolomite to contribute the essential calcium ions, and the climate is humid enough to maintain the lakes

D. Ford (✉)
School of Geography and Geology, McMaster University, Hamilton, ON L8S 4L8, Canada
e-mail: derekcliffordford@gmail.com

© Springer International Publishing Switzerland 2017
O. Slaymaker (ed.), *Landscapes and Landforms of Western Canada*, World Geomorphological Landscapes, DOI: 10.1007/978-3-319-44595-3_8

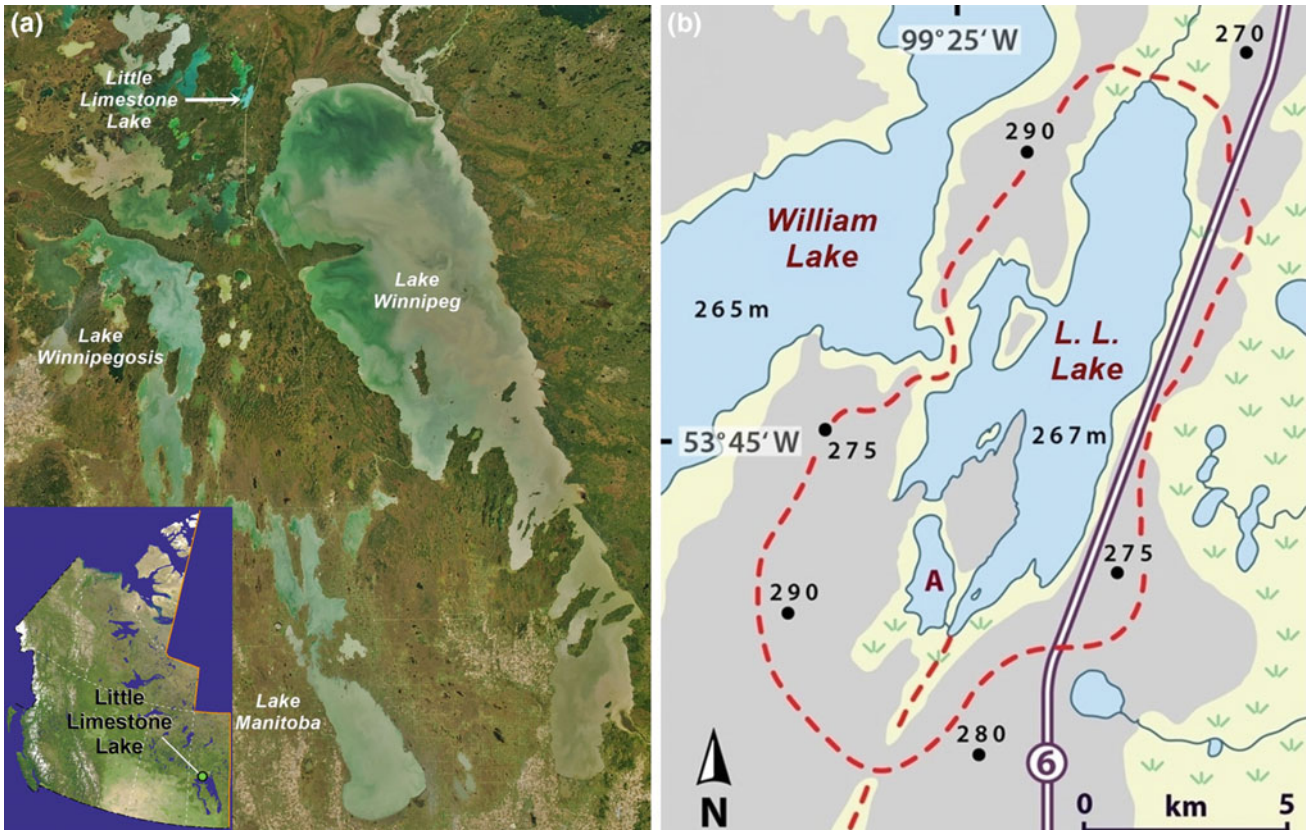

Fig. 8.1 **a** Portion of a moderate resolution imaging spectroradiometer (MODIS) image acquired 6 October 2004 covering the Interlake country, Manitoba. Little Limestone Lake stands out as a small but bright duck-egg blue lake west of the northern end of Lake Winnipeg. Highway 6 runs alongside it. The prominent transverse ridge is The Pas Moraine. *Source* Jacques Descloitres, MODIS Rapid Response Team, NASA/GSFC—extracted from Canada.A2004280.1915.250 m. *Inset image*: NASA, Visible Earth. **b** Schematic map of Little Limestone Lake and its basin

and keep the concentrations of dissolved solids in them below the levels where precipitation of gypsum and salt (evaporites) begins. Most climatically humid regions and the wetter fringes of the sub-humid/semi-arid regions qualify. However, it is recognised that a disproportionately large number of marl lakes are to be found in the glaciated regions, including perhaps a majority of the visually very attractive. Most marl lakes that have been described in the scientific literature are located in the glaciated regions of northern Europe and North America.

Following Pentecost (2009) the paths to the creation and deposition of marl may be inorganic or biogenic. Processes in a given lake may be completely dominated by one of them or by a mixture of both that may differ in their proportions as the seasons progress. The abiogenic is the simple process of limestone or dolomite inorganic dissolution, with crystallite precipitation following when CO_2 degasses from the Ca, Mg, HCO_3 solution due to warming or loss of pressure, or both.

Wholly biogenic deposits may arise because photosynthesis in freshwaters creates many species of microscopic algae and bacteria. Pentecost focuses on the common green alga *Chara* but there are a host of alternatives. In the first step: $-2HCO_3^- \rightarrow CH_2O_{(photosynthesis)} + O_2 + CO_3^{2-}$. There is abundant HCO_{3-} in karst lake waters, e.g. McConnaughey et al. (1994) found that macrophytes, chiefly *Chara*, extracted ~23 g C/m^2 during the growth season in a Minnesota marl lake. With abundant Ca^{2+} also being present via the inorganic path, step 2 proceeds: $-Ca^{2+} + CO_3^{2-} \rightarrow CaCO^{3(calcite)}$. 'Calcite begins to form in strongly alkaline surface regions of the internodal *Chara* cells and subsequently envelops almost the entire plant. During the later stages of calcification additional inorganic precipitation may be taking place but this has been little studied' (Pentecost 2009). The inorganic calcite probably accretes to the outer surface of the alga in the manner that it accretes to larger plants to form *tufa* deposits in many streams and lakes around the world. The algae remain very tiny, however, many species being plankton suspended in the water and scatter incident light and settle slowly downwards only if conditions become very calm.

8.2 Little Limestone Lake and Its Setting

Little Limestone Lake (Fig. 8.1; lat. 53°47′N, long. 99°19′ W) is the finest example of a marl lake that the author has seen in many years studying glaciated karst regions. It stands out sharply from neighbouring lakes in summertime colour satellite imagery, as illustrated. Viewed from the shore or in a boat, it is equally colourful (Fig. 8.2). For these reasons, the Manitoba chapter of the Canadian Parks and Wilderness Society argued for its protection for many years. The conservation branch of the provincial government requested an independent evaluation by a specialist (Ford 2010), which resulted in a park protection area being proclaimed in 2011.

The lake is situated in the Interior Low Plateaus geologic province, ~20 km west of Lake Winnipeg and draining to Hudson Bay. The bedrocks are platformal dolomites of Silurian age (Atikameg and East Arm Formations) totalling approximately 80 m in thickness and dipping very gently westwards (Bezys 1991; Bezys and Kobylecki 2003). Local relief upon them is never more than 70 m, created chiefly by glacial scour, or the deposition of glacial moraines during the recession of the last Laurentide ice sheet ~11,000 years ago. A sample bedrock section exposed to a road cut a few km south of the lake is shown in Fig. 8.3a. The strata are cyclic successions of regular beds varying from 'medium' (10 cm) to 'massive' (>100 cm) in thickness. The thicker beds are mechanically stronger and so survived glacier scour more readily. Clint and grike solutional pavement (epikarst) has developed on them in post-glacial times (Ford 1987; Ford and Williams 2007). They also have a high density of vugs, which can increase the matrix permeability of the rock and thus the quantities of dolomite taken into solution by groundwater permeating through it. Examples of the cliffs on massive dolomites and epikarst on thinner beds along the shores of Little Limestone Lake are shown in Fig. 8.4.

In Fig. 8.1b, the boundaries of the lake basin are drawn conventionally to follow the surface topographic divide because no karstic diversions of groundwater flow across divides are known. The basin is ~20 km in length and 5–8 km wide. It has an area of ~91 km^2, of which 36 km^2 is occupied by the lake itself. Pond A (~2 km^2; Fig. 8.1b) is a former arm of the lake that is now separated by wetlands but still drains into it; it has negligible groundwater supplies of its own, and its water is clear, not opaque and blue. The dry land area that is believed to contribute to the lake is ~53 km^2. Wetlands at or very close to the lake level occupy ~3.5 km^2 of this, and the balance consists of gentle side slopes and broad plateaus. The lake is at ~267 m above sea level, and the highest ground is around 290 masl.

There is no bathymetric map of Little Limestone Lake, and the bottom is always obscured by the suspended matter in summer. The geologic and physiographic setting indicates

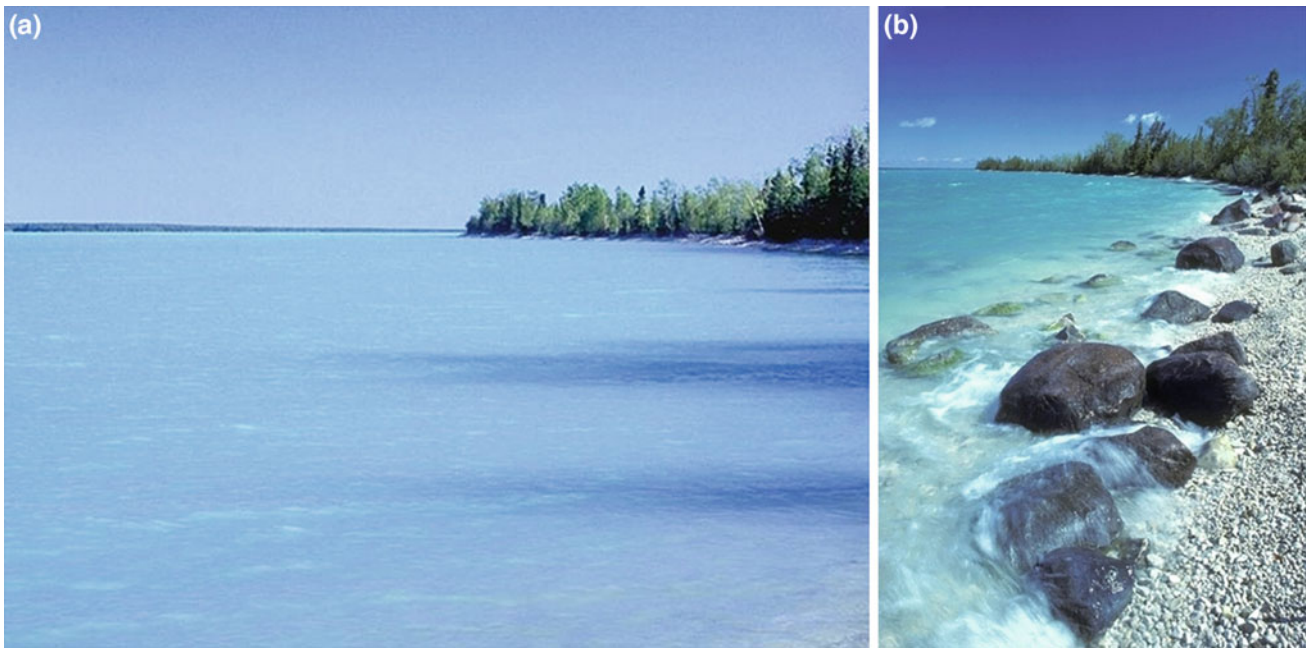

Fig. 8.2 To emphasise the strength of its blue colouration, Little Limestone Lake seen in both calm and windy weather. Boulders on the beach are shield erratics, and the fine-grained shingle is from the local dolomite (photos courtesy of Roger Turenne)

Fig. 8.3 **a** Cyclic dolomites of the Atikameg formation (Silurian) exposed in a Highway 6 road cut near Little Limestone Lake. The abrupt transitions of bed thicknesses between medium and massive are well seen here. The massive upper bed is weakly opened by solution down joints, forming 'grikes'. **b** Incipient grikes exposed by clearance for parking by the lake shore

that the lake is likely to be shallow everywhere. A few measured depths suggest that much of it has a flat floor at −7.0 to −7.5 m. This is comparatively deep for a marl lake but not as great as the deepest mentioned in Pentecost's (2009) sample of 100 such lakes in the British Isles. At −7.5 m the waters are fully in the photic zone. Sample cream-coloured carbonate oozes were dredged from the bottom there.

At its north end Little Limestone Lake is drained by a regular stream channel that passes through a wetland into a lake about 1 m lower (266 masl). A small spring-fed stream flows into the southern end. To the west William Lake, a much larger water body, is at 265 masl. To the east and south there are extensive wetlands and smaller dolomite plateaus draining 18–20 km eastwards into Lake Winnipeg at 217 masl. The important consequence is that the Little Limestone Lake basin, although it functions as a water-retaining shallow trough, can be envisioned as an elongated hydrological ridge or 'high' perched between drainage to lower lake levels around it. The lake plus pond A and associated wetlands occupy nearly 46 % of the basin, a very large proportion. Recharge from the remaining ∼54 % is almost entirely by groundwater that has passed through the dolomite. As a consequence, the basin is not prone to flushing by mud-laden flood waters from proportionally greater recharge areas, as the majority of other lakes in the region are. Under the natural conditions that have prevailed for at least some thousands of years here a delicate physical, chemical and (probably) biogenic balance has been able to build up and establish the remarkable marl blue colouration. The current climatic conditions are cool continental (Koppen type D). The mean annual temperature is ∼1.0 °C and precipitation is 475 mm/year. The natural vegetation is impoverished boreal forest.

Nearly flat plateau and bench surfaces in bedrock are predominant in the recharge areas. There is thin and discontinuous glacial till cover on them due to erosion by over-wash immediately after the ice receded. There is a nearly 100 % cover of mosses, lichens, flowers, juniper and other low shrubs, and forest litter. The trees are widely spaced, slow-growing or stunted in many places, reflecting the edaphic drought that occurs where the dolomite surfaces are efficiently drained by epikarst (Fig. 8.5). Forest fires have broken up the karst on thinner beds, increasing the efficiency of groundwater recharge. The greatest straight-line distance that groundwater must flow from these uplands to the lake is no more than 3–4 km, giving hydraulic gradients (depth/length gradients) of 5 m/km or more. There are some

Fig. 8.4 Three views of the shoreline that emphasise that discharge into the lake is from groundwater drainage through epikarst of differing local density

seepages in the cliffs and at the water line in the lake but most groundwater discharge is below that, perhaps because industrious beavers have raised the lake level by ~0.5 m in recent decades.

8.3 Water Chemistry

The water chemical characteristics of the lake itself have not been studied in detail. However, McRitchie (1994, 1995) carried out systematic sampling at springs and seeps in the dolomite escarpment immediately south of it, plus two water samples from springs on William Lake. Seventy water samples were analysed for the standard water quality variables plus trace concentrations of economic minerals and contaminants. All of the waters were simple calcium bicarbonate groundwaters typical of clean dolomite terrains. Total hardness ranged between 230 and 300 mg/L, Ca 40–60 mg/L and Mg 30–40 mg/L. The waters were saturated or supersaturated with respect to calcium carbonate under standard atmospheric conditions. Na, K, SO_4 and Cl were negligible in amount. At each site there was one-time sampling only and, in most cases, the water was taken from the spring itself before it had any opportunity to degas its CO_2 content or make other adjustments to open air conditions. McRitchie (1994) described what happened downstream, however—precipitates quickly appeared, as sand-sized particles at first but rapidly shrinking in size downstream and ceasing to form after 200–300 m of flow in the open channels. In the ponds at some springs there were organic-rich

Fig. 8.5 *Above* three scenes illustrating recharge conditions on the western plateau where the dolomite bedding is massive. The density of groundwater sink points is low. *Below* a recently burned area on the southern plateau where the bedding is of medium thickness and so readily broken up by frost and fire in addition to solution. The density of sink points is very high

mats of material. Downstream there was only cream-grey carbonate ooze, very like that collected from the bottom of Little Limestone Lake. The oozes were almost entirely $CaCO_3$, chiefly of inorganic origin although one of four samples may have contained as much as 10 % organics (i.e. from photosynthesis, as described above).

In September 2010, the author took one near-shore bulk water sample from the surface of Little Limestone Lake and a second from −2.0 m in the centre. Comprehensive standard analyses (ALS Laboratory, Winnipeg) found the two samples nearly identical, indicating that at least the upper two metres of the lake are uniform in composition. Na, K, Cl and SO_4 were negligible in amount. Total hardness (as $CaCO_3$) was 200 mg/L. This is significantly less than the values between 230 and 300 mg/L that Ritchie obtained at the springs and seeps from the dolomites. It suggests that the lake waters have degassed CO_2 and precipitated large amounts of their dissolved load. This explanation is substantiated by the Ca:Mg ratios of 26:33–34. In the large majority of published dolomite karst water compositions, the ratio is the reverse of this (60:40–80:20 in favour of Ca^{2+} until vigorous precipitation begins). The detection of 2–3 mg/L of CO_3^{2-} also indicates degassing, at a pH above 8.3. Determination of free CO_3 in the lake waters is a hint that photosynthesis was occurring.

Water temperature and electrical conductivity were measured at a depth of ∼1.0 m at 27 different points in the lake. A global 'best fit' equation for clean bicarbonate waters (salts + sulphates + nitrates + phosphates < 10 %; electrical conductivity <600 µS; see Krawczyk and Ford 2006) was used to calculate total hardness as mg/L $CaCO_3$. The principal finding was the uniformity of shallow water chemistry

everywhere on the lake proper. Despite a range of temperatures from 12.8 to 17.4 °C during the two days of sampling, EC was in the narrow range of 240–250 µS with one exception, yielding estimated $CaCO_3$ concentrations of 126–132 mg/L that place the lake waters comfortably in the mid-range that Pentecost (2009) cited in his sample of more than one hundred marl lakes and ponds in the British Isles. The one exception was the small spring-fed stream draining the southern epikarst. It entered the lake at a temperature of 11 °C, EC = 296 µS, and was clear (no blue opacity). Twenty metres further out into the lake sampling a few minutes later yielded T = 14.4 °C, EC = 247 µS. This suggested rapid warming with net precipitation of ~25 mg/L $CaCO_3$.

Concerning the stability of the density and hue of the colour, the author's previous visits to the lake (1984, 2004) were of short duration during warm sunny afternoons which led him to wonder whether there might be a daily 'blooming' of crystallites in response to solar warming, such as has been proposed for knee-deep water on the Bahamas Banks for example. It is now appreciated that this is not the case; the crystallites can have a duration of at least many weeks in suspension during the ice-free period on the lake, giving sufficient time for wind to mix them thoroughly across the surface. Further, many authorities contend that lakes that are as shallow as typical marl lakes do not develop strong thermal or other stratification (Pentecost 2009); the physical and chemical conditions are broadly similar from surface to the bottom. From the physical chemistry, some increase in the rate of precipitation is to be expected at the warmest times of the day: at Little Limestone Lake other observers have reported their qualitative impressions that there is some increase in density (opacity) then.

8.4 Conclusions and Recommendations

Little Limestone Lake has outstanding blue ('marl lake-type') colouration because its small and shallow, elongated basin is delicately perched between much larger basins draining to east and west respectively and thus is protected from flushing or clastic or organic detrital input by large surface streams during any strong thaw or rain flood events. The ratio of recharge area to lake area is low. Almost all annual recharge is from the combination of seasonal snowmelt and perennial groundwater flow directed through the enclosing dolomites. From current knowledge, it appears that the water chemical behaviour that determines the striking blue colouration of the lake during the summer is quite robust. The bulk of $CaCO_3$ crystallite precipitation appears to be of physical origin but the contribution of photosynthesis is not adequately understood at present.

The location is remote and the local population is very small. However, there are nickel exploration prospects in Canadian Shield rocks beneath the dolomites around William Lake that touch the western side of Little Limestone Lake. Physical threats to the lake could arise if the volumes of water flowing into it were substantially increased or diminished by any exploration or other development. Both could impact the colouration and its chemical stability in ways that are difficult to forecast. Chemical hazards could include acidification or introduction of other contaminants that kill off pertinent biota if biogenic activity is a crucial contributor to the carbonate precipitation. Heavy gasoline-powered boat traffic could also pose a threat. It is hoped that the creation of the provincial park will deal with these problems.

Acknowledgments The author is indebted to Roger Turenne and Ron Thiessen (Manitoba chapter, Canadian Parks and Wilderness Society), Ken Schykulski (Manitoba Conservation) and Chief Philip Buck of the Mosakahiken First Nation for their encouragement and support in the field.

References

Bezys RK (1991) Stratigraphic mapping (NTS 63F, 63K) and corehole programme 1991. Manitoba Energy and Mines, Report of Activities 1991, pp 61–73

Bezys RK, Kobylecki AJ (2003) Preliminary karst inventory of areas north and south Grand Rapids, Manitoba (NTS 63B and 63G). Manitoba Energy and Mines, Report of Activities 2003, pp 213–223

Ford DC (1987) Effects of glaciations and permafrost upon the development of karst in Canada. Earth Surf Process Landf 12:507–522

Ford DC (2010) Final report upon field studies and review at Little Limestone Lake Park Reserve. Parks and Natural Areas Branch, Manitoba Conservation, Canadian Parks and Wilderness Society, p 66

Ford DC, Williams PW (2007) Karst hydrogeology and geomorphology. Wiley, Chichester

Krawczyk WE, Ford DC (2006) Correlating specific conductivity with total hardness in limestone and dolomite karst waters. Earth Surf Process Landf 31:221–234

McConnaughey TA, Labaugh JW, Rosenberry DO, Striegl RG, Reddy MA, Schuster PF, Carter V (1994) Carbon budget for a groundwater-fed lake: calcification supports summer photosynthesis. Limnol Oceanogr 39:1319–1332

McRitchie WD (1994) GS-29. Spring water and marl geochemical investigations, Grand Rapids Uplands (NTS 63G). Manitoba Energy and Mines, Mineral Division, Report of Activities 1994, pp 148–162

McRitchie WD (1995) GS-22. Spring water and marl geochemical investigations, Grand Rapids Region, 1995 Status Report (NTS 63G). Manitoba Energy and Mines, Mineral Division, Report of Activities 1995, pp 109–119

Pentecost A (2009) The marl lakes of the British Isles. Freshw Rev 2009:167–197

Schurrenberger D, Russell J, Kelts K (2003) Classification of lacustrine sediments based on sedimentary components. J Paleolimnol 29:141–154

Landscapes of the Assiniboine River Watershed

9

W.F. Rannie

Abstract

The Assiniboine River watershed, 162,000 km^2 in area, contains five classic Prairie landscapes, namely (a) till plains characterized by hummocky terrain deposited by stagnating ice sheets, (b) closed depressions containing small lakes and sloughs of the Prairie Pothole region, (c) glacial spillways, (d) the flat floors of former ice-dammed glacial lakes, and (e) inactive sand dunefields. In addition, the watershed contains a large glacial delta and has undergone several extraordinary changes to its river network.

Keywords

Prairie landscape • Glacial spillways • Glacial lakes • Assiniboine River

9.1 Introduction

The Assiniboine River in east-central Saskatchewan and western Manitoba (Fig. 9.1) is the model Prairie stream. The river has a drainage area of 162,000 km^2. The structure and composition of the watershed's underlying geology and its surface materials are representative of most of the Prairies. Its climate ranges from subhumid continental in the east to semiarid in the west. All of the major ecosystems of the southern Prairies are found within the watershed. While most of the main stem of the river runs through the aspen parkland region, tributaries enter from the coniferous forests to the north and east and from a large area of much drier grasslands to the south and west. Till plains characterized by hummocky haphazard terrain deposited by stagnating ice sheets, abundant closed depressions containing small lakes and sloughs of the Prairie Pothole region, glacial spillways, the flat floors of former ice-dammed glacial lakes, and inactive sand dunefields are all classic Prairie landscapes. In addition, the watershed contains an unusually large glacial delta and has undergone several quite extraordinary changes to the configuration of its river network.

W.F. Rannie (✉)
Department of Geography, University of Winnipeg, 515 Portage Avenue, Winnipeg, MB R3B 2E9, Canada
e-mail: ranniebill@gmail.com

9.2 Geology

Apart from a very small region of Paleozoic sedimentary rocks below glacial sediments in the Manitoba Plain in the river's easternmost section and other small areas of Tertiary sandstones, the bedrock surface of the watershed consists of soft erodible shales deposited into a shallow seaway which extended through most of the North American interior in Cretaceous time. These shales are typical of those which underlie most of the southern Prairies. The formations of the Manitoba (Pembina) Escarpment and their equivalents continue westward to underlie much of the southern Prairies. Their dip is sufficiently gentle that they impart a virtually flat underlying structure to the entire southern Prairies (Klassen 1989). Originally, the shales extended much further eastward toward the Manitoba–Ontario boundary, but since Cretaceous time, they have retreated southwestward, forming the distinctive east-facing northwest–southeast-trending Manitoba Escarpment (Fig. 9.2). The escarpment relief above the adjacent lowlands is greatest (in excess of 300 m) in the Riding Mountain sector, reducing gradually to the south to less than 100 m in the vicinity of the Manitoba–North Dakota boundary.

The upper more resistant shale members have provided a cap rock which has protected the softer, weaker lower units which are generally thinly bedded, weakly indurated, and

© Springer International Publishing Switzerland 2017

O. Slaymaker (ed.), *Landscapes and Landforms of Western Canada*,
World Geomorphological Landscapes, DOI: 10.1007/978-3-319-44595-3_9

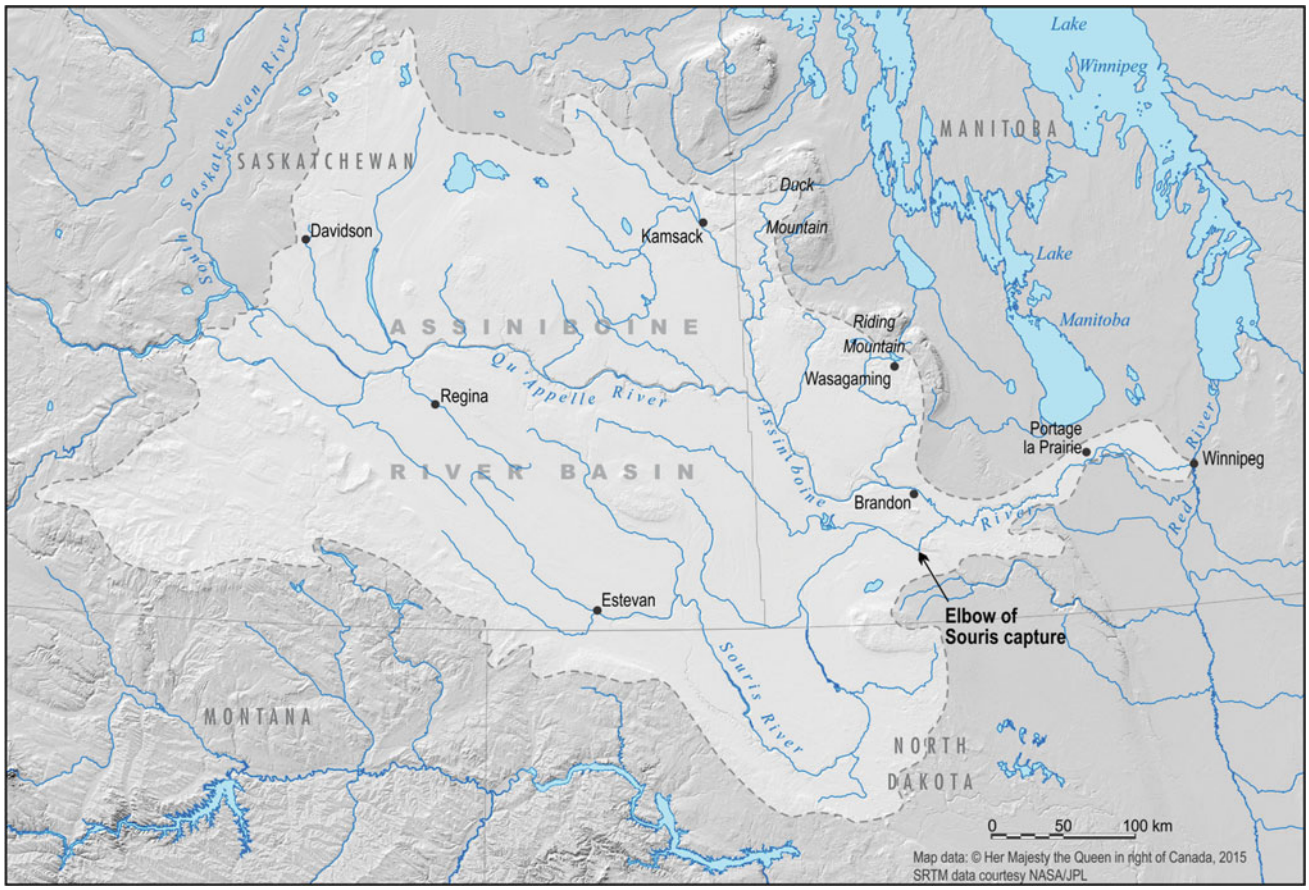

Fig. 9.1 The Assiniboine River watershed

contain abundant expansive montmorillonite (Bamburak and Nicolas 2010). The cap rock permitted the escarpment to maintain a coherent face as it retreated. It has also been suggested that the escarpment face has been maintained by sapping by springs at its base (Teller and Bluemle 1983) but also must have been trimmed by erosion during glacial advances and by the wave action of Lake Agassiz. The erodibility of the lower shales is exemplified by the fact that the unit suspended sediment yields of streams which dissect the eastern escarpment face are among the highest in Canada (Church et al. 1999).

The Manitoba Escarpment marks the division between the landscape units known as the First and Second Prairie Levels (Fig. 9.2). The lower First Prairie Level (or Manitoba Lowlands) lies east of the escarpment. The Second Prairie Level extends from the Manitoba Escarpment westward across the Saskatchewan Plains to the final step, the Third Prairie Level. The Third Prairie Level is marked by the Missouri Coteau, the Canadian portion of which begins west of Estevan, Saskatchewan, and extends northwestward into Alberta (Fig. 9.2). Superimposed on these Cretaceous units are isolated elevated Tertiary sandstone outliers of the Third Prairie level (Turtle Mountain, Moose Mountain, and the Touchwood Hills).

The Assiniboine River and its major tributaries, the Qu'Appelle and Souris rivers, rise on the Second Level in Saskatchewan and almost all of the watershed is at this level. Eastward from Brandon, the river begins its descent to the First Level through a progressively deeper post-glacial valley excavated into the sediments of the Assiniboine Delta/underflow fan, deposited into glacial Lake Agassiz when its margin lay along the Manitoba Escarpment. At Portage la Prairie, it emerges from the delta reach onto the Manitoba Lowlands.

Four landscape units dominate the surface of the watershed: till plains, glacial lake floors, glacial meltwater channels and spillways, and the Assiniboine Delta. The first three of these are typical of most of the southern Prairies. In addition to describing these units, this discussion will pay particular attention to the Assiniboine and Qu'Appelle valleys and to two unusual events which have dramatically altered the configuration of the river.

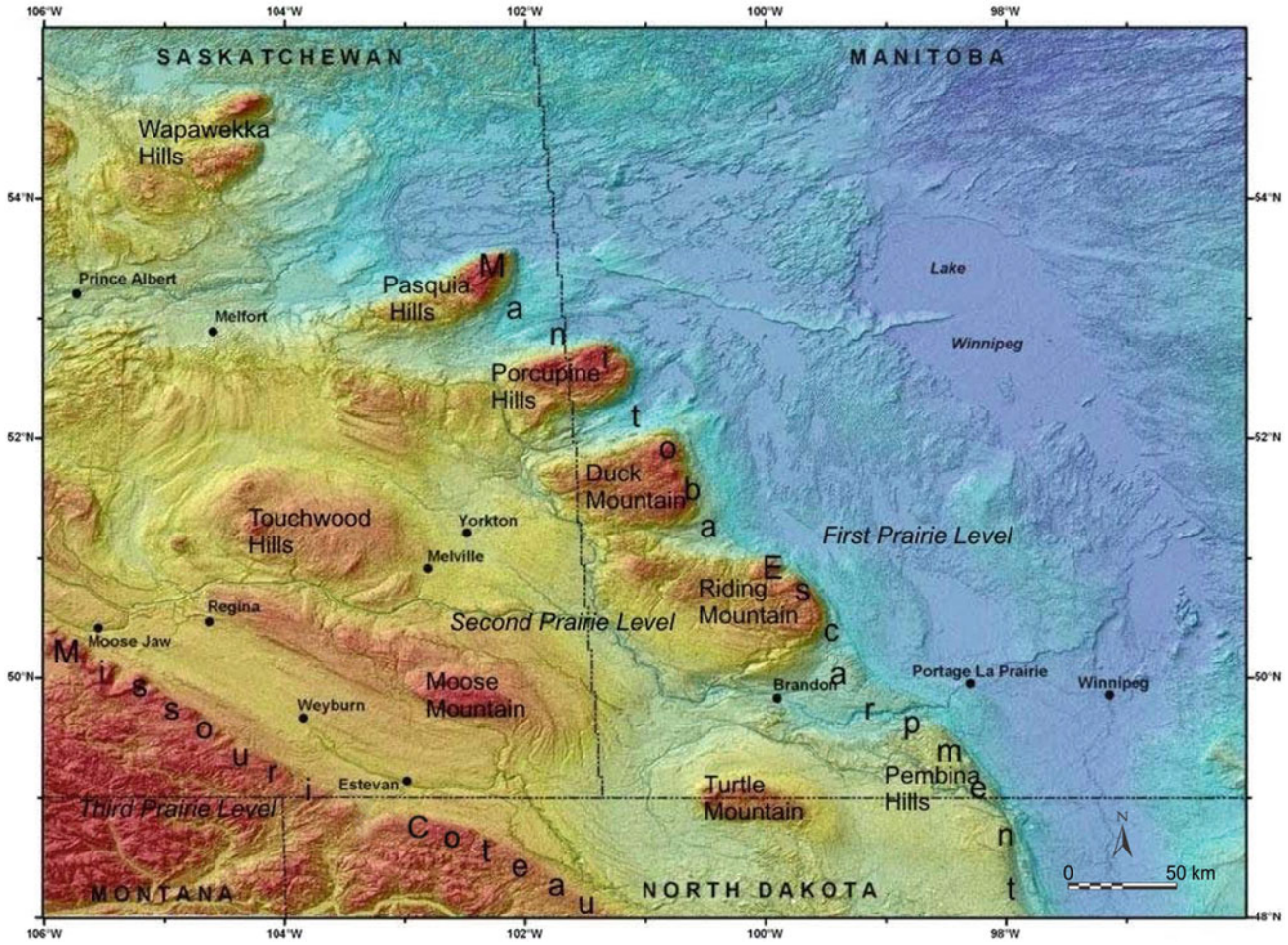

Fig. 9.2 The First, Second, and Third Prairie Levels, Manitoba Escarpment, and Missouri Coteau (after Bamburak and Nicolas 2010)

9.3 Till Plain

Much of the watershed surface consists of a low-relief till plain, much of which was deposited during the retreating phase of the last, late Wisconsinan (Klassen 1975; Christiansen 1979). The thickness of this till may be as little as a few meters in some places but is more generally greater than 50–100 m and locally may exceed 200 m (Fenton et al. 1994). The topography of the till plain is best described in such terms as subdued, undulating, disorganized, or hummocky. This hummocky ground moraine terrain was primarily a consequence of widespread ice stagnation during the retreating glacial phase, with downwasting of the ice surface buried under irregular thick supraglacial sediments. In some areas, the moraine takes the form of rimmed depressions, somewhat circular doughnut-like features with raised rims and central depressions, sometimes called Prairie mounds.

The effect of this topography is to produce a surface drainage dominated by closed basins which trap surface runoff in large or small, permanent or seasonal, standing water bodies commonly known as Prairie potholes (Fig. 9.3). Some of the potholes are fed by groundwater, others contribute to the water table below, and others receive or contribute groundwater on a seasonal basis. The semiarid to arid climate of the region causes many of these ponds and lakes to be ephemeral, filling with snowmelt in the spring and drying progressively over the summer (except in wet years). Many are saline and white salt flats are a common sight during dry years (Last and Slezak 1988; Last and Kelly 2002). The Assiniboine watershed lies at the center of the Prairie Pothole region, a distinctive terrain (Fig. 9.3) which extends in a broad arc from Iowa in the USA, through the Dakotas, Manitoba, and Saskatchewan, and into Alberta.

The wetlands in these potholes make this region one of the most important breeding areas and migration routes for North American waterfowl. They also play a crucial role in Prairie hydrology by complicating the normally simple concept of drainage area. In pothole regions, the myriad of closed basins trap a great deal of the potential surface runoff

Fig. 9.3 Prairie Pothole terrain near Indian Head, Saskatchewan (lat. 50°33′25.26″N and long. 103°48.0′0.75″W Google Earth 2002). *Dark areas* are ponded water in shallow depressions

and prevent it from reaching the main stream network (Lissey 1971). This reduces the gross drainage area, defined as the total area within the watershed boundary, to a smaller effective area, the area that actually might contribute surface runoff. The difference between gross and effective drainage areas confounds the understanding of virtually all aspects of Prairie streamflow which depend on watershed area. In the Assiniboine watershed, the difference can be very large. The major tributaries have effective drainage areas which are typically less than 40 % of the gross area—only 34.2 % for the Qu'Appelle and 35.5 % for the Souris River, for example (Mowchenko and Meid 1991). Only in streams draining the Riding Mountain region does the ratio of effective to gross area (slightly) exceed 50 %. As a consequence, actual runoff values are likely to be 2–3 times greater than those which are calculated from the standard use of gross drainage area. However, artificial drainage of the potholes integrates them into the broader stream network, thereby increasing the effective drainage area and runoff potential. In effect, with artificial drainage, the actual watershed area which contributes surface runoff grows without any change in the overall watershed boundary. Intensive artificial drainage systems have been in place for a century in the Red River Valley and may be playing a role in the increased flood frequency of the Red River in the late twentieth and early twenty-first centuries. In the Assiniboine watershed, artificial drainage has not been employed nearly as extensively until recently, but concerns have been raised about its role in increasing rates of runoff in the upper Assiniboine basin and as a contributing factor in flooding, for example, in the catastrophic floods of 2011 and 2014.

Within the overall till plain, there are areas of more organized glacial landforms, described in Abrahamsson (1972), Christiansen (1979), and Christiansen et al. (1981). The Tiger Hills near Holland, Manitoba, and the Condie Moraine near Regina are examples of end moraines. Small areas of low-relief washboard or corrugated moraine thought to have been formed parallel to the ice front are found at a number of locations within the region (for example, near Spy Hill, Saskatchewan). Subtle streamlined flutings and furrows occur on the margin of the Qu'Appelle Valley near Katepwa. The largest of all glacial features in southern Saskatchewan, ice-thrust or push moraines, occur along the Missouri Coteau just outside the Assiniboine watershed. Although these features can be found at many places along the Missouri Coteau from Saskatchewan to Alberta, the best example is the Dirt Hills south of Moose Jaw (Aber 2007).

9.4 Glacial Lake Floors

The second most common terrain features in the Assiniboine watershed are the floors of former ice-marginal lakes (Mollard and Janes 1983). At all stages of ice retreat, the continental ice sheet margin blocked the normal drainage toward the northeast and huge volumes of meltwater were ponded along the ice margin. These glacial lakes varied enormously in size and longevity. The largest was Lake Agassiz initially impounded in the southern Red River Valley of North Dakota, Minnesota, and Manitoba with its western margin against the Manitoba Escarpment (Fig. 9.4). As the ice margin retreated northward, the lake expanded with it. In total, 950,000 km^2 was covered at some time by Agassiz water although its maximum extent at any one time was 350,000 km^2 (Teller and Clayton 1983).

During its later stage, an eastern region in the James Bay region was added, bringing the total area ever covered by the lake to ~1.5 million km^2 (Leverington et al. 2002). Lake Agassiz existed from shortly before 10.9 ^{14}C ka (12.9 cal ka) to its final drainage through Hudson's Bay about 7.7 ^{14}C ka (8.5 cal ka) (Teller and Leverington 2004). The signatures of former glacial lakes are their featureless surfaces which range from absolutely flat to very gently rolling terrains which are often used to symbolize Prairie landscapes (Fig. 9.5).

This terrain is produced by the accumulation of fine-grained lacustrine sediments which, if they are thick enough, mask the underlying topography. In the centers of the largest palaeolake basins, the sediments may be 10–15 m thick, as in the vicinity of Regina where the lacustrine silts and clays of Glacial Lake Regina are 6–12 m thick (Christiansen 1961). If the sediments are too thin, perhaps because the lakes were small and/or short-lived, they may simply form a drape over the preexisting surface. Around the margins of the lakes, shoreline features such as beaches,

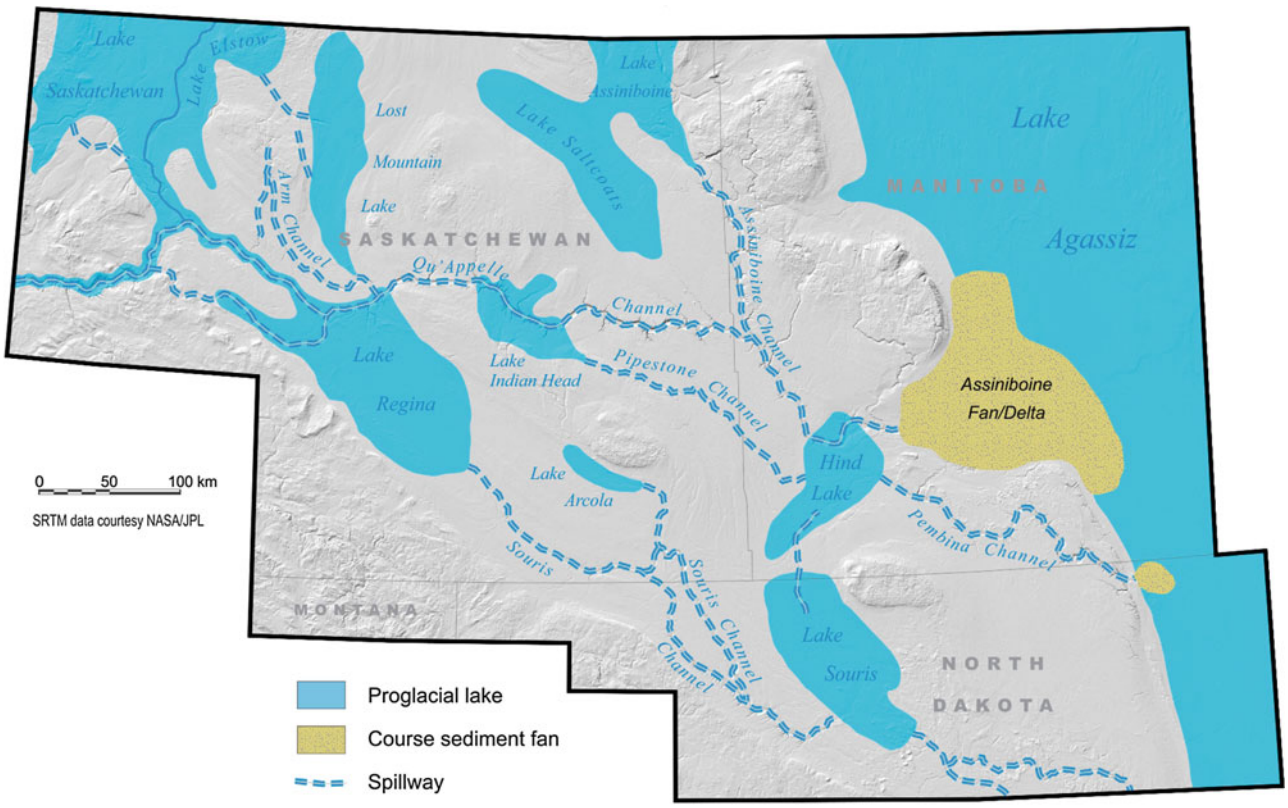

Fig. 9.4 Major glacial lakes and spillways in and near the Assiniboine watershed (after Kehew and Teller 1994)

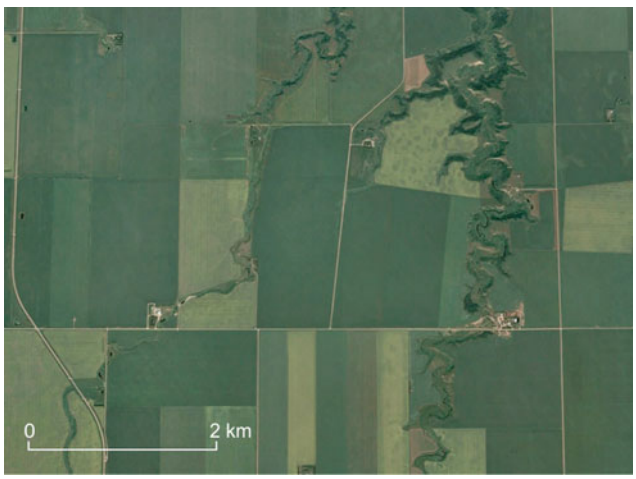

Fig. 9.5 Dissected flat lake-bed terrain near Indian Head, Saskatchewan, 70 km east of Regina (lat. 50°34′70″N and long. 103°38′20.79″ W Google Earth August 13, 2007)

wave-cut bluffs, or deltas mark the former lake's extent. Excellent examples of air photographs and LiDAR images of these and most other features of the Prairie landscape mentioned in this chapter (including giant iceberg scour marks) are contained in Mollard (1977); Mollard and Janes (1983) and Lepper et al. (2007).

9.5 Glacial Meltwater Channels and Spillways

The most impressive physiographic features in the watershed (and indeed on the entire Prairies) are the spillways and ice-marginal meltwater channels carved into the landscape in late glacial time. Not only do they dominate the landscape visually and topographically (Fig. 9.6), but they determine all of the main drainage lines of the Assiniboine River and most of its tributaries. Typical of spillways elsewhere, these channels are broad trenches, with steep sides and flat floors currently occupied by manifestly underfit streams. The spillways range in size from a few hundred meters across and a few tens of meters deep to as much as 5 km wide and more than 150 m deep in the case of the Assiniboine and Qu'Appelle valleys (Klassen 1975; Fig. 9.6). An inventory of spillways and their characteristics is given by Christiansen (1977).

Some spillways, especially the smaller ones, developed from normal drainage off the massive ice sheet, directed either away from or along the ice margin. However, many had a much more dramatic origin in the catastrophic drainage of ice-marginal glacial lakes. The idea was first proposed by Alan Kehew in 1979 to account for features of the

Fig. 9.6 Qu'Appelle Valley south of Esterhazy, Saskatchewan, 50 km west of junction with Assiniboine River at St. Lazare, Manitoba (photograph courtesy of Weldon Hiebert, Department of Geography, University of Winnipeg)

large Souris spillway in Saskatchewan and North Dakota (Kehew 1979; Kehew and Clayton 1983). It has been expanded into a megaflood concept in many subsequent studies (Kehew 1979; Kehew and Lord 1987; Lord 1991; Kehew and Teller 1994; Sun and Teller 1997; Kehew et al. 2009). In the megaflood concept, ice-dammed lakes were unstable, prone to catastrophic drainage in massive outburst floods (or jökulhlaups) when the dam failed abruptly due to movement of the ice margin or erosion of the lake outlet. The enormous volumes and high velocities of the water released in these outbursts were capable of rapid erosion of a new channel downstream from the point of release, often beginning as a broad scoured upland but rapidly evolving into a narrower, deeper inner channel which became the spillway proper. As the water released from one lake reached another lake downstream, the influx could cause the receiving lake to erode its outlet and release its water catastrophically, possibly into yet another lake downstream, triggering an outburst of that lake in turn. The first of these megafloods to be identified, and the best documented, was the outburst from Glacial Lake Regina which created the Souris Spillway (Fig. 9.7). Based on empirical relations between discharge and channel form, hydraulic formulae, and competence criteria, Kehew (1982) and Kehew and Clayton (1983) estimated that the water released from Lake Regina may have had a volume of 74 km^3 with discharges as much as 1.0×10^5 m^3 s^{-1} and velocities up to 12 m s^{-1}. Flood-streamlined elliptical hills and lags of large boulders provide additional evidence of the immense size of the flood. These waters flowed into Glacial Lake Souris and thence into Glacial Lake Hind and on to the Pembina Spillway (Sun and Teller 1997). Calculations by Kehew and Clayton (1983) suggest that the volume of water increased along the system to about 100 km^3 with discharge from Lake Souris as much as 2.5×10^5 m^3 s^{-1}. The larger valleys were partly filled by glacial outwash during the waning phase of the floods. Subsequent erosion by smaller post-glacial rivers left terraces along the valley margins. The number of spillways and their close association with glacial lakes shown in Fig. 9.7 indicates how widespread these megafloods must have been. Other features associated with some of the spillways (such as scoured and streamlined uplands, large-scale gravel bars, outsized bedforms) led Kehew to compare the spillway systems in this region with the catastrophic channeled scablands of Lake Missoula in eastern Washington.

9.6 The Qu'Appelle and Assiniboine River Valleys

The two largest spillways and the most impressive visual features in the Assiniboine watershed are the valleys occupied by the modern, greatly underfit, Assiniboine and Qu'Appelle Rivers (Fig. 9.6). The Assiniboine valley begins near Kamsack, Saskatchewan, as the outlet for Glacial Lake Assiniboine (Fig. 9.4). After it crosses into Manitoba, the valley has been dammed by the Shellmouth Dam which

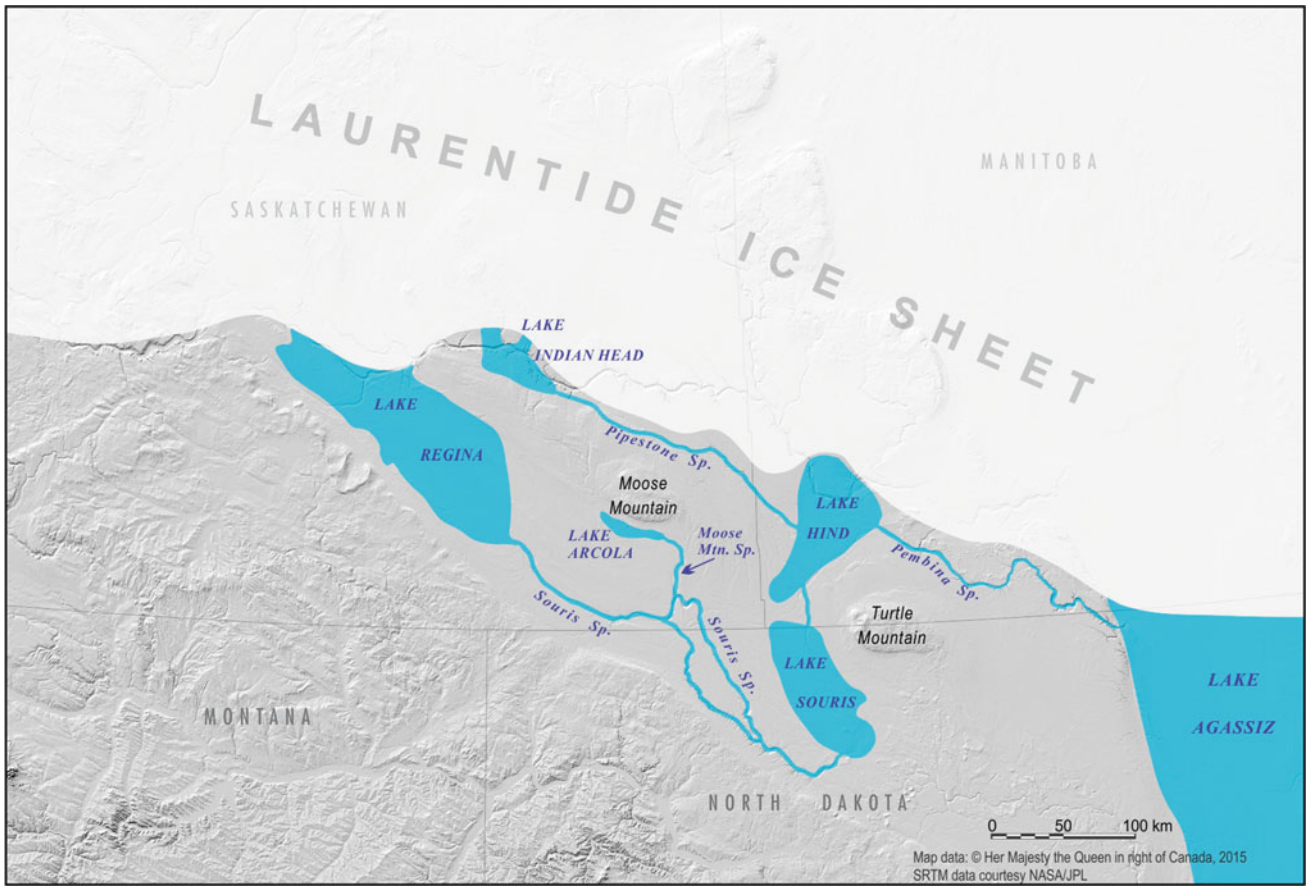

Fig. 9.7 A snapshot of glacial lakes and spillways along the ice margin that carried water from Lake Regina and other lakes to Lake Agassiz during the late glacial Lake Regina–Souris–Pembina drainage phase (after Kehew and Teller 1994)

impounds the 56-km-long reservoir Lake of the Prairies (Fig. 9.8). Completed in 1972 as part of a larger scheme to control flooding in Winnipeg, it also affords some flood protection for Brandon and Portage la Prairie and provides a pool of conservation water.

The Qu'Appelle Valley (Fig. 9.9) forms a 2.5–3-km-wide, 75–90-m-deep trench which runs for 440 km from Elbow, Saskatchewan, to its junction with the Assiniboine Valley (Klassen 1975). Other spillways—the Arm, Last Mountain, and Cutarm valleys—join the main valley from the north. The walls of the Qu'Appelle Valley have been subject to slope failure over much of their length, usually in the form of rotational slump blocks which may be up to 500 m long with pronounced ridges. Some mass movement is occurring at present, but Klassen concluded that most of the slumping occurred shortly following deglaciation. Such slumping of valley walls is characteristic of virtually all valleys on the Prairies where erosion has been sufficiently deep to expose weak shale bedrock.

The valley walls of the Assiniboine and Qu'Appelle valleys are marked everywhere by gullies at the mouths of which many alluvial fans have been deposited on the valley

Fig. 9.8 Shellmouth Dam and 56-km-long Lake of the Prairies Reservoir impounded in the Assiniboine Valley near Russell in western Manitoba (lat. 50°59′55.12″N and long. 101°24′37.49″W Google Earth September 26, 2010)

Fig. 9.9 Qu'Appelle glacial spillway containing the modern misfit Qu'Appelle River near Lumsden, Saskatchewan, 30 km north of Regina (lat. 50°43′40.41″ N and long. 104°42′24.76″W Google Earth August 7, 2014)

floor. The largest alluvial fans have formed dams on the small sluggish modern river, creating a string of lakes in the valley which provide important recreational areas. Last Mountain Lake in the Last Mountain Lake channel north of Regina is the largest natural lake in southern Saskatchewan. Other such lakes are found in the Pembina Valley in southern Manitoba. The Qu'Appelle and Assiniboine spillways join into a single valley at St. Lazare, Manitoba. From St. Lazare to Brandon, the valley of the combined spillways is up to 100 m deep and 3 km wide. At Brandon, the ancestral glacial river encountered glacial Lake Agassiz in an embayment or reentrant in the Manitoba Escarpment which had been eroded by the preglacial river system (Fig. 9.2). At this point, the river deposited a large delta/underflow fan.

9.6.1 Assiniboine Delta/Underflow Fan

The Assiniboine delta/underflow fan (Fig. 9.10) is the largest of several late glacial fan/deltas deposited by rivers entering Lake Agassiz from the west. From its apex near Brandon, it extends 140 km eastward to Portage la Prairie; at its distal end, it has a maximum breadth of about 75 km. The fan/delta covers an area of about 6400 km^2 and has a thickness up to 200 m (Teller and Bluemle 1983). The surface sediments of the fan/delta are coarsest in the vicinity of the apex (where they provide an important regional aquifer and display excellent steep foreset beds of gravel) and become finer and flat-lying toward the distal end. Over much of the surface, the sands of the upper underflow fan

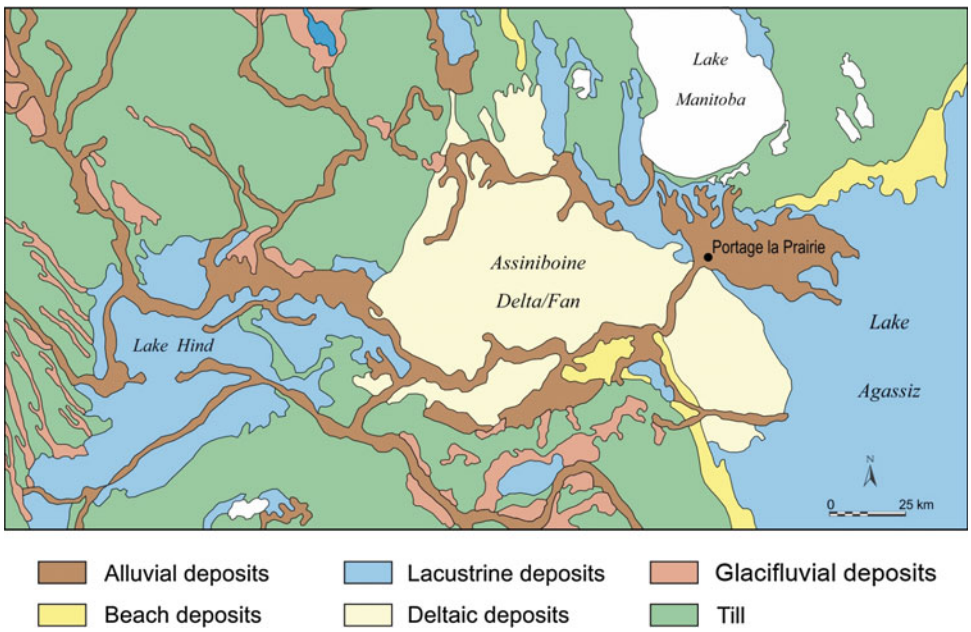

Fig. 9.10 The Assiniboine Delta and adjacent surficial materials (after Nielsen et al. 1981)

Fig. 9.11 The Assiniboine River and valley near Glenboro, Manitoba. Note the extreme meander amplitude in response to the steep gradient as the river descends from the Second to the First Prairie Level through the erodible materials of the Assiniboine Delta, and note also the active dunes of the Spirit Sands in Spruce Woods Provincial Park in lower left (lat. 49°40′51.23″N and long. 99°13′56.16″W Google Earth July 11, 2011)

surface have been subject to episodic aeolian activity with periods of active dune formation followed by intervals of stabilization and inactivity (David 1971; Wolfe et al. 2000; see Chap. 12). These cycles are marked by paleosols which reflect periods of dune stability and are common throughout the area; the most notable episodes of paleosol development occurred at 2300–2000, 1400–1000, and 600–500 ^{14}C BP (Wolfe et al. 2000). Most of the dunes are stable at present, but an area of active dunes occurs in the Spirit Sands in Spruce Woods Provincial Park, Manitoba (Fig. 9.11).

During the formation of the fan/delta, base level for the Assiniboine River was the level of glacial Lake Agassiz. The bulk of the delta materials was deposited when the lake was at its highest level. As new lake outlets opened periodically, lake levels fell causing the river to regrade its profile by cutting down through the deltaic sediments. The result of these adjustments was the incision of a large valley up to 75 m deep and 2 km across. The major lake still-stands are marked by prominent terrace segments, both paired and unpaired. Because the overall gradient of the valley floor through the delta section is about 3–4 times greater than in the spillway upstream of Brandon, the character of the river changes dramatically. Even though the discharges between the two sections are not greatly different, the increased gradient has caused the small meander amplitudes in the spillway section to become very large in the delta reach. As the river swings back and forth across the whole valley floor, it impinges on the erodible sandy deltaic materials of the valley walls at many places, producing cutbanks from which the river acquires much of its sediment load.

9.6.2 Capture of the Souris River

The modern Souris River originates in Saskatchewan and flows as an underfit stream in the Souris spillway in a large loop southward into North Dakota and then northward into Manitoba (Fig. 9.1) where it now joins the Assiniboine in the Assiniboine underflow fan section about 35 km east of Brandon. It was not always this way. Initially, the Manitoba section of the Souris River flowed along the Souris spillway, across the floors of Glacial Lakes Souris and Hind, and then southeast through its obvious continuation in the Pembina Valley/spillway (Fig. 9.7). It reached Lake Agassiz near Pembina, North Dakota, where it deposited a fan/delta smaller than but analogous to that of the Assiniboine. Early in post-glacial time, however, almost 90 % of the original Souris River watershed was diverted into the Assiniboine River by river capture, leaving the beheaded modern Pembina watershed only a small remnant of its former size. The site of the diversion was about 20 km southeast of Wawanesa, Manitoba, where the Souris River takes a sharp (90°) turn to the northeast. From this ‘elbow of capture,’ the new Souris course flows through a breach in the prominent Tiger Hills moraine and on to the Assiniboine. The sequence of events leading to this capture involved headward (southward) erosion by a small post-glacial tributary of the Assiniboine which had formed in a short glacial meltwater channel through the Tiger Hills moraine (Elson 1956, 1967). Eventually, this stream intersected the Souris Valley and the entire river was diverted northeastward. Subsequent erosion by the post-diversion Souris deepened its valley in the

vicinity of the diversion, leaving its former extension, the Pembina Valley, perched and without headwaters. The effect of the capture was dramatic. The drainage area of the Assiniboine was increased by 60 %, from about 100,000 km^2 to its current 162,000 km^2, and the area of the beheaded Pembina River was reduced from 70,000 to a mere 8500 km^2. This change had major consequences for the hydrology of the modern Assiniboine. The Souris River is a major source of water during large Assiniboine floods, such as in 1976, 2011, and 2014, and it is strongly implicated as a major contributor to the extreme historic floods of record in 1826 and 1852.

9.6.3 Channel Changes of the Lower Assiniboine

Throughout its entire length, the Assiniboine River is confined within large valleys, first in the spillway section upstream of Brandon and then in the deep valley of the delta reach. Near Portage la Prairie, however, it emerges from the confinement of the lower fan/delta onto the nearly flat floor of former glacial Lake Agassiz where it has been free to migrate through an arc of 180°. At this point, the river has constructed a large, low-angle alluvial fan with its apex just west of Portage la Prairie (Rannie 1990). During the construction of this fan, the river has adopted and abandoned many routes (Rannie et al. 1989). The initial courses were northward to Lake Manitoba, and for about 4000 years, the Assiniboine was not a tributary of the Red River. From 3000 ^{14}C BP onward, further avulsions directed the river eastward to the Red River, more than doubling the area of the Red River watershed area in the process. The first course to the Red River, however, was not its present one but along the La Salle channel to the south, joining the Red River at St. Norbert on the southern edge of Winnipeg. By 1300 ^{14}C BP, its course had shifted northward to its present confluence with the Red River at the Forks in downtown Winnipeg (Rannie et al. 1989).

9.6.4 The Portage Diversion and Recent Assiniboine River Floods

The gradients on the alluvial fan near Portage la Prairie are gentle, almost imperceptible, and the elevation of the fan apex is subtle. Nevertheless, it was this elevation that enabled the construction of the Portage Diversion, a 29-km artificial channel 1 km west of Portage la Prairie. Completed in 1970 as part of the flood control system for Winnipeg, it was designed to divert up to 700 m^3 s^{-1} to Lake Manitoba (an amount which exceeds the channel capacity of the river itself). Although it was constructed to reduce the hazard in Winnipeg from Red River floods, on three occasions (1976, 2011, and 2014), the diversion has been crucial to the management of disastrous floods on the Assiniboine itself. Each of these floods had very distinctive, contrasting origins.

In 1976, an unusually heavy, late-lying, snowpack, and a very rapid melt produced the largest flow since the beginning of records in 1913 and probably since at least 1852 (Rannie 2001). Maximum discharge at Portage la Prairie was 60 % higher than the previous peak (which had occurred only two years previously) and more than double the peak prior to the construction of the diversion. Of the water reaching Portage la Prairie, about half was contributed by the Souris River which was itself experiencing major flooding. With the diversion available to route 700 m^3 s^{-1} (about half of the total flow) to Lake Manitoba (Fig. 9.12), downstream flooding was minimal.

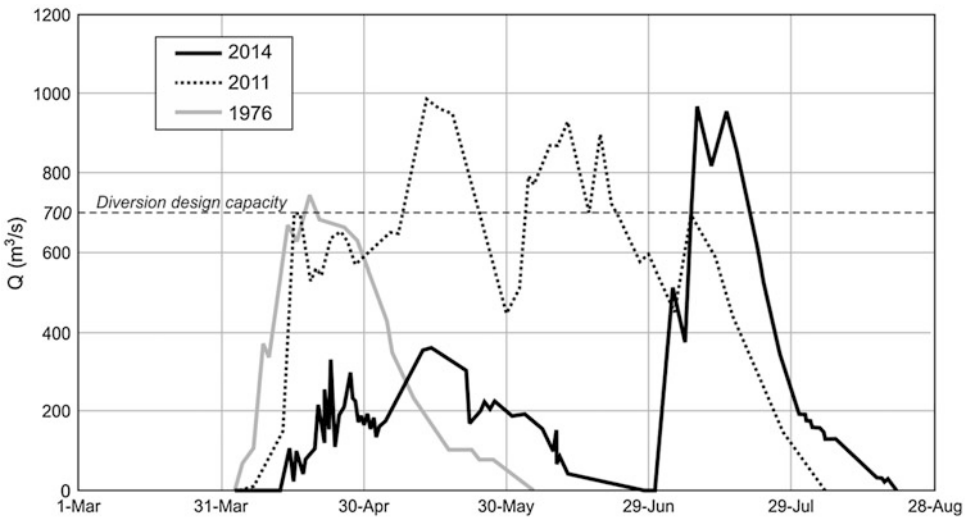

Fig. 9.12 Discharge through the Portage Diversion during the large Assiniboine River floods of 1976, 2011, and 2014 (after Ahmari et al. 2015)

In 2011, a flood with a peak flow slightly higher than the 1976 record brought the river to national attention (Government of Manitoba 2013a). This flood began as a major snowmelt event, but in contrast to 1976, it was extended for two months by exceptional rainfall throughout virtually the entire watershed (Government of Manitoba 2013b). Whereas the 1976 event had a normal flood hydrograph shape and duration, in 2011 the repeated passage of storms with heavy, widespread rainfall kept the river above flood level for several months, with several peaks. Through May, June, and much of July, the disaster spread to encompass the main river, the Qu'Appelle and Souris Rivers, and most of the tributaries. Again, the Souris River contributed almost 50 % of the peak flow at Portage la Prairie. In the decades since 1976, the capacity of the main channel below Portage la Prairie has diminished somewhat forcing the diversion to be used at up to 40 % above design capacity for extended periods (Fig. 9.12). This and the extremely long duration of the flood conditions led to the rerouting of an unprecedented volume of water from the Assiniboine into Lake Manitoba. Flood damages were sustained by communities along the Assiniboine and Souris Rivers (particularly in Brandon and Souris), but the most tragic and long-term consequences were to properties around the southern basin of Lake. Manitoba. There, exceptional lake levels were the result of a disastrous convergence of factors: a preexisting high lake level, high inputs from the lake's own watershed, the extraordinary volume of water diverted from the Assiniboine, and critically, the setup and waves from a wind storm at the end of May in which sustained 6-hr winds from the NNW reached 60 km h^{-1} with peak velocities of 90 km h^{-1} (Government of Manitoba 2013c). As of the spring of 2013, the total costs of preparations, flood fighting, repairs to infrastructure, and disaster assistance all aspects of the flood were estimated to have been $1.2 billion (Government of Manitoba 2013a).

Extreme flood conditions returned only 3 years later, in the summer of 2014. Although peak flows at Portage la Prairie were very similar to those in 1976 and 2011, the flood was particularly unusual in that it was a purely summer event generated entirely by exceptional rain in late June and early July falling on a watershed with saturated ground and nearly full wetlands. The peak flow reaching Portage la Prairie was comparable to that of 2011 but of much shorter duration (Fig. 9.12). Again, the Portage Diversion was used to divert a large volume of water to Lake Manitoba. The maximum rate of diversion virtually equaled that in 2011, reaching almost 40 % above design capacity, but because the 2014 flood duration was much shorter, the volume of water added to Lake Manitoba was only about one-third of the 2011 volume (but was nevertheless the second largest on record). Final assessment of flood damages is not yet complete but will exceed $1 billion (Ahmari et al. 2015). Most of these damages were incurred in agricultural regions and rural infrastructure.

Contemporary frequency curves indicate return periods for each of the 1976, 2011, and 2014 floods in excess of 300 years on the Assiniboine and its main tributaries and approached 400–500 years at some stations (Government of Manitoba 2013c). The 2011 and 2014 events were among the most serious Canadian floods in recent decades, and as large as the damages were, they would have been very much greater in the absence of the Portage Diversion. The decision to operate the diversion well beyond its design capacity and for such a long duration became a highly charged political issue for the inhabitants of the southern Lake Manitoba margin and on lakes downstream of the lake's outlet. Thus, after almost 40 years of effective use in reducing flood damages in Winnipeg and managing occasional high waters on the Assiniboine, the Portage Diversion has become a source of controversy and acrimony.

9.7 Conclusion

This chapter demonstrates the close interconnection between geomorphological landscapes formed during the Late Glacial and Early Holocene and the present-day river flooding hazard. It also demonstrates the uneven distribution of economic and social costs resulting from major investments in environmental engineering.

Acknowledgments The author is most grateful to Weldon Hiebert, cartographer at the University of Winnipeg, for his preparation and formatting of the figures and to Jim Teller for his constructive comments which improved the manuscript.

References

Aber JS (2007) Ice-thrust terrains of the Missouri Coteau. In: Thraves BD, Lewry ML, Dale JE, Schlichtmann H (eds) Saskatchewan: geographical perspectives. Department of Geography, University of Regina, Regina, pp 28–31

Abrahamsson KV (1972) Landforms of southern Saskatchewan. In: Paul AH, Dale EH, Schlichtman H (eds) Background papers to southern Prairies field excursion, 22nd Congress International Geographical Union, August, 1972. Department of Geography, University of Regina, Regina, pp 151–195

Ahmari H, Blais E-L, Greshuk J (2015) The 2014 flood event in the Assiniboine River basin: causes, assessment, and damage. Can Water Resour J. doi:10.1080/07011784.2015.1070695

Bamburak JD, Nicolas MPB (2010) Upper Cretaceous stratigraphy of the Pembina Hills area. Winnipeg: Manitoba Geological Survey

Christiansen EA (1961) Geology and groundwater resources of the Regina Area. Saskatchewan Research Council, Geol Div, Report No. 2

Christiansen EA (1977) Glacial spillways in the Prairies. EA Christiansen Consulting Ltd., Report No. 0004-002

Christiansen EA (1979) The Wisconsinan deglaciation of southern Saskatchewan and adjacent areas. Can J Earth Sci 6:913–938
Christiansen EA, Acton DF, Long RJ, Meneley WA, Sauer EK (1981) Fort Qu'Appelle geology: the valley's past and present. Saskatchewan Culture and Youth and Parks Canada, Regina
Church M, Ham D, Hassan M, Slaymaker O (1999) Fluvial sediment yield in Canada. Can J Earth Sci 36:1267–1280
David PP (1971) The Brookdale Road section and its significance in the chronological studies of dune activities in the Brandon Sand Hills of Manitoba. In: Turnock AC (ed) Geoscience studies in Manitoba. Geol Assoc Can Special Paper 9. The Geological Association of Canada, Toronto, pp 293–299
Elson JA (1956) Surficial geology of the Tiger Hills Region, Manitoba, Canada. Ph.D. Thesis Yale University, New Haven, Connecticut
Elson JA (1967) Geology of glacial Lake Agassiz. In: Mayer-Oakes WJ (ed) Life, land and water. Proceedings of the 1966 conference on environmental studies of the glacial Lake Agassiz Region. University of Manitoba Press, Winnipeg, pp 37–95
Fenton MM, Schreiner BT, Nielsen E, Pawlowicz IG (1994) Quaternary geology of the western plains. In: Mossop GD, Shetsen I (eds) Geological atlas of the Western Canada sedimentary basin. Can Soc Petrol Geol and Alberta Res Council. http://www.ags.gov.ab.ca/publications/wcsb_atlas/atlas.html. Accessed 18 Nov 2014
Government of Manitoba (2013a) Manitoba 2011 flood review task force report. Manitoba Infrastructure and Transportation, Winnipeg
Government of Manitoba (2013b) 2011 Flood: technical review of Lake Manitoba, Lake St. Martin and Assiniboine River water levels. Manitoba Infrastructure and Transportation, Winnipeg
Government of Manitoba (2013c) Manitoba 2011 flood review task force report. Appendix B, hydrological characteristics. Manitoba Infrastructure and Transportation, Winnipeg
Kehew AE (1979) Evidence for late Wisconsinan catastrophic flooding in the Souris River area, north central North Dakota. In: Proceedings North Dakota Acad Sci, Grand Forks, ND, p 32
Kehew AE (1982) Catastrophic flood hypothesis for the origin of the Souris spillway, Saskatchewan and North Dakota. Geol Soc Am Bull 93:1051–1058
Kehew AE, Clayton L (1983) Late Wisconsinan floods and development of the Souris-Pembina spillway system in Saskatchewan, North Dakota, and Manitoba. In: Teller JT, Clayton L (eds) Glacial Lake Agassiz, Geol Assoc Can Special Paper 26. The Geological Association of Canada, Toronto, pp 187–209
Kehew AE, Lord ML (1987) Glacial-lake outbursts along the mid-continent margins of the Laurentide Ice Sheet. In: Mayer L, Nash D (eds) Catastrophic flooding. Allen Unwin, Boston, pp 95–120
Kehew AE, Lord ML, Kozlowski A, Fisher TG (2009) Proglacial megaflooding along the margins of the Laurentide Ice Sheet. In: Burr D, Carling PA, Baker VR (eds) Megaflooding on earth and mars. Cambridge University Press, Cambridge, pp 104–127
Kehew AE, Teller JT (1994) History of late glacial runoff along the southwestern margin of the Laurentide Ice Sheet. Quat Sci Rev 13:859–877
Klassen RW (1975) Quaternary geology and geomorphology of Assiniboine and Qu'Appelle valleys of Manitoba and Saskatchewan. Geological Survey of Canada Bulletin, vol 228. Department of Energy, Mines and Resources, Ottawa
Klassen RW (1989) Quaternary geology of the southern Canadian Interior Plains. In: Fulton RJ (ed) Quaternary geology of Canada and Greenland. Geological Survey of Canada, Geology of Canada, no. 1. pp 138–174
Last WM, Kelly LI (2002) Salt lakes of the northern Great Plains. Post-conference field trip guide, Ann Mtg, Geol Assoc Can, May 27–29, 2002, Saskatoon
Last WM, Slezak LA (1988) The salt lakes of western Canada: a paleolimnological overview. Hydrobiologia 158:301–316
Lepper K, Fisher TG, Hajdas I, Lowell TV (2007) Ages for the Big Stone Moraine and the oldest beaches of glacial Lake Agassiz: implications for deglaciation chronology. Geology 35:667–670
Leverington DW, Mann JD, Teller JT (2002) Changes in the bathymetry and volume of glacial Lake Agassiz between 11,000 and 9300 ^{14}C yr B.P. Quaternary Res 57:244–252
Lissey A (1971) Depression-focused transient groundwater flow patterns in Manitoba. Ottawa, Ontario, The Queen's Printer, Geol Assoc Can Special Paper 9, pp 333–341
Lord ML (1991) Depositional record of a glacial-lake outburst: Glacial Lake Souris, North Dakota. Geol Soc Am Bull 99:663–673
Mollard J (1977) Landforms and surface materials of Canada stereoscopic air photo atlas and glossary, 6th edn. Jd Mollard and Associates, Regina
Mollard JD, Janes JR (1983) Air photo interpretation and the Canadian Landscape. Surveys and Mapping Branch, Department of Energy, Mines and Resources, Canada
Mowchenko M, Meid PO (1991) Addendum No. 5 to Hydrology Report No. 4. Prairie Farm Rehab Admin, Regina
Nielsen E, Ringrose S, Matile GLD, Groom HD, Mihychuk MA, Conley GG (1981) Surficial geological map of Manitoba. Manitoba Energy Mines, Mineral Resources Division, Geoscientific Map 81-1
Rannie WF (1990) The Portage la Prairie 'floodplain fan'. In: Rachocki AH, Church M (eds) Alluvial Fans: A Field Approach. Wiley, Chichester, England, pp 179–193
Rannie WF (2001) Assessment of the historic hydrology of the Assiniboine River and watershed, 1793–1870. Geol Surv Can Open-File 4087
Rannie WF, Thorleifsen LH, Teller JT (1989) Holocene evolution of the Assiniboine River paleochannels and Portage la Prairie alluvial fan. Can J Earth Sci 26:1834–1841
Sun CS, Teller JT (1997) Reconstruction of glacial Lake Hind in southwestern Manitoba, Canada. J Paleolim 17:9–21
Teller JT, Bluemle JP (1983) Geological setting of the Lake Agassiz region. In: Teller JT, Clayton L (eds) Glacial Lake Agassiz. Geol Assoc Can Special Paper 26. The Geological Association of Canada, Toronto, pp 3–5
Teller JT, Clayton L (1983) An introduction to Glacial Lake Agassiz. In: Teller JT, Clayton L (eds) Glacial Lake Agassiz, Geol Assoc Can Special Paper 26. The Geological Association of Canada, Toronto, pp 7–20
Teller JT, Leverington DW (2004) Glacial Lake Agassiz: a 5000 yr history of change and its relationship to the δ^{18}O record of Greenland. Geol Soc Am Bull 116:729–742
Wolfe SA, Muhs DM, David PP, McGeehin JP (2000) Chronology and geochemistry of late Holocene eolian deposits in the Brandon Sand Hills, Manitoba, Canada. Quat Int 67:61–74

Red River Valley, Manitoba: The Geomorphology of a Low-Relief, Flood-Prone Prairie Landscape

10

Gregory R. Brooks

Abstract

Located between the Manitoba Escarpment (known as the Pembina Escarpment in North Dakota) and a gentle topographic rise to late Quaternary glacial deposits, the Red River valley forms the southern extension of the Manitoba Lowlands. The dominant landform of the central valley is a low-relief clay plain composed of glacilacustrine deposits that accumulated in glacial Lake Agassiz. The north-flowing Red River is a low-energy, suspended sediment, mud-dominated, meandering stream that occupies a shallow stream-cut valley within the low-relief clay plain. Sedimentation along the convex banks of the meanders occurs as overbank and oblique accretion deposits. Significant sedimentation also occurs along the concave banks on the slopes of elongated zones of low-angled earth slides that are common along the river meanders between at least Emerson and St. Adolphe, Manitoba. The Red River is well known for its broad, slow-onset, spring floods. An array of artificial landforms have been constructed to mitigate the flooding hazard, ranging in scale from elevated pads and small ring dykes protecting isolated buildings, large ring dykes protecting towns, and the 48-km Red River Floodway that protects Winnipeg.

Keywords

Red River valley • Manitoba • Clay plain • Meandering river • Flood protection infrastructure • Flood hazards

10.1 Introduction

The Red River valley, Manitoba, is located in the southeastern corner of the Canadian Prairies on the eastern margin of the Great Plains of North America. The valley covers approximately 68,000 km^2 and is contained within the northward-flowing drainage basin of the Red River (known as the Red River of the North in the USA; Fig. 10.1). It straddles the Canada–USA border and is situated within the eastern portion of south-central Manitoba, Canada, eastern North Dakota, northwestern Minnesota, and the extreme northeastern corner of South Dakota, USA. The valley is an important agricultural area in the eastern Prairies, famous for its cereal and root crops. Winnipeg, the provincial capital of Manitoba, is located in the northern portion of the valley and is the largest urban centre. Important US urban areas in the valley are Fargo-Moorhead and Grand Forks-East Grand Forks, North Dakota, Minnesota. Notable geomorphic features and processes on the Red River valley, which are themes of this chapter, are the strikingly low-relief topography of the central valley, the meandering Red River, the broad, slow-moving, Red River floods, and an array of permanent anthropogenic landscape features constructed to mitigate the floods. Generalizations are made for the Red River valley as a whole, while specific details are drawn from the Manitoba portion of the valley, reflecting the Canadian theme of this volume and the experience of the author.

G.R. Brooks (✉)
Natural Resources Canada, Geological Survey of Canada,
601 Booth Street, Ottawa, ON K1A0E8, Canada
e-mail: greg.brooks@canada.ca

© Springer International Publishing Switzerland 2017

O. Slaymaker (ed.), *Landscapes and Landforms of Western Canada*,
World Geomorphological Landscapes, DOI: 10.1007/978-3-319-44595-3_10

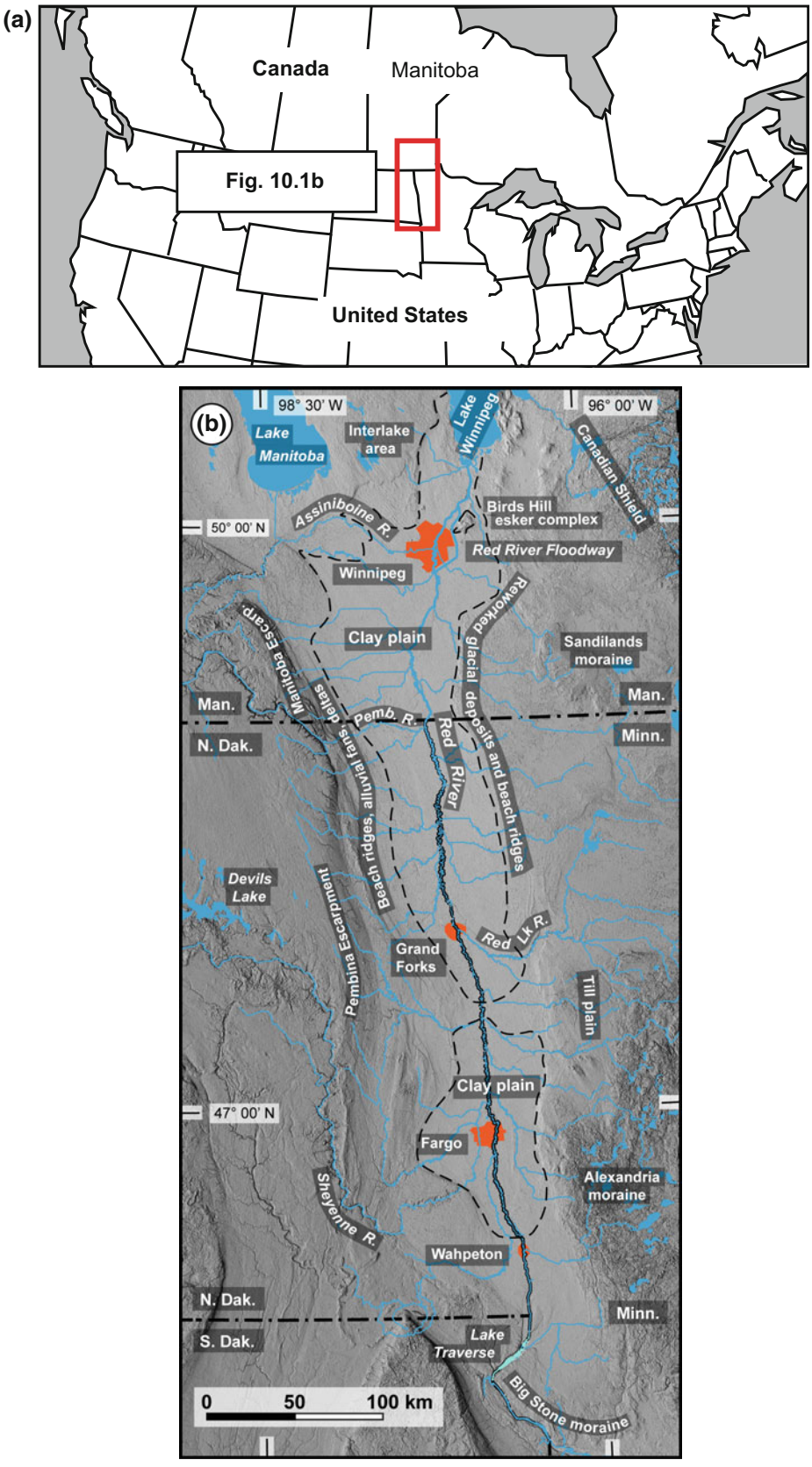

Fig. 10.1 **a** Map showing the location of **b** in southern Canada. **b** *Shaded* relief map of the Red River valley, Manitoba, North Dakota, Minnesota, and South Dakota (vertical exaggeration approximately ×15; DEM derived from NASA SRTM elevation data courtesy of USGS EROS Data Center). The major physiographic features, larger tributaries, and main urban areas that are mentioned in the text are labelled on the map. *Dashed lines* delineate the extent of the clay plain area

10.2 Red River Valley

The Red River valley is ~580 km long and up to ~140 km wide, extending from the Big Stone moraine in South Dakota, Minnesota, to the Lake Winnipeg, Interlakes area of Manitoba (Fig. 10.1b). The valley is the southern extension of the Manitoba Lowlands, a physiographic area of generally low relief that forms the lowest of three topographic steps to the southern Canadian Prairies (the Saskatchewan Plain and Eastern Alberta Plains are the others; Acton et al. 2012). The west side of the valley is well defined by the Manitoba Escarpment (known as the Pembina Escarpment in North Dakota) that is up to 200 m high (Fig. 10.2). The eastern margin is much less distinct and marked by a gentle topographic rise to late Quaternary glacial deposits.

Despite a name that suggests a direct link to the modern river, the morphology of the valley substantially predates the establishment of the river. Regional erosion during the Paleogene, Neogene and Quaternary periods produced a broad surface of low-relief and gentle northward slope across westerly-dipping Ordovician, Silurian, Devonian, and Jurassic bedrock, which underlies the Red River valley between the Manitoba Escarpment and the Precambrian Shield to the east (Fig. 10.2; Teller and Bluemle 1983). The Manitoba Escarpment is a preglacial feature that generally coincides with the eastern edge of westerly-dipping Cretaceous shale bedrock. Capped by hard siliceous shale, it has been more resistant to long-term erosion than the older Phanerozoic bedrock to the east (Fig. 10.2; Lauhn-Jensen 1994).

The contemporary topography of the Red River valley directly reflects the occurrence of the late Wisconsinan Glaciation during the late Quaternary. The valley was a corridor for ice feeding the Des Moines lobe of the Laurentide Ice Sheet that advanced into central Iowa by ~14.0 ka BP (~16.8 ka cal BP; Dyke et al. 2003). The combination of abrasion of the bedrock and existing sediments by streaming ice, and the aggradation of glacial deposits contributed to the subduing of bedrock relief in the valley. Ice subsequently retreated northwards, pausing or re-advancing at the southern end of the Red River valley by ~13.0 ka BP (15.6 ka cal BP) to form the Big Stone moraine at the present day drainage divide between the Red and Mississippi watersheds, the latter draining to the south (Fig. 10.1b; Fenton et al. 1983; Dyke et al. 2003). Other notable glacial deposits within or adjacent to the Red River valley are the Bird Hill esker complex near Winnipeg and the Sandilands and Alexandria moraines (Fig. 10.1b).

As glacial ice retreated down the Red River valley, meltwater became impounded between the ice front and the gentle northward slope of the valley landscape, forming a water body known as glacial Lake Agassiz. Persisting between ~11.7 and 7.7 BP (~13.4 and 8.45 ka cal BP; Teller and Leverington 2004; see Fig. 3.2), Lake Agassiz grew into the largest glacial lake in North America, extending far beyond the Red River valley. Over this period, the lake experienced substantial variations in size, shifts in outlet location, and catastrophic drainage events that were controlled by fluctuations in the regional margin of the Laurentide Ice Sheet, regional differential uplift, and outlet erosion (Teller and Clayton 1983; Teller 1985; Teller and Leverington 2004). The maximum extent of Lake Agassiz covered up to 841,000 km^2, including much of Manitoba, north-western Ontario, parts of eastern Saskatchewan and North Dakota, and north-western Minnesota (Teller and Bluemle 1983; Leverington et al. 2002).

The former presence of Lake Agassiz is strongly reflected in the contemporary geomorphology and surficial geology of the Red River valley. Glacilacustrine silt and clay deposits accumulated on the bed of Lake Agassiz, forming the broad clay plain that is the dominant landform of the central Red River valley. These deposits impart the strikingly low-relief topography, one of the flattest in North America

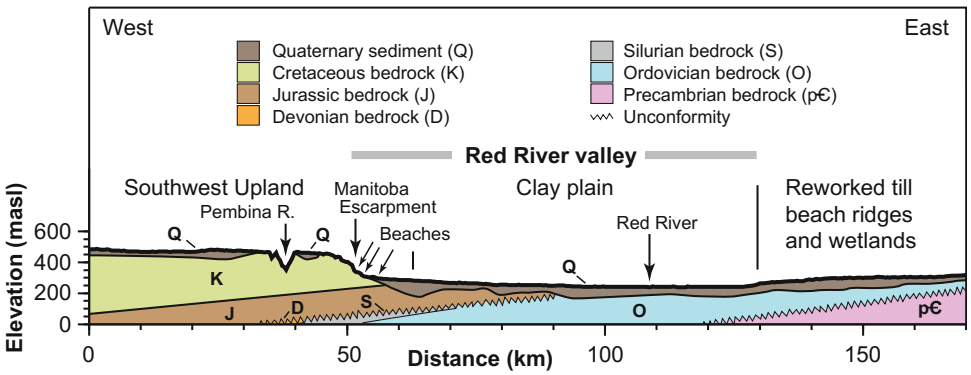

Fig. 10.2 West–east topographic profile across the Red River valley along the Canada–USA border (N 49°00′) with a schematic subsurface geology (vertical exaggeration ×30). The west side of the valley is well delineated by the Manitoba Escarpment, while the east side is defined by a slight rise to the glacial deposits. Topographic profile is derived from the DEM of Fig. 10.1b, and the subsurface geology follows MMRD (1979)

(Lauhn-Jensen 1994). Black grassland soils of the chernozemic and gleysolic (the latter where drainage is poor) orders developed on the clay plain following the recession of Lake Agassiz (Clayton et al. 1977). Prior to the introduction of European agriculture, numerous wetlands were present in poorly drained areas of the clay plain because of the combination of the low-relief topography and the low permeability of the soils (Warkentin and Ruggles 1970). Most of the wetland areas were drained artificially, beginning in the late nineteenth century and are now under cultivation (Hanuta 2001). The fertile soils of the Red River valley form an important agricultural area and have long been famous for cereal and root crops. Major crops grown in the Manitoba portion of the valley are wheat, soybean, canola and to a lesser extent corn, barley, and dry beans (Manitoba Agricultural Services Corporation 2014).

A series of wave-cut platforms and beach ridges are present along or adjacent to the Manitoba Escarpment and along the glacial deposits on the east side of the valley, each representing a former shoreline in the evolution of the Lake Agassiz (Figs. 10.1b, 10.2; Upham 1895; Johnston 1946; Teller and Thorleifson 1983). Best defined is the Upper Campbell Beach, which can be traced along the east and west margins of the Red River valley southwards to a former outlet channel in the Lake Traverse area, South Dakota, Minnesota, through which Lake Agassiz drained into the Mississippi watershed. The Lake Agassiz beaches are tilted, rising gradually to the NNE because of regional post-glacial differential uplift (Johnston 1946; Teller and Thorleifson 1983). Raised deltas splay into the valley along the Manitoba Escarpment where the proto-Assiniboine, Pembina, and Sheyenne rivers entered Lake Agassiz (Rannie et al. 1989; Rannie 2016). Later incision by these rivers into the deltaic deposits formed low-angled alluvial fans that splay onto the clay plain.

The incised courses of the Red River and its tributary network form the most obvious landforms on the clay plain, but other features are common. Virtually imperceptible on the ground, but readily visible on aerial photographs or satellite images, are clusters of subtle criss-crossing straight to slightly curved lineations, up to 150 m wide, and many kilometres in length. The lineations are interpreted to be the scour marks of icebergs that grounded on the bed of Lake Agassiz (Woodworth-Lynas and Guigné 1990; Matile 2005). Also difficult to see on the ground are linear clay ridges on the clay plain that are tens of kilometres long, up to 3 m high and spaced 1–3 km apart. Oriented parallel to the NNW–SSE direction of regional ice flow, the ridges are interpreted to be the subdued surface expression of fluted glacial deposits that are buried beneath the glacilacustrine deposits of the clay plain (Matile 2005). These ridges locally influence the course of some streams on the clay plain. Readily visible on the ground, however, are numerous elevated road and railroad beds, up to 1–2 m high, that form an intricate elevated topographic grid across the clay plain. In most landscapes, such elevated anthropogenic features are of minor importance geomorphically, but in the low-relief Red River valley, they form important linear rises in elevation that significantly accentuated the local stage of the 1997 Red River flood which inundated the clay plain (see below; Manitoba Water Commission 1998).

10.3 Fluvial Geomorphology of the Red River

Extending from the confluence of the Bois de Sioux and Otter Tail rivers at Wahpeton, North Dakota, to the river mouth at Lake Winnipeg, Manitoba, the meandering Red River is about 496 km long by valley length and about 880 km long by channel length (Fig. 10.1b). The watershed encompasses 290,000 km^2, including the Assiniboine River basin (163,000 km^2), which joins the Red River in Winnipeg (see Rannie 2016). Other major tributaries include the Red Lake, Sheyenne and Pembina rivers (Fig. 10.1b). Excluding the Assiniboine portion of the drainage basin, about 16 % of the Red River watershed is located in Canada.

Along the majority of its course, the Red River occupies a shallow stream-cut valley that is incised into the broad Lake Agassiz clay plain. The difference in elevation between Wahpeton and Lake Winnipeg (located about 496 km apart) is approximately 70 m, yielding an average valley gradient for the river of 0.00014. The width of the stream-cut valley is approximately the width of the meander belt (Figs. 10.3, 10.4). Within Manitoba, the stream-cut valley is up to 15 m deep, up to 2.5 km wide, and contains the genetic floodplain of the river (Brooks and Nielsen 2000; Brooks 2003b). Manitoba soil maps identify a belt of alluvial soil (Riverdale silty clay unit) that corresponds to the stream-cut valley, in contrast to the lacustrine and deltaic fine clay or silt clay soils (Red River, Osborne, and Emerson units) that dominate the clay plain (Ehrlich et al. 1953).

The shallow character of the stream-cut valley reflects the low-relief morphology and the gentle longitudinal gradient of the clay plain landscape, the combination of which inhibits stream incision. This character also reflects the development of the river, which extended its course progressively northward onto the clay plain as Lake Agassiz receded. The narrow valley, thus, did not convey a glacially influenced or glacial-lake-influenced hydrological regime, unlike other major rivers on or immediately marginal to the glaciated areas of the Great Plains, which are underfit and occupy meltwater spillways (see Kehew and Lord 1986; Kehew and Teller 1994; Rannie 2016).

Along the Red River meanders, a series of gentle ridges and swales undulate from the accreting portion of the convex

Fig. 10.3 Photograph of the meandering Red River, near Ste. Jean Baptiste, Manitoba, looking north. The stream-cut valley that is incised into low-relief clay plain is about the width of the meander belt, but is imperceptible in the photograph

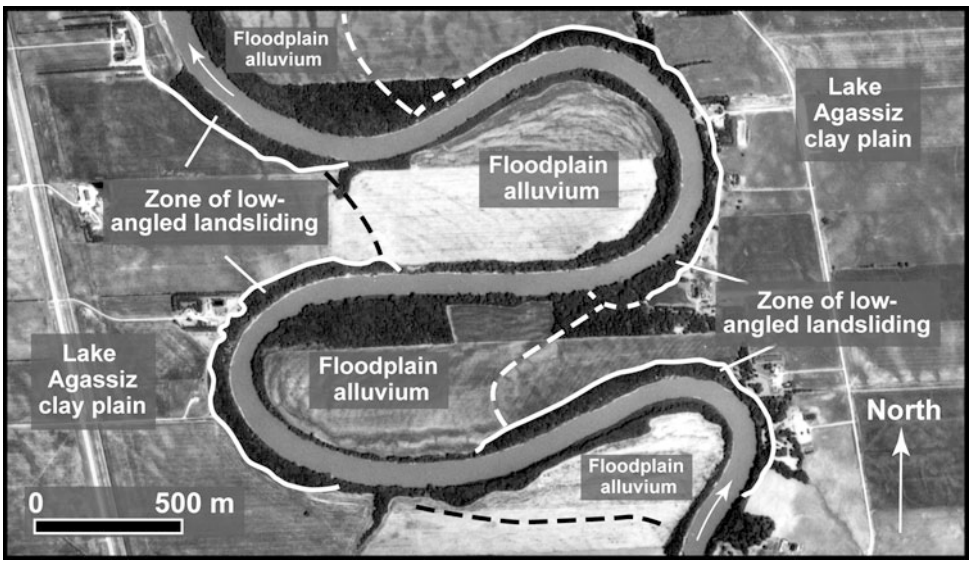

Fig. 10.4 Aerial photograph of three Red River meanders, near Ste. Jean Baptiste, Manitoba, showing the channel and alluvial floodplain within the stream-cut valley that is incised into the clay plain. The *black* and *white dashed lines* delineate the edge of the alluvial floodplain. Also shown are zones of low-angled landslides that experience rotational and translational earth sliding and are subject to concave overbank deposition [from Brooks (2005)]. The landslide zones are located where the concave side of the meanders are impinged against the glacilacustrine deposits that comprise the clay plain (NAPL A25476-51, taken on 19 June 1980)

bank to the distal area of the alluvial plain within the stream-cut valley, as commonly occurs along meandering river floodplains (Nanson and Croke 1992). However, only a single pattern of ridge and swale topography is present at most of the meanders along the river in Manitoba, where only nine cut-off meander scars and ox-bow lakes are present, as is apparent on LiDAR imagery. This geomorphic evidence indicates that most meanders have undergone only a single (and continuing) sequence of lateral migration, implying that lateral migration rates are low. Investigations of the floodplain confirm this observation. A reconstruction of the past inner bank channel positions at two meanders near Ste. Jean Baptiste, Manitoba, revealed that the meanders have extended outwards and rotated downvalley in a single sequence of lateral channel migration that spans the ~8900-year history of the river (Brooks 2003b). However, approximately half of the floodplain formed during the first third of the post-Lake Agassiz time period (~8900–6000 cal BP), when the rates of lateral channel migration were higher (0.35 and 0.18 m/year between 7850–7360 and 7360–6170 cal BP, respectively, compared to 0.08–0.04 m/year post-6170 cal BP; Brooks 2003b). The interval of higher lateral migration corresponds to the warmest-driest period of the Holocene in the eastern Prairies (Bradbury et al. 1993; Laird et al. 1996; Valero-Garcés et al. 1997; Grimm 2002) and is thought to reflect enhanced sediment supply to the river associated with the establishment of the drainage network on the clay plain by the drop in base level from the recession of Lake Agassiz (Brooks 2003b). The chronology of the floodplain also reveals that there has been active lateral channel migration over the past 1000 years, averaging ~0.04 m/year, which is difficult to discern from mid- to late-twentieth-century aerial photographs (Nielsen et al. 1993). There is no evidence that the river is straightening its course, which might be expected because of a long-term loss of valley gradient from regional post-glacial differential uplift (Schumm 1977), as has been suggested by some authors (Welsh 1973; Schumm et al. 2000).

Reflecting a setting within a gentle-sloped clay plain, the suspended sediment load of the Red River is composed of >90 % silt and clay (Glavic et al. 1988), and the overbank and channel deposits within the floodplain are composed predominately of silt (Brooks 2003a). The river, thus, represents a suspended load, mud-dominated stream within the continuum of river morphologies. Reflecting this, sedimentation processes along both convex and concave sides of the meanders impart a markedly different fluvial geomorphic character to the Red River compared to the sand- and gravel-bed alluvial rivers elsewhere in western Canada. Contemporary convex bank sedimentation occurs as overbank and oblique accretion deposition—the latter being silt-rich deposits that are draped on the steep face of the convex banks, 30°–40° in slope and 3–4 m high, and grade laterally into overbank deposits into the floodplain surface (Nanson and Croke 1992; Page et al. 2003). Large-scale rotational failures, up to several hundred metres wide and extending up to 30 m back from the channel, are common along the convex banks, although active failures are not necessarily present at a specific meander every year or during a period of years (Brooks 2005). These failures move slowly (up to ~1 m/year) and are driven by elevated pore water pressures associated with a relatively rapid draw-down of stage from the spring freshet or a secondary high summer flow (Baracos and Kingerski 1998). Subsidence associated with the rotational failures creates an elongated stepped-morphology, 1–2 m high and many tens of metres long, along the convex banks that parallel the channel.

Along the outer banks of meanders, significant "concave overbank" sedimentation occurs within areas of elongated, low-angled (<10°), landslide zones that are up to ~2 km long and extend up to 80 m from the channel edge. These zones are present where the channel impinges against Lake Agassiz glacilacustrine deposits (Fig. 10.4; Brooks 2005) and consist of a complex of multiple, adjacent, extremely slow to very slow, rotational to translational earth slides (terminology after Cruden and Varnes 1996). Landslide activity is localized and occurs intermittently both spatially and temporally within these zones with periods of activity or inactivity spanning multiple years. Causes of the instability include the undisturbed strength of the clays, a permanent loss in clay strength following disturbance, the removal of toe support by river erosion, and elevated pore water pressures generated by the relatively rapid draw-down of river stage similar to the failures along the convex banks (Baracos 1978; Kjartanson 1983; Baracos and Lew 2003). The landslide zones are subject to varying levels of inundation nearly annually during the freshet (depending on the stage of the peak flow), causing "concave overbank deposits" to aggrade (Fig. 10.5a). Adjacent to the channel, annual accretions, up to 0.21 m thick, have been observed as part of accumulations up to 4 m thick at the river edge (Fig. 10.5b; Brooks 2005). Both annual accretions and accumulated deposits generally thin with greater distance from the channel edge and increasing height up the landslide surface, reflecting decreasing frequency and duration of inundation. Concave overbank deposits extend continuously along the landslide zones, which are common to meanders along the river between at least Emerson to St. Adolphe, Manitoba. The deposition is not related to meander curvature or location along the meander apex, unlike that which occurs on features variously termed concave-bank benches, concave benches, and eddy accretion deposits present along other western

Fig. 10.5 **a** Desiccated concave overbank deposits on the lower slope of a landslide zone. *Arrows* mark an active fault scarp associated with slope movement towards the channel located on the *right*. **b** Concave overbank deposits ~4 m thick exposed along a cutbank of a landslide zone. A shovel provides scale (marked by an *arrow*). Both photographs were taken in 1999

Canadian rivers (see Hickin 1979, 1986; Burge and Smith 1999).

Concave overbank deposits have been interpreted to be part of a sediment recycling process occurring within the landslide zones, whereby sediments accumulate regularly on the landslide zones, are subsequently displaced gradually downslope from earth slide movement, and are eventually reworked at the channel edge (Brooks 2005). The aggradation represents a sediment supply to the landslide zone that partially compensates for the removal sediment along the channel, and thus, it contributes to the dampening of the lateral valley-side erosion by the river. The comparatively low rates of lateral channel migration along the Red River meanders thus are a function of several factors: low stream power (~6 W m^2 in the Ste. Jean Baptiste area); the cohesive character of the silt floodplain and clay valley-side deposits that form the outer side of the channel; and the aggradation of concave overbank deposits (Brooks 2005).

10.4 Red River Floods

Major Red River floods historically occur during the spring freshet as the product of snowmelt run-off. South of Winnipeg, such floods characteristically fill and overtop the shallow stream-cut valley and spread onto the clay plain to form a broad, shallow, elongated flood zone (Fig. 10.6). During the 1997 Red River flood, the largest since 1852

Fig. 10.6 Photograph of the 1997 Red River flood, looking downstream (northward) from near Emerson, Manitoba, at the Canada–USA border. Flood waters have inundated the stream-cut valley and extended onto the clay plain, forming a broad flood zone

(Bumsted 1997), the flood zone in southern Manitoba covered ~2000 km^2, was up to 40 km wide, and extended from Winnipeg to south of the Canada–USA border (Figs. 10.6, 10.7). The clay plain, thus, is a major part of the hydraulic floodplain of the Red River. Ice jamming commonly occurs during spring break-up and can cause localized flooding along the river, but is not a factor forming the broad flood zone that is characteristic of major Red River floods south of Winnipeg (Beltaos et al. 2000).

Major Red River floods resemble a wide, shallow lake, but in fact are slow-moving flows that take several weeks or more to descend the river course. As an example, the 1997 flood crested on April 6 at Wahpeton, North Dakota, and then 27 days later at Winnipeg, 430 km downstream, on May 3 (data from Manitoba Water Stewardship). The crests of major floods rise and fall slowly, as exemplified by flows in 1997 and 2009 that exceeded bankfull discharge at Emerson, Manitoba, for periods of 47 and 67 days, respectively (data from Water Survey of Canada). Major Red River flows thus are slow-onset floods compared to rivers draining similar-sized basins elsewhere in North America. This flood characteristic, coupled with outlook forecasts of spring flooding and evolving flow conditions upstream in the American portion of the basin, provides weeks of warning of impending spring flood conditions in southern Manitoba, allowing for significant flood emergency preparation and mitigation.

Although Red River floods are a product of hydrology, their wide extent and slow-moving progression are fundamentally a function of the geomorphology of the stream-cut valley and the clay plain. The flood characteristics arise because the stream-cut valley has insufficient capacity to contain extreme flows due to its shallowness and low gradient. The adjacent broad, low-relief clay plain allows overtopping river water to spread laterally for many kilometres on either side of the stream-cut valley. Despite such inundation, alluvial sedimentation on the clay plain is negligible.

Prior to the construction of the flood protection infrastructure at Winnipeg, the flood zone narrowed gradually northwards through the Winnipeg area until the flood waters became fully confined within the stream-cut valley. As an example, this confinement occurred ~10 km downstream of the Red-Assiniboine confluence during the 1950 flood (Clark 1950), which was the last major flood before Red River Floodway operations began to regulate of Red River flood flows into Winnipeg (see below). The confinement was caused by a gentle rise in the general level of the clay plain beginning just north (downstream) of the Assiniboine River confluence in conjunction with a slight steepening and shallowing of river flow in response to the increase in gradient across Lister Rapids. These rapids are located in Winnipeg where Ordovician carbonate bedrock outcrops along the river (MMRD 1979). Both factors increase the capacity of the stream-cut valley, allowing extreme flows to be confined entirely within the stream-cut valley. This change in channel capacity is apparent from the extent of the 1997 flood, which formed a broad flood zone south of

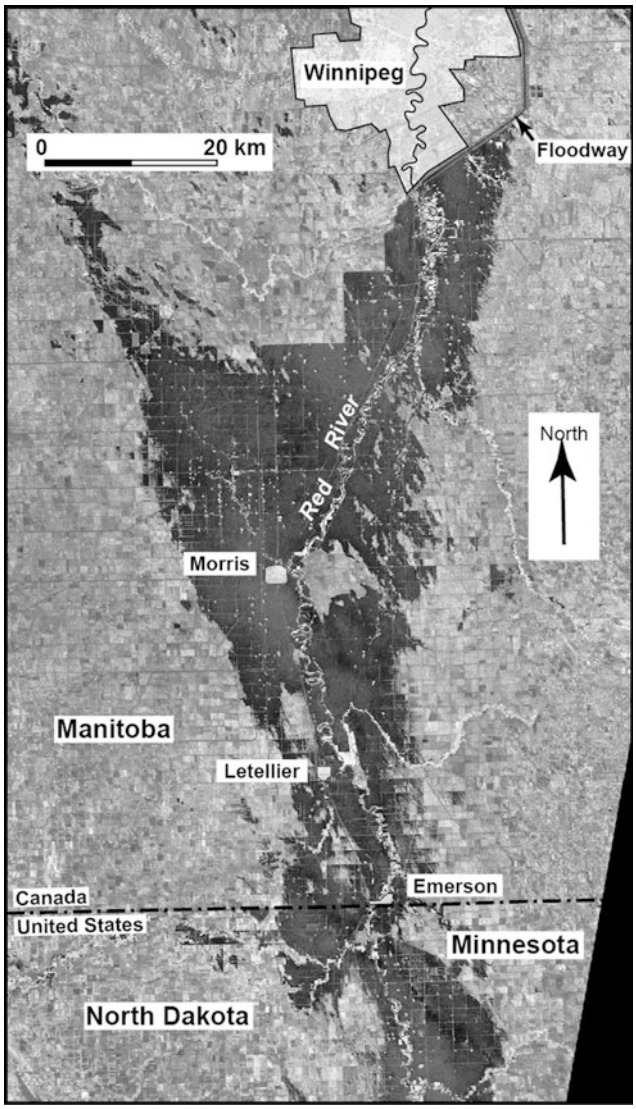

Fig. 10.7 *Radarsat* image of the flood zone during the 1997 Red River flood in southern Manitoba, showing the near-maximum extent of inundation (*dark* area on image; Radarsat-1 data acquired 4 May 1997, courtesy of Manitoba Remote Sensing Centre; © Canadian Space Agency 1997). The stepped, linear boundary at the north end of the flooding zone is formed against dykes protecting the southern area of Winnipeg

Winnipeg, but is absent north of the city downstream of the Floodway outlet where the river again carries the full flood discharge.

The occurrence of broad, slow-onset flooding is an intrinsic characteristic of the Red River valley and is not the product of modern alterations of the landscape (e.g. presence of cultivated fields, improvements to drainage, loss of wetlands, and the construction of raised road and railway beds; Brooks et al. 2005). This is demonstrated by historical accounts of broad Red River floods that extend back to the end of the eighteenth century in the records of fur-trading posts and early settlers (Bumsted 1997; Rannie 1998; St. George and Rannie 2003) The flood record has been further extended by dendrochronological investigations of bur oak trees (*Quercus macrocarpa* Michx.) that identified major eighteenth-century Red River flood years, based on the occurrence of "flood rings" within a continuous record of Red River valley tree rings that extends back to AD 1648 (St. George and Nielsen 2003). A flood ring contains anomalous structures in the early wood portion of the growth ring and is attributed to the occurrence of a major Red River spring flood of extended duration (St. George and Nielsen 2000; St. George 2010; Wertz et al. 2013).

10.5 Structural Flood Control Landforms

Red River floods have impacted the permanent settlements in the Red River valley on numerous occasions, causing major flood disasters in the springs of 1826, 1852, 1950, and 1997 (Bumsted 1997). The occurrence of the 1950 flood specifically, one of Canada's worst twentieth-century disasters (Bumsted 1997), initiated the establishment of integrated structural flood protection works within the Red River valley to mitigate similar or larger major floods in the future (Brooks and St. George 2015). This resulted in an array of artificial landforms of varying scale being built to mitigate Red River floods through several construction programmes, beginning in the early 1960s through 2014.

The largest and most important of these works is the Red River Floodway, a trapezoidal-shaped, diversion canal, about 48 km long and 160–370 m wide (Table 10.1). The floodway begins just upstream (south) of Winnipeg, extends north-easterly and then approximately northerly to bypass the city, before rejoining the river just downstream of Winnipeg (Figs. 10.1b, 10.7; see Weber 1967; Mudry et al. 1981). The Floodway Control Structure is situated immediately downstream of the Floodway entrance and regulates Red River stage through Winnipeg when discharge exceeds 900–1000 m^3/s, by raising submerged gates to divert a portion of flow into the Floodway channel. Built between 1962 and 1968 with a design capacity of 1700 m^3/s, the Floodway was enlarged significantly between 2005 and 2014, increasing the design capacity to 3960 m^3/s, which allows up to a 700-year flow to be mitigated. At the downstream (northern) end of the Floodway is the Floodway Outlet Structure that creates a ~4 m drop in the channel profile immediately prior to diverted flow rejoining the Red River (KGS Group 2001). This structure controls the energy gradient of flow upstream through the Floodway and allows water energy to dissipate rapidly.

The Floodway infrastructure also includes linear dykes that extend east and west of the Inlet Control Structure to

Table 10.1 Attributes of the expanded Red River Floodway (after Brooks and St. George 2015)

Length	~48 km[a]
Width	98–286 m base[b] 160–370 m top[b]
Depth	Up to 20 m (average 9.1 m)[a]
Channel shape	Trapezoidal, slopes ranging from 3H-1V to 10H-1V[b]
Design capacity	3960 m^3/s[b]
Design flow (natural flow)	Up to 7700 m^3/s[b,c,d]
Design flow return period	Up to 700 years[b,d]

[a]Mudry et al. (1981)
[b]Manitoba Floodway Authority, http://www.floodwayauthority.mb.ca/home.html and written communications, January–March 2012
[c]Flow within Winnipeg without the reducing effects of the Red River Floodway, Portage Division, and Shellmouth Dam
[d]Depending on character of the flood peak

arrest the northern extent of overland flooding to the south of Winnipeg, and direct flow through the Inlet Control Structure or Floodway channel. The East Dyke extends east of the Red River parallel to the Floodway (on the Winnipeg side) for about 10 km (KGS Group 2001). The West Dyke extends to the west of the Red River along a zig-zagging course for about 45 km. Earthen materials excavated from the channel during Floodway construction form a series of large, rectangular embankments, up to 10 m high, ~400 m wide, and several kilometres long, that parallel the Floodway channel.

South of Winnipeg, earthen ring dykes surround 18 rural towns and communities providing protection from Red River floods (Figs. 10.8, 10.9; Manitoba Ministry of Water Stewardship 2013). The height of a given ring dyke is constructed to at least the local stage of the 1997 Red River flood, plus a 0.6-m factor of safety. Short gaps in the ring dyke allow major roads to enter and exit the protected areas; these are in-filled with earth temporarily when threatening floods are forecast.

At a much smaller scale, over 1800 homes, businesses, and farms located outside of the ring dyked towns and

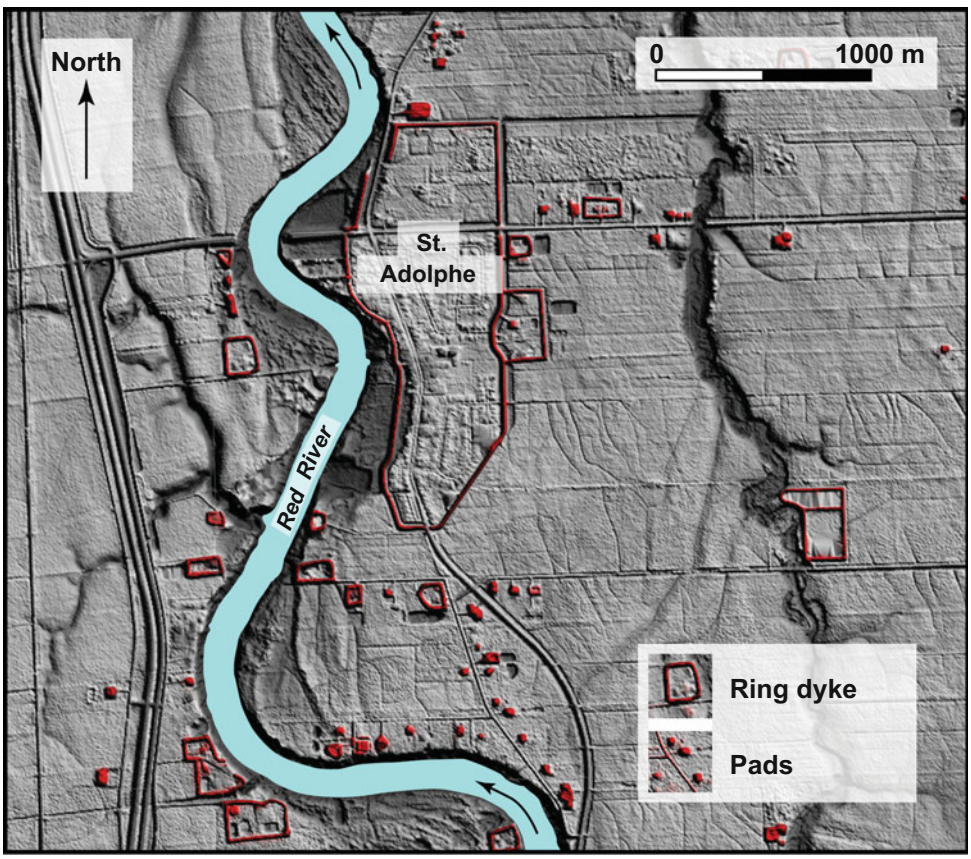

Fig. 10.8 Map showing ring dykes and pads of varying scale (highlighted with *red shading*) along the Red River in the vicinity of St. Adolphe, Manitoba (LiDAR image © Province of Manitoba, reproduced with permission)

Fig. 10.9 Town of Morris, Manitoba, protected from flooding by a ring dyke during the 1997 Red River flood (photograph taken 9 May 1997). Although appearing to be an island in the flood zone, the area within the town is lower than the level of flooding

communities are protected from flooding by a surrounding earthen ring dyke or by being situated on an elevated earthen pad (Fig. 10.9) that also is constructed to at least the level of the 1997 flood plus 0.6 m (Manitoba Ministry of Water Stewardship 2013). The clay soil used for the construction of an earthen ring dyke or pad is typically obtained by excavating a dug-out nearby. These depressions commonly fill with water becoming permanent ponds in the landscape. To a someone unfamiliar with the Red River flood hazard, the small-scale ring dykes and pads may seem an oddity on the low-relief landscape, especially where located kilometres from the river, but they are an important structural flood control. Ninety-five per cent of the homes, businesses, and farms in the flood zone south of Winnipeg are protected by structural flood control works (Manitoba Ministry of Water Stewardship 2013).

10.6 Conclusions

The exceptional low relief of the clay plain that forms the dominant landform of the Red River valley in combination with the low energy of the Red River imparts the impression of a benign landscape. Yet it is these very characteristics that result in the formation of the broad, slow-onset floods that have long afflicted the valley. This, in turn, has led to the construction of an array of anthropogenic landforms of varying scales that reduce the hazards of the flooding to communities and residents.

Acknowledgments Harvey Thorleifson (Minnesota Geological Survey) kindly provided information used in the compilation of Fig. 1. The chapter was improved from the helpful comments of Janet Campbell and Harvey Thorleifson. A significant portion of the Chapter draws upon geomorphic research in the Red River valley conducted between 1997 and 2003 that was supported by the Canada-Manitoba Agreement on Red River Valley Flood Protection Program, the Geological Survey of Canada, the Manitoba Geological Survey, and the Government of Canada's Climate Change Action Fund. The Chapter represents ESS Contribution Number 20140365.

References

Acton DF, Ryder JM, French H, Slaymaker O, Brookes IA (2012) Physiographic regions. The Canadian encyclopedia. http://www.thecanadianencyclopedia.ca/en/article/physiographic-regions/. Accessed 11 Nov 2014

Baracos A (1978) The effects of river levels, groundwater and other seasonal changes on river banks in Winnipeg. In: Proceedings of the 31st Canadian geotechnical conference, Winnipeg, MB, Canada

Baracos A, Kingerski D (1998) Geological and geotechnical engineering for urban development of Winnipeg, Manitoba. In: Karrow PF, White OL (eds) Urban geology of Canadian Cities. Geol. Assoc. Can. Special Paper No. 42, pp 171–190

Baracos A, Lew KW (2003) Geotechnical and related hydrology studies of the Red River banks through Winnipeg and upstream to the US border (1989–2001). In: Proceedings of the 56th Canadian geotechnical conference/4th joint IAH-CGS conference, Winnipeg, MB, Canada, pp 779–798

Beltaos SR, Pomerleau R, Halliday RA (2000) Ice-jam effects on Red River flooding and possible mitigation methods. Report prepared for the International Red River Basin Task Force, International Joint Commission. http://www.ijc.org/rel/pdf/icereport.pdf. Accessed 13 Nov 2012

Bradbury JP, Dean WE, Anderson RY (1993) Holocene climatic and limnologic history of the north-central United States as recorded in the varved sediments of Elk Lake, Minnesota: a synthesis. In: Bradbury JP, Dean WE (eds) Elk Lake Minnesota: evidence for rapid climate change in the north-central United States. Geol. Soc. Am Special Paper No. 276, pp 309–328

Brooks GR (2003a) Alluvial deposits of a mud-dominated river: the Red River, Manitoba Canada. Sedimentology 50:441–458

Brooks GR (2003b) Holocene lateral channel migration and incision of the Red River, Manitoba, Canada. Geomorphology 54:197–215

Brooks GR (2005) Overbank deposition along the concave side of the Red River meanders, Manitoba, and its geomorphic significance. Earth Surf Proc Land 23:1617–1632

Brooks GR, Nielsen E (2000) Red River, Red River Valley, Manitoba. Can Geogr 44:304–309

Brooks GR, George S (2015) Flooding, structural flood control measures, and a geomorphic context for the flood problem along the Red River, Manitoba, Canada. In: Hudson PF, Middelkoop H (eds) Geomorphic approaches to integrated floodplain management of lowland fluvial systems in North America and Europe. Springer, New York, pp 87–117

Brooks GR, Thorleifson LH, Lewis CFM (2005) Influence of loss of gradient from postglacial uplift on Red River flood hazard, Manitoba, Canada. Holocene 15:347–352

Bumsted JM (1997) Floods of the centuries: a history of flood disasters in the Red River Valley. Great Plains, Winnipeg 144 p

Burge LM, Smith DG (1999) Confined meandering river eddy accretions: sedimentology, channel geometry and depositional processes. In: Smith ND, Rogers J (eds) Fluvial sedimentology VI. Special Publication No. 28, International Association of Sedimentologists, Blackwell, Oxford, pp 113–130

Clayton JS, Ehrlich WA, Cann DB, Day JH, Marshall IB (1977) Soils of Canada, vols 1 and 2. Canada Department of Agriculture, Ottawa

Clark RH (1950) Notes on Red River floods with particular reference to the flood of 1950. Department of Mines and Natural Resources, Province of Manitoba

Cruden DM, Varnes DJ (1996) Landslide types and processes. In: Turner AK, Schuster RL (eds) Landslides investigation and mitigation. Special Report No. 247. National Academy Press, Washington, DC, pp 36–75

Dyke AS, Moore A, Roberston L (2003) Deglaciation of North America. Geol. Surv. Can. Open File No. 1574, 2 sheets; 1 CD-ROM. doi:10.4095/214399

Ehrlich WA, Poyser EA, Pratt LE, Ellis JH (1953) Reconnaissance soil survey of Winnipeg and Morris map sheet areas. Manitoba Soil Survey, Manitoba Department of Agriculture, Soils Report no. 5

Fenton MM, Moran SR, Teller JT, Clayton L (1983) Quaternary stratigraphy and history of the southern part of the Lake Agassiz basin. In: Teller JT, Clayton L (eds) Glacial Lake Agassiz. Geol. Assoc. Can. Special Paper No. 26, pp 49–74

George S (2010) Dendrohydrology and extreme floods along the Red River, Canada. In: Stoffel M, Bollschweiler M, Butler DR, Luckman BH (eds) Tree-ring reconstructions in natural hazards research: a state-of-the-art. Springer, London, pp 277–279

George S, Nielsen E (2000) Signatures of high-magnitude 19th century floods in *Quercus macrocarpa* tree rings along the Red River, Manitoba, Canada. Geology 28:899–902

George S, Nielsen E (2003) Paleoflood records for the Red River, Manitoba, Canada derived from anatomical tree-ring signatures. Holocene 13:547–555

George S, Rannie B (2003) Causes, progression, and magnitude of the 1826 Red River flood in Manitoba. Can Water Resour J 28:99–120

Glavic H, Day TJ, Yuzyk TR (1988) Interpretation of suspended sediment characteristics, Red River at Emerson Manitoba, 1978–1986. Report IWD-HQ-WRB-SS-88-3, Environment Canada

Grimm EC (2002) Trends and palaeoecological problems in the vegetation and climate history of the northern Great Plains, USA. Biol Environ 101:47–64

Hanuta I (2001) A reconstruction of wetland information in pre-settlement southern Manitoba using a geographical information system. Can Water Resour J 26:183–194

Hickin EJ (1979) Concave-bank benches on the Squamish River, British Columbia, Canada. Can J Earth Sci 16:200–203

Hickin EJ (1986) Concave-bank benches in the floodplains of Muskwa and Fort Nelson rivers, British Columbia. Can Geogr 30:111–122

Johnston WA (1946) Glacial Lake Agassiz, with special reference to the mode of deformation of the beaches. Geol. Surv. Bull. No. 7, Canada Department of Mines and Resources, Ottawa

Kehew AE, Lord ML (1986) Origin of large-scale erosional features of glacial-lake spillways in the northern Great Plains. Geol Soc Am Bull 97:162–177

Kehew AE, Teller JT (1994) History of late glacial runoff along the southwestern margin of the Laurentide ice sheet. Quat Sci Rev 13:859–877

KGS Group (2001) Flood protection studies for Winnipeg—main report. In: Report submitted to the Manitoba Conservation, Government of Canada, and City of Winnipeg

Kjartanson B (1983) Geological engineering report for urban development of Winnipeg. The University of Manitoba, Winnipeg

Laird KR, Fritz SC, Grimm EC, Mueller PG (1996) Century-scale paleoclimatic reconstruction from Moon Lake, a closed-basin lake in the northern Great Plains. Limnol Oceanogr 41:890–902

Lauhn-Jensen DM (1994) Geological highway map of Manitoba 1994, 2nd edn. Manitoba Minerals Division, Manitoba Energy and Mines, Winnipeg

Leverington DW, Mann JD, Teller JT (2002) Changes in the bathymetry and volume of glacial Lake Agassiz between 9200 and 7600 ^{14}C yr B.P. Quat Res 57:244–252

Manitoba Ministry of Water Stewardship (2013) Flood fighting in Manitoba, a history and background of Manitoba's flood protection works. http://www.gov.mb.ca/asset_library/en/spring_outlook/flood_fighting_2013.pdf. Accessed 18 Aug 2014

Manitoba Agricultural Services Corporation (2014) Yield Manitoba 2014. Farm Business Communications, Winnipeg. http://www.mmpp.com/mmpp.nsf/mmpp_publications.html. Accessed 12 May 2014

Manitoba Mineral Resources Division (MMRD) (1979) Geological map of Manitoba, scale 1:1,000,000, map 79-2

Manitoba Water Commission (1998) An independent review of actions taken during the 1997 Red River flood. In: Report to the Hon. J. Cummings, Minister of Natural Resources

Matile G (2005) Stop 1–3 landforms of Lake Agassiz—linear ridges and iceberg scours. In: Brooks GR, Grorge S (eds) Environmental

geoscience and geomorphic systems in the Red River valley, Manitoba, field trip guidebook. CANQUA, Winnipeg, pp 26–30

Mudry N, Reynolds PJ, Rosenberg HB (1981) Post-project evaluation of the Red and Assiniboine River flood control projects in the Province of Manitoba, Canada. In: methods of post-project evaluation: achievements and remedial measures, International Commission on Irrigation and Drainage: Special Session R. 9, Grenoble, Switzerland, pp 147–178

Nanson GC, Croke JC (1992) A genetic classification of floodplains. Geomorphology 4:459–486

Nielsen E, McKillop WB, Conley GC (1993) Fluvial sedimentology and paleoecology of Holocene alluvial deposits, Red River, Manitoba. Géog Phys Quat 47:193–210

Page KJ, Nanson GC, Frazier PS (2003) Floodplain formation and sediment stratigraphy resulting from oblique accretion on the Murrumbidgee River, Australia. J Sediment Res 73:5–14

Rannie WF (1998) A survey of hydroclimate, flooding, and runoff in the Red River basin prior to 1870. Geol. Surv. Can. Open File 3705

Rannie WF (2016) Landscapes of the Assiniboine River watershed. In: Slaymaker O (ed) Landforms and Landscapes of Western Canada. Springer, New York

Rannie WF, Thorleifson LH, Teller JT (1989) Holocene evolution of the Assiniboine River paleochannels and Portage la Prairie alluvial fan. Can J Earth Sci 26:1834–1841

Schumm SA (1977) The fluvial system. Wiley, New York

Schumm SA, Dumont JF, Holbrook JM (2000) Active tectonics and alluvial rivers. Cambridge University Press, Cambridge

Teller JT (1985) Lake Agassiz and its influence on the Great Lakes. In: Karrow PF, Calkin PE (eds) Quaternary evolution of the Great Lakes. Geol Assoc Can Special Paper No. 30, pp 1–16

Teller JT, Bluemle JP (1983) Geological setting of the Lake Agassiz region. In: Teller JT, Clayton L (eds) Glacial Lake Agassiz. Geol. Assoc. Can., Special Paper No. 26, pp 7–20

Teller JT, Clayton L (eds) (1983) Glacial Lake Agassiz. Geol. Assoc. Can., Special Paper 26

Teller JT, Leverington DW (2004) Glacial Lake Agassiz: a 5000 yr history of change and its relationship to $\delta^{18}O$ record of Greenland. Geol Soc Am Bull 116:729–742

Teller JT, Thorleifson LH (1983) The Agassiz–Lake Superior connection. In: Teller JT, Clayton L (eds) Glacial Lake Agassiz. Geological Association of Canada, Special Paper No. 26, pp 261–290

Upham W (1895) The Glacial Lake Agassiz. US Geol. Surv., Monograph 25

Valero-Garcés BL, Laird KR, Fritz SC, Kelts K, Ito E, Grimm EC (1997) Holocene climate in the Northern Great Plains inferred from sediment stratigraphy, stable isotopes, carbonate geochemistry, diatoms, and pollen at Moon Lake, North Dakota. Quat Res 48:359–369

Warkentin J, Ruggles RI (1970) Historical Atlas of Manitoba. Historical and Scientific Society of Manitoba, Winnipeg

Weber TE (1967) The Red River Floodway and related control works. In: International conference on water for peace, vol 7, planning and developing water programs. United States Government Printing Office, Washington, DC, pp 759–768

Welsh DM (1973) Channel form and bank erosion, Red River, Manitoba. In: Fluvial processes and sedimentation, proceedings of the hydrology symposium, University of Alberta, Edmonton, pp 284–293

Wertz EL, George S, Zelznik JD (2013) Vessel anomalies in *Quercus macrocarpa* tree rings associated with recent major floods along the Red River of the North, United States. Water Resour Res 49:630–634

Woodworth-Lynas CMT, Guigné JY (1990) Iceberg scours in the geological record: examples from glacial Lake Agassiz. In: Dowdeswell JA, Scourse JD (eds) Glacimarine environments: processes and sediments. Geological Society of London, Special Publications No. 53, pp 217–223

The Foothills Erratics Train Region

11

Lionel E. Jackson Jr.

Abstract

The Foothills erratics train (FET) region of Alberta includes a 580-km-long eponymous erratic boulder train, and an adjacent region underlain by drift whose lithology reflects past interaction between glaciers that entered the Foothills and nearby Interior Plains from the Rocky Mountains and the Laurentide Ice Sheet that brought rocks and minerals into this area from the Canadian Shield. Landforms in the region are a legacy of flowing glacial ice, ice stagnation and damming of drainage and re-establishment of eastward river drainage. The FET is the only known erratic boulder train to have been transported in a medial moraine position between mountain glaciers and a continental ice sheet. Based upon its rapid removal by human activities, it is suggested that other comparable erratic trains may have existed elsewhere but were erased by agriculture over the millennia.

Keywords

Erratic boulder train • Pleistocene geology • Glaciology • Laurentide Ice Sheet • Stonehenge

11.1 Introduction

The Foothills erratics train (FET) of Alberta is comprised of hundreds of angular quartzite boulders ranging from <1 m to the Big Rock near Okotoks with an estimated mass of 16,000 tonnes (Stalker 1956). It ranges from 1 to 22 km in width, and it can be traced over a distance of approximately 580 km (Fig. 11.1). Gaps in this erratic boulder train between the North Saskatchewan River and Edson coincide with a change of vegetation from grassland to forest so that erratic boulders would not be visible from the air or roads. Consequently, it is not known whether this gap is real or apparent. The Foothills erratics train region (FETR) includes a wider belt east and west of the eponymous FET wherein the underlying ground moraine has a pebble and heavy mineral lithology indicative of past interaction and coalescence between former valley glaciers that advanced from the Rocky Mountains and the Laurentide Ice Sheet (LIS). This zone of mixed provenance drift grades westward and eastward into purely montane and LIS drift, respectively (Jackson 1980). It parallels and commonly spans the eastern limit of the Rocky Mountain Foothills and the western limit of the Interior Plains between the Edson area and the Porcupine Hills. North of the Porcupine Hills, the mixed provenance drift in the FETR has a width of about 20 km, but landforms created by confluent glacial flow can be found 50 km or more from the FET.

South of the Porcupine Hills (A in Fig. 11.1), the FET leaves the edge of the Foothills and trends east–southeast. In this area, it parallels the northern margins of local uplands within the Interior Plains. These uplands form a continental divide between the Missouri River basin to the south and the South Saskatchewan River basin to the north. The FET ends

L.E. Jackson Jr. (✉)
Department of Earth Sciences, Simon Fraser University, 888 University Drive, Burnaby, BC V5A 1S6, Canada
e-mail: lionelj@sfu.ca

L.E. Jackson Jr.
Geological Survey of Canada, 1500–605 Robson Street, Vancouver, BC V6B 5J3, Canada

© Springer International Publishing Switzerland 2017
O. Slaymaker (ed.), *Landscapes and Landforms of Western Canada*, World Geomorphological Landscapes, DOI: 10.1007/978-3-319-44595-3_11

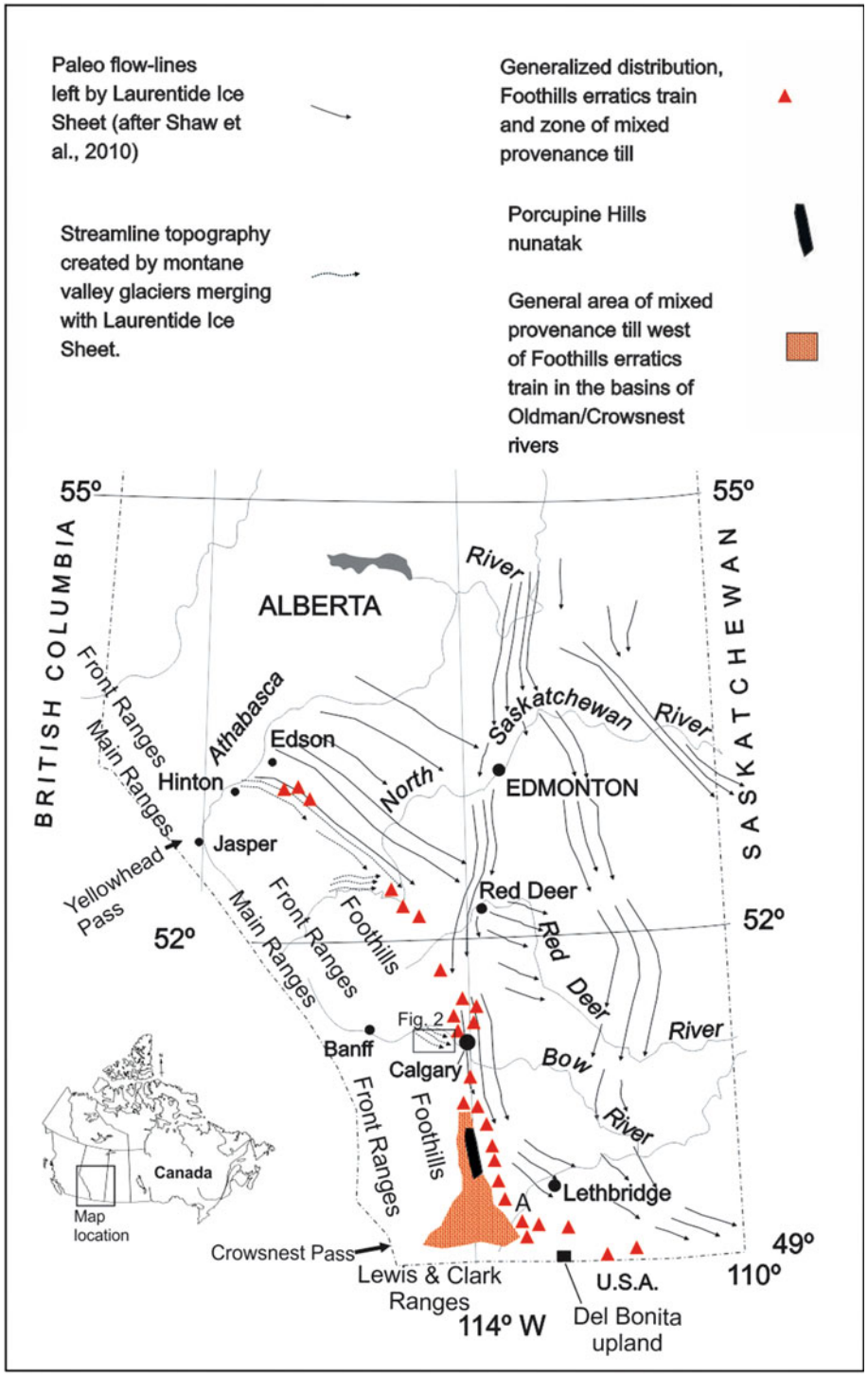

Fig. 11.1 Physiography and former ice flow directions as indicated by streamlined topography in central and southern Alberta. The *red triangles* generalize FET and zone of mixed provenance till north of the Porcupine Hills. South of them, the zone of mixed provenance till and erratics from the Canadian Shield extends much farther west due to asynchronous advances and retreats of montane glaciers and the LIS

near the international border in the area of the Coutts, Alberta/Sweetgrass, Montana border crossing (lat. 49°00′N, long. 112°40′W). The mixed provenance drift and landforms created by glacial interaction that defines the FETR extend all the way to the front of the Rocky Mountains in this area (see Fig. 11.1).

11.2 Recognition and Age of the Foothills Erratics Train

The occurrence of a linear train of large erratic boulders along the eastern edge of the Foothills was well known to the Siksikáwa people (better known as members of the

Blackfoot Confederacy) whose territory included the FETR at the time of contact with European explorers and traders. The Siksikáwa recognized that these boulders differed from the surrounding bedrock. They had oral traditions involving their Creator, Napi, which explained how this trail of similar and exceptionally large angular boulders came to be (Grinnell 1892).

Individual large erratic blocks within this erratic boulder train were first reported in the nineteenth century by James Hector of the Palliser Expedition (who erroneously reported them to be granite (Hector 1861)). These individual large bedrock blocks were variously interpreted as having been transported from the western edge of the Canadian Shield by icebergs during an incursion of the Arctic Ocean (Dawson 1885) or as an erosional remnant of a klippe in the case of the Big Rock (Hume 1931). The first regional synthesis of surficial geology for western Canada was carried out by Bretz (1943) using unpublished (and unacknowledged by him) maps by Geological Survey of Canada geologists P.S. Warren, W.A. Johnston and R.T.D. Wickenden. This compilation showed no indication of an erratic boulder train along the eastern margin of the Foothills. In fact, the mixed montane Canadian Shield provenance of drift in the FETR was recognized by Johnston and Wickenden (1931) before the FET was documented by the subsequent systematic mapping of Stalker (1956). Stalker recognized four properties of the rocks forming this erratic boulder train that led to the present understanding of its origin:

1. The blocks are highly indurated pebbly quartzite.
2. They are almost always angular and broken along bedding planes and joints (Fig. 11.2).
3. They rarely are striated or otherwise show evidence of being over-run by glacial ice.
4. They were derived from the Rocky Mountains and not from quartzite outcrops along the Canadian Shield in northeastern Alberta.

Stalker combined these observations with the distribution of the erratics in a narrow belt into the hypothesis that the erratic boulders initially fell onto a passing valley glacier from adjacent mountain cliffs in the headwaters of the Athabasca River. In this way, they were transported superglacially on a trunk glacier that exited from the Athabasca River valley. He further postulated that this glacier must have merged with the LIS along the eastern margin of the Foothills where their combined flow was in a southeast direction approximately parallel to the structural trend of hogback ridges that are erosional expressions of the northwest striking Foothills fold and thrust belt. Had this coalescence not happened, he reasoned, the erratics would have been deposited by a piedmont glacier in a fan-like pattern that would have been over-run by any subsequent advances of the LIS. His preliminary conclusions were subsequently supported by the discovery of the source of the erratics within the Lower Cambrian Gog Group in the Mt. Edith Cavell area of Jasper National Park (Roed et al. 1967) and subsequent regional mapping by Roed (1975), Harris and

Fig. 11.2 Glenwood erratic near Pincher Creek, Alberta (lat. 49° 24′53″N, long. 113°27′00″W). It lacks striations and shows the jointed nature of these blocks that suggest that they were transported supraglacially. A man stands along the left side of the erratic for scale. Photograph by Edward Little

Boydell (1972), Alley and Harris (1974), Jackson (1980) and Jackson et al. (2008).

Emplacement of the Foothills erratics train has been dated to the last glacial maximum (LGM) based upon cosmogenic chlorine-36 exposure dating of their upper surfaces (Jackson et al. 1999). Furthermore, stratigraphic investigations in central and southern Alberta have shown clearly that the coalescence of montane and continental ice that produced the Foothills erratics train was unique to the last glacial maximum. During all previous Neogene glaciations, broad ice-free corridors separated precursors of the LIS from piedmont glaciers along the eastern margin of the Cordillera (see Jackson et al. 2011 for a summary of past work by many workers).

11.3 Dominant Landforms in the FETR

Landforms in the FETR are the products of glaciation, deglaciation and post-glacial fluvial incision of the Foothills region. From oldest to youngest they are:

1. Ground moraine, streamlined bedrock ridges, whalebacks and drumlins created by active flow of coalesced valley glaciers from the Rocky Mountains and the LIS during the climax of the last glaciation.
2. Terraced gravel deposits on hillsides, former tunnel channels, hummocky ice stagnation moraine and glacial lake plains created by the thinning and stagnation of coalescent montane glaciers and the LIS during deglaciation.
3. Flights of terraces along extant streams that trend across the FETR. These were created when drainage from the Rocky Mountains re-established itself and incised through drift into pre-existing buried bedrock canyons or cut new courses during post-glacial time.

11.3.1 Ground Moraine (Till)

The zone of mixed provenance till that underlies the FETR is recognizable because there are no significant sources of plutonic or metamorphic rock within the Rocky Mountains east of the Great Divide (Alberta and British Columbia border). Consequently, till deposited by glaciers from the Rocky Mountains lack plutonic and metamorphic rocks. The only exceptions are rare clasts carried into the region by the valley glacier that crossed Yellowhead Pass in what is now Jasper National Park and rare granitic clasts from Mesozoic conglomerates that crop out in the Foothills. These orthoclase-dominated clasts are easily differentiated from the pink, plagioclase-rich plutonic rocks and high-grade metamorphic rocks that the LIS transported into the FETR from the Canadian Shield. Within the FETR north of the Porcupine Hills, plutonic and metamorphic pebbles decrease from about 1 % of total pebble content a few km east of the FET to non-existent within a few km west of it, whereas highly indurated orthoquartzite clasts from the Rocky Mountain Main Ranges become more common (Jackson 1980). With respect to the content of heavy minerals across the FETR, the total weight percentage of them decreases and green hornblende content drops from about 30 % of the non-opaque heavy mineral suite to zero: It is replaced by brown hornblende. Green hornblende dominates the heavy mineral suite of till deposited by the LIS in central Alberta (Bayrock 1962), whereas brown hornblende is the only type of hornblende that occurs within the clastic rocks of the Rocky Mountain Main and Front Ranges and the Foothills. This distribution of lithology and mineralogy indicates that a narrow zone of coalescence between glaciers from the Rocky Mountains and the LIS fluctuated within approximately 20 km east and west of the FET during the last glaciation.

This pattern changes abruptly in the area south of the Porcupine Hills. Plutonic and metamorphic rocks are found up to 65 km west of the FET in the Crowsnest River and Oldman River basins (Fig. 11.1). Jackson et al. (2008) and Jackson and Little (2008) found that glacial advances from the Rocky Mountains and two advances of the LIS were non-synchronous in this region: Valley glaciers advanced from the Front Ranges west of the Great Divide via Crowsnest Pass and from the Lewis and Clark Ranges during the early phase of the last glaciation. They terminated about 10 km west of Lethbridge. Montane valley glaciers retreated almost to the foot of the Rocky Mountains when the LIS reached the area. The margin of the LIS advanced far up into the Crowsnest and Oldman river basins where it reached the Rocky Mountain front and then retreated. Subsequently, there were readvances of montane valley glaciers and LIS creating a succession of mixed provenance tills interstratified with lake sediments (Holme et al. 2000; Jackson et al. 2008). The abrupt change in direction of the FET in the area of 'A' in Fig. 11.1 suggests that its superglacial transportation postdated the two advances of LIS into the Oldman and Crowsnest basins. The FET south and east of 'A' mark the direction of the last active flow within the LIS in that part of southern Alberta. Glacial ice to the west was apparently stagnating at that time.

11.3.2 Streamlined Landforms

The glacier transporting the FET boulders was part of a convergent flow of glacial ice formed by the coalescence of the Athabasca Valley glacier with the LIS to the east and confluent valley glaciers from major river basins that drain the

Continental Divide such as the North Saskatchewan and Bow River basins. The northwest trending bedrock ridges of the Foothills have been locally streamlined by glacial flow where valley glaciers were diverted parallel or subparallel to strikes of these hogback ridges. These glacially streamlined hills mark areas of major glacial coalescence. This topography is well developed south of the Athabasca River valley between Hinton and Edson (area or lat. 53°30′N, long. 117°00′W) and 30 km west of Calgary between Ghost Reservoir in the Bow River valley and Jumpingpound Creek (Fig. 11.3).

The minimum surface elevation of the glacial ice that produced these streamlined landforms can only be constrained as being $> \sim 1750$ masl. This is the elevation of highest glacial erratic found at the limit of glaciation along the north end of the Porcupine Hills which was a nunatak during the LGM. No former nunataks exist in the Foothills north of the Porcupine Hills that are useful for defining former ice surface gradients. However, south of the Porcupine Hills, Mathews (1974) reconstructed a glacial surface gradient of approximately 2 m/km using the upper limits of glaciation in southern Alberta and Saskatchewan and adjacent Montana. This is depicted in Fig. 11.4 between upper limits of erratic boulders from the Canadian Shield in the Porcupine Hills and the limit of glaciation at the north end of the Del Bonita upland which was a also a nunatak. This is a first-order approximation for the LGM. Subsequent work by Little et al. (2001) has shown that the surface gradient of the LIS along the Foothills south of the Porcupine Hills was complicated by ice dynamics. Regardless of actual maximum surface elevation and gradient of the coalescent montane glaciers with the LIS, the southeast coalescent glacier flow was sufficiently thick to inundate the topography of the Foothills and cross 12 major interfluves between streams that cross the Foothills. The highest of these interfluves is 1250 masl.

11.3.3 Glacial Lake Plains, Sub Aerial and Tunnel Channels and Ice Stagnation Topography

The FET records the pattern of ice flow immediately prior to the thinning glacial ice cover to the point that southward flow was no longer possible. Ice stagnation moraine complexes are common in many valleys where ice remained

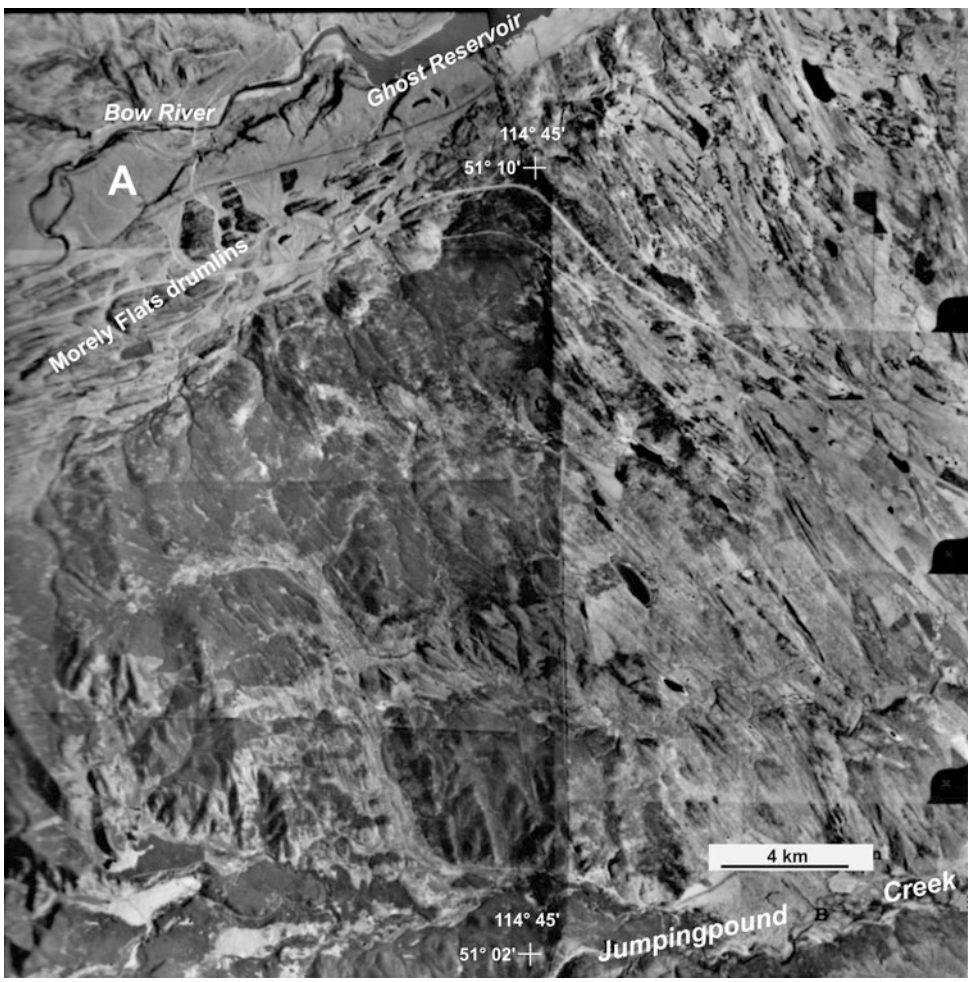

Fig. 11.3 Air photograph mosaic showing streamlined hogback ridges molded by the diversion of a valley glacier from the Bow River valley toward the southeast as it joined common flow with valley glaciers from farther north and the LIS during the last glacial maximum. The Morley Flats drumlins were deposited during a later phase of the same glaciation when the Bow Valley glacier was thinner and its flow was confined within the Bow River valley. The plain indicated by 'A' is a complex of gravel-dominated recessional outwash and paraglacial fill deposited during the early post-glacial period (air photographs courtesy of the Geomatics Canada)

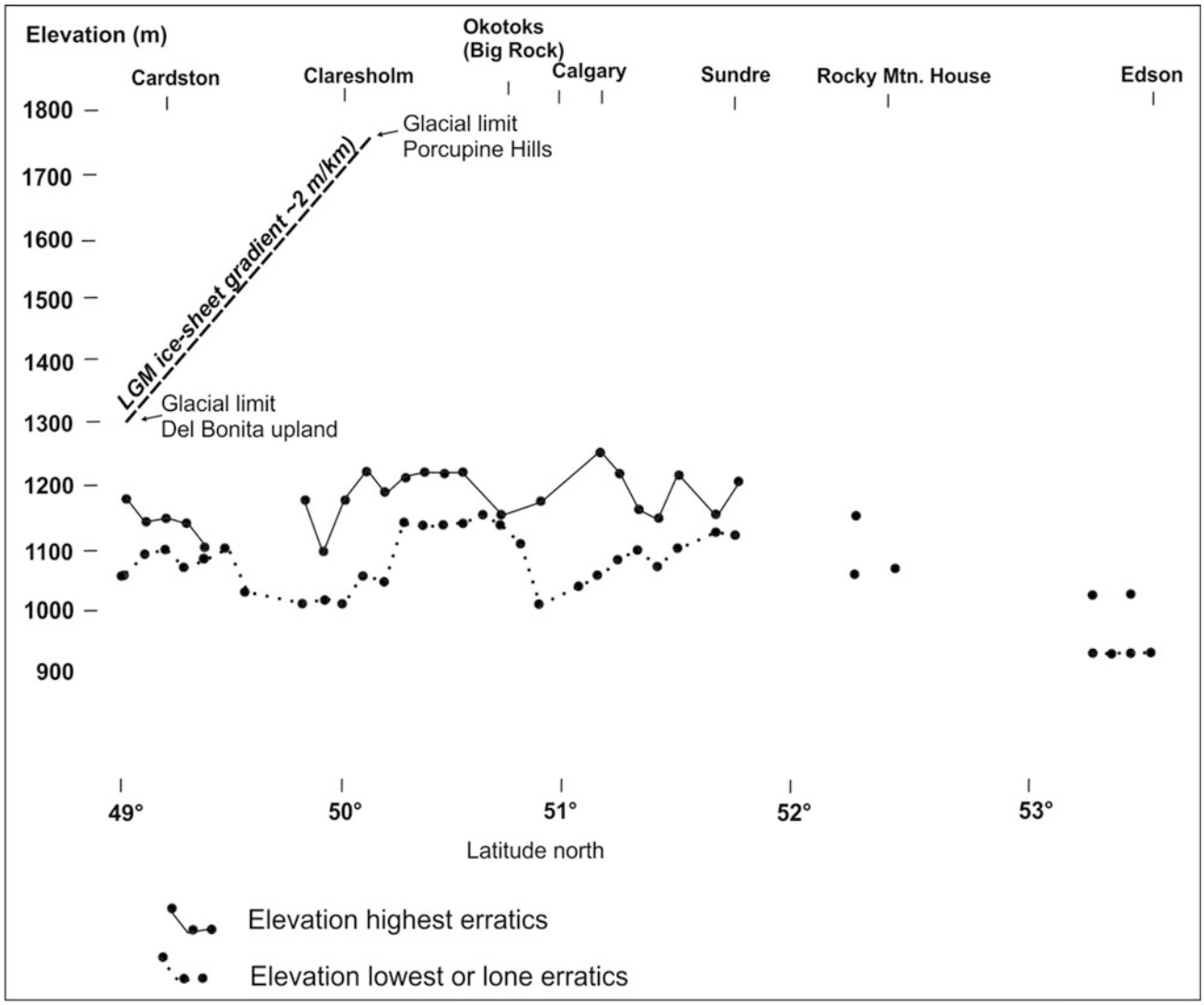

Fig. 11.4 A plot of the distribution of the FET by elevation of constituent erratic boulders. A hypothetical glacier surface (after Mathews 1974) is drawn between the limit of glaciation at the Del Bonita upland and the latitude of the highest erratic boulders on the Porcupine Hills, a former nunatak. This reconstructed surface can be regarded as having a maximum limiting elevation and gradient

relatively thicker as local upland hills and ridges emerged. This led to the formation of ice dams and ice-dammed lakes opposite valleys within the Foothills (Harris and Boydell 1972; Alley and Harris 1974; Roed 1975; Jackson et al. 2008). The Bow Valley in the area of present-day Calgary is a good example. It is underlain by sediments of Glacial Lake Calgary which was ponded at a succession of lake levels (Wilson 1983). Stalker (1956) noted that the absence of FET erratics in valleys like the Bow Valley coincided with glacial lake deposits, and he proposed that erratics were buried in the lake deposits due to calving of glacial ice into these lakes during recession of glacial ice eastward from the Bow Valley down the regional gradient. FET erratics have been found within these lake deposits. Water draining from glacial lakes and overall melting of the stagnating ice were transported through open or tunnel channels that generally were oriented northwest to southeast approximately normal to the present regional gradient. Figure 11.4 shows the range of elevations of FET erratics along the length of the erratics train. The difference between the elevations of the highest and lowest erratics is not more than 120–150 m at any latitude. This difference reflects the vertical wasting of glacier ice following stagnation so that erratics located over subglacial high topography were the first to be deposited, whereas those over low topography were the last at a given latitude. Ice stagnation produced belts of kame and kettle topography in intervening low areas. Locally, FET erratics are associated with flights of ice-walled channels where meltwater streams flowed in channels that had rock on one wall and glacial ice on the other as the ice surface wasted downward (Fig. 11.5).

Fig. 11.5 A succession of FET erratics resting on bedrock west of Claresholm, Alberta (*arrows* indicate erratics in the distance). The erratics are associated with a succession of gravel deposits. The gravel was deposited in the beds of streams at the margin of stagnating glacial ice so that one side of the channel had a bedrock wall and the other a wall of glacial ice. The closest erratic was the first to be deposited followed by those in the distance. Photograph by L. Jackson, Jr

11.3.4 Stream Terraces

As streams draining eastward from the Rocky Mountains re-established their courses, they incised through drift including ice stagnation complexes. Streams initially incised to bedrock but then aggraded filling valleys with gravel and sand. This peaked in the Bow River valley between c. 11,000 and 10,000 radiocarbon years before present (Jackson et al. 1982; Wilson 1983). This has been postulated to have been caused by the paraglacial effect (Church and Ryder 1972): Glaciation left large amounts of glacial debris in the Rocky Mountains as glaciers disappeared. Decrease in stream discharge coupled with a relative increase in sediment load caused streams to aggrade through earlier part of the Holocene. This was followed by incision and cutting of flights of terraces as erosion of relict glacial sediments dwindled causing sediment loads in rivers to diminish during the latter part of the Holocene (Jackson et al. 1982). Location 'A' in Fig. 11.3 shows the surface of such a late glacial/early Holocene fill.

11.4 Comparison of the FET with Other Extant and Possibly Vanished Erratic Boulder Trains

Darvill et al. (2015) compiled statistics on notable erratic boulder trains from the literature. Included were examples from North and South America and Antarctica. European examples were confined to Scotland. This compilation showed the FET to be without peers in two aspects:

1. It is by far the longest measured from source to most distant erratic at c. 580 km
2. It is the only known erratic boulder train to have been transported in a medial moraine position between mountain glaciers and a continental ice sheet.

The only extant erratic boulder trains that can said to be comparable are those in Tierra del Fuego (Darwin 1841; Darvill et al. 2015). Their combined lengths are 85 km, and individual blocks have been moved about 250 km from their source areas. The boulders in these trains fell onto valley glaciers from adjacent cliffs in their upper reaches, and they were transported supraglacially in a manner similar to the boulders of the FET.

It is interesting to note that in the compilation of Darvill et al. (2015), all of the erratic boulder trains identified are in remote, sparsely populated areas or areas where agriculture was introduced during the last 200 years: They largely have not been (as yet) erased by clearing of boulders from fields and pastures. It is fortuitous that the FET was mapped in the mid-twentieth century within a century after the introduction of agriculture. Many boulders of the FET have been subsequently removed by farmers due to their posing a nuisance to cultivation of fields. Even the 'Big Rock' near Okotoks, the largest erratic in the FET, was almost blown-up for rip-rap in the 1950s, and the Glenwood erratic (Fig. 11.2) was defaced by explosives for no apparent reason (Stalker 1975). Without heritage protection, these and many of the other erratics would surely have been erased without a trace.

With this in mind, it can be postulated that other extensive erratic boulder trains may once have existed in formerly

glaciated areas of the European continent but were destroyed as a result of agricultural clearing of boulders from fields or exploitation of them for building stone. John (2008) and John and Jackson (2009) noted that southwestern Wales lies along a former zone of eastward glacial ice flow convergence between successive Welsh ice caps and glaciers that covered what is now the Irish Sea during past glaciations. This zone of convergence encompasses widely spaced outcrops of a variety of volcanic and subvolcanic lithologies and micaceous sandstone that have been collectively called 'bluestones' at the Stonehenge ruin on the Salisbury Plain of southern England. Such a convergent flow would have carried plucked bedrock blocks from southwest Wales in a medial moraine position, analogous to the FET, into southwestern England a distance of up to 180 km where they would have formed a linear boulder train. John and Jackson and others before them suggested that such a boulder train would have provided a local source for the 'bluestone' megaliths. They may have been associated with supernatural events by Neolithic Britons in the same way that the boulders of the FET were by Neolithic indigenous Canadians. This was offered as an alternative to the man hauling up to 80 erratic bluestones, with masses of many tonnes over 200 km from Wales during the Neolithic (John 2008).

11.5 Summary

The 580-km FET is situated within a larger (FETR) region marked by landforms and drift that were shaped by interaction between glaciers from the Rocky Mountains and the LIS. Landforms in the region are a legacy of flowing glacial ice, ice stagnation, damming of drainage and re-establishment of eastward river drainage. The exceptional length of the FET and distance of transport of its boulders, compared to other known erratic boulder trains, may be more apparent than real. Others may have existed in Europe in such areas of the forelands north and south of the Alps, down-ice flow from the Norwegian mountains within the former Fennoscandian Ice Sheet and in southern England where medial moraine transport conditions were analogous to that in the FETR. Human modification of the landscape would have subsequently removed them during the post-glacial period. Conservation measures will be required to save the FET from a similar fate.

References

Alley NF, Harris SA (1974) Pleistocene lake sequences in the Foothills, southwestern Alberta, Canada. Can J Earth Sci 11:1220–1235

Bayrock LA (1962) Heavy minerals in till of central Alberta. J Alta Soc Petrol Geol 10:171–184

Bretz JH (1943) Keewatin end moraines in Alberta. Geol Soc Am Bull 54:31–54

Church M, Ryder JM (1972) Paraglacial sedimentation: a consideration of fluvial processes conditioned by glaciation. Geol Soc Am Bull 83:3072–3095

Darvill DM, Bentley MJ, Stokes CR (2015) Geomorphology and weathering characteristics of erratic boulder trains on Tierra del Fuego, southernmost South America: implications for dating of glacial deposits. Geomorphology 228:382–397

Darwin C (1841) On the distribution of the erratic boulders and on the contemporaneous unstratified deposits of South America. Trans Geol Soc Lond 2–6:415–431

Dawson GM (1885) Report on the region in the vicinity of the Bow and Belly rivers. Geological Survey and Natural History Survey of Canada, Report of Progress 1882-83-84:1c–169c

Grinnell GB (1892) Blackfoot lodge tales. Reprinted by CreateSpace Independent Publishing Platform (5 Sept 2013). http://www.createspace.com

Hector J (1861) On the geology of the country between Lake Superior and Pacific Ocean (between the forty eighth and fifty fourth parallels of latitude) visited by the government exploring expeditions under the command of Captain J. Palliser (1857–60). Quar J Geol Soc Lond 17:388–445

Harris SA, Boydell AN (1972) Glacial history of the Bow River and the Red Deer River areas and the adjacent foothills. In: Slaymaker O, McPherson HJ (eds) Mountain geomorphology: process studies in the Canadian Cordillera. Tantalus Press, Vancouver, pp 47–54

Holme PJ, Hickock SR, Jackson LE Jr (2000) Interaction of Laurentide and cordilleran ice in the Beaver Mines area, southwestern Alberta. Geogr phys Quat 54:209–218

Hume GS (1931) Overthrust faulting and oil prospects of the eastern Foothills of Alberta between the Bow and Highwood rivers. Econ Geol 26:258–273

Jackson LE Jr (1980) Glacial history and stratigraphy of the Alberta portion of the Kananaskis Lakes map area. Can J Earth Sci 17:459–477

Jackson LE Jr, Little EC (2008) A single continental glaciation of Rocky Mountain Foothills, south-western Alberta, Canada. In: Ehlers J, Gibbard PL (eds) Quaternary glaciations—extent and chronology. Elsevier, Amsterdam, pp 29–38

Jackson LE Jr, Wilson MC, MacDonald GM (1982) Paraglacial origin for terrace river sediments in Bow Valley, Alberta. Can J Earth Sci 19:2219–2231

Jackson LE Jr, Phillips FM, Little EC (1999) Cosmogenic 36Cl dating of the maximum limit of the Laurentide Ice Sheet in southwestern Alberta. Can J Earth Sci 36:1347–1356

Jackson LE Jr, Leboe ER, Little EC, Holme PJ, Hicock SR, Shimamura K, Nelson, FEN (2008) Quaternary stratigraphy and geology of the Foothills, southwestern Alberta. Geol Surv Can Bull 583:19–46 (CD-ROM)

Jackson LE Jr, Andriashek LD, Phillips FM (2011) Limits of successive Middle and Late Pleistocene continental ice sheets, Interior Plains of southern and central Alberta and adjacent areas. In: Ehlers J, Gibbard PL, Hughes PD (eds) Developments in quaternary science, vol 15. Elsevier, Amsterdam, pp 575–589

John B (2008) The bluestone enigma. Greencroft Books, Newport 160 p

John B, Jackson LE Jr (2009) Stonehenge's mysterious stones. Earth Mag 54(1):36–43

Johnston WA, Wickenden RTD (1931) Moraines and glacial lakes in southern Saskatchewan and southern Alberta, Canada. Trans R Soc Can Ser 325(4):25–44

Little EC, Jackson LE Jr, James TS, Hicock SR, Leboe ER (2001) Continental/Cordilleran ice interactions: a dominant cause of westward superelevation of the last glacial maximum continental ice limit in southwestern Alberta, Canada. Boreas 30:43–52

Mathews WH (1974) Surface profiles of the Laurentide ice sheet in its marginal areas. J Glaciol 19:37–42

Roed MA (1975) Cordilleran and Laurentide multiple glaciation, west-central Alberta. Can J Earth Sci 12:1493–1515

Roed MA, Mountjoy EW, Rutter NW (1967) The Athabasca Valley erratics train and ice movement across the Continental Divide. Can J Earth Sci 14:624–632

Shaw J, Sharp D, Harris J (2010) A flowline map of glaciated Canada based on remote sensing data. Can J Earth Sci 47:89–101

Stalker AM (1956) The Erratics train, Foothills of Alberta. Geol Surv Can Bull 37:1–28

Stalker AM (1975) The big rock. In: Evers HJ, Thorpe JE (eds) Structural geology of the Foothills between Savanna Creek and Panther River, S.W. Alberta, Canada. Canadian Society of Petroleum Geologists, Canadian Society of Exploration Geophysicists Exploration update, Calgary, pp 9–11

Wilson MC (1983) Once upon a river: archaeology and geology of the Bow River valley at Calgary, Alberta, Canada. Canadian National Museum of Man Mercury Series, Ottawa

The Prairie Dune Archipelago

12

Stephen A. Wolfe

Abstract

The Prairie dune archipelago describes the widely distributed dune fields extending across the Canadian Prairie Provinces. These dune fields have a common origin, with sediment supply derived from sandy outwash deposits associated with meltwaters of receding Laurentide and Cordilleran glacial ice. Wind reworked sediments soon after deglaciation, in a time-transgressive manner from south to north. Within the boreal forests of western Canada, post-glacial dune fields are well preserved with little to no remobilization during the Holocene. In contrast, dune fields of the southern Prairies reveal palimpsest landscapes, where dunes were reworked multiple times during the Holocene and presently display complex morphologies and depositional histories. Whereas relict and partially active stabilized parabolic dunes throughout the Prairies reflect primarily non-arid conditions, evidence exists for desert-like dunes on the southern Prairies developed during the Little Ice Age, possibly under reduced moisture conditions and shorter growing seasons. Historical accounts of dune fields indicate substantively more active dune fields in previous centuries than at present, raising issues as to the extent of past disturbances, including drought, fire, trampling and grazing on the activity of sand dunes. The few dune fields with presently active areas have also witnessed significant decline in this century, with a commensurate loss of plant and animal populations associated with these unique landscapes.

Keywords

Great plains • Dune fields • Parabolic dunes • Prairies

12.1 Introduction

Expansive regions of wind-blown sand are known as sand seas. Typical of the great deserts of the globe, these are large areas of actively shifting sand dunes, stabilized dunes or extensive low-profile sand sheets. On active dunes, the sand is generally loose and can be very difficult to cross. The term sand sea conjures images of expansive sand ripples and dunes.

Sand dunes are widespread on the Canadian Prairies, with more than 120 dune areas occupying roughly 40,000 km^2 in Alberta, Saskatchewan and Manitoba (Fig. 12.1). In contrast to sand seas, however, these individual dune fields are comparatively small and mostly stabilized by vegetation cover. The Brandon Sand Hills in Manitoba and the Great Sand Hills in Saskatchewan, for example, are two of the largest dune fields in southern Canada, each about 1200 km^2 in area and mostly stabilized, whereas many other dune fields may be less than 10 km wide.

These relatively small dune fields have a common paraglacial origin, derived from sandy outwash deposits associated with meltwaters of receding Laurentide and Cordilleran glacial ice. Rapidly changing ice limits, outwash channels and glacial lake levels restricted the amount of sand deposited in any one area. These discrete deposits were reworked into dunes soon after deglaciation. Within the

S.A. Wolfe (✉)
Geological Survey of Canada, Natural Resources Canada,
601 Booth St., Ottawa, ON K1A 0E8, Canada
e-mail: stephen.wolfe@canada.ca

© Springer International Publishing Switzerland 2017

O. Slaymaker (ed.), *Landscapes and Landforms of Western Canada*,
World Geomorphological Landscapes, DOI: 10.1007/978-3-319-44595-3_12

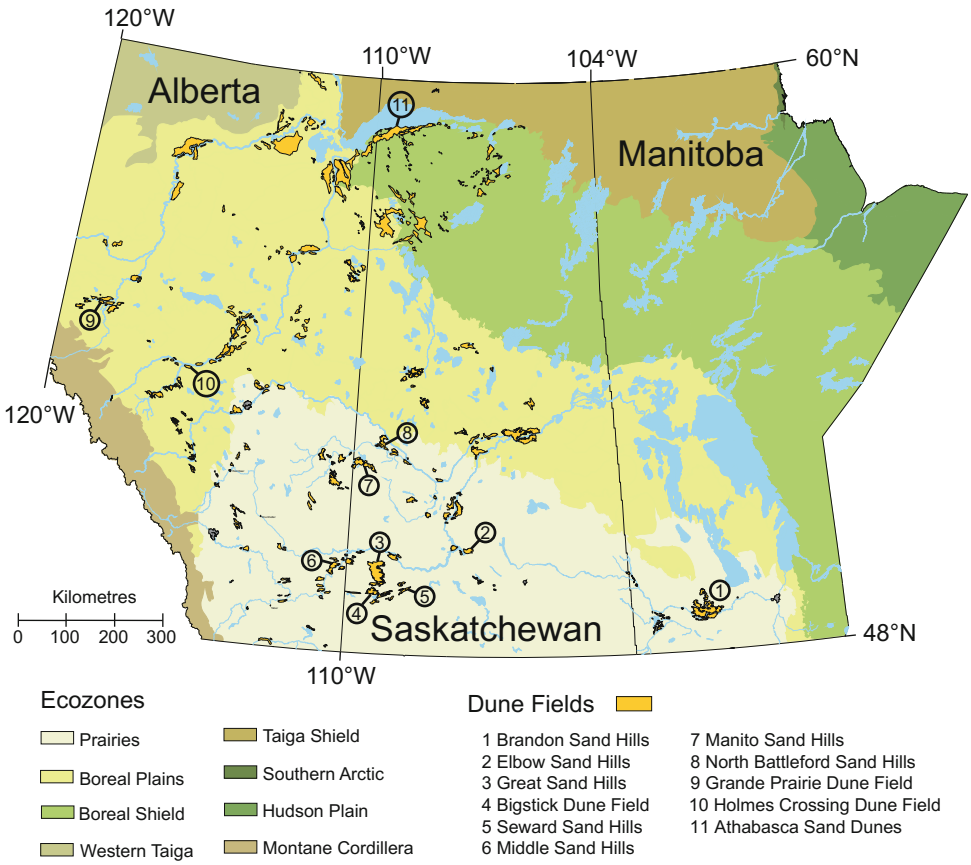

Fig. 12.1 Dune fields and ecozones in the Canadian Prairie Provinces (dune distribution after Wolfe 2001)

southern Prairies, the dune fields were subsequently reworked multiple times thereafter, creating a complex "palimpsest" landscape as older dunes were partially or completely replaced by younger ones. Historically, early explorers travelling across western Canada encountered areas of bare and active dunes amidst expanses of grasslands and forests. During droughts of the 1930s, agricultural lands in the south were lost to blowing soil and sand until countering conservation agricultural practices were put into place. Today, with the southern Prairies representing one of the most agriculturally productive regions in Canada, these dune fields may be viewed as "islands of biodiversity", home to isolated populations of native Prairie flora and fauna. For these reasons, the term dune archipelago, in contrast to sand sea, is used to describe these Prairie dune fields. Herein, the geographical and historical context, and the landforms and evolution of the prairie dune archipelago are described.

12.2 Geographical Context

The Prairie dune archipelago describes the relatively small but widely distributed dune fields scattered across the Canadian Prairie Provinces (Fig. 12.1). The presence of sand dunes in any environment is the result of three interacting parameters, namely wind strength, sediment supply and sediment availability. The occurrence of vegetation-stabilized dunes and active dunes within the Prairies attests to the fact that wind strengths were, and in some areas are still, sufficient to mobilize sandy sediments into dunes.

Unlike many dune fields, receiving modern inputs of sediment from coastal or fluvial sources, the sediment supply for Canadian Prairie dune fields are former glacilacustrine or glacifluvial outwash deposits that were associated with meltwaters from glacial ice (David 1977; Muhs and Wolfe 1999). These origins are significant, as supplies of sand for Canadian Prairie dune fields are therefore absolute, with no renewable supplies from external sources. Consequently, unlike dunes that are rejuvenated by additional supplies of sand (e.g. source-bordering dune fields), Canadian Prairie dune fields can only be reactivated by perturbations affecting the availability of existing sand, or by an increase in wind strength. This means that increases in dune activity are closely related to reductions in surface vegetation cover caused by drought, fire or natural and human disturbances, with stabilization related to suppression of such disturbances, an increase in vegetative cover and/or decrease in wind strength.

With the exception of a few ice-free uplands, such as the Cypress Hills (Fig. 12.2), the Canadian Prairies were

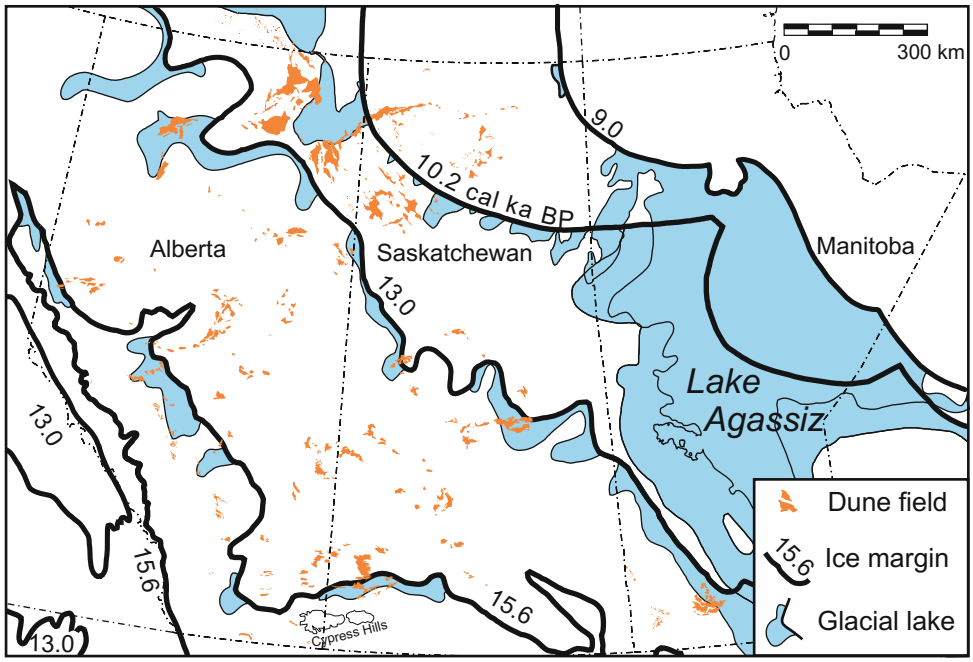

Fig. 12.2 Glacial limits and proglacial lakes at 15.6, 13.0, 10.2 and 9.0 cal ka BP (after Dyke et al. 2003) and distribution of dune fields (after Wolfe 2001) in the Prairie Provinces

covered by the Laurentide and Cordilleran ice sheets during the Late Wisconsinan glaciation. Thus, the maximum limiting age of Prairie dune fields follows the trend of receding Laurentide and Cordilleran ice sheets and the drainage of proglacial lakes and rivers (Fig. 12.2), with the oldest dune fields in the southern and western Prairies and progressively younger dune fields towards the northeast (Wolfe et al. 2004). With this in mind, dune fields such as the Bigstick and Seward Sand Hills in the southern Prairies are arguably two of the oldest dunes fields in western Canada, possibly older than 15 ka. The relatively small size of individual dune fields is due to the fact that the glacial outwash, from which most of these dune fields are derived, was limited in spatial extent by relatively short-lived intervals of deposition during glacial recession. In contrast, the Athabasca Sand Dunes, which the is largest dune field in Canada, is, perhaps, one of the few that continues to receive renewed supplies of sediment, via lake shore sands from the Peace–Athabasca delta and, based on receding ice and glacial lake levels, was likely formed less than 10 ka ago.

Lastly, Prairie dune fields have not migrated far from their original source areas (Fig. 12.3) as their transport distances have been controlled by wind regimes and vegetation cover, or both (Muhs and Wolfe 1999). Multiple episodes of dune activity have occurred on the Canadian Prairies and include initial activity, following deglaciation from about 15 to 10 ka ago, early to mid-Holocene activity ranging from about 8 to 5 ka ago, and late Holocene activity both within the last few thousand and within last few hundred years. Different regions of the Prairie dune archipelago have undergone different histories of activity since deglaciation, owing to regional variations in Late Pleistocene and Holocene environmental conditions. Within the boreal forest regions of western Canadian, post-glacial dune fields are well preserved with little to no remobilization during the Holocene. In contrast, dune fields on the southern Prairies represent palimpsest landscapes, where dunes were reworked multiple times during the Holocene and, as a result, presently display complex morphologies and depositional histories.

12.3 The Prairie Dune Archipelago

12.3.1 Relict Dune Fields of the Boreal Forest

Dune fields of the boreal forest ecozone are, with the exception of those in the Peace–Athabasca basin (Wolfe 2013), almost entirely stabilized by vegetation. These stabilized dune fields include parabolic, and occasionally transverse, dunes (Fig. 12.4a, b). Towards the western Cordillera, these dunes are aligned with winds from the northwest, similar to the direction of modern dune-forming winds. Towards the north and east, however, they are aligned with transporting winds from the southeast that have been ascribed to off-ice winds (Fig. 12.4c), which originated

Fig. 12.3 Active and stabilized sand dunes in the Great Sand Hills. Source sediments for these dunes are underlying glacifluvial sands that are reworked by the wind when exposed. Photograph by Stephen Wolfe

from a stationary high-pressure centre over the Laurentide Ice Sheet (David 1981; Wolfe et al. 2004). The majority of these stabilized dunes show little to no evidence of reactivation surfaces such as superimposed blowouts, and buried soil horizons are rare within dune exposures (Munyikwa et al. 2011; Wolfe et al. 2004). All of these dune fields appear to have undergone a primary dune-forming period, followed by rapid stabilization by either diminishing winds or vegetation cover, or both, and are presently relict dunes (Wolfe et al. 2004). This suggests that a single continuous episode of aeolian activity, though with varying net sediment transport directions, was succeeded by relatively abrupt stabilization. The apparent lack of reworking further suggests that these northern dune fields may generally contain

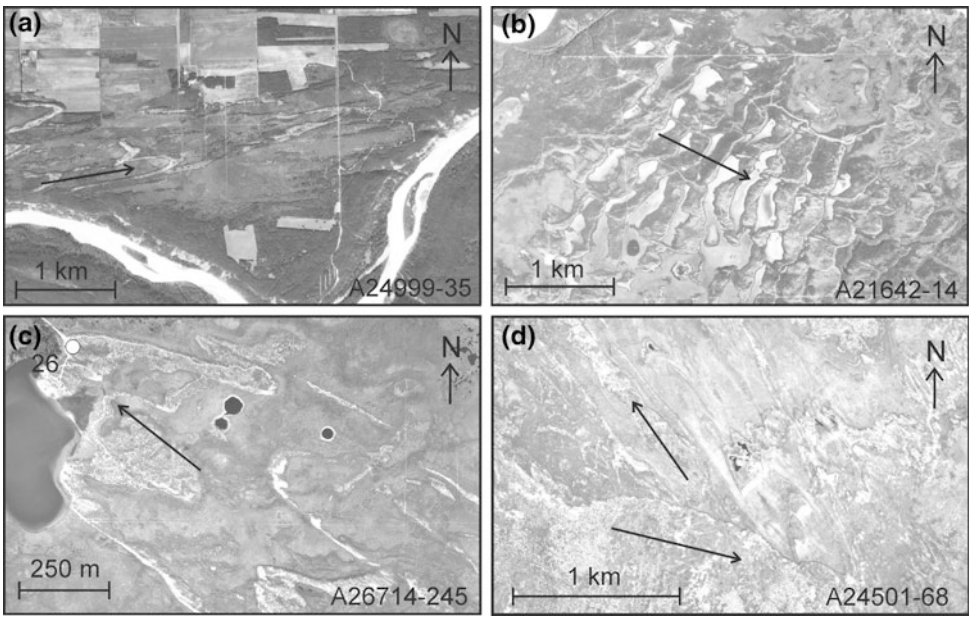

Fig. 12.4 Stabilized dunes of the boreal forest ecozone in north-western Alberta: **a** parabolic dunes of the Grand Prairie dune field; **b** transverse dunes of the Holmes Crossing dune field; **c** parabolic dunes of the Wood Buffalo Sand Hills with morphological evidence of transporting winds from the southeast related to off-ice winds from the Laurentide Ice Sheet; **d** dune field in northwestern Alberta with evidence of two transporting wind directions, suggesting transport from off-ice winds that were later replaced by transporting winds associated with Holocene northern hemispheric circulation. *Arrows* indicate direction of net sediment transport. *Air photographs*: National Air Photo Library, Natural Resources Canada, Ottawa

exclusively older aeolian records in contrast to those further to the south, as much of this northern region has been vegetated by boreal forest for 10–9 ka. A few dune fields show evidence of two transporting wind directions, suggesting transport from off-ice winds that were later replaced by transporting winds associated with Holocene northern hemispheric circulation (Fig. 12.4d).

The stabilized dunes of the boreal forest ecozone generally attest to dune formation during the Late Pleistocene, following deposition of glacifluvial deposits and drainage of proglacial lakes. Ages of dune fields in west-central Alberta indicate deposition primarily between 16 and 13 ka (Fig. 12.5a), corresponding to an ice-proximal setting along the margins of the retreating Laurentide and Cordilleran ice sheets (Wolfe et al. 2004; Munyikwa et al. 2011). Data further indicate that dune activity continued between 13 and 11 ka, as the Laurentide Ice Sheet retreated to the northeast (Fig. 12.5b). Dune activity appears to have terminated in a time-transgressive manner from the southwest at about 11 ka, to the northeast at about 9 ka, with the establishment of boreal forest cover and reduced wind strength (Wolfe et al. 2004). Notably, only dune fields situated in the east retain evidence of dune-forming winds originating from the southeast, and influenced by glacial off-ice winds (Fig. 12.5b). This suggests that such glacially influenced transport conditions may only have been well established after 13 ka, when the Laurentide and Cordilleran ice sheets were well separated, and that the effect on sediment transport by wind may have extended no more than about 200 km from the ice sheet.

12.3.2 Semi-arid Dunes of the Southern Prairies

Dune fields are abundant within the parkland and grassland-dominated dry sub-humid to semi-arid southwestern Canadian Prairies of Alberta, Saskatchewan and Manitoba (Figs. 12.1, 12.2). Dune orientations typically indicate transporting winds from the northwest or southwest that coincide with modern sediment-transporting wind directions, which are strongest in the spring and winter months (Wolfe and Lemmen 1999). Most of the dune fields in Canada that presently sustain active blowouts, isolated dunes and dune complexes are found within the southern Prairies, including the Brandon Sand Hills in Manitoba, the Great Sand Hills (Fig. 12.3) and Elbow Sand Hills in Saskatchewan, and the Middle Sand Hills in Alberta. Within individual dune fields, vegetation-stabilized dunes may show morphological evidence of reworking in the form of multiple blowouts, or no evidence of reworking since stabilization, indicating that multiple episodes of aeolian activity have occurred, but not uniformly, across dune fields.

Whereas the timing of glacial retreat in the central to southern Prairies infers that dune field formation could date to between 13 and 15 ka, or older, ages so far have been much younger. An AMS and conventional radiocarbon chronology from the Brandon Sand Hills based on dating of organic matter from palaeosols shows recurrent intervals of Holocene-aged aeolian activity and stability in the past 5 ka (Wolfe et al. 2000). Periods of most notable palaeosol development date to around 2.3–2, 1.4–1 ka and 600 to

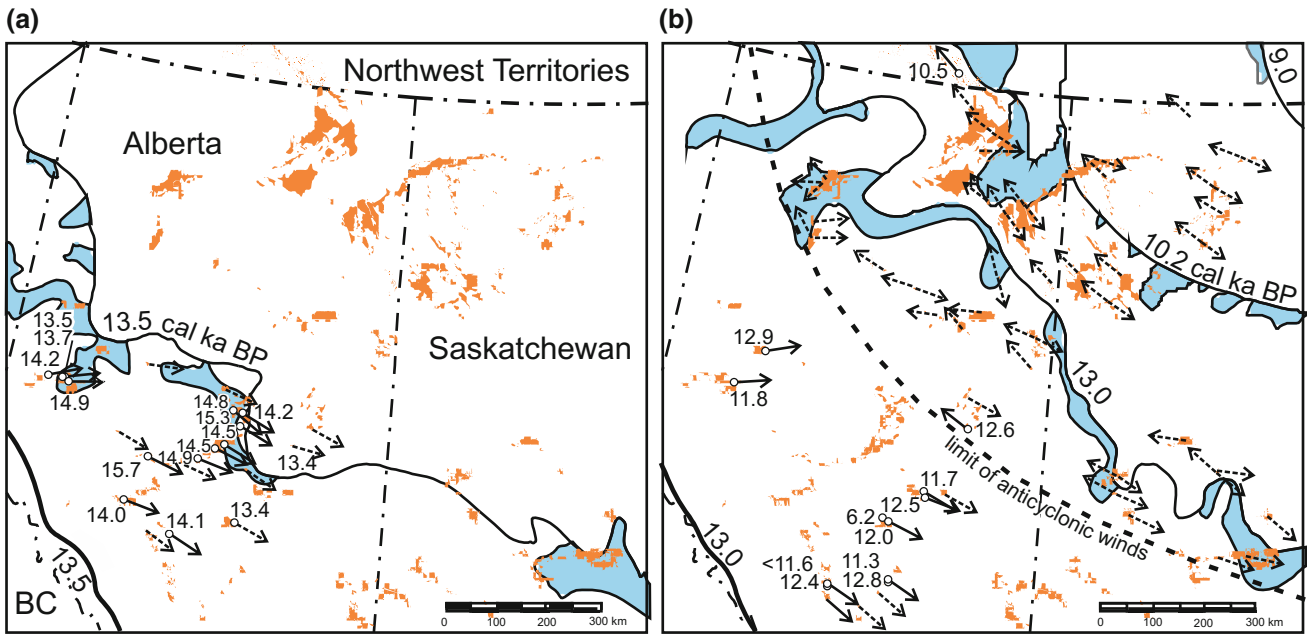

Fig. 12.5 Dune activity and wind directions in relation to glacial limits and proglacial lakes (after Dyke et al. 2003) for **a** ice position at 13.5 cal ka BP and **b** between 13.0 and 9.0 cal ka BP. Values shown are optical ages indicative of stabilization. *Solid arrows* indicate dune-forming wind directions derived from dune field orientations with age control, and *dashed arrows* indicate orientations with inferred timing

500 cal year BP with aeolian activity occurring before and after each of these periods. Luminescence ages are consistent with these radiocarbon ages, indicating aeolian activity at about 5.2, 4, 3.1 and 2 ka ago (Wolfe et al. 2002). Further north, luminescence ages from the Manito and North Battleford Sand Hills are some of the few that clearly record mid-Holocene aeolian deposition between 7000 and 5000 years ago (Wolfe et al. 2006). Luminescence ages from dune sands throughout the southern Prairies typically date to between 5.7 and 0.14 ka (Wolfe et al. 2002), and most notably, widespread recent dune activity is recorded from dune fields throughout the Prairie Grassland. Overall the aeolian chronology attests to recurrent dune activity on the southern Prairies during the Holocene.

Dune activity has declined dramatically in historical times due to a multitude of factors, but mostly due to changes in climate, including increased humidity with warmer temperatures, since the late 1700s (Hugenholtz et al. 2010; Wolfe and Hugenholtz 2009) and declines in disturbance, including reduced fires, aboriginal activity and wildlife grazing (Wolfe et al. 2007). All active areas within Prairie dunes fields have declined historically, at an average rate of about 9 ha per year. The most dramatic historical reductions have been in the Brandon Sand Hills and the Middle Sand Hills, where

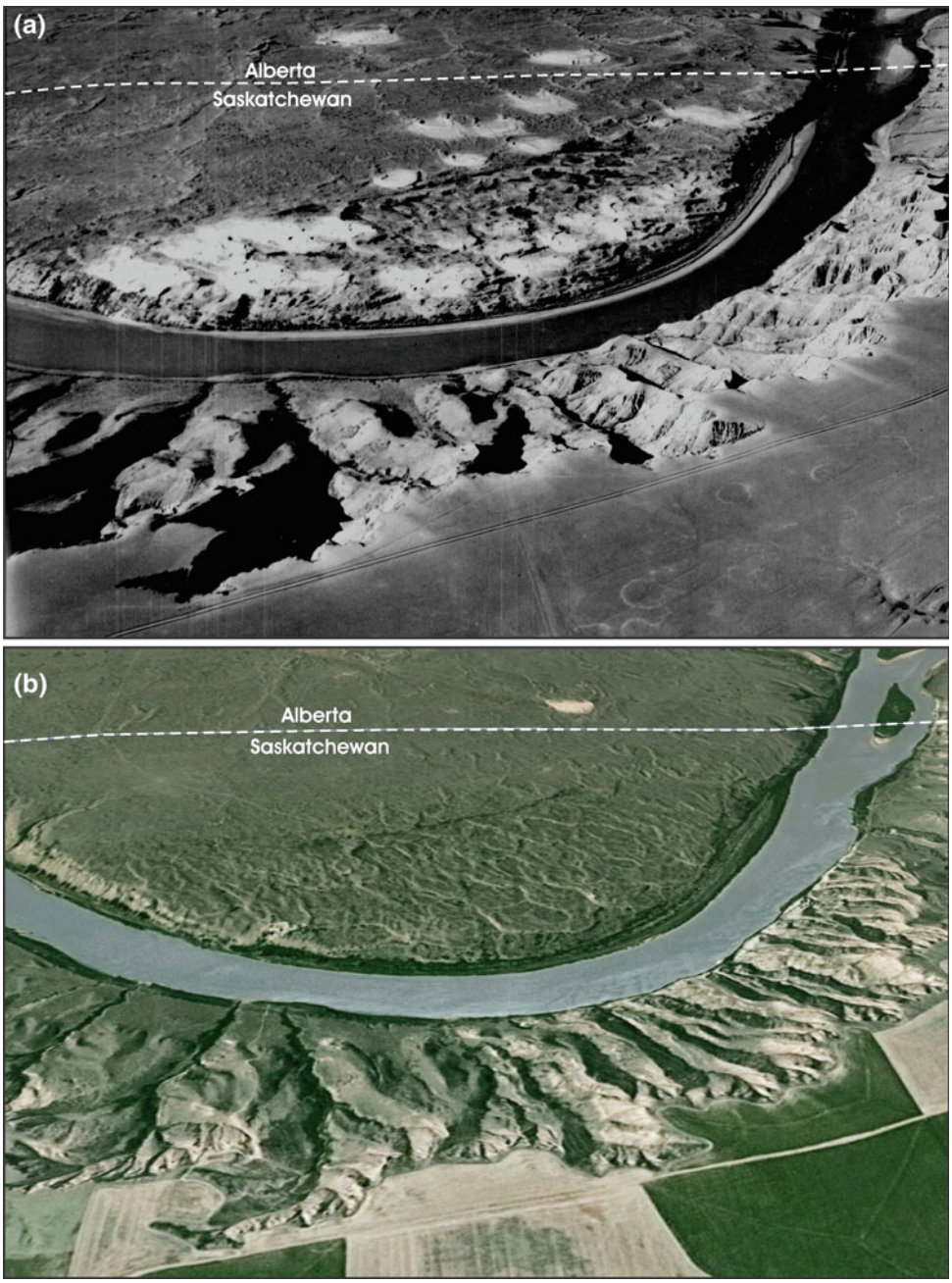

Fig. 12.6 Oblique images north of the Middle Sands Hills, along the Alberta–Saskatchewan border showing, (*upper*) active sand dunes descending into the South Saskatchewan River valley in 1937 (*source*: Canada's National Air Photo Library, Photo A5830-50). (*Lower*) One active dune remaining in 2006 (*source*: GoogleTM Earth)

the area of open sand has declined by as much as 95 % over a 70-year period through the twentieth century. These dune fields have gone from having several 100 ha of bare active sand to essentially, fully stabilized dune fields (Fig. 12.6a, b).

12.4 Desert Dunes on the Prairies?

Barchan dunes are characteristic of semi-arid and desert regions, typically with restrictive soil moisture or vegetation cover. Under unimodal wind regimes and moderate sand supply, dry, unconsolidated sand, typically without vegetation cover, forms crescent-shaped accumulations with slip-faces that, in planview, are concave downwind (Fig. 12.7).

There are presently no active barchan dunes on the Canadian Prairies. However, they were once abundant on the southern Prairies, particularly within the Great Sand Hills and, to a lesser extent, within surrounding dune fields including the Seward and Middle Sand Hills. Although all of the stabilized sand dunes in these areas are parabolic, many have morphologies characteristic of barchan dunes that transitioned into parabolic dunes during stabilization. Figure 12.8 illustrates the transition of a barchan dune into a parabolic dune, with the end stage showing a parabolic dune with preserved residual dune ridges representing the former base and position of the stoss slope of the dune. Topographic imagery of stabilized dunes in the Great Sand Hills reveals abundant stabilized parabolic dunes with residual dune ridges, indicative of the transition of barchan dunes to parabolic dunes during stabilization (Fig. 12.9). Luminescence dating of these dunes indicates that transformation of barchan to parabolic dunes occurred between AD 1810–1880 (Wolfe and Hugenholtz 2009), with the end of the Little Ice Age, indicating that barchan dunes stabilized under conditions of recent climate warming. This apparent contradiction was likely due to reduced moisture conditions and shorter growing seasons during the Little Ice Age, than occur today.

12.5 Historical Context

The Prairie dune archipelago, like western Canada itself, was encountered by earlier European explorers, progressively from east to west. The Brandon Sand Hills, on the eastern edge of the Canadian Prairies and the dune archipelago, was one of the first dune fields noted by many early explorers, including David Thompson in 1798, Alexander Henry in 1806 and Henry Hind in 1857. On 12 July 1806, the fur trader Alexander Henry gave a detailed account of the active dunes (Coues 1897, p. 297):

> At two o'clock we proceeded, and soon came to Montagne du Diable, the tops of which we had seen at Wattap river. This mountain, or rather ridge of barren, sandy hills, is a body of sand several miles in length; the principal hill is on the E., several miles in circumference, and level on top where no kind of vegetation grows. Our path led along the foot of this hill, which appears to be shifting its position eastward. Evidence of this may

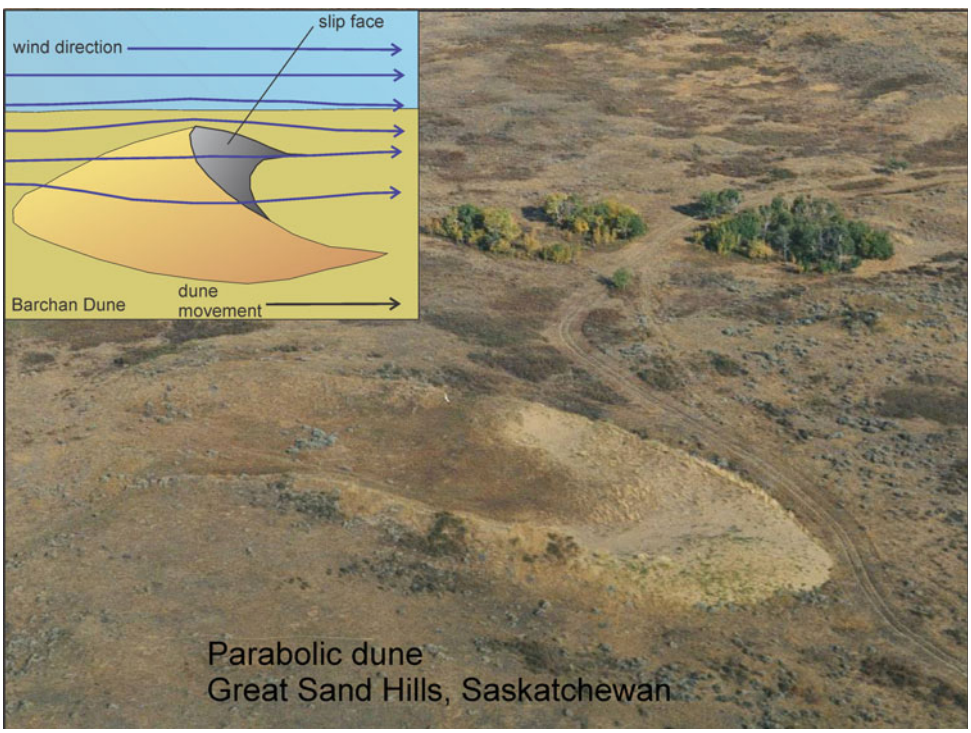

Fig. 12.7 Oblique views of a barchan dune and a parabolic dune

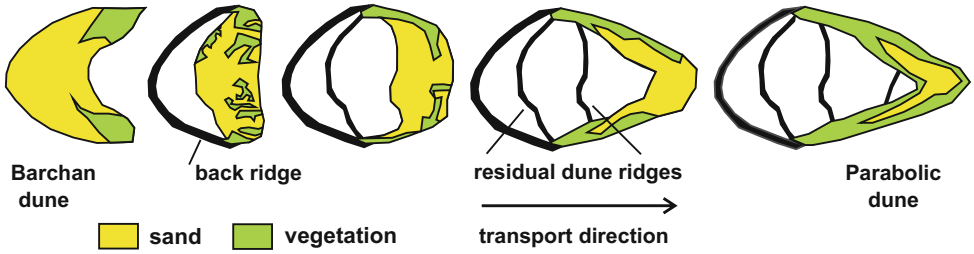

Fig. 12.8 Barchan-to-parabolic dune transformation under influence of vegetation (adapted from Durán et al. 2008) to illustrate residual dune ridges, representing preservation of vegetation-stabilized base of stoss slope of migrating dune

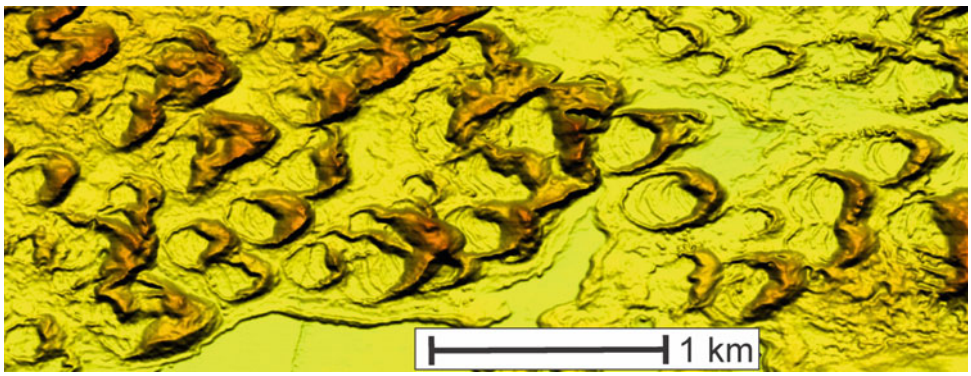

Fig. 12.9 Light detection and ranging (LiDAR)-based elevation model of stabilized sand dunes in the Bigstick Sand Hills showing dunes with residual dune ridges indicating transformation of barchan dunes to parabolic dunes during stabilization

> be seen in the state of trees on the E. side, where they are so deeply buried in sand that the very tops of some tall trees just peep through. Westward lies a sandy waste for three or four miles, where nothing grows but a few stunted épinettes, that tumble down when sands are blown about their roots. The principal reason why this body of sand may be said to move eastward is the strong westerly winds which prevail … In crossing those hills our horses sank up to their knees in many places.

For early explorers, this dune field was an impressive contrast to the surrounding parkland and forest of white spruce (*Picea glauca*), aspen (*Populus tremuloides*), balsam poplar (*Populus balsamifera*), bur oak (*Quercus macrocarpa*) and larch (*Larix lariana*). Today, less than 100 ha of open sand remains as a small remnant of the former expansive dunes.

In 1858–59, Henry Hind led a Canadian government commissioned exploration of the Assiniboine and Saskatchewan regions to document their suitability for settlement. Hind (1860: 54–55) describes the Elbow Sand Hills along the South Saskatchewan River:

> The Sand Hills commence on the north side about two miles west of Sand Hill Lake as it appears in summer. They are drifting dunes, and many of them present a clear ripple marked surface without any vegetation, not even a blade of grass. They have invaded the Great Valley, and materially lessened its depth…
>
> On the morning of Thursday, 29th, we prepared to visit the main body of the Cree camp at the Sandy Hills … Soon after breakfast we crossed the valley and threaded our way between sand dunes; one which we measured was 70 feet high, quite steep on one side, beautifully ripple-marked by the wind, and crescent-shaped. Sand dunes are on both sides of the valley.

Hind's observations are particularly notable, as the extent of active dunes at that time is greater than today, as open sand is presently confined only to the crests and south slopes of some dune ridges, and to a single large area in the northwesternmost section of the dune field.

Also notable are Hind's accounts of impoundments, used by the Cree to entrap bison (Fig. 12.10), and that were formed within the small valleys between the sand dunes. Hind describes one pound that:

> "was formed in a pretty dell between sand hills, about a half mile from the first, and leading from it in two diverging rows, the bushes they designate dead men, and which serve to guide the buffalo when at full speed, were arranged. The dead men extended a distance of four miles in the Prairie, west of and beyond the Sand Hills. They were placed about 50 feet apart, and between the extremity of the rows might be a distance of from one and a half to two miles."

These observations raise the question to what extent did disturbances such as fire, trampling and grazing influence the activity of sand dunes within the Prairie dune archipelago. Aboriginal occupation, including the use of dunes for impounding bison, may have perpetuated dune activity, as did Euro-Canadian settlement, with later land use emphasizing conservation encouraging more recent stabilization (Wolfe et al. 2007).

Fig. 12.10 "Plains Cree Driving Buffaloes into a Pound." Chromoxylograph from a sketch by John Fleming. Printed by Spottiswood and Co., New-Street Square London (Facing page 358) In: Hind (1860) Narrative of the Canadian Red River Exploring Expedition of 1857 and of the Assiniboine and Saskatchewan Exploring expedition of 1858. Vol. 1. Longman, Green, Longman, and Roberts, London. © Public Domain

Perhaps the most influential of early European explorers of the Canadian Prairies was Captain John Palliser who led the British Exploration Expedition of 1857–1860, for a detailed assessment of western Canada for the suitability of agriculture and settlement. Whereas the Palliser expedition observed some of the same dune fields as Hind, they explored areas north of the southern Prairies, later re-entering the Prairies and documenting their encounter with the Middle Sand Hills south of Red Deer River on 19 July 1859 (Palliser 1862, p. 413):

> …one of our carts broke down in going over a succession of sand-hills … We were now halted on a salt lake, the only water we could find. The Doctor had a severe spell with the carts in the sand-hill … We drank a little water by digging a pit, and drinking through a silk handkerchief; the men and horses we in great want of water, and the heat was very great while travelling through miles of burning sand. In the evening left the high broken country and descended into a valley running north and south, which was the direction in which Amoexepeta ought to have taken them, i.e. in a direct line and avoiding the sand-hills, which had been all but impassable to the carts, and fearfully severe on the horses.

Following the British Exploration Expedition of 1857–1860, Captain John Palliser described the southern Canadian Prairies as a 'central desert forming a triangle, having its base the 49th parallel from longitude 100° to 114°W, with its apex reaching to the 52nd parallel of latitude'. Within this 'central desert' Palliser further wrote that 'The large belt of country embraces districts, some of which are valuable for the purposes of the agriculturalist, while others will forever be comparatively useless'. Wolfe et al. (2013) contend that it was the condition of dune fields, and Palliser's inference of their extent, that influenced his perception of a 'central desert'. Today, this 'central desert' is referred to as Palliser's Triangle (Fig. 12.1), but contrary to Palliser's predictions, it is Canada's productive dryland agricultural region with only a few, isolated active dunes acting as remnants of a once arid environment.

12.6 Present and Future Status

Perhaps the most significant implication of declining wind erosion on sand dunes is the loss of specialized habitat and, potentially, the wildlife species that depend on these habitats (Hugenholtz et al. 2010). Nearly a dozen dune-dependent plant and animal species, including smooth goosefoot (*Chenopium subglabrum*), western spiderwort (*Tradescantia occidentalis*), hairy-Prairie clover (*Dalea villosa* var. *villosa*), gold-edged gem (*Schnia avemensis*), small-flowered sand verbena (*Tripterocalyx micranthus*), Ord's kangaroo rat (*Dipodomys ordii*), Prairie skink (*Eucmeces septentriolnalis*) and a variety of moths are listed as threatened or endangered western Prairie species. Whereas increased aridity or windiness might have detrimental effects on agriculture, without such changes that are conducive to wind erosion and dune activity, management interventions to increase disturbance by fire, grazing, trampling or mechanical means might be the only mechanism to conserve habitat for dune-dependent species within the Canadian Prairie dune archipelago.

12.7 Conclusions

The Prairie dune archipelago is a unique result of post-glacial meltwater deposition of sand and late Pleistocene to Holocene erosion and redeposition by wind. The resultant dune fields are widespread, but comparatively small, extending across the vast Canadian Prairies,

analogous to an island chain or archipelago in contrast to extensive sand seas. As revealed by complex morphologies and accompanying chronologies, these dune fields represent some of the most dynamic components of the Prairie landscape. Here, dune activity is controlled mainly by sediment availability and wind strength, rather than renewed inputs of sand. Thus, changes affecting the protective vegetation cover, such as drought and surface disturbances, have been the main drivers of dune activity since deglaciation. The present landscape of the Prairie dune archipelago is thus a reflection of complex changes in past wind regimes, climate and land use.

References

Coues E (1897) New light on the early history of the greater northwest: the manuscript journals of Alexander Henry, Fur Trader of the Northwest Company and of David Thompson, Official Geographer and Explorer of the Same Company, p 1799–1814

David PP (1977) Sand dune occurrences of Canada: a theme and resource inventory of eolian landforms in Canada. Ottawa: Indian and Northern Affairs National Parks Branch Contract No. 74-230, p 193

David PP (1981) Stabilized dune ridges in northern Saskatchewan. Can J Earth Sci 18:286–310

Durán O, Silva MVN, Bezerra LJC, Herrmann HJ, Maia LP (2008) Measurements and numerical simulations of the degree of activity and vegetation cover on parabolic dunes in north-eastern Brazil. Geomorphology 102:460–471

Dyke AS, Moore AJ, Robertson L (2003) Deglaciation of North America. Geol Surv Can Open File 1574, 2 map sheets

Hind HY (1860) Narrative of the Canadian red river exploring expedition of 1857 and of the Assiniboine and Saskatchewan exploring expedition of 1858, vol 1, Longman, Green, Longman and Roberts London [Republished in 1969 by Greenwood Publishing, New York]

Hugenholtz CH, Bender D, Wolfe SA (2010) Declining sand dune activity in the Southern Canadian Prairies: Historical context, controls and ecosystem implications. Aeol Res 2:71–82

Muhs DR, Wolfe SA (1999) Sand dunes of the northern great plains of Canada and the United States. In: Lemmen DS, Vance RE (eds) Holocene climate and environmental change in the Palliser triangle: a geoscientific context for evaluating the impacts of climate change on the Southern Canadian Prairies. Geological Survey Canadian Bulletin 534. Geological Survey of Canada, Ottawa p 183–197

Munyikwa K, Feathers JK, Rittenour TM, Shrimpton HK (2011) Constraining the Late Wisconsinan retreat of the Laurentide ice sheet from western Canada using luminescence ages from post-glacial aeolian dunes. Quat Geochronol 6:407–422

Palliser J (1862) Journals, detailed reports and observations relative to Captain Palliser's exploration of a portion of British North America. In: Spry IM (ed) 1968, The Papers of the Palliser Expedition, Toronto, The Champlain Society, p 694

Wolfe SA (2001) Eolian deposits in the Prairie Provinces. Geol Surv Can Open File 4118, 1 map sheet

Wolfe SA (2013) Cold-climate aeolian environments. In: Shroder JF (Editor-in-chief), Lancaster N, Sherman DJ, Baas ACW (eds) Treatise on geomorphology, vol 11, Aeolian Geomorphology. Academic Press, San Diego, p 375–394

Wolfe SA, Hugenholtz CH (2009) Barchan dunes stabilized under recent climate warming on the northern Great Plains. Geology 37:1039–1042

Wolfe SA, Lemmen DS (1999) Monitoring of dune activity in the Great Sand Hills region, Saskatchewan. In: Lemmen DS, Vance RE (eds) Holocene climate and environmental change in the Palliser Triangle: a geoscientific context for evaluating the impacts of climate change on the southern Canadian Prairies. Geological Survey Canadian Bulletin 534. Geological Survey of Canada, Ottawa p 199–210

Wolfe SA, Muhs DR, David PP, McGeehin JP (2000) Chronology and geochemistry of late Holocene eolian deposits in the Brandon Sand Hills, Manitoba, Canada. Quat Int 67:61–74

Wolfe SA, Huntley DJ, Ollerhead J (2002) Optical dating of modern and late Holocene dune sands in the Brandon Sand Hills, southwestern Manitoba. Géogr Phys Quat 56:203–214

Wolfe SA, Huntley DJ, Ollerhead J (2004) Relict late Wisconsinan dune fields of the Northern Great Plains, Canada. Géogr phys Quat 58:323–336

Wolfe SA, Ollerhead J, Huntley DJ, Lian OB (2006) Holocene dune activity and environmental change in the Prairie parkland and boreal forest regions of central Saskatchewan, Canada. Holocene 16:17–29

Wolfe SA, Hugenholtz CH, Evans C, Huntley DJ, Ollerhead J (2007) Potential aboriginal occupation-induced dune activity, Elbow Sand Hills, northern Great Plains, Canada. Great Plains Res 17:173–192

Wolfe SA, Hugenholtz CH, Lian OB (2013) Palliser's Triangle: reconstructing the 'central desert' of the southwestern Canadian Prairies during the late 1850s. Holocene 25:699–707

The Polar Desert Landscape of Prince Patrick Island

13

Hugh M. French

Abstract

The landscape of Prince Patrick Island is fashioned by intense cold and aridity. At the macroscale, the landscape is structurally controlled. Frost action is restricted to the disintegration of exposed frost-susceptible bedrock. Patterned ground and mass wasting processes are restricted to snowbank localities. Vegetation is sparse, and diversity is limited; cover is typically 5–10%. Snow, removed from interfluves and bare surfaces, is concentrated in gullies and stream channels in the winter months, enhancing the effectiveness of snowmelt runoff in the spring. The presence of continuous and thick permafrost is indicated by widespread thermal contraction cracking and sand wedge polygons, but other evidence for permafrost and ground ice is largely lacking.

Keywords

Deserts • Aridity • Frost action • Fluvial activity • Permafrost • Sand wedge polygons • Canadian arctic islands

13.1 Introduction

Prince Patrick Island is a remote landmass located north of the mainland between latitudes 74°N and 77°N in the western Canadian Arctic (Fig. 13.1). It forms part of the western Queen Elizabeth Islands and covers an area of ~17,000 km^2. From a geomorphic perspective, the landscape is best described as a cold desert where aridity limits the effectiveness of some cold-climate processes and enhances others. The island is uninhabited and rarely visited.

H.M. French (✉)
Departments of Geography and Earth Sciences, University of Ottawa, Ottawa, ON K1N 6N5, Canada
e-mail: hmfrench@shaw.ca

H.M. French
Department of Geography, University of Victoria, Victoria, BC V8R 3R4, Canada

13.2 What Is a Polar Desert?

Deserts of the world are often described by terms such as 'hostile,' 'barren' and 'inhospitable.' Two categories of cold desert are recognized in the well-known climatic classification of Köppen-Geiger: either *Bwk* (areas that experience annual average temperatures less than 18 °C) or *Dwc* (areas that experience dry winters, less than 4 months above 10 °C and the coldest month being lower than −3 °C).

The cold deserts of the high latitudes differ from the cold deserts of the mid-latitudes because the relationship between temperature and precipitation is not straightforward. This is due largely to the 'polar night,' the period of time during which there is 24-h darkness for several months of the year. Under these conditions, the uniformly cold and dry climate limits photosynthesis and plant growth. Thus, the polar desert landscape consists of rocky and sparsely vegetated alluvial surfaces, interfluves and bedrock-controlled uplands. Typically, vegetation cover is less than 10 %. Areas of tundra are restricted to depressions, late-lying snowbanks and sheltered areas adjacent to drainage channels and along coastlines. The polar desert vegetation shows little variation from place to

© Springer International Publishing Switzerland 2017

O. Slaymaker (ed.), *Landscapes and Landforms of Western Canada*,
World Geomorphological Landscapes, DOI: 10.1007/978-3-319-44595-3_13

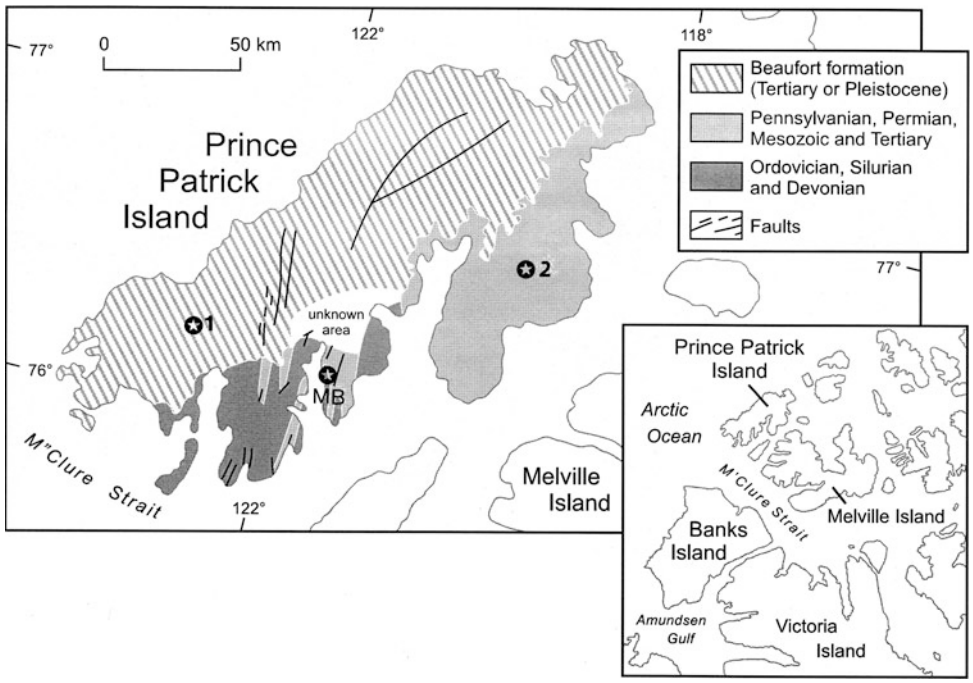

Fig. 13.1 Location map of Prince Patrick Island, Western Canadian Arctic, showing the geology and major physiographic regions (after Tozer and Thorsteinsson 1962). Legend: *MB* Mould Bay; *1* Elf Dyer Bay I-59 exploratory well site; *2* Elfex et al Wilkie Point J-51 exploratory well site

place. Plants are small, close to the ground and often widely separated with bare soil or rock in between. The tundra is technically a type of cold desert, even though it is relatively well vegetated and capable of supporting a limited but productive ecosystem.

Closely related to cold temperature and low precipitation amounts is the question of aridity (Table 13.1). Moisture availability is the central issue, here defined as the balance between water supply, provided by precipitation (*P*, rain or snow), and water loss due to evapotranspiration (PE_t, both evaporation from water and transpiration from plants and near-surface sediment).

Aridity complicates any interpretation of the polar desert landscape. Low temperature not only reduces evaporation but also enhances sublimation and hence the direct removal of moisture (snow) to the atmosphere. Further complications are that a sparse vegetation cover reduces evapotranspiration losses and the presence of a frozen, largely impermeable, substrate (permafrost) reduces infiltration into the ground. These enhance the overall effectiveness of precipitation and

Table 13.1 Desert climates according to temperature regime and moisture availability (from Thomas 2011)

	Annual temperature regime				
	Hot	Mild winter	Cool winter	Cold winter	Cold Desert[a]
Coldest month (°C)	10–30	10–20	0–10	<10	<−20?
Warmest month (°C)	>30	10–30	10–30	10–30	>10

Classification	Aridity Index[b] (A/I) range	Precipitation characteristics	Precipitation limits[c]
Hyper-arid	<0.5	12 months without rain; 100 % interannual rainfall variability	<25 mm year
Arid[b]	0.05 to <0.20	Low and unreliable rainfall; 50–100 % interannual rainfall variability	25–200 mm year
Semi-arid	0.20 to <0.50	Seasonal rainfall; 25–50 % interannual rainfall variability	200–500 mm year
Dry subhumid	0.50 to <0.65	Reliable season rainfall; 25 % interannual rainfall variability	500–1000 mm year

[a]Cold deserts are arbitrarily defined as being area where the warmest month >10 °C and the coldest month < −20 °C

[b]Aridity Index (AI) = P/PE_t, where P = annual precipitation and PE_t = potential evapotranspiration based upon Thornthwaite's 1948 Index of Moisture Availability (I_m)

[c]For Prince Patrick Island, total precipitation (see Table 13.2) includes rain, snow, fog and freezing drizzle

surface runoff in spite of the general aridity. Finally, the presence of snow, unevenly distributed across the landscape because of transport by wind and persisting for many months in snowbank localities, introduces spatial and temporal complexities to the landscape-forming processes.

13.3 The Polar Desert Climate of Prince Patrick Island

Climate records at Mould Bay (Table 13.2, see Fig. 13.1 for location) indicate the island experiences a High Arctic periglacial climate (see French 2007, 34–37). The mean annual air temperature approximates −18 °C and temperatures plunge to well below −30 °C for several months of the year. They rarely rise above 5 °C during the summer. Thus, the climate fits within each of the Köppen categories described earlier as well as the arbitrary definition of a cold desert stated in Table 13.1. As regards moisture, the total mean annual precipitation (rain and snow equivalent) is approximately 180–185 mm, the majority falling as snow. Clearly, the island falls within the 'arid' category. Moisture may oscillate seasonally between its liquid (rain) and solid (snow and ice) states with associated heat transfer linked to sublimation and evaporation.

13.4 The Transition from Tundra to Polar Desert

While the polar desert environment dominates the landscape of Prince Patrick Island, the tundra is also present in a few select localities. This mixing is largely controlled by topography, parent material and drainage. Snowbed locations are favoured sites for vegetation growth and the formation of 'patchy wetlands' (Fig. 13.2). Other favoured habitats are gullies, poorly drained valley bottoms and low level fluvial terraces. There are striking but simple relationships between topography, soil and vegetation on Prince Patrick Island (Tedrow 1974, 1977) (Fig. 13.3). The typical ecological change consists of a progressive transition from lowland terrain dominated by cryptogam-herb and moss graminoid assemblages to simple herb barrens on the uplands (Bliss 1997). So-called 'hummocky soils' mark the transition (see Fig. 13.4a). The extensive lush tundra of adjacent Banks Island does not exist. Instead, the extreme growth environments are late-lying snowbanks (Fig. 13.4b) and windswept ridges and interfluves. At these sites, plants tend to be either cryptogams (mosses) in snowbed sites or crustose lichens on ridges and summits. Saline and alkaline soil conditions are characteristic of the polar desert terrain; typically, salt crusts and efflorescence form after several days of rain-free, windy conditions and carbonates may be precipitated on the lower sides of rock fragments.

13.5 Geomorphic Features

It is generally agreed that Prince Patrick Island is located beyond the western limits of the NW Laurentide and Innuitian ice sheets (England et al. 2006, 2009). The presence of scattered erratics, meltwater channels and outwash fans suggests older, possibly local, ice caps prior to the last cold period (Fyles 1965). The range of landscapes present on Prince Patrick Island is illustrated in Fig. 13.5a–d.

Table 13.2 Average monthly temperature and precipitation data and frost statistics for Mould Bay, Prince Patrick Island, 76° 15′N; 133° 2′W, 15.2 masl (1948–1970) (from Maxwell 1980)

Month	Temperature (°C)	Precipitation		Frost data	
		Rain (mm)	Snowfall (cm)		
Jan	−33.9	–	3.8	Thawing degree-days (TDD)	~200
Feb	−36.0	–	10.4	Freezing degree-days (FDD)	~7,000
Mar	−33.2	–	22.1	Frost-free period (days)	23
Apr	−23.8	–	31.5	Number of Freeze-thaw cycles, annual average	13.4
May	−11.4	0.3	34.5		
Jun	−0.2	3.1	37.6		
Jul	+3.3	16.0	40.1		
Aug	+1.4	29.5	42.4		
Sept	−6.9	31.5	45.5		
Oct	−17.3	31.5	48.5		
Nov	−26.8	–	56.1		
Dec	−31.4	–	59.9		
Average	−17.8	–	–		

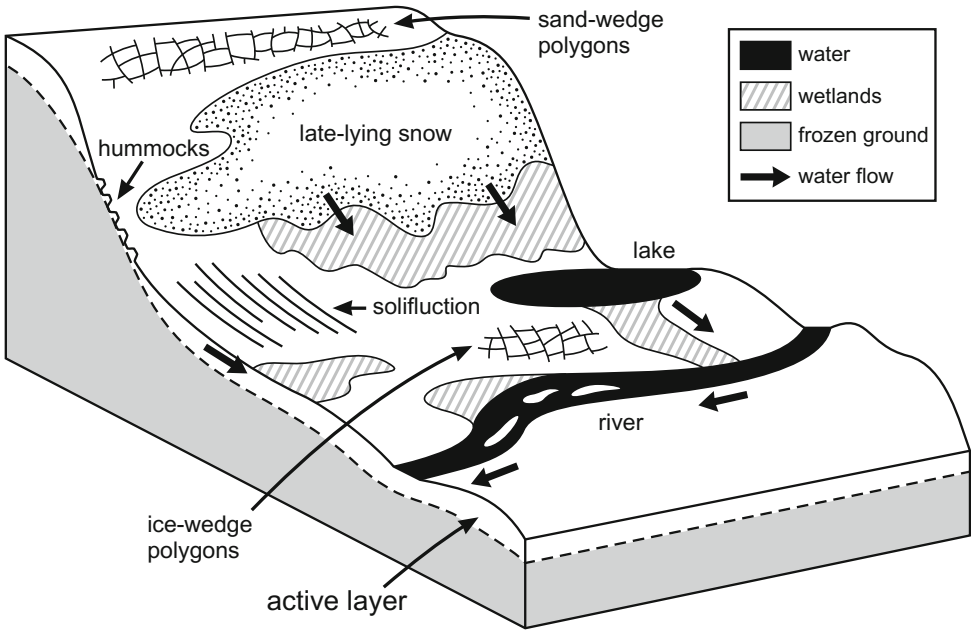

Fig. 13.2 A conceptualized topographic model of terrain characteristics and occurrence of 'snowbed' or 'patchy wetland' sites in the polar desert landscape (modified after Woo and Young 2003)

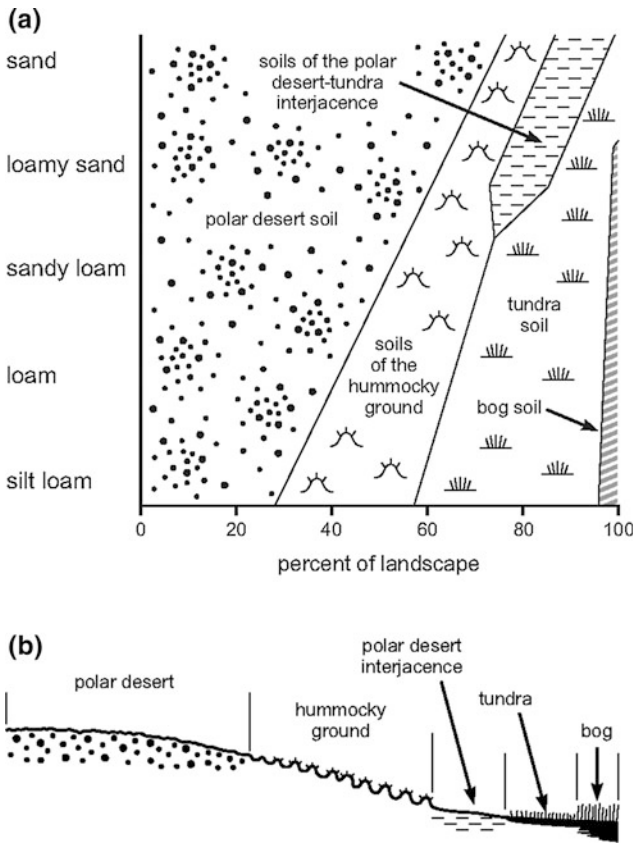

Fig. 13.3 Terrain transition from tundra to polar desert conditions on Prince Patrick Island. **a** The relationship between soils and grain-size composition. **b** A simplified mesotopographic profile from bog-tundra in valley bottoms to polar desert terrain on wind-swept interfluves and uplands (modified from Tedrow 1974, 1977; Tedrow et al. 1968)

In most deserts of the world, the major landscape control relates to geology. This is certainly the case for Prince Patrick Island. For example, outcrops of Paleozoic shale and sandstone on the eastern half of the island produce structurally controlled uplands subject to frost action and weathering. Here, the terrain is typically covered with a veneer of angular frost-shattered debris. By contrast, western and central parts of the island are underlain by weakly consolidated sand and gravel of the Beaufort Formation (Tozer and Thorsteinsson 1964; Fyles 1990). This gives rise to undulating terrain characterized by gentle slopes and broad shallow drainage channels with a maximum relative relief of 100–200 m (Fig. 13.5a). This terrain merges into extensive, largely featureless, sandy outwash surfaces and braided fluvial plains that grade westward toward the Beaufort Sea. These form barren landscapes devoid of distinct macro- and meso-scale landforms.

The aridity of the landscape means that the frequency and magnitude of geomorphic processes differ from similar processes in more humid, cold-climate environments. For example, features characteristics of intense frost action are restricted mainly to the eastern side of the island where Paleozoic bedrock is exposed. Frost wedging (ice segregation) is an effective mechanism but others, such as either thermal stress or 'explosive shattering,' may be equally important in this arid environment. In areas of silty regolith, and where sufficient moisture is present, annual freezing and thawing can lead to the formation of sorted and non-sorted circles. But, in general, the polar desert terrain of Prince Patrick Island lacks widespread development of the patterned ground features that characterize more humid cold environments. Tundra terrain is restricted to small areas in sheltered locations on the east coast (Fig. 13.5b).

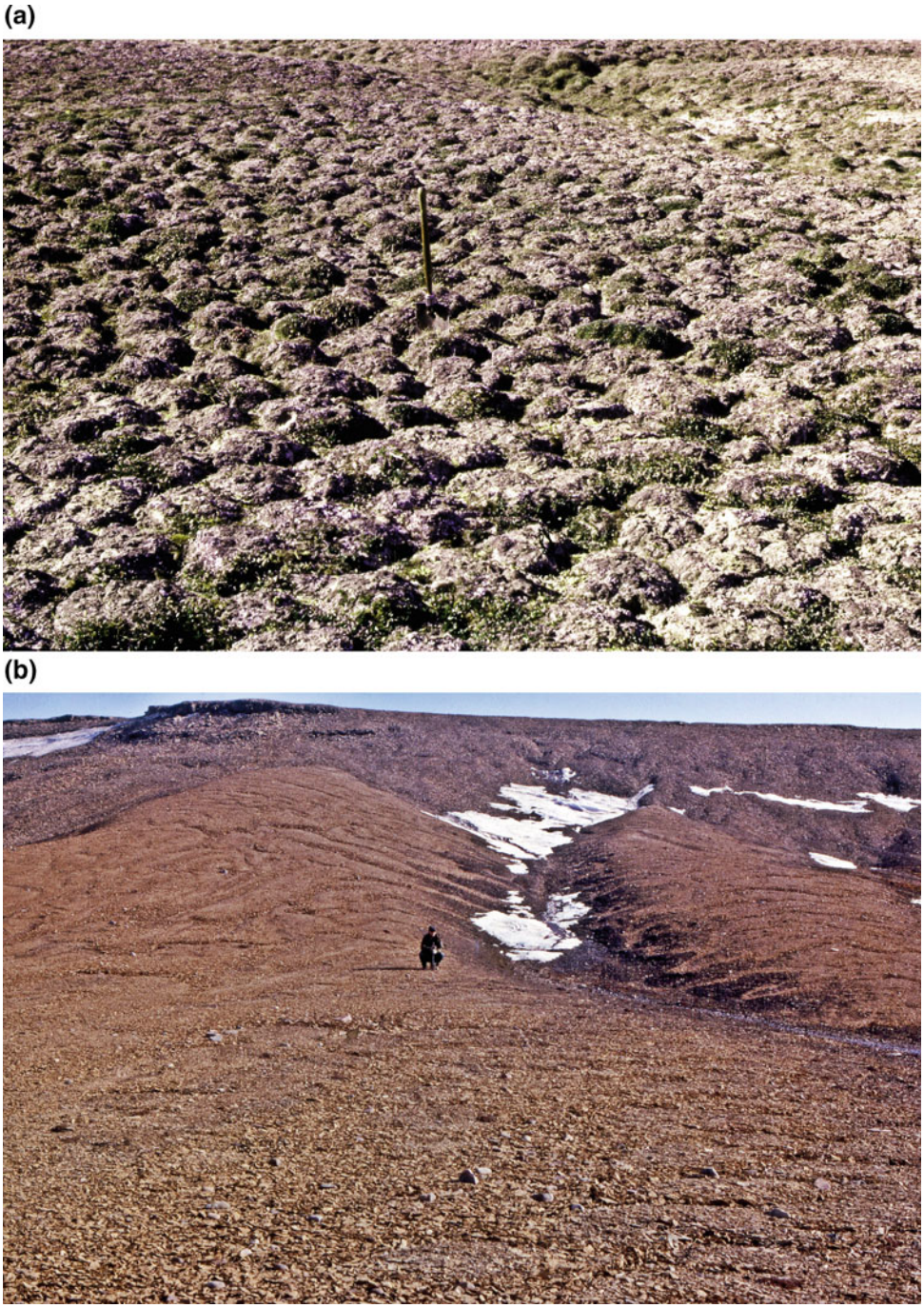

Fig. 13.4 Examples of the terrain transition from tundra to polar desert conditions on Prince Patrick Island. **a** Soil hummocks, 30–60 cm in size and 20–40 cm high, occur on sloping terrain 5 km north of Mould Bay. They mark the transition between lowland (vegetated) tundra and upland (unvegetated) polar desert conditions. *Photograph*—H. M. French. **b** Extreme growth positions in the polar desert relate to late-lying snowbanks and sheltered gullies and stream banks. The location is upland terrain ~10 km north of Mould Bay. *Photograph*—H. M. French

The traditional importance attached to wind in the polar deserts should be downplayed when one considers Prince Patrick Island. Many of the early accounts that stress the effects of wind action in the polar regions are from ice-free areas that are adjacent to either large ice sheets or high mountains, or both, such as Antarctica and northern Greenland (see French 2007, 264–268). As a result, strong katabatic winds are characteristic of these areas. Prince Patrick Island is not in a similar location. Equally, corrasion by blowing snow crystals is also cited as an important wind-abrading agent in polar regions. This is because the hardness of ice particles increases as temperatures decrease. On Prince Patrick Island, winter temperatures drop below −25 to −30 °C for several months each year. Therefore, a Mohs hardness of 3–4 might reasonably be expected for blowing ice crystals. But monthly wind speeds at Mould Bay during that period are less than 20 km/hr (see Table 13.2). Furthermore, in the December–February period, there is only a 5 % probability of hourly wind speed in excess of 44 km/h at Mould Bay (Table 13.3). This may explain why

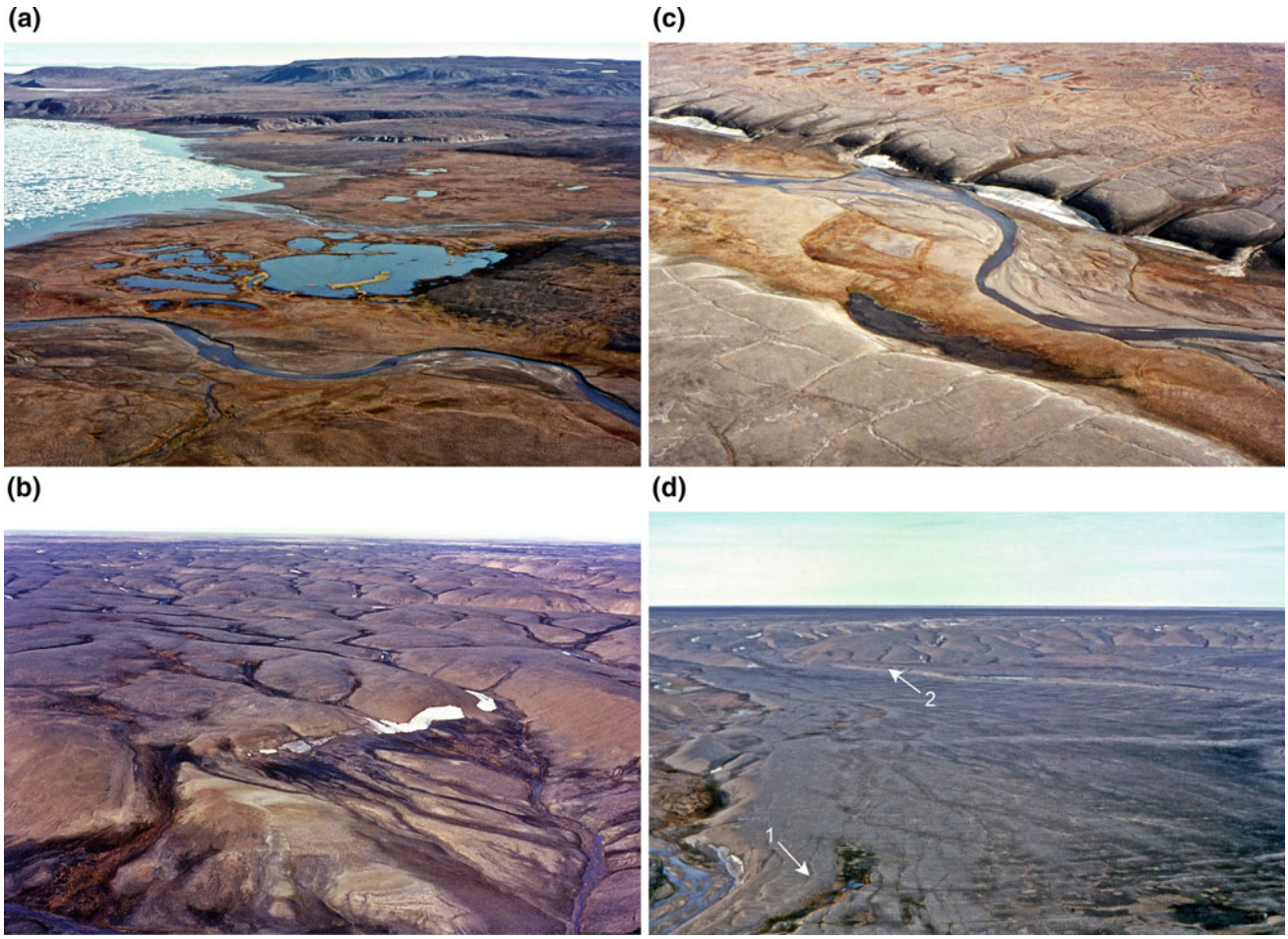

Fig. 13.5 Landscapes of Prince Patrick Island are structurally controlled and fluvial-dominated. **a** The central and western parts of the island constitute a gentle west-sloping plain that is underlain by sand and gravel of the Beaufort Formation. A network of ephemeral streams dissects the surface. The interfluves and uplands are largely bare of vegetation. Photograph—H. M. French. **b** The Mould Bay Inlet illustrates the transition from tundra in poorly drained lowland areas to polar desert terrain on surrounding better drained uplands. Ephemeral streams drain into the bay. Photograph—H. M. French. **c** A small box-shaped stream channel, incised within a low fluvial terrace, contains a braided stream channel. The location is ~3 km north of the Mould Bay weather station. Each year, for a period of between 1–3 weeks in late May and early June, rapid snowmelt results in bankfull discharge. The photograph was taken in late June 1968 after snowmelt 3–4 weeks previously. Photograph—H. M. French. **d** An outwash fan 10 km northwest of Mould Bay suggests that local ice caps may have existed prior to the last cold period. The alluvial surface (mid-foreground#1) is marked by large sand wedge polygons. Snowmelt runoff in spring is eroding small gullies (mid-background#2) along the lines of weakness presented by these sand wedges. Photograph—H. M. French

Table 13.3 Wind speed (km/hr) and duration (values of hourly wind speed (km/hr) equaled or exceeded at a given probability level, Mould Bay (1953–1972) (from Maxwell 1980)

Percent probability	Period			
	Dec-Jan-Feb	Mar-Apr-May	Jun-Jul-Aug	Sept-Oct-Nov
1	61	50	50	52
5	44	35	37	39
10	34	29	31	32
20	24	23	24	24
50	10	10	15	13
70	2	3	10	5
90	–	–	3	1
98	–	–	–	–

wind-abraded pebbles (ventifacts) are not found. In all probability, current wind-induced erosion is either negligible or extremely slow in those polar deserts, such Prince Patrick Island, that are far removed from continental ice sheets or high mountain ranges.

It is clear that the main geomorphic effect of the wind on Prince Patrick Island is via deflation (Pissart 1966). Fine particles are removed from the extensive snow-free and sparsely vegetated surfaces during the winter months and deposited in lee-slope positions and gullies as either cover-sand or localized niveo-aeolian sediment. The wind also encourages the formation of saline and alkaline soils through the rise and evaporation of capillary moisture and promotes desiccation cracking wherever silty and fine-grained sediment are present at the ground surface. Perhaps the most important indirect effect of the wind is that gullies and stream channels become snow-choked by early spring. This accentuates the short snowmelt runoff season.

In summary, the collective result is that, in spite of aridity, fluvial processes appear to dominate the landscape. In spring, the thawing active layer is quickly saturated and the underlying impermeable permafrost does not allow snowmelt runoff to infiltrate. This leads to approximately 80–90 % of annual runoff occurring within a short 2–3-week period in early spring. As temperatures rise, the snow that has accumulated within valleys becomes progressively more saturated, localized slushflows may appear, and then the snow melts as air temperatures rise above zero (Pissart 1967b). Following this short period of high discharge and erosive activity, stream channels are largely dry for the remainder of the summer months (Fig. 13.5c). Today, evidence of this fluvial activity is indicated by the widespread occurrence of small gullies, often exploiting lines of weakness presented by sand wedges. In certain areas, the large paleosandur surfaces and alluvial fans that were formed by higher discharges in the past are currently being dissected (Fig. 13.5d).

Features reflecting the presence of permafrost and ground ice are largely lacking from the polar desert landscape, even though the mean annual ground temperature at the depth of zero annual amplitude is approximately −14 °C and permafrost is probably several hundred meters thick. Typically, the ground surface thaws for less than 6–8 weeks, usually in July and August. But in the absence of a vegetation cover, maximum thaw penetration (the active layer) can reach 50 to 75 cm in sandy sediments and exposed bedrock. Solifluction, sheetwash and mass wasting processes are limited to small areas in close proximity to snowbanks. The clearest evidence for permafrost is seen in thermal contraction-crack polygons, 10–20 m in size. They characterize the sandy and gravelly surfaces of the western part of the island. Polygons of this nature, first described from Antarctica (Péwé 1959), are underlain by wedges of sand and gravel rather than ice. Limited field observations on Prince Patrick Island by both A. Pissart in 1965 (Pissart 1966, 199, 1968) and by the author in 1974 (see Fig. 13.6a) indicate the wedges are less than 1.2 m deep and 0.6 m wide (Pissart 1966, 1968). Smaller polygons, 2–5 m in size, which occur on shale bedrock on the eastern part of the island, may be the result of desiccation.

There are few water bodies or rivers of sufficient size to induce the formation of unfrozen zones or 'taliks.' But a number of partially collapsed mounds that occur on low terraces along the west coast near Satellite Bay (Pissart 1967a) suggest linear taliks may have existed in the recent geological past. Some of the mounds are elongate and similar to features on Banks Island (Pissart and French 1976). Shallow excavations made in the summers of 1965 and 1966 by A. Pissart revealed irregular bodies of massive ice. Although detailed information as to the nature of the ice core is lacking, it is probable that these mounds are the remnants of closed-system pingos. They would have formed following the freezing of unfrozen zones that would have formed beneath the deeper parts of stream channels at times of greater discharge and/moisture availability.

More puzzling are a number of low circular mounds that occur inland at higher elevations along the summit of the island. They appear to be aligned along deep-seated faults in the underlying Paleozoic rocks. Their origin and age are problematic; one suggestion is that they are ancient ice hydrolaccoliths that formed when groundwater, trapped by the faulted bedrock, moved upward along the fault lines and then froze as permafrost aggraded (Pissart 1967a; Pissart and French 1977). Other visible signs of ground ice, such as thermokarst lakes and the typical ice wedge polygon relief that is characteristic of tundra areas such as the Mackenzie Delta lowlands, are either restricted to coastal lowlands, infrequent or completely lacking on Prince Patrick Island.

Collectively, all these observations reflect the general aridity of the climate. In the absence of more detailed field investigations, one must assume that the permafrost terrain on Prince Patrick Island is ice-poor. Typical ice volumes within the upper 5–10 m are probably as little as 10–15 %. This assumption is supported by the minimal levels of terrain disturbance that occurred during the drilling of exploratory oil wells in the 1970s at a number of polar desert sites in the Canadian Arctic islands (French 1978, 21–22). For example, on Prince Patrick Island, the Elf Dyer Bay I-59 well was located on a sandy gravelly outwash surface underlain by sand and gravel of the Beaufort Formation. Drilling and site restoration were completed without significant environmental or terrain problems (Fig. 13.6a; Table 13.4). A similar situation occurred at the Elfex et al Wilkie Point J-51 well (Fig. 13.6b), located on terrain underlain by sandstone and sand of the Wilkie Point Formation. Both sites are excellent examples of the barren and inhospitable nature of much of the polar desert landscape of Prince Patrick Island.

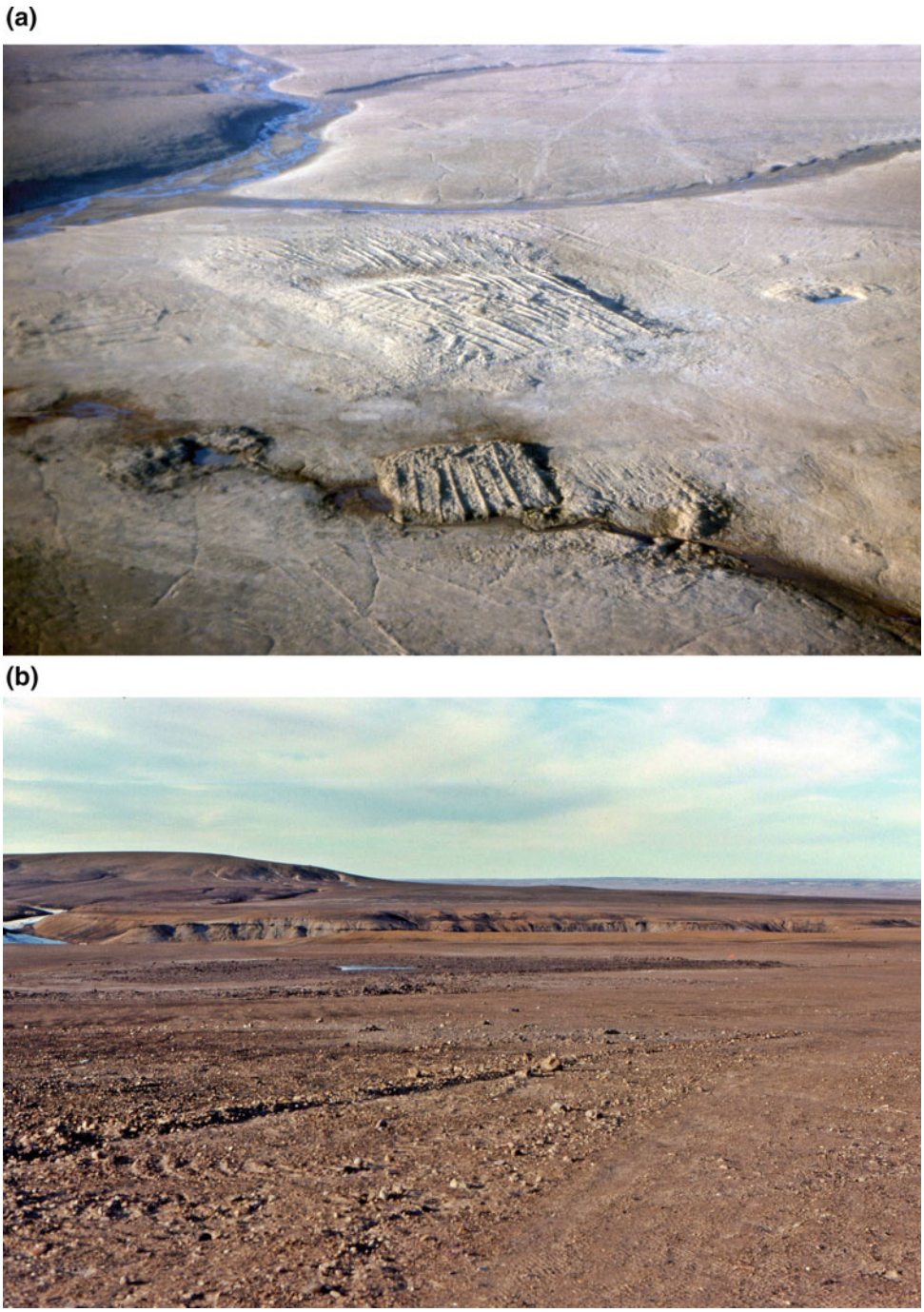

Fig. 13.6 Oil exploration activity indicates that polar desert terrain, underlain by frozen bedrock with low ground ice amounts and largely lacking surface vegetation, is not susceptible to high levels of environmental and terrain disturbance (see Table 13.4). **a** Air view of the site of the Dyer Bay I-59 exploratory well (lat 76° 08′N, long 121°48′W), drilled in the winter of 1975–1976. The location is a sandy outwash surface derived from Beaufort Formation sediments and completely bare of vegetation. The site is an interfluve between two shallow ephemeral stream channels. Sand-wedge polygons are visible in bottom left corner of the picture. **b** The terrain adjacent to the airstrip at the Wilkie Point J-51 exploratory well (lat 75° 30′N, long 117° 19′ W) is underlain by shale and sandstone of the Wilkie Point Formation. The well was drilled during the 1974–1975 winter. The ground is covered with a veneer of angular rock fragments. Vegetation cover is <5 %. Both photographs were taken in mid-August 1976. *Photographs* —H. M. French

Table 13.4 Temperatures (°C) and thaw depths (cm) measured in the active layer in disturbed and undisturbed terrain at the Wilkie Point J-51 and Dyer Bay I-59 well sites. The data indicate little difference between disturbed and undisturbed sites (from French 1978)

Depth (cm)	Wilkie Point J-51		Dyer Bay I-59	
	Undisturbed	Disturbed (sump)	Undisturbed	Disturbed (sump)
Surface	5.0	4.5	1.5	2.0
10	4.5	4.0	3.5	3.5
20	4.0	2.5	4.5	4.0
30	2.5	1.0	4.0	3.5
40	1.0	–	3.0	2.5
Frost Table (16-08-1976)	47.0	35.0	75.0	75.0
Vegetation	Polar desert <5 %		Polar desert, bare	
Geology	Sandstone and shale, Wilkie Point Formation		Sand and gravel, Beaufort Formation	

13.6 Conclusions

The landscape of Prince Patrick Island is typical of a cold, polar desert. Geology exerts a fundamental control. The combination of aridity and extreme cold limits plant growth. The range of cold-climate landforms is restricted because of the paucity of snow and the relative absence of ground ice. Thermal contraction cracking results in sand wedges, and the resulting polygons characterize extensive surfaces. Wind is the cause of deflation activity on these exposed surfaces and the desiccation of near-surface sediments. Wind also concentrates snow in gullies and depressions during the winter months; this leads to rapid snowmelt and a short period of fluvial activity in the spring.

Acknowledgements Fieldwork conducted on Prince Patrick Island in the summers of 1968 and 1974 was supported by The Geological Survey of Canada, NSERC, PCSP, Elf Aquitaine, Panarctic Oils, and the Arctic Petroleum Operators Association. Professor M-K. Woo is thanked for his review and his clarification of the concept of a cold desert. Figures 13.1, 13.2, 13.3, 13.5b, c and 13.6b are also available in Cuadernos de Investigación Geográfica (No 42(2), 321–340), published by Universidad de La Rioja (Spain) (pulicaciones.unirioja.es/revistas/cig).

References

Bliss LC (1997) Arctic ecosystems of North America. In: Wielgolaski FE (ed) Ecosystems of the World 3, polar and alpine tundra. Elsevier, New York, pp 551–683

England JH, Atkinson N, Bednarski J, Dyke AS, Hodgson DA, O'Cofaigh C (2006) The Innuitian Ice Sheet: configuration, dynamics and chronology. Quat Sci Rev 25:689–703

England JH, Furze MFA, Doupe JP (2009) Revision of the NW Laurentide Ice Sheet: implications for paleoclimate, the northeast extremity of Beringia, and the Arctic Ocean sedimentation. Quat Sci Rev 28:1573–1596

French HM (1978) Sump studies: 1, Terrain disturbances. Environmental Studies No 6, Department of Indian Affairs and Northern Development, Ottawa, 52 p

French HM (2007) The periglacial environment, 3rd edn. Wiley, Chichester

Fyles JG (1965) Surficial geology, western Queen Elizabeth Islands. Geol Surv Can Paper 65–1:3–5

Fyles JG (1990) Beaufort Formation (Late Tertiary) as seen from Prince Patrick Island, Arctic Canada. Arctic 43:393–403

Maxwell JB (1980) The climate of the Canadian Arctic islands and adjacent waters. Climatological Studies, 30, Atmospheric Environment Service, Environment Canada

Péwé TL (1959) Sand-wedge polygons (tessellations) in the McMurdo Sound region, Antarctica. Amer J Sci 257:545–552

Pissart A (1966) Le rôle géomorphologique du vent dans la région de Mould Bay (Ile Prince Patrick, NWT, Canada). Zeits Geomorph 10:226–236

Pissart A (1967a) Les pingos de l'île Prince Patrick (76°N–120°W). Geogr Bull 9:189–217

Pissart A (1967b) Les modalités de l'écoulement de l'eau sur l'île Prince Patrick. Biuletyn Peryglacjany 16:217–224

Pissart A (1968) Les polygons de fente de gel de l'île Prince Patrick. Biuletyn Peryglacjany 17:171–180

Pissart A, French HM (1976) Pingo investigations, north-central Banks Island, Canadian Arctic. Can J Earth Sci 13:937–946

Pissart A, French HM (1977) The origins of pingos in regions of thick permafrost, Western Canadian Arctic. Questiones Geographicae 4:149–160

Tedrow JCF (1974) Soils of the high arctic landscape. In: Smiley TL, Zumberge JH (eds) Polar deserts and modern man. University of Arizona Press, Arizona, pp 63–69

Tedrow JCF (1977) Soils of the polar landscape. Rutgers University Press, New Jersey 638 p

Tedrow JCF, Bruggeman PF, Walton GF (1968) Soils of Prince Patrick Island. Arctic Institute of North America Research Paper 44, Washington D.C., 82 p

Thomas DSG (2011) Arid environments: their nature and extent. In: Thomas DSG (ed) Arid zone geomorphology. Blackwell, Oxford, pp 3–16

Tozer ET, Thorsteinsson R (1964) Western Queen Elizabeth islands, Arctic Archipelago. Geol Surv Can Memoir 332, 222 p

Woo M-L, Young KL (2003) Hydrogeomorphology of patchy wetlands in the High Arctic polar desert environment. Wetlands 23:291–309

Cold Climate, Canyons and Karst Along the Canol Road Corridor, Mackenzie Mountains, NWT

14

D.C. Ford and J.P. Hamilton

Abstract

Geomorphic landscapes along a transect from the Plains of Abraham 90 km inside the Mackenzie Mountains eastwards to the edge of the Mackenzie Valley are exceptionally rich in their variety of forms, processes and causes. They are linked together by a similarly rich physical history of sedimentation, diagenesis and tectonic deformation in the bedrocks, of glacier advances and retreats across them at the cold arid limits of Quaternary glacierization, and by the historical construction of the Canol Road. The distinctive landforms include (1) never glaciated dolomite plateaus dominated by periglacial processes but exhibiting some karst drainage today; (2) pedimentation and karst polje development linked to the limits of Wisconsinan glacial penetration: inside the limits (3) active and relict river canyons with vigorous mass wasting; (4) limestone pavements and a solution breccia landscape that is unique; (5) a late glacial spillway chopped into many pieces of different size, form and function by post-glacial processes. This transect is worthy of adoption as a national park and promotion for UNESCO World Heritage status.

Keywords

Mackenzie Mountains • River canyons • Spillways • Karst • Poljes • Dolomite pavement • Territorial Park

14.1 Introduction

14.1.1 The Mackenzie Mountains

The Mackenzie Mountains are a complex of ranges extending between latitudes 60° and 67°N, dividing Pacific drainage (Yukon) from that to the Mackenzie River and Arctic Ocean (Northwest Territories). They are scarcely peopled. Along the spine, batholithic rocks of Cretaceous age are carved into typical alpine topography—the 'Backbone Ranges'. They supported extensive Cordilleran valley glaciers during the ice ages and preserved a few extant glaciers and small ice caps today. To the east, thick sequences of Upper Proterozoic and Paleozoic sedimentary rocks were deformed by the plutonic injections into fold and overthrust topographies, with rivers flowing eastwards across them—the 'Canyon Ranges'. Their western parts were invaded by Cordilleran valley glaciers, with some limited extensions eastwards. The Laurentide Continental Ice Sheet was able to override the most easterly. In between, there is a corridor of rarely to never glaciated terrain that widens to the north (Ford 1974; Duk-Rodkin and Lemmens 2000). It contains magnificent river canyon landscapes, principally in resistant limestone and dolomite formations. There are also resistant sandstone formations, weaker shales, calcareous shales and siltstones. Gypsum interbeds are common in the dolomites, and also present with salt at depth. As a result, there are many different geomorphic styles to be seen in the mountains, consequences of the differing

D.C. Ford (✉)
School of Geography and Geology, McMaster University, Hamilton, ON L8S 4L8, Canada
e-mail: derekcliffordford@gmail.com

J.P. Hamilton
Department of Geography, Wilfred Laurier University, Waterloo, ON N2L 3C5, Canada

© Springer International Publishing Switzerland 2017

O. Slaymaker (ed.), *Landscapes and Landforms of Western Canada*, World Geomorphological Landscapes, DOI: 10.1007/978-3-319-44595-3_14

composition, lithology, geologic structure, glacial and/or periglacial history.

14.1.2 The Canol ('Canadian Oil') Road

Following the declaration of war in December 1941, the US Navy feared that Japanese forces might be able to cut off the fuel supplies it needed to defend Alaska. Very hastily, it was decided to run a 4-in. pipeline from the small oil field at Norman Wells, NT, to Whitehorse, YT, crossing the uninhabited Mackenzie Mountains (Fig. 14.1). A rough dirt road was bulldozed through swamps, canyons and over high mountains into the Yukon Valley. It was abandoned in 1944. The Territorial portion has partly survived natural processes and is now conserved as the 'Canol Heritage Trail'.

A journey along the trail from the Plains of Abraham in the interior of the Canyon Ranges to the mouths of the river canyons debouching into the Mackenzie Valley passes through a wide variety of sedimentary rocks and of geological structures. It begins in an area probably never glaciated but subject to intensive periglacial conditions during the glacial periods. It retains deep permafrost today. The trail next traverses a zone of fluvial, periglacial and old, muted glacial morphology before entering an eastern mountain front sector where there is strong visual evidence of glacial invasion and scouring during the last (Wisconsinan) advances of the Laurentide Ice Sheet. During the recession,

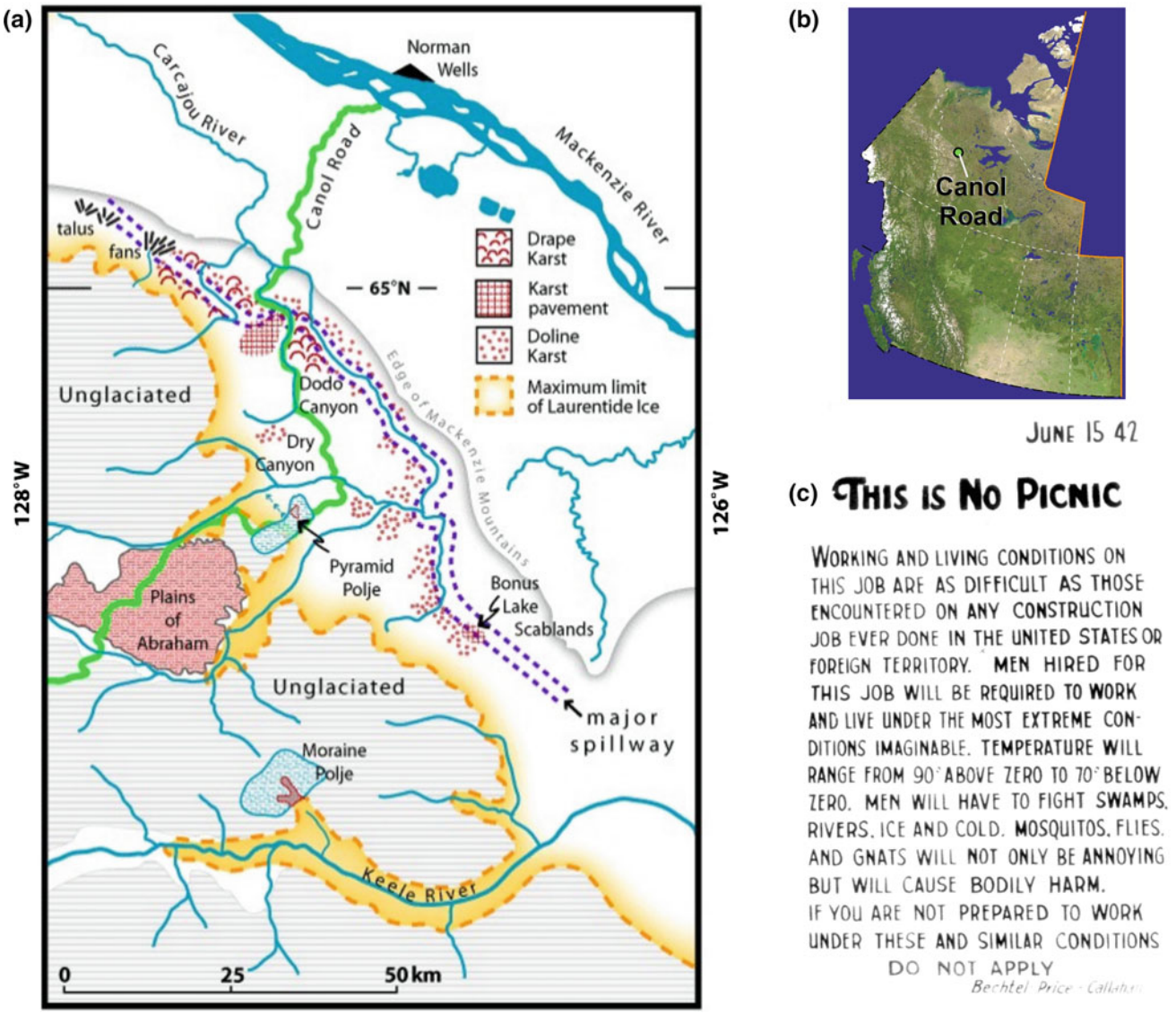

Fig. 14.1 **a** Diagrammatic sketch map of the geomorphic landscapes along the Canol Road. **b** Location of Canol Road corridor, Mackenzie Mountains, Northwest Territories. *Background image* NASA, Visible Earth. **c** 'Truth in advertising'! In 1942, the Bechtel Corporation seeks workers to construct the road (Courtesy of the Norman Wells Museum)

ice margin melt rivers then carved a series of deep spillways (canyons) into the bedrocks just inside the eastern edge of the mountains. Several of them linked up as a nearly continuous feature, the Great Spillway (Fig. 14.1). The variety of the rocks and of the geomorphic processes able to attack them has combined to produce a rich mixture of physical landscapes. This essay highlights a selection of them. It is based on the doctoral study of the karst processes and landforms by Hamilton (1995) and on later commissioned reports to the government of the Northwest Territories by Ford (2008, 2012).

14.2 Lithology, Geologic Structure, Glacial History and Modern Climate

In this region, the rocks of the Canyon Ranges are mixtures of clastic, carbonate and evaporite sediments extending from Upper Proterozoic to Cretaceous in age. There is much local variation in facies and thicknesses within them that is further complicated by a history of complex folding and overthrusting. However, for the transect being considered here, the variety can be reduced to just five formations from the Cambrian to Devonian in age and to a few simple structures. In sequence from the chronologic base upwards, the formations are as follows:

(a) The Saline River Formation (Upper Cambrian) composed of 800 + m of redbeds, varicoloured siltstones and shales, gypsiferous shales with abundant salt casts: intact halite and anhydrite beds are found in deep cores (Aitken and Cook 1974; Aitken et al. 1982; Meijer Drees 1986). Most of these strata are mechanically weak and thus recessive. Only ~130 m of the upper beds are exposed in our transect (in Dodo Canyon), but there are thick sequences in subcrop. The occurrence of salt springs as warm as 8–9°C at the mouth of Carcajou Canyon (the local base level) suggests that that there is significant regional groundwater circulation to great depths in this formation and possibly below it.

(b) The Franklin Mountain Formation (Cambro–Ordovician) consists of ~400+ m of varied dolomites. Above basal redbeds, there are irregular thicknesses of relatively weak argillaceous dolomites including bright orange-weathering strata. These are succeeded by stronger, buff- to grey-weathering, dolomites that become siliceous, cherty and dark-weathering towards the top of the formation (Macqueen 1970). There is an unconformity at the top of the formation that displays orange- to red-weathering earths at a few sites. It may represent a palaeokarst but has not been studied.

(c) The Mount Kindle Formation (Silurian–Devonian). The type section is far to the south in the Franklin Mountains. In the Canol Trail region, the formation consists of up to 250–300 m of medium to massively bedded and resistant dolomites, including well-developed cyclic sequences. Lower units are siliceous, cherty and dark grey-weathering; upper units become paler in colour and quite fossiliferous, including small patch reefs. The fossils are silicified and may stand out prominently on karst pavements. An apparent unconformity with up to forty metres of relief can be seen at the top of the formation in Dodo Canyon. Elsewhere its relationship with the overlying rocks appears to be merely disconformable, due to extreme brecciation in the strata above it.

(d) The Bear Rock Formation (Lower and Middle Devonian) extends >50,000 km^2 in subcrop under the Mackenzie Valley and the Mackenzie and Franklin mountains (Morrow and Meijer Drees 1981). The Canol transect is in its central area, longitude 64–66°N, latitude 125–130°W. Where it has been cored during oil exploration deep beneath the valley, the intact formation consists of a regular sequence of dolomite and anhydrite beds (a typical supratidal or 'sabkha' facies) totalling 250–300 m in thickness and becoming disturbed (slightly brecciated) towards the top (Meijer Drees 1986, 1993). On the flanks of the mountains east and west of the Mackenzie Valley, it is always found to be a solution megabreccia, typically reduced to ~200 m or less in thickness beneath outcrops of the overlying Hume Formation and thinning to zero where it becomes exposed upslope of them. Brecciation is due to preferential solution of the sulphate beds (anhydrite and gypsum) by circulating groundwater, with consequent fracture and settling of the overlying carbonate beds. Brecciation and recementation are complete to the base of the formation. It is now a mixture of chiefly (i) 'pack' breccias (Stanton 1966) where the carbonate beds, although fractured, have retained much of their stratigraphic order, with fragments that are similar in size, uniformly and firmly recemented and thus are comparatively resistant, and (ii) 'float' breccias that are highly disordered due to greater break-up and displacement, and are physically and chemically much weaker due to the wider mixture of grain sizes and strengths of the recementation. In bulk terms, much of the original dolomite has been replaced by limestone during the brecciation and cementation processes ('dedolomitization') but some dolomite remains. Water chemistry data indicate that trace quantities of gypsum survive except close to the surface. A particularly resistant pack breccia several metres in thickness, the Landry Member, is seen at depth in some sections and elsewhere draped on the open surface as individual blocks many square metres in area, perched above or

sliding into solutional depressions in the underlying weaker breccias. Evidently, the solution, brecciation and cementation processes have been caused by circulation of meteoric groundwaters, commencing in the mid-Tertiary and continuing to the present (Hamilton 1995; Hamilton and Ford 2002). The Bear Rock Formation is one of the most striking solution breccias that the first author has seen in a lifetime of karst studies around the world. Some of the landscapes created in it appear to be morphologically unique.

(e) The Hume Formation (Devonian) consists of ~90–150 m of platformal limestones that are shaly and recessive at the base, becoming thick to massively bedded and resistant above (Aitken et al. 1982). They weather buff to light grey or blue-grey. They are prominent only along eastern fringe of the study area.

The geologic structure of folding and thrusting is complex in detail but, for the purposes of this review, can be described as being gently monoclinal along the trail in the west ('Plains of Abraham'; Fig. 14.1), shallowly synclinal at Pyramid Polje in the middle, and then traversing a series of broad anticlines and synclines along the strike of the Canyon Ranges (Fallas and MacNaughton 2014). The anticlines rise to a crest more than 900 m above local base levels before bringing the Mackenzie Mountains to a close by dipping below the valley floor along the eastern flank. There is sharper structural deformation to the north and south of the route.

The history of glaciations as they are presently understood is indicated in Fig. 14.1a. In this north-west sector, maximum penetration of the Laurentide Ice Sheet into the Mackenzie Mountains is believed to have occurred during the Wisconsinan Glaciation, not in any of the earlier glacials that saw much deeper advances along the southern margins of the ice (Lemmen et al. 1994; Duk-Rodkin and Hughes 2000; Duk-Rodkin and Lemmens 2000; Duk-Rodkin 2002). Based on ^{14}C ages of trees buried by glacial deposits, the maximum ice extent was reached sometime after 35 ka BP and recession had begun by ~21 ka BP (Katherine Creek Stage). Entrenchment of spillways will have begun later and may have lasted through the Early Lake Mackenzie Stage, ~11.5 ka BP. After that the ice receded across the Mackenzie Valley (Smith 1992).

The length of the transect along the trail is approximately 90 km. Elevations increase from 220 m above sea level on the edge of the Mackenzie Valley to 2000 m on the highest ground in the west. The mean annual temperature at Norman Wells Airport (75 masl) is −5.1 °C (Environment Canada 2015): values on the higher ground are expected to range from −8.0 to −15.0 °C or lower. Annual mean precipitation is ~290 mm in the valley, increasing to 600+ mm in the mountains; there is usually a distinct summer maximum, which may include violent rain storms. Heginbottom and Radburn (1992) mapped terrain below ~600 m along the canyons as displaying extensive but discontinuous permafrost. It is presumed to become (technically) continuous at higher elevations, but subject to all the variations of depth and ice content caused by differing rocks and soils, vegetation cover and aspect. Ground below 600 m is placed in a High Subarctic ecoclimatic category (Ecoregions Working Group 1989) where impoverished boreal forest may grow on suitable soils; ground between 600–1000 m is categorized as Subalpine Northern Subarctic Cordilleran with boreal forest confined to the most sheltered places. Above 1000 m, it is Alpine Northern Subarctic with limited flora below 1500 m and a sparse display of alpine plants above.

All of the karstic rocks mentioned in this summary (limestone, dolomite, gypsum, solution breccias, salt) can be seen undergoing modern dissolution along the traverse, and there are many other geomorphic processes vigorously at work on both the soluble and the insoluble strata. It is a region of outstanding geologic and geomorphic interest that also offers landscapes of great aesthetic appeal.

14.3 Geomorphological Landscapes

14.3.1 The Plains of Abraham

The Plains of Abraham are a plateau ~400 km^2 in area in the central unglaciated zone of the mountains (Fig. 14.2a). They are formed on regularly bedded dolomites of the Mt Kindle Formation underlain by Franklin Mountain rocks. The strata dip very gently eastwards, with elevations descending from ~1800 to 1500 masl. The plains are dissected by shallow stream valleys that form regular dendritic (consequent) channel patterns, but with low drainage density. It appears that actual flow in many of the channels is limited to peak melt times and occasional summer storms, except in the downstream reaches. The plains themselves are in the Alpine Subarctic ecozone but lusher herbaceous and shrub tundra is seen in sheltered sites in the valleys, especially where fluvial or colluvial debris has accumulated.

The high plains surfaces are a landscape of frost-shattered and frost-sorted dolomite debris. There is little native or allogenic fine-grained soil but there is variety in the form and scale of surface features that is determined by the following: (1) slight differences in the susceptibility of individual dolomite beds to frost shattering or dissolution, (2) microclimate or (3) hydraulic gradient factors in the seasonal active layer. Above 1600 masl, a few patches of well-formed patterned ground, chiefly circular or elliptical in shape are scattered amongst broader areas of simple shatter (felsenmeer). Stone stripes are well developed on gentle slopes

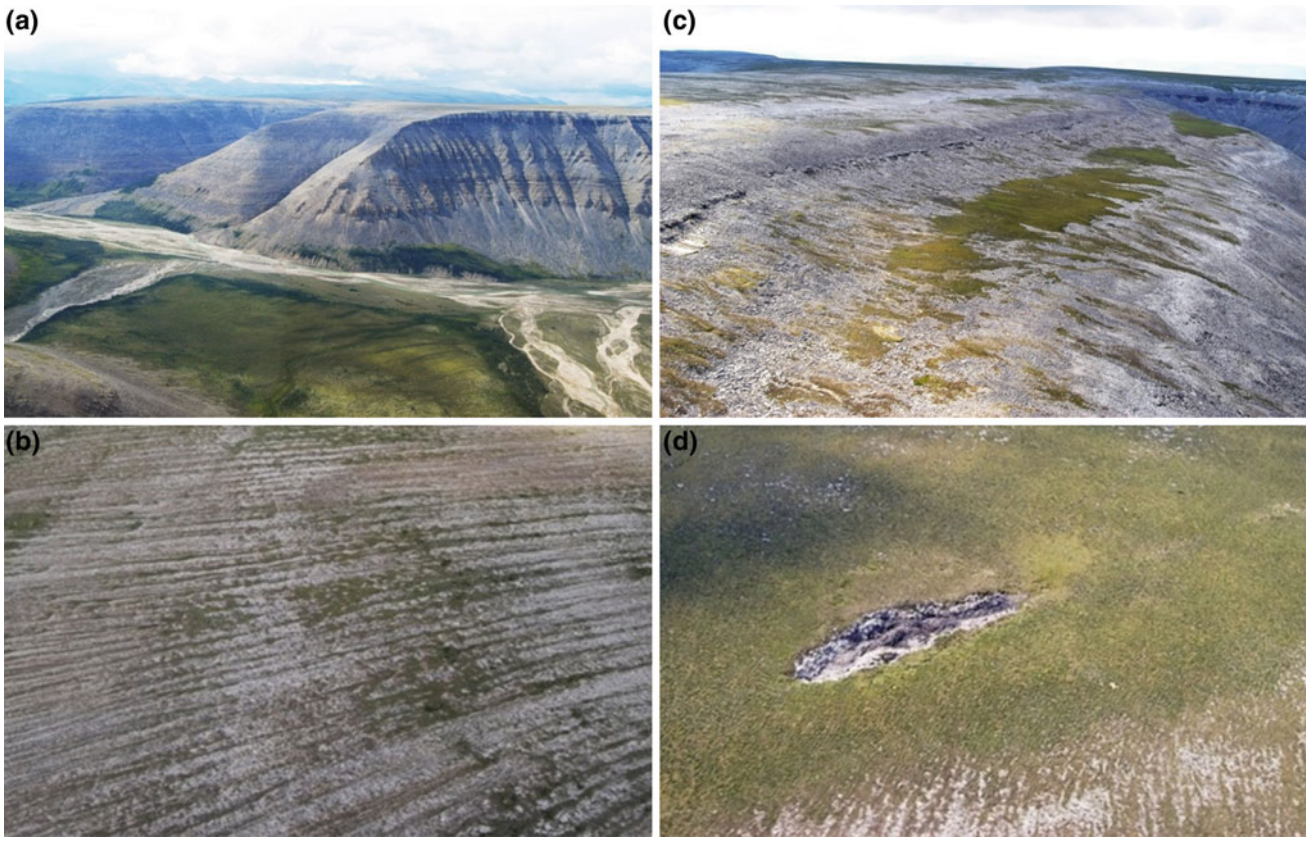

Fig. 14.2 **a** Approaching the Plains of Abraham, with the Carcajou River at their foot. **b** Stone stripes on the plains. **c** An example of the altiplanation terracing. **d** A karst sinkhole that captures the active layer drainage from a patch of stone stripes

(Fig. 14.2b). Regular frost polygons up to a few metres in diameter are limited to some exposures of more massively bedded dolomite. Altiplanation terraces develop along the edges of such beds, where there are low scarp faces that locally steepen groundwater hydraulic gradients and so deepen the active layer, allowing bedrock solution and frost to work together (Fig. 14.2c). Below ~1600 masl where alpine plant cover is more abundant, there is some development of solifluction lobes.

Despite the severe climate and permafrost that is presumably deeper than 50 m, there is some evidence of karstic drainage such as small sink points, even on plateau tops. Figure 14.2d shows a sinkhole ~50 m in length developed along a joint that catches active layer drainage from a patch of stone stripes upslope of it. Figure 14.3 shows the finest example of a springhead sapping feature ('steephead' or 'pocket valley'; Fr, 'reculée') that the writers have seen anywhere in the arctic or subarctic. The location is latitude 64°33′39″N, longitude 127°49′09″W. The Canol Road passes by the crest. Channelled groundwater is flowing from points along the foot of the arcuate cliff of resistant dolomite, sapping it back primarily by solution. The water emerges as springs at the base of the talus, creating an oasis. Its floor is at 1450 masl. In Fig. 14.3d, a line of tiny, truncated solution caves can be seen in the prominent bedding plane at the base of the massive dolomite bed. Their pattern is typical of focused karstic flow in the early stages of cave development. Although now abandoned because the groundwater has moved down to a similar exit plane at the oasis level, these caves indicate that the history of karst development here is ancient. However, as this is the only example of a significant steephead seen in the plains it appears to have been of local scale only, rather than integrated regional groundwater flow as described below in Dodo Canyon. The cliffs are north-facing. A tiny glacier or firn field was able to form below them during the Wisconsinan glacial, aiding the process of arcuate recession and leaving a small terminal moraine in the mouth of the cirque.

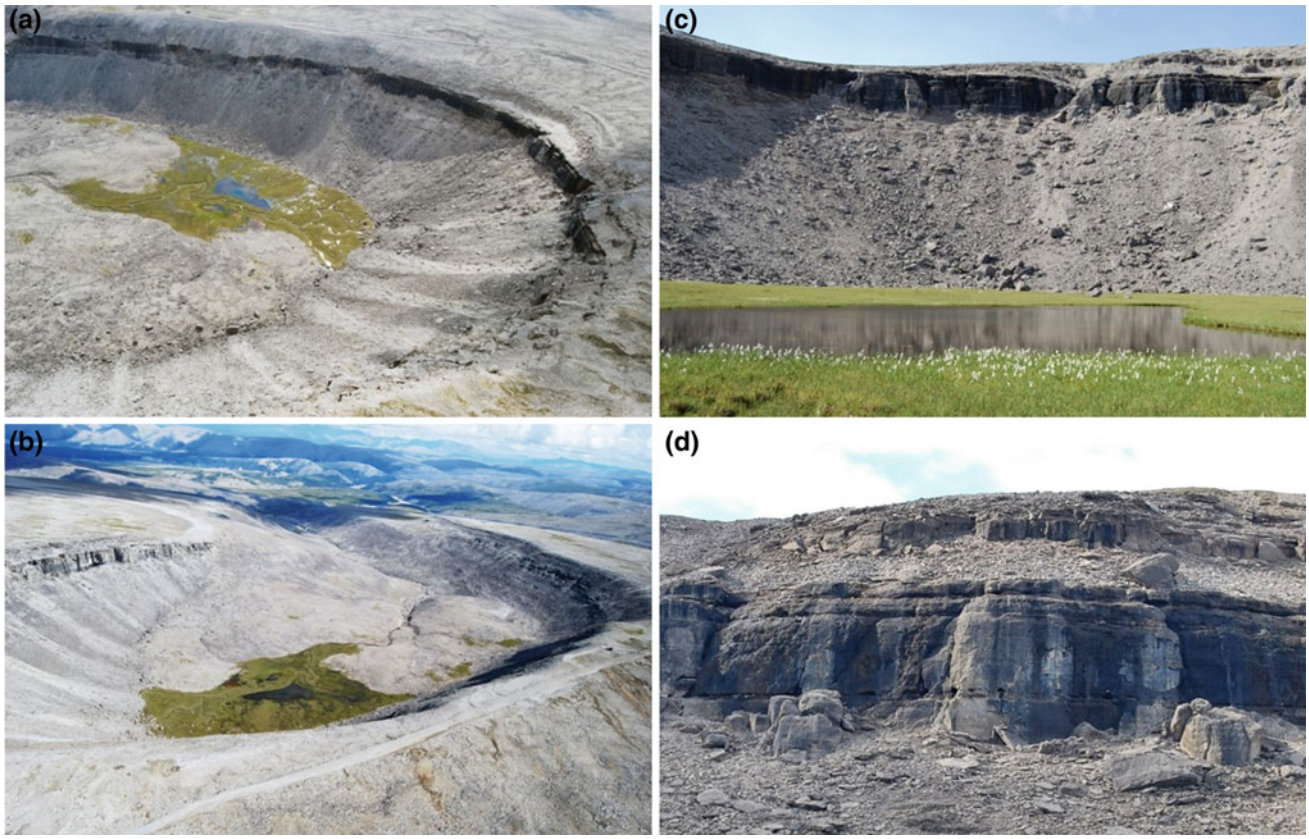

Fig. 14.3 Four views of a karst springhead sap ('steephead') in the plains; see the text for details. The Canol Road is seen along the brow

14.3.2 Moraine Polje

Moraine Polje (Figs. 14.1, 14.4) is located 25 km southeast of the Plains of Abraham and the Canol Road. Despite this geographical separation, it is included in this account because it is a most spectacular piece of geomorphology.

At its furthest incursion into the Keele River Valley, a lobe of the Laurentide Ice Sheet advanced upstream in a tributary until it was halted at a narrows created by a pair of bedrock spurs in Mount Kindle Formation dolomite. It built a terminal moraine there (Fig. 14.4a) that blocked surface stream flow out of the valley. Upstream of the moraine, the valley has never been glaciated. It became partly filled with alluvial detritus and the water developed an underground karst drain through the dolomites (Ford 1987).

Blockage of drainage by terminal moraines is a common phenomenon in glaciated regions. In almost every case, however, the area behind the barrier fills and overflows, so entrenching a channel through the moraine ridge and draining any temporary lake. At Moraine Polje, the moraine ridge shows no evidence of entrenchment, indicating that the impounded lake quickly opened an alternative underground karst drainage route. The basin created behind the moraine is $\sim$90 km^2 in area. It is entirely in the Mount Kindle Formation, which here weathers grey to rusty red. Its thalweg follows the axis of a steep-sided V-form syncline aligned down the centre of the basin (see Fig. 14.4a). In becoming alluviated and drained underground in the downstream direction, it is technically a 'rand' (border) polje, a large-scale, flat-floored karst landform receiving allogenic drainage (Ford and Williams 2007; p. 363). There are a few tors on the ridge crests around the basin perimeter and an extensive periglacial erosional pediment which bevels the steeply dipping strata (Fig. 14.4c). The contrast with the morphology in the same dolomite formation on the Plains of Abraham could scarcely be greater! It is due primarily to the synclinal folding, which is centred in thinner, weaker beds lower in the formation than those that are exposed on most of the surface of the plains. Curiously, the main creek draining the basin sinks underground into a rock spur *upstream* of the impounded alluvial flats, instead of into the same strata on the downstream (southern) side which are much closer to any likely spring outlet. The sink point is at

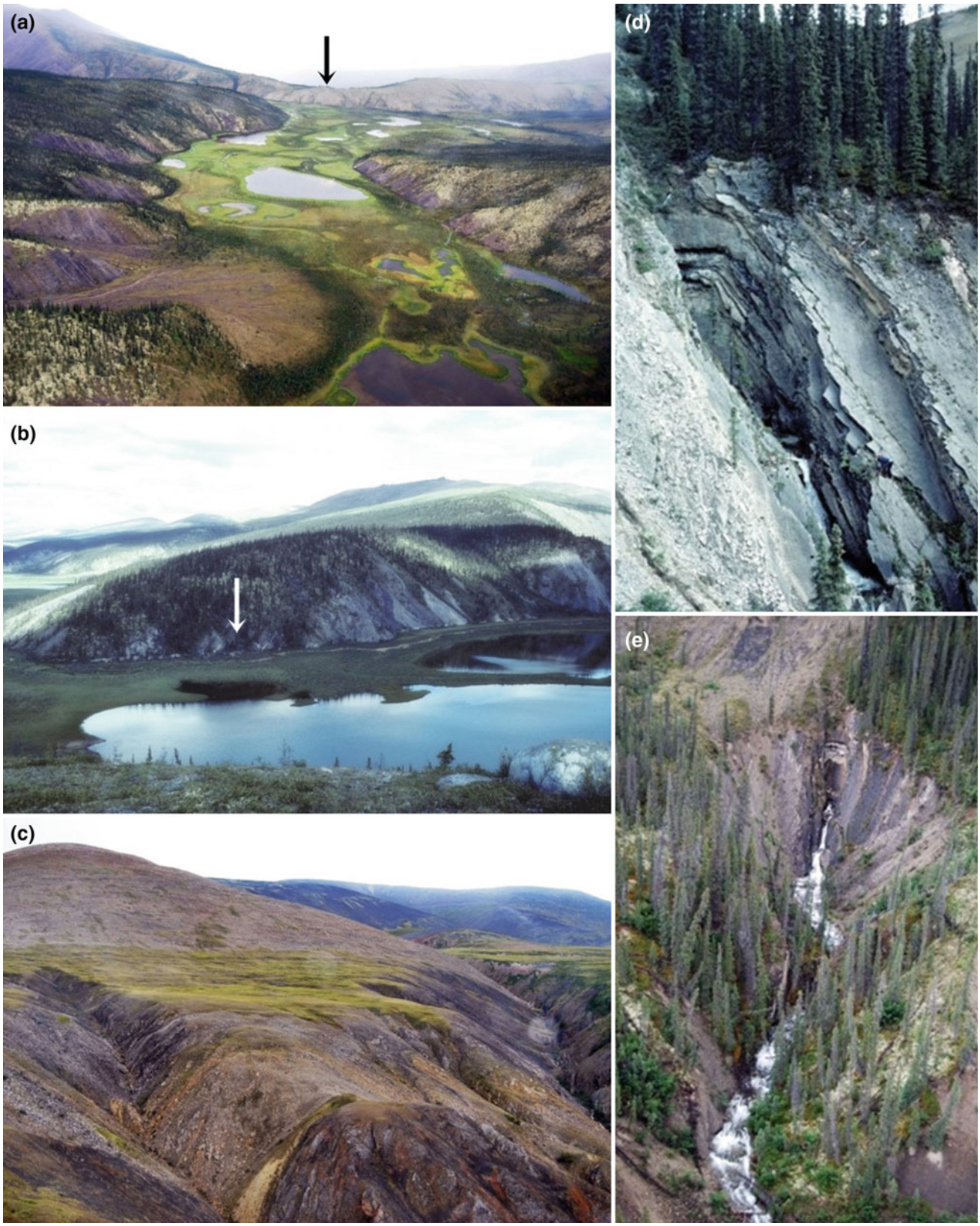

Fig. 14.4 Moraine Polje. **a** The alluvial floor of the polje looking downstream. The arrow mark the end of the Wisconsinan glacial terminal moraine that blocked the drainage, creating the polje. Note the very steep dip of Mount Kindle Formation dolomites on either flank in the foreground, forming a V-shaped syncline down the valley axis. **b** Looking up the polje from a stance on the terminal moraine. The *arrow* indicates the entrance to a cave that drains all stream flow in the polje. **c** A fine example of periglacial pedimentation truncating steeply dipping dolomites on the west flank of the polje. **d**, **e** Two views of 'Giant Fist Spring' where the cave water resurges

~975 masl. It is possible to follow the stream through a cave for 50 m before it becomes impassably wet under summer flow conditions. The cave morphology is simple and youthful, without any deposits such as stalagmites.

The stream resurges approximately 1600 m south of the sink at ~775 masl at a spring that the first author has named, with some justification, 'Giant Fist Spring' (Fig. 14.4d, e). It appears that the groundwater first burst out at this point under explosively high pressure; it is one of the most remarkable spring orifices we have seen. In dry weather in 1983, fluorescein tracer dye injected at the stream sink was observed at the spring 5 h later. This result gives a minimum groundwater flow rate of 300 m/h. The actual rate will be faster because the flow will not follow a simple straight line. It indicates that the cave must be a solutional pipe large enough throughout its course to permit vigorous turbulent flow.

Moraine Polje is the best example the first author has seen of glacial moraine blockage creating a large karst landform. It is an outstanding example of karstic drainage exploiting an obstruction to surface river flow to capture the water underground, all the more remarkable because it happened very rapidly in dolomite, the least soluble of the common karst rocks.

14.3.3 Pyramid Lake Polje

Pyramid Lake (Fig. 14.5a) is located at latitude 64°42′N, longitude 127°15′W. The lake surface is ~786 masl,

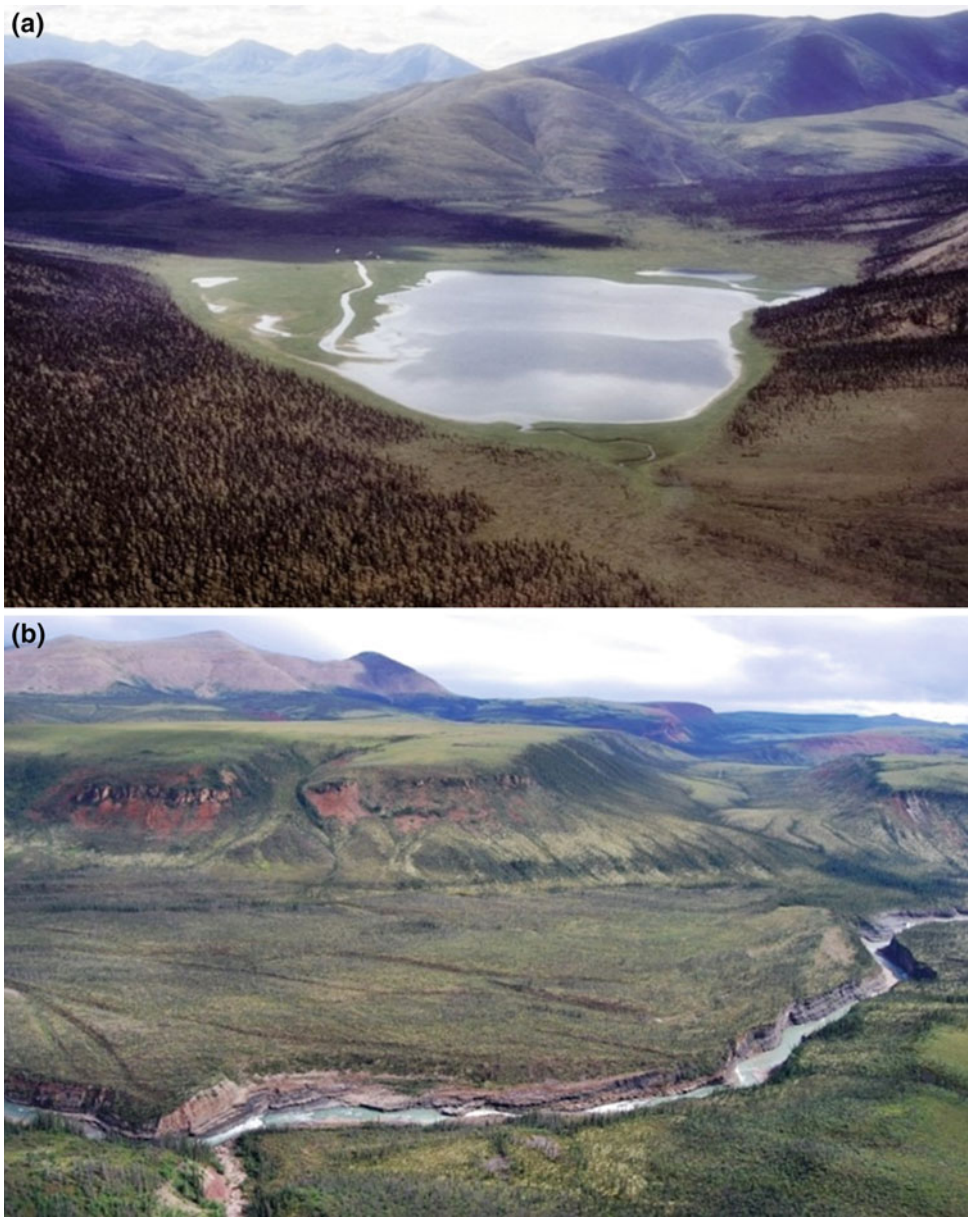

Fig. 14.5 **a** Pyramid Lake, a karst lake drained underground along a syncline in the Franklin Mountain Formation dolomites. The Canol Road traverses the foot of the slopes behind the lake. **b** From Pyramid Lake the Canol Road winds north across the Little Keele River, which has been captured by knickpoint recession from a tributary of Carcajou River; the capture gorge, in Mount Kindle Formation dolomites, is seen here with stratiform cryopedimentation beyond it

fluctuating a little seasonally. It occupies an alluvial lowland depression that is topographically closed and drained underground karstically, and thus functions as a karst polje. The view in Fig. 14.5a looks west across it towards the Plains of Abraham. The Canol Trail crosses the scene at the foot of the hills behind the lake.

The polje has a catchment basin of 34.4 km^2 and is fed by a series of small channels. Surface water in the basin enters the karst drainage system via two sets of pathways. Flow from the largest channel to the polje was observed to sink in the creek bed upstream of the lake. Other water that enters the basin sinks into bedrock at the south-western apex of the lake. A dye trace established a route from the losing section of the stream to 'Horseshoe Springs' (unofficial name) located almost 6 km to the north-east, with a flow time of 4 days or ~1500+ m/day. The underground flow broadly follows a synclinal downfold in Franklin Mountain Formation dolomites: this is a polje determined chiefly by geological structure rather than by morainic obstruction. Supposedly, the area was glaciated during the ancient Katherine Creek glacial stage of the Wisconsinan but escaped later glacier action. It is predominantly a periglacial landscape of intense solifluction creating long, gentle footslopes (cryopediments). It displays many morphological similarities with Moraine Polje but has a different origin. This pair of large, subarctic poljes thus contrast neatly in genetic terms.

14.3.4 Dodo Dry Canyon

The large tributary river shown immediately north of the Plains of Abraham in Fig. 14.1a is the Little Keele River. The Pyramid Lake Polje drains into it through Horseshoe Springs. Until the Katherine Creek glacial stage or some time later Little Keele River formed the headwaters for all flow into modern Dodo Canyon. It was then captured via knickpoint recession from a tributary of Carcajou River (see Fig. 14.5b). This capture left a 10 km stretch of the former course without any major surface streams to supply it; the lower two-thirds of this is a canyon entrenched into the Franklin Mountain and Mount Kindle dolomites, 'Dodo dry canyon' (Fig. 14.6).

At the head of the dry canyon the approaches to a paleo-waterfall that was 40 m in height have been converted into a karst sinkhole for local streams. Below it there are continuous cliffs along the upper walls while the canyon floor is occupied by coalescent talus slopes and cones interspersed with a few shorter stretches of alluvial deposits (Figs. 14.6a, b). A seasonal pond forms in talus below the paleo-falls, there is a longer lake (~600 m; Fig. 14.6c) at the mouth of the dry canyon that may be a permanent feature, and a few shallow ponds in the alluvial sections in between. However, there are no continuous channels, or visible suggestions of continuous underflow in the talus and alluvium that fill the canyon floor. The locations of any springs have not been established.

One striking feature halfway along the canyon is the occurrence of apparently weakly consolidated or unconsolidated fill within or at the top of the Franklin Mountain strata. These have the appearance of *terra rossa* and *terra fusca* soils and thus may be an ancient palaeokarst (Fig. 14.6b). A second striking feature of this canyon is the presence of torrential debris flow channels in some of the larger talus cones, as shown in Fig. 14.6b, c. Those in Fig. 14.6b are conveying clasts from the Franklin Mountain infillings; those in Fig. 14.6c are in the lower Mount Kindle dolomites. Further debris flow channels are seen in Bear Rock breccias in the Great Spillway but space does not permit us to illustrate them. The channelled debris flows probably occur during the occasional but intense summer storms.

14.3.5 Dodo Creek Canyon

Modern Dodo Creek follows the course created when it was augmented by flow from the Little Keele River and meltwater from the Laurentide Ice Sheet. For a distance of 17 km, it crosses a major anticline (MacDougal Anticline) more or less directly. As a consequence, it first entrenches through progressively older rocks until the anticlinal axis is reached, after which the channel cuts through the formations in reverse order towards the canyon mouth. The thalweg descends from 610 masl at the head to 325 masl at the exit into the Mackenzie Valley, a very steep mean gradient of 17 m/km. No bedrock is exposed in the channel bottom; the creek flows on abundant coarse debris supplied from the canyon walls to the alluvial channel. The walls range 120–400 m in height over the lower half of the course, where enclosing mountains rise to maxima of 900–1100 masl behind them.

As Fig. 14.7 suggests, it is a very colourful journey. Figure 14.7a looks downstream across upper beds of the Saline River Formation. Red, brown and black shales, yellow and orange siltstones are exposed in rapid succession along the course due to tight anticlinal folding with local thrust fault displacements. It will be observed that the channel has carved a tightly meandering 'valley-in-valley' in these readily erodible strata that represents the net entrenchment since Dodo Creek lost the Little Keele flow, leaving it an underfit in the broader valley above. This

Fig. 14.6 **a** View up Dodo dry canyon from its midpoint. **b** Apparent palaeokarst fills in the canyon west wall at the midpoint, with torrential debris flow channels seen in the talus cones below. **c** The mouth of the dry canyon with a small lake, and view into the modern active canyon downstream

underfit form is lost lower down, where the creek is augmented by major tributaries.

Figure 14.7b–d show off the most spectacular parts of Dodo Canyon, where it is entrenched into the eastern dip slope of the anticline and so passes progressively upwards through the stratigraphic succession again. In Fig. 14.7b, the redbeds are at the Saline River–Franklin Mountain juncture with basal dolomites of the latter formation standing up as vertical cliffs above them. One block has dropped prominently: it is not known whether this is an incipient rotational landslide due to some failure within the redbeds, or attributable to salt and anhydrite solution below them. The arrow indicates remains of one of the largest Canol camps; the pipeline and road were taken straight up the canyon here.

Figure 14.7c shows the orange-weathering beds of the middle Franklin Mountain Formation dolomites dipping below the canyon floor. There are a dozen bright pinnacles in the cliffs here, which rise 250 m. In the background, the grey-weathering Mount Kindle dolomites succeed them. In Fig. 14.7d, regularly bedded Mount Kindle dolomites in foreground dip below the canyon floor in their turn and are succeeded by 140 m cliffs in the highly disordered breccias of the Bear Rock Formation. It is a canyon of many colours!

14.3.6 The Dodo West Dolomite Pavements

On the west side of lower Dodo Canyon, the resistant dolomites of the upper Mount Kindle Formation are exposed over a tract of approximately 6 km^2 between 800 and 600 masl, dipping gently towards the Mackenzie Valley (Fig. 14.8a). They were scoured vigorously by the Wisconsinan ice, so it is interesting to contrast their appearance with that of essentially the same strata in the unglaciated zone shown in Fig. 14.2. The dolomites here are cyclic sequences of massive beds with many vugs and thinner, more fossiliferous beds (Fig. 14.8b). This alternation allowed the ice to strip the layers by bulldozing along the weaker interbeds, creating a stepped landscape of a type well studied in the Alps where it is known as ‘schichttreppen (staircase) karst’ (Lundberg and Ford 1994).

Many of the principal types of karren (small solution forms) found on pavements of pure limestone such as

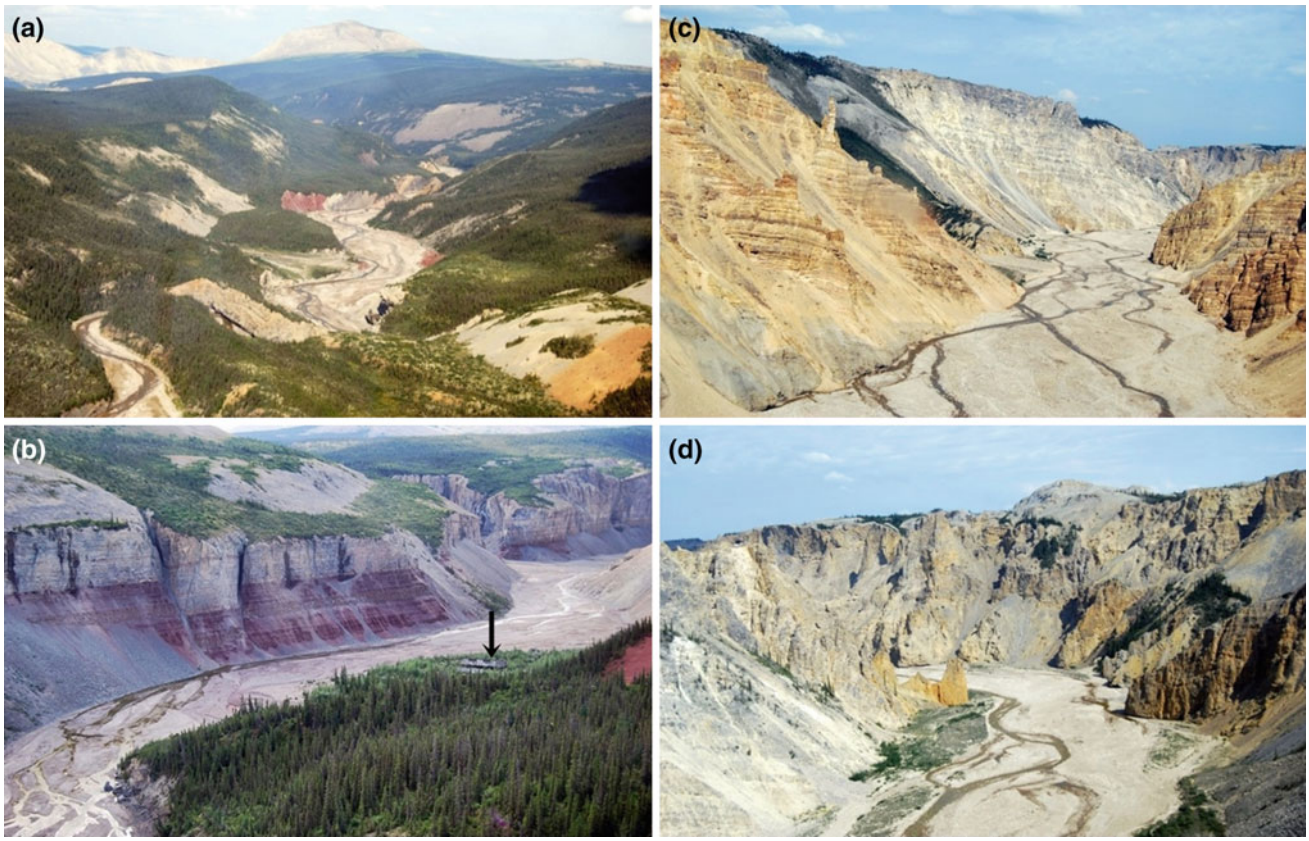

Fig. 14.7 **a** The 'valley-in-valley' form where Dodo Creek entrenches rocks of the Saline River Formation across the crest of an anticline. **b** Dodo Canyon at the contact between the Saline River and Franklin Mountain formations. The *arrow* indicates the remnants of a Canol Road construction camp. **c** Franklin Mountain Formation dolomites dip below the canyon floor in the foreground, Mount Kindle Formation dolomites in rear. **d** Mount Kindle Formation dolomites dip below the canyon floor, Bear Rock Formation breccias (*in rear*) are entered through a portal. See the text for further details

solution pits, flat-floored pans and linear troughs along joints (grikes) are to be seen on the Dodo pavement (Fig. 14.8c), but there is a dearth of the simple channel forms such as tiny rills or more robust runnels on the clints (surfaces between the joints). This is characteristic of dolomites in our experience, attributable to their lesser solubility. Instead, channelled dissolution is represented by a few subglacial 'p-forms' (Fig. 14.8d). However, the morphology of the clint surfaces is richly variable due to the substantial compositional changes that occur up the succession of massive beds: some are homogeneous planar surfaces, others are richly fossiliferous with projecting siliceous coral heads and solutional pitting of the fine-grained dolomite in between.

The glacial scour and subsequent overwash by melt water as the ice front receded were efficient. There is remarkably little erratic material of any size on the dolomite surfaces, and the lack of fines limits the growth of tundra. The Dodo west pavements are exceptionally clean in this regard, the finest examples of schichttreppen karst known to us in the arctic and subarctic regions.

14.3.7 The Bear Rock Drape Karst of Dodo Canyon

Between Dodo Canyon and Carcajou Canyon to the east of it, the Bear Rock Formation breccias are exposed in a roughly rectangular block measuring 3 × 3 km. It extends down the dip slope of the anticline from ~600 masl (the 'zero sub-edge' of the breccia outcrop because upslope all of it has been lost to solution) to 300 masl, where it enters a relict section of the Great Spillway before passing below overlying limestones of the Hume Formation. Features seen in this block may be considered characteristic of landforms that develop on Bear Rock outcrops elsewhere, for example, on the Bear Rock itself, near Tulita 170 km to the southeast. But the intensification of solutional, glacial and periglacial processes at this particular locality has combined to produce a morphologically fantastical landscape not described anywhere else in the world. It was the dramatic appearance of this landscape on air photos that drew the first author to reconnoitre the region in 1983. Meltwaters from the

Fig. 14.8 **a** A general view of the Dodo west karst pavements on the Mount Kindle Formation dolomites. **b** Illustrating the cyclic deposition of the dolomites. **c** A typical 'clint-and-grike' karst pavement. **d** A relict P-form subglacial channel on the pavement

Laurentide Ice Sheet formed spillway channels and related forms. This was succeeded by the post-glacial development of permafrost competing with the circulation of meteoric groundwater through the breccias. Collectively, these processes have scoured corridors and formed sinkholes into the breccias, preferentially sapping or destroying its softer parts and leaving large fragments of more resistant, hardened surface crusts such as the Landry Member draped on ridges and sliding down into solutional depressions—the 'drape karst', a unique landscape (Fig. 14.9a).

Hamilton (1995) divided the karst into three broadly parallel belts: (a) upslope, a belt of comparatively weak scour by Laurentide meltwaters where allogenic streams flow into the karst and sink, subsidence troughs create dry valleys and scattered lesser sinkholes develop; (b) a central, more dissected, belt of closed depressions that are highly

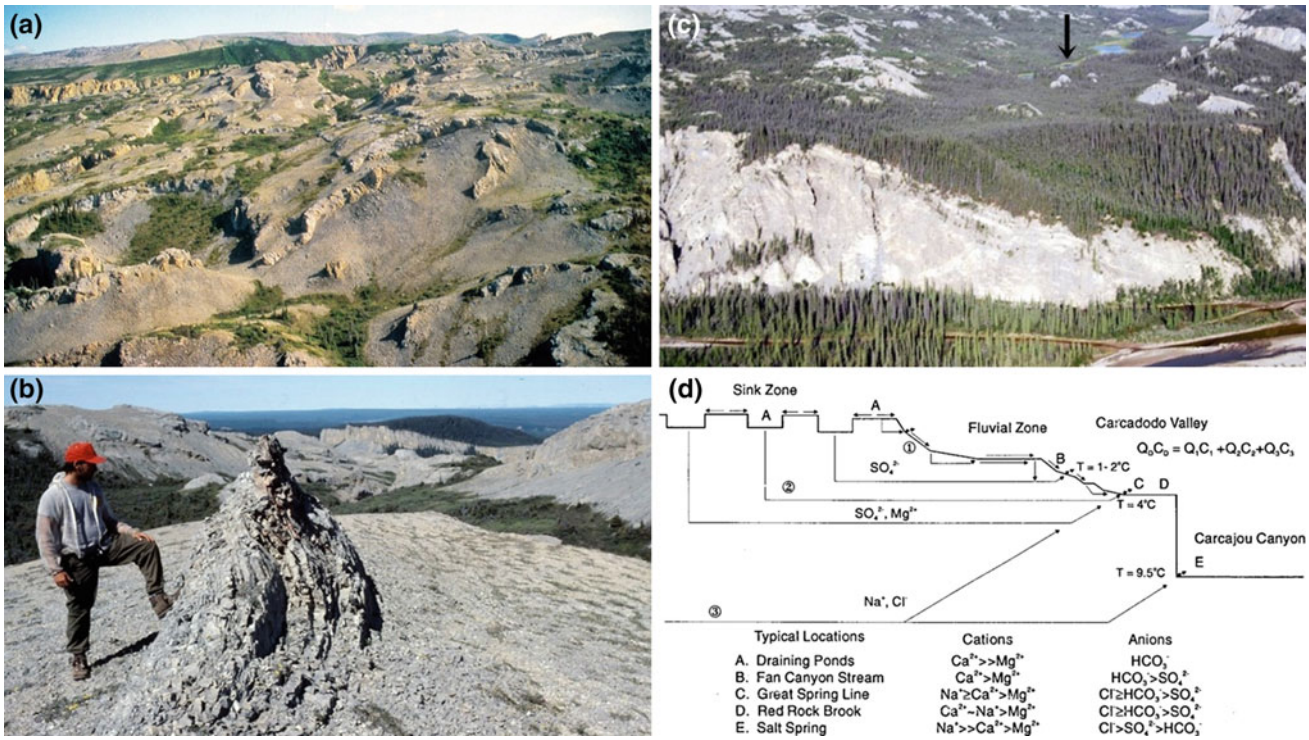

Fig. 14.9 **a** A general view of the central area of the Bear Rock Formation drape karst. **b** An example of a block of resistant 'pack breccia' that has been rotated into the vertical by a combination of solutional undermining and frost heave. **c** View along the line of springs that drain the drape karst. The *arrow* indicates where the waters sink underground again, to rise in the floor of Carcajou Canyon in the foreground; the deeply stained waters there are salt springs. **d** Model of the chemistry of the karst groundwaters (Hamilton 1995). See the text for further details

irregular in form and depth that is exemplified by Fig. 14.10; and (c) 'Carcadodo Valley', a part of The Great Spillway (below) where much of the water that sinks in belts (a) and (b) returns as springs, only to sink again at the east end of the valley and rise as freshwater and salt springs in Carcajou Canyon (Fig. 14.9c). There are also small caves formed by seepage and frost action in cliffs ('frost pockets') and stream caves blocked by detritus or ice. Periglacial processes attack all features, partially filling them with talus and solifluction lobes or establishing patterned ground.

Hydrological and water chemical conditions were investigated over three melt seasons (Hamilton 1995; pp. 249–338). Early in the season surface flows fed by spring waters have a $Ca + HCO_3$ ionic composition representing the dominance of shallow circulating meltwaters. In mid-season, the larger springs change to a $Mg + SO_4$ composition with water temperatures as great as 4 °C, indicating the discharge of deeper waters that are accomplishing dedolomitization. The few perennial springs (which create winter 'icings' or *naledi*) have a significant Na + Cl component and temperatures up to 9 °C, showing deep circulation. Modelling suggests that there are three components to the groundwater circulation system involving the Bear Rock Formation and the underlying dolostones and salt-bearing units (Fig. 14.9 d). The sulphate concentrations from springs at the base of the Bear Rock Formation show that the brecciation processes continue today. Analysis of oxygen isotope patterns in the precipitation, sinking streams and springs, indicates that mean residence times of the central, $Mg + SO_4$ groundwaters are 40–90 days.

14.3.8 'Bonus Lake' Karst in the Great Spillway

'Bonus Lake' is the authors' unofficial name for a lake at latitude 64°32′N, longitude 126°40′W. On all published maps, and Google Earth and similar imagery, it is shown as a normal lake drained by a surface stream at its north end, with the water surface stable at ~519 masl. Like Moraine Polje, it is at some distance from the Canol Trail (Road) traverse (Fig. 14.1). However, it is genetically linked by its location in the late glacial 'Great Spillway', and the fact that the lake is a seasonal feature and karstic, as Figs. 14.11a, b clearly show. There is a prominent limestone cave above the west

Fig. 14.10 Pond sinkholes and dry solution troughs in the highly disordered central zone of the drape karst. This is a unique landscape

shore of Bonus Lake (Fig. 14.11d); so the name 'Grotto Lake' is used by some local visitors.

This distinctive landscape is best understood by referring to Fig. 14.11a, b. The former was taken looking upstream to the south-east up the spillway; in it the right bank is in Hume Formation limestone underlain by Bear Rock Formation breccias, both dipping eastwards into the channel. The left bank is in later Devonian clastic rocks, also dipping eastwards and thus away from the channel. The rugged topography seen on the right bank (Fig. 14.11a) is developed in the Hume Formation and is due to the combination of lateral rotational landsliding into the channel, undermining of the resistant limestone caprock by solution directed downwards into the breccias underneath it and to glacial meltwater scour. Individual slumping blocks are up to hundreds of metres in length and tens of metres in breadth. Their integrity is maintained as they tilt eastwards and settle downwards, as shown in Fig. 14.11d by the preservation of the large, intact solutional cave in the limestone. The natural arch in Fig. 14.11c is entirely in the breccia, indicating that it too can support channelled flow underground. Other distinctive features in the photographs are the occurrence of three large (100+ m diameter) scour holes (depressions) rather uniformly distributed along the limestone bank of the lake (Fig. 14.11b) and a highly streamlined, barchan-like limestone block downstream of it, detached from the main mass and possibly transported *en masse* to its present position. These are taken to indicate that at least one scabland-type megaflood swept down the spillway when it was active.

The lake is a ponding that was created by the extension of a large alluvial fan across the spillway downstream of it. The channel scour holes have been adapted to function as karst ebbing-and-flowing wells (Fr—*estavelles*), discharging water into the lake under wet conditions and swallowing it in droughts. The upstream scour feature in Fig. 14.11b was discharging groundwater weakly when the photograph was taken in August 2007 but the scours downstream of it were swallowing its output and the lake was slowly shrinking in volume. Quite possibly, the scours themselves are enlargements of pre-existing karst sinks. Today, the groundwater moves by conduit flow through the Bear Rock and Hume formations to springs 3–4 km downstream of the fan and ~10 m lower in elevation (Hamilton 1995; pp. 339–373).

Fig. 14.11 **a**, **b** Two views of the 'Bonus Lake' karst terrain in the Great Spillway. **c** A natural arch in the Bear Rock Formation breccias. It is 10 m in height. **d** A solution cave in Hume Formation limestone perched on top of the breccias. It has an impressive entrance but shrinks rapidly, pinching out in a fill of permafrozen silt about fifteen metres inside. See the text for further details

14.3.9 Features of the Great Spillway

By 12 ka BP, the marginal spillway that had been carved by surface melt runoff from the Laurentide Ice Sheet just inside the front of the Mackenzie Mountains lost its flow due to the recession of the ice (Dyke et al. 2003). It was oriented essentially across the paths of the energy flows of the wide variety of geomorphic processes moving water, solutes and solid debris down the mountain front into the Mackenzie Valley. These processes have chopped the spillway into pieces of different size, form and function today. The karst developments at Bonus Lake described above is one example. This review concludes with four others, each different in form and function, to further underline the rich diversity of landscapes along the Canol Trail. They are illustrated in Fig. 14.12.

Carcajou River is the largest river in this region. It maintained a steady northeasterly flow from the Plains of Abraham (Fig. 14.1) until it was within 3 km of the Mackenzie Valley, where it was abruptly turned through 90° to follow the Great Spillway for 30 km inside the mountain front before finally breaking out. The mean channel gradient along this reach is 3.7 m/km today, a sharp contrast to the 17 m/km of Dodo Creek which was able to maintain its northeasterly trend almost directly into the valley. At its outlet, Carcajou River has entrenched ~63 m below the original floor in the spillway. Along its course, the canyon walls rise up to 300–500 m above the river, exposing upper Franklin Mountain Formation and Mount Kindle Formation dolomites and many tens of metres of the Bear Rock breccia (Fig. 14.12a).

Carving of the Spillway into the foot of the Bear Rock drape karst created an inescapable spring line there, its karst water initially joining the Laurentide melt water to flow to the north. Following glacial recession, entrenchments by the Carcajou River to the south and Dodo Creek to the north left this short section of the spillway hanging at both ends. The southern entrenchment is much deeper, so the direction of flow along the spillway has been reversed by a combination of karst captures to the Carcajou River springs (Fig. 14.9c) and encroachment by alluvial fans (Fig. 14.12b).

Figure 14.12c shows 3 km of the Great Spillway between the Dodo west pavements and Katherine Creek, which intercepts it to the north. Here it is 500 m wide and 150 m deep, entrenched into Mount Kindle Formation dolomites. Its form and magnitude are better appreciated in this scene than elsewhere because it has remained largely untouched since it was abandoned. The rotational landslide is another

Fig. 14.12 **a** A section of the Great Spillway that was adopted by Carcajou River. The canyon walls here are ~450 m in height, in Franklin Mountain and Mt Kindle Formation dolomites topped by remnants of the Bear Rock breccias. **b** The spillway remnant collecting spring flow at the foot of the drape karst. Cliffs to the right are in the Hume Formation limestones. **c** The Great Spillway between Dodo Canyon and Katherine Creek, showing a large rotational landslide. **d** The spillway north of Katherine Creek, where it becomes overwhelmed by debris flow from the Bear Rock breccia cliffs to the west (*left*)

'textbook' example of a specific landform, with six successive slice failures; it is the more remarkable because rotational landsliding is very rare in massive dolomites.

North of Katherine Creek, the Great Spillway was carved along the contact between the Bear Rock Formation breccias and the Hume Formation limestone, as it was at the foot of the drape karst. The dip of the breccias is much steeper here, however, with bare slopes 250–350 m in height that are deeply gullied. As a consequence, the spillway becomes increasingly aggraded by torrentially deposited detrital fans and with its footwall in the limestone breached by their runoff (Fig. 14.12d) until, at the end, one particularly large fan destroyed it completely.

14.4 Conclusions

It has been shown that the geomorphic landscapes along this transect from the Plains of Abraham to the edge of the Mackenzie Valley are exceptionally rich in their variety of forms, processes and causes. They are linked together by a similarly rich physical history of sedimentation, diagenesis and tectonic deformation in the rocks, of glacier advances and retreats across them at the cold arid limits of Quaternary glacierization, and by the historical construction of the Canol Road. As noted, the road is now designated as the Canol Heritage Trail by the Territorial government, while the planning board of the Sahtu First Nation has proposed that the eastern half of the transect should be protected as the Doi T'oh Territorial Park.

In 2010, the first author recommended that this Territorial Park be extended along the road to include the Pyramid Lake country and Plains of Abraham, plus two annexes (outliers) to recognize and protect Moraine Polje and the Bonus Lake karst (Ford 1993). It was further argued that, once established, the park should be put forward for recognition as a UNESCO 'World Heritage' natural (landscape) property. There are ten different criteria for this highest level of international recognition. Qualification under any one of them is sufficient. The first six criteria are cultural (pertaining to particular buildings, sites, towns, etc. that are meritorious), the other four natural. Criterion VII reads that a site

('property') may be inscribed in the World Heritage list if it is judged 'to contain superlative natural phenomena or areas of exceptional natural beauty and aesthetic importance', and Criterion VIII. '…to be outstanding examples representing stages in earth's history, including the record of life, significant ongoing geological processes in the development of landforms, or significant geomorphic or physiographic features' (see chap 29).

In 1978, South Nahanni River National Park Reserve was one of the first four natural properties to be placed on the World Heritage list, based in good part on the evidence presented by the first writer here (Ford 1974). Since that time much further experience has been gained, in advising national committees preparing proposals for natural properties and advising UNESCO on the quality of other proposals. The Canol Road transect is not as large or as visually spectacular as South Nahanni but it is more than sufficient to qualify for the World Heritage list under both criteria, VII and VIII. It is especially important because subarctic mountain landscapes in general are poorly represented on the list, and certain of the karst landforms described here are believed to be truly unique.

Acknowledgments Our primary acknowledgement is to our companions in the field in this remote region. Most of the fieldwork was supported by research grants to Ford by the Natural Science and Engineering Research Council of Canada. The Protected Areas Strategy Group, Ministry of Environment and Natural Resources, Government of the Northwest Territories, and Ducks Unlimited are thanked for their support in 2007.

References

Aitken JD, Cook DG (1974) Carcajou Canyon map area, District of Mackenzie, Northwest Territories. Geol Surv Can, Paper 74-13

Aitken JD, Cook DG, Yorath CJ (1982) Upper Ramparts River (106G) and Sans Sault Rapids (106H) map areas, District of Mackenzie, Northwest Territories. Geol Surv Can, Memoir 38

Duk-Rodkin A (2002) Surficial geology, Norman Wells, District of Mackenzie, Northwest Territories. Geol Surv Can, Map 1989A, scale 1:250,000

Duk-Rodkin A, Hughes OL (2000) Surficial geology, Carcajou Canyon, District of Mackenzie, Northwest Territories. Geol Surv Can, Map 1788A, scale 1:250,000

Duk-Rodkin A, Lemmens DS (2000) Glacial history of the Mackenzie region. In: Dyke LD, Brooks GR (eds) The physical environment of the Mackenzie Valley, Northwest Territories: a base line for the assessment of environmental change. Geol Surv Can Bull 547:11–20

Dyke AS, Moore A, Robertson L (2003) Deglaciation of North America, Geol Surv Can Open File 1574

Ecoregions Working Group (1989) Ecoclimatic regions of Canada, first approximation. Environment Canada, Ottawa

Environment Canada (2015) Canadian monthly climate data and 1981–2010 normals (online). Ottawa, ON. http://climate.weather.gc.ca/climate_normals/. Accessed 11 Feb 2015

Fallas KM, MacNaughton RB (2014) Geology, Carcajou Canyon (northwest), Northwest Territories. Geol Surv Can, Canadian Geoscience Map 94, Scale 1:100,000

Ford DC (1974) Geomorphology of South Nahanni National Park, N. W.T. Contract 72-32B, Parks Canada, 186 p, 7 map plates

Ford DC (1987) Effects of glaciations and permafrost upon the development of karst in Canada. Earth Surf Process Landf 12:507–522

Ford DC (1993) Karst in the cold environments. In: French HM, Slaymaker O (eds) Canada's cold environments. McGill-Queen's University Press, Quebec, pp 199–222

Ford DC (2008) Report upon a survey of Karst Landforms around Norman Wells, Northwest Territories. Protected Areas Strategy Group, Ministry of Environment and Natural Resources, Government of the Northwest Territories, Yellowknife

Ford DC (2012) Mapping known and potential karst areas in the Northwest Territories, Canada. Environment and Natural Resources, Government of the Northwest Territories, Yellowknife

Ford D, Williams P (2007) Karst Hydrogeology and Geomorphology. Wiley, Chichester, p 562

Hamilton JP (1995) Karst geomorphology and hydrogeology of the northeastern Mackenzie Mountains, District of Mackenzie, N.W.T., Canada. PhD thesis, McMaster University

Hamilton J, Ford DC (2002) Karst geomorphology and hydrogeology of the Bear Rock formation—a remarkable dolostone and gypsum megabreccia in the continuous permafrost zone of Northwest Territories, Canada. Carbonates Evaporites 17:114–115

Heginbottom JA, Radburn LK (1992) Permafrost and ground ice conditions of northwestern Canada. Geol Surv Can, Map 1691A. Scale 1:1,000,000

Lemmen DS, Duk-Rodkin A, Bednarski JM (1994) Late glacial drainage systems along the northwest margin of the Laurentide Ice Sheet. Quat Sci Rev 13:805–828

Lundberg J, Ford DC (1994) Dissolutional pavements. Can Geogr 38:271–275

Macqueen RW (1970) Lower Paleozoic stratigraphy and sedimentology, eastern Mackenzie Mountains, northern Franklin Mountains (96C, D, E, F; 106G, H). Geol Surv Can, Paper 70-1A, pp 225–230

Meijer Drees, NC (1986) Evaporitic deposits of Western Canada. Geol Surv Can Paper 85–20

Meijer Drees NC (1993) The Devonian succession in the subsurface of the Great Bear and Great Slave Plains, Northwest Territories. Geol Surv Can Bull 393

Morrow DW, Meijer Drees NC (1981) The Early to Middle Devonian Bear Rock Formation in the type section and other surface sections, District of Mackenzie. Geol Surv Can, Paper 81-1A, pp 107–114

Smith DG (1992) Glacial Lake Mackenzie, Mackenzie Valley, Northwest Territories, Canada. Can J Earth Sci 29:1756–1766

Stanton RJ (1966) The solution brecciation process. Geol Soc Am Bull 77:843–848

The Many Landscapes of South Nahanni National Park

15

D.C. Ford

Abstract

South Nahanni National Park comprises the S. Nahanni and Ram River basins, c. 38,000 km^2 in area and extending from the continental divide (Yukon boundary) eastwards to the margins of the Mackenzie River plains. Elevations range from 2500 masl (polar desert ecozone) to 200 masl (boreal forest). Continuous permafrost conditions begin c. 600 masl. The geomorphic landscapes are exceptionally rich and diverse, including (1) rugged Cordilleran glacial landforms (cirques, arêtes, horn peaks, etc.) in resistant batholithic rocks of Cretaceous age in the west; (2) broader glacial troughs and V-form fluvial tributaries in weak, structurally deformed Lower Paleozoic sedimentary strata in the centre; (3) deep antecedent river canyons, stripped anticlines and synclines in stronger Upper Paleozoic limestones and dolostones in the east, with (4) an inter-basin belt of karst landforms and caves, the most accentuated reported in any sub-arctic or arctic region; (5) thick deposits of sand, silt and clay in proglacial lakes created by Laurentide continental ice blocking the river outlets to the Mackenzie plains: the deposits are terraced or dissected and, in the last 25 years, beginning to display widespread slumping that is due to the thawing of ground ice.

Keywords

Alpine and continental glaciations • Antecedent river canyons • Proglacial lakes • Karst and caves

15.1 South Nahanni National Park

A full transect of South Nahanni National Park from the Backbone Ranges to the Mackenzie Valley at latitude 61°–62°N is presented here. The topography and extent of the Park (Fig. 15.1) are shown. It has a complicated foundational history, being first suggested in the late 1960s to protect against hydroelectric developments that were proposed for the South Nahanni River below Virginia Falls. In 1972 a 'Nahanni National Park Reserve' corridor was established along the river from Rabbitkettle Lake at the edge of the batholithic rocks ('Ragged Range') downstream to 'The Splits', a braided segment of the river just above the community of Nahanni Butte on the junction with the Liard River. One year earlier, the writer was invited to evaluate newly discovered limestone caves in the First Canyon and from that experience undertook to compile what was known of the bedrock geology in the Reserve and study its geomorphology and hydrology, on behalf of Parks Canada (Ford 1974a, b). Scotter et al. (1971) similarly appraised the flora, fauna and ecological zoning. Based on this documentation, in 1978 the Reserve was inscribed as one of the first four UNESCO World Heritage natural sites.

It was always the plan of Parks Canada to expand the national park to encompass the conventional (topographically defined) drainage basin of South Nahanni River when

D.C. Ford (✉)
School of Geography and Earth Sciences, McMaster University, Hamilton, ON L8S 4K1, Canada
e-mail: derekcliffordford@gmail.com

© Springer International Publishing Switzerland 2017
O. Slaymaker (ed.), *Landscapes and Landforms of Western Canada*,
World Geomorphological Landscapes, DOI: 10.1007/978-3-319-44595-3_15

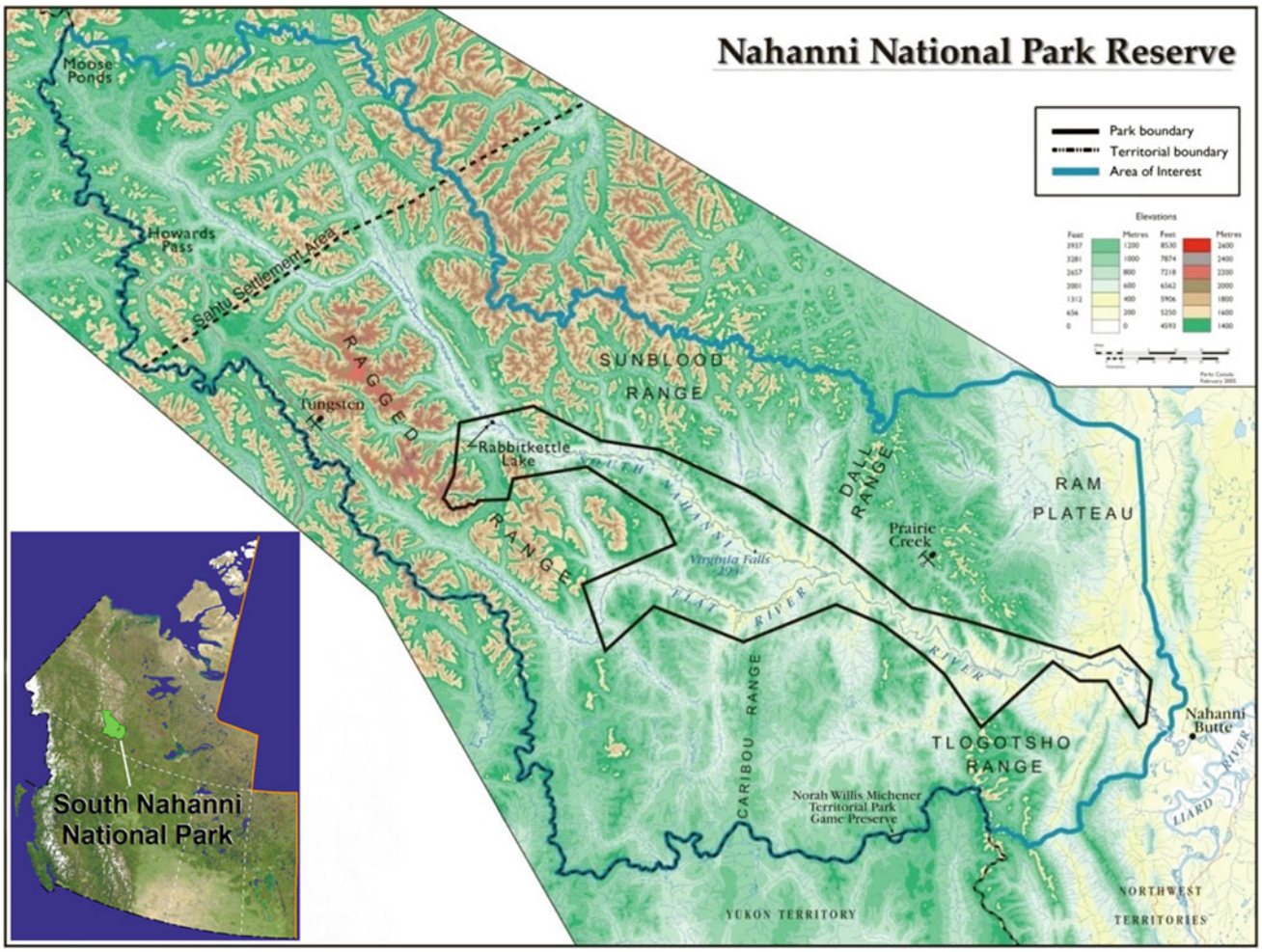

Fig. 15.1 The location and topographic features of the Nahanni National Park, Northwest Territories, Canada. The *blue lines* denote the hydrological boundaries of the South Nahanni and Ram River basins, excluding only their downstream extremities. Following legislation in 2009 and 2012, they have also become the boundaries of the much enlarged South Nahanni National Park (east of the Sahtu Settlement line) and Naats'ihch'oh National Park (west). The *black boundaries* denote 'Nahanni National Park Reserve', an initial protected area established in 1972. *Inset image* NASA, Visible Earth

feasible (Gimbarzevsky et al. 1979). In 1974 the writer advocated including the Ram River basin to the north of it in addition because there was karstic groundwater flow of unknown extent between the two basins (Ford 1972, 1974a; Brook and Ford 1975). In 2009 the Ram basin and all of the South Nahanni basin that is within the domain of the Deh'cho First Nation were incorporated, and in 2012 that of the Sahtu First Nation was added as the Naats'ihch'oh National Park at the head of the basin. There are exclusions around two mineral properties, Cantung (tungsten) on Flat River, the principal south bank tributary of the South Nahanni, and on Prairie Creek (zinc, lead, silver) an important tributary on the north bank.

15.2 A Geomorphological Transect from the Ragged Range to First Canyon

A trip of c. 300 km down the South Nahanni River from Rabbitkettle Lake to The Splits exposes the voyager to a singularly rich variety of erosional and depositional landforms—glacial, periglacial, fluvial, karstic, pseudo-karstic, mass-wasted, even thermal: only aeolian dunes and coastal cliffs seem to be missing from a representative global geomorphic typology—although there are blowouts in soft sandstones southeast of First Canyon and careful search around the margins of some of the large proglacial lakes that formed during the Wisconsinan glaciation will probably turn

up local wave-cut benches and cliffs. Space limitations permit only a summary of some of the highlights here; for more details, see Ford (1984, 2008) and Ford and Worthington (2009).

15.2.1 Simplified Geology, Structure and Glacial History

A highly schematic picture of the bedrock geology along the transect is presented (Fig. 15.2). The Ragged Ranges are a dissected batholith of Cretaceous age, composed chiefly of massive and resistant quartz monzonites and granodiorites. They were injected into, and greatly deformed, Lower Paleozoic (Late Cambrian–Silurian) clastic and carbonate strata totalling c. 2200 m that are now dominant in outcrop between the Rabbitkettle hot springs and the middle of Third Canyon. These strata are mostly thin-bedded limestones, dolomites, sandstones, shales and calcareous shales that are generally weak and readily erodible, especially in the valley of the Flat River, but include the Sunblood Formation (Middle Ordovician) which has a thick and resistant limestone member at the base that supports Virginia Falls and much of Third Canyon.

Further east the outcrops are dominated by resistant carbonates and sandstones of Devonian and Carboniferous age. At the First and Second Canyons and beneath the main sector of the Nahanni karstlands north of them, the base is composed of two successive dolomite formations, the Arnica and the Manetoe, with a total thickness of 1000 m or more. The bedding is medium to massive, with visually striking colour banding in some sub-units. Further north, these thick and resistant dolomites are replaced by a similar thickness of argillaceous limestones and calcareous shales (Headless and Funeral formations) that are much weaker, with important consequences for the development of the landforms.

The strata that host most of the karst landforms and all of the known caves are limestones of the Nahanni Formation (Middle Devonian), $\geq$180 m of ideal karstic rock, pure, thick- to massively bedded and resistant. Overlying it are c. 1500 m of recessive limestones, calcareous shales, shales, mudstones and sandstones (Horn River, Fort Simpson, and Yohin formations; Late Devonian–Carboniferous) that are locally exposed in low cuestas in a syncline between First Canyon and the Front Range. The sequence is concluded by the Mattson Formation (Carboniferous), a classic red sandstone caprock: it supports the Tlogotsho Range, a fine example of a dissected tundra plateau south of the Reserve, but is not prominent elsewhere in the Park.

From air photograph analysis and excursions on foot from bases along the South Nahanni River and in the eastern Ram basin, Ford (1973, 1974a, b) reported that, during the Quaternary glaciations, Cordilleran valley glaciers that accumulated in the Ragged Ranges were able to extend eastwards down the Reserve as far as the head of the Third Canyon on the River. The Laurentide Ice Sheet, advancing westwards up the Reserve, was halted at about 1400 masl on Nahanni Plateau (the unroofed anticline entrenched by the First Canyon, Fig. 15.2), but edged around it on lower ground to the south to reach the exit of the Second Canyon and abrade a low limestone spur there. The terrain in between was part of the never-glaciated corridor found down the central Mackenzies. Based on more recent images and survey by helicopter, Duk-Rodkin and Lemmens (2000) have proposed that in the Wisconsinan Glaciation there was much deeper penetration by the Laurentide Ice Sheet and that it met the Cordilleran glaciers as far upstream as Virginia Falls (see Figs. 15.1, 15.2): if that is correct, it must be stressed that there is little or no morphological evidence of glacial erosion in the landscapes of the corridor, which are those of fluvial dissection, frost, glacilacustrine deposition and its subsequent partial removal by rivers and streams.

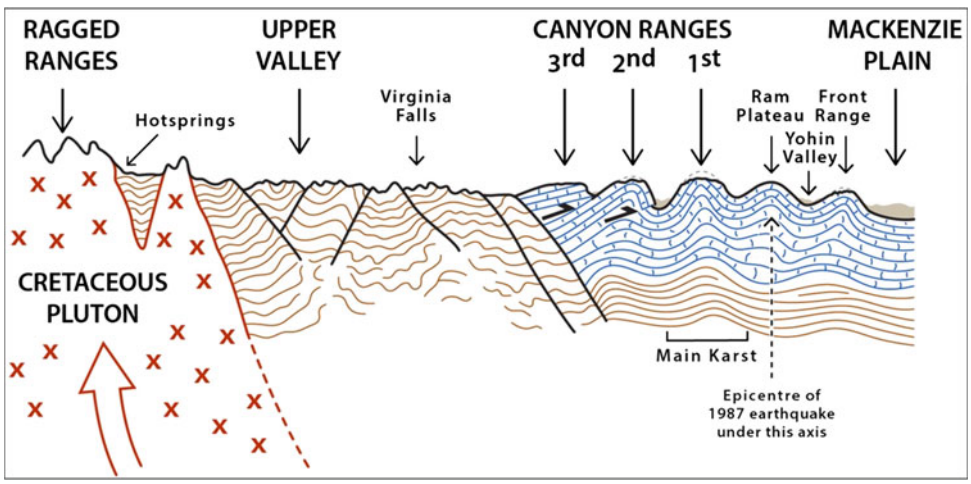

Fig. 15.2 Schematic geologic section of the park reserve from the Ragged Range east to the Front Range

15.2.2 Alpine Morphology of the Ragged Range and the Rabbitkettle Hotsprings Mounds

The landscape of the Ragged Range around the western extremities of the reserve is that of textbook 'temperate' mountain glaciation, namely cirques enclosed by arêtes and horn peaks, U-shaped valleys, hanging valleys, etc. (e.g. Fig. 15.3a). Many scenes are reminiscent of the classical alpine landscape in granite around Chamonix, French Alps. Elevations range between 700 and 1000 masl in the trunk valley floors, rising to 2250–2750 masl at crest lines. Fresh

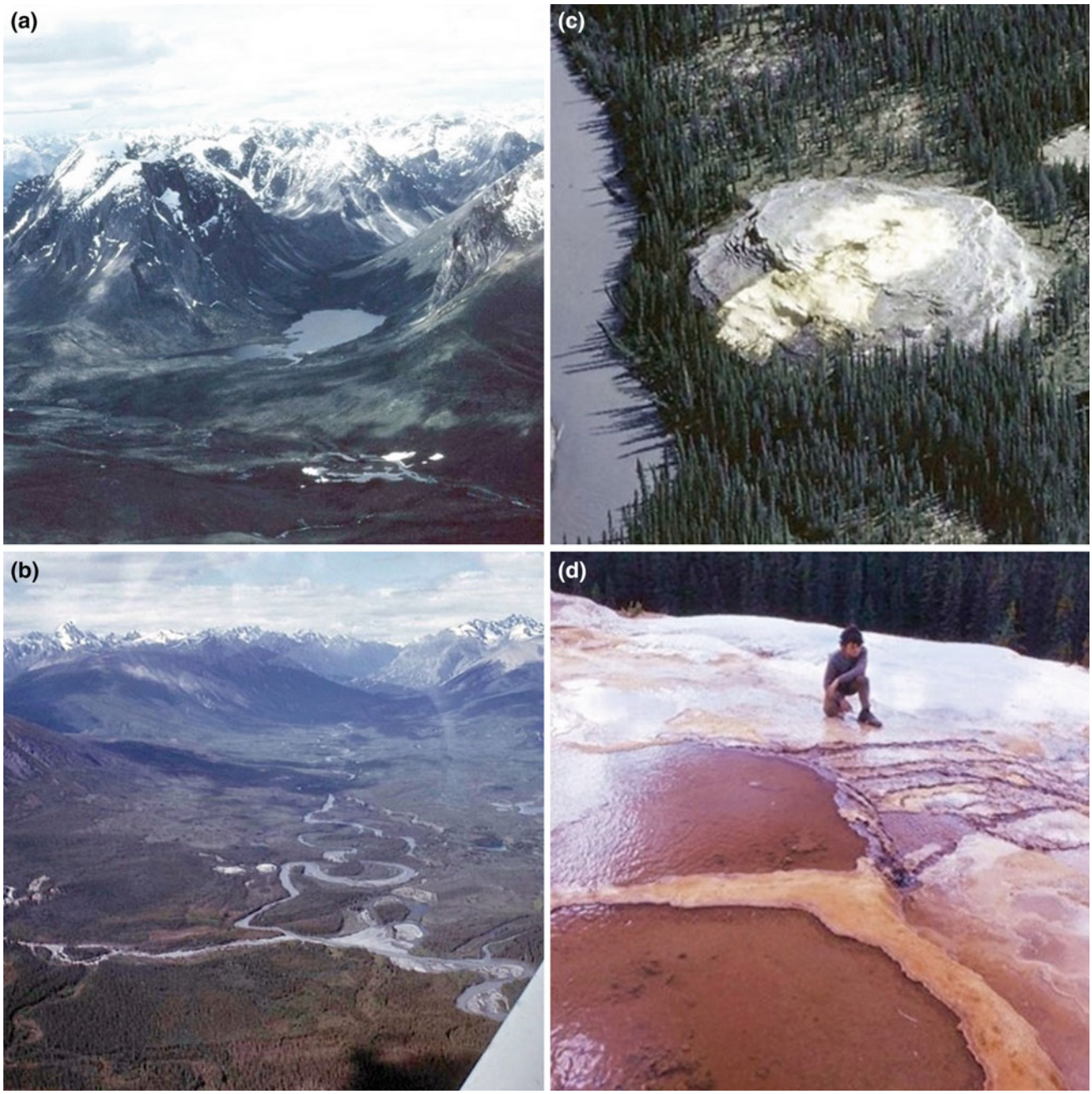

Fig. 15.3 **a** Hole-in-the-Wall valley at the eastern end of the Ragged Range. **b** Rabbitkettle River draining from the Ragged Range. The two *white* features in the *centre* are the hotsprings travertine mounds. **c** The northern mound. **d** Fresh flowstone with gour dams (rimstone) on the active sector of the mound

(Wisconsinan) trimlines are 440–600 m above the floors, with older and fainter evidences 40–80 m higher in some instances.

There is a smaller outlier of the quartz monzonites a few km to the east that rises only to 2100–2200 masl along its crestline. It is downwind in the rain/snow shadow of the Ragged Ranges. Its western slopes display glacial valleys of the polar type (e.g. no wet-bottom glacier rotational over-deepening that will leave tarns upon deglaciation) and major solifluction lobes. The eastern slopes are dissected into incipient cirque forms only, some much degraded by frost because they were probably not occupied by ice during the last regional glaciation. Alpine sculpting by source glaciers here and further east in the reserve thus has been strictly limited by aridity.

The Cordilleran valley glaciers were certainly able to extend far to the east and southeast of their sources in the Ragged Range (Fig. 15.1). The upper halves of both the South Nahanni and the Flat River basins were originally drained southwards into the valley of what is now Borden Creek, and onwards into the Pacific Ocean. Glacial erosion deranged their flow, breaching divides in the comparatively soft Paleozoic rocks and directing it eastwards into the Mackenzie River catchment via sharp elbows of capture.

The nature and evolution of the Rabbitkettle Hotsprings Mounds are illustrated (Fig. 15.3b–d). The springs are the most prominent of several groups that emerge from the sedimentary rocks around the Ragged Range batholith and which can be considered to represent the last vestiges of the Cretaceous batholithic injection energy. The Rabbitkettle Mounds are built of travertine (calcite) which precipitates rapidly in the open air, forming flowstones with rimstone dams (Fig. 15.3d). These are the largest such structures known in Canada. The north mound, which looks like a giant wedding cake (Fig. 15.3c), has a diameter of about 80 m, a depth of 15+ m and a mass of c. 15,000 m^3. Water flows out of two vents at its centre (620 masl) at a constant 21.5 °C. Total dissolved solids are steady in the range, 475–550 mg/L expressed as $CaCO_3$, and there is minor Mg plus other elements in trace amounts (Brown and Wright 1979). These values are above those expected in simple meteoric karst waters at these latitudes. The D/H and $^{16}O/^{18}O$ isotope ratios indicate that the waters are of meteoric origin but enriched by exhalative CO_2 from the pluton. The mean annual environmental temperature here is estimated to be below −5 °C, suggesting that the water is circulating to depths in excess of 1500 m. However, this is hot karst in a cold climate. Vagaries of the rimstone build-up redirect the spilling waters from time to time, abandoning the fragile travertine structures to frost action. Frost polygons of fragmented travertine shown appear just 15 m from the thermal water outlet on the lesser south mound.

15.2.3 The Upper South Nahanni Valley and Virginia Falls

Below Rabbitkettle Hotsprings South Nahanni River flows for c. 100 km in a broad, rather straight valley in the weak Lower Paleozoic sedimentary rocks, descending gently from 590 masl to 520 m at the top of Virginia Falls. The valley form is highly modified by glacial action (Fig. 15.4a). Many spurs are truncated by glacial scour; survivors display fragmentary ice marginal channel entrenchments up to 100 m in depth, with modern karst sinkhole drainage where they are in limestone. The upper valley sides are deeply dissected by ravines. The valley floor is filled to unknown depths with glacial and fluviglacial deposits, topped off with glaciolacustrine silts that are now shallowly entrenched by the modern flood plain (Fig. 15.4c). There are some spectacular meanders in the channel (Fig. 15.4d).

The crests of the enclosing mountains are generally less than 1850 masl, too low to support source glaciers in the shadow of the Ragged Range. The South Nahanni valley was repeatedly invaded by Cordilleran valley glaciers from the Ragged Range (Fig. 15.4a). The Sunblood hills, by contrast and immediately adjacent, display simple V-form fluvial entrenchments with solar aspect modifications attributable to periglacial processes (Fig. 15.4b). They are a part of the unglaciated corridor country in the park.

Virginia Falls and gorge (Fig. 15.5) include the high falls (90 m in height) and the low falls (52 m). With the rapids above, the total fall is about 110 m. In the summer season base flow over the falls is c. 500 m^3/s, rising to $\geq$ 1500 m^3/s in the heaviest rain storms.

The falls and gorge were created by a mixture of entrenchment and knickpoint recession in the resistant Virginia Falls Member of the Sunblood Formation, which here is dipping c. 8° in the downstream direction. A first falls was created by recession to the arrow (Fig. 15.5a). It and the gorge were then buried beneath sediments of Glacial Lake Nahanni to c. 560 masl, 40 m above the top of the rapids. When exhuming the gorge after the lake had drained, the new river channel was offset some 600 m north of the buried falls and has since carved a new gorge by knickpoint recession from them to its present position. The buried falls have become the portage route.

15.2.4 Glacial Lake Nahanni and Glacial Lake Tetcela Landscapes

Advances of the Laurentide Ice Sheet into the Mackenzie Mountains obstructed the eastwards flow of the rivers, backing them up as narrow lakes along the valleys until they

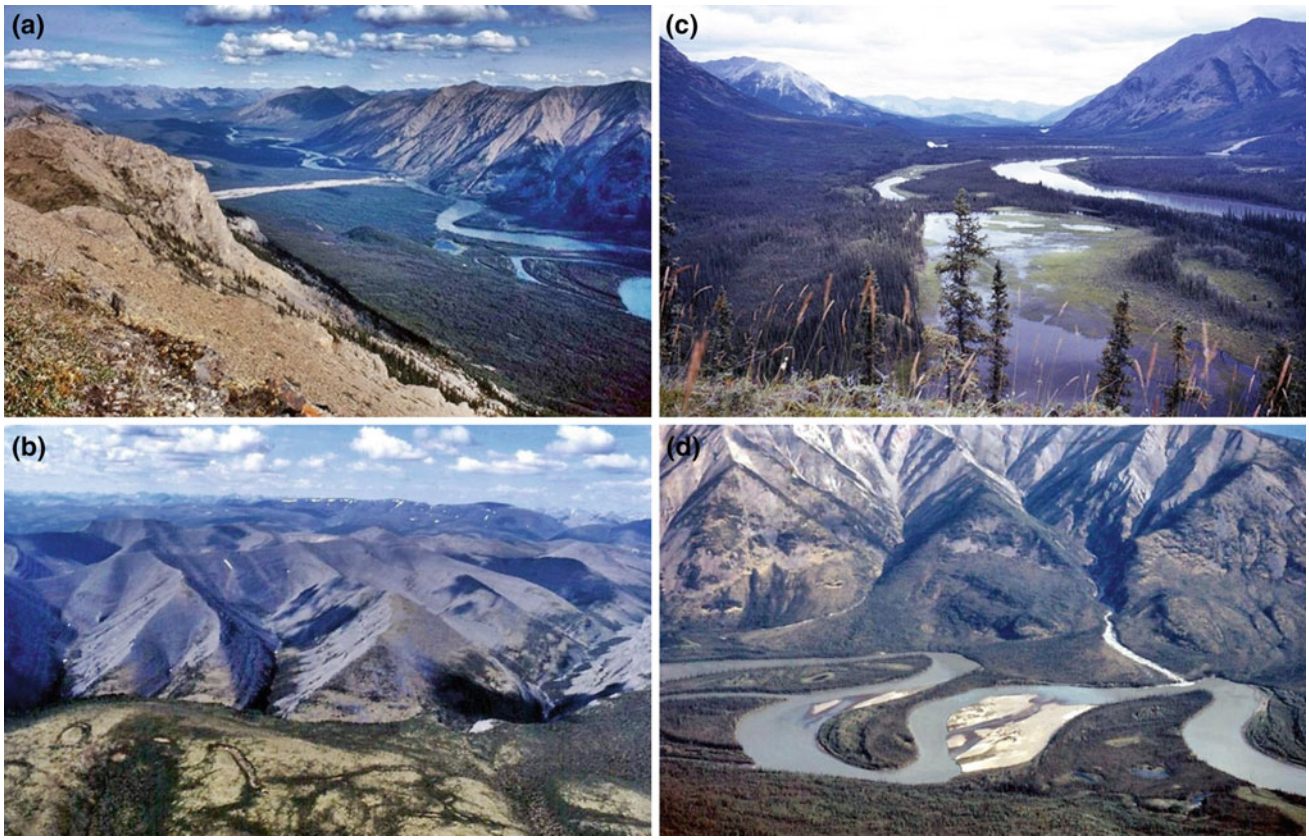

Fig. 15.4 Four scenes in the upper valley of the South Nahanni River. **a** A view looking southeast down the valley from the crest of the ridge on its northern side. Glaciers have removed most spurs, straightening the course. The floor is deeply infilled. **b** View north from the same camera position reveals a V-form fluvial and periglacial landscape with no morphological evidence of glacier action. **c** Wetlands on the floodplain. There were four moose in the ponds when this shot was taken on a hot day. **d** A shapely delta fan and meanders on the upper river

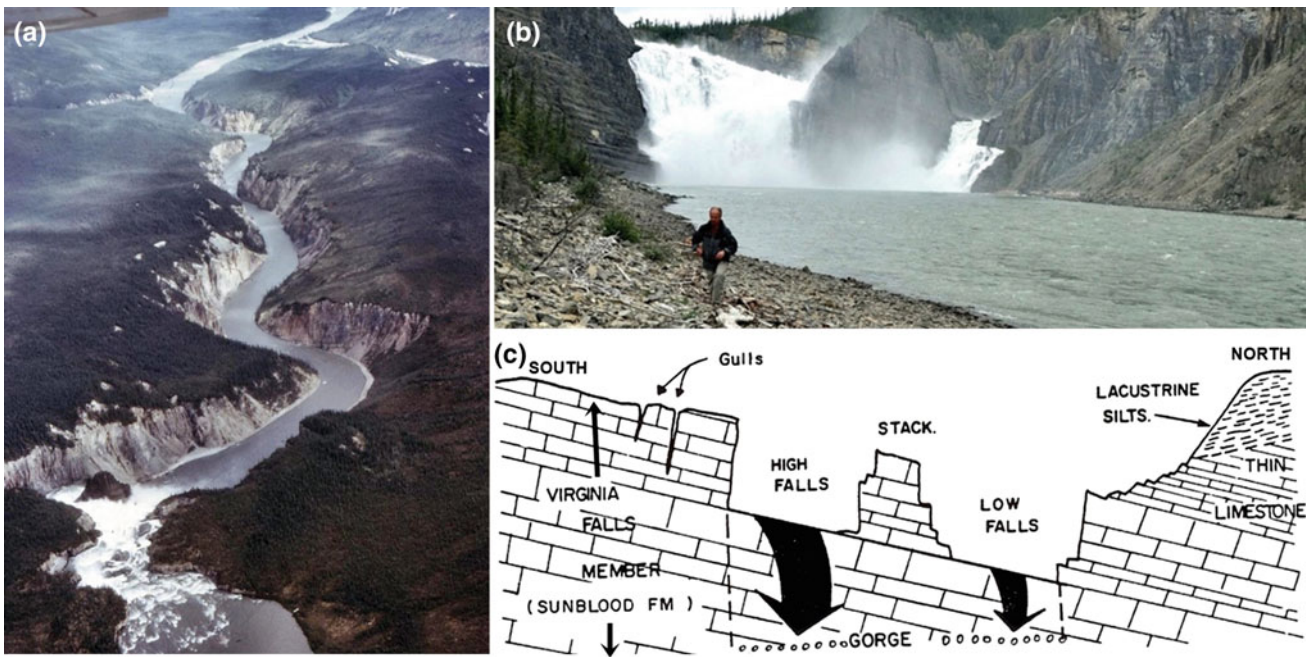

Fig. 15.5 Virginia Falls. **a** Aerial view looking down the recessional gorge. The *arrow* indicates the location of the falls before they were inundated by Glacial Lake Nahanni. **b** The modern falls seen from below. **c** Geology of the Falls (Ford 1984)

were able to overspill to the north or south. There are abundant evidences of two such lakes in the original reserve. First was Glacial Lake Nahanni, which rose to c. 600 masl to overspill southwards via Mary Creek. It then had a maximum depth of 360 m (Ford 1974b). Weirich (1978) suggests that this lake basin filled at least twice, with a lengthy period of erosion occurring in between. Following both events, Glacial Lake Tetcela (named for Tetcela River in the Yohin syncline between First Canyon and the Front Range) rose to c. 400 masl and discharged to the north via Fishtrap Creek. It had a maximum depth of about 200 m but shrank considerably when its outlet was eroded, lowering the water level to c. 275 masl.

Large volumes of glacilacustrine sediments were deposited in both lakes, then exposed and dissected as they were drained. Their yields of fines still keep the South Nahanni waters turbid below Virginia Falls today. Glacial Lake Nahanni deposits are best seen between the Falls and Third Canyon and, especially, in the gentle relief of the lower reaches of the Flat River. As a result of the prevalence of shaley strata and quieter backwater conditions in a broader lake there, the deposits tend be darker and more regularly bedded than on the South Nahanni (Fig. 15.6a). Silt and clay are predominant. Weirich (1978) mapped five well-formed terraces in them, created as the river cut down to its modern level of 450 masl from a paleo-lake floor at 580–550 m. Along the South Nahanni itself, there are thick but poorly bedded deposits of buff-coloured silts with drop-stones, in some places resting upon bedrock or discontinuous patches of till above the modern waterline, at others extending to

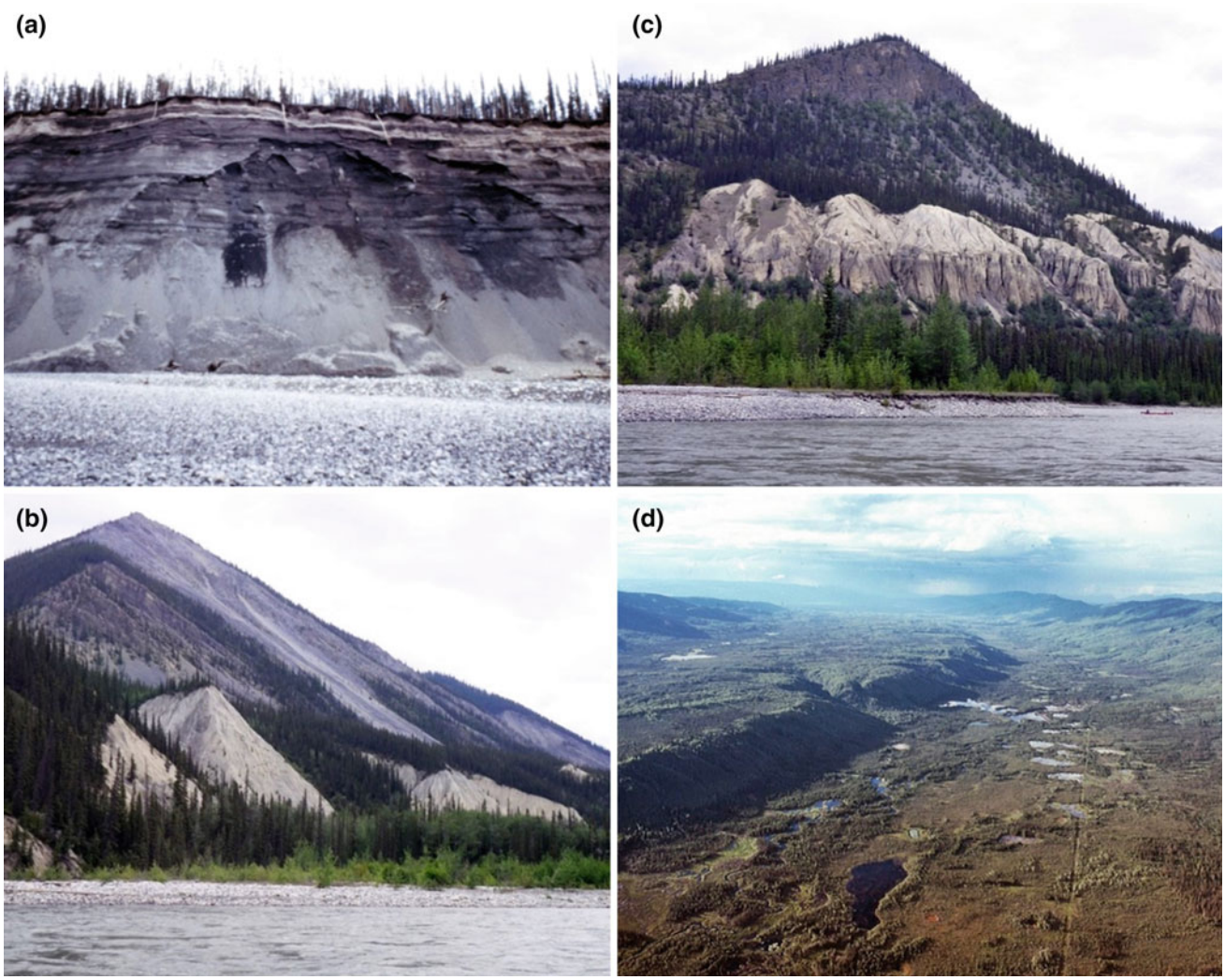

Fig. 15.6 Views of dissected proglacial lake sediments in the Reserve. **a** Dark, thin-bedded deposits of Glacial Lake Nahanni along Flat River. **b** Typical dissection of the poorly bedded buff silts with drop-stones that are dominant along the South Nahanni River between the falls and Third Canyon. Here, the base of the silts is below the level of the modern floodplain. **c** A delta fan of darker sediments buried by the buff silts. **d** Glacial Lake Tetcela sediments at 400 masl entrenched by a spillway in the Fishtrap River valley

Fig. 15.7 Deadmen Valley, a synform between First Canyon (*right*) and Second Canyon. Prairie Creek dissects the western flank for the First Canyon antiform with an antecedent canyon. The creek delta is the finest seen in the Reserve and of notable ecological interest. Glacial Lake Tetcela deposits at c. 400 masl are preserved to its right. In the foreground, these deposits are buried by periglacial sludge from shales below Tlogotsho Plateau, which is beneath the aircraft

unknown depths below it (Fig. 15.6b). A deltaic deposit of darker silts is seen beneath the buff sediments at one point (Fig. 15.6c).

Deposits of later Glacial Lake Tetcela can be traced to the head of Third Canyon but are visually impressive only in Deadmen Valley between the First and Second Canyons and in the Yohin synclinal lowlands downstream of them (Fig. 15.6d). In Deadmen Valley[1] they are partly destroyed by a spectacular delta where Prairies Creek discharges from the mountains on the north bank (Fig. 15.7) and are buried by periglacial sludge from shales beneath the Mattson sandstones on the south bank. Where preserved near the mouth of Second Canyon, there is active rotational slumping into the river: the silts here are well drained as a consequence and support the best wild raspberries in the Reserve, a finding that has not escaped the notice of the local grizzly bears.

Downstream of First Canyon the Tetcela sediments lap upon and partly bury some earlier kame-and-kettle dead ice topography containing lenses of gravels. Sinkholes formed in the lake silts where the latter could be piped away through the gravel are the finest examples of this form of pseudo-karst that the writer has seen in Canada. In a narrow strip between the river and Yohin Lake there are more than forty funnel-shaped sinkholes, 20–200 m in diameter and 6–30 m in depth. They may be dry or partly water-filled. Amalgamation has created three larger closed depressions about 800 m in length. Further east the c. 400 masl Glacial Lake Tetcela floor is beautifully preserved on the west side of the Fishtrap River valley but destroyed on the east side by the final spillway of the glacial retreat sequence (Fig. 15.6d).

15.2.5 The Antecedent River Canyons

The antecedent canyons in the expanded park are the finest known to the writer anywhere in Canada. First, Second and Third Canyons on South Nahanni River (named in that order

[1]The somewhat ominous place names in this part of the Park ('Deadmen Valley', 'Headless Range', 'Funeral Range', 'Sombre Range') may be traced to mishaps that befell white explorers at the beginning of the twentieth century; see Patterson (1966).

by western explorers coming up-river) are the longest and deepest, but there are other impressive examples where Ram River crosses Ram Plateau, and on lesser tributaries such as Meilleur River, Clearwater Creek and Prairie Creek. Most are carved directly across rising structural antiforms, but Prairie Creek is incised along the strike of the First Canyon/Nahanni Plateau anticline (as seen in Fig. 15.7).

Asymmetric (or in-growing) meandering river entrenchment across rising land is illustrated in principle (Fig. 15.8) and in the Nahanni canyons themselves (Figs. 15.9, 15.10). Third Canyon is developed in the Sunblood rocks and weaker limestone shales above them (Fig. 15.8c). Strictly fluvial morphology is maintained to c. 900 m above the River (where mass wasting processes take over), but a greater

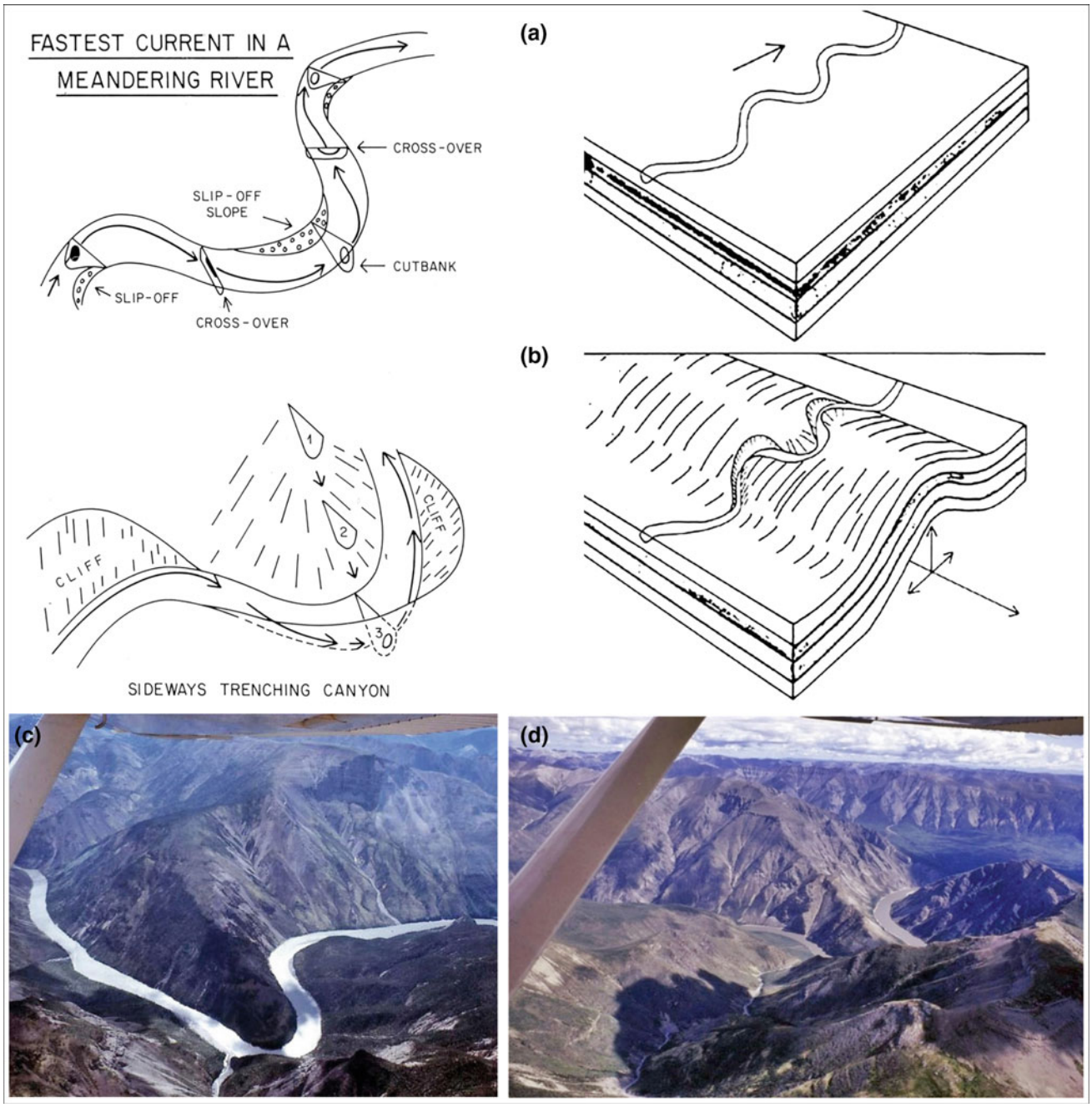

Fig. 15.8 **a**, **b** Illustrating the nature of antecedence and in-growing meander entrenchment. **c** An in-growing spur in Sunblood Formation dolomites, Third Canyon. **d** In the Devonian limestone and dolomite, the in-growing spur of Second Canyon. Its crest is 1320 m above the modern river

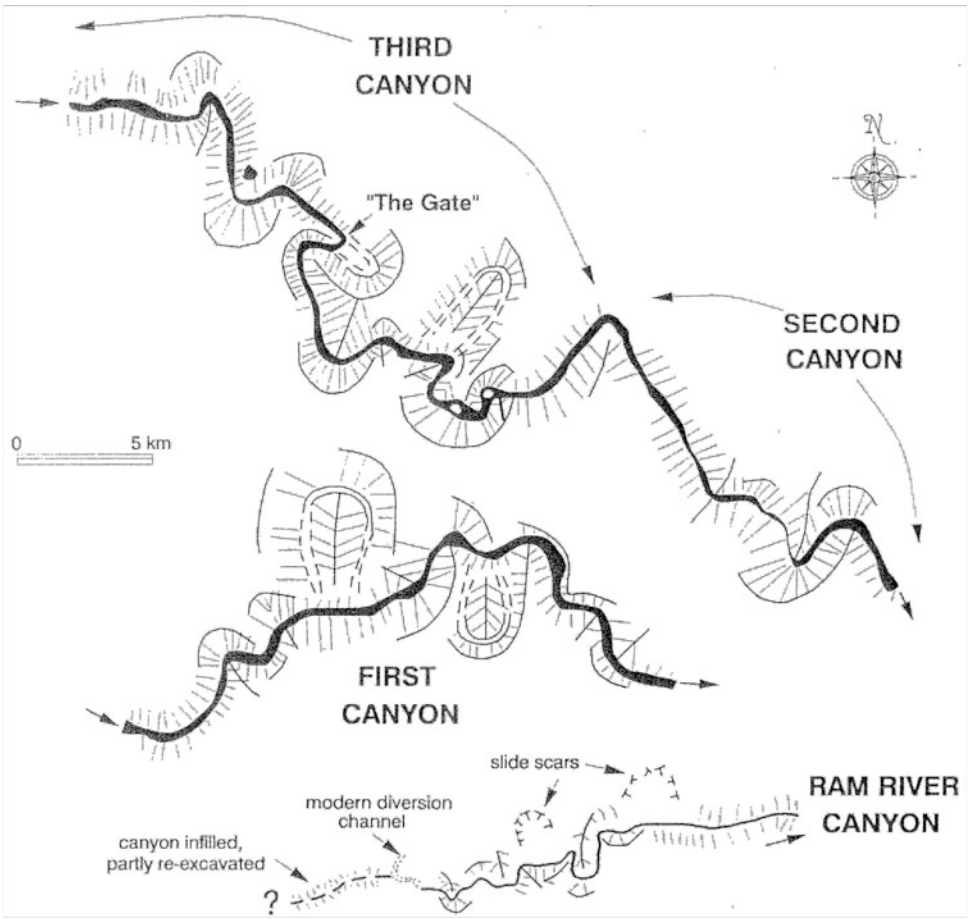

Fig. 15.9 Meander form of First, Second and Third Canyons on the South Nahanni River, and Ram Canyon on Ram River; see the text for details (From Ford 1991)

verticality in the entrenchment between 600 and 650 masl may be attributed to some trimming of these comparatively weak strata by the waters of Glacial Lake Nahanni. The other canyons do not display this effect. 'The Gate' is a famous cut-off of a hairpin meander at modern river level in Third Canyon that probably began as a cavern through the resistant Virginia Falls beds of the Sunblood Formation. The eastern cut-off, in shaley rocks, is 230 m above the river today.

Second Canyon begins with a straight section where the River follows the strike of a major overthrust in the Nahanni limestone, then turns across the thrust axis to entrench it (Fig. 15.8d). The simple symmetrical spur created by this entrenchment rises 1320 m above the modern river channel, which itself is perched on an unknown depth of glacilacustrine sediments: it is the greatest single testament to sustained antecedent entrenchment in the park.

A majority of voyagers consider First Canyon to be the most impressive. It is carved across the steeply plunging nose of the First Canyon/Nahanni Plateau anticline (Fig. 15.10a). A southerly channel diversion of only 10 km in Deadmen Valley would have carried the river around the anticline in lowlands instead. The length of the modern channel is 26 km. The 9-km-long western cut-off at 490 m above the river and the eastern of 6 km at 150 m increase the length of the original antecedence to c. 41 km. The Nahanni limestone dips down to form vertical cliffs at river level at each end of the canyon (Fig. 15.10c, e). In between, the Arnica and Manetoe dolomites form steep to vertical cliffs with impressive talus slopes below (Fig. 15.10d). Occasional landslides expose remnants of the buff Glacial Lake Tetcela sediments beneath the darker talus. Fluvial morphology relief extends to c. 1200 m above the river.

No bedrock is exposed anywhere in the river channel in these canyons. Instead, the river maintains a steady gradient of 1.3–1.5 m/km on a veneer of bedload (including large boulders) resting on Glacial Lake Tetcela silts of unknown depth. Local rapids and riffles along the river course are due to build-out of gravel deltas by local tributary streams and are short-lived.

The course of the Ram River across Ram Plateau (a beautifully symmetrical anticline) is distinctly different (see

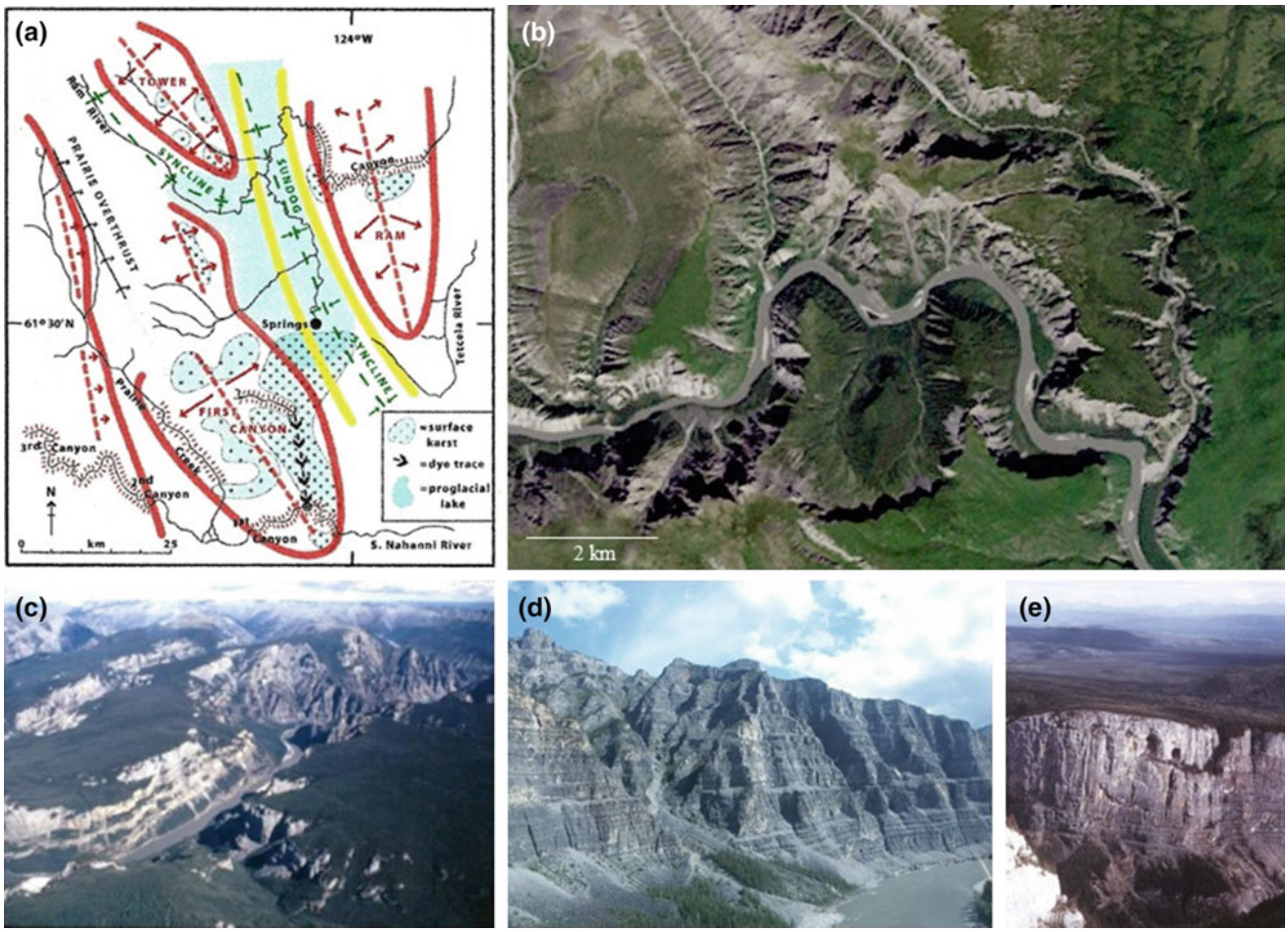

Fig. 15.10 **a** Highly schematic diagram of the anticlines and synclines in the eastern park, noting the location of principal karst areas and springs. **b** Air photograph view of First Canyon showing both cut-off meanders and the beginning of karst corridor entrenchment of the Nahanni Limestone in the eastern half. Lafferty Canyon is the deep tributary on the north side. **c** The river entering First Canyon anticline. Nahanni Limestone (buff) is seen on the flank, but has been eroded off of the top. **d** Resistant Arnica and Manetoe dolomites support great cliffs in the centre of First Canyon. **e** On the east flank of the anticline the Nahanni Limestone dips beneath clastic rocks in the Yohin syncline. The Nahanni Front range is seen in the far background. Grotte Andre is typical of the relict stream caves stranded by uplift of the anticline

Fig. 15.9). Only at its centre, which would be the first uplifted part to be encountered by a meandering antecedent river, is asymmetric entrenchment. Both the east and west ends are straight, which is attributed to the onset of Quaternary cold conditions greatly increasing the volumes of bedload to be transported (Ford 1991). The western straight section was later infilled with deltaic sediments (Glacial Lake Sundog—see 15.4), and post-glacial flow was diverted northwards to re-enter the mid-canyon at a high falls that has receded as a knickpoint to create 'Scimitar Canyon', a most spectacular youthful feature (see Sect. 15.3.6). There are bedrock falls in the Ram Canyon channel in its eastern straight sector as well, plus landslides and moraine ridges that leave no doubt that the Laurentide ice intruded into it: such features are not seen in the South Nahanni River canyons.

15.3 Karstlands of the Nahanni and Ram Basins

15.3.1 Tectonic and Physiographic Settings

The structural features of the eastern Park are bold and simple (Fig. 15.10a). The three anticlines are broad, symmetrical domal forms with gentle stratal dips. Ram Plateau retains a cover of the Nahanni Limestone, which passes beneath limestone shales of the Horn River Formation north of the river canyon. The limestone is removed from the crest of the First Canyon/Nahanni Plateau anticline, exposing the Arnica dolomites there. The Tower anticline is gutted. It is most important to appreciate that these structures have been active during neotectonic times. The epicentre of the strongest earthquake experienced anywhere in continental Canada

during the past 50 years (Richter 6.9 in 1987) was at shallow depth on the Ram anticlinal trend 40 km further north; it triggered a major landslide in the limestone there.

At its greatest extent the Laurentide Ice Sheet buried Ram Plateau and the Sundog syncline and extended up to elevations of c. 1400 masl on the eastern flanks of the First Canyon and Tower anticlines (Ford 1974a, Brook 1976). In a later stage, ice advanced up the syncline to a terminus south of the northern springs (Fig. 15.10a), impounding proglacial 'Lake Sundog' at c. 900 m asl to the north. Deposition of up to 100 m of lacustrine silts buried much pre-existing karst there. The lake drained abruptly at some time after 40 ka BP (based on a ^{14}C date of tree wood in the silts—A. Duk-Rodkin, personal communication 2006): it cut a broad spillway through the silts and into the top of the karst beneath it, including some channeled scablands forms.

Karst landforms are found scattered for 50 km along a broad belt from eastern First Canyon to 'Bubbling Springs' at the head of Sundog Creek, a major tributary of Ram River (Fig. 15.10a). There are also the ruins of a once extensive karst terrain on the Tower anticline, lesser displays west of it and on the oldest exposed parts of Ram Plateau to the east. Together, they amount to the most accentuated and morphologically diverse karst features that the writer is aware anywhere in the arctic and sub-arctic regions of our planet.

15.3.2 The Relict Caves of First Canyon

More than 200 relict karst solution caves (i.e. caves drained of their formative waters) have been found in the region, but most are sealed off within a few metres of their entrances by ground ice, fallen rock or frozen lacustrine silts. The lengthiest open systems are preserved along the north (up dip) wall of First Canyon, near its mouth (Fig. 15.11). Their form is of dendritic drainage, from the sink points of streams flowing from shale cover that is now largely or entirely removed. Flow was down-dip into the river channel at and just below the contemporary water tables. A first example, Grotte Valerie, has two kilometres of passages now stranded in cliffs 450 m above the river. It has partial fillings of lacustrine silts, and winnowings of an older till cemented by calcite (Ford 1973). The cave entrances are south-facing with the result that, in the summer, cold air drains from a low exit, sucking in warm air to replace it through an entry that is 40 m higher. This creates (1) a 'warm entrance cave' (+6 to +1 °C in summer) where there is active deposition of small calcite speleothems today; this supplies moist air to (2) a 'cool exit cave' (0 to −1.5 °C) covered with ice and hoar frost: behind and below both is (3) a 'permafrost cave' receiving only the cold air of winter, dry and dusty, without speleothems or ice but preserving the remains of 80 or more wild sheep (Figs. 15.11b–c). It is an exceptional example of cold climate zonation in a cave (Ford and Williams 2007, 294–298). Nearby, Grotte Mickey has more than three kilometres of galleries at several different levels between 250 and 400 m above the river. This multi-level, multi-phase pattern points to extended development that kept pace with the entrenchment of First Canyon for a long while (Schroeder 1977, 1979).

An important feature of these caves and some in the Labyrinth (below) is the occurrence of large, highly ornamented stalagmites, columns and flowstones of calcite. They are no longer growing (modern growth is limited to very small deposits without ornamentation), and most are weathered, partly eroded by invading streams or shattered by freezing. They are indicative of warmer conditions in the past which (allowing for cave truncation by cliff recession since) extended much further into cave interiors than today. There was abundant uranium in the cover shales which, re-precipitated in the calcite, has made the speleothems particularly suitable for U series dating. This region saw much of the pioneer dating work as a consequence (e.g. Harmon et al. 1977). The large majority of samples proved to be >350 ka BP in age (the limit of the dating method using 1970s alpha spectrometer technology), although they were <1.25 Ma. The first application of U series speleothem dating to a geomorphic problem was by the writer, who showed that the mean rate of South Nahanni River entrenchment below Grotte Valerie could not be more than 0.8 m/ka and that there had been possibly as much as 350 m of uplift on the First Canyon anticlinal axis since c. 1.5 Ma BP (Ford 1973). Work in progress at time of writing, using much improved spectrometry with laser ablation technology, has determined that Sample 72030 of frost-shattered flowstone from Grotte Valerie (Fig. 14.11e) grew briefly around 120 ± 0.6 ka BP, 356 ± 6 ka BP and during at least six warm climate episodes between 596 ± 12 and 695 ± 14 ka BP (Smith et al. 2011): growth had begun before this, but the base of the sample is too weathered to be used. In the near future, speleothem dating and stable isotope analysis at Nahanni and similar sites will determine much of the climatic history of the past one million years or more in the Canadian North.

15.3.3 Springs

The main belt of karst terrain (Fig. 15.10a) drains to just two sets of springs. At the north end, 'Bubbling Springs' (700 masl) rise where the stratigraphic top of the Nahanni Limestone dips under impermeable cover shales in the Sundog syncline. They drain perhaps the northern one-third of the belt, with discharges >10 m^3/s during wet summer spells. In contrast, 'White Spray', the southern springs, discharge at 240 masl in First Canyon, from dolomites that

Fig. 15.11 Scenes from Grotte Mickey and Grotte Valerie in the First Canyon. These are relict stream caves now raised high above the river in the canyon walls. **a** The portal of Grotte Mickey, looking down on the river (photograph courtesy of Jacques Schroeder). **b** Glacilacustrine silts on the floor of the main passage, Grotte Valerie. **c** Looking down into the permafrost cave, occupied by a lake of cold, stagnant winter air. **d** Flowstone sample 72030 was a frost-shattered clast collected in situ a few metres from the scene in (**c**). U series and U–Pb dating reveal that it grew intermittently between 120 and c. 700 ka BP; see the text for details. **e** Hoarfrost and floor ice in the (airflow) downstream sector of Grotte Valerie. Photograph taken by the writer in 1973; in 2014 the ice was reported to be highly degraded by regional warming

are stratigraphically c. 580 m below the base of the Nahanni Limestone. Most of their discharge is into the river bed and is strong enough to keep this stretch of the river free of ice throughout the winter, a unique feature; 'White Spray' itself, spouting from a cliff foot a few metres above the river is merely a summer overflow spring. These springs must drain much of the First Canyon dome, including Canal Canyon (30 km in length and up to 1000 m deep) where a stream

Fig. 15.12 Looking west up Canal Canyon in the east flank of First Canyon anticline. The canyon is aggraded by alluvial and colluvial deposits behind a moraine ridge blocking its mouth. All of the ponds are sinkholes that pipe water into Nahanni limestone and Arnica dolomite. The outlet springs are 19 km to the south in the floor of First Canyon

sinks into both bedrock and alluvial fill behind a blocking terminal moraine (Fig. 15.12). Dye traces from there (Fig. 15.10a) and a lake further north proved underground flow of 21+ km at mean rates >3500 m/day on a hydraulic gradient of 0.03 (Ford and Worthington 2009). Although no enterable caves have been found in them yet, the dolomites can thus develop integrated systems of underground solutional conduits quite rapidly.

15.3.4 The Nahanni Labyrinth

The Nahanni Labyrinth is in a spillway of Glacial Lake Sundog where the outflow has partially exhumed and modified a pre-existing, rugged karst terrain in the Nahanni Limestone that was buried by >100 m of lacustrine silts (Fig. 15.13a, Area A). East of the labyrinth a plateau on the Horn River limestone shales that rises above the glacial lake level is pitted with large and deep solutional and collapse sinkholes (Fig. 15.13a, Area B). West of it in Area C the silt still buries the limestone karst but is drained into it by suffosion sinkholes. Area A is the largest example of karstic labyrinth morphology reported in the Northern Hemisphere. The outstanding landforms are dissolutional corridors ('streets') that follow major joints (Brook 1976, Brook and Ford 1978). Individual corridors are 20–100 m deep, 15–100 m wide and up to 6 km in length. For a distance of 13 km they intersect one another to form a natural labyrinth. The walls recede from frost shattering, causing some parallel corridors to amalgamate into broader closed depressions, like squares in a pattern of city streets; the greatest measures 800 × 400 m. Isolated towers are preserved within them. Floor profiles of corridors and squares are highly irregular, with local streams sinking into depressions between talus accumulations or into bedrock shafts. In the labyrinth and elsewhere on the limestone are large, vertical-walled sinkholes and smaller, elliptical solutional shafts (Fig. 15.13c). Many trap the water of successive melt seasons, its depth increasing slowly until pressure bursts

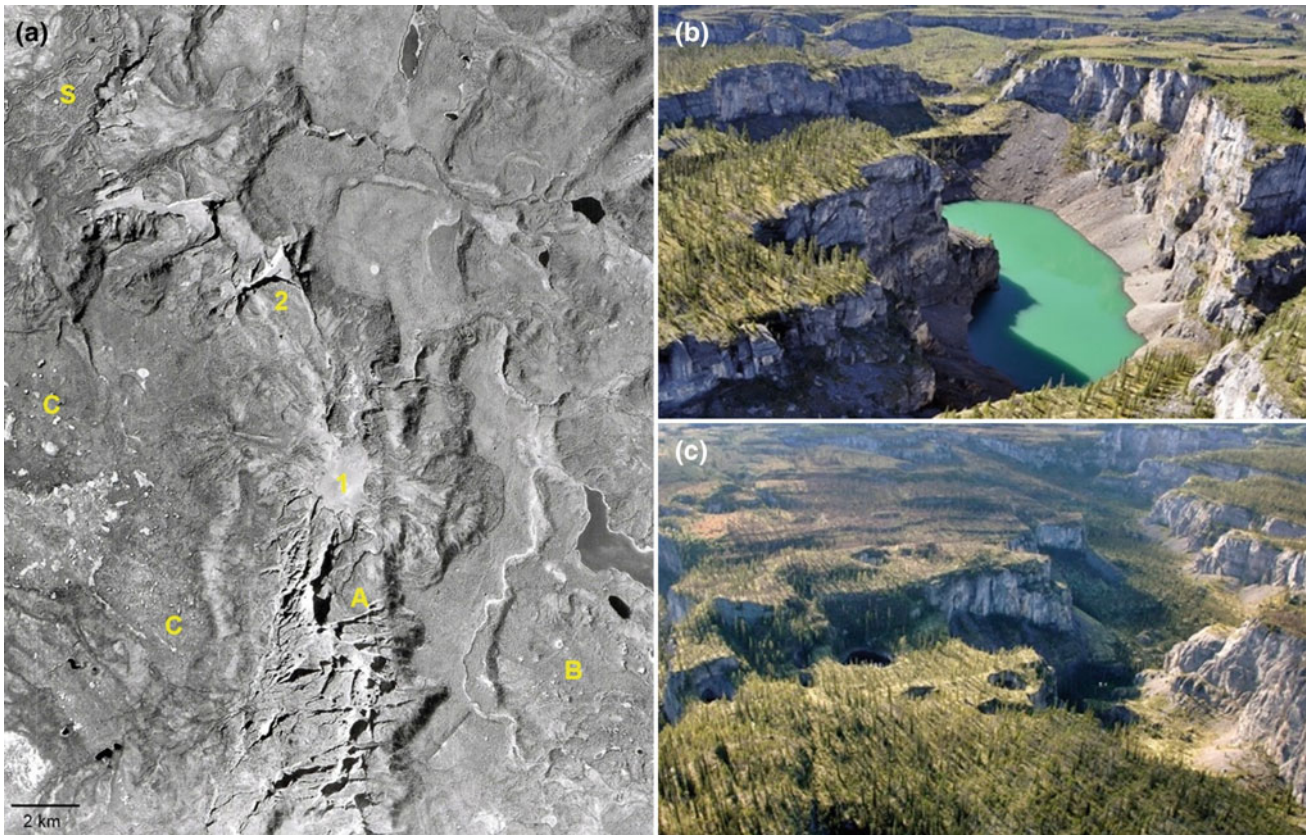

Fig. 15.13 **a** Air photograph covering the Nahanni Karst Labyrinth in the Sundog syncline; see the text for identification of the numbered and lettered features. **b** Raven Lake, a sinkhole in the Nahanni Limestone, 300 m long and 130 m deep, seen here with c. 40 m of summer flood water. **c** Multiple sinkholes and a closed depression 800 m in length in the labyrinth (photograph courtesy of Paul Sanborn)

an ice plug below and the features then drain with catastrophic rapidity. Raven Lake, an unusually large doline within a corridor (Fig. 15.13b), is 300 m in length and 130 m deep; under flood conditions waters rise >75 m at rates up to 3 m/day. At the north end of the labyrinth the shale cover and glacilacustrine silts encroach to reduce the limestone outcrop to a narrow spillway with three small (<2.5 km^2) but elegant poljes developed in it. Brook (1976) showed that the lake and poljes function as one well-integrated karst groundwater system draining to Bubbling Springs.

Relict caves in the Labyrinth include some with speleothems known to be >350 ka BP in age. Glacial Lake Sundog drained <40,000 years ago (Duk-Rodkin, op. cit). The extent to which the pre-existing surface karst landforms were increased in density and enlarged in size by catastrophic flood burst processes such as those described in the Channeled Scablands in the state of Washington (Baker 2010) remains incompletely determined but was likely substantial.[2]

15.3.5 Tower Anticline Contrasted with Tower Syncline and Ram Plateau

The limestone morphologies on the northern structures (Fig. 15.10a) offer some striking contrasts with each other and with that in the main karst belt (including the Labyrinth) to the south. Tower anticline was upraised and stripped of its cover of Horn River limestone shales at broadly the same time as the First Canyon anticline, probably Late Miocene–Pliocene. But it did not have the strong, karstifiable dolomites of First Canyon in support beneath the limestone. Due to lateral facies changes there are weak calcareous shale strata of the Headless and Funeral formations instead. Tower anticline developed an extensive plateau epikarst with

[2]*Pb:U dating of speleothem samples from this area of the Nahanni karst is just beginning. In a first result Professor Jon Woodhead (Geology, University of Melbourne) has reported an age of 2.32 +/- 0.02 Ma from Sample 73052 (Woodhead, personal communication, March 2016). This was a fragment of frost-shattered flowstone from a relict cave three km south of the Labyrinth and just above the level of Glacial Lake Sundog. This age indicates that, at the beginning of the Quaternary here, there was well-established karst with at least some river caves that were already abandoned.

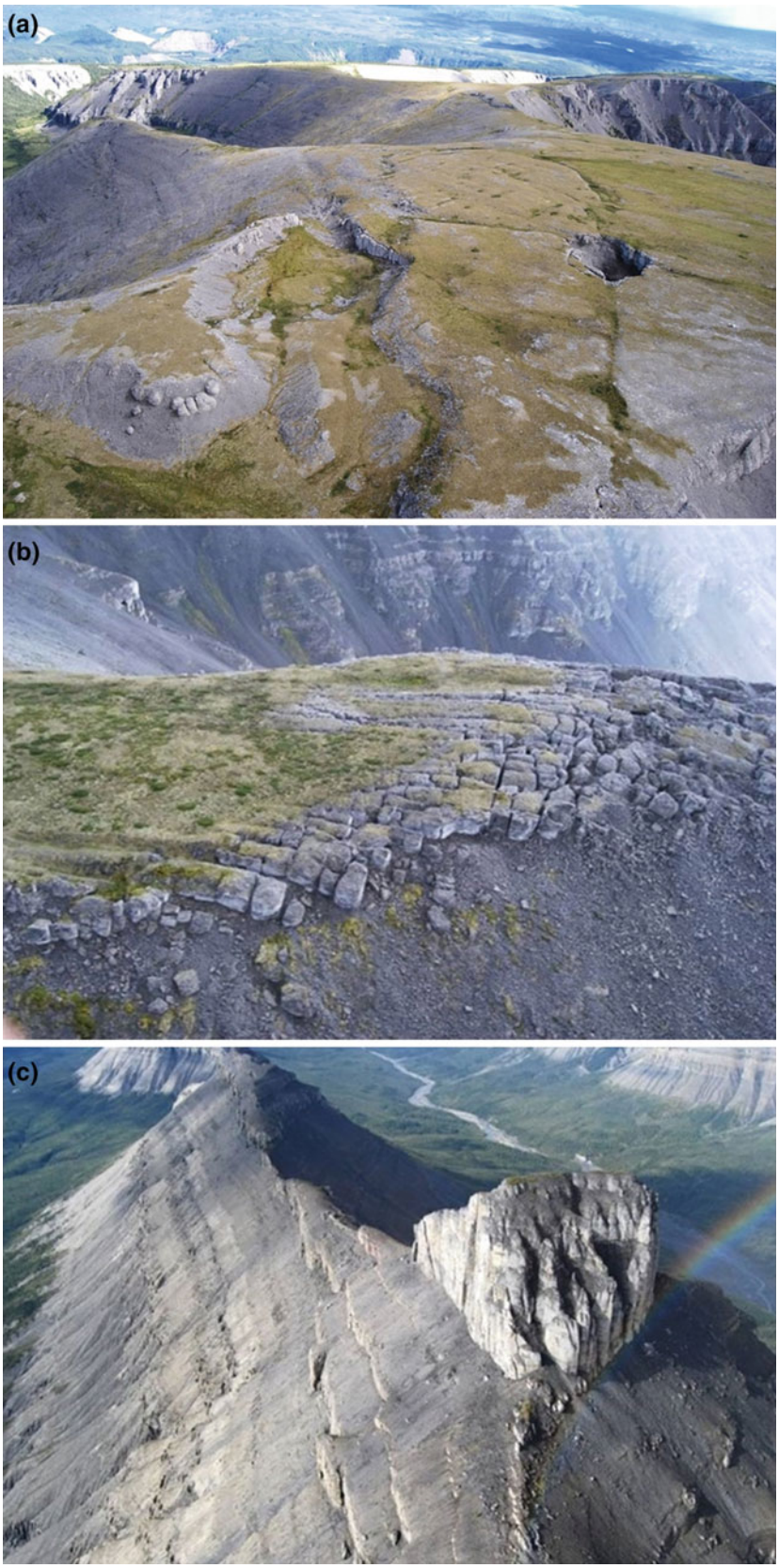

Fig. 15.14 Three scenes in the gutted karst on Tower anticline. **a** Looking down into the Sundog syncline across glaciated pavement with dolines on the well-preserved southeast end of the structure. **b** Relict pavement on the gutted crest of the anticline. **c** A final remnant at the western end

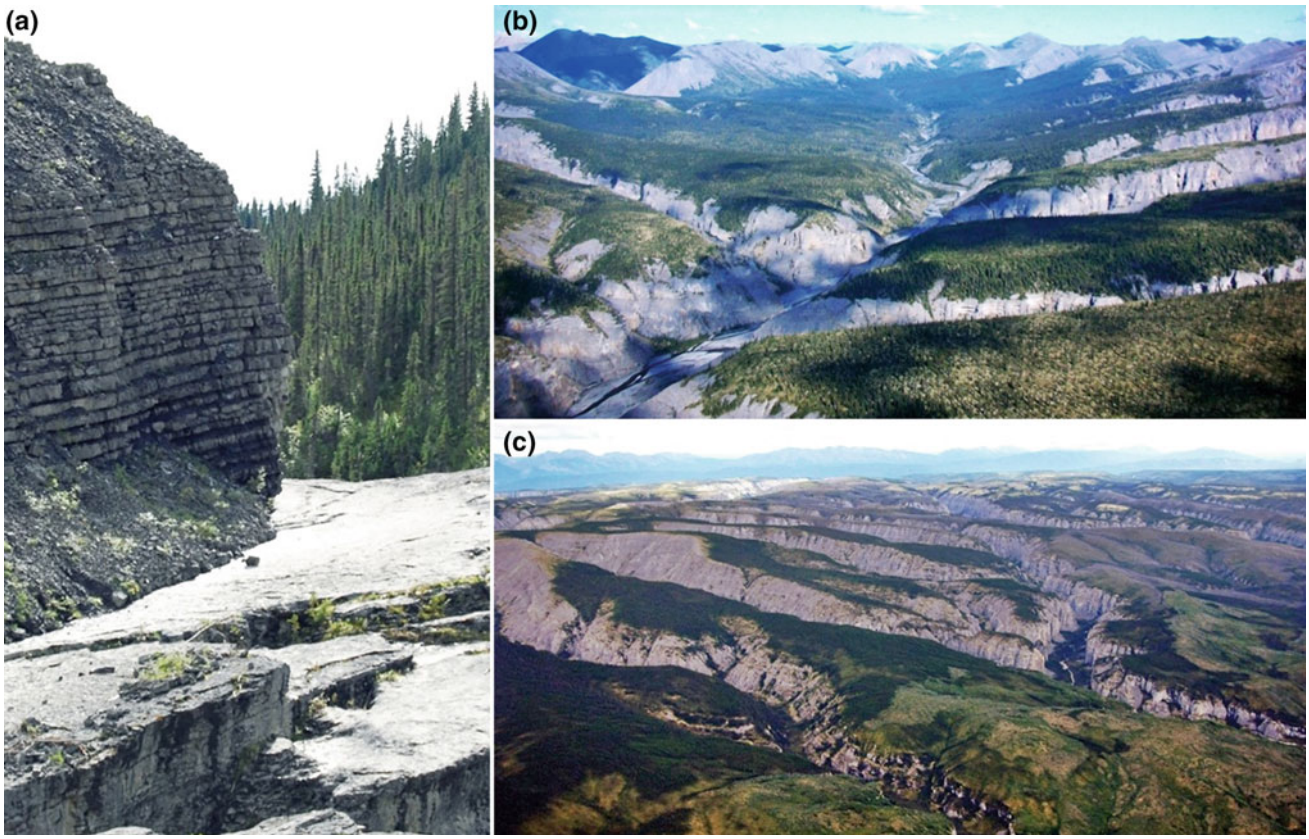

Fig. 15.15 **a** Stripping the weak Horn River limestone shales off of the resistant Nahanni limestone; a scene in the chutes of Ram River at its entry to the Sundog syncline. **b** The Nahanni limestone at the head of the Tower syncline, stripped of its shale cover and dissected by consequent canyons (photograph courtesy of Steve Worthington). **c** The same morphogenetic situation occurs on the southern half of the Ram Plateau anticline (photograph courtesy of Paul Sanborn)

limestone pavement and dolines that are preserved (with glacial scour up to 1200 masl) at the east end (Fig. 15.14a). To the west, the plateau and its karst have been almost entirely destroyed by headward and lateral enlargement of flash flood canyons in the underlying shales (Fig. 15.14b, c).

In strongest contrast to the geomorphic evolution on Tower anticline, stripping of the overlying Horn River limestone shales came significantly later in the Tower syncline because of its lower elevation, and on Ram Plateau because the tectonic uplift there came later to due to its more easterly location (as noted in Fig. 15.9). The consequences appear to have been that exposure of the limestone largely occurred under permafrost climatic conditions (Ford 2008). Except in a few places of early stripping, karst groundwater systems could not be established in the Nahanni Limestone before the rock became frozen. Instead of karst, classical consequent stream channel patterns with canyons were carved into the dipping limestone slopes on both the syncline and anticline (Fig. 15.15).

15.3.6 Scimitar Canyon

As noted, the upstream end of Ram Canyon was infilled with glacial and proglacial sediments from the Sundog syncline (Crosbie 1978). After the proglacial lake there had drained, the new Ram River took a lengthy hairpin course north of the buried canyon before returning to it via a spillway through the Horn River strata (Fig. 15.16a). This discharged over the northern limestone wall of the canyon as a waterfall

Fig. 15.16 **a** View looking south from the head of Scimitar Canyon. The broad entrenchment is in Horn River rocks, the slot below in the Nahanni Limestone. Some very fresh landslides can be seen on the *right* where permafrost is thawing in the upper Horn River slopes. **b** Scimitar limestone canyon, here about 120 m deep; see the text for details

approximately 150 m in height. The falls have since retreated five kms, creating the spectacular 'Scimitar Canyon' (Fig. 15.16b) which breaks into multiple knickpoints at its head.

Karst capture is in process of returning much of Ram River to its original routes into the head of Ram Canyon, however. There are fresh springs spouting from limestone cliffs there that are probably taking all of the base flow of the river. Adjoining tracts of higher terrain on the Horn River and glacilacustrine sediment surfaces are also becoming karstified because the groundwater hydraulic gradients through the underlying limestone into the canyon are steep; the process is being abetted by widespread thawing of permafrost.

15.3.7 The Castellated Karst

Some more complex geologic structure is preserved where tectonic forces of the Prairie Overthrust and First Canyon anticline merge near the entry of Ram River into the Sundog syncline (Fig. 15.10a). On ridges above 1150 masl there are many attractive tors in the limestone, their morphology changing as the dip of the resistant beds ranges from horizontal through steep to vertical. It is invigorating walking country above treeline where the writer's favourite tor is located, a natural version of an Iron Age fortress (Fig. 15.17).

15.4 Impacts of Global Warming?

To conclude with a further personal note the writer saw much of the Nahanni landscape each summer, 1971–1977, and then again in the summers of 2006–2010. In the former period the only thawing permafrost observed in the reserve and the karst occurred where river channels were eroding their banks in frost-susceptible soils (only two examples). Over 2006–2010 forty-four landslides caused by ground ice melt were noted in the area of the Sundog glacial silts or underlying Horn River shales alone. None of these were due to river action. The largest single example is illustrated (Fig. 15.18).

Fig. 15.17 'The Iron Age Fort', a fine example of tor development with permafrost creep features in the Castellated Karst

Fig. 15.18 **a** Second Polje seen in flood in July 2007. **b** Seen dry in June 2010, but after a landslide into it in 2008 caused by permafrost thawing in the Glacial Lake Sundog silts remaining above the Nahanni

Acknowledgments The writer is deeply indebted to his research students and other colleagues in the many years of field work, especially thanks to George Brook, Mary Lynn Crosbie (deceased), Russ Harmon, Darlene Johnston, Jacques Schroeder, Frank Weirich and Stever Worthington. Parks Canada was consistently supportive in logistics and with some grants. Other costs were met by grants in aid of research from the Natural Sciences and Engineering Research Council of Canada.

References

Baker VR (2010) Channeled scablands: a megaflood landscape. In: Migon P (ed) Geomorphological landscapes of the world. Springer, Dordrecht, pp 21–28

Brown MC, Wright D (1979) The geography of Rabbitkettle Hotsprings, S. Nahanni National Park. Parks Canada. Unpublished report

Brook GA (1976) Karst terrains of the South Nahanni area, MackenzieMountains, N.W.T. Ph.D. thesis, McMaster University

Brook GA, Ford DC (1975) The karstlands of the South Nahanni region, N.W.T. Contract 72-32C, Parks Canada, 501 pp

Brook GA, Ford DC (1978) The nature of labyrinth karst and its implications for climaspecific models of tower karst. Nature 275:493–496

Crosbie ML (1978) Glaciolacustrine deposits of the Ram River Canyon area, Mackenzie Mountains, N.W.T. MSc thesis, Geography, McMaster University

Duk-Rodkin A, Lemmens DS (2000) Glacial history of the Mackenzie Region. In: Dyke LD, Brooks GR (eds) The physical environment of the Mackenzie Valley, Northwest Territories: a base line for the

assessment of environmental change. Geological Survey of Canada, Bulletin 547, pp 11–20

Ford DC (1972) Cavern and associated research in the First Canyon area, South Nahanni River, N.W.T. Contract report, Parks Canada, 115 pp

Ford DC (1973) Development of the canyons of the South Nahanni River, N.W.T. Can J Earth Sci 10:366–378

Ford DC (1974a) Geomorphology of South Nahanni National Park, N.W.T. Contract 72-32B, Parks Canada, 186 pp, 7 map plates

Ford DC (1974b) Evidences of multiple glaciation in South Nahanni National Park, Mackenzie Mountains, N.W.T. Can J Earth Sci 13:1433–1445

Ford DC (1984) Section 3-Geology, Section 4-Geomorphology, Section 5-Hydrology. In: Barlow J (ed) Nahanni National Park Reserve; Resource analysis and description. Parks Canada, pp 3.1–31; 4. 1–126; 5.1–60

Ford DC (1991) Antecedent canyons of the South Nahanni River. Can Geogr 35:426–431

Ford DC (2008) Report upon the Expansion of South Nahanni River National Park Reserve, Mackenzie Mountains, Northwest Territories. Unpublished report to Parks Canada

Ford DC, Williams PW (2007) Karst Hydrogeology and Geomorphology. Wiley, Chichester

Ford DC, Worthington SRH (2009) Final Report upon Cave and Karst Research and Evaluation in the South Nahanni and Ram river basins (NT, Canada). Unpublished report to Parks Canada

Gimbarzevsky P, Peaker JP, Addison P, Talbot S (1979) Nahanni National Park, North West Territories; integrated survey of biophysical resources. Parks, Canada

Harmon RS, Ford DC, Schwarcz HP (1977) Interglacial chronology of the Rocky and Mackenzie Mountains based upon $^{230}Th/^{234}U$ dating of calcite speleothems. Can J Earth Sci 14:2543–2552

Patterson RM (1966) The dangerous river. Gray's Publishing, Sydney

Schroeder J (1977) Les formes de glaces des grottes de la Nahanni, T.N.O. Can J Earth Sci 14:1179–1185

Schroeder J (1979) Le développement des grottes dans la région du Premier Canyon de la rivière Nahanni Sud, T.N.-O. University of Ottawa, PhD thesis

Scotter GW, Simmons NM, Simmons HL, Zoltai SC (1971) Ecology of the South Nahanni and Flat River areas. Unpublished report to Canadian Wildlife, Edmonton

Smith CJM, Richards DA, Smart PL, Farrant AR, Parrish RR, Horstwood SA, Ford DC (2011) Preliminary U–Pb LA-ICPMS analyses of a late Quaternary age speleothem from the Mackenzie Mountains. In: 6th Conference on the Karst Record, Birmingham, UK

Weirich FA (1978) Geomorphology of the central sector of South Nahanni national Park, with special reference to the glaciolacustrine sediments. M.Sc thesis, McMaster University

Castleguard Cave and Karst, Columbia Icefield, Alberta and British Columbia

16

D.C. Ford and C.C. Smart

Abstract

Castleguard Cave and alpine karst are developed in a limestone benchland that abuts and underlies the Columbia Icefield, Alberta/British Columbia. Castleguard Mountain (3083 masl) and other peaks rise above it, with lesser glaciers that also drain into the karst. On the surface, typical karst landforms such as karren fields, solution and suffosion sinkholes are abundant but comparatively small in size, reflecting erosion or infilling by expanded Little Ice Age glaciers that are now in rapid retreat. The explored cave, 'Castleguard I', has 24 km of mapped passages, the longest currently known in Canada and the foremost example anywhere of a modern cave beneath glaciers. Most of it is now a hydrological relict, basal meltwaters from the central Icefield and lesser glaciers passing down through it into an inaccessible lower system, 'Castleguard II'. Relict inlet passages are blocked by plugs of ice or till. Six km of central passages pass through the mountain as down dip/up joint looping conduits with alternating vadose and phreatic morphology known to be >780 ka BP in age. Outlet passages can still flood with catastrophic rapidity during summer melt, despite being $\geq$ 360 m above basal, perennial, springs in the Castleguard River valley below. Cumulative karst discharge is c. 20 m^3/s^{-1}, most of it weakly turbid melt from the base of the central Icefield.

Keywords

Alpine glaciation • Karst processes • Geologic structure • Speleogenesis • Meltwater flood extremes

16.1 Introduction

Castleguard Cave and alpine karst have developed in a limestone benchland abutting the eastern side of the Columbia Icefield and extending beneath it. Castleguard Mountain (latitude 50°06′30"N, longitude 117°15′10″W; elevation 3083 masl) is approximately at the centre of the karst (Fig. 16.1). The icefield and its valley glacier outlets are c. 320 km^2 in area, the largest glacier ice body remaining in the Rocky Mountains today (see Chap. 17, this volume). The explored cave has 24 km of mapped passages, the longest currently known in Canada, and is the foremost example anywhere of a modern cave beneath glaciers. It displays many striking morphologic and speleogenetic features, interactions between glaciers and karst aquifers, and a complex modern climate. In 1983 a comprehensive report involving many specialists was published as a full issue of the journal, *Arctic and Alpine Research,* and is the basis of most of the summary being presented here (Ford 1983); see also Muir and Ford 1985.

D.C. Ford (✉)
School of Geography and Geology, McMaster University, Hamilton, ON L8S 4L8, Canada
e-mail: derekcliffordford@gmail.com

C.C. Smart
Department of Geography, University of Western Ontario, London, ON N6G 2V4, Canada

© Springer International Publishing Switzerland 2017

O. Slaymaker (ed.), *Landscapes and Landforms of Western Canada*,
World Geomorphological Landscapes, DOI: 10.1007/978-3-319-44595-3_16

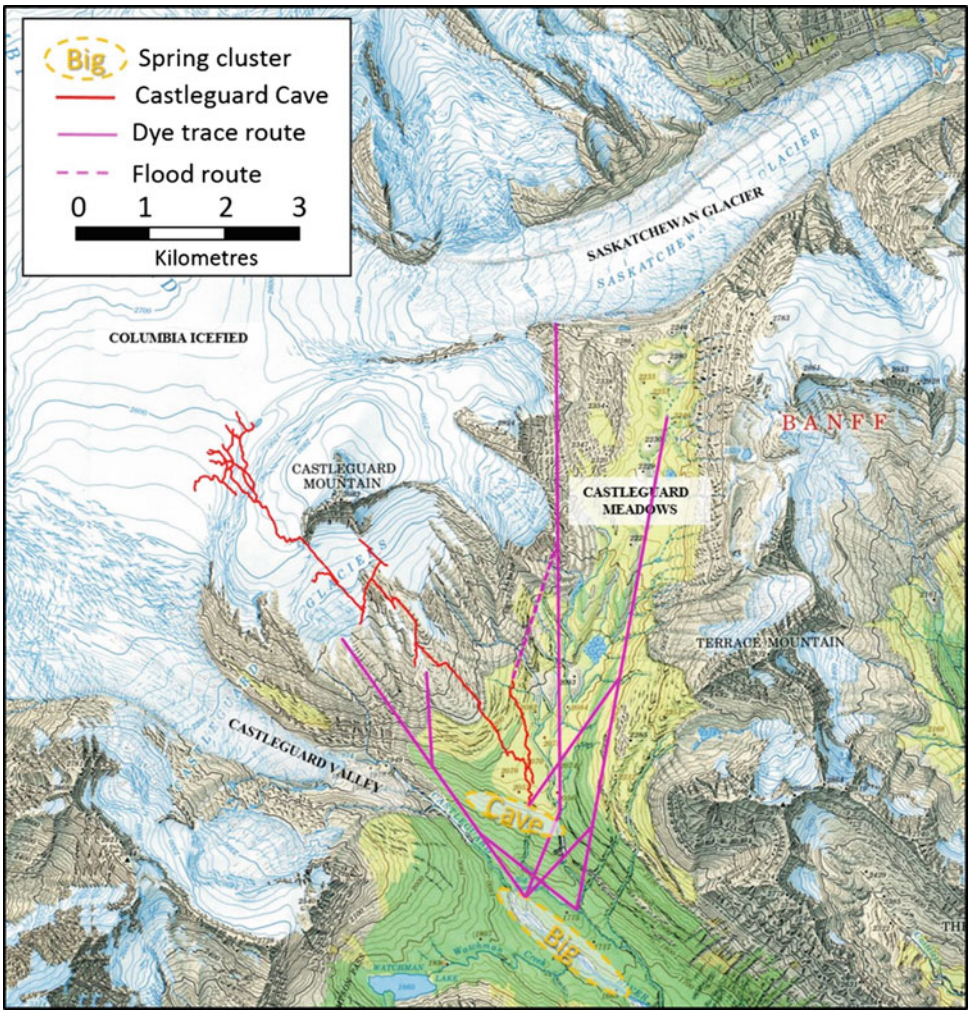

Fig. 16.1 Shaded topographic relief map of the Columbia Icefield and adjoining mountains. The Banff-to-Jasper ('Icefields') Parkway lies a few km to the north of the map. The location of Castleguard Cave (passing beneath Castleguard Mountain) is shown in *red* and a selection of the ground water traces in *purple*. Castleguard Meadows (alpine) extend between Saskatchewan Glacier and the Castleguard River valley in the south

16.2 Regional Physiography, Geology and Glaciology

The Columbia Icefield region is a 'textbook example' of alpine glacial morphology, with horn peaks, arêtes, cirques, trough-head valleys, a plateau ice cap with radiating valley glaciers, medial and recessional moraines, outwash terraces and braided river channel deposits downstream of glacier snouts in the trunk valley bottoms. The local relief from valleys to peaks is 1400–1600 m.

The glaciers rest upon a pedestal of sedimentary rocks dipping gently to the southeast (Fig. 16.2). Caves and karst features are developed in a platform carbonate rock sequence of Middle Cambrian age that has been divided into four distinct formations (Douglas et al. 1970). Their aggregate thickness in the locality is at least 560 m, the base lying unseen below the alluvial floor of the Castleguard River valley. At the bottom of the sequence, the Cathedral Formation has a main member consisting of very uniform, massively bedded and resistant, crystalline limestones overlain by an upper member that is also massive but more varied in composition, including dolomitic mottling and one strikingly blue porcellanous bed. The main member hosts the bulk of the groundwater channels that are active today. The upper member displays excellent surface karst landforms in the northern meadows (e.g. Fig. 16.3b).

The overlying Stephen Formation is a mixture of shaley limestones and calcareous shales with pyrite. These strata are thinner bedded, mechanically recessive and significantly less soluble than the limestones above and below. They serve as an aquitard, obstructing the passage of karst waters through them but not prohibiting it. Above them, the Eldon and Pika formations are limestones of intertidal origin, thick to massively bedded, but with frequent orange-weathering dolomite partings that protrude on weathering surfaces and have also tended to obstruct groundwater flow. Many limestone beds are strongly rippled: overridden by ice flow that is nearly normal to the axes of ripple crests, the ripples may be dissected into spectacular displays of micro-rock drumlins (see Fig. 16.4).

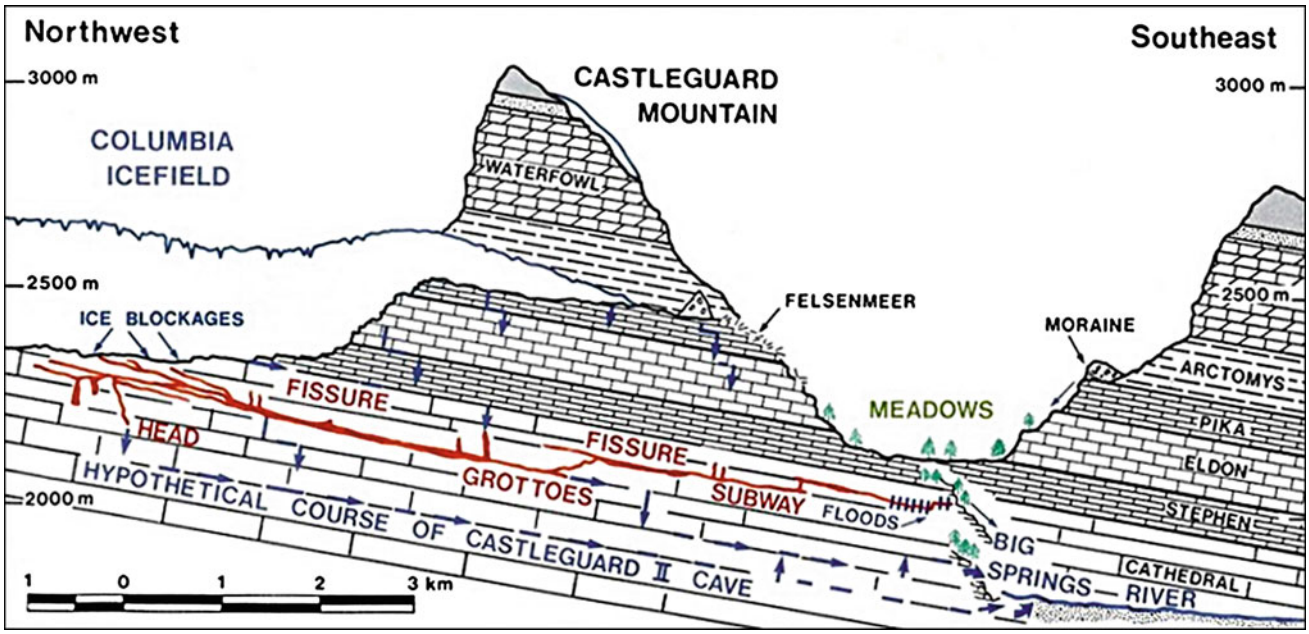

Fig. 16.2 Sketch geological section of Castleguard Mountain and Meadows showing the stratigraphic formations and the approximate locations of the known Cave, the inaccessible channels ('Castleguard II') beneath it, and the outlet springs

Fig. 16.3 **a** Inside the Little Ice Age moraine, freshly scoured Pika limestone with Castleguard Mountain in background. **b** Outside the moraine, Cathedral limestone pavement at the head of the meadows. **c** Inside; a small sinkhole modified by glacial plucking on the up-ice (*left*) side and scour down-ice. It is the morphological converse of a *rôche moutonnée!* **d** Outside, a suffosion doline in medial moraine: flowing water is piped down into underlying epikarst in the limestone

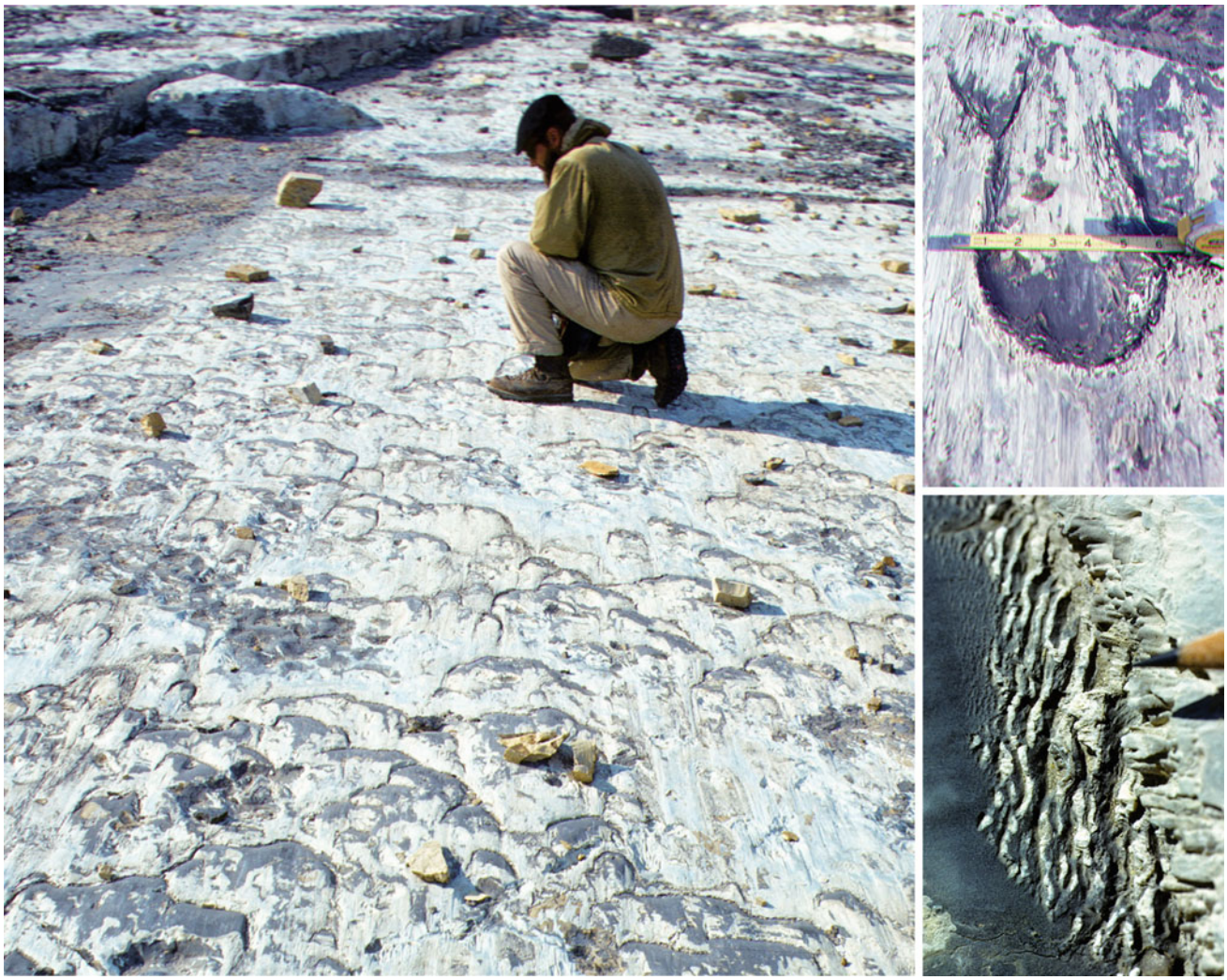

Fig. 16.4 As the Little Ice Age glaciers are receding across the rather smooth benches of Cathedral and Pika limestones, there is net scour and solution on prominences at the glacier base, and prompt precipitation of sub glacial calcite (*white*) where the pressure is relieved. It is shown here at three different scales on the South Castleguard bench. This is amongst the finest sites reported in the literature

Above the Pika Formation, a thick, purple-maroon shale (the Arctomys Formation) is impermeable and so terminates the karst carbonate sequence. It is overlain by several hundred metres of other shales, sandstones and dolomites of Upper Cambrian-Ordovician age that are mechanically weak and compose narrow summit masses enclosing glaciers that rest on the upper carbonates. They supply copious clastic debris.

The karst area lies on the axis of a broad anticlinal structure plunging southeast. Stratal dips on Castleguard Mountain and meadows are regularly 4°–6° SSE. Where the cave extends under the icefield, the dip appears to be reduced. Joints are few, but long and deep, in two sets oriented north–south and northwest–southeast (Hooyer et al. 2012). There are widely spaced deep, south-trending sedimentary dikes and fractures associated with hydrothermal mineralisation at depth. These features imply deep hydrothermal groundwater circulation, possibly associated with the Laramide orogeny when the area was deeply buried and undergoing tectonic thrusting (Bodenhamer 2007). The bedding planes exposed in the cave are extensively modified by slickensides and local shear structures indicative of modest displacement accommodated by bedding plane shear (Ford et al. 2000).

This area was a major centre for glacier ice formation and dispersal during each buildup of the Cordilleran Ice Sheet. Distribution of erratics indicates that all cirques, benches and valleys were occupied by flowing ice at the peak of the last major ice age, the Wisconsinan. Trimlines are poorly preserved but suggest maximum ice elevations 750–800 m above the current floors of trunk valleys such as that of Saskatchewan Glacier, the source of the North Saskatchewan River.

During the Wisconsinan recession, interlobate sediments were left along the axis of the upper meadows, including a small ice dammed lake (Henoch et al. 1979). A ^{14}C date of 9480 ± 95 years on a sample of red squirrel midden from the head of the cave (Wildberger 1987, personal communication) and calcite speleothem (6100 ± 200 BP) from benches south of Castleguard Mountain suggest that, contrary to our earlier opinion, the icefield and neighbouring glaciers may have almost entirely disappeared during the Hypsithermal phase of the early Holocene.

The ice returned after c. 5000 BP. Around 200 years ago, during the Neoglacial ('Little Ice Age'), the icefield and valley glaciers expanded substantially. Cirque and bench glaciers around Castleguard Mountain extended c. 1000 m, bulldozing surface debris into sharp terminal moraines up to 50 m in height. The earliest photographs (1918) show the ice still standing at these moraines but considerably thinned from the inferred maxima. Ice fronts have now receded an average of 500–600 m from them (e.g. Fig. 16.3a), exposing scoured bedrock platforms. Saskatchewan Glacier has receded 2.4 km and thinned more than 100 m from the Neoglacial maximum. Luckman (2016) (see Chap. 17, this volume) provides details of the distal recessional history of the Athabasca Glacier, another major glacier outlet of the icefield. From radio echo traverses modern ice depths range 100–365 m over the icefield itself and in the upper valley glaciers (Waddington and Jones 1977). From cave survey data, the icefield is c. 300 m thick over the head of Castleguard Cave.

The modern tree line is between 2000 and 2150 masl. There is a wealth of periglacial landforms above it, primarily felsenmeer on Eldon and Pika limestone benches outside of the Neoglacial moraines. Sedimentary deposits have been remobilised by solifluction and streams to encroach upon or bury some karren fields and sinkholes (e.g. Fig. 16.3).

16.3 Surface Karst Landforms

Karst landforms are found on all of the carbonate formations. Small-scale solution features ('karren' and limestone pavements) are common on exposed bedrock surfaces outside of the Neoglacial moraines. A typical small patch of pavement is shown in Fig. 16.3b. Varieties of sinkholes (dolines) are the principal larger features, numbering more than one hundred in the meadows. On the Pika, Eldon and Stephen rocks, they are narrow, vertical shafts elongated along guiding joints, up to 30 m in depth and at least early postglacial in age. On the more purely calcitic Cathedral limestone, circular or elliptical shafts predominate and are considered to originate subglacially, or represent existing dolines truncated by glacial erosion. There are also a few more typical funnel-shaped dolines that may have survived glaciation, or opened up by postglacial frost shattering. Where sediments overlie karst, 'suffosion dolines' can form where the sediment is being carried into an underlying fissure. Such features can switch from a pond to an open sinkhole depending on runoff and choking of the outlet. Figure 16.3d shows an example formed in proglacial lake sediments that now conveys a vigorous stream, as evidenced by the calibre of the bedload.

A rare class of small karst features is a deposits of calcite that is precipitated subglacially and then exposed as the ice recedes (Fig. 16.4). The Castleguard deposits appear to be more extensive, larger and more varied morphologically than those of many other sites (Ford et al. 1970; Hallet 1976), because the glacier ice is largely debris-free, reducing the impact of abrasion. The deposits are typically c. 1–2 mm thickness, streamlined to accord to the flow directions of basal melt films of water, and may cover 80 % of a polished rock surface freshly exposed by glacier recession. Basal glacier ice encountering obstacles melts to provide water to dissolve the limestone. Where pressure is relieved—such as on the lee side of obstacles—the meltwater freezes, precipitating calcite laminae and spicules. The entire cycle (pressure melt + limestone solution → transverse micro-furrows dissolved in dark grey limestone → refreezing + calcite precipitation → light coloured laminae and spicules) is illustrated at the scale of the tip of a pencil (Fig. 16.4c). Unfortunately, exposed subglacial precipitates are vulnerable to frost shattering and dissolution and only persist a few decades after ice retreat.

16.4 Castleguard Cave

16.4.1 'The Explorers' Cave

The cave that is highlighted in red in Figs. 16.1 and 16.2 is that which is accessible to cavers and has been mapped, 'Castleguard I'. From the hydrological perspective, it is now a relict cave, equivalent to a terrace in a fluvial geomorphic system. In the warmer seasons, seepage and small streams enter overhead at many points and pass down through it via shafts, or flow along the floor for a few tens or hundreds of metres before disappearing into tiny new solutional passages. They are carrying the water into 'Castleguard II', an underlying active system of solutional conduits that conveys up to 20 m^3/s meltwater from the Columbia Icefield (Fig. 16.2). 'Castleguard III' is a second active system of similarly complex geometry that conveys karst water from the meadows and upper Saskatchewan Glacier (Smart and Ford 1986).

Earliest karst dissolution is represented by the hydrothermal fracture fill deposits associated with north–south fractures through the cave. These features imply deep

groundwater circulation under entirely different topography probably associated with the Laramide orogeny 40–70 Ma ago (e.g. Bodenhamer 2007). Erosion into the Pleistocene created a suite of glacial troughs first exposing the Cathedral limestone along the axis of the Castleguard Meadows where the initial meteoric water cave is expected to have formed aligned along a north–south fracture. This development provided a discharge outlet for groundwaters encountering the Cathedral limestone to the northwest.

The explored Castleguard I is an excellent example of a limestone dissolutional cave. Cavers can enter the cave only at its downstream end, which is at 1970 masl in the north wall of Castleguard River valley, more than 300 m above the valley floor. From there, the cave ascends more than 380 m to terminations underneath the icefield. There are three distinct morphologic sections: (i) A headward complex of small inlet passages beneath the modern icefield, created by repeated blockage and re-routing of sinking waters in the past (labelled 'HEAD' in Fig. 16.2). The passages are plugged by glacier ice or debris today. (ii) A downstream complex of low tunnels in two major bedding planes, created by flooding and obstructions by glacier ice in Castleguard Valley in the past ('FLOODS' in Fig. 16.2). (iii) In between, the central cave is a sequence of remarkably long, straight conduits created where one master bedding plane is intersected by vertical joints that are linked by small number of north–south fractures and a sedimentary dike (Grottoes Dike) crossing them (Fig. 16.5a). In the bedding plane, there is some evidence of crushing and shearing, indicating that a few cm of differential slip related to flexure in strata to the south opened it up a little, permitting groundwater to penetrate at its juncture with the joints and dike. It is not clear if the cave developed as a single link between a recharge zone north of the present Castleguard Mountain and the Castleguard Valley, or whether a series of progressive cross-links developed between north–south fractures. All north–south segments in the cave exhibit modern drains to lower levels.

Initially, the explored cave may have functioned as a single phreatic (water-filled) loop that descended more than 370 m below a palaeo-watertable, requiring water to discharge upwards through the Stephen Aquitard (presumably along faults) to reach ancient springs in the Castleguard Valley. More certainly, as Castleguard Valley was entrenched below the Stephen Formation, the cave became largely drained and enlarged to nearly its modern dimensions, as shown in Fig. 16.5b. It was then comprised of two shallow principal loops with vadose canyon entrenchments up to 20 m deep at their upstream ends (Fig. 16.6a, d), grading downstream into phreatic tubes four to five m in diameter and of beautiful circularity where the water-filled cave persisted (Fig. 16.6b, e). The downstream loop discharged into the downstream complex, by a vertical lift of 24 m up a shaft of phreatic origin (Fig. 16.6f). Following further entrenchment of the valley, the main cave headwaters were diverted into a new, lower cave (Castleguard II) and the local recharge waters drained through constricted under-capture passages in the bottoms of the loops (Fig. 16.5c) and cross-rifts.

The downstream complex is the meeting point of Castleguard I and a complementary cave that still conveys summer floods and sustains a perennial spring near the cave entrance (Smart and Ford 1986). The latter cave has recently been dived for 845 m northwards to air-filled passage (Groves 2010) and is inferred to deliver melt and rain waters from the upper Meadows and Saskatchewan Glacier.

16.4.2 Clastic Sediments in Castleguard Cave

Fluvial boulders, gravel and sand are encountered in the headward complex in the cave (Fig. 16.7b). These deposits have been variously cemented by calcite and eroded, indicating a long history of filling and removal (Schroeder and Ford 1983).The modern subglacial catchment of the cave generates surprisingly little sediment, consistent with limited subglacial fluvial action in the upper accumulation zone of glaciers. The headwater fluvial sediments are most consistent with interglacial conditions, when proglacial streams mobilised exposed glacial sediments and transported them intermittently into the cave.

In contrast, in both the vadose and phreatic passages throughout the cave, there are fragments or substantial sections of laminated silts and clays up to several metres in thickness that represent multiple episodes of deposition (Fig. 16.7c, d). There appears to be no consistent stratigraphy or longitudinal gradient in these deposits. They exhibit varied lamina thickness. Although predominantly still water drapes, there are occasional sedimentary structures indicative of water flow (e.g. cross-bedding) and erosion (e.g. scour trenches and rip-up clasts). Deposition in vadose (air-filled) passages and interbedded calcite deposits including occasional stalagmites demonstrate drained conditions prior to emplacement. Such fine sediments would traditionally be assigned as 'slackwater deposits' arising from still water conditions, typically in backwater tributary passages. These voluminous still water deposits are challenging to interpret as they occupy many kilometres of previously drained cave with a relatively steep overall gradient over hundreds of metres of elevation head. Single event flooding and ponding through the cave is improbable. A source for the fine sediments is required, as is a mechanism for generating piecemeal ponding and sediment deposition throughout the cave.

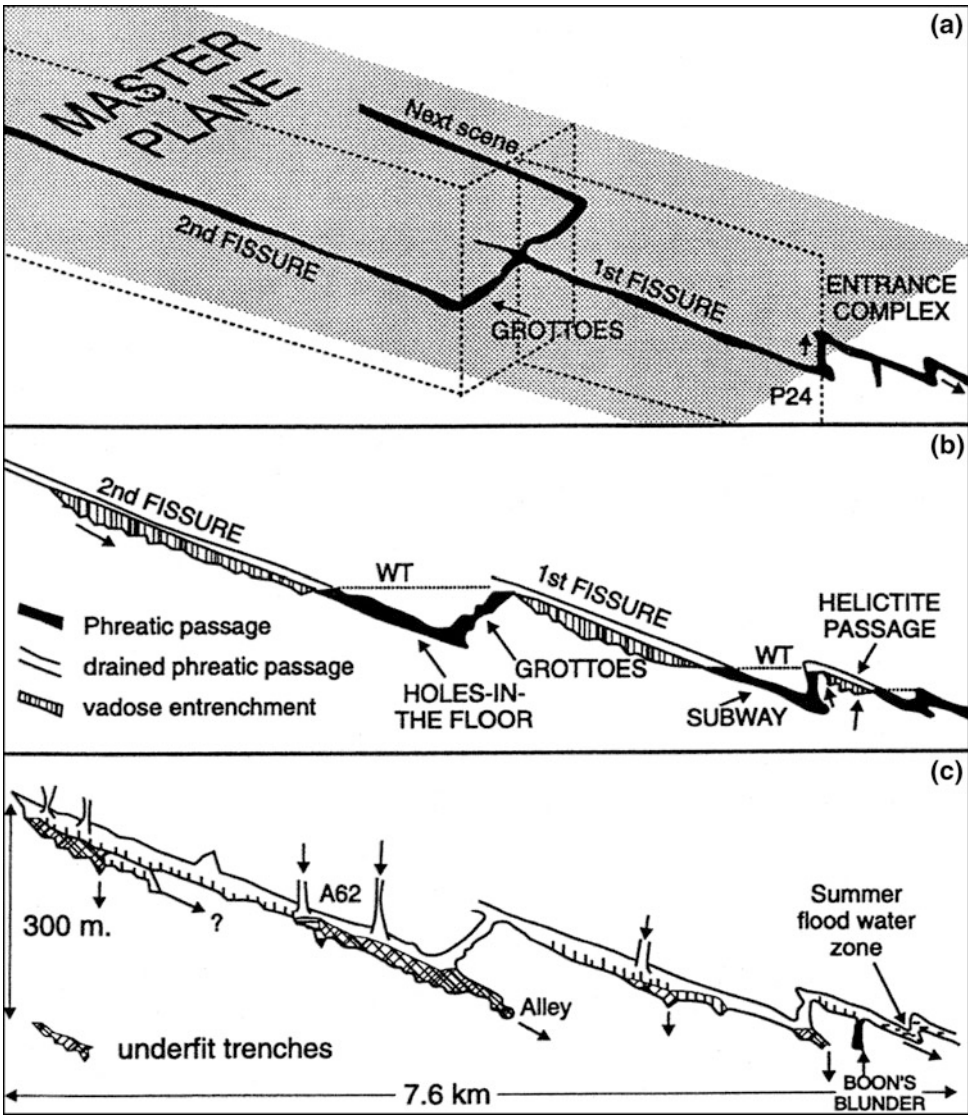

Fig. 16.5 The basic architecture of Castleguard Cave. **a** The cave developed where three particularly penetrable bedding planes 6 and 24 m apart in the Cathedral limestone are intersected by lengthy joints oriented aslant the 5° dip. The lowest, 'Master,' plane guides most of the central cave. As passages enlarged (**b**), the water table was lowered to the minimum elevations required to maintain circulation into the upper planes and out of the mountain, ="phreatic loops." Glacial and fluvial entrenchment of the Cathedral River valley (**c**) then led to capture into lower caves (Castleguard II) that are inaccessible

Each lamina requires stagnant water, yet multiple laminae and local erosional episodes indicate repeated, occasionally energetic flushes with fresh turbid water. Glaciation provides a likely source of fine sediments as glacier flour and is also likely to have raised the water table in Castleguard Valley, not only flooding previously drained cave passage but also seasonally reducing the overall hydraulic gradient through the cave. Turbid glacial meltwater may pass through the cave in summer, and stagnate in winter, allowing deposition of a layer of the fine grained sediments. Subsequent flushing and even periodic drainage will leave the cohesive sediments largely intact. This cycle may eventually result in local blockage of the cave, so that various sectors pond and drain, sometimes catastrophically as barriers rupture and reform, so accounting for the incoherent stratigraphy.

A most unusual instance of cave sedimentary dynamics occurs at P8, an eight metre shaft just one hundred metres inside the cave. Over the course of the fall → winter → spring thermal cycle, frost-shattering sends fresh clasts from the walls down to a talus slope at the foot. In summer floods, when there is flow ≥ 6 m^3/second *up* the shaft, flood pulsing re-works this talus into a storm shingle beach like that seen on rocky open sea coasts (Fig. 16.7e). Shingled clasts, when reduced to about seven cm in length, are swept up the shaft and out of the cave (Schroeder and Ford 1983).

16.4.3 Speleothems in the Cave

Despite its location beneath glaciers or alpine tundra, the cave beyond the modern entrance flood zone is well decorated with precipitated speleothems. Very pure, white calcite in the form of stalactites, stalagmites, and flowstone on the

Fig. 16.6 Illustrating the architecture shown in Fig. 16.5. **a** Second Fissure, a gravitational ('vadose') entrenchment drains into—**b** 'Holes-in-the-Floor', a subwater table ('phreatic') tube that descends to feed. **c** The Grottoes, an ascending phreatic passage. This spilled over into **d** First Fissure, a vadose entrenchment draining to **e** The Subway, a phreatic tube straight as a die for 450 m and descending gently to **f** 24 m Pot, a vertical shaft created by solution up a small fault ('phreatic lift') to deliver the water to Helictite Passage, so completing the D–E–F loop

walls is overwhelmingly predominant (Fig. 16.8a, b). In the warmer central sector (temperature of +2 to +3 °C, relative humidity of ≥ 93 % in the driest season), there are small evaporative aureoles of aragonite, huntite, hydromagnesite, gypsum, mirabilite, and epsomite; evaporation in these extreme conditions is due to strong drafts blowing through the cave when it is not in flood (Harmon et al. 1983). The richest growth is in the central grottoes, but there are even widespread juvenile straw stalactites growing in the headward passages under the icefield itself, where temperatures

Fig. 16.7 Sedimentary deposits in the cave. **a** Underneath the Icefield, many passages become blocked by regelation ice or **b** glacier bedload. During glacial phases, the phreatic areas and lower parts of many vadose passages were filled with varved clays (**c**), most of which have been sapped into underfit stream trenches today (**d**). **e** View up the 8 m shaft, 100 m from the cave entrance and within the modern flood zone. Winter frost and summer flood pulses work local clasts into a shingle beach (foreground) until they are small enough to be swept up and out of the cave

are close to 0 °C. Cave pearls are widespread in the cave—inferred to be the product of drip water disturbing a gradually growing sphere of calcite. A remarkable variant occurs in the Second Fissure where a double layer of calcite sub-cubical pearls 5–7 mm in diameter is found; it is one of only four instances known in the world (Roberge and Caron 1983; Hill and Forti 1997).

There has been speculation about the causes of the modern calcite deposition because in most other caves this is due primarily to extra acidity supplied to the drip water by high concentrations of soil CO_2 overhead. There are no soils above most of Castleguard Cave. Atkinson (1983) analysed the conditions and concluded that the extra acid derived from oxidation of pyrite in shales of the Pika Formation, a conclusion supported by analysis of the sulphur isotopes (Yonge and Krouse 1987). Stalactites in the headward complex may be associated with elevated CO_2 in the refreezing water film at the bed of the glacier, a subterranean analogue of the precipitates found on the surface (Fig. 16.4).

Although the large majority of speleothems appear to postdate the latest phase of varved clay deposition, there are some interbedded stalagmites and remains of older massive calcite deposits that suffered erosion during subsequent floods (Fig. 16.8c). Uranium series dating and palaeomagnetic studies of some of the oldest examples show that the cave became relict (i.e. Castleguard II was already well

Fig. 16.8 Calcite speleothems in the cave. **a** Stalactites and straw stalactites are abundant in the central cave, many growing into the constant draft. **b** Larger stalagmites and flowstones in The Grottoes. **c** Also in the Grottoes, a large modern stalactite grows from the remnants (*yellow-buff*) of a predecessor removed by solution during a glacial inundation. **d** High in First Fissure (vadose canyon) a stalagmite is being destroyed by dripping seepage water that earlier created it. A sample from its base was magnetically reversed (>780,000 years in age), helping to establish the antiquity of the cave

developed) more than 780,000 years ago (Fig. 16.8d; Gascoyne et al. 1983). The varved clays are younger. Such antiquity appears to be typical of multi-level alpine caves.

16.5 The Karst Hydrology of the Columbia Icefield, the Castleguard Caves and Meadows

The Castleguard Valley contains numerous springs that discharge, *in toto*, up to 20 m^3/s of remarkably clear water in high summer. Flow decreases very rapidly in cold weather, and approaches zero in late winter. In contrast, the few small glacial meltwater streams and closed drainage basins in the upper meadows and on the benches around Castleguard Mountain supply only a maximum of c. 1 m^3/s to the karst aquifer. It has long been recognised that this imbalance implies that the majority of the recharge comes from the Columbia Icefield, although the location and mechanism of recharge was unclear (Ford 1983).

Winter cave exploration beneath the icefield revealed dry vertical shafts passing through the cave and descending to constrictions tens or hundreds of metres below. Many shafts showed sharply etched, clean-washed walls implying meltwater flow in the summer. Steady air flow up the shafts showed that warm cave air was able to reach the surface

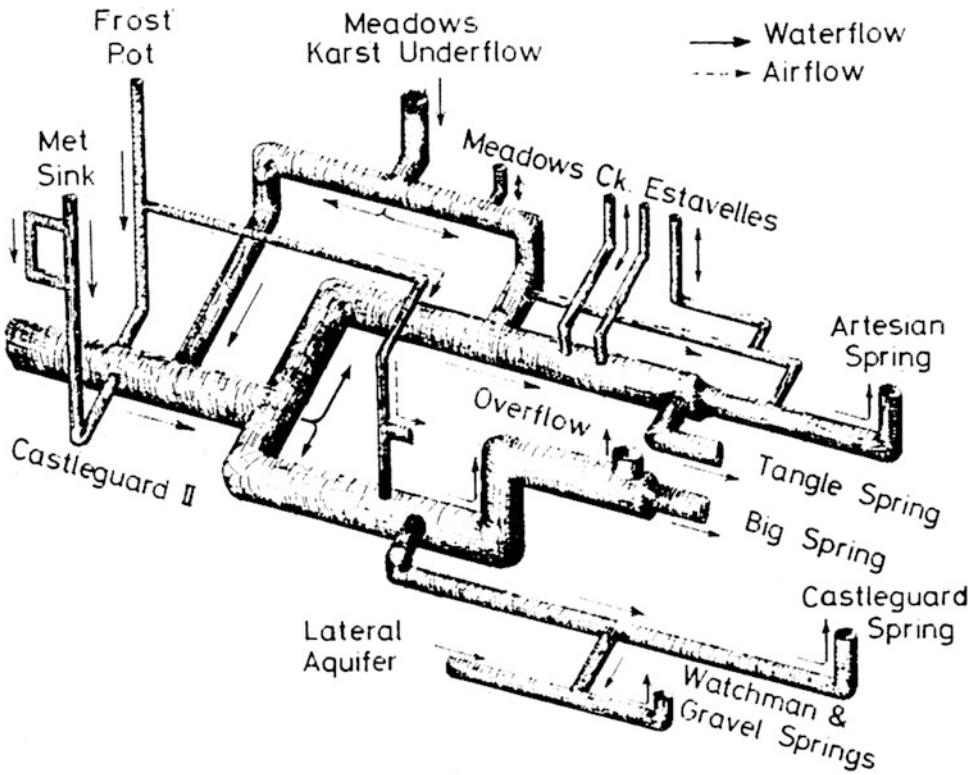

Fig. 16.9 Castleguard II, the inaccessible modern floodwater cave. This model illustrates the complex connections between the glacial and other groundwater sinks, the inaccessible conduits in the strata below the explored cave, and the outlet springs. The pipe diameters are proportional to their discharges. The connections and capacities were determined by dye tracing, chemical and isotopic water sampling and discharge measurements by Smart (1983)

through c. 300 m of glacier ice. It was inferred that the meltwater descended to the lower level cave, 'Castleguard II' linked to the springs in Castleguard Valley (Fig. 16.9).

A water tracing program was undertaken in 1979–81, using small quantities of fluorescent dyes to track meltwater from the Saskatchewan Glacier and Castleguard benches to the valley springs, supporting the glacial origin of the meltwater (Smart 1983; Fig. 16.10). Traces from the upper meadows fed a set of springs around the cave entrance, as well as being detected in the Castleguard Valley Springs. Careful analysis of the tracer timing revealed very rapid flushing of dye through the aquifer, implying well-developed (i.e. mature) karst conduits.

Glacial meltwater has relatively limited capacity to dissolve limestone. The constrictions of the erosional shafts explored in the cave reflect this limited capacity, but their sharp etching implies water newly encountering bedrock, i.e. an origin on the glacier surface. Observations of the flow rate in the springs demonstrated strong daily variation, closely matching icefield melt rates, again confirming a surface origin and very rapid transmission of water.

The Valley Springs extend for 4–5 km, varying from large conduit outlets (e.g. Big Spring ≤ 5 m^3/s), through bubbling artesian springs to small quick sand boils and seeps. Observations of flow and dye recovery showed that these springs operated as two somewhat independent spring groups, each of which extended spatially and vertically as flows increases and new overflows became activated. Such a widely distributed set of restricted springs might be taken as a feature of a rather immature karst aquifer.

The overall picture is one of surface melt descending through crevasses in the icefield to reach limestone bedrock, forming vertical shafts that descend to Castleguard II. The crevasses are formed where ice deforms over a series of bedrock steps in the flanks of a cirque north of Castleguard Mountain. The various recharge inlets all unite into a trunk conduit before being divided again to be distributed to the numerous springs.

The restricted vertical shafts and numerous springs in the valley are characteristic of an immature karst system, as might be expected with glacial meltwater as the agent of dissolution. But the rapid flow and inferred common conduit suggest otherwise. It is concluded that the immaturity of the shafts (and much of the complexity of the headward complex in the cave) results from progressive retreat of the bedrocks steps, episodically reorganising the position of crevasses over time and contributing to the tangled network of cave passages in this area. The widely distributed spring system is inferred to have resulted from glacial erosion and post-glacial infilling disrupting the spring outlets. A very similar situation has arisen at the outlet of the Maligne Karst near Jasper (Smart 1988a, b).

In addition to summer floods of several m^3/s emerging from the cave entrance, there are intermediate floodwater springs and one perennial ('Red') spring that shows no response to the flood events. This is surprising given its

Fig. 16.10 Illustrating the karst hydrology. **a** A glacial melt stream sinks into a youthful shaft at c. 2480 masl in the Pika limestone. **b** Floodwaters pouring out of the entrance to Castleguard Cave at 1970 m. **c** The Big Springs discharging from an outlet at 1800 m, hanging 40 m above the alluvial valley floor. **d** 'Watersmeet' at 1710 masl; tinted only with a little glacier flour, karst ground waters from the central Icefield, Saskatchewan Glacier, Castleguard Mountain and Meadows (left-hand channel) combine to push aside the very turbid, but lesser, melt river from the snout of the South Castleguard Glacier

position 340 m above the floor of the Castleguard Valley. There is no obvious geological explanation for flow emerging at this level, so it was inferred that the conduits feeding the spring are ancient features, reactivated in some way. Monitoring of these phenomena implied a large flooded (hydrologically perched) passage maintained through a combination of the massive bedrock and sedimentary fill (Smart and Ford 1986). Slow drainage over winter sustained the Red Spring, but in summer, cave floods were inferred to also use this conduit. The trigger for floods appears to be overflow further upstream during days of high runoff. The recent, very challenging, cave diving has confirmed some aspects of this model, including the volume of the flooded conduit.

16.6 Conclusions

Castleguard Cave has provided an astonishing natural laboratory facilitating understanding of cave development, glacier hydrology and alpine hydrochemistry. The site also hosts unique invertebrates and promises further insights into natural evolution in isolated refugia (Holsinger et al. 1983).

Although one of the most studied alpine karst systems in the world, the age, origin and full function of the cave remains poorly understood. In part this is a reflection of the total inaccessibility of much of the functional cave, and severe difficulties accessing the more remote reaches of the cave and icefield. The cave was possibly initiated at some depth in the deep past when climate and topography were very different and plate tectonic forces were acting. The hydrological interaction between glaciers and adjacent karst aquifers is also poorly understood, despite this having been the predominant condition over much of the last two million years.

Given the understanding gained from the site, and the many mysteries that remain, it is fortunate that it has for long been under the protection of Parks Canada, and is a component of the Mountain Parks World Heritage Site.

Acknowledgements The primary debt of all researchers in Castleguard Cave is to their companions in the field. It is a severe and hazardous place, yet there never has been a lack of volunteers to work very hard. Financial aid was chiefly from Natural Scientific and Engineering Research Council of Canada grants to Ford and Smart. Parks Canada has given much encouragement and practical assistance in kind. A major scientific expedition to the cave in 1980 was supported by the Crestview Foundation (Calgary), Hudson's Bay Oil and Gas Co. and the Royal Canadian Geographical Society.

References

Atkinson TC (1983) Growth mechanisms of speleothems in Castleguard Cave, Columbia Icefields, Alberta, Canada. Arctic Alpine Res 15:523–536

Bodenhamer HG (2007) Preglacial development of caves at structural duplexes on the Lewis Thrust, Glacier National Park, Montana. J Cave Karst Stud 69:326–341

Douglas RJW, Gabrielse H, Wheeler JO, Stott DF, Belyea HR (1970) Geology of Western Canada. In: Douglas RJW (ed) Geology and Economic Minerals of Canada. Geological Survey of Canada, Ottawa, pp 365–488

Ford DC (ed) (1983) Castleguard Cave and Karst, Columbia Icefields Area, Rocky Mountains of Canada: a symposium. Arctic Alpine Res 15:425–554

Ford DC, Fuller PJ, Drake JJ (1970) Calcite precipitates at the soles of temperate glaciers. Nature 226:441–442

Ford DC, Lauritzen S-E, Worthington S (2000) Speleogenesis of Castleguard Cave, Rocky Mountains, Alberta, Canada. In: Klimchouk A, Ford DC, Palmer AN, Dreybrodt W (eds) Speleogenesis: Evolution of Karst Aquifers. National Speleological Society of America, Huntsville, Alabama, pp 332–337

Gascoyne M, Latham AG, Harmon RS, Ford DC (1983) The antiquity of Castleguard Cave. Arctic Alpine Res 15:463–470

Groves M (2010) Castleguard cave diving expedition 2010. Official report to Ghar Parau Foundation (http://www.gharparau.org.uk/wp-content/uploads/Castleguard-Official-Report-2010.pdf)

Hallet B (1976) Deposits formed by subglacial precipitations of $CaCO_3$. Geol Soc Am Bull 87:1003–1015

Harmon RS, Atkinson TC, Atkinson JL (1983) The mineralogy of Castleguard Cave, Columbia Icefields, Alberta, Canada. Arctic Alpine Res 15:503–516

Henoch WES, Luckman BH, Baranowski S (1979) A new Holocene locality from Castleguard Meadows, Banff National Park. Z Geomorphol 23:383–395

Hill CA, Forti P (1997) Cave minerals of the world. National Speleological Society of America, Huntsville

Holsinger R Jr, Mort JS, Recklies AD (1983) The Subterranean Crustacean Fauna of Castleguard Cave, Columbia Icefields, Alberta, Canada, and its Zoogeographic Significances. Arctic Alpine Res 15:543–549

Hooyer TS, Cohen D, Iverson NR (2012) Controls of glacial quarrying by bedrock joints. Geomorphology 153–154:91–101

Luckman BH (2016) Glacier landscapes in the Canadian Rockies. In: Slaymaker O (ed) Landforms and landscapes of Western Canada. Springer, Berlin

Muir RD, Ford DC (1985) Castleguard. Parks Canada Centennial Publication. Department of Supply and Services, Gatineau, Quebec

Roberge J, Caron D (1983) The occurrence of an unusual type of pisolite: The cubic cave pearls of Castleguard Cave, Columbia Icefields, Alberta, Canada. Arctic Alpine Res 15:517–522

Schroeder JJ, Ford DC (1983) Clastic sediments in Castleguard Cave. Arctic Alpine Res 15:451–461

Smart CC (1983) The hydrology of the Castleguard Karst, Columbia Icefields, Alberta, Canada. Arctic Alpine Res 15:471–486

Smart CC (1988a) Quantitative tracing of the Maligne Karst System, Alberta Canada. J Hydrol 98:185–204

Smart CC (1988b) Artificial tracer techniques for the determination of the structure of conduit aquifers. Groundwater 26:445–453

Smart CC, Ford DC (1986) Structure and function of a conduit aquifer. Can J Earth Sci 23:919–929

Waddington ED, Jones TDP (1977) A radio echo ice thickness survey on the Columbia Icefield. Unpublished report, Parks Canada

Wildberger A (1987) Personal communication of carbon-14 dating. Switzerland

Yonge C, Krouse HR (1987) The origin of sulphates in Castleguard Cave, Columbia Icefields, Canada. Chem Geol 65:427–433

Glacier Landscapes in the Canadian Rockies

17

Brian Henry Luckman

Abstract

This paper provides a descriptive account of selected glacier forefields in the central Canadian Rockies. A map of landforms in the forefield of the Athabasca Glacier is presented, updated to 2014, together with a brief summary of the glacier history since the Little Ice Age maximum extent in the 1840s. Brief descriptions are given of the formation of the major lateral moraines, small annual moraines and the evolution of the proglacial drainage into Sunwapta Lake. The adjacent, debris-covered Dome Glacier is also illustrated. Landforms in these forefields are developed on easily deformed, fine-grained sediments. Angel Glacier is a cirque glacier at Mount Edith Cavell with a hanging tongue that formerly contributed to Cavell Glacier—a larger, reconstituted glacier fed by avalanches descending the sheer north face of Mount Edith Cavell. Glacier deposits at this site are formed from quartzite blocks and sandy materials and host the lichen *Rhizocarpon geographicum* which has been used to date the well-developed multiple lateral and terminal moraines. The lake at the toe of Cavell Glacier has expanded since 1960 producing a vertical calving ice front that displays internal glacier structures. Rockfall and avalanche debris, accumulating on the glacier surface, have resulted in ice-cored ablation forms due to differential ablation. The Ramparts are a quartzite mountain ridge that hosts complex assemblages of small glaciers, rock glaciers and rockslides at the foot of its precipitous north- and east-facing cliffs. The differing relationships between these landforms are illustrated, and it is suggested that the rockslides and rock glacier material that confine some of the glaciers may have a paraglacial origin dating from the earliest phase of deglaciation.

Keywords

Canadian Rockies • Glacier forefields • Athabasca Glacier • Mount Edith Cavell • The Ramparts • Rock glaciers • Ablation mounds

17.1 Introduction

The central Canadian Rockies (Fig. 17.1) provide the most accessible examples of glacierised landscapes in Canada and have been visited by tourists and scientists for over 100 years. During the last glaciation valley glaciers from the Rockies flowed eastwards to approximately the mountain front, probably coalescing with the Laurentide Ice Sheet, but little is known of their detailed history and/or chronology. Ice advanced across the Jasper townsite after 26,000 years BP, and sites just outside the Little Ice Age (LIA) moraines were ice free by 11,300 years BP at Crowfoot Glacier in Banff National Park. There is evidence for a glacier advance (the Crowfoot Advance) of equivalent age to the Younger Dryas (10,000–11,000 years BP), but, at most sites, evidence for the Crowfoot Advance was overridden during the LIA. As glaciers have receded from their LIA maxima during the twentieth century, organic remains (mainly trees)

B.H. Luckman (✉)
Department of Geography, The University of Western Ontario, London, ON N6A 5C2, Canada
e-mail: Luckman@uwo.ca

© Springer International Publishing Switzerland 2017

O. Slaymaker (ed.), *Landscapes and Landforms of Western Canada*,
World Geomorphological Landscapes, DOI: 10.1007/978-3-319-44595-3_17

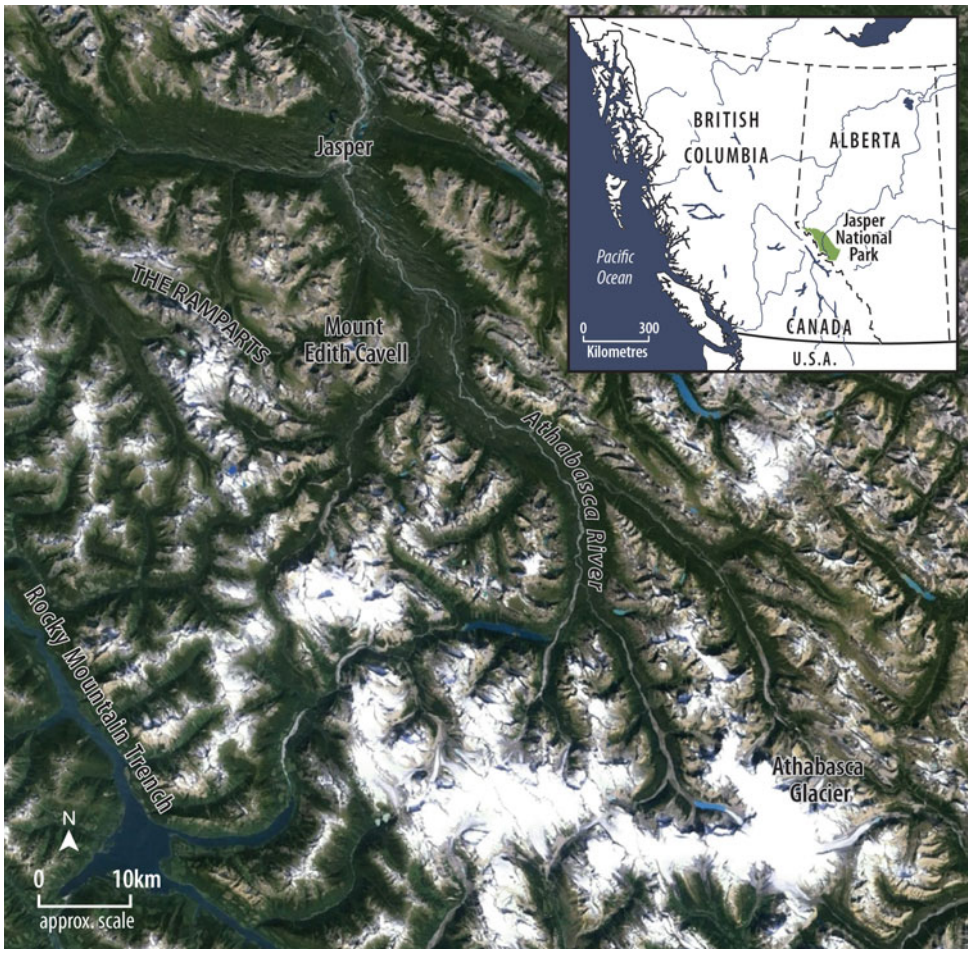

Fig. 17.1 Google Earth Image 7.1.5.1557 (9 April 2013) of the southern half of Jasper National Park in the central Canadian Rocky Mountains showing the principal localities referred to in this essay. The *inset map* shows the location of Jasper National Park in Western Canada

have been exposed within glacier forefields providing evidence of multiple periods of glacier advance during the last 10,000 years. However, there is little direct landscape evidence for this history as, at almost all sites, glacier advances appear to have been progressively more extensive during the Holocene, overriding evidence of the earlier events and culminating in the LIA advances of the 1700s and 1800s. This paper will concentrate on selected examples of the landforms and history of three sites that demonstrate the range of landscapes developed in these glacier forefields during the last few centuries.

17.2 Columbia Icefield Area

The Columbia Icefield (approximately latitude 52°10′N, longitude 117°20′W) is the largest in the Canadian Rockies and feeds glaciers and rivers that flow to Hudson Bay (North Saskatchewan River), the Arctic Ocean (Athabasca River) and the Pacific Ocean (Bush River to Columbia River). The central icecap and glaciers covered an area of c. 200 km^2 in 2009 (Tennant and Menounos 2013) having lost approximately 20 % of their estimated area since 1917 (259 km^2). The icefield feeds several large outlet glaciers, namely the Saskatchewan (c. 9.5 km),[1] Athabasca (c. 5.5 km), Columbia, Stutfield, Dome (all c. 5 km) and Castleguard (c. 4 km). All descend steeply via icefalls from the Icefield margin. Dome and Stutfield Glaciers are principally reconstituted glaciers below major rock cliffs.

17.2.1 Athabasca Glacier

The Athabasca Glacier (Fig. 17.2) has been easily accessible by road for almost 80 years, and currently about 250,000 people visit the glacier toe every year.[2] The underlying geology consists mainly of sedimentary rocks of Cambrian age. The Athabasca is a relatively clean glacier. A series of three icefalls between 2700 and 2250 masl feed the c. 800-

[1]Length from the icefield edge or headwall.
[2]Each year about 1,200,000 tourists travel the Icefields Parkway and view the glacier from the road.

Fig. 17.2 Athabasca Glacier from Wilcox Peak, view south, September 2000 (photograph by D.J. Smith). Note the sharp-crested lateral moraines of Athabasca and the eastern lateral of Dome Glacier on the *right*

to 900-m-wide gently sloping, c. 3-km-long, glacier tongue that terminates at c. 1980 masl. Downvalley of the present terminus the former glacier tongue widened and turned slightly westwards as it extended across the Sunwapta Valley and terminated against the gently upslope flank of Wilcox Ridge. Collie's 1899 map (Stutfield and Collie 1903) indicates that the margins of Athabasca and Dome Glaciers were confluent at that time.

The western 20 % of Athabasca Glacier is completely covered with debris derived from supraglacial moraine emerging below the icefalls plus rock cliffs and lateral moraine along the western valley side. This debris cover has resulted in marked differences in the glacier morphology and terminus over the last 150 years. Differential ablation has resulted in the debris-covered section of the snout being up to 20 m higher and extending further downvalley than the gently sloping, relatively debris-free, glacier tongue. For most of the twentieth century, the position of the debris-covered terminus was poorly defined and, in fact, was not mapped as glacier ice on the Environment Canada glacier maps of the 1950–1980s (e.g. Environment Canada 1982). In 2003, the main proglacial drainage shifted from the eastern to the western side of the clean glacier snout (see Fig. 17.3) and now runs across the front of the debris-covered snout exposing a near-vertical ice cliff in places up to 10–15 m high.

17.2.2 Lateral Moraines at Athabasca Glacier

The most conspicuous landforms in the forefield are the two prominent lateral moraines that tower up to 150 m above the present glacier toe. These are simple, single, sharp-crested ridges built against the valley walls where the glacier is confined but change in character downvalley (Fig. 17.2). The high eastern lateral terminates where it is crossed by the stream from "Little Athabasca" Glacier, and the former eastern margin is poorly defined downvalley, mainly by a change in

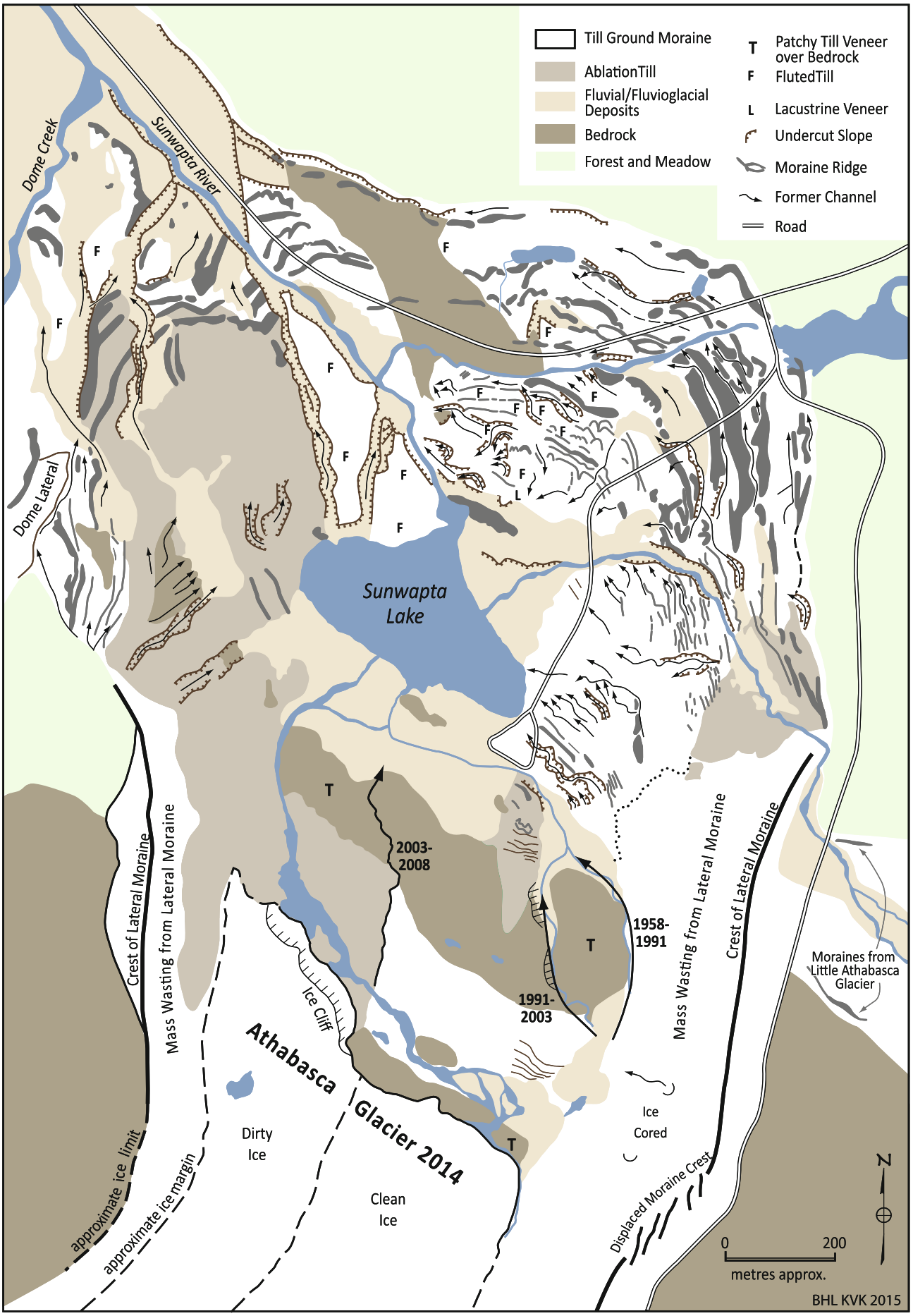
Till Ground Moraine
AblationTill
Fluvial/Fluvioglacial Deposits
Bedrock
Forest and Meadow
T Patchy Till Veneer over Bedrock
F FlutedTill
L Lacustrine Veneer
Undercut Slope
Moraine Ridge
Former Channel
Road
Dome Creek
Sunwapta River
Dome Lateral
Sunwapta Lake
Crest of Lateral Moraine
Mass Wasting from Lateral Moraine
2003-2008
1958-1991
1991-2003
Ice Cliff
Athabasca Glacier 2014
Dirty Ice
Clean Ice
Ice Cored
Displaced Moraine Crest
Moraines from Little Athabasca Glacier
approximate ice limit
approximate ice margin
N
0
200
metres approx.
BHL KVK 2015

◀ **Fig. 17.3** Landforms of the Athabasca Glacier forefield. Modified and updated from Luckman 1988 using 1999 and 2014 air photographs plus field observations. Many of the landforms north of the road were reconstructed from 1959 air photography as part of this area is now a parking lot. The *scale* is approximate

vegetation cover (Fig. 17.4). The terminal moraine is a low ridge, barely one metre high, built against the lower slopes of Mount Wilcox at the lower forest boundary and colonised by trees. It has been dated from a tree growing out of the moraine face that was tilted by the glacier in the winter of 1843–1844 (Luckman 1988). The western lateral has several minor ridges on the crest as it leaves the valley wall and meets the east lateral of Dome Glacier. In 1953, Calvin Heusser sampled a tree at the foot of this moraine that was tilted by the glacier in 1714 (Heusser 1956). However, elsewhere the outer LIA margins of both Dome and Athabasca Glaciers date from the 1840s advance. The local chronology of a maximum LIA advance in the 1820–1850s and/or an event in the early 1700s is typical of most glaciers in the Canadian Rockies (Luckman 2000; Menounos et al. 2009).

All three of the major laterals in Fig. 17.2 have a simple outer face, 10–30 m high, formed by debris that spilled over the moraine crest. The inner slopes are much higher and dissected by debris flows and slumping which occasionally exposes buried glacier ice. The earliest photographs show that the glacier ice adjacent to these moraines was heavily debris covered and as the glacier surface downwasted, differential ablation has preserved ice beneath the debris cover lying against the proximal slope of the moraine at the glacier margin (see the east lateral in Fig. 17.3). These high moraines are not ice-cored moraines: they are actually composite features built up over the Holocene and last occupied during the LIA advance. No datable material has been found in the moraines at Athabasca Glacier, but sections at Stutfield Glacier nearby (Osborn et al. 2001) and elsewhere in the cordillera show composite stratigraphies indicating that these moraines have been built up over a series of glacier events during the Holocene. The lateral margin of these glaciers is confined by the valley walls, and the moraine is reoccupied during subsequent events that extend further downvalley and can overtop the pre-existing moraine crest spilling fresh debris down the distal face. However, although no wood has been exposed in these laterals at Athabasca Glacier, detrital wood has been washed out of the glacier snout, derived from an unknown valley floor location upvalley. Radiocarbon dates of c. 6090 and between 7700 and 8200 ^{14}C years BP indicate two periods when an earlier, smaller, glacier may have advanced into a forested area on the present valley floor.

A 540-m-long section of the eastern lateral of Athabasca (Fig. 17.3) is unusual in that it has undergone progressive gravitational deformation since the early 1950s and the moraine crest has been displaced up to 55 m downslope (c. 37 m horizontally, 41 m vertically) between 1967 and 2006. This mass wasting is attributed to a combination of debutressing of the moraine due to glacier recession, the movement of a mobile, debris-mantled slope and rock glacier impinging on the upslope side plus possible anthropogenic influences due to heavy traffic and modifications of the access road running parallel to and outside the lateral moraine (Hugenholtz et al. 2008).

17.2.3 Landforms in the Glacier Forefield

The difference in debris cover of the glacier has resulted in two distinctive forefield landscapes (Fig. 17.3). Much of the western third of the forefield is blanketed with ablation moraine mainly consisting of black angular debris of Middle Cambrian limestones that contrast sharply with the grey and brownish till debris elsewhere in the forefield that forms small-scale minor landforms resulting from active glacier flow. There are three conspicuous moraine fragments in the northeast section of the forefield (cut by the access road) formed between the 1840s and 1906s (Fig. 17.4). Several subparallel arcuate moraines of probable similar age occur in the northwestern portion of the forefield near the former confluence of Athabasca and Dome Glaciers. Elsewhere the relatively fine-grained deformable till shows traces of small fluting forms. Small annual moraines, usually less than one metre high, have been preserved marking ice front positions from the 1920–1930, 1960–1980 and the 1999–2007 periods (Figs. 17.3 and 17.5). These are formed where the winter advance of the glacier front was pushing over relatively gently sloping surfaces of till or other loose materials rather than bedrock. These features are only preserved at sites where there is a net recession of the ice front from year to year.

Recession of the glacier was mapped on an annual (1945–1950) or biannual basis (1950–1980) by the Water Survey of Canada. Earlier recession (1906–1945) has been estimated from documentary sources and aerial photography (see Luckman 1988, Table 6). Annual recession ranged from c. 20 to 35 m/year from 1938 to the mid-1960s during the period where part of the glacier front was calving into Sunwapta Lake. Once the glacier tongue became land based and was receding upslope during the 1960s–1980s, annual recession was often only 3–5 m/year. The annual moraines from 1978 to 1982 are less than a few metres apart, and there was little recession of the toe over this period. No detailed measurements are available since 1980 although spacing of the annual moraines indicates rates of 6–8 m/year from 1999 to 2007. From 2010 to 2014, frontal recession has been more

Fig. 17.4 Detail of the eastern margin of Athabasca Glacier, July 1978. The eastern lateral terminates at the stream crossing, and the former ice margin is marked by a change in vegetation and followed by the line of the road from the smaller parking lot to the road junction. The irregular moraines cut by the toe access road were formed between 1844 and 1906. The main proglacial drainage from the glacier is from the east portal at this time. Photograph by B. Luckman. Unless otherwise specified, all photographs in this chapter were taken by the author

irregular, up to 20 m/year in places, as bedrock ridges emerge from beneath a relatively thin glacier tongue.

The forefield also shows considerable evidence of former and ongoing fluviglacial activity. The Athabasca Glacier occupies a tributary of the Sunwapta Valley and, at its maximum extent, blocked that valley forcing the drainage from Sunwapta Pass to flow either around or, at times, through the glacier tongue until the glacier receded sufficiently to establish the present stream course bypassing Sunwapta Lake. Unfortunately, most evidence of these small channels has been removed by subsequent tourist development (Fig. 17.3).

17.2.4 Sunwapta Lake and Proglacial Drainage Changes

Sunwapta Lake is a prominent feature that occupies a shallow basin in the middle of the forefield. Prior to 1938, the main proglacial drainage occupied a former channel west of the present lake outlet. The lake and present channel began to form c. 1940 or 1941 as the glacier receded and the lake continued to expand until about 1968 when the glacier front receded to the bedrock ridge immediately upvalley of the tourist parking lot. The maximum area of the lake at that time was probably about 13.5 ha with a depth of 10–12 m in two basins. Delta formation from the proglacial drainage of Little Athabasca and Athabasca Glaciers has progressively filled the lake reducing it to c. 4.5 ha and maximum depth of c. 7 m in the single, northern basin in 2000 (Challies et al. 2002). The lake surface area was estimated to be c. 4 ha in 2014.

A bedrock ridge c. 20–30 m high running across the valley was first exposed at the glacier snout in 1968 and has been a major control of the course of proglacial drainage into the lake. From c. 1958 to 1991, the main proglacial outlet was a stable channel from the eastern edge of the glacier, progressively building the delta on which the parking lot is presently located. Throughout the period from the 1950s, a smaller proglacial stream also flowed into the lake from an ice cave at the western end of the debris-covered ice front.

Fig. 17.5 Annual moraines at Athabasca Glacier, July 1993. These moraines were formed between c. 1962 and 1981 by the winter advances of the glacier ploughing into loose sediments. No well-defined ridges were formed as the glacier subsequently withdrew over the bedrock ridge in front of the glacier until suitable conditions occurred east of the glacier snout again between 1999 and 2007 (see Fig. 17.3). In 1991, the proglacial drainage shifted from the east portal (Fig. 17.4) to pass through a gap in the bedrock ridge, cutting a new channel through the till, visible on the *left*

Recession of the ice front across the ridge in the 1980s opened up a new stream course c. 150 m west in 1991 (Figs. 17.3 and 17.5) which shortcut the route to the southeast delta and eroded a new channel across the till below the rock ridge, delivering considerable new material to the delta. In 2003, the proglacial river abandoned this course and flowed westwards beneath the clean glacier snout, emerging at the junction with the debris-covered glacier front. It then flowed along the front of the debris-covered snout, developing an ice cliff before crossing a low point in the rock ridge and building a new delta into the lake. Continued recession of the clean glacier snout completely exposed the former subglacial stream course by 2011. Gradual recession of the ice cliff and undercutting of the debris-covered section of the snout by the river finally breached the ice-cored moraine between the two proglacial streams in 2008 and diverted the main proglacial drainage westwards to join the western outlet. The entire proglacial drainage now flows into the prograding delta at the western end of the lake (Fig. 17.3). It seems likely that this will remain the main outlet for proglacial drainage for the foreseeable future as it is the lowest section of the confining ridge and a second crossvalley ridge has emerged from beneath the glacier in 2013–2014. A similar complex history of changing proglacial drainage can be deduced from several abandoned proglacial channels, active between c. 1900 and 1940, that occur in the northwestern part of the forefield (Fig. 17.3).

17.2.5 Dome Glacier

Dome Glacier (Fig. 17.6) is a debris-covered glacier in the valley immediately west of the Athabasca Glacier and completely different in character. It is formed from the confluence of three glaciers from the Columbia Icefield that spill over bedrock cliffs 700–1000 m high at the head of the Dome Valley. The main glacier tongue upvalley has a broad central debris-covered rounded ridge flanked by relatively

clean ice and two ice-cored lateral ridges below the lateral moraines. Downglacier the debris cover merges laterally, and the toe becomes completely debris covered. The main glacier tongue has a relatively smooth surface with a relative relief of 10–30 m between the three parallel debris-covered ridges and intervening depressions. The glacier front is a smooth debris-covered ramp with a lateral ice cliff, but the glacier tongue is increasingly being dissected by supraglacial stream incision. A crossvalley bedrock ridge confines the outwash downstream of the glacier snout, and part of the proglacial drainage upwells as siphons into small ponds and kettle holes. Glacial landforms in the lower forefield have mainly been removed by fluviglacial erosion except for a small well-marked section of terminal moraine, up to 2 m high, adjacent to the former Athabasca terminus. A tree on the lateral margin was tilted and scarred in 1846 (Luckman 1988) indicating that the LIA maximum advance of Dome Glacier was synchronous with Athabasca Glacier.

17.3 Mount Edith Cavell

Mount Edith Cavell (lat. 52° 42′N, long. 118° 03′W; 3356 masl) is one of the highest mountains in Jasper National Park. The mountain is underlain by the Lower Cambrian Gog Quartzites outcropping on the eastern limits of a shallow syncline. Cavell Creek occupies a NNW-SSE trending asymmetric valley developed along the strike between the massive Gog Quartzites and the Precambrian Miette Argillites. The valley is tributary to and "hangs" above the wide glacial trough occupied by the Astoria River.

The Cavell Creek valley contains several glaciers of quite different character. The main valley hosts several small glaciers nestled in the shadow of the 1000- to 1500-m-high precipitous east face of the mountain. The largest of these is Cavell Glacier, a gently sloping, partially debris-covered glacier fed by avalanching from the adjacent cliffs. During the LIA, it expanded downvalley, forming the well-developed

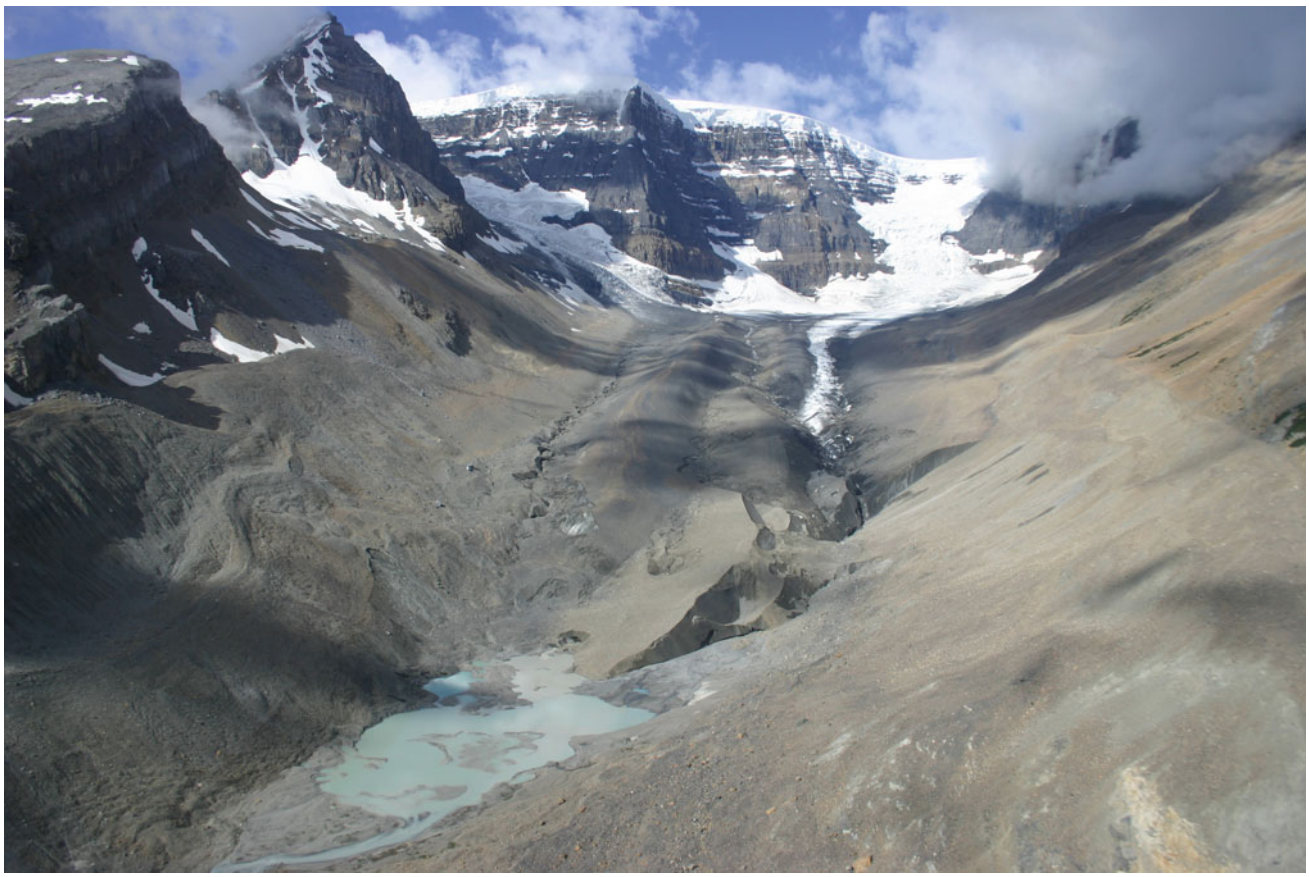

Fig. 17.6 Dome Glacier, 16 July 2006. The lower glacier is debris covered and being dissected by a supraglacial stream on its western flank (*right*). Active kettle formation occurs in the proximal outwash and within the proglacial lake

lateral moraine complex on the east side of the valley and a series of terminal moraines downvalley. At its LIA maximum, it was probably about 1.5 km^2 in area and has downwasted about 100 m at the position of the present snout.

17.3.1 Angel Glacier

Angel Glacier (Fig. 17.7) is a small hanging glacier that spills out of a classic cirque carved into the east face of Mount Edith Cavell. It has an accumulation area of c. 1 km^2 on the cirque floor between 2430 and 2735 masl. When first visited in the early 1900s, this glacier extended onto and merged with Cavell Glacier and early accounts assumed the LIA moraines were associated with Angel Glacier rather than a much expanded Cavell Glacier. Recession of Angel Glacier led to its separation from Cavell Glacier c. 1946 (Ms. Guild pers. comm. in Luckman 1977) and the hanging tongue receded upslope or was stable through the 1960s and 1970s. However, between 1979 and 1981, the tongue advanced onto the talus cone below (Fig. 17.8) before resuming its upslope recession. Several other small glaciers, including one from Mount Athabasca, also advanced at about this time (Luckman et al. 1987). By 2013, the hanging tongue terminated about halfway between the top of the talus and the lip of the cirque (Fig. 17.9).

17.3.2 Cavell Glacier

Moraines at Cavell are quite different in character from those at Athabasca as they are formed exclusively of debris from the Gog Formation and consist of angular quartzite clasts, with blocks up to several m^3, in a sandy matrix. Unlike many moraines in the Rockies which are composed of calcareous debris, these quartzite materials host the lichen *Rhizocarpon geographicum* that has been used to provide dates for moraine formation at Cavell and elsewhere (Luckman 1977). During the LIA Cavell Glacier produced contrasting examples of lateral and terminal moraines. On the eastern flank, the lateral moraines consist of a series of intersecting complex ridges 1–5 m high, banked against the shale slope of the eastern valley side (Fig. 17.8). These show a complex pattern of ice marginal fluctuations, but the oldest ridge dates from the early 1700s. However, some 2 km upvalley, a small section of much older moraines is preserved extending out from beneath the LIA material. The oldest of these ridges has a total lichen cover and is quite possibly Crowfoot (early Holocene) age. On the west side, there is a single well-defined lateral moraine crest from which subsidiary ridges diverge downslope and downvalley to connect with four well-marked terminal moraines that cross the valley dating from c. 1705, 1720, 1860 and 1890. Recession from the latter moraine is estimated between 14–18 m/year from 1927 to 1947 and 12–14 m/year from 1947 to 1963 (Luckman 1977). Between 1947 and 1960s, the ice front was receding up a low rounded till ridge that crosses the valley at the point where the north margin of the former, extended, Angel Glacier would have covered Cavell Glacier. Possibly, this is a former moraine that was overridden during the LIA. Recession of Cavell Glacier after c. 1960 led to the development of a small lake that drained either over or through the ridge. As recession and downwasting continued, the front of Cavell Glacier has been transformed from a gently sloping surface to a vertical, calving, ice cliff, bordering the expanding lake. The ice front was approximately 30 m from the north shore of the lake in 1976 and over 400 m in 2013. The lake area was approximately 1.5 ha in 2012, drains in winter and when full is up to 27 m deep (Wedgwood 2013).

The snow avalanches that feed Cavell Glacier also transport debris onto the glacier surface. In addition, larger rockfalls onto the glacier surface are incorporated into the snow and buried in the accumulation zone. These former debris-covered surfaces emerge downglacier (Figs. 17.6–17.8) as gently inclined debris bands with a shallow upglacier dip. Differential ablation beneath the patches of thicker emerging debris cover (c. 0.3–0.6 m) leads to the development of dirt cones or larger, debris-covered ice domes. Ice covered by the larger or thicker deposits grows in relative height above the adjacent cleaner ice surface as it moves downglacier through the ablation zone. Larger rockfall deposits may result in mounds that are 10–15 m above the adjacent cleaner ice. Through the 1970–1990s, two of these ice domes slowly moved downglacier towards the receding calving front and were truncated (Fig. 17.8) and subsequently consumed by the calving ice front. Thin, possibly annual, debris layers appear as narrow bands on the glacier surface and are also exposed in the calving front (Fig. 17.9) illustrating differences in the pattern of accumulation and age of the glacier ice.

17.3.3 Ghost Glacier Collapse

Ghost Glacier was a small glacierette that formerly clung to the east face of Mount Edith Cavell, below the summit. It gradually diminished in size over the twentieth century, and on the night of 9–10 August 2012, the vestigial mass, estimated at 125,000 m^3, released and fell c. 1000 m onto the

Fig. 17.7 Angel and Cavell Glaciers from the east, 1970, showing the classic cirque that hosts Angel Glacier. The partially debris-covered Cavell Glacier extends downvalley below the tongue of Angel with debris bands emerging at its surface. Three ablation mounds are visible on its surface with a new debris source emerging upslope of the largest mound

glacier and into the lake. This triggered a major flood wave that travelled downvalley, greatly expanding the previous outlet stream channel, burying tourist facilities and removing part of the terminal moraine (Wedgwood 2013). Fortunately, this occurred at night when there were no visitors at the site. However, it provides a graphic illustration of the continued hazard associated with some glacier sites.

17.4 The Ramparts

Rock glaciers are relatively common in the Canadian Rockies, but there have been few detailed studies of this phenomenon in the region. The Ramparts (lat. 52° 42′N, long. 118° 20′W) are a massive narrow, curving ridge of mountains formed in Gog Quartzites running generally NW

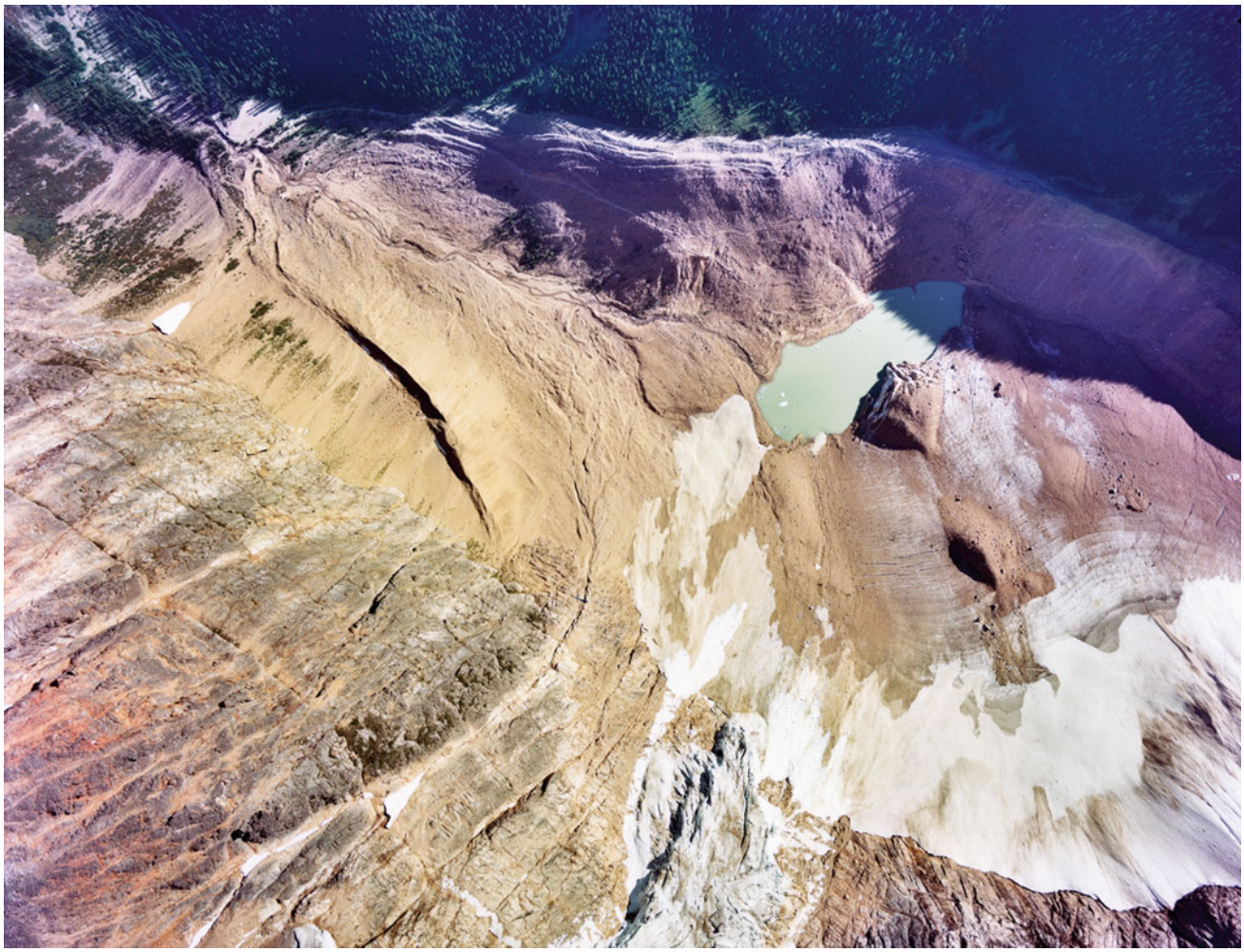

Fig. 17.8 Angel and Cavell Glaciers, aerial photograph A31240-30, 1979. The east (*right*) lateral moraine shows the complex series of ridges that date between 1700 and the early 1900s. The western lateral is a simple ridge leading into the series of terminal moraines downvalley. The downglacier ablation mound rises c. 10 m above the adjacent ice surface and is calving into the lake. The upslope edge of the second mound has merged with the emerging debris patch further up ice (see Fig. 17.7). The emerging debris bands are clearly visible on the glacier surface. The toe of Angel Glacier (*centre*, *bottom*) has advanced to the top of the talus. It is one of several small glaciers in the region that advanced during the 1970s and early 1980s (Luckman et al. 1987)

to SE and reaching elevations of 3000–3600 masl. The ridge is about 10 km long, and its northeast face towers 1000–1400 m above the broad flanking lowlands of the Tonquin Valley (Alberta) and Tonquin Creek (BC). Several small glaciers (up to 1 km^2) nestle in the shadow of these cliffs, hidden behind massive Little Ice Age moraines up to 100 m high. There are also extensive rock glaciers and rockslide deposits derived from these mountain walls. Relationships between these phenomena are complex and offer tantalising insights into the Holocene history of coarse debris landforms in this region.

Several small mounds of fluviglacial material and a small esker occur in the floor of Tonquin Pass and are interpreted as deposits of the last phase of Late Wisconsinan Cordillera Ice Sheet that stagnated on the Continental Divide (these deposits contain metamorphic erratics derived from the west). Radiocarbon dates from bogs on the valley floor of the pass (Kearney and Luckman 1983) indicate it was ice free prior to 9300 C^{14} years BP, and therefore all of these coarse debris landforms are Holocene in age.

17.4.1 Relationships Between Rockslides, LIA Moraines and Rock Glaciers

Based on soil development, vegetation and/or lichen cover, the rockslides or rock avalanches identified at the foot of these cliffs appear to be the oldest features. The large rockslide below Bastion Peak (Fig. 17.10) is particularly instructive. Here, a large rockslide deposit is overridden by a

Fig. 17.9 Angel and Cavell Glaciers, 22 August 2013. The lichen trimline below Angel Glacier indicates its extent at the LIA maximum. Note the upslope recession of the glacier toe. The large ice mounds on Cavell Glacier in the previous images have moved down ice and were destroyed at the calving front. Large crevasses are opening up in the face of Cavell Glacier as it calves into the lake. The exposed ice cliff is between 5 and 10 m high and extends underwater at least 20 m to the lake bed. The *enlarged image* of the ice cliff clearly shows the relationship between the dirt bands in the ice and at the glacier surface

Fig. 17.10 Coarse debris landforms below Bastion Peak at the Ramparts along the Alberta-British Columbia boundary. The large rockslide in the foreground extends into Moat Lake and is covered by a later rock glacier and Little Ice Age moraines from two small glaciers. The superimposition of these phenomena provides a potential scenario for the Holocene development of coarse debris landforms at this site

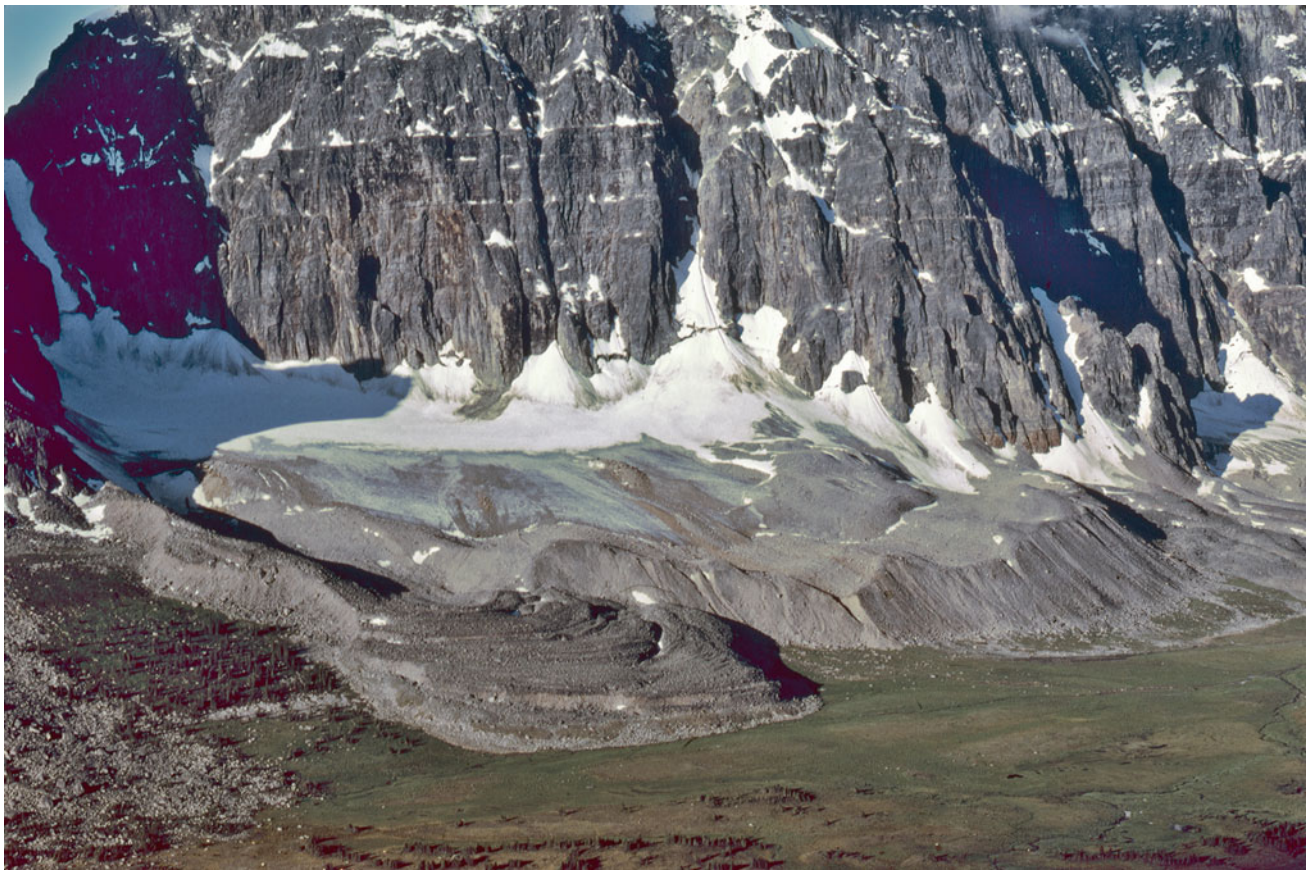

Fig. 17.11 Little Ice Age moraine and rock glacier below Turret Mountain. The eastern (*left*) edge of the glacier rode up onto the rock glacier, reorienting some of the surface blocks to a vertical position. The steep, western face of the rock glacier (similar in appearance to the eastern flank shown) passes beneath the terminal moraine of the glacier without obvious signs of disturbance. This suggests that the rock glacier is inactive

small rock glacier which in turn is overlain by the LIA lateral and terminal moraines of a small glacier and an active snow avalanche-modified talus slope. This indicates that, at least at this site, rock glacier development postdates significant instability in the adjacent cliffs.

Elsewhere the moraines and rock glaciers rest on till which dates from the last glaciation. These features are exclusively composed of quartzite debris that hosts *Rhizocarpon geographicum,* and lichen sizes on debris can be used to differentiate LIA from older materials. The moraines are characteristically high, relatively simple, single-crested, sharp ridges with distal slopes of 30–35°. Photographs taken in 1915 indicate glacier fronts were at or near these moraine crests and would have been last occupied by a glacier during the LIA. In a few cases, short sections of the moraine crest have multiple small ridges, some of which can be dated back to the sixteenth century by lichenometry (Luckman and Osborn 1979). This suggests that these moraines have been reoccupied by successive LIA and perhaps earlier advances, each advance adding a fresh supply of morainic debris.

The contrasts in morphology, grainsize and lichen cover between glaciers and rock glaciers are clear and sharp. About half of the glaciers clearly override rock glaciers with apparently minimal disturbance of the material. On the large complex flanking Turret Mountain (Fig. 17.11), the glacier margin appears to have pushed onto the rock glacier material and the zone of contact is marked by a series of ridges of indeterminate origin. In some cases, the morphology, grainsize and fabric of the deposits suggest that the rock glacier material has been pushed or thrust into ridges, whereas elsewhere the ridges resemble moraines in form and grainsize but have a much older lichen cover. In other cases, the LIA glaciers were clearly confined by the rock glacier deposits and have shrunk back into the large headward pits upslope (Fig. 17.12).

The rock glacier debris itself is 15–30 m thick and consists of large, heavily lichen-encrusted blocks with maximum lichen diameters ranging up to 230–270 mm indicating ages of several thousand years. An unidentified (probably Mazama) tephra was recovered from one of the outer rock

Fig. 17.12 View west down Tonquin Creek, BC showing the glacier/rock glacier complexes below Mount Geikie (*left*) and Barbican Peak. The glaciers below Mount Geikie were confined behind the rock glaciers and unable to override them. Two rockslides and large lobate rock glacier are visible in the distance, downvalley

glacier surfaces at Mount Geikie (Luckman and Osborn 1979) indicating minimally an early Holocene age for these features. In several cases, the classic micro-relief features of rock glaciers are well developed (longitudinal and transverse ridges and furrows, conical pits up to 20 m deep, overriding lobes and arcuate ridges). Some rock glacier fronts are steep (up to 42°) with well-defined debris slopes, but more frequently the fronts are less steep, apparently stable slopes of large heavily lichen-covered blocks. No traces of buried ice have been found, and none of the rock glaciers terminating in Amethyst Lake showed any evidence of recent slumping.

Examination of the distribution and plan shape of the rock glaciers and glaciers suggest that their position and size were controlled by slightly different factors. Three of the large rock glaciers have not been subsequently overridden by glaciers, have no trace of a former glacier between the rock glacier and the cliff and appear to have developed from talus slopes. Many others have headward "pits" occupied by glaciers or vestigial snow or ice patches that were glaciers during the Little Ice Age (e.g. Fig. 17.12). At some localities, the general shape and plan of the glaciers and rock glaciers are similar, but elsewhere the crosscutting relationships of glaciers and rock glaciers suggest that they had different centres of movement. In some cases, rock glaciers were almost completely overridden, whereas in others the massive rock glacier deposits clearly confined the downslope extent of the glaciers.

The entire complex of glacier, rock glacier and rockslide materials at this site is Holocene in age. The original interpretation of these features was that most of the rock glaciers were inactive and older (based on morphology and lichen cover probably several thousand years old). During the Little Ice Age, these sites were only occupied by glaciers and there is no evidence of contemporary rock glacier activity. The great range and variety of coarse debris landforms raise interesting questions about their origin and classification of these features that cannot be addressed here. However, these sites contain a vast quantity of coarse rock debris derived from a discrete source which raises important questions

about the magnitude and frequency of debris provision to cliff-foot zones during the Holocene. There is considerable indirect evidence that much of this cliff-foot debris is immediately postglacial in age. Studies of rockfall accumulation rates based on lichen cover of talus slopes in the Bennington valley on the west face of the Ramparts and similar talus slopes elsewhere in the Rockies (Luckman and Fiske 1997) indicate that rockfall accumulation during the last 2–300 years is at least an order of magnitude too slow to develop these slopes during the Holocene. This suggests that considerably higher rates of rockfall provision may have prevailed in the past, and it is therefore possible that much of this coarse debris accumulated shortly after regional deglaciation when lateral support was removed from these quartzite cliffs, i.e. rockslide, and rock glacier formation may have been initiated during a phase of "paraglacial" activity.

17.5 Conclusion

The great range of landforms in the glacier forefields of the Canadian Rockies reflects the diversity of topographic settings, glaciological and geomorphic environments that host glaciers across this region. The examples herein range from the outlet/valley glaciers from the Columbia Icefield to small reconstituted glaciers or glacierettes at the Ramparts and Mount Edith Cavell. The constituent geology also plays a role in the development of these landform suites. The glacial deposits in the forefields of glaciers at the Ramparts and Mount Edith Cavell are developed from hard resistant quartzites that yield blocky or sandy deposits. The forefields at Athabasca and Dome contain glacigenic landforms developed in more malleable and deformable tills derived from the argillaceous and calcareous rocks. The latter situation is probably more typical of sites in the Rockies, e.g. the forefields of Robson and Saskatchewan Glaciers, not discussed here. However, this short essay can only give a selective sample of these landscapes.

Acknowledgements The research on which this essay is based has been supported by NSERC and Parks Canada over many years. I am grateful to Karen van Kerkoerle for preparing Fig. 17.1 and redrafting Fig. 17.3 and to Parks Canada personnel in Banff and Jasper for making available preliminary copies of the 2014 imagery of the Athabasca Glacier forefield.

References

Challies M, Cormier L, Fric C, George LA, Laroque CP, Smith DJ (2002) Historical sedimentation in Sunwapta Lake, Columbia Icefield Area, Canadian Rocky Mountains. Unpublished manuscript Geography, University of Victoria

Environment Canada (1982) 1978–1980 Survey of the Athabasca and Saskatchewan Glaciers. Internal Report, Water Survey of Canada, Calgary Office

Heusser CJ (1956) Postglacial environments in the Canadian Rocky mountains. Ecol Monogr 36:263–302

Hugenholtz CH, Moorman BJ, Barlow J, Wainstein PA (2008) Large scale morainic deformation at the Athabasca Glacier, Jasper National Park, Alberta, Canada. Landslides 5:251–260

Kearney MS, Luckman BH (1983) Postglacial vegetational history of Tonquin Pass, British Columbia. Can J Earth Sci 20:776–786

Luckman BH (1977) Lichenometric dating of Holocene moraines at Mount Edith Cavell, Jasper, Alberta. Can J Earth Sci 14:1809–1822

Luckman BH (1988) Dating the moraines and recession of Athabasca and Dome Glaciers, Alberta, Canada. Arct Alp Res 20:40–54

Luckman BH (2000) The Little Ice Age in the Canadian Rockies. Geomorphology 32:357–384

Luckman BH, Fiske CJ (1997) Holocene development of coarse debris landforms in the Canadian Rockies. Paläoklimaforschung 19: 283–297

Luckman BH, Osborn GD (1979) Holocene glacier fluctuations in the middle Canadian Rockies. Quat Res 11:52–77

Luckman BH, Harding KA, Hamilton JP (1987) Recent glacier advances in the Premier Range, British Columbia. Can J Earth Sci 24:1149–1161

Menounos B, Osborn G, Clague J, Luckman BH (2009) Latest Pleistocene and Holocene glacier fluctuations in western Canada. Quat Sci Rev 28:2049–2074

Osborn GD, Robinson BJ, Luckman BH (2001) Holocene and latest pleistocene fluctuations of Stutfield Glacier, Canadian Rockies. Can J Earth Sci 38:1141–1155

Stutfield HM, Collie JN (1903) Climbs and exploration in the Canadian Rockies. Longmans, Green and Co., London

Tennant C, Menounos B (2013) Glacier change of the Columbia Icefield, Canadian Rocky Mountains, 1919–2009. J Glaciol 59: 671–686

Wedgwood R (2013) Gone like a Ghost: the ghost glacier failure and subsequent outburst flood, Mt. Edith Cavell, Jasper National Park. Unpublished ms, Parks Canada, Jasper

The Northern Interior Yukon: An Example of Periglaciation

18

Hugh M. French

Abstract

Much of the northern interior Yukon Territory was never glaciated during the Quaternary. Frost action, aided by wind, is the dominant geomorphic process. Running water and permafrost are relatively minor factors in landscape modification. Because the landscape has experienced continental, cold and arid conditions for several millions of years, it may closely approximate a truly periglacial landscape. However, the presence of cryopediments and cryoplanation terraces, two landforms where a periglacial origin appears problematic, suggests that the complete footprint of periglacial landscape modification may not have been achieved.

Keywords

Periglacial • Frost action • Wind • Cryoplanation • Eagle plain • Barn mountains • Northern Yukon

18.1 Introduction

Northern interior Yukon constitutes a vast upland area lying between latitude 64°N–68°N and longitude 132°N–141°W (see Fig. 18.1). Two landscapes are described in this chapter: (a) Eagle Plain, an upland area in the south-central part of the Porcupine Plateau, and (b) Barn Mountains, a range of hills that connect the northern end of the Richardson Mountains with the eastern end of the British Mountains. The southern part of Eagle Plain is crossed by the Dempster Highway, the 1100-km-long gravel road that links Dawson City in the Yukon with Inuvik in the NWT; otherwise, the rest of the Porcupine Plateau and the Barn Mountains are largely inaccessible except by aircraft.

This chapter also distinguishes between *periglacial environments* and *periglacial landscapes*. Periglacial environments are those in which cold, non-glacial processes dominate. It is generally recognized that frost action and the presence of either seasonally or perennially frozen ground (permafrost) are central characteristics (French 2007). Periglacial landscapes are fashioned by cold non-glacial processes, and the term *periglaciation* refers to the degree to which a landscape is, or has been, modified by such processes.

18.2 Quaternary History

It is generally agreed that drainage of the area was probably initiated on a Tertiary age peneplain (Duk-Rodkin and Hughes 1994). Today, the Porcupine Plateau is drained by rivers that flow, via the Old Crow Basin, to the Yukon River and, ultimately, the Pacific Ocean. The southern part of the Porcupine Plateau is drained by the Peel River that flows east to the Mackenzie River and, ultimately, the Arctic Ocean. Smaller streams drain the British and Richardson mountains.

During the cold periods of the Pleistocene, the area was part of the eastern extremity of Beringia, the ice-free land

H.M. French (✉)
Departments of Earth Sciences and Geography, University of Ottawa, Ottawa, ON K1N 6N5, Canada
e-mail: hmfrench@shaw.ca

H.M. French
Department of Geography, University of Victoria, Victoria, BC V8R 3R4, Canada

© Springer International Publishing Switzerland 2017
O. Slaymaker (ed.), *Landscapes and Landforms of Western Canada*, World Geomorphological Landscapes, DOI: 10.1007/978-3-319-44595-3_18

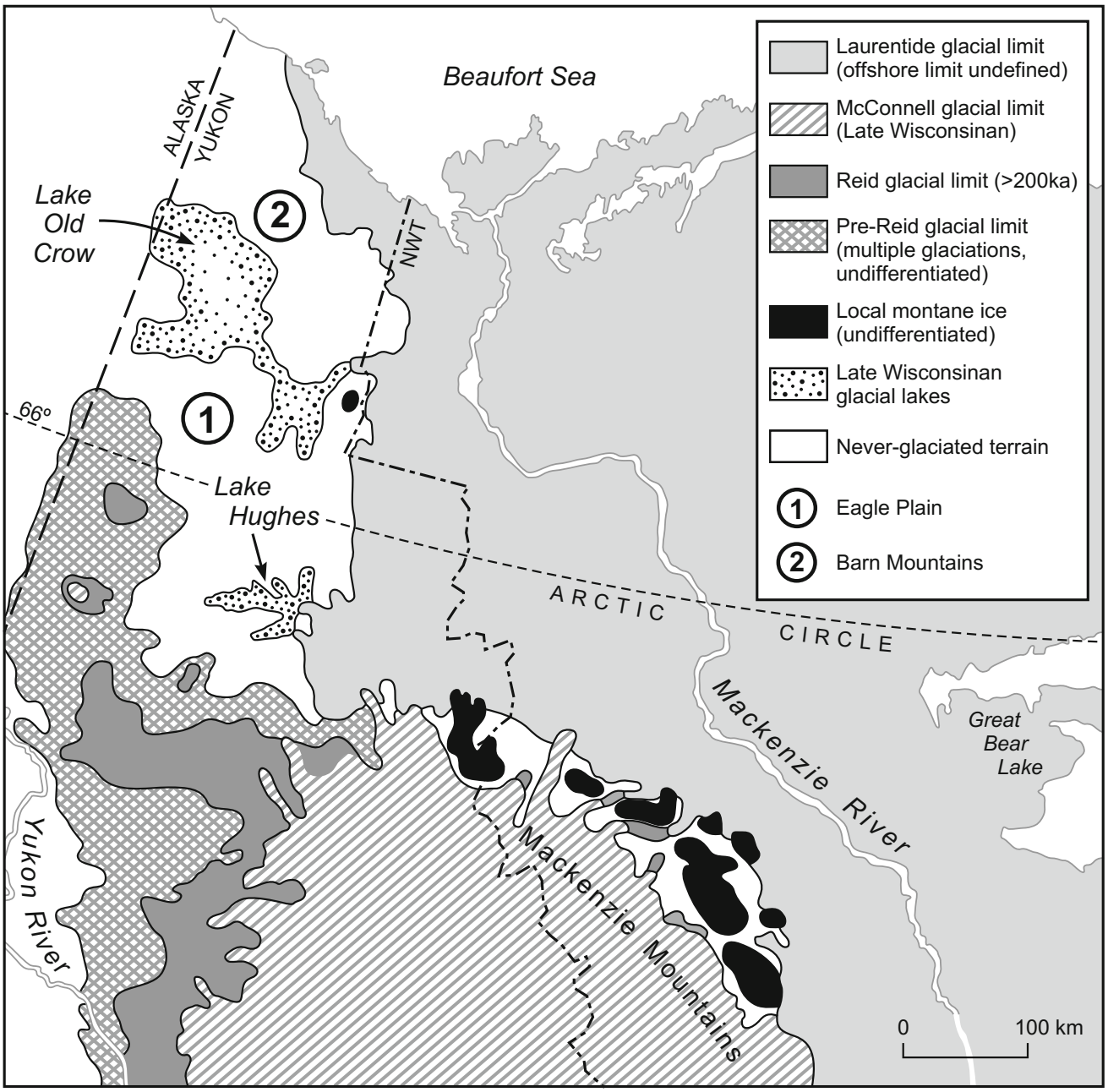

Fig. 18.1 Map of northern interior Yukon showing locations of Eagle Plain and Barn Mountains, major drainage systems and maximum extent of Quaternary ice sheets (after Hughes 1972; Norris 1977; Rampton 1982; Duk-Rodkin et al. 1996). Never glaciated terrain is unshaded

that joined the North American and Eurasian landmasses (Hopkins et al. 1982; Froese et al. 2000). The limits of the various Cordilleran ice sheets and the Laurentide glacial limit are indicated on Fig. 18.1 together with the extent of Late Wisconsinan glacial lakes. In the Klondike area, paleomagnetic evidence dates the onset of periglacial conditions and the formation of permafrost to at least 2.58 Ma (Gauss normal chron) and ice-wedge pseudomorphs in the Upper White Channel gravel even suggest a late Pliocene age (Froese et al. 2000). It is reasonable to assume, therefore, that both Eagle Plain and Barn Mountains have been ice-free and subject to intense periglaciation for several millions of years.

18.3 Climate

The current climate of the region can only be approximated due to sparse data. What can be said is that it is continental, cold and semiarid. Observations at the Eagle Plain Lodge,

Table 18.1 Climatic data for selected stations in the northern interior Yukon

	Jan	Feb	Mar	Apr	May	Jun	Jul	Aug	Sep	Oct	Nov	Dec	Year
Eagle Plain[a]													
Temperature (mean, °C)	−22.6	−23.3	−19.2	−9.2	1.1	10.6	13.3	10.6	2.6	−9.3	−16.3	−21.3	−6.9
Precipitation													
Snow (cm)	19.7	19.3	14.5	20.3	3.7	1.0	0.5	1.5	14.7	25.6	25.5	18.1	164.6
Rain (mm)	–	–	–	–	11.5	82.7	84.5	70.5	22.4	5.7	–	–	277.3
Old Crow[b]													
Temperature (mean, °C)	−29.2	−26.5	−21.2	−10.1	2.7	12.9	14.6	10.9	3.5	−8.8	−22.9	−25.1	−8.3
Precipitation													
Snow (cm)	15.4	16.4	16.6	9.7	6.6	2.7	–	1.0	9.25	23.0	21.6	18.9	141.4
Rain (mm)	13.1	13.8	14.4	9.5	14.4	37.2	43.5	46.7	29.0	22.1	18.1	16.7	154.7
Dawson[c]													
Temperature (mean, °C)	−25.9	−21.5	−12.1	−0.8	8.2	14.0	15.7	12.3	5.8	−4.7	−18.1	−22.9	−4.1
Precipitation													
Snow (cm)	27.6	18.2	12.0	7.2	2.5	–	–	0.4	4.5	26.7	36.3	31.0	166.4
Rain (mm)	–	–	–	2.5	28.4	38.2	49.0	43.1	29.7	9.4	–	–	201.3

Sources Wahl et al. 1987 (Eagle Plain), AES Climate Canada Normals 1981–2010, station data (Old Crow, Dawson)
[a]Eagle Plain—lat. 66°26′N, long. 136°45′W; 716 masl
[b]Old Crow—lat. 67°34′N, long. 139°50′W; 250 masl
[c]Dawson—lat. 64°02′N, long. 139°07′W; 370 masl

located on the rolling uplands of the Porcupine Plateau at ~700 masl, are most representative, but only 5 years of recorded data are available (Table 18.1). During winter, cold air is entrapped by the surrounding mountains and air temperatures drop below −20 °C for more than 3–4 months each year. Summer temperatures rise to between 10 and 15 °C. As might be expected, the data from Eagle Plain Lodge mask considerable variation; for example, more long-term data from the settlements at Old Crow and Dawson (see Table 18.1), both lowland localities, indicate colder temperatures in winter due to cold air drainage from the uplands and warmer temperatures in the summer months. One must assume much colder conditions at higher elevations in the Barn Mountains, and certainly in the Richardson and British Mountains.

Recorded data at Eagle Plain Lodge indicate approximately 250–300 mm of rain and about 150 cm of snow fall annually. However, these amounts are probably overestimates because another short-term station (Rock River) just 50 km to the north indicated total precipitation that was one tenth of the amount recorded at Eagle Plain Lodge (Wahl et al. 1987). Probably more typical for the interior northern Yukon area are the long-term records from Shingle Point and Komatuk Beach, both located on the Yukon coast, that indicate total annual precipitation (rain and snow) of only 125–175 mm.

18.4 Permafrost and Frozen Ground

Permafrost is continuous throughout the area, but quantitative data to substantiate this are few. Geotechnical investigations in Dawson City in the early 1970s indicated discontinuous permafrost to a depth of 60 m with a mean annual ground temperature (MAGT) of between −3 and −5 °C (EBA 1977). Drilling prior to the construction of the Eagle River bridge on Eagle Plain in 1976 indicated that permafrost on the north-facing slope of the Eagle River valley was >90 m thick with a MAGT of -3 °C, but a near-isothermal tálik (unfrozen zone) existed beneath the river (Johnston 1980). Only one exploratory well, the Socony Mobil Cath B-62, has been logged for temperature in the area (Taylor and Judge 1974). Measurements indicate a permafrost thickness of approximately 100 m and a MAGT of between 0 and −2 °C. In more recent years, permafrost and Quaternary studies in the Klondike area suggest permafrost in that area may be Pleistocene in age (Froese et al. 2008). As such, there may be no direct correlation between permafrost occurrence and current climate in the never glaciated Yukon. Therefore, one must assume that permafrost is probably widespread at higher elevations on Eagle Plain and continuous in the Barn Mountains. There is little indication of ground ice.

The intensity of frost action depends not only on lithology but also the ground thermal regime. Eagle Plain is underlain by sandstone, and the Barn Mountain foothills are composed of shale, siltstone and sandstone. These lithologies have relatively high thermal conductivity values. If bedrock is exposed at the surface, numerical simulation of the seasonal pattern of frost penetration on Eagle Plain indicates the active layer may reach as much as 2.5 to 3.0 m in thickness (Fig. 18.2a). At the same time, field measurements indicate that the active layer beneath well-vegetated colluvium on lower slopes and in valley bottoms may be as little as 30–50 cm (Fig. 18.2b). As regards freeze thaw, the annual cycle dominates, while the number of diurnal (near-surface) cycles probably does not exceed 10–15 at the 10 cm depth. Similar relationships are to be expected in the Barn Mountains where the barren uplands are capped by sandstone and siltstone and the better-vegetated lowlands are underlain by shale.

18.5 The Landscape of Eagle Plain

Eagle Plain is an extensive intermontane plateau between 650 and 800 masl located between latitudes 65°N–67°N. It is formed by near-horizontal sandstone and siltstone of Cretaceous age (Norris et al. 1963). These strata are well bedded, porous and frost susceptible. The southern edge of the plateau is marked by a prominent escarpment formed by a resistant member of the Eagle Plain Formation (Norris et al. 1963). Vegetation consists of stunted and open boreal forest which changes to shrub tundra at higher elevations. The alpine tree line decreases northwards in elevation from approximately 850 m in the south to 600 m in the north. Field observations indicate active layer thicknesses vary from as little as 30–40 cm beneath icy organic-rich sediments in valley bottoms to more than 1.0–3.0 m on exposed bedrock on the uplands (French 1977).

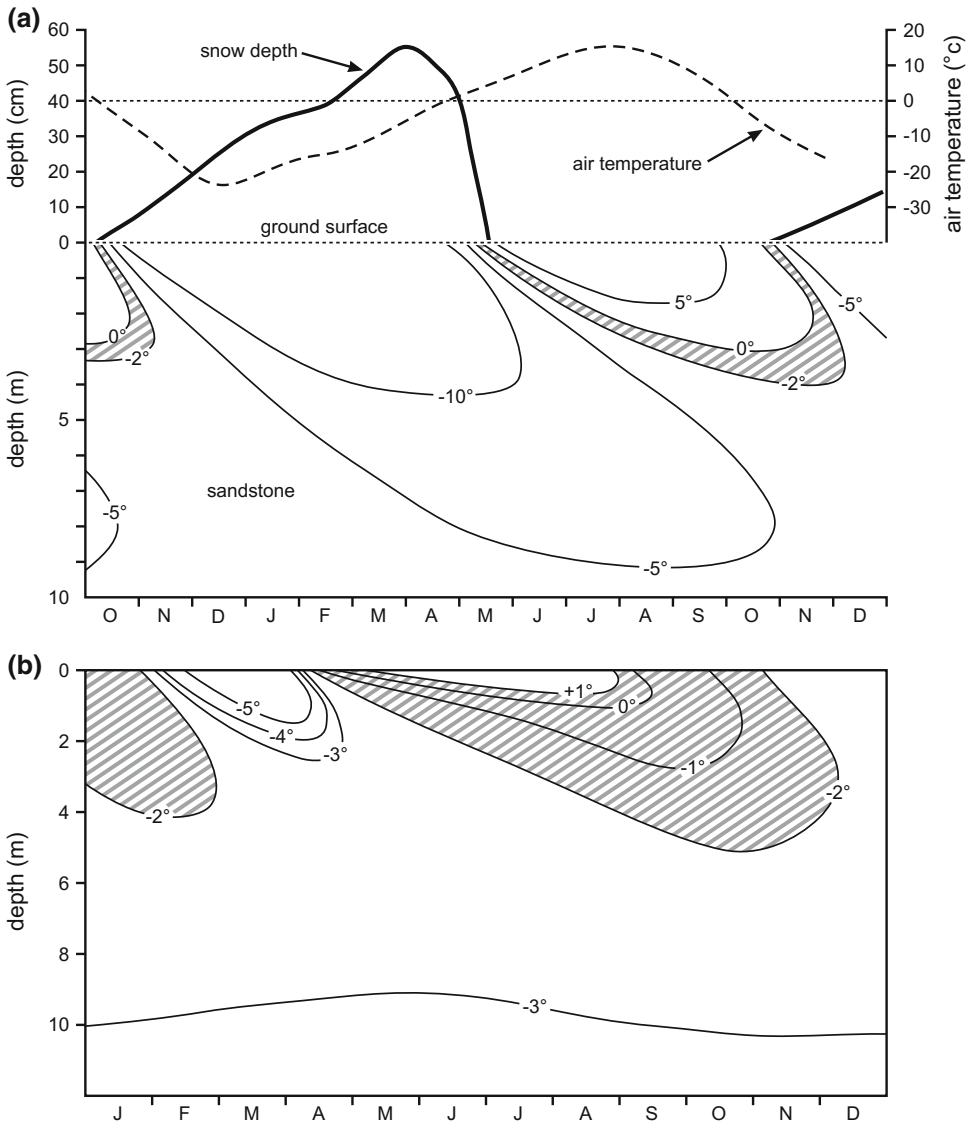

Fig. 18.2 Annual ground thermal regime on Eagle Plain: **a** numerical modeling of ground thermal regime of a bare horizontal sandstone surface on Eagle Plain. The analysis was undertaken by WH Pollard in 1979. From French (1981). **b** The ground thermal regime observed, between 1974 and 1976, in fine-grained sediments on the Eagle River floodplain adjacent to the bridge on the Dempster Highway that crosses the river valley. Data supplied by G. H. Johnston, NRCC, in 1979

Fig. 18.3 Eagle Plain landscape: **a** general view of the upland surface of Eagle Plain. Vegetation consists of shrub tundra on interfluves with open black spruce woodland on sloping terrain (lat. 66°16′N, long. 137°10′W. *Photograph*—H.M. French. **b** Non-sorted circles and nets formed in angular rock-rubble near Eagle Plain Lodge (lat. 66°22′N, long. 136°38′W. *Photograph*—H.M. French. **c** Frost-widened joints are exposed in shale bedrock in a borrow pit at km 366, Dempster Highway. *Photograph*—H.M. French. **d** A small tributary stream with beaded drainage indicates icy permafrost occurs in the colluvial valley bottom deposits, Chance Creek (lat. 66°15′N, long. 137°25′W). *Photograph*—H.M. French

The plain is currently dissected by broad shallow valleys which drain northwards to the Old Crow Basin via the Porcupine and Eagle Rivers (Fig. 18.3a). Slopes are gentle, and bedrock outcrops are rare. Evidence of glaciation is lacking. Although fluvial sediments are present within the Eagle River valley, they were probably deposited when Laurentide ice blocked eastward drainage of the proto-Peel drainage system and meltwater crossed Eagle Plain via this valley toward the glacial lake in the Old Crow Basin (see Fig. 18.1).

The long and uninterrupted period of cold conditions on Eagle Plain had produced an extensive veneer of frost-shattered angular rock-rubble. This mantles the interfluves and upper surfaces and is as much as 2–3 m thick. Often, the regolith has been reworked by frost sorting (Fig. 18.3b). The underlying bedrock is rarely exposed, but borrow pits located along the Dempster Highway reveal frost-widened joints in the bedrock (Fig. 18.3c) caused by the freezing of downward-percolating water (French 1981). Thermal contraction cracking of the bedrock is not readily apparent, and other diagnostic signs of permafrost and ground ice are absent. However, if fine-grained alluvial and/or colluvial sediments are present in valley bottoms, beaded drainage (Fig. 18.3d) indicates ice-rich permafrost and, in places, poorly developed ice-wedge polygon networks are present. In summary, the Eagle Plain landscape is a structurally controlled bedrock surface of low relative relief that has been subject to intense frost action. Running water, wind and permafrost are of relatively minor importance in fashioning the landscape.

18.6 The Landscape of the Barn Mountain Foothills

The Barn Mountains lie north of Eagle Plain and are centered upon latitude 68°30′N and longitude 138°30′W. They form NW-SE trending uplands between the Blow and Babbage river valleys (see Fig. 18.1) and are north of tree line. They rise to elevations in excess of 1200 masl. The dominant

control over relief is that of geological structure; the foothills consist of sequences of gently folded Mesozoic age shale and sandstone that produce curving anticlinal escarpments and synclinal ridges separated by broad valleys (Norris 1977, 1984). By contrast, the main range of the Barn Mountains is more rugged and consists of faulted Paleozoic shale and limestone interbedded with quartzite, chert and conglomerate. Precambrian rocks occur in the nearby Buckland Hills to the north, and granitic intrusions occur both to the north (Mount Sedgwick) and to the south (Mount Fitton). Evidence of glaciation, in the form of glacially derived sediments and glacially sculptured landforms, is absent.

The most striking characteristic of the Barn Mountain foothills is their rounded nature (Fig. 18.4a). The convex-shaped hills and gentle escarpments of the foothills form distinctive non-glacial topography. A second characteristic is that the upland surfaces, usually formed in either siltstone or sandstone, are veneered with angular frost-shattered debris (Fig. 18.4b). Third, near-planar, gently sloping concave surfaces, or pediments, constitute lowlands that surround the structurally controlled ridges and uplands (Fig. 18.4c). The surfaces are developed predominantly upon shale bedrock and are dissected by the current drainage network; the latter is frequently characterized by terraces incised 10–15 m into the underlying bedrock. Fourth, the lowlands are separated from the upland massifs by relatively sharp angular junctions. Typically, the pediment surfaces grade at angles of between 5° and 9°.

A final characteristic of the Barn Mountain foothills is the presence of isolated inselberg-like hills that possess a

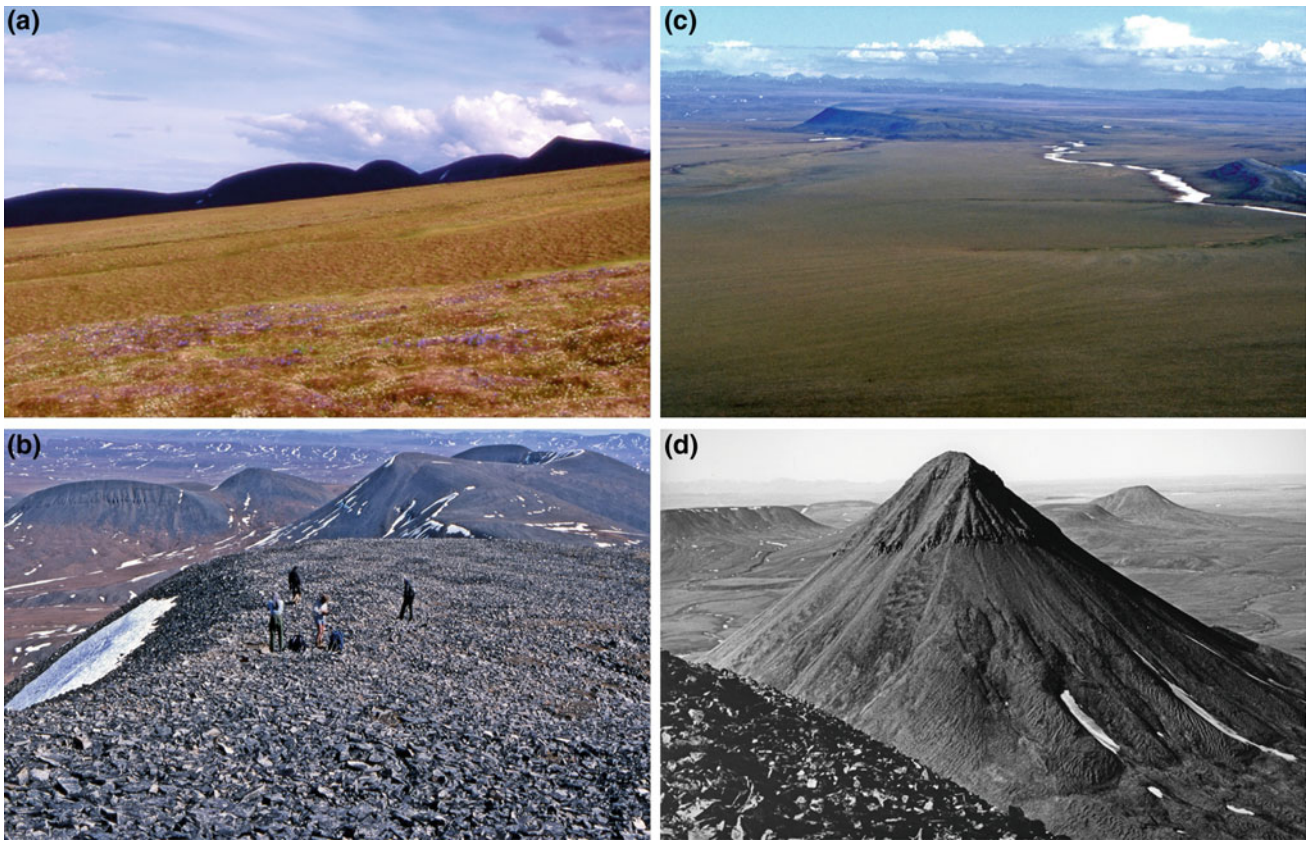

Fig. 18.4 Landscape of the Barn Mountain foothills: **a** Rounded and convex hills are surrounded by gentle planar slopes (lat. 68°42′N, long. 138°16′W). Typically, the slopes are covered with tussock tundra vegetation and possess a hummocky micro-relief, 30–40 cm in height. The hummocks often extend down slope into linear ridges that are several tens of meters in length and up to one meter in width. *Photograph*—H.M. French. **b** The upland surfaces, usually formed in siltstone or sandstone, are planar or gently convex in plan and are mantled with a veneer of angular rock-rubble (lat. 68°42′N, long. 138°19′W). Non-sorted circles may form where the regolith is fine-grained. *Photograph*—H.M. French. **c** Extensive pediment-like surfaces surround the uplands. This photograph shows the southern flank of the Barn Mountains, viewed from near Sam Lake (lat. 68°24′N, long. 138°16′N). They grade at angles of between 5° and 9° and are separated from the upland massifs by relatively sharp angular junctions. Shallow seepage lines outlined by willow-birch shrub may also be present. *Photograph*—H.M. French. **d** Sleepy Mountain, an isolated inselberg-like hill, is a well-known landmark in the Barn Mountains (lat. 68°43′N, long. 138°21′W). The free face is developed in resistant beds of Cretaceous age sandstone and quartzite. Below the free face is a near-rectilinear slope, between 30 and 35° in angle, developed upon softer shale and siltstone of Jurassic age. Active debris flows are present on the lower slopes, and talus material forms a shallow basal concavity. *Photograph*—H.M. French

dramatic steepening of slopes at their boundary with the surrounding lowlands. The most striking is Sleepy Mountain (Fig. 18.4d).

Quite different relief characterizes the summits of the two granitic intrusions of Mount Fitton and Mount Sedgwick. On Mount Fitton (Fig. 18.5a), the ridges and summits possess angular bedrock outcrops and the surrounding slopes are covered with a mantle of boulders and fine-grained quartz and feldspar fragments ('growan'). In places, current frost action and mass-wasting processes, aided by wind action, are stripping and exhuming deeply weathered bedrock (Fig. 18.5b). By contrast, on Mount Sedgwick, the broad summit appears planated and is covered with a veneer of angular rock fragments.

18.7 Discussion

Given that these two uplands have experienced uninterrupted cold-climate conditions for at least 1–3 Ma, it is reasonable to assume that these landscapes are close approximations to truly periglacial landscapes. However, two landforms that occur in these never glaciated uplands are described in more detail because they are often uncritically attributed to frost action processes.

1. Cryoplanation terraces or ancient erosional benches?

The bevelled summit of Mount Sedgwick is just one of a number of erosional benches cut within bedrock in the

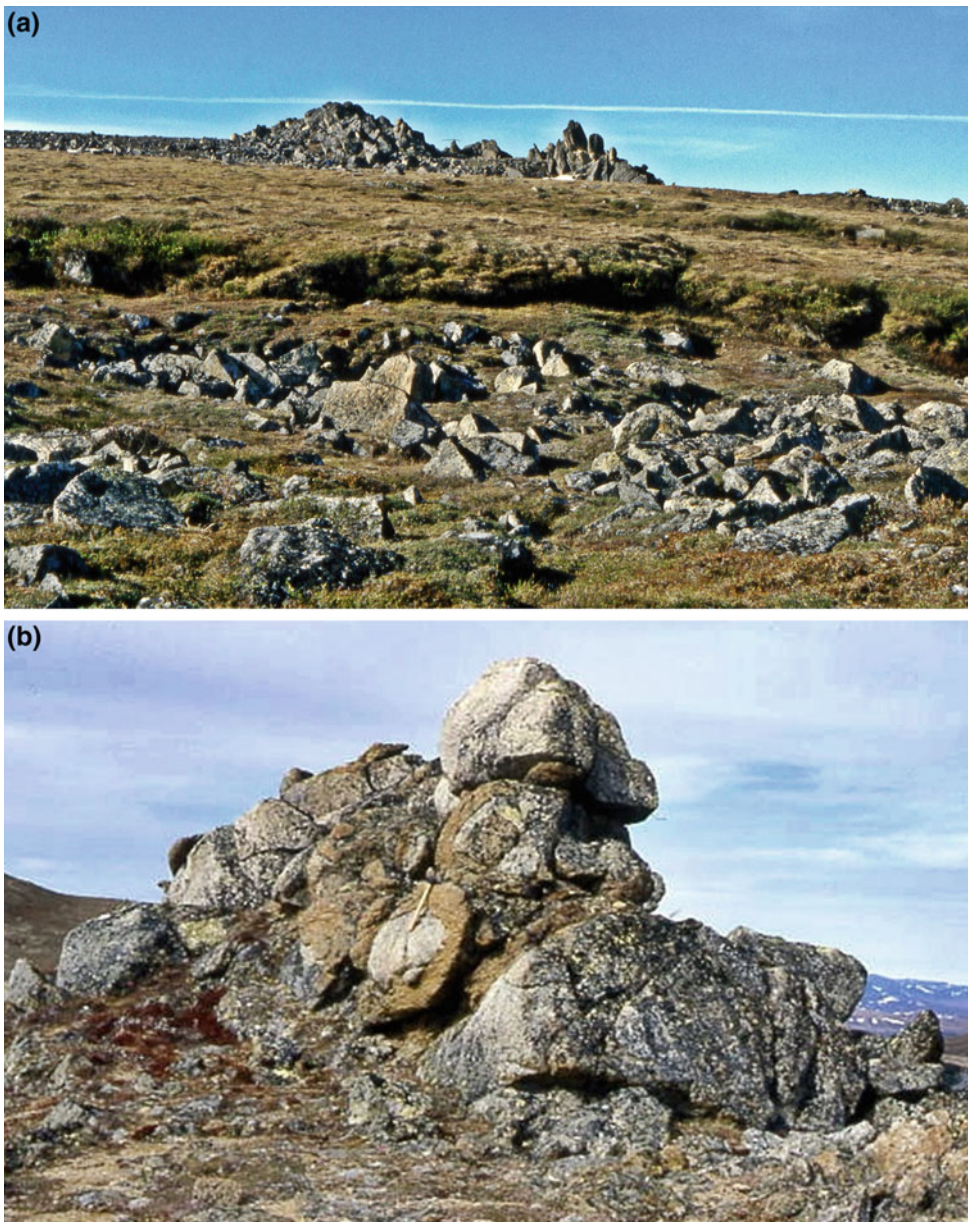

Fig. 18.5 Granitic landscape of Mount Fitton (lat. 68°30′N, long. 138°00'W): **a** Summit and hillslope tors are surrounded by slopes covered with a mantle of siliceous fragments and weathered granitic debris ('growan'). *Photograph*—H.M. French. **b** A summit tor is being exposed by frost action and mass wasting aided by wind to reveal a deeply weathered bedrock surface, of probable Tertiary age. *Photograph*—H.M. French

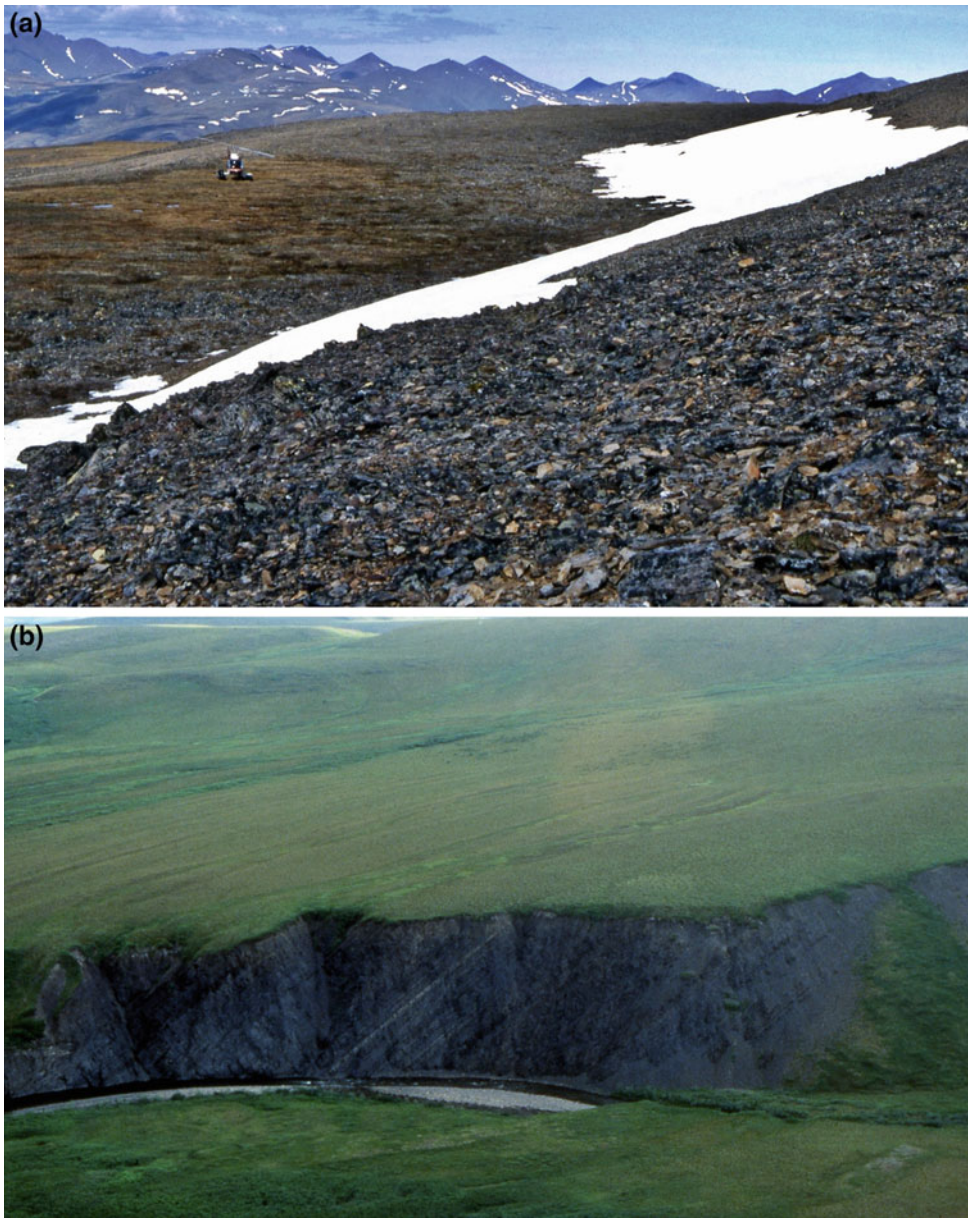

Fig. 18.6 Pediment-like surfaces (cryopediments) and erosional benches (cryoplanation terraces) are of ambiguous periglacial significance: **a** Bedrock terrace developed upon argillite and chert of Pre-Cambrian age, Buckland Hills, Barn Mountains (lat. 68°57′ N; long. 139°30′W). The helicopter provides scale. *Photograph*—H.M. French. **b** Oblique air view of the Anker Creek pediment, upper Canoe Creek drainage basin (lat. 68°40′ N, long. 138°51′W) showing how the pediment surface truncates the underlying shale bedrock (Kingak Formation). A thickness of 1–4 m of a cold-climate diamicton, described in French and Harry (1992, 150–152), covers the pediment surface. *Photograph*—H.M. French

uplands of northern interior Yukon. For example, in the adjacent Buckland Hills (Fig. 18.6a), upper slopes are bevelled by large bedrock terraces, 30–100 m wide with bedrock risers of 10–15 m. These flat surfaces are developed in highly resistant argillites and chert of the Pre-Cambrian Neruokpuk Formation. Similar bedrock benches occur elsewhere in Yukon (Hughes 1990).

The traditional explanation of these bevelled hilltops and erosional benches, first advanced by Russian geologists working in Siberia, highlights the critical role thought to be played by the combined action of frost action and snow in promoting the mechanical disintegration of resistant bedrock. When combined with mass wasting (solifluction), the process was central to the periglacial 'cycle' of landscape evolution initially proposed by Peltier (1950). Subsequently, the concept was termed cryoplanation by European and North American geomorphologists (see French 2007, 244–246). However, field investigations in Yukon fail to demonstrate the active formation of these erosional surfaces. For example, the nature and rate of weathering of quartzite blocks on a cryoplanation terrace in the Old Crow Basin indicates that bench formation may be mid-Pleistocene or earlier (Lauriol et al. 1997; Bjornson and Lauriol 2001) and a recent investigation of the impressive 'giant steps' of Bug Creek of the adjacent Richardson Mountains concluded that '… present day processes…allow them to persist but do not seem capable of having initiated them ' (Lauriol et al. 2006, p 274).

It is probable, therefore, that so-called cryoplanation terraces are either structurally controlled benches that currently favor snow accumulation or the remnants of ancient erosional surfaces that would have formed when the Late Tertiary peneplain began to be eroded by the ancestors of the current hydrographic network.

2. Cryopediments or pediments?

The origin and age of pediments, especially those in the hot arid regions of the world, have long been the subject of speculation. Over 50 years ago, Dylik (1957) remarked upon the similarity of landforms in the hot and cold deserts of the world. The pediments of the Barn Mountain foothills are best described as 'covered' pediments (Twidale 1981), that is, they carry a protective veneer of detritus derived from upslope. Field observations suggest that current activity on the Barn Mountain pediments is limited to cryoturbation and earth hummock formation in the seasonally thawed material that veneers the surface (French and Harry 1992).

The pediments are also erosional in nature. This is because the pediment surfaces truncate the dip of the underlying shale bedrock. Occasionally, they either cross fault lines or encroach upon the adjacent sandstone that forms the uplands. For example, undercutting of the pediment in Anker Creek, a small tributary of the Caribou Creek drainage network, shows that the surface cuts across Mesozoic age shale (Fig. 18.6b). Moreover, a perennially frozen diamicton, ~2–4 m thick, lies unconformably over the bedrock surface yet the current active layer is only between 30 and 60 cm in thickness (French and Harry 1992). For the most part, the diamicton consists of a shale-silt matrix that encloses angular and subangular sandstone fragments. There is a marked absence of organic material and faunal remains; in fact, the diamicton appears to be cryogenic in origin, similar to the 'head' deposits of temperate latitudes. Because the diamicton rests unconformably upon the underlying shale bedrock, it is unrelated to the erosion of the planar surface upon which it lies.

Similar pediment-like surfaces occur elsewhere in the northern interior Yukon. All appear to truncate bedrock. By far the most extensive occurs south of the British and Barn Mountains and flank outcrops of limestone, dolomite and sandstone of Carboniferous and Proterozoic age (Norris 1977). At lower elevations in the Old Crow Basin, these surfaces are covered by Quaternary age lacustrine sediments. Other pediment-like surfaces flank the western slopes of the Richardson Mountains and the northern slopes of the British Mountains in areas beyond the limits of early Wisconsin glaciation (Hughes 1972; Rampton 1982). On the basis of surficial geology mapping, the Tulugaq pediment is thought to be pre-Early Wisconsin in age (Rampton 1982). One must conclude that the pediments that surround the Barn Mountains are not necessarily fashioned by cryogenic processes. Instead, they merely acted as slopes of debris transport at times of more intense frost action than present.

18.8 Conclusions

The landscapes of Eagle Plain and the Barn Mountains foothills illustrate the manner in which long-continued periglaciation acts to modify bedrock terrain. Weathering and frost action have resulted in a veneer of angular bedrock derived debris that mantles the upland surfaces. Stripping of previously weathered debris has also occurred. The landscapes may be some of the closest approximations to periglacial landscapes that exist today. But the preservation of pediments and the remnants of possible ancient erosional surfaces indicate that the complete footprint of periglacial landscape modification has not been achieved.

Acknowledgments Field work on Eagle Plain between 1977 and 1983 was supported by the Arctic Land Use Research (ALUR) program (Indian and Northern Development, Ottawa), Aquitaine of Canada Ltd, and the Natural Sciences and Engineering Research Council. Field work in the Barn Mountains between 1985 and 1988 was supported by the Natural Sciences and Engineering Research Council and the Geological Survey of Canada.

References

Bjornson J, Lauriol BM (2001) Météorisation des blocs de granites à la surface des pediments dans le nord du Yukon, Canada. Perma Perigl Proc 12:289–298

Duk-Rodkin A, Hughes OL (1994) Tertiary-Quaternary drainage of the pre-glacial Mackenzie Basin. Quat Intern 22(23):221–241

Duk-Rodkin A, Barendregt RW, Tarnocai C, Phillips FM (1996) Late tertiary to late quaternary record in the Mackenzie Mountains, Northwest Territories, Canada: stratigraphy, paleosols, paleomagnetism and chlorine-36. Can J Earth Sci 33:875–895

Dylik J (1957) Tentative comparison of planation surfaces occurring under warm and under cold semi-arid conditions. Biul Peryglac 5:175–186

EBA (1977) Geotechnical investigation of utilities design, Dawson City, Yukon. Consultants report, EBA Engineering Consultants Ltd., vol 2, pp 27–28, with supplementary data

French HM (1977) Permafrost and terrain report: Aquitaine Alder well site, Eagle Plain, Yukon Territory (65°52′N; 136°52′W). Consultants Report, Aquitaine of Canada ltd., Calgary

French HM (1981) Sump studies IV: permafrost terrain disturbances adjacent to exploratory well sites, northern Yukon Territory. Environmental Studies, No. 19. Northern Affairs Program, Indian and Northern Development, Ottawa

French HM (2007) The periglacial environment, 3rd edn. Wiley, London

French HM, Harry DG (1992) Pediments and cold-climate conditions, Barn Mountains, unglaciated northern Yukon, Canada. Geogr Ann 74A:145–157

Froese DG, Barendregt RW, Enkin RJ, Baker J (2000) Paleomagnetic evidence for multiple late Pliocene-early Pleistocene glaciations in the Klondike area, Yukon Territory. Can J Earth Sci 37:863–877

Froese DG, Westgate JA, Reyes AV, Enkin RJ, Preece SJ, (2008) Ancient permafrost and a future, warmer Arctic. Science 321:1648

Hopkins DM, Matthews JV, Schweger CE (eds) (1982) Paleoecology of Beringia. Elsevier, Amsterdam

Hughes OL (1972) Surficial geology of northern Yukon Territory and northwestern District of Mackenzie, Northwest Territories. Geol Surv Can Paper 69–36, Map 1319A

Hughes OL (1990) Surficial geology and geomorphology, Aishihik Lake, Yukon Territory. Geol Surv Can Paper 87–29

Johnston GH (1980) Permafrost and the Eagle River bridge, Yukon Territory, Canada. In: Proceedings, permafrost engineering workshop, National Research Council of Canada, Ottawa, Technical memorandum, vol 130, pp 12–28

Lauriol BM, Lalonde AE, Dewez V (1997) Weathering of quartzite on a cryoplanation terrace in northern Yukon, Canada. Perma Perigl Proc 8:147–153

Lauriol BM, Lamirande I, Lalonde AE (2006) The giant steps of Bug Creek, Richardson Mountains, N.W.T., Canada. Perma Perigl Proc 17:267–275

Norris DK (1984) Geology Northern Yukon and Northwestern District of Mackenzie. Geol Surv Can Map 1581A. Scale: 1:1,000,000

Norris DK (1977) Blow River and Davidson Mountains, Yukon Territory—District of Mackenzie. Geol Surv Can Map 1516A. Scale: 1:250,000

Norris DK, Price RA, Mountjoy EW (1963) Geology, northern Yukon Territory and northwestern District of Mackenzie. Geol Surv Can Map 10-1963. Scale: 1:1,000,000

Peltier LC (1950) The geographic cycle in periglacial regions as it is related to climatic geomorphology. Ann Assoc Am Geogr 40:214–236

Rampton VN (1982) Quaternary geology of the Yukon Coastal Plain. Geol Surv Can Bull 317

Taylor AE, Judge AS (1974) Canadian geothermal data collection—northern wells, 1955 to February 1974. Geothermal Series No 1, Geothermal Service of Canada, Earth Physics Branch, Energy, Mines and Resources, Ottawa

Twidale CR (1981) Origins and environments of pediments. J Geol Soc Aust 28:423–434

Wahl HE, Fraser DB, Harvey RC, Maxwell JB (1987) Climate of Yukon. Climatological Studies No. 40, Environment Canada

Old Crow Flats: Thermokarst Lakes in the Forest–Tundra Transition

19

Pascale Roy-Léveillée and Christopher R. Burn

Abstract

Old Crow Flats, in northern Yukon, is a 5600 km^2 Arctic wetland surrounded by mountains. It contains thousands of thermokarst lakes. The area was not glaciated during the Wisconsinan but was submerged by a glacial lake that drained catastrophically 15,000 years ago. Today the glacilacustrine plain is underlain by continuous permafrost and is within the forest–tundra ecotone of northern Yukon. Lakes cover approximately 35 % of the plain area. Many lakes have rectilinear shores and are oriented northeast–southwest or northwest–southeast where tundra vegetation dominates the ground cover. Where taiga and tall shrubs dominate the vegetation cover, lakeshores tend to be irregular. Drained lake basins are abundant in the Flats. Overlapping basins indicate that several generations of thermokarst lakes have formed and drained over the last 15,000 years. In tundra areas, drained basins generally have wet, depressed margins surrounding a slightly elevated centre. Ice wedge polygons are ubiquitous in the tundra and are often strikingly orthogonal near lakes and drained basins. The Flats are incised by Porcupine and Old Crow rivers which meander 20–50 m below the plain level. Effects of climatic warming on the Flats may threaten the traditional activities and food security of the Vuntut Gwich'in.

Keywords

Oriented lakes • Patterned ground • Permafrost • Thermokarst

19.1 Introduction

Old Crow Flats (OCF) is a 5600 km^2 Arctic wetland in eastern Beringia that is surrounded by mountains (Fig. 19.1). Thousands of shallow lakes cover more than one-third of the surface and form a freshwater landscape recognized as a wetland of international significance (The Secretariat of the Convention on Wetlands 2014). Many of the lakes of OCF have rectilinear shorelines and are oriented either northeast–southwest or northwest–southeast. The lakes of OCF exhibit key features of the thermokarst lake cycle, such as lake expansion and drainage followed by permafrost recovery and lake reinitiation. Signs of lake expansion by thawing of ground ice include steep undercut banks with dangling peat curtains, spruce trees leaning towards the water on bank tops, and partly submerged shrubs and trees at the edge of the lakes (Roy-Léveillée and Burn 2010). There are many drained lake basins throughout the Flats, commonly with deeply incised outlets, suggesting that catastrophic lake drainage may occur.

Old Crow Flats is within the forest–tundra transition of northern Yukon and forms a patchy mosaic of water, forest, and tundra incised by entrenched meandering rivers. It has long been a refuge for arctic wildlife (Wolfe et al. 2011). The river bank bluffs have yielded a rich fossil record, including

P. Roy-Léveillée (✉)
School of Northern and Community Studies,
Laurentian University, 935 Ramsey Lake Rd., Sudbury,
ON P3E 2C6, Canada
e-mail: proyleveillee@laurentian.ca

C.R. Burn
Department of Geography and Environmental Studies,
Carleton University, 1125 Colonel By Drive, Ottawa,
ON K1S 5B6, Canada
e-mail: Christopher.burn@carleton.ca

© Springer International Publishing Switzerland 2017

O. Slaymaker (ed.), *Landscapes and Landforms of Western Canada*,
World Geomorphological Landscapes, DOI: 10.1007/978-3-319-44595-3_19

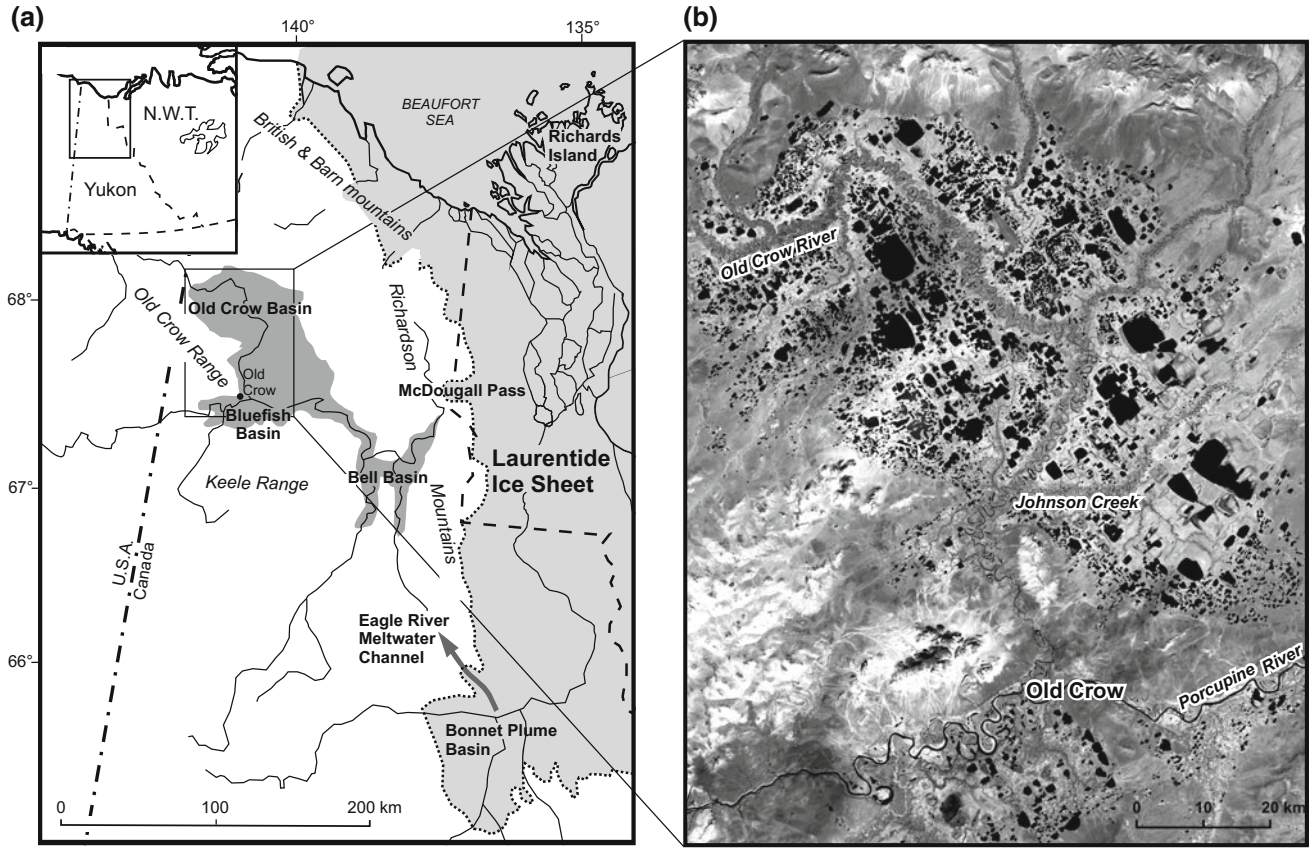

Fig. 19.1 Location map of Old Crow Flats showing **a** northern Yukon with extent of Glacial Lake Old Crow in Bell, Bluefish, and Old Crow basins. The approximate maximum limit of the Laurentide Ice Sheet is shown in *light grey* (after Zazula et al. 2004, Fig. 1 and Lauriol et al. 2009, Fig. 1) and **b** Landsat ETM orthoimage of Old Crow Flats and surrounding areas acquired on 30 August 2001. Waterbodies are in *black* (© Department of Natural Resources Canada. All rights reserved)

possible indications of human presence in the area as long as 40,000 to 35,000 years ago (Morlan 2003). Today Old Crow Flats are a key part of the Traditional Territory of the Vuntut Gwitchin First Nation (VGFN), and local observations indicate that the Flats are undergoing pronounced changes in temperature, precipitation, vegetation cover, lake water levels, and wildlife distribution (Wolfe et al. 2011). VGFN members are concerned that these environmental changes threaten the traditional activities and food security of their citizens (Wolfe et al. 2011).

19.2 Physiography and Climate

OCF is located within a bowl-shaped structural depression formed as the surrounding topography was uplifted, during orogenic events in the Devonian and late Cretaceous to Tertiary Periods (Lane 2007). To the north, OCF is separated from the arctic coast by British (max. elevation 1655 m) and Barn mountains (max. elevation 1109 m). To the east, Richardson Mountains (max. elevation 1671 m) rise between OCF and Mackenzie Delta. OCF is bordered by Old Crow Range (max. elevation 1270 m) to the west, and the Keele and Dave Lord ranges extend to the south (max. elevation 1395 m).

The mountainous terrain to the north separates OCF from the maritime influence that moderates air temperatures at the Arctic coast (Wahl 2004; Burn 2012). Mean January temperature at Old Crow is −29 °C, the lowest in Yukon, and mean air temperature in July is 15 °C, with mean daily maximum temperatures $\geq$20 °C in June, July, and August. Approximately 60 % of the annual precipitation falls between May and September, and on average only 108 mm of precipitation falls as snow, between October and April. In winter and spring, coniferous trees absorb more solar radiation than snow-covered shrubs and grasses, resulting in significant differences in atmospheric heating between areas dominated by taiga and tundra (Roy-Léveillée et al. 2014). The resulting difference in air temperature increases with incoming solar radiation and continues to increase in May for a short period

after disappearance of the snow cover, due to persistence of lake ice until early June on large lakes in tundra areas (Roy-Léveillée et al. 2014).

A composite record of regional temperature indicates that, between 1930 and 2000, winter, spring, and summer temperatures increased by 1.9, 1.6, and 1.2 °C, respectively, which is consistent with local observations of climatic and environmental change (Wolfe et al. 2011; Porter and Pisaric 2011). Simulations by coupled general circulation models for the twenty-first century generally predict increases of 4–5 °C in summer temperature and 9–12 °C in winter temperature near Old Crow; precipitation is also predicted to increase. Thermokarst landscapes such as OCF, which are shaped by interactions between permafrost and surface water, may be particularly sensitive to such changes in air temperature and precipitation.

19.3 Surficial Deposits and Permafrost

Old Crow Flats was not glaciated during the Wisconsinan glacial stage, but advances of the Laurentide Ice Sheet about 30 ka BP and again about 17 ka BP blocked eastward drainage at McDougall Pass and in Bonnet Plume Basin (Fig. 19.1). Glacially dammed water in Bonnet Plume Basin was diverted through the Eagle River meltwater channel towards Glacial Lake Old Crow, which formed in the Bell–Old Crow–Bluefish basins (Fig. 19.1) (Zazula et al. 2004). The glacial lake had a maximum extent of approximately 13,000 km^2, and the elevation of palaeoshorelines around OCF indicates water depths ranging from a few metres to more than 50 m (Rocheleau 1997). These palaeoshorelines constitute ridges of poorly sorted local material, indicating that Glacial Lake Old Crow only persisted for short periods of time (Rocheleau 1997). The glacial lake deposited up to 10 m of unfossiliferous glacilacustrine silts and clays over the thick-layered sands and silts which had accumulated in the basin during the Pleistocene (Lichti-Federovich 1973). It finally drained westward into Yukon River basin at The Ramparts between 16.4 and 14.9 ka BP, establishing the present-day westward drainage of Porcupine River (Zazula et al. 2004).

Beneath the glacilacustrine deposits, ice wedge pseudomorphs and involutions are visible in river bank exposures in a stratigraphic unit that is possibly >2.48 Ma. This suggests that permafrost was present in OCF during the late Pliocene (Pearce et al. 1982; Burn 1994). It is likely that permafrost degraded completely beneath Glacial Lake Old Crow and aggraded again in the exposed glacilacustrine sediments following lake drainage (Lauriol et al. 2009). Measurements in a geotechnical borehole drilled at Old Crow, in the Porcupine River valley, indicated a permafrost thickness of 63 m. In OCF, permafrost temperatures at the depth of zero annual amplitude are −3.1 to −4.0 °C in the taiga along Porcupine and Old Crow rivers, and vary between −5.1 °C beneath low shrubs and −2.6 °C beneath tall shrubs on the Flats (Roy-Léveillée et al. 2014). River bank exposures indicate that the distribution of excess ground ice in the upper 40 m of deposits is limited to the glacilacustrine sediments deposited by Glacial Lake Old Crow (Matthews et al. 1990). Surface features indicative of ice-rich permafrost in the Flats include thermokarst ponds with rapidly receding lake shores, drunken forest, and extensive ice wedge polygon networks.

19.4 Thermokarst Lakes and Drained Basins

Old Crow Flats includes over 2500 thermokarst lakes. Thermokarst lakes form as thawing of ice-rich permafrost leads to settlement of the ground surface and formation of depressions where water tends to accumulate. Many of the lakes of OCF likely formed during the early Holocene climate optimum (Mackay 1992; Burn 1997), when July temperatures in OCF were approximately 6 °C higher than today (Lauriol et al. 2002a). However, some of the earliest lakes may have developed from remnant ponds after the drainage of Glacial Lake Old Crow (Ovenden 1985). The lakes of OCF are generally flat bottomed and shallow, with an average depth of 1–1.5 m and a maximum depth of 4 m. Over 80 % of the lakes are smaller than 10 hectares in area but large lakes, up to 36 km^2, occur throughout the Flats. The lakes tend to expand laterally because conduction of heat from the lake into the bank sediment results in the progressive subsidence of shore banks. Shore recession is accelerated by thermo-mechanical erosion where wave action reaches exposed permafrost and rates of shore recession up to 3.9 m/year have been observed under such conditions (Roy-Léveillée and Burn 2010).

Many of the lakes and drained basins of OCF are oriented either parallel or perpendicular to the dominant summer wind, NE–SW or NW–SE, respectively. Lakes between 1 ha and 1 km^2 are commonly oriented parallel to the dominant wind direction, whereas lakes larger than 10 km^2 are almost exclusively oriented NW–SE. The proportion of oriented lakes increases with lake size, indicating that lake orientation is controlled by processes associated with shore erosion and lake expansion. In areas where the vegetation cover is dominated by low shrubs and grasses, the shorelines of oriented lakes tend to be rectilinear due to wave erosion and redistribution of sediment by longshore currents (Fig. 19.2a, c, e) (Roy-Léveillée and Burn 2015). Where taiga and tall shrubs dominate the landscape, vegetation can remain anchored in the sediment after subsidence of shore banks beneath water and form a barrier protecting the shore from wave action and ice push, thereby hindering the redistribution of sediment by wind-generated currents. In these areas, shorelines are generally irregular and thaw subsidence is the dominant process affecting lake expansion (Fig. 19.2b, d, f).

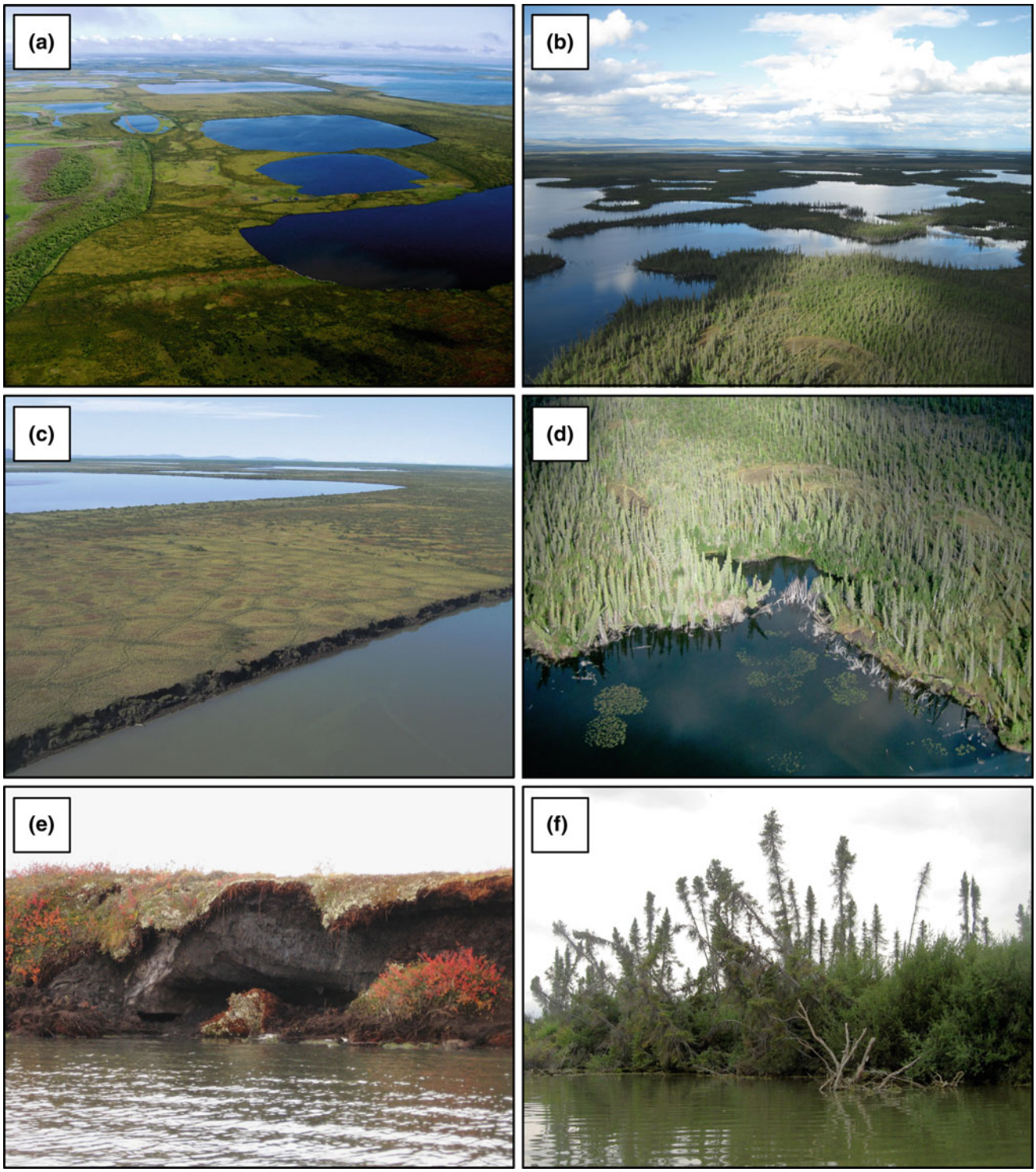

Fig. 19.2 Lake geometry and shore erosion in tundra and taiga areas. **a** Oriented lakes with rectilinear shorelines in an area where the vegetation cover is dominated by low shrubs and grasses; **b** lakes with irregular shorelines in an area where the vegetation cover is dominated by taiga; **c** rectilinear shoreline affected by thermo-mechanical erosion; **d** irregular shore affected by thaw subsidence where trees have remained anchored in the sediment after submergence; **e** shore section with overhanging peat curtains and thermo-erosional niche; **f** shore section protected from thermo-mechanical erosion by partly submerged trees and tall shrubs. Photographs © P. Roy-Leveille

Fig. 19.3 Zelma Lake (12 km^2, in the background) and two smaller adjacent lakes, drained catastrophically in June 2007. Photograph © T. Pretzlaw, used with permission

Despite the expansion of the lakes, residents of Old Crow report decreasing lake water levels and increasing frequency of catastrophic lake drainage (Wolfe et al. 2011). These observations are consistent with remote sensing analyses, which indicate that there was a 3.5 % decrease in lake surface area in OCF between 1972 and 2001, associated with the catastrophic drainage of two large lakes and a negative water balance from 1988 to 2001 (Labrecque et al. 2009). The hydrological regime of the OCF lakes differs depending on the characteristics of the surrounding vegetation (Turner et al. 2010). Where taiga and tall shrubs dominate the vegetation cover, the lake water balance is dominated by input from snowmelt until mid-summer and the lakes are susceptible to catastrophic drainage due to overflow and erosion of ice wedges (Lantz and Turner 2015). In tundra areas where the vegetation cover is dominated by dwarf shrubs and grasses, the snow cover is redistributed by wind during winter, and the main water input for the lakes is rainfall. Lakes in the latter category, as well as lakes with smaller catchments, are particularly vulnerable to water level drawdown by evaporation during summer and many have decreased in size since the 1950s (Bouchard et al. 2013; Turner et al. 2014). The frequency of catastrophic drainage in OCF increased between 1951 and 2009 and may reflect recent increases in precipitation (Lantz and Turner 2015). Increased precipitation levels may raise the intensity of thermo-mechanical erosion of shores or lead to overflow and drainage initiation by ice wedge erosion (Fig. 19.3).

Drained lake basins abound throughout OCF and, in certain areas, overlap of basins and lakes suggest that several generations of thermokarst lakes have developed and drained since Glacial Lake Old Crow. In parts of Old Crow Flats dominated by tundra vegetation, the centre of drained basins is generally slightly raised and better drained than the depressed margins, where ponding is common (Fig. 19.4). This topography results from the transport of fine sediment away from eroding lake margins during lake expansion. Over time, this transport results in the deposition of more

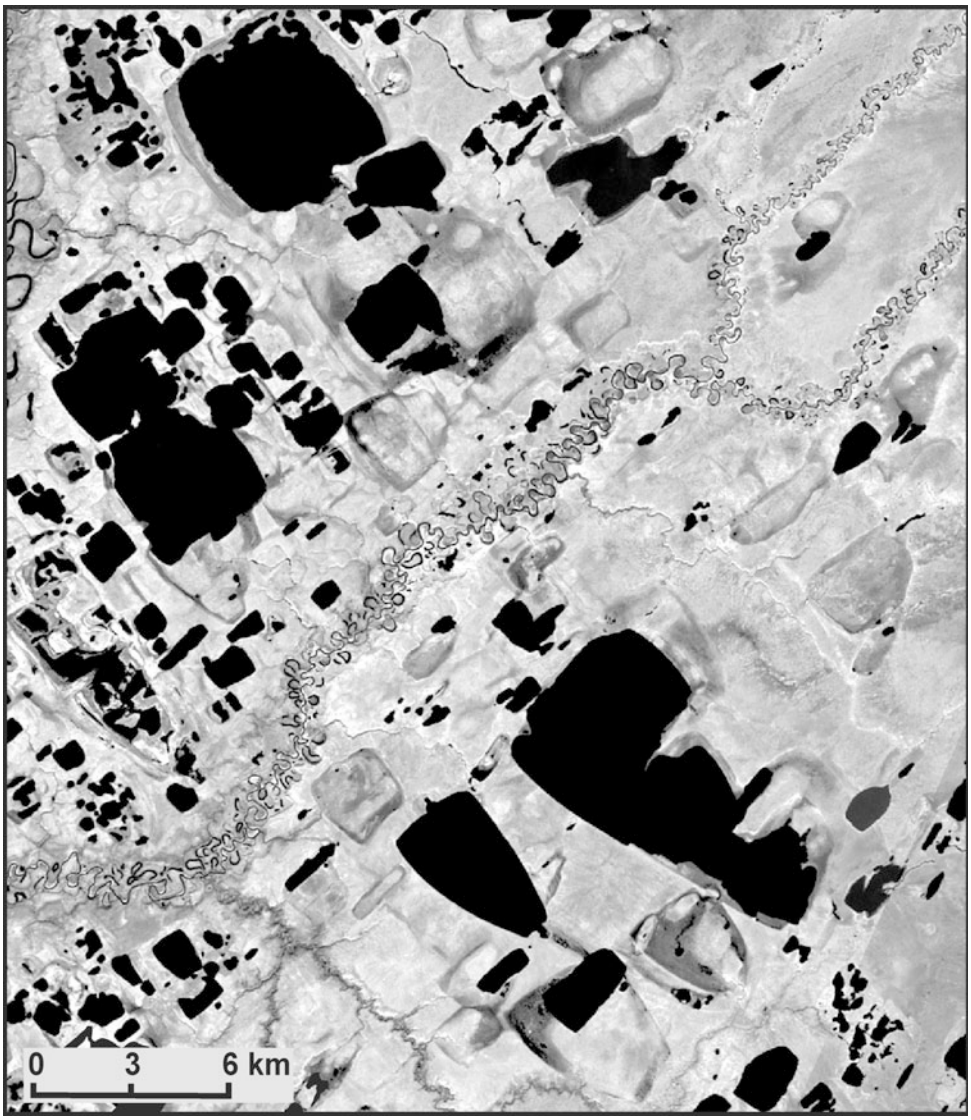

Fig. 19.4 Landsat ETM orthoimage of a part of Old Crow Flats dominated by low-shrub tundra, near Johnson Creek, where several drained lake basins are visible. Areas with high moisture contents generally appear in *darker shades* of *grey*, and waterbodies are in *black* (© Department of Natural Resources Canada. All rights reserved)

sediment in the central parts of lakes, where the lake bottom has been submerged for longer and has subsided below wave base, than at the shallow margins, where resuspension by wave action occurs frequently (Roy-Léveillée and Burn 2016) (Fig. 19.5a). This difference in sediment volume is revealed after drainage, when permafrost aggrades in the lake-bottom sediment and underlying talik (Fig. 19.5b).

19.5 Ice Wedge Polygons

In the tundra of OCF, patterned ground resulting from the development of ice wedges is omnipresent and clearly visible from the air (Fig. 19.6). Ice wedges are massive bodies dominantly composed of foliated ice which form through the repeated infiltration and freezing of snowmelt in thermal contraction cracks (Mackay 1974). They are typically interconnected in a network forming a polygonal pattern at the surface. In Old Crow Flats, ice wedges are occasionally exposed in cross section in rapidly eroding lakeshore banks. The ice wedge networks are strikingly orthogonal over extensive areas around the lakes and drained lake basins (Fig. 19.6). Orthogonal ice wedge networks develop where a source of heat in the landscape, such as a water body, reduces the thermal stress in one direction and causes ground cracking to occur at 90° to the edge of the heat source (Lachenbruch 1962). In OCF, ice wedge networks are widespread in areas where tundra vegetation dominates, but they are rare in areas dominated by tall shrubs and taiga (Roy-Léveillée and Burn 2010). This difference in ice wedge

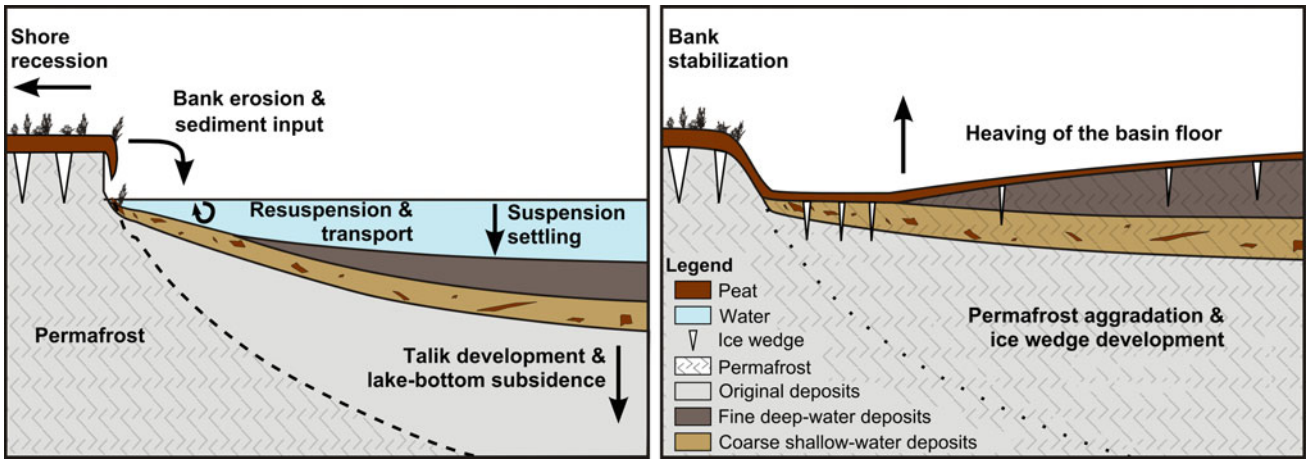

Fig. 19.5 Conceptual model of sedimentation patterns near receding thermokarst lakeshores (*left*) and resulting topography after lake drainage and permafrost agradation (*right*). A *light grey* pattern indicates sediments that are in permafrost (Roy-Léveillée and Burn 2016)

Fig. 19.6 Orthogonal ice wedge polygons near oriented lakes. Note that alders and willows grow almost exclusively on the ice wedge ridges, where the ground is slightly elevated and better drained than the polygon centres. Photograph © C.R. Burn

Fig. 19.7 Meanders on the Old Crow River near the centre of Old Crow Flats. Note the vegetation patterns inside the first meander indicating previous channel positions. The eroding bluffs are approximately 30 m high. At this location, the width of the Old Crow River valley varies between 1.2 and 2.5 km. Photograph © K. Turner

abundance between taiga and tundra likely reflects differences in snow cover characteristics and ground temperature (Roy-Léveillée et al. 2014).

19.6 Meandering Rivers

The Flats are incised by Porcupine and Old Crow rivers which meander 20–50 m below the plain level (Fig. 19.7). Intense fluviglacial discharge from the Laurentide ice sheet led to the rapid incision of the Porcupine and Old Crow river valleys approximately 12,000 years ago. During this period, the Porcupine River attained a depth of 50 m and a width of 5 km over a distance of 30 km in less than 1000 years (Lauriol et al. 2002b). Today the Porcupine and Old Crow rivers run along a fill-cut terrace formed by the aggradation of 5 to 10 m of sediment, between 8 and 4 ka BP, and subsequent channel incision in the deposit. River migration across the valley bottoms formed oxbows lakes and meander scars on the terrace providing evidence of former river courses (Lauriol et al. 2002b). Porcupine and Old Crow river bank bluffs contain geological records of environmental change spanning several million years and have yielded the richest Ice Age fossil record in Canada, including bones of woolly mammoths, steppe bison, horses, lions, ground sloths, and camels (Harington 1977).

19.7 Conclusion

Protected by its mountainous surroundings, Old Crow Flats forms a striking freshwater landscape where thermokarst lakes, drained lake basins, ice wedge polygon networks, and deeply entrenched meandering rivers form intricate patterns that vary through the forest–tundra transition. The area provides important habitat for over 500,000 waterbirds and numerous other species including moose, wolverine, and muskrats which are important to the traditional subsistence activities of the Vuntut Gwich'in. Local residents report that the Flats are undergoing pronounced changes in temperature,

precipitation, vegetation cover, lake water levels, and wildlife distribution (Wolfe et al. 2011). VGFN is concerned that these environmental changes are linked to climatic warming and threaten the traditional activities and food security of their citizens. Despite its multi-layered significance, sensitive environment, and rapidly changing climate, OCF remains an understudied area as it is remote and difficult to access.

Acknowledgements Our research on permafrost in the Old Crow Flats has been funded by the Natural Science and Engineering Research Council of Canada, the Canadian International Polar Year Program, the Polar Continental Shelf Program (Natural Resources Canada), and the Northern Scientific Training Program (Indigenous Affairs and Northern Development Canada). Essential logistical support has been provided by the Vuntut Gwitchin First Nation Government, the Yukon Field Unit of Parks Canada Agency, and the Aurora Research Institute, Inuvik. Several field assistants contributed to data collection including A.J. Jarvo, A.L. Frost, B. Brown, D. Charlie, E. Tizya-Tramm, K. Tetlichi, L. Nagwan, M. Frost Jr., S. Njoutli, S. Frost, and C.Z. Braul.

References

Bouchard F, Turner KW, MacDonald LA, Deakin C, White H, Farquharson N, Medeiros AS, Wolfe BB, Hall RI, Pienitz R, Edwards TWD (2013) Vulnerability of shallow subarctic lakes to evaporate and desiccate when snowmelt runoff is low. Geophys Res Lett 40:6112–6117. doi:10.1002/2013GL058635

Burn CR (1994) Permafrost, tectonics, and past and future regional climate change, Yukon and adjacent Northwest Territories. Can J Earth Sci 31:182–191

Burn CR (1997) Cryostratigraphy, paleogeography, and climate change during the early Holocene warm interval, western Arctic coast, Canada. Can J Earth Sci 34:912–925

Burn CR (2012) Climate. In: Burn CR (ed) Herschel Island Qikiqtaryuk: a natural and cultural history of Yukon's Arctic Island. Wildlife Management Advisory Council, Whitehorse, pp 48–53

Harington CR (1977) Pleistocene mammals of the Yukon Territory. Ph. D. Thesis, University of Alberta

Labrecque S, Lacelle D, Duguay CR, Lauriol B, Hawkings J (2009) Contemporary (1951–2001) evolution of lakes in the Old Crow Basin, Northern Yukon, Canada: remote sensing, numerical modeling, and stable isotope analysis. Arctic 62:225–238

Lachenbruch AH (1962) Mechanics of thermal contraction cracks and ice-wedge polygons in permafrost. Geological Society of America Special Papers 70

Lane LS (2007) Devonian-Carboniferous paleogeography and orogenesis, northern Yukon and adjacent Arctic Alaska. Can J Earth Sci 44:679–694

Lantz TC, Turner KW (2015) Changes in lake area in response to thermokarst processes and climate in Old Crow Flats, Yukon. J Geophys Res Biogeosci 120:513–524. doi:10.1002/2014JG002744

Lauriol B, Cabana Y, Cinq-Mars J, Geurts M-A, Grimm FW (2002a) Cliff-top eolian deposits and associated molluscan assemblages as indicators of Late Pleistocene and Holocene environments in Beringia. Quatern Int 87:59–79

Lauriol B, Duguay CR, Riel A (2002b) Response of the porcupine and Old Crow rivers in northern Yukon, Canada, to Holocene climatic change. Holocene 12:27–34

Lauriol B, Lacelle D, Labrecque S, Duguay CR, Telka A (2009) Holocene evolution of lakes in the Bluefish Basin, northern Yukon, Canada. Arctic 62:212–224

Lichti-Federovich S (1973) Palynology of six sections of late Quaternary sediments from the Old Crow River, Yukon Territory. Can J Bot 51:553–564

Mackay JR (1992) Lake stability in an ice-rich permafrost environment: examples from the western Arctic coast. In: Robarts RD, Bothwell ML (eds) Aquatic ecosystems in semi-arid regions: implications for resource management, August 27–30, 1990, Saskatoon, Canada. National Hydrology Research Institute, Environment Canada, Saskatoon, pp 1–25

Mackay JR (1974) Ice-wedge cracks, Garry Island, Northwest Territories. Can J Earth Sci 11:1366–1383

Matthews JV, Schweger CE, Janssens JA (1990) The last (Koy-Yukon) interglaciation in the northern Yukon: evidence from Unit 4 at Ch'ijee's Bluff, Bluefish Basin. Géogr Phys Quatern 44:341–362

Morlan RE (2003) Current perspectives on the Pleistocene archaeology of eastern Beringia. Quat Res 60:123–132

Ovenden L (1985) Hydroseral histories of the Old Crow peatlands, Northern Yukon. Ph.D. Thesis, University of Toronto

Pearce GW, Westgate JA, Robertson S (1982) Magnetic reversal history of Pleistocene sediments at Old Crow, northwestern Yukon Territory. Can J Earth Sci 19:919–929

Porter TJ, Pisaric MFJ (2011) Temperature-growth divergence in white spruce forests of Old Crow Flats, Yukon Territory, and adjacent regions of northwestern North America. Glob Change Biol 17:3418–3430

Rocheleau M (1997) Sédimentologie des paleoplages de la plaine d'Old Crow, territoire du Yukon, Canada. M.A. Thesis, Université d'Ottawa

Roy-Léveillée P, Burn CR (2010) Permafrost conditions near shorelines of oriented lakes in Old Crow Flats, Yukon Territory. In: Proceedings, GEO2010: 63rd Canadian geotechnical conference and 6th Canadian permafrost conference, Calgary, Sept. 12–16, 2010. Can Geotech Soc, Richmond, pp 1509–1516

Roy-Léveillée P, Burn CR (2015) Geometry of oriented lakes in Old Crow Flats, northern Yukon. In: Proceedings, GEOQuebec2015: 68th Canadian geotechnical conference and 7th Canadian permafrost conference, Quebec City, Sept. 21–23, 2015. Can Geotech Soc, Richmond

Roy-Léveillée P, Burn CR (2016) A modified landform development model for the topography of drained thermokarst lake basins in fine-grained sediments. Earth Surf Proc Land 41:1504–1520. doi:10.1002/esp.3918

Roy-Léveillée P, Burn CR, McDonald ID (2014) Vegetation-permafrost relations within the forest–tundra ecotone near Old Crow, Northern Yukon, Canada: permafrost temperatures within the forest–tundra near Old Crow, YT. Permafr Periglac Proc 25:127–135

The Secretariat of the Convention on Wetlands (2014) The list of Wetlands of international importance. http://ramsar.org/ pdf/sitelist.pdf

Turner KW, Edwards TWD, Wolfe BB (2014) Characterising runoff generation processes in a lake-rich thermokarst landscape (Old Crow Flats, Yukon, Canada) using $\delta^{18}O$, $\delta^{2}H$ and d-excess measurements. Permafr Periglac Proc 25:53–59

Turner KW, Wolfe BB, Edwards TWD (2010) Characterizing the role of hydrological processes on lake water balances in the Old Crow Flats, Yukon Territory, Canada, using water isotope tracers. J Hydrol 386:103–117

Wahl HE (2004) Climate. In: Smith CAS, Meikle JC, Roots CF (eds) Ecoregions of the Yukon Territory: biophysical properties of Yukon landscapes. Agric Agri-Food Can, Summerland, pp 19–23

Wolfe BB, Humphries MM, Pisaric MF, Balasubramaniam AM, Burn CR, Chan L, Cooley D, Froese DG, Graupe S, Hall RI, Lantz T, Porter TJ, Roy-Léveillée P, Turner KW, Wesche SD, Williams M (2011) Environmental change and traditional use of the Old Crow Flats in northern Canada: an IPY opportunity to meet the challenges of the new northern research paradigm. Arctic 64:127–135

Zazula GD, Duk-Rodkin A, Schweger CE, Morlan RE (2004) Late Pleistocene chronology of glacial Lake Old Crow and the north-west margin of the Laurentide ice sheet. In: Ehlers J, Gibbard PL (eds) Quaternary glaciations-extent and chronology part II: North America. Elsevier, London, pp 347–362

The Deglacial Landscape of the Southern Fraser Plateau, British Columbia

20

Tracy A. Brennand and Andrew J. Perkins

Abstract

Until recently, the prevailing view of late glacial Cordilleran Ice Sheet (CIS) decay over the interior plateaus was one of regional stagnation attributed to a rapid rise in equilibrium line altitude (ELA). A new model of late glacial CIS decay has emerged from recent landform mapping and classification across the southern Fraser Plateau, facilitated by the availability of higher resolution terrain data, geophysical surveys and sedimentology at available exposures. Patterns of palaeoglacial lake evolution and moraines suggest an active ice margin systematically retreating northwestward back towards the Coast Mountains, consistent with the pattern of eskers, ice-marginal channels, and reconstructed glaci-isostatic tilt from palaeolake shorelines. Lake effects likely enhanced glacier retreat, at least partially decoupling it from broader climate patterns. Ice-margin retreat was accompanied by thinning recorded by the presence of nested ice-marginal channels and supraglacial eskers. A rapidly rising ELA and lake effects enhanced melt rates allowing supraglacial lakes to form on the ice surface and drain through crevasses or moulins forming subglacial meltwater corridors and glacial lake outburst flood eskers. Pockets of localized stagnation, supported by the presence of hummocky terrain, crevasse-fill ridges and ice-walled canyon eskers, existed during regional retreat across the southern Fraser Plateau.

Keywords

Cordilleran Ice Sheet • Deglaciation • Retreat • Meltwater channels • Tunnel valleys • Eskers • GLOFs • Ice-marginal lakes • Spillways • Moraines • Crevasse-fill ridges

20.1 Introduction

The southern Fraser Plateau (Fig. 20.1) is a largely forested, sparsely populated landscape accessible mainly by gravel roads. These conditions have presented a challenge to geomorphologists and geologists in their attempts to map and decode the deglacial landscape of the region. Early work at the reconnaissance scale (1:250,000) identified major landforms and sediments (pitted terrain, 'drift ridges of uncertain origin', eskers, meltwater channels and lake deposits) from aerial photographs and limited ground observations during bedrock mapping campaigns (Tipper 1971). More recent work mapped similar landforms and sediments (with the addition of crevasse-fill ridges and moraines) at the 1:50,000 scale using satellite and digital elevation model data, aerial photographs and ground observations (Plouffe et al. 2011

T.A. Brennand (✉) · A.J. Perkins
Department of Geography, Simon Fraser University, 8888 University Drive, Burnaby, V5A 1S6, BC, Canada
e-mail: tabrenna@sfu.ca

A.J. Perkins
e-mail: ajp7@sfu.ca

© Springer International Publishing Switzerland 2017
O. Slaymaker (ed.), *Landscapes and Landforms of Western Canada*,
World Geomorphological Landscapes, DOI: 10.1007/978-3-319-44595-3_20

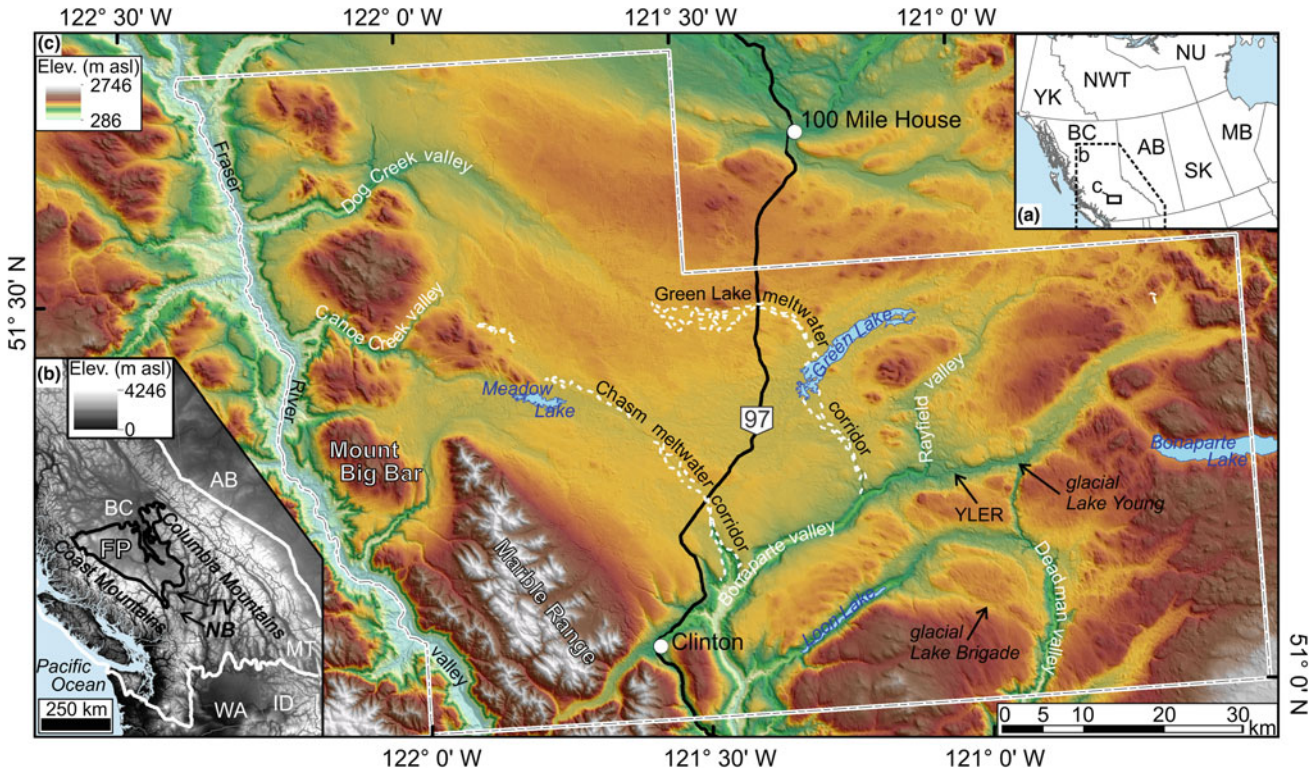

Fig. 20.1 *a* Location of study area within the context of western Canada (extent of '*b*' noted by *dashed line*, extent of '*c*' noted by *solid line*). *AB* Alberta; *BC* British Columbia; *MB* Manitoba; *NU* Nunavut; *NWT* Northwest Territories; *SK* Saskatchewan; *YK* Yukon. *b* Elevation (Geobase®), non-synchronous Cordilleran Ice Sheet extent at local last glacial maximum (*white solid line*; Clague and James 2002), the extent of the Fraser Plateau (*black solid line*; Holland 1976) in BC, and the location of the map in (*c*) (*white dashed box*). *FP* Fraser Plateau; *ID* Idaho; *MT* Montana; *WA* Washington; *TV* Thompson Valley; *NB* Nicola Basin; *Elev. masl* Elevation in m above sea level. *c* Physiographic features and population centres on and around the southern Fraser Plateau; *YLER* Young Lake esker-like ridge

and references therein). Meltwater channels were not classified on the maps by origin (i.e. subglacial, proglacial, ice-marginal or spillway) although differences in origin were acknowledged and used to infer ice retreat patterns (Plouffe et al. 2011). Because the morpho-sedimentary relationships of eskers and moraines were not explored (drift dispersal being the primary mandate for that campaign), neither were they classified by origin and thus the ice dynamics associated with their formation remained unexplored. Our work has focussed on mapping putative deglacial landforms and sediments at the $\leq$1:40,000 scale from aerial photographs and digital terrain models [DTMs; 25 m horizontal grid cells, 1 m vertical resolution (90 % of measurements within 5 m of true elevation), Geobase®)] in a c. 8000 km^2 region of the southern Fraser Plateau near Clinton, British Columbia (BC) (Fig. 20.1c), and near the geographic centre of the last Cordilleran Ice Sheet (CIS) at its maximum. Sedimentology at available exposures and selective application of shallow geophysics has facilitated genetic interpretations and a refined understanding of deglacial pattern and style in the region. The results of this work are summarized in this chapter.

20.2 The Canvas on Which Deglaciation Took Place

The southern Fraser Plateau is located between the Coast and Columbia mountain ranges in south-central British Columbia (BC), Canada (Tipper 1971; Holland 1976) (Fig. 20.1b). The subdued topography of the plateau (average elevation c. 1175 m asl) is a result of the infilling of intrusive igneous and sedimentary basement topography by basaltic lava flows and subsequent tectonic warping during the Neogene (Mathews 1989). In places, the plateau has been incised by streams, such as the Fraser River, forming deep valleys that are filled with thick sequences of glacial sediments (e.g. Eyles and Clague 1991; Huntley and Broster 1994; Lian and Hicock 2001), some of which were deposited in the Early or Mid-Pleistocene (Lian et al. 1999). However, the vast majority of bedrock on the plateau is mantled by glacial sediment deposited during the last glaciation (marine isotope stage (MIS) 2) (cf. Fulton and Smith 1978; Huntley and Broster 1994, 1997; Lian and Hicock 2000, 2001; Plouffe et al. 2011). The regional MIS 2 drift blanket, including Kamloops Lake till (Fulton and Smith 1978), is generally

less than 20 m thick (Andrews et al. 2011), with most outcrops typically 1–2 m thick. Exposed bedrock exhibits striae and rock drumlins, and the drift blanket exhibits ribbed terrain (Tipper 1971; Brennand et al. 2014; Perkins 2015) and/or streamlined bedform fields mainly attributed to ice flow around local last glacial maximum (LLGM) (Tipper 1971; Plouffe et al. 2011). There has been speculation that some streamlined bedforms may have been formed during deglaciation (Kleman et al. 2010).

20.3 Glacial History

Growth of the last CIS in BC was diachronous, beginning c. 35–30 cal ka BP and reaching the southern Fraser Plateau sometime after 24 cal ka BP (Clague and James 2002). Regional ice flow history, reconstructed from the orientation of streamlined glacial bedforms, meltwater channels, till geochemistry, and pebble lithologies and supplemented by striae orientations (Tipper 1971; Plouffe et al. 2011), indicates that during MIS 2 ice flowed onto the plateau from source areas in the Coast Mountains to the west and the Cariboo Mountains (a sub-range of the Columbia Mountains) to the east (Fig. 20.1b), eventually coalescing somewhere east of the Fraser River and forcing flow north and south (e.g. Tipper 1971; Huntley and Broster 1997; Clague and James 2002; Plouffe et al. 2011). The southern part of the CIS reached its maximum extent at c. 17 cal ka BP (LLGM) when its margin terminated in a series of lobes that extended into northern Washington, Idaho and Montana (Clague and James 2002) (Fig. 20.1b). At this time, the southern Fraser Plateau was covered by ice at least 600 m thick (Huntley and Broster 1994), as recorded by the maximum elevation of glacial trimlines and minimum elevation of relict periglacial landforms (Huntley and Broster 1997; Lian 1997), and possibly >1000 m thick, as recorded by erratics on the summit of the Marble Range (Margold et al. 2014; see also Lian 1997) (Fig. 20.1). Consequently, dissecting valleys (e.g. Fraser and Thompson valleys) may have contained >1000 m (Huntley and Broster 1994) and possibly >1900 m (Margold et al. 2014) thick ice. Due to increased ice thickness and, thus, increased porewater pressure in the glacier bed, the initially cold-based CIS margin is thought to have shifted to a temperate thermal regime over the southern Fraser Plateau by LLGM (cf. Huntley and Broster 1993; Lian and Hicock 2000).

Limited radiocarbon and ^{10}Be exposure ages suggest that ice sheet decay over southern interior BC was relatively rapid, commencing as early as c. 15 cal ka BP and almost entirely complete by c. 11.5 cal ka BP (Clague and James 2002; Margold et al. 2014). During deglaciation, the ice was thought to have regionally stagnated (a passive top-down decay causing ice to recede from the Coast Mountains) because of a rapid rise in equilibrium line altitude (ELA) (Fulton 1991) (Fig. 20.2a), with minor (complex) frontal backwasting across the interior plateaus (Fulton 1967; Clague and James 2002). This concept is supported by the presence of hummocky topography interpreted as ice-disintegration moraine and a perceived lack of recessional moraines across the plateau surface, as well as the presence of ice-dammed lakes in major valleys, such as the Thompson Valley (Fulton 1967; Tipper 1971). However,

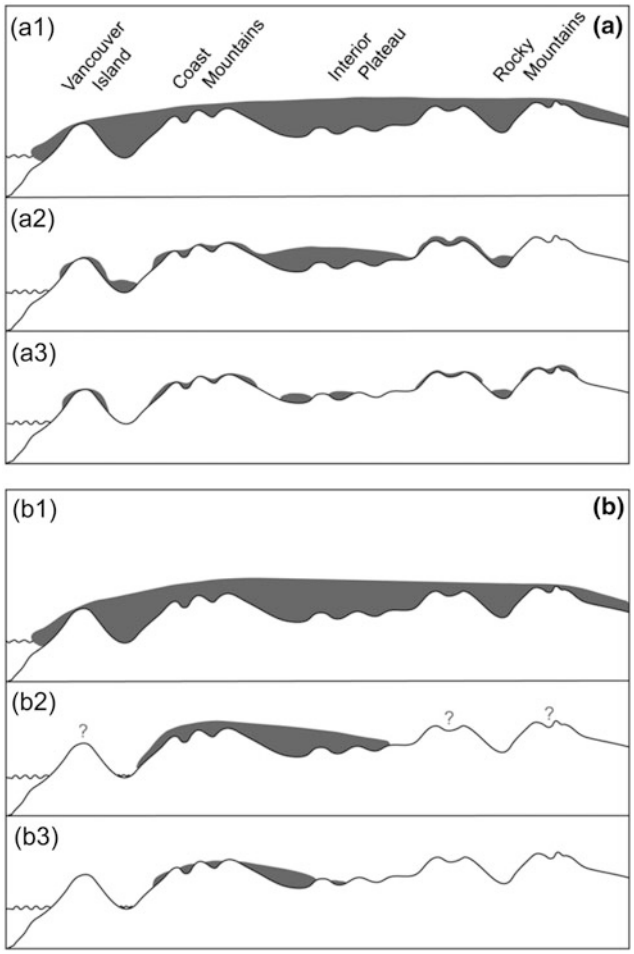

Fig. 20.2 Schematic cross sections of the Cordilleran Ice Sheet from local last glacial maximum (LLGM) (**a**) to early (**b**) and late (**c**) stages of deglaciation (Margold et al. 2013, with permission from Wiley). **a** Conceptual model of CIS decay adapted from Fulton (1991: Fig. 7, p. 285); *a1* at LLGM, a dome is centred over central British Columbia; *a2* a rapid rise in ELA results in passive downwasting over the plateaus, and thicker, active ice remains in the deep valleys; *a3* alpine glaciers persist in the high mountains, and scattered stagnant ice masses remain on the interior plateau and the deepest valleys. **b** Schematic reconstruction of the CIS according to Margold et al. (2013); *b1* at LLGM, the CIS covered most of the highest mountains and had an asymmetric profile with an ice divide over the interior plateau east of the Coast Mountains; *b2* the ice divide shifted west to the Coast Mountains as the ELA rose and the western margin retreated rapidly by calving; *b3* nunataks expanded in the mountains as the remnant ice sheet retreated into the Coast Mountains; stagnating ice fringed the retreating ice sheet

reconstructions of glaci-isostatic rebound from palaeoglacial lake shoreline deformation in the Thompson Valley (Johnsen and Brennand 2004) (Fig. 20.1b), explication of the distribution of meltwater landforms recording ice-margin positions and ice surface slopes in interior BC (Plouffe et al. 2011; Margold et al. 2013), and reconstructions of late glacial ice-marginal lake evolution, and discovery and explanation of numerous moraine ridges on the southern Fraser Plateau together suggest a systematic northwestward pattern of ice-margin retreat, accompanied by regional thinning (Perkins et al. 2013; Perkins and Brennand 2014; Brennand et al. 2014) in the area.

Ice sheet decay is recorded by glacilacustrine and outwash sediments (e.g. Eyles and Clague 1991; Lian and Hicock 2001; Plouffe et al. 2011; Burke et al. 2012a, b; Perkins et al. 2013; Perkins and Brennand 2014) and by subglacial, ice-marginal and proglacial meltwater channels, eskers, moraine ridges, hummocky terrain, crevasse-fill ridges, deltas, subaqueous fans, and spillways (e.g. Tipper 1971; Plouffe et al. 2011; Burke et al. 2012a, b; Perkins et al. 2013; Perkins and Brennand 2014). As deglaciation progressed several large, well-documented late glacial ice-dammed lakes filled with thick glacilacustrine sediments in the narrow, deep valleys that transect the plateau (e.g. Fulton 1969; Johnsen and Brennand 2004) and with thinner sediment accumulations in broader, shallower ice-dammed lakes in the broad basins on the plateau (Bednarski 2009; Huscroft 2009; Plouffe 2009a, b; Perkins et al. 2013; Perkins and Brennand 2014). Eventually, the lakes drained, some catastrophically (Blais-Stevens et al. 2003; Johnsen and Brennand 2004; Perkins and Brennand 2014), and were replaced by streams that subsequently incised their glacial valley fills leaving behind a series of terraces. These terraces are typically capped by fluvial sand and gravel, paraglacial alluvial and colluvial fans, and finally up to several metres of aeolian silt and sand (Ryder 1971; Lian and Huntley 1999; Lian and Hicock 2001).

20.4 Subglacial Meltwater Corridors and Eskers

Subglacial meltwater corridors are characterized by reaches with upslope long profiles, associations with subglacial landforms (e.g. contain subglacial eskers and truncate subglacial bedforms), and bedrock or till walls (e.g. Brennand and Shaw 1994; Greenwood et al. 2007). They are numerous on the southern Fraser Plateau, but are likely underrepresented on maps because many were reoccupied by proglacial streams during ice retreat (and are thus mapped as proglacial channels). The majority are oriented NW–SE and are relatively short (averaging c. 2 km in length). They record erosion and deposition in subglacial canals (meltwater channels incised down into subglacial substrates and up into the overlying ice; cf. Ng 2000).

Two prominent, northwest to southeast orientated (similar to LLGM ice flow direction, cf. Plouffe et al. 2011) meltwater corridors (spaced c. 10–15 km apart and 45–55 km long) terminate in large bedrock cataracts (with plunge pools at their heads) that were carved in a headward fashion from the Bonaparte valley walls (Burke et al. 2012a) (Figs. 20.1c, 20.3a, 20.4). The bedrock cataracts are up to 6 km long, 1.5 km wide (some post-glacial widening associated with mass wasting has occurred), and 0.3 km deep (Fig. 20.4). The meltwater corridors are up to 55 km long and 2.5 km wide and relatively straight with undulating long profiles that include significant upslope reaches (Fig. 20.3a, c). Downflow (southeast) sections of the corridors are defined by discontinuous (and not always well-defined) troughs irregularly cut (up to 20 m deep) into the underlying substrate (till and/or bedrock). The trough heads are defined by double horseshoe-shaped recessional cataracts (c. 0.5 km wide, >10 m deep) and plunge pools (Fig. 20.3b). The upflow sections of the meltwater corridors are characterized by broad (up to 2.5 km wide) zones of scabbed terrain that include erosional remnants aligned with the corridor axes (Fig. 20.3b). The discontinuous troughs contain eskers (up to 32 km long, 20 m high, and 300 m wide) along most of their length, and the eskers drape gravel sheets and dunes (Burke et al. 2012a, b; Perkins et al. 2016) (Fig. 20.3a, d). Because these meltwater corridors have low sinuosity, undulating long profiles with long upslope segments, and till and bedrock walls and contain eskers, they are interpreted as tunnel channels/valleys that operated as efficient canals (Burke et al. 2012a). The gravel sheets and dunes are consistent with high-magnitude subglacial meltwater flows (Burke et al. 2012a).

The eskers are dominated by single ridges; anabranched reaches are infrequent. Individual esker ridges exhibit round-crested and flat-crested segments (Fig. 20.4a–c) that contain ridge-scale macroforms (composite bedforms) and vertically accreted gravel sheets, respectively (Burke et al. 2012b; Perkins et al. 2016). This sedimentary architecture, the limited presence of flow-parallel faulting, long upslope reaches, and association with a tunnel channel/valley suggest that the eskers were mainly deposited by glacial lake outburst floods (GLOFs) in subglacial ice tunnels or low englacial conduits (Burke et al. 2012b; Perkins et al. 2016). It also suggests that the ice tunnel depositional environment was dynamic (Burke et al. 2012b). Under thinning ice, creep closure rates would have been low, so the ice tunnels evolved through feedbacks between conduit growth via frictional melting and mechanical excavation, and conduit closure due to sediment infilling rather than ice creep. Anabranched reaches formed where the ice tunnel roof collapsed as the ice thinned forming crevasses and

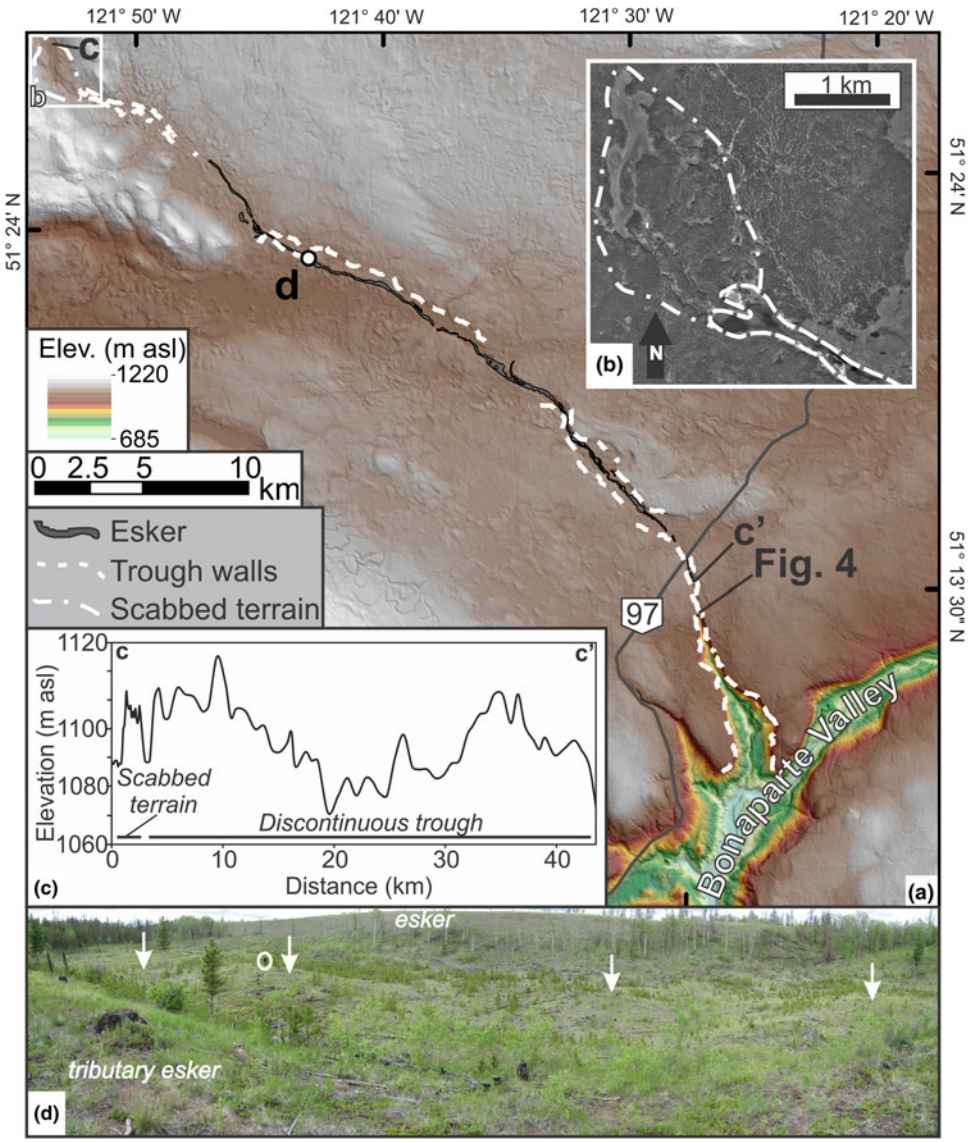

Fig. 20.3 **a** Geomorphology of the Chasm meltwater corridor. *White box* locates scabbed terrain and recessional cataract shown in (**b**). *c*–*c*′ corresponds to upflow and downflow ends of the elevation profile presented in (**c**) masl—m above sea level. **d** View of the corridor fill (eskers and hummocks) at '*d*' in (**a**). The hummocks (*arrowed*) are gravel dunes. Note person (c. 1.8 m tall) for scale (*circled*). After Burke et al. (2012a) with permission from Elsevier

Fig. 20.4 Panoramic photograph looking downflow (south) from the head of the Chasm bedrock cataract (location in Fig. 20.3a). Here, the cataract is c. 500 m wide and 100–200 m deep

meltwater flow followed the path of these structural weaknesses, and/or due to tunnel blockage (Burke et al. 2012a, b). Flat-crested segments (Fig. 20.4c) dominated by vertically accreted gravel sheets record local unroofing of the ice tunnel within thin ice in the final stages of esker formation (Burke et al. 2012b). Finally, the flanks of the eskers collapsed (faulted and slumped) as the ice walls melted away.

It is possible that the bedrock cataracts formed by meltwater flows over multiple glaciations (Plouffe et al. 2011) and acted as low-pressure sinks that focused seasonal subglacial water flow. However, the meltwater corridors most likely formed and filled from canal flow (cf. Ng 2000) during a single GLOF following LLGM because: (1) they are mainly incised into till deposited during the last glacial period (cf. Huntley and Broster 1994, 1997; Lian and Hicock 2000, 2001; Plouffe et al. 2011); (2) they are single-thread systems, consistent with a point water source; (3) their walls are discontinuous, suggesting broad water discharge through the corridors was short lived; (4) they contain extensive corridor-wide gravel sheets and dunes, and eskers composed of ridge-wide macroforms, testament to high-magnitude deposition (Brennand 1994; Burke et al. 2010, 2012b) and, by extension, erosion of the corridor (Burke et al. 2012a); (5) they do not exhibit time-transgressive fans along their length; and (6) the broad corridor fill has not been reworked following deposition nor is it buried by waning stage fines. This is consistent with rapid collapse of the broad flow that deposited the dunes into an esker-forming ice tunnel on the waning stage of the flood (Burke et al. 2012a).

Subglacial hydraulic potential modelling is able to produce a subglacial lake upflow of the corridors, though the parameters required are fairly unrealistic (Burke et al. 2012a). It seems more likely that supraglacial lake drainage through crevasses or moulins produced the landsystems (Burke et al. 2012a). This scenario is consistent with rapid melting associated with a late glacial rapid rise in ELA (Fulton 1991; Clague and James 2002) and observations of supraglacial lake drainage from the Greenland Ice Sheet today (e.g. Bartholomew et al. 2011; Leeson et al. 2014). At the point of water input to the bed, a well-established drainage network was absent and so floodwaters slowly propagated as a broad floodwave (inefficient drainage coinciding with the scabbed topography, Fig. 20.3a, b), which channelized downflow when it encountered a pre-existing (seasonal) ice tunnel (cf. Dow et al. 2015). Focusing of the broad floodwave into the ice tunnel was like 'pulling the plug' on this slowly propagating floodwave, increasing the flow velocity of water, eroding the scabbed terrain, causing headward erosion of the trough-head cataract, and rapidly enlarging a canal in order to efficiently evacuate the GLOF. As flow waned, initial deposition was canal-wide (gravel sheets and dunes) but soon collapsed into esker-forming ice tunnels (cf. Burke et al. 2012a, b), perhaps facilitated by roof collapse and crevassing in thin ice (perhaps <100 m thick).

Shorter (perhaps near-marginal) subglacial meltwater channels and low sinuosity subglacial eskers (<6 km length; mean sinuosity c. 1.1) occur across the southern Fraser Plateau (Fig. 20.5a). However, not all eskers were deposited in subglacial ice tunnels. Differences in geomorphic context, ridge geomorphology, and sedimentary architecture revealed in ground-penetrating radar reflections define two additional esker types (Perkins et al. 2016).

Supraglacial eskers are short (<7 km), dominantly sharp-crested, and continuous and highly sinuous (typically >1.3, occasionally up to 1.9) ridges (Fig. 20.5a, d), indicating deposition in a supraglacial channel (cf. Price 1966 and high sinuosity values for supraglacial streams in Marston (1983)) or high (near ice surface)-englacial conduit (cf. Gulley 2009; Gulley et al. 2009). The dominance of a tabular sedimentary architecture that supports open-channel flow in a braided stream suggests non-GLOF discharges. Extensive post-depositional faulting in flow-parallel and perpendicular directions and ubiquitous slumping of ridge flanks indicates substantial melt-out of underlying ice. The continuity of supraglacial eskers may reflect relatively thin ice and thus a limited height of let-down. They typically occur downflow of ice-marginal channels (Fig. 20.6a) and take paths consistent with topographic and inferred ice slopes. The path of a supraglacial channel or high-englacial conduit with water flow under atmospheric pressure is theoretically controlled by ice surface slope (Shreve 1972), but in reality may be disrupted by crevasses (cf. Hooke 1984; Gulley 2009; Gulley et al. 2009). On the flanks of the Marble Range, where most of the supraglacial eskers are found (Fig. 20.6a), the ice surface likely sloped down towards the southeast, because regional ice-margin retreat was northwestward (Perkins and Brennand 2014). Supraglacial eskers on the southern Fraser Plateau formed in near-marginal channels atop thin ice that discharged water derived from ice-marginal streams and/or supraglacial melt (Perkins et al. 2016).

Ice-walled canyon eskers (e.g. Young lake esker-like ridge, Figs. 20.1b, 20.5a; Perkins et al. 2013) were formed in ice-walled channels or re-entrants where water supply was likely contributed from subglacial, supraglacial, and ice-marginal sources. They are found in deeply incised valleys and are surrounded by enclosed depressions (kettle holes) recording the melting of detached ice blocks (ridge flanks contain significant faulting and slumping). The ridges are relatively short (2–6.5 km long), largely flat-crested, and highly continuous, with low-trunk esker sinuosity (c. 1.1) that mimics that of the enclosing valley. They terminate in flat to low-gradient segments resembling fans or deltas (Perkins et al. 2013). Sedimentary architecture is largely tabular, recording deposition by open-channel meltwater

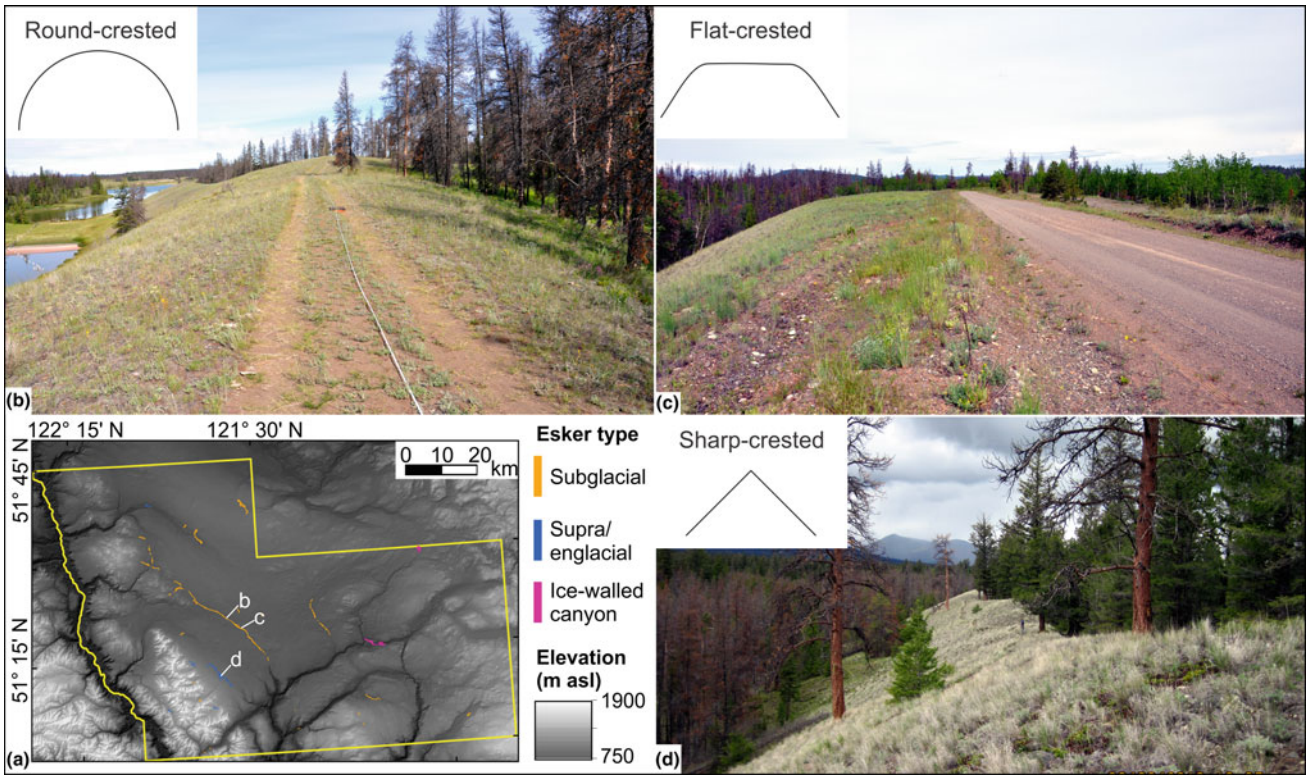

Fig. 20.5 **a** Esker types on the southern Fraser Plateau (after Perkins et al. 2016). masl—m above sea level. **b** Round-crested. **c** flat-crested, and **d** sharp-crested esker morphology. Refer to '*a*' for locations

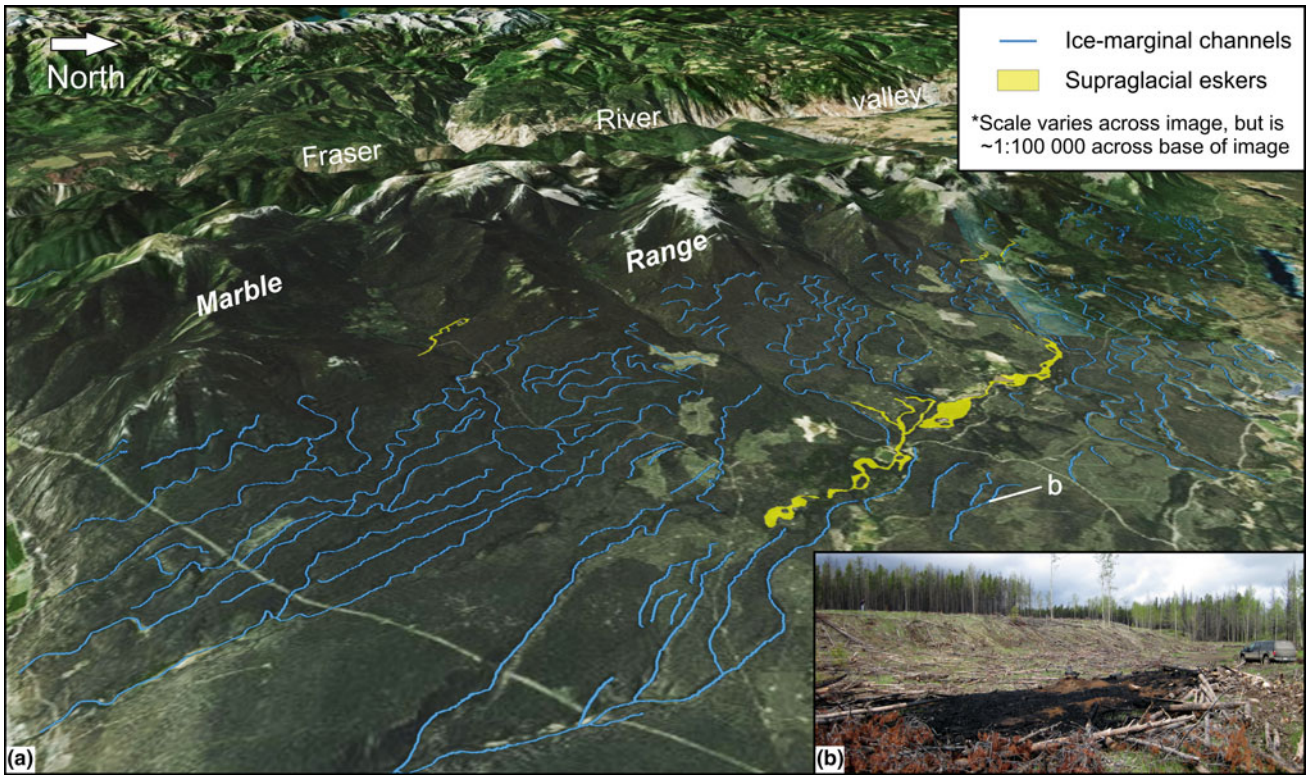

Fig. 20.6 **a** Ice-marginal channels and supraglacial eskers on the flanks of the Marble Range record a thinning and recessing ice sheet. *b* Single-walled ice-marginal channel. Vehicle is 1.8 m high. Refer to '*a*' for location

flows. Ice-walled canyon eskers on the southern Fraser Plateau record localized ice stagnation in topographic basins (Perkins et al. 2013, 2016).

20.5 Proglacial and Ice-Marginal Meltwater Channels

Proglacial meltwater channels are double-walled channels eroded into bedrock or sediment that follow the topographic slope away from an ice margin (cf. Kehew 1982). Ice-marginal meltwater channels are single (Fig. 20.6b) or double-walled channels that typically exhibit paths perpendicular or oblique to topographic slope (Greenwood et al. 2007). They record locations on hillsides where water flow along the topographic gradient was blocked by ice. As such, nested ice-marginal channels record the lateral and vertical evolution in ice surface slope and the position of the ice margin during ice sheet decay (Syverson and Mickelson 2009). On the southern Fraser Plateau, proglacial channels were ubiquitous, typically partially filled with outwash sand and gravel, some supporting present-day streams and others dry. The largest examples are the Fraser, Bonaparte, Rayfield, and Deadman valleys (Fig. 20.1c). Large groups of nested ice-marginal channels occur on the NE slopes of the Marble Range (Fig. 20.6a), the eastern slopes of Mount Big Bar, on the slopes south of Loon Lake, and north of Bonaparte Lake (Fig. 20.1c) (Tipper 1971; Plouffe et al. 2011 and references therein, Margold et al. 2013). They are an average of 1500 m in length and 2–32 m deep and are horizontally spaced 100–300 m apart and vertically separated by $\sim$30 m. The orientation and slope of nested ice-marginal channels indicate that ice was retreating towards the northwest as the ice surface lowered. The highest nested channels began forming when ice was c. 500 m thick on the plateau surface, and the lowest nested channels may still have been forming when the ice was a few 10's of metres thick (based on their elevation above the adjacent plateau). Many ice-marginal channels terminate in deltas or subaqueous fans at the margins of palaeolake basins, suggesting that water in them followed the ice margin until it emptied into an extant ice-dammed lake, which acted as local base level.

20.6 Palaeo Ice-Marginal Lakes and Spillways

Ice-marginal palaeolake systems exist where water is dammed between the ice margin and a topographic barrier (e.g. Carrivick and Tweed 2013). When the ice dam is removed, the palaeolake drains, leaving a record of its existence in remnant lake deposits (e.g. lake-bottom sediments) and landforms including deltas, subaqueous fans, shorelines, and spillways.

The presence of palaeoice-marginal lakes on the southern Fraser Plateau is known from the patchy presence of mapped lake-bottom sediments (cross-laminated sand and horizontally laminated sand, silt, and clay; Perkins and Brennand 2014) within broad basins (Tipper 1971; Bednarski 2009; Huscroft 2009). Modern drainage in each of these basins is to the west or northwest, and thus, an ice margin is required in the northwest sector of each basin in order for palaeolakes to have formed (earthen dams are rare in these positions, and those that are present are grounding-line moraines formed near the ice margin, Perkins and Brennand 2014). Lake stage extent has been modelled using a DTM (Geobase®) and primary (at water level) and secondary (constraining) palaeo water-plane indicators: deltas, spillways, ice-marginal channels, subaqueous fans, and lake-bottom sediments identified from aerial photographs and DTMs combined with field observations of geomorphology and sedimentology, and ground-penetrating radar (GPR) surveys to confirm landform classification (Perkins and Brennand 2014). Lake extents are constrained by the elevation of water plane indicators, the position at which the reconstructed water plane intersects topography and the position of palaeodams (ice or sediment dams). Ice-contact indicators, such as ice-marginal channels, grounding-line moraines, and hummocky terrain, further constrain ice-margin positions.

Palaeo ice-marginal lake systems developed largely in the western sector of the southern Fraser Plateau where adverse topography likely encouraged lake formation against the retreating ice margin (e.g. glacial Lake Meadow, glacial Lake Dog; Perkins and Brennand 2014) (Figs. 20.1c, 20.7a); smaller, valley-bottom lakes developed in the eastern sector (e.g. glacial Lake Young, glacial Lake Brigade, Fig. 20.1c; Perkins et al. 2013; Perkins and Brennand 2014). All lake systems developed a pattern of higher elevation stillstands in the east evolving to lower elevation stillstands in the west (Perkins and Brennand 2014). Classic, gilbert-style deltas occur in the largest palaeolake system, glacial Lake Dog, and only on the north-east side of the basin, underscoring the northern source of meltwater and sediment supply (Fig. 20.7a). Subaqueous fans occur in most of the lake basins and again typically on their north side (Fig. 20.7a). Spillways mainly drained lakes to the south and west (Fig. 20.7a).

Because topography is subdued, palaeoice-marginal lakes were relatively shallow (average 18 m) and expansive (average 27 km^2; max. 116 km^2) (Perkins and Brennand 2014). Broad spatial exposure to potential spillways resulted in numerous lakes and lake stages, helpful in reconstructing the relative position of the ice margin over time (Fig. 20.7a). Within basins, successive lake stages evolved by expansion,

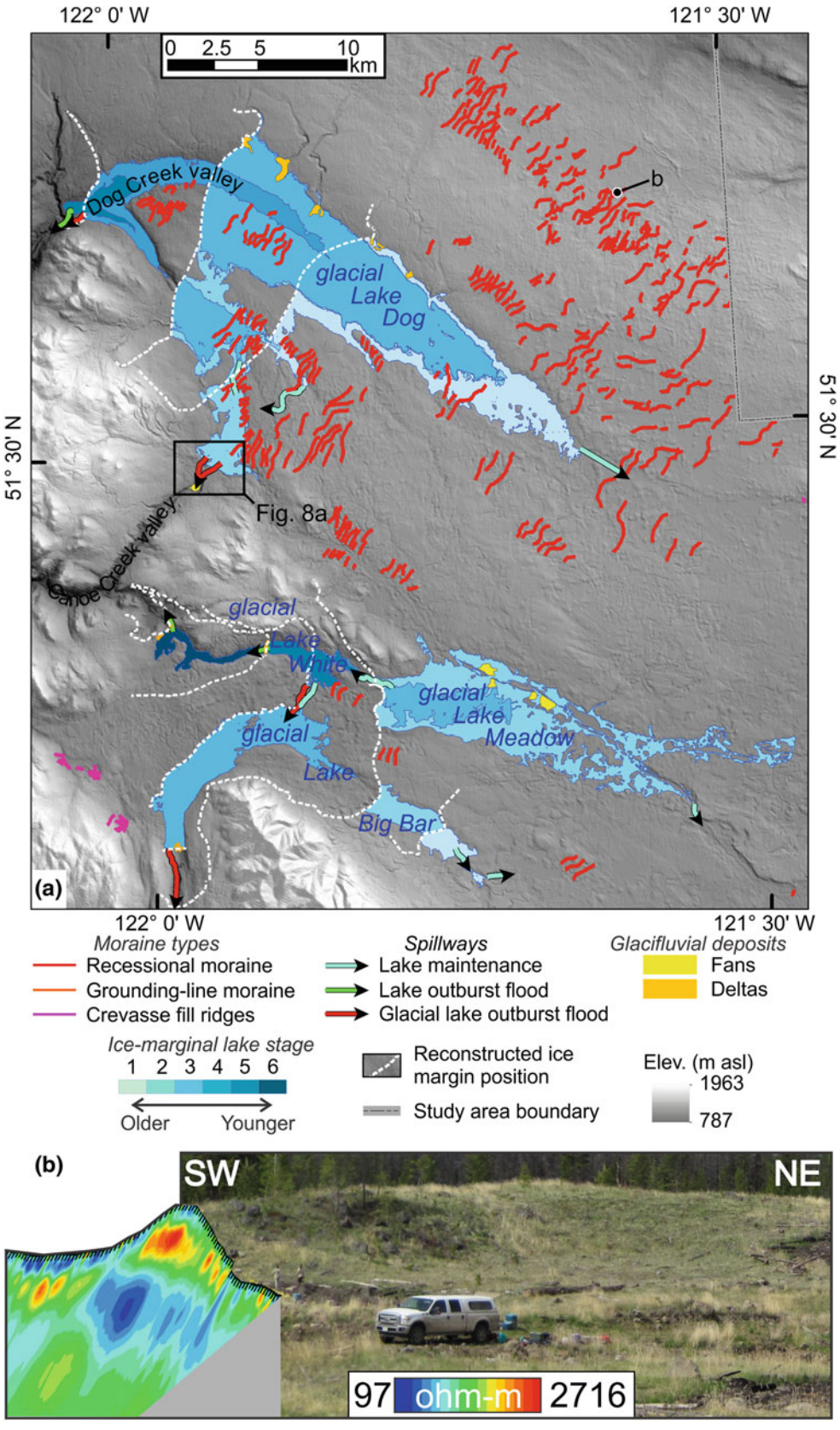

Fig. 20.7 **a** Late glacial lakes, recessional and grounding-line moraines, crevasse-fill ridges, and subaqueous fans and deltas on the southern Fraser Plateau (Perkins 2015). Ice-margin positions associated with palaeolakes are shown (after Perkins and Brennand 2014). **b** Perspective view of recessional moraine (located in '*a*') and processed Electrical Resistivity Tomography (ERT) profile showing internal composition and architecture. The moraine is approximately 14 m high. Diamicton (low resistivity, *blue*) drapes gravel (high resistivity, *red*) on the moraine's proximal (NW) slope. The gravel was pushed into a ridge prior to the deposition of subglacial till (Perkins 2015)

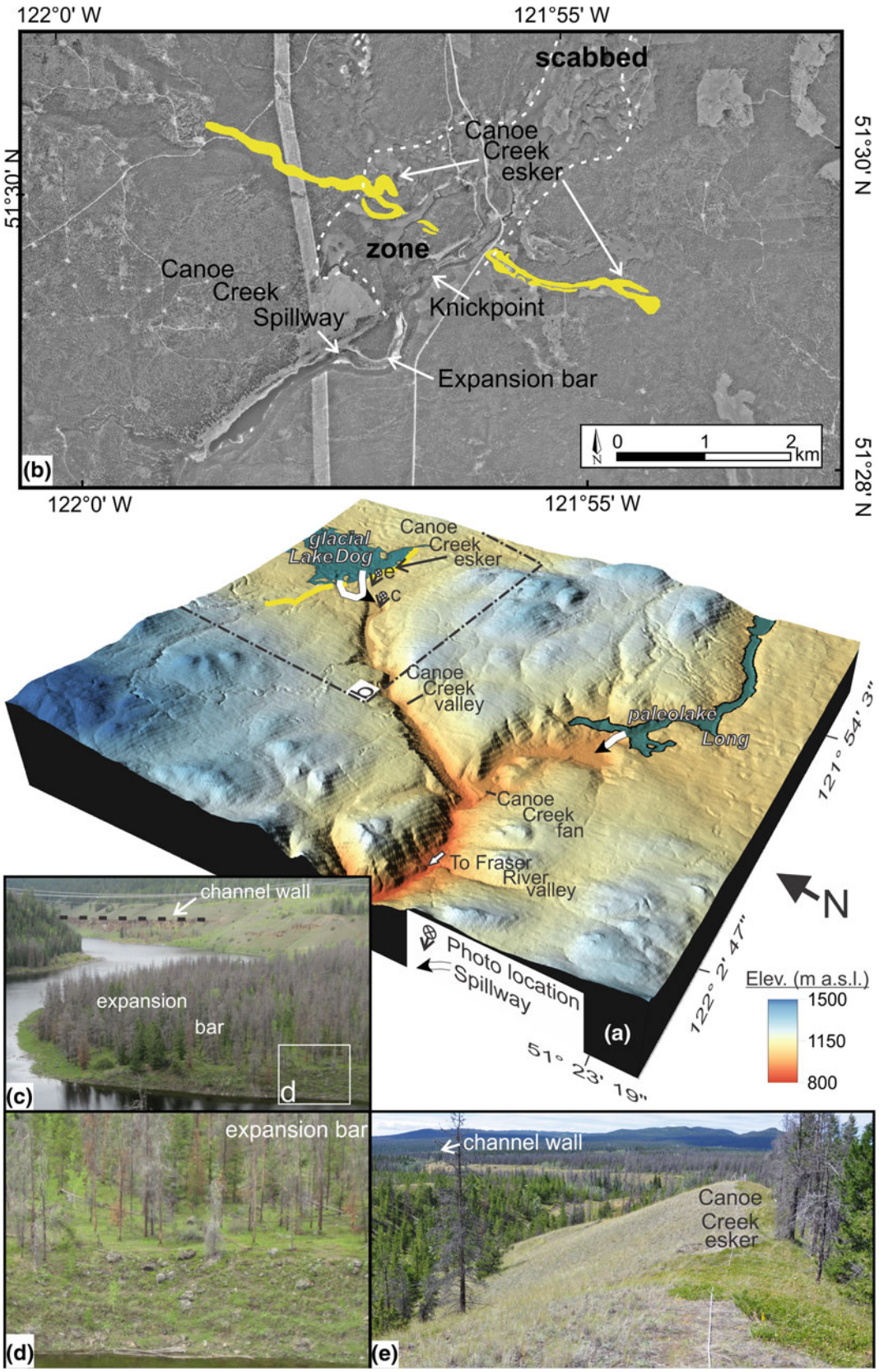

Fig. 20.8 **a** Canoe Creek spillway is characterized by a straight, 8.5 km long, 250–600 m wide, recessional cataract (knickpoint) averaging c. 60 m deep at its head. The near-vertical walls of the cataract are composed of columnar basalt (below *black dashed line*) (Campbell and Tipper 1971) overlain by till (**c**). A wide, flat-bottomed, and scabbed system of braided channels occurs upflow (north) from the cataract (**b**). These channels are largely incised into glacilacustrine silts from glacial Lake Dog (Fig. 20.7a) but also cut through the Canoe Creek esker (**b**, **e**). The trees in the foreground are c. 1.2 m high. Immediately downflow (south) of the knickpoint is a boulder bar (**c**, **d**) comparable to the expansion bars commonly associated with outburst floods (cf. Maizels 1997)

decanting or drainage from southeast to northwest, implicating a northwestward backwasting, and/or retreating ice margin (Perkins and Brennand 2014). Some lakes maintained stable lake levels (stillstands) for some time, their heights maintained by spillways cut in bedrock or bouldery till and the low slopes of the plateau surface (Perkins and Brennand 2014). Others drained catastrophically when their earthen or ice dams were breached forming spectacular GLOF spillways, such as that at Canoe Creek (Figs. 20.7a, 20.8). GLOF spillways contain coarse gravel deposits (Carling 2013) and landforms associated with outburst flood discharges, including scabbed topography (Kehew 1982), expansion bars (Maizels 1997), and deeply incised canyons (Lamb and Fonstad 2010) (Fig. 20.8). Consequently, reconstructed lake systems were dynamic and transitory and probably had significant effects on the dynamics of ice-margin retreat (cf. Carrivick and Tweed 2013).

A glaci-isostatic tilt could not be defined from primary water-plane indicators on the southern Fraser Plateau (Perkins and Brennand 2014). A zero tilt was also inferred on glacial lake water planes in the nearby Fraser River valley (Huntley and Broster 1994). Thin ice and zero tilt on glacial lake water planes on the southern Fraser Plateau may suggest that glaci-isostatic rebound was locally complete prior to lake development, confirming that rebound must have occurred rapidly as suggested for most of southern British Columbia (cf. Clague and James 2002). Should zero tilt be real, and not an artefact of the limited spatial (and temporal) resolution of the data, the fact that glacial lakes in the Thompson and Nicola valleys (Fig. 20.1b) to the south record significant rebound (Fulton and Walcott 1975; Johnsen and Brennand 2004) suggests that the timing of those lakes was just early enough to be affected by glaci-isostatic rebound. Sufficient time must have elapsed between the formation of these southern valley lakes and the development of the plateau lake systems for the majority of glaci-isostatic rebound on the southern Fraser Plateau to be complete. That is, the glacial lakes on the southern Fraser Plateau were younger than the glacial lakes in the Thompson and Nicola basins. This reasoning reinforces the interpretation of regional northwestward ice retreat across the Nicola and Thompson basins and the southern Fraser Plateau, rather than regional downwasting into valleys (cf. Fulton 1967, 1991).

20.7 Moraines and Crevasse-Fill Ridges

Large linear moraine systems are rare on the southern Fraser Plateau (Tipper 1971; Plouffe et al. 2011). Their absence has been attributed to regional stagnation and downwasting of the MIS 2 CIS (e.g. Fulton 1967, 1991; Ryder et al. 1991; Clague and James 2002; Plouffe et al. 2011). However, the availability of DTMs, large-scale stereo-photograph pairs, and high-resolution orthophotographs has facilitated the identification of numerous smaller moraine ridges on the southern Fraser Plateau (Bednarski 2009; Huscroft 2009; Plouffe 2009a, b; Brennand et al. 2014; Perkins 2015). Based on their composition, sedimentary architecture, geomorphology, geomorphic context, and orientation, they have been classified as glacitectonic (push) moraines, grounding-line moraines, and crevasse-fill ridges and relatively dated (by association to ice-marginal lakes and inferred ice flow directions, cf. Plouffe et al. 2011) to MIS 2 ice advance or retreat (Perkins 2015).

Recessional glacitectonic (push) moraines on the southern Fraser Plateau are round-crested (Fig. 20.7b), relatively narrow (80–250 m wide compared to 400–1100 m wide for overridden, ice advance moraines; Perkins 2015), arcuate to sinuous ridges oriented SW-NE (Fig. 20.7a), and perpendicular to subglacial and proglacial meltwater channels and eskers (Fig. 20.5a). They are typically 6–18 m high and 0.5–4 km long, occurring as a field of >300 ridges on the interfluves and slope flanks around Dog Creek basin and singularly elsewhere across the southern Fraser Plateau (Fig. 20.7a). They contain sheared and stacked diamicton, gravel, silt, and/or sand units (Fig. 20.7b) characteristic of glacitectonic push (Bennett 2001) at an active ice margin. Episodic (perhaps annual, cf. Krüger 1995) readvances of the ice margin formed the recessional moraine field against the adverse topography surrounding the Dog Creek basin (Perkins 2015).

Grounding-line moraines are relatively sharp, narrow-crested, and single linear ridges with gentle ice-proximal (up to 15°) and steep ice-distal (up to 20°) slopes. They average c. 280 m in length (max. 630 m long) and are up to 15 m high and 90 m wide. They are restricted to valley bottoms associated with palaeolake basins (Fig. 20.7a) and contain closed circular depressions, indicating post-depositional melt-out of buried ice blocks. Ridges are composed of a range of materials including moderately sorted, subrounded pebble to cobble gravel, laminated silt and fine sand, and diamicton containing angular clasts exhibiting minor glacigenic wear features such as bullet noses and plucked ends (cf. Krüger 1984). They are interpreted as grounding-line moraines because of their cross-valley orientation, asymmetric topographic profiles, kettled surface, and composition (Sharpe and Cowan 1990; Benn 1996). They were deposited mainly from meltwater flows as an apron beyond the grounded ice-margin peripheral to a lake and consequently record an ice-margin position before ice-contact glacial lake drainage.

Crevasse-fill ridges are low-relief (1–2 m), reticulate ridges containing moderately sorted, subrounded pebble to cobble gravel interbedded with lenses of well sorted, silty fine sand (Perkins 2015). They average 390 m long (but may be up to 1500 m) and 2–3 m wide and are located on the

flanks of Mount Big Bar (Fig. 20.7a). Some overlie a glacitectonic moraine ridge formed during glacier advance (Perkins 2015), and others are separated by enclosed, lake-filled depressions interpreted as kettle holes (Huntley 1996). These ridges are interpreted as crevasse-controlled eskers because they are composed of waterlain stratified sediment, and their distribution in a rectilinear pattern suggests channelized meltwater flow within crevasses near the ice margin. The relative continuity of the ridges supports formation in subglacial rather than supraglacial crevasse systems. Longitudinal and transverse crevassing is attributed to ice-margin oscillation and flexure in a large proglacial ice-dammed lake directly east of the ridges (glacial Lake Big Bar, Perkins and Brennand 2014) (Fig. 20.7a).

Pitted (hummocky) terrain is characterized by a low-relief landscape of plains (or mounds) and depressions (kettle holes). Tipper (1971) reported three fields of pitted terrain between Green Lake and the Marble Range (Fig. 20.1c) within the study area and interpreted them as evidence of regional ice stagnation (passive downwasting). However, this interpretation is at odds with the presence of recessional glacitectonic (push) moraine (two of Tipper's pitted terrain fields are reinterpreted thus) and successive grounding-line moraine in the area, both recording active ice retreat. Rather, the kettle holes that occur in association with recessional moraines may be attributed to downwasting following advance on a seasonal or episodic cycle (Krüger 1995; Bennett 2001). Smaller patches (0.5–5 km^2) of hummocky terrain are found in association with crevasse-fill ridges and ice-walled canyon eskers (Perkins 2015). Limited exposures indicate an internal composition of heterogeneous diamicton, likely till, or stratified sand and gravel. These localized patches of hummocky terrain record the decay of dirty or buried stagnant ice (Benn 1992; Huntley 1996).

20.8 Conclusion: A New Model of Late Glacial CIS Decay on the Southern Fraser Plateau

Until recently, the prevailing view of late glacial CIS decay over the interior plateaus was one of regional stagnation (a passive top-down decay causing ice to recede from the Coast Mountains) because of a rapid rise in ELA (Fulton 1991) (Fig. 20.2a), with minor (complex) frontal backwasting across the interior plateaus (Fulton 1967; Clague and James 2002). A new model of late glacial CIS decay has emerged from recent landform mapping and classification for the southern Fraser Plateau, facilitated by the availability of higher resolution terrain data. Patterns of palaeoglacial lake evolution and push moraines suggest an active ice margin systematically retreated northwestward back towards the Coast Mountains (Fig. 20.2b), consistent with the pattern of eskers (Plouffe et al. 2011) and ice-marginal channels (Margold et al. 2013), and numerical and thermo-mechanical modelling (Roberts 1991, Tarasov and Peltier 2006; Seguinot et al. 2016). The presence of an active ice margin during retreat implies that the ice surface sloped down towards the southeast as deglaciation progressed. Based on retreat direction, this places the maximum ice thickness to the northwest, affirming previous inferences of an ice divide near the southern Fraser Plateau based on landform interpretations (Wilson et al. 1958; Tipper 1971) and reconstructions of glaci-isostatic tilt from palaeolake shorelines (Fulton and Walcott 1975; Johnsen and Brennand 2004). Transient ice-marginal lakes within depressions on the plateau encouraged the formation of grounding-line moraines in topographic lows during ice retreat and may have facilitated the formation of recessional glacitectonic moraines on the surrounding topographic highs due to the transference of basal pressure to these grounded areas. Furthermore, the lower albedo and low thermal conductivity of proglacial lakes (in contrast to bare sediment or ice) would have moderated local air temperatures and contributed to enhanced thermo-mechanical melting of the in-contact ice margin (e.g. through notching just below water level, Carrivick and Tweed 2013), increasing melt rates for lake-terminating ice on the southern Fraser Plateau and accounting for the complex and transitory evolution of the lake systems. The implication of these effects was to enhance glacier retreat, at least partially decoupling it from broader climate patterns (cf. Carrivick and Tweed 2013; Margold et al. 2014).

Ice thinning was contemporaneous with ice-margin retreat. This thinning is recorded by the presence of nested ice-marginal channels and supraglacial eskers. A rapidly rising late glacial ELA (Fulton 1991; Clague and James 2002) and lake effects (op. cit.) enhanced melt rates and allowed supraglacial lakes to form on the ice surface. Drainage of these lakes through crevasses or moulins formed the subglacial meltwater corridors and GLOF eskers. Pockets of localized stagnation, supported by the presence of hummocky terrain, crevasse-fill ridges, and ice-walled canyon eskers, likely existed during regional retreat across the southern Fraser Plateau. This interpretation of the decay of the last CIS is similar in style and pattern to that proposed for the last Fennoscandian Ice Sheet (Boulton et al. 2001) and is reminiscent of the decay of the Greenland Ice Sheet today (e.g. Chu 2014; Enderlin et al. 2014).

Acknowledgements Research was funded by National Science and Engineering Research Council (NSERC) of Canada Discovery (194107) and Research Tools and Instruments grants to Brennand, and by a Geological Society of America Graduate Student Research Award to Perkins.

References

Andrews GDM, Plouffe A, Ferbey T, Russell JK, Brown SR, Anderson RG (2011) Bedrock elevation and the thickness of Neogene and Quaternary cover across the Interior Plateaus, Intermontane Belt, British Columbia: analysis of water-well drill records and implications for exploration potential. Can J Earth Sci 48:973–986

Bartholomew I, Nienow P, Sole A, Mair D, Cowton T, Palmer S, Wadham J (2011) Supraglacial forcing of subglacial drainage in the ablation zone of the Greenland Ice Sheet. Geophys Res Lett. doi:10.1029/2011GL047063

Bednarski JM (2009) Surficial geology, Bridge Lake, British Columbia, scale 1:50 000. Geol Surv Can Open File 5839

Benn DI (1992) The genesis and significance of 'hummocky moraine': evidence from the Isle of Skye, Scotland. Quat Sci Rev 11:781–799

Benn DI (1996) Subglacial and subaqueous processes near a glacier grounding line: sedimentological evidence from a former ice-dammed lake, Achnasheen, Scotland. Boreas 25:23–36

Bennett MR (2001) The morphology, structural evolution and significance of push moraines. Earth-Sci Rev 53:197–236

Blais-Stevens A, Clague JJ, Mathewes RW, Hebda RJ, Bornhold BD (2003) Record of the late Pleistocene outburst floods preserved in Saanich Inlet sediments, Vancouver Island, Canada. Quat Sci Rev 22:2327–2334

Boulton GS, Dongelmans P, Punkari M, Broadgate M (2001) Palaeoglaciology of an ice sheet through a glacial cycle: the European ice sheet through the Weichselian. Quat Sci Rev 20:591–625

Brennand TA (1994) Macroforms, large bedforms and rhythmic sedimentary sequences in subglacial eskers, south-central Ontario: implications for esker genesis and meltwater regime. Sediment Geol 91:9–55

Brennand TA, Shaw J (1994) Tunnel channels and associated landforms, south-central Ontario: their implications for ice-sheet hydrology. Can J Earth Sci 31:505–522

Brennand TA, Lian OB, Perkins AJ (2014) The life and times of the Cordilleran Ice Sheet around the southern Fraser Plateau, British Columbia. In: Dashtgard S, Ward B (eds) Trials and tribulations of life on an active subduction zone: field trips in and around Vancouver, Canada. Geol Soc Am Field Guide, New York, pp 101–124. doi:10.1130/2014.0038(06

Burke MJ, Woodward J, Russell AJ, Fleisher PJ, Bailey PK (2010) The sedimentary architecture of outburst flood eskers: a comparison of ground-penetrating radar data from Bering Glacier, Alaska and Skeiðarárjökull, Iceland. Geol Soc Am Bull 122:1637–1645

Burke MJ, Brennand TA, Perkins AJ (2012a) Evolution of the subglacial hydrologic system beneath the rapidly decaying Cordilleran Ice Sheet caused by ice-dammed lake drainage: implications for meltwater-induced ice acceleration. Quat Sci Rev 50:125–140

Burke MJ, Brennand TA, Perkins AJ (2012b) Transient subglacial hydrology of a thin ice sheet: insights from the Chasm esker, British Columbia, Canada. Quat Sci Rev 58:30–55

Campbell RB, Tipper HW (1971) Geology of Bonaparte Lake map area, British Columbia. Geol Surv Can Memoir 363

Carling PA (2013) Freshwater megaflood sedimentation: What can we learn about generic processes? Earth-Sci Rev 125:87–113

Carrivick JL, Tweed FS (2013) Proglacial lakes: character, behaviour and geological importance. Quat Sci Rev 78:34–52

Chu VW (2014) Greenland ice sheet hydrology: a review. Prog Phys Geogr. doi:10.1177/0309133313507075

Clague JJ, James TS (2002) History and isostatic effects of the last ice sheet in southern British Columbia. Quat Sci Rev 21:71–87

Dow CF, Kulessa B, Rutt IC, Tsai VC, Pimentel S, Doyle SH, van As D, Lindbäck K, Pettersson R, Jones GA, Hubbard A (2015) Modeling of subglacial hydrological development following rapid supraglacial lake drainage. J Geophys Res Earth. doi:10.1002/2014JF003333

Enderlin EM, Howat IM, Jeung S, Noh M-J, van Angelen JH, van den Broeke MR (2014) An improved mass budget for the Greenland Ice Sheet. Geophys Res Lett. doi:10.1002/2013GL059010

Eyles N, Clague JJ (1991) Glaciolacustrine sedimentation during advance and retreat of the Cordilleran Ice Sheet in central British Columbia. Géogr Phys Quat 45:137–331

Fulton RJ (1967) Deglaciation studies in Kamloops region an area of moderate relief, British Columbia. Geol Surv Can Bulletin 154

Fulton RJ (1969) Glacial lake history, southern Interior Plateau, British Columbia. Geol Surv Can Paper 69–37

Fulton RJ (1991) A conceptual model for growth and decay of the Cordilleran Ice Sheet. Géogr Phys Quat 45(3):281–286

Fulton RJ, Walcott RI (1975) Lithospheric flexure as shown by deformation of glacial lake shorelines in southern British Columbia. Geol Soc Am Mem 142:163–173

Fulton RJ, Smith GW (1978) Late Pleistocene stratigraphy of south-central British Columbia. Can J Earth Sci 15:971–980

Greenwood SL, Clark CD, Hughes ALC (2007) Formalising an inversion methodology for reconstructing ice-sheet retreat patterns from meltwater channels: application to the British Ice Sheet. J Quat Sci 22:637–645

Gulley JD (2009) Structural control of englacial conduits in the temperate Matanuska Glacier, Alaska, USA. J Glaciol 55:681–690

Gulley JD, Benn DI, Screaton E, Martin J (2009) Mechanisms of englacial conduit formation and their implications for subglacial recharge. Quat Sci Rev 28:1984–1999

Holland S (1976) Landforms of British Columbia—a physiographic outline. In: B.C. Department of Mines and Petroleum Resources, Bulletin No. 48

Hooke RL (1984) On the role of mechanical energy in maintaining subglacial water conduits at atmospheric pressure. J Glaciol 30:180–187

Huntley DH (1996) The late Wisconsinan glaciation of east-central Taseko Lakes, British Columbia. Unpublished doctoral thesis, University of New Brunswick

Huntley DH, Broster BE (1993) Polyphase glacigenic deformation of advance glaciofluvial sediments, near Big Creek, British Columbia. Géogr Phys Quat 47:211–219

Huntley DH, Broster BE (1994) Glacial Lake Camelsfoot: a Late Wisconsinan advance stage proglacial lake in the Fraser River Valley, Gang Ranch area, British Columbia. Can J Earth Sci 31:798–807

Huntley DH, Broster BE (1997) The Late Wisconsinan deglacial history of the east-central Taseko Lakes area, British Columbia. Can J Earth Sci 34:1510–1520

Huscroft CA (2009) Surficial geology, Criss Creek, British Columbia, scale 1:50 000. Geol Surv Can Open File 5932.

Johnsen TF, Brennand TA (2004) Late glacial lakes in the Thompson basin, British Columbia: paleogeography and evolution. Can J Earth Sci 41:1367–1383

Kehew AE (1982) Catastrophic flood hypothesis for the origin of the Souris spillway, Saskatchewan and North Dakota. Geol Soc Am Bull 93:1051–1058

Kleman J, Jansson K, de Angelis H, Stroeven AP, Hättestrand C, Alm G, Glasser N (2010) North American ice sheet build up during the last glacial cycle, 115-21 kyr. Quat Sci Rev 29:2036–2051

Krüger J (1984) Clasts with stoss-lee form in lodgement tills: a discussion. J Glaciol 30:241–243

Krüger J (1995) Origin, chronology and climatological significance of annual-moraine ridges at Myrdalsjökull, Iceland. Holocene 5:420–427

Lamb MP, Fonstad MA (2010) Rapid formation of a modern bedrock canyon by a single flood event. Nat Geosci 3:477–481

Leeson AA, Shepherd A, Briggs K, Howat I, Fettweis X, Morlighem M, Rignot E (2014) Supraglacial lakes on the Greenland Ice Sheet advance inland under warming climate. Nat Clim Change. doi:10.1038/NCLIMATE2463

Lian OB (1997) Quaternary geology of the Fraser Valley area, Big Bar Creek to Pavillion, southcentral British Columbia. Unpublished doctoral thesis, University of Western Ontario

Lian OB, Barendret RW, Enkin RJ (1999) Lithostratigraphy and paleomagnetism of pre-Fraser glacial deposits in south-central British Columbia. Can J Earth Sci 36:357–1370

Lian OB, Hicock SR (2000) Thermal conditions beneath parts of the last Cordilleran Ice Sheet near its centre as inferred from subglacial till, associated sediments, and bedrock. Quat Int 68–71:147–162

Lian OB, Hicock SR (2001) Lithostratigraphy and limiting optical ages of the Pleistocene fill, Fraser valley, near Clinton, south-central British Columbia. Can J Earth Sci 38:839–850

Lian OB, Huntley DJ (1999) Optical dating of post-glacial aeolian deposits from the south-central Interior of British Columbia, Canada. Quat Sci Rev 18:1453–1466

Maizels J (1997) Jökulhlaup deposits in proglacial areas. Quat Sci Rev 16:793–819

Margold M, Jansson KN, Kleman J, Stroeven AP, Clague JJ (2013) Retreat pattern of the Cordilleran Ice Sheet in central British Columbia at the end of the last glaciation reconstructed from glacial meltwater landforms. Boreas 42:830–847

Margold M, Stroeven AP, Clague JJ, Heyman J (2014) Timing of terminal Pleistocene deglaciation at high elevations in southern and central British Columbia constrained by ^{10}Be exposure dating. Quat Sci Rev 99:193–202

Marston RA (1983) Supraglacial stream dynamics on the Juneau Icefield. Ann Assoc Am Geogr 73:597–608

Mathews WH (1989) Neogene Chilcotin basalts in south-central British Columbia: geology, ages, and geomorphic history. Can J Earth Sci 26:969–982

Ng FSL (2000) Canals under sediment-based ice sheets. Ann Glaciol 30:146–152

Perkins AJ (2015) Pattern and style of deglaciation on the southern Fraser Plateau, British Columbia. Unpublished doctoral thesis, Simon Fraser University

Perkins AJ, Brennand TA, Burke MJ (2013) Genesis of an esker-like ridge over the southern Fraser plateau, British Columbia: implications for paleo-ice sheet reconstruction based on geomorphic inversion. Geomorphology 190:27–39

Perkins AJ, Brennand TA (2014) Refining the pattern and relative timing of Cordilleran Ice Sheet retreat: paleogeography, evolution and implications of lateglacial ice-marginal lake systems on the southern Fraser Plateau, British Columbia. Boreas 44:319–342

Perkins AJ, Brennand TA, Burke MJ (2016) Towards a morphogenetic classification of eskers: implications for modelling ice sheet hydrology. Quat Sci Rev 134:19–38

Plouffe A (2009a) Surficial geology, Loon Lake, British Columbia, scale 1:50 000, vol 5933. Geol Surv Can Open File

Plouffe A (2009b) Surficial geology, Green Lake, British Columbia, scale 1:50 000, vol 5939. Geol Surv Can Open File

Plouffe A, Bednarski JM, Huscroft CA, Anderson RG, McCuaig SJ (2011) Late Wisconsinan glacial history in the Bonaparte Lake map area, south-central British Columbia: implications for glacial transport and mineral exploration. Can J Earth Sci 48(6):1091–1111

Price RJ (1966) Eskers near the Casement glacier, Alaska. Geogr Ann 48:111–125

Roberts BL (1991) Modeling the Cordilleran Ice Sheet. Géog Phys Quat 45:287–299

Ryder JM (1971) The stratigraphy and morphology of para-glacial alluvial fans in south-central British Columbia. Can J Earth Sci 8:279–298

Ryder JM, Fulton RJ, Clague JJ (1991) The Cordilleran Ice Sheet and the glacial geomorphology of southern and central British Columbia. Géogr Phys Quat 45:365–377

Seguinot J, Rogozhina I, Stroeven AP, Margold M, Kleman J (2016) Numerical simulations of the Cordilleran Ice Sheet through the last glacial cycle. The Cryosphere 10:639–664

Sharpe DR, Cowan WR (1990) Moraine formation in northwestern Ontario: product of subglacial fluvial and glaciolacustrine sedimentation. Can J Earth Sci 27:1478–1486

Shreve RL (1972) Movement of water in glaciers. J Glaciol 11: 205–214

Syverson KM, Mickelson DM (2009) Origin and significance of lateral meltwater channels formed along a temperate glacier margin, Glacier Bay, Alaska. Boreas 38:132–145

Tarasov L, Peltier WR (2006) A calibrated deglacial drainage chronology for the North American continent: evidence of an Arctic trigger for the Younger Dryas. Quat Sci Rev 25:659–688

Tipper HW (1971) Glacial geomorphology and Pleistocene history of central British Columbia, Geol Surv Can Bulletin 196

Wilson JT, Falconer G, Mathews WH, Prest VK (1958) Glacial map of Canada, scale 1:3 801. Geological Association of Canada, Map 1253A 600

The Diverse Landscapes of Haida Gwaii

21

Alexandre Bevington, John J. Clague, Thomas Millard, Ian J. Walker, and Marten Geertsema

Abstract

The archipelago of Haida Gwaii, formerly known as the Queen Charlotte Islands, is one of the most dynamic geomorphic environments in Canada. Climatic and geophysical forces have combined to shape the unique landscape of the archipelago. Strong cyclonic storms from the Pacific Ocean are frequent and are accompanied by heavy rainfall. The two strongest earthquakes in Canadian history happened on the Queen Charlotte Fault just west of the archipelago in the Pacific Ocean. Coastal landscapes on the west coast are rugged and rocky, whereas the north and east coasts are formed in thick glacial sediments that are being rapidly eroded by waves. The mountainous spine that runs the length of Haida Gwaii is susceptible to landslides and other mass wasting processes. Slope failures are the primary agent of natural disturbance in these mountains and occur at rates that are among the highest in Canada. They are triggered by heavy rainfall, forestry activities, and earthquakes.

Keywords

Haida Gwaii • Gwaii Haanas • Queen Charlotte fault • Earthquake • Climate • Glaciation • Refugia • Crustal forebulge

21.1 Setting

21.1.1 Physiography

Haida Gwaii is an archipelago of more than 200 islands with a total land area of nearly 10,000 km^2, lying off the coast of the British Columbia mainland (Fig. 21.1). The two largest islands, Graham Island on the north (6400 km^2) and Moresby Island on the south (2600 km^2), account for ninety percent of the surface area of the archipelago. There is an instructive contrast between coastal landscapes on the west coast that are rugged and rocky, and those on the north and east coasts that are formed in rapidly eroding glacigenic sediments (Fig. 21.2). The three main physiographic regions are the Queen Charlotte Ranges, the Queen Charlotte Lowlands, and Skidegate Plateau (Fig. 21.3; Sutherland Brown 1968).

The Queen Charlotte Ranges supported ice caps and valley and cirque glaciers during the last Pleistocene glaciation. The mountains are a complex assemblage of sedimentary, volcanic, and intrusive igneous rocks that support shallow soils. The Queen Charlotte Lowland of northeastern Graham Island is mostly below 100 masl and is developed on middle to late Tertiary sedimentary rocks and overlying glacial sediments, including till, outwash, and glacimarine sediments. Parts of

A. Bevington (✉) · M. Geertsema
BC Ministry of Forests, Lands and Natural Resource Operations, Prince George, BC V2N 4W5, Canada
e-mail: Alexandre.Bevington@gov.bc.ca

J.J. Clague
Department of Earth Sciences, Simon Fraser University, 8888 University Drive, Burnaby, BC V5A 1S6, Canada

T. Millard
BC Ministry of Forests, Lands and Natural Resource Operations, Nanaimo, BC V9T 6E9, Canada

I.J. Walker
School of Geographical Sciences & Urban Planning, and School of Earth & Space Exploration, Arizona State University, PO Box 875302, Tempe, AZ 85287-5302, United States

© Springer International Publishing Switzerland 2017
O. Slaymaker (ed.), *Landscapes and Landforms of Western Canada*, World Geomorphological Landscapes, DOI: 10.1007/978-3-319-44595-3_21

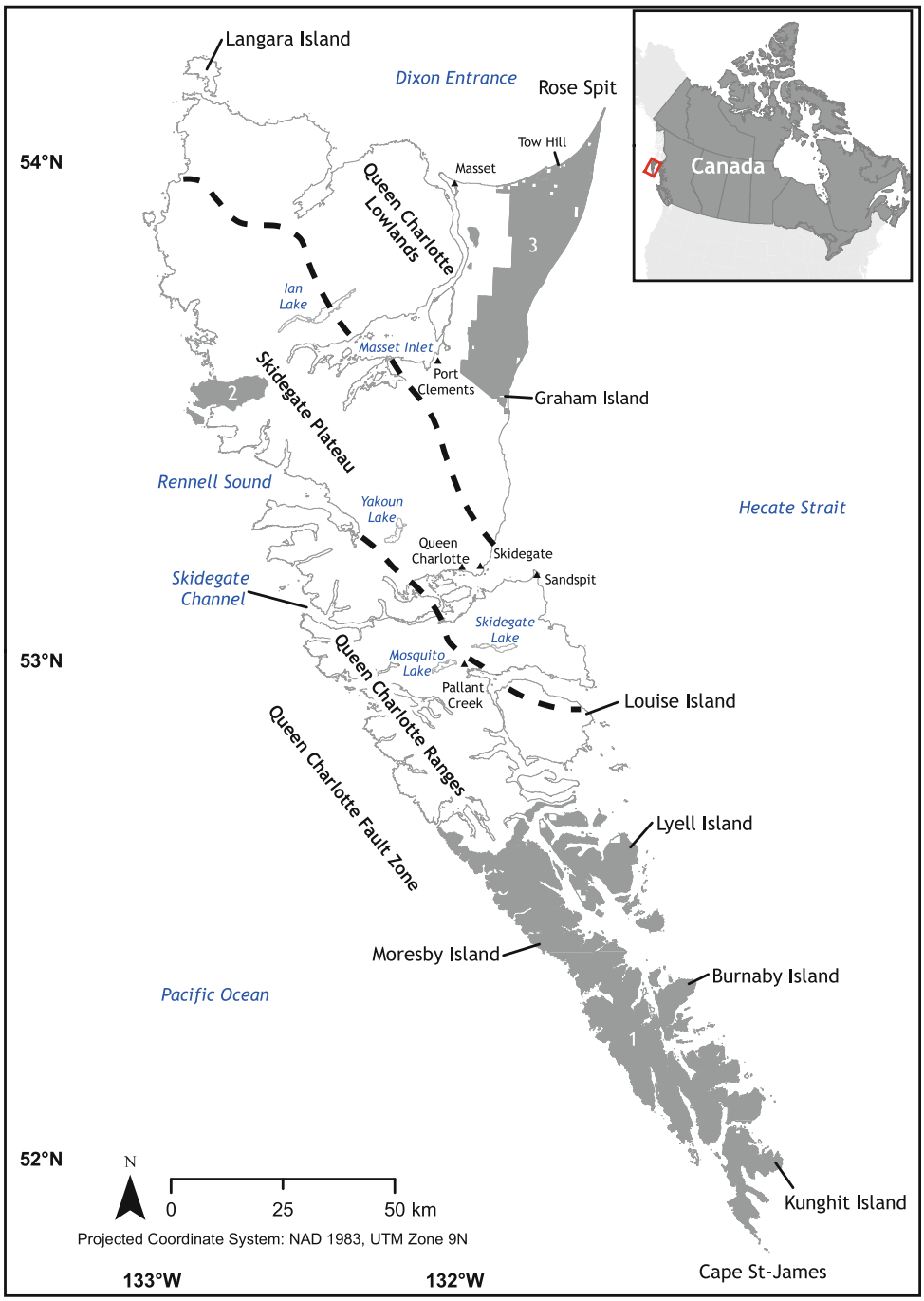

Fig. 21.1 Location of Haida Gwaii, British Columbia. The three physiographic regions are shown, as are the most important ecological reserves: *1* Gwaii Haanas National Park Reserve, *2* V.J. Krajina Ecological Reserve, and *3* Naikoon Provincial Park

this region are poorly drained and covered in muskeg, and the coastline is dynamic. Skidegate Plateau is a hilly region on northern Graham Island, separating the Queen Charlotte Ranges and Queen Charlotte Lowland. It is underlain by felsic and mafic volcanic rocks of early to late Tertiary age. Skidegate Plateau is separated from the Queen Charlotte Ranges by the Rennell Fault and from the Queen Charlotte Lowlands by the Sandspit Fault.

21.1.2 Earthquakes

Haida Gwaii owes its origin to collision and accretion of 'exotic' terranes to the margin of ancestral North America during the late Mesozoic Era, followed by northwestward movement of the archipelago along strike-slip faults during the Cenozoic Era (<66 Ma). Today, the Queen Charlotte Fault marks the boundary between the North American and

Fig. 21.2 **a** Photograph of the rugged shoreline of western Haida Gwaii (photograph by A. Bevington in 2015). **b** Photograph of the rapidly eroding shoreline of northeastern Haida Gwaii (photograph by A. Bevington in 2015)

Pacific plates. It is dominantly a dextral strike-slip fault with an average horizontal displacement rate of 50–60 mm/year. About 3 mm/year of convergence and underthrusting occur along the southern part of the fault (Cassidy et al. 2014; Fig. 21.4). Most earthquakes affecting Haida Gwaii have sources on this fault. Submarine valleys and canyons on the edge of the continental shelf off Haida Gwaii are truncated at mid-slope depths (1200–1400 m) by this fault (Harris et al. 2014), and sediment movement off the continental shelf into abyssal depths may be influenced by active faulting (Barrie et al. 2013). Canada's two largest recorded earthquakes have occurred on the Queen Charlotte Fault—one northwest of Haida Gwaii in 1949 (M 8.1) and the other west of Moresby Island in 2012 (M 7.7) (Fig. 21.2; Rosenberger et al. 2013; Fig. 21.4).

21.1.3 Climate

Haida Gwaii has a marine west coast cool climate (Köppen classification Cfb) with strong longitudinal and altitudinal temperature and precipitation gradients caused by the orographic effects of the Queen Charlotte Ranges and Skidegate Plateau. The temperate climate of Haida Gwaii reflects its offshore location and the barrier of the Coast Mountains on the mainland to the east, which protect the archipelago from cold winter and hot summer continental air masses.

Monthly air temperatures at the Sandspit Airport (6.4 masl) range from 4.0 °C in January to 14.5 °C in August; mean annual air temperature is 8.6 °C. Modeled air temperatures show that higher elevation areas have mean annual

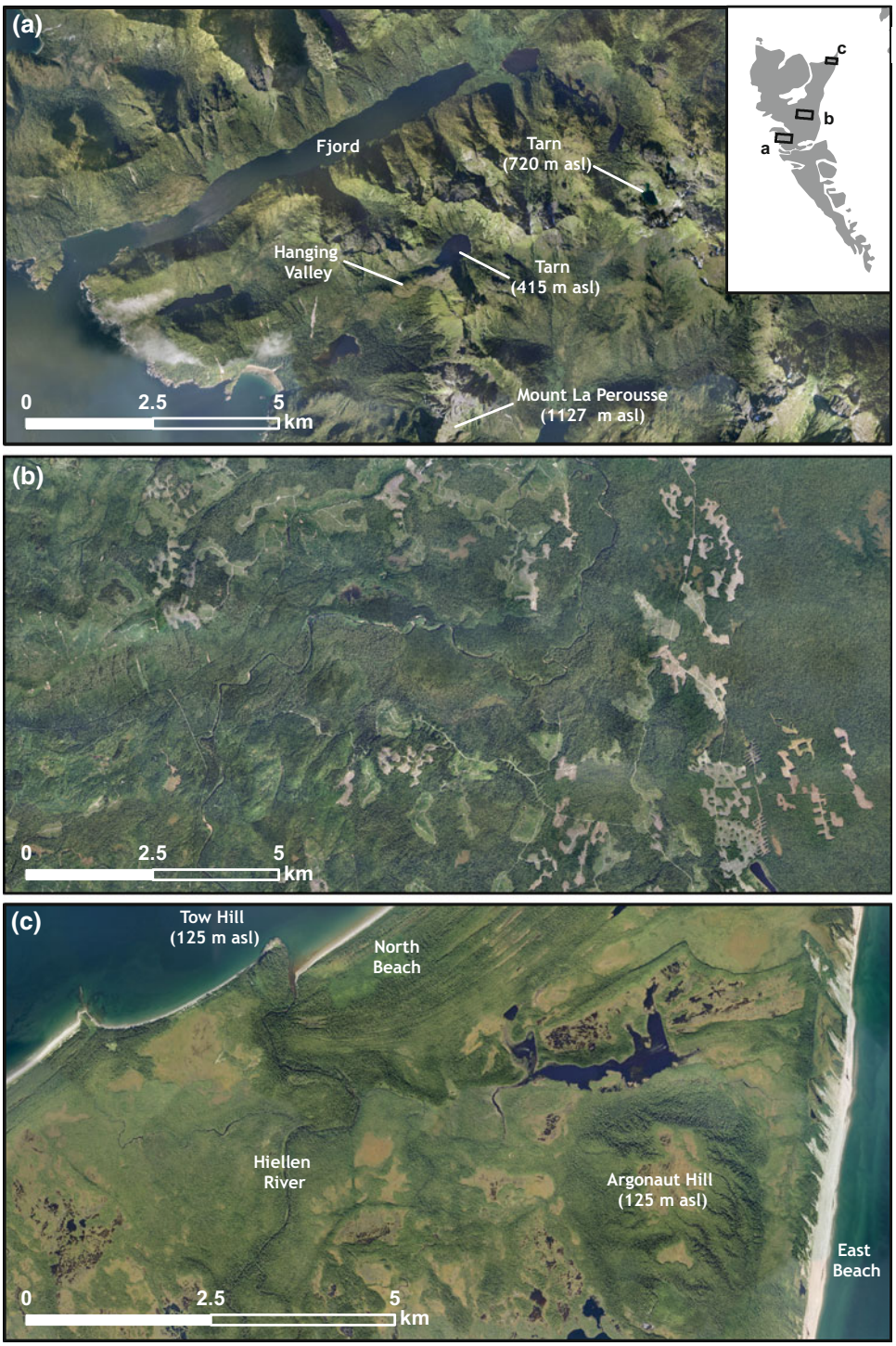

Fig. 21.3 2007 Aerial photography illustrating the three main physiographic regions of Haida Gwaii: **a** the Queen Charlotte Ranges; **b** Skidegate Plateau; and **c** the Queen Charlotte Lowlands (imagery source: British Columbia Ministry of Forests, Lands and Natural Resource Operations 2015)

temperatures below 7 °C (Fig. 21.5). Annual precipitation at the Sandspit Airport is 1408 mm, of which 1370 mm falls as rain, mostly from October to April. About 30 km to the south-west, mean annual precipitation at Pallant Creek is 3336 mm, of which 3256 mm is rain and 80 mm is snow. There are no climate stations at high elevations, but precipitation is likely greater than 5000 mm on the western (windward) side of the Queen Charlotte Ranges (Fig. 21.5; Wang et al. 2012). Wind conditions and exposure also differ greatly across the islands due to topographic effects and exposure to dominant winds from the Pacific Ocean and Hecate Strait. Average annual wind speeds at Sandspit Airport and in Hecate Strait are, respectively, 19 km/h and 31 km/h. A maximum hourly wind speed of 177 km/h and a maximum wind gust speed of 193 km/h were recorded at the Cape St. James weather station in February 1978.

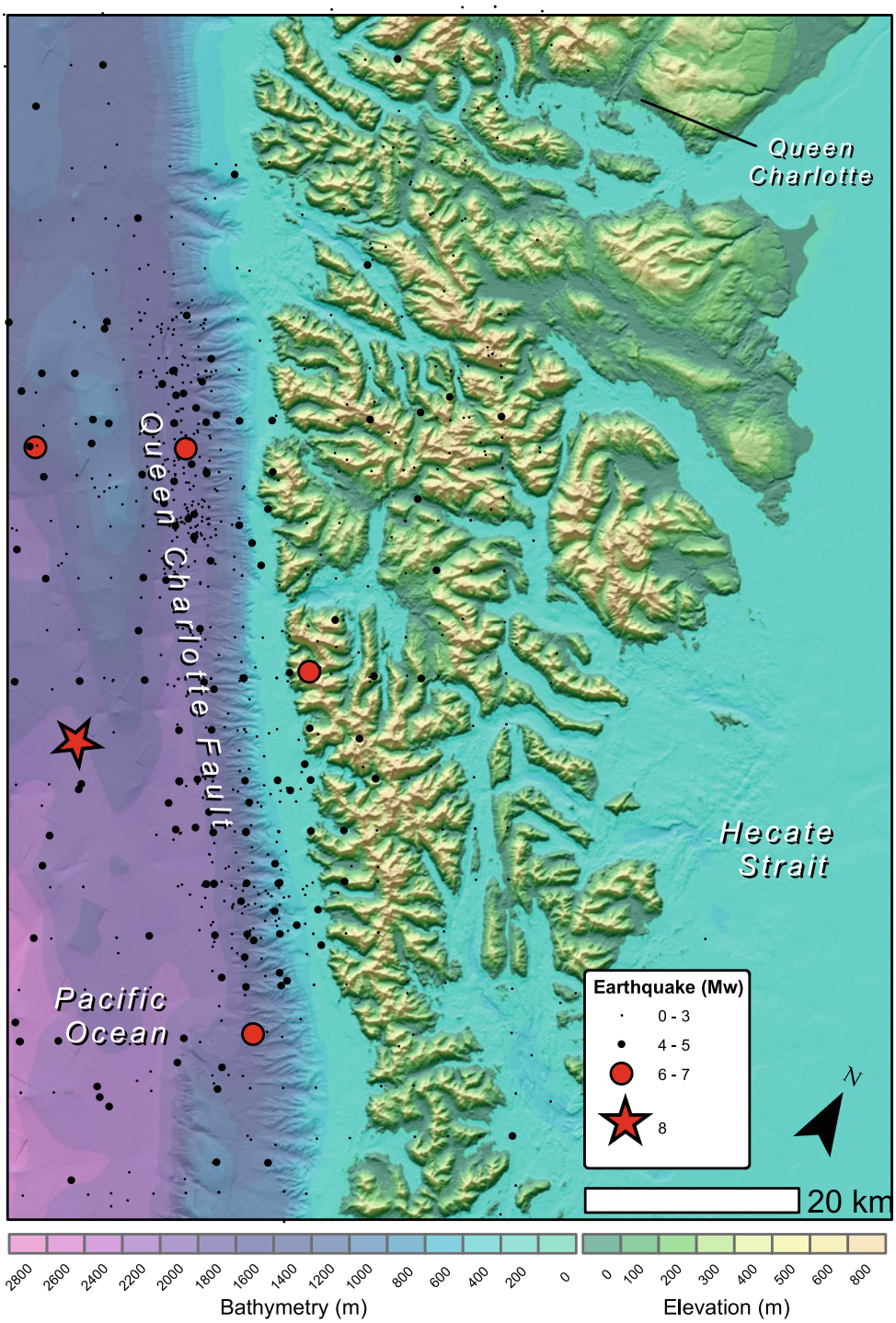

Fig. 21.4 Bathymetry of the ocean floor surrounding Haida Gwaii and epicenters of the October 2012 M 7.7 earthquake and its aftershocks (bathymetry data source: Gwaii Haanas National Park Reserve, National Marine Conservation Area Reserve, and Haida Heritage Site 2015; seismic data: Natural Resources Canada 2015)

21.1.4 Glaciation and Sea Level History

The Quaternary history of Haida Gwaii differs from that of mainland British Columbia in three respects: glacier cover was relatively brief; some areas remained ice free as refugia; and the sea level history is unique to Haida Gwaii. Geomorphic evidence supports the existence of valley glaciers sourced in the Queen Charlotte Ranges during the late Pleistocene. Stratigraphic evidence from the Cape Ball area on eastern Graham Island indicates that the western margin of the Cordilleran Ice Sheet coalesced with valley glaciers flowing from the Queen Charlotte Ranges at the peak of the last glaciation about 18 ka ago (Clague et al. 1982; Warner et al. 1984). At that time, global sea level was about 125 m lower than today and Haida Gwaii was situated on a crustal forebulge created by lateral displacement of the asthenosphere from beneath the center of the load of the

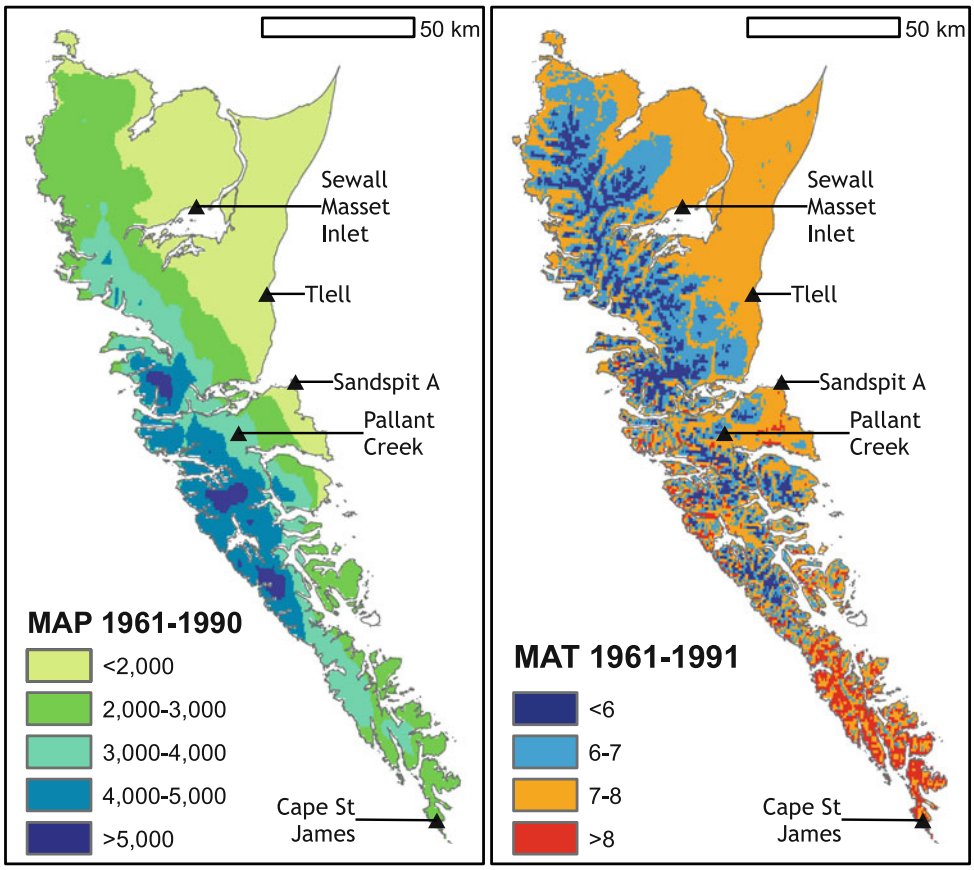

Fig. 21.5 Modeled mean annual precipitation (MAP, mm) and mean annual air temperature (MAT, °C) based on 1961–1990 climate normals (Wang et al. 2012). Environment Canada weather stations with climate normals are shown as *black triangles*

Cordilleran Ice Sheet to the east. This crustal forebulge lowered relative sea level along the shores of the archipelago. Lobes of the Cordilleran Ice Sheet covered Queen Charlotte Sound, Hecate Strait, and Dixon Entrance during the last glaciation (Clague et al. 1982). Local piedmont ice was deflected northward over Argonaut Plain by the western edge of the Cordilleran Ice Sheet (Sutherland Brown 1968; Clague et al. 1982). A thick sequence of glacial outwash deposited by meltwater streams from advancing glaciers underlies thin till from the last glaciation on Argonaut Plain (Clague 1989). Cape Ball was deglaciated 16–17 ka ago (Warner et al. 1984), and the continental shelf was completely free of ice by 14 ka ago. Deglaciation of Hecate Strait was rapid due to the combination of isostatic adjustments (forebulge collapse), eustatic sea level rise, rapid ice flow caused by drawdown of the Cordilleran Ice Sheet, and extensive calving along the western margin of the ice sheet (Barrie and Conway 2002). Sea level rose rapidly at the end of the Pleistocene and reached 15–20 m above the present datum about 9.5 ka ago (Clague et al. 1982; Clague 1989; Wolfe et al. 2008). Geomorphic evidence of this high stand can be found on Naikoon Peninsula on northeastern Graham Island. About 9 ka ago, relative sea level fell from the local marine limit and Rose Spit (Fig. 21.6) began to extend northeastward into Dixon Entrance (Wolfe et al. 2008).

Some areas on or near Haida Gwaii appear to have been refugia for plants and animals during the last glaciation (Warner et al. 1982). Because all but the highest peaks in the Queen Charlotte Ranges were ice-covered at the Last Glacial Maximum, it is likely that exposed parts of the continental shelf fringing the present landmass were the sites of these refugia (Hetherington et al. 2003). Terrestrial plant communities on the continental shelf in Hecate Strait and Queen Charlotte Sound were drowned as sea level rose (Lacourse et al. 2003).

21.2 Landslides

21.2.1 Landslide Distribution

Landslides and to a lesser degree windthrow are the primary disturbance agents on Haida Gwaii. Wildfires, the major disturbance agent in most Canadian forests, are extremely rare on the archipelago. Wind damage is significant on certain susceptible slopes, but Pearson et al. (2005) estimate that stand-replacing windthrow impacts only 0.3 % of the Haida Gwaii's forested landscape—much less than that impacted by landslides. Gimbarzevsky (1988) inventoried more than 8000 landslides on Haida Gwaii using 1:50,000

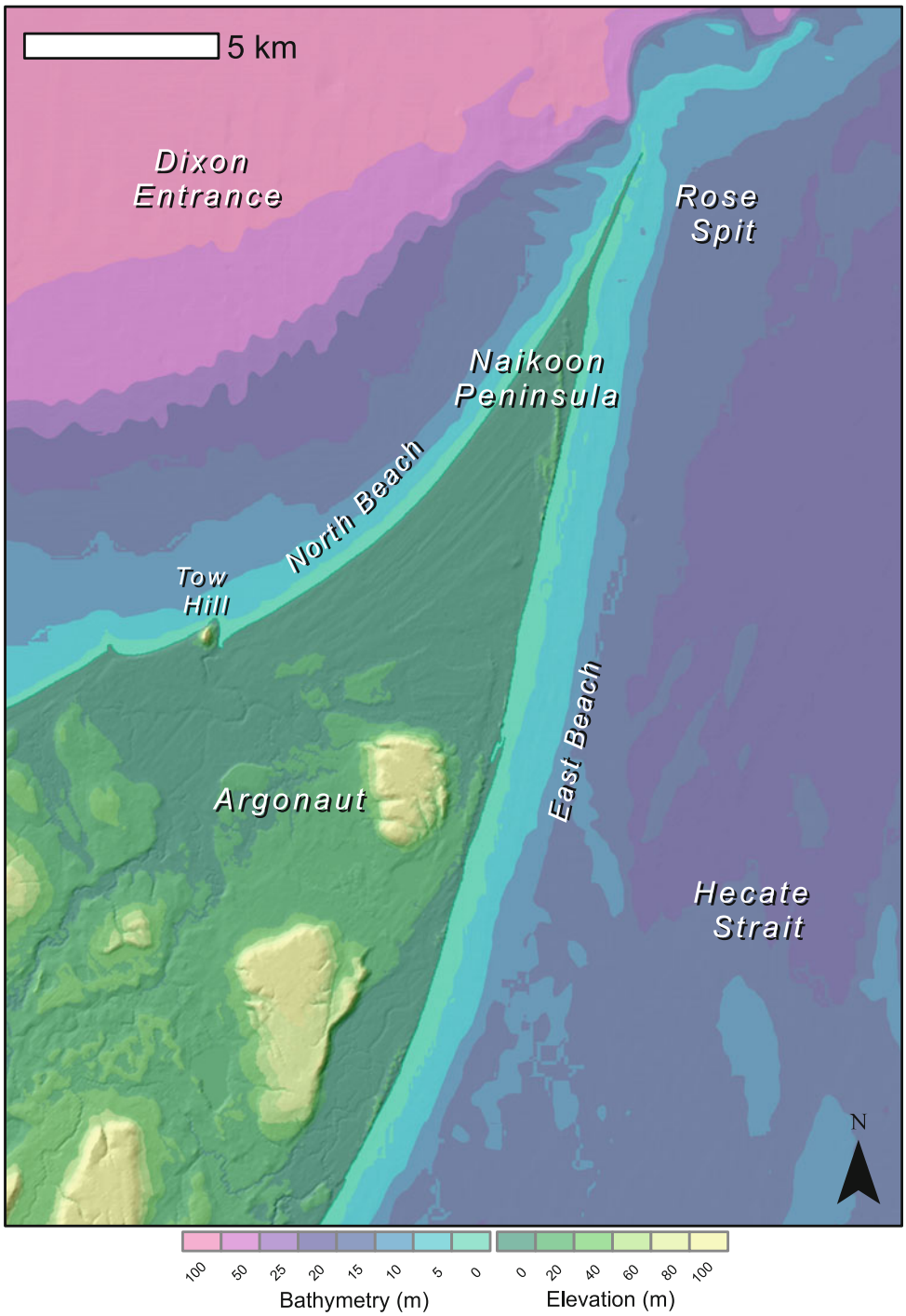

Fig. 21.6 Argonaut Plain and bathymetry of the seafloor off northeastern Graham Island (bathymetry data source: Gwaii Haanas National Park Reserve, National Marine Conservation Area Reserve, and Haida Heritage Site 2015)

aerial photographs and supplemented these data with inventories based on larger-scale photographs. He concluded that about 10,500 landslides, or an average of 1.5 landslides/km^2, have occurred on Haida Gwaii during the historic period. The Queen Charlotte Ranges, with only 28 % of the land area, account for 58 % of the landslides, and most of the remainder are on Skidegate Plateau; only 0.4 % of the landslides are in the Queen Charlotte Lowlands. Debris slides, rockslides, debris flows, and debris avalanches are the main types of mass movements (Jagielko et al. 2012). Weak and steep bedrock, shallow soils, high precipitation rates, abundant forest growth on steep slopes, proximity to a fault, and earthquakes are the main controls on the distribution of landslides in the region (Jagielko et al. 2012). Many landslides initiate on upland organic soils (Folisols) lying on bedrock.

21.2.2 Human Influences

Although most landslides are natural, slope failure is exacerbated by harvesting of forests on Skidegate Plateau and the Queen Charlotte Ranges. Rood (1984) inventoried more than 1300 landslides on Haida Gwaii and found that more than 30 % were in clear-cut logged areas and nearly 10 % were along roads. He estimated that clear-cut areas have a 30× higher rate and roads a 76× higher rate, of landslides than forested areas, 3–10× higher than rates determined for forested regions elsewhere on the Pacific coast. This finding is consistent with findings elsewhere in the province (e.g., Millard et al. 2002; Wolter et al. 2010).

21.2.3 Seismic and Tectonic Influences

Earthquakes contribute to the high incidence of landslides on Haida Gwaii. Reconnaissance flights shortly after the October 2012 earthquake showed almost 100 new landslides, most of them on southern Moresby Island near the epicenter (Fig. 21.7). Ninety percent of the landslides were debris slides; the remainder were rock falls, rock slides, and debris flows (Millard et al. 2012). Soils were relatively dry when the earthquake occurred. Had the earthquake happened during wetter weather, the number of landslides might have been much larger. Ongoing, follow-up research suggests that the 2012 earthquake may have had a delayed effect, lowering

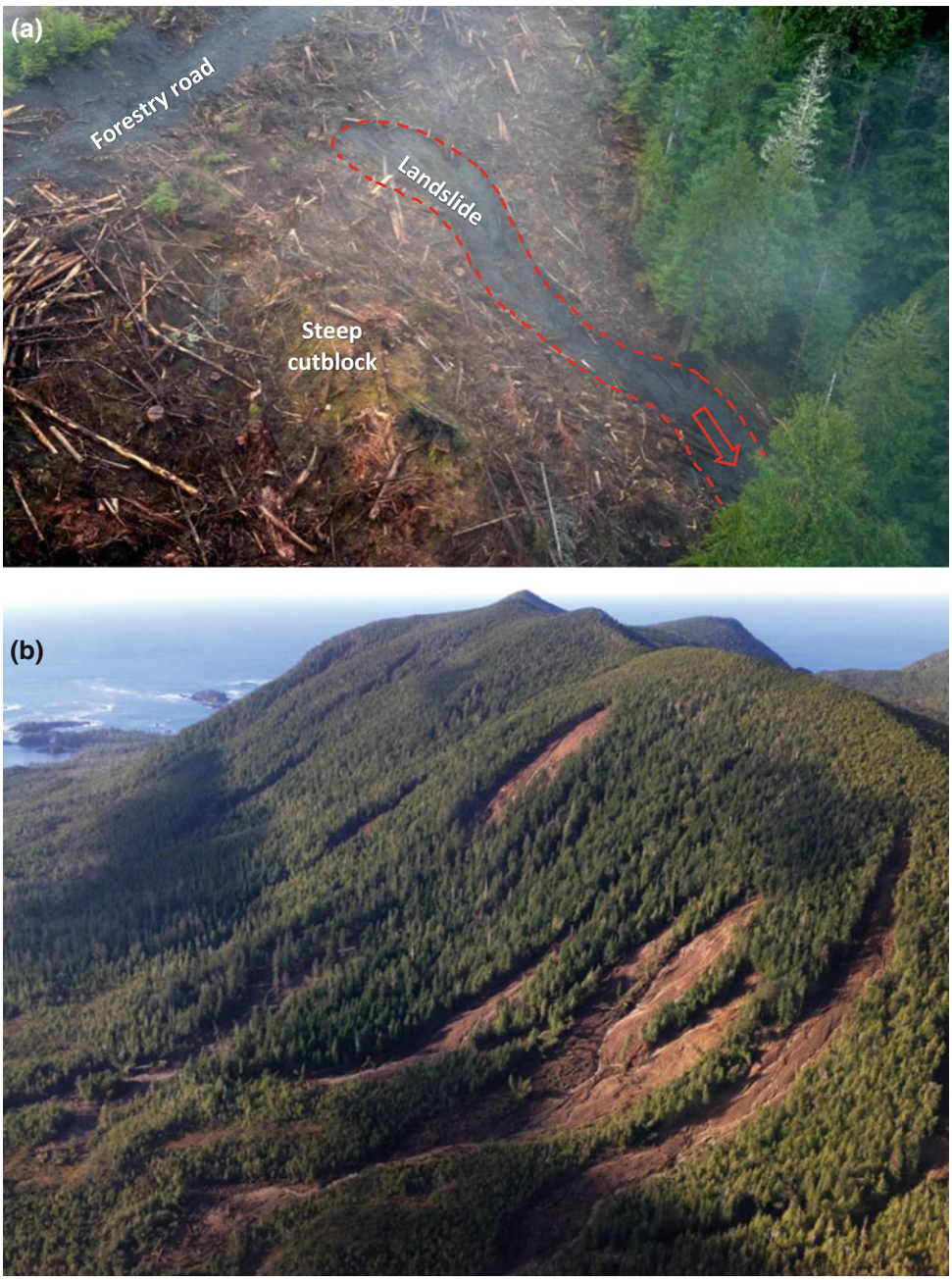

Fig. 21.7 **a** A landslide initiation zone located in the cutblock on Moresby Island (photograph by Bevington in 2015). **b** Landslide on Moresby Island triggered by the 2012 earthquake (photograph by M. Geertsema in 2012)

the threshold for the initiation of new landslides, as many additional landslides have occurred since the initial failures.

21.2.4 Geomorphic Implications

Landslides play an important role in maintaining soil, site, and habitat diversity (Geertsema et al. 2009) and introducing large woody debris (LWD) to streams. Research on Haida Gwaii has shown the importance of old-growth forests and LWD on sediment storage and channel processes in both steep gullies and along streams on valley bottoms. Steep gullies are typically excavated to bedrock during a debris flow. LWD promotes sediment storage in gullies, and debris flow volumes are therefore dependent on LWD inputs (Bovis et al. 1998). Woody debris and woody debris jams strongly affect channel morphology along Haida Gwaii fish streams (Hogan 1987). The long-term effect of woody debris depends on the size of stream (whether it is capable of moving the woody debris) and the sources of the woody debris (bank erosion, windthrow, or debris flows).

LWD is also extensive on beaches throughout Haida Gwaii and plays important roles in beach and dune morphodynamics and sediment budgets (Walker and Barrie 2006). On East Beach and Rose Spit, deposits of LWD can be massive, at many sites extending more than 150 m into the backshore and fronting foredunes and bluffs. These deposits can be several meters thick and fill quickly with aeolian sand and swash deposits. As such, these LWD jams are important sources of sediment in the backshore for incipient dune growth; buffering established dunes and bluffs from wave attack and storm surges; barricading backshore rivers, lakes, and wetlands; and providing important habitat for backshore species (Walker and Barrie 2006).

21.3 The Coastal Landscape

21.3.1 Wave Regime, Tides, and Currents

The wave climate around Haida Gwaii is among the most energetic in North America (Harper 2006). Open exposed fetches in the northeast Pacific Ocean generate large swell waves that reach the western and northern shores, and frequent storms generate large waves in Hecate Strait, which impact the eastern shores, especially in winter. Annual significant wave height (H_S) in Hecate Strait is 1.8 m, and individual waves exceeding 20 m have been recorded numerous times there (Harper 2006). Average tidal amplitude on Haida Gwaii is 4–5 m. However, the tidal wave propagates over the shallower waters of Dogfish Banks in Hecate Strait, amplifying the tidal range on the east coast of Graham Island to over 7 m (Robinson 2006). Currents in Hecate Strait and Dixon Entrance are driven mainly by tidal forcing; coastal topographic effects are only locally important (Amos et al. 1995). Reversing flood–ebb tidal currents occur as water floods into Dixon Entrance, around Rose Spit, and then into Hecate Strait, before reversing at high tide. River discharge and winds appear to have minimal effect on tidal currents except during intense storms when wind-shear currents can approach 0.25 m/s (Strong et al. 2002).

21.3.2 Beach Environments

The coastal geomorphology of Haida Gwaii is diverse and highly dynamic (Fig. 21.2). Shores on northern Graham Island host a variety of landforms including low gradient dissipative beaches backed by relict and modern foredunes (e.g., North Beach near Tow Hill, Fig. 21.8a); reflective cuspate cobble beaches with sandy low tide terraces (Rose Spit, Fig. 21.8b); multiple-barred beaches backed by foredunes and active parabolic dunes (northern East Beach, Fig. 21.8c, d); eroding sediment bluffs (East Beach near Cape Fife and Cape Ball (Fig. 21.8e, f); actively meandering river outflows (Sangan and Hiellen rivers on North Beach and the Tlell and Oeanda rivers on East Beach, Fig. 21.8g); and the Rose Spit complex (Fig. 21.8h).

Rose Spit, also known as ‘Naikun’ or ‘pointy nose’ in Haida culture, is located at the convergence of North Beach and East Beach and is one of the Canada’s most spectacular coastal landforms (Fig. 21.8h) and British Columbia’s longest spits (Fig. 21.6). The spit extends from the larger Rose Point complex, which is a flat, vegetated cobble-gravel plain capped by aeolian sand. Rose Point is bounded on East Beach by 1- to 5-m-high, driftwood-laden foredunes that grade to wave-cut scarps toward the end of the plain. Beyond this, Rose Spit proper extends another few kilometers as a steep-faced intertidal cobble beach. The modern spit complex is maintained by convergence of two regional circulation gyres—one rotating counterclockwise in Dixon Entrance and flowing eastward along North Beach and the other rotating clockwise in Hecate Strait and flowing northward from Cape Ball along East Beach (Amos et al. 1995). Strong wave and tidal currents are superimposed on this circulation system and combine to transport appreciable amounts of sediment in the littoral zone. During southeasterly storms, currents flow westward through a gap in the spit into Dixon Entrance. Rose Bar is located to the east of this gap and on the steep northern edge of Dogfish Banks where it meets the deeper waters of Dixon Entrance. Rose Bar has been interpreted to be a nearshore ‘storm ridge’ (Swift et al. 1981) maintained by northward storm-driven sand transport from East Beach combined with topographic steering of tidal and wind-driven currents along the edge of Dogfish Banks (Amos et al. 1995). North of Cape Ball, bluffs developed in late Pleistocene

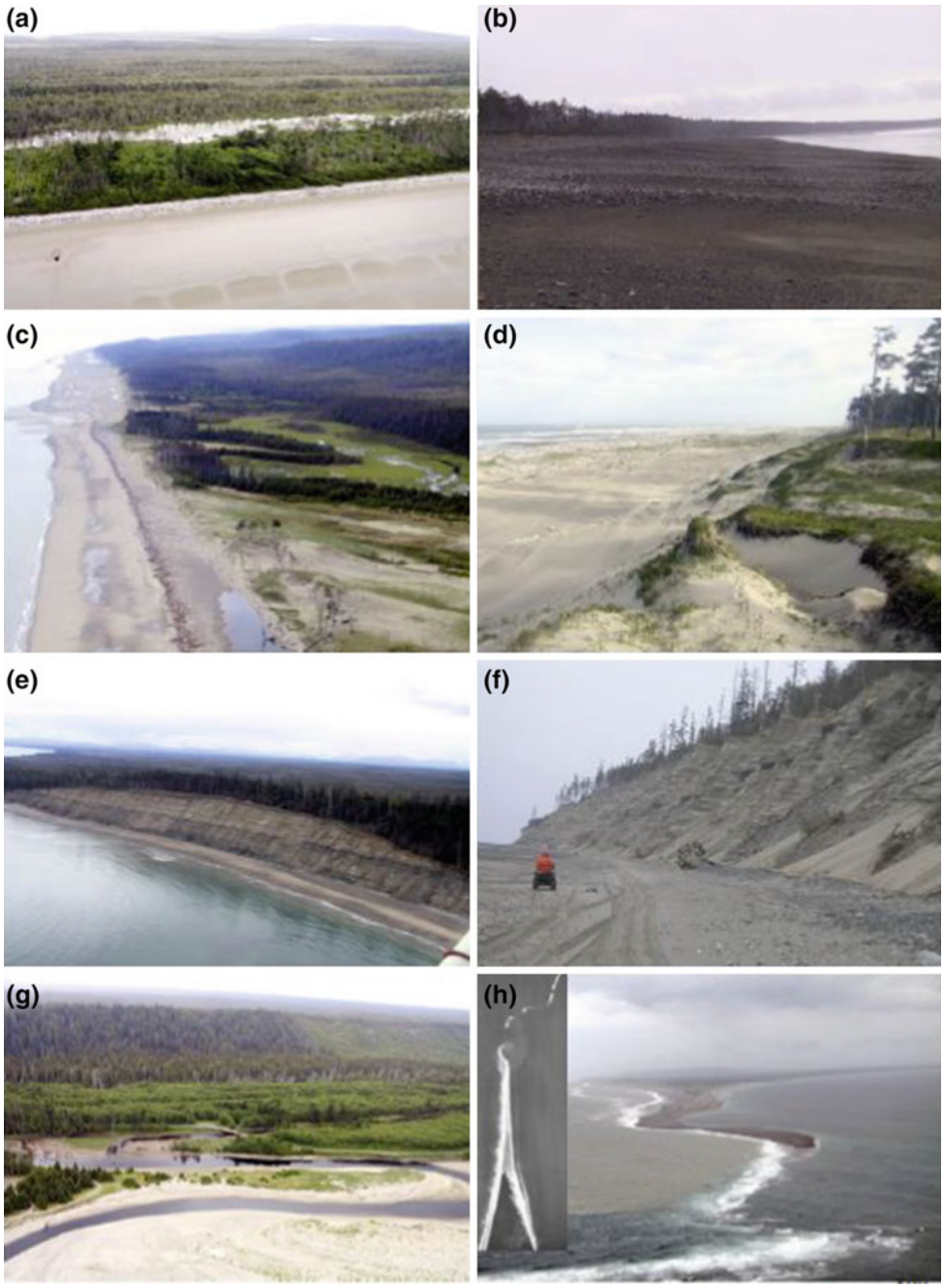

Fig. 21.8 Coastal landscapes of northeastern Graham Island. **a** North Beach near Tow Hill; **b** Rose Spit; **c**–**d** northern East Beach; **e**–**f** East Beach near Cape Fife and Cape Ball; **g** Oeanda River on East Beach; and **h** the Rose Spit complex (photographs by I. Walker)

glacial and glacifluvial sediments are locally capped by early Holocene to modern aeolian sediments (bluff-top dunes). The bluffs generally decline in height toward Rose Spit. North of Oeanda River, toward Rose Spit, an active and continuous foredune system backs the beach and is marked by numerous erosional blowouts and large (up to 1.2 km long), partly stabilized landward parabolic dune systems, particularly south of Kumara Lake (Fig. 21.8c, d). The parabolic dunes extend hundreds of meters inland and transgress muskeg on a former coastal platform.

Nearshore sediments are cycled in shore-parallel, inter- to sub-tidal, northward-migrating bars on East Beach. The bars are maintained by intense swash action and strong longshore tidal currents. Bars occasionally weld obliquely to the beach and can be reworked by storm waves (Anthony and Orford 2002). Comparison of aerial photographs taken 1980 and 1997 near Cape Fife indicates about 5 km of northward migration of an extensive intertidal bar complex. Erosion of beaches and bluffs occurs inshore of the northerly edges of these bars as wave energy is focused onshore. This process,

coupled with erosion by storm waves, likely caused the drainage of Kumara Lake between 1980 and 1994 (Conway and Barrie 1994). These bars also provide a supply of sand to backshore dune systems, and as they migrate, they may activate dune growth in the backshore.

21.3.3 Coastal Erosion

Currently, East Beach is retreating at an average rate of 1–3 m/year (Conway and Barrie 1994) and faster following extreme events such as the 1997–1998 El Niño that raised sea level off Haida Gwaii 0.4 m and triggered up to 12 m of shoreline retreat (Barrie and Conway 2002). Erosion is mostly localized at bluffs with narrow backshores, although dune-backed reaches of coastline also experience erosion and retreat despite high onshore aeolian sand delivery (Figs. 21.8a, c, d). The more dissipative shores of North Beach have been, until recently, prograding at rates of 0.3–0.6 m/year (Harper 1980). This progradation has been occurring for at least the past 1200 years, as evidenced by ages on a series of relict foredune ridges landward of North Beach (Wolfe et al. 2008; Fig. 21.8a). Sediment supplying this progradation originates either from longshore transport from the west toward Rose Spit or from East Beach during strong southeasterly storms when littoral transport is funneled through a nearshore channel at Rose Spit, to be carried onshore to North Beach later by northwesterly waves and winds (Amos et al. 1995). A network of erosion monitoring profiles established on East Beach shows that most of that section of the coast has experienced notable erosion in response to recent high-water events. These events are increasing at more than twice the rate of regional sea level rise and are linked to El Niño–Southern Oscillation (ENSO) and the Pacific Decadal Oscillation (PDO) events (Abeysirigunawardena and Walker 2008).

21.4 Conclusion

Haida Gwaii is one of the most dynamic landscapes in Canada. It is strongly impacted by coastal processes and slope failures. The glacial history of the archipelago also influences the geomorphic processes that operate in the different regions. For example, the Queen Charlotte Ranges, with their steep glacially scoured slopes, are particularly susceptible to landslides. In contrast, the Queen Charlotte Lowlands, which have low relief and are partly a product of glacial deposition, have few landslides, although its shores are constantly changing due to waves, currents, and tides. Strong earthquakes are common on the Queen Charlotte Fault and impact slopes and shorelines, causing landslides and tsunamis. Heavy rainfall and strong winds also trigger landslides. Large waves and a tidal range up to 7.5 m are major shapers of the coastline.

References

Abeysirigunawardena DS, Walker IJ (2008) Sea level responses to climate variability and change in northern British Columbia. Atmos Ocean 46:277–296

Amos CL, Barrie JV, Judge JT (1995) Storm enhanced sand transport in a macrotidal setting, Queen Charlotte Islands, British Columbia, Canada. In: Flemming BW, Bartoloma A (eds) Tidal signature in modern and ancient sediments. Special Publication of the Int. Assoc. of Sedimentologists, vol 24, pp 53–68

Barrie JV, Conway KW (2002) Rapid sea-level change and coastal evolution on the Pacific margin of Canada. Sediment Geol 150:171–183

Barrie JV, Conway KW, Harris PT (2013) The Queen Charlotte fault, British Columbia: seafloor anatomy of a transform fault and its influence on sediment processes. Geo-Mar Lett 33:311–318

Bovis MJ, Millard TH, Oden ME (1998) Gully processes in coastal British Columbia: the role of woody debris. In: Hogan DL, Tschaplinski PJ, Chatwin S (eds) Carnation Creek and Queen Charlotte Islands Fish/Forestry Workshop. Province of British Columbia: Land Management Handbook # 41, pp 49–75. https://www.for.gov.bc.ca/hfd/pubs/docs/Lmh/Lmh41.htm

Cassidy JF, Rogers GC, Hyndman RD (2014) An overview of the 28 October 2012 Mw 7.7 earthquake in Haida Gwaii, Canada: a tsunamigenic thrust event along a predominantly strike-slip margin. Pure Appl Geophys 171:3457–3465

Clague JJ (1989) Quaternary geology of the Canadian Cordillera. In: Fulton RJ (ed) Quaternary geology of Canada and Greenland. Geological Survey of Canada, Geology of Canada, no. 1, pp 15–96

Clague JJ, Mathewes RW, Warner BG (1982) Late Quaternary geology of eastern Graham Island, Queen Charlotte Islands, British Columbia. Can J Earth Sci 19:1786–1795

Conway KW, Barrie JV (1994) Coastal erosion on the east coast of Graham Island, Queen Charlotte Islands, British Columbia. Geol Surv Can Curr Res 1994-E, 53–58

Geertsema M, Highland LM, Vaugeois L (2009) Environmental impact of landslides. In: Sassa K, Canuti P (eds) Landslides—disaster risk reduction. Springer, Berlin, pp 585–604

Gimbarzevsky P (1988) Mass wasting on the Queen Charlotte Islands. Land management report 29. Province of British Columbia, Victoria

Gwaii Haanas National Park Reserve, National Marine Conservation Area Reserve, and Haida Heritage Site (2015) Compilation of bathymetric data. Parks Canada (draft dataset)

Harper JR (1980) Coastal processes on Graham Island, Queen Charlotte Islands, British Columbia. Geol Surv Can Curr Res 80(1A):13–18

Harris PT, Barrie JV, Conway KW, Greene HG (2014) Hanging canyons of Haida Gwaii, British Columbia, Canada: fault-control on submarine canyon geomorphology along active continental margins. Deep-Sea Res Part II 104:83–92

Hetherington R, Barrie JV, Reid RG, MacLeod R, Smith DJ, James TS, Kung R (2003) Late Pleistocene coastal paleogeography of the Queen Charlotte Islands, British Columbia, Canada, and its implications for terrestrial biogeography and early postglacial human occupation. Can J Earth Sci 40:1755–1766

Hogan DL (1987) The influence of large organic debris on channel recovery in the Queen Charlotte Islands, British Columbia, Canada. In: Beschta RL, Blinn T, Grant GE, Ice GG, Swanson FJ (eds) Erosion and sedimentation on the Pacific Rim. Proceedings of the Corvallis symposium, Internat Assoc Hydrol Sci Pub, vol 165, pp 343–354

Jagielko L, Martin YE, Sjogren DB (2012) Scaling and multivariate analysis of medium to large landslide events: Haida Gwaii, British Columbia. Nat Hazards 60:321–344

Lacourse T, Mathewes RW, Fedje DW (2003) Paleoecology of late-glacial terrestrial deposits with in situ conifers from the submerged continental shelf of western Canada. Quat Res 60:180–188

Millard T, Rollerson TP, Thomson B (2002) Post-logging landslide rates in the Cascade Mountains, southwestern British Columbia. Province of British Columbia, Nanaimo Technical Report 23

Natural Resources Canada (2015) Earthquakes Canada. http://www.earthquakescanada.nrcan.gc.ca/

Pearson AF, Mitchell, SJ, Lanquaye N, Heath J (2005) Patterns of wind disturbance in Haida Gwaii. South Moresby forest replacement account final report, University of British Columbia, Department of Forest Sciences, Vancouver BC and Terrasaurus Ltd., Vancouver, BC

Robinson CLK (2006) Oceanography. In: Sloan NA (ed) Living marine legacy of Gwaii Haanas. V: coastal zone values and management around Haida Gwaii, Parks Canada technical reports in Ecosystem Science, pp 148–164

Rood KM (1984) An aerial photograph inventory of the frequency and yield of mass wasting on the Queen Charlotte Islands, British Columbia. Province of British Columbia, Victoria, Land Management Report 34, pp 1–55

Rosenberger A, Bird A, Turek ME, Huffman S, Rogers G, Cassidy J, Mulder T (2013) Strong motion data from the magnitude 7.7 "Haida Gwaii" earthquake on October 27, 2012 (local time). Geol Surv Can Open File 7324:1–32

Sutherland Brown A (1968) Geology of the Queen Charlotte Islands, British Columbia. British Columbia Department of Mines and Petroleum Resources Bulletin 54

Swift DJP, Young RA, Clarke TL, Vincent CE, Niedoroda A, Lesht B (1981) Sediment transport in the Middle Atlantic Bight of North America: synopsis of recent observations. In: Nio S-D, Shüttenhelm RTE, Van Weering TJCE (eds) Holocene marine sedimentation in the North Sea Basin. Blackwell Publishing Ltd., Oxford. doi:10.1002/9781444303759.ch26

Walker IJ, Barrie JV (2006) Geomorphology and sea-level rise on one of Canada's most 'sensitive' coasts: northeast Graham Island, British Columbia. J Coast Res 39:220–226

Wang T, Hamann A, Spittlehouse DL, Murdock TQ (2012) Climate WNA-high-resolution spatial climate data for western North America. J Appl Meteorol Climatol 51:16–29

Warner BG, Mathewes RW, Clague JJ (1982) Ice-free conditions on the Queen Charlotte Islands, British Columbia, at the height of late Wisconsin glaciation. Sci 218(4573):675–677

Warner BG, Clague JJ, Mathewes RW (1984) Geology and paleoecology of a mid-Wisconsin peat from the Queen Charlotte Islands, British Columbia, Canada. Quat Res 21:337–350

Wolfe S, Walker IJ, Huntley D (2008) Holocene coastal reconstruction, Naikoon peninsula, Queen Charlotte Islands, British Columbia. Geol Surv Can Curr Res 2008–12:1–18

Wolter A, Ward B, Millard T (2010) Instability in eight sub-basins of the Chilliwack River valley, British Columbia Canada: a comparison of natural and logging-related landslides. Geomorphology 120:123–132

Lillooet-Harrison Drainage Basin: Variable Landscapes Within the Coast Mountains

22

Olav Slaymaker, John J. Clague, Robert Gilbert, Pierre A. Friele, Peter Jordan, Brian Menounos, and Erik Schiefer

Abstract

The Lillooet-Harrison watershed (7870 km^2 in area, of which 459 km^2 is glacierized) contains recurring morphological landscape elements that differ in terms of their level of connectivity with Lillooet River. First, ridge tops with low local relief are connected to Lillooet River primarily through dissolved solids moving along subsurface pathways. Second, small glaciers have little direct connection with Lillooet River because of their numerous proximal lakes, whereas larger valley glaciers are directly linked to Lillooet River. Third, hillslopes subject to infrequent, large mass movements are episodically connected, and fourth, debris flow channels are directly linked with valley-bottom rivers. Fifth, mid-valley and lower valley-bottom sites are sediment storage areas that are episodically coupled to the adjacent river channel. The Mount Meager Volcanic Complex dominates the supply of coarse clastic sediment to Lillooet River and is primarily responsible for the rapid rates of Lillooet delta progradation and aggradation. The 6 % of the watershed that is glacierized provides a high proportion of the fine clastic sediments to Lillooet and Harrison lakes, whereas solute production that has little influence on morphological elements is important in assessing the overall rate of landscape denudation in the Lillooet-Harrison watershed. More frequent extreme rainfall events and rapid glacier

O. Slaymaker (✉)
Department of Geography, University of British Columbia, 1984 West Mall, Vancouver, BC V6T 1Z2, Canada
e-mail: olav.slaymaker@ubc.ca

J.J. Clague
Department of Earth Sciences, Simon Fraser University, 8888 University Drive, Burnaby, BC V5A 1S6, Canada

R. Gilbert
Department of Geography and Planning, Queen's University, Mackintosh-Corry Hall, Kingston, ON K7L 3N6, Canada

P.A. Friele
Cordilleran Geoscience, Consultant, 1021 Raven Drive, P.O. Box 612, Squamish, BC V8B 0A5, Canada

P. Jordan
B.C. Forest Service, #401-333 Victoria St., Nelson, BC V1L 4K3, Canada

B. Menounos
Geography Program and Natural Resources and Environmental Studies Institute, University of Northern British Columbia, 3333 University Way, Prince George, BC V2N 4Z9, Canada

E. Schiefer
Department of Geography, Planning and Recreation, Northern Arizona University, Flagstaff, AZ 86011-5016, USA

© Springer International Publishing Switzerland 2017
O. Slaymaker (ed.), *Landscapes and Landforms of Western Canada*, World Geomorphological Landscapes, DOI: 10.1007/978-3-319-44595-3_22

retreat together with intensified human occupancy in the valley can be expected to increase the coupling of each of the morphological elements to Lillooet River and expedite the movement of water, sediments, and solutes through the watershed.

Keywords
Coupling • Solutes • Glaciers • Mass movements • Lake sedimentation • Human occupancy

22.1 Geological and Hydroclimatic Context

The Lillooet-Harrison watershed is an elongate, 7870 km^2 river basin (c. 250 × 30 km) that is a part of the Fraser River watershed (Fig. 22.1). As of 2005, approximately 459 km^2 of the watershed is glacierized. The basin incorporates a representative range of the landforms and landscapes of British Columbia's Pacific Ranges, part of the southern Coast Mountains. The major geological structures in the basin include Mid-Cretaceous to Early Tertiary west- and east-vergent contraction faults, right-lateral strike-slip faults, and Eocene extension faults. Accretion of terranes was accompanied by compression and by northwestward displacement of accreted rocks along high-angle reverse faults and strike-slip faults that resulted in a strong northwest-southeast structural and topographic grain (Monger and Journeay 1994; Fig. 22.1).

Mesozoic granitic and metamorphic rocks dominate the watershed, but Mount Meager is a major Quaternary volcanic center that figures prominently in our subsequent discussion of slope instability and sediment yield. Uplift in Late Cenozoic time led to a cycle of fluvial canyon cutting that further accentuated the northwest-southeast topographic grain. During the Pleistocene Epoch, the Lillooet-Harrison valleys were widened and deepened by glacier ice embedded within the Cordilleran Ice Sheet. A cirque landscape developed at higher elevations, whereas below about 2200 masl rounded ridges and roche moutonnée features were sculpted by the Cordilleran Ice Sheet. An erosional legacy of glaciation is an extensive system of steep undercut slopes, many of which have joints, foliation, and faults that are favorably oriented for modern-day mass movement (Ryder 1981).

The hydroclimatic environment is influenced greatly by the NW-SE alignment of the major divides of the Pacific Ranges. Atmospheric circulation over the North Pacific Ocean brings most precipitation from the southwest, thereby imposing a strong rain shadow effect on the Lillooet-Harrison basin. Temperature, precipitation, streamflow, and glacierization decline dramatically from west to east across the basin. The presence of Interior Douglas fir on the northeastern slopes of Lillooet Valley marks the visible onset of more arid conditions in the Interior Cordillera (Fig. 22.2). Furthermore, the equilibrium line altitude rises from southwest to northeast in response to increased continentality and the moisture gradient. Ryder (1981) and Evans (1990) have discussed the implications of this gradient for the distribution and morphology of cirques. The large, medium, and microscale morphology and regolith control the pathways of water and sediment between alpine, subalpine, and temperate landscape components (Teti 1984; Gallie and Slaymaker 1985; Barrett and Slaymaker 1989).

In 1972, Church and Ryder introduced their paraglacial model of sedimentation, which emphasized the role of non-glacial processes conditioned by glaciation. Although they made no reference to sedimentation in Lillooet Valley, all subsequent geomorphic study in British Columbia has had to take into account the implications of the paraglacial model. The Lillooet basin is a specific case of punctuated paraglaciation that has expanded our understanding of the basic model (Ballantyne 2002; Friele and Clague 2009).

22.2 Original Research Objectives

The original motivation for a geomorphic research program in the Lillooet-Harrison basin was fourfold (Slaymaker 1972; Slaymaker and Gilbert 1972): (1) to determine the rate of denudation of the Pacific Ranges; (2) to determine sediment sources, fluxes, and sinks based on a semiquantitative sediment budget for the Lillooet-Harrison River basin; (3) to elaborate the paraglacial model of postglacial landscape evolution; and (4) to consider natural hazards associated with contemporary geomorphic, hydrologic, and anthropogenic processes in the Lillooet-Harrison system. Several seminal papers, in addition to those discussed in the body of this chapter, have furthered these objectives, most notably the following three: Parrish (1983) determined by fission track dating that, averaged over millions of years, rates of

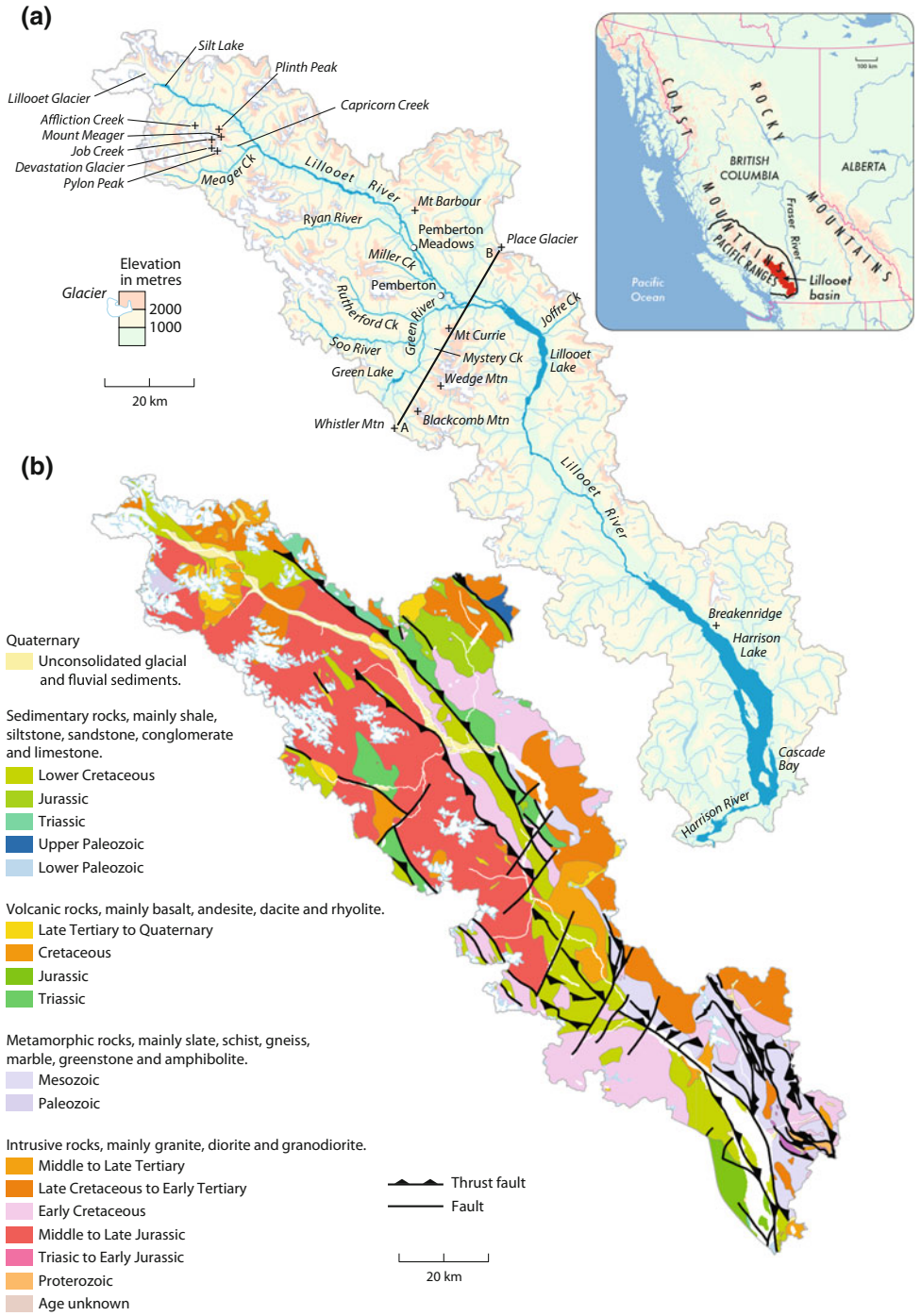

Fig. 22.1 Topography and geology of the Lillooet-Harrison drainage basin and sites mentioned in the text (National Topographic System and Monger and Journeay 1994). The line A–B is the transect illustrated in Fig. 22.2

tectonic uplift of the Coast Mountains have far exceeded rates of contemporary denudation; Clague (1986) emphasized the temporal discontinuities of active geomorphic processes in the Canadian Cordillera; and Mathews (1991) provided a magisterial summation of pre-Quaternary landscape evolution in the Canadian Cordillera.

22.3 Coupling: The Central Concept in This Study

Coupling involves the transmission of water, sediment, and dissolved solids through a system from hillslope and headwater sources to the river system (Schumm 1977; Harvey

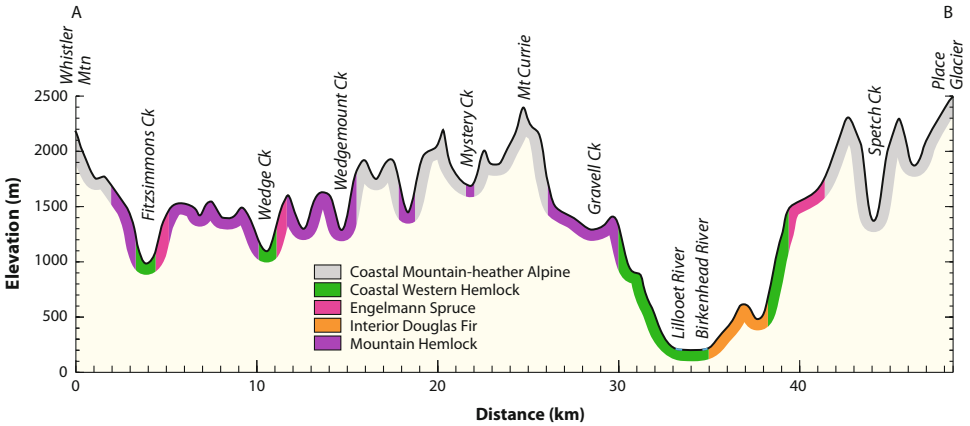

Fig. 22.2 Hydroclimatic and ecological gradient from Whistler Mountain to Place Glacier in the Pacific Ranges of the Coast Mountains, British Columbia

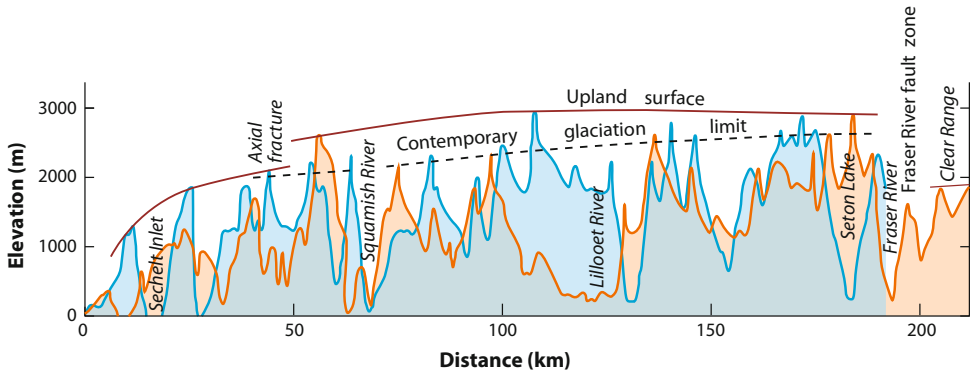

Fig. 22.3 Tertiary erosion surface, accordance of summit levels, and contemporary glaciation limit in the Pacific Ranges of the Coast Mountains (Ryder 1981). The pink and light blue transects are taken from the Strait of Georgia to the Fraser Valley, British Columbia

2002). Where hillslopes and river channels are tightly coupled, there is a continuous or semicontinuous flow of water, sediment, and dissolved solids from slopes to channels. Water and dissolved solids commonly follow preferred pathways from headwaters to the outlet of a river basin, and clastic sediments accumulate at preferred locations within the basin, such as slope breaks or lakes. The rate at which morphological changes propagate through the system depends directly on the degree of this coupling. Tight coupling implies a high level of connectivity; decoupling implies no connectivity.

Five broad morphological elements can be defined within the Lillooet-Harrison system based on their coupling to Lillooet Valley. First, ridge tops with low local relief are coupled to Lillooet Valley primarily through dissolved solids moving along subsurface pathways. Clastic sediments are commonly decoupled on ridge tops (Sect. 22.4). Second, small glaciers, like Place, Joffre, and Fitzsimmons, are decoupled from Lillooet Valley by numerous proximal lakes, whereas larger valley glaciers, including Lillooet and Ryan, are directly coupled to Lillooet River (Sect. 22.5). Third, hillslopes subject to infrequent large mass movements are episodically coupled (Sect. 22.6). Fourth, debris flow channels directly couple hillslopes with valley-bottom rivers (Sect. 22.7). Fifth, mid-valley and lower valley sites are sediment storage areas or sinks that are also episodically coupled with the adjacent river channel (Sects. 22.8 and 22.9).

22.4 Solute Fluxes and the Preservation of Ancient Erosion Surfaces

The presence of an ancient erosion surface of moderate relief (Mathews 1958, 1991; Ryder 1981) was first inferred by George Dawson (1896) (Fig. 22.3). More recently, Tribe (2005) explored the Eocene palaeophysiography in the adjacent southern Interior Plateau. She examined the distribution and depositional palaeoenvironment of Eocene rocks and crosscutting relations between regional-scale geomorphology and bedrock geology. She confirmed that fragments of a Tertiary erosion surface and associated summit levels are present in the Pacific Ranges and argued that Lillooet Valley has Late Cretaceous ancestry.

Major topographic divides, accordant summit levels, and ridge tops are commonly viewed as being decoupled from Lillooet Valley (Fig. 22.4a). But weathering products from the dominant coarse crystalline rocks in these settings use

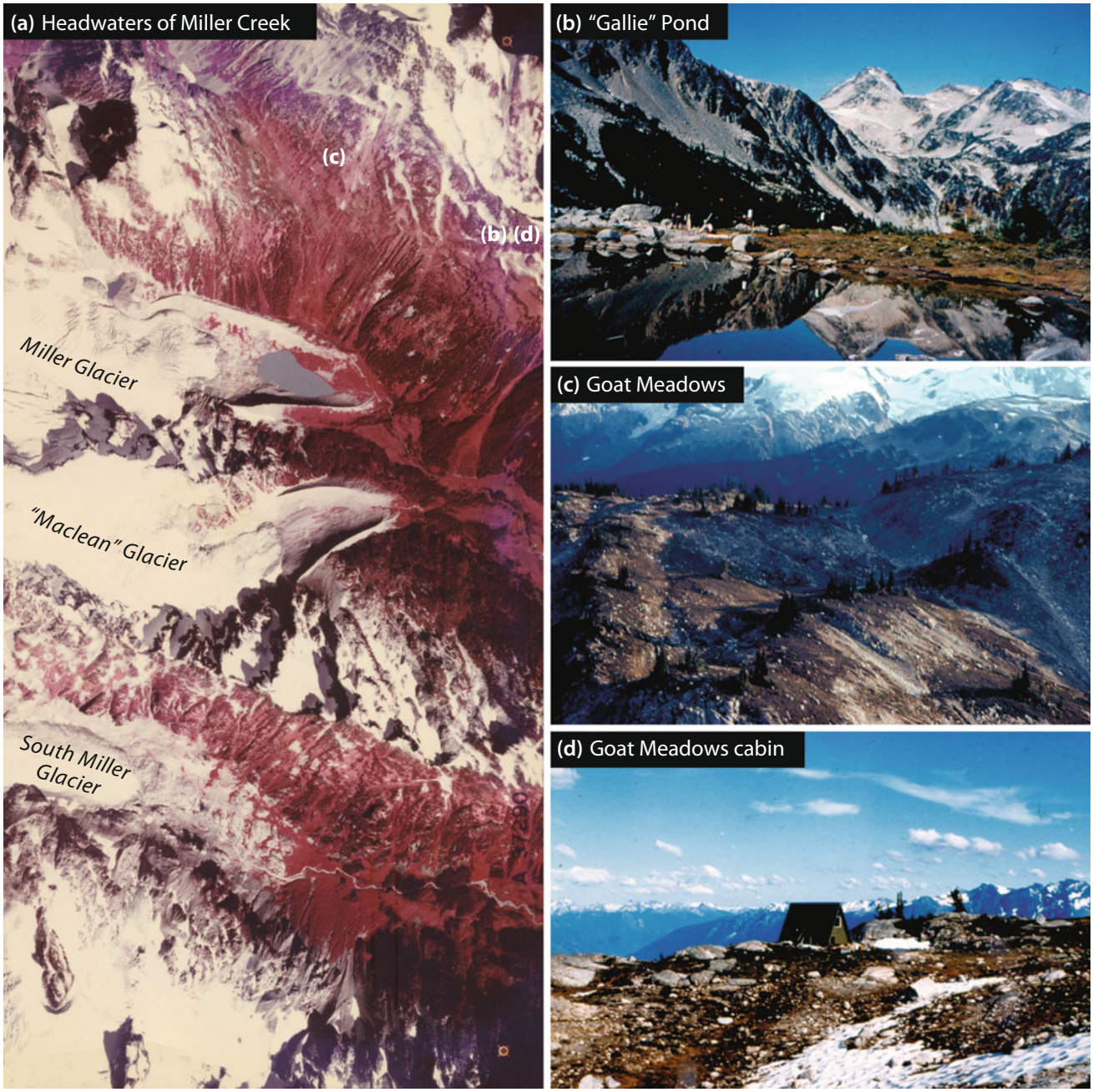

Fig. 22.4 Overview of the 15 % glacierized Miller Creek watershed, part of the Lillooet River basin, British Columbia

subsurface hydrologic pathways to reach adjacent rivers. Ridge tops exhibit widespread evidence of toppling along well-developed, preexisting joints that permit preferred access of water and solutes to deep groundwater reservoirs (Fig. 22.4b). High precipitation, both snow and rain, drives denudation by solution in and around these ridge tops. The precipitation moves through three major reservoirs with differing residence times: bedrock pathways (43 %); soils (29 %); and surface detention (28 %) (Gallie and Slaymaker 1985).

A series of studies (Souch 1989; Owens and Slaymaker 1992; Laudon and Slaymaker 1997) carried out at ten ridge-top sites (1976–1995) around Goat Meadows (Fig. 22.4c) demonstrated that the net rate of contemporary bedrock weathering averages c. 3 Bubnovs (B), where 1 B is defined as 1 mm ka^{-1} of surface lowering (Fischer 1969). This rate implies c. 30 m of surface lowering over the 10 Ma of latest Miocene, Pliocene and Quaternary time (Fig. 22.4d).

Measured dissolved solids fluxes in the Coast Mountains imply that c. 30 % of the regional total denudation in granitic terrain is due to solution (Slaymaker 1987). By contrast, in headwater systems, such as Green Lake, which has been monitored for over a half-century, only 15 % of total denudation is accounted for by solution (Schiefer et al. 2010). There is a chain of dissolved solids transfers that moves material from ridge tops and hillslopes toward a local base level or stream channel. The ridge tops are coupled with the valley, and the mass flux represented by these processes, distributed across the landscape, is significant. The morphological impact of denudation by solution is, however, not so immediately apparent.

22.5 Sediment Production by Glaciers

Subglacial erosion is maximized under thick temperate glaciers because high driving stresses promote rapid rates of basal sliding. Erosion and reworking of fine-grained sediments beneath temperate glaciers and within their recently deglaciated forefields may likewise explain why sediment export from glacierized watersheds is typically higher than that from adjacent non-glacial basins (Church et al. 1999). Several studies implicate glaciers as major sediment sources in the Canadian Cordillera (Leonard 1997; Hodder et al. 2006, 2007; Schiefer and Gilbert 2008). Desloges and Gilbert (1994a) and Heideman (2013) note that glaciers are one of the primary sources of sediment in the Lillooet basin. However, sediment delivery by glaciers to the southernmost end of Harrison Lake is more uncertain and raises the question of the role of lakes in decoupling the lower end of the Lillooet-Harrison system from Lillooet Valley north of the Lillooet delta.

Glaciers in the southern Coast Mountains achieved their maximum Holocene extent about 200–300 years ago during the climactic advances of the Little Ice Age (Menounos et al. 2009). Since then, and especially in the twentieth century, glaciers have thinned and receded in response to warmer, dryer conditions. Between 1985 and 2005, glacier cover in the Lillooet basin shrank from 521 to 459 km^2 (Bolch et al. 2010). Glacier cover in nearby Garibaldi Provincial Park during the Little Ice Age was about twice that of today (Koch et al. 2009), likely comparable in magnitude to the ice loss experienced in the Lillooet basin. Glacier retreat has exposed forefields and unstable lateral moraines that can be reworked by fluvial and hillslope processes (Figs. 22.4a, 22.5).

22.5.1 Glacier Stream Channel Coupling: Small Glaciers Versus Valley Glaciers

In the case of glacierized basins with high sediment yields, the single factor that is most responsible for differences in sediment yield rates is the degree of coupling of glacial sediments and stream channels. In this case, coupling depends on the presence or absence of sediment-trapping lakes. In the Lillooet basin, a first-cut distinction can be made between small glaciers, like Place, Joffre, and Fitzsimmons, that are largely decoupled from Lillooet River, and valley glaciers, like Lillooet and Ryan, that are highly coupled to Lillooet River.

Fig. 22.5 Oblique view from Goat Meadows to "Maclean" Glacier and its 100 m-high north-facing Neoglacial moraine (photograph by O. Slaymaker)

(a) Small Glaciers Joffre, Miller, Overlord, and Fitzsimmons glaciers are small glaciers in the Lillooet basin for which measurements and field observations are available (Fig. 22.6a). Place Glacier is unique in this basin in that it has a relatively long record of mass balance measurements (Fig. 22.6b).

Sediment-laden meltwater from Overlord and Fitzsimmons glaciers flows into Green Lake. Distinct and anomalously thick varves deposited in Green Lake from 1930 to 2000 have been attributed to rapid glacial recession during the early twentieth century, floods caused by major late summer and autumn rainstorm floods, and rapid snowmelt during late spring and summer (Schiefer et al. 2006, 2007). Similar decadal trends in Fitzsimmons Creek bedload transport have been reconstructed from rates of delta progradation. A reactivated deep-seated landslide in lower Fitzsimmons Creek valley has been implicated in the case of the thickest varve (1991) (Mierzejewski et al. 1993).

Average lake-wide accumulation in Green Lake for the period 1930–2000 is 68 Mg km^{-2} a^{-1} or c. 28 B, which is typical of lightly to moderately glacierized catchments in the Coast Mountains (Desloges and Gilbert 1994b; Schiefer et al. 2001). This value, however, is at least an order of magnitude less than the contemporary sediment yield in the heavily glacierized Silt Lake catchment at the head of the watershed (Schiefer 2006; see below). The degree to which these upland valleys are coupled to the sediment cascade of lower Lillooet River is largely controlled by the presence and size of intervening lakes. This observation has no bearing on the primary factors controlling sediment yield from glaciers, such as driving stress, quarrying, and abrasion rates, but simply the extent to which intervening lakes alter the channel coupling.

(b) Valley Glaciers Ryan and Lillooet glaciers are the largest valley glaciers in the Lillooet basin. Lillooet Glacier is by far the more important of the two in terms of sediment production. It is the source of Lillooet River and dominates the uppermost part of Lillooet Valley (Fig. 22.7). In the vicinity of Silt Lake in the forefield of Lillooet Glacier, the valley bottom is bounded by sharp-crested Little Ice Age lateral moraines up to about 200 m high (Reyes and Clague 2004). Within the glacier forefield, the valley contains glacifluvial outwash, till, and bedrock exposures. Schiefer and Gilbert (2007) used sequential air photographs (Fig. 22.8) to quantify a half-century (1947–1997) of landscape change in this upper reach of Lillooet Valley, which we update here using recent satellite imagery. In 1947, the site of Silt Lake was covered by up to 140 m of glacier ice. Silt Lake formed during retreat of Lillooet Glacier between 1947 and 1973. The glacier has retreated a further 1.8 km up the valley since 1973, but Silt Lake has decreased in area from a maximum of 0.75–0.45 km^2 because of outwash progradation. The proximal sides of the lateral moraines have been deeply

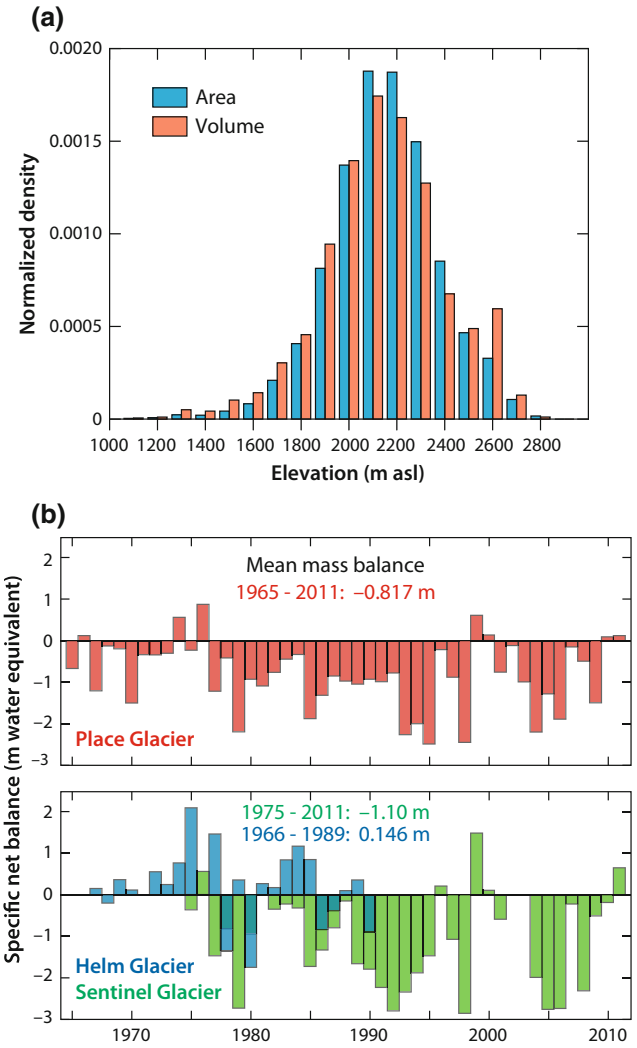

Fig. 22.6 **a** Glacier area and volume in the Lillooet-Harrison basin as a function of elevation. **b** Place Glacier and combined Helm and Sentinel glacier mass balances (data from www.wgms.ch) (courtesy of B. Menounos)

eroded, contributing significantly to sediment delivery to the lake (Fig. 22.8). Colluvium was redistributed by Lillooet Glacier until the late 1960s and then by Lillooet River following glacier retreat. Reconstruction of gully evolution indicates that erosion rates were highest from 1963 to 1973, when the slope became debuttressed as a result of Lillooet Glacier's retreat. Denudation was moderately high immediately before and after that period, a pattern of sediment delivery consistent with the paraglacial concept at the local scale (Church and Ryder 1972). This gully development is a previously unaccounted for source of contemporary sediment production in the Lillooet basin (Jordan and Slaymaker 1991). Recent air photographs show that the morainal slopes have largely stabilized since the late 1970s despite an increase in flood-producing rainstorms since 1980 (Gilbert et al. 2006b). This observation suggests that destabilization

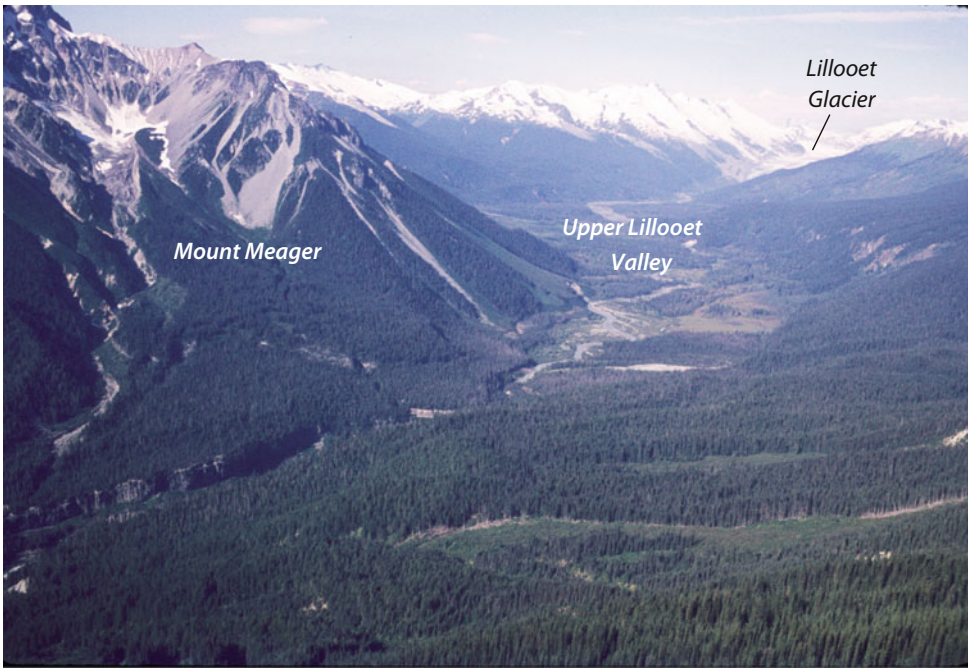

Fig. 22.7 Upper Lillooet Valley with Lillooet Glacier in the distance. The Mt. Meager massif is at the left center (photograph by P. Jordan)

was initiated by debuttressing and perhaps interstitial ice melt rather than high runoff.

Schiefer and Gilbert (2008) examined Silt Lake sediments to determine its trapping efficiency and to characterize sediment delivery from its heavily glacierized catchment. The first sediments deposited in the lake indicate a rapid transition from outwash to varve deposition. Accumulation rates decreased nonlinearly as the lake became free of ice in the early 1970s. The uppermost varves, however, indicate increased deposition attributable to progradation of an outwash plain and delta into the lake. Average contemporary yield of fine sediment in Silt Lake is estimated to exceed 10^3 Mg km^{-2} a^{-1} (or >400 B), a value much higher than long-term yields estimated from lake sediments elsewhere in the Canadian Cordillera (Schiefer et al. 2001) and higher than the non-glacial regime envelope based on fluvial data (Church and Slaymaker 1989). Such a yield exceeds that previously estimated for Lillooet watershed glaciers by Jordan and Slaymaker (1991). The formation and rapid subsequent infilling of Silt Lake have likely had a significant influence on downstream sediment transfers, and the lake has acted as a decoupling agent over the past half-century.

22.6 Hillslopes Experiencing Large Mass Movements

Mass movements in the Lillooet basin form a continuum of sackung, toppling, rockfall, rock avalanches, and debris flows, but only debris flows provide regular and strong coupling of hillslopes to channels.

22.6.1 Sackung

Sackung ("slope sag" in German) is deep-seated, slow movement in rock that typically involves distributed shear. They commonly are manifested by surficial toppling and rockfall, by the formation of sets of uphill- and downhill-facing scarps and grabens and by bulging at the toes of deforming slopes. Sliding, however, is the primary movement mechanism (Bovis 1982; Bovis and Evans 1995, 1996). Sackung occurs where faults, joints, foliation, or bedding in the rock mass allow for slow downslope movement along one or more surfaces at depth (Bovis and Evans 1996). Surficial flexural toppling is self-stabilizing, but deep-seated movements of a rock mass can, in some cases, generate debris flows and debris floods, such as at Mt. Barbour northwest of Pemberton (Fig. 22.9). Many sackung sites identified in the Lillooet basin are situated on the north side of northwest-trending valleys in which there are major faults, notably Mt. Breakenridge along the Breakenridge fault, and several sites between Railroad Pass and North Creek aligned with the Owl Creek fault.

One of the best-documented, slow, deep-seated rockslope movements in the watershed is at Affliction Creek in the Mount Meager Volcanic Complex (MMVC). Radiocarbon dating of buried soils suggests that observed cracks are less than 4300 years old and that movement initiated first in the north and propagated southward, consistent with the direction of retreat of the alpine glacier near the site (Bovis 1990). Instrumented movements indicate spreading of individual cracks of 50–300 cm over a seven-year period, with variations attributed to differences in groundwater conditions

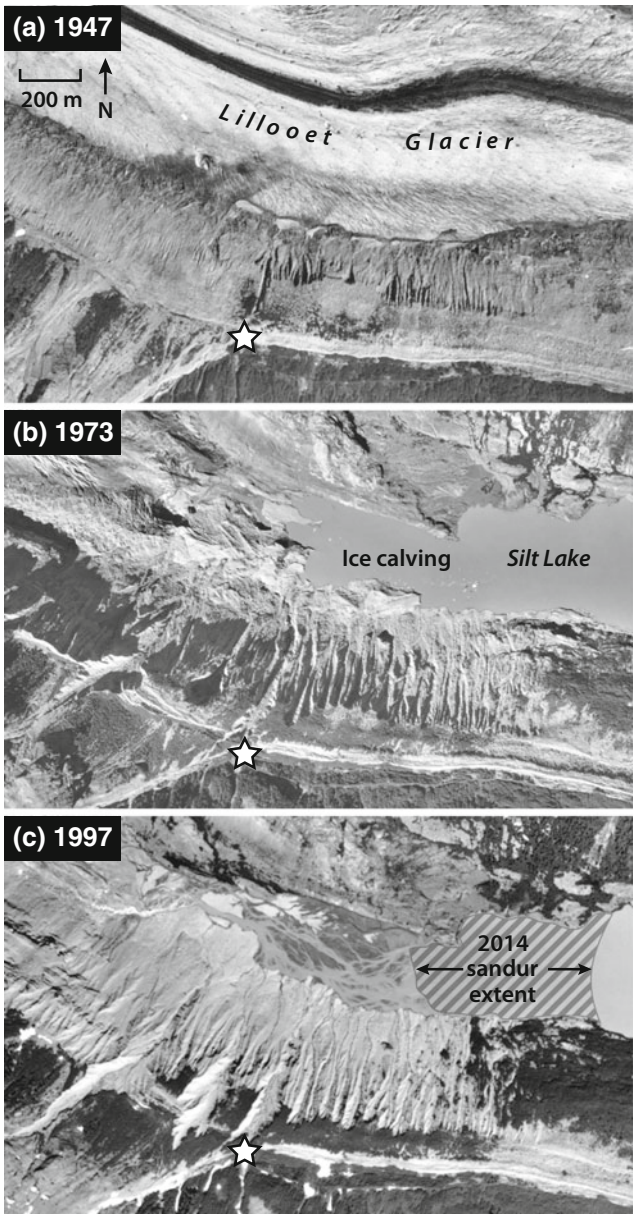

Fig. 22.8 Landscape change at Silt Lake from **a** 1947 to **c** 1997 (courtesy of E. Schiefer). The photographs show a half-century of geomorphic change in the vicinity of the Silt Lake and the lower Lillooet Glacier, including rapid ice retreat, moraine incision, and valley sandur progradation. Georectified imagery from Province of British Columbia aerial photographs X 37:6 BC 79099: 97 and BC B97021:117. Crown Copyright reserved

(Bovis 1990). Similarly, for the Mount Currie sackung near Pemberton, Evans (1987) and Bovis and Evans (1995) reported instrumented movement of several centimeters over a four-year period. Thompson et al. (1997) trenched the main antislope scarp at Mount Currie and demonstrated ongoing movement over thousands of years. Using InSAR, van der Kooij and Lambert (2002) documented displacements of several centimeters per year at the Devastation East site in the MMVC.

22.6.2 Rock Avalanches and Related Debris Flows in Volcanic Rocks

The MMVC is susceptible to edifice collapse (Siebert 1984). A rock avalanche deposit at the foot of Pylon Peak with a hummocky surface that is elevated 130–150 m above Meager Creek has been dated to about 8700 years ago (Friele and Clague 2004). Inset into this deposit, and forming a prominent terrace, is a second rock avalanche deposit that is about 4400 years old. The two rock avalanches had volumes of the order of 2×10^8 m^3. Friele and Clague (2004) hypothesized that now-populated areas in Lillooet Valley, 30–75 km downstream from Pylon Peak, were affected by volcanic debris flows originating from these edifice collapses. To test this idea, Friele et al. (2005) conducted a drilling program in Pemberton Meadows north of Pemberton. They found three discrete volcanic debris flow units at the most upstream site, 32 km from Mt. Meager, dated to 7200, 4400, and 2500 years ago (Simpson et al. 2006). These debris flows were extremely mobile and far-reaching, with travel angles of 2–4°, and were clearly coupled to Lillooet River.

22.6.3 Rock Avalanches in Granitic Rocks

Large rock avalanches in granitic rocks in the Lillooet basin differ from the volcanic landslides in the MMVC in that they are more extensively distributed in the landscape, are less frequent, are smaller by at least an order of magnitude, are composed of coarser fragments, and have steeper travel angles. Their coupling to the river system ranges from nil to substantial.

A well-documented example is the large Mystery Creek rock avalanche (4.0×10^7 m^3) sourced on the northwest ridge of Mount Currie (Eisbacher 1983; Jordan 1987; Nichol et al. 2002). The main body of the deposit straddles Green River valley, is 1.5 km wide, and covers an area of 1.2 km^2. The rock avalanche had sufficient momentum to rise 140 m up the southwest wall of the valley and spill over a ridge between Green and Soo rivers to the present location of Highway 99.

The lowermost 3–4 km of the valley occupied by Salal Creek is filled with up to 100 m of rock avalanche debris derived from Athelstan Peak to the east. The deposits are deeply incised by Salal Creek, but there remains an extensive, low-gradient river flat that extends 1.5 km upstream from the edge of the debris. Wood recovered from lacustrine silt exposed in the riverbank within this area yielded an age of 8100 years, which is a maximum age for the landslide. This event formed a persistent barrier that for a long time interrupted the transfer of sediment from upstream sources.

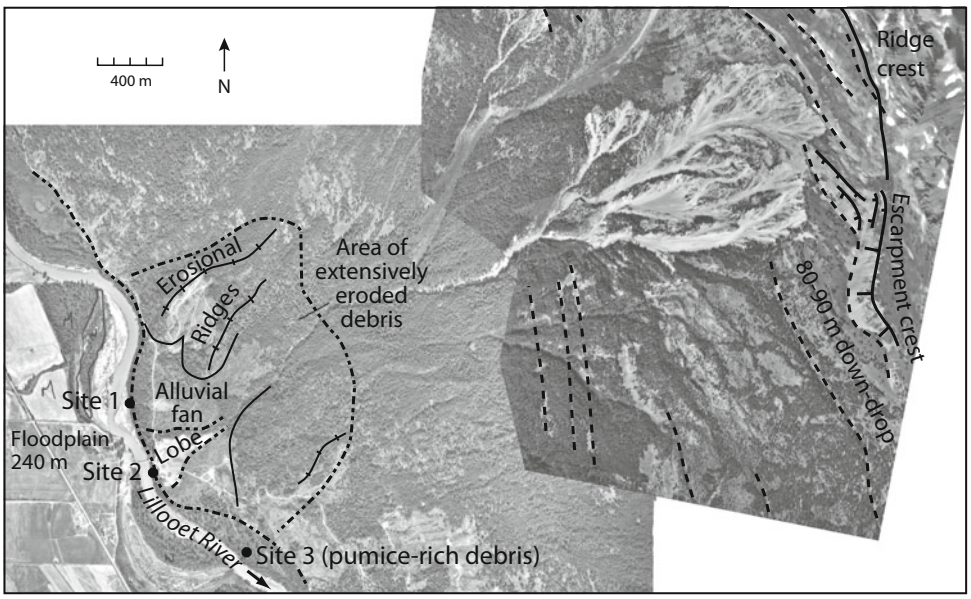

Fig. 22.9 Debris flow channels at Mt. Barbour (courtesy of P.A. Friele)

Another dated landslide in granitic rocks is located 7.5 km downstream from the confluence of Lillooet River and Meager Creek. This event is sourced on the north side of the valley. It left a hummocky deposit elevated 140 m above the modern floodplain that covers an area of 1.5 km^2. The landslide forced Lillooet River to the opposite valley wall. A so-called barrier-defended terrace (cf. Hewitt 1998) preserved at the side of this deposit is underlain by a sequence of lahar and hyperconcentrated flow deposits derived from the MMVC. The base of the sediment sequence dates to about 7000 years ago, which is a minimum age for the landslide.

22.7 Debris Flow Channels

22.7.1 Overview

Debris flows are the dominant sediment transfer mechanism linking upland sediment sources with river channels in the Lillooet basin (Jordan and Slaymaker 1991). Local relief from ridge tops to adjacent river valley floors is about 1500 m, achieved over distances of 3 to 6 km; thus, most small, valley-side channels are on slopes (10–30°) that can transport debris flows. In some parts of the watershed, steep valley-side slopes have structurally controlled bedrock instabilities or Neoglacial moraines that provide abundant sediment to channels. Debris flows are frequent within these channels, with return periods of typically a decade to a century.

In the MMVC, there is abundant sediment related to colluvial activity in incompetent bedrock and to oversteepening of slopes by contemporary glaciers (Holm et al. 2004). Almost all steep stream channels in the MMVC are loci of frequent, often very large debris flows (Jordan 1994; Jakob 1996). Although the volcanic complex occupies only 2 % of the Lillooet basin upstream of Lillooet Lake, volcanic sediments dominate the Lillooet River valley fill (Friele et al. 2005). Read (1990) refers to the MMVC as the most unstable landscape in Canada.

The mobility of debris flows is dependent on water content and the texture of the debris matrix and is especially sensitive to clay content (Jordan 1994). Debris flows originating in granitic rocks typically have a matrix dominated by sand and have negligible clay. On losing confinement, these flows drain rapidly and typically come to rest on slopes of 8°–15°. When such a flow enters a stream channel, it readily mixes with water and changes to a debris flood. In contrast, the hydrothermally altered pyroclastic rocks of the MMVC produce clay-rich debris, and large debris flows from this source are much more mobile, often flowing long distances on gradients of 1°–5°.

Many steep tributary streams have built large fans on the Lillooet Valley floor. Some or all of the sediment delivered by debris flows from tributary basins is in temporary or long-term storage in these fans. Typically, large debris flows deliver most of their sediment to the periphery of the fan or to the river channel, whereas smaller events deposit much of their sediment near the fan apex. The proportion of sediment delivered directly to a trunk stream depends on the form of its channels. The larger rivers (Lillooet, Ryan, and Green) have wide, low-gradient reaches in which the active channel migrates laterally on timescales of decades to centuries. Debris flow sediment may be stored at fan margins in such situations for centuries before being mobilized and carried downstream. In contrast, many tributary streams, for

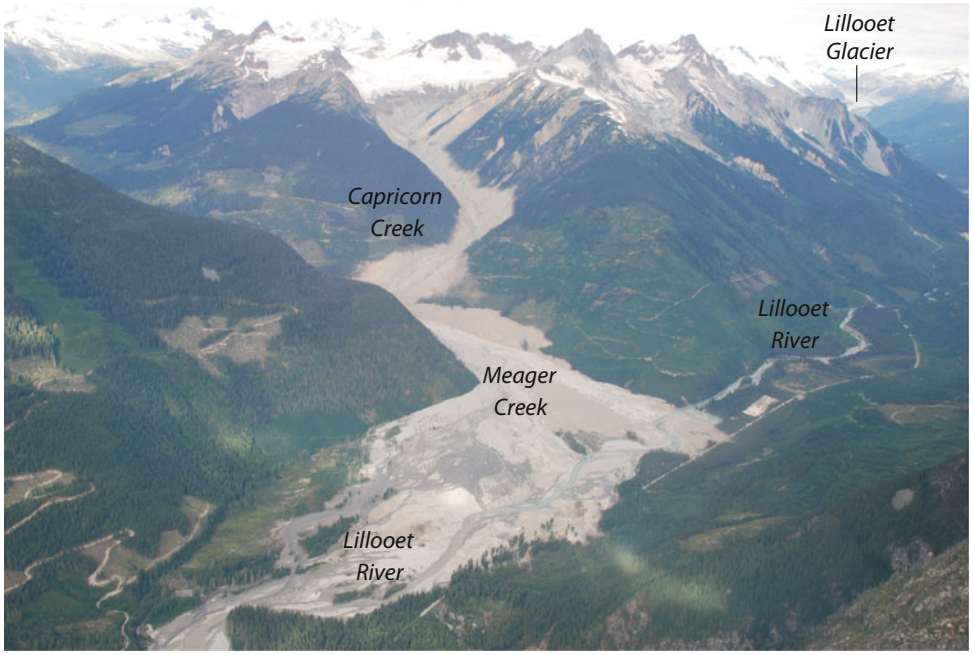

Fig. 22.10 The 2010 Capricorn debris avalanche and debris flow in the Mount Meager Volcanic Complex (oblique photograph taken on August 29, 2010, by J. J. Clague)

example North, South, Pebble, and Salal creeks, are confined, and debris flow sediment is more likely to be delivered directly to the channels.

22.7.2 Large Debris Flows

Large debris flows (10^5 m^3 or larger) in the MMVC typically result from deep-seated landslides in the hydrothermally altered pyroclastic rocks (Friele and Clague 2004), or from the thick colluvium derived from these rocks (Bovis and Jakob 2000). To evolve into debris flows, these landslides must have or incorporate sufficient water for the failed debris to flow.

Prior to the 2010 Mt. Meager landslide (Guthrie et al. 2012), the largest historic landslide in the Lillooet River watershed was the 1975 Devastation Glacier event (12×10^6 m^3), which caused four fatalities (Mokievsky-Zubok 1977). The latter landslide dammed Meager Creek but did not evolve into a debris flow (Jordan 1994). Another large landslide (3×10^6 m^3) flowed down the valley of Meager Creek in 1932 (Carter 1932) and entered Lillooet River. Flow surges were noted 15 km downstream at South Creek during this event (Fougberg et al. 1977). In July 1998, partial collapse of a talus apron that had been debuttressed by alpine glacier retreat spawned a 1×10^6 m^3 debris flow that overran the Capricorn Creek fan and blocked Meager Creek, forming a temporary lake (Bovis and Jakob 2000). The most recent event was the August 6, 2010, Capricorn Creek debris flow (4.8×10^7 m^3) caused by the collapse of the southwest flank of Mount Meager into Capricorn Creek. The flow descended Capricorn Creek, entered the valley of Meager Creek, ran 270 m up the opposing wall, and split into two lobes, one of which ran 3 km up Meager Creek and the other descended Meager Creek and spread out into Lillooet Valley (Guthrie et al. 2012) (Fig. 22.10).

The August 2010 hydrograph of Lillooet River at Pemberton records an initial blockage, followed by partial recovery as the river overtopped and gradually incised its barrier and then, 20 h later, an outburst flood as the barrier on Meager Creek was overtopped and breached. Initial barrier incision mobilized some sediment, and the subsequent outburst flood washed over much of the landslide surface, marking the first stage of fluvial reworking of the deposit. A series of storms in late September 2010 further eroded the barriers and the landslide deposit in Lillooet Valley. These floods induced downstream transport of sediment, leading to deposition of 0.5–1.5 m of sand on bar surfaces along the length of Lillooet River to the delta (Hancock 2011).

22.8 Mid-Valley Sediment Storage Areas and Lillooet Valley Fill Architecture

Lillooet Valley was occupied by a 75-km-long fjord lake at the end of the Pleistocene (Friele and Clague 2004; Friele et al. 2005). Over the past 11,000 years, Lillooet River has infilled the lake over a distance of 50 km to the present head of Lillooet Lake. Assuming an average yield of 400 B, calculated using a sediment budget approach (Slaymaker

1993), Lillooet River has deposited on the order of 15 km^3 of sediment over this period. Friele et al. (2005) inferred the architecture of the Lillooet Valley sediment fill from cores recovered from 12, 10–40 m boreholes on the valley floor between Pemberton and the upvalley end of Pemberton Meadows. The boreholes penetrated the subaerial portion of the postglacial valley fill, which included channel fill, overbank, hyperconcentrated flow, and debris flow facies. Friele et al. (2005) concluded that the cored sediments overlie delta slope and foreslope deposits, which likely comprise a thick sequence of silt and sand. The bedrock floor of the valley has not been mapped, but almost certainly lies well below sea level. The character and origin of the sediments below the lacustrine sequence are unknown, although it is likely that Late Pleistocene ice contact deposits and till occur at depth, and there may be older lacustrine, or even marine, sediments beneath deposits of the last glaciation.

Friele et al. (2005) documented the punctuated nature of sediment deposition on the Lillooet Valley floor. Average long-term (1000–7200 years) aggradation rates are of the order of 1.4–6.0 mm a^{-1}, based on radiocarbon ages obtained from plant remains in drill cores. Valley-wide aggradation of decimeters to meters occurred during extreme events such as hyperconcentrated flows and debris flows triggered by very large landslides in the MMVC. Debris flows deposited valley-wide sheets that were meters thick over valley lengths of many tens of kilometers in minutes to hours. Recorded thicknesses of debris flow deposits in boreholes range from 2 to 8 m. Hyperconcentrated flows left sediment sheets up to 1 m thick in overbank settings and up to 6 m thick in river channels. Friele et al. (2005) also used radiocarbon ages from the boreholes to estimate the position of the Lillooet delta front at different times during the Holocene (Fig. 22.11). Some of the radiocarbon samples were recovered from near the same elevation as Lillooet Lake and could be used directly to define delta front positions, with the caveat that the level of the lake did not change significantly during the Holocene. At most sites, however, the deepest samples were above mean lake level. In these cases, Friele et al. (2005) assumed that the dated sample represents the age of a particular palaeofloodplain surface graded to mean lake level. The corresponding delta front position was determined by projecting the dated sample downvalley to mean lake level along the slope of the modern floodplain surface.

The data indicate average delta progradation rates ranging from 3 to 13 m a^{-1}. The average rate between about 4800 and 3800 years ago is twice that during the interval 7200–5600 years ago. The period with the higher rate includes a flank collapse at the MMVC about 4400 years ago (Friele and Clague 2004) and is recorded by debris flow and hyperconcentrated flow deposits at three of the drill hole sites. The average progradation rate increased over threefold between 2700 and 1800 years ago, a period that includes a large debris flow and an eruption at Mount Meager 2400 years ago. This debris flow is recorded at seven of the drill hole sites by a 2–4-m-thick, valley-filling sheet of diamicton. Hyperconcentrated flow deposits also record the eruption and an associated outburst flood at five of the sites.

Event, or "pulse," progradation rates were much larger than suggested by the average values cited above. Much of the sediment delivered to the delta front may have arrived in periods of hours or a day during large debris flows and hyperconcentrated flows, or in a few decades following these events as the deposits were reworked by Lillooet River. In

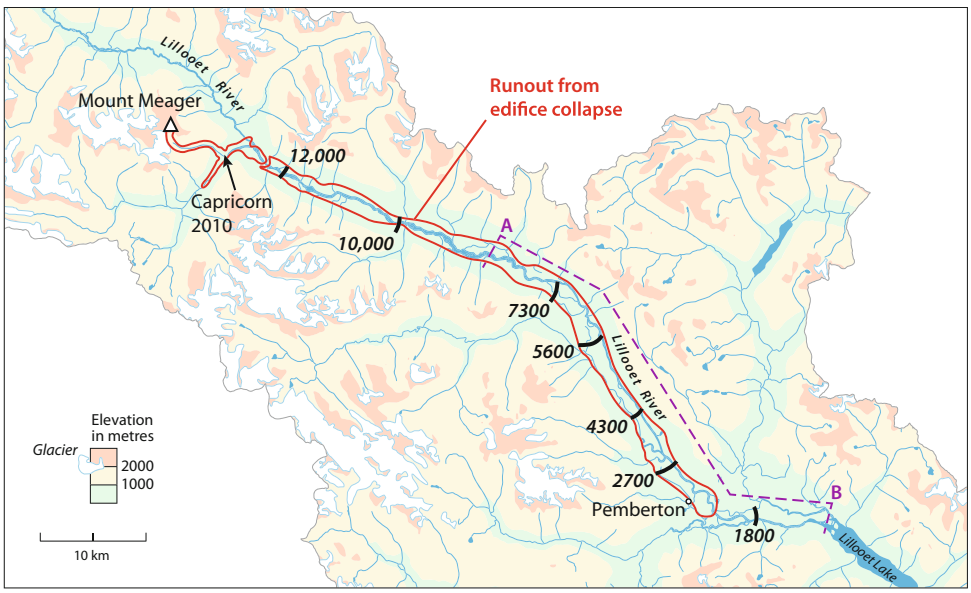

Fig. 22.11 Rate of progradation of Lillooet delta during the Holocene Epoch (courtesy of P.A. Friele and J.J. Clague)

the case of the 4400-year-old landslide, the estimated pulse rate over 50 years is 105 m a^{-1}. The estimated pulse rate for the landslide and eruption 2400 years ago is about 150 m a^{-1} (Fig. 22.11).

Assuming a long-term delta progradation rate of 6 m a^{-1} (Friele and Clague 2004; Friele et al. 2005), the delta front was 60 km upstream 10,000 years ago soon after the valley was deglaciated. However, the stratigraphy reported by Friele et al. (2005) provides no information on postglacial aggradation and delta progradation prior to 7200 years ago. It seems likely that the volume of sediment delivered to the protolake in the upper part of Lillooet Valley during and immediately after deglaciation far-exceeded that deposited during the past seven millennia, and it is likely that the delta front at the time of deglaciation was even farther than 60 km from its present location (Fig. 22.11).

22.9 The Sedimentary Record of Lillooet and Harrison Lakes

Lillooet and Harrison lakes are the two most important sediment reservoirs in the Lillooet River catchment. Lillooet Lake (area 30.4 km^2, maximum depth 137 m) is very much smaller than Harrison (area 223 km^2, maximum depth 270 m), but it is the more significant sediment repository because it is upstream (Fig. 22.12) and because its watershed directly links to both more and larger glaciers and to the very large point source of sediment in the MMVC.

Studies of the sediment fills in the two lakes over more than 40 years using seismic, acoustic, and limnologic techniques in combination with coring have provided insights into the processes operating in the lakes, and the deposits and their relation to their drainage basins. In Harrison Lake, the upper acoustic facies represents accumulation since Lillooet Lake became glacier-free (c. 11.5 ka); the lower facies represents the previous c. 0.4 ka when trunk glaciers were directly connected to the lake. In Lillooet Lake, the upper acoustic facies represents accumulation since 0.90 ka; the lower facies spans the period between 0.90 and 2.50 ka (Desloges and Gilbert 1994a; Friele et al. 2005).

The cores record modern rates of accumulation (Gilbert 1975; Desloges and Gilbert 1991; Desloges and Gilbert 1994b). Accumulation at the delta front was calculated from (a) the geometry of the foreset beds, which slope at an angle of repose to 8 m depth, below which the slope is c. 8°, and (b) rates of horizontal advance indicated in Fig. 22.12 (Gilbert 1975; Jordan and Slaymaker 1991). In October 2003, the largest flood on record deposited sediments across the lake floor in a few days (Gilbert et al. 2006a).

Early Holocene sediments in Lillooet Lake have not been resolved, but two prominent Late Holocene acoustic facies are distinguished by strong reflectors indicative of sediment

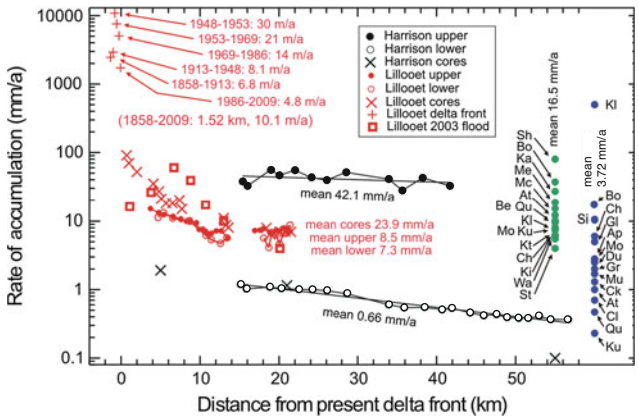

Fig. 22.12 Mean annual rates of sediment accumulation in Harrison Lake (*black*) and Lillooet Lake (*red*) (courtesy of R. Gilbert). The *green dots* represent accumulation based on the maximum thickness of lacustrine sediment in selected lakes of the Canadian Cordillera (see Gilbert et al. 2006a). The *blue dots* represent modern rates of accumulation in selected lakes of the Cordillera (Gilbert and Desloges 1987, 2012; Menounos et al. 2005; Hodder et al. 2006; Schiefer and Gilbert 2008; Gilbert and Crookshanks 2009; Chakraborty et al. 2010; Tunnicliffe et al. 2012). *Ap* Ape; *At* Atlin; *Be* Bennett; *Bo* Bowser; *Ch* Chilko; *Ck* Cheakamus; *Cl* Chilliwack; *Du* Duffy; *Gl* Glacier; *Gr* Green; *Ka* Kalamalka; *Kl* Kluane; *Ki* Kinaskan; *Kt* Kitsumkalum; *Ku* Kusawa; *Mc* McDonald; *Me* Meziadin; *Mo* Moose; *Mu* Mud; *Qu* Quesnel; *Sh* Shuswap; *Si* Silt; *St* Stave; *Wa* Waterton

of coarse texture (Hodder et al. 2006; Gilbert and Desloges 2012). These horizons have been inferentially dated to a major debris flow 900 years ago in upper Lillooet Valley and to the 2500-year-old eruption of Mt. Meager (Desloges and Gilbert 1994a; Friele et al. 2005). Uncorrected for compaction, these data indicate that the rate of sediment accumulation in Lillooet Lake has increased only slightly during the Late Holocene (Fig. 22.12). The higher rate in the past 900 years and the significantly higher modern rate in the proximal part of the lake as measured in sediment cores are more likely due to the advance of the Lillooet River delta than to greater sediment input. Nevertheless, these values are much larger than the modern rates in almost all the other lakes in the Canadian Cordillera (Fig. 22.12). Only in the proximal region of Kluane Lake, Yukon, is accumulation significantly larger (Gilbert and Crookshanks 2009). Even in Silt Lake in front of Lillooet Glacier, the mean rate of 10.5 mm a^{-1} (Schiefer and Gilbert 2008) is less than half the modern rate in Lillooet Lake.

The average rate of advance of the delta into Lillooet Lake during the past 150 years (10 m a^{-1}) compares well with the longer-term rates of Friele et al. (2005), except during pulse progradation events following catastrophic events in the basin. Only the advance of the Slims River delta into Kluane Lake (modern maximum = 74 m a^{-1}; mean since deglaciation = 48 m a^{-1}) exceeds that of the Lillooet delta (Gilbert and Crookshanks 2009). The

significantly lower rate in the late twentieth century may be due more to deepening and widening of Lillooet Lake in 1948 (Slaymaker and Gilbert 1972) than to reduced sediment input.

The amount of clastic sediment that continues through Lillooet Lake and on to Harrison Lake is not known, but based on models (e.g. Brune 1953), it is inferred to be less than 5 %. Turbidity currents that are so efficient in routing large quantities of sediment through some lakes with simple basins do not reach the outlet of Lillooet Lake due to the presence of sills along its length. As well, the assumption that some at least of the finest sediment remains in suspension long enough to be transported through the lake have been called into question by work that shows that flocculation rapidly scavenges most of this fine sediment from the water column (Hodder and Gilbert 2007). These factors, in combination with the lower relief, fewer glaciers, and absence of large amounts of catastrophically derived sediment, mean that modern rates of sediment accumulation in Harrison Lake are among the lowest in the Canadian Cordillera (only Kusawa and Quesnel lakes have lower measured rates). This condition has existed since Lillooet Lake was deglaciated more than 11,000 years ago (Fig. 22.11). Moreover, the consistent downlake decrease in sediment accumulation rates indicates that Lillooet River is a more important sediment source than lakeside sources.

22.10 Implications of Intensified Human Occupancy and Climate Change

The geomorphology of the Lillooet-Harrison basin is well understood based on the evidence presented above. By contrast, the potential effects of intensified human occupancy and climate change on natural processes operating within the watershed are less clear. Human use of the Lillooet-Harrison basin includes development associated with the resort community of Whistler, road and rail transportation through the Green River valley corridor linking the coast with Lillooet Valley, the road network in the valley itself, and the communities of Pemberton and Mount Currie. The growing population on the floodplain of Lillooet River is at the greatest risk, not only from floods (Fig. 22.13) but also from rare volcanic eruptions (Hickson et al. 1999) and landslides. Between 2001 and 2011, there was a 15 % increase in the population of the Squamish-Lillooet Electoral Area C, which includes Whistler and Pemberton. River training starting in 1948 and continuing through the 1950s has elevated the flood risk to residents in Lillooet Valley (Weatherly and Jakob 2014). As the evidence for more frequent extreme rainfall events and warming mounts (e.g. Brooks 2001) and the population and related infrastructure

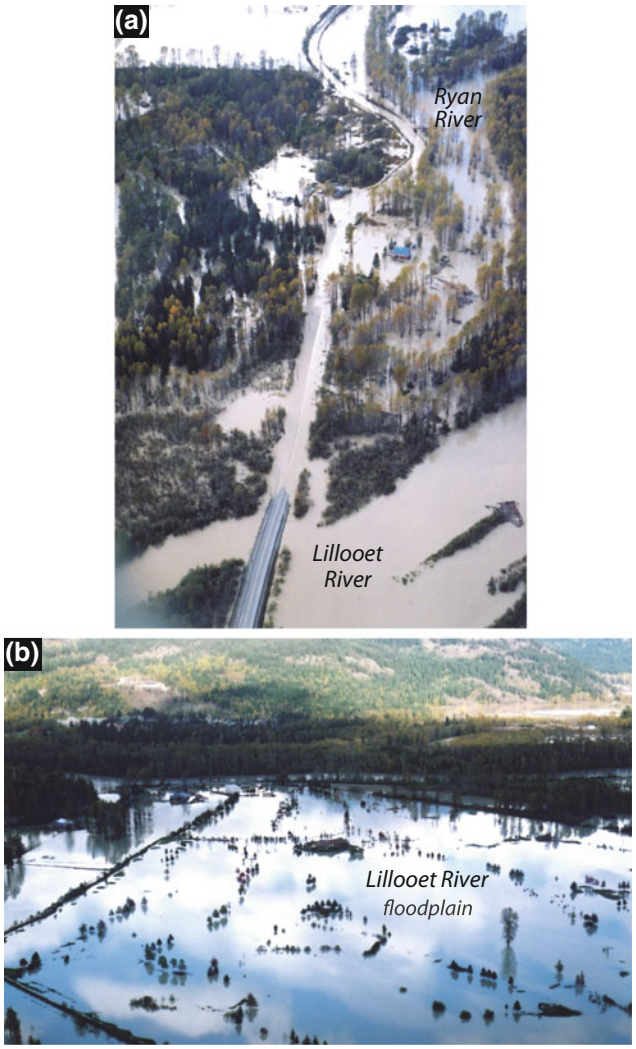

Fig. 22.13 Lillooet Valley under water in October 2003. **a** Junction of the Ryan and Lillooet rivers and **b** floodplain of Lillooet River (photographs by B. Menounos)

in the valley continues to grow, natural hazards and associated risks can be expected to increase (Heideman 2013).

Future climate change scenarios indicate that surface temperatures will rise 2–4 °C by the end of this century, with the result that glaciers throughout western Canada will experience substantial mass loss (Moore and Demuth 2001; Radić et al. 2013). Assuming an adiabatic lapse rate of -0.0065 C m^{-1}, the transient snowline and, by inference, the equilibrium line altitude (ELA) could rise between 300 and 600 m by AD 2100. Even a moderate (20 %) increase in winter precipitation over this period would do little to substantially reduce this rise in the ELA for glaciers in the Lillooet basin. Given the current hypsometry of glaciers in the watershed, few are likely to survive (Fig. 22.14).

The changes that glacier retreat will have on the Lillooet sediment cascade are complex. Rapid glacier retreat may

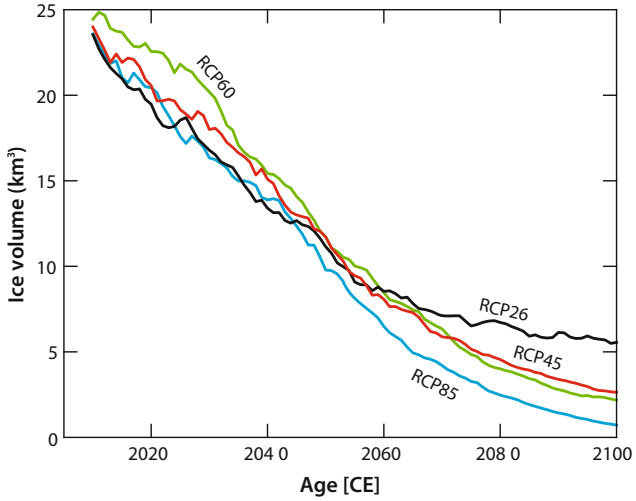

Fig. 22.14 Life expectancy of Lillooet-Harrison watershed glaciers (Clarke et al. 2013, 2015). RCP refers to representative CO_2 concentration pathways, which are modeled scenarios based on increases in radiative forcing by 2100 relative to preindustrial value

initially expose unstable sediment sources, but these surfaces will be quickly vegetated. Proglacial lakes similar to Silt Lake can also form near toes of receding glaciers and act as sediment traps. We hypothesize that deglaciation coupled with rapid revegetation will lead to decreased fluxes of glacigenic sediment in the basin over the remainder of the century. Natural hazards presented by sudden draining of transient ice-dammed and ice-marginal lakes that may appear during glacier recession should also be considered.

Landslides and slowly deforming rock slopes are also inherently natural hazards, and knowledge about their locations and activity is important, especially where population centers might be impacted, such as near Mount Currie near Pemberton and Mount Breakenridge on the east side of Harrison Lake. Despite the potential hazard, only the Affliction Creek linear structural features and the Mount Currie fault scarp have been studied in any detail.

22.11 Conclusions

The juxtaposition of coupled, extremely active and decoupled, relatively inactive sites and their extreme variability over time have proven to be the most distinctive and intriguing finding arising from four decades of intensive research in the Lillooet River basin. The role of ubiquitous, slow, deep-seated gravitational rock slope movements in the watershed as a long-term landscape-shaping process has yet to be fully explored, but is clearly important and may be more important than currently thought (Bovis and Evans 1995, 1996). In addition to the role of sackung in modifying the landscape, it is also the case that sets of uphill- and downhill-facing scarps that facilitate toppling also encourage the deep penetration of groundwater and associated movement of dissolved solids. The role of solution in denudation of the Coast Mountains has a minimal influence on morphology, but mass flux of dissolved solids is important in assessing the overall rate of landscape denudation. Large infrequent events such as rock avalanches are clearly more important in terms of landscape dissection and morphology. Preferred pathways for sediment and solute movement control the location and geomorphic effectiveness of extremely active sites.

A second conclusion concerns the lessons learned from successive conceptual models of the history of paraglacial sediment supply. The paraglacial sediment supply model (Church and Ryder 1972; Church and Slaymaker 1989), which applies to much of the British Columbia landscape, is less applicable in valleys draining Quaternary volcanoes. In these settings, extensive volcaniclastic deposits must be considered characteristic elements of the depositional environment, and any long-term decrease in sediment supply exceeds the span of the postglacial period and is punctuated by sedimentation spikes caused by large landslides. The Jordan and Slaymaker (1991) model drew attention to the importance of volcanic sediment sources and anthropogenic activity in modifying the Church and Ryder model. The model of Friele and Clague (2009), however, suggests that the MMVC dominates the supply of sediment to Lillooet River and that its presence is primarily responsible for the rapid rates of Lillooet delta progradation and aggradation, both over the historic period and through the Holocene. The model of Dadson and Church (2005) is a stochastic model of sediment production that estimates the magnitude and duration of the paraglacial sediment pulse in the Lillooet basin. These evolving conceptual models reinforce the understanding that landscape evolution is hierarchical in the sense that specific spatial and temporal scales must be identified and explicit representation of large landslides and channel network structure must be incorporated in order to improve the predictive capacity of such models (Fig. 22.15).

A third conclusion concerns the role of lake sedimentation in interpreting contemporary and Holocene environmental change, which was pioneered at Lillooet Lake by Gilbert (1975). Lillooet Lake contains one of the finest varve records in the world. Large intra-annual variations in these varves are linked to individual events of nival, glacial, or storm-induced inflow (Gilbert 2003). In addition, large events are clearly distinguishable in the record. For example, the largest flood on record, which occurred in October 2003, deposited in the mid-regions of the lake significantly more sediment in only a few days than in most other entire years (Fig. 22.12). Menounos et al. (2005, 2006), Schiefer and Gilbert (2007), and Schiefer et al. (2006, 2010) have analyzed the varved sediments of Green and Silt lakes. They

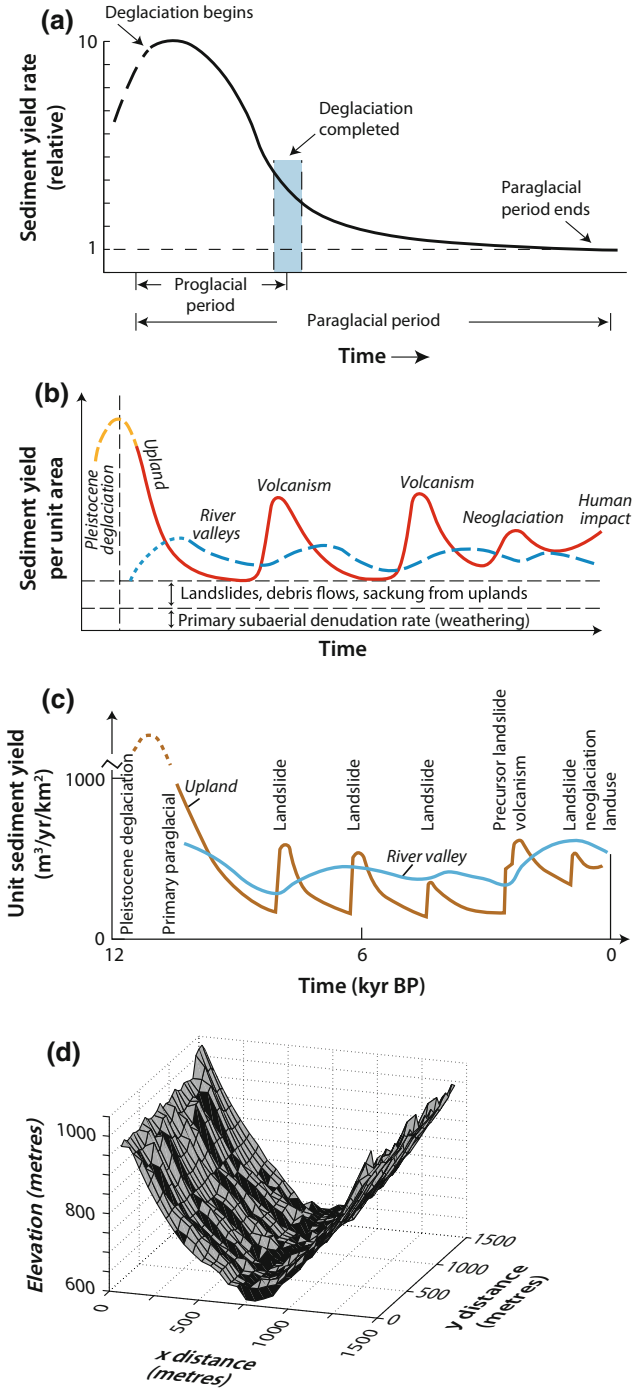

Fig. 22.15 Models of evolution of Lillooet-Harrison basin landscape. **a** General paraglacial model (Church and Ryder 1972). **b** Model of paraglacial sediment yield per unit area specifically for the Lillooet basin (Jordan and Slaymaker 1991). **c** Paraglacial activity at Quaternary volcanoes: an end member in the spectrum of landscape response to Pleistocene deglaciation (Friele and Clague 2009). **d** Stochastic model of sediment production for the Lillooet basin (Dadson and Church 2005)

established a chronology of annual sediment accumulation covering the past 125 years that shows a higher frequency of extreme runoff-sediment yield events after 1940. This change parallels a documented change in climate in the region after 1945 (Desloges and Gilbert 1994b).

A fourth and final conclusion is more tentative. In spite of the intensive research conducted over the past four decades, there remain a number of uncertainties with respect to the hazard and risk implications of intensified human occupancy of the Lillooet Valley floodplain and with respect to climate change. As more frequent extreme rainfall events, rapid glacier retreat, and intensified human occupancy in the valley can be expected to increase the coupling of each of the morphological elements to Lillooet River, the movement of water, sediments, and solutes through the watershed will be expedited. In such a case, risks associated with extreme geophysical events will likely increase.

References

Ballantyne CK (2002) Paraglacial geomorphology. Quat Sci Rev 21:1935–2017

Barrett G, Slaymaker O (1989) Identification, characterization and hydrological implications of water repellency in mountain soils, southern British Columbia. Catena 16:477–489

Bolch T, Menounos B, Wheate R (2010) Landsat-based inventory of glaciers in western Canada, 1985–2005. Remote Sens Environ 114:127–137

Bovis MJ (1982) Uphill-facing (antislope) scarps in the Coast Mountains, southwest British Columbia. Geol Soc Amer Bull 93:804–812

Bovis MJ (1990) Rock slope deformation at Affliction Creek, southern Coast Mountains. Can J Earth Sci 27:243–254

Bovis MJ, Evans SG (1995) Rock slope movements along the Mount Currie "fault scarp", southern Coast Mountains, British Columbia. Can J Earth Sci 32:2015–2020

Bovis MJ, Evans SG (1996) Extensive deformation of rock slopes in southern Coast Mountains, southwestern British Columbia. Eng Geol 44:163–182

Bovis MJ, Jakob M (2000) The July, 1998 debris flow and landslide dam at Capricorn Creek, southwestern British Columbia. Can J Earth Sci 37:1321–1334

Brooks GR (ed) (2001) A synthesis of geological hazards in Canada. Geol Surv Can Bull 548

Brune GM (1953) Trap efficiency of reservoirs. Trans Amer Geophys Union 34:407–418

Carter NM (1932) Exploration in the Lillooet River watershed. Can Alpine J. 21:8–18

Chakraborty K, Finkelstein SA, Desloges JR, Chow NA (2010) Holocene paleoenvironmental changes inferred from diatom assemblages in sediments of Kusawa Lake, Yukon Territory, Canada. Quat Res 74:15–22

Church M, Ryder JM (1972) Paraglacial sedimentation: a consideration of fluvial processes conditioned by glaciation. Geol Soc Amer Bull 83:3059–3072

Church M, Slaymaker O (1989) Holocene disequilibrium of sediment yield in British Columbia. Nature 327:452–454

Church M, Ham D, Hassan M, Slaymaker O (1999) Fluvial sediment yield in Canada. Can J Earth Sci 36:1267–1280

Clague JJ (1986) The Quaternary stratigraphic record of British Columbia: evidence for periodic sedimentation and erosion controlled by glaciation. Can J Earth Sci 23:885–894

Clarke GKC, Anslow FS, Jarosch AH, Radić V, Menounos B, Bolch T, Berthier E (2013) Ice volume and subglacial topography for western Canadian glaciers from mass balance fields, thinning rates, and a bed stress model. J Climate 26:4282–4303

Clarke GKC, Jarosch AH, Anslow FS, Radic V, Menounos B (2015) Projected deglaciation of western Canada in the twenty-first century. Nature Geosci. doi:10.1038/NGEO2407

Dadson SJ, Church M (2005) Postglacial topographic evolution of glaciated valleys: a stochastic landscape evolution model. Earth Surf Proc Landforms 30:1387–1403

Dawson GM (1896) Report on the Area of the Kamloops Map Sheet. Geol Surv Can Ann Rep 1894, NS7B

Desloges JR, Gilbert R (1991) Sedimentary record of Harrison Lake: implications of deglaciation in southwestern British Columbia. Can J Earth Sci 28:800–815

Desloges JR, Gilbert R (1994a) The record of extreme hydrological and geomorphological events inferred from glaciolacustrine sediments. In: Olive LJ, Loughran RJ, Kesby JA (eds) Variability in stream erosion and sediment transport. In: Proceedings of the canberra symposium, vol 224. Internat Assoc Hydrol Sci, pp 133–142

Desloges JR, Gilbert R (1994b) Sediment source and hydroclimate inferences from glacial lake sediments: the post-glacial sedimentary record of Lillooet Lake, British Columbia. J Hydrol 159:375–393

Eisbacher GH (1983) Slope stability and mountain torrents, Fraser lowland and southern coast mountains. Geol Assoc Can, Victoria Section, Field Trip Guidebook no. 15

Evans IS (1990) Climatic effects on glacier distribution across the southern Coast Mountains, B.C. Canada. Ann Glaciol 14:58–64

Evans SG (1987) Surface displacement and massive toppling on the northeast ridge of Mount Currie, British Columbia. Geol Surv Can Pap 87-1A, 181–189

Fischer AG (1969) Geological time-distance rates: the Bubnov unit. Geol Soc Amer Bull. 80:549–552

Fougberg F, Ronayne M, Decker M (1977) Pemberton: the history of a settlement. Pemberton Pioneer Women, Pemberton

Friele PA, Clague JJ (2004) Large Holocene landslides from Pylon Peak, southwestern British Columbia. Can J Earth Sci 41:165–182

Friele PA, Clague JJ (2009) Paraglacial geomorphology of Quaternary volcanic landscapes in the southern Coast Mountains, British Columbia. In: Knight J, Harrison S (eds) Periglacial and Paraglacial Processes and Environments. Geol Soc London Special Publication vol 320, pp 219–233

Friele PA, Clague JJ, Simpson K, Stasiuk M (2005) Impact of a Quaternary volcano on sedimentation in Lillooet River valley, B.C. Sed Geol 176:305–322

Gallie TM, Slaymaker O (1985) Hydrologic controls on alpine stream chemistry. In: Proceedings of hydrol symposium. Nat. Res. Council Can, Quebec City, PQ, 15, pp 288–306

Gilbert R (1975) Sedimentation in Lillooet Lake, British Columbia. Can J Earth Sci 12:1697–1711

Gilbert R (2003) Varves. In: Middleton GV (ed) Encyclopedia of sedimentology and sedimentary rocks. Kluwer Acad. Publ, Dordrecht, pp 764–766

Gilbert R, Crookshanks S (2009) Sediment waves in a modern high energy glacilacustrine environment. Sedimentology 56:645–659

Gilbert R, Desloges JR (1987) Sediments of ice-dammed, self-draining Ape Lake, British Columbia. Can J Earth Sci 24:735–1747

Gilbert R, Desloges JR (2012) Late glacial and Holocene sedimentary environments of Quesnel Lake, British Columbia. Geomorphology 179:186–196

Gilbert R, Crookshanks S, Hodder K, Spagnol J, Stull RB (2006a) The record of an extreme flood in the sediments of montane Lillooet Lake, British Columbia. J Paleolimnol 35:737–745

Gilbert R, Desloges JR, Lamoureux SF, Serink A, Hodder KR (2006b) The geomorphic and paleoenvironmental record in the sediments of Atlin Lake, northern British Columbia. Geomorphology 79:130–142

Guthrie RH, Friele P, Allstadt K, Roberts N, Evans SG, Delaney KB, Roche D, Clague JJ, Jakob M (2012) The 6 August 2010 Mount Meager rock slide-debris flow, Coast Mountains, British Columbia: characteristics, dynamics, and implications for hazard and risk assessment. Natural Hazards Earth System Sci 12:1–18

Hancock CA (2011) Geomorphic Changes to Lillooet River Due to the 2010 Mount Meager Landslide. Honours BSc thesis, Simon Fraser Univ, Burnaby, British Columbia

Harvey A (2002) Effective timescales of coupling in geomorphology. Geomorphology 44:175–201

Heideman M (2013) Flood Hazard and Risk, Lillooet River Basin. PhD thesis, Simon Fraser Univ, Burnaby, British Columbia

Hewitt K (1998) Catastrophic landslides and their effects on the Upper Indus streams, Karakoram Himalaya, northern Pakistan. Geomorphology 26:47–80

Hickson CJ, Russell JK, Stasiuk MV (1999) Volcanology of the 2350 BP eruption of Mount Meager volcanic complex, British Columbia: implications for hazards from eruptions in topographically complex terrain. Bull Volcanol 60:489–507

Hodder KR, Gilbert R (2007) Evidence for flocculation in glacier-fed Lillooet Lake, British Columbia. Water Res 41:2748–2762

Hodder KR, Desloges JR, Gilbert R (2006) Pattern and timing of sediment infill at glacier-fed Mud Lake: implications for Late-Glacial and Holocene environments in the Monashee Mountain region of British Columbia, Canada. Holocene 17:705–716

Hodder KR, Gilbert R, Desloges JR (2007) Glaciolacustrine varved sediment as an alpine hydroclimatic proxy. J Paleolimnol 38:365–394

Holm K, Bovis M, Jakob M (2004) The landslide response of alpine basins to post-Little Ice Age glacial thinning and retreat in southwestern British Columbia. Geomorphology 57:201–216

Jakob M (1996) Morphometric and Geotechnical Controls of Debris Flow Frequency and Magnitude. PhD thesis, Univ. British Columbia, Vancouver, British Columbia, 232 p

Jordan P (1987) Impacts of mass movement events on rivers in the Southern Coast Mountains, British Columbia. Environ. Canada. Inland Waters Dir, Summary Rep IWD-HQ-WRB-SS-87-3

Jordan P (1994) Debris flows in the southern Coast Mountains, British Columbia: Dynamic Behaviour and Physical Properties. PhD thesis, Univ. British Columbia, Vancouver, British Columbia

Jordan P, Slaymaker O (1991) Holocene sediment production in Lillooet River basin: a sediment budget approach. Géogr Phys Quatern 45:45–57

Koch J, Menounos B, Clague JJ (2009) Glacier change in Garibaldi Provincial Park, southern Coast Mountains, British Columbia, since the Little Ice Age. Global Planet Change 66:161–178

Laudon H, Slaymaker O (1997) Hydrograph separation using stable isotopes, silica and electrical conductivity: an alpine example. J Hydrol 201:82–101

Leonard E (1997) The relationship between glacial activity and sediment production: evidence from a 4450-year varve record of Neoglacial sedimentation in Hector Lake, Alberta. J Paleolimnol 17:319–330

Mathews WH (1958) Geology of the Mount Garibaldi map area, southwestern British Columbia. Geol Soc Amer Bull 69:179–198

Mathews WH (1991) Physiographic evolution of the Canadian Cordillera. In: Gabrielse H, Yorath CJ (eds) Geology of the Cordilleran orogen in Canada. Geol Surv Can, Geology of Canada vol 4, pp 403–418

Menounos B, Clague JJ, Gilbert R, Slaymaker O (2005) Environmental reconstruction from a varve network in the southern Coast Mountains, British Columbia. Holocene 15:1163–1174

Menounos B, Osborn G, Clague JJ, Luckman BH (2009) Latest Pleistocene and Holocene glacier fluctuations in western Canada. Quat Sci Rev 28:2049–2074

Menounos B, Schiefer E, Slaymaker O (2006) Nested temporal scale sediment yield estimates, Green Lake, Whistler, British Columbia. Geomorphology 79:114–129

Mierzejewski JK, Labridis C, Campbell G, Rice A (1993) The Fitzsimmons Creek slide and its potential downstream impact at Whistler Village. In: Chantler AG (ed) Whistler and Water: Building a City in the Mountains. BiTech Publ Ltd., Richmond, pp 105–114

Mokievsky-Zubok O (1977) Glacier caused slide near Pylon Peak, British Columbia. Can J Earth Sci 15:1039–1052

Monger JWH, Journeay JM (1994) Guide to the geology and tectonic evolution of the Southern Coast Mountains. Geol Surv Can Open File 2490

Moore RD, Demuth MN (2001) Mass balance and streamflow variability at Place Glacier, Canada, in relation to recent climate fluctuations. Hydrol Process 15:3473–3486

Nichol SL, Hungr O, Evans SG (2002) Large-scale brittle and ductile toppling of rock slopes. Can Geotech J 39:773–788

Owens PN, Slaymaker O (1992) Late Holocene sediment yields in small alpine and sub-alpine drainage basins. In: Walling DE, Davies TR, Hasholt B (eds) Proceedings of the Chengdu Symposium; Erosion, Debris Flows and Environment in Mountain Regions. Internat Assoc Hydrol Sci 209, pp 147–154

Parrish RR (1983) Cenozoic thermal evolution and tectonics of the Coast Mountains of British Columbia, 1: fission track dating, apparent uplift rates and patterns of uplift. Tectonics 2:601–631

Radić V, Bliss A, Beedlow A, Hock R, Miles E, Graham Cogley J (2013) Regional and global projections of twenty-first century glacier mass changes in response to climate scenarios from global climate models. Clim Dyn 42:37–58

Read PB (1990) Mount Meager complex, Garibaldi Belt, southwestern British Columbia. Geosci Can 17:167–170

Reyes AV, Clague JJ (2004) Stratigraphic evidence for multiple Holocene advances of Lillooet Glacier, southern Coast Mountains. Can J Earth Sci 41:903–918

Ryder JM (1981) Geomorphology of the southern part of the Coast Mountains of British Columbia. In: Slaymaker O (ed) High Mountains. Zeitscrift Geomorphol Supp Vol 37, pp 120–147

Schiefer E (2006) Contemporary sedimentation rates and depositional structures in a montane lake, Coast Mountains. Earth Surf Proc Land 31:1311–1324

Schiefer E, Gilbert R (2007) Reconstructing long-term morphometric change in a proglacial landscape using historical aerial photography and automated DEM generation. Geomorphology 88:167–178

Schiefer E, Gilbert R (2008) Proglacial sediment trapping in recently formed Silt Lake, upper Lillooet Valley, Coast Mountains. Earth Surf Proc Land 33:1542–1556

Schiefer E, Hassan M, Menounos B, Pelpola C, Slaymaker O (2010) Inter-decadal controls of total sediment yield in a montane catchment, Coast Mountains. Geomorphology 118:207–212

Schiefer E, Menounos B, Slaymaker O (2006) Extreme sediment delivery events recorded in the contemporary sediment record of a montane lake, southern Coast Mountains. Can J Earth Sci 43:1777–1790

Schiefer E, Menounos B, Wheate R (2007) Recent volume loss of British Columbian glaciers. Geophys Res Letters 34:1–6

Schiefer E, Slaymaker O, Klinkenberg B (2001) Physiographically controlled allometry of specific sediment yield in the Canadian Cordillera: a lake sediment-based approach. Geogr Ann 83A:55–65

Schumm SA (1977) The fluvial system. Wiley, New York 338 p

Siebert L (1984) Large volcanic debris avalanches: characteristics of source areas, deposits, and associated eruptions. J Volcanol Geotherm Res 22:163–197

Simpson KA, Stasiuk M, Shimamura K, Clague JJ, Friele P (2006) Evidence for catastrophic volcanic debris flows in Pemberton Valley, British Columbia. Can J Earth Sci 43:679–689

Slaymaker O (1972) Sediment yield and sediment control in the Canadian Cordillera. In: Slaymaker O, McPherson HJ (eds) Mountain Geomorphology. Tantalus, Vancouver, pp 235–245

Slaymaker O (1987) Sediment and solute yields in British Columbia and Yukon: their geomorphic significance reexamined. In: Gardiner V (ed) Geomorphology '86. Wiley, Chichester, pp 925–945

Slaymaker O (1993) The sediment budget of the Lillooet River basin. Phys Geogr 14:304–320

Slaymaker O (2009) Proglacial, periglacial or paraglacial? In: Knight J, Harrison S (eds) Periglacial and Paraglacial Processes and Environments. Geol Soc London Special Publication vol 320, pp 71–84

Slaymaker O, Gilbert RE (1972) Geomorphic processes and land use changes in the Coast Mountains of British Columbia. In: Macar P, Pissart A (eds) Processus Periglaciaires Ėtudiés sur le Terrain. Univ. Liège, Belgium, pp 269–279

Souch C (1989) Holocene sedimentary environments of the Goat Meadows watershed southern Coast Mountains, British Columbia. Géogr Phys Quatern 43:77–85

Teti P (1984) Time variant differences in chemistry among four small streams. Water Resour Res 20:347–359

Thompson SC, Clague JJ, Evans SG (1997) Holocene activity of the Mt. Currie scarp, Coast Mountains, British Columbia, and implications for its origin. Environ Eng Geosci 3:329–348

Tribe S (2005) Eocene paleo-physiography and drainage directions, southern Interior Plateau, British Columbia. Can J Earth Sci 42:215–230

Tunnicliffe J, Church M, Enkin RJ (2012) Postglacial sediment yield to Chilliwack Lake, British Columbia. Boreas 41:84–101

van der Kooij M, Lambert A (2002) Results of processing and analysis of large volumes of repeat-pass InSAR data of Vancouver and Mount Meager, B.C. In: Proceedings of the international geoscience remote sensing symposium. Inst. Electrical Electronics Eng, New York, vol. 2, pp 1228–1230

Weatherly H, Jakob M (2014) Geomorphic response of Lillooet River, British Columbia, to meander cutoffs and base level lowering. Geomorphology 17:48–60

Mackenzie Delta: Canada's Principal Arctic Delta

23

C.R. Burn

Abstract

Mackenzie Delta, in Canada's western arctic, is North America's largest arctic delta. For over half the year, the rivers and lakes of this vast alluvial plain are ice covered. Permafrost is ubiquitous in the delta and the surrounding landscape. The tree line traverses the delta, separating closed-canopy white spruce forests in southern parts from low shrub tundra and sedge wetlands at the Beaufort Sea coast. The extension of the delta northwards into the ocean is the net result of 128 Mt of sediment brought annually to the delta by Mackenzie and Peel rivers, of which about two-thirds is deposited offshore. The permafrost of the uplands adjacent to the delta is ice rich, with numerous tabular bodies of almost pure ice that formed when the ground originally froze. Throughout the region, the terrain surface is criss-crossed by networks of ice-wedge polygons, initiated by water freezing in cracks opened by ground contraction during winter cooling. A large number of pingos—ice-cored, conical hills up to 50 m high—have developed in the sandy sediments of drained lakes in the area. These features grow as permafrost aggrades in saturated lake sediments. Continual uplift of these little hills demonstrates the enormous forces that can be generated by ground freezing.

Keywords

Ground ice • Ice-wedge polygons • Mackenzie Delta • Permafrost • Pingos

23.1 Introduction

Mackenzie River's delta is North America's largest arctic delta, and, with an area of 13,000 km^2, the world's second largest Arctic delta, smaller than only the delta of the Lena River in Russia. Mackenzie Delta is a maze of lakes and sinuous channels, carrying the discharge of Mackenzie and Peel rivers to the Beaufort Sea (Fig. 23.1). For over half the year, the rivers and lakes are ice covered, and in this period roads and trails can be constructed to connect points accessible in summer only by boat or aircraft (Fig. 23.2). The tree line crosses the delta, with spruce forest covering the southern portions, and willow bushes and sedge wetlands and marshes to the north. The delta is an alluvial plain with lakes occupying up to half of the total area (Mackay 1963). It is 210 km long and on average 62 km wide. The elevation at Point Separation, at its apex (Fig. 23.1), is only about 15 m asl (Mackay 1963). A few bedrock "islands" are exposed in the southeast portion of the delta, the highest being about 30 m above the delta plain.

C.R. Burn (✉)
Department of Geography and Environmental Studies, Carleton University, 1125 Colonel By Drive, Ottawa, ON K1S 5B6, Canada
e-mail: Christopher.Burn@carleton.ca

© Springer International Publishing Switzerland 2017
O. Slaymaker (ed.), *Landscapes and Landforms of Western Canada*, World Geomorphological Landscapes, DOI: 10.1007/978-3-319-44595-3_23

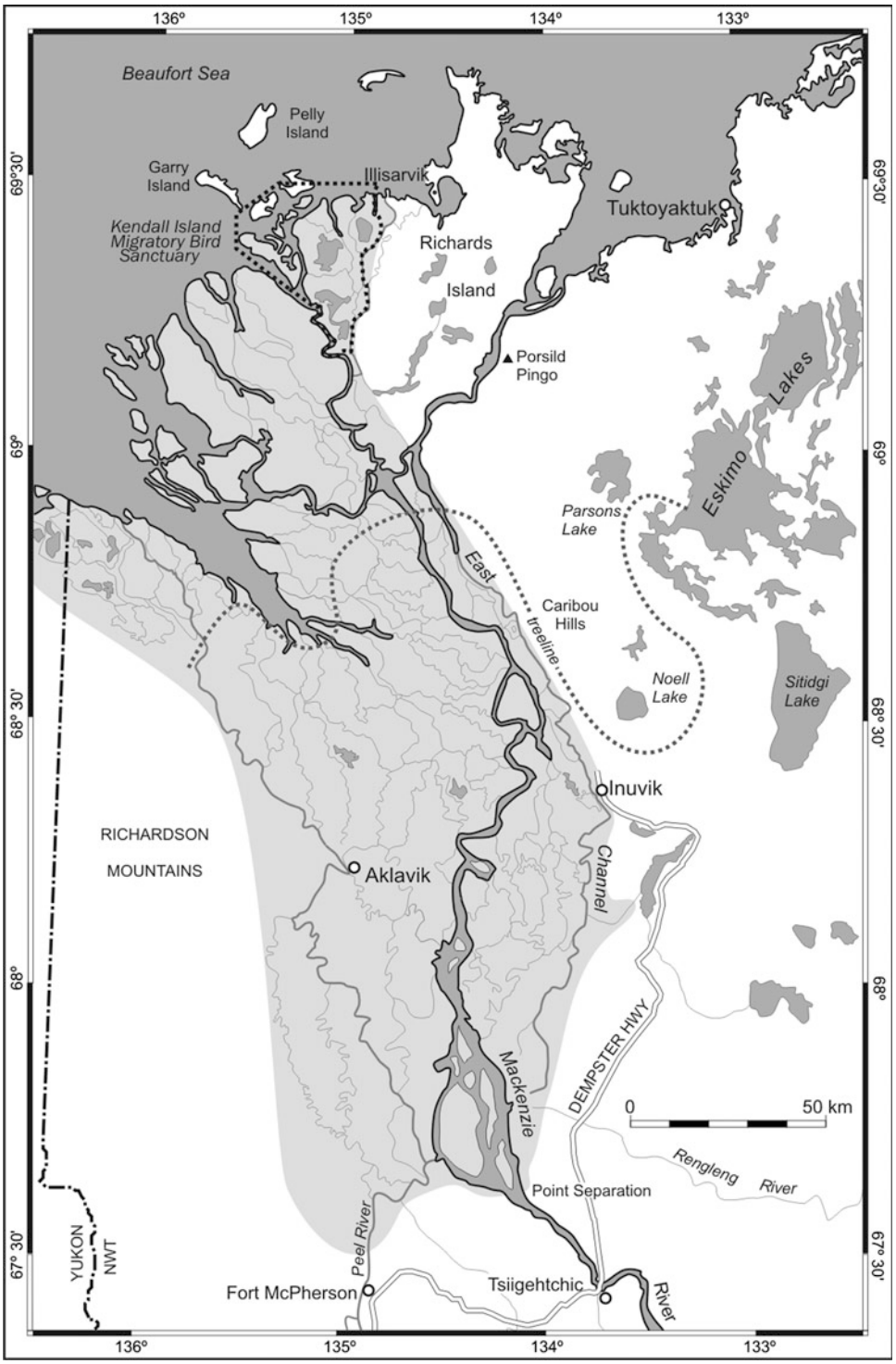

Fig. 23.1 Location map of the Mackenzie Delta area. The tree line is from Mackay (1963; Fig. 70). Cartography by Christine Earl

Fig. 23.2 The Mackenzie Delta in summer, showing part of the network of channels and lakes that dominate the floodplain. Water bodies connected to the silt-laden Mackenzie's discharge are distinguishable by their brown color. The Caribou Hills are in the distance (see Fig. 23.1). Photograph © C.R. Burn

The northern portion of the delta, adjacent to the Beaufort Sea, and the area to the east form the Tuktoyaktuk Coastlands, a rolling, lake-rich plain only a few tens of meters above sea level. The area is a treasure trove of landforms created by the ubiquitous presence of permafrost, ground that remains at or below 0 °C for 2 or more years. A large population of pingos—small, conical, ice-cored hills—is found here (Fig. 23.3), and over vast swaths of the terrain the ground surface is dissected by networks of ice-wedge polygons (Fig. 23.4). Landforms caused by the thawing of permafrost are also abundantly distributed over the landscape, especially where wave erosion along lake shores or at the coast has exposed ice-rich ground (Fig. 23.5).

Mackenzie Delta is a post-glacial feature, building out into the southeastern Beaufort Sea (Fig. 23.1). Most of the ground in the delta is underlain by permafrost, but there are patches, or taliks, of unfrozen ground due to the influence of shifting river channels on ground temperatures (Smith 1976). The Beaufort Delta region is the northernmost extent of the Western Canada Sedimentary Basin that contains considerable discovered and anticipated reserves of oil and gas (Dixon et al. 1994). The delta is an arctic wetland of international significance, providing critical habitat for numerous fish and mammals, and for thousands of migratory birds, as recognized through establishment of the Kendall Island Bird Sanctuary in 1960 (Fig. 23.1). Each summer,

Fig. 23.3 Porsild Pingo, named for Canada's most distinguished arctic botanist, has grown in a lake basin since 1920. The pingo's height is increasing at about 19 cm/year, and it is now over 11 m high (Mackay 1979, 1988). Photograph © C.R. Burn

hundreds of beluga whales use the warm water in the near offshore for calving. Inuvik is the principal settlement in the region, established in 1958 as an alternative to Aklavik, which is flooded in spring about once in every 10 years.

23.2 Geographical Setting

Mackenzie Delta lies at the northern margin of North America. The land to the east and south of the delta is the northwest corner of the Interior Plains of Canada, a sedimentary basin between the Western Cordillera and the Canadian Shield. The hilly uplands east of the delta are generally <100 m above sea level. The western side of the delta is bounded by Richardson Mountains, which rise to over 1500 m and are part of the northernmost ranges in the Western Cordillera. At the foot of Richardson Mountains, the delta fills part of Mackenzie Trough, which trends northwest into the Beaufort Sea (Rampton 1988). The most northern portion of the delta, around the Kendall Island Bird Sanctuary, lies north of Mackenzie Trough. In this area, the hilly uplands have been partially eroded in response to sea level rise and degradation of the ice-rich permafrost that underlies the upland terrain. In the last 1500 years, the area between the remaining hills has been incorporated into the distributary system of the delta.

Fig. 23.4 Ice-wedge polygons in the outer Mackenzie Delta. The growth of ice wedges deforms the adjacent ground, raising the soil on either side of the wedge. The vegetation on these ridges is modified from the plant community that grows in the saturated ground in the middle of the polygons (Morse and Burn 2013). Photograph © C.R. Burn

The climate of the region is bounded by conditions at Fort McPherson and Tuktoyaktuk, where the mean annual air temperatures and total precipitation are −7.3 and −9.8 °C and 310 and 151 mm, respectively (Burn and Kokelj 2009). The ecological gradient evident across the tree line is associated with the climatic gradient through the region, controlled by latitude and proximity to the Beaufort Sea (Burn 1997). The snow cover is established throughout the area by early October, but while it melts at Fort McPherson before the end of May, it remains into June at Tuktoyaktuk, where the presence of sea-ice offshore in early summer lowers coastal temperatures during on-shore winds. Mean annual air temperatures have increased recently throughout northwest Canada, and the rate of change is relatively high in the delta area. The regional temperature was relatively stationary between 1926 and 1969, but subsequently the annual mean air temperature at Inuvik has increased at a rate of 0.77 °C per decade, with the warming primarily in winter. These observations are consistent with projections for climate warming in northern Canada being greatest in winter and least in summer.

Fig. 23.5 Retrogressive thaw slumps on the coast of Pelly Island, outer Mackenzie Delta. These features, formed by thawing of permafrost, are initiated by coastal erosion exposing ice-rich ground. The islands of the outer delta are ice-rich remnants of a surface that has been inundated by the Beaufort Sea. Photograph © C.R. Burn

23.3 Glaciation and Sedimentation

Most of the bedrock beneath the delta is sandstone and shale, and, in the middle of the delta, lies approximately 80 m below the ground surface (Johnston and Brown 1965). The area was entirely covered by the northwest corner of the Laurentide Ice Sheet for several thousand years during the last glaciation, with the maximum extent perhaps reached about 30,000 years ago (Duk-Rodkin and Lemmen 2000). Portions of the outer delta area and Richards Island were ice-free for much of the glaciation, but the Inuvik area was not deglaciated until about 14,500 years ago (Ritchie 1985). Mackenzie Delta has been building seaward for about the last 14,000 years. It is a result of drainage diversion, for before glaciation most of Mackenzie River basin drained eastwards and emptied into the Atlantic Ocean (Duk-Rodkin and Lemmen 2000).

Mackenzie Delta receives about 128 Mt of sediment each year, with 83 % supplied by Mackenzie River and the remainder by Peel River (Carson et al. 1998). About two-thirds of the sediment load is deposited in the ocean and the balance is added to the delta, mostly in the outer margins. The sediment is dominantly silt (Fig. 23.6).

Fig. 23.6 Adventitious roots exposed in a channel bank of central Mackenzie Delta. The development of these roots indicates the active sedimentation in the delta. Photograph by J.R. Mackay

Sea level has risen since glaciation (Hill et al. 1985), and there has been considerable inundation of low-lying areas, erosion of ice-rich ground, and, in total, coastal retreat of about 100 km. As a result, there are four depositional histories for terrestrial sites in the area. First, there is upland terrain that has remained above water level since glaciation. In these areas, the ground is characteristically covered by sand or glacial till. Several hills in the Kendall Island Bird Sanctuary represent such terrain. Second, parts of the outer delta have been submerged by sea level rise, but have emerged as a result of sedimentation (Taylor et al. 1996). Third, in most of the delta the surface has built up over time, emerged from the ocean, and ground level has kept pace with sea level. Finally, in some parts of the hilly terrain, peat deposits have accumulated in low-lying ground.

23.4 Hydrology

The flooding hydrology of Mackenzie Delta creates the stark contrast between the wetlands of the delta plain and the dry terrain of the surrounding uplands. Peak water levels occur in late May or early June, as snow melt from the Mackenzie basin, which extends southwards to Alberta and British Columbia, reaches the coast. There is relatively modest precipitation locally during summer, and discharge into the delta responds to frontal precipitation in Mackenzie River valley and the Peel River basin. Great Slave and Great Bear lakes are permanent reservoirs for Mackenzie River, so there is a constant discharge into the delta in winter, and the water level in the Delta rises as distal channels freeze through.

In late summer, when water levels in the delta are low, storm surges may advance upstream to Point Separation and beyond (Marsh and Schmidt 1993). These surges may inundate the outer delta, but they are rarely sufficient to flood areas south of tree line. Instead, the principal flood hazard occurs in late May and early June when ice jamming may raise water levels to flood much of the delta. The frequency and duration of flooding has systematic effects on vegetation development, so that specific forest communities in the delta are associated with flooding regimes, in addition to the vegetation succession that may be anticipated on aggrading point bars (Pearce et al. 1988). The hydrology of lakes in the delta is closely associated with the hydrograph, for the annual water balance of the area is negative, and over time water bodies will dry up, unless refilled by flooding (Marsh and Hey 1989).

23.5 Channel Migration

Mackenzie Delta is a maze of shifting channels and lakes (Fig. 23.2). Channel migration can be inferred from the vegetation succession on the edges of channels, especially at

Fig. 23.7 Massive ground ice exposed near Tuktoyaktuk. This ice formed after melting of glacial ice from the landscape, as permafrost developed in the exposed sediments. The ice grew from water injected under pressure from below toward the growing permafrost. Sand below the ice was the conduit through which a water supply was maintained to feed the ice body as it grew. Photograph by J.R. Mackay

point bars, which are commonly opposite cut banks. The vegetation succession in the forested areas of the delta follows a path from horsetail (*Equisetum* spp.) in newly emerged river bars, through willow and alder associations (*Salix* spp., *Alnus crispa*), to white spruce forest (*Picea glauca*) (Pearce et al. 1988). Channel migration undercuts the surface vegetation, which then floats away. Flooding commonly leads to sediment deposition on the forest floor, and over time adventitious roots may extend out from tree trunks (Fig. 23.6). However, aggradation of the delta is primarily by infilling of channels, because forest vegetation, particularly logs, are rarely encountered while drilling.

23.6 Permafrost and Ground Ice

Perennially frozen ground is ubiquitous north of tree line and beneath forested surfaces in the middle and upper delta. Permafrost is absent beneath lakes and river channels that do not freeze to the bottom, where the water maintains a mean annual temperature above 0 °C (Smith 1976). Along the edges of channels, permafrost may not be formed where willows capture snow blown off river or lake ice in winter to create deep snow banks that keep summer heat in the ground. In forested terrain, the mean annual ground temperature is about −2 °C. This is considerably higher than the

Fig. 23.8 An ice-wedge exposed near Tuktoyaktuk. The wedge is about 3 m tall. A thermal contraction crack penetrates the wedge. The growth of the wedge, by repeated thermal contraction cracking and infilling with snow melt water, has deformed the sediments on each side of the wedge. Photograph © C.R. Burn

mean annual air temperature, due to the proximity of "warm" water bodies, and because snow in the forest does not drift, but accumulates steadily through the winter. In contrast, in the tundra of the outer delta, where the snow depth is reduced by wind scour, the mean annual ground temperature is about −6 °C (Burn and Kokelj 2009).

Permafrost thicknesses in the delta may be divided into three categories. First, in places that were unglaciated for much of the last 100,000 years, the thickness is on the order of 500 m or more. These environments include parts of the outer delta that were submerged relatively recently, and have now emerged due to sedimentation (Taylor et al. 1996). Second, in much of the delta itself, the thickness is <100 m, as a result of relatively warm ground at depth, due to the abundance of water bodies (Smith 1976). Third, permafrost is thin in the emerging sedimentary environments of Mackenzie Trough, where it is beginning to develop.

Although the permafrost in the delta contains ice throughout its depth, most of the sediments, having been laid down in river channels, were not exposed at the ground surface. As a result, the majority of the permafrost contains ice in the sediment pore spaces only. However, high ice contents develop beneath exposed surfaces, as water is drawn into permafrost from thawed, saturated soil near the ground surface at the end of summer. Characteristically, the uppermost 2–3 m of permafrost are ice rich and release water upon thawing, but below this the soil ice content is close to the pore volume only (Williams 1968).

In the glacial outwash sediments of the outer delta area and Tuktoyaktuk Coastlands, there are extensive bodies of massive ground ice (Fig. 23.7) that formed after deglaciation as permafrost grew in the exposed ground. In some places, glacier ice may lie buried under a veneer of till. Retrogressive thaw slumps, up to 200 m wide, commonly form where such ground ice is exposed by erosion (Fig. 23.5), and the warmth of summer conditions begins to thaw the permafrost.

Ice wedges develop under contemporary conditions in the outer delta, where the winter cold is sufficient to lead to ground contraction and cracking. These linear cracks are filled with snow melt water, leading to veins of ice in the ground. After many years of repeated cracking, the veins develop into wedge-shaped bodies of almost pure ice (Fig. 23.8). Characteristically, these wedges form polygonal networks, with a distance across each polygon of 10–20 m. Ice-wedge polygons are visible in much of the outer delta, but there are also similar features in the forest. In tundra lowlands, these networks are readily visible (Fig. 23.4), but in uplands the appearance is less common, because slope movement obscures their surface expression on hillsides. Ice-wedge polygons are best developed in drained-lake basins, which may cover several square kilometers (Fig. 23.3). Ice wedges in the forests of the delta do not crack under the present ground climate, although they were active until early in the twentieth century (Kokelj et al. 2007).

23.7 Pingos

The landforms of the Mackenzie Delta area have stimulated a considerable amount of the geocryological research in the region, because they are natural indicators of the

Fig. 23.9 Ibyuk Pingo near Tuktoyaktuk. Ibyuk Pingo at 50 m is the tallest pingo in Canada and is currently growing higher at about 3 cm/year (Mackay 1998). Ice-wedge polygons are visible in the drained-lake basins in the lower right of the photograph. Photograph © C.R. Burn

geotechnical behavior of permafrost. The most well known are the closed-system pingos of the Tuktoyaktuk Coastlands (Fig. 23.3), which demonstrate the efficacy of pore-water expulsion during ground freezing to deform permafrost (Mackay 1998).

Pingos—the name is derived from the Inuvialuktun word for a hill—are generally conical, ice-cored hills, which reach up to heights of 50 m, and may be >100 m in basal diameter. In the Mackenzie Delta area, most of the pingos occur in drained-lake basins (Fig. 23.3). There are about 1350 pingos in the region, with the largest being Ibyuk Pingo, a few kilometers south of Tuktoyaktuk (Fig. 23.9). These landforms grow because of the ubiquitous permafrost, the sandy sediments, and the presence of about 5000 lakes in the Tuktoyaktuk Coastlands.

Each year one or two of the lakes drain as the permafrost retaining the water is eroded (Fig. 23.10). Usually, drainage occurs in a matter of hours, and commonly small ponds are left in depressions on the drained-lake bottom. Prior to drainage, permafrost is absent beneath the lake if the water

Fig. 23.10 A small tundra pond on Richards Island that drained in summer 2006. The pond was about 40 m in diameter. Photograph © C.R. Burn

depth is sufficient to prevent freezing of the lake bottom sediments. But after drainage, permafrost invades the talik and the saturated lake bottom sediments freeze. During freezing, water expands as it turns to ice, leading to a greater volume of pore contents than pore space in the unfrozen, saturated sediments. The excess volume is accommodated by expelling water from the location of freezing, and this builds up a pressure inside the talik, because the excess water is confined by the surrounding permafrost (Fig. 23.11). In some cases, pore water has been ejected from the ground along fractures, but in others sufficient pressure develops to deform the aggrading permafrost, leading to heave of the ground surface (cf. Figure 4 in Mackay 1998). The ground is domed up by a lens of water, which freezes over time to form the pingo's core of ice (Fig. 23.12) (Mackay 1978). Pingos may keep growing while the talik continues to freeze: Ibyuk Pingo (Fig. 23.9), which is over 1200 years old, is still growing. In some cases, more than one pingo may form in a drained-lake basin. The pressures involved in lifting a pingo the size of Ibyuk are

Fig. 23.11 Release of water under pressure from the water lens beneath a pingo's ice lens. The geyser flowed when the pingo was punctured by drilling (Mackay 1998). Photograph by J.R. Mackay

remarkable, for the weight of this 50 m high hill is equivalent to that of a 50-story building and demonstrates the forces generated by permafrost aggradation.

The first scientific reports on pingos were provided by Sir John Franklin and Sir John Richardson during their journeys to the Mackenzie Delta area in 1825–1826 and in 1848, but the vast majority of our knowledge of these features and of permafrost in the Mackenzie Delta area comes from the pioneering field research of the late Professor J.R. Mackay, which began in 1951 and continued through to 2012 (e.g., Mackay 1963, 1997; Mackay and Burn 2002).

23.8 Conclusion

Mackenzie Delta is ecologically the most productive landscape in arctic Canada, fundamentally nourished by the annual flood of the Mackenzie River. For millennia, it has provided nesting and staging grounds for thousands of migratory birds and calving grounds for beluga whales. It has sustained a population of indigenous people, hunting and trapping for food and clothing. Analysis of the development of landforms in the region has contributed a large portion of our knowledge concerning the behavior of freezing ground and permafrost. For the last 50 years, there has been considerable interest in the energy resources of the region, especially the significant reservoirs of natural gas, held both in conventional reservoirs and as hydrates. Exploitation of these resources poses substantial engineering challenges, principally due to the presence of permafrost and ground ice in a deltaic setting. These issues are perhaps matched in difficulty by the challenges of managing industrial development in a remote but ecologically critical environment.

Fig. 23.12 Ice core of a pingo exposed in a coastal bluff north of Tuktoyaktuk, August 1955. Photograph by J.R. Mackay

Acknowledgments The research program on permafrost in the Mackenzie Delta area is supported by the Natural Sciences and Engineering Research Council of Canada, Transport Canada, the Polar Continental Shelf Project of Natural Resources Canada, and the Aurora Research Institute, Inuvik, NWT. This chapter is a revised version of Burn (2010), which incorporates helpful suggestions from the editor, Professor Olav Slaymaker, and Professor Piotr Migon.

References

Burn CR (1997) Cryostratigraphy, paleogeography, and climate change during the early Holocene warm interval, western Arctic coast, Canada. Can J Earth Sci 34:912–925

Burn CR (2010) The Mackenzie Delta: an archetypal permafrost landscape. In: Migon P (ed) Geomorphological landscapes of the world. Springer, Dordrecht, pp 1–12

Burn CR, Kokelj SV (2009) The environment and permafrost of the Mackenzie Delta area. Permafr Periglac Proc 20:83–105

Carson MA, Jasper JN, Conly FM (1998) Magnitude and sources of sediment input to the Mackenzie Delta, Northwest Territories, 1974–1994. Arctic 51:116–124

Dixon J, Morrell GR, Dietrich JR (1994) Petroleum resources of the Mackenzie Delta and Beaufort Sea. Part 1: Basin analysis. Geol Surv Can Bull 474, Ottawa

Duk-Rodkin A, Lemmen DS (2000) Glacial history of the Mackenzie region. In: Dyke LD, Brooks GR (eds) The physical environment of the Mackenzie valley, Northwest Territories: a base line for the assessment of environmental change. Geol Surv Can Bull 547, Ottawa, pp 11–20

Hill PR, Mudie PJ, Moran K, Blasco SM (1985) A sea-level curve for the Canadian Beaufort Shelf. Can J Earth Sci 22:1383–1393

Johnston GH, Brown RJE (1965) Stratigraphy of the Mackenzie River Delta, Northwest Territories, Canada. Geol Soc Am Bull 76:103–112

Kokelj SV, Pisaric MFJ, Burn CR (2007) Cessation of ice-wedge development during the 20th century in spruce forests of eastern Mackenzie Delta, Northwest Territories, Canada. Can J Earth Sci 44:1503–1515

Mackay JR (1963) The Mackenzie Delta area, N.W.T. Dep Mines Tech Surv, Geogr Branch Mem 8, Ottawa

Mackay JR (1978) Sub-pingo water lenses, Tuktoyaktuk Peninsula, Northwest Territories. Can J Earth Sci 15:1219–1227

Mackay JR (1979) Pingos of the Tuktoyaktuk Peninsula area, Northwest Territories. Géogr phys Quat 33:3–61

Mackay JR (1988) The birth and growth of Porsild Pingo, Tuktoyaktuk Peninsula, District of Mackenzie. Arctic 41:267–274

Mackay JR (1997) A full-scale field experiment (1978–1995) on the growth of permafrost by means of lake drainage, western Arctic coast: a discussion of the method and some results. Can J Earth Sci 34:17–33

Mackay JR (1998) Pingo growth and collapse, Tuktoyaktuk Peninsula area, western Arctic coast, Canada: a long-term field study. Géogr phys Quat 52:271–323

Mackay JR, Burn CR (2002) The first 20 years (1978/79 to 1998/99) of ice-wedge growth at the Illisarvik experimental drained lake site, western Arctic coast, Canada. Can J Earth Sci 39:95–111

Marsh P, Hey M (1989) The flooding hydrology of Mackenzie Delta lakes near Inuvik, N.W.T., Canada. Arctic 42:41–49

Marsh P, Schmidt T (1993) Influence of a Beaufort Sea storm surge on channel levels in the Mackenzie Delta. Arctic 46:35–41

Morse PD, Burn CR (2013) Field observations of syngenetic ice-wedge polygons, outer Mackenzie Delta, western Arctic coast, Canada. J Geophys Res Earth Surf 118:1320–1332

Pearce CM, McLennan D, Cordes LD (1988) The evolution and maintenance of white spruce woodlands on the Mackenzie Delta, N. W. T., Canada. Holarct Ecol 11:248–258

Rampton VN (1988) Quaternary geology of the Tuktoyaktuk Coastlands, Northwest Territories. Geol Surv Can Mem 423, Ottawa

Ritchie JC (1985) Late-Quaternary climatic and vegetational change in the Lower Mackenzie Basin, northwest Canada. Ecology 66:612–621

Smith MW (1976) Permafrost in the Mackenzie Delta, Northwest Territories. Geol Surv Can Pap 75-28, Ottawa

Taylor AE, Dallimore SR, Judge AS (1996) Late Quaternary history of the Mackenzie-Beaufort region, Arctic Canada, from modeling of permafrost temperatures. 2. The Mackenzie Delta—Tuktoyaktuk Coastlands. Can J Earth Sci 33:62–71

Williams PJ (1968) Ice distribution in permafrost profiles. Can J Earth Sci 5:1381–1386

Herschel Island (Qikiqtaryuk), Yukon's Arctic Island

24

C.R. Burn

Abstract

Herschel Island (Qikiqtaryuk) is Canada's westernmost arctic island, 3 km north of the Yukon coast. The island is underlain by permafrost, in which near-surface temperature increased by 2–3 °C during the twentieth century. Herschel Island was originally a ridge, with a high point currently 182 m above sea level. The ridge was glacially up-thrust from Herschel Basin, a depression in the continental shelf to the east. The ground materials are coastal sediments excavated from the shelf and glacial till. The island is separated from the mainland by a narrow and shallow strait that is <1600 years old. Herschel Island has been a key place for Inuvialuit subsistence activities for hundreds of years, because it shelters the ocean to the east from moving pack ice, creating landfast ice on its eastern side that is habitat for ringed seals. The sea near the island is productive due to upwelling of nutrient-rich water from the deep ocean. Pauline Cove, the only anchorage on the northern coasts of Alaska and Yukon with protection from moving pack ice, became a principal base for overwintering of the western arctic whaling fleet in 1890–1910. The ground contains extensive sheets of buried glacier ice and other massive ice, visible in the headwalls of large retrogressive thaw slumps. The northern coastal bluffs, fully exposed to the ocean, have erosion rates of up to 3 m/year.

Keywords

Beaufort Sea • Yukon Coastal Plain • Coastal erosion • Permafrost • Sea level rise

24.1 Introduction

Herschel Island, *Qikiqtaryuk* ("it is an island") in the Siglit dialect of Inuvialuktun, is 116 km^2 of continuous permafrost that lies on the Yukon-Alaskan continental shelf of the southeastern Beaufort Sea. It is separated from the mainland by 3 km of shallow water in Workboat Passage (Fig. 24.1). The island was named on 15 July 1826 by Capt. John Franklin, who, standing at Kay Point (Fig. 24.2), saw an island "about 15 Miles distant" to which he gave "the distinguished name of Herschel" (Franklin 1828). The Herschels were the premier scientific family of late Georgian England (Burn 2009). Franklin named many features visible along the coast for scientists, especially astronomers and geologists, practitioners of two rapidly developing branches of enquiry, astronomy then breaking the limits of space and geology the limits of time (Fig. 24.2) (Burn 2013). He thereby introduced a remote part of British North America to western science in comfortably metropolitan terms. The island had been inhabited by indigenous people for at least 600 years before Franklin arrived, although artefacts of prior colonizers may have been washed away by the sea (Friesen 2012).

The island shelters the ocean to the east from the prevailing northwest storm winds. A natural harbour, Pauline Cove, has formed near the northeastern tip, bounded by the island, a Holocene alluvial fan that has built out onto the continental shelf, and a spit formed by longshore drift

C.R. Burn (✉)
Department of Geography and Environmental Studies, Carleton University, 1125 Colonel By Drive, Ottawa, ON K1S 5B6, Canada
e-mail: Christopher.Burn@carleton.ca

© Springer International Publishing Switzerland 2017
O. Slaymaker (ed.), *Landscapes and Landforms of Western Canada*, World Geomorphological Landscapes, DOI: 10.1007/978-3-319-44595-3_24

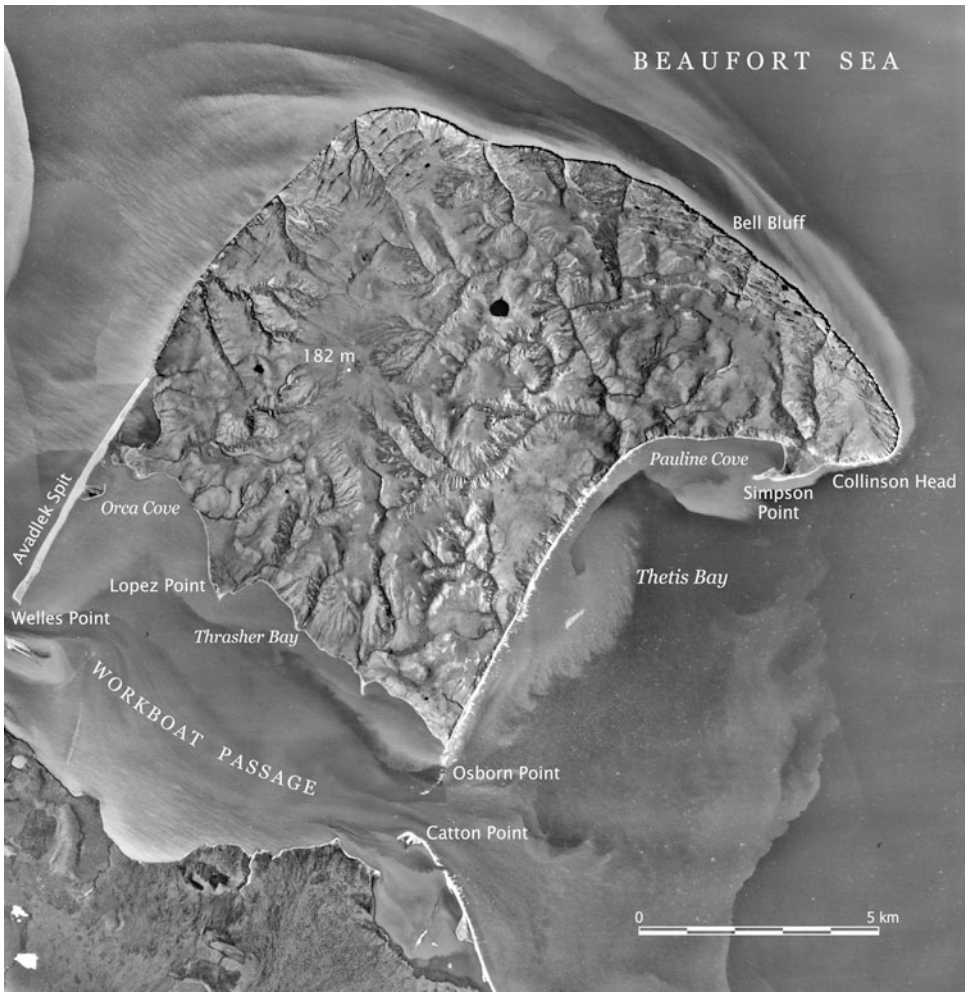

Fig. 24.1 Aerial photograph mosaic of Herschel Island from photographs A22974 212, 213, 214, and A22975 23, 24, 25 (Burn 2012b, Fig. 14). The mosaic was assembled by Jon Tunnicliffe

(Fig. 24.1). This natural harbour was recognized by the western arctic whaling fleet in 1889 (Burn and Hattendorf 2011), and for about 20 years (1890–1910) was a principal depot of the industry (Bockstoce 1986). Subsequently, it became an important point in the western arctic fur trade. Thetis Bay, the ocean sheltered by Qikiqtaryuk, was a winter base for Gulf Canada's vessels during offshore petroleum exploration in the 1970s and 1980s. At present, the settlement at Pauline Cove is the focus of Herschel Island Qikiqtaruk Territorial Park, a contribution of the Government of Yukon to the Inuvialuit Final Agreement (the western Arctic land claim).

The island occupies a strategic position for both indigenous livelihoods and national sovereignty. The ocean near Qikiqtaryuk is remarkably productive due to upwelling at the edge of the continental shelf and the relatively warm water near shore in summer contributed by Mackenzie River. As a result, both fish and marine mammals—ringed and bearded seals, beluga and bowhead whales, and polar bears—are commonly present offshore. Co-management of these resources, and the caribou and grizzly bears that roam the island, is a demonstration of environmental stewardship shared between federal and territorial governments and the Inuvialuit.

24.2 Geographical Setting

The present landscape began to emerge about 110 Ma ago, when the rock masses in what are now the Canadian Arctic islands moved away from the Yukon coast to open up a depression that, over time, became the Beaufort Sea. The

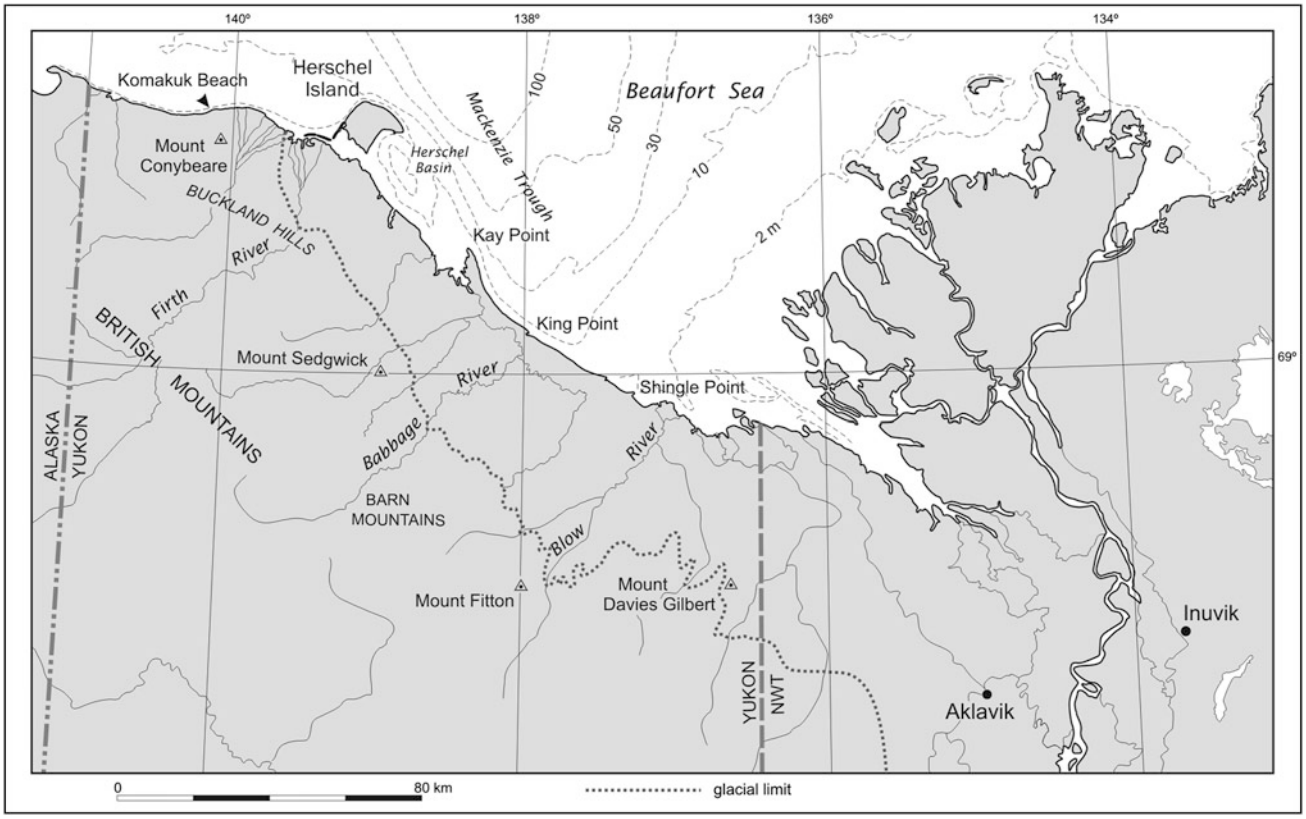

Fig. 24.2 The western Arctic coast of Canada between Mackenzie Delta and the international border. Cartography by Christine Earl

British Mountains of northern Yukon took on their present form between 70 and 45 Ma ago, pushed up by collision between northern Yukon and Alaska and by tectonic forces to the south. Streams eroding these rising mountains deposited their sediment loads in ancestral Beaufort Sea to a thickness of between three and over 12 km. These materials form the bedrock that underlies about a kilometre of unconsolidated sediment on the continental shelf and, having been folded and faulted in the last 10 Ma, contain the traps that hold petroleum reserves. The upper, unconsolidated sediments are of similar origin, but settled out in the ocean as beach or marine deposits.

The continental shelf near Herschel Island is separated by Mackenzie Trough between the Yukon-Alaskan and Canadian Beaufort shelves. The trough is a broad, deep, submarine canyon that rises southeastward, cutting the shelf to make it relatively narrow at Herschel Island (Fig. 24.2). In fact, the island covers most of the shelf. As a result, coastal water must either pass through Workboat Passage or flow over the narrow shelf north of the island. If the surface water moves offshore, it is replaced with cold water welling up from the deeper ocean.

The climate of Herschel Island is bounded by conditions at Shingle Point and Komakuk Beach (Fig. 24.2), where the mean annual air temperatures and total precipitation are −9.9 and −11.0 °C and 254 and 161 mm, respectively (Burn 2012a). Trees are found on the mainland a few tens of km south of the island, but at the coast, the proximity of sea ice lowers early summer temperatures (Burn 1997), and so the growing season is relatively short and the island is covered by dwarf-shrub tundra. As a result, snow thickness is controlled by the topography. Little snow is trapped by vegetation on the wind-swept uplands (Fig. 24.3), but it may accumulate to several metres depth in valleys. The snow cover is established by early October, but while the uplands may be clear by early June, snow banks linger in valleys until late July and August.

Fig. 24.3 View from Collinson Head looking towards Pauline Cove, April 22, 2005. The thin and patchy snow cover is evident (Burn 2012a, Fig. 6). Photograph © C.R. Burn

Mean annual air temperatures have increased recently throughout northwest Canada, and the rate of change is relatively high in the western Arctic (Burn and Kokelj 2009). The first year-round records of air temperature from the Canadian Arctic were collected on Herschel Island by the Rev. Isaac Stringer and his successor missionary, Rev. Charles Whittaker. These records allow calculation of annual mean air temperatures for 1899–1903 and 1905, which are about 3 °C lower than values collected on the island since 1995 (Burn and Zhang 2009). The change is consistent with data from 1898 to the present for Dawson City, the only location in the Canadian North with a continuous record over this period. The warming has been concentrated in late autumn and winter (November–January), with little change in the summer months.

24.3 Glaciation and Sedimentation

Herschel Island is a glacially upthrust moraine, formed during the last glaciation when the Laurentide Ice Sheet reached its maximum extent in NW Canada (Fig. 24.2) (Rampton 1982). At the time, sea level was 100 m or more below its present position and the continental shelf was exposed (Hill et al. 1985). Deformed bedding in the sediments exposed in the island's northern cliffs has been reported for some time (e.g. O'Neill 1921), but the glaciotectonic origin of the island was identified by Ross Mackay (1959), who recognized the deformation of sediments and faulting visible at the surface (Fig. 24.1) to be indicative of upthrust beds. He pointed out several examples of similar stratigraphy along the Yukon coast. Mackay also discovered

Herschel Basin, a depression on the continental shelf east of the island, whose volume below the shelf's surface is approximately the same as that of the island. He pointed out that, with the exception of the coastal bluffs, the bathymetric slope from the basin to the island's coast is continuous with hill slopes leading to the island's high point at 182 m asl. Mathews and Mackay (1960) presented a geotechnical analysis of the glacitectonic deformation, in particular assessing the pore water pressure conditions required to allow permafrost beds to be upthrust at the margin of the ice sheet. The deformed sediments are mostly beach sands and marine silts and clays. Ice wedges and veins in these deposits 20–60 m below the surface indicate that the ground was upthrust as permafrost (Fig. 24.4) (Mathews and Mackay 1960).

The skull of a Yukon horse (*Equus lambei*) found near the top of a high bluff on the northern coast by Stephen Wolfe in 1986 was determined to be between 16 and 17,000 years old (Zazula et al. 2009), indicating that the ridge had been deglaciated by then. For several thousand years the island would, therefore, have been part of Beringia, roamed by woolly mammoths and other members of the distinct fauna that occupied unglaciated NW North America and Siberia, and whose bones have been found on the island (Zazula 2012).

Sea level has risen since glaciation. The current rate of sea level rise is 3.3 mm/year, slightly faster than the late Holocene average (Campeau et al. 2000). Workboat Passage is <3 m deep, so the island was probably only separated from the mainland in the last 1600 years, perhaps as recently as 600 years ago (Burn 2009). The late Inuvialuit elder Jean Tardiff of Aklavik recalled that the people who lived on what is now the island used to be called *Nuvuuyaqmiut* ("people of the point") but were later known as *Qikiqtaryukmiut* ("people of the island") (Nagy 1994).

Throughout the island the ground is covered by a veneer of till, remnant from the ice sheet. The till lies in many places above massive ground ice, some of which is relict glacier ice (Fig. 24.5) (Fritz et al. 2011). The massive ice is concentrated in the upper 15 m of the ground. Extensive retrogressive thaw slumps have developed in this remnant glacier ice, especially along the eastern coast of the island (Fig. 24.6) (Lantuit and Pollard 2008). They resemble the "megaslumps" of the Peel Plateau to the southwest of Mackenzie Delta that are also developed in such relict ice (Kokelj et al. 2015).

Fig. 24.4 Northern bluffs of Herschel Island, with ice wedges at depth in deformed bedding and blocks that have fallen to the bottom of the cliffs. Photograph © Mary Beattie, April 2009, used with permission

The surficial materials have been exposed to the elements for millennia, so most salts have been leached from the seasonally thawed active layer. In the upper metre or so of permafrost the salinity is higher, because this stratum was part of the active layer only during the early Holocene, 10,000–8000 years ago, when the region's summer climate was warmer than at present (Burn 1997). But below the thaw unconformity which marks the maximum active layer thickness, the sediments are saline (Kokelj et al. 2002). These soils may be released from permafrost by thaw slumps to form a fresh surface for plant colonization. However, the

Fig. 24.5 Exposed ground ice in a thaw slump on the coast of Thetis Bay. The massive ice below the V-shaped ice wedges is ice remnant from the last glaciation (Burn 2012b, Fig. 8). Photograph © Louis Schilder, August 2008, used with permission

salt-tolerant plants that thrive on such surfaces are quite distinct from those that grow in undisturbed tundra (Kennedy 2012).

24.4 Upwelling and Bathymetry

Mackenzie Trough enhances upwelling from the deep ocean on to the continental shelf, especially when the surface stress on the ocean is from the east. At these times, flow of surface water off the shelf is partially replaced by upwelling water, which flows more easily up the submarine canyon than over the abrupt margin of the rest of the shelf. The surface flow may be generated by wind or sea-ice movement, and ocean water may be uplifted over 600 m from its original depth (Williams and Carmack 2012). The upwelling water moves westwards past the northern cliffs of Herschel Island, as evident on Fig. 24.7, a visible-spectrum satellite image taken during an upwelling event. Figure 24.8 shows the sea-surface temperature on the same day as Fig. 24.7 was taken. The warm Mackenzie outflow is visible, as is extremely cold water that has emerged from Mackenzie Trough and is flowing off the north coast of Herschel Island. In winter the situation is reversed, with upwelling water being relatively "warm" in comparison with the surface layers. In that season, upwelling breaks up surface sea ice, so that conditions to the north and west of the island are extremely rough, while the landfast ice in Workboat Passage and to the east is smooth (Fig. 24.9). The smooth ice forms viable habitat for ringed seals.

24.5 Coastal Erosion

The unconsolidated and, in places, ice-rich, sediments of the western arctic coastlands are amongst the most erodible coastal sediments in Canada (Solomon 2005). Coastal erosion at Herschel Island varies between its four sides due to

Fig. 24.6 Retrogressive thaw slumps on the coast of Thetis Bay, July 2015. Reactivation of stabilized slumps is caused by coastal erosion. The upper feature is about 400 m across. Photograph © C.R. Burn

relative exposure to storms, which are strongest from the NW. The high northern and western bluffs contribute the most sediment per linear metre of coastal retreat, commonly collapsing as frozen, undercut blocks (Fig. 24.4). The retreat rates are highest on these coasts and at Collinson Head (up to 3 m/year), as they are the most exposed to the Beaufort Sea (Lantuit and Pollard 2008). The most stable coast is in Workboat Passage, a strait protected by gravel spits at each end (Fig. 24.1), and therefore relatively calm water (Hill 1990). The spits themselves are the product of longshore drift of till eroded from the island and winnowed of fines by the sea. The spit at Pauline Cove is a thaw-stable surface on which buildings have been erected, including the Yukon's oldest frame structure, built in 1893 by the Pacific Steam Whaling Company. The spit formed from erosion of Collinson Head (Fig. 24.1). The longest spit is Avadlek, a feature on which several ancestral Inuvialuit dwellings have been excavated (Friesen 2012).

Retrogressive thaw slumps, initiated by coastal erosion, are common in the glacially up-thrust permafrost beds between Shingle and Kay points (Fig. 24.2) and are well developed along the Thetis Bay coast of Herschel Island. Headwall retreat rates of up to 15 m/y have been measured for these features, which are developed in massive icy sediments (Lantuit and Pollard 2008). Several generations of slumps may occur in the same area, because coastal erosion rejuvenates stabilized slumps (Fig. 24.6).

As we have seen, sea level rise is responsible for the island itself through creation of Workboat Passage. However, Herschel Basin is separated from Mackenzie Trough by Herschel Sill, a submarine ridge that has a maximum depth of about 14 m below sea level. Coastal erosion would not have affected the east side of the island until well after the Beaufort Sea reached this level, likely about 3500 years ago (Hill et al. 1993). In the last few decades, sea level rise has begun to threaten the infrastructure on

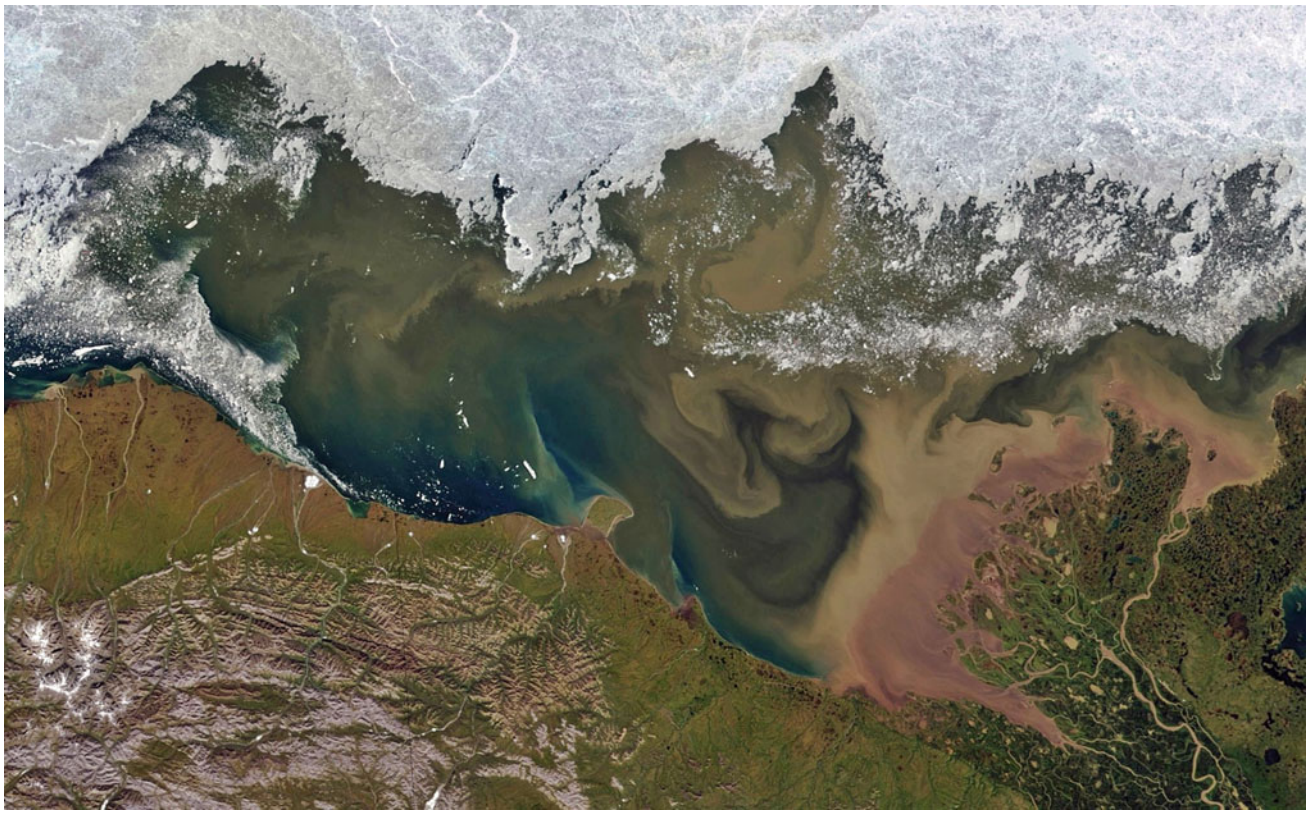

Fig. 24.7 Satellite image for July 26, 2006, showing the sediment plume of Mackenzie Delta and sediment streaming off Herschel Island (Williams and Carmack 2012, Fig. 2). Image prepared by Bill Williams and used with permission

Simpson Spit. Strong east winds blowing for several days may raise the water level in Pauline Cove to flood the spit (Fig. 24.10).

24.6 Permafrost and Ground Ice

Permafrost on Herschel Island is continuous and is found beneath a shallow active layer, commonly <60 cm thick. The temperature at 15-m depth, close to the depth of zero annual amplitude has been measured since 2002 at a site on Collinson Head. The value, of −8 °C, is representative of many sites on the windswept uplands of the island where little snow accumulates (Fig. 24.3). At series of 10 instrumented sites leading up to Collinson Head, the annual mean temperature in 2003–2006 varied between −8 and −4 °C, with the warmest location in a small valley where snow, blown off the top of the island accumulates early in winter (Burn and Zhang 2009). The thickness of permafrost at Herschel Island is unknown, but the regional geothermal flux of 0.05 W/m^2 translates into a geothermal gradient of about 40 m/°C. Under present surface conditions, we might then expect an equilibrium thickness of over 300 m, but if near-surface conditions were cooler in the past, the thickness would be greater.

The early Holocene thaw unconformity, described above, is a key indicator of permafrost history on the island. The horizon between the bottom of the present active layer and the unconformity represents ground in which permafrost has aggraded over the last 8000 years. The ice content in this layer is limited over large tracts of the island because summer conditions on the island are relatively dry. In contrast, the alluvial fan at Pauline Cove presents extremely high ice contents in the near-surface permafrost that has aggraded beneath a moist surface as sediment has accumulated on the fan (Fig. 24.11).

Numerous ice wedges, the products of long-term thermal contraction cracking in permafrost, have been observed in the head walls of thaw slumps (Fig. 24.5). However, tundra polygons, the most readily identified surface expression of ice-wedge development, are not common in the island's

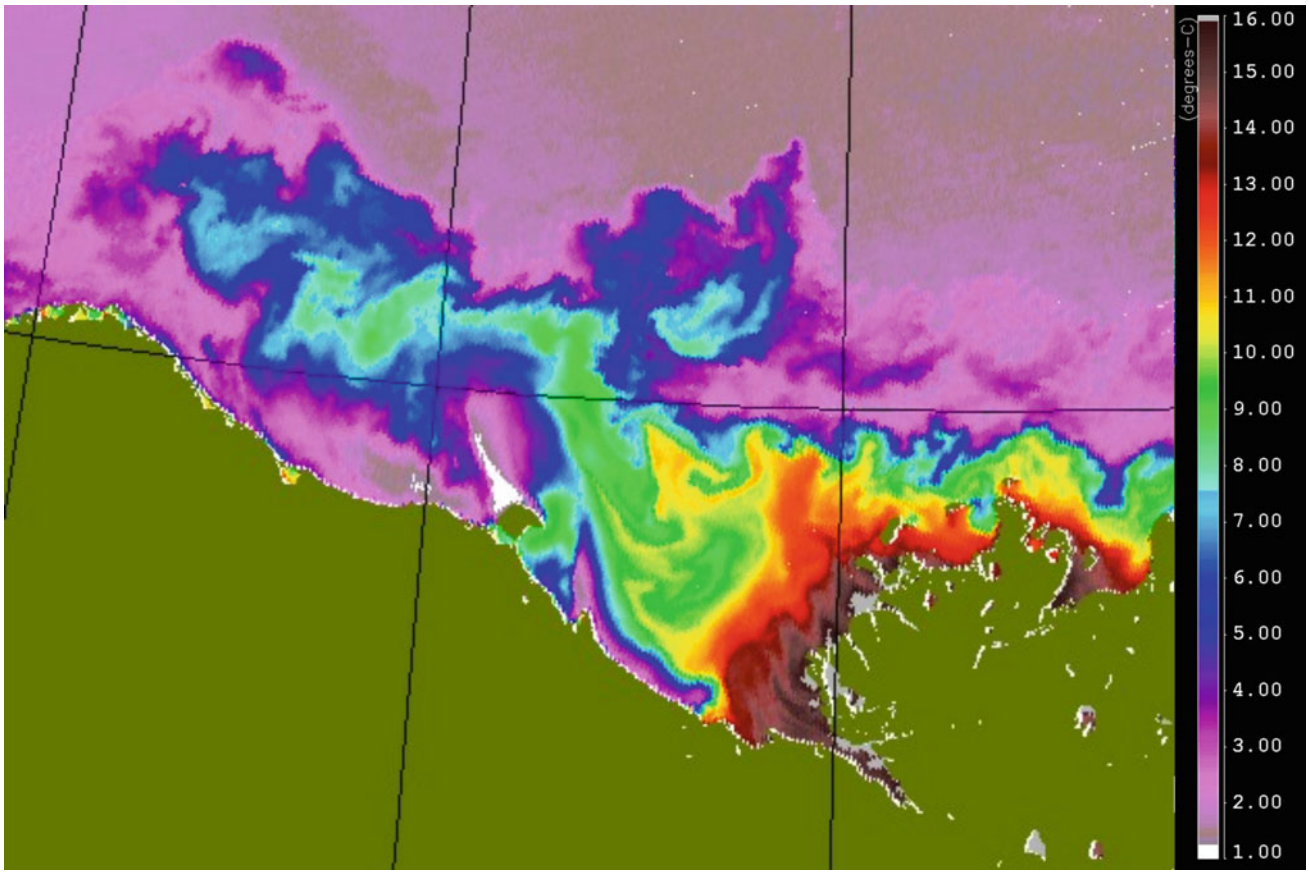

Fig. 24.8 Sea-surface temperature on July 26, 2006, the same day Fig. 24.7 was taken (Williams and Carmack 2012, Fig. 3). Frigid water is streaming off Herschel Island. Image prepared by Bill Williams and used with permission

rolling terrain. Instead, many of the ice wedges develop on hill slopes, where the surface is slowly eroded by slope movement. The soil creep obscures the troughs above the ice wedges that are characteristic of lowland polygons. In the few places where troughs are well developed on the hill sides, they are several metres in width, because they have formed from melting of the wedges, which are wide at the ground surface (Fig. 24.5).

The whalers recognized the permafrost as a medium in which they could store meat and other items that would benefit from remaining frozen. In March 1891, they built the first of several ice cellars, blasted out of the ground at Pauline Cove, and covered with a sod roof. One of these remains viable today as a natural freezer, but five others have collapsed. The functioning cellar is about 3 m deep by 3 m wide by 4 m long. The temperature within the cellar rises to about −2 °C in summer and drops to about −12 °C in winter.

24.7 Climate Change Effects

There are three principal elements of the arctic environment that we anticipate will be significantly altered as climate change continues and, likely, accelerates. These are sea level, the extent of sea ice, and the state of permafrost. Changes in the extent of sea ice in summer are already evident and well recognized (Stroeve et al. 2007). In the vicinity of Herschel Island, little ice may be visible from mid July until September. The reduction in sea-ice extent has been accompanied by an increase in the length of the ice-free season. The whaling ships kept records of the date they were frozen fast in Pauline Cove, which in 1890–1900 was on average October 8. Amundsen's *Gjoa* spent the third winter of her transit of the Northwest Passage at King Point (Fig. 24.2), where she was frozen in on September 7, 1905. Amundsen recorded that he could walk around his ship on September 9th that year. Comparable sea-ice conditions in 2000–2010 were observed

Fig. 24.9 **a** Rough ice on the west coast of Herschel Island, and **b** landfast ice in Thetis Bay, where the SDC offshore drilling platform was berthed for winter 2008–09. Photographs by Mary Beattie, April 2009, used with permission

annually by satellite between October 22 and November 17. Data on advances in the date of break-up are less clear, because the whalers used dynamite to blast their way out of Pauline Cove. Since the greatest increase in mean monthly temperature has occurred in late autumn, we may expect further delay in freeze-up if such change continues.

A longer open-water season is key to anticipating an increase in the rate of coastal erosion at Herschel Island. Rising sea level is the factor that most threatens the infrastructure on the island (Fig. 24.10). During the first 20 years of the twentieth century, the Royal North-West Mounted Police reported flooding of the spit at Pauline Cove only once. In 1995–2014, the spit has been flooded every 2 or 3 years for periods of up to 10 days. The rate of sea level rise in the Beaufort Sea is increasing: at present the incremental change is 3.3 mm/year, while in the late Holocene the rate was closer to 1 mm/year (Campeau et al. 2000; Manson and Solomon 2007).

The ground temperature profile in permafrost is unequivocal evidence of long-term climate warming in the

Fig. 24.10 The spit at Pauline Cove inundated by a storm surge in August 2010 (Olynyk 2012, Fig. 14). Photograph used with permission of Govt. of Yukon

western Arctic (Burn and Zhang 2009). The profile was obtained by drilling to 42 m depth on Collinson Head and installing thermistors throughout the distance between the depth of where the temperature does not fluctuate annually, about 15 m, and the bottom of the hole (Fig. 24.12). The profile has been reconciled numerically with the change in climate since the beginning of the twentieth century that has been described above. The numerical simulation suggests that the ground temperatures have been affected to about 120 m depth and that the change in temperature at 20 m has been 3 °C. The mean annual ground temperature, −8 °C, is low enough for it to be sensitive to climate warming because little ice melts as temperature rises in such cold ground. The deep thermistor cables on the island are well suited to monitoring the continuing effects of climate change on ground temperatures.

Changes to the active layer have been measured in the period since 1987, when the first soil surveys were made on the island. The terrain surface in the uplands was then dominated by mud hummocks (Fig. 24.3), but now the ground has a well-developed vegetation cover (Kennedy 2012). Active layer thicknesses have increased from about 30 cm in the late 1980s to 50 cm in similar terrain at present (Smith et al. 1989; Burn and Zhang 2009). Thawing of

Fig. 24.11 Ice-rich permafrost in the upper metre of ground at the alluvial fan near Pauline Cove. The ice wedge has grown upwards with deposition of sediment. The trowel is 22 cm long. Photograph © C.R. Burn

ice-rich, near-surface permafrost has accompanied this deepening. The greening of the island may be due to nutrients released into the active layer from the degrading permafrost, because the summer climate has changed little recently. Active layer thickening is driven by warming of winter conditions, which prevent the ground from cooling as much as before and so facilitate greater thawing in summer (Burn and Zhang 2010).

24.8 Conclusion

Herschel Island is a relic of the last glaciation, slowly being eroded by the sea. Its location and interaction with the Beaufort Sea has endowed it with cultural significance for the Inuvialuit and economic prominence in the region's recent history. It is now protected as a Territorial Park to respect its importance for the Inuvialuit, and this also allows research, especially on the permafrost coast, to flourish there. Along with Ivvavik and Vuntut national parks on the adjacent mainland, the island forms a reserve in the extreme northwest corner of Canada that is critical for the sustainability of the Porcupine Caribou herd and is legislated into regional land claim agreements. The waters offshore, however, are not similarly protected. Herschel Island's anchorages may become strategically important as marine traffic increases in the Arctic Ocean and may be used again if development of petroleum resources beneath the Beaufort Sea proceeds.

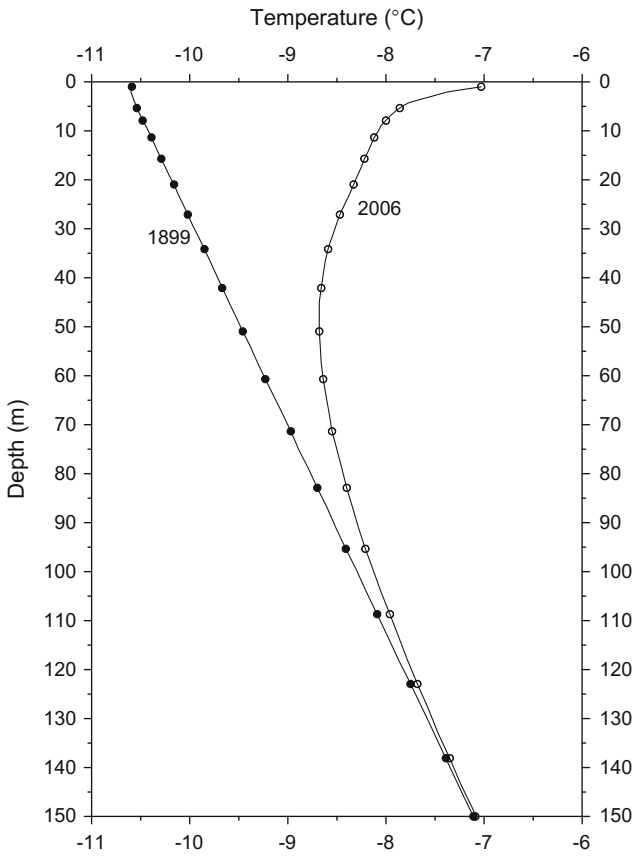

Fig. 24.12 Temperature profile in the upper 42 m of the ground at Collinson Head measured in 2006 and its projected extension downwards, and an equilibrium temperature profile drawn from surface conditions at the beginning of the twentieth century

Acknowledgements The research program on permafrost at Herschel Island has been supported by the Natural Sciences and Engineering Research Council of Canada; the Polar Continental Shelf Project, Natural Resources Canada; Herschel Island Territorial Park; the Aurora Research Institute; and Parks Canada Agency. I acknowledge with gratitude assistance in preparation of the figures from Jon Tunnicliffe and Christine Earl.

References

Bockstoce JR (1986) Whales, ice, and men: the history of whaling in the western Arctic. University of Washington Press, Seattle

Burn CR (1997) Cryostratigraphy, paleogeography, and climate change during the early Holocene warm interval, western Arctic coast, Canada. Can J Earth Sci 34:912–925

Burn CR (2009) After whom is Hershel Island named? Arctic 62:317–323

Burn CR (2012a) Climate. In: Burn CR (ed) Herschel Island Qikiqtaryuk: a natural and cultural history of Yukon's Arctic island. Wildlife Management Advisory Council (North Slope), Whitehorse, pp 48–53

Burn CR (2012b) Physical setting. In: Burn CR (ed) Herschel Island Qikiqtaryuk: a natural and cultural history of Yukon's Arctic island. Wildlife Management Advisory Council (North Slope), Whitehorse, pp 30–37

Burn CR (2013) *Calton* Point or *Catton* Point? A Misprinted Toponym on the Yukon Coast. Arctic 66:459–462

Burn CR, Hattendorf JB (2011) Toponymy of Herschel Island (Qikiqtaryuk), western Arctic coast, Canada. Arctic 64:459–464

Burn CR, Kokelj SV (2009) The environment and permafrost of the Mackenzie Delta area. Permafr Periglac Proc 20:83–105

Burn CR, Zhang Y (2009) Permafrost and climate change at Herschel Island (Qikiqtaruk), Yukon Territory, Canada. J Geophys Res Earth Surf 114:F02001

Burn CR, Zhang Y (2010) Sensitivity of active-layer development to winter conditions north of treeline, Mackenzie Delta area, western Arctic coast. In: Proceedings, GEO2010: 63rd Canadian geotechnical conference and 6th Canadian permafrost conference, Calgary, Sept. 12–16, 2010. Can Geotech Soc, Richmond, pp 1458–1465

Campeau S, Héquette A, Pienitz R (2000) Late Holocene diatom biostratigraphy and sea-level changes in the southeastern Beaufort Sea. Can J Earth Sci 37:63–80

Franklin J (1828) Narrative of a second expedition to the shores of the polar sea in the years 1825, 1826, and 1827. John Murray, London

Friesen M (2012) Inuvialuit archaeology. In: Burn CR (ed) Herschel Island Qikiqtaryuk: a natural and cultural history of Yukon's Arctic island. Wildlife Management Advisory Council (North Slope), Whitehorse, pp 146–150

Fritz M, Wetterich S, Meyer H, Schirrmeister L, Lantuit H, Pollard WH (2011) Origin and characteristics of massive ground ice on Herschel Island (western Canadian Arctic) as revealed by stable water isotope and hydrochemical signatures. Permafr Periglac Proc 22:26–38

Hill PR (1990) Coastal geology of the King Point area, Yukon Territory, Canada. Mar Geol 91:93–111

Hill PR, Héquette A, Ruz M-H (1993) Holocene sea-level history of the Canadian Beaufort shelf. Can J Earth Sci 30:103–108

Hill PR, Mudie PJ, Moran K, Blasco SM (1985) A sea-level curve for the Canadian Beaufort Shelf. Can J Earth Sci 22:1383–1393

Kennedy C (2012) Vegetation. In: Burn CR (ed) Herschel Island Qikiqtaryuk: a natural and cultural history of Yukon's Arctic island. Wildlife Management Advisory Council (North Slope), Whitehorse, pp 80–86

Kokelj SV, Smith CAS, Burn CR (2002) Physical and chemical characteristics of the active layer and permafrost, Herschel Island, western Arctic coast, Canada. Permafr Periglac Proc 13:171–185

Kokelj SV, Tunnicliffe J, Lacelle D, Lantz TC, Chin KS, Fraser R (2015) Increased precipitation drives mega slump development and destabilization of ice-rich terrain, northwestern Canada. Glob Planet Change 129:56–68

Lantuit H, Pollard WH (2008) Fifty years of coastal erosion and retrogressive thaw slump activity on Herschel Island, southern Beaufort Sea, Yukon Territory, Canada. Geomorphology 95:84–102

Mackay JR (1959) Glacier ice-thrust features of the Yukon coast. Geog Bull 13:5–21

Mathews WH, Mackay JR (1960) Deformation of soils by glacier ice and the influence of pore pressures and permafrost. Trans R Soc Can Ser 3(54):27–36

Manson G, Solomon SM (2007) Past and future forcing of Beaufort Sea coastal change. Atmos-Ocean 45:107–122

Nagy MI (1994) Yukon North Slope Inuvialuit oral history. In: Hude Hudän Series, Occasional Papers in Yukon History No. 1. Heritage Branch, Government of Yukon, Whitehorse

Olynyk D (2012) Buildings. In: Burn CR (ed) Herschel Island Qikiqtaryuk: a natural and cultural history of Yukon's Arctic island. Wildlife Management Advisory Council (North Slope), Whitehorse, pp 202–209

O'Neill JJ (1921) The geology of the Arctic coast of Canada, west of Kent Peninsula. In: Report of the Canadian Arctic Expedition 1913–1918, vol XI, Geology and Geography, Part A. King's Printer, Ottawa

Rampton VN (1982) Quaternary geology of the Yukon Coastal Plain. Geol Surv Can Bull 317, Ottawa

Smith CAS, Kennedy CE, Hargrave AE, McKenna KM (1989) Soil and vegetation of Herschel Island, Yukon Territory. Yukon Soil Survey Report 1. Land Resource Research Centre. Agriculture Canada, Ottawa

Solomon SM (2005) Spatial and temporal variability of shoreline change in the Beaufort-Mackenzie region, Northwest Territories, Canada. Geo-Mar Lett 25:127–137

Stroeve J, Holland MM, Meier W, Scambos T, Serreze M (2007) Arctic sea ice in decline: faster than forecast. Geophys Res Lett 34:L09501

Williams B, Carmack E (2012) Ocean water and sea ice. In: Burn CR (ed) Herschel Island Qikiqtaryuk: a natural and cultural history of Yukon's Arctic island. Wildlife Management Advisory Council (North Slope), Whitehorse, pp 54–59

Zazula G (2012) Ice Age. In: Burn CR (ed) Herschel Island Qikiqtaryuk: a natural and cultural history of Yukon's Arctic island. Wildlife Management Advisory Council (North Slope), Whitehorse, pp 60–64

Zazula GD, Hare PG, Storer JE (2009) New radiocarbon-dated vertebrate fossils from Herschel Island: implications for the palaeoenvironments and glacial chronology of the Beaufort Sea coastlands. Arctic 62:273–280

The Landslide-Modified Glacimarine Landscape of the Terrace–Kitimat Area, BC

25

Marten Geertsema, David M. Cruden, and John J. Clague

Abstract

Low-gradient landslides (spreads and flows) involving sensitive clays have modified the uplifted glacimarine landscape of the Terrace–Kitimat area in northern coastal British Columbia. Broad, shallow landslide depressions are clustered throughout the area, along streams, delta fronts, and lake shores, with some occupied by wetlands. Several large landslides have occurred in the past century, and there are earlier oral First Nation's accounts of landslides. Radiocarbon analyses indicate that one-third of dated landslides plot between 3500 and 1900 years ago, perhaps relating to a period of wetter climate. The presence of quick clays, continued stream incision into sensitive sediments, and a projected wetter future climate suggest that this landscape will continue to be modified by low-gradient landslides.

Keywords

Landslide • Glacimarine sediment • Quick clay • Radiocarbon dating • *Naxnox* • British Columbia

25.1 Introduction

Fjord valleys dissect the Coast Mountains of British Columbia including the Coast Mountains near Kitimat and Terrace (Fig. 25.1). At the peak of the last Pleistocene glaciation, thick ice of the Cordilleran Ice Sheet isostatically depressed the underlying crust. During deglaciation, the sea transgressed far inland on the isostatically depressed landscape. One arm of the sea expanded eastward up Skeena River, and the other reached northward from Kitimat past Terrace. The inland seas, however, were short-lived. Rapid isostatic rebound lifted the drowned landscape above sea level, subjecting thick glacimarine sediments to stream incision, lateral erosion, and, over time, to large, low-gradient landslides. The landslides modified the landscape, in many cases forming wetlands that persist to the present. The landslides also play a role in First Nation's oral histories. Today they pose challenges for settlements and infrastructure.

25.2 Setting

25.2.1 Physiography

The Terrace area is located in the Kitimat Ranges, which is one of the ranges of the Coast Mountains of British Columbia (Holland 1976). It occupies a broad, relatively flat-bottomed and steep-walled valley known as the Kitimat–Kitsumkalum trough, which ranges in width from 1 to 15 km (Clague 1984). The valley does not have a single major river along length. Skeena River cuts orthogonally

M. Geertsema (✉)
Ministry of Forests, Lands and Natural Resource Operations, Prince George, BC V2N 4W5, Canada
e-mail: marten.geertsema@gmail.com

D.M. Cruden
Department of Civil and Environmental Engineering, University of Alberta, Edmonton, AB T6G 1H9, Canada

J.J. Clague
Department of Earth Sciences, Simon Fraser University, 8888 University Drive, Burnaby, BC V5A 1S6, Canada

© Springer International Publishing Switzerland 2017
O. Slaymaker (ed.), *Landscapes and Landforms of Western Canada*, World Geomorphological Landscapes, DOI: 10.1007/978-3-319-44595-3_25

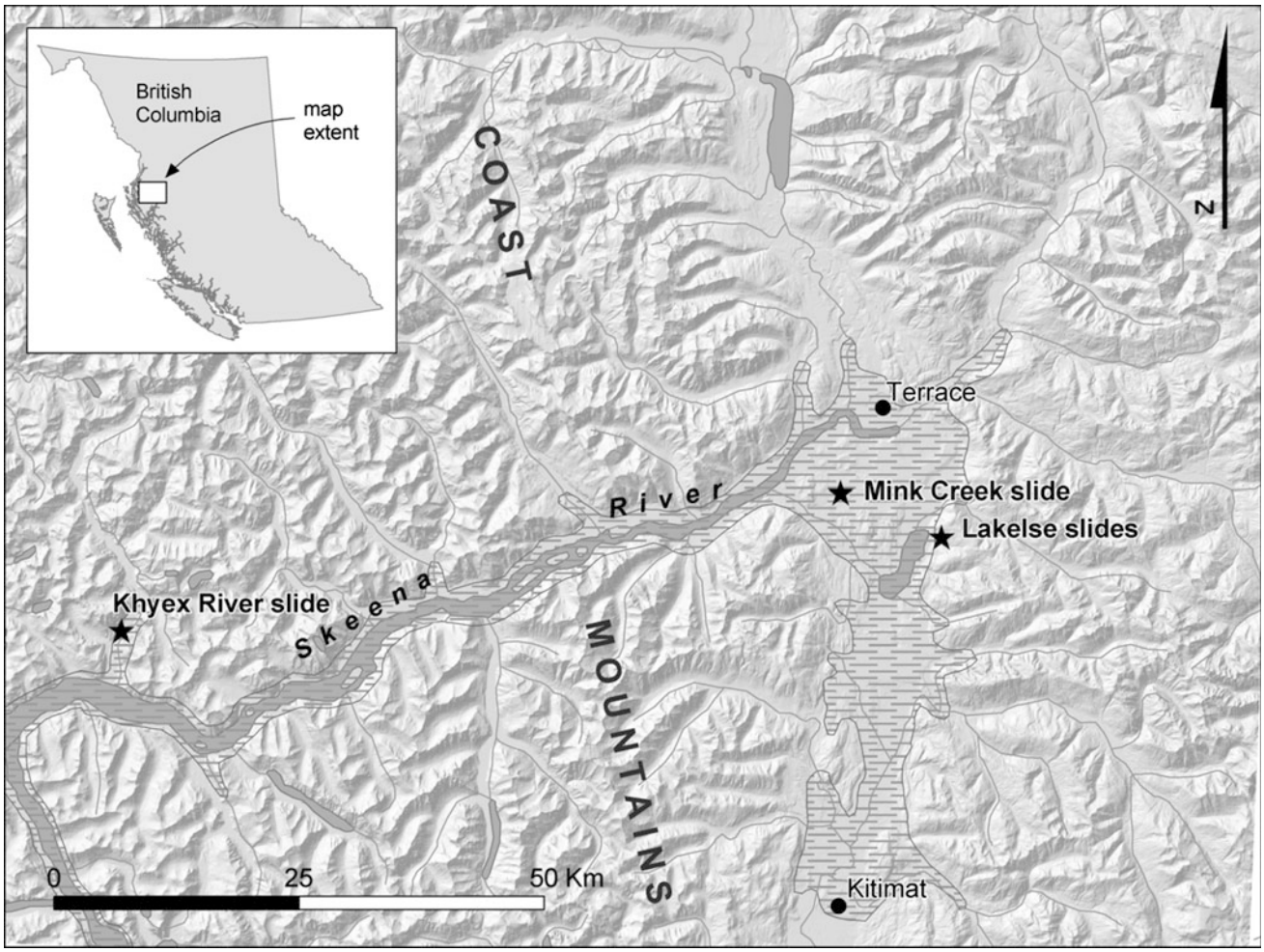

Fig. 25.1 Map of the study area. Note the locations of the 1993–1994 Mink Creek landslide and the 1962 Lakelse landslides. Glacimarine sediments occur within the patterned area (from Geertsema 2004)

across the trough, and Kitimat River enters the valley north of Kitimat. Lack of a major integrated drainage network suggests a formative drainage system different from that of today (Duffel and Souther 1964; Clague 1984).

The forest-covered Kitimat–Kitsumkalum trough is characterized by rolling to flat terrain, composed of gullied glacial and post-glacial sediments and isolated bedrock hills. Most of the valley fill consists of glacial sediments, including glacimarine mud, glacifluvial gravel, and till. Glacimarine sediments are locally more than 50 m thick and deeply gullied. Post-glacial landforms include alluvial floodplains and fans, bogs and fens, and slopes mantled with colluvium. The largest water body in the study area is Lakelse Lake. Steep rock slopes border the Kitimat–Kitsumkalum trough, culminating in peaks up to 1500 m in elevation. Bedrock includes Cretaceous granitic rocks and older Mesozoic and older volcanic and sedimentary rocks (Duffel and Souther 1964).

25.2.2 Climate

The climate of the study area is wet sub-maritime. Mean annual precipitation ranges from 2300 mm at Kitimat to about 1300 mm near Terrace; more than three-quarters of the precipitation falls between October and April. Mean annual temperature ranges from 5.9 °C near Terrace to 6.4 °C at Kitimat. Respective extremes are about −27 and 36 °C near Terrace, and −25 and 36 °C at Kitimat (British Columbia Ministry of Forests 1997).

25.2.3 Deglacial History

At the end of the last (Fraser) glaciation, ice flowing down Skeena Valley bifurcated near Terrace; one lobe flowed southward towards Kitimat and the other flowed westward towards Prince Rupert. The termini of both glaciers were in

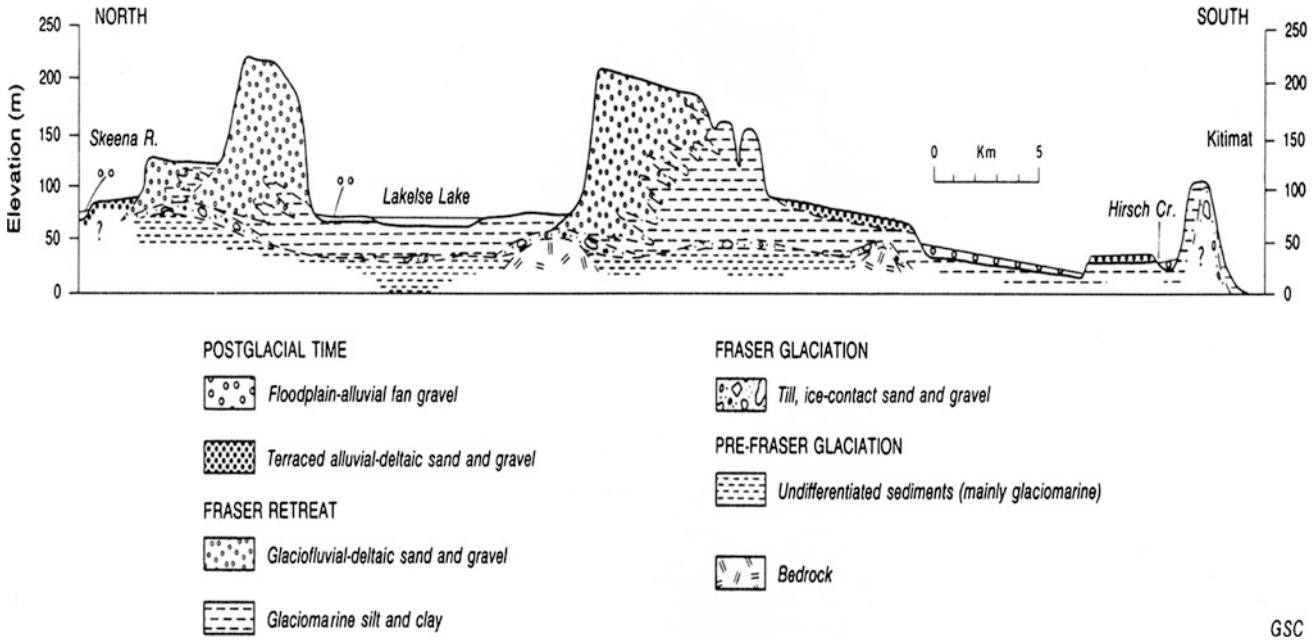

Fig. 25.2 Schematic longitudinal cross section of the valley between Terrace and Kitimat. Note the terminal moraine at Kitimat and two ice-contact deltas graded to late-glacial high sea levels (From Clague 1984)

contact with the sea. The snout of the south-flowing glacier retreated from the present location of Kitimat towards Terrace about 12,500 years ago. Terrace was ice-free by about 11,000 years ago. Recession, although rapid, was interrupted by three significant stillstands. The first is marked by a large arcuate end moraine at the present location of Kitimat. The second stillstand occurred about 20 km north of Kitimat, producing a large ice-contact delta that blocked the northward transgression of the sea. The third stillstand was near Terrace, where another delta was built into the sea (Fig. 25.2).

Isostatic rebound continued for about another 2000 years following deglaciation. Local sea level fell from its highest level at about 200 masl to at or below present sea level by 9000–8500 years ago (Clague 1984). During and soon after deglaciation, the landscape experienced significant change due to paraglacial sediment transfers (Church and Ryder 1972). Floodplains, fans, and deltas formed and evolved rapidly. Paraglacial deposits were subsequently incised in response to falling base level and a reduction in sediment delivery, and many fans and side-valley deltas are now relict features.

25.3 Conditions for Sensitive Clay Development

In most freshwater environments, clay particles settle more slowly than silt and accumulate in stacks of plates parallel to one another. In contrast, in salt water silt and clay particles form aggregates (small floccules) that settle together in a random pattern (Torrance 1983). This random alignment of particles gives the sediment a higher-than-normal amount of pore space and interstitial water. Such floccules formed in the late-glacial sea near Terrace (Geertsema and Torrance 2005).

When interstitial porewater has a high salt content, interparticle bonds are strong. Leaching or diffusion by freshwater gradually lowers the salinity in marine and glacimarine sediments. Some types of clays and mixtures of silt and clay are prone to structural collapse once the salinity of the porewater falls below a threshold value because repulsive forces between the particles increase (Rosenqvist 1953; Bjerrum 1954; Quigley 1980; Torrance 1983). A remarkable characteristic of these fine sediments is the large difference in strength between the undisturbed and disturbed (remoulded) sediment—the remoulded material behaves as a fluid. Clays that exhibit this type of behaviour are called *sensitive clays*, where 'sensitivity' is defined as the quotient of the undisturbed shear strength divided by the disturbed shear strength. In extreme cases, where sensitivity exceeds 30 and remoulded shear strength is less than 0.5 kPa, the deposits are called *quick clays* (Torrance 1983).

25.4 Landslides

25.4.1 Landslide Depressions

Scars of low-gradient landslides are common on the valley floor between Terrace and Kitimat (Fig. 25.3; Geertsema

Fig. 25.3 The Mink Creek landslide occurred 7 km south-west of Terrace on a broad glacimarine plain, 100 m above sea level. The travel angle of the landslide was 2°. Photograph courtesy of British Columbia Ministry of Forests, Lands, and Natural Resource Operations

and Schwab 1997). The landslides have happened in glacimarine mud (Fig. 25.4), although in some instances the mud is covered with post-glacial alluvium or glacifluvial gravel (Fig. 25.5). The landslides can be large, with volumes of up to 10 million m^3 and areas up to 2 km^2. They tend to have high ratios of horizontal retrogression to the height of the scarp above the main rupture surface, thus forming broad, shallow depressions. The travel angles can be <1° (Geertsema and Cruden 2008, 2014), with movement on nearly flat ground.

The landslides are largely translational, and in some cases upright trees are transported over distances of hundreds of metres (Fig. 25.6). The Kitsumkalum people have an oral tradition of the *naxnox*, a supernatural being. One of the ways that *naxnox* would manifest itself is through trees travelling upright into rivers or lakes (Alex Bolton, Kitsumkalum Band, personal communication 1997).

25.4.2 Landslide Distribution

Many of the landslides in the Kitimat–Kitsumkalum trough occur in clusters. Landslides are particularly abundant around Mink Creek (Fig. 25.1), the foreslope of the Onion Lake delta (Figs. 25.7, 25.8) and the Nalbeelah wetlands (Fig. 25.9).

As on the foreslope of the delta fronting the St. Narcisse moraine in Quebec (Lebuis et al. 1983), the abundance of landslides at the front of the Onion Lake delta may be related to the presence of a confined aquifer with water-bearing delta foreslope deposits lying beneath glacimarine mud. Even without excess pore pressures, the movement of water through the aquifer removes salt from the water of the overlying mud, increasing its sensitivity (La Rochelle et al. 1970; Carson 1983). Bank erosion by Kitimat River may be a factor contributing to the large number of landslides in this area.

In contrast, the foreslope of the large delta northwest of Lakelse Lake (Fig. 25.3) has few large landslides. The absence of a major eroding stream in this area may partly explain the lower frequency of landslides. The largest landslides in the area are historic and include two Lakelse landslides in 1962 that destroyed a highway (Clague 1978; Evans 1982; Geertsema 1998) and the Mink Creek landslide in 1993 (Geertsema et al. 2006). Such large landslides undoubtedly have occurred in the prehistoric past, but

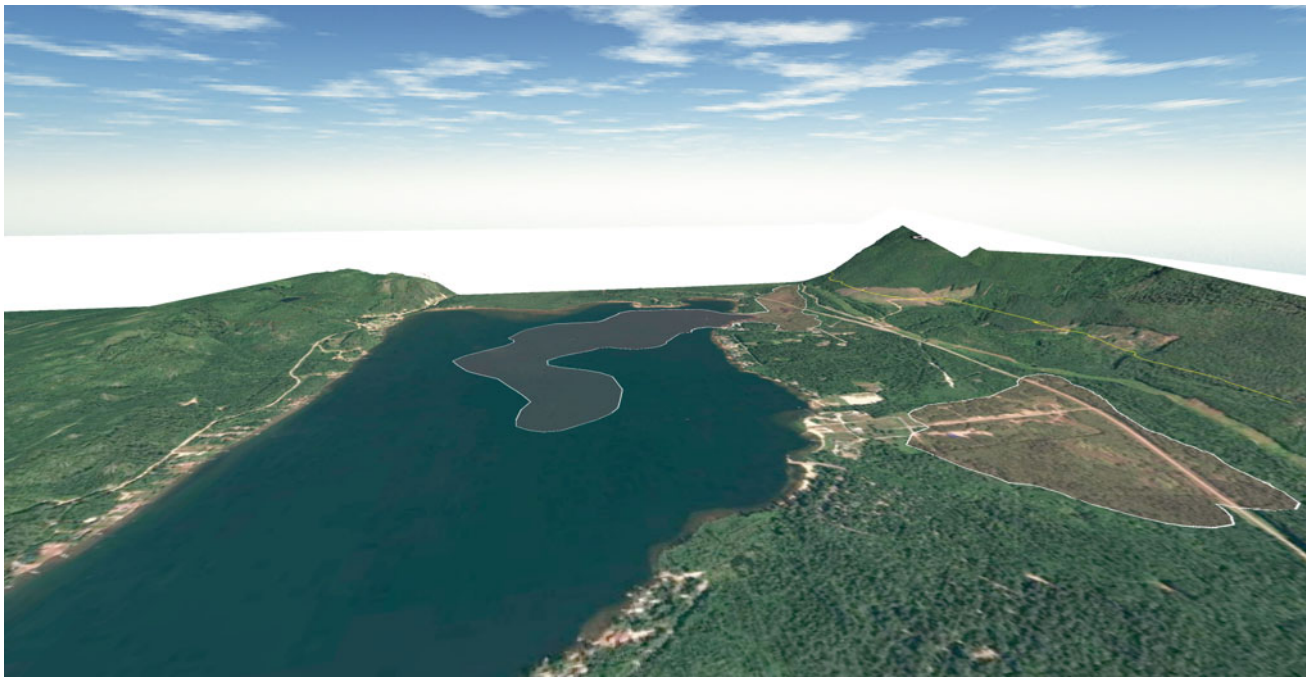

Fig. 25.4 Two (*grey shaded*) landslides that were triggered by highway construction occurred in 1962 on a LiDAR digital elevation model. The landslides both had rupture surfaces <1° gradient, but volumes in excess of 10 million m^3 (Geertsema and Cruden 2014), but only one of them entered Lakelse Lake. The distal (north end of Lakelse Lake is 2.2 km wide. The *yellow* line represents the 200 m marine limit. View north. Data on file at British Columbia Ministry of Forests, Lands, and Natural Resource Operations

Fig. 25.5 Prehistoric earth flow with a bottleneck shape on Nalbeelah Creek—the term bottleneck to describe a landslide was first used by Sharpe (1938). *Dotted line* delineates the headscarp and lateral margins of the landslide. The outlet is 70 m wide. Note the gully to the left of the landslide. This gully may have limited the retrogression of the landslide along its *left side* (from Geertsema 2004)

evidence for them has been lost due to subsequent sliding, gully erosion, or revegetation. Large hanging landslide depressions, presumably prehistoric, are preserved in mud blanketed with glacifluvial gravel (Fig. 25.5). The absence of mapped landslides at the north and southeast ends of Lakelse Lake does not necessarily imply that no landslides

Fig. 25.6 Trees rafted in near-vertical position by the 1993–1994 Mink Creek landslide (from Geertsema 2004)

have occurred there. There are local accounts of trees buried in clay that were exposed during excavations in these areas. The scarps may become obliterated over time by alluvium and organic deposits in these low-lying, flood-prone areas.

25.4.3 Landslide Ages

Radiocarbon ages are available for 16 prehistoric landslides (Fig. 25.10; and tables in Geertsema and Schwab 1997; Geertsema 2004). With one exception, the ages are on basal peat in landslide depressions and thus are minima for the ages of the landslides (Fig. 25.9; Geertsema 1996). The one exception is an age on plant material found along an excavated rupture surface. Although the dated landslides are a small percentage of the total landslides mapped, more than one-third of them appear to have happened between 3500 and 1900 years ago. The largest cluster of peat-filled landslide depressions is the Nalbeelah wetland east of Kitimat River (Fig. 25.9). A landslide at Hirsch Creek in glacimarine clay blanketed by glacifluvial gravel happened before 10,000 years ago, shortly after deglaciation. Although it is an anomaly in Fig. 25.10, other nearby landslides north of Hirsch Creek (Fig. 25.5) may also be early post-glacial in age.

25.4.4 Landslide Legacies

Landslides can have both short-term and enduring impacts on soil, site, and landscape diversity (Geertsema and Pojar 2007; Geertsema and Schwab 1996). Readily apparent effects of flows and spreads include the formation of large scars or scallops (Cruden and Varnes 1996), the filling of valleys with displaced material (Fig. 25.11), and the formation of landslide-dammed lakes. Landslide-dammed lakes may be short-lived or may endure for decades or longer (Fig. 25.3), depending in large part on stream power. Sometimes these lakes transform into peat-filled wetlands. Where the rupture surfaces of these landslides are below the

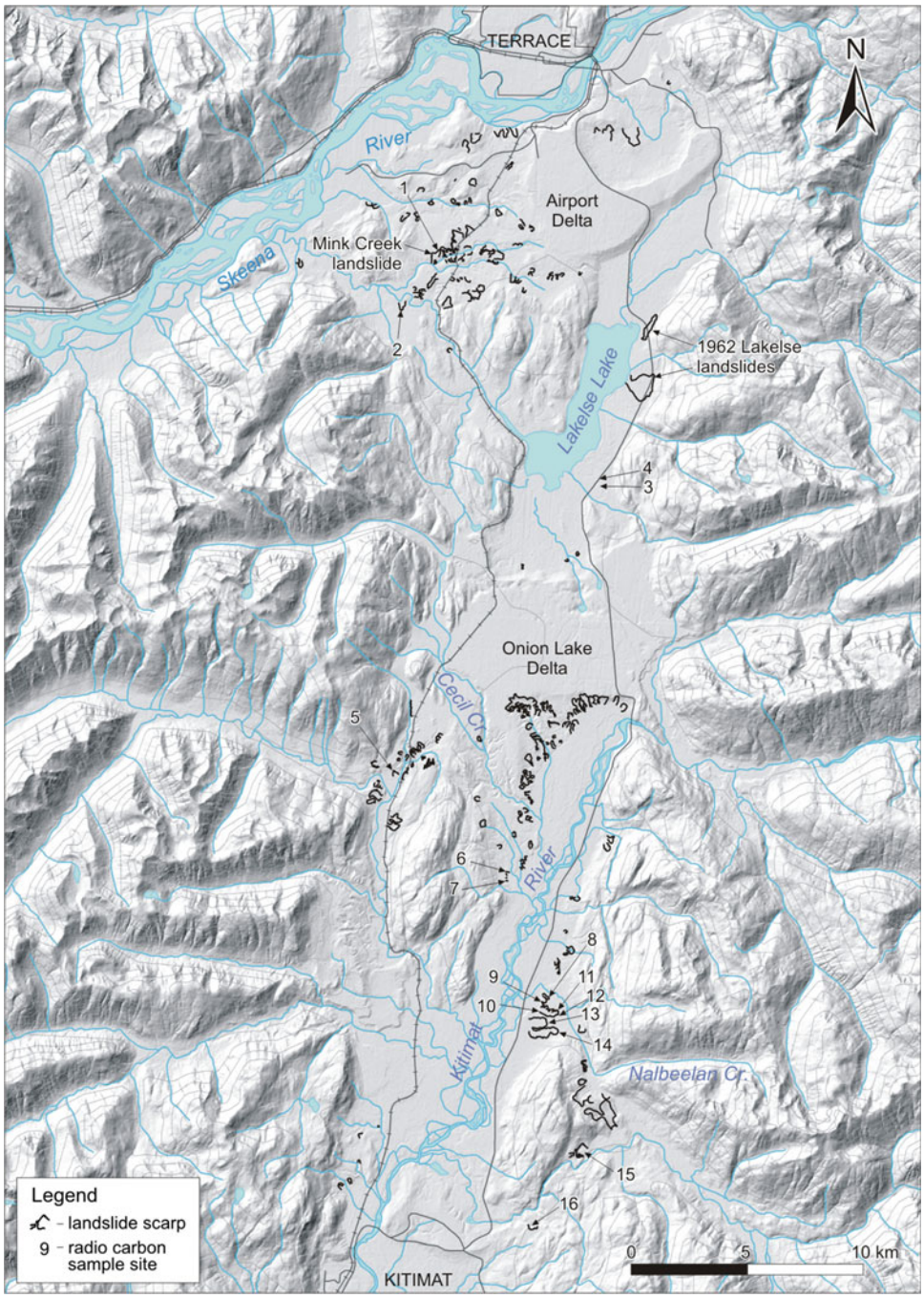

Fig. 25.7 Distribution of landslide scarps in glacimarine sediment in the Terrace–Kitimat area (from Geertsema and Schwab 1997)

water table, wetlands may develop within the bodies of landslides (Fig. 25.9).

Contributions to biophysical diversity may come from mixing of materials by landslides. Figure 25.12 shows a mosaic of patches of brown surface soil interspersed with deeper grey clay at the Mink Creek landslide. The surface soil has a pH lower than 5, whereas the grey clay has a pH above 8 (Geertsema and Pojar 2007).

25.5 Controls on Landsliding

25.5.1 Influence of Valley Formation

Stream erosion is the most common cause of retrogressive landslides in glacimarine sediments (Bjerrum et al. 1969; Lebuis et al. 1983; Viberg 1983). Both Bjerrum et al. (1969) working in Norway and Lefebvre (1986) working in Quebec

Fig. 25.8 View to the northeast of the slope of the late Pleistocene Onion Lake delta (Fig. 25.7). The delta slope is heavily scarred by landslides. Note logging roads on the scarps of some of the landslides. Photograph by M. Geertsema

Fig. 25.9 Wetland-filled earth flows at Nalbeelah Creek (sites 12–14; Fig. 25.7). British Columbia Ministry of Forests, Lands, and Natural Resource Operations imagery

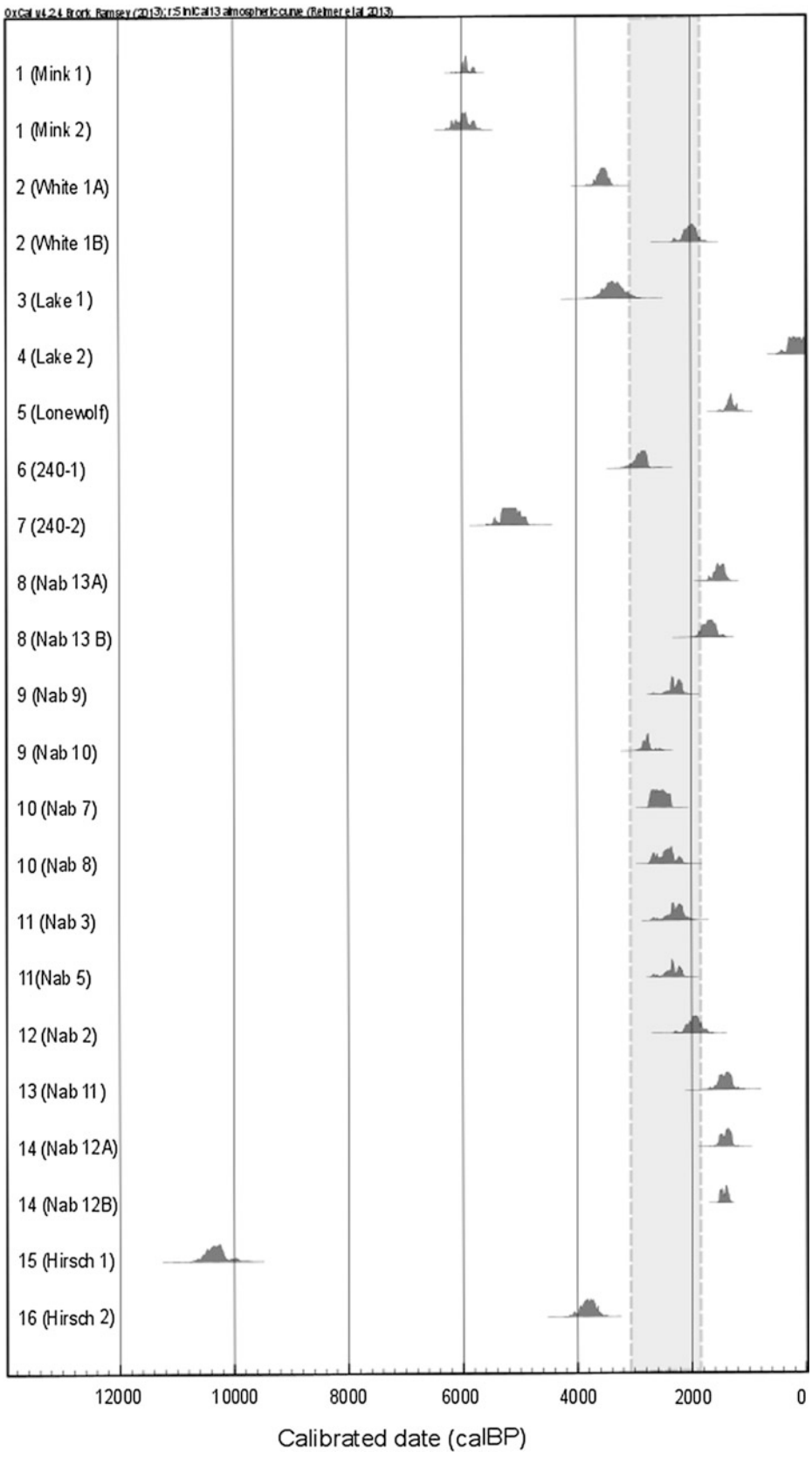

Fig. 25.10 Calibrated radiocarbon age distribution of basal peats from the zones of depletion of landslides (see Fig. 25.7 for locations). The upper two samples (Mink Creek) were not from peats, but organics along a buried rupture surface. Calibration done using OxCal 4.2.4 (Bronk Ramsey 2013). The shaded column represents a cool, wet period identified by Clague and Mathewes (1996). More than one-third of the dates fall within this period

Fig. 25.11 Muddy landslide material completely filling the valley of Mink Creek following the 1993–1994 landslide. Photograph courtesy of British Columbia Ministry of Forests, Lands, and Natural Resource Operations imagery

used landscape evolution approaches involving stream incision to map zones of earthflow potential in sensitive clay areas (Geertsema 2013).

Bjerrum et al. (1969) assumed that stream bank erosion is the main cause of quick clay failures; they proposed equilibrium gradients for streams from which future erosion might be predicted. They defined three zones of stream erosion. The lowest zone is no longer actively downcutting and is characterized by old slide scars and localized cutbank failures at stream bends. This zone is mature, and the danger of quick clay landslides is small. An intermediate zone exists where the stream is flowing almost exclusively on landslide deposits and is eroding back to its old level. Bjerrum et al. (1969) argue that the risk of quick clay failures in this zone is low. However, the Saint–Jean–Vianney slide in Quebec (Tavenas et al. 1971; Potvin et al. 2002) and the Mink Creek landslide at least partly involved remobilization of old landslide deposits. The third, uppermost zone is the original land surface where streams are cutting into undisturbed clay. Bjerrum et al. (1969) termed the boundary between this zone and intermediate zone the 'front of aggression' and argued that the risk of failure is greatest there. When an earth flow carries material into the valley, the intermediate zone is extended and the front of aggression moves upstream.

Working in Quebec, Lefebvre (1986) described three phases of valley formation and associated groundwater flow. An early phase is characterized by relatively shallow stream incision into thick marine mud and groundwater flow that is not influenced by underlying permeable till. An intermediate phase is characterized by moderate valley incision and strong artesian pressures, which facilitate large, retrogressive failures. A late phase is marked by stream incision through permeable till and downward groundwater flow. Only small landslides are expected during this late phase of valley formation. Most streams in the Kitimat–Kitsumkalum trough are incising thick glacimarine sediments (Geertsema 1998, 2013). The area thus is in the early and intermediate stages of valley formation, and large landslides are still occurring there.

Although the zones proposed by Bjerrum et al. (1969) do not relate directly to Lefebvre's (1986, 1996) phases of valley formation, the intermediate zones in both studies have the greatest likelihood of retrogressive flowsliding. Lefebvre's valley formation approach may more applicable to the Terrace–Kitimat area because prehistoric landslides are ubiquitous throughout the area (Fig. 25.7), and large landslides are occurring in areas that have experience retrogressive landslides in the past.

25.5.2 Influence of Climate

The 1993–1994 Mink Creek landslide happened after 8 years of increased precipitation, 9 years of increased warming, and a warmer than average fall and early winter (Geertsema et al. 2006). These hydroclimatic conditions likely contributed to high ground water and stream levels, setting up the landslide. Such conditions have been shown to be important contributors to other large landslides (Patton 1984). Studies of landslide–climate relationships in British Columbia have largely been restricted to shallow debris slides and debris flows in steep mountainous terrain (Schwab 1983; Church and Miles 1987; Evans 1989; Hogan and Schwab 1991). Bovis and Jones (1992), however, showed that large deep-seated earth flows in southern British Columbia were active during wet periods in the Holocene Epoch.

According to Geertsema et al. (2006), most global circulation models predict warmer and wetter conditions for the Terrace area later in this century. Conditions that contributed to the Mink Creek landslide could become more common in

Fig. 25.12 Mosaic of vegetation and soils on the surface of the Mink Creek landslide. Acidic brown soils and mildly alkaline grey clay ridges provide a rich diversity of ecosystems. Photograph by M. Geertsema

the future—a decade of increasing precipitation and temperature and mild wet falls.

Most of the dated prehistoric landslides (Fig. 25.10) happened during a cool wet period (Clague and Mathewes 1996). There might have been more frequent flowslides during Neoglacial time (the last 5000 years) than earlier in the Holocene when it was warmer and drier (Pielou 1991).

25.5.3 Controls on Landslide Size

Glacimarine landslide size is controlled by a number of factors including material characteristics and strength, leaching and diffusion of salt from porewater, topography, and the inclination of bedding (Geertsema and L'Heureux 2014). One of the main requisites for landslide growth is that displaced material must leave the zone of depletion (Carson 1977, 1979; Carson and Lajoie 1981). For continued growth of retrogressive landslides, the failed material must move away from the headscarp and sidescarps to prevent buttressing. Evacuation of sediment from developing scarps is influenced by the ability of material to flow and by the ability of the valley to accommodate the displaced material.

Mitchell and Markell (1974) and Trak and Lacasse (1996) related the length of glacimarine flows and spreads (or the distance of retrogression) to Janbu's stability number, Ns. They found that the stability number ($Ns = \gamma H/su$, where γ is the bulk unit weight of the soil, H is the height of the slope, and su is the undrained shear strength) must exceed some threshold value (usually 6) for retrogressive movement to occur. Below the threshold, movement becomes rotational and arrests further landslide growth, forming a stable main scarp.

Rupture surfaces in many glacimarine flows and spreads develop along bedding planes. The dip of the strata can play a role in how far a landslide will penetrate into a slope. Counterintuitively, flatter strata allow larger landslides to develop because limiting thresholds are achieved over longer distances along the rupture surfaces (Fig. 25.13). With nearly horizontal rupture surfaces, the limiting Ns threshold may not be met. At Lakelse Lake in 1962, the slopes were gentle and strata were nearly flat; the landslides penetrated

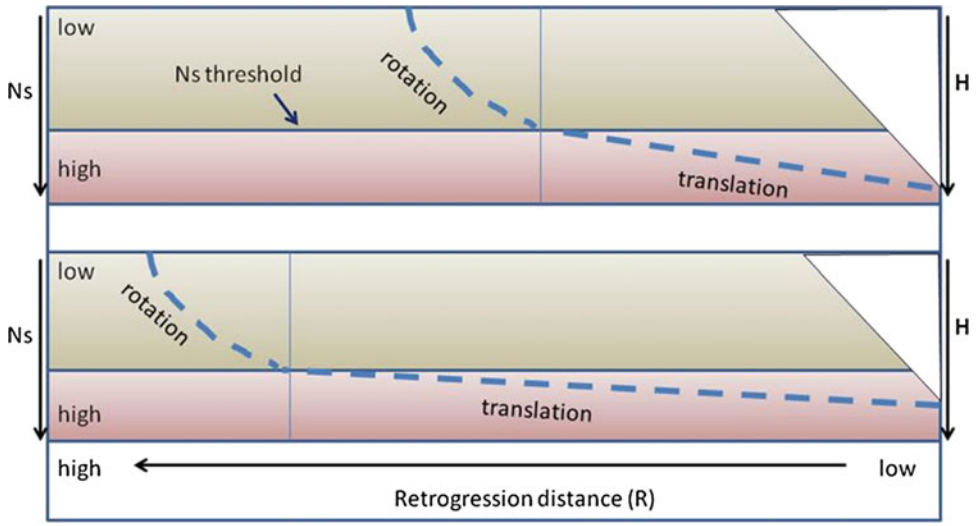

Fig. 25.13 Influence of the inclination of the rupture surface (*dashed blue lines*) on retrogression distance. Steeper inclinations intersect the Ns threshold over a shorter distance than do more gently sloped rupture surfaces. Once the threshold is reached movement transforms from translation to rotation. The intersection of the rotational surface with the ground surface is generally the crown of the landslide (figure adapted from Geertsema and L'Heureux 2014)

along the rupture surface until they encountered the rising bedrock slope on the valley wall (Geertsema and L'Heureux 2014).

Many landslides are bounded by pre-failure gullies (Fig. 25.5). Gullies limit landslide size in three main ways. Gullies provide a negative topography that reduces lateral earth pressure and Ns. They can lower the water table. And a weathered crust can develop in the interfluve areas between gullies, imparting strength deeper into the sediment.

25.6 Conclusions

There are many historic and prehistoric low-gradient translational landslides in glacimarine sediments in the Terrace–Kitimat area. Rapid landslides moving on essentially flat ground typically are not expected, and trees moving in the vertical position in landslides are even less so. Oral histories of *naxnox* manifested as upright moving trees may provide further evidence of these landslides.

These landslides leave a variety of geomorphic traces in the landscape, including landslide-dammed lakes and wetlands, peat-filled landslide depressions, and a mosaic of soil types.

The landslides are especially abundant near Mink Creek, on the foreslope of the Onion Lake delta, and in the Nalbeelah Creek area. The most common trigger for large earth flows is bank erosion, and many prehistoric failures in the Terrace–Kitimat area happened during a period when rivers eroded slopes formed of glacimarine sediments. Streams in this area are still in the early-to-intermediate phases of valley formation when large landslides are most likely.

Three interesting points can be made about climate. First, about one-third of the dated prehistoric landslides in the Kitimat–Kitsumkalum trough occurred during a wet period. Second, almost a decade of increasing precipitation and temperature and a wet warm fall and early winter preceded the large Mink Creek landslide. Third, future climate in the Terrace–Kitimat area is likely to be wetter and warmer than today.

Given the current state of valley formation in the Terrace–Kitimat area, the history of previous landslides, and the clear relation between climate and instability, there is every reason to think that large landslides will happen in the future.

References

Bjerrum L (1954) Geotechnical properties of Norwegian marine clays. Geotechnique 4:49–69

Bjerrum L, Løken T, Heiberg S, Foster R (1969) A field study of factors responsible for quick clay slides. In: Proceedings, 7th ICSMFE. Mexico, 2, pp 531–540

Bovis MJ, Jones P (1992) Holocene history of earthflow mass movements in south-central British Columbia: the influence of hydroclimatic changes. Can J Earth Sci 29:1746–1755

British Columbia Ministry of Forests (1997) Climate data summaries for the biogeoclimatic zones of British Columbia, Version 4. Unpublished Excel file, B.C. Ministry of Forests, Victoria, BC

Bronk Ramsey C (2013) OxCal version 4.2.2

Carson MA (1977) On the retrogression of landslides in sensitive muddy sediments. Can Geotech J 14:582–602

Carson MA (1979) Le glissement de Rigaud (Quebec) du 3 Mai 1978: Une interpretation du mode de rupture d'apres la morphologie de la cicatrice. Géog Phys Quatern 33:63–92

Carson MA (1983) Influence of porefluid salinity on instability of sensitive marine clays; a new approach to an old problem. Earth Surf Process landf 6:499–515

Carson MA, Lajoie G (1981) Some constraints on the severity of landslide penetration in sensitive deposits. Géog Phys Quatern 35:301–316

Church M, Miles MJ (1987) Meteorological antecedents to debris flows in southwestern British Columbia; some case studies. In: Costa JE, Wieczorek GF (eds) Debris flows/avalanches: process, recognition, and mitigation. Geol Soc Am. Reviews in Engineering Geology 7:63–79

Church M, Ryder JM (1972) Paraglacial sedimentation: a consideration of fluvial processes conditioned by glaciations. Geol Soc Am Bull 83:3059–3071

Clague JJ (1978) Terrain hazards in the Skeena and Kitimat River basins, British Columbia. In: Current research, part A. Geological Survey of Canada, Paper 78-1A, pp 183–188

Clague JJ (1984) Quaternary geology and geomorphology, Smithers–Terrace–Prince Rupert area, British Columbia. Geol Surv Can Mem 413

Clague JJ, Mathewes RW (1996) Neoglaciation, glacier-dammed lakes, and vegetation change in northwestern British Columbia, Canada. Arct Alp Res 28:10–24

Cruden DM, Varnes DJ (1996) Landslide types and processes. In: Turner AK, Schuster RL (eds) Landslides investigation and mitigation. National Research Council, Transportation Safety Board, Special Report 247, pp 36–75

Duffel S, Souther JG (1964) Geology of the Terrace map-area, British Columbia (103I E 1/2). Geol Surv Can Mem 329

Evans SG (1982) Landslides and surficial deposits in urban areas of British Columbia: a review. Can Geotech J 19:269–288

Evans SG (1989) Rain-induced landslides in the Canadian Cordillera, July 1988. Geosci Can 16:193–200

Geertsema M (1996) Earthflow generated wetlands. B.C. Ministry of Forests, Extension Note No. 20

Geertsema M (1998) Flowslides in waterlain muds of northwestern British Columbia, Canada. In: Moore DP, Hungr O (eds) Engineering geology and natural hazards. Proceedings, 8th IAEG Congress. Vancouver, BC, 3, pp 1913–1921

Geertsema M (2004) A composite earth flow—spread in glaciomarine sediments near Terrace, British Columbia. M.Sc. thesis. Department of Earth and Atmospheric Sciences, University of Alberta

Geertsema M (2013) Quick clay landslides, landscape evolution, and climate change: a perspective from British Columbia. In: Margotinni C, Canuti P, Sassa K (eds) Landslide science and practice, vol 4. Springer, Berlin, pp 115–120

Geertsema M, Cruden DM (2008) Travels in the Canadian Cordillera. In: 4th Canadian conference on geohazards. Quebec PQ

Geertsema M, Cruden DM (2014) Further travels in the Canadian Cordillera. In: Proceedings, 6th Canadian conference on geohazards. Kingston, ON

Geertsema M, L'Heureux J-S (2014) Controls on the dimensions of landslides in sensitive clays. In: L'Heureux JS, Locat A, Leroueil S, Demers D, Locat J (eds) Landslides in sensitive clays, chapter 9. Springer, Netherlands, pp 105–117

Geertsema M, Pojar JJ (2007) Influence of landslides on biophysical diversity—a perspective from British Columbia. Geomorphology 89:55–69

Geertsema M, Schwab JW (1996) A photographic overview and record of the Mink Creek Earthflow, Terrace, British Columbia. B.C. Ministry of Forests Research Report 08

Geertsema M, Schwab JW (1997) Retrogressive flowslides in the Terrace–Kitimat, British Columbia area: from early post-deglaciation to present—and implications for future slides. In: Proceedings of the 11th Vancouver geotechnical society symposium. pp 115–133

Geertsema M, Torrance JK (2005) Quick clay from the Mink Creek landslide near Terrace, British Columbia: geotechnical properties, mineralogy, and geochemistry. Can Geotech J 42:907–918

Geertsema M, Cruden DM, Schwab JW (2006) A large, rapid landslide in sensitive glaciomarine sediments at Mink Creek, northwestern British Columbia, Canada. Eng Geol 83:36–63

Hogan DL Schwab JW (1991) Meteorological conditions associated with hillslope failures on the Queen Charlotte Islands. B.C. Ministry of Forests, Land Management Report 73

Holland SS (1976) Landforms of British Columbia. A physiographic outline. British Columbia Department of Mines and Petroleum Resources, Bulletin No. 48

La Rochelle P, Chagnon YJ, Lefebvre G (1970) Regional geology and landslides in the marine clay deposits of eastern Canada. Can Geotech J 7:145–156

Lebuis J, Robert J-M, Rissmann P (1983) Regional mapping of landslide hazard in Quebec. In: Bergren B, Lindgren J (eds) Symposium on slopes on soft clays. Swedish Geotechnical Institute, Report 17:205–262

Lefebvre G (1986) Slope instability and valley formation in Canadian soft clay deposits. Can Geotech J 23:261–270

Lefebvre G (1996) Soft sensitive clays. In: Turner AK, Schuster RL (eds) Landslides investigation and mitigation. National Research Council, Transportation Safety Board, Special Report 24, pp 607–619

Mitchell RJ, Markell AR (1974) Flowsliding in sensitive soils. Can Geotech J 11:11–31

Patton FD (1984) Climate, groundwater pressures and stability analyses of landslides. In: Proceedings, 4th international symposium on landslides, Toronto, ON, 3, pp 43–59

Pielou EC (1991) After the ice age—the return of life to glaciated North America. University of Chicago Press, Chicago

Potvin EC, Pellerin F, Demers D, Robitaille D, La Rochelle P, Chagnon, J-Y (2002) Revue et investigation complementaire du site du glissement de Saint–Jean–Vianney. In: Proceedings—2001; an earth Odyssey. Canadian Geotechnical Society, Calgary, AB, pp 792–800

Quigley RM (1980) Geology, minerology, and geochemistry of Canadian soft soils: a geotechnical perspective. Can Geotech J 17:261–285

Rosenqvist ITh (1953) Considerations on the sensitivity of Norwegian quick-clays. Géotechnique 3:195–200

Schwab JW (1983) Mass wasting: October–November 1978 storm, Rennell Sound, Queen Charlotte Islands, British Columbia. B.C. Ministry of Forests, Research Note 91

Sharpe CFS (1938) Landslides and related phenomena. Columbia University Press, New York

Tavenas F, Chagnon J-Y, La Rochelle P (1971) The Saint–Jean–Vianney landslide: observations and eyewitnesses accounts. Can Geotech J 8:463–478

Torrance JK (1983) Towards a general model of quick clay development. Sedimentology 30:547–555

Trak B, Lacasse S (1996) Soils susceptible to flow slides and associated mechanisms. In: Proceedings, seventh international symposium on landslides. Trondheim, Norway. Balkema, Rotterdam, 3, pp 497–506

Viberg L (1983) Experiences of mapping and classification of stability conditions. Swedish Geotechnical Institute, Report No. 17, pp 455–461

The Fraser Lowland: A Polygenetic Paraglacial Landsystem

26

Dori J. Kovanen and Olav Slaymaker

Abstract

The Fraser Lowland is a landsystem that has been modified in its entirety by non-glacial processes conditioned by glaciation. The Late Pleistocene and Holocene paraglacial processes of landform modification include slope erosion, glacimarine, marine, glacifluvial, fluvial, glacilacustrine, lacustrine, organic, mass movement, and aeolian. This complex paraglacial landsystem has transitioned from proglacial through marine to its present dominantly fluvial character. Landforms representative of each sediment redistribution process are described, and a conceptual model is developed with relative sea level and sediment source changes as the primary drivers. Accelerated anthropogenic modification during the past two centuries (the Anthropocene) has complicated the paraglacial story and is shown to impact the incidence of natural hazards, especially in the context of hydroclimate change.

Keywords

Paraglacial • Landscape • LiDAR • Natural hazards • Fraser Lowland

26.1 Introduction

In formerly glaciated regions, postglacial landscape evolution can be conceptualized by a model of paraglacial landscape response, which describes the readjustment of a landscape from glacial to non-glacial conditions over time (Ryder 1971; Church and Ryder 1972; Church and Slaymaker 1989; Ballantyne 2002). The withdrawal of ice exposes large sediment stores that are in unstable or metastable states and consequently become available for modification, erosion, and sediment transport at rates exceeding background denudation rates. Ballantyne (2002) expanded understanding of paraglacial geomorphology by including rock slopes, drift-mantled slopes, glacier forelands, alluvial and lacustrine landforms, and coasts as interlinked paraglacial landsystems. Each landsystem consists of a series of sediment cascades by which glacigenic drift is reworked, transferred, stored, remobilized, and deposited in terrestrial, lacustrine, and coastal environments (Fig. 54 in Ballantyne 2002).

Slaymaker (2009) proposed that paraglacial environments should be viewed as 'transitional landscapes' that are not fully adjusted to regional hydroclimate or present sea level. The sequence of landscape change is broadly recognized as pleniglacial, proglacial, and paraglacial. The paraglacial processes responsible for the transitions include relative sea level change; marine, lacustrine, and fluvial transportation/redistribution of sediments; relaxation of steep slopes by mass movements; and aeolian processes, each of them conditioned by glaciation. The complex paraglacial landsystem becomes progressively more dominated by non-glacial processes over time (Kovanen and Slaymaker 2015).

Here, we present a new perspective on the geomorphology of the Canadian sector of the Fraser Lowland (Fig. 26.1). All the landscape, landforms, and surface materials are viewed through the filter of paraglaciation. This area was overridden by the Cordilleran Ice Sheet during the

D.J. Kovanen (✉) · O. Slaymaker
Department of Geography, University of British Columbia, 1984 West Mall, Vancouver, BC V6T 1Z2, Canada
e-mail: djkovanen@comcast.net

O. Slaymaker
e-mail: olav.slaymaker@ubc.ca

© Springer International Publishing Switzerland 2017
O. Slaymaker (ed.), *Landscapes and Landforms of Western Canada*, World Geomorphological Landscapes, DOI: 10.1007/978-3-319-44595-3_26

Pleistocene, differentially eroded by outflow glaciers, and blanketed by till. It is the extent to which these glacial landforms and sediments have been modified by 'non-glacial processes conditioned by glaciation' (Church and Ryder 1972) that is the central theme of this chapter. The documented increase in natural hazards (Brooks 2001) during the second half of the twentieth century may be sufficiently disruptive of the paraglacial landsystem as to constitute a new disturbance regime (Slaymaker 2012).

26.2 Regional Setting

26.2.1 Background Information

The Fraser Lowland extends west from Hope between the Coast Mountains and North Cascade Range to the Strait of Georgia (Fig. 26.2) and consists of relatively low relief terrain. Regional relief is largely the result of tectonic uplift of the Coast Mountains and Cascades and continuing subsidence of the Fraser Lowland during the Tertiary period. Most of the details of the Fraser Lowland stratigraphy were caused by repeated episodes of intense glacial erosion and deposition during the Pleistocene (Clague 1986). The landforms today are largely conditioned by the last (Fraser) glaciation (e.g. Church et al. 1999; Booth et al. 2004).

The lower Fraser River is the region's primary river which discharges into the Strait of Georgia. Fraser River continues to build its delta, the form of which is strongly dependent on anthropogenic processes (Fig. 26.3). Contemporary modification of the Fraser delta includes dredging the riverbed to maintain navigation channels and to supply construction aggregate. The effect of this confinement is to channelize flow and sediment deposition at the river mouth.

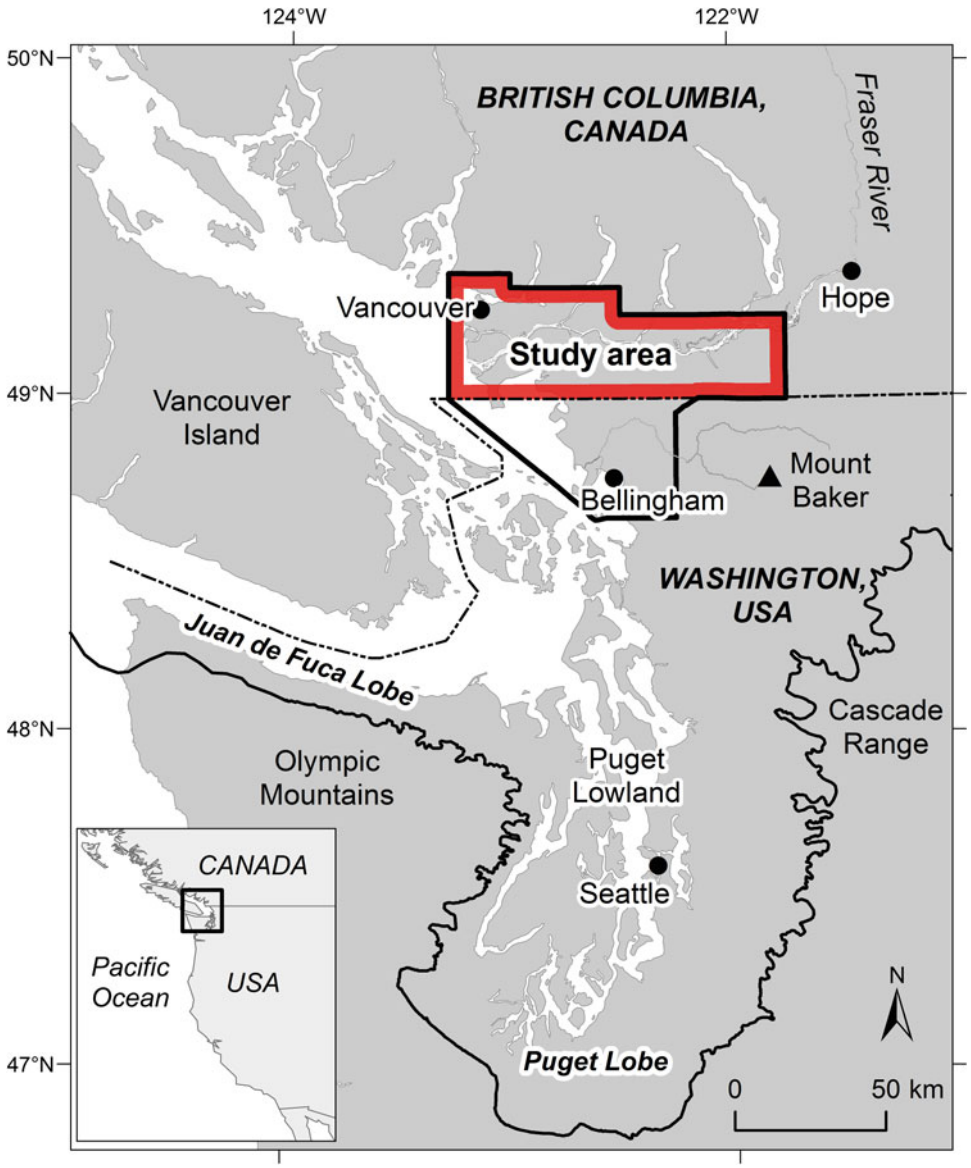

Fig. 26.1 Location of the study area, southwestern British Columbia is delimited by the *red frame*. Also shown is the maximum extent of the Puget lobe, which drained the southwestern margin of the Cordilleran Ice Sheet during the late Pleistocene. The Juan de Fuca lobe terminated on the continental shelf (modified from Kovanen and Slaymaker 2015)

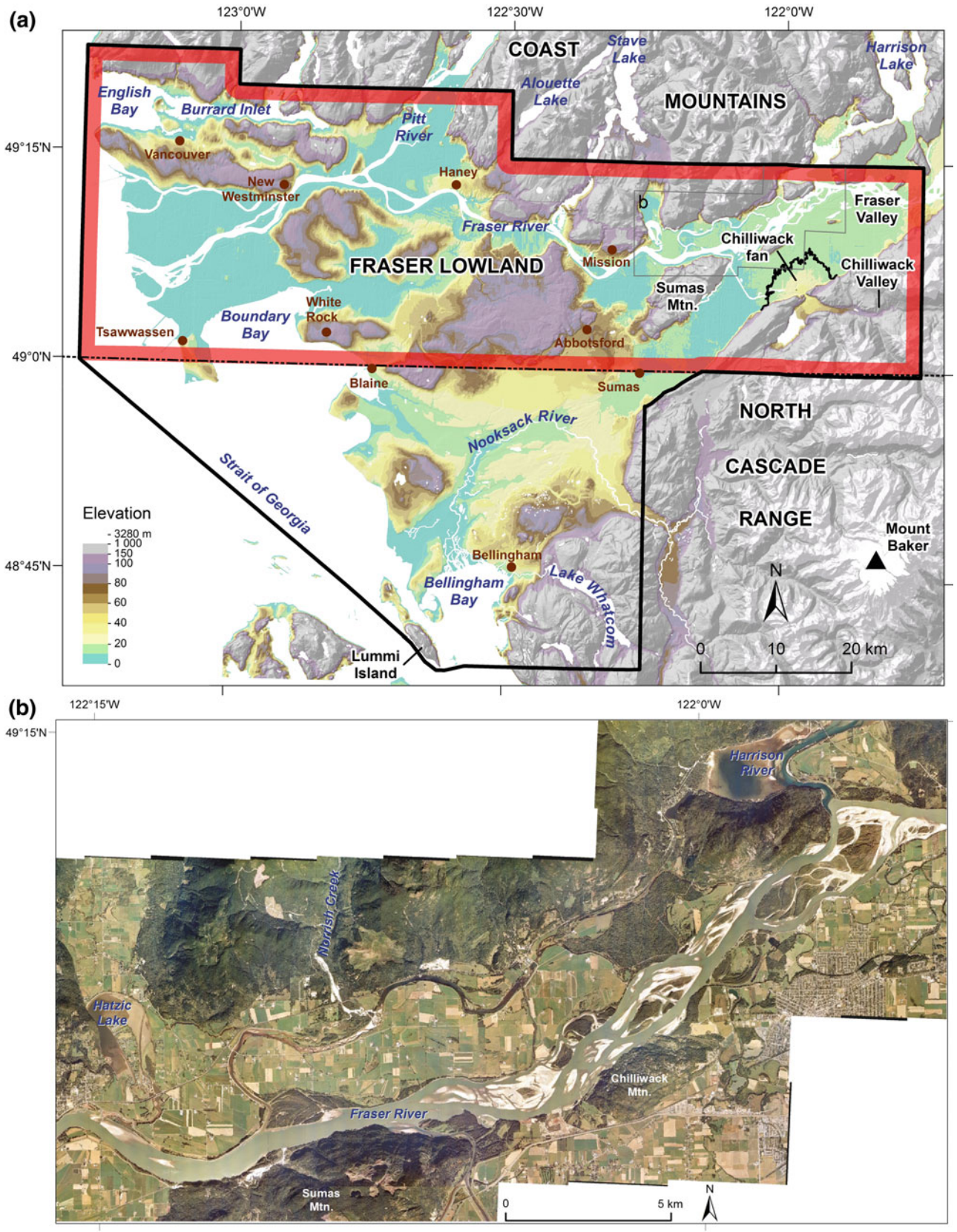

Fig. 26.2 **a** Topography of the study area (c. 3721 km^2) centered on the Fraser Lowland. The Chilliwack fan is delimited by the 15 m contour (modified from Kovanen and Slaymaker 2015). **b** Air photograph of the lowest braided reach of Fraser River. Downstream from this point Fraser River adopts a meandering habit. The location is shown in (**a**). *Photograph* regional_mosaics_bc_fraser-hope_xc1m_bcalb_1995, from British Columbia Imagery WMS. Contains information licensed under the Open Government License—British Columbia

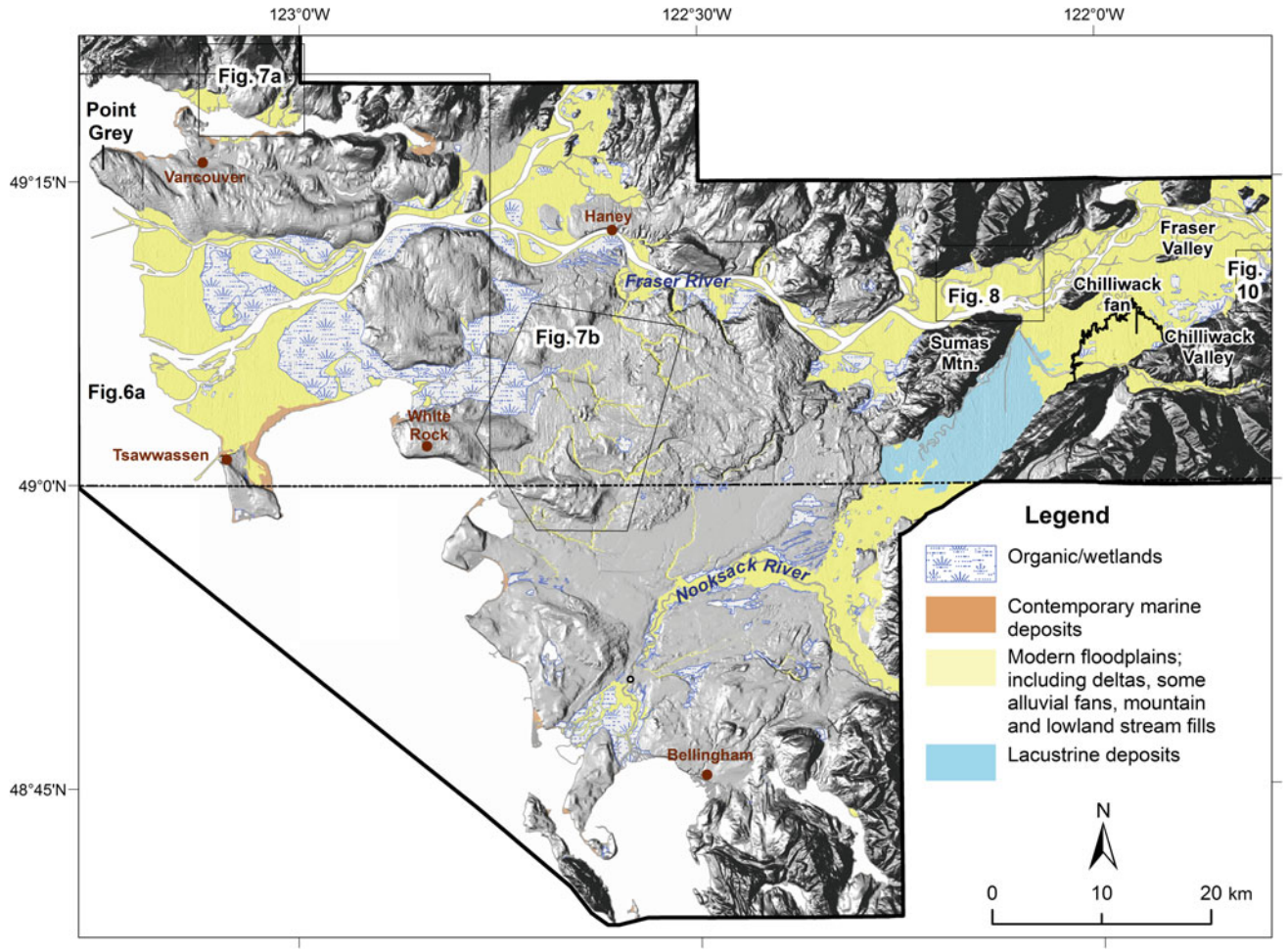

Fig. 26.3 Hillshade image showing landforms of Fraser River including the delta, alluvial fans, mountain and lowland stream fills, organic wetlands, and lacustrine deposits. The locations of detailed maps used to describe representative paraglacial landforms are indicated (modified from Kovanen and Slaymaker 2015)

This accumulating sediment fails by mass movement at the delta front. Sand that formerly replenished the tidal flats at the delta front is now lost to deep water.

The dominant characteristic of tributaries of Fraser River is one of fluvial dissection of glacial deposits and paraglacial sediments, forming valleys whose broad cross sections were established by the glacial meltwaters of the last glaciation. They are in almost all cases 'misfit' streams, with discharges that rarely fill the valley cross sections under the present hydrologic regime (Collins and Montgomery 2011).

26.2.2 Glacial Conditioning of the Fraser Lowland During the Late Pleistocene

During the last (Fraser) glaciation, glaciers flowed from the Coast Mountains of BC, streamed down fjords and valleys, coalesced to form a piedmont lobe, and extended to fill the isostatically depressed coastal lowlands between the Olympic Mountains and Cascade Range (Fig. 26.1). At its peak by c. 14,550 ± 70 ^{14}C year BP (17,530–17,940 cal year BP; Porter and Swanson 1998), ice was up to c. 1800 m thick over the Fraser Lowland (Easterbrook 1963).

Glacially conditioned sediment transport and storage commenced with deglaciation and locally proceeded through four stages:

1. Rapid frontal retreat and downwasting, facilitated by changing relative sea level, flooded coastal lowlands, and created embayments as the glaciers calved back to fjord heads. The opening accommodation space led to the deposition of glacimarine and marine deposits (Fig. 26.4a; Armstrong 1957 and 1981; Easterbrook 1963; Dethier et al. 1995). Sediments deposited in the glacimarine setting were derived from a variety of

sources and modes of transport by ice (Dethier et al. 1995), but the modification of these sediments was by marine processes. By c. 12,200 ± 170 ^{14}C year BP (marine reservoir corrected age; 13,480–15,170 cal year BP; GSC-2193; Armstrong 1981), the coastline was at a present elevation of at least 175 m asl—the elevation of the highest delta near Vancouver (Armstrong 1957, pg. 6).

2. Rapid isostatic rebound exposed the land surface, and the glacier that persisted in the Fraser Valley became land based (Clague et al. 1997). By c. 11,810 ± 60 ^{14}C year BP (13,480–13,760 cal year BP; B-135696), the sea had fallen to at least 67 m asl and occupied the lower reaches of many paleovalleys (Kovanen 2002).
3. Multiple readvances of the ice margin separated by brief periods of retreat occurred shortly before and after c. 11,300 ± 80 ^{14}C year BP (13,030–13,310 cal year BP; TO-4056; Clague et al. 1997; also see Armstrong 1957; Kovanen and Easterbrook 2002; Kovanen and Slaymaker 2003), resulting in the deposition of moraines, meltout debris, and glacifluvial deposits in valleys, terraces, raised deltas terraces, and large fans. At times, the advances blocked the natural drainage of adjacent basins where proglacial lakes developed (e.g. Saunders et al. 1987; Kovanen et al., unpublished results; Fig. 26.4b).
4. Outburst floods originating from ice- or moraine-dammed lakes (e.g. Blais-Stevens et al. 2003; Johnsen and Brennand 2004) scoured and entrenched many surfaces in low-lying areas by c. 10,245 ± 90 ^{14}C year BP (11,620–12,400 cal year BP; AA-27057; Kovanen and Easterbrook 2002). Fraser River established its present course between c. 11,000 and 9000 year BP, following deglaciation (Armstrong 1981; Clague et al. 1983).

26.2.3 Relative Sea Level and Sediment Redistribution Changes as Drivers of Change in the Paraglacial Fraser Lowland

As sea level changed following retreat of the Cordilleran Ice Sheet, the paraglacial sediment-to-sink cascade was supplied by glacigenic sediment sources and fluvial aggradation was the initial response.

As indicated by a suite of cores from the Fraser delta and floodplain—studied by Mathews et al. (1970), Clague et al. (1982), and Williams and Roberts (1989)—emergence of the land surface culminated during the early Holocene with shorelines that were at least 13 m below present sea level by 8360 ± 170 ^{14}C year BP (8780–9700 cal year BP). The lowstand was followed by a gradual rise in sea level (eustatic) until c. 7000 ^{14}C year BP when it had risen to c. −5 m. Emergence of the land surface increased the gradients of streams (e.g., increased incision) and made sediment sources that had previously become temporary storage sites available for erosion and transportation by those streams. As sediment storage areas were transformed into sediment sources, the entire range of non-glacial processes of sediment redistribution (marine, fluvial, mass movement, and aeolian) were activated. By c. 2080 ± 110 ^{14}C year BP (1830–2330 cal year BP; TO-409; Williams and Roberts 1989), the modern coastline position and modern sedimentary conditions were established (e.g. Clague 1998). Consequently, the paraglacial landscape transformation was achieved in a regime of fluctuating sea level and new sediment sources becoming exposed to the major subaerial processes of erosion and sedimentation.

By defining paraglacial sedimentation as the work of 'non-glacial processes conditioned by glaciation,' Church and Ryder (1972) considered glaciation extrinsic to the paraglacial system. Ballantyne (2002) argued that relative sea level is also an extrinsic process. His argument is that glaci-eustatic effects have been documented around all of Earth's oceans, and if relative sea level change is regarded as intrinsic to paraglaciation, this opens up the possibility that all coastlines are paraglacial. We take the view that relative sea level change is intrinsic to the paraglacial system in locations influenced by both glaci-eustasy and glaci-isostasy and that this criterion ensures that relative sea level changes are a 'non-glacial process conditioned by glaciation.' Other sediment redistribution processes—which are not conditioned by glaciation, such as tectonism, hydroclimatic change, and anthropogenic activity—are considered external to the paraglacial process. Their influence on the Fraser Lowland will be considered later in the chapter.

26.3 The GIS Framework and Paraglacial Landform Units

Table 26.1 shows the hierarchical framework of this study. Landform units are defined by terrain attributes, genesis, and time and constitute the first level of the hierarchy.

These units were registered in the GIS framework as polygon features. Their attributes contain descriptive information associated with our analyses and classification hierarchy. In short, the elements of the landforms were assigned a symbol, a description, whether glacial or paraglacial, most recent process of terrain modification, and whether Holocene or Late Pleistocene. The integration of spatial and attribute data resulted in 5262 paraglacial landform units.

At the second level of the hierarchy, landforms and their associated sediments from the two digital sources were simplified, reclassified, and ultimately merged. These data were then aggregated, defined by dominant surficial

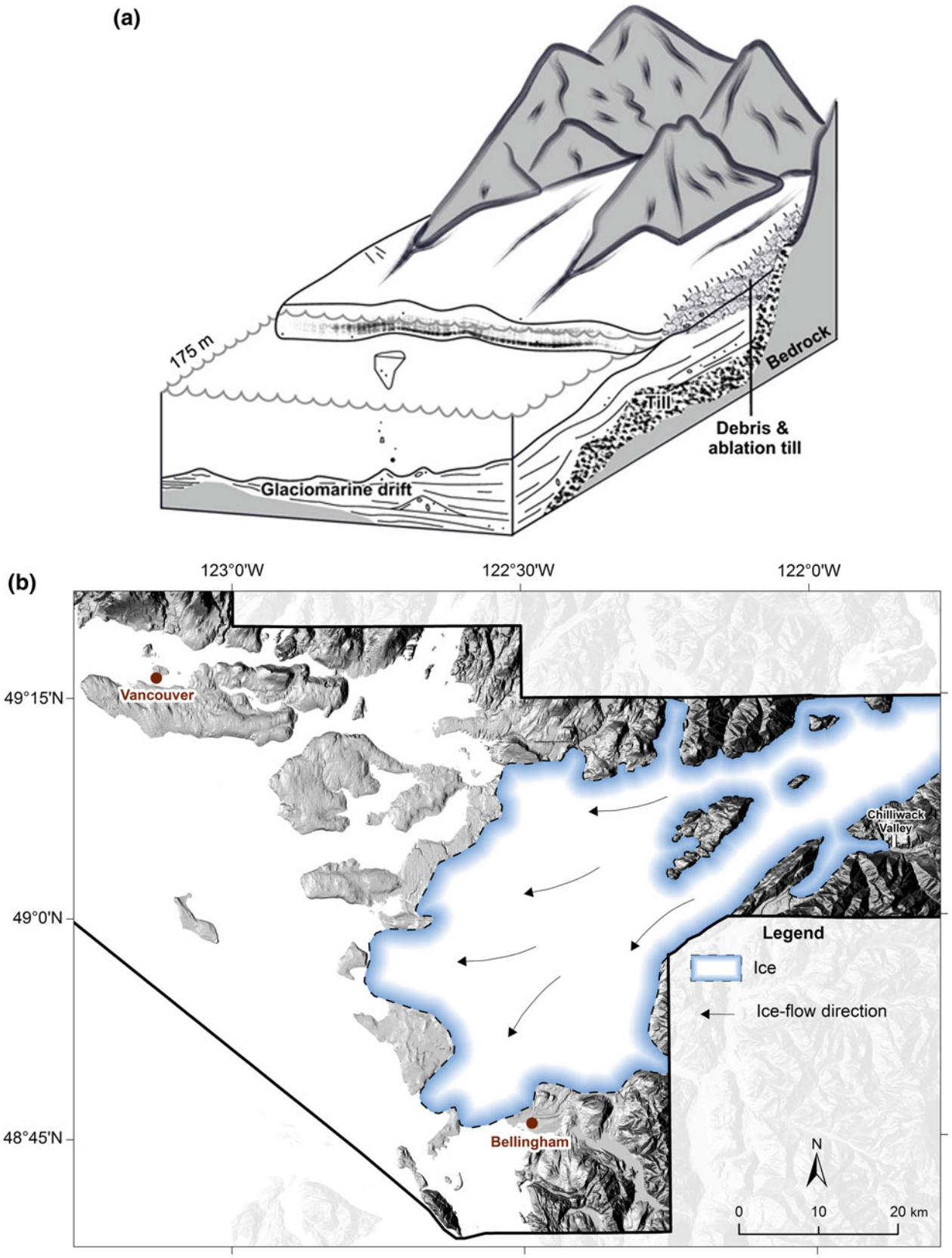

Fig. 26.4 **a** Diagram showing deposition of late Pleistocene glacimarine sediments by marine-based ice sheet nourished by mountain glaciers. Thick deposits of glacimarine and marinesediment drape over the preexisting seafloor. **b** Maximum extent of ice during a readvance following initial deglaciation. Along the western margin, uplifted shorelines are cut by and also lap onto moraines, suggesting that a part of the glacier was calving into the sea (sea level was probably lower than c. 41 m and at least as high as c. 36 m) (Kovanen and Slaymaker 2015)

Table 26.1 Methodological framework (Kovanen and Slaymaker 2015)

Paraglacial hierarchy (number of units)	Level of hierarchy	Definition
Landsystem (1)	3	Defined as the sum of all paraglacial landforms and sediments
Landforms and their sediments (10)	2	Defined by dominant surface materials and time
Landform units (5262)	1	Units defined by terrain attributes, genesis, and time

sediment type, morphology, and inferred process and form the basis of thematic maps that show the distribution of paraglacial landforms and their sediments occurring in the Fraser Lowland. There are just ten of these morphogenetic units.

The third and highest level of the hierarchy is the landsystem. The term landsystem refers to a grouping of landforms and related sediments. Such an approach has been favored by geomorphologists and glacial geologists as a means of identifying, classifying, and explaining landform–sediment associations (Eyles 1983; Benn and Evans 2010; see Sect. 26.4.2). In this case, we have defined the whole Fraser Lowland in British Columbia as a single paraglacial landsystem.

26.4 Paraglacial Landforms and Their Sediments

26.4.1 The Paraglacial Morphogenetic Units

In their original discussion of paraglacial environments, Church and Ryder (1972) envisaged a paraglacial period that commenced with and included a proglacial period. This proglacial period was characterized by glacimarine, glacifluvial, and glacilacustrine sedimentation, which were also seen as paraglacial processes because they are 'non-glacial processes conditioned by glaciation.' They discussed explicitly the role of glacifluvial sedimentation during the proglacial period, but glacimarine and glacilacustrine would also qualify as non-glacial processes on the ground that the dynamic processes of sedimentation are (respectively) fluvial, marine, and lacustrine. Paraglacial landforms and their sediments in this study can be divided into 10 morphogenetic units: (1) Late Pleistocene modified glacial; (2) Late Pleistocene glacimarine; (3) Holocene marine; (4) Late Pleistocene glacifluvial; (5) Holocene fluvial; (6) Late Pleistocene glacilacustrine; (7) Holocene lacustrine; (8) Holocene organic accumulation; (9) Holocene mass movement; and (10) Holocene aeolian (Fig. 26.5a). Below, the paraglacial landscape is described with the aid of landforms and sediments representative of each morphogenetic category. We have grouped the morphogenetic units subject to similar sediment redistribution processes. Histograms of the relative area of each unit within the total Fraser Lowland (Fig. 26.5b) and that which is confined to the Fraser Lowland in BC (Fig. 26.5c) have been calculated. These histograms demonstrate that the Fraser Lowland in BC is reasonably representative of the total Fraser Lowland (for details, see Kovanen and Slaymaker 2015).

1. **Late Pleistocene Modified Glacial Units** Modified glacigenic sediments are paraglacial in so far as they have been modified by subaerial processes over the past 14,000 years or so. The distribution of modified glacial units is shown in Fig. 26.5a. These units cover an area of c. 25 % of the map area and are the largest single morphogenetic group. They contain material transported and deposited at the margin, or scoured and abraded at the base, of the former Cordilleran Ice Sheet. In the lowland and along the flanks of the mountains, within the limits of stage (3) mentioned in Sect. 26.2, characteristic landforms include moraines, kame terraces, and streamlined lineations composed of glacial drift. These were deposited during readvance and final retreat of the ice from the area. All glacial units have been modified by running water, soil creep, and sheetwash. The rate of operation of these processes is low (ranging from 1 to 25 m^3 km^{-2} $year^{-1}$ according to Roberts and Church 1986), but gullying at select locations can be one to two orders of magnitude more rapid (Campbell and Church 2003).
2. **Late Pleistocene Glacimarine Units** During the deglacial phase of inundation, the retreating glacier deposited ice-marginal diamicton against valley sides and glacimarine sediments produced by marine reworking of glacigenic deposits. The glacimarine drift includes mixtures of stony, silty clay, which is unsorted and may show faint, irregular stratification. This morphogenetic unit comprises c. 729 km^2 of the map area and is the third most extensive component of the paraglacial landsystem (Fig. 26.5a). Beach ridges that typically fringe uplands beyond the maximum extent of the last glacial resurgence may exhibit a vertical relief up to c. 1 m, especially on relatively flat slopes, and range in altitude from c. 150 to 11 masl. They are spatially

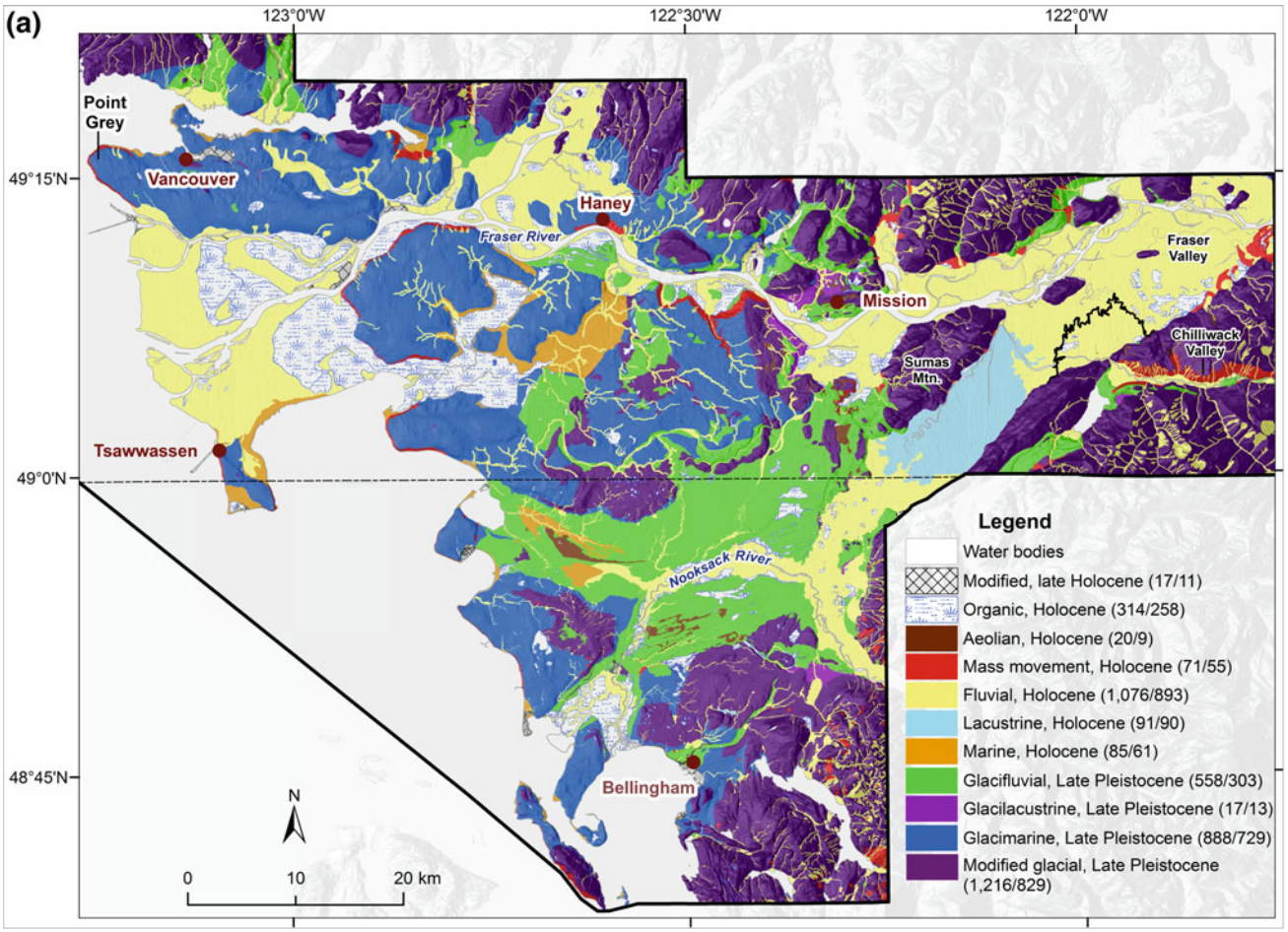

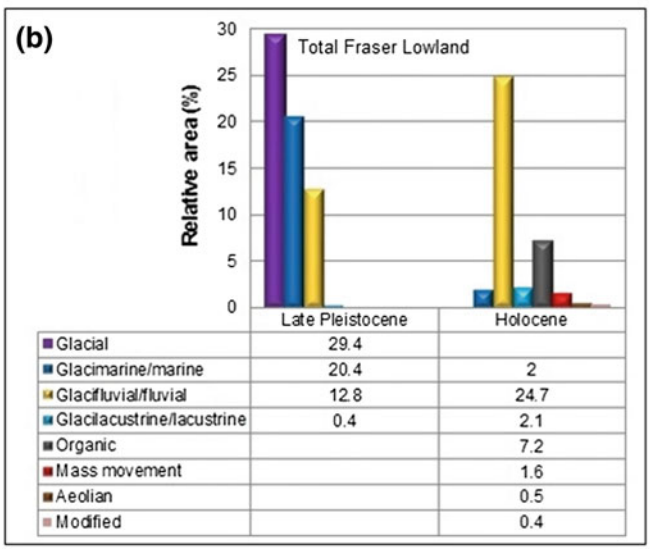

	Late Pleistocene	Holocene
Glacial	29.4	
Glacimarine/marine	20.4	2
Glacifluvial/fluvial	12.8	24.7
Glacilacustrine/lacustrine	0.4	2.1
Organic		7.2
Mass movement		1.6
Aeolian		0.5
Modified		0.4

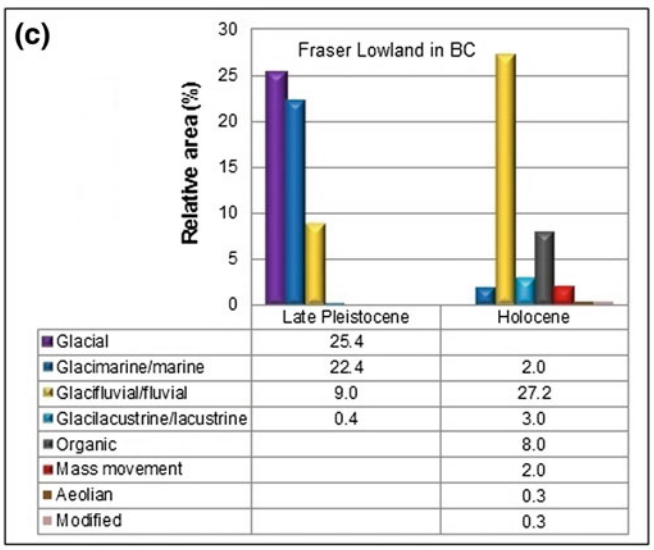

	Late Pleistocene	Holocene
Glacial	25.4	
Glacimarine/marine	22.4	2.0
Glacifluvial/fluvial	9.0	27.2
Glacilacustrine/lacustrine	0.4	3.0
Organic		8.0
Mass movement		2.0
Aeolian		0.3
Modified		0.3

Fig. 26.5 **a** Distribution of Late Pleistocene and Holocene paraglacial landforms and sediment (area, km^2: total area/in BC). **b**, **c** Chart showing relative area (%) of paraglacial landforms and sediments in the contemporary landscape (**a** and **b**, modified from Kovanen and Slaymaker 2015)

discontinuous and best developed where the underlying glacigenic and glacimarine deposits provided a local sediment source and where fluvial, glacial, and/or marine erosion have not degraded them. These glacimarine landforms and sediments continue to be modified in the contemporary landscape by fluvial erosion and mass movement.

3. **Holocene Marine Units** As mentioned above, sea level was at least 13 m below its present level during the early Holocene, followed by a steady rise and mid-Holocene stabilization c. 7000 ^{14}C year BP to within 5 m of present (e.g. Clague et al. 1982; Clague and James 2002). The modern shoreline can be characterized as follows (e.g. Shipman 2008):
   (a) Sandy or gravelly beaches—mainly depositional beaches characterized by active transport of sediment by wave action and longshore drift (Fig. 26.6). These features include spits, bars, and sand ridges. Also, much of a beach-ridge complex deposited over the Boundary Bay tidal flats (Figs. 26.5a and 26.6) has formed since 2080 ± 110 ^{14}C year BP (1830–2330 cal year BP; TO-409; Williams and Roberts 1989) in equilibrium with modern sea level (Engels and Roberts 2005).
   (b) Embayments, such as protected estuaries and lagoons—the Nicomekl and Serpentine river estuaries (Fig. 26.6a) are good examples.
   (c) The Fraser River delta onlaps the former island of Tsawwassen (Figs. 26.5a, 26.6a).
   (d) Rocky shorelines include rocky platforms and pocket beaches of gravel and cobbles protected by bedrock headlands as exemplified on the western end of the North Shore along English Bay (Figs. 26.2a and 26.6a).
   (e) Coastal bluffs—at Point Grey bluffs up to 70-m-high bluffs have been retreating at rates up to 50 cm year^{-1} during the 1960–1980 period. In addition to normal coastal retreat, torrential rains occasionally accelerate gullying, such as in January 1935 when about 100,000 m^3 of sand were removed over a period of two days at Point Grey (Clague 1982).
4. **Late Pleistocene Glacifluvial Units** Glacifluvial deposits cap many valley fills, accumulated in meltwater channels, and rest against steep slopes. Characteristic features include (a) erosional landforms—meltwater channels that contain misfit streams and outburst flood-scoured surfaces; and (b) depositional landforms—outwash plains, kames, terraces, large fans that may coalesce, and aggrading floodplains produced by reworking of glacigenic sediment. Thick Pleistocene fills occur in many mountain valleys that are tributary to the Fraser Lowland. Emergence from the early postglacial highstand has entrenched and reworked these deposits to produce a series of lower deltaic and fluvial terraces, wave-cut terraces, and lag deposits at the mouth of many mountain streams. Representative examples of these landforms are found along the lower Capilano and Seymour rivers and Lynn Creek (Fig. 26.7a; Armstrong 1981). Marine shells collected from a raised delta at an elevation of 154 m asl yielded an age of 12,200 ± 170 ^{14}C year BP (marine reservoir corrected age, 13,480–15,170 cal year BP; GSC-2193; Armstrong, 1981), indicating that emergence and reworking of the deltaic deposits, as well as channel incision and lake drainage, probably occurred after c. 12,400 ^{14}C year BP until sea level fell to its present datum c. 11,000 ^{14}C year BP ago (Clague et al. 1982). A representative delta is the Campbell River delta, which occurs south of Langley (Fig. 26.7b). Water from a late Pleistocene ice margin, c. 16 km to the east, incised and flowed through the meltwater channel occupied by the modern Campbell River and built the delta at c. 40 m above modern sea level (e.g. Armstrong 1981; Clague and Luternauer 1983) prior to 11,413 ± 75 ^{14}C year BP (13,100–13,410 cal year BP; AA-27063; Kovanen and Easterbrook 2002).
5. **Holocene Fluvial Units** 27 % of the Fraser Lowland in BC consists of Holocene fluvial landforms and sediments. This morphogenetic group is the second most extensive in the Fraser Lowland. The aggradational floodplain and major delta of Fraser River are the dominant fluvial landforms. Other characteristic landforms include:
   (a) Alluvial fans—the Chilliwack fan dominates the eastern half of the Fraser Lowland (Fig. 26.3). A mix of debris flow and fluvial sediments deposited where streams emerge from steep, narrow valleys onto flatter ground. Many alluvial fans are dissected relict features in the present landscape and date from early postglacial time.
   (b) Gullies—steep incised channels that convey water, sediment, and woody debris and are associated with channelized debris flows. Gullies in the colluvial deposits on hillslopes and the fluvial channel reaches on the valley floor within the mountain front have become the main sources of sediment (e.g. Figs. 26.7a and 26.8). Contemporary rates of mobilization of sediment from these basins are estimated at around 330 m^3 km^{-2} year^{-1} based on the dense gully networks in the adjacent Coast Mountains (Campbell and Church 2003). The contemporary contribution to streams from channelized debris flows is estimated at c. 170 m^3 km^{-2} year^{-1} (Brardinoni et al. 2003).
   (c) Deltas—Fraser delta has developed as a tidally influenced sedimentary body, prograding westward into the Strait of Georgia entirely within the Holocene over the past 10,000 years (Fig. 26.9). The subaerial portion of the Fraser River delta ranges from 1 to 5 m asl and comprises a dyked floodplain that extends 23 km westward from a gap in the Pleistocene uplands at New Westminster (Figs. 26.2a, 26.3, and 26.9a, b) and is mantled by

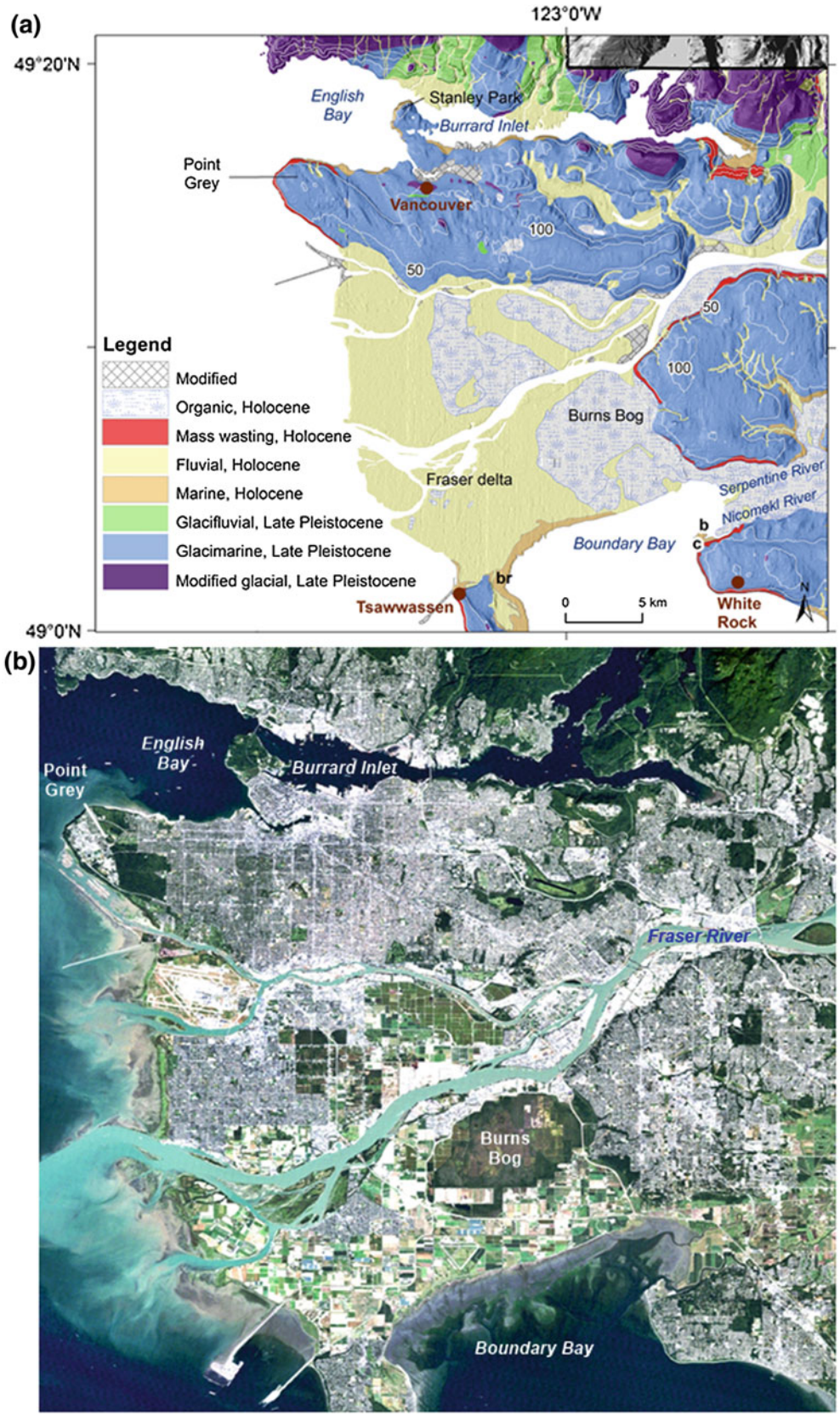

Fig. 26.6 **a** Modern shoreline configuration showing embayments that deeply indent the mainland, spits, and a portion of the Fraser River delta. 'br'—beach ridges; 'c'—Crescent Beach; and 'b'—Blackie Spit, a remnant tip of the larger Crescent Beach spit system. Also, shown are the estuaries of the Nicomekl and Serpentine rivers and a portion of the Fraser River estuary. See Fig. 26.3 for location. **b** Landsat image of the Vancouver metropolitan area, 2011. *Source* NASA GSFC Landsat/LDCM EPO Team

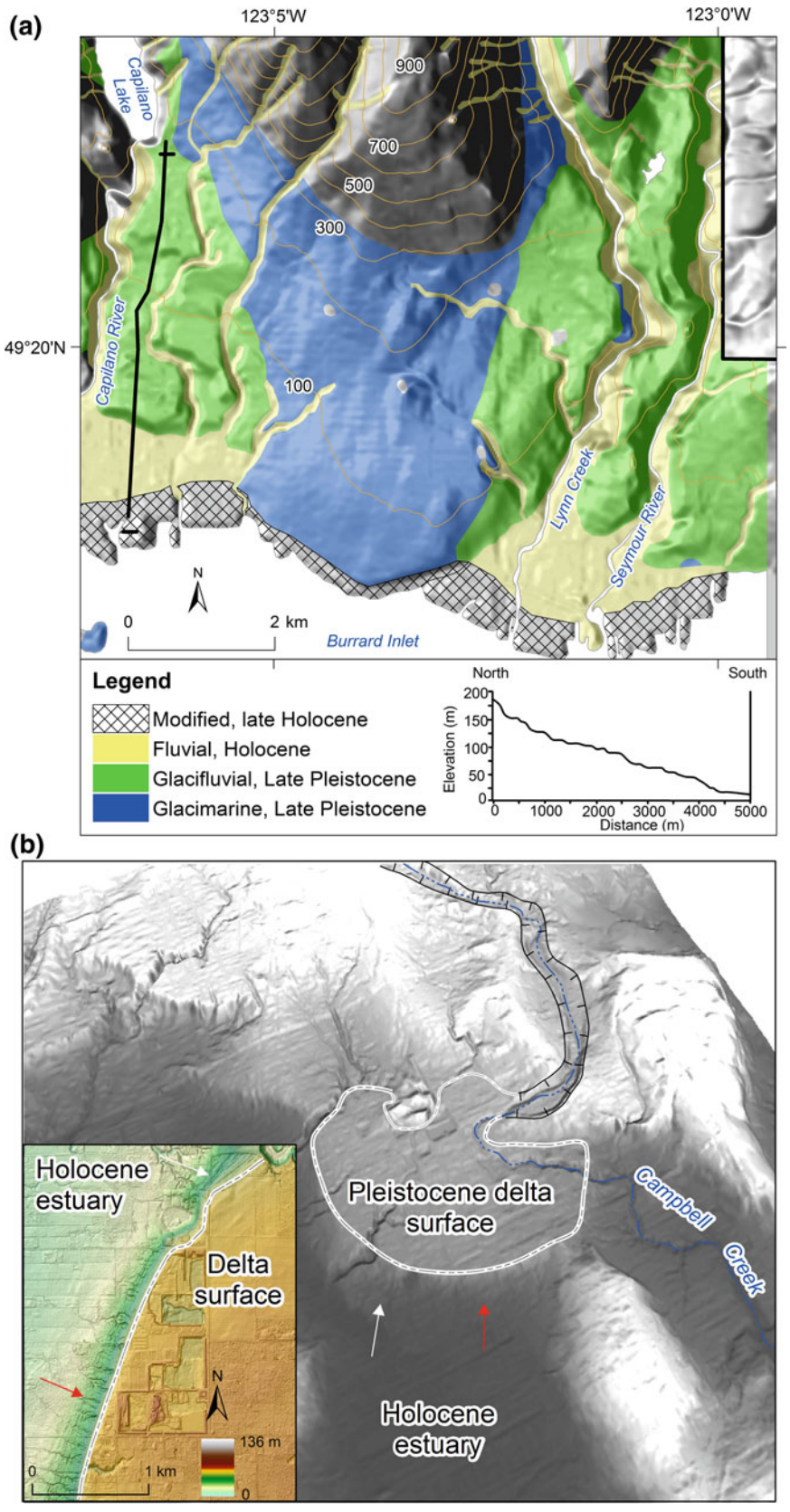

Fig. 26.7 Glacifluvial landforms in the Fraser Lowland. **a** North Vancouver area showing terraces that formed as rate of isostatic uplift outpaced eustatic sea level rise following retreat of glacial ice (*base data source* The District of North Vancouver GIS Department 2014). Contour interval is 100 m. **b** Perspective view of the Campbell Creek delta and a portion of its feeder meltwater channel. The delta surface rises to the southeast from 40 to c. 60 masl at the apex. *Arrows* point toward raised shorelines that descend to the earliest Holocene sea floor shown in the inset image (*LiDAR data source* City of Surrey 2014) (Kovanen and Slaymaker 2015)

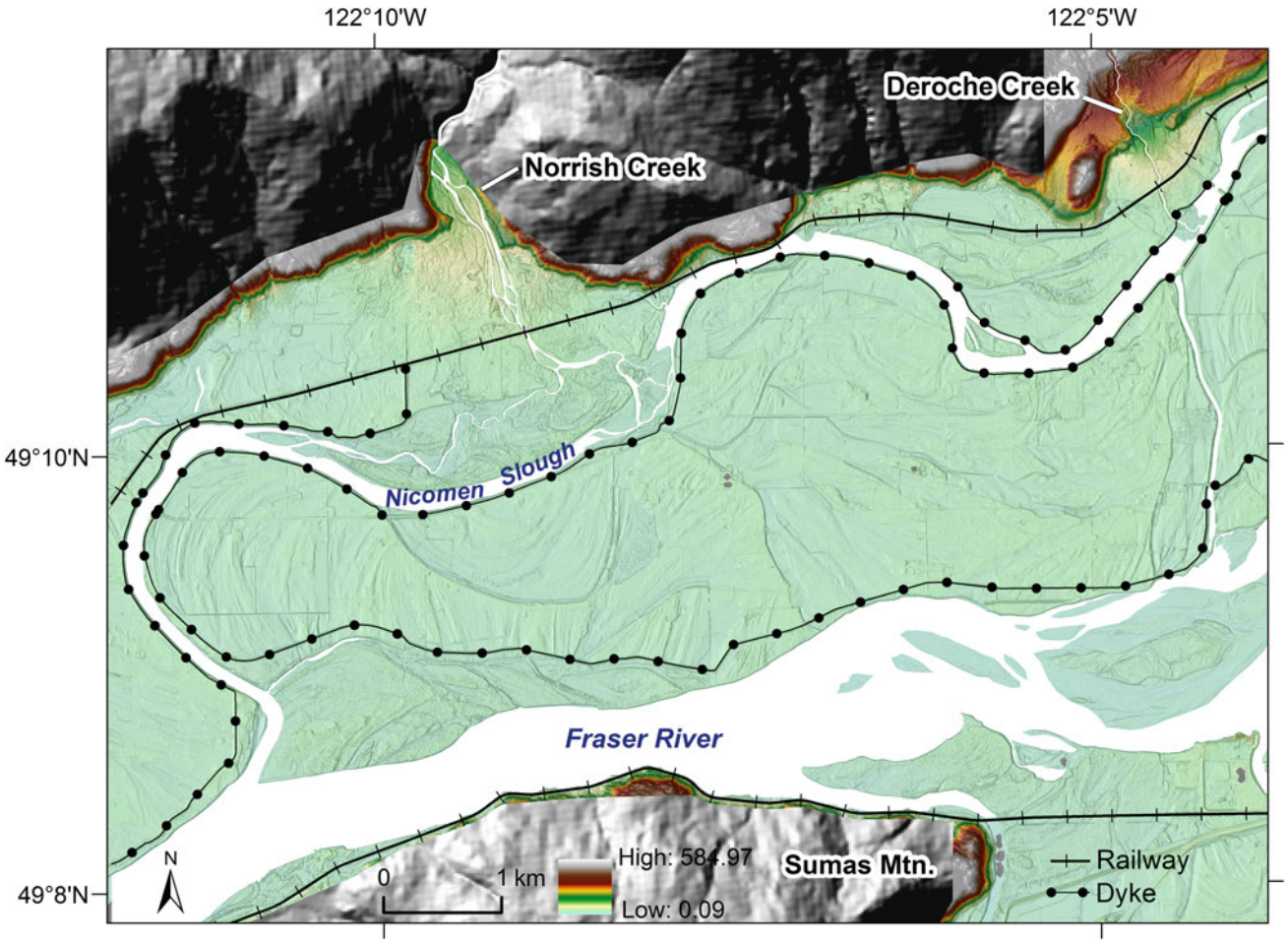

Fig. 26.8 Fluvial landforms in the Fraser Lowland. **a** Norrish and Deroche creek areas showing a debris torrent fan and a portion of the lower Fraser River floodplain. The *shaded* relief image of the floodplain is derived from LiDAR data (*LiDAR data source*, Fraser Basin Council 2008) and draped over a terrain model of coarser resolution. The vertical scale is exaggerated eight times; see Fig. 26.3 for locations

silt and peat. The delta conformably overlies late Pleistocene glacial drift. Since deltaic sedimentation commenced, local relative sea level has risen at least 13 m (Clague et al. 1998). Rising base level caused accelerated aggradation of the delta and the floodplain, such that the rate of sediment accumulation kept pace with the rate of sea level rise (Williams and Roberts 1989; Monahan et al. 1993). Dykes now control the course of the South, Middle and North arms of Fraser River, effectively preventing further channel migration and concentrating sedimentation.

6. **Late Pleistocene Glacilacustrine Units** Glacilacustrine sediments were deposited in ice- or moraine-dammed lakes that were confined in tributary valleys or against topographic highs during or shortly after deglaciation (Fig. 26.5a). These sediments consist mainly of silt and fine sand. Relict lake shorelines are erosional features where wave action cut a terrace into the valley side. Hence, the map shows areas of relict lake shorelines associated with terraces that are underlain by lacustrine sediments. The raised lake terraces at Mission and in the Chilliwack Valley are two of the best-developed examples within the map area. In these glacilacustrine sediments, altered drainage conditions can produce piping and gullying.
7. **Holocene Lacustrine Units** Holocene lacustrine sediments are associated with lake deltas with fine grained forests and with bottomsets. Sumas Lake once filled the valley south of Sumas Mountain (Fig. 26.5a), and its shorelines are evident on both sides of the border. The paraglacial Chilliwack alluvial fan (Tunnicliffe et al. 2012) intersects the drained Sumas Lake shoreline deposits at its western end. The lake was drained in the 1920s (Environment Canada 1992).
8. **Holocene Organic Units** Peat has accumulated in poorly drained areas in surface depressions or valley bottoms. Although the geomorphological sites range in

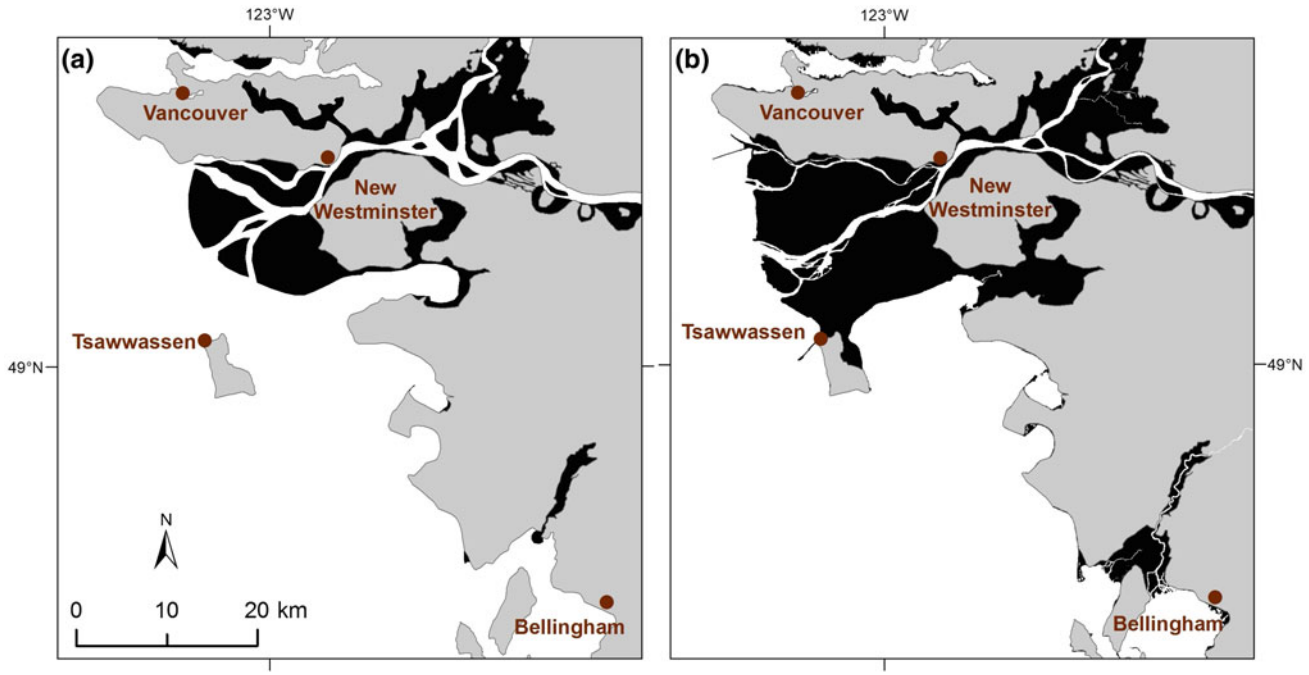

Fig. 26.9 **a** Reconstruction of the Fraser delta c. 5000 years ago (Clague et al. 1991). **b** Present-day extent of the Fraser delta (area, c. 625 km^2) (Kovanen and Slaymaker 2015)

age from Late Pleistocene (glacial outwash) to Holocene (river floodplains), the organic units themselves are Holocene in age. Organic deposits accumulated in kettles, glacially eroded depressions, backswamps, abandoned channels, abandoned channel–levee complexes on floodplains, bogs and fens, and on delta and coastal marshes and estuaries. Burns Bog, a raised dome peat bog (Fig. 26.6a), is the largest urban green space in greater Vancouver with an area of c. 40 km^2 (Ward 1992). Even though the deltas and floodplains of the Fraser Lowland have been dramatically changed over the past century (North and Teversham 1997), areas of organic accumulation remain some of the most valuable natural areas in the region.

9. **Holocene Mass Movement Units** Mass movement units include failure scars, debris cones, flows, slumps, landslides, and rock fall deposits. Three groups of surficial materials are especially prone to slope failure in the study area, namely glacimarine sediments, glacilacustrine sediments, and glacial till and colluvium mantling steep mountain slopes (Evans 1982). Mass movement landforms in the Fraser Lowland are generally associated with (a) steep slopes along the foothills of the Coast Mountains and the Cascades and (b) the modern coastline where the glacigenic bluffs have eroded landward. On January 30, 1880, a large failure occurred in glacimarine deposits on the eroding north bank of Fraser River at Haney (Figs. 26.2a and 26.5a). The slide, which partially blocked Fraser River, resulted in one fatality and substantial property damage (Evans 1982). The largest catastrophic mass movement event within the Fraser Lowland is the Cheam rock avalanche, which delivered an estimated 175 million m^3 to a glacifluvial terrace at the base of Mount Cheam about 5000 years ago (Fig. 26.10; Naumann and Savigny 1992; Orwin et al. 2004).
10. **Holocene Aeolian Units** This unit includes sand sheets and dunes and is normally only a thin mantle. The unit is most extensive on outwash surfaces. The source of the sand is the adjacent sandy glacifluvial outwash deposits, which suggests that they have not migrated far from their original sources and that their mobility has been controlled by wind strength and/or vegetation cover. We have inadequate dating control to discriminate between late Pleistocene and Holocene aeolian landforms.

26.4.2 The Paraglacial Landsystem

The Fraser Lowland paraglacial landsystem comprises the 10 morphogenetic units described above. It is a landsystem that is in transition. When the Cordilleran Ice Sheet covered the Fraser Lowland, the landscape was fully glacial. Initially, marine processes dominated the redistribution of primary glacigenic sediments with the flooding of the lowland because of glaci-isostatic crustal depression and glaci-eustatic sea level rise. Since ice sheet retreat, fluvial

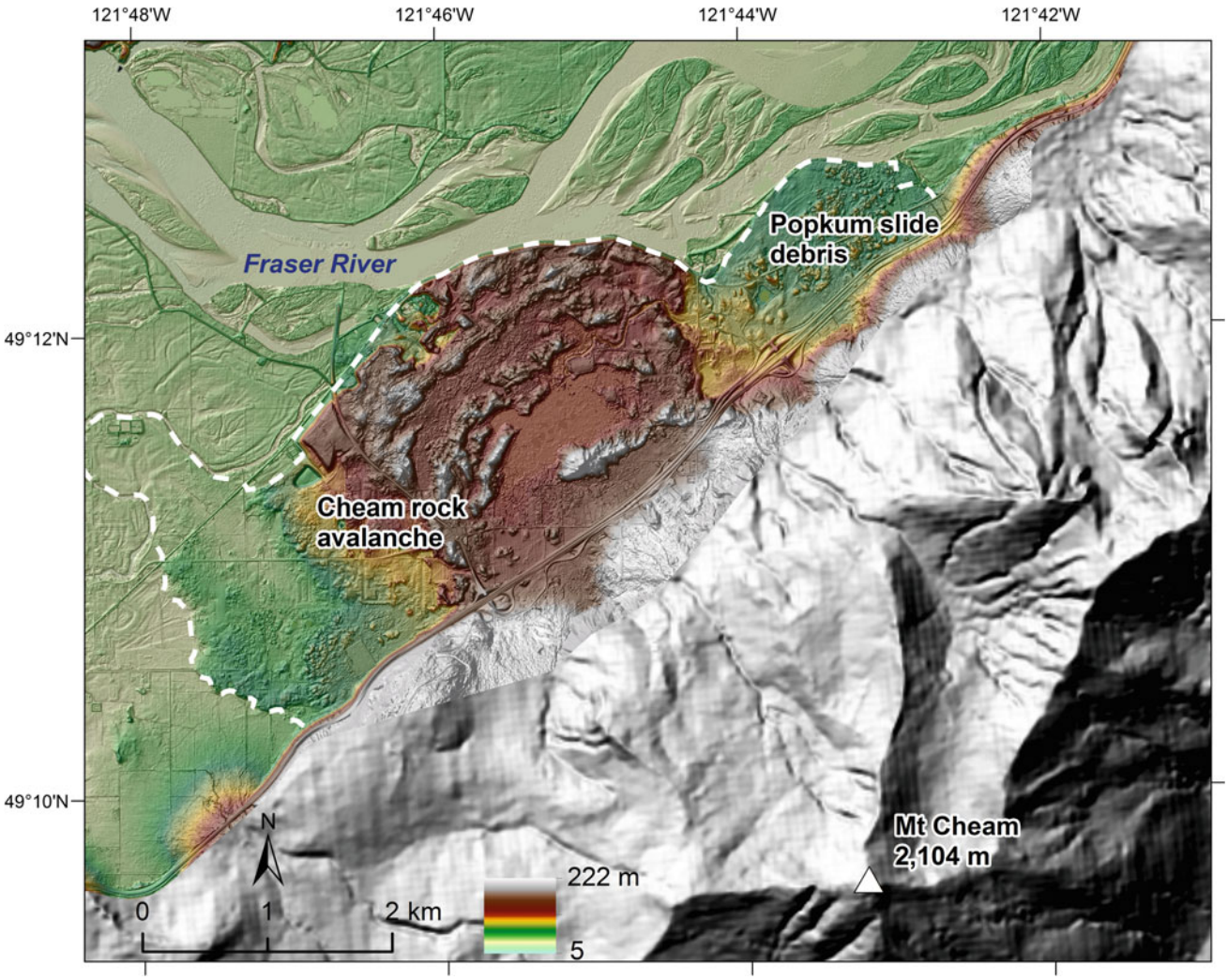

Fig. 26.10 Cheam rock avalanche and Popkum slide complex extent (modified from soil mapping in Orwin et al. 2004). The *shaded* relief image of the floodplain is derived from LiDAR data (*LiDAR data source*, Fraser Basin Council 2008) and draped over a terrain model of coarser resolution. The vertical scale is exaggerated eight times; see Fig. 26.3 for location (Kovanen and Slaymaker 2015)

processes—redistributing primary and secondary reworked glacigenic sediments—have become progressively more dominant.

Quantitatively, the proportional area of the contemporary Fraser Lowland occupied by each of the morphogenetic units described in Sect. 26.4.1 gives a first-order estimate of the changing importance of the major paraglacial sediment redistribution processes. Qualitatively, the landsystem transition is conceptualized as resulting from one or a series of sediment waves that produce a continuously decreasing delivery of sediment. This cascade of sediment is increasingly dominated by fluvial sediment redistribution processes over time. Both primary glacigenic sediments and secondary reworked storage areas within the Fraser Lowland and throughout the Fraser River basin are the sediment sources.

Near the end of the Pleistocene, the Fraser Lowland was a glacially overdeepened embayment, with glaciers calving directly into the embayment; later, it was an active outwash coastal plain fronting advancing or retreating glaciers. We envisage four distinct phases of sediment redistribution that coincide approximately with the historical stages of glacial conditioning identified in Sect. 26.2.2: (1) sediment deposition in a glacimarine environment when the land was still depressed from the load of the Late Pleistocene ice mass; (2) marine redistribution of glacigenic sediments in a falling sea level regime—at the same time as an influx of reworked glacigenic sediment from bordering tributary valleys; (3) a wave of glacigenic sediment moving from the retreating glacier front during final deglaciation and stores of modified glacigenic sediment becoming progressively exhausted over time; and (4) one or more jökulhlaups associated with glacier dam bursts from upstream.

Many sediment redistribution processes that remain strongly coupled, such as the gully–debris–flow–fluvial

aggradation continuum and the landslide–coastal–erosion–longshore drift coupling are highly sensitive to changing relative sea level and local base-level changes (see Fig. 26.6). We envisage that if the relative sea level remains constant, each morphogenetic unit will become more stable over time. But the extrinsic processes of tectonism, hydroclimate, and land-use change have the potential to perturb this semi-stable state.

26.5 Discussion

In this section, we discuss two aspects of this study: (1) the transitional landscapes of the Fraser Lowland from full glacial through proglacial and marine to fluvial are considered as a function of the two primary drivers, relative sea level and sediment source changes, and (2) we ask the question whether contemporary hydroclimate or land-use changes are sufficient to initiate a new disturbance regime as discussed in Slaymaker (2012).

26.5.1 The Paraglacial Landsystem as Influenced by the Intrinsic Process of Relative Sea Level and Sediment Source Changes

The past 14,000 years of geological history have seen dramatic changes in the landscape of the Fraser Lowland. Relative sea level and sediment source changes were the drivers of those changes (Fig. 26.11) and are here regarded as intrinsic to the paraglacial landsystem (as discussed in Sect. 26.2.3). The importance of Late Pleistocene and Early Holocene relative sea level change is associated with raised

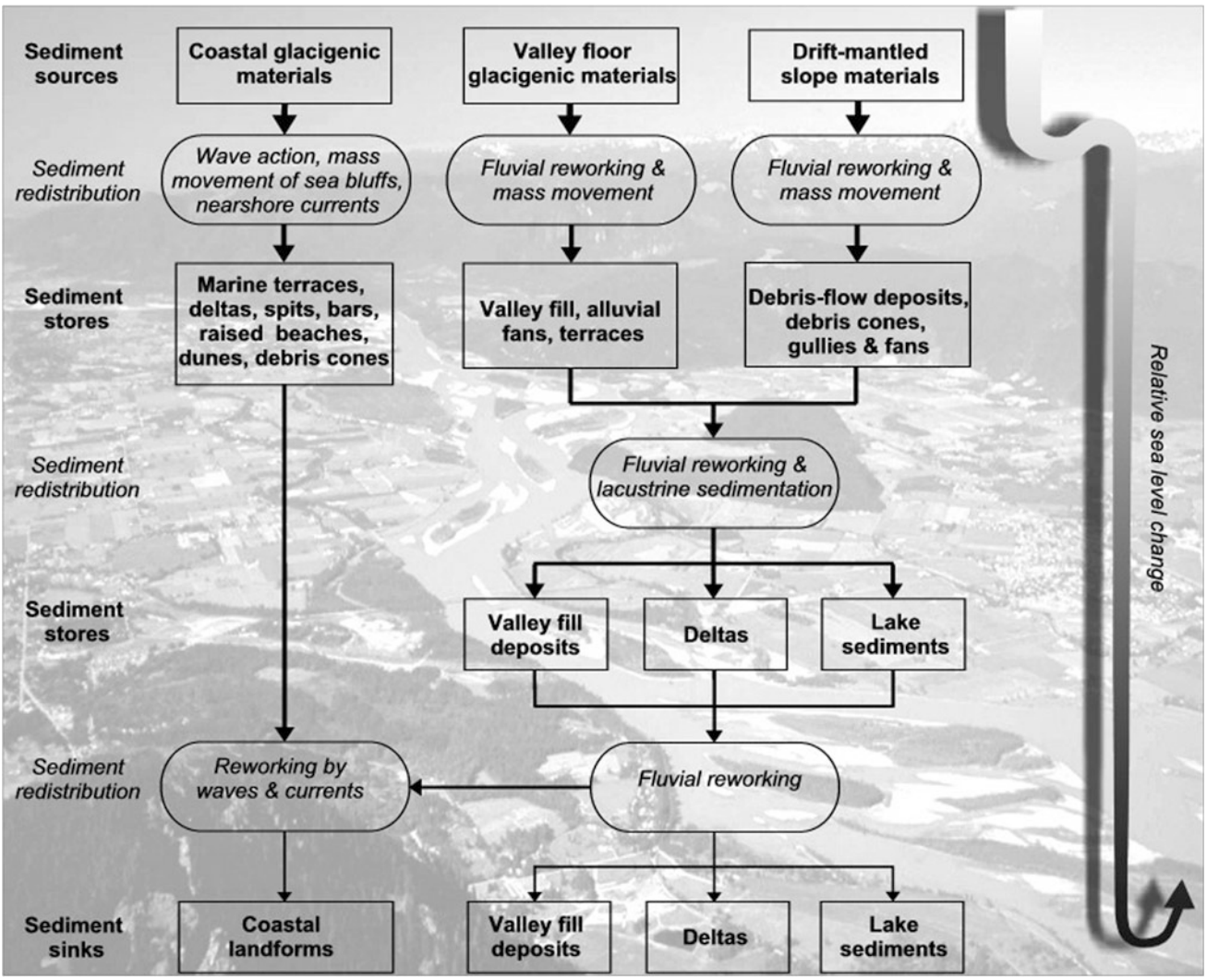

Fig. 26.11 Conceptual flow diagram of paraglacial landsystem indicating sediment pathways, redistribution processes, and sinks (Kovanen and Slaymaker 2015)

shorelines at >175 m asl. As relative sea level declined, the increasing importance of the reworking of glacigenic sediments and the complexity of the sources, transport pathways, and sinks of reworked glacigenic sediments became the primary controller of sediment redistribution processes as illustrated in Fig. 26.11. Three primary sediment sources were identified: (1) drift-mantled slope materials, (2) valley floor glacigenic materials, and (3) coastal glacigenic materials. The entire present surface of the Fraser Lowland is paraglacial in the sense that it has been modified by non-glacial processes that are identified in the vertical columns of Fig. 26.11. During the period 14,000–10,000 years BP, glacial, proglacial, and glacimarine environments succeeded one another, but during the past 10,000 years, fluvial environments have become increasingly dominant. In theory, the transition to a totally fluvial paraglacial environment is anticipated to continue until all reworked glacigenic sediments in the Fraser Lowland have been mobilized and transported to the ocean. In summary, relative sea level and sediment source changes have determined the balance between aggradation and degradation in the evolving paraglacial landscape, and the full range of paraglacial processes of sediment redistribution is responsible for the fine detail of the contemporary polygenetic paraglacial landscape (Fig. 26.11).

26.5.2 Extrinsic Perturbation of the Fraser Lowland Paraglacial Landsystem

In the absence of major disturbances by intrinsic processes such as relative sea level and sediment source changes, sediment flux would be expected to decline over time. But extrinsic processes such as tectonism, hydroclimate, and anthropogenic activity are not static. Tectonism, which is a primary control of landform evolution over geological time scales, has not strongly influenced sediment fluxes over the last 10,000 years in the Pacific Northwest. In contrast, hydroclimate and anthropogenic activity are increasingly important in modifying the paraglacial landsystem.

During the past century, anthropogenic disturbances of the landscape have contributed to sediment redistribution. Evidence of anthropogenic landscape modification is shown in modified urban land (Fig. 26.5); marina, estuarine, and spit modification (Fig. 26.6); urban shoreline modification (Fig. 26.7a); and debris torrent from Norrish and Deroche creeks interacting with the transportation network (Fig. 26.8). Around the landward perimeter of the Fraser Lowland, landslides and debris torrents provide massive input of sediments, infrequently and at specific sites (Jordan and Slaymaker 1991; Brardinoni et al. 2003; Campbell and Church 2003). Figure 26.10 is the extreme example of mass movement interacting with human settlement on one of the Fraser terraces. Stolo Nation oral history suggests that the debris from the Mount Cheam rock avalanche buried a village, causing the first known landslide fatalities in Canada (Orwin et al. 2004).

In addition to anthropogenic activity, a second extrinsic perturbation that of hydroclimate must be considered. Hydroclimatic changes in western British Columbia are increasingly well documented. For example, only three significant flood disasters, measured in terms of damage in millions of dollars, occurred in western BC between 1900 and 1948, and 13 such events occurred between 1949 and 1997 (Brooks 2001). Data are available for the incidence of natural dam failures in British Columbia, which result from hydroclimate change: either glacier recession or permafrost thaw. The statistics for glacier dam failures from 1900 to 1948 compared with 1949 to 1997 are possibly 10 versus at least 60 (Brooks 2001). This change is primarily a function of climate warming.

In sum, the interacting processes of rapid population growth during the past century and potential changes in hydroclimate have made the paraglacial landsystem more polygenetic and therefore more vulnerable to natural hazards. Human activity and hydroclimate change in the Fraser Lowland may well produce a disturbance regime landscape, analogous to that described for the adjoining mountains (Slaymaker 2012).

26.6 Conclusion

We have presented a new perspective on the geomorphology of southwestern British Columbia and northwestern Washington. New mapping, using LiDAR and GIS, provides highly resolved terrain information, which allows a semi-quantitative assessment of the extent to which this highly glaciated landscape has transitioned toward a fluvially dominated polygenetic paraglacial landsystem. The most rapid paraglacial changes were substantially completed by 10,000 years BP, but this paper provides further evidence that paraglacial adjustments continue in the present landsystem, as proposed by Church and Slaymaker (1989). Finally, the frequency and magnitude of natural hazards are likely to increase because anthropogenic activity has made the paraglacial landsystem more vulnerable to changes driven by climate change. We conclude that the recent history of the Fraser Lowland can be summarized in two periods: the Holocene, which has seen the dominance of paraglacial processes, and the Anthropocene, which will be seen as increasingly dominated by anthropogenically and hydroclimatically induced fluvial processes.

Acknowledgments We thank Steve Litke of the Fraser Basin Council for use of raw LiDAR data. We also acknowledge helpful discussions

with Colin Ballantyne and Mike Church. Figures 26.4, 26.7, 26.8, 26.9, 26.10, and 26.11 and Table 26.1 are reprinted from Geomorphology, Vol. 232, Kovanen and Slaymaker, The paraglacial geomorphology of the Fraser Lowland, southwest British Columbia and northwest Washington, 78–93, 2015, with permission from Elsevier. Cartography by D. Kovanen.

References

Armstrong JE (1957) Surficial geology of New Westminster map-area. British Columbia. Geol Surv Can Map 57-5:25

Armstrong JE (1981) Post-Vashon Wisconsin glaciation, Fraser Lowland, British Columbia. Geol Surv Can Bull 322:34

Ballantyne CK (2002) Paraglacial geomorphology. Quat Sci Rev 21:1935–2017

Benn DI, Evans DJA (2010) Glaciers and glaciation. Arnold, London

Blais-Stevens A, Clague JJ, Mathewes RW, Hebda RJ, Bornhold BD (2003) Record of large, late Pleistocene outburst floods preserved in Saanich Inlet sediments, Vancouver Island, Canada. Quat Sci Rev 22:2327–2334

Booth DB, Troost K, Clague JJ, Waitt RB (2004) The Cordilleran ice sheet. In: Gillespie AR, Porter SC, Atwater BF (eds) Developments in Quaternary Science volume 1, the Quaternary Period in the United States. INQUA, Elsevier International, Amsterdam, pp 17–43

Brardinoni F, Slaymaker O, Hassan MA (2003) Landslide inventory in a rugged forested watershed: a comparison between remotely sensed and field survey data. Geomorphology 54:179–196

Brooks GR (ed) (2001) A synthesis of geological hazards in Canada. Geol Surv Can Bull 548:281

Campbell D, Church M (2003) Reconnaissance sediment budgets for Lynn Valley, British Columbia: Holocene and contemporary time scales. Can J Earth Sci 40:701–713

Church M, Ryder JM (1972) Paraglacial sedimentation: a consideration of fluvial processes conditioned by glaciation. Geol Soc Am Bull 83:3059–3072

Church M, Slaymaker O (1989) Disequilibrium of Holocene sediment yield in glaciated British Columbia. Nature 337:452–454

Church M, Ham D, Hassan M, Slaymaker O (1999) Fluvial sediment yield in Canada. Can J Earth Sci 36:1267–1280

City of Surrey (2014) 2009 bare earth DEM, 1 m resolution DEM Grid. Provided by iGi Consulting, Coquitlam, BC under contract with City of Surrey. http://data.surrey.ca

Clague JJ (1982) Erosion at Point Grey, British Columbia. Geosci Can 9:129–131

Clague JJ (1986) The Quaternary stratigraphic record of British Columbia—evidence for episodic sedimentation and erosion controlled by glaciation. Can J Earth Sci 23:885–894

Clague JJ (1998) Geological setting of the Fraser River delta. In: Clague JJ, Luternauer JL, Mosher DC (eds) Geology and natural hazards of the Fraser River delta, British Columbia. Geol Surv Can Bull 525:1–6

Clague JJ, James TS (2002) History and isostatic effects of the last ice sheet in southern British Columbia. Quat Sci Rev 21:71–87

Clague JJ, Luternauer JL (1983) Late Quaternary geology of southwestern British Columbia. Field Trip Guidebook, GAC-MAC, CGU, p 112

Clague JJ, Haper JR, Hebda RJ, Howes DE (1982) Late Quaternary sea levels and crustal movements, coastal British Columbia. Can J Earth Sci 19:597–618

Clague JJ, Luternauer JL, Hebda RJ (1983) Sedimentary environments and postglacial history of the Fraser Delta and lower Fraser Valley, British Columbia. Can J Earth Sci 20:1314–1326

Clague JJ, Luternauer JL, Pullan SE, Hunter JA (1991) Postglacial deltaic sediments, southern Fraser River delta, British Columbia. Can J Earth Sci 28:1386–1393

Clague JJ, Mathewes RW, Guilbault JP, Hutchinson I, Rickets BD (1997) Pre-Younger Dryas resurgence of the southwestern margin of the Cordilleran Ice Sheet, British Columbia, Canada. Boreas 26:261–277

Clague JJ, Luternauer JL, Mosher DC (eds) (1998) Geology and natural hazards of the Fraser River delta, British Columbia. Geol Surv Can Bull 525:7–16

Collins BD, Montgomery DR (2011) The legacy of Pleistocene glaciation and the organization of lowland alluvial process domains in the Puget Sound region. Geomorphology 126:174–185

Dethier DP, Pessel F Jr, Keuler RF, Balzarini MA, Pevear DR (1995) Late Wisconsinan glaciomarine deposition and isostatic rebound, northern Puget Lowland, Washington. Geol Soc Am Bull 107:1288–1303

Easterbrook DJ (1963) Late Pleistocene glacial events and relative sea-level changes in the northern Puget Lowland, Washington. Geol Soc Am Bull 74:1465–1484

Engels S, Roberts MC (2005) The architecture of prograding sandy-gravel beach ridges formed during the last Holocene highstand: southwestern British Columbia. Can J Sedim Res 75:1052–1064

Environment Canada (1992) State of the environment for the lower Fraser River Basin. State of the Environment Report No 92-1, Ottawa

Evans SG (1982) Landslides and surficial deposits in urban areas of British Columbia: a review. Can Geotech J 19:269–288

Eyles N (1983) Glacial geology: a landsystems approach. In: Eyles N (ed) Glacial geology. Pergamon, Oxford, pp 1–18

Fraser Basin Council (2008) Bare earth topographic LiDAR: lower Fraser Basin Floodplain. Provided by Terra Remote Sensing Inc, Sidney, BC, under contract with Fraser Basin Council

Johnsen TF, Brennand TA (2004) Late-glacial lakes in the Thompson Basin, British Columbia: paleogeography and evolution. Can J Earth Sci 41:1367–1383

Jordan P, Slaymaker O (1991) Holocene sediment production in Lillooet river basin: a sediment budget approach. Géogr Phys Quatern 45:45–57

Kovanen DJ (2002) Morphologic and stratigraphic evidence for Allerød and Younger Dryas age glacier fluctuations of the Cordilleran Ice Sheet, British Columbia, Canada and northwest Washington, USA. Boreas 31:163–184

Kovanen DJ, Easterbrook DJ (2002) Extent and timing of Allerød and Younger Dryas age (ca. 12.5–10.0 ^{14}C kyr BP) oscillations of the Cordilleran Ice Sheet in the Fraser Lowland, Western North America. Quat Res 57:208–224

Kovanen DJ, Slaymaker O (2003) Lake Terrell upland glacial resurgences and implications for late-glacial history, northwestern Washington State, USA. Can J Earth Sci 40:1767–1772

Kovanen DJ, Slaymaker O (2015) The paraglacial geomorphology of the Fraser Lowland, southwest British Columbia and northwest Washington. Geomorphology 232:78–93

Mathews WH, Fyles JG, Nasmith HW (1970) Postglacial crustal movements in southwestern British Columbia and adjacent Washington State. Can J Earth Sci 7:690–702

Monahan P, Luternauer JL, Barrie JV (1993) A delta plain sheet sand in the Fraser River delta, British Columbia, Canada. Quat Int 20:27–38

Naumann CM, Savigny KW (1992) Large rock avalanches and seismicity in southwestern British Columbia. In: Paper presented at the 6th international symposium on landslides, Christchurch, New Zealand, 10–14 Feb 1192

North M, Teversham J (1997) The vegetation of the floodplain of the Fraser, Serpentine and Nicomekl rivers, 1859–1890. Syesis 17:47–66

Orwin JF, Clague JJ, Gerath RF (2004) The Cheam rock avalanche, Fraser Valley, British Columbia, Canada. Landslides 4:289–298

Roberts R, Church M (1986) The sediment budget in severely disturbed watersheds, Queen Charlotte Islands, British Columbia. Can J For Res 16:1092–1106

Ryder JM (1971) The stratigraphy and morphology of paraglacial alluvial fans in south-central British Columbia. Can J Earth Sci 8:279–298

Saunders IR, Clague JJ, Roberts MC (1987) Deglaciation of Chilliwack River valley, British Columbia. Can J Earth Sci 24:915–923

Shipman H (2008) A geomorphic classification of Puget Sound nearshore landforms. Puget Sound Nearshore Partnership Report No. 2008–01. Published by Seattle District, U.S. Army Corps of Engineers, Seattle, Washington

Slaymaker O (2009) Proglacial, periglacial or paraglacial? In: Knight J, Harrison S (eds) Periglacial and paraglacial processes and environments special publication 320. The Geological Society of London, pp 71–84

Slaymaker O (2012) Geomorphic change in Canada's temperate mountains. In: French H, Slaymaker O (eds) Changing cold environments: a canadian perspective. Wiley, Chichester, pp 222–246

The District of North Vancouver GIS Department (2014) Contours 1 m. http://geoweb.dnva.org.data. Accessed Apr 2014

Tunnicliffe J, Church M, Clague JJ, Feathers JK (2012) Postglacial sediment budget of Chilliwack Valley, British Columbia. Earth Surf Process 37:1243–1252

Ward P (1992) Wetlands of the Fraser Lowland, 1989. Summary Report, Canadian Wildlife

Williams HF, Roberts MC (1989) Holocene sea-level change and delta growth: Fraser River delta, British Columbia. Can J Earth Sci 26:1657–1666

Fraser River: History in a Changing Landscape

27

Michael Church

Abstract

The Fraser River of British Columbia is among the longest montane rivers in the world. Draining a mainly wildland catchment, its hydrology is dominated by the annual snowmelt freshet and sediment yield by material recruited along the banks of the river from Pleistocene valley fills. The upper course of the river was captured from arctic drainage in late Quaternary time. Another Quaternary legacy is one of the world's greatest salmonine fisheries. As it approaches the sea, gradient declines and the gravel load of the river is deposited, creating a wandering-braided channel zone that supports an exceptionally rich aquatic ecosystem. But it also presents a potentially escalating flood hazard to settlements along the river and to major arteries of communication. In the sand-bed deltaic reach of the river, persistent dredging for navigation has created the reverse problem of riverbed degradation and loss of sand recruitment to the delta front. Natural history and human development are intertwined in complex ways along the lower course of this river.

Keywords

Fishery • Flooding • Fluvial sedimentation • Fraser river • Quaternary history • River management

27.1 Introduction

Fraser River drains 232,000 km^2 of south-central British Columbia—the heartland of Canada's westernmost province (Fig. 27.1). About 80 % of the province's population resides in the Fraser drainage, most of it within the Lower Fraser Valley. The source of the river is traditionally placed near Mt. Robson, the highest peak in the Canadian Rocky Mountains; in fact it rises 90 km southeast in the Rocky Mountain Trench. It flows 1375 km to the sea at Vancouver, Canada's principal Pacific coast city. It is the seventy-seventh largest river in the world by discharge and the largest river draining from British Columbia into the Pacific Ocean. About 70 % of its drainage area consists of the Nechako, Fraser and Thompson Plateaus, the uplands that lie between the Rocky and Cariboo mountains to the east and the Coast Mountains to the west (Fig. 27.1). These are regions of ranching, logging and mining, activities that form the economic base of interior British Columbia life. Only two tributaries have been impounded, and the free-running river is host to the greatest remaining runs of Pacific salmon (*Oncorhyncus* spp.). The native cultures of the region have depended on the salmon for the more than 10,000 years they have been present, as do major commercial and recreational fisheries today.

In 1792, the English captain, George Vancouver, managed to miss the river while producing otherwise highly accurate charts of the Strait of Georgia and much of the British Columbia coast, but in that same year, the Spanish navigators Dionisio Galiano and Cayetano Valdés y Flores located and anchored in the North Arm on Fraser delta. The first European overland explorer, Alexander Mackenzie, travelled the tributaries of the upper river on his way to the Pacific Ocean at Bella Coola in 1793, but another North West Company fur

M. Church (✉)
Department of Geography, The University of British Columbia, 1984 West Mall, Vancouver, BC V6T 1Z2, Canada
e-mail: mchurch@geog.ubc.ca

© Springer International Publishing Switzerland 2017

O. Slaymaker (ed.), *Landscapes and Landforms of Western Canada*,
World Geomorphological Landscapes, DOI: 10.1007/978-3-319-44595-3_27

Fig. 27.1 Map of Fraser River basin showing principal places mentioned in the text. Dashed arrows denote routes of prehistoric drainage. *Inset* position of Fraser River drainage basin in Canada

trader made the first descent of the forbidding canyons of the middle river: Simon Fraser—for whom the river is named—and John Stuart reached the sea in 1808. Fifty years later, after the establishment of a British colony on Vancouver Island, placer gold was discovered on a river bar near Yale, precipitating a gold rush that began fifty years of mining along the river, and the establishment of the colony of British Columbia. Ultimately, the greatest strikes were made along tributaries of the Cariboo, Cottonwood and Willow rivers, themselves left bank tributaries of Fraser River in the Cariboo Plateau (Sutherland Brown and Ash 2009). In response to the gold fever, paddlewheel river boats began to ply the lower river and the Cariboo wagon road was pushed north and eventually forced through the canyons. In the 1880s, the Canadian Pacific Railway laid track through the lower canyons, an engineering triumph of its day. This feat was largely achieved by indentured Chinese laborers whose descendants have remained a significant part of British Columbia society. Today, the river still directs the patterns of provincial commerce and lies at the center of environmental management issues in the province. It has been a dominating factor in many of the events of British Columbia's history.

27.2 The History of the River

The hydrography of the river is remarkable. North of Latitude 51 °N the tributaries, and eventually the Fraser itself, flow toward the north (Fig. 27.1). Elements of the drainage history were first interpreted in studies of the Cariboo placers (Lay 1940). The ancestral drainage is traced back more than 10 Ma to a mid-Miocene landscape of moderate relief (Mathews 1991) when a northward flowing river occupied a broad valley in the northern two-thirds of the basin. Cobble conglomerates near 51.5 °N, directly overlying mid-Miocene lavas, indicate northeasterly drainage, while palynomorphs indicate a warm climate (Mathews and Rouse 1984). That river drained to the Peace-Mackenzie system via what is today the Crooked River valley north of Prince George, where the divide remains less than 50 m high. The ancestral valley remains present in the mid-Fraser basin as a broad terrace (Figs. 27.2a, 27.3), still with its northerly gradient (made somewhat steeper by subsequent tectonic delevelling), above the incised Pleistocene valley.

The Neogene history of the interior plateau has been punctuated by episodes of volcanism that produced more or less extensive basalt flows. Dating the lavas demarcates the antiquity of intercalated fluvial, lacustrine and, latterly, glacial deposits. End-Pliocene lavas (2.8 Ma: Andrews et al. 2012) dammed the ancestral river at Dog Creek (Mathews and Rouse 1986) at the same time that the Coast Mountains to the west were being rejuvenated. At 1.0 Ma, the lava dam event was repeated. This lava overlies an early glacial till (Fig. 27.3: inset). These events impounded lakes to the south of the dam that might have spilled to the south.

The actual reason for the reversal of the northern drainage remains obscure. It could be directly due to lava blockage, or to glacial derangement of drainage. Or the rejuvenated Coast Mountains may have steepened a south flowing stream to the point that it pirated the system by aggressive headward erosion. Recently, evidence has been discovered of minerals from the northeastern Rocky and Omineca Mountains in the Nitinat sea fan, the submarine repository of the fine fraction of Fraser sediments, lying off the mouth of the Strait of Juan da Fuca (Andrews et al. 2012). The 0.76 Ma age of the fan constrains the drainage reversal to have occurred sometime between 0.76 and 1.0 Ma; the more recent date would associate drainage reversal with marine isotope stage 16 continental glaciation.

South of Dog Creek the river follows the Fraser Fault (which may have been influential in the act of piracy), dividing the Coast Mountains from the Cascade Mountains to the east, until it escapes toward the sea west of Hope, BC, at the gap between the two mountain belts. The reach along the fault zone consists of a series of deep canyons, collectively known as 'Fraser Canyon,' in which the river may have downcut at rates of up to 150–200 m Ma^{-1} (Andrews et al. 2012), thus securing the southward drainage.

A notable legacy of the Pleistocene glaciations, during which ice repeatedly emanated from both the eastern and western mountains to coalesce near Fraser River and form the Cordilleran Ice Sheet, is the major lakes occupying montane valleys on either edge of the plateau (Fig. 27.1). The lakes were created by valley-directed ice streams that carried ice out of the mountains. Today Fraser River is deeply incised below the interior plateaus (Fig. 27.2a). The Quaternary inner valley of the river and the valleys of its major tributaries are filled with a complex sequence of Pleistocene lacustrine sediments, tills and outwash, in places capped by Holocene alluvial fans, debris flow deposits or slopewash, through which the rivers have degraded onto or near rock (Fig. 27.2b). Fraser River now flows in a trench within the Quaternary valley, itself inset into the Miocene valley, and in places between high rock walls (Fig. 27.2c). Upstream from Soda Creek (52°20′N), in contrast, and west of Hope, it flows unconfined in a broad valley with floodplain (Fig. 27.2d): in the north, Fraser River occupies its ancestral valley.

Fig. 27.2 Views of Fraser River: **a** Fraser River near 51°46′N, view northward (*upstream*) north of the confluence with Chilcotin River, prominently showing the broad Miocene valley; Iron Canyon in the *middle* ground (photograph by J. M. Ryder); **b** incised into Pleistocene sediments, north of Lillooet; **c** the White Canyon. Both views near 50° 50′N; **d** Fraser River in the gravel-bed reach of lower Fraser Valley, view looking downstream (west) east of Chilliwack, BC (photograph by A. Zimmermann)

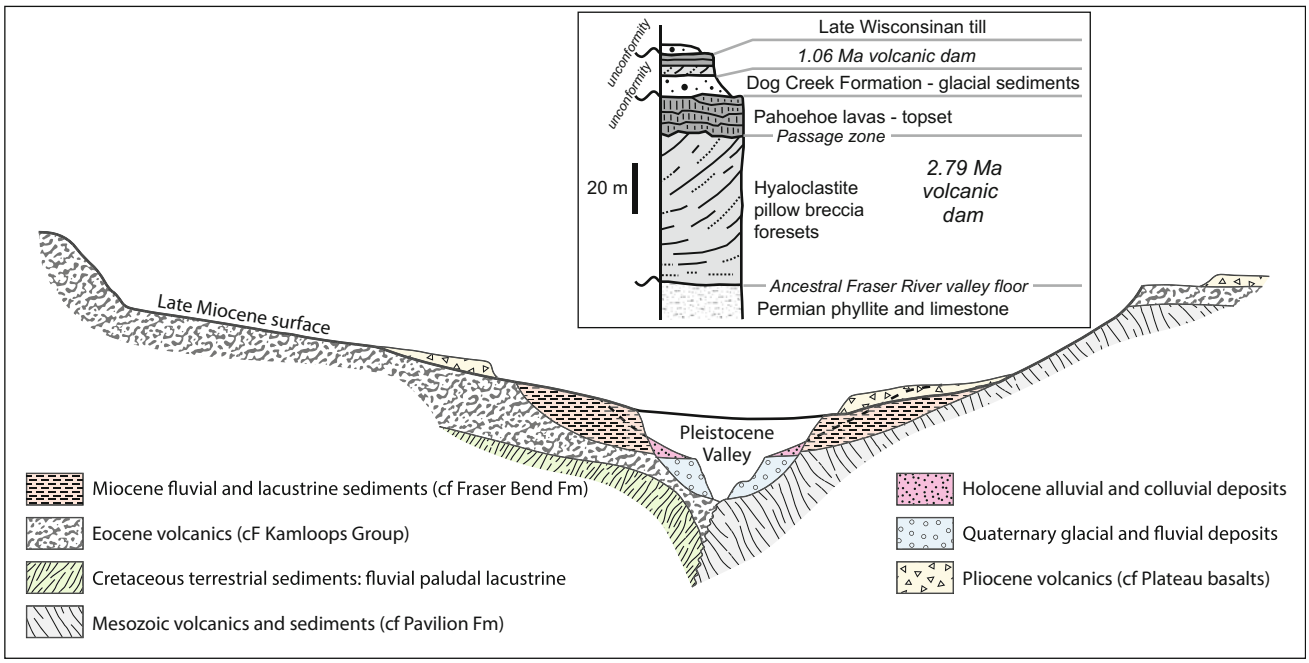

Fig. 27.3 Schematic cross section of Fraser Valley in the interior plateau country (after W.H. Mathews): *Inset* stratigraphic details at Dog Creek (after Andrews et al. 2012, their Fig. 2b)

27.3 The Contemporary River: Hydrology and Sedimentation

The plateaus lie within the rain shadow of the Coast Mountains and are subhumid. Little runoff is generated in summer, but they accumulate a substantial snow load in winter and, in the surrounding mountains, heavy accumulation occurs. Snowmelt on the plateaus (1000–1300 masl) occurs synchronously over a wide area in spring, producing the major hydrological event of the year. Nival melt dominates the flow regime to the extent that the annual hydrograph in most years resembles a single-event hydrograph (Fig. 27.4). High flow occurs throughout late May, June and early July and recedes in August and September. Water yield from the basin is relatively high, around 0.8 m depth per annum from the mountain headwaters (Table 27.1: Fraser at Hansard) and more than 1 m near the coast, declining to less than half that value in the plateaus. The mean annual flow at Mission, the farthest downstream gauge on the river, is 3410 m^3s^{-1} and the mean annual flood is 9790 m^3s^{-1} (McLean et al. 1999). The 1894 flood, in which flows are estimated to have reached 17,000 ± 1000 m m^3s^{-1} at Hope (NHC 2008), is the historic flood of record (the Hope gauge, established in 1912, contributes the longest record of flow on the river: see Fig. 27.5d). Without the large lakes in the basin, the flood regime would be more extreme. Winter flows in the lower river dip to values less than 1000 m^3s^{-1}, for an annual range of about 10×. The significance of the Thompson River, the largest tributary, is evident in that, with one-quarter of the combined drainage area at the confluence, it increases the mean flow by about 45 % and the annual flood by more than 50 %. In 1952, a diversion (for hydroelectric power generation) across the mountains from the Nechako River, a northern tributary, effectively reduced the size of the basin by 5.6 % and mean annual flows by 3 %. Since then, however, mean flows in the river have actually increased by 6 %, probably as a consequence of the secular increase in precipitation that has affected the province over the course of the twentieth century. The flood sequence, however, shows no persistent trend, though throughout the twentieth century the river experienced decades-length periods of greater floods and lesser ones under the influence of the oscillating thermal condition of the North Pacific Ocean and the weather that it creates (Mantua et al. 1997).

Projections for the future envisage significant increases—up to order 100 %—in spring runoff in the mountains as the result of accelerated melt of a heavy snowpack, itself the consequence of increased winter snowfall. On the plateaus, however, spring runoff is expected to decline by up to 25 %, the consequence of increased portions of the early and late winter precipitation falling as rain, leaving a reduced snowpack (M. Schnorbus, personal communication, October 2014; see also Shrestha et al. 2012). The net projected effect is for little change in flood frequency over the bulk of the range, but an order 10 % increase in the greatest floods, bringing 15,000 m^3s^{-1} (Hope flow) to within 100 years'

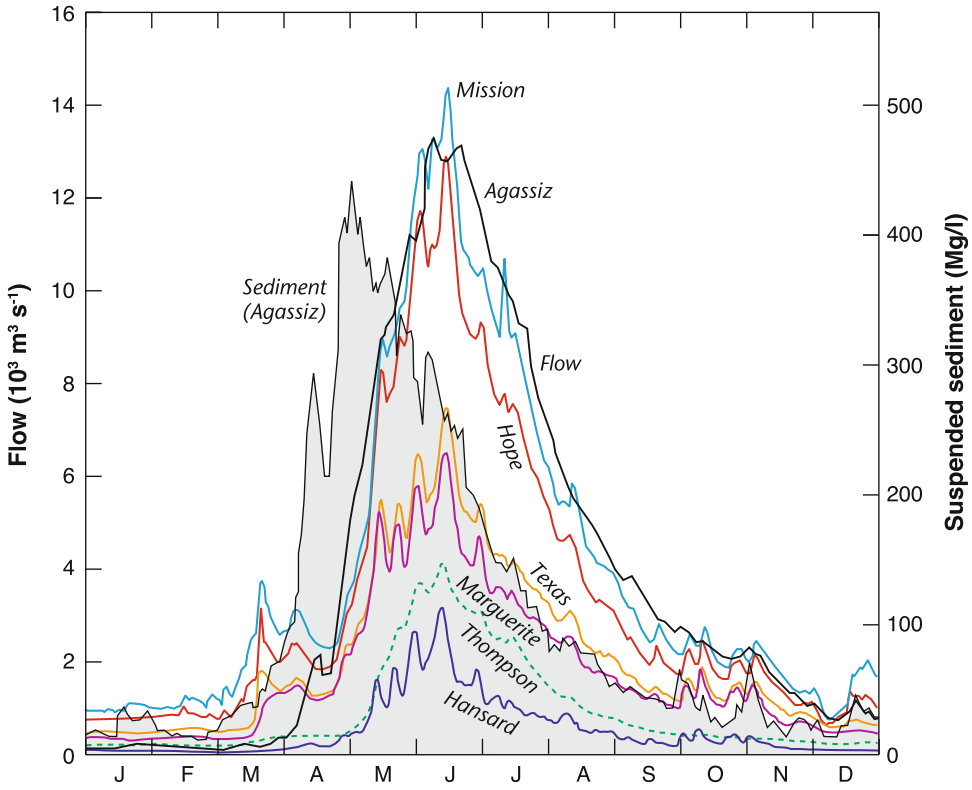

Fig. 27.4 The 1972 annual hydrograph at principal gauges along Fraser River and on Thompson River (station details in Table 27.1) and graph of suspended sediment concentration at Agassiz. Agassiz is located 130 km from the mouth of the river in the 'gravel reach' of the Lower Mainland (Fig. 27.1)

Table 27.1 Flow and suspended sediment in Fraser River

Station	WSC No.	Drainage area (km^2)	Mean annual flood (m^3s^{-1})	Mean flow (m^3s^{-1})	Water yield ($m^3km^{-2}a^{-1}$)[a]	Mean susp. sed. conc. (mg l^{-1} = g m^{-3})	Mean sediment load (Mg a^{-1})	Sediment yield (Mg $km^{-2}a^{-1}$)
At Hansard	08KA004	18,000	1999	480	841×10^3	197	2990,000`	166
Near Marguerite	08MC018	114,000	4477	1460	404	235	10,800,000	95
Above Texas Crk.	08mF040	154,000	5030	1736	355			
Thompson R at Spences Bridge	08LF051	55,400	2740	772	439			
At Hope	08MF005	217,000	8,665[b]	2730	390	212	18,100,000	83
Mission	08MF024	228,000	9790	3410	471	159	17,200,000	75
Silverhope Crk.	08MF009	350	86[c]	14.4	1300	9.1	4120	11.8

Flow data typically cover the period 1951–present, except Hope. Sediment data may not be comparable between stations because of different periods of record and varying sampling effort. Most sediment data were collected between 1966 and 1986. WSC: Water Survey of Canada
[a]Divide by 10^6 to obtain runoff depth in meters
[b]1951–2012 only: record extends to 1912
[c]9 years only

recurrence. Conversely, winter flows are expected to increase from typically less than 1000 m^3s^{-1} (Hope) to greater than that figure.

The Pleistocene valley fills throughout the Fraser River basin and Tertiary and Cretaceous sediments along the valleysides—particularly lacustrine silts and volcanic clays—are erosion prone in the freeze-thaw environment of the regional winter. The older formations give rise to massive, slow-moving earthflows lubricated by the annual, snowmelt-driven variation in groundwater, many of which descend down the steep slopes from the plateaus to the river (Bovis 1985), while in a few places along the middle river,

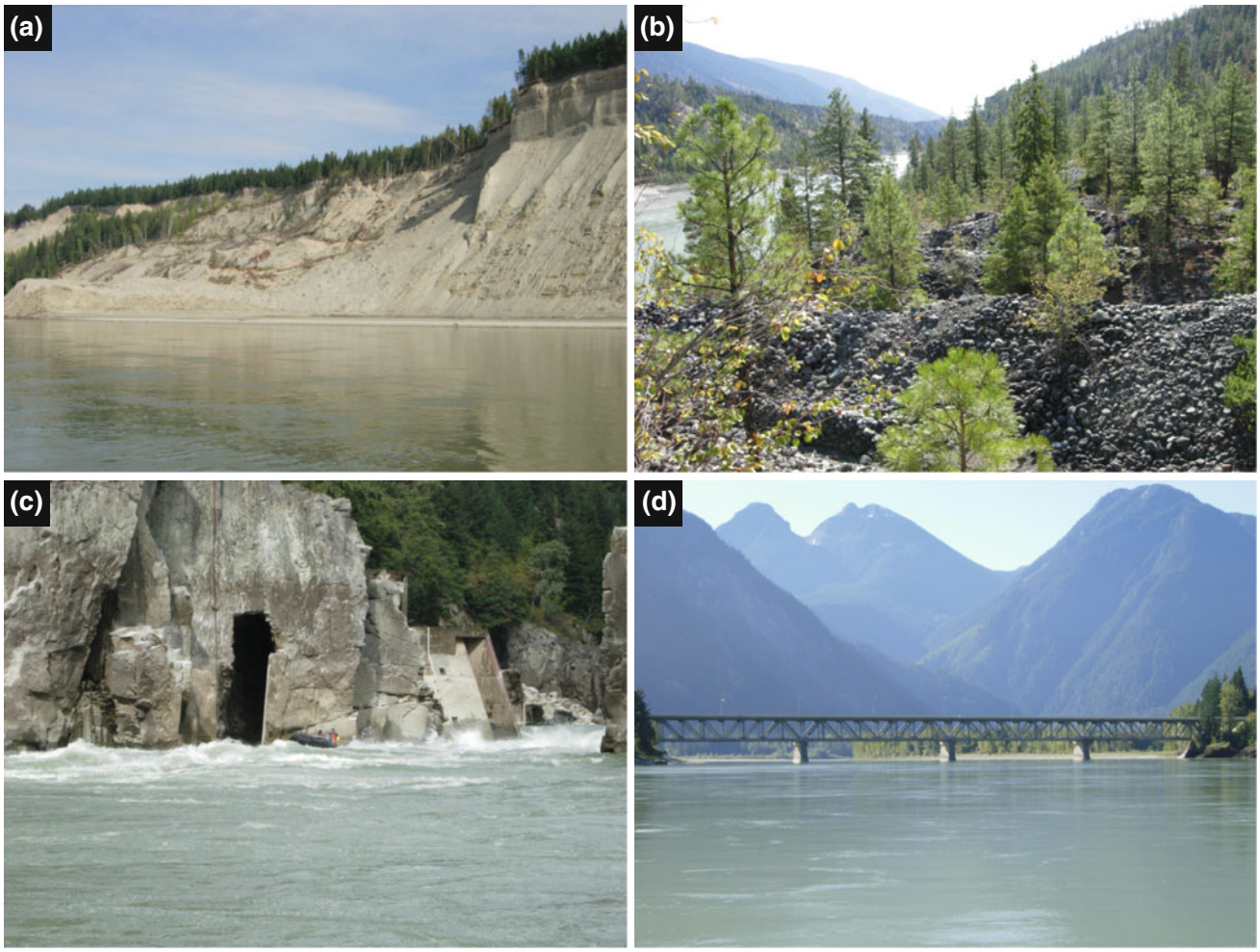

Fig. 27.5 Fraser River landscapes: **a** retrogressive landslide, left bank, about 10 km south of Quesnel, a prolific source of sediment to the river; **b** nineteenth-century placer workings at Browning's Bench, south of Lillooet, a significant transient source of sediment; **c** Hell's Gate, 30 km north of Yale, where the river is only 35 m wide but about 60 m deep at high flow, when water velocities may exceed 10 m/a; **d** view downstream to the gauge section at Hope, where the river enters its lower, fully alluvial course

massive, chronically retrogressing landslides occur in glacilacustrine silts that are common from north of Dog Creek into the Prince George area (Tipper 1971) (Fig. 27.5 a). The dominant forest and range landscape contributes relatively little sediment, so most of the sediment carried by the river originates in the riverbanks from the earthflows and from Pleistocene valley fill. Through autumn and winter, dry ravel delivers material to river level from noncohesive deposits, while frost heave prepares cohesive surfaces for subsequent erosion. With the first rise of the nival melt, this material is mobilized by the river. By the time of peak runoff, much of the available material, including sand deposited along the river edge in the preceding year, has been re-entrained. River banks under direct attack and susceptible to repeated, retrogressive failure, continue to contribute material throughout the flood, but the peak of suspended sediment concentration precedes the runoff peak by a month or more (Fig. 27.4) and the annual pattern of suspended sediment yield is markedly clockwise hysteretic.

The suspended sediment budget of the river from three stations with a history of measurements is given in Table 27.1. The load is modest in comparison with that of many major rivers of the world (see the compilation in Milliman and Meade 1983). Unit area sediment yield decreases steadily down the system, but load per kilometer along the channel actually increases. Areal sediment yield recorded at the mainstem stations is an order of magnitude higher than yields measured in a gauged montane tributary of the river (Table 27.1), consistent with the sources of sediment being along the banks of the river itself.

The river is a steep mountain river—remarkably steep for its size—averaging 0.0009 in gradient through the canyons (Fig. 27.5c) where it is able to move large cobbles and boulders. After the river enters the lower valley

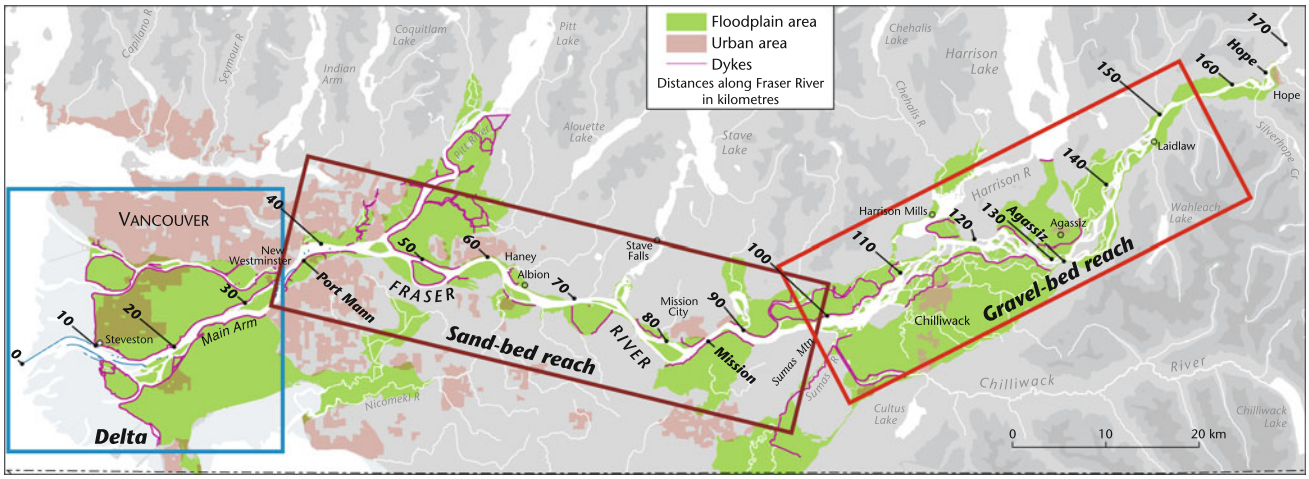

Fig. 27.6 Map of Lower Fraser River, showing the gravel- and sand-bed reaches, and the delta

Table 27.2 Sediment budget of the Lower Fraser River (mean annual load, 10^3 Mg a^{-1})

Station	WSC	Suspended load				Bedload			Total
	Station	Clay	Silt	Sand	Total	Sand	Gravel	Total	Load
Agassiz (gravel bed)	08MF035	2750	8590	5190	16,530	49	227	276	16,806
Mission (sand bed)	08MH024	2690	8280	6080	17,050	154	–	154	17,204
Sand Heads[a]	*Estimated*	*2700*	*8200*	*3000*	*13,900*	*1300*	–	*1300*	*15,200*

[a]Sand Heads is the mouth of the river. Measurements at Agassiz and Mission were conducted between 1966 and 1986

(Figs. 27.5d and 27.6), the gradient declines as it approaches the sea. The cobble–gravel portion of the sediment load is deposited in a 48-km reach between Laidlaw and Sumas Mountain on what amounts to an extended, low-angle, alluvial fan, confined between mountains to the north and south (Rice et al. 2009; Church and Rice 2009; Ham and Church 2012). At Sumas Mountain, 100 km from the sea, the river undergoes an abrupt gravel–sand transition (Venditti and Church 2014). Once unconfined, the river in the gravel-bed reach exhibits a wandering, low-order braid morphology with islands (Fig. 27.2d). After the transition to sand, it flows in a single-thread channel to the head of its delta near Port Mann, 35 km from the sea. The sediment budget for the gravel and sand-bed reaches was established by McLean et al. (1999) on the basis of a sampling program conducted by the Water Survey of Canada over a period of 20 years and is shown in Table 27.2. Clay and silt loads are today essentially unchanged all the way to the sea (to within measurement error), though in former times substantial silt was lost to the floodplain and delta surface. However, there appears to be an increment of sand in the lower river, while the gravel load is lost in the gravel-bed reach. While McLean et al. estimated the gravel budget to be about 227,000 Mg a^{-1}, further investigation has led to a higher consensus figure of about 400,000 Mg a^{-1} as the gravel influx (Ferguson and Church 2009).

The sand budget of the lower river is thought before the mid-twentieth century to have been in approximate equilibrium, with the 6 million Mg passing Mission mostly reaching the delta front, about half as washload (grain size finer than 0.18 mm) and half as bed material load. Extensive dredging in the latter half of the twentieth century to improve deep-draft navigation below Port Mann (Fig. 27.6) has removed an average of 3 million Mg from the river bed each year. This has prompted upstream-progressing bed degradation (McLean et al. 2006), mobilizing about 1 million Mg a^{-1}, so that about 1 million Mg a^{-1} of bed material now arrives to nourish the delta front, a reduction of 67 %. It should be emphasized that these figures are all inferential and hence may be subject to significant error.

The delta itself provides a long-term perspective on the sediment budget of the river. At the close of the last glacial period c. 13,000 cal. years ago, the sea flooded into the Lower Mainland space now occupied by the lower river and its floodplain. The river rapidly filled this shallow marine embayment with sediment and about 10,000 radiocarbon years ago—that is 11,000 actual years—began to deposit the modern delta from New Westminster seaward (Clague et al. 1983). Today the delta occupies about 1000 km^2 and has an

average sediment thickness of about 120 m (Mathews and Shepard 1962), so that the volume of deltaic sediments is approximately 1.2×10^{11} m^3. Given 11 ka of sedimentation, the mean annual sediment influx has been about 10 million m^3 or 16 million Mg (with bulk density 1.6 Mg m^{-3}). This is comparable with the (pre-dredging) sediment yield of the river (18.2 million Mg a^{-1}), but most of the clay-sized sediment and part of the silt will have escaped the identified delta body. The implication is that past (particularly, one supposes early post-glacial) sediment yield was greater than that of today, but not dramatically so. One concludes that the size of the system effectively buffers the mainstem from perturbations in sediment yield that may afflict smaller tributaries as the consequence of fire, insect pests in the forest, a major landslide, Neoglacial sediment production in the mountain rims or, latterly, human land use. The persistence of the principal sediment sources along the banks of the river itself also contributes to the apparent long-term consistency of sediment yield (Church and Slaymaker 1989). To be sure, there must have been some major spikes in sediment yield along the river; the Fraser mainstem itself has been blocked by landslides at least twice (Ryder et al. 1990). There is evidence, however, that the river is able to transport considerably more than its historical load of sediment (see below).

27.4 Contemporary Problems of River Management

27.4.1 Floods and the Fishery

The river today remains one of the world's great producers of salmonine fish (Northcote and Larkin 1989) because of its mountain headwaters, which produce fast, clean water from annual snowmelt, because of the major lakes in the system that provide spawning and rearing habitat for some species, because of the gravel substrates that the fish use for spawning, produced by erosion of the valley fills throughout the basin, and because of moderate turbidity that protects the fish from predators. The bounty is, then, a product of Quaternary history and the geomorphology of the river. The fish themselves have evolved into their modern form and families with the growth of the mountains and the river over millions of years (Montgomery 2000) and so are peculiarly adapted to the environment of the river. The Pink salmon (*O. gorbuscha*) run in the gravel reach of the Fraser River may exceed 10 million fish in some years. (Pinks return to spawn in the Fraser River only in odd-numbered years.) The large side channels of the gravel reach are important Chum salmon (*O. keta*) spawning habitats, while Sockeye (*O. nerka*) spawn in the many lakes and their outlet channels. The gravel reach habitats also contribute to large-value fisheries outside this area: the large bars in the gravel reach of the Fraser River may be the most productive of all instream rearing habitats within the watershed for Chinook salmon (*O. tshawytscha*). The river also harbors populations of the iconic Northern White Sturgeon (*Acipenser transmontanus*) with further populations upstream. Altogether there are 42 native species of fish in the river, 31 of which are found in the lower river.

Gravels deposited in the lower river sustain the system of bars and multiple channels (Fig. 27.2d) that create the rich range of aquatic habitats. But it is supposed that the deposited gravels systematically raise the bed of the river, thence the water surface. Sedimentation in the gravel-bed reach in the latter half of the twentieth century suggests that this does in fact occur (Fig. 27.7). To the population of the

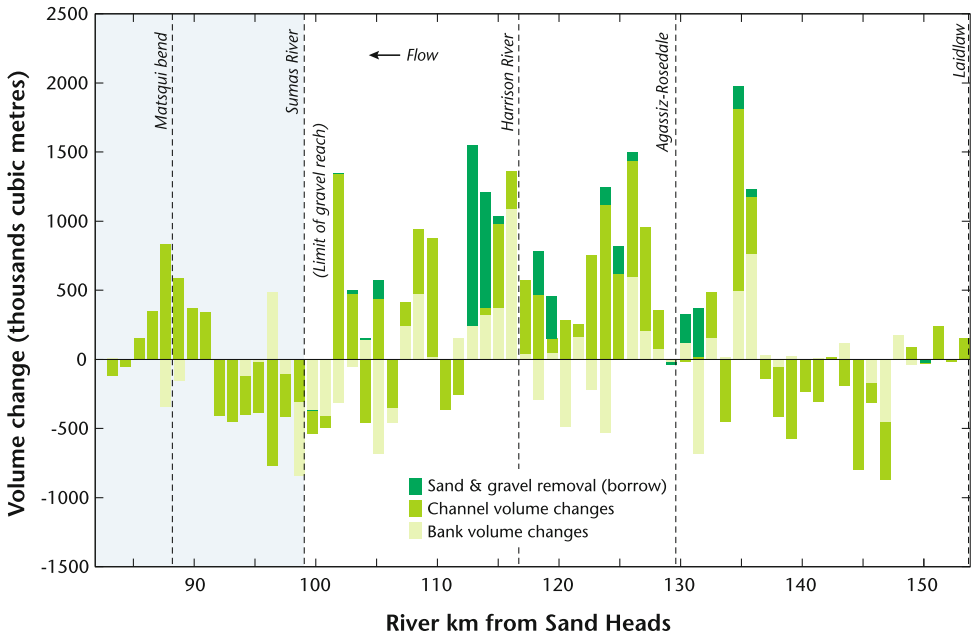

Fig. 27.7 Bed material sediment budget of the gravel-bed reach of lower Fraser River, 1952–1999

rapidly urbanizing lower valley, this gives the appearance of a steadily escalating risk of flooding.

There is a history of disruptive floods in the lower valley (Watt 2006). The great flood of 1894 inundated most of the valley floor and prompted the commencement of a century of dyke building and dyke improvements. Yet in 1948, the dykes failed in several places and flooding occurred again. In 1972 (Fig. 27.4) and in recent years, there have been concerns for dyke security during high spring runoff. How to manage this perceived hazard in the long term—in particular, whether to remove gravel from the river—raising the possibility of severe damage to the fish habitat—is the subject of an important public debate. Both elements of the problem are predicated on hydrological and geomorphological conditions that must be well understood in order to find a resolution. In particular, the problem requires that the pattern of sedimentation in the gravel-bed reach be well understood and it requires the projection of trends in flow and in gravel recruitment in the long term.

27.4.2 Floods and the Community

The river provides other values to society than the fishery. First, it is a central element in the culture of First Nations resident along the river, all of whom sustain a traditional focus on the fishery. For many residents of Fraser Valley, the river is an important site for recreational boating, picnicking and nature study. Most important, perhaps, the river and its remaining riparian zone are the most significant elements of the landscape to provide relief from the increasingly pervasive urbanism of the lower Fraser Valley. With the population of the region projected to grow by more than 40 % in the next 25 years from 2.7 million (2011 census) to a projected 3.9 million (www.bcstats.gov.bc.ca/data/pop/pop/popproj.asp), the river will more and more become the central element in the maintenance of a 'liveable environment.' These reasons, as well as concern for the fishery, argue for the maintenance of the river in its natural state, with as little human interference as possible. The contemporary lower river is, then, caught in a classic problem posed by the opposition of social development and environmental stewardship. Again, it is vital to understand patterns of sedimentation and sound projections for future flows.

On the best currently available analysis, the distribution of spring flood flows in the future—discussed above—is not expected to change significantly, but it is expected that floods with recurrence interval in the order of a century may increase in magnitude, though not beyond the estimated 1894 flow of 17,000 m^3s^{-1}, the reference flow for design of the dykes. But an additional factor enters consideration of flood defenses, that is, the residual risk to communities, infrastructure and lives posed by a flood that exceeds the designed level of protection or breaches a dyke (Jakob and Church 2011). Near the mouth of the river the city of Richmond, with an increasing population currently of 175,000, is built on an island of Fraser delta, as is Vancouver's airport. Considering also the towns in the lower valley, it is clear that the investment, level of economic activity and concern for lives justify a level of protection against floods that extends well beyond the provincially mandated level of 200 years or even the current flood of record. This might lead to further upgrading of river dykes and confinement of the river. An alternative more in keeping with the river environment would be to set dykes back in order to increase conveyance in an adequate channel zone, but that would expose floodplain properties to inundation.

It is commonly imagined that gravel moves carpet like along the bed of the stream and, when deposited, raises the streambed more or less uniformly. That is not true. Gravel moves in short hops, from a point of erosion in the river bank or bed, to a point of deposition in the next encountered bar (Pyrce and Ashmore 2003). Bar growth obstructs the channel and forces it to move laterally, prompting new erosion and onward movement of the sediment load. While the aggradation during the latter half of the twentieth century was, on average, 8.6 cm (but reduced to 2.1 cm net by gravel mining), gravel accumulations actually occur locally where aggressive bar building occurs and may amount to 1 or 2 m of change in mean bed elevation. This has two important consequences. First, the threat posed by high water levels is, in the short term, a local one, not a general one. Extra high water occurs in the backwater upstream of an expanding bar, the zone of backwater influence being in the order of a kilometer. In some places, the construction of dykes and their attendant protection has aggravated problems by constricting the channel zone of the river; about 70 % of the outer channel banks in the gravel reach are now hardened by riprap placement, even where the dykes are set back from the river. Second, bars steer the river—they determine the channel alignment. The flow resistance generated by channel bends is a much more important mediator of water level along the channel than is any individual bar. So it appears that gravel removal, if it should occur at all, should be locally focused to defuse locally generated instances of high water.

27.4.3 Anticipating History

An important question is whether—should gravel be removed from the river—it will be replaced. If not, the

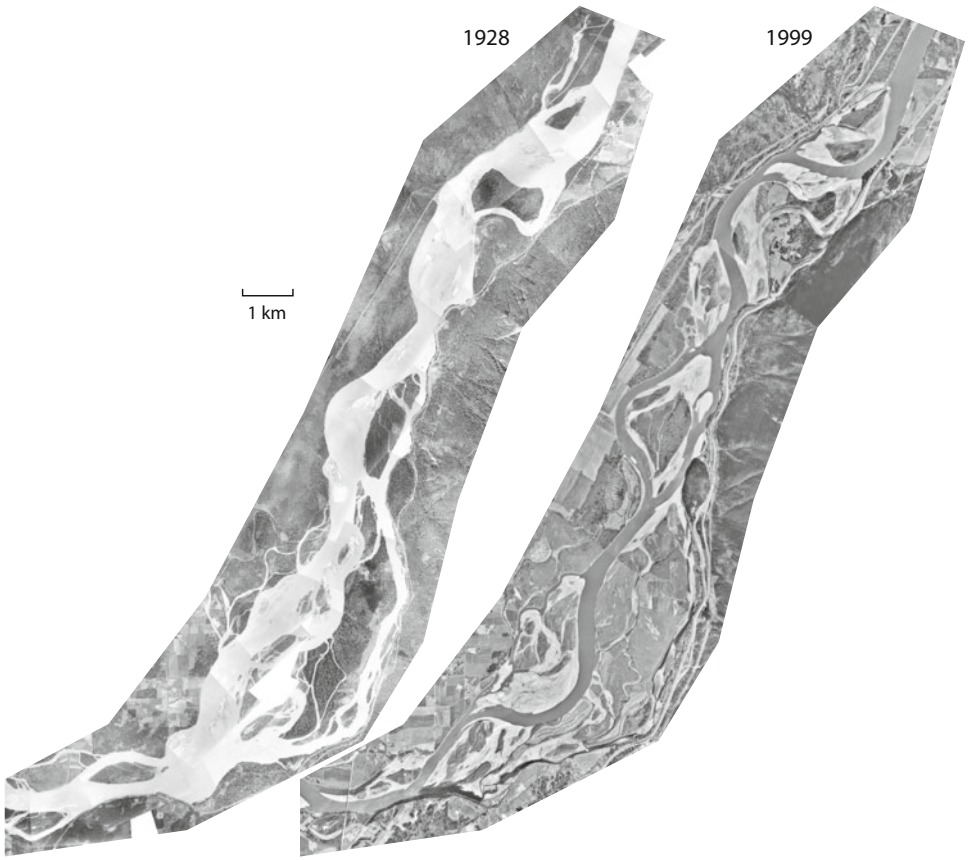

Fig. 27.8 Proximal part of the gravel-bed reach of Lower Fraser River, 1928 (*left*) and 1999. Simplification of the channel is evident between the two dates, corresponding with the degradational trend of sedimentation during the period (see Fig. 27.7: 135–148 km)

channel will be simplified by repeated removals; secondary channels and islands will disappear, and the important diversity of habitat types that supports the rich fishery will be impoverished. Indeed, the morphology of the upper part of the gravel reach has become considerably simplified over the past century, suggesting a reduction in bed material transport through the reach. That reach has slightly degraded during this period (Fig. 27.8). These observations suggest, in turn, that the yield of bed material from the upper basin has declined during the twentieth century. The nineteenth-century activities of Europeans who came into the region provide a plausible reason why this may be so. The first major intersection between European settlement and the river was the gold rush. After the first rush of 1858 to Yale, miners extensively worked both the active river bars and the terraces along the river (Fig. 27.5b) as far upstream as the Cottonwood River, a reach of some 500 km length. From the terraces, an estimated 58 million m^3 of tailings—of which about 65 % (or about 70 million Mg) consisted of cobbles, gravel and coarse sand—were dumped into the river (Nelson and Church 2012) with the peak influx occurring after 1880 when the new railway permitted the import and operation of heavy hydraulic mining equipment. Mining on the active bars loosened the bed and increased the mobilization of instream deposits. Construction of the railway and, in the early twentieth century, a second railway, dumped further, unmeasured amounts of sediment into the river. The result was an estimated order of magnitude increase in the bed material load of the middle river. A numerical model of the transfer downstream of the mining waste (Ferguson et al. 2015) shows that the bulk of the mining debris had been flushed into the terminal gravel wedge below Agassiz by 1910 and that, after 1920, slight degradation of the reach immediately upstream indeed had begun to occur (Figs. 27.7 and 27.8).

The speed with which the mining waste was evacuated from the source reaches to the terminal gravel wedge is startling. Three circumstances combined to effect it: First, the river is steep and powerful throughout the canyon reaches through which the material was transported; second, the waste material was substantially finer than the streambed sediments along the upstream and canyon reaches; hence, the river was competent to transport it all; and third, the influx of a substantial surcharge of relatively fine sediment had the effect of fining the bed surface, which then increased the bedload transport capacity of the river (Ferguson et al. 2015). There is no such large-scale disturbance along the middle or upper river today, and the prospect for land use change is such that none is likely to recur; hence, we may reasonably expect bed material

recruitment in future to be similar to or smaller than that of the present day and the rate of gravel accumulation in the lower river to decline.

27.4.4 The Delta

Human activity has generated the converse problem in the delta of Fraser River where the channel naturally shoals as it approaches the sea and sand is deposited to the channel bed: The natural depth over riffles was as little as 6 m, compared with a mean depth of about 12 m in the sand-bed reach. Dredging to accommodate deep-draft marine navigation, discussed above, has prompted upstream-progressing degradation that, it is calculated, will reach upstream past Mission and re-equilibrate the reach only after about a century, supposing that no further changes occur.

At the same time, the removal of sand from the navigation channel has reduced sand delivery to the tide flats and delta front—prospectively by as much as two-thirds (see Sect. 27.3)—so that the capacity of the delta to raise its front surface level in pace with the rate of twenty-first-century sea level rise is substantially reduced. Future wave attack on the sea dykes may be correspondingly more severe than it otherwise might be.

27.5 Final Thoughts

Most of Canada remains largely empty of people, and the natural processes that shape the landscape continue as they always have. The 12,000 years of aboriginal occupation made very limited changes in this condition. Yet everywhere people with advanced engineering capabilities have settled, the landscape at local to regional scales has been subjected to a set of changes more rapid and powerful than those produced by the normal water- and gravity-driven processes of Earth's surface environment. Thus are effected significant changes in erosion, sediment transfer and sedimentation and, ultimately, in the entire landscape. Fraser River is no exception. In only 100 years, Fraser River has been subjected to an epicycle of sedimentation deriving from nineteenth-century gold mining and railway building, the effect of which today fuels concerns for river stability and protection from flooding hazards along the lower river. Engineering measures that might be taken to secure the lower valley from floods pose a risk to the viability of the exceptionally rich aquatic ecosystem of the river. Farther downstream, in the Fraser delta, dredging over half a century to secure deep-draft navigation has set in train a different set of river responses entailing degradation throughout the sand-bed reach. The contemporary evolution of the lower river—that part of the river where human settlement and activity are overwhelmingly focused—is driven by human activity, not by the natural forces of Nature. But still the canyons of the middle river remain remote, inaccessible and wild.

Acknowledgment I thank the editors for helpful guidance and acknowledge the cartographic skills of Eric Leinberger who drew all the figures in final form.

References

Andrews GDM, Russell JK, Brown SR, Enkin RJ (2012) Pleistocene reversal of the Fraser River, British Columbia. Geology 40:111–114

Bovis MJ (1985) Earthflows in the Interior Plateau, southwest British Columbia. Can Geotech J 22:313–334

Church M, Rice SP (2009) Form and growth of bars in a wandering gravel-bed river. Earth Surf Proc Land 34:1422–1432

Church M, Slaymaker O (1989) Holocene disequilibrium of sediment yield in glaciated British Columbia. Nature 337:452–454

Clague JJ, Luternauer JL, Hebda RJ (1983) Sedimentary environments and postglacial history of the Fraser River delta and lower Fraser Valley, British Columbia. Can J Earth Sci 20:1314–1320

Ferguson RI, Church M (2009) A critical perspective on 1D modeling of river processes: gravel load and aggradation in lower Fraser River. Water Resour Res 45(15):W11424. doi:10.1029/2009WR007740

Ferguson RI, Church M, Rennie CD, Venditti JG (2015) Reconstructing a sediment pulse: modeling the effect of placer mining on Fraser River, Canada. J Geophys Res 120:1436–1454

Ham DG, Church M (2012) Morphodynamics of an extended bar complex, Fraser River, British Columbia. Earth Surf Proc Land 37:1074–1089

Jakob M, Church M (2011) The trouble with floods. Can Water Resour J 36:287–292

Lay D (1940) Fraser River Tertiary drainage history in relation to placer gold deposits. BC Dept Mines, Victoria. Bulletin 3:30

Mantua NJ, Hare SR, Zhang Y, Wallace JM, Francis RC (1997) A Pacific interdecadal climate oscillation with impacts on salmon production. B Meteorol Soc 78:1069–1079

Mathews WH (1991) Physiographic evolution of the Canadian Cordillera. In: Gabrielse H, Yorath CJ (eds) Geology of the Cordilleran Orogen in Canada. Geol Surv Can, Geology of Canada, vol 4, p 403–418

Mathews WH, Rouse GE (1984) The Gang Ranch—Big Bar area, south-central British Columbia: stratigraphy, geochronology and palynology of the Tertiary beds and their relationship to the Fraser Fault. Can J Earth Sci 21:1132–1144

Mathews WH, Rouse GE (1986) An early Pleistocene proglacial succession in south-central British Columbia. Can J Earth Sci 23:1796–1803

Mathews WH, Shepard FP (1962) Sedimentation of the Fraser River delta, British Columbia. Am Assoc Petrol Geol Bull 46:1416–1438

McLean DG, Church M, Tassone B (1999) Sediment transport along lower Fraser River. 1. Measurements and hydraulic computations. Water Resour Res 35:2533–2548

McLean DG, Mannerström M, Lyle T (2006) Impacts of human interventions on the lower Fraser River. Can Water Resour Assoc, BC Div, Ann Conf, Vancouver, Oct 24–25

Milliman JD, Meade RH (1983) World-wide delivery of sediment to the oceans. J Geol 91:1–21

Montgomery DR (2000) Coevolution of the Pacific salmon and Pacific Rim topography. Geology 28:1107–1110

Nelson AD, Church M (2012) Placer mining along Fraser River, British Columbia: the geomorphic impact. Geol Soc Am Bull 124:1212–1228

NHC (Northwest Hydraulics Consultants) (2008) Comprehensive review of Fraser River at Hope, Flood hydrology and flows—scoping study, Report for BC Min Env

Northcote TG, Larkin PA (1989) The Fraser River: a major salmonine production system. In: Dodge DP (ed) Proc Int Large River Symp (LARS). Can Dept Fisheries Oceans, Ottawa. Can Special Pub Fisheries Ocean Sci 106, pp 172–204

Pyrce RS, Ashmore PE (2003) The relation between particle path length distributions and channel morphology in gravel-bed streams: a synthesis. Geomorphology 56:167–187

Rice SP, Church M, Wooldridge CL, Hickin EJ (2009) Morphology and evolution of bars in a wandering gravel-bed river: lower Fraser River, British Columbia, Canada. Sedimentology 55: 709–736

Ryder JM, Bovis MJ, Church M (1990) Rock avalanches at Texas Creek, British Columbia. Can J Earth Sci 27:1316–1329

Shrestha RR, Schnorbus MA, Werner AT, Berland AJ (2012) Modelling spatial and temporal variability of hydrologic impacts of climate change in the Fraser River basin, British Columbia, Canada. Hydrol Process 26:1840–1860

Sutherland Brown A, Ash CH (2009) Great Mining Camps of Canada 3. The History and of the Cariboo Goldfield, Barkerville and Wells. BC. Geosci Can 36:1–31

Tipper HW (1971) Glacial geomorphology and Pleistocene history of central British Columbia. Geol Surv Can Bull 196:89 pp + folded maps

Venditti JG, Church M (2014) Morphology and controls on the position of a gravel-sand transition: Fraser River, British Columbia. J Geophys Res 119:1959–1976

Watt KJ (2006) High water: living with the Fraser floods. Dairy Industry Hist Soc BC, Abbotsford, BC

Landscapes of the Alberta Oil Sands

28

Nigel Atkinson

Abstract

Alberta's oil sands underlie about 142,000 km^2 of the Athabasca, Cold Lake and Peace river areas in northern Alberta. Up to 80 % of this deposit is buried too deeply to be recoverable by traditional mining techniques. However, shallow bitumen deposits in the Athabasca oil sands area north of the city of Fort McMurray have been extracted within open-pit mines since the mid-twentieth century. The surface mineable area occupies approximately 4800 km^2 of lowlands flanking the Athabasca River. The morphology of these lowlands largely reflects a fluvial landscape, superimposed by sediments and landforms relating to advance and retreat of the Laurentide Ice Sheet and the subsequent effects of deglacial meltwater drainage. Oil sand within this area is currently mined using electric and hydraulic shovels and transported to processing facilities where it is mixed with hot water and diluent to separate the bitumen from the sand. Water and sand are then transferred to settling basins and storage facilities that are impounded by tailings dams. To date, up to 844 km^2 of land has been disturbed by development activities, making this one of the largest mining developments in the world. This chapter reviews the pre-development landscape of the Athabasca oil sands area and the geomorphic impacts of current landscape modification, as well as comments on future changes to the landscape associated with post-mine closure and reclamation.

Keywords

Athabasca oil sands • Surface mining • Engineered landscapes • Landscape evolution • Geomorphology

28.1 Introduction

Cordilleran-derived clastic successions within the Albertan portion of the Western Canada Sedimentary Basin host 10 % of the basin's conventional oil reserves, over 25 % its natural gas reserves and almost all its supergiant bituminous oil sands deposits (Mossop and Shetsen 1994; Hein et al. 2013). These bitumen deposits comprise a naturally occurring biodegraded heavy oil and occur within the Athabasca, Cold Lake and Peace river areas, which collectively underlie 142,000 km^2 of northern Alberta (Fig. 28.1) and account for >95 % of the in-place bitumen resources in North America (Hein 2000, 2006, 2013). The largest of these deposits occurs within the Athabasca oil sands area, which extends across 46,000 km^2 of northeast Alberta (Fig. 28.2). Most of the oil sand deposits in this area are hosted in the Early Cretaceous McMurray Formation, which comprises a succession (up to 150 m thick) of shale, sandstone and bitumen-impregnated sand deposited in fluvial to fluvial estuarine or marginal marine settings (Conly et al. 2002; Hein et al. 2013). Approximately 80 % of the McMurray Formation is buried too deeply to be recoverable by traditional mining techniques and is instead extracted by in situ

N. Atkinson (✉)
Alberta Geological Survey/Alberta Energy Regulator,
4th Floor Twin Atria Building, 4999-98 Avenue,
Edmonton, AB T6B 2X3, Canada
e-mail: nigel.atkinson@aer.ca

© Springer International Publishing Switzerland 2017
O. Slaymaker (ed.), *Landscapes and Landforms of Western Canada*,
World Geomorphological Landscapes, DOI: 10.1007/978-3-319-44595-3_28

methods. The remaining 20 % of the oil sand within this formation is accessible in open-pit mines north of the city of Fort McMurray, where deposits are overlain by less than 75 m of non-bituminous Cretaceous bedrock and Quaternary sediment.

The remaining established reserves of Alberta's crude bitumen are estimated to be 27 billion m^3 (170 billion barrels of oil; Alberta Energy and Resources Conservation Board 2013), of which about 13 % by area is under active development. Approved schemes in Athabasca oil sands area include eight surface mines (Fig. 28.3). Based on the capital investment required to build and sustain oil sands operations, these reserves rank among the world's costliest to develop. Nevertheless, investment in oil sands projects has accelerated rapidly since the mid-1990s, increasing from over $1 billion annually in 1996, to $4.2 billion in 2000. This growth was sustained over the last decade, averaging over $16 billion per year from 2006 to 2008 (Gosselin et al. 2010). To appreciate the landscape impacts of these surface mines, it is important to understand the properties of oil sands deposits. Compared with conventional and heavy crude oil, bitumen has a lower hydrogen-to-carbon ratio, higher molecular weight, greater specific gravity and higher sulphur, nitrogen and metal content. Typical ore in the Athabasca oil sands contains between 8–14 wt% bitumen and 3–5 wt% water, with the remaining material comprising coarse sand, silt and clay.

This chapter describes how landscape evolution in northeast Alberta, primarily the result of fluvial erosion by Paleogene river systems, augmented by high-magnitude glacial meltwater discharge, exposed the McMurray Formation at the modern land surface, thereby enabling the economic viability of bitumen extraction within open-pit mines. It also addresses how engineered features and landforms within the surface mineable area have contributed to the modification of the current landscape, as well as how this will continue to evolve with post-mine closure and reclamation activities.

28.2 Setting

The Athabasca oil sands surface mineable area flanks the Athabasca River and occupies approximately 4800 km^2 of the Northern Alberta Lowlands and Northern Plains regions of the Interior Plains of Canada (Pettapiece 1986). Topographically, this area is characterized as subdued to locally variable, with flat to undulating relief and numerous small lakes, streams, marshes, bogs and peatlands. Surface drainage is captured by tributaries of the northward flowing Athabasca River, and the westward flowing Clearwater River, which converge at the city of Fort McMurray (Figs. 28.1 and 28.2; Pettapiece 1986). The major physiographic features include the McMurray Lowland (220 masl), which is flanked by the Birch Mountains (860 masl) to the northwest, and Muskeg Mountain (650 masl) to the east (Pettapiece 1986). Less prominent features include the Fort Hills and the locally high relief of the Firebag Hills Uplands along the Alberta–Saskatchewan border.

The surface mineable area is located in the Central Mixedwood natural subregion of Alberta's boreal forest (Downing and Pettapiece 2006). Upland vegetation comprises stands of aspen, poplar and white spruce. Lowland boreal forest or muskeg contains peat and non-peat wetlands comprising willows and sedges, and forest fens dominated by tamarack, trembling aspen, white and black spruce and pine. Patterned fens are common across lowlands, with bogs containing black spruce and sphagnum moss occurring as islands in large fens (Johnson and Miyanishi 2008).

28.3 The Pre-development Landscape

The Athabasca oil sands surface mineable area comprises a range of geomorphic terrains and associated surficial geological units (Figs. 28.3, 28.4 and 28.5). Karst is a common feature throughout the area, primarily occurring as active and relict sinkholes, especially around McClelland Lake on the southern Embarras Plain (Fig. 28.2). These features relate to collapse of the strata overlying the pre-Cretaceous unconformity due dissolution of the underlying Devonian Prairie Evaporite Formation (Schneider et al. 2012; Schneider and Grobe 2013). The flat to gently undulating terrain of the McMurray Lowland largely reflects a fluvial landscape eroded by Paleogene river systems. This terrain evolved within part of a broad peneplain across a basin-wide unconformity following regional uplift associated with the Laramide orogeny prior to the first Laurentide glacial advance into the region (Fenton et al. 2004; Leckie 2006). During ongoing uplift and associated changes in base level, northeastward flowing river systems continued to incise this peneplain, leaving the Birch and Muskeg mountains as remnant bedrock uplands above a younger regional planation surface.

This surface is unconformably overlain by a succession of Quaternary sediments that range in thickness from 0 to 100 m (Atkinson et al. 2013; MacCormack et al. 2015). Remnant uplands in the region are in places mantled by multiple till sequences deposited during successive advances of the Laurentide Ice Sheet into northern Alberta prior to the last glaciation (Andriashek and Barendregt 2016). However, most glacial sediment–landform associations described in this chapter are inferred to be related to the configuration and dynamics of the Laurentide Ice Sheet during its build-up to the Late Wisconsinan glacial maximum and subsequent retreat during the early Holocene.

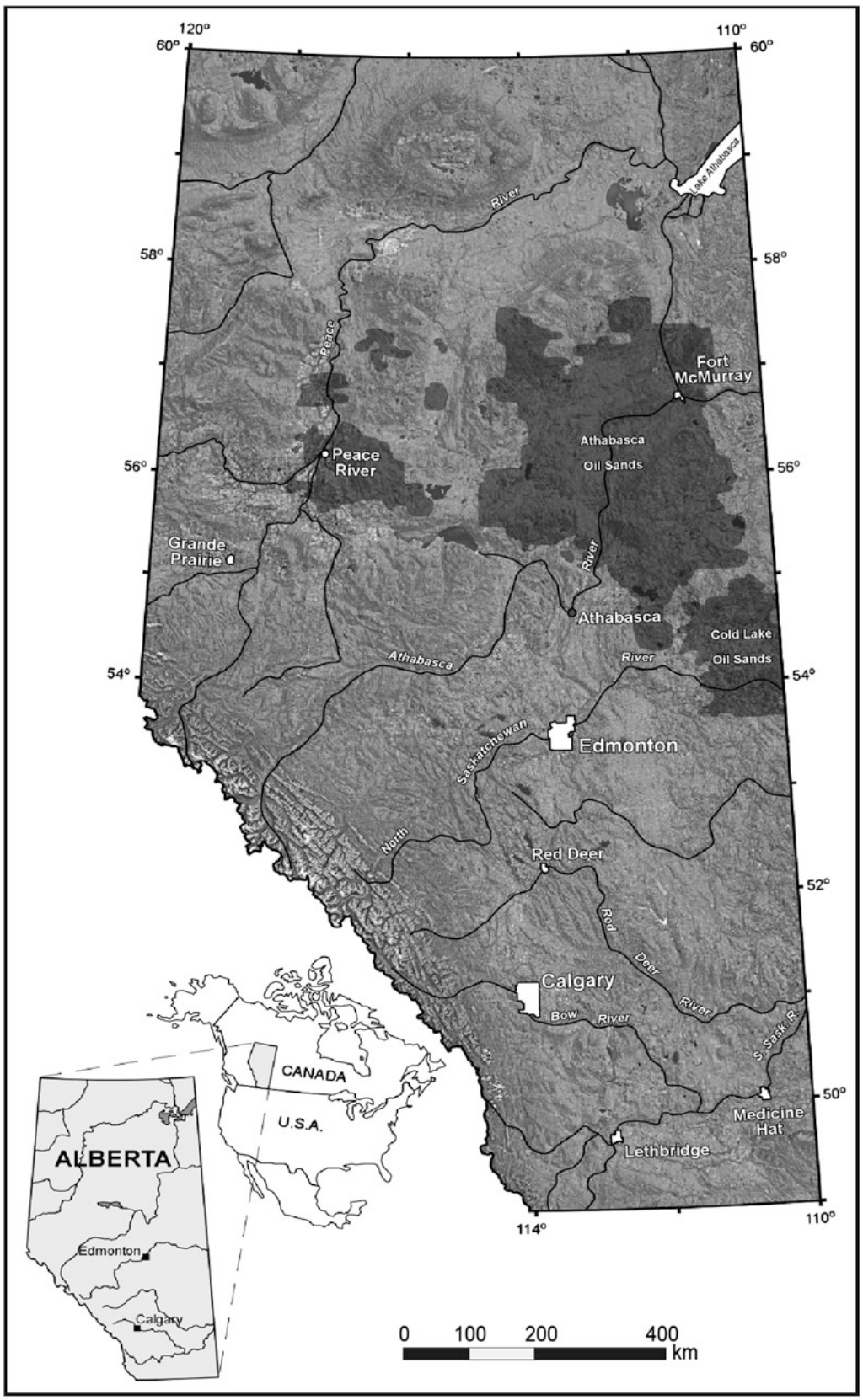

Fig. 28.1 Digital elevation model (DEM) of Alberta showing place names used in the text. Major oil sands deposits are shaded *grey*

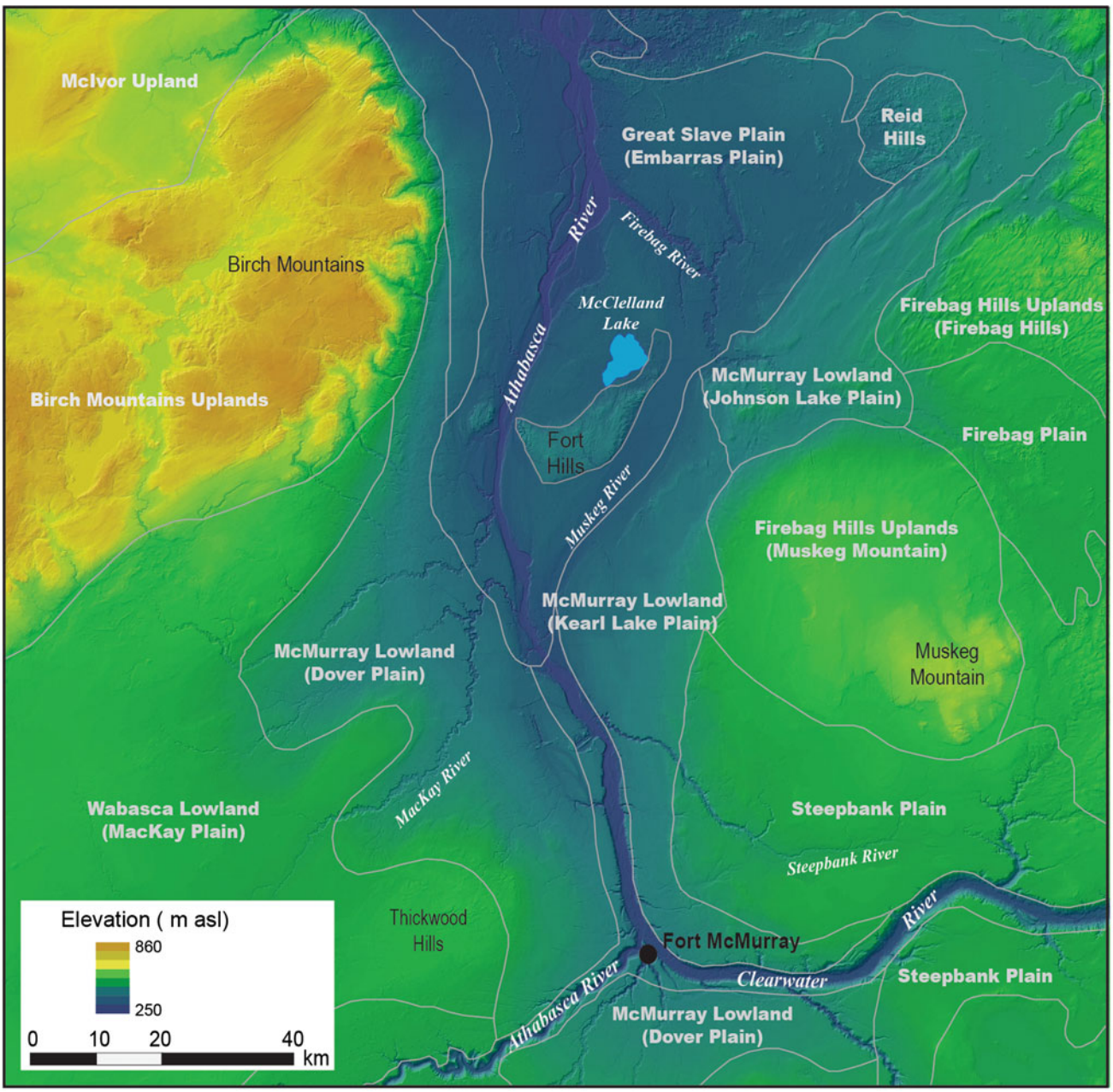

Fig. 28.2 Digital elevation model (DEM) showing the relief and physiographic regions of northeast Alberta, and place names used in the text (modified from Pettapiece 1986)

On the Johnson Lake and Firebag plains, east of the Athabasca River, tracts of parallel-sided to tapered flutings and mega-scale glacial lineations have cross-cut and partially overprinted small (<1 km long) equidimensional drumlins on the Firebag Hills (Fig. 28.6a). These tracts of streamlined subglacial bedforms are superimposed by eskers and crevasse-fill ridges and are commonly associated with well-developed moraines and ice-marginal meltwater channels (Atkinson et al. 2014). Similarly, the Birch Mountains Uplands to the west exhibit eskers superimposed on tracts of mega-scale glacial lineations that terminate at arcuate moraines (Fig. 28.6b). Collectively, these streamlined subglacial bedforms document a major Laurentide ice flow trajectory that extended southwestward across the region and deposited till across the surface mineable area and the surrounding regions of northeast Alberta (Fenton et al. 2013; Atkinson et al. 2014). The terrain down-ice of these bedform tracts is commonly associated with irregular topography, hill–hole pairs and composite, arcuate ridges which collectively demonstrate the influence of glacitectonics within the Quaternary sediments and shallow bedrock on the pre-development landscape of the surface mineable and

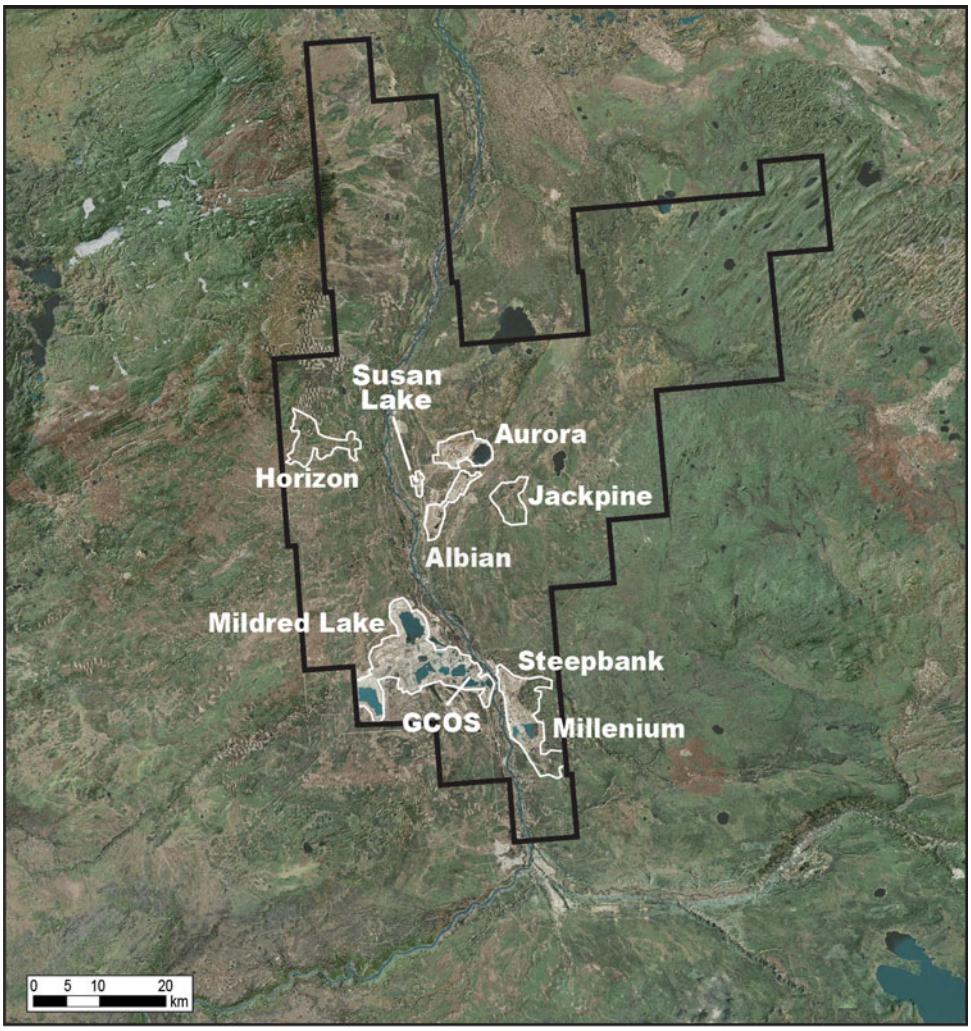

Fig. 28.3 *Colour* orthophoto draped over the LiDAR bare-earth DEM to emphasize the physiographic features of northeast Alberta, and the extent of the surface mineable area (*black outline*) and locations of current surface mines and mine-related operations (*white outlines*; *GCOS* Great Canadian Oil Sands). *Image courtesy* of the Alberta Geological Survey. *Source* Esri, DigitalGlobe, GeoEye, Earthstar Geographics, CNES/Airbus DS, USDA, USGS, AEX, Getmapping, Aerogrid, IGN, IGP, swisstopo, and the GIS User Community

adjacent areas (Fig. 28.6c; Andriashek and Atkinson 2007). This influence is particularly evident at the Fort Hills, which comprises an ice-contact feature of glacifluvial and ice thrust material (Fig. 28.6d).

The McMurray Lowlands (Fig. 28.2) comprise flat to gently rolling plains overlain by a suite of ice-marginal and proglacial sediment–landform associations that relate to the retreat of the Laurentide Ice Sheet from the region at c. 10.5 ka BP (Fisher et al. 2009). As the Laurentide Ice Sheet retreated northeastwards and down drainage from the Fort McMurray area, it exposed this lowland basin, into which subaerial and glacial meltwater drainage systems converged to form a proglacial lake. This lake is demarcated by glacilacustrine sediments that mantle the southern and western margins of the surface mineable area (Fig. 28.5). These glacilacustrine sediments form part of a larger expanse of deposits relating to spatial and temporal evolution of glacial Lake McMurray, which occupied successive proglacial positions as the retreating Laurentide Ice Sheet exposed progressively lower basins to the north (Fisher et al. 2009).

A major geomorphic feature in the region is the Clearwater Lower Athabasca Spillway, which scours though the central portion of the surface mineable area (Fig. 28.5; Smith and Fisher 1993; Fisher and Smith 1994; Fisher 2007; Fisher et al. 2009). This spillway extends 170 km westwards from Saskatchewan into Alberta along a 1.5 km wide, c. 110-m-deep anastomosed valley complex (Smith and Fisher 1993). The spillway bends northward at the confluence of the present-day Clearwater and Athabasca rivers and continues for a further 75 km, where it widens to 12 km and bifurcates around the Fort Hills, with one channel extending along the Muskeg and Firebag river valleys and the other following the modern course of the Athabasca River valley (Figs. 28.2, 28.5 and 28.6d). The spillway terminates north of the Fort Hills at the apex of the lower Athabasca braided delta that prograded into Glacial Lake McConnell at the end of the last glaciation (Rhine and Smith 1988). The Clearwater Lower Athabasca Spillway was incised by the high-magnitude discharge of meltwater from proglacial lakes in northwest Saskatchewan. This discharge has been

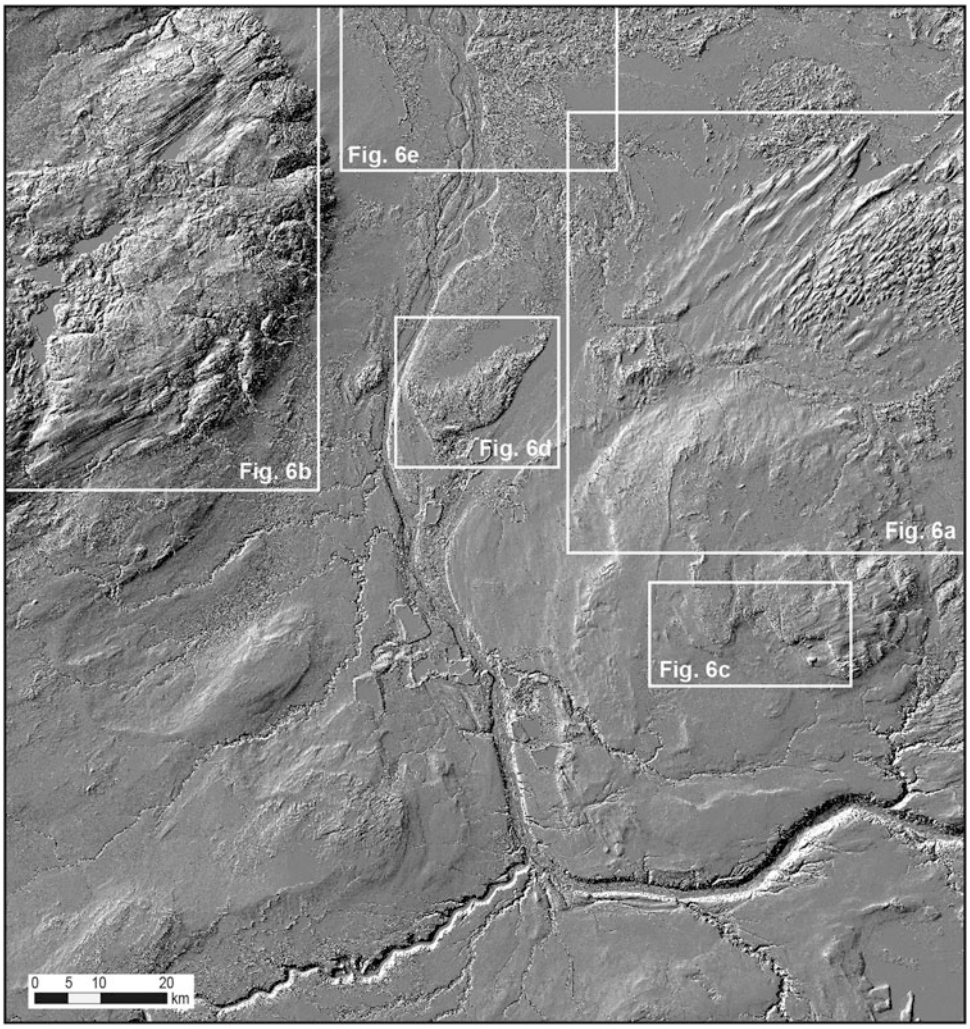

Fig. 28.4 Hillshade image of northeast Alberta derived from the LiDAR bare-earth DEM. The location of specific landform examples is provided in Fig. 28.6. *Image courtesy* of the Alberta Geological Survey

chronologically linked to a rapid 50-m drop in the level of glacial Lake Agassiz following the incision of a drainage divide near the Alberta–Saskatchewan border (Smith and Fisher 1993; Fisher and Smith 1994), although subsequent work suggests that this discharge originated from a regional lake which was at the time separated from Lake Agassiz by ice or topography (Fisher et al. 2009). Deposits in the surface mineable area that relate to this discharge are characterized by glacifluvial sand and gravel comprising massive to planar-bedded boulder gravel containing rip-ups and rafts of bituminous McMurray Formation, and extensive sheets of upper flow regime plane-bedded sand and pebbles that mantle the scoured outer zone of the spillway. These deposits typically overlie bedrock, indicating that discharge along the spillway eroded much of the Quaternary sediment in the central part of the surface mineable area. Ongoing postglacial modification of the McMurray Lowland by the Athabasca and Clearwater rivers has continued the erosion of the Quaternary sediment and Cretaceous bedrock along the flanks of these valleys, further exposing bitumen-bearing McMurray Formation at the modern land surface.

Postglacial aeolian reworking of these glacifluvial deposits is responsible for the formation of extensive sand sheets and dune complexes north of the surface mineable area (David 1977). Dune complexes comprise longitudinal and parabolic paleodunes which include the largest reported examples in Alberta, ranging from 1 to 3 km apart, up to 15 km long and up to 20 m high (Fig. 28.6e; Allen et al. 2003). Dunes characteristically have steep slopes and sharp crests and include areas of active blowouts and deflation troughs that are commonly filled with vegetated wetlands.

28.4 The Developed Landscape

The Athabasca oil sands have experienced significant growth in development and land disturbance over the last decade, with current mine site footprints extending across

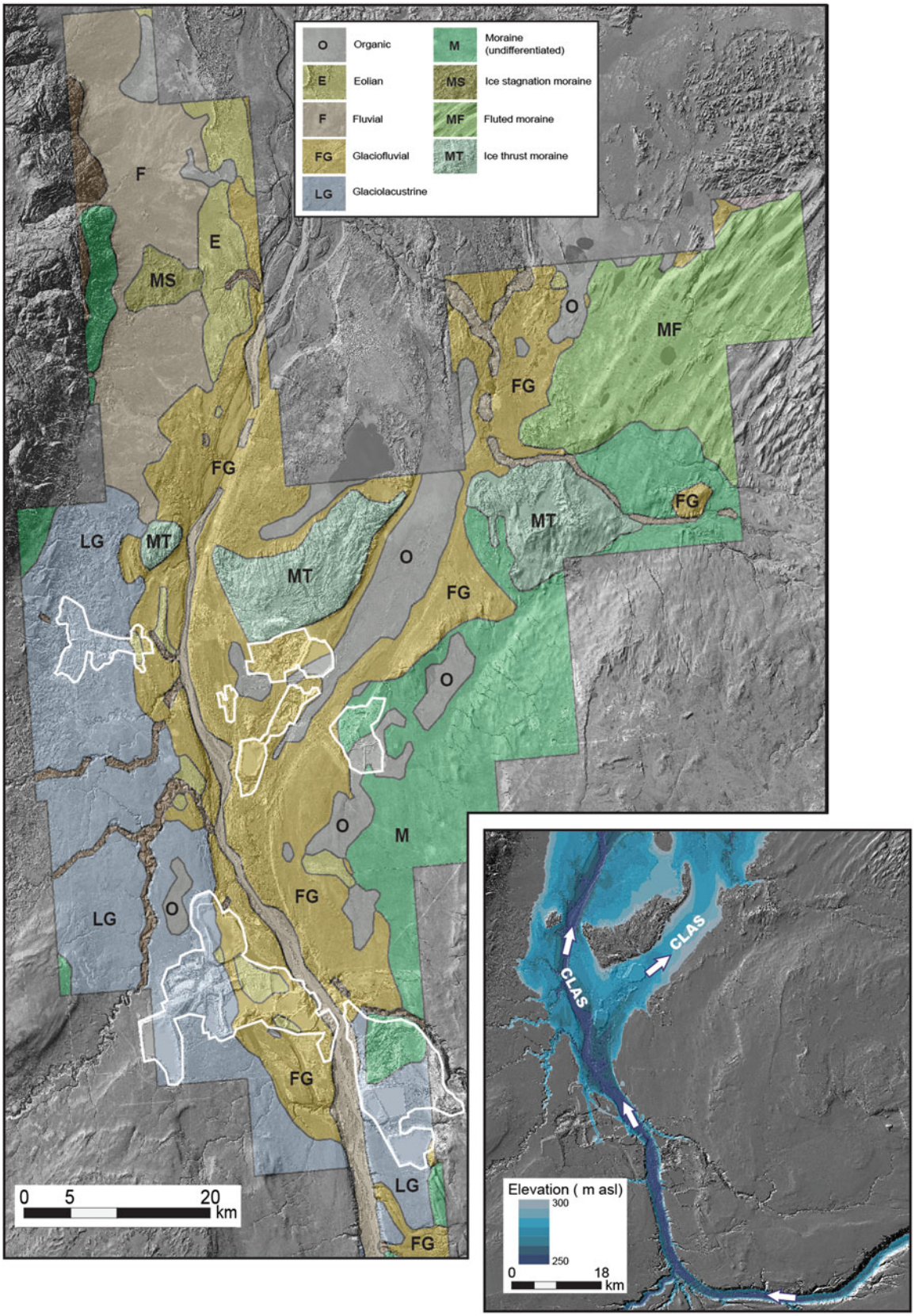

Fig. 28.5 Surficial geology and mine site footprints (*white outlines*) of the surface mineable area (Fenton et al. 2013) draped over the LiDAR bare-earth DEM of the region. *Inset* shows the extent and flow paths of the Clearwater Athabasca Spillway (CLAS; modified from Smith and Fisher 1993)

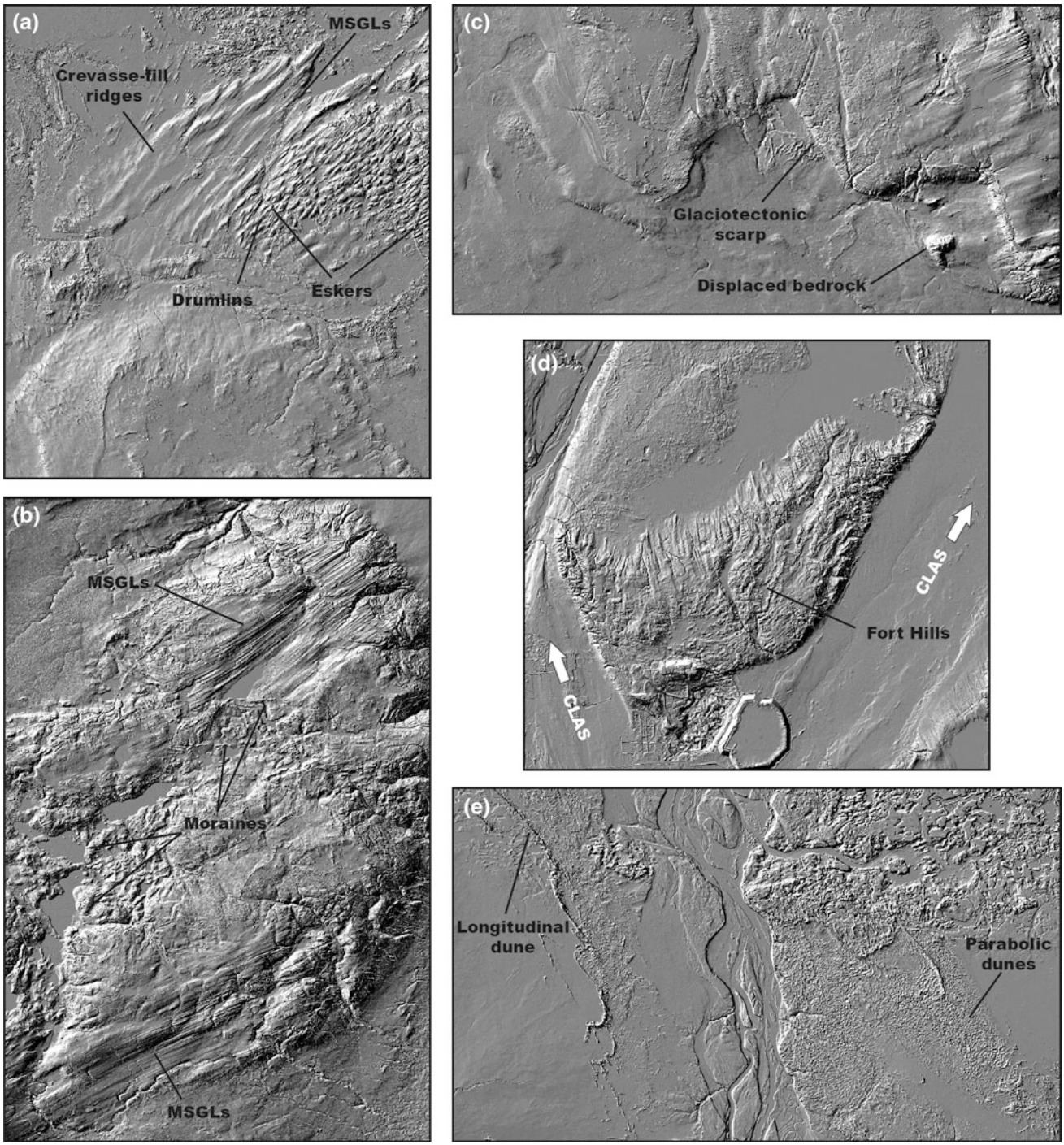

Fig. 28.6 Specific landform examples referred to in text. **a** Small drumlins partially overprinted by flutings and mega-scale glacial lineations (MSGLs) and superimposed by eskers and crevasse-fill ridges, **b** eskers superimposed on mega-scale glacial lineations that terminate at arcuate moraines on the Birch Mountains, **c** glacitectonically displaced bedrock on the southern flank of Muskeg Mountain, **d** the Fort Hills, an ice-contact feature of glacifluvial and ice thrust material, **e** longitudinal and parabolic paleodunes flanking the Athabasca River. See Fig. 28.4 for site locations. Images courtesy of the Alberta Geological Survey

844 km^2 of the surface mineable area (Fig. 28.7). Prior to 2002, there were only two open-pit mines in production. However, by the end of 2012, these mines had both significantly increased their capacities, and an additional four mines had commenced production, with a further two proposed surface mines having received regulatory approval. Collectively, production from these mines has risen from 197 million barrels of oil in 2002, to 356 million barrels in

2013 (Alberta Energy Resources Conservation Board 2013). This accounts for 47 % of total bitumen production, although in 2012 production from surface mines was exceeded for the first time by output from in situ projects (362 million barrels), a trend that is expected to continue.

The Athabasca oil sands surface mines are primarily located within the Clearwater Athabasca Spillway, since high-magnitude meltwater discharge along the spillway eroded Quaternary sediment and non-bituminous Cretaceous bedrock, resulting in the McMurray Formation being accessible at a shallow enough depth for it to be economically viable to operate open-pit mines. Each mine contains a range of interrelated facilities, including: active and mined-out pits, mine waste dumps, ore processing and upgrading facilities, tailings sand storage facilities and fine tailings settling basins, worker accommodation (Fig. 28.8) and, at the northern mines, landing strips for commercial aircraft. The developed landscape of the surface mineable area comprises a range of engineered features and landforms, the design and location of which are constrained by ore extraction requirements and the need to accommodate storage space for mine waste within lease boundaries. Mining begins with clearing the land, which requires the removal of the vegetation, organic and mineral soils, as well as Quaternary sediment and Cretaceous bedrock to expose the underlying McMurray Formation. Clearing activities are staged and may begin up to 5 years before mining commences. Once vegetation is cleared, rivers and streams are diverted, and ditches dug to dewater the muskeg wetlands, which may take up to 3 years depending on drainage conditions (Fig. 28.9a). When the soil and muskeg are sufficiently dewatered for handling, they are removed and stockpiled at storage areas for use in future reclamation activities. Muskeg removal is scheduled for the winter months and typically occurs at least one year prior to the commencement of surface mining. The Quaternary sediments and underlying, non-bituminous Cretaceous bedrock are subsequently mined in a series of benches to remove overburden. These materials are managed separately based on their suitability for the construction of tailings dams, haul roads and other mine site projects. The remaining material is stored in overburden dumps, which form large features on the developed landscape, ranging from tens of metres high to several kilometres long.

Following the removal of this material and exposure of the McMurray Formation, which in the surface mineable area generally occurs within 75 m of the land surface, bituminous oil sands deposits are mined. Oil sands were originally mined using a system of dragline excavators and bucket wheels which dug directly into the pit face. Material was then loaded onto a series of conveyor belts and transported to ore processing facilities (Fig. 28.9b). This system was superseded in 2006 by the use of large electric and hydraulic front shovel excavators, which dump material into 400-ton haul trucks (Fig. 28.9c). These enable higher grades of oil sand to be transported to the processing facilities, while leaving deposits below the cut-off grade in place. The open-pit mines comprise a series of benches, each up to 15 m high (Figs. 28.8 and 28.9d). The use of multi-bench mining, where excavators are located on more stable, lower-grade sand facies within the McMurray Formation, or on the underlying Devonian limestone, utilizes bulldozers to trim the bench and push material downslope towards the loading area. The height of the mining face makes this use of bulldozers a critical factor in operational safety.

From the mining face, material is transported to processing facilities where it is crushed and cleaned by mixing the ore with hot water and diluent to separate the bitumen from the sand. The production of 1 m^3 (6.3 barrels) of crude oil requires approximately 11 tonnes of oil sands (at 90 % bitumen recovery) and 2.5 m^3 (16 barrels) of water, of which up to 85 % is recycled, typically from the uppermost three metres of the tailings ponds. After bitumen separation and recovery, approximately 3.3 m^3 of waste product remains. This mixture of water, sand, silt, clay and residual bitumen, termed tailings slurry, is hydraulically pumped to settling basins and sand storage facilities that are impounded by large embankment dams (Figs. 28.8 and 28.9a).

Tailings are stored in a combination of settling basins which include external-to-pit retention ponds constructed above the surrounding ground surface adjacent to the mine, and smaller, internal-to-pit retention ponds which are impounded within mined-out portions of the active pit and get sequentially flooded as the mine progresses (Fig. 28.7). Within external-to-pit retention ponds, the starter dyke is constructed with overburden materials, with compacted tailings sand being used to complete the embankment as mining and waste production advances. These embankment dams are by volume among the largest in the world. Some dams like those at the Albion, Aurora and Jackpine mines form self-contained features on the landscape. However, to reduce land disturbance and material handling costs, other dams including examples at the Mildred Lake, Horizon and Millennium mines have been constructed against the slopes of adjacent hills, to incorporate local topography as part of the retention structure.

Tailings slurry is poured into cells and beaches where the sand is quickly deposited along the edge of the ponds, and the fine-fluid tailings (silt, clay, bitumen and water) are carried further out into the settling basin (Fig. 28.10). By volume, the fine tailings suspension is typically 85 % water and 15 % fines, which settles and dewaters to form mature fine tailings (MFT). These typically have a solids content of up to 35 %. Mature fine tailings settle very slowly and may remain fluid-like for decades or centuries. As a consequence of the intensive use of water in oil sands processing, and the

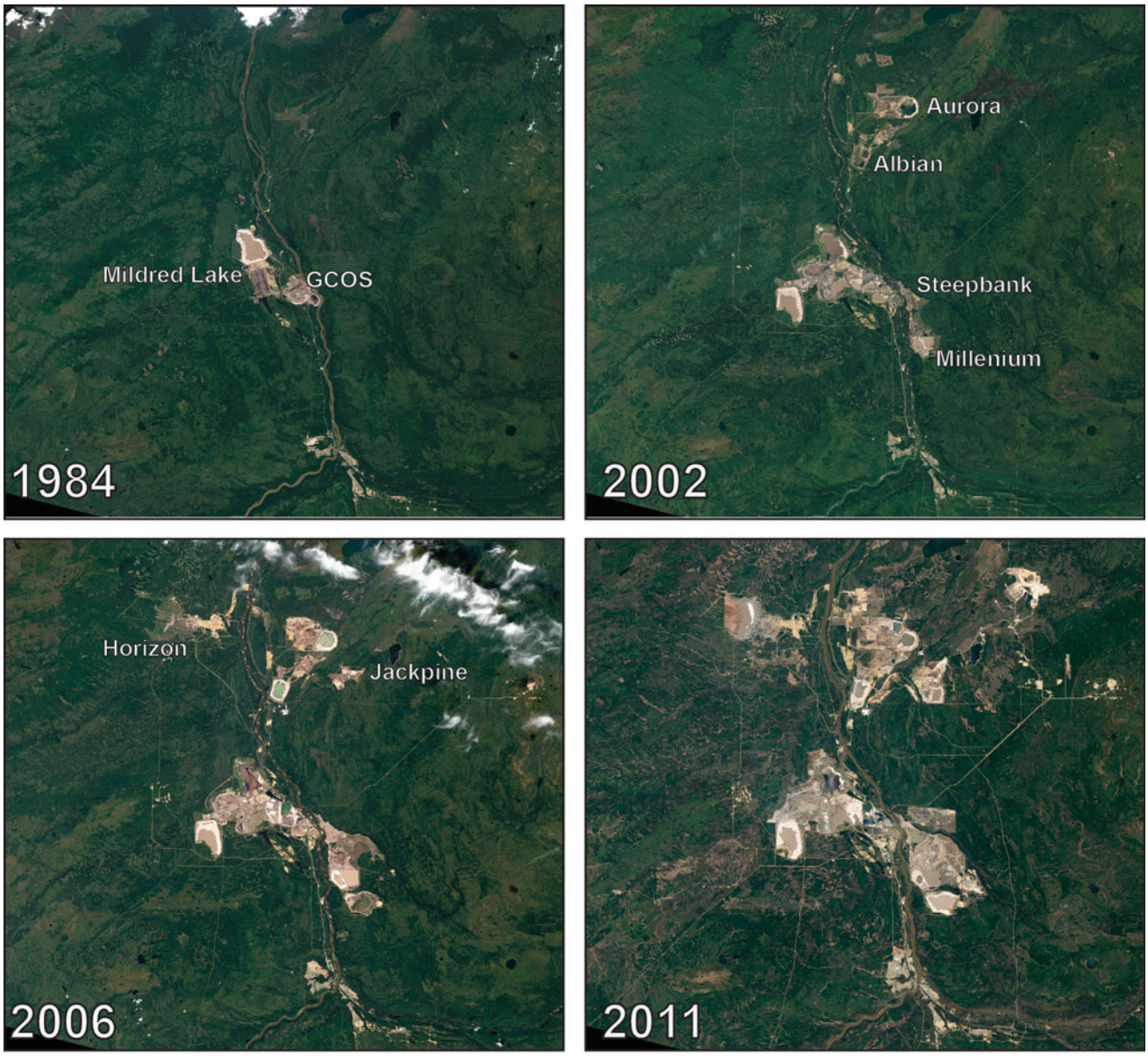

Fig. 28.7 Landsat satellite images showing the spatial and temporal changes in mine site footprints in the surface mineable area between 1984 and 2011. *Image courtesy* of NASA's Earth Observatory

desire to reduce the area of mineable land sterilized by tailings storage, operators strive to develop MFT remediation technologies that reduce the footprint of settling basins and maximize the volume of water available for recycling.

Seepage water from settling basins is managed with perimeter ditches, sumps and recovery wells. Drainage channels constructed at the toe of the embankment dams collect seepage, and monitoring wells are used to assess potential off-site migration of process-affected water. Settling basins can remain part of an active mine operation for 30–40 years, either for the retention of tailings slurry or for the storage of water for recycling. To date, there are at least 16 major basins within the Athabasca oil sands area, with a combined storage volume of 750 million m^3. Of the 844 km^2 of land disturbed by oil sands mining activity (including mine site footprints and cleared land), 176 km^2 is currently occupied by settling basins (Oil Sands Information Portal 2015).

The largest oil sands mine operates at daily material handling rates approaching 1.5 million tonnes of mined ore, waste and tailings, with primary extraction and ore processing capacity exceeding 500,000 tonnes per day (Suncor Energy Inc. 2010a, b). These production values place the Athabasca oil sands mines among the largest mines in the world and make their primary extraction facilities the largest processing plants globally. Oil sands mines are waste constrained, insofar

Fig. 28.8 Semi-transparent SPOT image draped over the LiDAR bare-earth DEM to illustrate examples of facilities and engineered features and landforms within an Athabasca oil sands surface mine. *1*—active pit; *2*—external-to-pit settling basin; *3*—internal-to-pit settling basin; *4*—reclamation area; *5*—ore processing facility; *6*—mine waste/overburden dump; and *7*—tailings sand storage facility. *Image courtesy* of the Alberta Geological Survey

that the widespread distribution of mineable bitumen-rich facies within the McMurray Formation limits the amount of space available across the lease to store mined waste and tailings without sterilizing the deposit. Waste planning is therefore the most significant non-regulatory constraint in mine development. Consequently, the management of mining

Fig. 28.9 Examples of engineered features and mining operations in the surface mineable area. **a** Mine site footprint in initial stages of development, **b** machinery used in pre-2006 mining operations, including dragline excavators, bucket wheels and conveyor belts, **c** since 2006, front shovel excavators have been used to load higher grade oil sand into 400-ton haul trucks, **d** multiple benches within a surface mine. Images courtesy of the Alberta Geological Survey

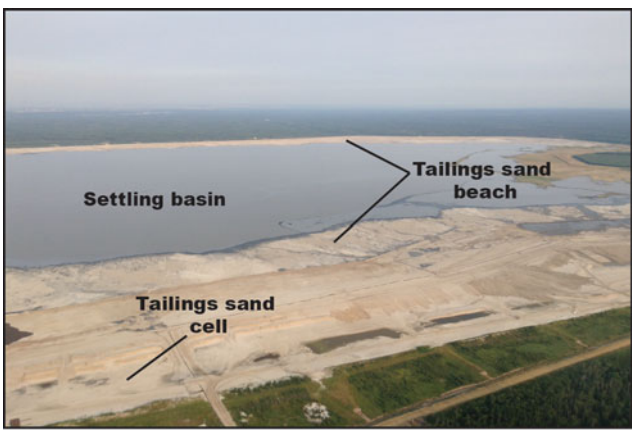

Fig. 28.10 Tailings sand deposited in cells and beaches around the margin of a fine-fluid tailings settling basin. *Image courtesy* of the Alberta Geological Survey

waste and tailings has a significant impact on the sequencing of oil sands mining activities compared with conventional open-pit operations. Successful oil sands waste management is dependent on the interaction between overburden planning, ore planning and extraction control and tailings planning. The medium- to long-term tailings plan must meet predicted tailings containment requirements and ensure that sufficient water is available for recycling back into the ore processing facilities.

In addition to the land disturbance directly associated with mining operations, these projects place significant demands on aggregate availability, with annual requirements ranging from 5 to 8 million tonnes for plant construction and 500,000 to 1 million tonnes for road building and maintenance and other infrastructure development in the Fort McMurray region. The Susan Lake gravel pit, located within the Clearwater Lower Athabasca Spillway, south of the Fort Hills (Fig. 28.3), is the largest single aggregate operation in North America and provides the majority of gravel to oil sands operators in the area. Between 2003 and 2011, annual aggregate production from this pit averaged 6.20 million tonnes, which increased to 7.75 million tonnes in 2011.

28.5 Post-mine Closure and Reclamation

According to Alberta's Environmental Protection and Enhancement Act, areas that are no longer required for mining activities are deemed suitable for closure and reclamation. The objective of reclamation is to return the mine site footprint to a land capability that is equivalent to pre-disturbance conditions and capable of maintaining diverse and self-sustaining boreal forest ecosystems (Alberta Environment and Water 2012). Reclaimed ecosystems are intended to be able to support a variety of end uses. Given the scale of these mine site footprints, current reclamation strategies involve the construction of full ecosystems at the landscape scale (Johnson and Miyanishi 2008; McKenna 2009).

The major mine site features that require reclamation in the Athabasca oil sands area include inactive pits, overburden storage and mine waste dumps, tailings sand dykes and fine-fluid tailing settling basins (Fung and Macyk 2000). Reclamation of these features incorporates a range of upland and wetland landscaping and engineering strategies (Quagraine et al. 2005) depending on mine site constraints and the planned end uses of the reclaimed landscape.

28.5.1 Upland Strategies

Reclamation proceeds from the removal and decontamination of buildings and other mine-related infrastructure, followed by the reconstruction and stabilization of the land surface (Beckingham and Archibald 1996). This process involves several stages, depending on the location of the reclamation area within the mine site, and includes the hauling and placement of salvaged reclamation materials, application of fertilizer, revegetation, monitoring and certification (Syncrude 2006).

Reclamation of the pit utilizes stockpiled overburden and waste materials from dumps and tailings sand beaches and dykes to backfill the site, either up to the level of the original ground surface or to a level that surface water can drain without ponding. To further promote drainage, the reconstructed land surface is contoured and revegetated to stabilize the reclamation area. Soil reconstruction is an important component of this process and utilizes organic and mineral mixtures from stockpiles created during initial land clearing.

Reclamation of overburden dumps and tailings sand dykes began in the early 1970s (Alberta Environment 2010). Since these features are elevated above the surrounding landscape, they act as local watersheds, draining water to lower parts of the landscape. The objective of early reclamation strategies was to therefore stabilize the erodible sandy slopes of the dykes by seeding them with grass and legumes. However, as reclamation strategies evolved from erosion control to developing self-sustaining ecosystems, revegetation plans increasingly focussed on using tree species best suited to local soil moisture and nutrient conditions, as well as the topography of the reclamation area (Bridge and Johnson 2000).

Settling basins containing large volumes of fluid tailings present significant closure and reclamation challenges in the mined landscape. For example, fine-fluid tailings within the bottommost layers of the setting basins contain a mixture of clay and water which can take up to 30 years to separate, dewater and consolidate into mature fine tailings. Consequently, regulatory directives seek to reduce the volume of fine-fluid tailings stored within tailings ponds. Consolidated tailings are an engineered product containing coagulating agents such as gypsum and polymers that alter the physical characteristics of fine-fluid tailings to enable them to form non-segregating mixtures when added with sand. The production of consolidated tailings helps expend fine-fluid tailings and tailings sand and represents a significant part of ongoing reclamation activities. Consolidated tailings have sand-to-fines ratios between 3:1 (to allow dewatering and consolidation) and 5:1 (to utilize adequate quantities of fines). Regulatory directives require that consolidated tailings have the shear strength, stability and structure necessary to establish a trafficable surface within 5 years of the cessation of tailings discharge into the settling basin. To reclaim consolidated tailings as a solid landscape, it requires a substrate capable of supporting heavy equipment. Hydraulic sand capping is a technique that involves discharging large volumes of tailings sand across mature and consolidated tailings to create 2- to 5-m-thick deposits that help stabilize the decommissioned settling basin prior to revegetation. However, tailings sand provides a poor substrate for plant growth (Fung and Macyk 2000), and crusting of the sand cap can inhibit water infiltration. Therefore, a blend of salvaged reclamation material including mineral soil, peat and overburden stockpiled during initial mine clearance is applied over the sand cap prior to revegetation. This cover enhances the physical, chemical and biological properties of the substrate, which improves the establishment of vegetation needed to return fine tailings deposits to productive ecosystems in a terrestrial landscape (Naeth and Wilkinson 2004).

Salinity and moisture are the greatest limitations to germination and establishment of vegetation on soft tailings (Naeth and Wilkinson 2004). Therefore, engineered substrates are designed to be sufficiently thick to ensure that saline water released during tailings consolidation does not enter the rooting zone of revegetated reclamation areas (cf. Purdy et al. 2005). Salt-tolerant grasses such as barley, wheatgrass and wild rye are typically used in the initial reclamation of fine tailings (Renault et al. 2003, 2004). Shrub species such as willow show relatively high salt tolerance, although conifer species like white spruce and jack pine exhibit significant growth reductions on substrates with elevated salt concentrations.

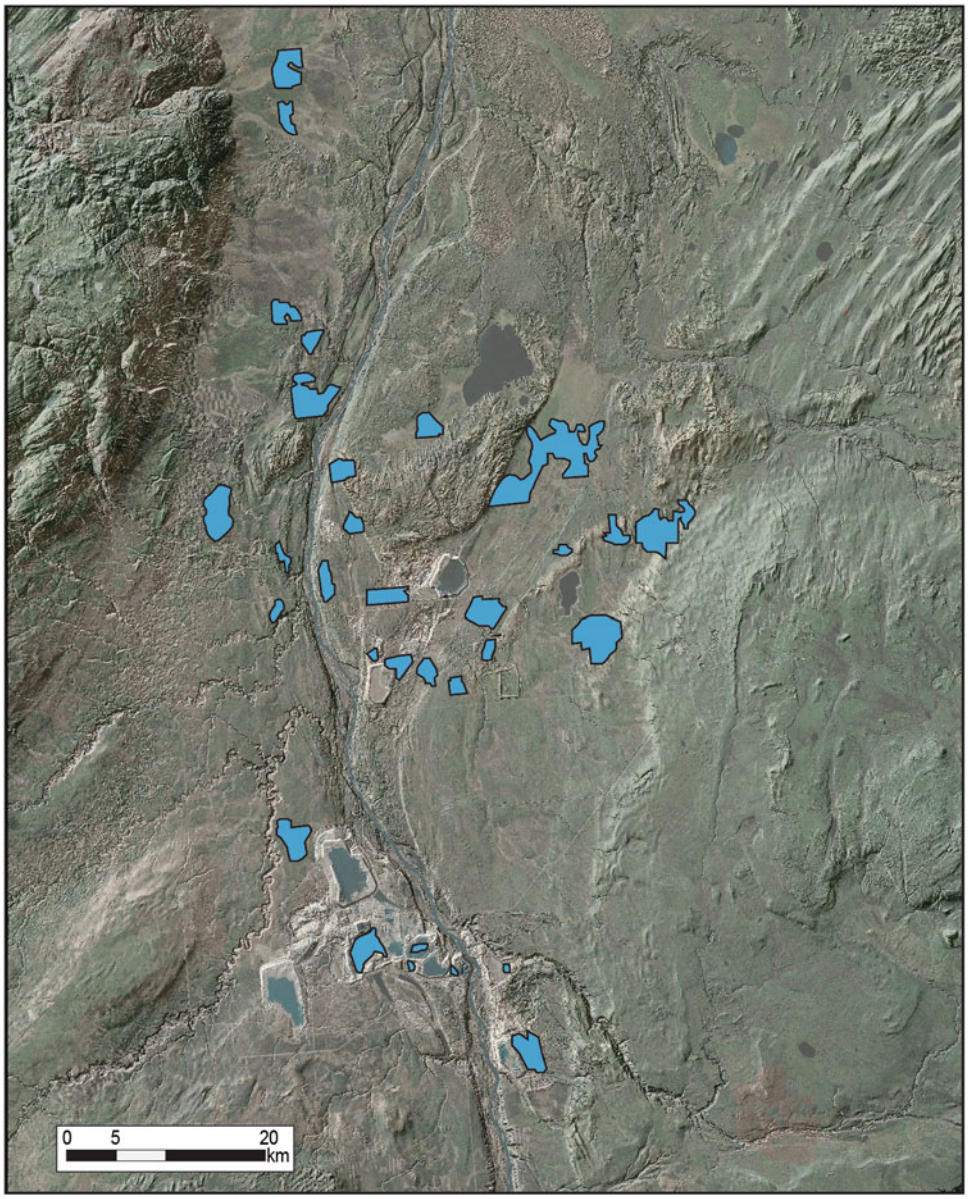

Fig. 28.11 Locations of planned end pit lakes (*blue* polygons) in the Athabasca oil sands area based on closure plans submitted before December 2011 (modified from CEMA 2012)

Managing moisture deficits and excesses, including seepage zones from overburden dumps and settling basins, pose challenges to revegetation strategies. Strategies incorporate a range of engineered features and meso-topographic landforms such as plateau, hummocks, ridges and slopes. These topographic controls are designed to maintain a water table at least 2 m below the reconstructed land surface to mitigate over saturation and salinization of the rooting zone. Seepage management includes the creation of wetlands at the toes of overburden dumps and settling basins to remediate groundwater discharge, as well as the construction of streams and swales to control the storage and movement of runoff across the reclaimed landscape.

28.5.2 Wetland Strategies

At the end of a mine's life cycle, the final pit including internal-to-pit retention ponds is allowed to fill with surface runoff and groundwater discharge to form a water body termed an end pit lake (EPL). These engineered lakes serve as important reclamation tools to remediate tailings waste and process-affected water to meet water quality guidelines prior to being discharged to the downstream environment. End pit lakes are designed to be permanent features in the reclaimed landscape of the Athabasca oil sands area, with at least 25 planned within the next 60 years (Fig. 28.11; Westcott and Watson 2007). Unlike the shallow tailings ponds, EPLs are designed to be 65–100 m deep.

End pit lakes that incorporate flooded internal-to-pit retention ponds are designed as multi-layer features that comprise a substrate of overburden, tailings sand and low-grade oil sands, an intermediate layer of mature fine tailings, and an overlying cap of fresh water at least 5 m thick. End pit lakes that do not incorporate tailings storage require fewer design and management considerations. These EPLs can store process-affected and remediated waters and other mine waste materials where there is insufficient overburden material available to backfill the pit to a terrestrial landscape.

Due to their spatial extent, mine site footprints can be considered landscape-scale features, covering 20–200 km^2, often incorporating several watersheds. At this scale, many of the activities within the mine site have impacts on EPL design, construction, operation and performance. Therefore, once established, EPLs will become central features in the reconstructed landscape, influencing many of the reclamation activities both upstream and downstream of the lake. They typically occupy the lowest topographic position in the mine site, and to ensure adequate volumes of freshwater inflow, reconstructed land surfaces are contoured to direct surface runoff towards the lake, while their outlet elevation ensures properly regulated outflow of remediated water. Landscape design therefore considers upland and wetland topographic ratios and contains a mosaic of natural and engineered meso-scale landforms in order to establish a closed surface water drainage system that maintains water balance within the EPL watershed (Flint 2005). It is anticipated that EPLs will become viable aquatic ecosystems with active littoral and pelagic zones, inlets, outlets and islands, as well as shoreline and riparian areas that support biological activity.

Peat-forming wetlands extended across 43 % of the pre-disturbance landscape and were an important component of the pre-development ecosystem, providing a range of functions including water storage, flow attenuation, vegetation and wildlife habitat. Wetlands are therefore desirable reclamation features within the surface mineable area, and design guidelines have been developed for their construction over decommissioned settling basins (Westcott and Watson 2007). Designs may be complicated by topographic constraints, ongoing tailings consolidation, the erodibility of reclamation materials, the management of solute transport and the accumulation of salts in the landscape.

28.6 Conclusion

To date, a 1.04-km^2 area called Gateway Hill has been fully reclaimed, insofar as terrestrial and/or wetland performance objectives have been met, and regulators have issued a final certification for the site to be returned to the Crown as public land. An additional 80 km^2 is currently undergoing active reclamation (Oil Sands Information Portal 2015). Although reclamation may not return the landscape to pre-development conditions, land is returned to an equivalent capacity. For example, areas of wetland may be converted to upland, and the invasion of natural species may proceed more slowly than introduced species, particularly if these are better suited to the prevailing conditions of the reconstructed land surface.

References

Alberta Energy and Resources Conservation Board (2013) ST98-2013: Alberta's energy reserves 2012 and supply/demand outlook 2013–2022. Calgary, Alberta

Alberta Environment and Water (2012) Best management practices for conservation of reclamation materials in the mineable oil sands region of Alberta. Terrestrial Subgroup of the Reclamation Working Group of the Cumulative Environmental Management Association, Fort McMurray, Alberta

Allen L, Hunter D, Nordstrom W, Vujnovic D (2003) Richardson River Dunes Wildland Provincial Park—a synthesis of biophysical information. Parks and Protected Areas Division, Alberta Community Development, Edmonton

Andriashek LD, Atkinson N (2007) Buried channels and glacial-drift aquifers in the Fort McMurray Region, Northeast Alberta. Alberta Energy Utilities Board/Alberta Geological Survey Earth Sciences Report 2007-01, p 160

Andriashek LD, Barendregt RW (2016) Evidence for Early Pleistocene glaciation from borecore stratigraphy in north-central Alberta. Alberta Energy Regulator/Alberta Geological Survey Report 92, p 34

Atkinson N, Andriashek LD, Slattery SR (2013) Morphological analysis and evolution of buried tunnel valleys in northeast Alberta, Canada. Quat Sci Rev 65:53–72

Atkinson N, Utting DJ, Pawley SM (2014) Landform signature of the Laurentide and Cordilleran ice sheets across Alberta during the last glaciation. Can J Earth Sci 51:1067–1083

Beckingham JD, Archibald JH (1996) Field guide to ecosites of Northern Alberta. National Resources Canada, Canada Forest Service, Northwest Region, Edmonton

Bridge SRJ, Johnson EA (2000) Geomorphic principles of terrain organization and vegetation gradients. J Veg Sci 11:57–70

Cumulative Environmental Management Association (2012) End pit lakes guidance document Alberta Environment (2010) Guidelines for reclamation to forest vegetation in the Athabasca oil sands region. Terrestrial Subgroup of the Reclamation Working Group of the Cumulative Environmental Management Association. Fort McMurray, Alberta

Conly FM, Crosley RW, Headley JV (2002) Characterizing sediment sources and natural hydrocarbon inputs in the lower Athabasca River, Canada. J Environ Eng Sci 1:187–199

David PP (1977) Sand dune occurrences of Canada. Indian and Northern Affairs, National Parks Branch pp 183

Downing DJ, Pettapiece WW (2006) Natural regions and subregions of Alberta. Natural Regions Committee, Government of Alberta Publication T/852, p 264

Fenton MM, Pawlowicz J, Paulen R, Prior G, Olson R (2004) Quaternary geology of northern Alberta: implications for kimberlite exploration. In: Abstracts of the 8th international kimberlite conference

Fenton MM, Waters EJ, Pawley SM, Atkinson N, Utting DJ, Mckay K (2013) Surficial geology of Alberta. Alberta Geological Survey, AER/AGS Map 601

Fisher TG (2007) Abandonment chronology of glacial Lake Agassiz's northwestern outlet. Palaeogeogr Palaeocl 246:31–44

Fisher TG, Smith DG (1994) Glacial Lake Agassiz: its northwest maximum extent and outlet in Saskatchewan (Emerson phase). Quat Sci Rev 13:845–858

Fisher TG, Waterson N, Lowell TV, Hajdas I (2009) Deglaciation ages and meltwater routing in the Fort McMurray region, northeastern Alberta and northwestern Saskatchewan, Canada. Quat Sci Rev 28:1608–1624

Flint L (2005) Bitumen recovery technology: a review of long term research and development opportunities. Natural Resources Canada, Devon

Fung MRP, Macyk T (2000) Reclamation research for various uses in the oil sands region of Alberta, Canada. In: Global land reclamation/remediation 2000 and beyond. Proceedings of the Canadian Land Reclamation Associations 25th Annual Meeting. Edmonton, Alberta

Gosselin P, Hrudey SE, Naeth MA, Plourde A, Therrien R, van der Kraak G, Xu Z (2010) The Royal Society of Canada expert panel: environmental and health impacts of Canada's oil sands industry. The Royal Society of Canada, Ottawa, p 414

Hein FJ (2006) Heavy oil and oil (tar) sands in North America: An overview and summary of contributions. Nat Resour Res 15:67–84

Hein FJ (2000) Historical overview of the Fort McMurray area and oil sands industry in northeast Alberta. Alberta Energy Resources Conservation Board/Alberta Geological Survey Earth Sciences Report 2000–2005, p 32

Hein FJ, Leckie, DA, Larter, S, Suter JR (2013) Heavy oil and bitumen petroleum systems in Alberta and beyond: the future is nonconventional and the future is now. In: Hein FJ, Leckie D, Larter S, Suter JR (eds) Heavy oil and oil-sand petroleum systems in Alberta and beyond. American Association of Petroleum Geologists, Tulsa, OK, USA, pp 1–21

Johnson EA, Miyanishi K (2008) Creating new landscapes and ecosystems: the Alberta oil sands. Year in ecology and conservation biology 2008. Ann NY Acad Sci 1134:120–145

Leckie DA (2006) Tertiary fluvial gravels and evolution of the western Canadian Prairie landscape. Sedim Geol 190:139–158

MacCormack K, Atkinson N, Lyster S (2015) Sediment thickness of Alberta. Alberta Geological Survey, AER/AGS Map 603

McKenna G (2009) Techniques for creating mining landforms with natural appearance. In: Proceedings of the tailings and mine waste conference, Banff, Alberta. 1–4 Nov 2009

Mossop GD, Shetsen I (1994) Geological atlas of the western Canada Sedimentary Basin. Canadian Society of Petroleum Geologists and Alberta Research Council

Naeth MA, Wilkinson S (2004) Revegetation research in the Athabasca oil sands: a literature review. Prepared for Suncor Energy Inc

Oil Sands Information Portal (2015) Oil sands information portal. http://osip.alberta.ca/. Accessed 1 Feb 2015

Pettapiece WW (1986) Physiographic subdivision of Alberta. Agric Can Scale 1:500,000

Purdy BG, Macdonald SE, Lieffers VJ (2005) Naturally saline boreal communities as models for reclamation of saline oil sand tailings. Restor Ecol 13:667–677

Quagraine EK, Peterson HG, Headley JV (2005) In situ bioremediation of naphthenic acids contaminated tailing pond waters in the Athabasca oil sands region-demonstrated field studies and plausible options: a review. J Environ Sci Heal A 40:685–722

Renault S, MacKinnon MD, Qualizza C (2003) Barley, a potential species for initial reclamation of saline composite tailings of oil sands. J Environ Qual 32:22–45

Renault S, Qualizza C, MacKinnon MD (2004) Suitability of altai wildrye (*Elymus angustus*) and slender wheatgrass (*Agropyron trachycaulum*) for initial reclamation of saline composite tailings of oil sands. Environ Pollut 128:339–349

Rhine JL, Smith DG (1988) The late Pleistocene Athabasca braid delta of northeastern Alberta, Canada: a paraglacial drainage system affected by aeolian sand supply. In: Nemec W, Steel RJ (eds) Fan Deltas: sedimentology and tectonic settings. Blackie and Son, Glasgow, pp 158–169

Schneider CL, Mei S, Grobe M, Haug K (2012) Beneath the oil sands: stratigraphy and structural features of the Devonian of northeast Alberta. Canadian Society of Petroleum Geologists, Geoconvention, p 4

Schneider CL, Grobe M (2013) Regional cross-sections of Devonian stratigraphy in northeastern Alberta (NTS 74D, E). Alberta Energy Regulator/Alberta Geological Survey Open File Report 2013-05, p 25

Smith DG, Fisher TG (1993) Glacial Lake Agassiz: the northwestern outlet and paleoflood. Geology 21:9–12

Suncor Energy Inc (2010a) 2011 Mine & tailings plan: Millennium, North Steepbank Extension, Lease 86/17. ERCB Annual Submission

Suncor Energy Inc (2010b) 2011 Mine & tailings plan: Millennium, North Steepbank Extension, Lease 86/17. ERCB Annual Submission

Syncrude Canada Ltd (2006) Syncrude 2006 closure and reclamation plan. Submitted by Syncrude Canada Ltd., Fort McMurray, Alberta to Alberta Environment

Westcott F, Watson L (2007) End Pit Lakes technical guidance document. Clearwater environmental consultants for CEMA end Pit Lakes subgroup, Project 2005-61

Part III

The Intrinsic Value of Our Geomorphological Heritage

Geomorphological Landscapes and Geoconservation

29

Olav Slaymaker, Norm Catto, and Dori J. Kovanen

Abstract

The intrinsic value of geomorphological landscapes is considered in the context of aesthetics, culture, socio-economics, and ecology as well as geoscience. Geoconservation has become more urgent as geodiversity, biodiversity, and cultural diversity have declined. The evolution of western Canada's parks and natural heritage sites is a story of alternating successes and failures to achieve geoconservation in the face of hostile economic and political visions. The recent emergence of tribal parks and geoparks is yet further evidence of the lively debate that continues. The common element in these debates is the increasing awareness of the intrinsic value of the geoheritage of which geomorphological landscapes are a central part.

Keywords

Geomorphological landscapes • Parks • Natural heritage sites • Geoheritage • Intrinsic value

29.1 Landscapes, Art, and Culture

Humanity has a connection with its natural surroundings often reflected in love of landscape (Goudie and Viles 2010). Feeling for landscape can be translated into art, poetry, spiritual and religious values, and other cultural affirmations of scenery and landforms (Goudie 2002). This may lead to enhanced sensitivity to the need for conservation of sites for future generations. This whole subject area can well be called cultural geomorphology (Gregory 2000). Managing, enhancing or conserving the landscape implies an understanding of the cultural context. For example, if we wish to improve the management of river systems, it is important to understand the cultural relationship that local people have with their rivers. Where land is of religious significance as among the First Nations of western Canada, forest management, power development projects, and oil and gas exploration must respect local wisdom.

Writers and artists as diverse as the orthodox English clergyman, Ronald Blythe (1922) and the controversial Austrian artist Gustav Klimt (1862–1918) have been inspired by landscape. Blythe (1986) writes "Britain is an old country and among its landscapes there is scarcely one that has not been hallowed over the centuries by poet or saint". He is a scholar with an artist's eye. Klimt's landscape paintings are representative of the Viennese Art Nouveau school. His Lake Attersee paintings from the late 1890s reveal "landscapes that are characterized by the same refinement of design and emphatic patterning as his figural pieces" (Koja 2006).

The Group of Seven (1920–1933) is best known for paintings inspired by the Canadian landscape, and initiated the first major Canadian national art movement. Emily Carr (1871–1945) was associated with the group from 1927 onwards. She

O. Slaymaker (✉) · D.J. Kovanen
Department of Geography, University of British Columbia, 1984 West Mall, Vancouver, BC V6T 1Z2, Canada
e-mail: olav.slaymaker@ubc.ca

D.J. Kovanen
e-mail: djkovanen@comcast.net

N. Catto
Department of Geography, Memorial University of Newfoundland, St. John's, NL A1B 3X9, Canada
e-mail: ncatto@mun.ca

© Springer International Publishing Switzerland 2017

O. Slaymaker (ed.), *Landscapes and Landforms of Western Canada*, World Geomorphological Landscapes, DOI: 10.1007/978-3-319-44595-3_29

was an iconic Canadian artist, initially directly inspired by the First Nations of the Pacific Northwest. As her artistry evolved, she moved from aboriginal themes to west coast forest landscapes in particular. Some of her most profound work interprets the partially logged temperate rain forest landscape, which simultaneously evokes the mysterious work of the Creator and the destructive impact of "progress". The human-modified landscapes painted by Emily Carr are echoed to the east in Tom Thomson's paintings of Algonquin Provincial Park, which was logged intensively prior to Thomson's work during the period 1830–1890. Jack pines, the symbol of the area as painted by Thomson, were an insignificant component of the forest prior to the removal of more commercially desirable species. Pre-industrial modifications of Canadian landscapes have been significant locally. Modification of terrain by First Nations people did occur prior to 1500 AD, particularly from impacts of burning (Ryan et al. 2013). Traditional use since 1500 has resulted in significant changes in beaches and coastal terrain (e.g. Catto and Catto 2012).

The sense of place and human connectivity with landscape has led to the desire for conservation or preservation of terrain. Initially in western Canada in the later nineteenth century, the focus was on individual features (such as the hot springs at Banff and Radium), often those of immediate interest for tourism promotion. Parks were established along railway lines with tourism in mind, rather than for the preservation of characteristic landscapes. The pattern set with Banff (1885) and Jasper (1907) national parks was replicated with later parks established along transportation routes elsewhere in Canada [e.g. Algonquin Provincial Park (1893) and Terra Nova National Park (1957)]. It has only been relatively recently in Canada that national (and to a lesser extent, provincial) parks have been established with conservational or preservational objectives as the sole or absolutely dominant criterion. Establishment of national parks since 1970 in northern Canada (e.g. Nahanni, Vuntut, and Aulavik) has considered biodiversity and geodiversity as dominant factors, as is also the case for newer parks in more southern areas (e.g. Grasslands, Gros Morne).

Landscapes are a finite resource that have their own intrinsic value, independent of their role as providers of services. Geodiversity is therefore worthy of protection, and there are ethical reasons for wishing to preserve land with its accompanying geodiversity and outstanding natural beauty for the benefit of future generations. Understanding of the science of geomorphology or "landscape science" provides appropriate time and space scales for the analysis of landscape stability. Any attempt to assess the sustainability of landscape requires careful attention to the sensitivity and vulnerability of that landscape to environmental change.

29.2 Geodiversity

Geodiversity is a term that attempts to describe the geoscientific basis for understanding the immense variety of geomorphological landscapes. Geodiversity can be defined as the natural diversity of landscapes, landforms, soils, rocks, and minerals. It includes their assemblages, relations, interpretations, and systems (Gray 2004).

The Geological Survey of Canada (Berger and Iams 1996) developed the geoindicator index in response to the challenge of finding a metric to express environmental change quantitatively. As defined by the International Union of Geosciences, geoindicators are "measures (magnitudes, frequencies, rates, trends) of geological processes and phenomena, occurring at or near the Earth's surface and subject to changes that are significant for understanding environmental change over periods of 100 years or less". Identification of geoindicators in particular environments (such as individual national parks) thus stresses short-term geomorphic processes. Geodiversity takes its lead from the idea of biodiversity which emphasizes the importance of diversity over uniqueness (Thomas 2011). An emphasis on uniqueness, such as that favoured by, for example, Ollier (2012) has been a major obstacle to establishing parks in areas such as the Canadian Prairies and Boreal Forest, where the terrains "all look the same", without geomorphic features perceived by policy makers and the general public as conspicuous and unique.

Geodiversity was initially intended to be the geological (or geomorphological) equivalent of biodiversity, with the acknowledgement that biological activity is influenced by soils, terrain, and topographic influences on climate (Gray 2005). Terrain cannot be separated from local climate, vegetation, soil development, agriculture, settlement, transportation, or any form of life on Earth. Indeed, over evolutionary timescales, biodiversity, and cultural diversity have become possible only because of the existence of geodiversity.

The term "geoheritage" is said by some to broaden the scope of "geodiversity" to include human use and perceptions of the landscape (Dixon 1996; Calder and Badman 2009; Bruno et al. 2014). Essentially, whereas geodiversity implies cataloguing and assessing geomorphology from a scientific viewpoint, a geoheritage view treats landscapes as environments perceived by people, linking humans to geomorphology. Indeed, the international journal "Geoheritage" embraces among its central themes identification of geoheritage, geodiversity in nature conservation and land-use policies, geoparks, conservation, and geotourism.

29.3 Geoconservation

"Geoconservation" refers to procedures or active management that might be used to maintain the qualities of a particular geoheritage site (Sharples 2002; Brocx and Semeniuk 2007). Here, we distinguish between "conservation"—allowing a site to evolve with only the intervention necessary, and "preservation"—taking measures to attempt to halt change, in the belief that the site's unique qualities will be destroyed if change is permitted to occur. Generally, although geoconservation is our preferred path, irreversible geological processes in sites deemed more vulnerable and sensitive to external pressures may require a preservation approach (Vasiljevic et al. 2010).

Over the past five decades, the balance of emphasis has shifted towards biological systems and away from physical and cultural systems (Bruschi and Cendrero 2005). Nevertheless, in any assessment of the importance of land and landscapes, it is vital that the values enshrined in geosystems, ecosystems, and cultures be preserved. We maintain that cultures, ecosystems, and geosystems are intimately interconnected and that, unless demonstrated to be dysfunctional, should all be conserved '(Kareiva et al. 2007)'.

29.3.1 The Intrinsic Value of Landscape

Our ability to pass on a legacy of wild places is challenged by the extent to which human activities are altering the planet (Burek and Prosser 2008). Viable wilderness areas of more than 500 km^2 no longer exist in most of southern Canada. Wood Buffalo,at nearly 45,000 sq.km., is western Canada's largest national park (Fig. 29.1). The expansion of logging operations and pulp mills outside the park and the construction of an upstream dam on the Peace River threaten this World Heritage Site.

The significance of landforms and surface processes for biological and ecological processes is that they underpin these processes, contribute to the high degree of endemism, and explain the mosaic of habitats and specific environmental adaptations in the living world. Individual landforms and landscapes provide information about the evolution of the Earth surface in different time spans, from the most recent Quaternary (active volcanoes) to the Precambrian. Hence, landforms may play a role somewhat analogous to the one played by key geological exposures—stratotypes (type sections)—and complement the geological record written in rocks and structures. In sum, the more complete the story told, the better understood the origin of a landform complex, and the more accurately it is dated, the more significant such a landform complex becomes. Another aspect of significance is related to the role of a type locality played by a landform/landscape. Certain geomorphic localities are sites of "milestone" discoveries in the history of Earth science. Landforms offer valuable insights into the power of certain land-forming processes and may prove to be significant for establishing the magnitude and frequency of operation of those processes.

Badman (2010) referred to the framework of "Thirteen Earth Science themes" (Dingwall et al. 2005) which provides guidance to IUCN in assessing nominations. He concluded that there is a need for better integration of geodiversity and biodiversity, a suggestion which parallels recent conceptual developments in the science of geomorphology (Goudie and Viles 2010).

29.3.2 The Cultural and Aesthetic Value of Landscape

There are aesthetic reasons for valuing landscape. Areas of outstanding natural beauty are recognized as part of our World Heritage (UNESCO 1972). Social and cultural views of particular landforms within landscapes also vary widely. Volcanoes are personified in many areas of the world (e.g. "Fuji-san"), with several examples of volcanic goddesses and gods (e.g. Mefitis (Roman); Pele (Hawai'ian); Surtur (Norse)). Cultures which tend to personify volcanoes, using terms such as "awaken" or "grumble", often do not extend the same treatment to other natural hazards or landforms (e.g. Pasquarè and Pozetti 2007). The frequent personification of rivers and individual mountains (such as the "Sleeping Giant" near Thunder Bay) in Canada indicates the connections felt by people for geomorphology. Although not necessarily significant on their own, landforms nevertheless are the background of many cultural landscapes or inseparable components of sites of special cultural, religious, or historical significance. These linkages are epitomized in the concept of a sacred mountain. The wider cultural significance includes history, architecture, general landscape aesthetics, art, and religion, and is embedded in the concept of geoheritage.

29.3.3 The Economic and Functional Value of Landscape

Banff National Park has become a symbol of Canada, providing Parks Canada with an instantly recognizable, well-defined image. This popularity has a significant price, however: "The Banff townsite is more an icon to commercialization than a shrine to the birthplace of Canada's national parks" (McNamee and Kraulis 1994). The 3.2 million plus paying visitors who swarm through Banff annually have a large impact on the natural environment. Development pressures are strong within the park, especially for winter skiing facilities, hotels, summer campgrounds,

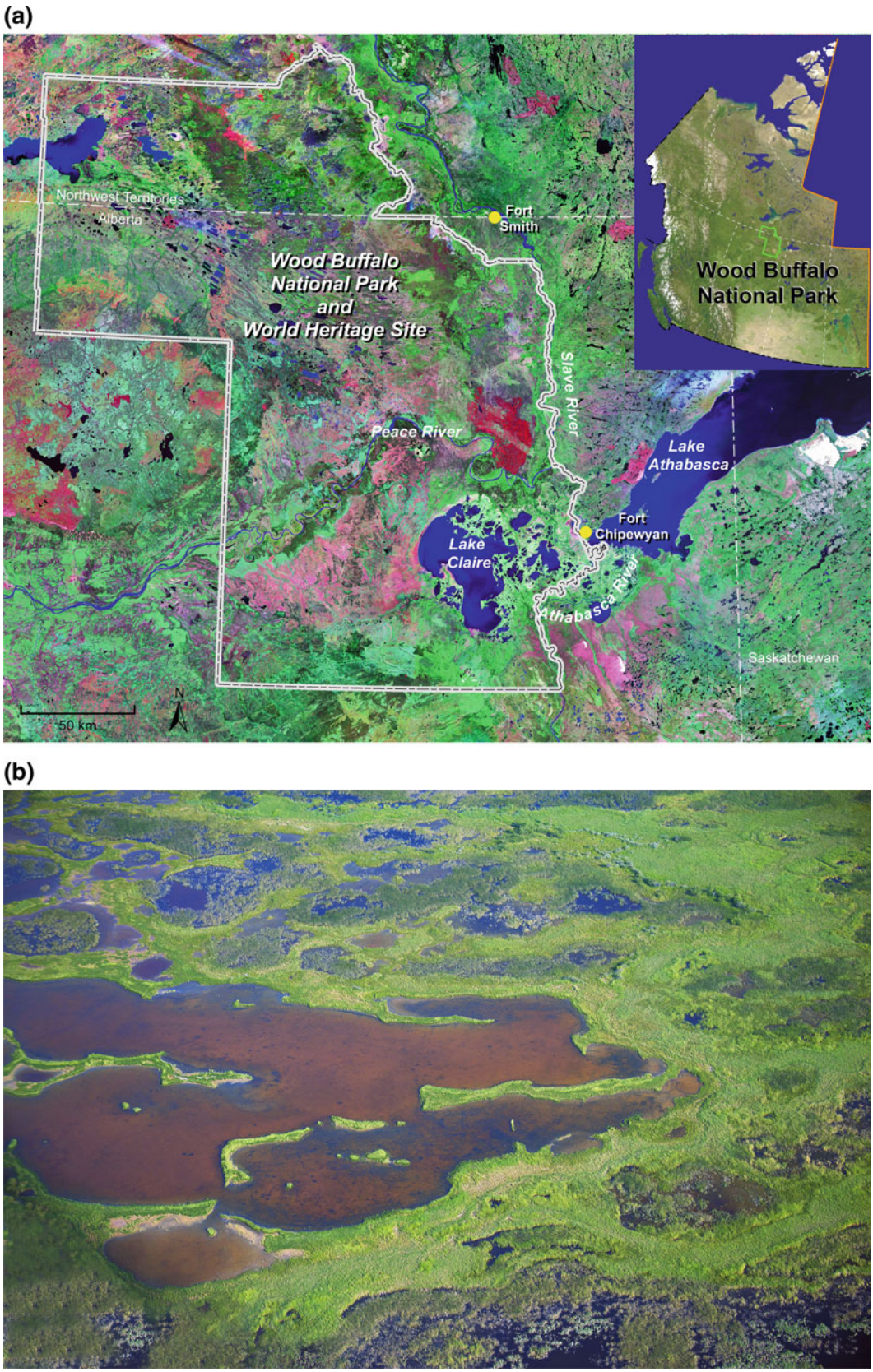

Fig. 29.1 **a** Wood Buffalo National Park and World Heritage Site is Canada's largest national park (44,802 km^2). It contains the world's largest freshwater inland river deltas, the Peace-Athabasca Delta and sustains the world's largest herd of wood bison. *Source* MDA Federal (2004). **b** Wood Buffalo National Park is the most ecologically complete and largest example of the Great Plains-Boreal grassland ecosystem. ©Ko Hon Chiu Vincent/*source*: UNESCO World Heritage Centre. The *inset* image is extracted from NASA, Visible Earth (Stöckli et al. 2005)

and tourist amenities. In addition, the park's position straddling the major transportation artery from Calgary to Vancouver results in large amounts of through traffic. Traffic volumes, with over 9 million people per year, have grown to the point where the Trans-Canada Highway through the park must be converted to a four-lane expressway. Prior to the construction of overpasses (6) and underpasses (38) for animals, significant (and ever-growing) numbers of wildlife–vehicle collisions occurred during the summer months. In the twenty-first century, there are 9 million visitors to the western Canadian National Parks each year; 36 million visit the top 10 National Parks in the USA each year. The twin mandate of use and protect that many feel to be irreconcilable objectives has been present from the beginning.

29.4 The Evolution of Western Canada's National Parks

29.4.1 The Beginning: 1885–1910

The first national parks in western Canada were established in the 1880s, and their distribution as of 2015 is illustrated in Fig. 29.2 More than 14,000 km^2 of relatively undisturbed land is being protected from resource exploitation for the benefit of future generations. This represents about 3 % of western Canada's land area.

Shortly after the establishment of Banff, Glacier, and Yoho national parks, the discovery of mineral hot springs in the Bow Valley formed the basis for the first Rocky Mountain Park Act (1887). Banff Park was created as a public park or pleasure ground for the benefit and enjoyment of the people. Logging, mining, grazing, and hunting were also permitted. The first parks were created to be islands of civilization in a sea of wilderness. Waterton Lakes and Jasper national parks followed, but Jasper National Park has succeeded in remaining more pristine than the other four parks, as illustrated in Figs. 29.3 and 29.4.

29.4.2 Expansion to the Prairies: 1911–1929

The Dominion Parks Branch (now called Parks Canada) was created in 1911 as the first national parks service in the world, predating the US National Parks Service by 2 years. The first commissioner of the Dominion Parks Branch (JB Harkin) combined a mystical reverence for wilderness with a pragmatic view of its economic value. He wrote that national parks were created so that, "every Canadian citizen may satisfy his soul craving for nature". In 1911, there were five mountain national parks in western Canada, by the time Harkin's career came to an end Elk Island, Mount Revelstoke, Kootenay, Wood Buffalo, Prince Albert, and Riding Mountain had been added to the national parks inventory. More significantly, the first national parks in Saskatchewan (Prince Albert), Manitoba (Riding Mountain), and the North-west Territories (Wood Buffalo) had come into being.

29.4.3 Stagnation: 1930–1969

The signal achievement of Harkin was Parliament's passing of the National Parks Act in 1930. The Act prohibited logging, mining, oil and gas exploration, and recreational hunting inside park boundaries. However, no organization of a public constituency to watch over the parks was created in Canada, in contrast to the USA (under the influence of Franklin D. Roosevelt). A process of erosion of Canada's national parks commenced in 1930 when the boundary of Rocky Mountain National Park was amended to allow damming of the Kananaskis and Spray valleys. In 1947, the size of Waterton Lakes and Prince Albert parks was reduced and logging was permitted in Wood Buffalo Park. During the 1930–1970 period, there was stagnation and no new parks were created in western Canada. In the late 1930s, the area of the former "Buffalo National Park", established at Wainwright (Alberta), was requisitioned for tank manoeuvres. The Plains bison were evacuated to several locations, including Wood Buffalo, and the area is now Canadian Forces Base (CFB) Wainwright. Similarly, Wawaskesy National Park, northeast of Medicine Hat, was requisitioned for military purposes in 1941 as CFB Suffield. The former Menissawok National Park (Saskatchewan) and Nemiskam National Park (southern Alberta) were delisted in 1947, and the land returned to private use. "The Canadian public's sensitivity to and enthusiasm for wilderness lags at least two generations behind opinion in the United States" (Nash 1968). In 1963, the National and Provincial Parks Association of Canada (NPPAC) was formed, and this marked the beginning of a new environmental consciousness in Canada that bore fruit in subsequent decades.

29.4.4 Renewal: 1970–1984

After 40 years of inactivity, Jean Chretien set in motion a process of expansion which included the Pacific Rim Reserve, Grasslands, Kluane, Nahanni Reserve, and Ivvavik.

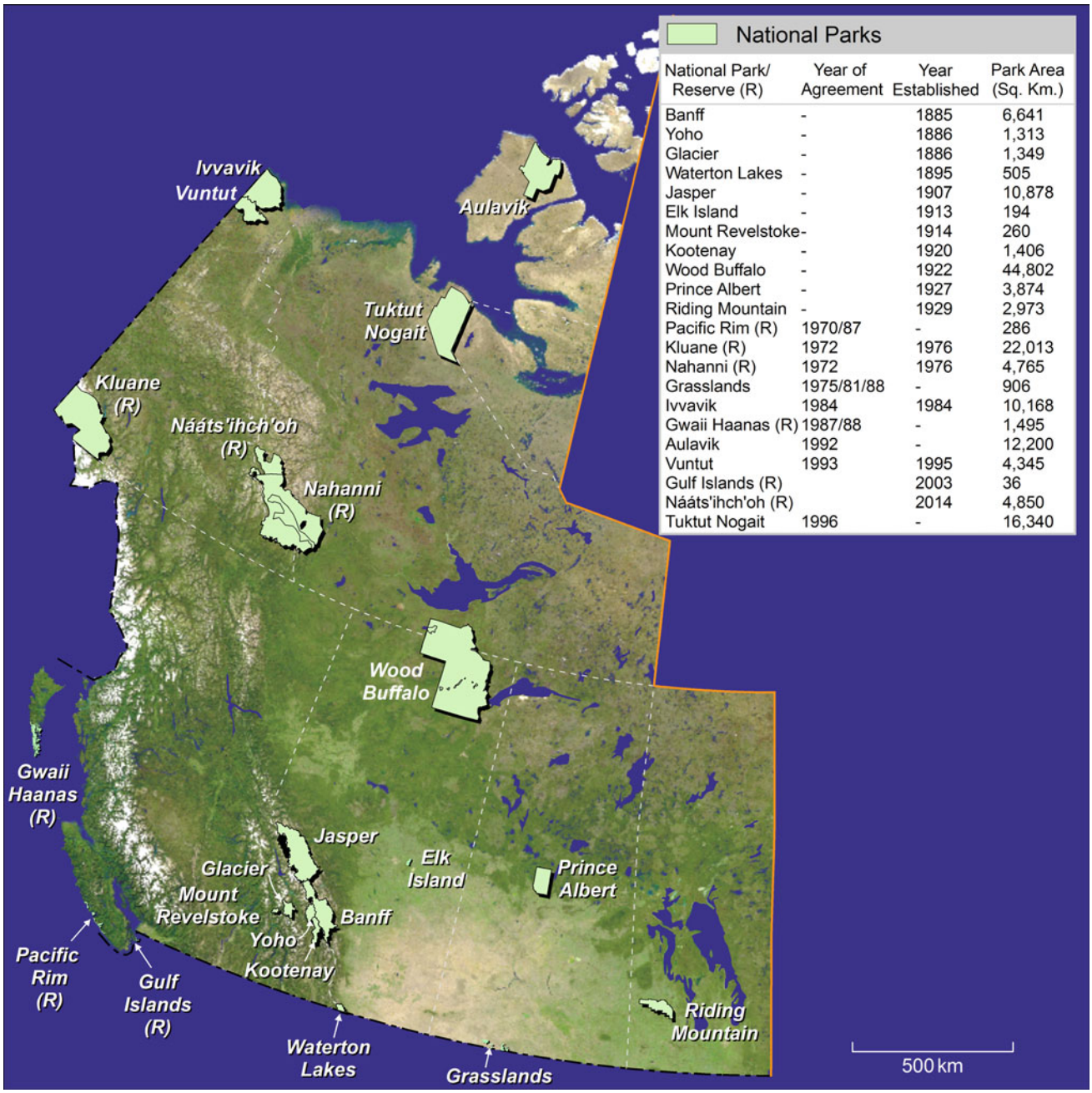

Fig. 29.2 Distribution of National Parks in western Canada. *Source* background image; NASA, Visible Earth. National Park boundaries; IUCN and UNEP-WCMC (2015), available at: www.protectedplanet.net

Chretien vowed "that there will never be mineral development in the spectacular landscape of Kluane National Park, just as Virginia Falls on the South Nahanni river will never be the site of a hydroelectric development" project.

Grasslands National Park, for example, is an area of mixed grass prairie on the Montana/Saskatchewan border that has been left relatively undisturbed. The rolling terrain covered with long and short varieties of grasses includes deep wooded coulees in the north, extensive grasslands to the south, and badlands in the east (Fig. 29.5). This was a prime buffalo hunting area for the migrant tribes, ancestors of the Assiniboine, the Cree and the Blackfoot. In 1870, the

Fig. 29.3 Maligne Lake, Jasper National Park, Alberta. Reproduced with the permission of Natural Resources Canada, 2015 (*photograph* NRCan 2002-582 by Réjean Couture, Gianluca Bianchi Fasani). See Fig. 29.2 for location

newly formed Canadian government began to promise free land to European settlers. The effect of European settlers on the ecology was drastic for two reasons. The wholesale slaughter of wildlife and the wide-scale ploughing under the grassland to satisfy the Dominion Lands Act which stipulated 10 acres be cultivated annually, in time, destroyed habitats, disrupted interdependent ecosystems, and led to the extinction of entire species.

Kluane National Park, by contrast with the highly disturbed Prairie grasslands, contains areas of pristine wilderness that surely qualify as superlative on any criterion (Fig. 29.6). Mountains and glaciers are the essence of the park taking up 82 % of the surface area. Mount Logan is Canada's highest point (5959 masl) with Mount Steele, Mount St. Elias, and Mount Lucania all above 5000 m. Together with the boundary ranges of the Coast Mountains, the Icefield Ranges contain a network of over 2000 valley glaciers. Steep slopes, cliffs, and rapid mass wasting characterize those parts of the landscape that are not covered by ice.

29.4.5 Continued Stuttering Growth: 1985–Present

1985 was the centennial of Canada's national park system, but the newly elected Conservative government provided no resources for its celebration. However, they did achieve a huge environmental victory in the creation of Gwaii Haanas Reserve. Subsequently, expansion has been slow and 27 years have produced only 6 new national parks in

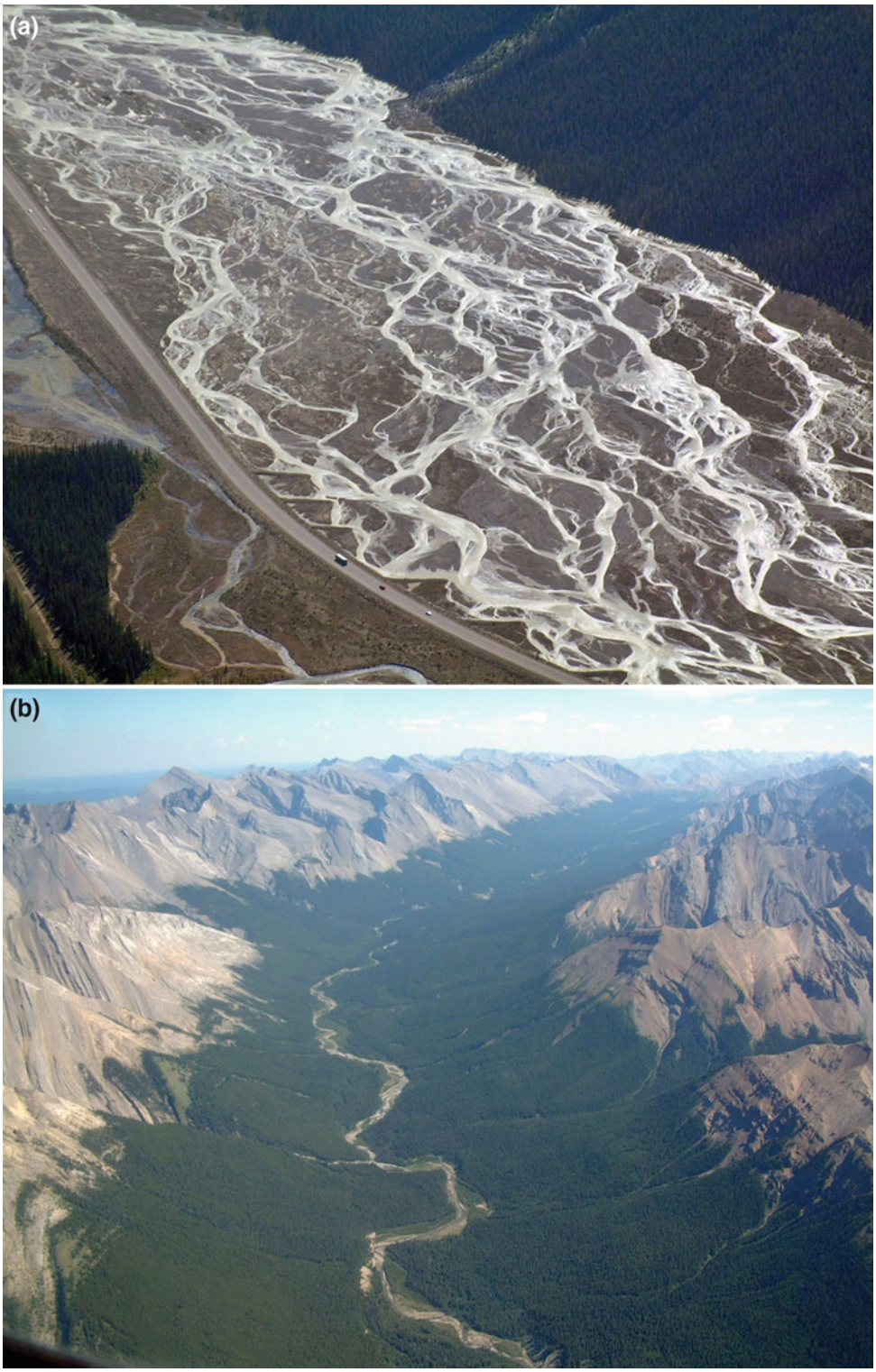

Fig. 29.4 **a** *Upstream* complexly braided channel of Sunwapta River forming a sandur along the Ice Fields Parkway, southern part of Jasper National Park, Alberta. **b** *Downstream* meandering Rocky River, Jasper National Park, Alberta. Reproduced with the permission of Natural Resources Canada, 2015 (*photographs* NRCan 2002-597 by Réjean Couture, Gianluca Bianchi Fasani, and NRCan 2002-596 by Réjean Couture). See Fig. 29.2 for location

western Canada: Aulavik on Banks Island; Vuntut in Yukon; Tuktut Nogait in Northwest Territories; Gulf Islands Reserve in British Columbia; and Nááts'ihch'oh Reserve in Northwest Territories.

Gulf Islands National Park Reserve is scattered over 15 islands and numerous islets and reefs in the southern Strait of Georgia (Fig. 29.7). The Gulf Islands themselves are an island chain between Nanaimo in the northwest and

Fig. 29.5 Frenchman River Valley, Grasslands National Park, Saskatchewan. **a** Photograph courtesy of D. J. Sauchyn. **b** *Source* Reproduced with the permission of Natural Resources Canada, 2015 (*photograph* NRCan 1999-042B by D. J. Sauchyn). See Fig. 29.2 for location

southeastwards to the international boundary. They display a strong northwest to southeast elongation, as do many of the promontories and bays. The Late Cretaceous Nanaimo group of sandstones, shales, and conglomerates are variably resistant and tilted mainly to the northeast giving rise to numerous cuestas. Where a sandstone or conglomerate is at the surface, the land tends to stand high and form cliffs along the shoreline and ridges inland. Softer beds, such as shale, form valleys and embayments. The islands support many plant and animal species at the northern limit of their range. On land, hillsides of Douglas fir forest, the distinctive red-barked arbutus trees, and meadows of the endangered Garry oak ecosystem speak to the diversity of island habitats.

29.5 Evolution of Provincial and Territorial Parks

The national park system is not alone in protecting Canada's landscapes. In the Canadian Federal system, provinces and territories have the authorization to establish parks. The quality of landscapes protected by the provinces and territories is no less impressive than that overseen by the national parks. The major difference is the level of protection that is guaranteed by the provinces and territories vis-à-vis the federal government. The eastern provinces of Ontario and Québec were the first to exercise this right. Beginning in 1911 with Strathcona Provincial Park, British Columbia has established large parks at Mt. Assiniboine (1922),

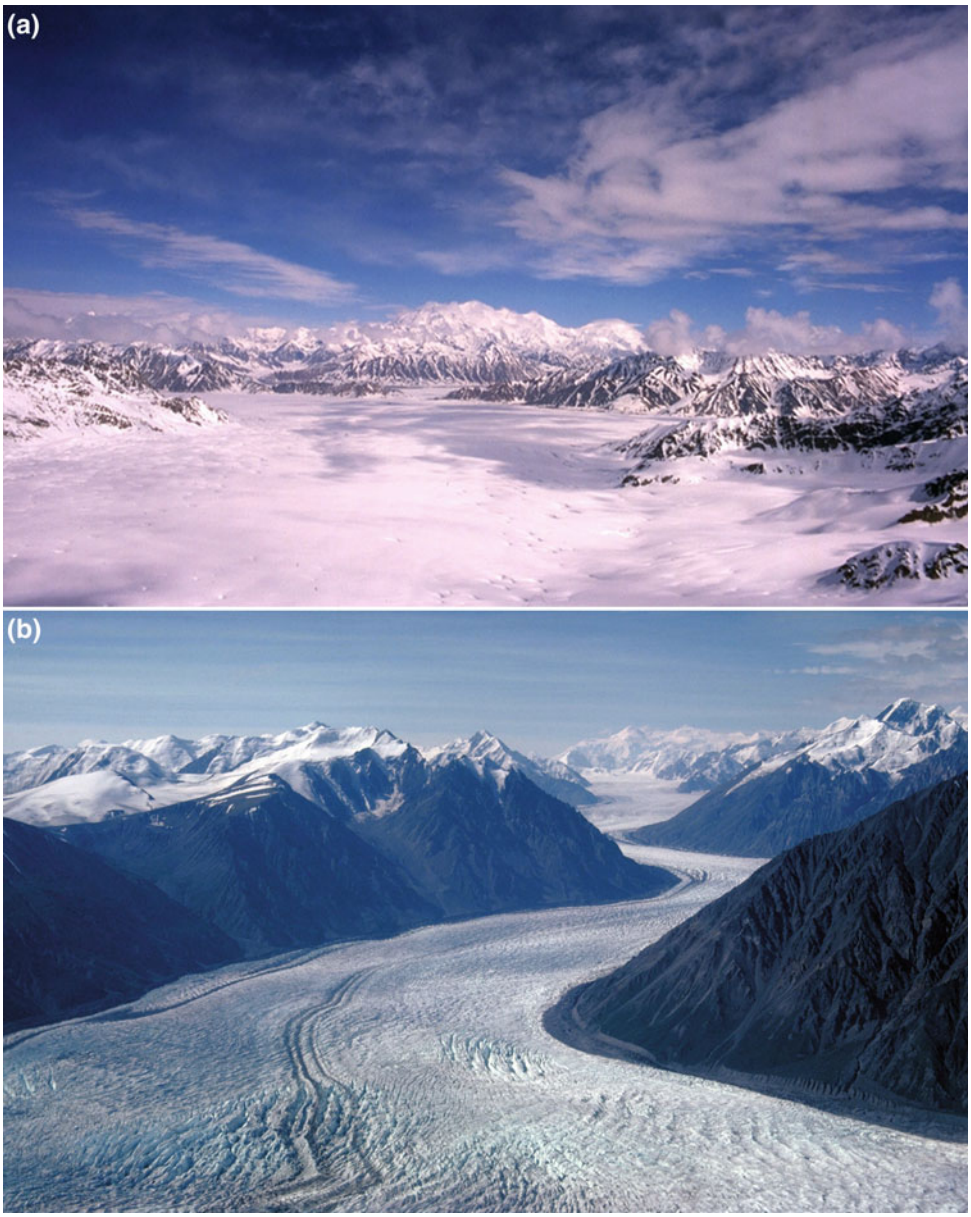

Fig. 29.6 **a** Mountain landscape, Icefield Ranges, Kluane National Park and Reserve, Yukon. Mount Logan (5959 masl) the highest mountain in Canada at centre back. **b** Meandering valley glacier, St. Elias Mountains, Kluane National Park, Yukon. Reproduced with the permission of Natural Resources Canada, 2015 (*photographs* NRCan 2001-049E by Christian Zdanowicz and NRCan 2002-677 by R. Bélanger). See Fig. 29.2 for location

Tweedsmuir South (1938), Wells Gray (1939), Mount Edziza (1972), Tatshenshini-Alsek (1993), Itcha-Ilgachuz (1995), Height of Rockies (1995), Northern Rocky Mountains (1999), and Foch-Gilttoyees (2004).

Mt. Assiniboine Provincial Park (Fig. 29.8), for example, is a magnificent place of lakes, glaciers, peaks, and alpine meadows in British Columbia's Rocky Mountains. World renowned Mount Assiniboine, at an elevation of 3618 masl, is situated along the continental divide near the south-east corner of the park and has defined mountain splendour in the Canadian Rockies for over 100 years. The peak is often compared favourably with the Matterhorn in the Swiss Alps. There are no roads in this unspoiled wilderness, with trails providing the only land access.

Mt. Edziza Provincial Park encloses a large volcanic complex (described in Chapters 1 and 2) that includes four central volcanoes: Mt. Edziza, Ice Peak, Armadillo Peak, and the Spectrum Range (Fig. 29.9). At the southern end of the Mount Edziza volcanic complex, volcanism constructed the Spectrum Range 3–2.5 Ma ago. Named for its extensive colouration, this nearly circular lava dome is up to 650 m thick and more than 10 km wide. Since its formation, the

Fig. 29.7 Saturna and Tumbo islands are two of the 15 islands represented in the Gulf Islands Reserve, British Columbia. *Source* ©Parks Canada (available at parkscanada.gc.ca.). See Fig. 29.2 for location

Spectrum Range lava dome has been deeply cut by erosion, forming an extensive valley system. This park is equally unspoiled wilderness.

Northern Rocky Mountains Provincial Park contains spectacularly exposed geological structures, including huge folds, thrust faults, castellated peaks, glacially sculpted valleys, cirques, and hanging valleys. In comparison with the southern Rockies, the Muskwa Ranges show evidence of more complex tectonic deformation. The escarpments and chevron folds in Sleeping Chief Mountain, Mt. Sylvia, and Mt. Mary Henry are notable. Hoodoos at Wokkpash Gorge are up to 90 m high and flank the sides of the valley over a distance of 5 km above Wokkpash Lake (Fig. 29.10a) Although few measurements of rates of mass movement have been taken in this park, observations of fresh landslides and active alluvial and colluvial fans are strongly indicative of rapid and currently active processes (Fig. 29.10b, c). At elevations exceeding 2400 masl, glaciers and perennial ice patches are common though threatened by recent warming trends (Clarke et al. 2015). The Lloyd George ice field is the largest. The park lies within the Northern Boreal Mountains Ecoprovince.

Large provincial parks in Alberta include Dinosaur (1955; a UNESCO World Heritage Site); Cypress Hills (1951; joined to Saskatchewan's in 1989); Peter Lougheed (Kananaskis 1977); and Spray Valley (2000). In addition, Alberta has designated wilderness areas and wildland provincial parks, both of which have more restrictions on usage than the provincial parks. Saskatchewan's large provincial parks, all in the north, include Steele Narrows, Clearwater River, Lac La Ronge, and Athabasca Sand Dunes. Manitoba's large provincial parks include Caribou River, Sand Lakes, Numaykoos Lake, Grass River, Duck Mountain, Whiteshell, Atikaki, and Nopiming. Yukon has territorial parks at Qikiqtaruk (Herschel Island; see Chap. 24) in the Beaufort Sea, Ni'inlii Njik along the Fishing Branch River, and Tombstone along the Dempster Highway, along with others in the process of being established as of September 2015. Northwest

Fig. 29.8 Mt. Assiniboine Provincial Park, British Columbia. Photograph by Adam Gibbs

Territories have several small parks focused on specific landform features, primarily waterfalls and lakes. At Tuktoyaktuk, eight of the largest pingos, including Ibyuk (49 m high, 300 m diameter), are protected in the federally designated "Pingo Canadian Landmark", administered by Parks Canada. Ibyuk has been used by the Inuvialuit residents of the Tuktoyaktuk area as a lookout for migrating caribou and marine life, and as an aid to navigation, and thus is a geoheritage site.

Height of the Rockies Provincial Park (542 km^2) plays an important role in contributing to the ecological integrity and viability of the large block of national and provincial parks extending along the spine of the Rocky Mountains. There are numerous small lakes and outstanding natural features from the lower elevations, such as the Palliser River valley at 1300 masl, to Mount Joffre at 3449 masl. The park is an alpine environment with forested bottomland including the Palliser River valley, the Middle Fork of the White River, the Limestone Lakes plateau (Fig. 29.11), Conner Lakes, and the Royal Group of mountains. It encompasses 26 peaks over 3000 masl and has internationally significant biodiversity values.

29.6 World Cultural and Natural Heritage Site Selection

The Convention Concerning the Protection of the World Cultural and Natural Heritage was adopted by the UNESCO General Conference in 1972. Canada ratified the Convention in 1976, and Parks Canada was designated as the lead agency for implementation of the convention in Canada. The Convention is overseen by the World Heritage Committee, composed of 21 countries elected by the States Parties. The 1992 UN Convention on Biological Diversity (CBD) also contributes to the worldwide system of protected areas.

The World Heritage Convention (1972) set up 10 criteria for World Heritage Site selection, whether cultural, natural,

Fig. 29.9 Mt. Edziza Provincial Park (Spectrum Range), British Columbia. Photograph by Adam Gibbs

or "mixed". In order to qualify as a "natural" world heritage site, one or more of the following criteria must be satisfied:

(vii) Superlative natural phenomena or areas of exceptional natural beauty and aesthetic importance.
(viii) Outstanding examples of major stages of Earth history including significant geomorphic or physiographic features.
(ix) Outstanding examples of ongoing ecological and biological processes.
(x) Most significant natural habitats for in situ conservation of biological diversity, including threatened species of outstanding universal value (Table 29.1).

In Chap. 15 of this volume, Ford provides valuable insights into the process of moving from the status of a Nahanni National Park Reserve to South Nahanni World Heritage Site as he, in his role as expert karst geomorphologist, was one of the prime movers for the establishment of UNESCO World Heritage Sites. In Chap. 14, he also describes his continuing efforts to establish a new World Heritage Site in the Mackenzie Mountains, Northwest Territories. Canadian geomorphology has achieved global prominence through Ford's lifelong commitment to the cause of geoconservation (Fig. 29.12).

29.6.1 Dinosaur Provincial Park and World Heritage Site

Dinosaur Provincial Park and World Heritage Site is situated in the valley of the Red Deer River, which is noted for its striking badland topography (Fig. 29.13a). The park was established as a UNESCO World Heritage Site on 26 October 1979 both for its nationally significant badlands (Fig. 29.13b, c) and riverside riparian habitats, and for the international importance of the fossils found here. The park is well known for being one of the richest dinosaur fossil locales in the world. The fossil assemblage of nearly 500 species of life, from microscopic fern spores to large carnivorous dinosaurs, justified its becoming a World Heritage Site in 1979.

Fig. 29.10 Muskwa Ranges in the Northern Rocky Mountains Provincial Park and Protected Area, British Columbia **a** Wokkpash Lake. **b** Paternoster lakes northwest of Devereux Peak. **c** Mass movement processes and limestone structure southeast of Wokkpash Lake. Photographs by Gary Fiegehen

Fig. 29.11 Limestone Lakes plateau, Height of Rockies Provincial Park, British Columbia. Photograph by Russ Heinl, BC, Canada

The sediments exposed in the badlands at Dinosaur Provincial Park were laid down over a period of about 2.8 million years during the Late Cretaceous and belong to three different geologic formations. The terrestrial Oldman Formation is overlain by a complete section of the terrestrial Dinosaur Park Formation, which is in turn overlain by the base of the marine Bearpaw Formation. The Dinosaur Park Formation, which contains most of the articulated dinosaur skeletons, was laid down between about 76.5 and 74.8 Ma ago. It was deposited in floodplain and coastal plain environments by river systems that flowed eastward and southeastward to the Western Interior Seaway.

29.6.2 The Burgess Shale Fossil Site

The Burgess shale fossil site is located in Yoho National Park which is also a part of the Canadian Rocky Mountains World Heritage Site (Fig. 29.14a). From Emerald Lake in Yoho Park, the site of the world's most prolific middle Cambrian soft-bodied fossils can be seen. This moment in evolutionary history, known as the Cambrian explosion of life, refers to the sudden appearance in the fossil record of animals with mineralized skeletal remains possibly the most important evolutionary event in the history of the world. The beginning of the explosion is generally placed at 542 Ma ago, the same time the Ediacarans disappeared. The Burgess shale at 505 Ma old records the tail end of this explosion. The explosion is particularly remarkable because all major animal body plans appeared during this time, changing the biosphere forever. The Burgess shale site has been the object of research since 1909 when Walcott discovered it in the course of routine geological mapping in the region (Fig. 29.14b).

29.6.3 Peyto Lake

Peyto Lake is a glacier-fed lake located in Banff National Park and is also a part of the Canadian Rocky Mountains World Heritage Site. The lake itself is easily accessed from the Icefields Parkway. During the summer, significant

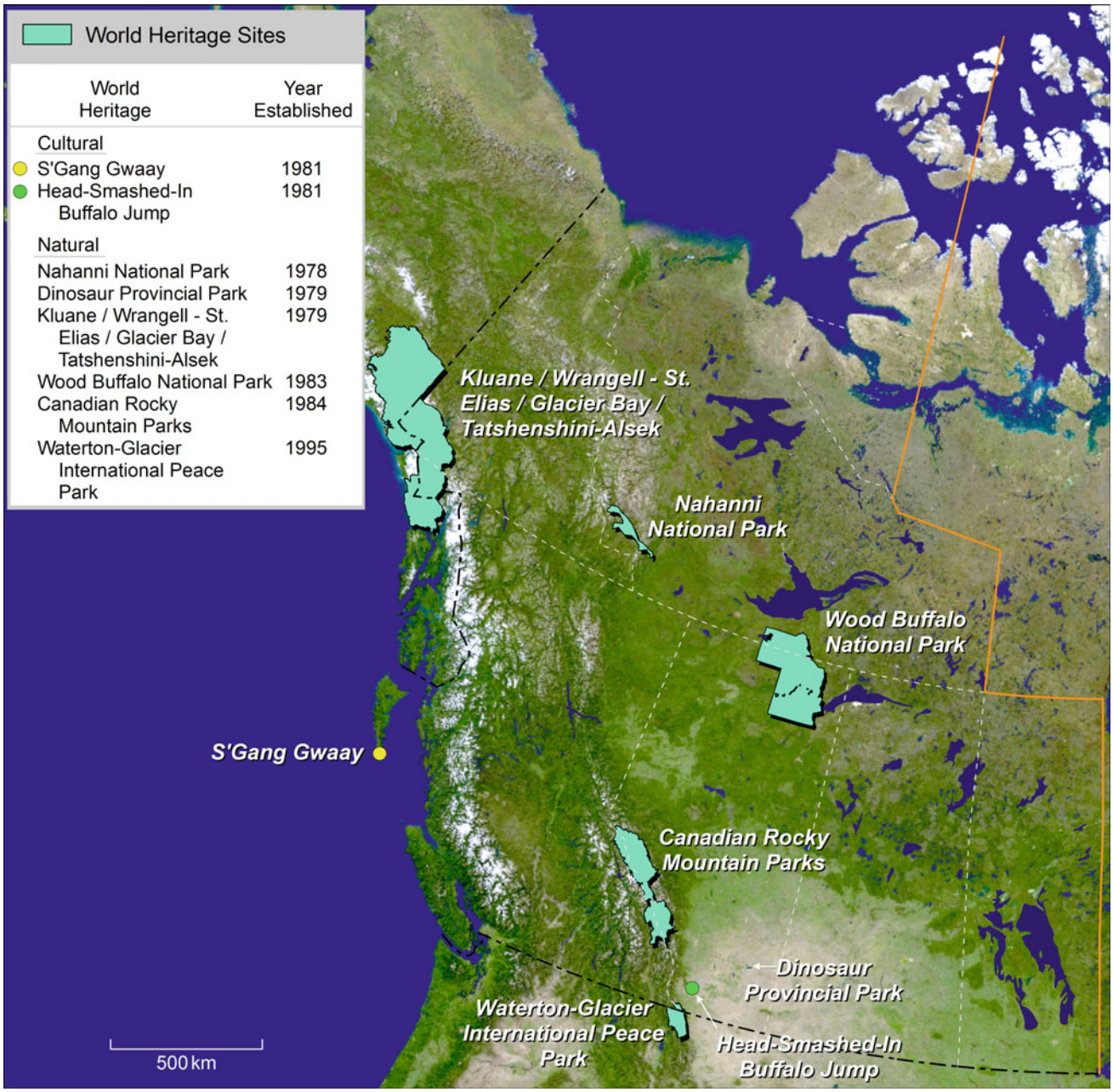

Fig. 29.12 Distribution of World Heritage Sites in western Canada. *Source* background image; NASA, Visible Earth. World Heritage Sites; IUCN and UNEP-WCMC (2015), available at: www.protectedplanet.net

amounts of glacial rock flour flow into the lake, and these suspended rock particles give the lake an unusually bright, turquoise colour. The lake is best seen from Bow Summit, the highest point on the Icefields Parkway (Fig. 29.15).

29.6.4 Head-Smashed-in Buffalo Jump

Head-Smashed-In Buffalo Jump is designated as an exclusively cultural World Heritage site, although its cultural significance is entirely dependent on its geomorphology. The eastern margin of the Porcupine Hills is marked by steep, terraced escarpments 10–60 m high. Prior to the arrival of the horse c. 1500 AD, these escarpments played a vital role in the culture of indigenous people. Bison herds were stampeded towards the cliffs, often by young men dressed in bison robes, along drive lanes marked by stones. The herd, once stampeded, would continue to run blindly over the escarpment. The majority of the people would camp below the cliff face, killing any wounded animals and butchering

Table 29.1 Criteria for the natural properties of World Heritage Site selection (UNESCO 2011a). Statements particularly relevant to geomorphology are emphasized in bold

No.	Criteria for natural properties
vii	To contain **superlative natural phenomena or areas of exceptional natural beauty** and aesthetic importance
viii	To be outstanding examples representing major stages of earth's history, including the record of life, **significant ongoing geological processes in the development of landforms, or significant geomorphic or physiographic features**
ix	To be outstanding examples representing significant ongoing ecological and biological processes in the evolution and development of terrestrial, freshwater, coastal and marine ecosystems, and communities of plants and animals
x	To contain the most important and significant natural habitats for in situ conservation of biological diversity, including those containing threatened species of outstanding universal value from the point of view of science or conservation

Fig. 29.13 Badlands topography carved in flat-lying Upper Cretaceous strata, Alberta. **a** Dinosaur Provincial Park and World Heritage Site. ©Ko Hon Chiu Vincent/*source* UNESCO World Heritage Centre. **b** Horseshoe Canyon. Photograph by D. Kovanen. **c** Hoodoo at Drumheller. Reproduced with the permission of Natural Resources Canada, 2015 (*photograph* NRCan-1819). See Fig. 29.12 for location

the casualties. Several of these bison jumps were routinely used between 7000 and 1000 years ago in southern and central Alberta. Head-Smashed-In, the largest of these jumps, is located 10 km northwest of Fort Macleod. The site, managed and operated by the Piegan (Blackfoot) First Nation, is a classic example of geoheritage.

29.6.5 Superlative Natural Phenomena

The wording of criterion vii states that properties to be inscribed on the World Heritage List have either to contain "superlative natural phenomena", or they need to be valued as of "exceptional natural beauty and aesthetic importance",

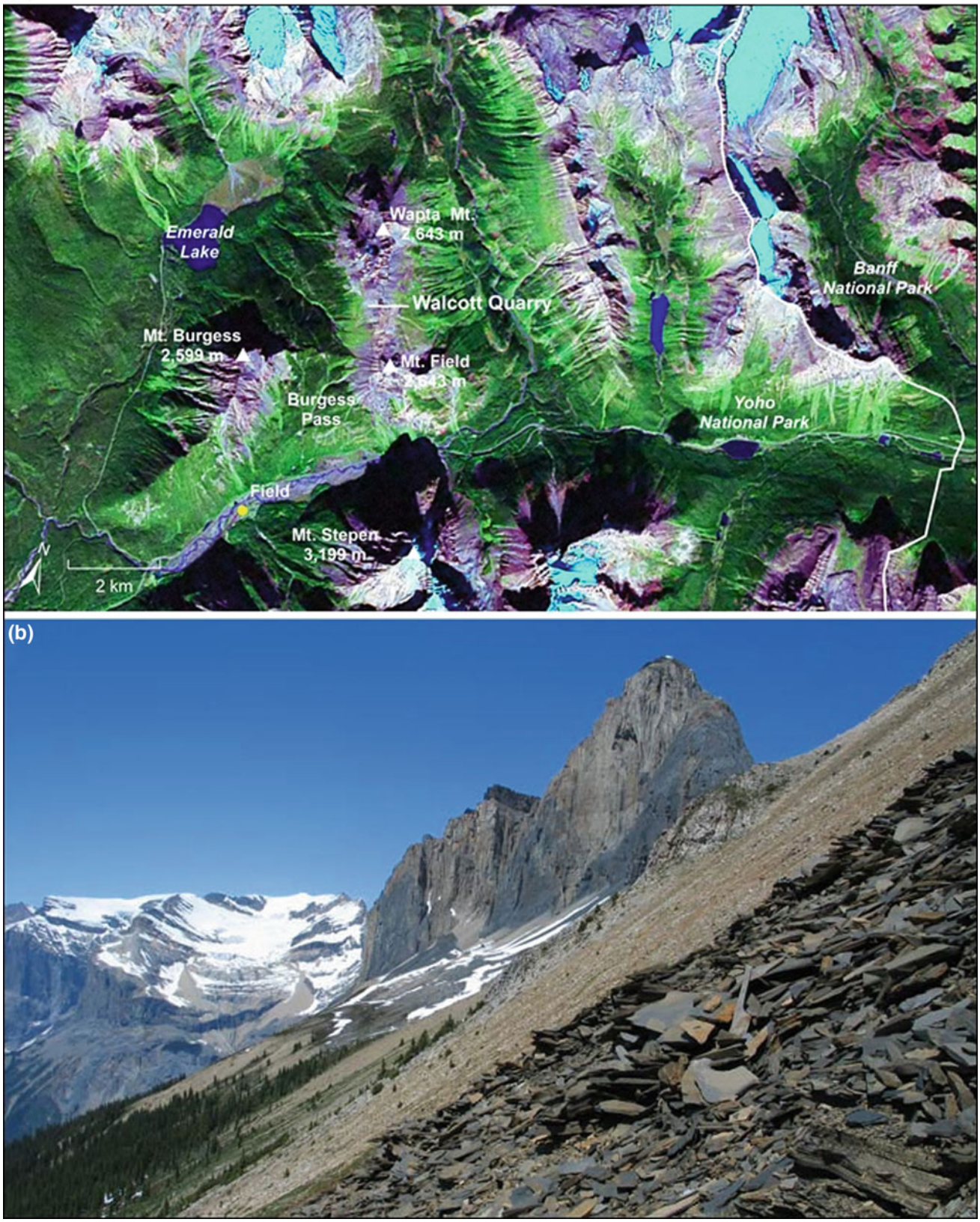
(a)
Emerald Lake
Wapta Mt.
2,643 m
Walcott Quarry
Banff National Park
Mt. Burgess
2,599 m
Mt. Field
Burgess Pass
Yoho National Park
Field
Mt. Stephen
3,199 m
N
2 km
(b)

◀ **Fig. 29.14** Canadian Rocky Mountain Parks, Alberta and British Columbia. **a** On a mountain ridge in Yoho National Park, British Columbia is one of the world's most celebrated fossil deposits: the Burgess Shale at the Walcott Quarry (2336 m). *Source*: background image; MDA Federal (2004). **b** The Burgess Shale (of the Stephen Formation) at Walcott's Quarry is in the lower right foreground. The prominent peak in the middle background is Mount Wapta. This consists of the Eldon Formation, which stratigraphically overlies the Burgess Shale. The beige areas on this mountain indicate areas of dolomitization. The snowy mountain in the background at the left is the Vice President and the Emerald Glacier. *Photograph* ©Parks Canada/John Niddrie. See Figs. 29.2 and 29.12 for location

Fig. 29.15 Peyto Lake in Banff National Park, Alberta. © Maureen J. Flynn/*source* UNESCO World Heritage Centre. See Figs. 29.2 and 29.12 for location

or possibly both. "Superlative" in this context means that the property has more of the particular quality than anything else of the same type and is the best among examples of similar kind. This sounds simple, but operationally it is considerably more complicated and opens the space for various interpretations (see Migoń 2014). Two main issues emerge here. First, which natural phenomena may be considered superlative? Second, how to objectively measure/assess whether they are superlative or not. Although the 2011 edition of *Preparing World Heritage Nominations* (UNESCO 2011b) indicates that "superlative natural phenomena can often be objectively measured and assessed (e.g. deepest canyon, highest mountain, largest cave system, highest waterfall)", this in reality is quite restrictive and applies to selected physical phenomena only rather than to landscapes as a whole. A recent review of World Heritage properties inscribed under criterion vii has revealed that attempts to provide an objective (i.e. measurable) judgement have been rare (Mitchell et al. 2013).

Many unique natural sites are still not admitted to the UNESCO World Heritage List. For example, the "true desert" environment of Osoyoos Lake in British Columbia is

the northernmost extension of the Great American Desert. The incomplete ground cover, unique flora, and fauna confirm the long-term hydroclimatic record of true desert conditions as defined by Köppen (Kottek et al. 2006). There are three variations in desert climate on Köppen's scheme, of which the mild desert climate (BWn) characterizes the immediate vicinity of Osoyoos. Less than 250 mm annual precipitation and mean annual temperature between 18 and 0 °C are the defining criteria.

The past practice in applying the World Heritage Convention shows that superlative natural phenomena were of two main kinds. First, is living nature, particularly ancient undisturbed forests, pristine grasslands, herds of freely roaming animals, and bird and fish sanctuaries. In this context, undisturbed and pristine generally imply "not significantly affected by large-scale or industrial human activity", although indigenous residents of western Canada have utilized and managed these geoheritage areas since their arrival. However, in recent years, this biotic component has been more thoroughly elaborated for properties nominated and inscribed under the criteria ix and x (see Table 29.1). The second common theme is the physical landscape. The examination of 56 inscriptions from the past two decades (1992–2012) indicates that natural phenomena referred to most often to support the nomination were spectacular physical landscapes (Williams 2008), mainly mountainous, active volcanic (Wood 2009), and coastal (Mitchell et al. 2013). These practices mirror those involved in the initial establishment of Canadian national parks.

Likewise, geomorphic processes themselves (as opposed to landforms) are rarely highlighted as a justification of World Heritage nomination or inscription. One of the likely reasons is that processes as such cannot be demonstrated in a way similar to static landforms that is viewed by an observer not trained in geomorphology (e.g. Bruno et al. 2014). This is either because they are episodic (e.g. mass movements), extremely slow (e.g. limestone dissolution), or microscopic (e.g. biogeochemical soil formation). Coastal cliffed heritage areas are not designated because they are undergoing coastal erosion, but because specific landforms such as arches and stacks are present. The implication is that such features will remain forever, unless they are threatened by a destructive process, such as coastal erosion (see Catto and Catto 2012). Usually, processes are inferred from landforms: the argument goes that if the resultant landforms are significant and outstanding, the forces responsible for them had to be significant and outstanding, and perhaps even unique.

The various measures of geodiversity (Gray 2004) are yet to be consistently applied. Intermediate and larger scale geomorphology remains relatively neglected, compared with local-scale studies. Complex regional and local geomorphological studies are not really encouraged. As an outcome, a vital part of each World Heritage nomination and evaluation, which is comparative analysis, is often missing. The International Association of Geomorphologists has spearheaded an initiative to define "geomorphosites" as a quantitative basis for determining the uniqueness of geomorphological landscapes (Migoń 2009; Reynard and Coratza 2013).

29.7 Tribal Parks and Geoparks

29.7.1 Tribal Parks

The full story of tribal parks in western Canada has yet to be told. In 1984, the Meares Island Tribal Park Declaration was announced unilaterally by the Tla-o-éi-aht (Clayoquot) and Ahousaht First Nations Bands of the Nuu-Chah-Nulth people of Clayoquot Sound on Vancouver Island, British Columbia. The original motivation was a defence against the proposed logging of old growth forests before there had been any settlement of Indian land claims. Since that time, the tribal park model has been expanded by the Tla-o-qui-aht people in their own territory and has inspired First Nations protected areas around the world.

In 2015, the Tsilhqot'in (Chilcotin) Nation declared unilaterally the Dasiqox Tribal Park to protect cultural and spiritual areas from inappropriate industrial development. The area is about 125 km southwest of Williams Lake, British Columbia, and covers about 3000 km^2 of spectacular wilderness and prime wildlife habitat (Fig. 29.16). This particular tribal park initiative is now supported by a recent Supreme Court of Canada decision that gave the Chilcotin Nation strong powers to govern their lands and waters.

In the mean time, the Indigenous Peoples and Community Conserved Territories and Areas (ICCA) consortium is an international organization promoting indigenous people's conservation areas globally (Borrini-Feyerabend et al. 2004). Increasingly, tribal parks are seen as one mechanism for promoting all that is vital to the maintenance of indigenous cultures. "We regard fish as a value, the serenity of our lands and spiritual practices that we have to do there as all vital for our culture" (Saya Masso, Clayoquot band councillor and resource manager).

29.7.2 Geoparks

A geopark advances the protection and use of geological heritage in a sustainable way, and promotes the economic well-being of the people who live there. Geoparks use that heritage to promote awareness of key issues facing society in the context of environmental change (Mc Keever and Zouros 2005). Many geoparks promote awareness of geohazards, and many help prepare disaster mitigation strategies among

Fig. 29.16 Taseko Lakes in Dasiqox Tribal Park. Photograph by Jeremy Williams/River Voices

local communities. Geoparks are educators on current climate change as well as adopters of a best practise approach to utilizing renewable energy and employing the best standards of green tourism. Geoparks also inform about the sustainable use and need for natural resources, while at the same time promoting respect for the environment and the integrity of the landscape. Geoparks are not a legislative designation though the key heritage sites within a geopark are often protected under local, regional, or national legislation as appropriate. The multidisciplinary nature of the concept of geopark and tourism promotion in geoparks differentiates itself from other models of sustainable tourism.

There is a Canadian National Committee for Geoparks (CNCG) that was formed in 2009 under the auspices of the Canadian Federation of Earth Sciences (CFES). Only one geopark (Stonehammer Geopark) in New Brunswick has so far been established in Canada, but a second aspirant has recently come forward. The Tumbler Ridge Aspiring Geopark is located in British Columbia in the Eastern Cordillera and has a number of outstanding geoheritage assets. Outstanding geodiversity of mountain geomorphology, extraordinary waterfalls, dinosaur fossils and trackways and activities ranging from motoring tourism, hiking, and wilderness experiences. This proposal was presented to UNESCO's Division of Ecological and Earth Sciences in October of 2013. The sustainability goals of geoparks are admirable and may well succeed in injecting jobs and socio-economic prosperity in regions that are otherwise economically disadvantaged. But the basic tension between environmental conservation, preservation, and exploitation remains troubling.

29.8 The Land Ethic

Aldo Leopold's land ethic (Leopold 1949) offered this general principle of land management: "A thing is right when it tends to preserve the integrity, stability and beauty of the biotic community. It is wrong when it tends otherwise". Land to Leopold had a broad meaning. It included soils, water, plants, and animals. The boundaries included people as a part of Nature. Leopold's lifelong land ethics journey led from a stewardship of resources management mentality to stewardship entwined with an ecological conscience.

Geomorphology imposes certain constraints on how people should act towards the land if they wish to preserve

its integrity. Understanding of geomorphology also challenges the unspoken assumptions of an unwisely managed neoliberal society, which accepts uncritically the role of the marketplace. Proper evaluation of the sustainability of land and landscape is rapidly being eroded as environmental assessment protocols are being loosened. It seems clear that the removal of soil cover is an unsustainable practice and will ultimately reduce livelihood options for people and agriculture, as well as other organisms. The careful management of land and its biogeochemical as well as its aesthetic properties is an ethical obligation for a sustainable society. To have "outstanding universal value" determined solely by application of a physical science-based checklist of quantifiable criteria is not enough. Equally important are fulfilling the condition of integrity of the land, and adjacent water, and sound management plans which would ensure that the geoheritage value receives adequate protection.

It is evident that geomorphologists should play a pivotal role in defining the significance of landforms, landform assemblages, and landscapes. Our contribution resides in at least six interrelated aspects: (a) assessing the variable sensitivity of landscape and its vulnerability to disturbance; (b) the assessment of geodiversity and involvement in investigating geoheritage; (c) determining the representativeness of the geodiversity, biodiversity, and cultural diversity of a specific landscape; (d) providing archives and records of events that shaped landforms at the surface of the Earth in the past; (e) giving examples of particular types of landforms—in terms of size, position, visibility, and clarity of expression and state of research; and (f) recording milestones in the history of geomorphology. It is precisely because of this multiple significance that we have an ethical obligation to geoconserve landforms and landscape diversity for future generations (Slaymaker et al. 2009).

Acknowledgment Cartography by D. Kovanen.

References

Badman T (2010) World Heritage and geomorphology. In: Migoń P (ed) Geomorphological landscapes of the world. Springer, Dordrecht, pp 357–368

Berger AR, Iams WJ (eds) (1996) Geoindicators. Assessing rapid environmental changes in earth systems. Balkema, Rotterdam

Blythe R (1986) Divine landscapes. Harcourt Brace Jovanovich Publishers, San Diego

Borrini-Feyerabend G, Kothari A, Oviedo G (2004) Indigenous and local communities and protected areas: towards equity and enhanced conservation. Best practice protected area guidelines series no. 11. IUCN, Gland, Switzerland and Cambridge

Brocx M, Semeniuk V (2007) Geoheritage and geoconservation—history, definition, scope and scale. J R Soc West Aust 90:53–87

Bruno DE, Crowley BE, Gutak JM, Moroni A, Nazarenko OV, Oheim KB, Ruban DA, Teiss G, Zorina SO (2014) Paleogeography as geological heritage: developing geosite classification. Earth Sci Rev 138:300–312

Bruschi VM, Cendrero A (2005) Geosite evaluation; can we measure intangible values? Il Quat 18:293–306

Burek CV, Prosser CD (2008) The history of geoconservation: an introduction. Geol Soc Lond Spec Publ 300:1–5

Calder J, Badman T (2009) Earth heritage: a common past … and future. World Herit 52:6–15

Catto N, Catto G (2012) Landscape response to human impact in coastal Newfoundland, Canada: 29,000 km of "untouched" coastline. In: Landscape archaeology conference, LAC 2012, Topoi, special volume 3, pp 225–227

Dingwall P, Weighell T, Badman T (2005) Geological world heritage: a global framework. IUCN, Gland

Dixon G (1996) Geoconservation: an international review and strategy for Tasmania. Occasional paper 35, Parks and Wildlife Service, Tasmania, Australia

MDA Federal (2004) Landsat GeoCover ETM+ 2000 Edition Mosaics Tiles N-11-50, N-12-55. ETM-EarthSat-MrSID, 1.0, USGS, Sioux Falls, South Dakota, 2000. Data available at the Global Land Cover Facility. www.landcover.org

Goudie AS (2002) Aesthetics and relevance in geomorphological outreach. Geomorphology 47:245–249

Goudie AS, Viles H (2010) Landscapes and geomorphology: a very short introduction. Oxford University Press, Oxford

Gray M (2004) Geodiversity. Valuing and conserving abiotic nature. Wiley, Chichester

Gray M (2005) Geodiversity and geoconservation: what, why, and how? George Wright Forum 3

Gregory KJ (2000) The changing nature of physical geography. Arnold, London

IUCN and UNEP-WCMC (2015) The world database on protected areas (WDPA) (Online), (October 2015). UNEP-WCMC, Cambridge. www.protectedplanet.net

Kareiva P, Watts S, McDonald R, Boucher T (2007) Domesticated nature: shaping landscapes and ecosystems for human welfare. Science 316:1866–1869

Koja S (ed) (2006) Gustav Klimt: landscapes. Prestel Verlag, Munich

Kottek M, Grieser J, Beck C, Rudolf B, Rubel F (2006) World Map of the Köppen–Geiger climate classification updated. Meteorol Z 15:259–263. doi:10.1127/0941-2948/2006/0130. Retrieved 01 June 2013

Leopold A (1949) Sand county almanac. Oxford University Press, Oxford

Mc Keever PJ, Zouros N (2005) Geoparks: celebrating earth heritage, sustaining local communities. Episodes 28:274–278

McNamee T, Kraulis JA (1994) The national parks of Canada. Key Porter Books, Toronto

Migoń P (2009) Geomorphosites and the World Heritage List of UNESCO. In: Reynard E, Coratza P, Regolini-Bissig G (eds) Geomorphosites. Verlag Dr. Friedrich Pfeil, München, pp 119–130

Migoń P (2014) Stories behind superlative scenery. World Heritage 63:22–27

Mitchell N, Leitão L, Migoń P, Denyer S (2013) Study on the application of criterion (vii): considering superlative natural phenomena and exceptional natural beauty within the World Heritage Convention. IUCN World Heritage Study no. 10, Gland, Switzerland

Nash R (1968) The American environment: readings in the history of conservation. Addison Wesley, Boston

Ollier CD (2012) Problems of geotourism and geodiversity. Quaest Geogr 31:57–61

Pasquarè F, Pozetti M (2007) Geological hazards, disasters and the media: the Italian case study. Quat Int 173–174:1661–1671

Reynard E, Coratza P (2013) Scientific research on geomorphosites. A review of the activities of the IAG Working Group on geomorphosites over the last twelve years. Geogr Fis Din Quatern 36:159–168

Ryan KC, Knapp EE, Varner JM (2013) Prescribed fire in North American forests and woodlands: history, current practice, and challenge. Front Ecol Environ 11(Online Issue 1):e15–e24. doi:10.1890/120329

Sharples C (2002) Concepts and principles of geoconservation tasmanian parks and wildlife service website, version 3. http://www.dpiw.tas.gov.au/internnsf/Attachments/SJON-57W3YM/$FILE/geoconservation.pdf

Slaymaker O, Spencer T, Dadson S (2009) Landscape and landscape-scale processes as the unfilled niche in the global environmental change debate: an introduction. In: Slaymaker O, Spencer T, Embleton-Hamann C (eds) Geomorphology and global environmental change. Cambridge University Press, Cambridge, pp 1–36

Stöckli R, Vermote E, Saleous N, Simmon R, Herring D (2005) The Blue Marble Next Generation—a true color earth dataset including seasonal dynamics from MODIS. NASA, Earth Observatory

Thomas MF (2011) A geomorphological approach to geodiversity—its applications to geoconservation and geotourism. Quaest Geogr 31:81–89

UNESCO (1972) World Heritage sites. World Heritage Centre, UNESCO

UNESCO (2011a) Operational guidelines for the implementation of the World Heritage convention. UNESCO, Paris

UNESCO (2011b) Preparing world heritage nominations, 2nd edn. UNESCO, Paris

Vasiljević DA, Marković SB, Hose TA, Smalley I, Basarin B, Lazić L, Jović G (2010) The introduction to geoconservation of loess-palaeosol sequences in the Vojvodina region: significant geoheritage of Serbia. Quat Int 240:108–116

Williams P (2008) World heritage caves and karst. IUCN, Gland

Wood C (2009) World heritage volcanoes. IUCN, Gland